

NASA TECHNICAL
MEMORANDUM

NASA TM X-2326

001

LOAN COPY: RET 0152053
AFWL (DO)
KIRTLAND AFB



TECH LIBRARY KAFF, NM

DEPLOYMENT LOADS DATA FROM
A FREE-FLIGHT INVESTIGATION OF
ALL-FLEXIBLE PARAWINGS HAVING
371.612 METERS² (4000 FEET²)
OF WING AREA

by Delwin R. Croom

Langley Research Center
Hampton, Va. 23365

NATIONAL AERONAUTICS AND SPACE ADMINISTRATION • WASHINGTON, D. C. • NOVEMBER 1971



0152053

1. Report No. NASA TM X-2326	2. Government Accession No.	3. Recipient's Catalog No.	
4. Title and Subtitle DEPLOYMENT LOADS DATA FROM A FREE-FLIGHT INVESTIGATION OF ALL-FLEXIBLE PARAWINGS HAVING 371.612 METERS² (4000 FEET²) OF WING AREA		5. Report Date November 1971	6. Performing Organization Code
7. Author(s) Delwin R. Croom		8. Performing Organization Report No. L-7843	10. Work Unit No. 117-07-04-07
9. Performing Organization Name and Address NASA Langley Research Center Hampton, Va. 23365		11. Contract or Grant No.	13. Type of Report and Period Covered Technical Memorandum
12. Sponsoring Agency Name and Address National Aeronautics and Space Administration Washington, D.C. 20546		14. Sponsoring Agency Code	
15. Supplementary Notes			
16. Abstract A free-flight test program to determine the deployment characteristics of all-flexible parawings was conducted at the Joint Parachute Test Facility, El Centro, California, under NASA Contract NAS 1-7467.			
 Both single-keel and twin-keel parawings having a wing area of 371.612 m ² (4000 ft ²) with a five-stage reefing system were tested by use of a bomb-type instrumented test vehicle. Several twin-keel-parawing tests were also made by using an instrumented controllable sled-type test vehicle. The systems were launched from either a C-130 or a C-119 carrier airplane, and a programer parachute was used to bring the test vehicle to a proper dynamic pressure and near-vertical flight path prior to deployment of the parawing system.			
 This paper presents without discussion the free-flight deployment loads data obtained under this contract in the form of time histories of individual suspension-line loads and total loads.			
17. Key Words (Suggested by Author(s)) Parawing technology Flight operations Space vehicle		18. Distribution Statement Unclassified – Unlimited	
19. Security Classif. (of this report) Unclassified	20. Security Classif. (of this page) Unclassified	21. No. of Pages 509	22. Price* \$6.00

DEPLOYMENT LOADS DATA FROM A FREE-FLIGHT INVESTIGATION OF
ALL-FLEXIBLE PARAWINGS HAVING 371.612 METERS²
(4000 FEET²) OF WING AREA

By Delwin R. Croom
Langley Research Center

SUMMARY

A free-flight test program to determine the deployment characteristics of all-flexible parawings was conducted at the Joint Parachute Test Facility, El Centro, California, under NASA Contract NAS 1-7467.

Both single-keel and twin-keel parawings having a wing area of 371.612 m² (4000 ft²) with a five-stage reefing system were tested by use of a bomb-type instrumented test vehicle. Several twin-keel-parawing tests were also made by using an instrumented controllable sled-type test vehicle. The systems were launched from either a C-130 or a C-119 carrier airplane, and a programer parachute was used to bring the test vehicle to a proper dynamic pressure and near-vertical flight path prior to deployment of the parawing system.

This paper presents without discussion the free-flight deployment loads data obtained under this contract in the form of time histories of individual suspension-line loads and total loads.

INTRODUCTION

The National Aeronautics and Space Administration has been investigating all-flexible fabric wings to define and evaluate their performance, stability, control, and deployment characteristics. The results of wind-tunnel investigations of several single-keel and twin-keel parawing configurations are reported in references 1 to 6. Reference 7 reports the highlights of a wind-tunnel and free-flight investigation of all-flexible parawings at small scale that were obtained under NASA Contract NAS 1-7467. All the free-flight deployment loads data obtained on parawings with a wing area of 37.16 m² (400 ft²) under this contract are documented in reference 8. Reference 9 reports the highlights of a free-flight investigation of all-flexible parawings having a 371.612-m² (4000-ft²) wing area that were obtained under the same contract. An analysis of the total loads, canopy filling time, and line load distribution during each stage of canopy inflation is presented

in reference 9. Inasmuch as emphasis was given to analysis of the deployment data in reference 9, the total-load time histories presented were considerably compressed in order to provide an overall picture of events and peak loads. These condensed load time histories, however, are not suitable for a detailed analysis of deployment and inflation characteristics.

The present paper has been prepared to document in detail all the free-flight deployment loads data obtained on the 371.612-m²- (4000-ft²-) wing-area parawings under NASA Contract NAS 1-7467. The data are presented without discussion and are in the form of time histories of individual suspension-line loads and total loads. No summary or analysis plots have been included inasmuch as this information is available in reference 9.

SYMBOLS

Measurements were taken in U.S. Customary Units. Values are given in both the International System of Units (SI) and U.S. Customary Units.

a_x, a_y, a_z	longitudinal, lateral, and vertical accelerations, respectively (measured along vehicle axis system), g units
b_0	parawing flat-pattern span, m (ft)
$C_{F,t}$	total force coefficient, F_t/qS
F	force, N (lb)
F_{aft}	force in aft riser, N (lb)
F_{fwd}	force in forward riser, N (lb)
F_{left}	force in left riser, N (lb)
F_{right}	force in right riser, N (lb)
F_t	total force $(F_{aft} + F_{fwd} + F_{left} + F_{right})$, N (lb)
h	altitude above mean sea level, m (ft)
l_k, l_{le}, l_{te}	flat-pattern length of keel, leading edge, and trailing edge, respectively, m (ft)

l_r	effective reefing-line length, including end attachments for noncontinuous reefing lines, m (ft)
l_r/l_k	effective reefing ratio
q	dynamic pressure, N/m^2 (lb/ft^2)
s	flat-pattern parawing area ($0.69148l_k^2$ for single-keel parawings, $0.7726l_k^2$ for twin-keel parawings), m^2 (ft^2)
t	time, sec
v	velocity, m/sec (ft/sec)
w_D	descent weight, N (lb)
w_p	suspended weight, N (lb)
	NOTE: The two swing-arm disconnect assemblies weigh 102 N (23 lb) each and are not included in the suspended weight.
γ	flight-path angle measured from horizon, deg

Suspension-line designations:

k, le, te keel, leading-edge, and trailing-edge suspension lines, respectively.
 (Prefix L or R indicates left side or right side, and numerical suffix indicates canopy attachment location.)

Riser designations:

aft,fwd,left,right aft, forward, left, and right riser, respectively

Event designations:

PD,LS,1DR,2DR,3DR,LT programer-parachute disconnect, line stretch, first disreef, second disreef, third disreef, and line transfer, respectively

DESCRIPTION OF PARAWINGS

General

The 371.612-m²- (4000-ft²-) wing-area parawings used in the aerial-drop-test program consisted of seven versions of the twin-keel parawing and one version of the single-keel parawing. Changes in the twin-keel parawing were mainly structural modifications to the canopy. In addition, functional and structural improvements were made to the reefing system and some minor changes were made in suspension-line lengths.

Structural Arrangement

Basic canopy structures for the single-keel and the twin-keel parawings were similar in design. The canopies were constructed of 76.288-g/m² (2.25-oz/yd²) low-permeability nylon sailcloth, with the warp running parallel to the wing trailing edges.

The cloth permeability was less than $0.15 \frac{\text{m}^3/\text{min}}{\text{m}^2} \left(0.5 \frac{\text{ft}^3/\text{min}}{\text{ft}^2}\right)$ at a pressure of 1.27 cm

(0.5 in.) of water. Main structural canopy seams were parallel to the trailing edges of the wing, joining the leading-edge suspension-line or reefing-ring attachment points with the adjacent keel-line attachment points. These seams were reinforced with layers of nylon tape as required. All the outer edges and the keels of the canopies were reinforced with multiple layers of the nylon tape. Highly stressed areas, such as the suspension-line and reefing-ring attachments, were reinforced with semicircular- or elliptical-shaped load distribution patches fabricated from the basic canopy material. Where necessary, additional patch reinforcement was provided by overlaid radial tapes.

Twin-Keel Parawing

The planform layout and structural design for the seven versions of the twin-keel parawing are shown in figures 1 to 6. The suspension-line lengths and rated strengths for all versions are given in table I. Version I, as shown in figures 1 and 3, was the basic version from which all other versions were created by modification. Version I had a total of 42 suspension lines: six lines equally spaced along each leading edge, 12 lines located along each keel, and three lines spaced along the trailing edge of each outer section. The version II model was identical with version I except for tip suspension lines Lle6 and Rle6, which were made 1.031 m (40.6 in.) longer in order to provide a complete range of tip-control-line travel when used with the controllable test vehicle.

The version III model shown in figures 2 and 4 was identical with version II except for the addition of five leading-edge suspension lines to each outer section, larger semicircular load distribution patches at leading-edge-line attachment locations $2\frac{1}{2}$ to $4\frac{1}{2}$, and

four longitudinal ripstop tapes sewn on each outer section. Version IV, shown in figures 2 and 5, was identical with version II except for the addition of five suspension lines to the leading edge of each outer section, five longitudinal ripstop tapes added to the wing center section, 16 diagonal ripstop tapes added to each outer section, and load distribution patches added at leading-edge-line attachment locations 3, $3\frac{1}{2}$, and 4. Version V was identical with version IV except for the tip suspension lines Lle6 and Rle6 being 1.031 m (40.6 in.) shorter on version V. Version VI, shown in figures 2 and 6, was identical with version IV except that the outer section radial tapes on the Lkl and Rkl reinforcing patches were lengthened to terminate at the intersections of two diagonal ripstop tapes. Version VII was identical with version VI except for the tip suspension lines Lle6 and Rle6 being 1.031 m (40.6 in.) shorter on version VII.

The nominal weights of the parawing subsystems and the actual preflight weight of the complete parawing for each of the parawings are given in table II. Table II also identifies the parawing and structural version used in each of the flight tests.

Single-Keel Parawing

The planform layout and structural design for the single-keel parawing are shown in figures 7 and 8, respectively. The single-keel parawing had a total of 32 suspension lines: six lines equally spaced along each leading edge, 12 lines spaced along the keel, and four lines equally spaced along each trailing edge. The length and rated strength of each suspension line are given in table III.

RIGGING ARRANGEMENT

The parawing was attached to the test vehicle with four risers located as shown in figure 9. Each riser was attached to a group of suspension lines with a connector link. Multiple riser legs were used where necessary to accommodate a large number of lines. The number of riser legs at each attachment location is identified in figures 10, 11, and 12. The suspension-line—riser arrangements are shown in figures 13, 14, 15, and 16. To provide for the equal-suspension-line-length configuration required during the reefed phase of deployment, each suspension line was provided a bypass loop located equidistant from the canopy skirt. These loops were attached to the swing-arm release fittings located at the main forward and aft attach points. The excess length of each suspension line in the deployment configuration was stowed in individual sleeves attached to the suspension line above the bypass loop. These stowed line segments were deployed after the line transfer event. The arrangements of the attachment of the parawing to the test vehicle during the deployment phase and during the gliding-flight phase are shown in figures 17 and 18, respectively.

REEFING SEQUENCES

General

The basic reefing sequences used in tests of the 371.612-m²- (4000-ft²-) wing-area parawings were developed in the small-scale-parawing program reported in reference 7. Both the twin-keel and the single-keel parawing reefing sequences were developed with the objective of limiting peak opening loads during deployment to 3g. The reefing systems served to accomplish this objective by allowing the drag area of the system to increase in discrete steps.

A number of different reefing schemes for varying the drag area in a stepwise manner were evaluated in wind-tunnel tests (ref. 7) early in the small-scale-parawing program. The most promising reefing systems from this initial investigation, one each for the single-keel and the twin-keel parawing models, were subsequently tested and suitably modified in aerial drop tests conducted at El Mirage Dry Lake, California (2 tests) and at the Joint Parachute Test Facility, El Centro, California (16 tests). The resulting reefing systems were incorporated in the design of the 371.612-m²- (4000-ft²-) wing-area single-keel and twin-keel parawings. Detailed descriptions of these reefing systems are presented in a subsequent section.

Both tests of the 371.612-m²- (4000-ft²-) wing-area single-keel parawing were conducted with the same reefing sequence. In the tests of the 371.612-m²- (4000-ft²-) wing-area twin-keel parawing, some modifications were made to the reefing sequence originally developed in the small-scale-parawing program. The reefing sequences used in the present tests are described in the following paragraphs.

Twin-keel-parawing reefing sequence.- The twin-keel-parawing reefing sequence consisted of four stages of reefing, followed by the gliding-configuration stage. The following paragraphs provide a stage-by-stage description of the reefing sequence.

Stage 1: The wing surface was reefed into three lobes by use of a separate reefing line around the periphery of each section of the wing (i.e., the center and the two outboard sections) and by gathering the wing trailing edges with a separate reefing line. For those tests in which nose reefing was employed, the center-section nose area of the wing was also gathered with a separate reefing line. Suspension lines were shortened to the length of the tip suspension lines, the shortest suspension lines on the wing. This shortening was done to (a) align the inlets to the three lobes in a plane perpendicular to the air-stream, (b) eliminate loose suspension lines and their possible entanglement during the deployment process, (c) prevent abrasion damage of keel suspension lines against the skirt reinforcing band, and (d) provide a more uniform suspension-line loading.

During stage 1, the parawing inflated to a three-lobed balloon shape. Figure 19 shows a view looking up into the canopy with the wing fully inflated in the first reefed

stage. As shown, three air inlets – one for each lobe – are formed by the reefing lines around the leading edges, the keels, and the trailing edges. In this stage the parawing performed basically as a drag device, similar to a parachute.

Stage 2: To establish stage 2, the reefing lines on the periphery of the outboard sections of the wing were severed. The parawing inflated to the planform shape shown in figure 19. Note that the center lobe maintained its balloonlike shape between the more fully inflated outboard lobes. During this stage the wing continued to perform basically as a drag device.

Stage 3: To establish stage 3, the reefing line on the periphery of the center section of the wing was severed. The wing planform for this stage is shown in figure 19. Two planforms are illustrated, one with and one without reefing of the center-section nose area of the wing. During this stage the wing began gliding in a rearward direction.

Stage 4: To achieve stage 4, the trailing-edge gathering line and, if used, the nose gathering line were severed. For this stage all reefing lines were removed and the wing inflated to the planform shown in figure 19. The wing underwent a transition to forward gliding flight during this stage.

Full open: The suspension lines were released to their gliding-flight lengths, and the wing made a transition to the gliding-flight planform shown in figure 19.

Single-keel-parawing reefing sequence.– The single-keel-parawing reefing sequence consisted of four stages of reefing, followed by the gliding-configuration stage. The following paragraphs provide a stage-by-stage description of the reefing sequence.

Stage 1: The wing surface was reefed into two lobes by reefing lines routed around the leading edge and trailing edge of each section and by separate reefing lines which gathered the keel and the trailing edges of the wing. Suspension lines were shortened to the length of the tip suspension lines for the reasons previously mentioned in the description of the twin-keel reefing sequence.

During stage 1, the parawing inflated to a two-lobed balloon shape. Figure 20 shows a view looking up into the canopy with the wing fully inflated in the first reefed stage. As shown, two lobes were formed with the gathered keel serving as a partition between the lobes. In this stage the parawing performed basically as a drag device.

Stage 2: To establish stage 2, the reefing lines around the leading edge and trailing edge of each lobe were released, so that the leading edges were allowed to inflate fully. Figure 20 shows a planform view (from below) of the canopy in this stage. During this stage the wing continued to perform basically as a drag device.

Stage 3: To achieve stage 3, the keel gathering line was severed. Figure 20 shows the planform for this stage. During this stage the wing began gliding in a rearward direction.

Stage 4: For stage 4, the trailing-edge gathering line was severed, which removed all reefing lines from the wing. A transition to forward gliding flight occurred during this stage. The planform for this stage is shown in figure 20.

Full open: The suspension lines were released to their gliding-flight lengths, and the wing made a transition to the gliding-flight planform shown in figure 20.

Reefing Systems Used for Free-Flight Deployment

Twin-keel-parawing reefing system A.- The basic reefing system for the twin-keel parawing, designated "reefing system A," was the four-stage system defined in figure 21. The first-stage reefing system consisted of a separate line for reefing each outer lobe. The two reefing lines were connected to keel beackets forward of Lk12 and Rk12, passed through all the outboard keel reefing rings and the leading-edge reefing rings, and terminated at a connector loop located between Rk12 and Lk12. The connector loop passed through a reefing cutter and reefing ring at Rk12 and at Lk12. At cutter firing, the connector loop was severed, which provided simultaneous disreef of both outer lobes.

The second-stage reefing system consisted of reefing the center lobe with one reefing line. The line was attached to a keel becket located forward of Lk12 and passed through all the left inboard keel reefing rings, nose reefing rings, and the right inboard keel reefing rings. The end of the line was attached to a becket located forward of Rk12. The line passed through two second-stage reefing cutters at Rk2.

The third-stage reefing system consisted of a single reefing line used to gather the wing trailing edges. Each end of the line was attached to a becket located at Lle6 and at Rle6. The line was passed through all the trailing-edge reefing rings and the third-stage reefing cutters located at Rk12 and Lk12.

The fourth-stage reefing system equalized the suspension-line lengths to the length of the tip lines. Although not a conventional reefing-system arrangement, the line equalization was a separate stage in the deployment process and is, in this report, identified as a separate reefing stage. Initiation of deck-mounted, pyrotechnic-operated, swing-arm disconnects released the suspension-line bypass loops, deployed the stowed suspension-line lengths, and allowed the wing to assume a gliding-flight configuration.

Twin-keel-parawing reefing system B.- Reefing system A was improved by adding a separate third-stage nose reefing line to reduce third-stage loads and reduce localized loads in the center section of the wing, particularly in the nose area. The first-stage connector loop was routed through the reefing rings located at Lle6 and at Rle6 to eliminate possible hang-up of the first-stage reefing line at Lle6 and Rle6. This system was designated "reefing system B" and is shown in figure 22.

Twin-keel parawing reefing system C. - Further improvement was made in the third-stage reefing system by relocating the trailing-edge reefing cutters at the tip-suspension-line locations Lle6 and Rle6. The reefing cutters in their original location could move relative to the trailing-edge gathering line, which could cause abrasion of this line. The original reefing-cutter location also required that the cutters be capable of severing two thicknesses of the line because of the proximity of the reefing-line eye splice to the cutter hole. With the third-stage reefing cutters relocated in the reefing-line eye splice at the wing tips, only one thickness of line was cut by each reefing-line cutter. This permitted use of a stronger trailing-edge gathering line. Also, the abrasion problem of the gathering line against the reefing cutter was eliminated with the cutters secured to each end of the gathering line. The reefing system which incorporated this third-stage change was designated "reefing system C" and is shown in figure 23.

Single-keel-parawing reefing system. - The single-keel parawing used a four-stage reefing system, as shown in figure 24. The first-stage reefing system consisted of a separate reefing line for each of the two lobes of the canopy. Each line was connected to the reefing ring at k1, passed through all the leading-edge reefing rings, and terminated at a connector loop located at k12. The connector loop passed through two reefing-line cutters and the reefing ring at k12. At reefing-cutter firing, the connector loop was severed, which provided simultaneous disreef of both lobes.

The second-stage reefing system consisted of a single reefing line used to gather the keel between k1 and k12. The reefing line was connected to a snubber loop on the left side of the keel at k11 and passed through all the reefing rings on the left side forward through k1 and then back through the keel reefing rings on the right side to a second snubber loop at k11. Each snubber loop was connected to its respective keel becket. These beackets were both located between k11 and k12 on the keel. Both snubber loops passed through two reefing cutters located at k11. At cutter firing, both snubber loops were severed, which freed both ends of the keel reefing line.

The third-stage reefing system consisted of one reefing line used to gather the trailing edges of the canopy. The line was attached to a tip becket at Lle6 and at Rle6 and passed through all the trailing-edge reefing rings, including two reefing cutters at k12. At cutter firing, the reefing line was severed in the center of the line, which allowed the aft section of the wing to open and inflate.

As with the twin-keel parawing, the fourth-stage reefing system was the suspension-line-length-equalization arrangement. Initiation of deck-mounted, pyrotechnic-operated, swing-arm disconnects released the suspension-line bypass loops, deployed the stowed suspension-line lengths, and allowed the wing to assume a gliding-flight configuration.

TEST VEHICLES AND INSTRUMENTATION

The two types of test vehicles used in the 371.612-m^2 - (4000-ft²-) wing-area-parawing flight-test program, together with their associated instrumentation, are described in this section. The first was a bomb-type test vehicle, designed and built for use in parawing aerial deployment tests. The second was a sled-type controllable test vehicle, designed and built by the NASA Manned Spacecraft Center for use in parawing-controlled aerial gliding-flight tests.

Bomb-Type Test Vehicle

General description. - Two identical cylindrical bomb-type vehicles were built which had hemispherical noses and flared-cone—cylinder aft sections. The vehicle had an overall length of 3.556 m (140 in.), a forebody diameter of 0.940 m (37 in.), and an aft-section maximum diameter of 1.499 m (59 in.). It was capable of being ballasted from a minimum weight of approximately 11 565 N (2600 lb) to a maximum weight of approximately 26 689 N (6000 lb). The vehicle was equipped with a pair of skids for landing and for support and attachment to the extraction sleds used with either a C-119 or a C-130 launch airplane. Figure 25 shows a sketch of this vehicle.

The basic bomb-type test-vehicle structure consisted of a heavy-steel-pipe central core, to which were mounted a hemispherical nose; forward, center, and aft bulkhead assemblies; and an aft deck assembly. These sections were designed to be slipped onto the central pipe core and then securely fastened to the core. The major subassemblies of the bomb structure are illustrated in figure 26.

Gross weight changes in the vehicle were accomplished by adding semicircular steel disks to (or removing them from) the center bulkhead assembly. These ballast disks were normally added in pairs, one on each side of the bulkhead, in order to maintain the vehicle center-of-gravity position at the center bulkhead station. Small weight adjustments to the vehicle were made by adding lead shot in (or removing it from) four compartments located in the hemispherical nose section.

The aft deck assembly served several functions. First, it provided an enclosure for the packed parawing system and the deployment system, including the programmer parachute and the parawing pilot parachute. Second, it provided a structural deck for attachment of the parawing and programmer parachute to the vehicle and for retention of the parawing, programmer parachute, and pilot parachute packs. Third, the flared shape of this assembly provided aerodynamic stability to the test vehicle after vehicle separation from the launch airplane and after programmer-parachute disconnect.

Instrumentation. - The instrumentation module, containing the battery power supply, the sequencing unit, the telemetry unit, and the three-axis accelerometer package, was

mounted in the nose section of the vehicle. This module was installed in the vehicle by removal of a cover plate in the forward end of the nose. Aft-mounted instrumentation and pyrotechnics, such as the total load transducers, the individual suspension-line load transducers, and the cartridges for initiating programmer-parachute disconnect and parawing line transfer, were connected to the instrumentation module through electrical cables between the aft structural deck and the module. An aft-looking 16-mm camera, located just forward of the structural deck, was also electrically connected to the instrumentation module. Table IV is a list of the instrumentation used for a typical bomb-type vehicle test.

In addition to the aforementioned instrumentation, the bomb-type vehicle was equipped with lanyard-actuated sequencer switches, ground checkout switches, and test indicator lights, all mounted in the vehicle nose section.

Controllable Sled-Type Test Vehicle

General description.- The controllable sled-type test vehicle was developed by the NASA Manned Spacecraft Center for controllable parachute testing in the 22 240-N (5000-lb) payload range. Two basically identical vehicles were designed and fabricated for use. The two vehicles differed only in their weight range capability. The serial no. 1 vehicle had a weight range from 13 816 N (3106 lb) to 16 218 N (3646 lb), whereas the serial no. 2 vehicle had a weight range from 16 507 N (3711 lb) to 25 115 N (5646 lb).

The controllable-test-vehicle structure had a rectangular-planform base consisting of two large skids fabricated from 0.381-m (15-in.) steel channel. To the base was mounted a load-bearing structure consisting of four 1.194-m- (47-in.-) long sections of 0.127-m- (5-in.-) diameter steel pipe, coupled with stabilization braces, as shown in figure 27.

Atop the load-bearing structure was an upper deck. This upper deck was circular in planform, 1.321 m (52 in.) in diameter and was constructed of 0.006-m (1/4-in.) steel plate. The deck was supported by a square framework of 0.102-m (4-in.) H-beams through which parawing loads were transmitted to the vehicle structure.

Between the upper deck and the base was a large instrumentation pallet, to which was mounted all load-sensitive equipment. The pallet rested on two blocks of aluminum honeycomb. The pallet was free to move vertically, guided by the four main structural steel pipes, with the blocks of honeycomb serving as an impact attenuation subsystem. The basic vehicle structure measured 3.099 m (122 in.) in overall length, 1.397 m (55 in.) in width, and 1.212 m (47.7 in.) in height.

Vehicle weight changes were accomplished by adding steel plates and lead weights at four locations on the heavy steel skids, as indicated in figure 27.

When rigged for flight, the parawing risers were connected to attachment hardware on the upper deck. This attachment hardware was similar to that used with the bomb-type test vehicle, except for the additional feature of parawing disconnect. The disconnect system served to separate the parawing from the vehicle at impact to prevent dragging of the vehicle or to jettison the parawing prior to deployment of the emergency recovery system.

The parawing pack itself was mounted on top of the upper deck and held in place with a retention system. The programmer-parachute pack was mounted to the support structure forward of the upper deck, with harness attachment to disconnect fittings on the upper deck. Figure 28 shows a photograph of the serial no. 1 controllable test vehicle rigged for flight prior to test 250T.

The controllable test vehicle was equipped with a radio-command-activated emergency recovery system. This system was designed to recover the test vehicle in the event of failure of the parawing test specimen. The emergency system consisted of a drogue gun, a pilot parachute, and a 25.603-m- (84-ft-) diameter ringsail parachute. This system was located on the aft end of the test vehicle below the upper deck.

Instrumentation.- The instrumentation system for the vehicle was designed to measure onboard parameters and events and to telemeter this information to a ground receiving station. Table V is a list of the instrumentation used for the deployment phase of the controllable vehicle tests. In addition, the vehicle was equipped with a vertically mounted camera to record the parawing deployment process.

TEST PROCEDURE

Launch Airplanes

The two types of airplane used for the bomb-type vehicle tests were the C-119 and the C-130. For the controllable sled-type vehicle tests only the C-119 airplane was used.

Parawing Deployment System and Test Sequence

Bomb-type test vehicle.- For purposes of discussion in this section of the report, the deployment system is defined as all the equipment used from airplane launch of the test system until the parawing-test-specimen line stretch event. Figure 29 shows a typical test sequence with the bomb-type test vehicle and illustrates the various components in the deployment system. For launch from the airplane, the bomb-type test vehicle was initially mounted on a platform. The platform was a standard cargo delivery platform, sized to fit the rollers and guide rails on the floor of the airplane. Launch of the test system from the drop airplane was initiated by deploying an extraction parachute to the rear of the airplane. This parachute in turn pulled the platform with the attached test

vehicle from the airplane. As the bomb and platform moved away from the airplane, another parachute called the cutter parachute was static-line deployed. This parachute was used to sever the lashings which held the bomb to the platform.

After the bomb restraint lashings were cut, the extraction parachute pulled the platform away from the bomb. As the bomb separated from the platform a static line from the platform deployed a pilot parachute which in turn deployed the programer parachute. The function of the programer parachute was to establish the proper dynamic pressure and flight-path angle prior to deployment of the parawing test specimen. After a predetermined length of programer-parachute operating time, the programer parachute was released and used to deploy the parawing pilot parachute. The pilot parachute in turn extracted the parawing pack from the aft section of the bomb-type vehicle and deployed the parawing from its deployment bag. At this point in the sequence, the parawing began the disreefing sequence previously described. The time interval for each stage of the reefing sequence was controlled by pyrotechnic reefing-line cutters. These cutters had a time-delay powder train which was lanyard initiated at parawing line stretch. At the end of the fixed time delay, the powder train ignited an explosive charge which actuated the reefing-line cutter blade. Upon completion of the deployment sequence, the parawing—bomb-vehicle system made an uncontrolled gliding descent.

During the flight, test data were telemetered from onboard instrumentation to a ground receiving station. Also, camera coverage and phototheodolite data were obtained.

Controllable sled-type test vehicle.—Figure 30 illustrates a typical sequence with the controllable sled-type test vehicle. The vehicle was carried in the launch airplane on an inclined ramp. Launch of the vehicle was initiated by release of the shackles which held the test vehicle to the launch ramp. Releasing the shackle allowed the test vehicle to slide down the inclined ramp and out of the airplane. As the test vehicle separated from the airplane, a static line deployed a programer parachute. As with the bomb-type vehicle tests, the purpose of the programer parachute was to establish the proper conditions for deployment of the parawing test specimen. After a predetermined period of time, the programer parachute was disconnected from the test vehicle and used to deploy the parawing pilot parachute. The pilot parachute in turn lifted the parawing pack off the test-vehicle upper deck and deployed the parawing test specimen from its deployment bag. The parawing then proceeded through the previously described reefing sequence until the fully inflated gliding-flight configuration was established, and then the vehicle made a controlled gliding descent. Flight-test data from onboard instrumentation were telemetered to a ground receiving station during the flight. Motion-picture coverage and phototheodolite tracking data were also obtained.

PARAWING CANOPY FAILURES AND FAILURE ANALYSES

General

In the course of the 371.612-m²- (4000-ft²-) wing-area parawing flight-test program, a number of tests resulted in significant parawing-canopy structural failures which could influence the deployment load histories. Analysis of these canopy failures indicated that the failures could be grouped by failure mode, with probable causes identified for each failure mode. The significant canopy structural failures which occurred are identified, the failure modes are established, the corrective actions taken are cited, and the efficacy of the corrective actions is discussed.

It is significant that despite the major canopy damage incurred during the deployment process in several of the flight tests, all the damaged wings did open and achieve a steady gliding configuration. This fact clearly demonstrates the positive opening characteristics of the parawing. Also, all damaged wings achieved a low vertical rate of descent prior to touchdown of the test vehicle.

Significant Parawing Canopy Failures and Failure Modes

Significant canopy structural failures occurred in seven of the parawing aerial tests. These tests were single-keel-parawing test 201S and twin-keel-parawing tests 202T, 205T, 203T, 208T, 211T, and 206T; figures 31 to 37, respectively, show the major parawing canopy damage incurred in these tests. Figure 38 shows a photograph of the test 206T parawing in steady gliding flight, with some of the canopy damage in evidence.

From analyses of the canopy failures which occurred in these tests, a total of four failure modes were identified. All the significant canopy damage in the seven tests cited could be related to these four failure modes. Table VI presents the four failure modes, the time of their occurrence in the deployment process, the apparent cause of the failure mode, the test occurrence and damage identification for each failure mode, and the corrective actions taken.

Efficacy of the Corrective Actions

For three of the four failure modes shown in table VI – namely, modes 2, 3, and 4 – the corrective actions taken were successful. For failure mode 1, the corrective action was only partially successful.

In the instance of failure mode 2, 11 flights were flown after the corrective actions had been implemented on the test wings, with no recurrence of this failure mode. (Of the 11 flights, the first three flights – 207T, 250T, and 251T – were flown with added lines and larger patches and the last eight tests were flown with added lines, larger patches,

and the ripstop tape matrix.) For failure mode 3, 11 flights were flown after the corrective actions had been implemented, with little if any significant damage in the contoured nose area of the wing. For failure mode 4, five tests were flown after the corrective action had been implemented, with no further tear damage in the forward area of the side lobes.

For failure mode 1, the corrective action, consisting of addition of a ripstop tape matrix, was designed to prevent extensive tear propagation of the cloth damage but not necessarily to eliminate the occurrence of localized cloth damage. The corrective action did perform its design purpose, as demonstrated in 11 tests, beginning with test 207T. However, localized damage to canopy cloth continued to occur in these 11 tests, with the amount of such damage increasing at the higher deployment dynamic pressures. In two tests, notably 211T and 206T, canopy-cloth tears occurred with tear propagation confined by the ripstop tapes. These tears, although confined, resulted in holes of significant size in the wing canopies which degraded both the deployment and gliding-flight performance of the wings.

REDUCTION OF DATA

The altitude, flight-path angle, and velocity relative to the ground were obtained from the phototheodolite tracking data. The movement of the ambient air relative to the ground and the atmospheric density were obtained by Rawin sounding balloons. Wind corrections were applied to the velocity and dynamic pressure.

Onboard instrumentation provided force measurements which were telemetered to the ground receiving station and recorded on magnetic tape as force time histories of the flight.

In the data-reduction process, the analog data on magnetic tapes were converted to a digital tape. The digital tape was then processed to convert the data to engineering units and then into coefficient form. Data noise and dropouts were sometimes present in the analog data because of telemetry system problems; however, no effort was made in the data-reduction process to remove spurious signals or interpret data during these periods. The spurious signals usually appear in the data presented in figures 39 to 58 as spikes.

PRESENTATION OF DATA

The free-flight deployment loads data on parawings having 371.612 m^2 (4000 ft^2) of wing area that were obtained under NASA Contract NAS 1-7467 are presented without discussion in figures 39 to 58 as time histories of individual suspension-line loads and total loads. A detailed listing of each component measured is given in table VII and a

summary of the test conditions and event times with comments on the tests extracted from reference 9 is given in table VIII.

Langley Research Center,
National Aeronautics and Space Administration,
Hampton, Va., September 7, 1971.

REFERENCES

1. Naeseth, Rodger L.; and Fournier, Paul G.: Low-Speed Wind-Tunnel Investigation of Tension-Structure Parawings. NASA TN D-3940, 1967.
2. Bugg, Frank M.; and Sleeman, William C., Jr.: Low-Speed Tests of an All-Flexible Parawing for Landing a Lifting-Body Spacecraft. NASA TN D-4010, 1967.
3. Gainer, Thomas G.: Investigation of Opening Characteristics of an All-Flexible Parawing. NASA TN D-5031, 1969.
4. Ware, George M.: Wind-Tunnel Investigation of the Aerodynamic Characteristics of a Twin-Keel Parawing. NASA TN D-5199, 1969.
5. Libbey, Charles E.; Ware, George M.; and Naeseth, Rodger L.: Wind-Tunnel Investigation of the Static Aerodynamic Characteristics of an 18-Foot (5.49-Meter) All-Flexible Parawing. NASA TN D-3856, 1967.
6. Naeseth, Rodger L.: Low-Speed Wind-Tunnel Investigation of a Series of Twin-Keel All-Flexible Parawings. NASA TN D-5936, 1970.
7. Linhart, E. M.; and Buhler, W. C.: Wind Tunnel and Free Flight Investigation of All-Flexible Parawings at Small Scale. Contract No. NAS 1-7467, Northrop Corp., June 1969. (Available as NASA CR-66879.)
8. Croom, Delwin R.: Deployment Loads Data From a Free-Flight Investigation of All-Flexible Parawings at Small Scale. NASA TM X-2307, 1971.
9. Moeller, J. H.; Linhart, E. M.; Gran, W. M.; and Parson, L. T.: Free Flight Investigation of Large All-Flexible Parawings and Performance Comparison With Small Parawings - Final Report. Contract No. NAS 1-7467, Northrop Corp., Mar. 1970. (Available as NASA CR-66918.)

TABLE I.- TWIN-KEEL-PARAWING SUSPENSION-LINE LENGTHS AND RATED STRENGTHS

(a) International System of Units

Suspension line	Version I		Version II		Versions III, IV, and VI		Versions V and VII	
	Length, m (a)	Rated strength, N	Length, m (a)	Rated strength, N	Length, m (a)	Rated strength, N	Length, m (a)	Rated strength, N
Rle1 and Lle1	20.4089	24 465	20.4089	24 465	20.4089	24 465	20.4089	24 465
Rle1 $\frac{1}{2}$ and Lle1 $\frac{1}{2}$	-----	-----	-----	-----	20.2336	15 567	20.2336	15 567
Rle2 and Lle2	19.9695	24 465	19.9695	24 465	19.9695	24 465	19.9695	24 465
Rle2 $\frac{1}{2}$ and Lle2 $\frac{1}{2}$	-----	-----	-----	-----	19.7510	20 017	19.7510	20 017
Rle3 and Lle3	19.5326	44 480	19.5326	44 480	19.5326	24 465	19.5326	24 465
Rle3 $\frac{1}{2}$ and Lle3 $\frac{1}{2}$	-----	-----	-----	-----	18.9840	20 017	18.9840	20 017
Rle4 and Lle4	18.5445	24 465	18.5445	24 465	18.5445	24 465	18.5445	24 465
Rle4 $\frac{1}{2}$ and Lle4 $\frac{1}{2}$	-----	-----	-----	-----	17.7749	15 567	17.7749	15 567
Rle5 and Lle5	17.1171	24 465	17.1171	24 465	17.1171	24 465	17.1171	24 465
Rle5 $\frac{1}{2}$ and Lle5 $\frac{1}{2}$	-----	-----	-----	-----	16.1747	15 567	16.1747	15 567
Rle6 and Lle6	13.2334	24 465	14.2646	24 465	14.2646	24 465	13.2334	24 465
Rk1 and Lk1	21.3970	20 017	21.3970	20 017	21.3970	20 017	21.3970	20 017
Rk2 and Lk2	21.7272	20 017	21.7272	20 017	21.7272	20 017	21.7272	20 017
Rk3 and Lk3	21.6154	20 017	21.6154	20 017	21.6154	20 017	21.6154	20 016
Rk4 and Lk4	21.3970	20 017	21.3970	20 017	21.3970	20 017	21.3970	20 017
Rk5 and Lk5	21.3970	20 017	21.3970	20 017	21.3970	20 017	21.3970	20 017
Rk6 and Lk6	21.3970	20 017	21.3970	20 017	21.3970	20 017	21.3970	20 017
Rk7 and Lk7	21.1785	20 017	21.1785	20 017	21.1785	20 017	21.1785	20 017
Rk8 and Lk8	21.1785	20 017	21.1785	20 017	21.1785	20 017	21.1785	20 017
Rk9 and Lk9	21.0668	20 017	21.0668	20 017	21.0668	20 017	21.0668	20 017
Rk10 and Lk10	20.8483	20 017	20.8483	20 017	20.8483	20 017	20.8483	20 017
Rk11 and Lk11	20.4089	20 017	20.4089	20 017	20.4089	20 017	20.4089	20 017
Rk12 and Lk12	19.2761	24 465	19.2761	24 465	19.2761	24 465	19.2761	24 465
Rte1 and Lte1	23.4950	15 567	23.4950	15 567	23.4950	15 567	23.4950	15 567
Rte2 and Lte2	23.4950	15 567	23.4950	15 567	23.4950	15 567	23.4950	15 567
Rte3 and Lte3	20.5232	15 567	20.5232	15 567	20.5232	15 567	20.5232	15 567

^aLength from skirt-band attachment to riser-leg connector link (riser dimensions in fig. 18), except for Rk12 and Lk12 which were attached to an extension riser 1.66 meters long. The length of Rk12 and Lk12 from the skirt-band attachment to the riser-leg connector links where all other suspension lines were attached was 20.94 meters.

TABLE I.- TWIN-KEEL-PARAWING SUSPENSION-LINE LENGTHS AND RATED STRENGTHS - Concluded

(b) U.S. Customary Units

Suspension line	Version I		Version II		Versions III, IV, and VI		Versions V and VII	
	Length, in. (a)	Rated strength, lb	Length, in. (a)	Rated strength, lb	Length, in. (a)	Rated strength, lb	Length, in. (a)	Rated strength, lb
Rle1 and Lle1	803.5	5 500	803.5	5 500	803.5	5500	803.5	5500
Rle1 $\frac{1}{2}$ and Lle1 $\frac{1}{2}$	-----	-----	-----	-----	796.6	3500	796.6	3500
Rle2 and Lle2	786.2	5 500	786.2	5 500	786.2	5500	786.2	5500
Rle2 $\frac{1}{2}$ and Lle2 $\frac{1}{2}$	-----	-----	-----	-----	777.6	4500	777.6	4500
Rle3 and Lle3	769.0	10 000	769.0	10 000	769.0	5500	769.0	5500
Rle3 $\frac{1}{2}$ and Lle3 $\frac{1}{2}$	-----	-----	-----	-----	747.4	4500	747.4	4500
Rle4 and Lle4	730.1	5 500	730.1	5 500	730.1	5500	730.1	5500
Rle4 $\frac{1}{2}$ and Lle4 $\frac{1}{2}$	-----	-----	-----	-----	699.8	3500	699.8	3500
Rle5 and Lle5	673.9	5 500	673.9	5 500	673.9	5500	673.9	5500
Rle5 $\frac{1}{2}$ and Lle5 $\frac{1}{2}$	-----	-----	-----	-----	636.8	3500	636.8	3500
Rle6 and Lle6	521.0	5 500	561.6	5 500	561.6	5500	521.0	5500
Rk1 and Lk1	842.4	4 500	842.4	4 500	842.4	4500	842.4	4500
Rk2 and Lk2	855.4	4 500	855.4	4 500	855.4	4500	855.4	4500
Rk3 and Lk3	851.0	4 500	851.0	4 500	851.0	4500	851.0	4500
Rk4 and Lk4	842.4	4 500	842.4	4 500	842.4	4500	842.4	4500
Rk5 and Lk5	842.4	4 500	842.4	4 500	842.4	4500	842.4	4500
Rk6 and Lk6	842.4	4 500	842.4	4 500	842.4	4500	842.4	4500
Rk7 and Lk7	833.8	4 500	833.8	4 500	833.8	4500	833.8	4500
Rk8 and Lk8	833.8	4 500	833.8	4 500	833.8	4500	833.8	4500
Rk9 and Lk9	829.4	4 500	829.4	4 500	829.4	4500	829.4	4500
Rk10 and Lk10	820.8	4 500	820.8	4 500	820.8	4500	820.8	4500
Rk11 and Lk11	803.5	4 500	803.5	4 500	803.5	4500	803.5	4500
Rk12 and Lk12	758.9	5 500	758.9	5 500	758.9	5500	758.9	5500
Rte1 and Lte1	925.0	3 500	925.0	3 500	925.0	3500	925.0	3500
Rte2 and Lte2	925.0	3 500	925.0	3 500	925.0	3500	925.0	3500
Rte3 and Lte3	808.0	3 500	808.0	3 500	808.0	3500	808.0	3500

^aLength from skirt-band attachment to riser-leg connector link (riser dimensions in fig. 18), except for Rk12 and Lk12 which were attached to an extension riser 65.4 inches long. The length of Rk12 and Lk12 from the skirt-band attachment to the riser-leg connector links where all other suspension lines were attached was 824.3 inches.

TABLE II.- WEIGHT BREAKDOWN OF PARAWING SYSTEMS TESTED

(a) International System of Units

Parawing serial number	Structural version	Test	Nominal weight, N						Measured complete parawing system weight, N	
			Canopy		Suspension system		Reefing system	Complete parawing system		
			Cloth	Reinforcements	Lines	Risers				
Twin-keel parawing										
1	I	200T	334	356	453	120	89	1352	1353.1	
1	I	202T	334	356	453	120	89	1352	1339.8	
1	III	207T	334	418	525	142	89	1508	1508.8	
1	III	250T	334	418	525	142	89	1508	1503.5	
1	III	251T	334	418	525	142	89	1508	1512.4	
2	I	204T	334	356	453	120	89	1352	1357.2	
2	I	205T	334	356	453	120	89	1352	1366.5	
2	IV	252T	334	556	525	142	89	1646	1647.2	
2	VI	253T	334	556	525	142	89	1646	1661.0	
2	VI	254T	334	556	525	142	89	1646	1654.3	
2	VI	255T	334	556	525	142	89	1646	1664.5	
3	I	201T	334	356	453	120	89	1352	1313.1	
3	II	208T	334	356	453	120	89	1352	1377.6	
4	I	203T	334	356	453	120	89	1352	1357.2	
4	V	209T	334	556	525	142	89	1646	1637.8	
4	V	211T	334	556	525	142	89	1646	1624.5	
4	VII	206T	334	556	525	142	89	1646	1646.7	
4	VII	210T	334	556	525	142	89	1646	1660.1	
Single-keel parawing										
1		200S	334	222	436	102	67	1161	1162.8	
2		201S	334	222	436	102	67	1161	1166.3	

TABLE II.- WEIGHT BREAKDOWN OF PARAWING SYSTEMS TESTED – Concluded

(b) U.S. Customary Units

Parawing serial number	Structural version	Test	Nominal weight, lb						Measured complete parawing system weight, lb	
			Canopy		Suspension system		Reefing system	Complete parawing system		
			Cloth	Reinforcements	Lines	Risers				
Twin-keel parawing										
1	I	200T	75	80	102	27	20	304	304.2	
1	I	202T	75	80	102	27	20	304	301.2	
1	III	207T	75	94	118	32	20	339	339.2	
1	III	250T	75	94	118	32	20	339	338.0	
1	III	251T	75	94	118	32	20	339	340.0	
2	I	204T	75	80	102	27	20	304	305.1	
2	I	205T	75	80	102	27	20	304	307.2	
2	IV	252T	75	125	118	32	20	370	370.3	
2	VI	253T	75	125	118	32	20	370	373.4	
2	VI	254T	75	125	118	32	20	370	371.9	
2	VI	255T	75	125	118	32	20	370	374.2	
3	I	201T	75	80	102	27	20	304	295.2	
3	II	208T	75	80	102	27	20	304	309.7	
4	I	203T	75	80	102	27	20	304	305.1	
4	V	209T	75	125	118	32	20	370	368.2	
4	V	211T	75	125	118	32	20	370	365.2	
4	VII	206T	75	125	118	32	20	370	370.2	
4	VII	210T	75	125	118	32	20	370	373.2	
Single-keel parawing										
1		200S	75	50	98	23	15	261	261.4	
2		201S	75	50	98	23	15	261	262.2	

TABLE III.- SINGLE-KEEL-PARAWING SUSPENSION-LINE DESIGN
LENGTHS AND RATED STRENGTHS

(a) International System of Units

Suspension line	Design length, m (a)	Rated strength, N
Rle1 and Lle1	25.0596	26 689
Rle2 and Lle2	23.8557	26 689
Rle3 and Lle3	22.8448	44 482
Rle4 and Lle4	21.2039	26 689
Rle5 and Lle5	20.1143	26 689
Rle6 and Lle6	18.0721	26 689
k1	24.0970	20 017
k2	24.6278	20 017
k3	24.8666	20 017
k4	24.3865	20 017
k5	23.8074	20 017
k6	23.6144	20 017
k7	23.6144	24 465
k8	23.6144	24 465
k9	23.6144	24 465
k10	23.2766	24 465
k11	21.5265	24 465
k12	19.9999	24 465
Rte1 and Lte1	25.2222	15 569
Rte2 and Lte2	26.4262	15 569
Rte3 and Lte3	25.5422	15 569
Rte4 and Lte4	21.6865	15 569

^aLength from skirt-band attachment to riser-leg connector link. (See fig. 18 for riser dimensions.)

TABLE III.- SINGLE-KEEL-PARAWING SUSPENSION-LINE DESIGN

LENGTHS AND RATED STRENGTHS – Concluded

(b) U.S. Customary Units

Suspension line	Design length, in. (a)	Rated strength, lb
Rle1 and Lle1	986.6	6 000
Rle2 and Lle2	939.2	6 000
Rle3 and Lle3	899.4	10 000
Rle4 and Lle4	834.8	6 000
Rle5 and Lle5	791.9	6 000
Rle6 and Lle6	711.5	6 000
k1	948.7	4 500
k2	969.6	4 500
k3	979.0	4 500
k4	960.1	4 500
k5	937.3	4 500
k6	929.7	4 500
k7	929.7	5 500
k8	929.7	5 500
k9	929.7	5 500
k10	916.1	5 500
k11	847.5	5 500
k12	787.4	5 500
Rte1 and Lte1	993.0	3 500
Rte2 and Lte2	1040.4	3 500
Rte3 and Lte3	1005.6	3 500
Rte4 and Lte4	853.8	3 500

^aLength from skirt-band attachment to riser-leg connector link. (See fig. 18 for riser dimensions.)

TABLE IV.- INSTRUMENTATION FOR A TYPICAL
BOMB-TYPE-VEHICLE TEST (200T)

IRIG TM channel	Parameter measured	Sensor range	
18	Outboard riser load (left)	0 to 5000 lb	(22 241 N)
17	Suspension-line load Lk12	0 to 5000 lb	(22 241 N)
16	Suspension-line load Lle7	0 to 5000 lb	(22 241 N)
13	Main riser load (aft)	0 to 15 000 lb	(66 723 N)
12	Suspension-line load Lle6	0 to 5000 lb	(22 241 N)
11	Suspension-line load Lle1	0 to 5000 lb	(22 241 N)
10	Outboard riser load (right)	0 to 5000 lb	(22 241 N)
9	Main riser load (forward)	0 to 15 000 lb	(66 723 N)
8	Z-axis acceleration	-1g to +4.5g	
7	Y-axis acceleration ^a	-2.30g to +3.50g	
6	X-axis acceleration ^a	-2.31g to +3.89g	
5	Events	-----	

^aSuspension-line loads were measured in place of accelerations on some tests.

TABLE V.- INSTRUMENTATION USED DURING CONTROLLABLE-VEHICLE
DEPLOYMENT TESTS

(a) Continuous data

IRIG TM channel	Parameter measured	Sensor range
13	Aft main riser load	0 to 15 000 lb (66 723 N)
12	Forward main riser load	0 to 15 000 lb (66 723 N)

(b) Commutated data (IREG E channel)^a

Commutator switch position	Parameter measured	Sensor range
3, 18, 33, 48, 63, and 78	Left riser load	0 to 5000 lb (22 241 N)
4, 19, 34, 49, 64, and 79	Right riser load	0 to 5000 lb (22 241 N)

^aThese data were commutated by using a 90 by 10 commutator. The sensors were attached to six switches each and thus were commutated at 60 samples/sec.

TABLE VI.- PARAWING-CANOPY FAILURE MODES, TEST OCCURRENCES, AND CORRECTIVE ACTION

Failure mode	Time of occurrence in the deployment process	Apparent cause of failure	Test occurrence and damage identification		Corrective action (a)
1. Localized canopy cloth damage, often followed by propagating tears in the cloth until stopped by heavier canopy structure.	Initial parawing deployment and first-stage reefed inflation.	Localized cloth abrasion damage during initial canopy stretchout and first-stage reefed inflation and/or localized cloth overload during first-stage reefed inflation.	201S 205T 208T 211T 206T	Panel tearout in right-hand lobe. Longitudinal tear in right-hand lobe. Holes in center and right-hand lobe. Large hole in right-hand lobe. Large holes in left-hand, center, and right-hand lobes.	Matrix of ripstop tapes sewn on canopy to limit tear propagation.
2. Structural failure in the central areas of the wing leading edges, often followed by propagating tears in the cloth until stopped by heavier canopy structure.	Second-stage reefed inflation.	High concentrated loads at the number 3 and 4 leading-edge-line attachment locations, with inadequate canopy structure in the direction of the loads.	201S 203T 208T	Two-panel tearout in left-hand lobe. Panel tearout in right-hand lobe; torn gusset at Rle4. Three-panel tearout in right-hand lobe.	(a) Ten leading-edge lines (five on each leading edge) added between existing lines 1 and 6. (b) Larger semicircular load distribution patches added in the central and leading-edge-line attachment locations. (c) Alignment of ripstop tapes to provide structure in the direction of load during second-stage inflation
3. Holes, burns, and tears in the contoured nose section of the wing.	Holes and burns – probably during initial parawing deployment; tears probably during third-stage reefed inflation.	Cloth burn/abrasion damage from contact with leading-edge skirt band and/or nose snubber lines; tears due to dynamic loading condition following second-stage disreef.	202T 205T	Two large tears and numerous burn holes and burn areas in contoured nose panel. Numerous small holes in contoured nose panel.	(a) Encasement of the five nylon nose snubber lines in cotton sateen sleeves. (b) Separate reefing added for the nose section of the wing.
4. Tears in the forward areas of the side lobes, between the leading-edge skirt band and the edge of the forward keel-line fan patch.	Second- or third-stage reefed inflation.	Marginal canopy structural strength in the direction of load during second- or third-stage reefed inflation.	211T	Tears in forward portion of left-hand lobe, between the leading-edge skirt band and the forward keel-line fan patch.	Four fan-patch tapes extended to the intersection of existing ripstop tapes.

^aAccomplished on the twin-keel parawing only.

TABLE VII.- INSTRUMENTATION SUMMARY

Test	Test sequence	Parawing	Data figure	Riser load link				Suspension-line load link on line -				Acceleration along axis				
				Fwd	Aft	Left	Right	k12	k7	Lle1	Lle6	---	---	X	Y	Z
200S	3	1	39	1	1	1	1	k12	k7	Lle1	Lle6	---	---	X	Y	Z
201S	4	2	40	1	1	1	1	k12	k7	Lle1	Lle6	---	---	X	Y	Z
200T	1	1	41	1	1	1	1	Lk12	Lk7	Lle1	Lle6	---	---	X	Y	Z
201T	5	3	42	1	1	1	1	Lk12	Lle1	Lle3	Lle6	---	---	X	Y	Z
202T	6	1	43	1	1	1	1	Lk12	Lk7	Lle1	Lle6	---	---	X	Y	Z
203T	8	4	44	1	1	1	1	Lk12	Lle1	Lle3	Lle6	---	---	X	Y	Z
204T	2	2	45	1	1	1	1	Lk12	Lk7	Lle1	Lle6	---	---	X	Y	Z
205T	7	2	46	1	1	1	1	Lk12	Lk7	Lle1	Lle6	---	---	X	Y	Z
206T	16	4	47	1	1	1	1	Lk12	Lle1	Lle2	Lle3	Lle4	Lle6	-	-	Z
207T	10	1	48	1	1	1	1	Lk12	Lk7	Lk3	Lle1	Lle6	Lte3	-	-	Z
208T	9	3	49	1	1	1	1	Lk12	Lle1	Lle2	Lle3	Lle4	Lle6	-	-	Z
209T	13	4	50	1	1	1	1	Lk12	Lle1	Lle2	Lle3	Lle4	Lle6	-	-	Z
210T	18	4	51	1	1	1	1	Lk12	Lle1	Lle2	Lle3	Lle4	Lle6	-	-	Z
211T	14	4	52	1	1	1	1	Lk12	Lle1	Lle2	Lle3	Lle4	Lle6	-	-	Z
250T	11	1	53	1	1	1	1									
251T	12	1	54	1	1	1	1									
252T	15	2	55	1	1	1	1									
253T	17	2	56	1	1	1	1									
254T	19	2	57	1	1	1	1									
255T	20	2	58	1	1	1	1									

TABLE VIII.- TEST CONDITIONS, EVENT TIMES, AND COMMENTS FOR INTERMEDIATE-SCALE PARAWING TESTS

Test	Conditions at programmed parachute disconnect				Suspended weight, w_p		Descent weight, w_d		Event time, sec after launch					Reefing		Comments on deployment phase of test (a)
	q_{PD}		h_{PD}		N	lb	N	lb	t_{PD}	t_{LS}	t_{IDR}	t_{2DR}	t_{3DR}	t_{LT}	Version	t_r/t_k
	N/m ²	lb/ft ²	m	ft												
200S	794.8	16.6	1582	5 190	11 392	2561	12 758	2868	23.87	25.97	32.17	34.98	38.29	41.74	0.116	Good deployment test.
201S	857.1	17.9	885	2 905	20 809	4678	22 228	4997	26.19	28.08	34.32	37.99	40.74	44.87	.120	Major canopy damage during deployment.
200T	814.0	17.0	1524	5 000	11 214	2521	12 806	2879	23.87	25.61	31.76	34.85	38.43	39.61	A	Abbreviated fourth reefed stage, otherwise good deployment test.
201T	919.3	19.2	1227	4 025	20 871	4692	22 392	5034	26.13	27.92	33.99	37.22	40.71	44.74	A	Left trailing edge failed to disreef.
202T	2734.0	57.1	4444	14 580	15 320	3444	16 868	3792	27.35	28.69	35.29	37.94	41.36	45.26	A	.100 Some canopy damage in nose area.
203T	2858.5	59.7	4560	14 960	15 364	3454	16 925	3805	27.36	28.76	35.06	38.12	41.58	45.23	A	Major canopy damage in right lobe during deployment.
204T	1623.1	33.9	5828	19 120	15 271	3433	16 841	3786	28.98	30.45	36.97	39.57	43.08	47.00	A	.140 Some vehicle oscillation after first-stage inflation, otherwise good deployment test.
205T	3231.9	67.5	4496	14 750	20 809	4678	22 379	5031	26.25	27.57	33.96	36.82	40.63	44.16	A	.100 Some canopy damage in nose area plus a 0.508-m (20-inch) tear in right lobe.
206T	4366.7	91.2	5627	18 460	20 395	4585	22 246	5001	22.54	23.86	29.96	32.84	36.62	40.83	C	.080 Moderate canopy damage in all three lobes during deployment, otherwise good deployment test.
207T	1489.1	31.1	4625	15 175	20 502	4609	22 214	4994	29.48	30.02	37.37	40.12	43.32	48.42	B	.100 Good deployment test.
208T	885.8	18.5	5848	19 185	20 764	4668	22 348	5024	29.33	30.99	37.42	40.19	43.01	48.26	A	.100 Major canopy damage in right lobe during deployment.
209T	2724.4	56.9	4432	14 540	15 106	3396	16 952	3811	27.44	28.82	35.07	No data	b35.41	45.47	B	.080 Third-stage trailing-edge reefing line failed in second stage, otherwise good deployment test.
210T	2614.3	54.6	5794	19 010	15 097	3394	16 961	3813	23.12	24.54	30.74	35.64	36.99	42.43	C	.080 Some vehicle oscillation during deployment, otherwise good deployment test.
211T	2034.9	42.5	5692	18 675	24 897	5597	26 729	6009	23.49	24.90	31.03	34.30	38.00	41.68	B	.100 Moderate canopy damage during deployment, otherwise good deployment test.
250T	732	15.3	5899	19 353	13 613	3060	15 320	3444	10.74	12.68	19.40	22.14	25.70	32.98	B	.100 Good deployment test.
251T	1044	21.8	6399	20 995	15 975	3591	17 691	3977	10.61	32.99	41.99	46.08	-----	33.76	B	.100 Prolonged parawing-pack hang-up, resulting in abnormal deployment.
252T	790	16.5	6905	22 655	15 975	3591	17 824	4007	10.61	12.41	18.77	21.77	24.96	32.55	B	.100 Good deployment test.
253T	1139	23.8	6989	22 931	20 428	4592	22 290	5011	10.56	12.27	18.38	21.27	c24.11	32.63	C	.100 Good deployment test. d24.30
254T	1216	25.4	6834	22 420	24 881	5593	26 738	6011	10.62	12.33	18.43	21.30	24.72	32.32	C	.100 Good deployment test.
255T	1446	30.2	7193	23 600	24 881	5593	26 752	6014	10.46	12.08	18.46	21.12	24.26	32.27	C	.100 Good deployment test.

aThese comments taken from reference 9.

bThird-stage trailing-edge line failed at $t = 35.41$ sec, resulting in premature third-stage disreef. Second-stage disreef not distinguishable.cCenter-section nose disreef at $t = 24.11$ sec.dTrailing-edge disreef at $t = 24.30$ sec.

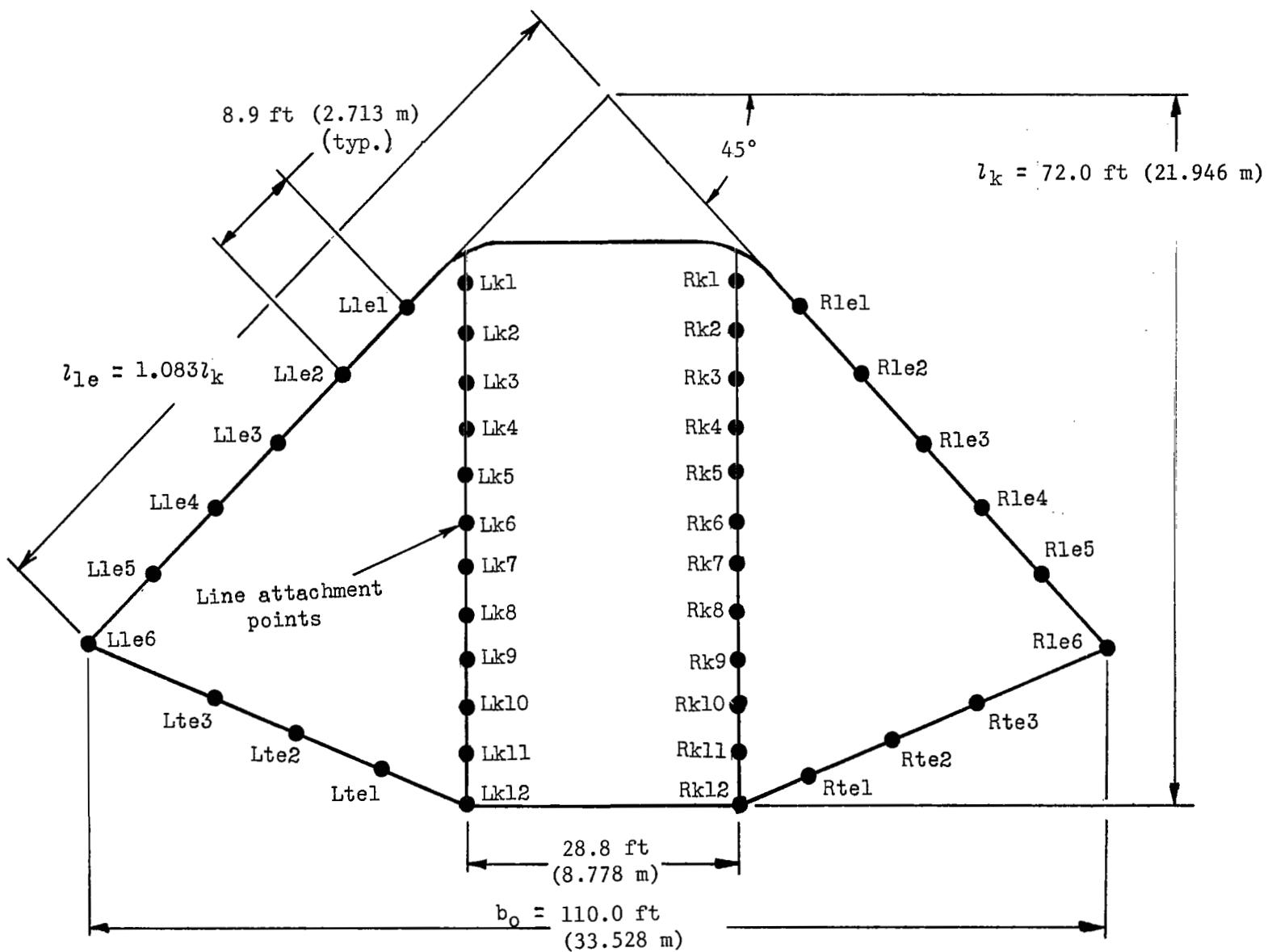


Figure 1.- Planform layout for versions I and II of 371.612-m²- (4000-ft²-) wing-area twin-keel parawing.

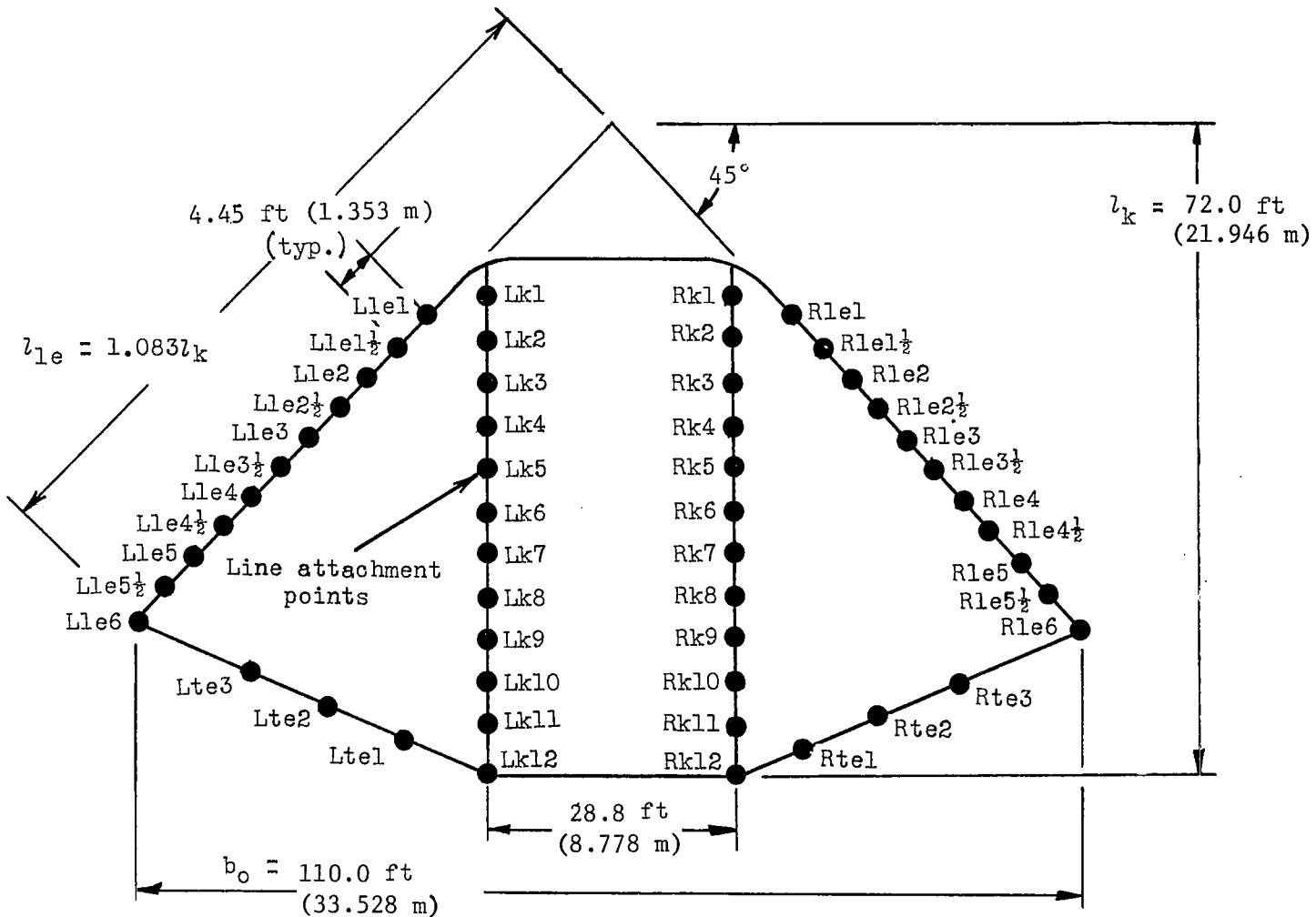


Figure 2.- Planform layout for versions III, IV, V, VI, and VII of 371.612-m²- (4000-ft²-) wing-area twin-keel parawing.

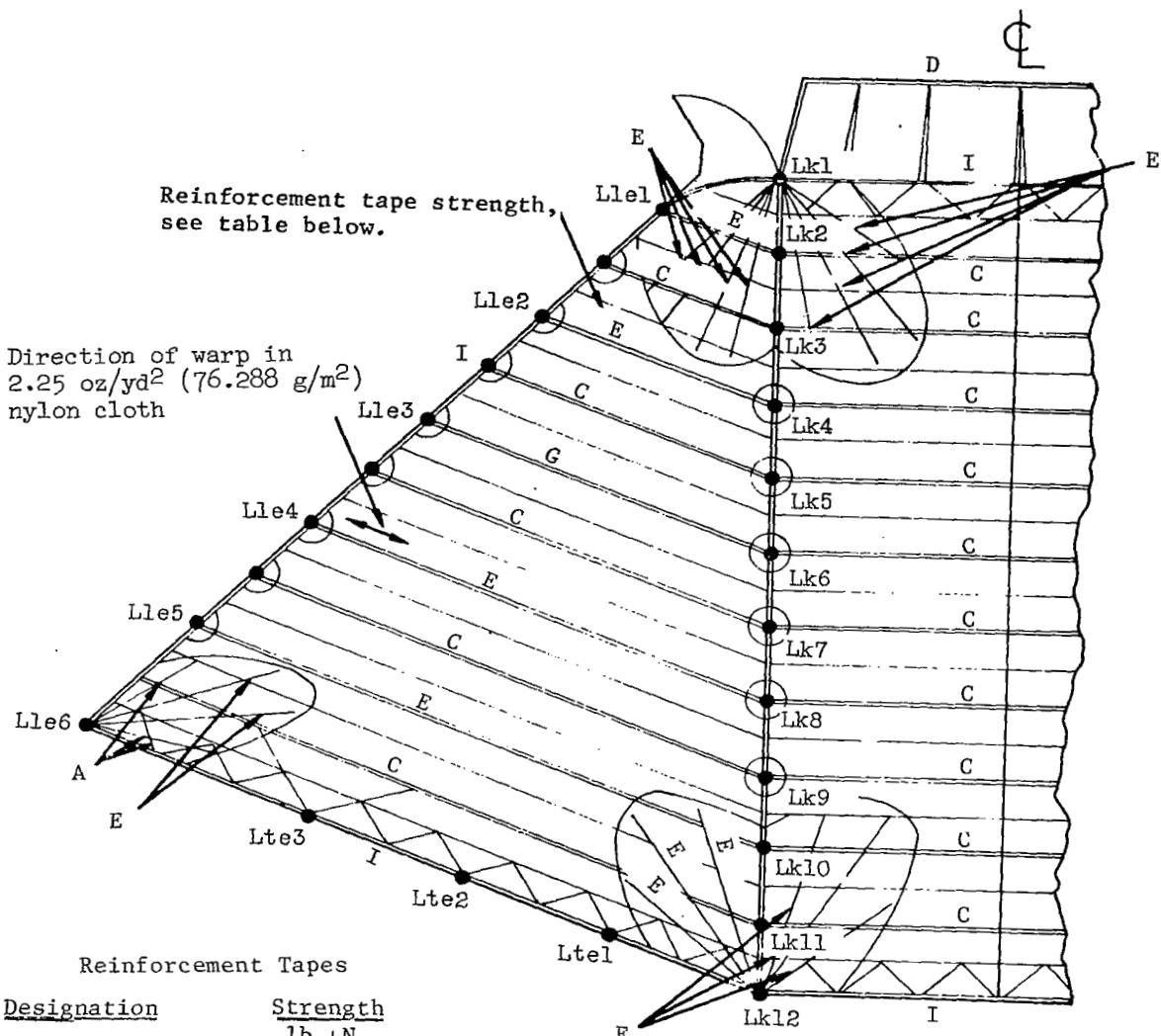


Figure 3.- Structural diagram for versions I and II of twin-keel parawing.

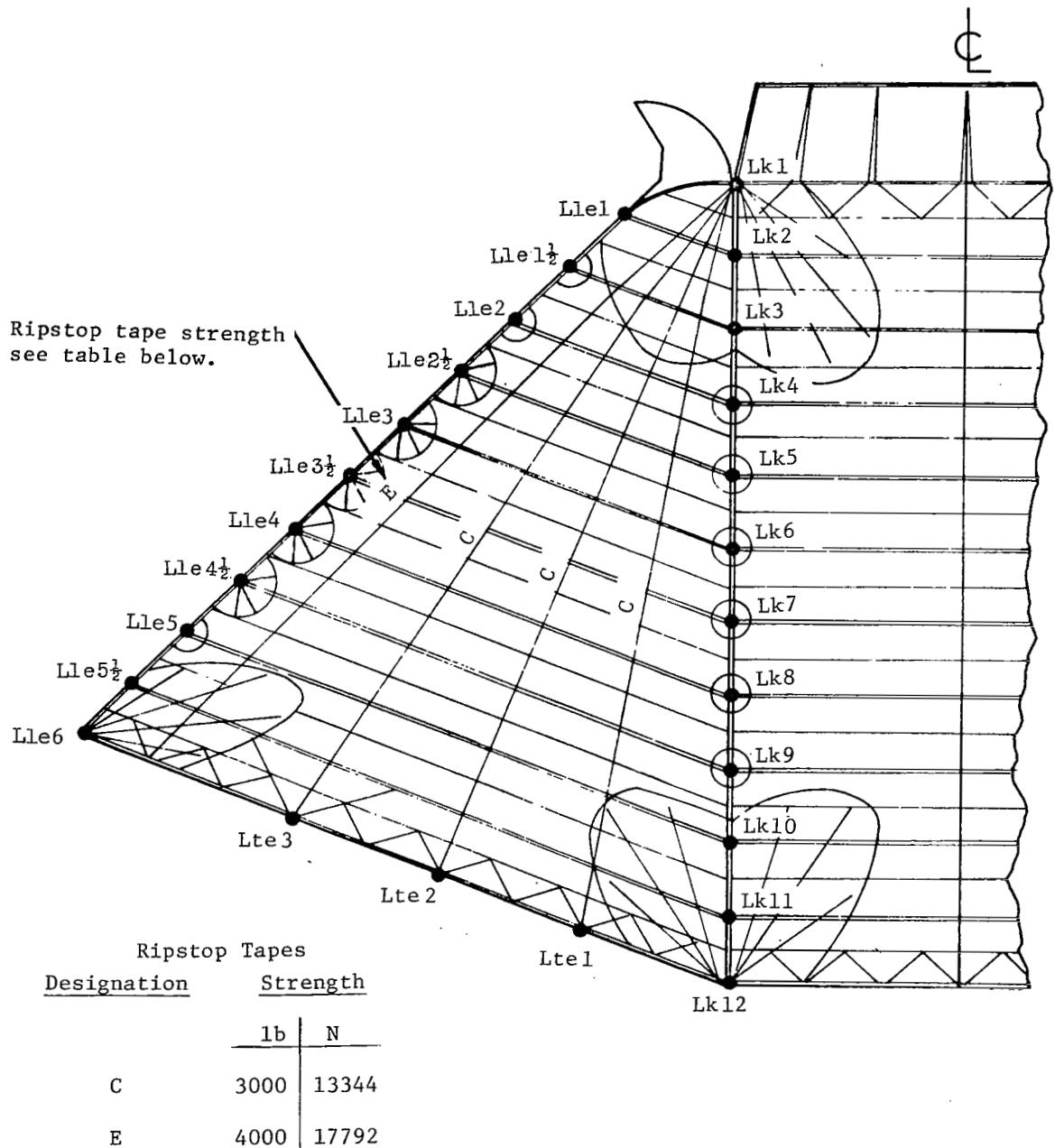


Figure 4.- Structural diagram for version III of twin-keel parawing. (Identical with versions I and II, except as noted.)

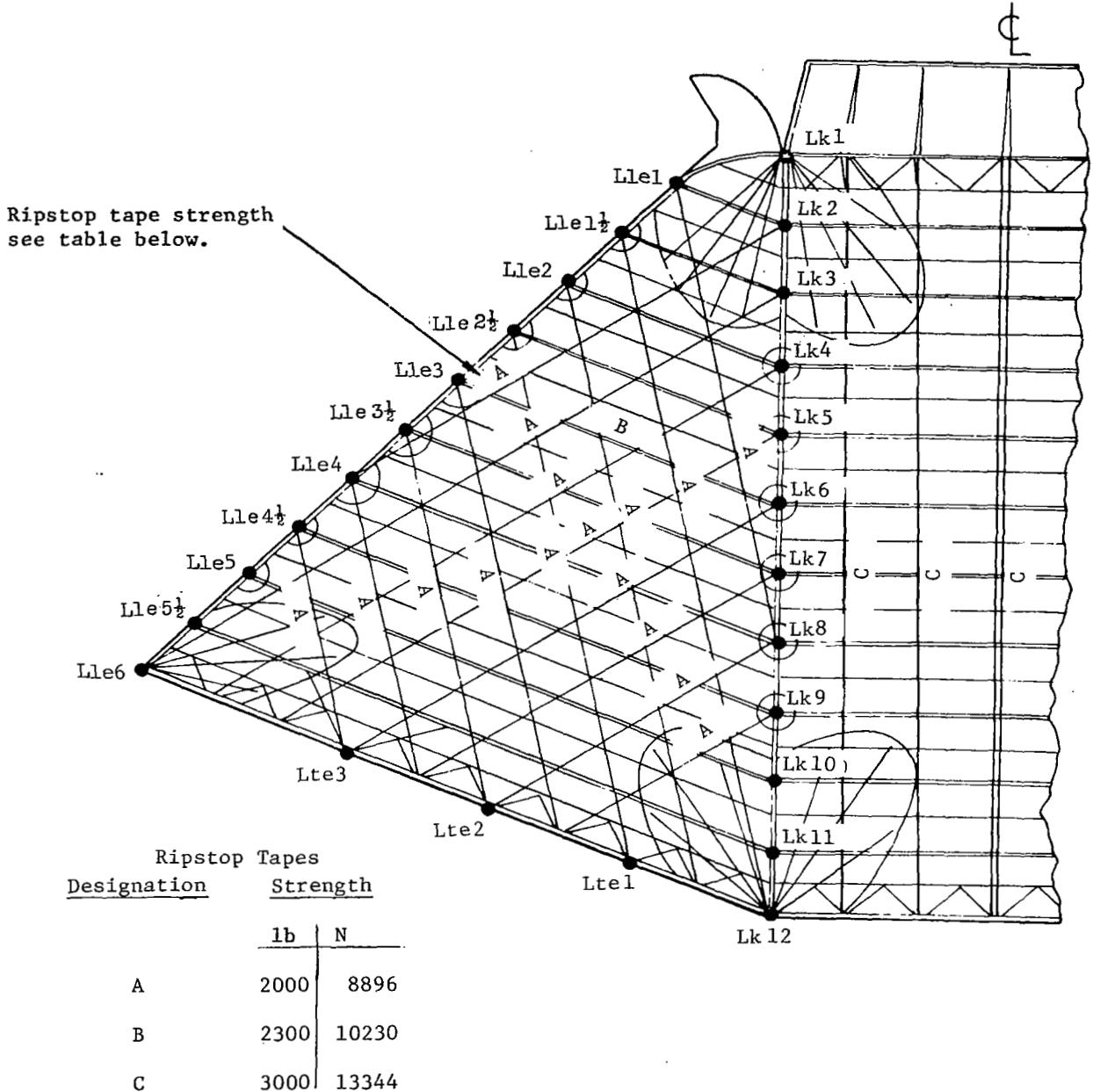
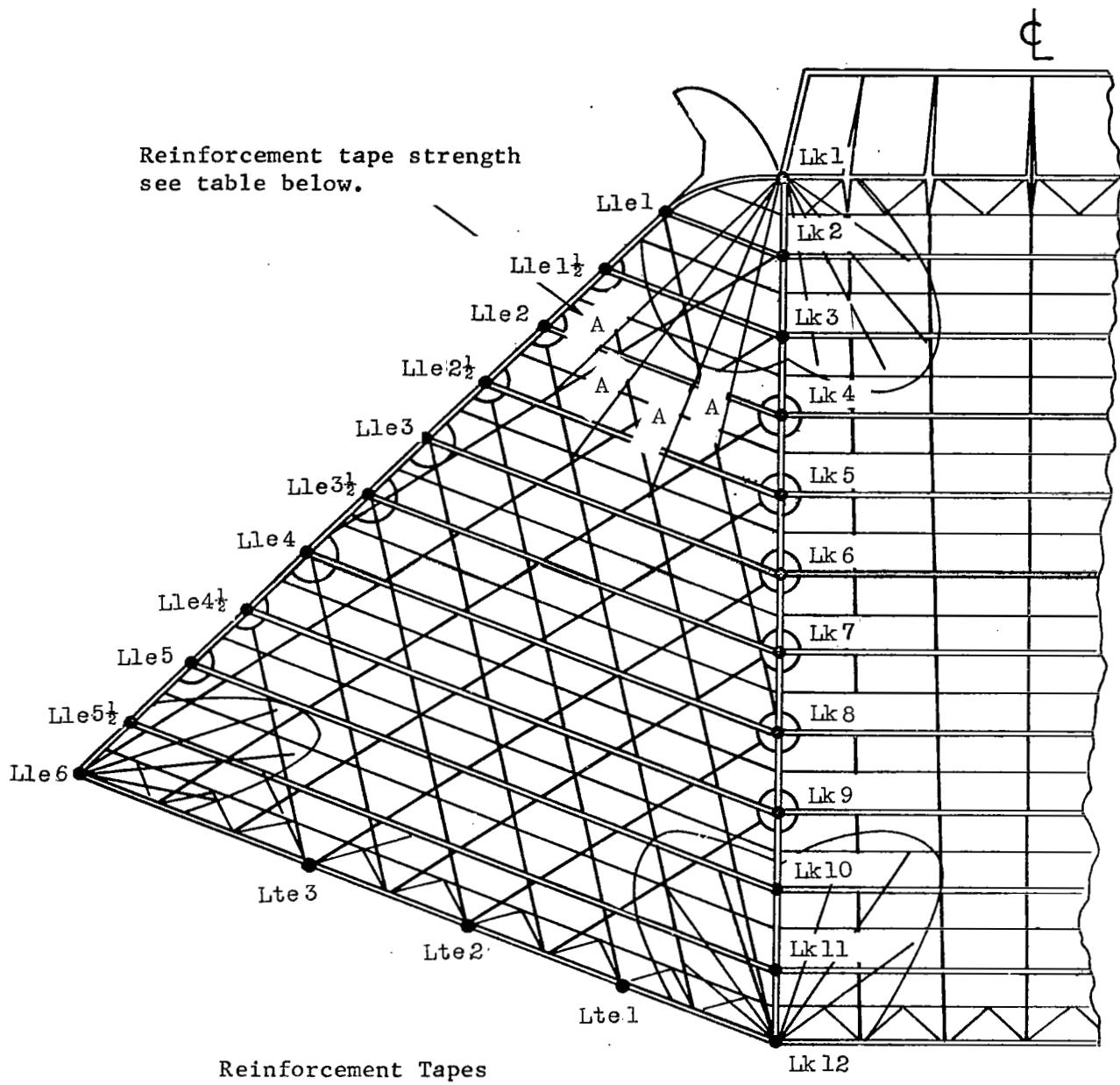


Figure 5.- Structural diagram for versions IV and V of twin-keel parawing. (Identical with versions I and II, except as noted.)



<u>Designation</u>	<u>Strength</u>	
	lb	N
A	2000	8896

Figure 6.- Structural diagram for versions VI and VII of twin-keel parawing. (Identical with versions IV and V, except as noted.)

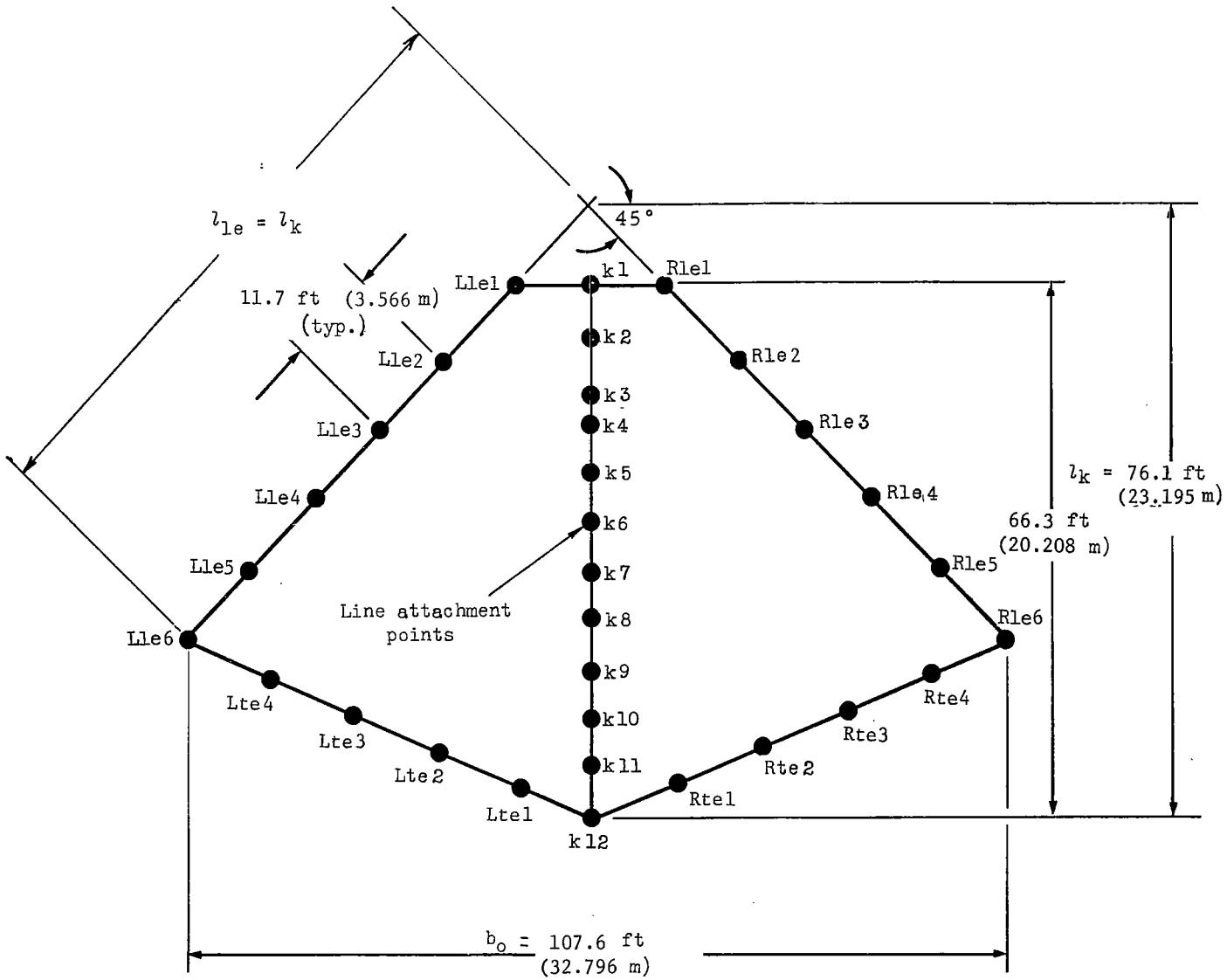


Figure 7.- Planform layout for 371.612-m²- (4000-ft²-) wing-area single-keel parawing.

Reinforcement tape strength
see table below.

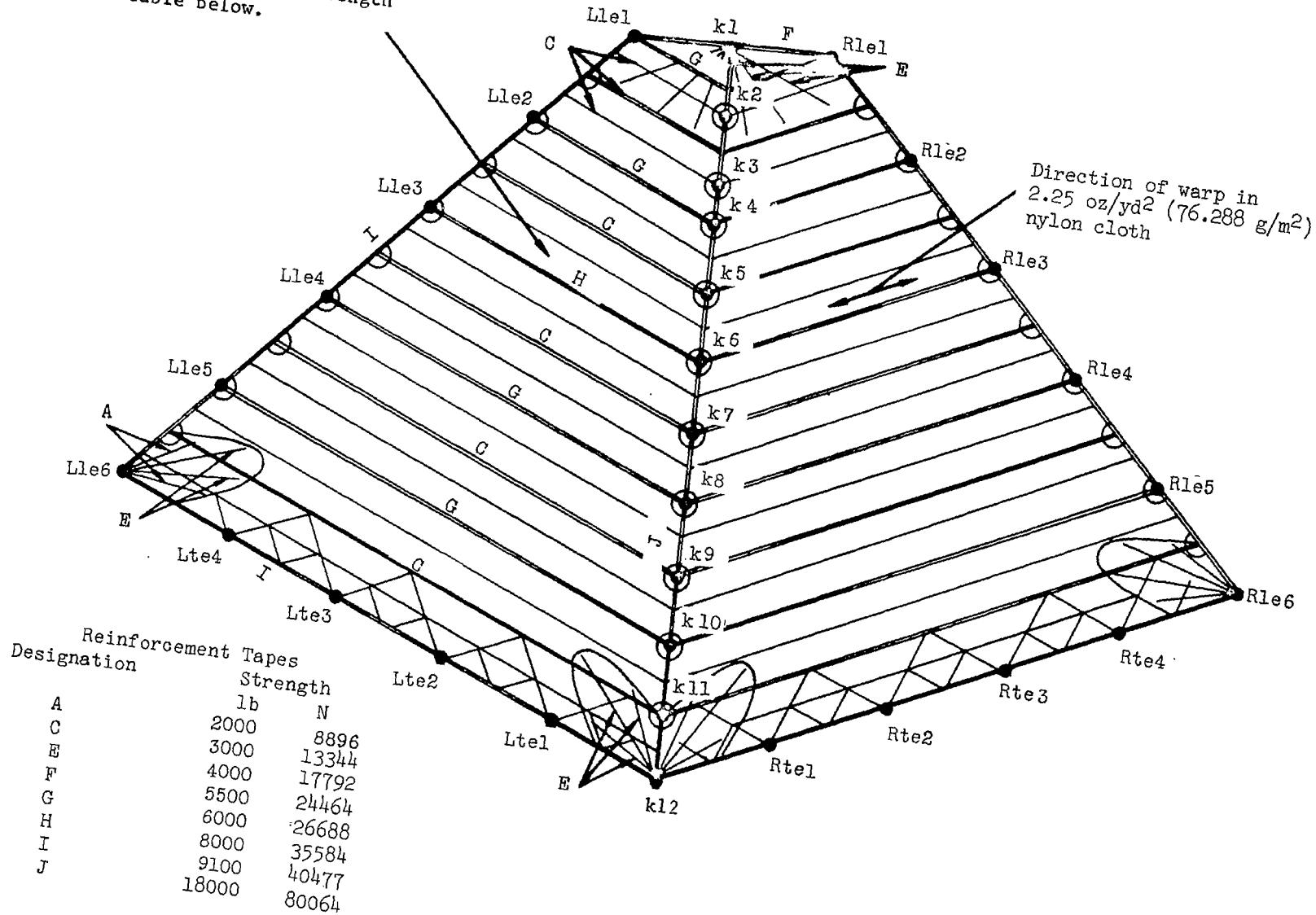


Figure 8.- Structural diagram for single-keel parawing.

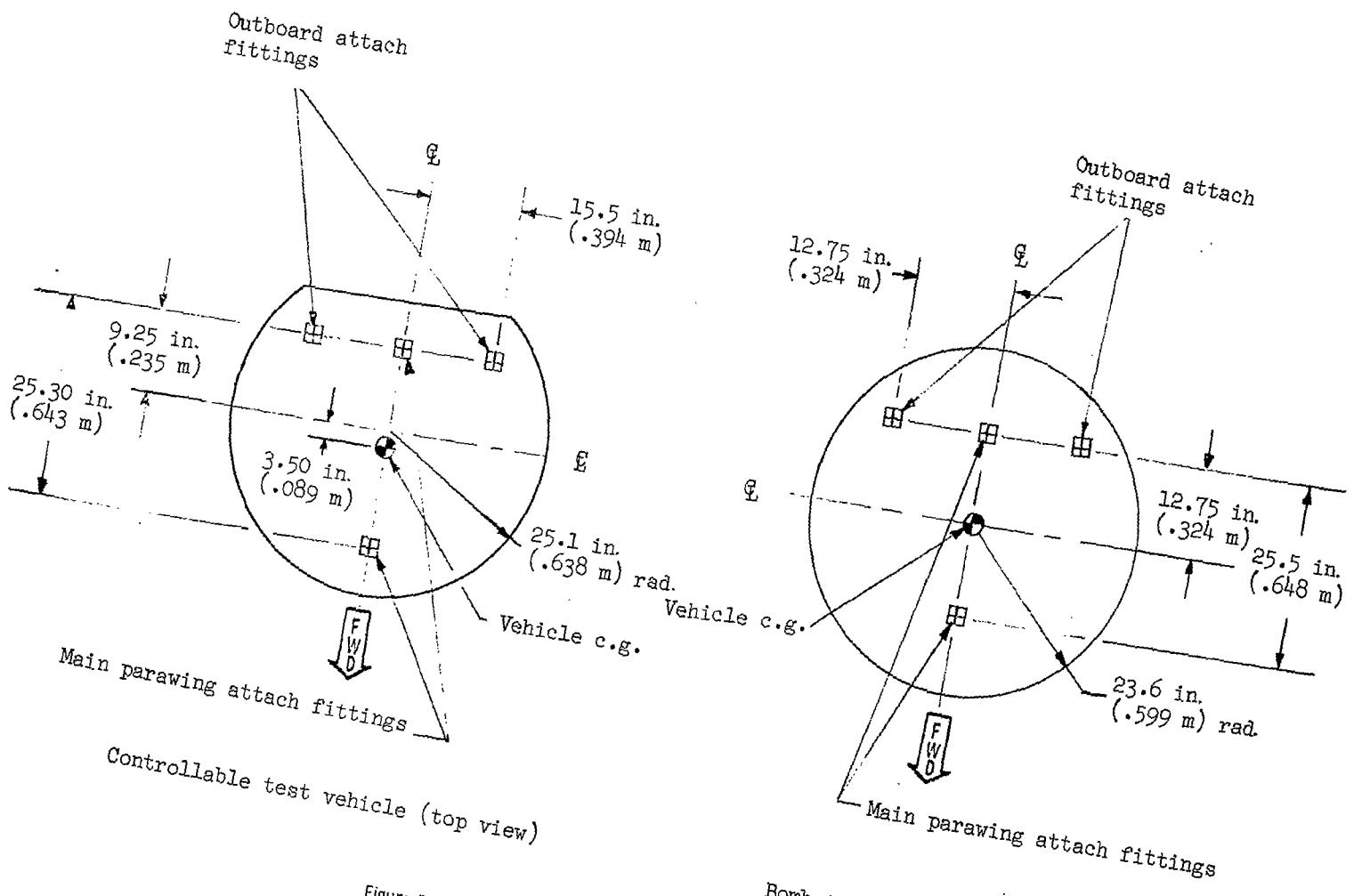


Figure 9.- Parawing attach-fitting locations on test vehicles.

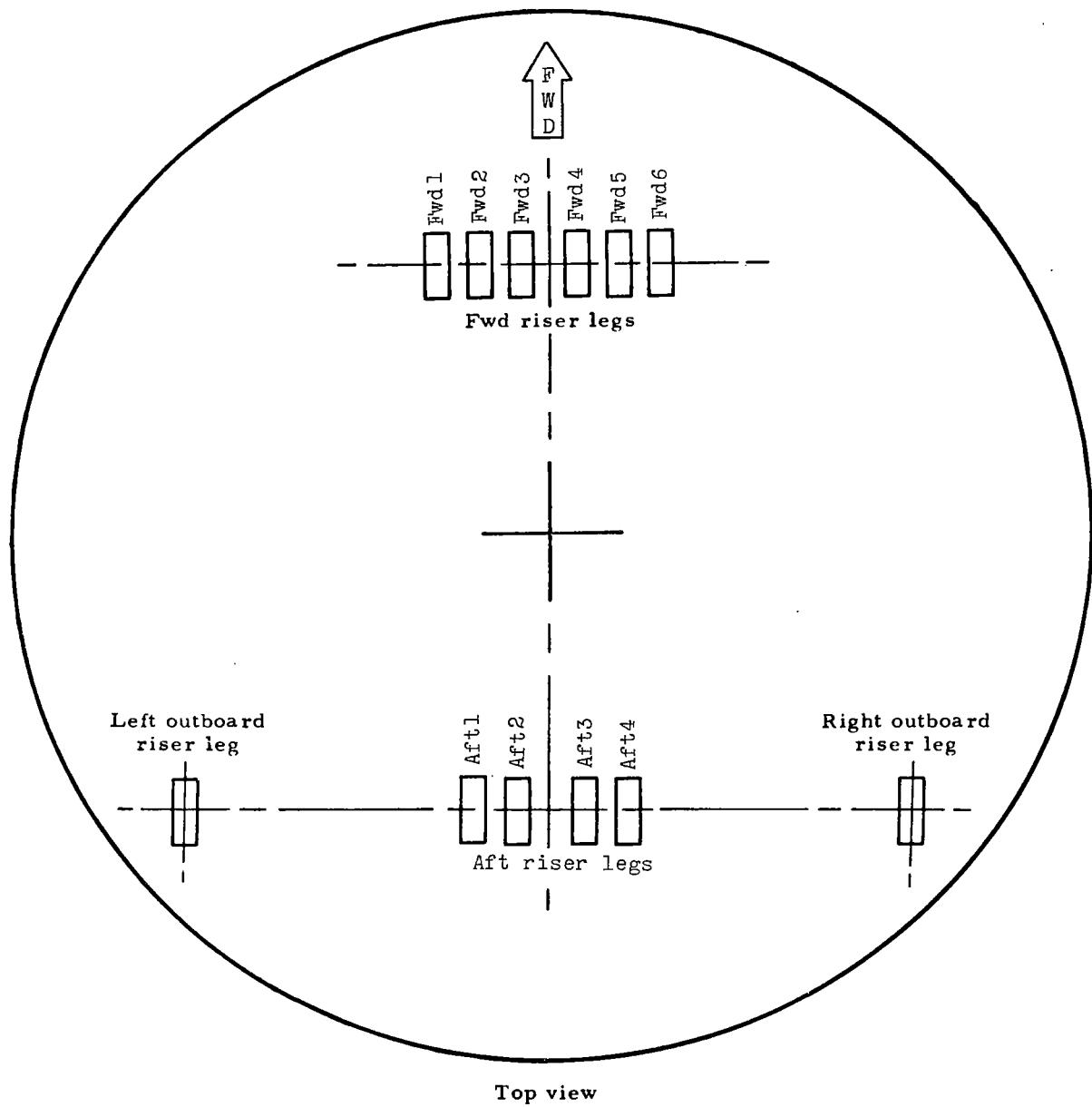


Figure 10.- Riser arrangement for versions I and II of twin-keel parawing.

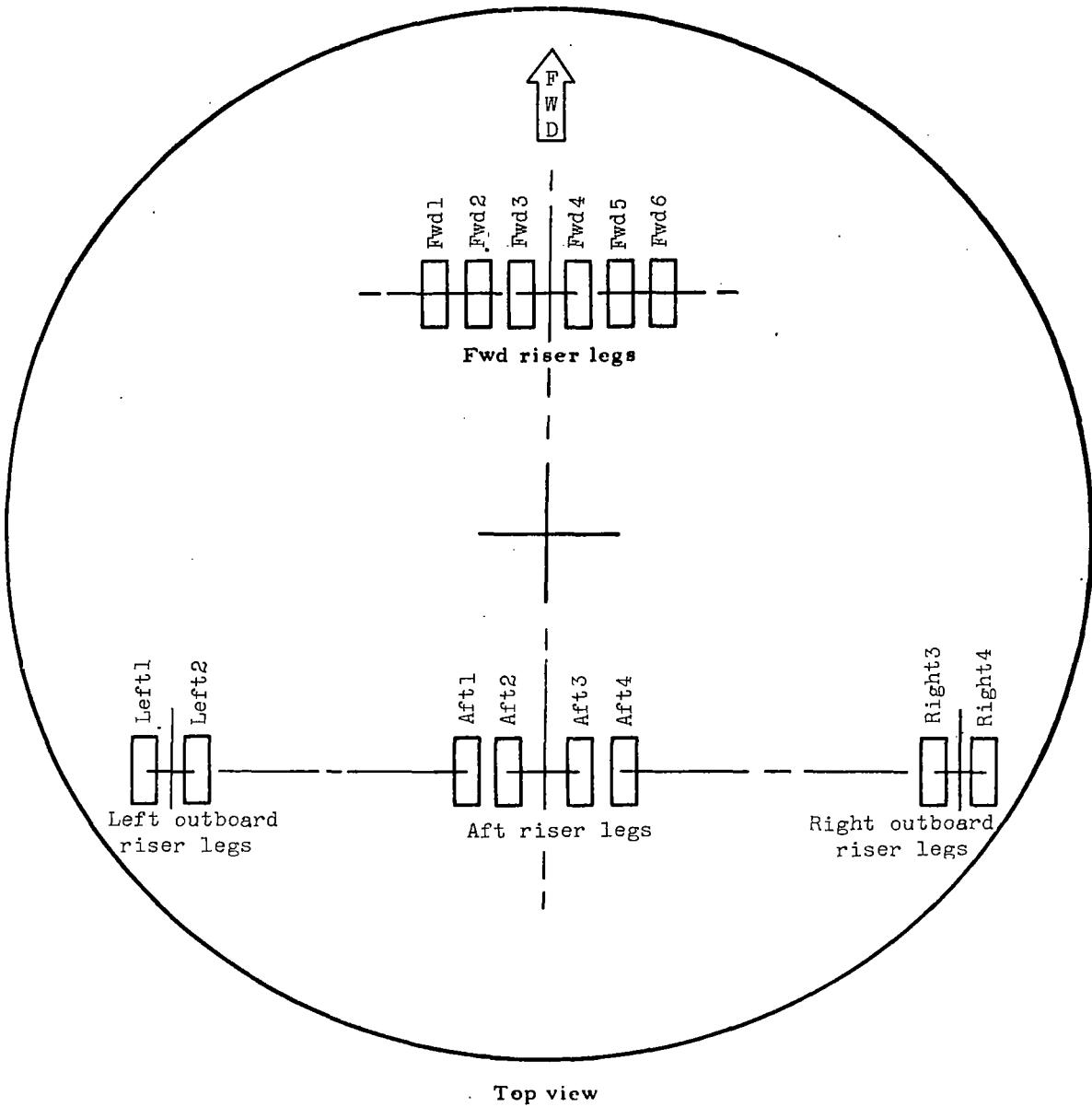


Figure 11.- Riser arrangement for versions III to VII of twin-keel parawing.

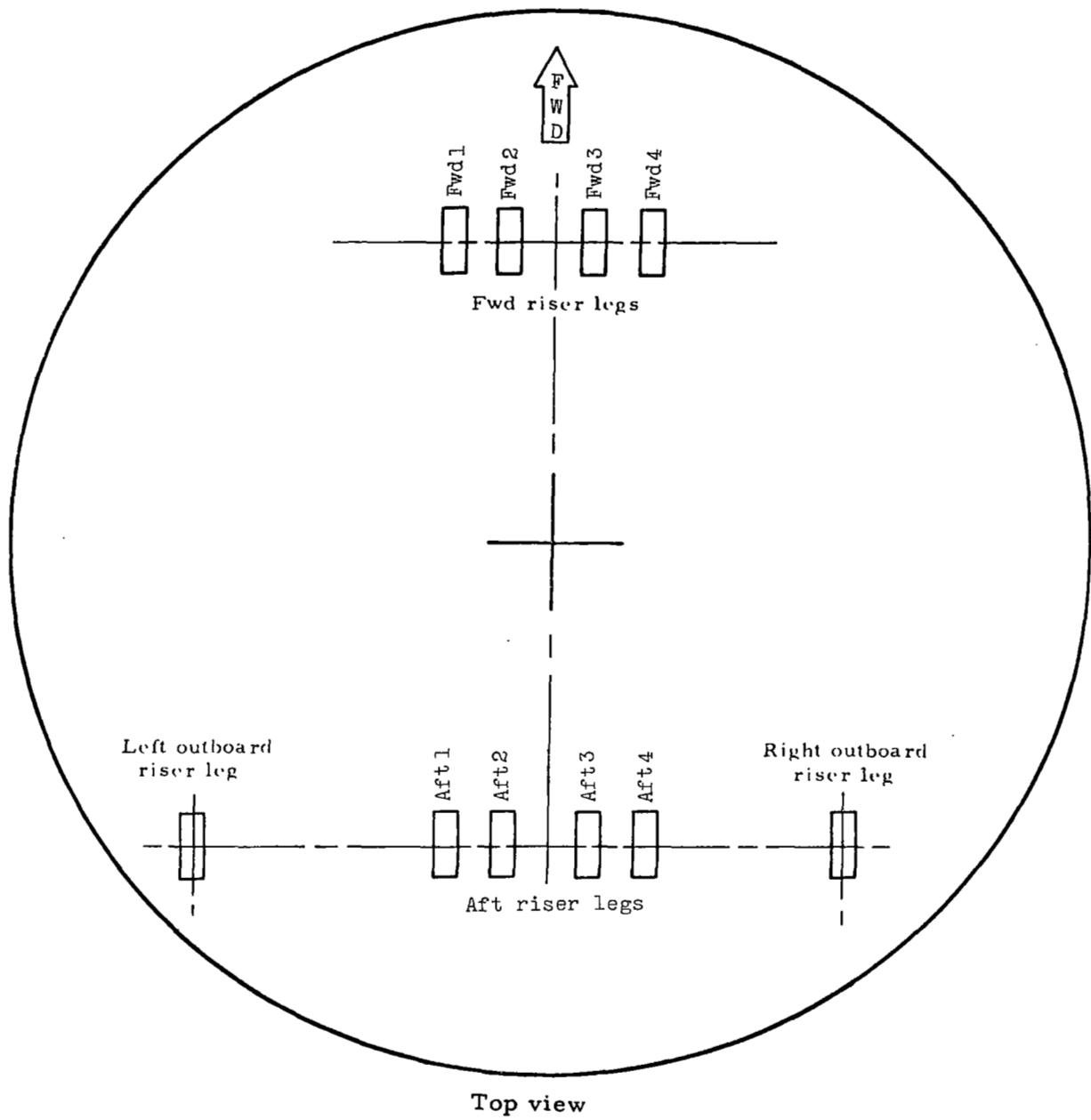
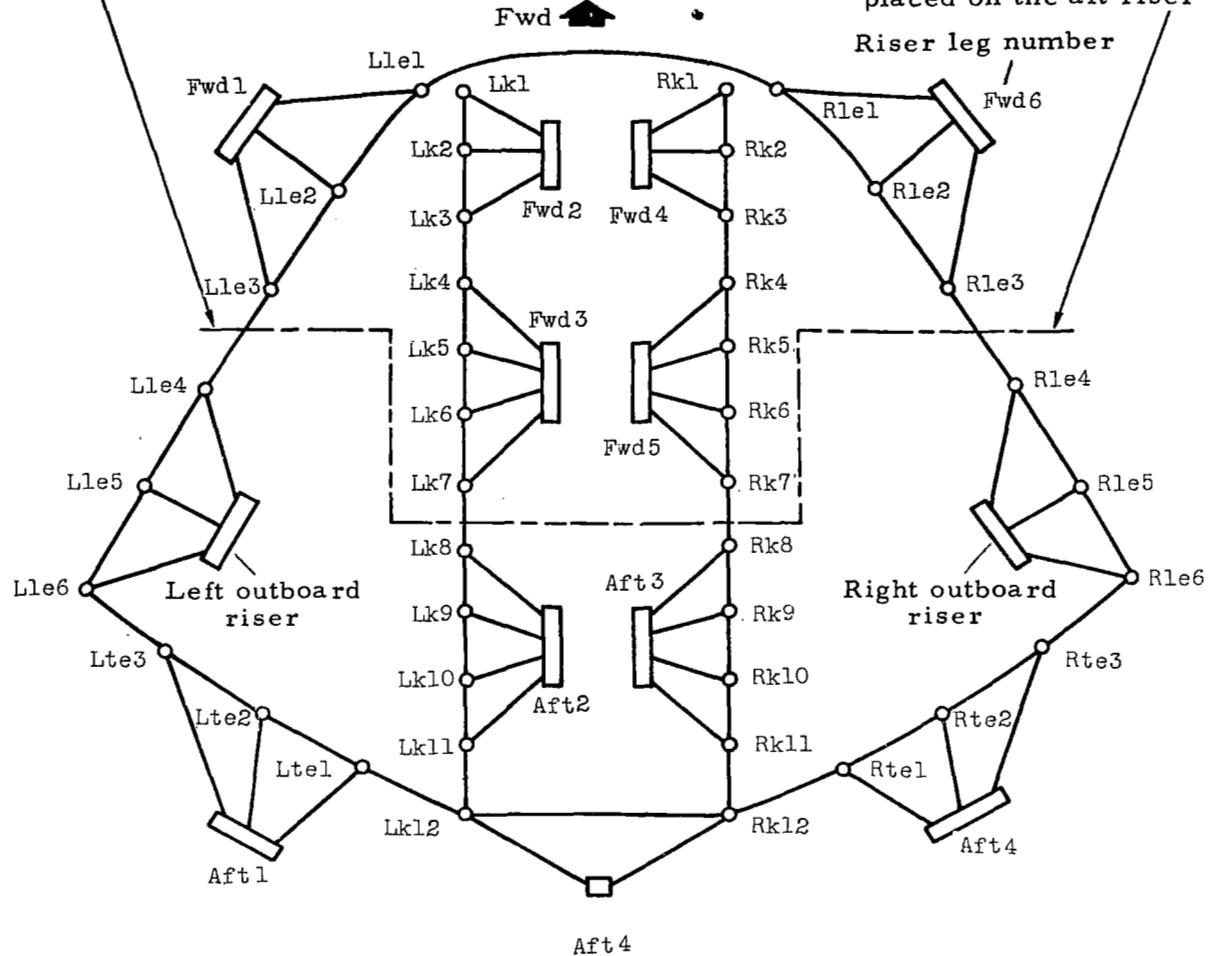


Figure 12.- Riser arrangement for single-keel parawing.

NOTE: All lines forward of this line placed on the forward riser

All lines aft of this line placed on the aft riser
Riser leg number



View from above

Figure 13.- Suspension-line-riser attachment arrangement for version I of twin-keel parawing.

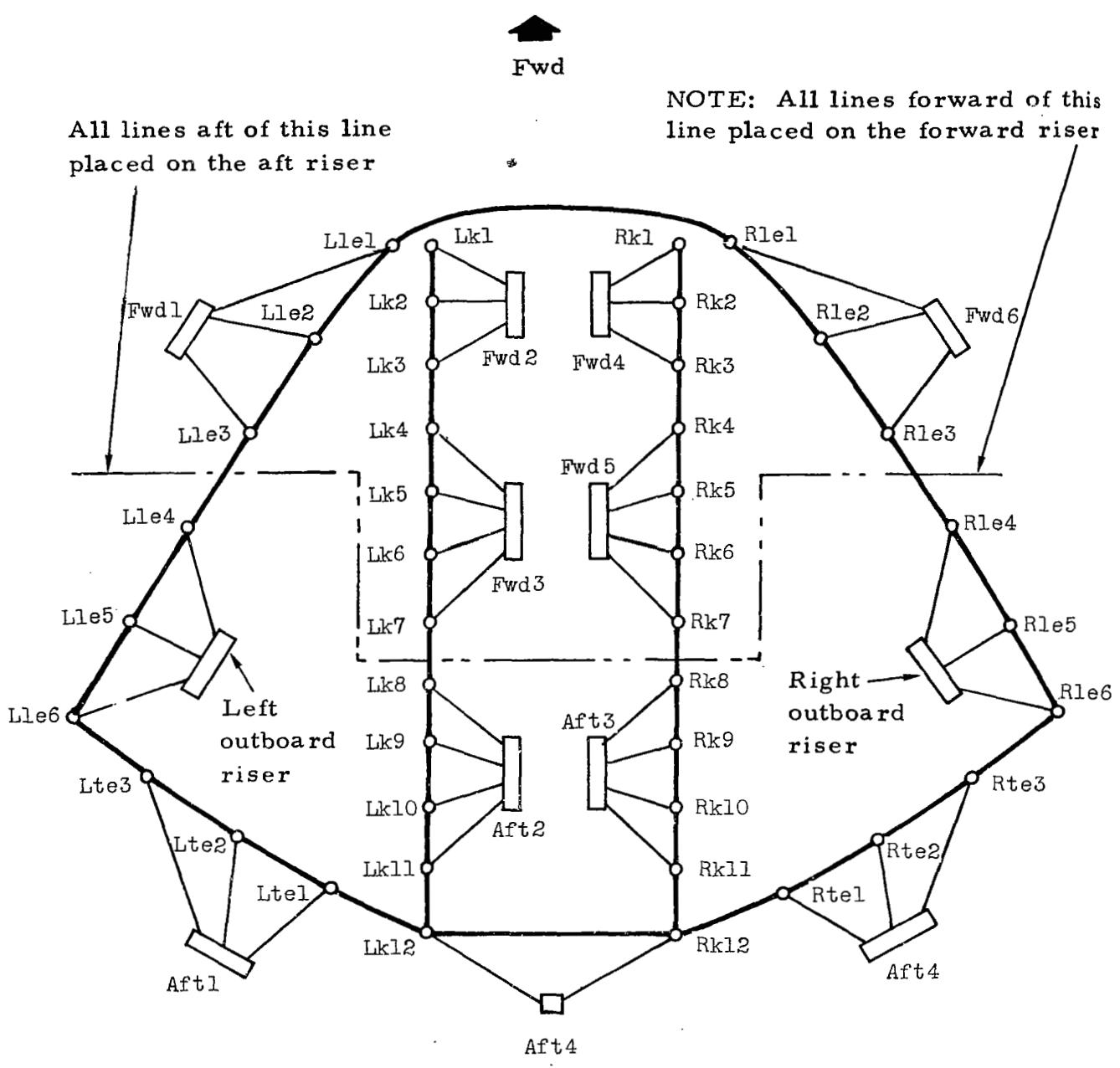
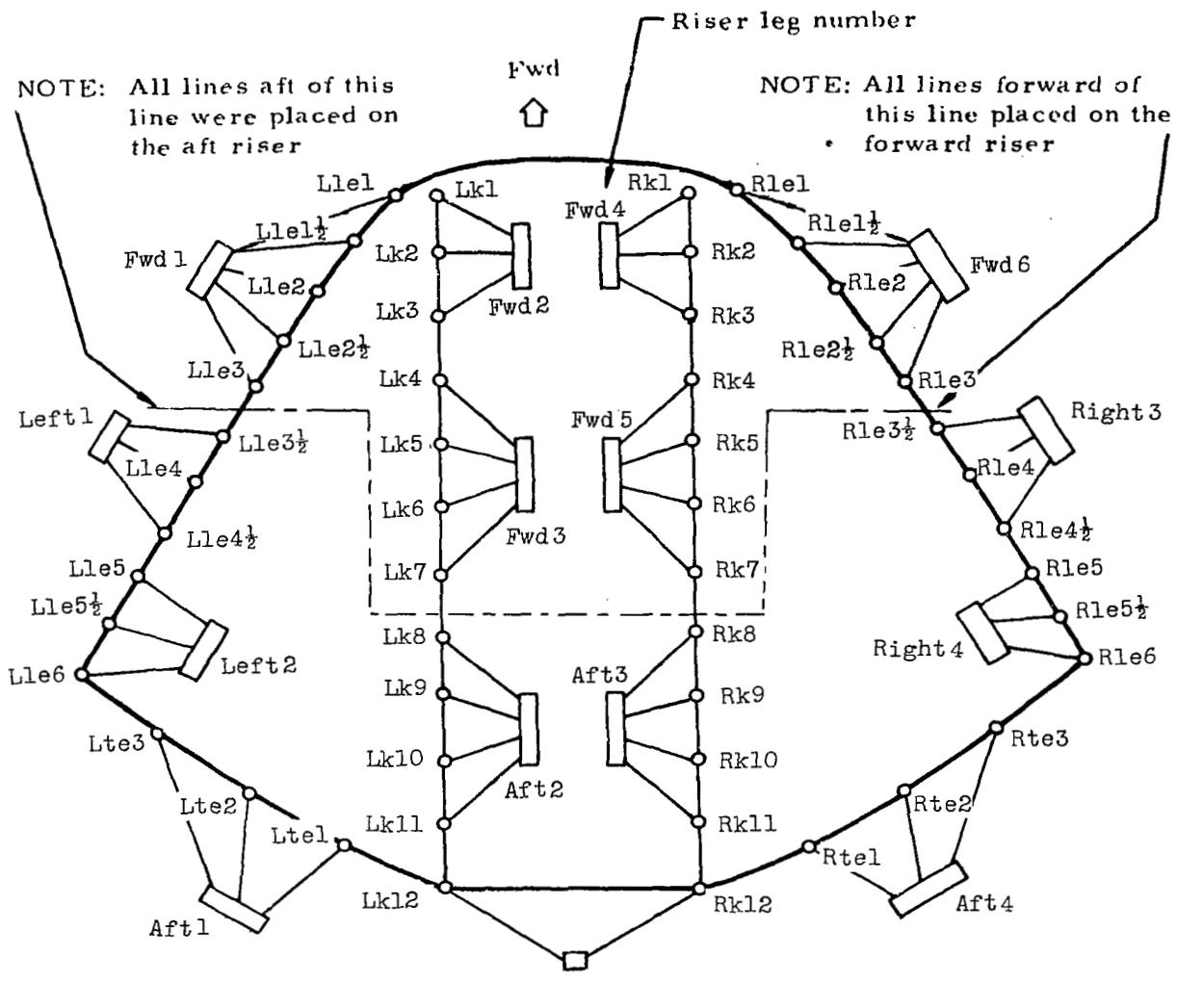


Figure 14.- Suspension-line-riser attachment arrangement for version II of twin-keel parawing.



View from above

Figure 15.- Suspension-line-riser attachment arrangement for versions III, IV, V, VI, and VII of twin-keel parawing.

NOTE: All lines forward of this line were placed on the forward riser

NOTE: All lines aft of this line were placed on the aft riser

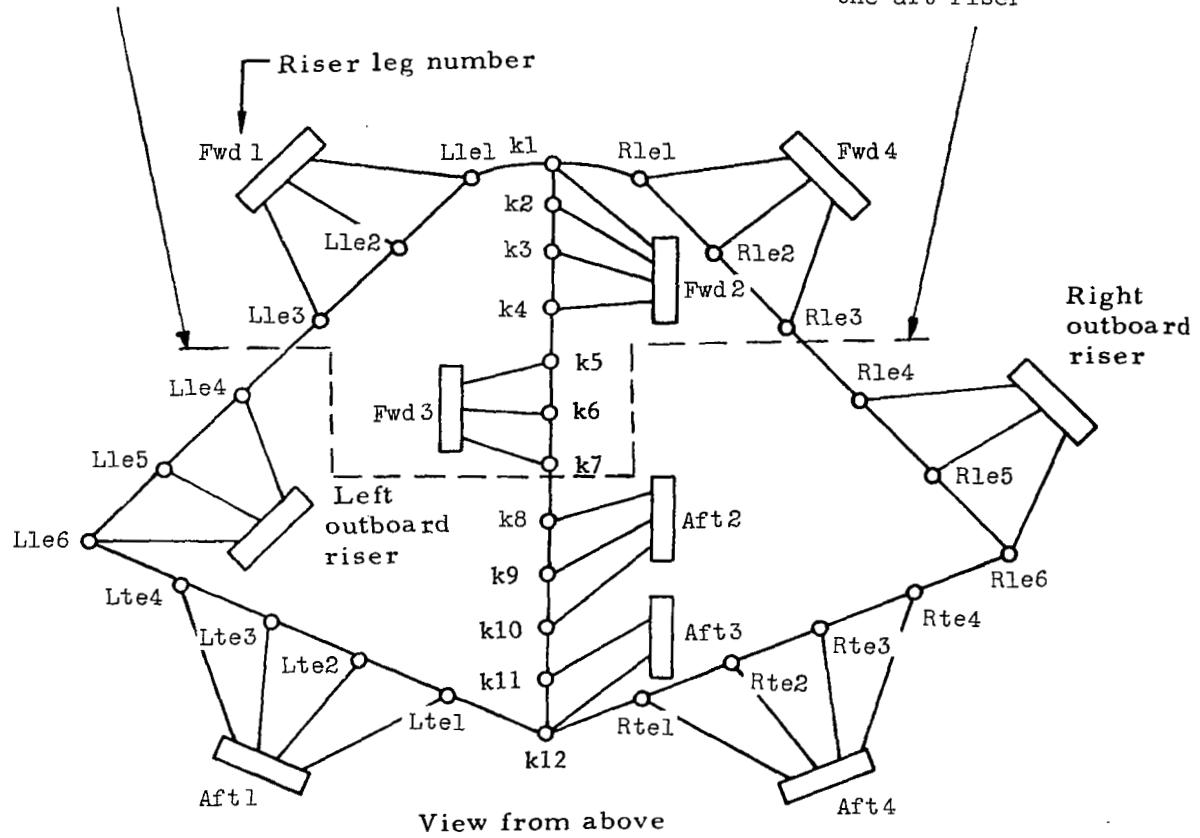


Figure 16.- Suspension-line-riser attachment arrangement for single-keel parawing.

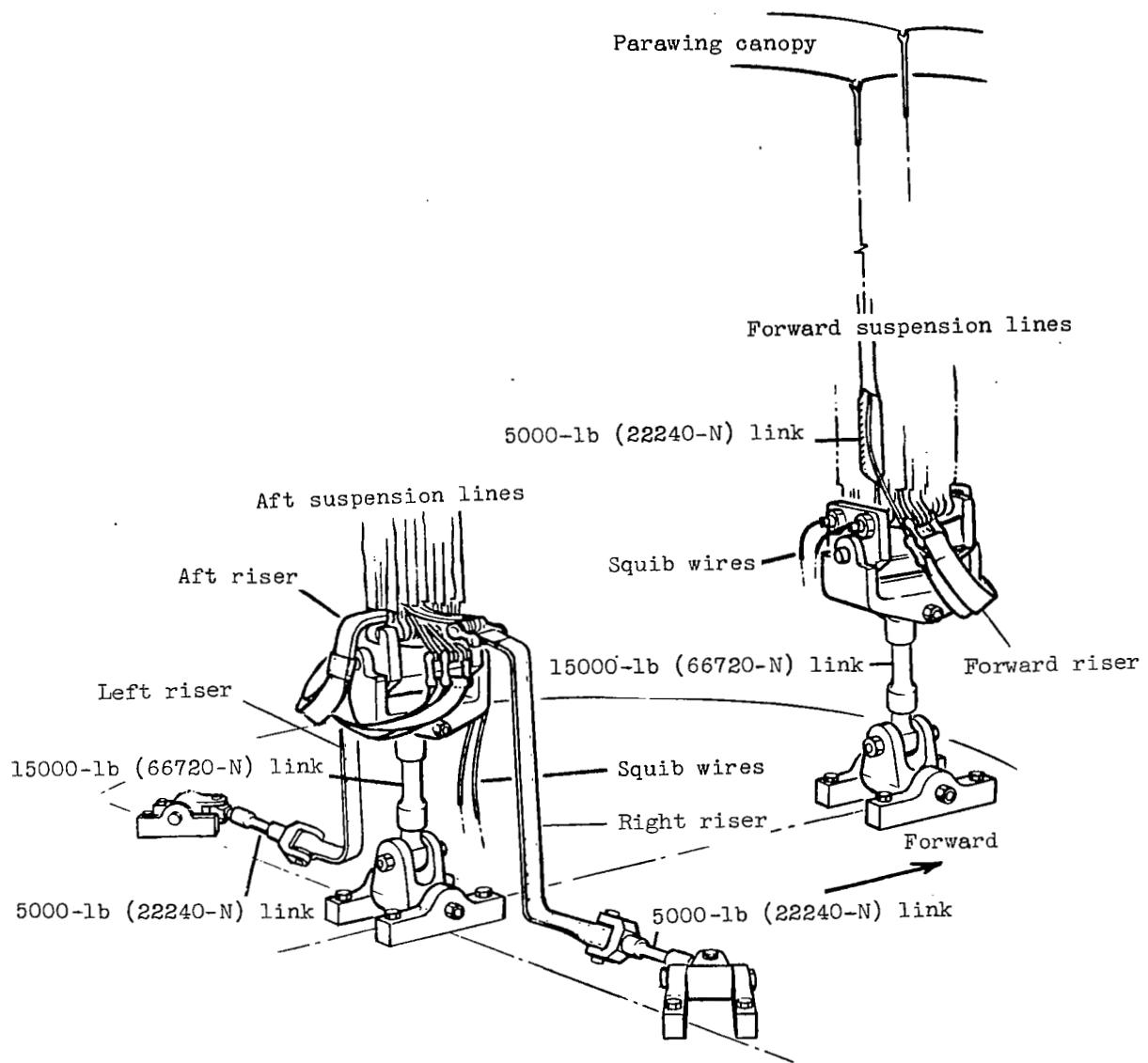


Figure 17.- Parawing deck attachment and load instrumentation arrangement before line transfer.

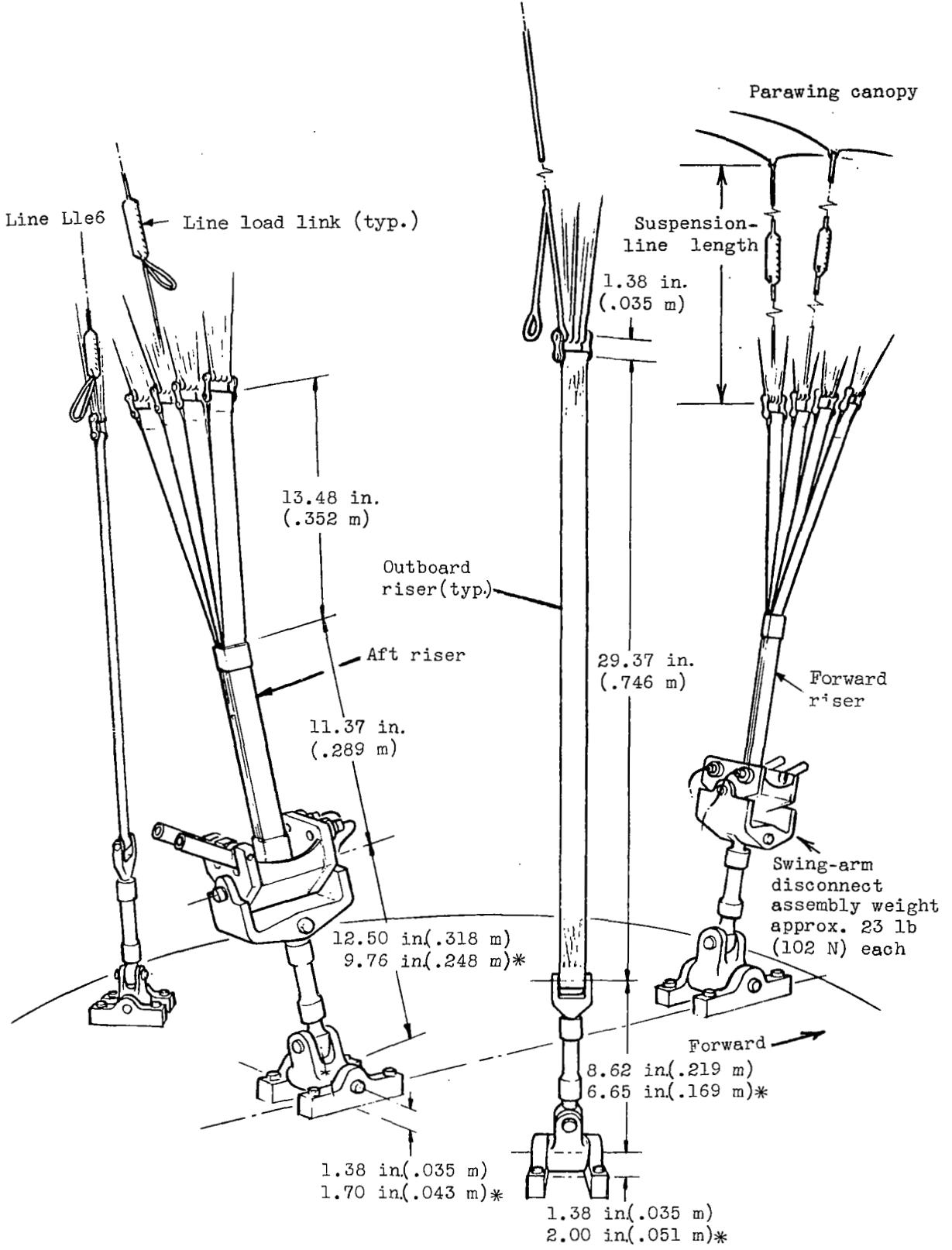


Figure 18.- Parawing deck attachment arrangement after line transfer. Dimensions for controllable test vehicle denoted with *.

NOTE: All views are looking up into canopy;
all views are for fully inflated
canopy during a stage.

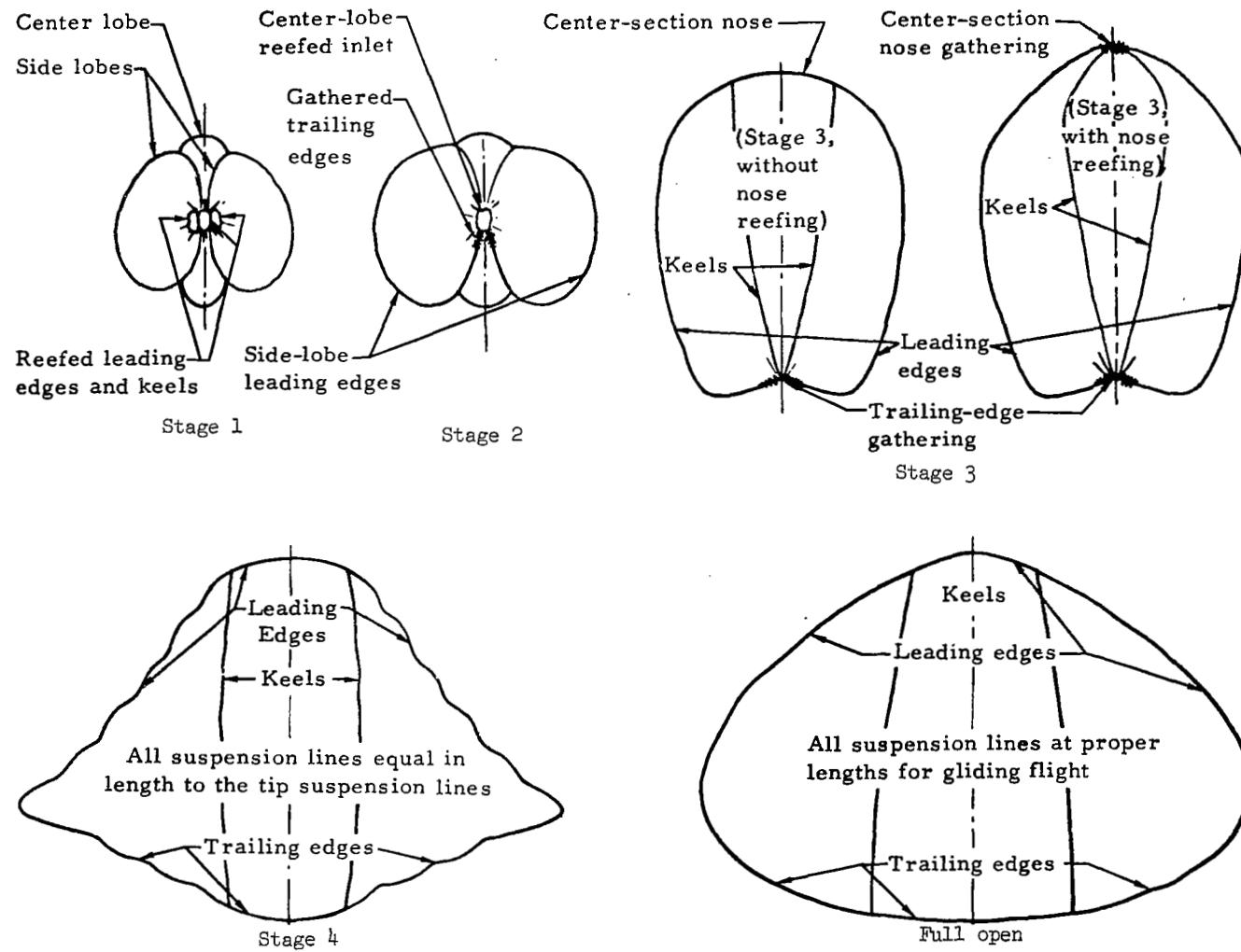


Figure 19.- Typical planforms during reefing sequence for twin-keel parawing.

NOTE: All views are looking up into canopy;
all views are for fully inflated
canopy during a stage.

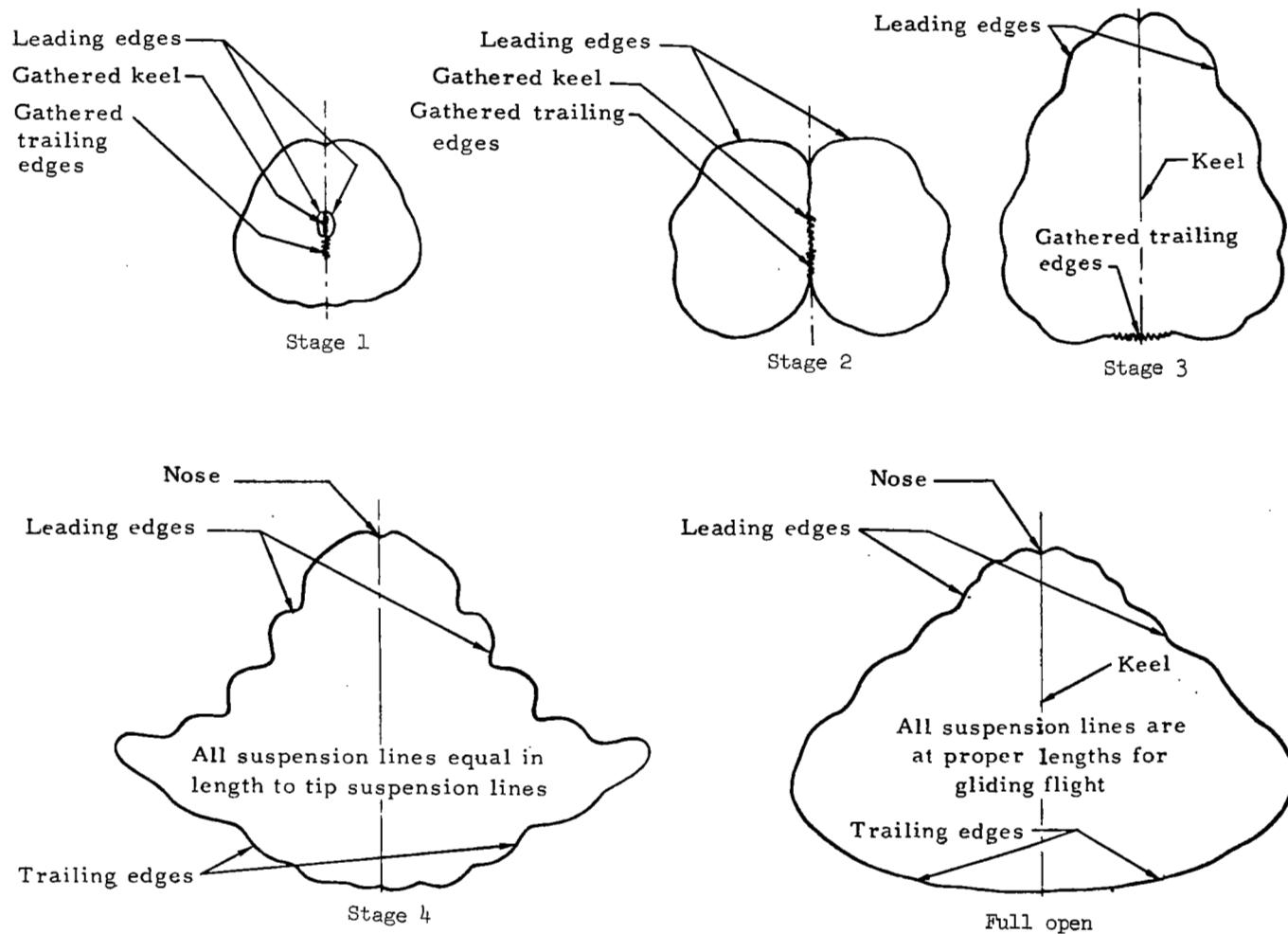
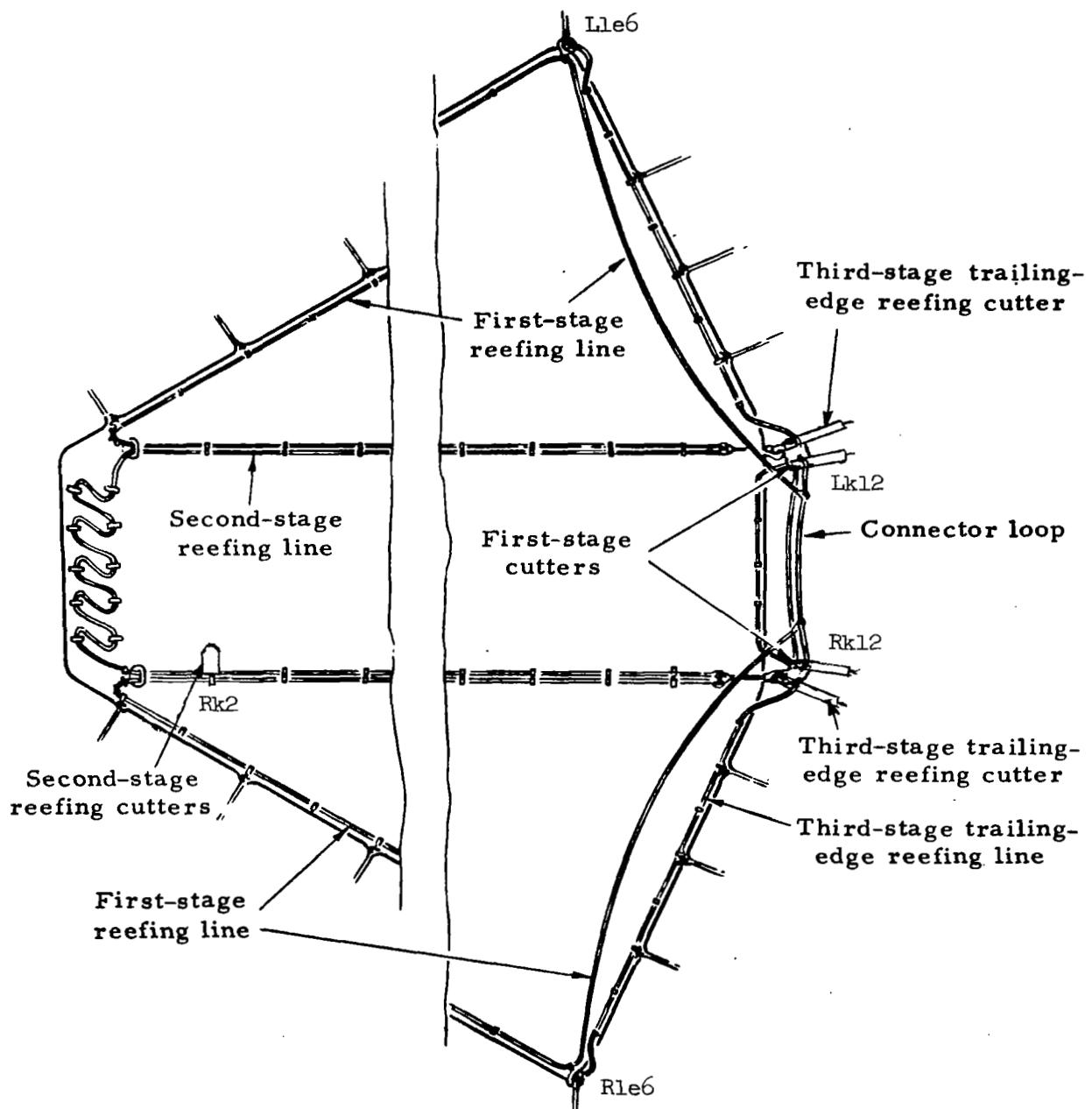
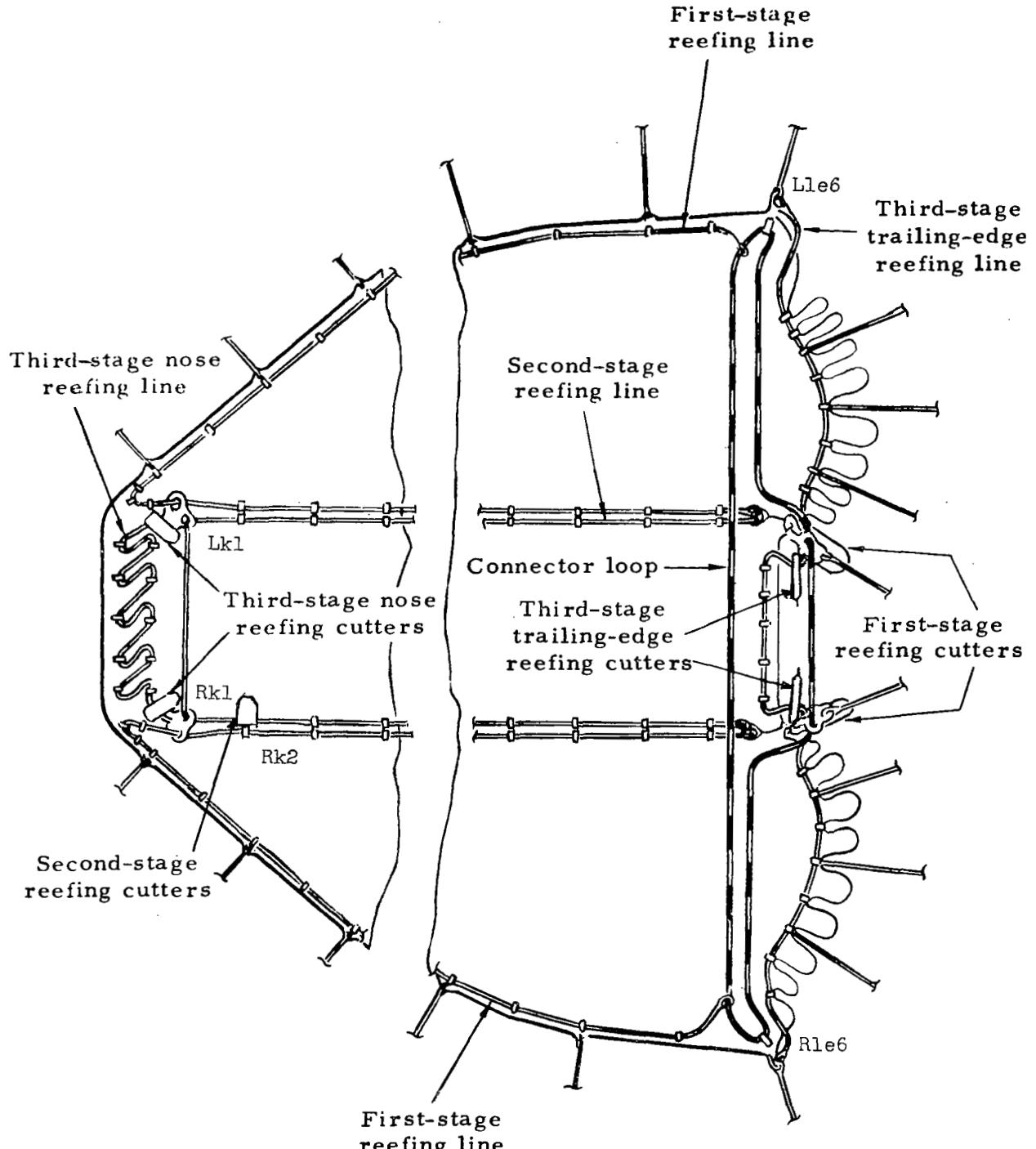


Figure 20.- Typical planforms during reefing sequence for single-keel parawing.



Viewed from below

Figure 21.- Reefing system A for twin-keel parawing.



Viewed from below

Figure 22.- Reefing system B for twin-keel parawing.

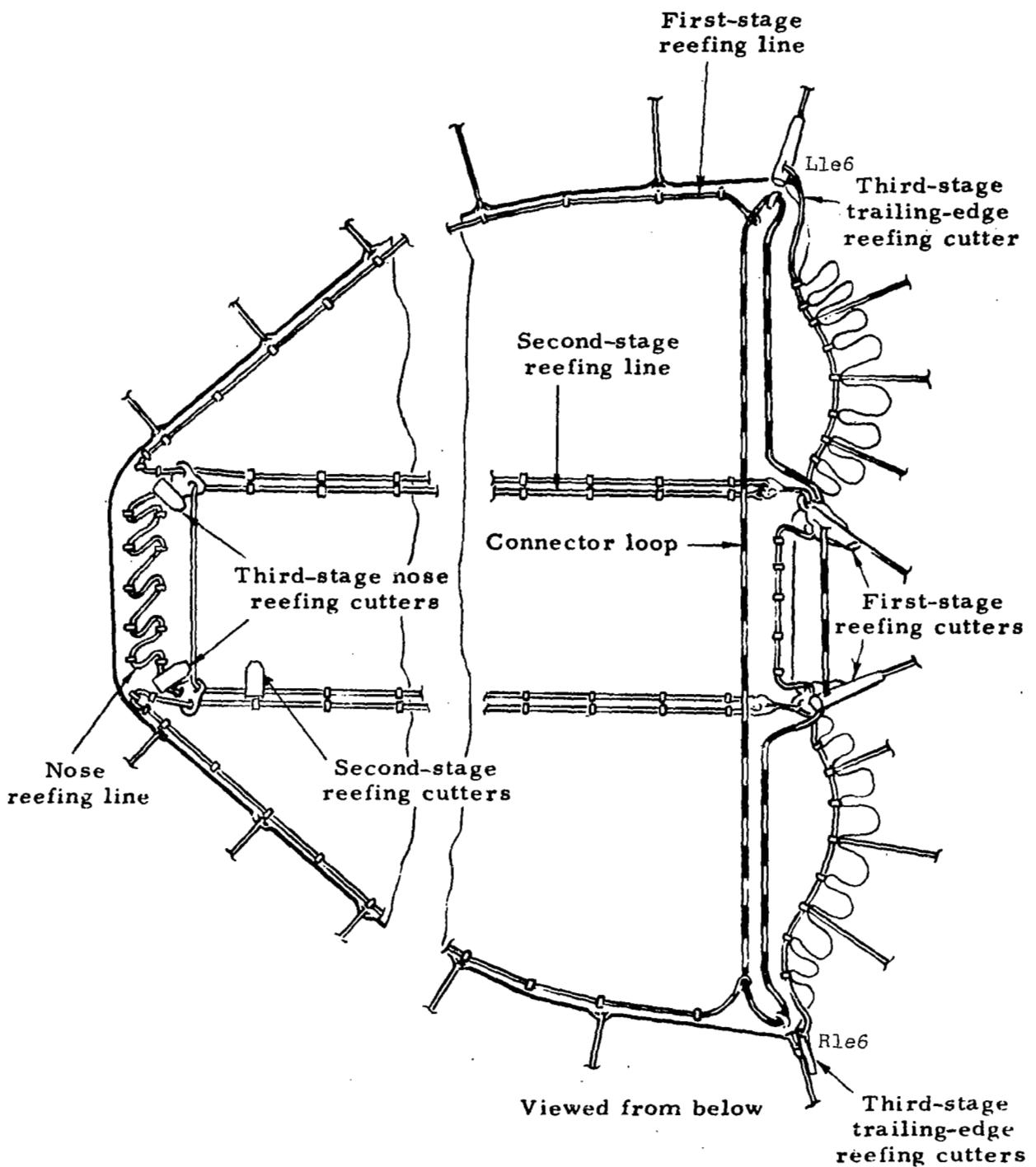
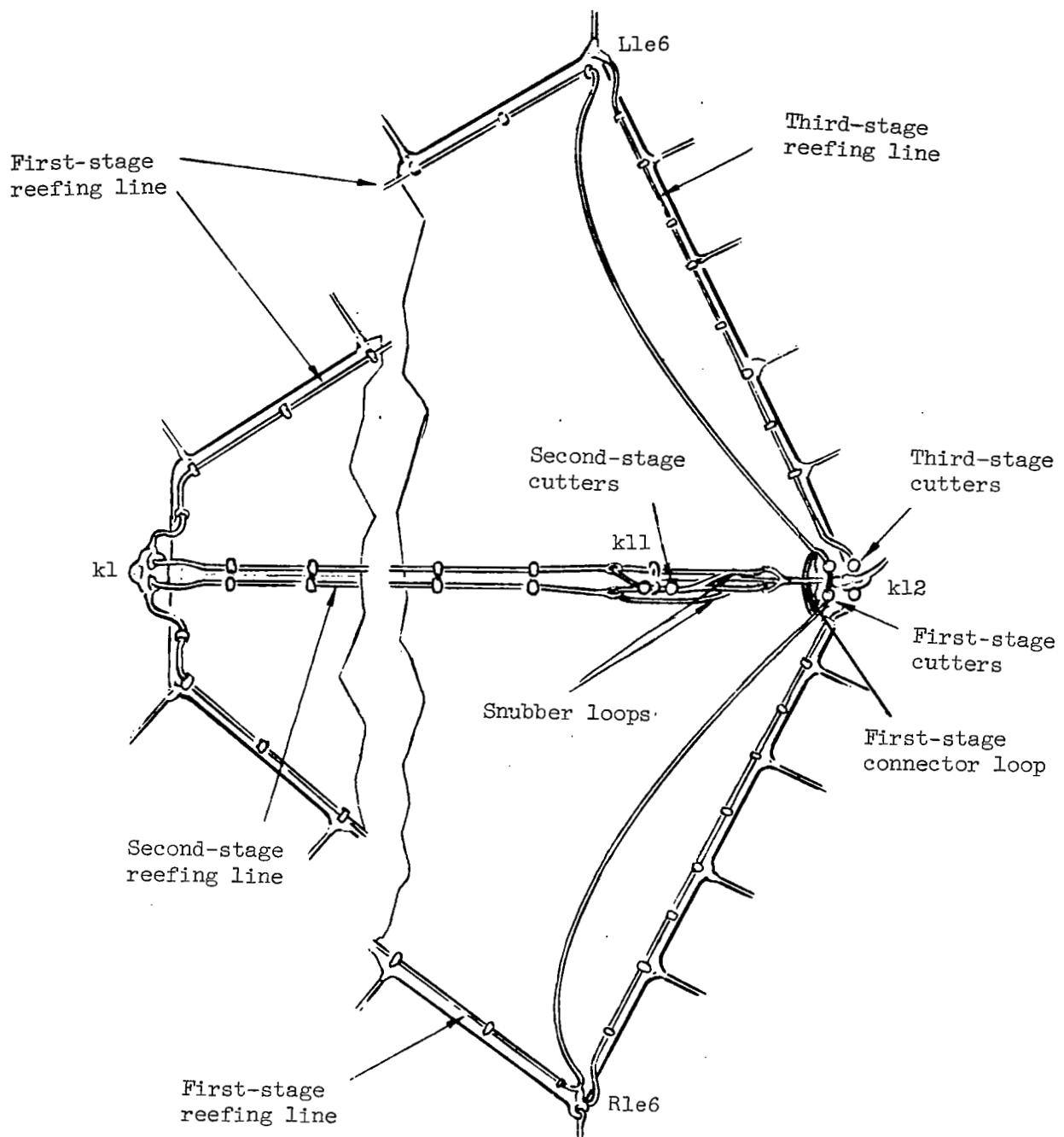


Figure 23.- Reefing system C for twin-keel parawing.



Viewed from below

Figure 24.- Reefing system for single-keel parawing.

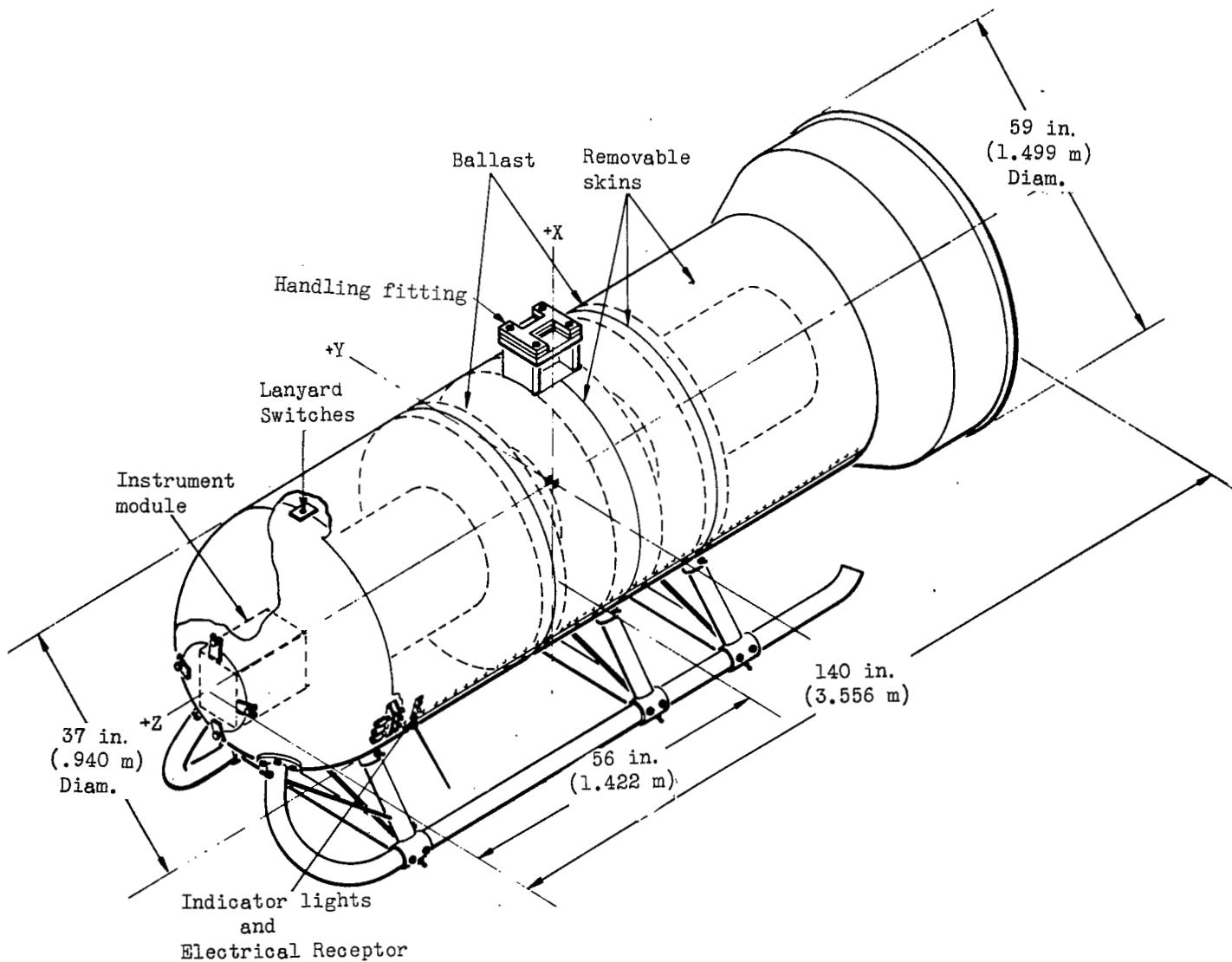


Figure 25.- Bomb-type test vehicle.

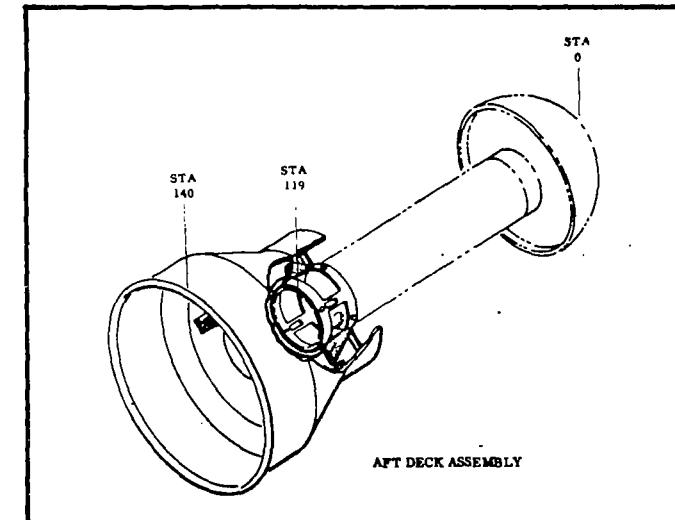
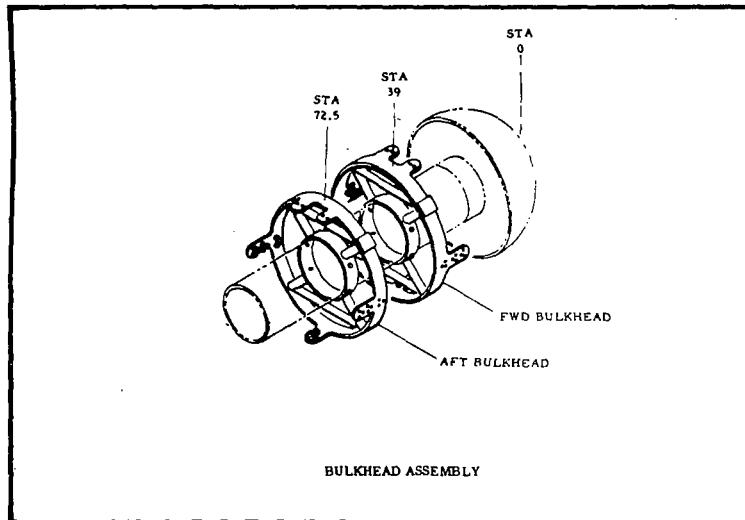
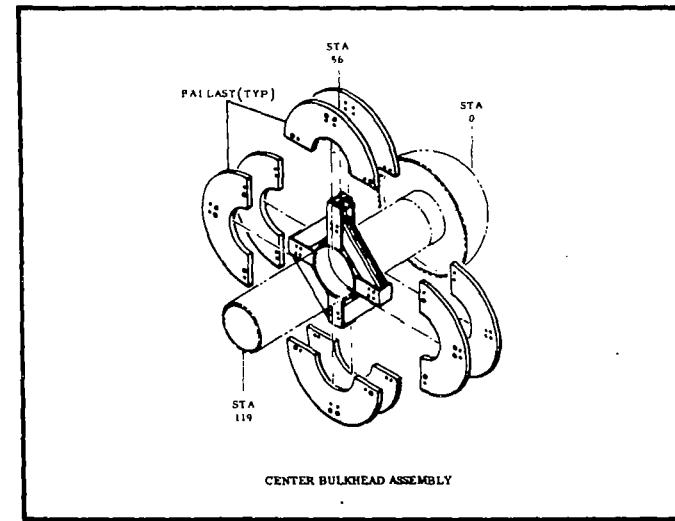
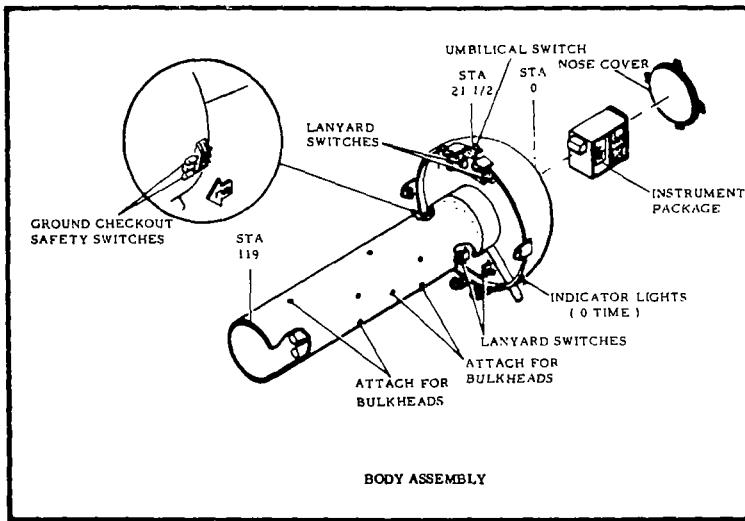
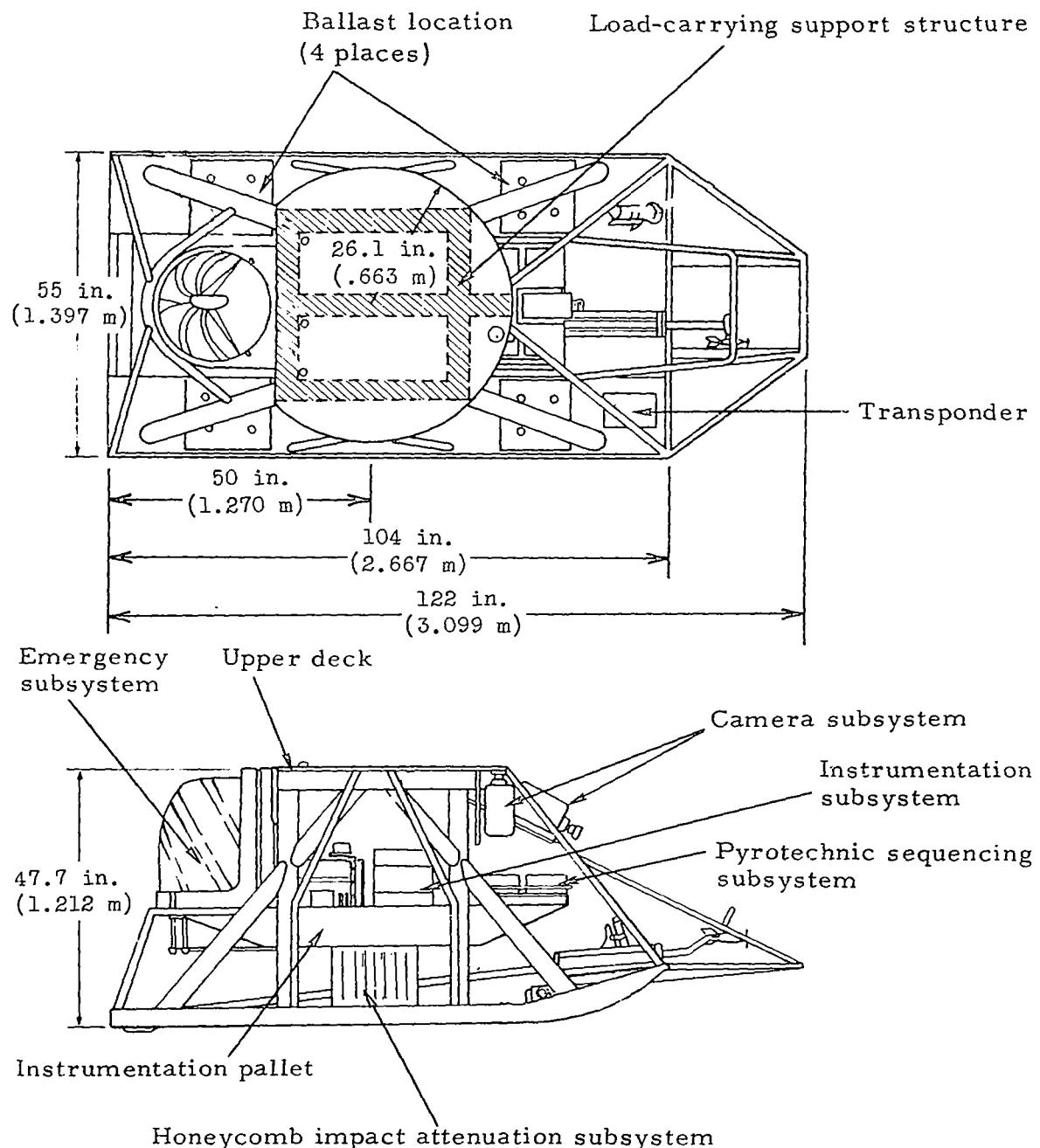


Figure 26.- Major structural subassemblies of bomb-type test vehicle.



- Note:
1. Not to scale
 2. Dimensions given in inches
(meters) are approximate

Figure 27.- Controllable sled-type test vehicle, showing location of principal subsystems.

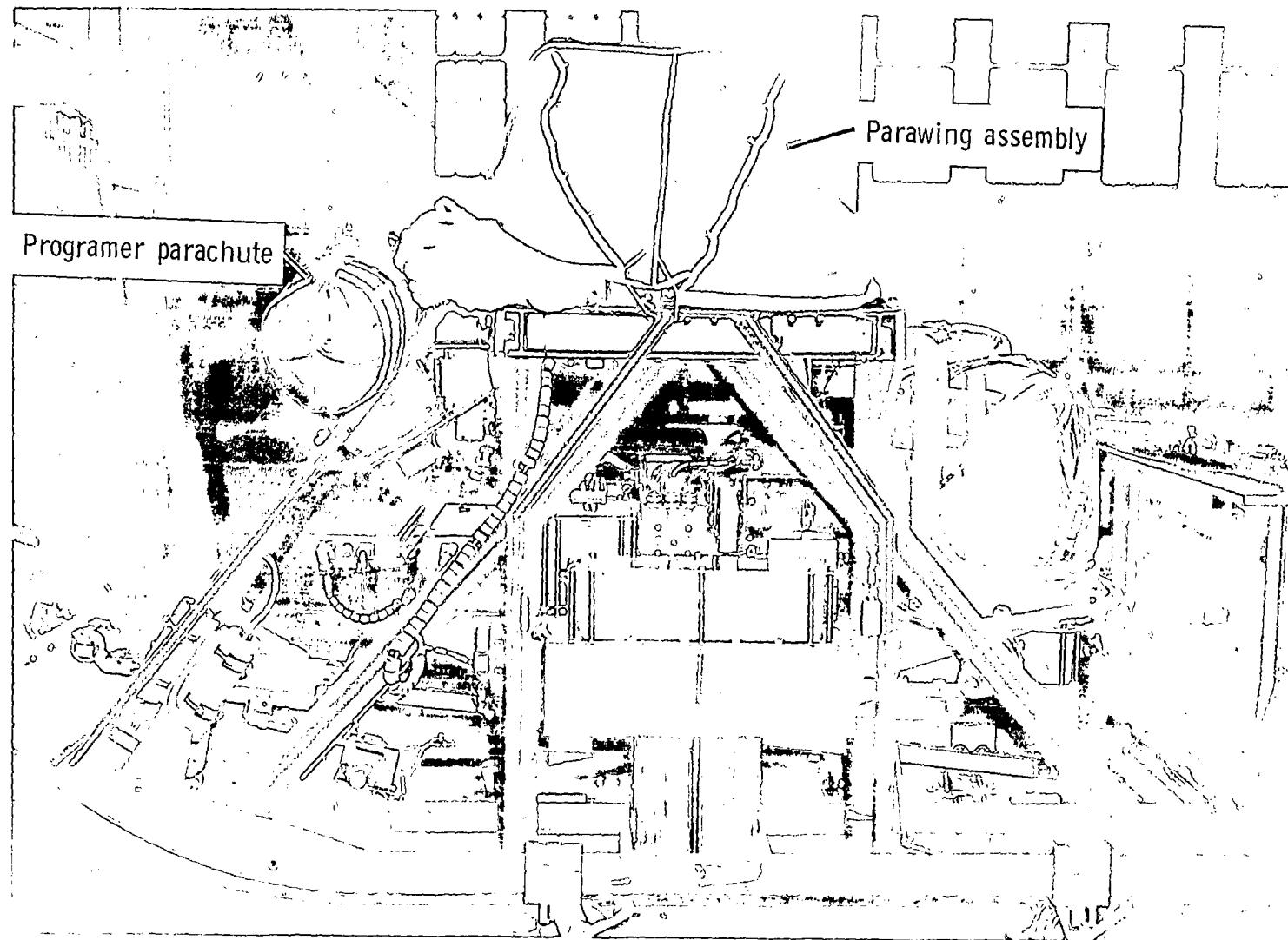


Figure 28.- Controllable sled-type test vehicle rigged for test 250T.

L-71-697

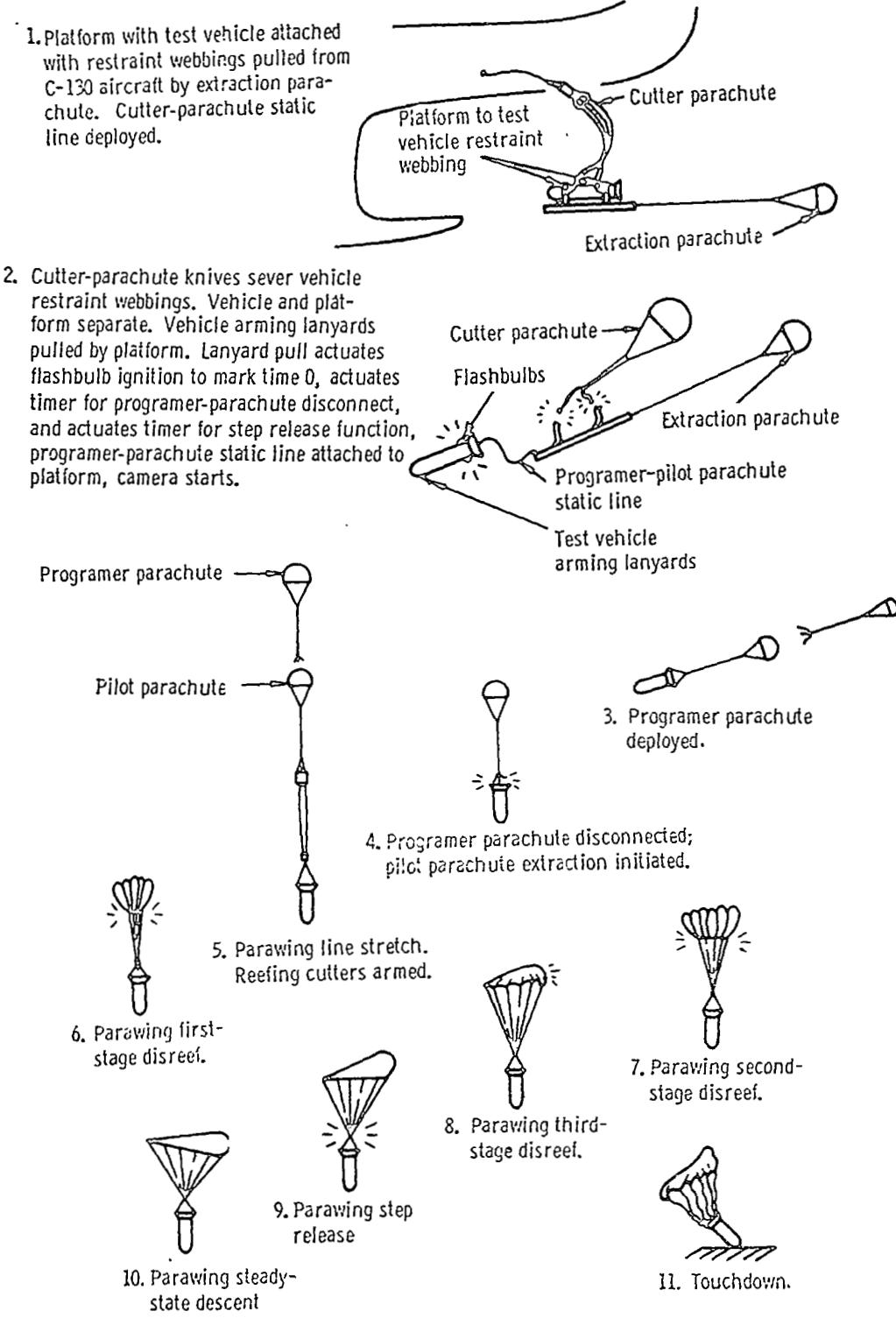
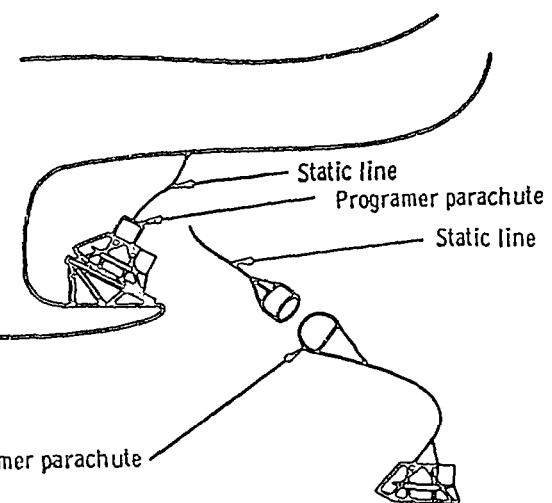


Figure 29.- Sequence of events in C-130 and C-119 airplane launch of bomb-type test vehicle.

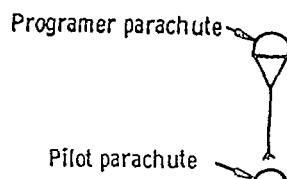
1. Ramp with test vehicle mounted in C-119 aircraft. Programer-parachute static line deployed. Arming lanyard pulled at launch. Sequence timers start.



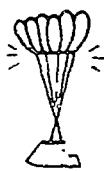
2. Programer parachute deployed by static line.



3. Programer parachute deployed.



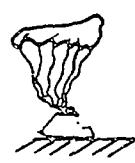
4. Programer parachute disconnected. Lanyard starts onboard camera. Pilot parachute extraction initiated.



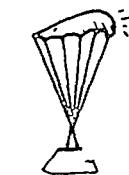
6. Parawing first-stage disreef.



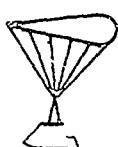
5. Parawing line stretch, Reefing cutters armed.



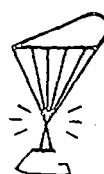
7. Parawing second-stage disreef.



8. Parawing third-stage disreef.



10. Parawing steady-state descent.



9. Parawing step release.

11. Touchdown.

Figure 30.- Sequence of events in C-119 airplane launch of controllable test vehicle.

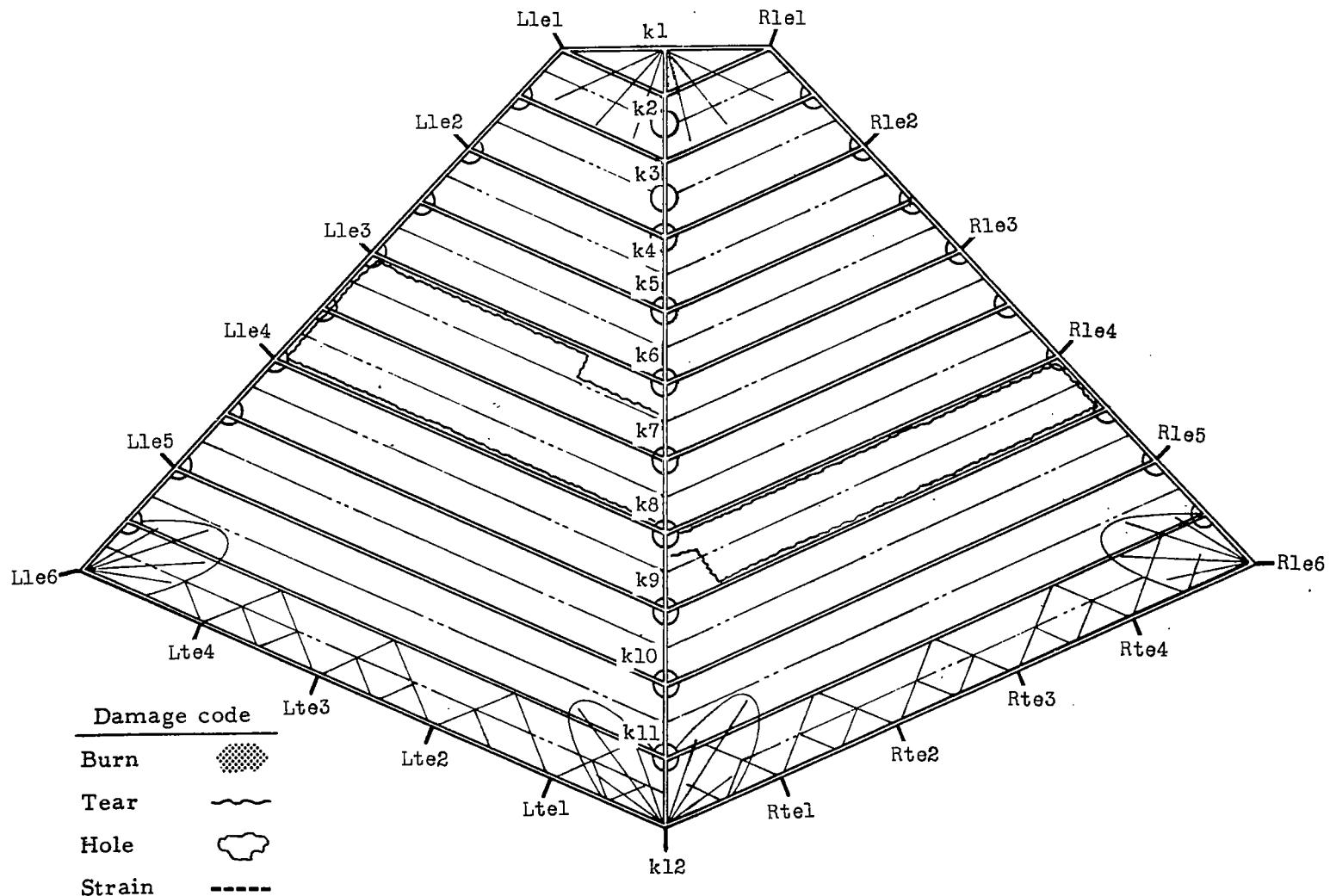


Figure 31.- Major canopy damage, test 201S.

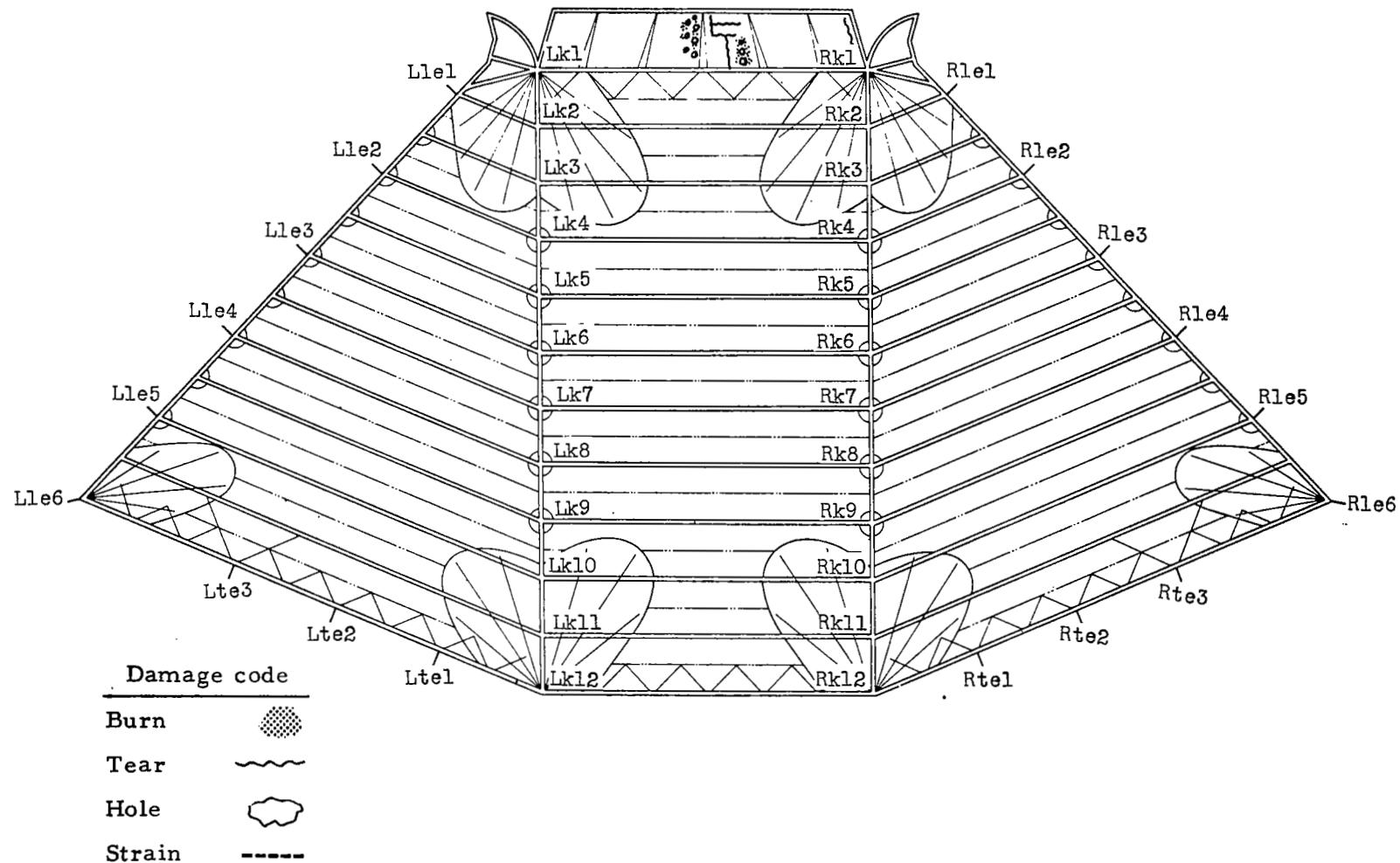


Figure 32.- Major canopy damage, test 202T.

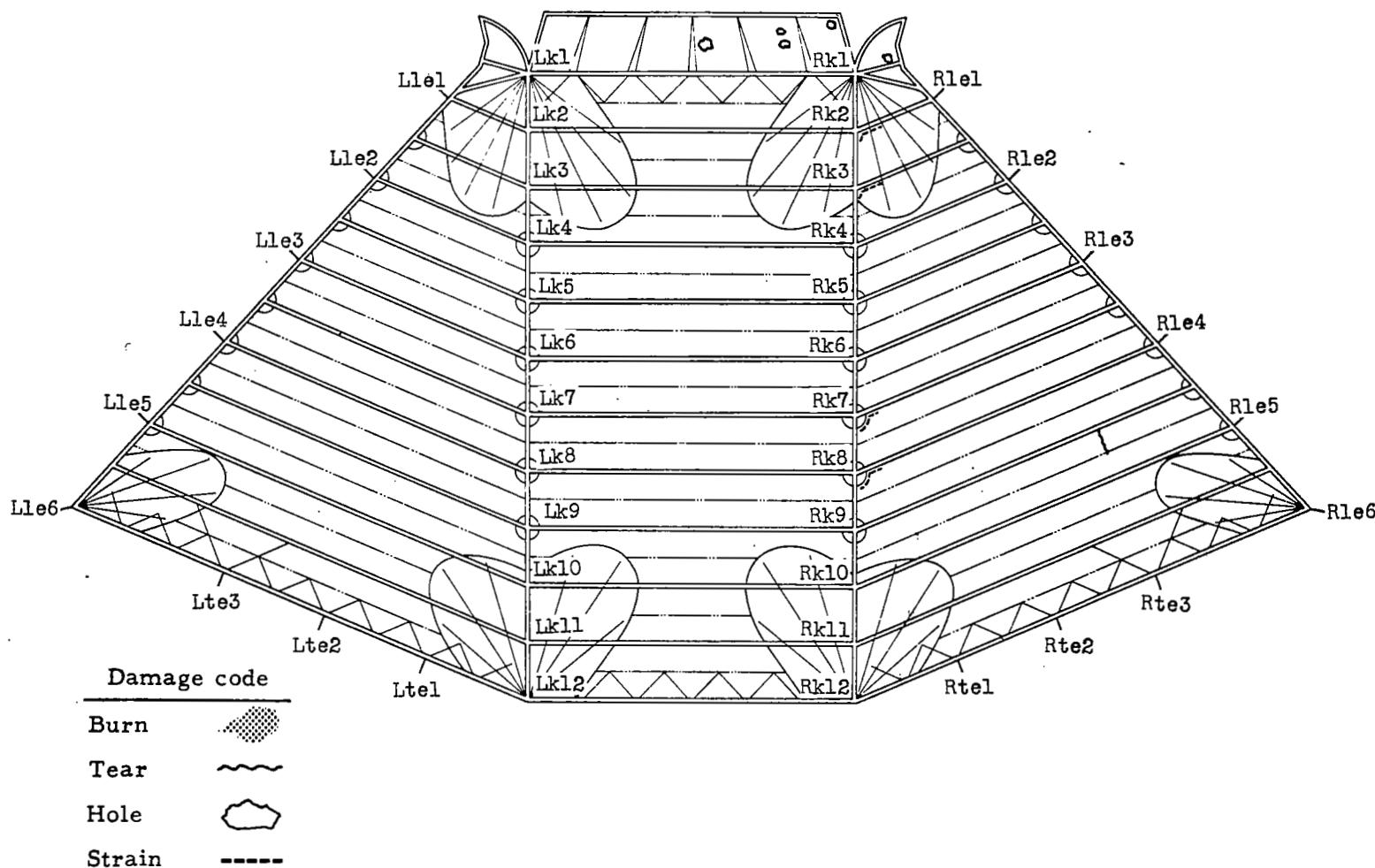


Figure 33.- Major canopy damage, test 205T.

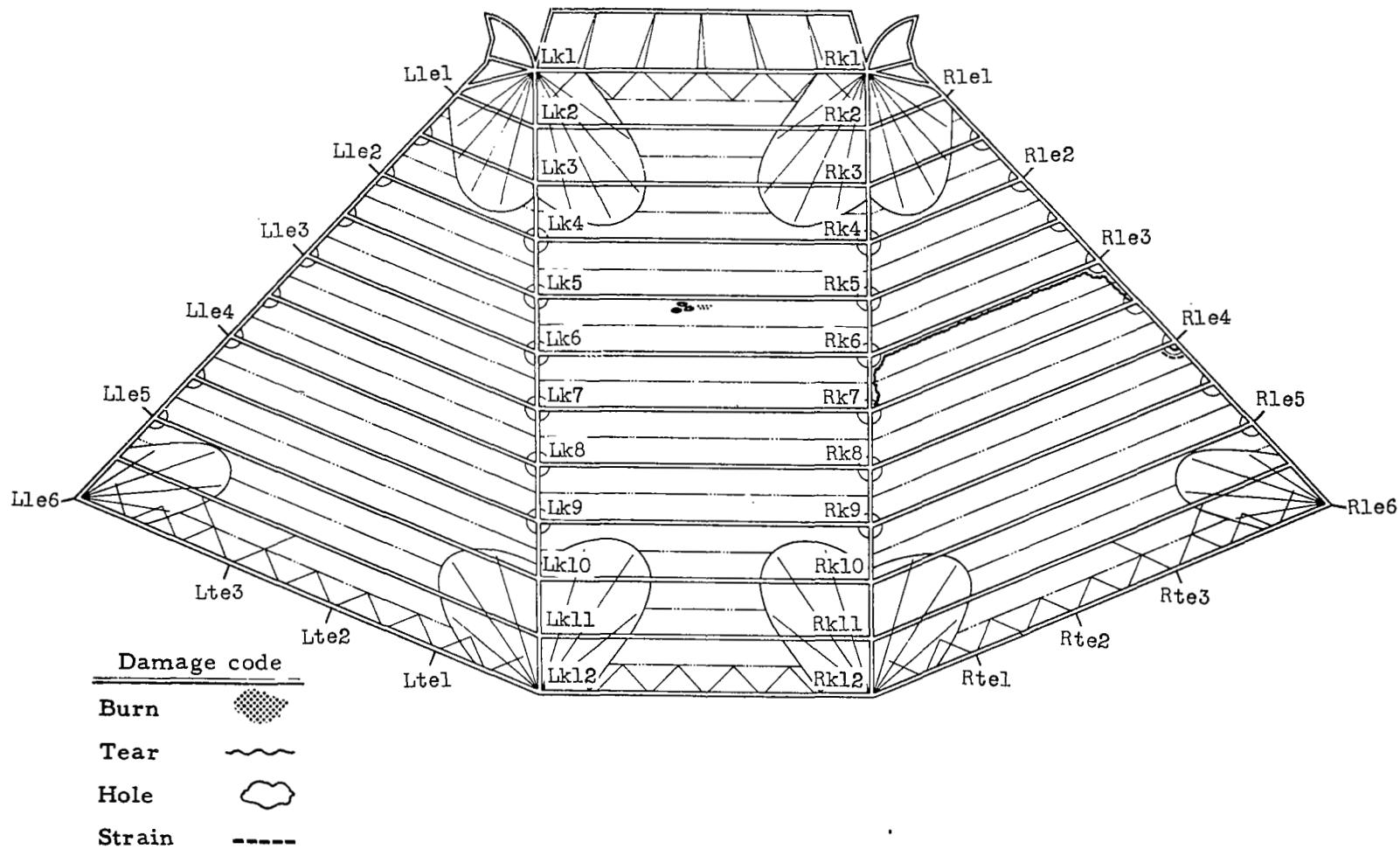


Figure 34.- Major canopy damage, test 203T.

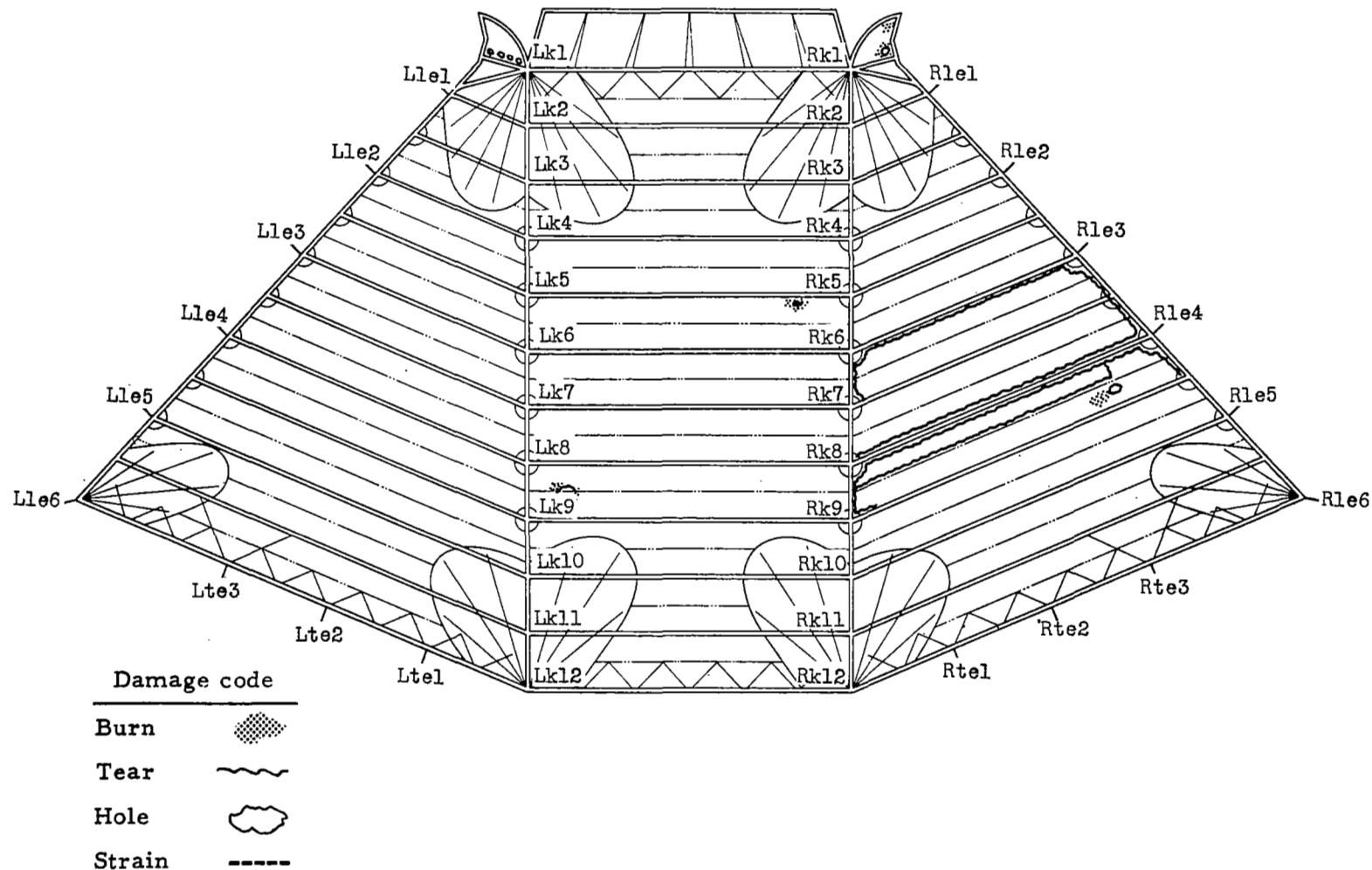


Figure 35.- Major canopy damage, test 208T.

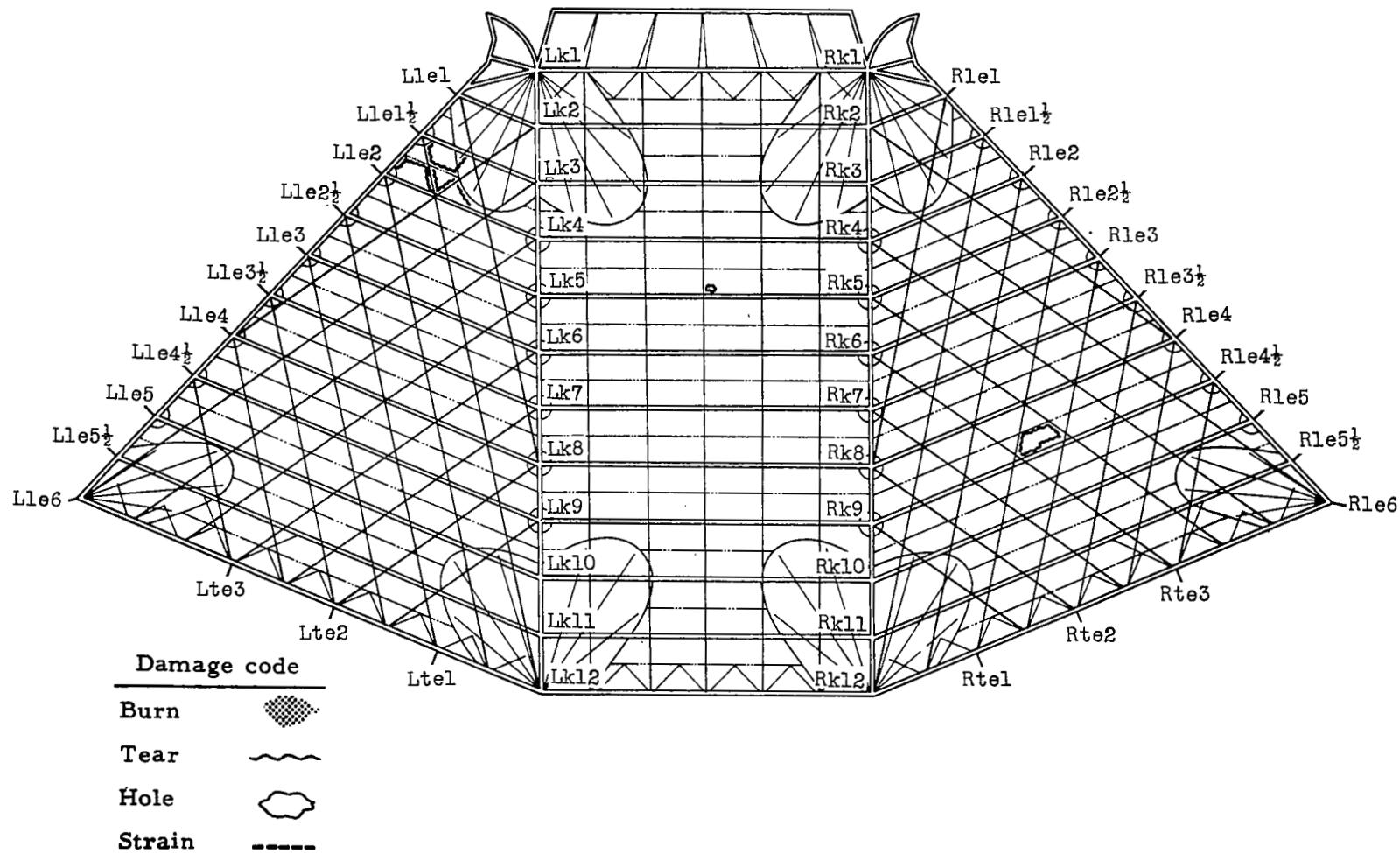


Figure 36.- Major canopy damage, test 211T.

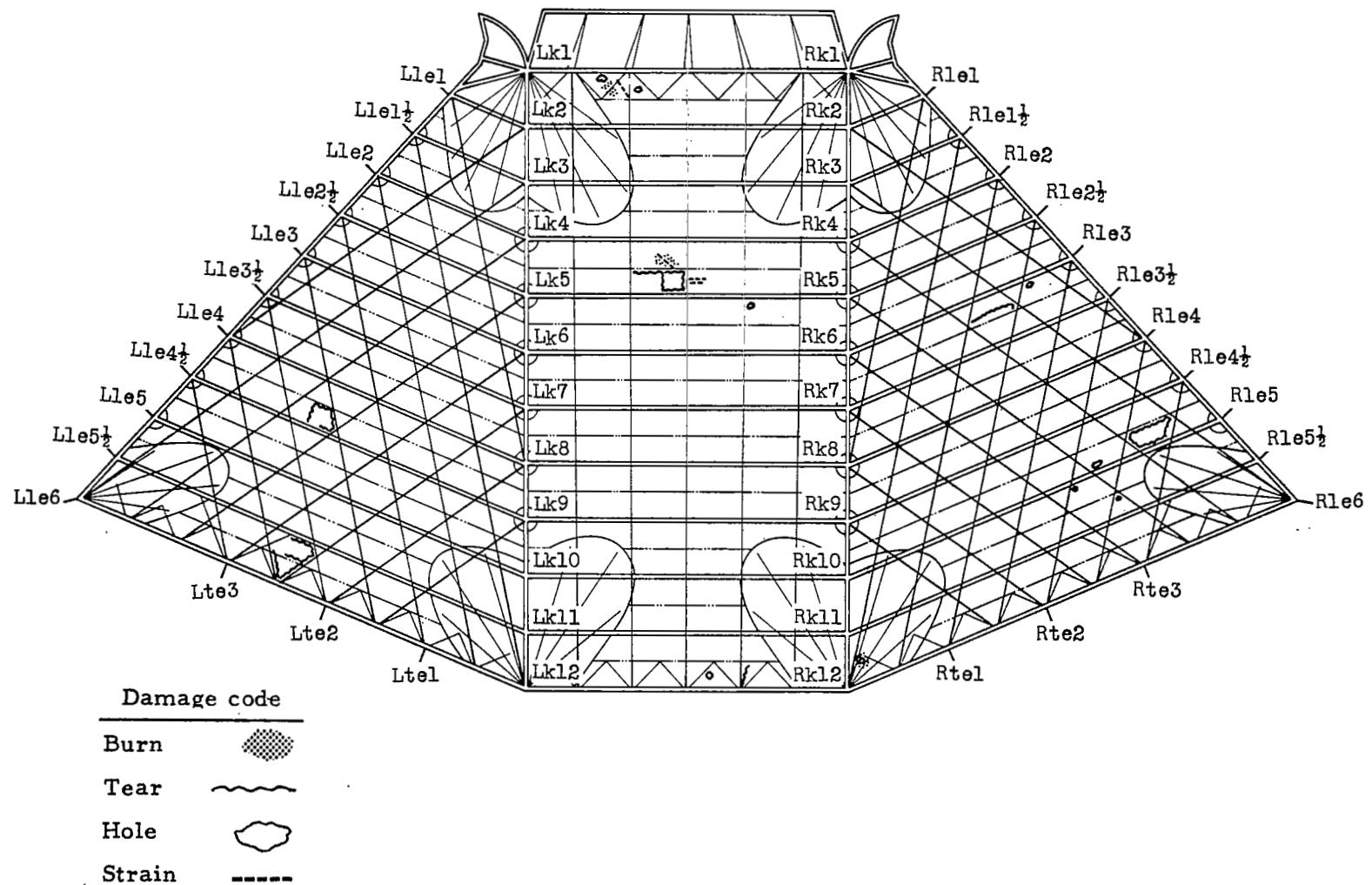


Figure 37.- Major canopy damage, test 206T.

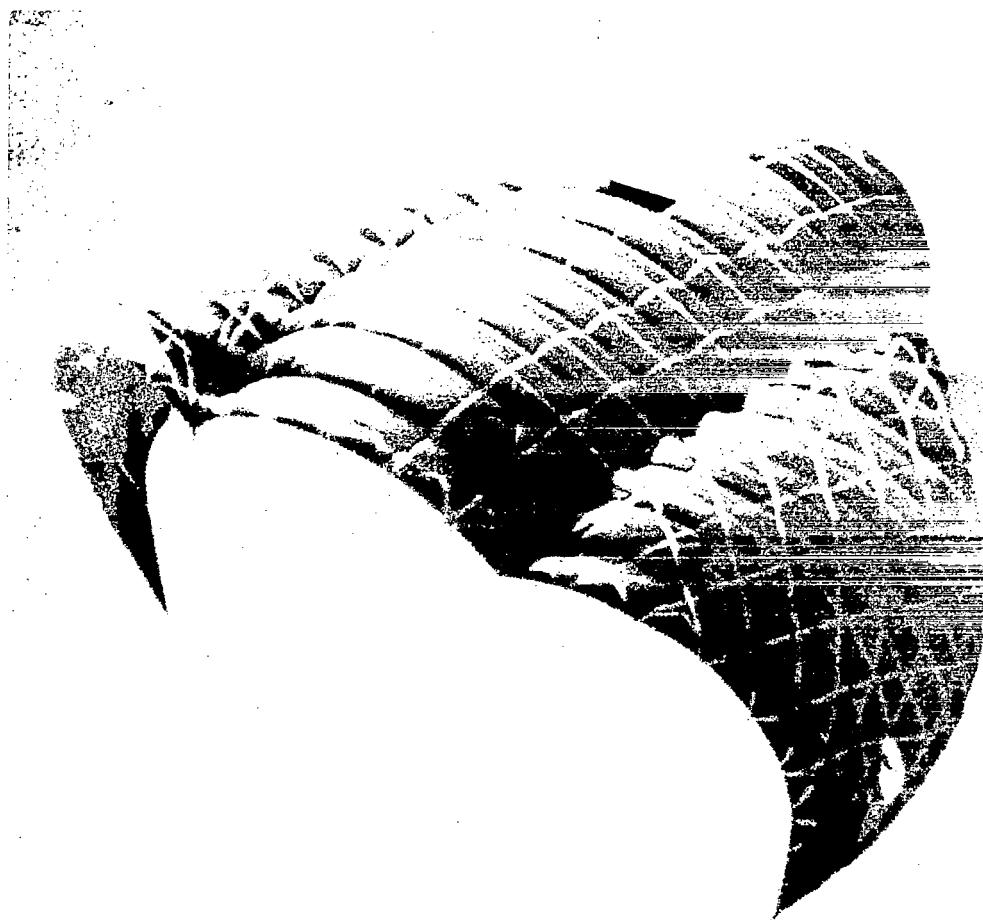
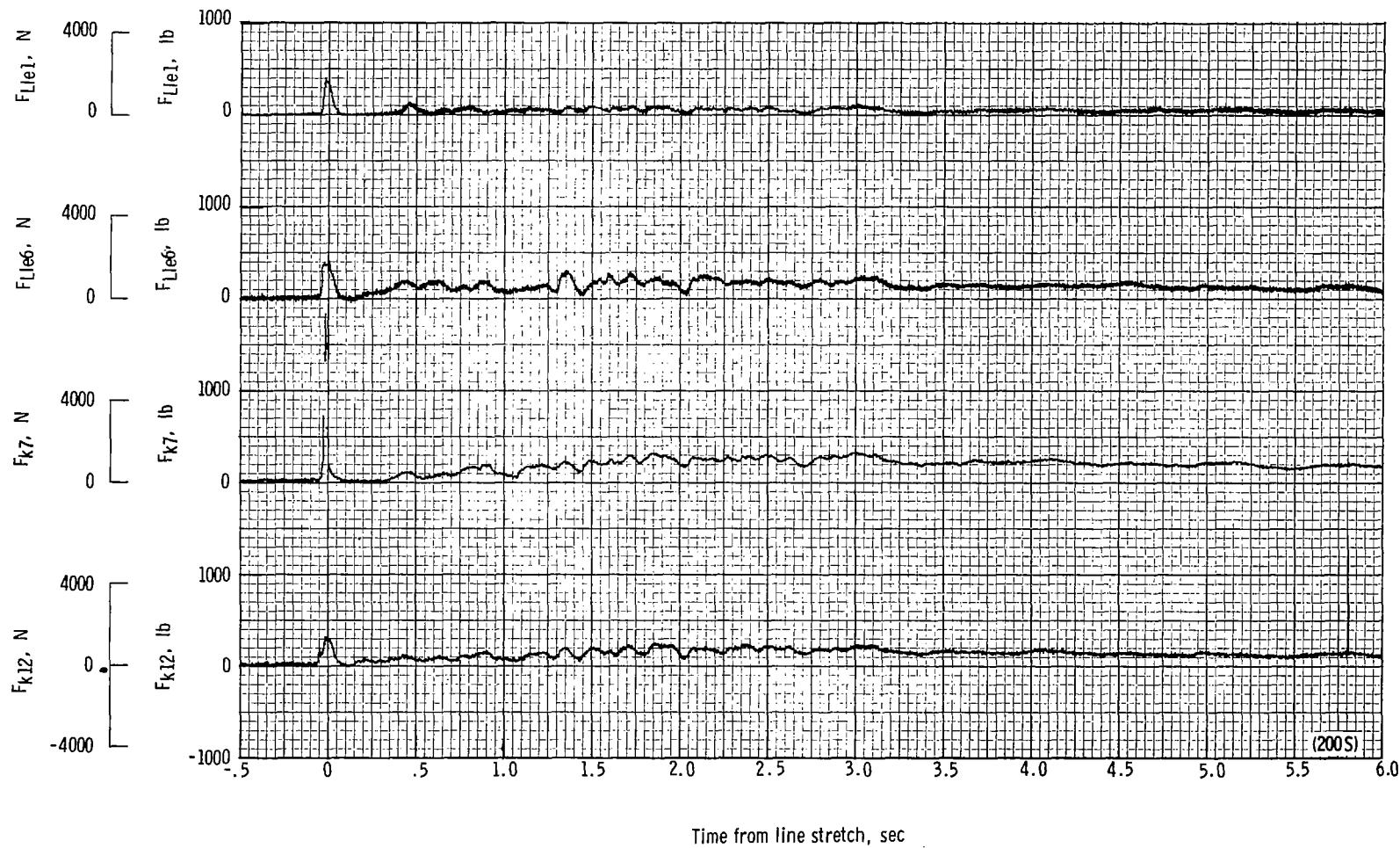


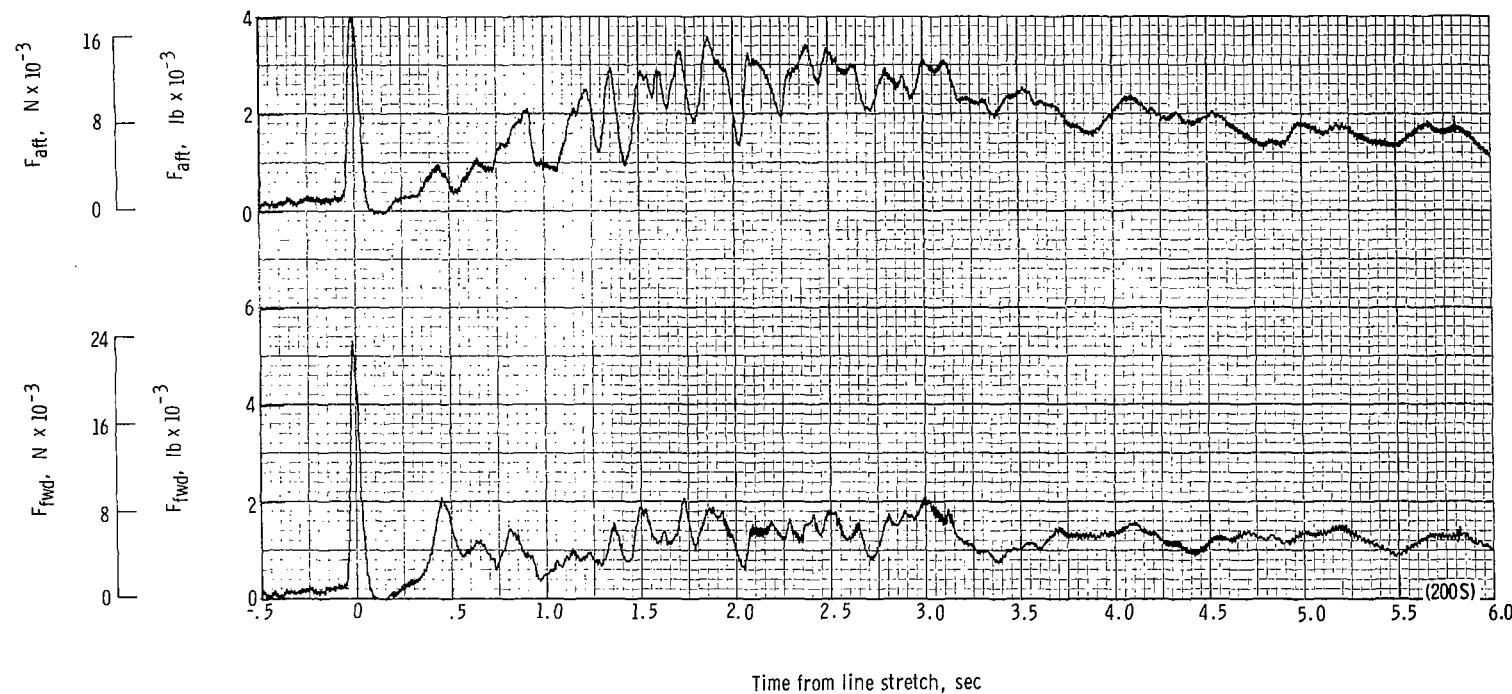
Figure 38.- Test 206T parawing in gliding flight, showing some of the canopy damage.

L-71-698



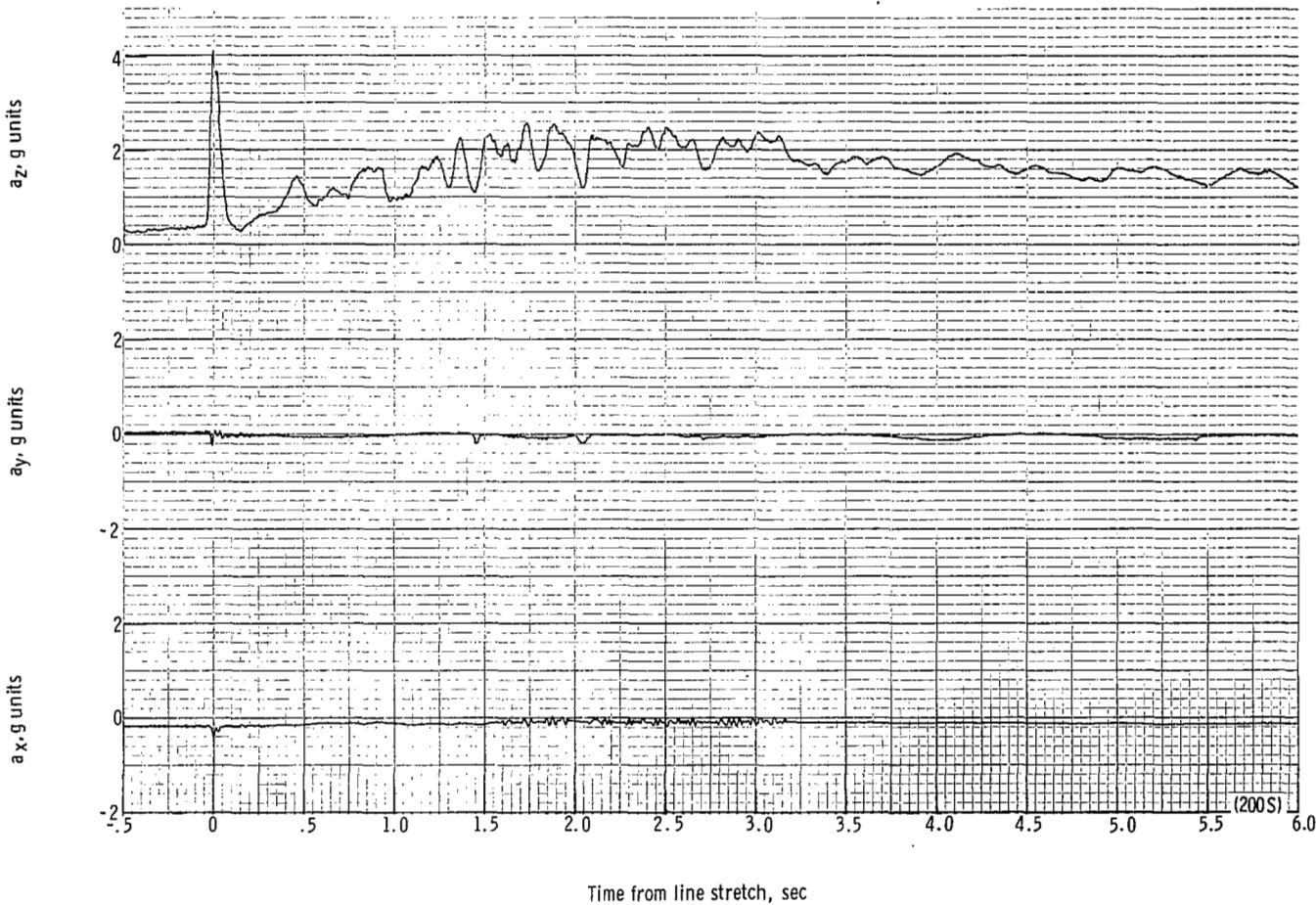
(a) Individual suspension-line loads F_{k12} , F_{k7} , F_{Lle6} , and F_{Lle1} plotted against time from line stretch. Time = 0 second corresponds to 25.97 seconds after launch.

Figure 39.- Time history of single-keel parawing deployment data for test 200S. $W_D = 12\,758\text{ N}$ (2868 lb); $W_P = 11\,392\text{ N}$ (2561 lb); $q_{PD} = 794.8\text{ N/m}^2$ (16.6 lb/ft²); $h_{PD} = 1582\text{ m}$ (5190 ft); $l_r/l_k = 0.116$.



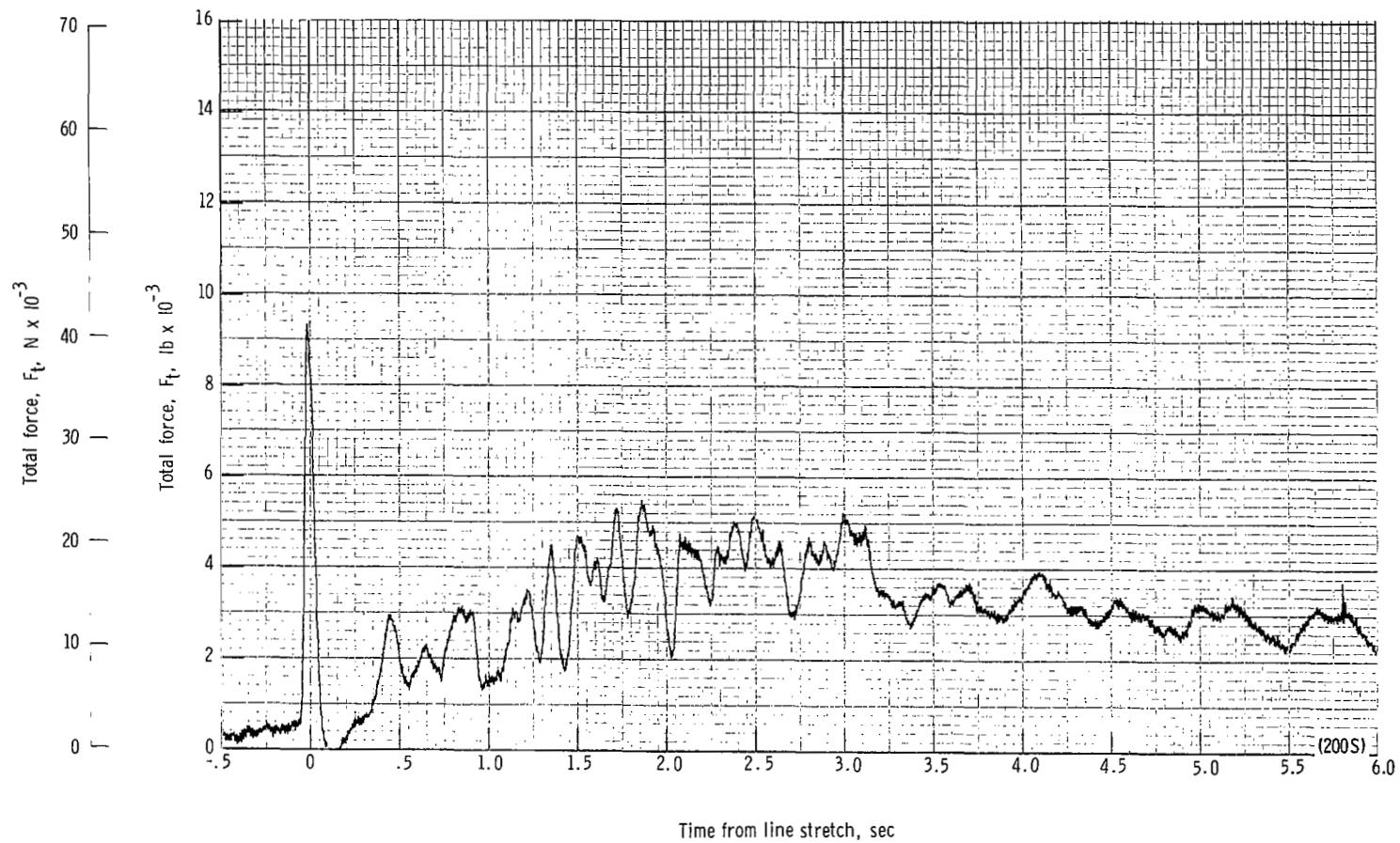
(b) Forward and aft riser loads plotted against time from line stretch. Time = 0 second corresponds to 25.97 seconds after launch.

Figure 39.- Continued.



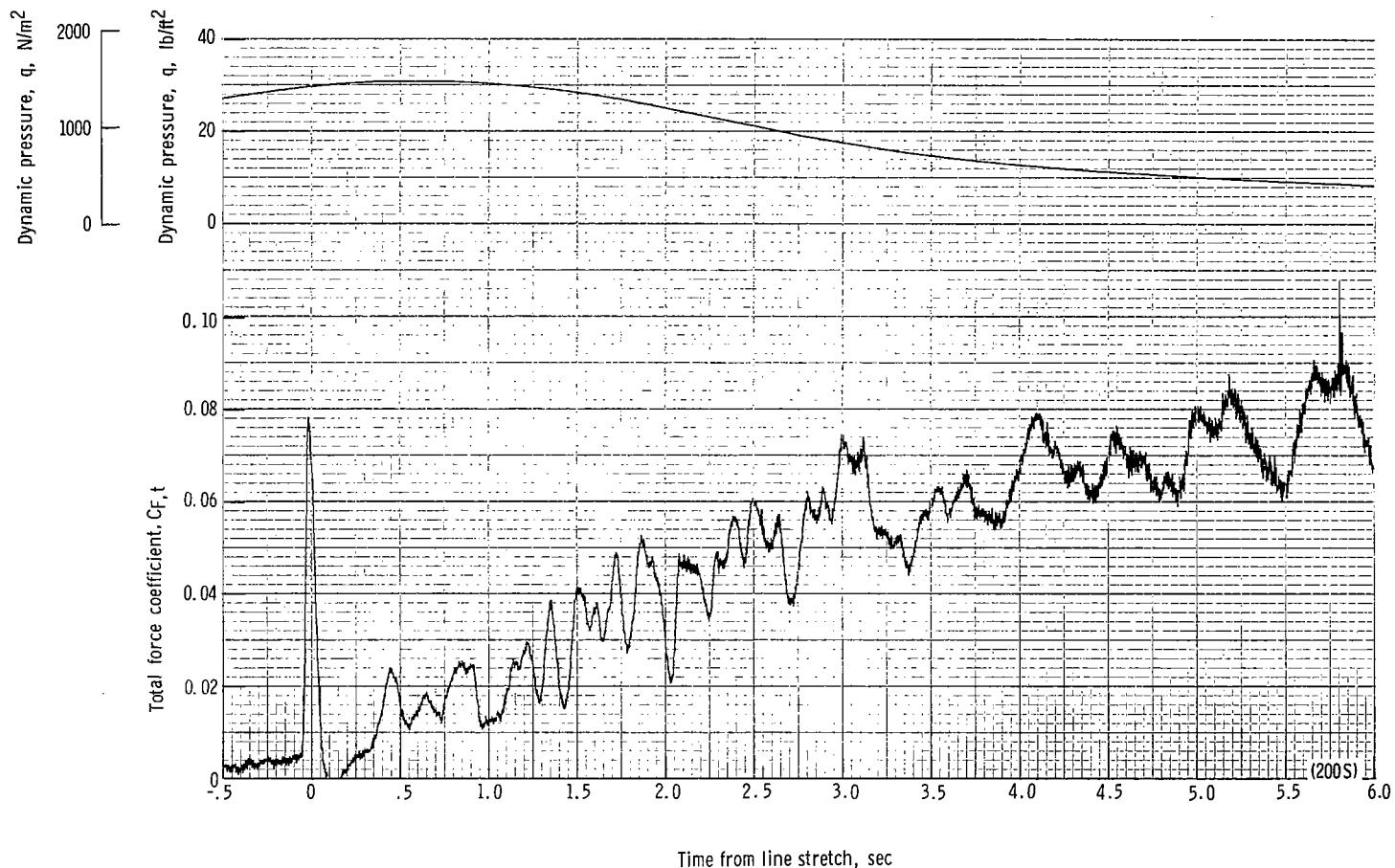
(c) Accelerations a_x , a_y , and a_z plotted against time from line stretch. Time = 0 second corresponds to 25.97 seconds after launch.

Figure 39.- Continued.



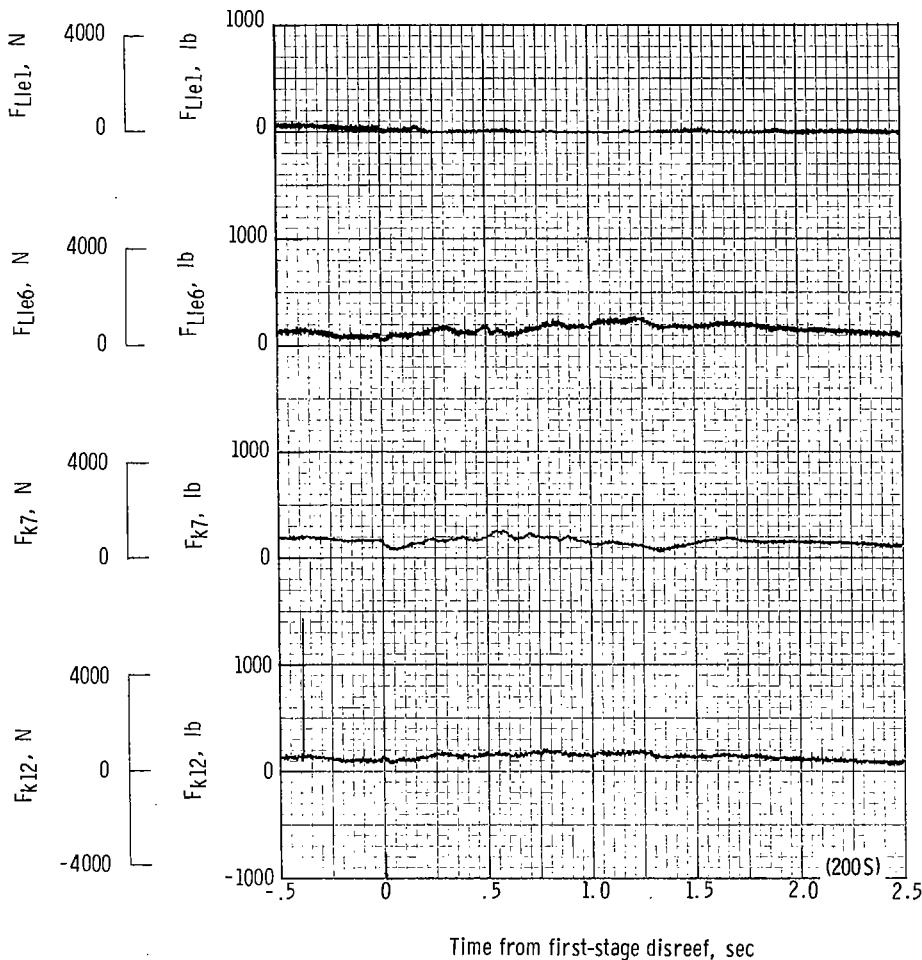
(d) Total force F_t plotted against time from line stretch. Time = 0 second corresponds to 25.97 seconds after launch.

Figure 39.- Continued..



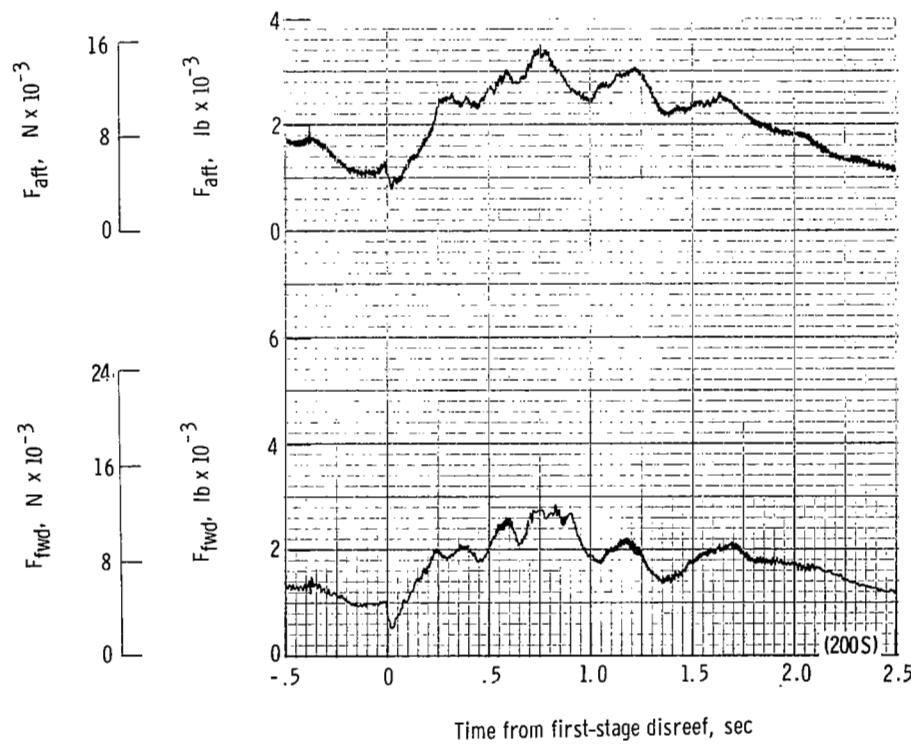
(e) Total force coefficient $C_{F,t}$ and dynamic pressure q plotted against time from line stretch. Time = 0 second corresponds to 25.97 seconds after launch.

Figure 39.- Continued.



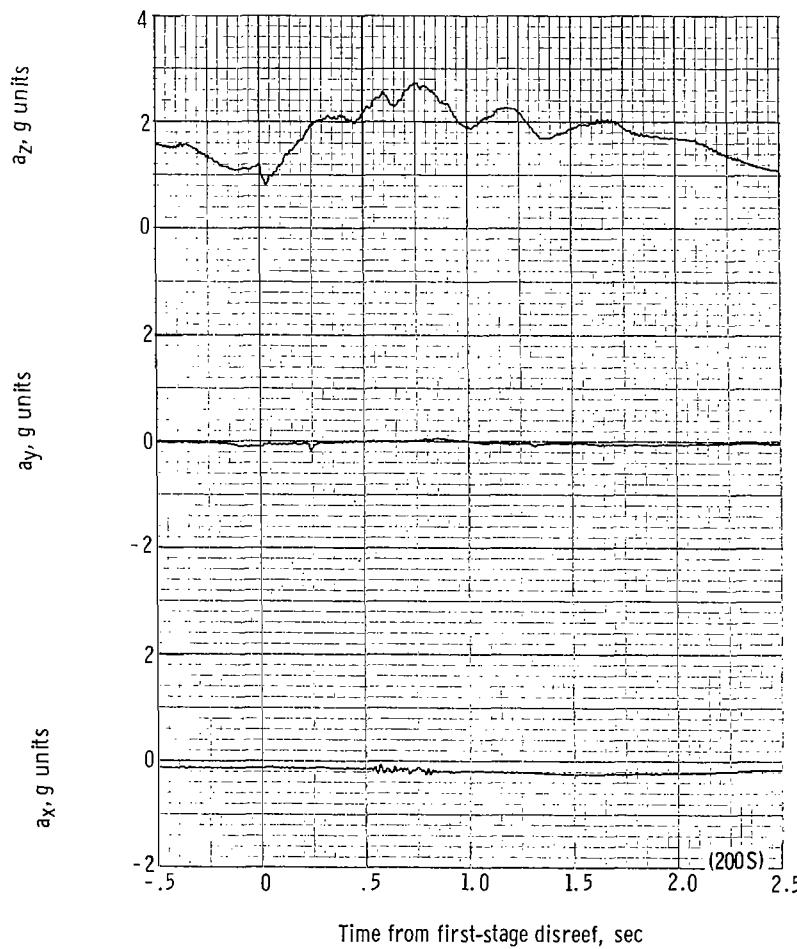
(f) Individual suspension-line loads F_{k12} , F_{k7} , F_{Lle6} , and F_{Lle1} plotted against time from first-stage disreef. Time = 0 second corresponds to 32.17 seconds after launch.

Figure 39.- Continued.



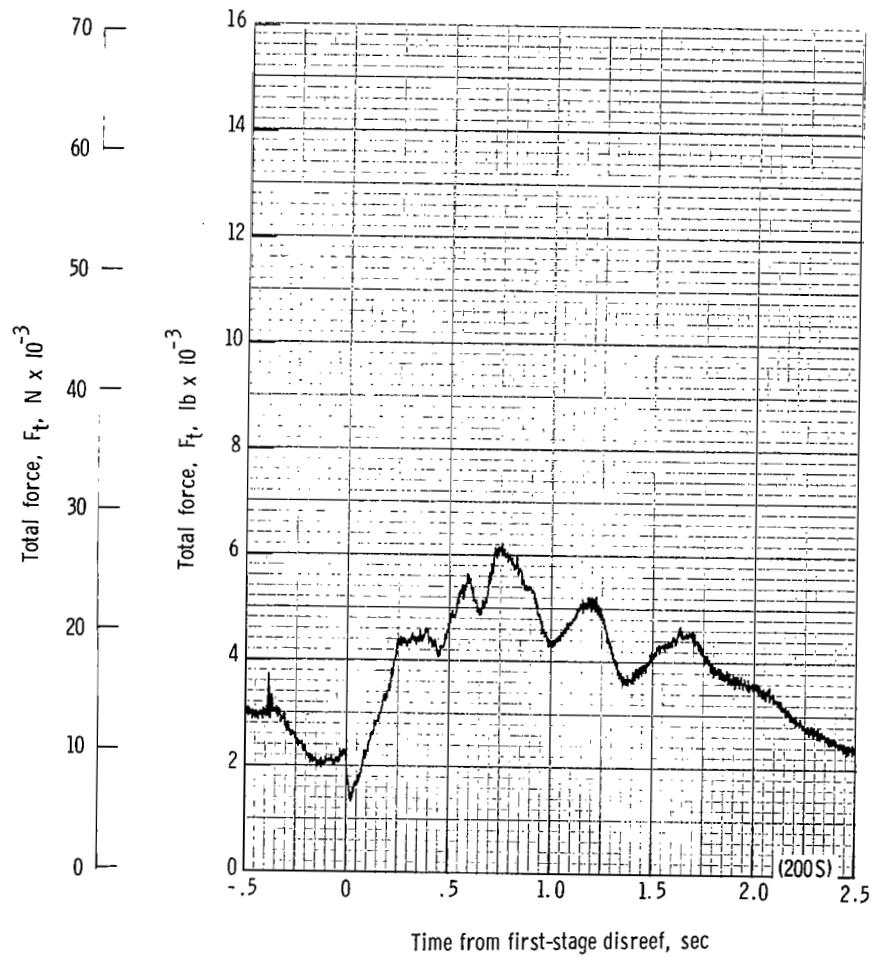
(g) Forward and aft riser loads plotted against time from first-stage disreef. Time = 0 second corresponds to 32.17 seconds after launch.

Figure 39.- Continued.



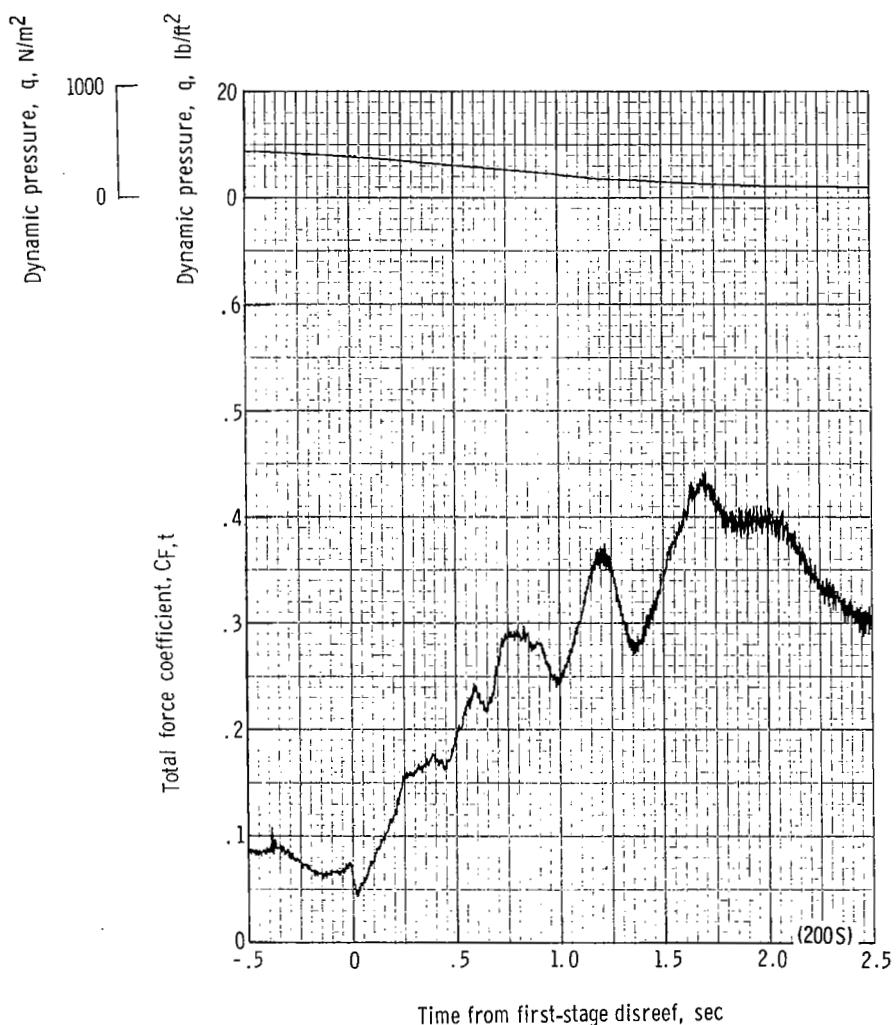
(h) Accelerations a_x , a_y , and a_z plotted against time from first-stage disreef. Time = 0 second corresponds to 32.17 seconds after launch.

Figure 39.- Continued.



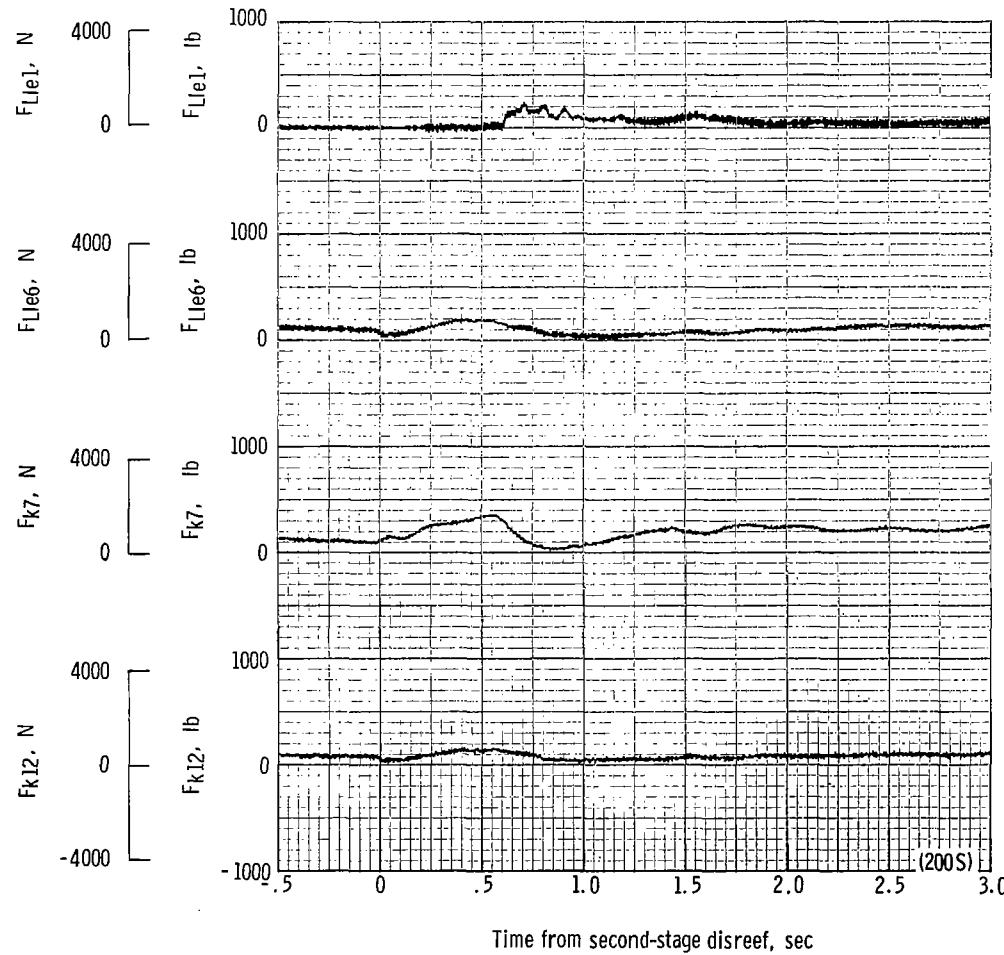
(i) Total force F_t plotted against time from first-stage disreef. Time = 0 second corresponds to 32.17 seconds after launch.

Figure 39.- Continued.



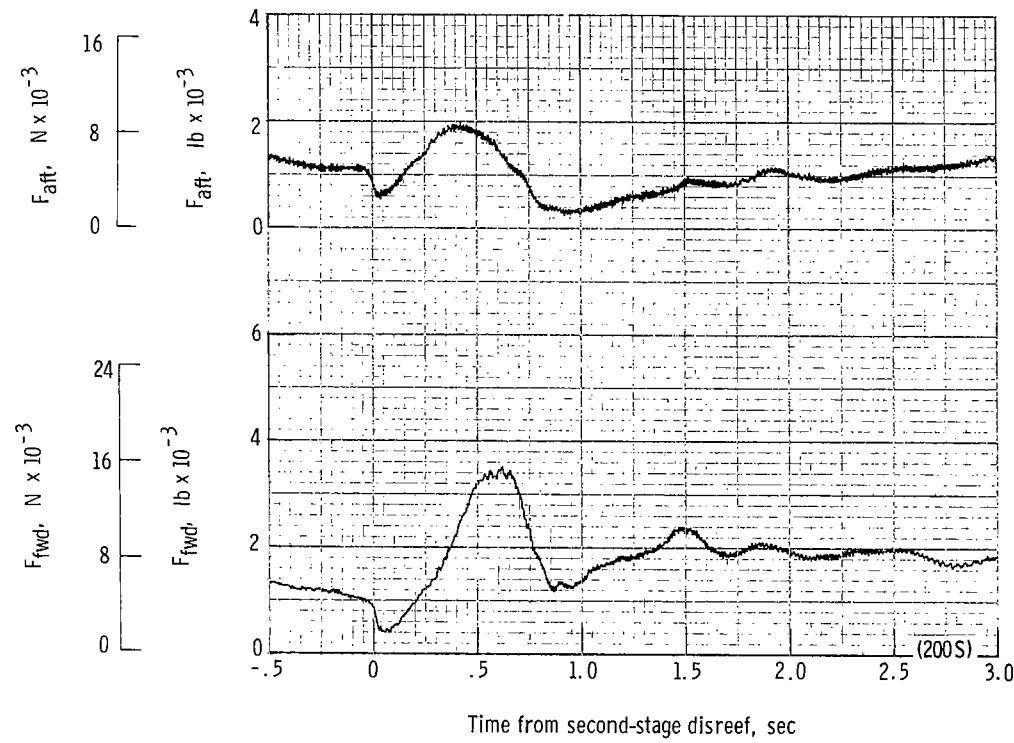
(j) Total force coefficient CF_t and dynamic pressure q plotted against time from first-stage disreef. Time = 0 second corresponds to 32.17 seconds after launch.

Figure 39.- Continued.



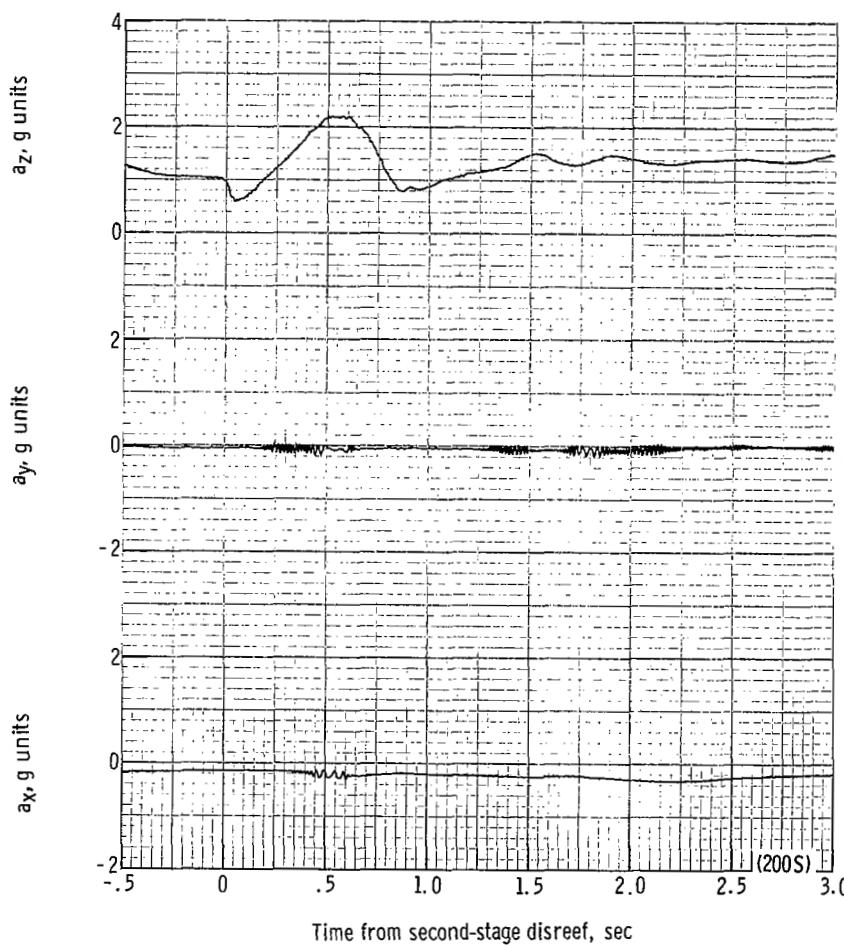
(k) Individual suspension-line loads F_{k12} , F_{k7} , F_{Lle6} , and F_{Lle1} plotted against time from second-stage disreef. Time = 0 second corresponds to 34.98 seconds after launch.

Figure 39.- Continued.



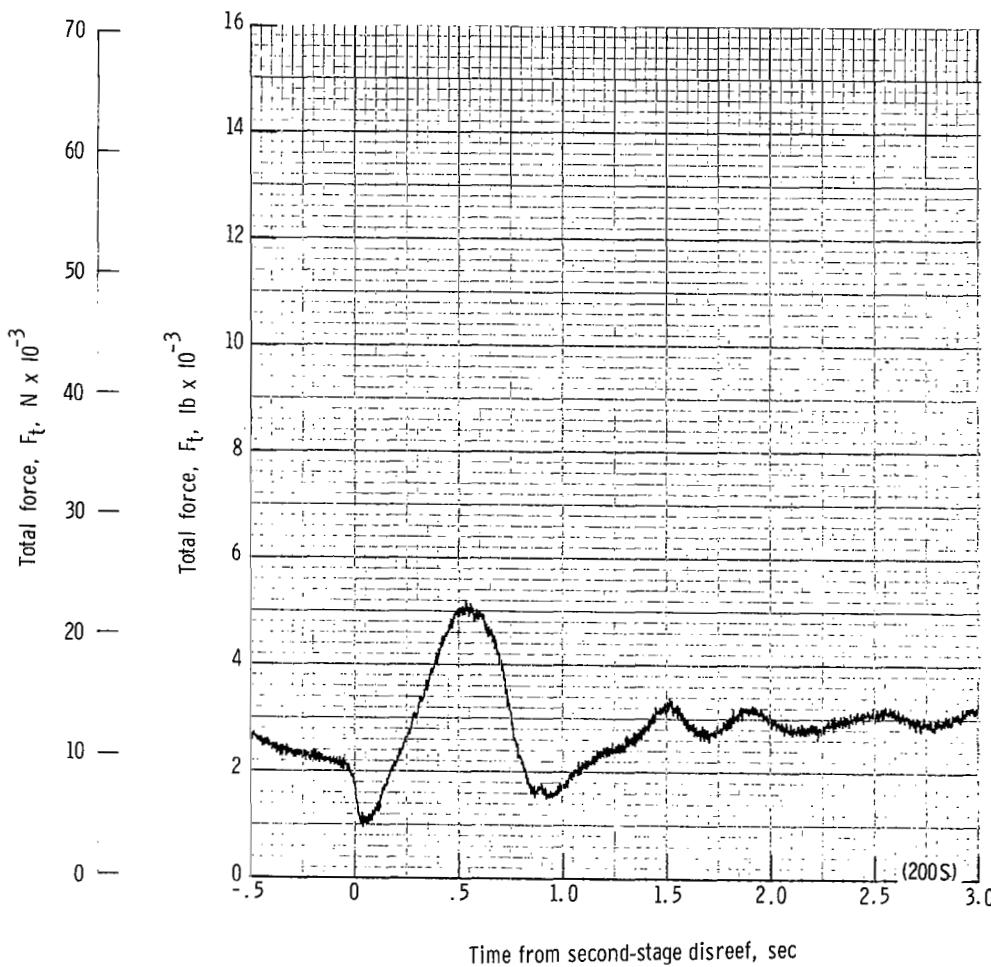
(I) Forward and aft riser loads plotted against time from second-stage disreef. Time = 0 second corresponds to 34.98 seconds after launch.

Figure 39.- Continued.



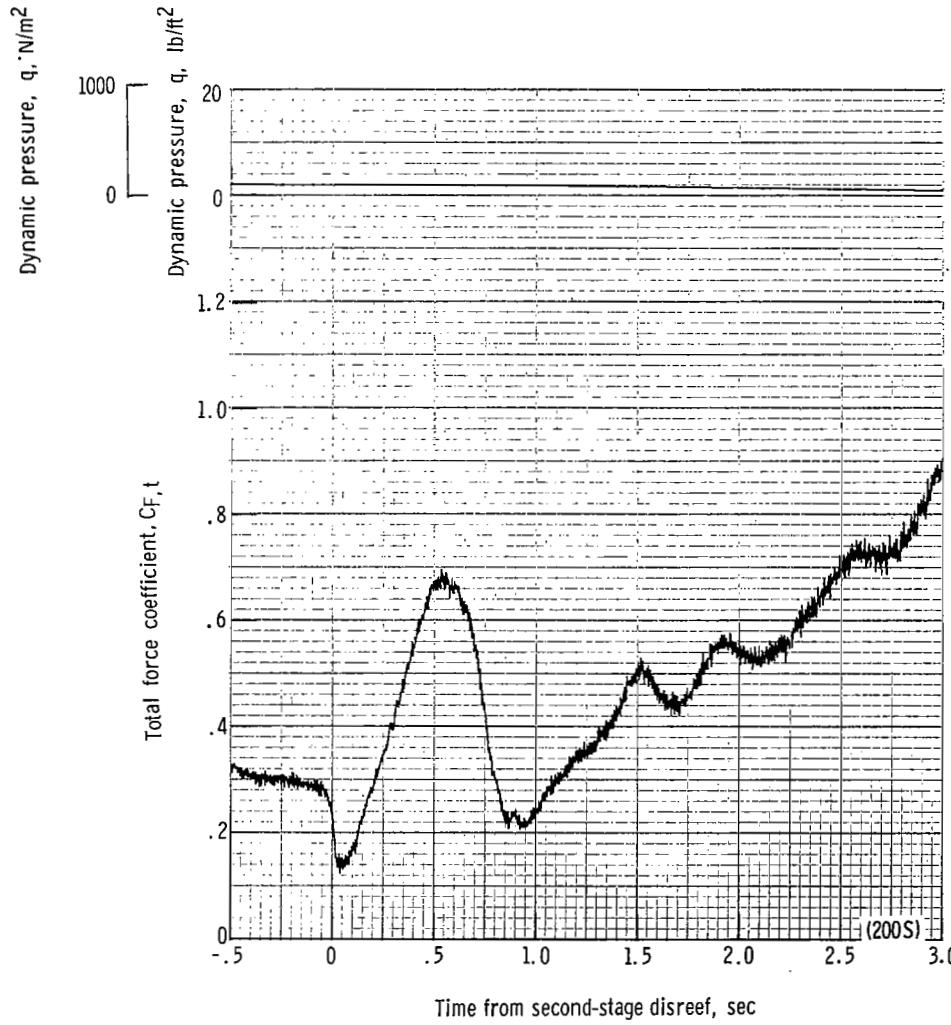
{m} Accelerations a_x , a_y , and a_z plotted against time from second-stage disreef. Time = 0 second corresponds to 34.98 seconds after launch.

Figure 39.- Continued.



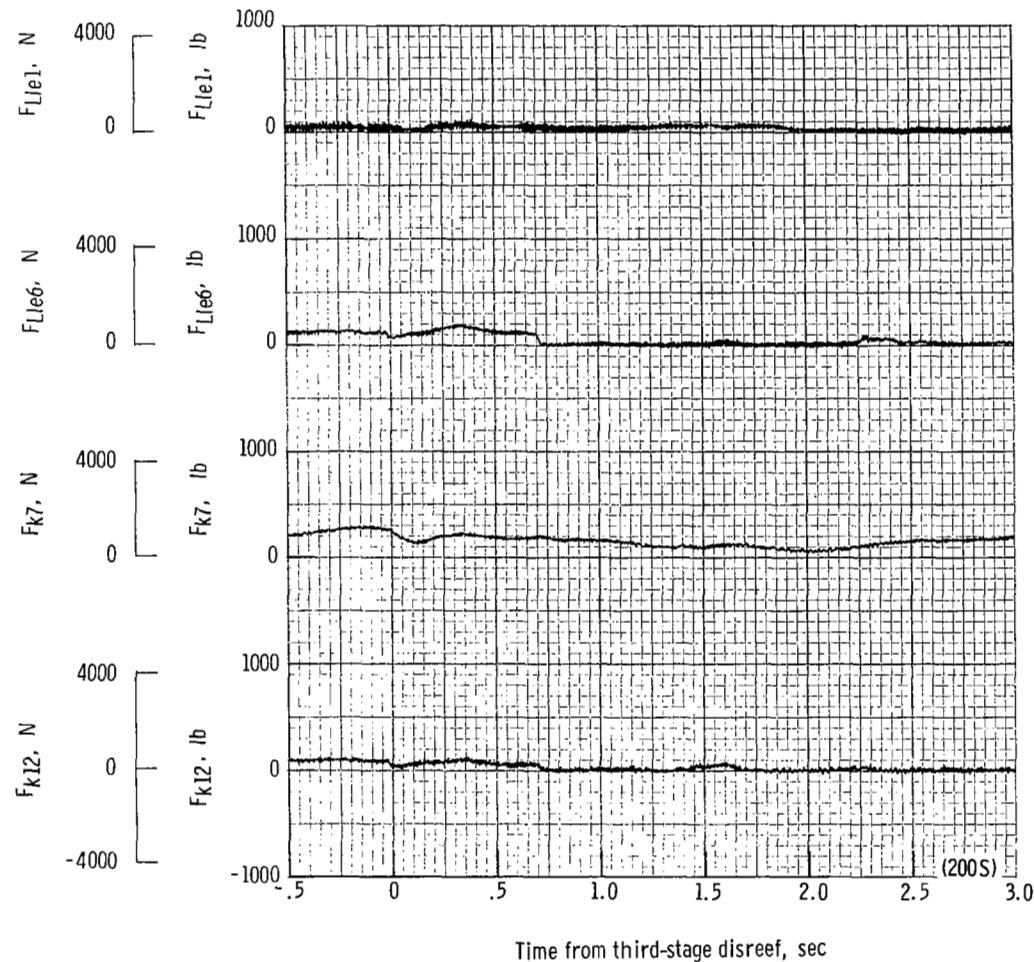
(n) Total force F_t plotted against time from second-stage disreef. Time = 0 second corresponds to 34.98 seconds after launch.

Figure 39.- Continued.



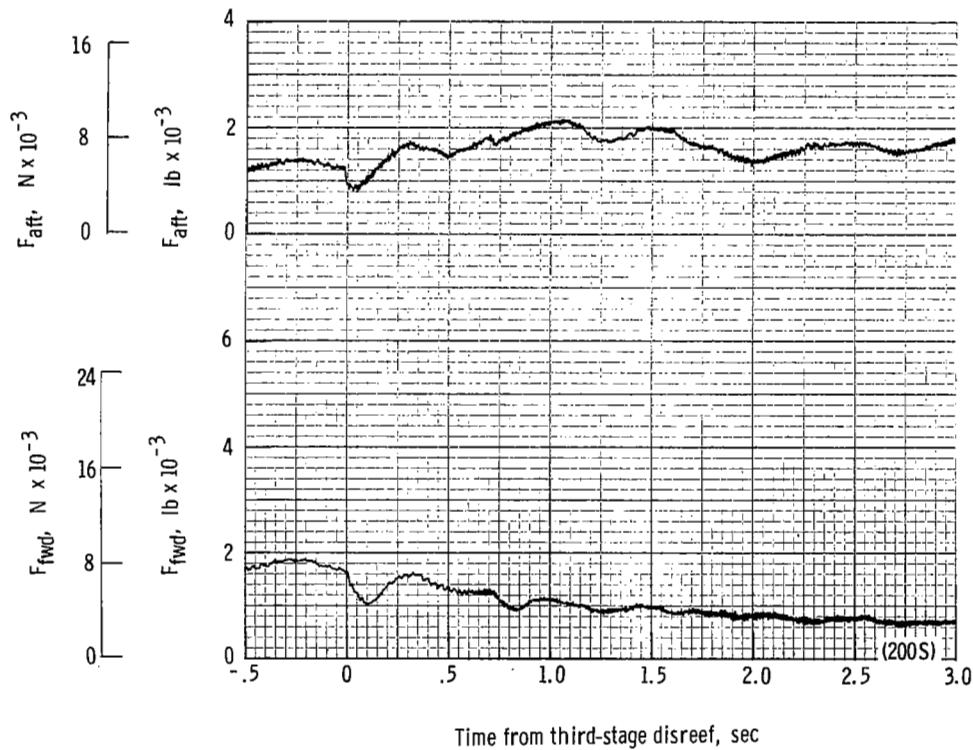
(o) Total force coefficient $C_{F,t}$ and dynamic pressure q plotted against time from second-stage disreef. Time = 0 second corresponds to 34.98 seconds after launch.

Figure 39.- Continued.



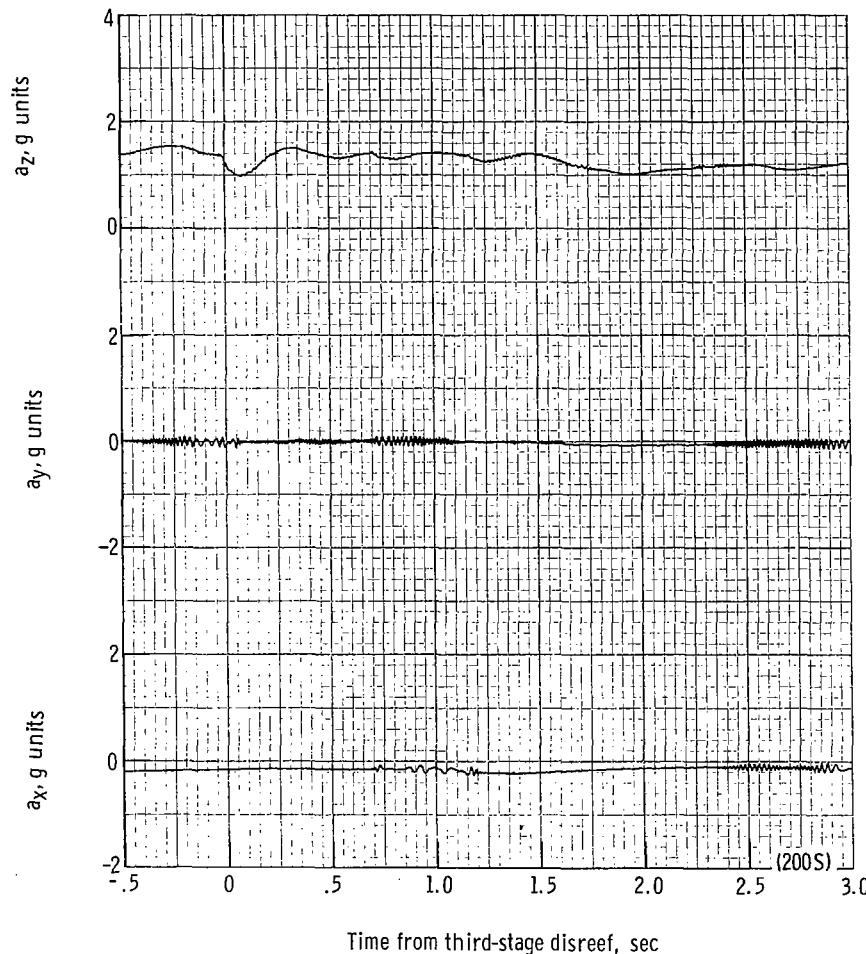
(p) Individual suspension-line loads F_{k12} , F_{k7} , F_{Lle6} , and F_{Lle1} plotted against time from third-stage disreef. Time = 0 second corresponds to 38.29 seconds after launch.

Figure 39.- Continued.



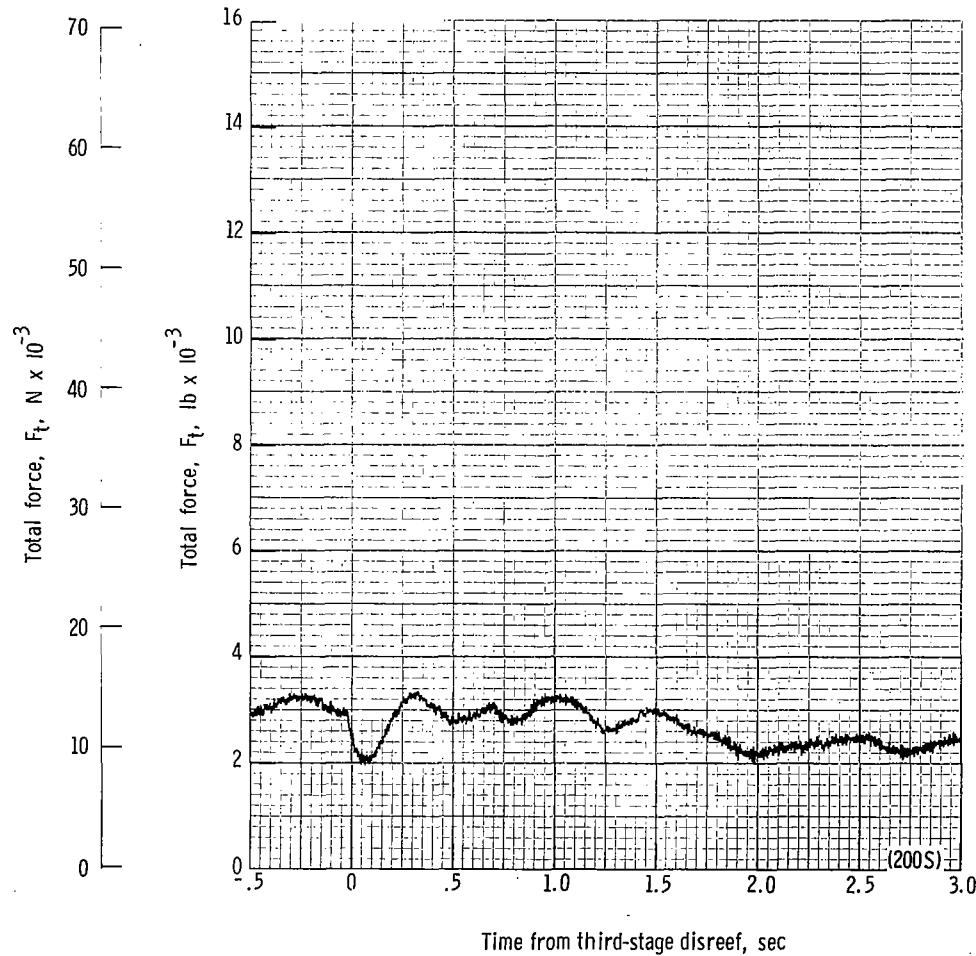
(q) Forward and aft riser loads plotted against time from third-stage disreef. Time = 0 second corresponds to 38.29 seconds after launch.

Figure 39.- Continued.



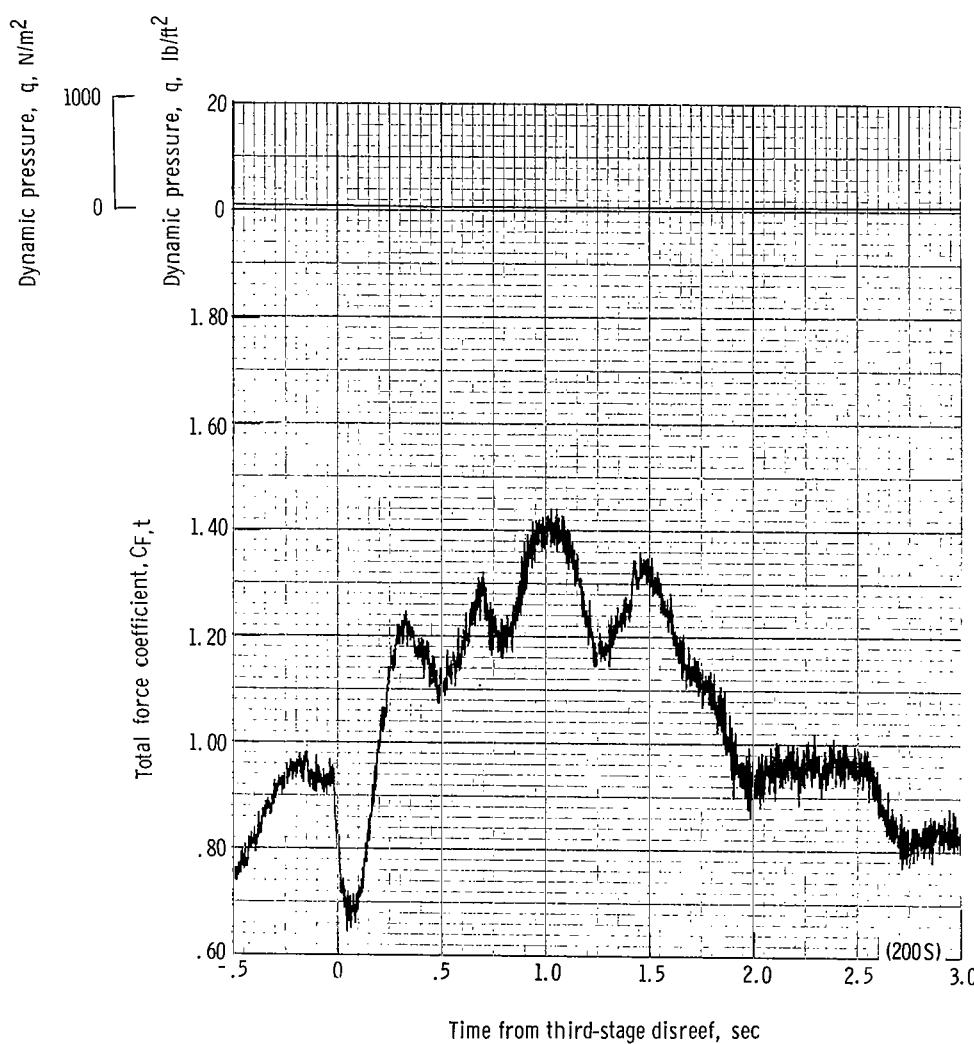
(r) Accelerations a_x , a_y , and a_z plotted against time from third-stage disreef. Time = 0 second corresponds to 38.29 seconds after launch.

Figure 39.- Continued.



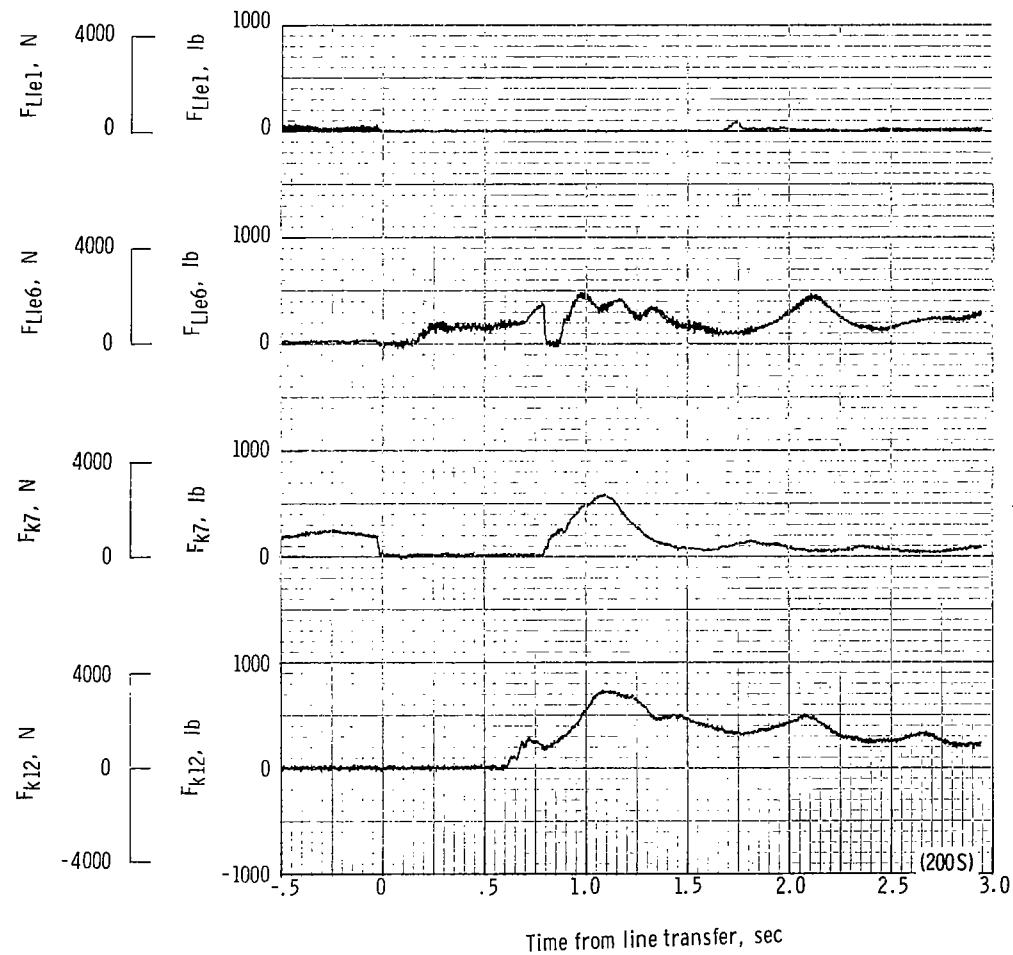
(s) Total force F_t plotted against time from third-stage disreef. Time = 0 second corresponds to 38.29 seconds after launch.

Figure 39.- Continued.



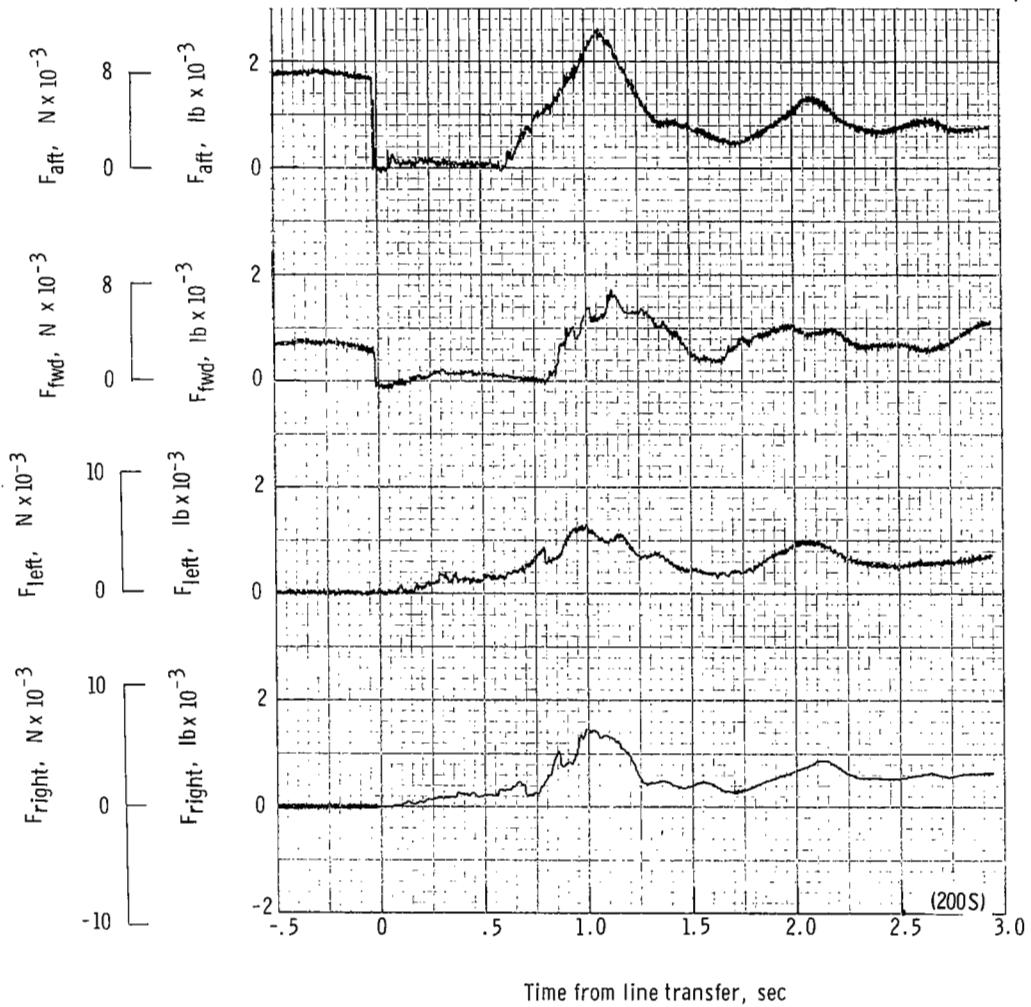
(t) Total-force coefficient $C_{F,t}$ and dynamic pressure q plotted against time from third-stage disreef. Time = 0 second corresponds to 38.29 seconds after launch.

Figure 39.- Continued.



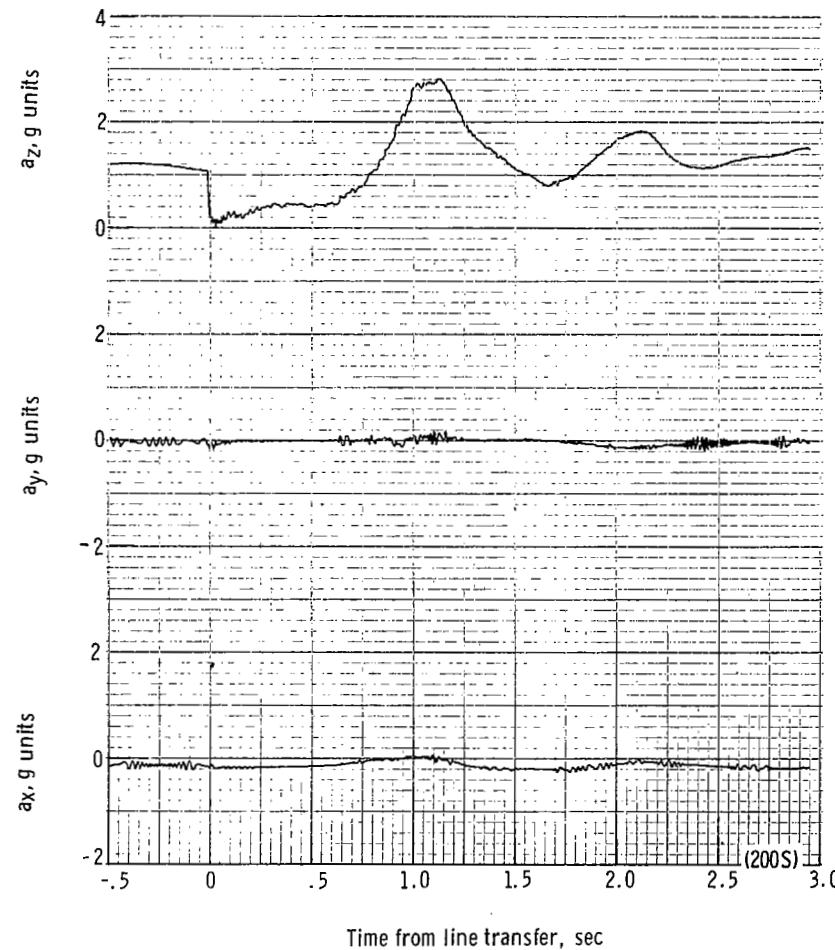
(u) Individual suspension-line loads F_{k12} , F_{k7} , F_{Lle6} , and F_{Lle1} plotted against time from line transfer. Time = 0 second corresponds to 41.74 seconds after launch.

Figure 39.- Continued.



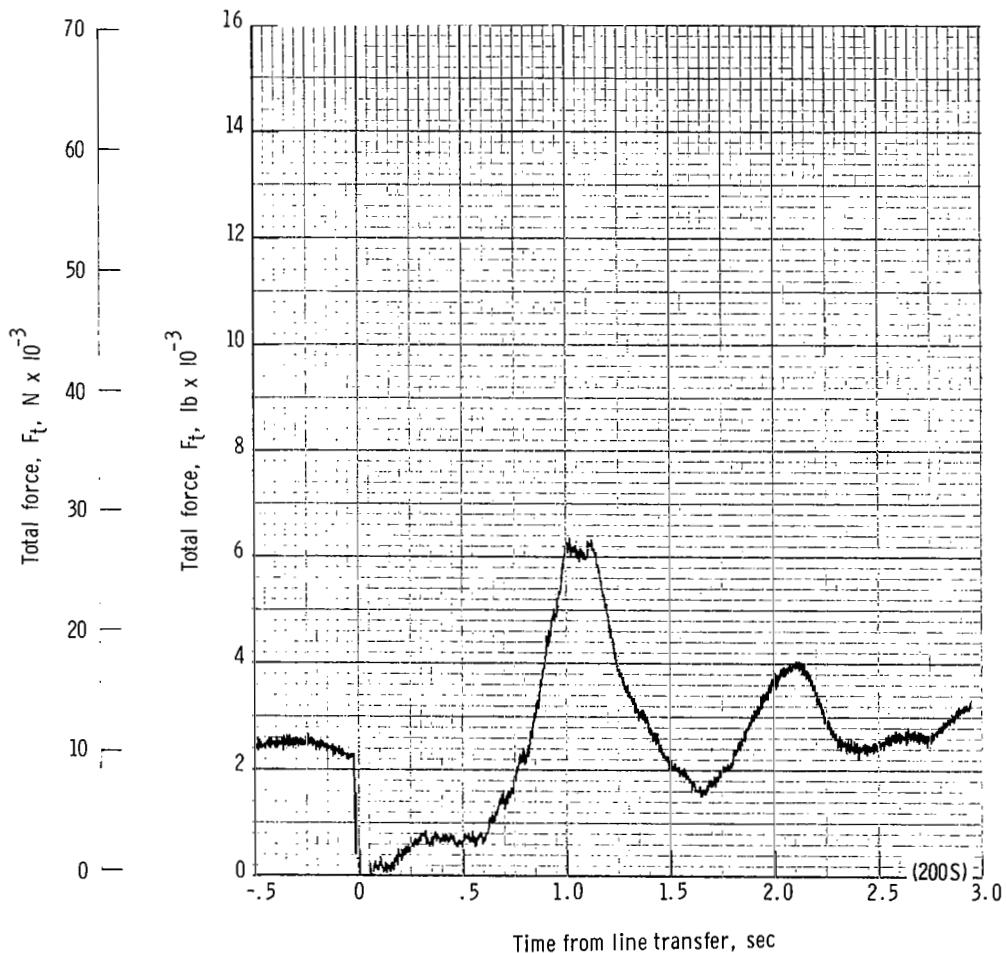
(v) Right, left, forward, and aft riser loads plotted against time from line transfer. Time = 0 second corresponds to 41.74 seconds after launch.

Figure 39.- Continued.



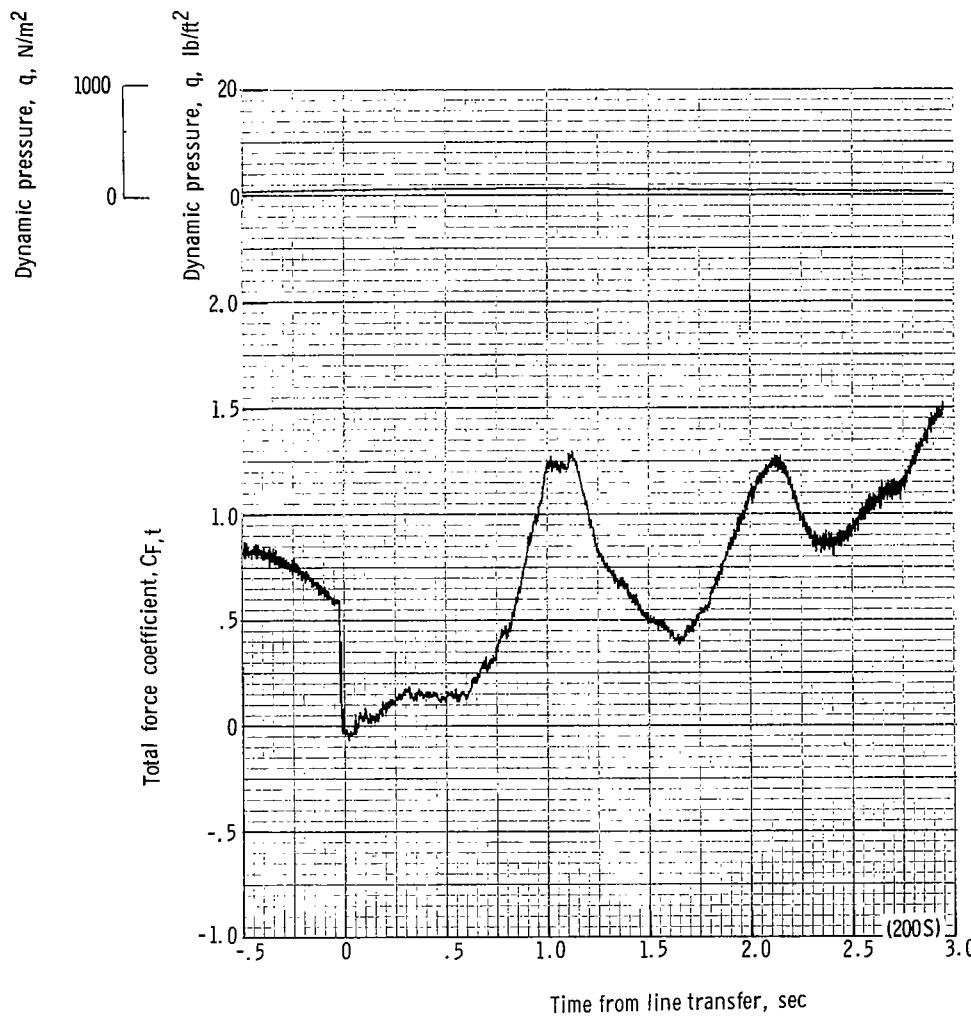
(w) Accelerations a_x , a_y , and a_z plotted against time from line transfer. Time = 0 second corresponds to 41.74 seconds after launch.

Figure 39.- Continued.



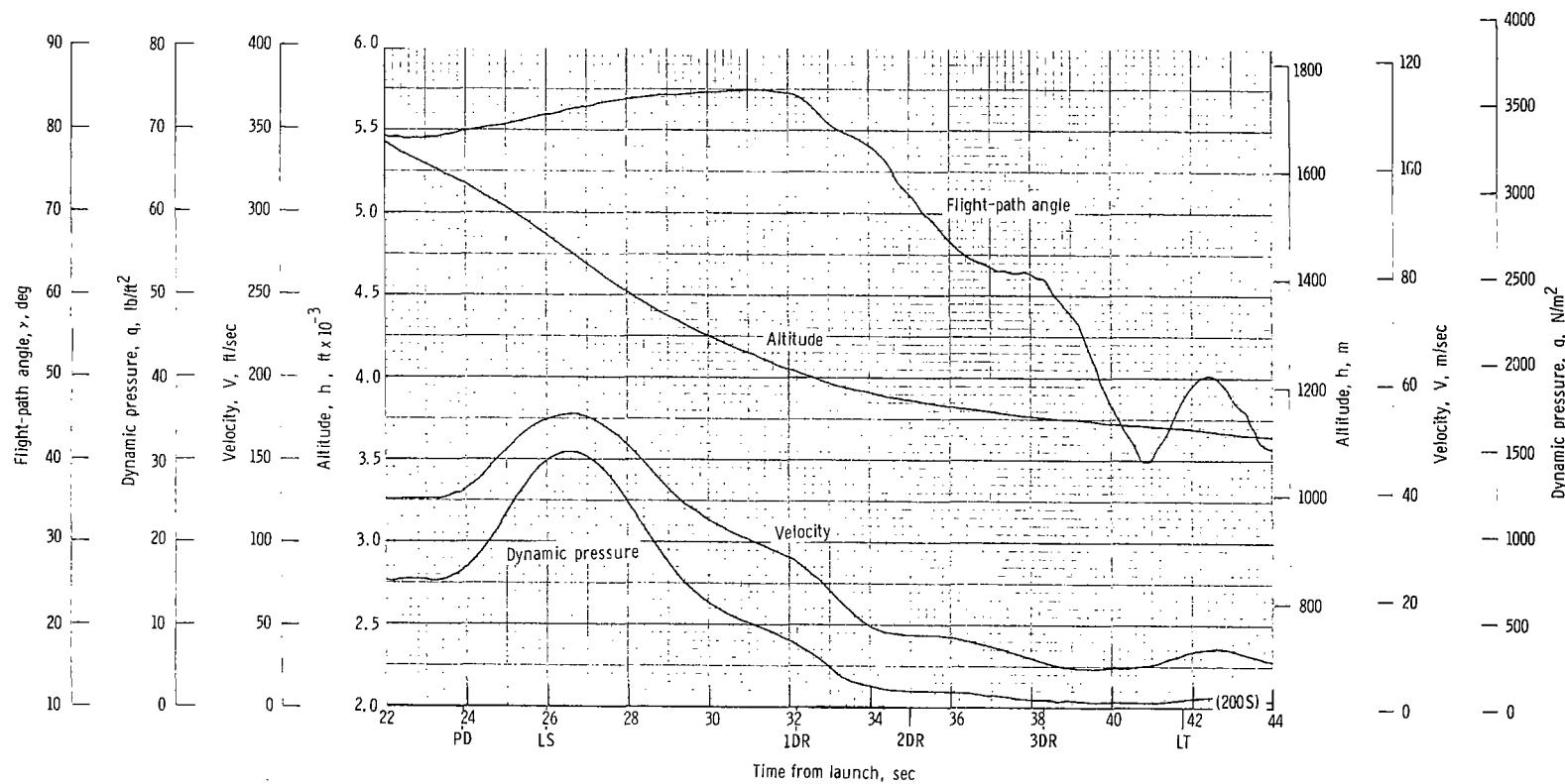
(x) Total force F_t plotted against time from line transfer. Time = 0 second corresponds to 41.74 seconds after launch.

Figure 39.- Continued.



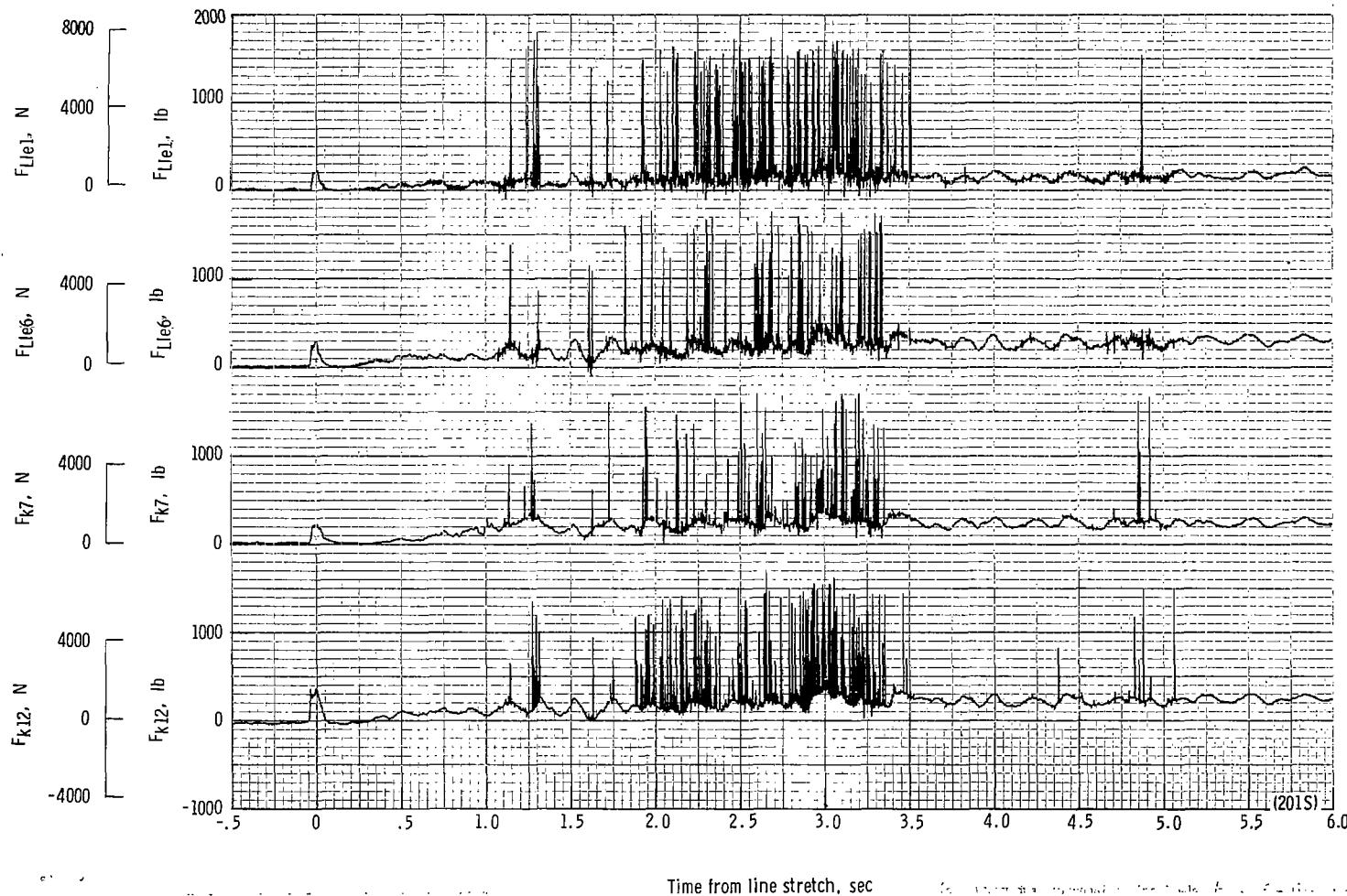
(y) Total force coefficient $C_{F,t}$ and dynamic pressure q plotted against time from line transfer. Time = 0 second corresponds to 41.74 seconds after launch.

Figure 39.- Continued.



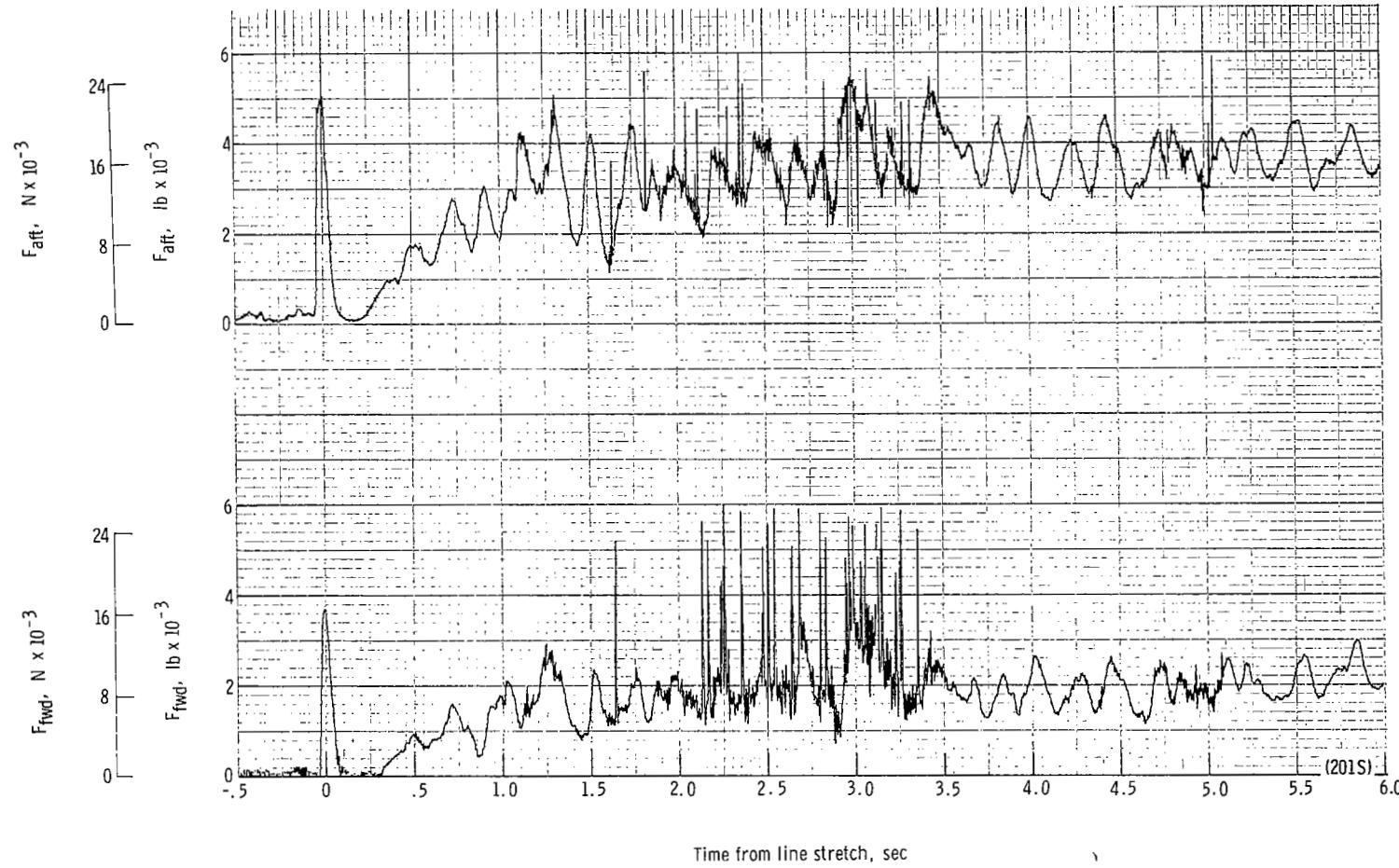
(z) Flight-path angle γ , dynamic pressure q , velocity V , and altitude h plotted against time from launch.

Figure 39.- Concluded.



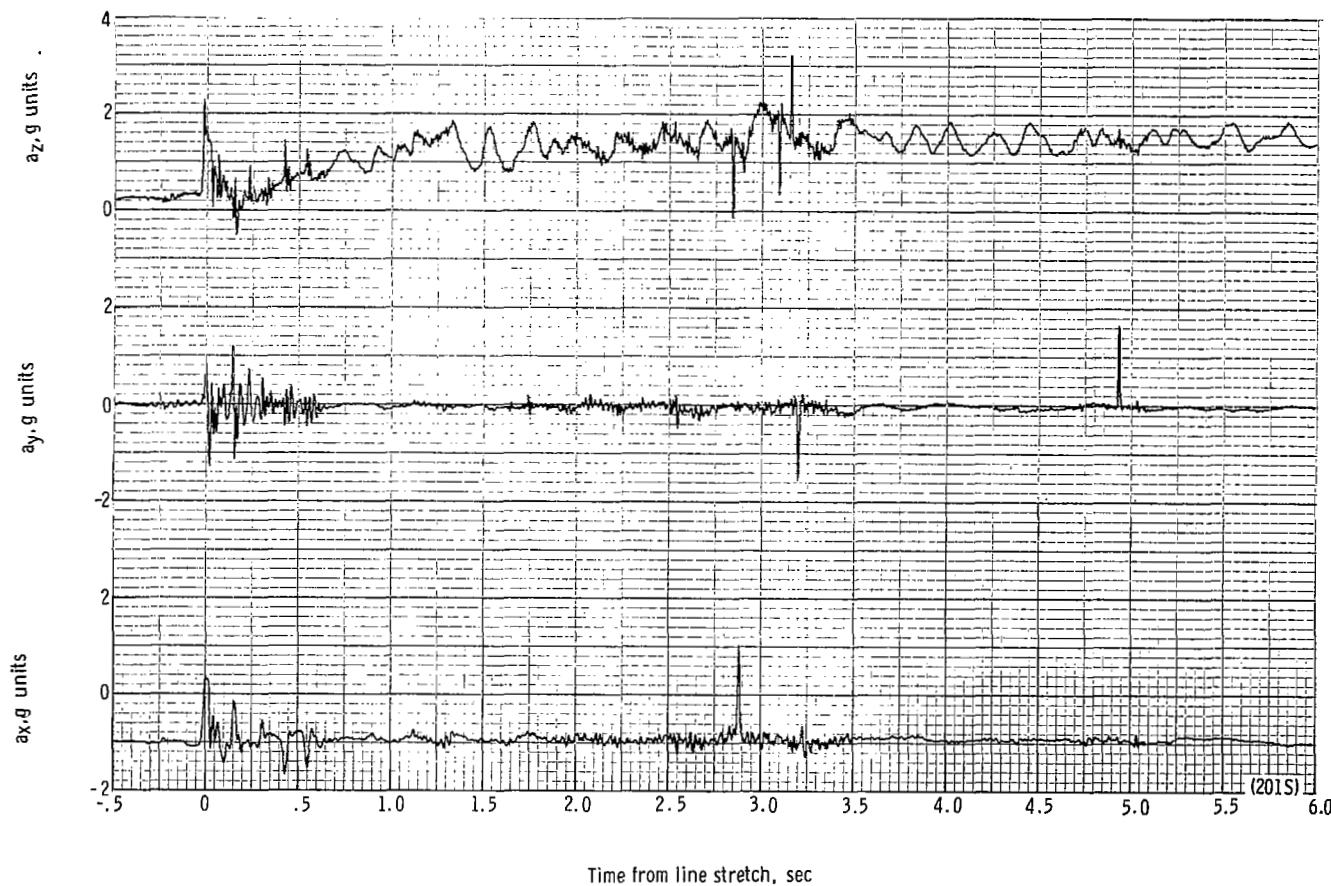
(a) Individual suspension-line loads F_{k12} , F_k7 , F_{Lle6} , and F_{Lle1} plotted against time from line stretch. Time = 0 second corresponds to 28.08 seconds after launch.

Figure 40.- Time history of single-keel parawing deployment data for test 201S. $W_D = 22\ 228\ N$ (4997 lb); $W_P = 20\ 809\ N$ (4678 lb); $q_{PD} = 857.1\ N/m^2$ (17.9 lb/ft²); $h_{PD} = 885\ m$ (2905 ft); $l_r/l_k = 0.120$.



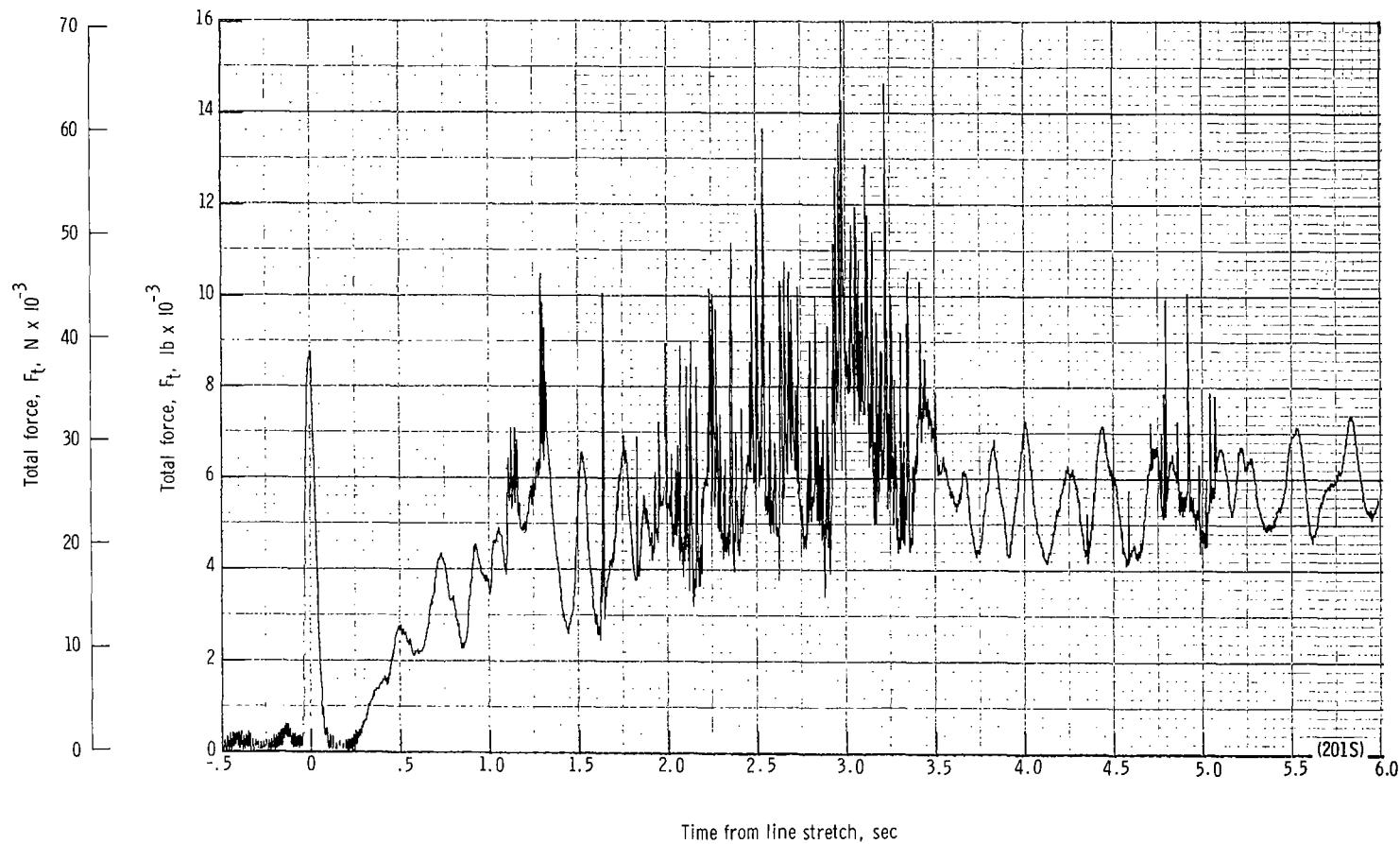
(b) Forward and aft riser loads plotted against time from line stretch. Time = 0 second corresponds to 28.08 seconds after launch.

Figure 40.- Continued.



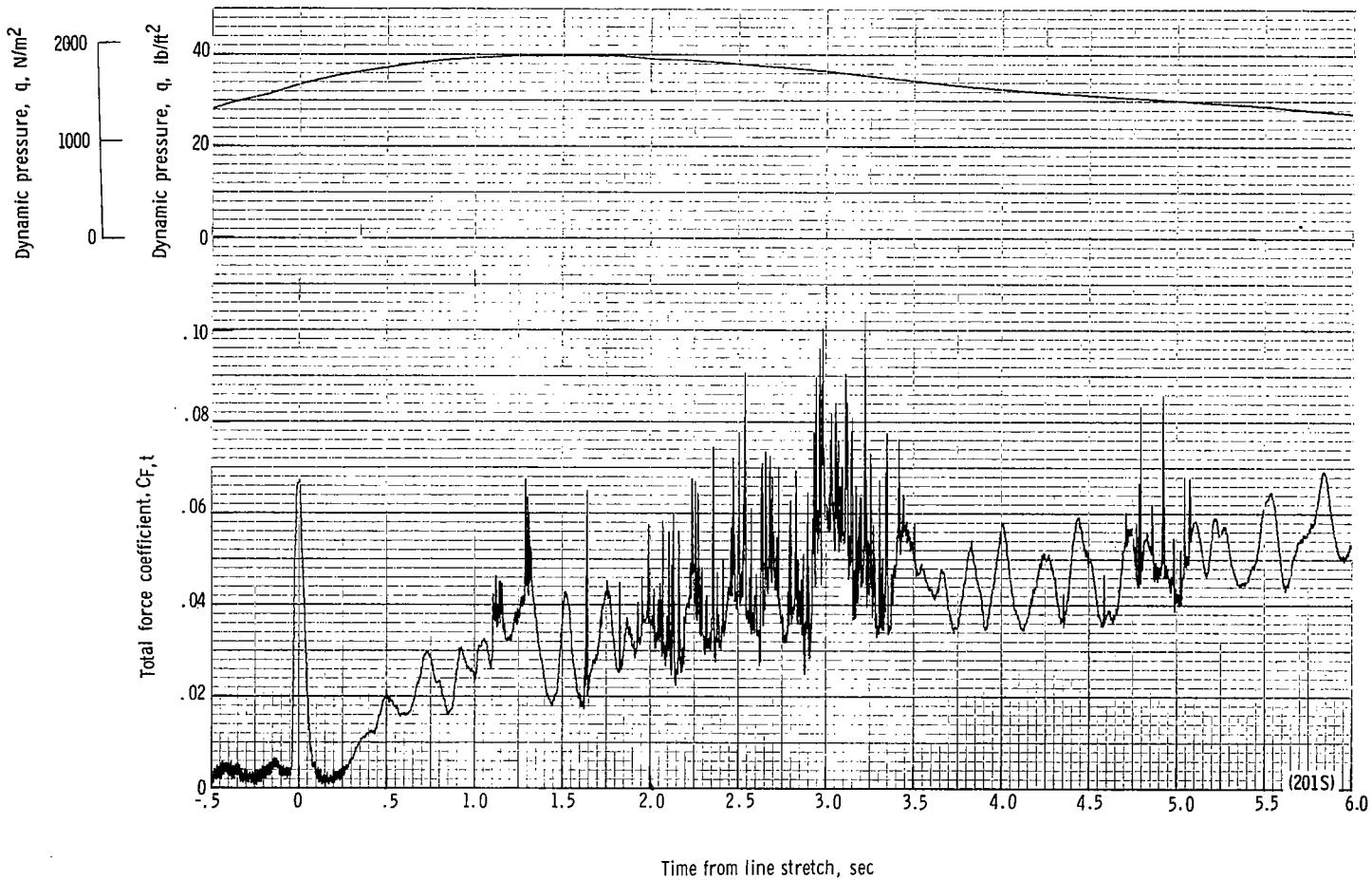
(c) Acceleration a_x , a_y , and a_z plotted against time from line stretch. Time = 0 second corresponds to 28.08 seconds after launch.

Figure 40.- Continued.



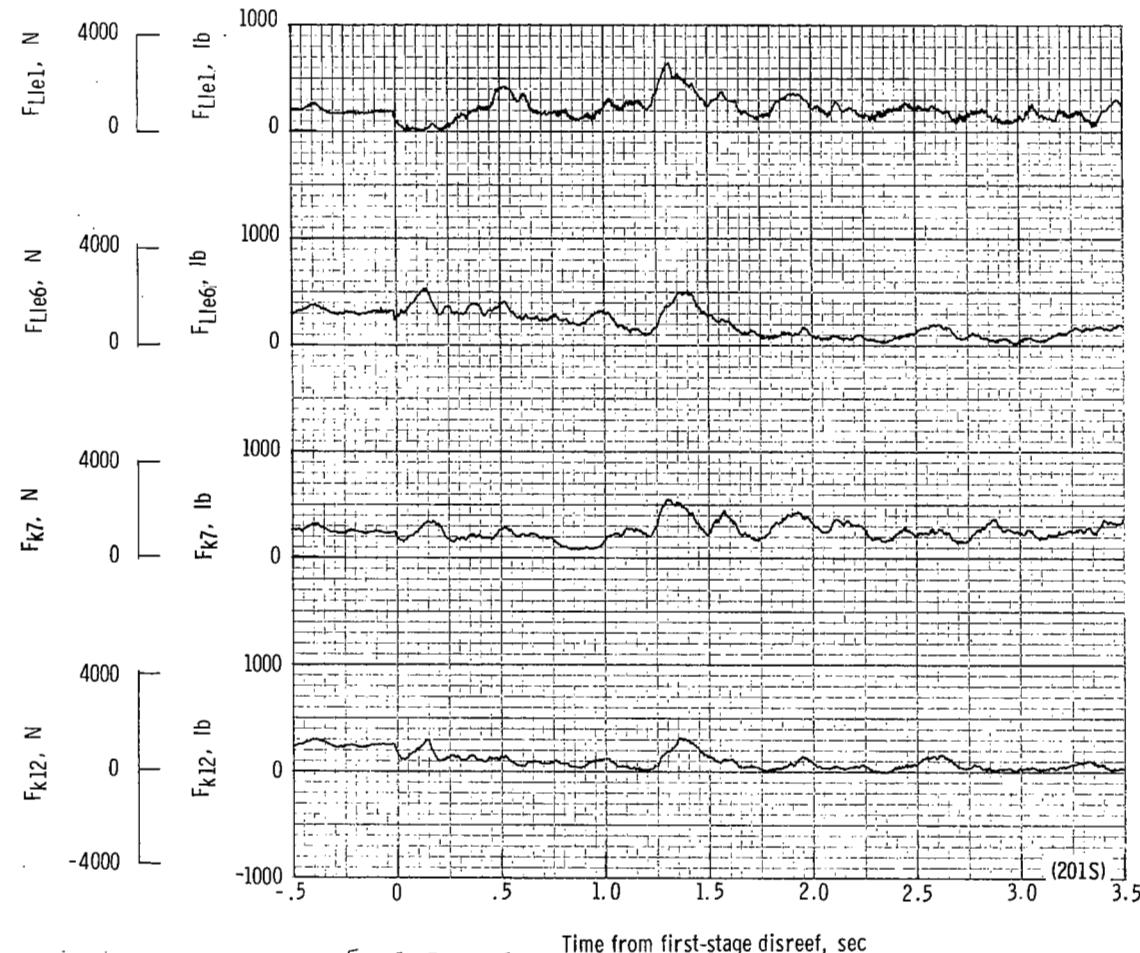
(d) Total force F_t plotted against time from line stretch. Time = 0 second corresponds to 28.08 seconds after launch.

Figure 40.- Continued.



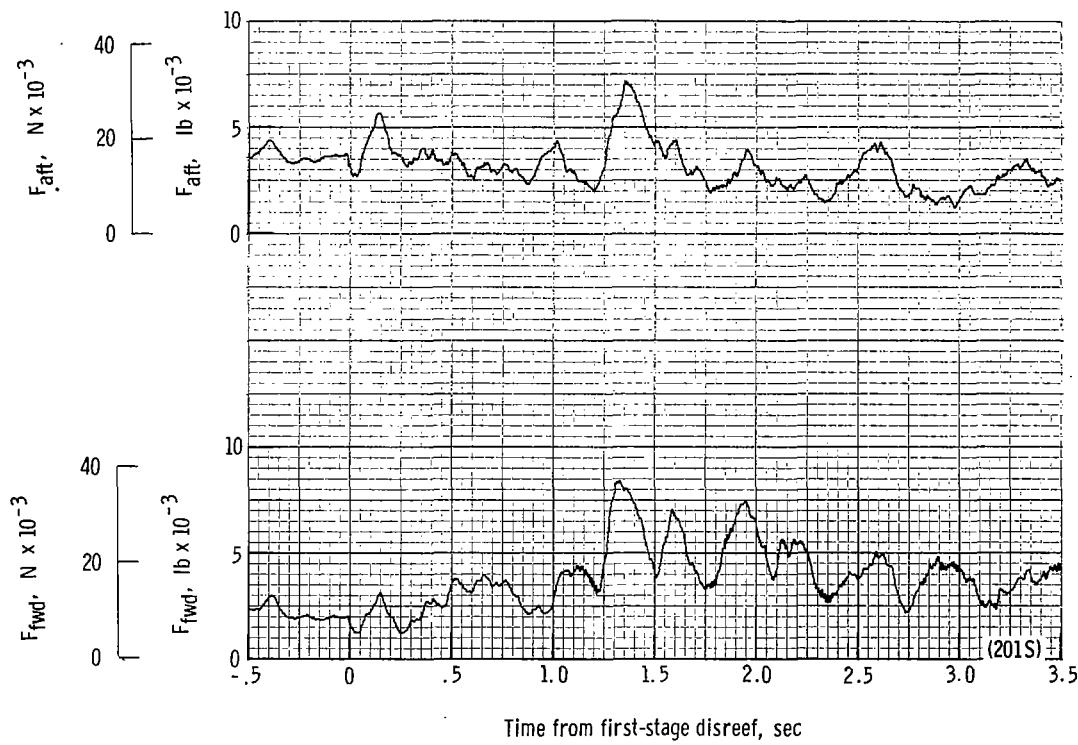
(e) Total force coefficient $C_{F,t}$ and dynamic pressure q plotted against time from line stretch. Time = 0 second corresponds to 28.08 seconds after launch.

Figure 40.- Continued.



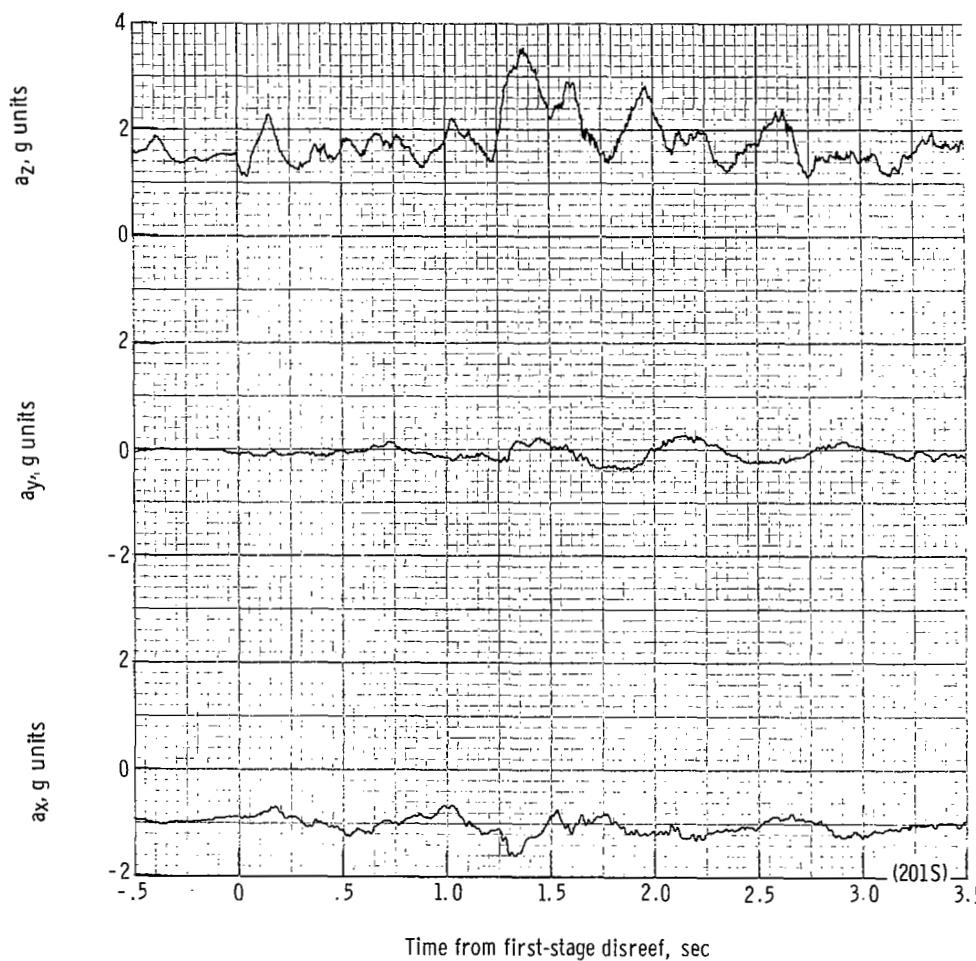
(f) Individual suspension-line loads F_{k12} , F_{k7} , F_{Lle6} , and F_{Lle1} plotted against time from first-stage disreef. Time = 0 second corresponds to 34.32 seconds after launch.

Figure 40.- Continued.



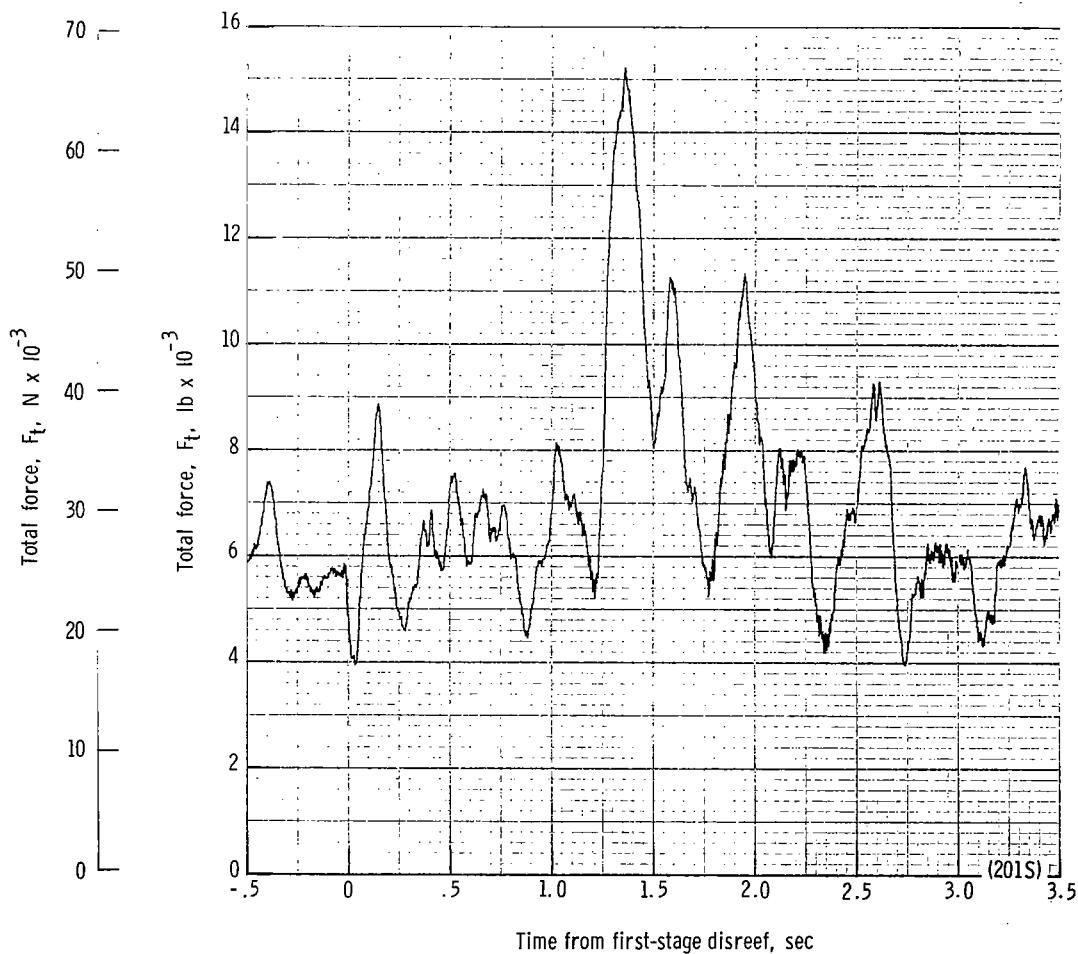
(g) Forward and aft riser loads plotted against time from first-stage disreef. Time = 0 second corresponds to 34.32 seconds after launch.

Figure 40.- Continued.



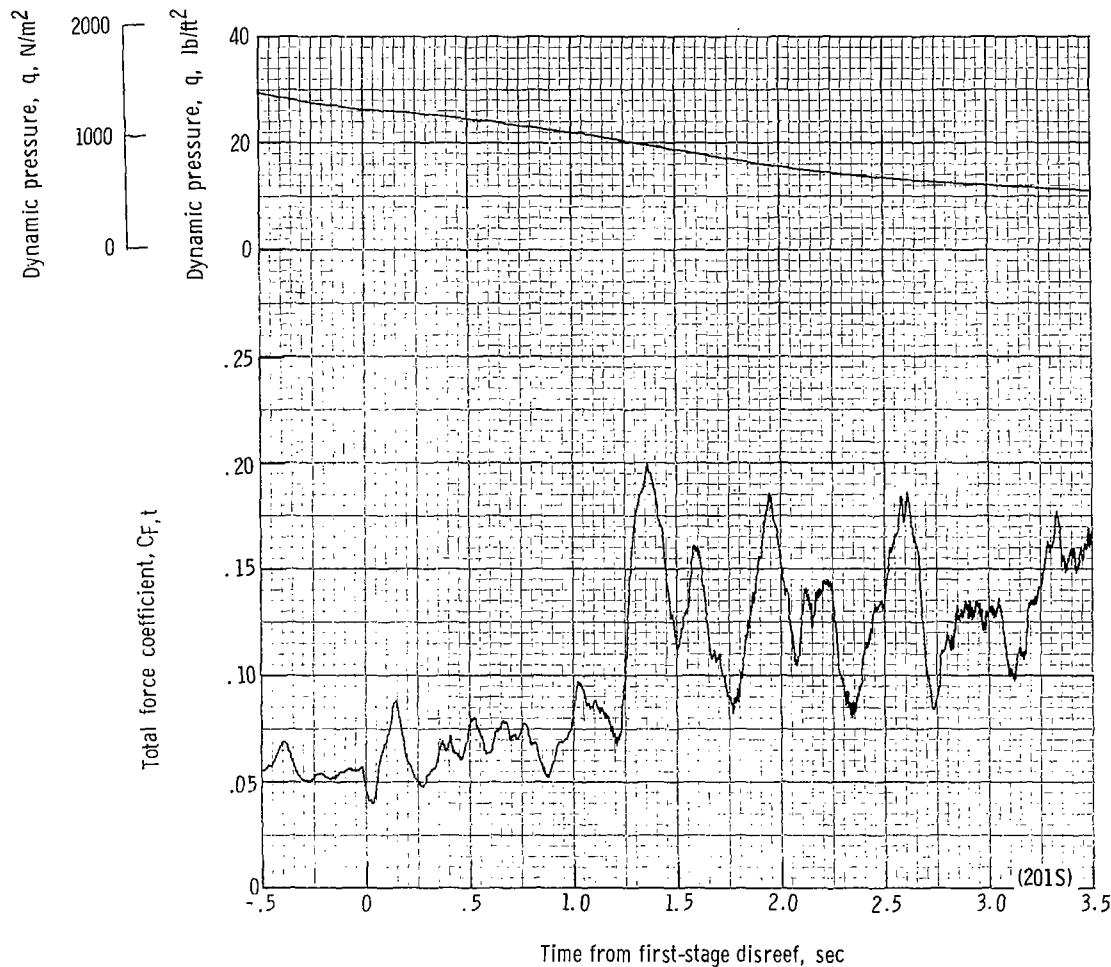
(h) Accelerations a_x , a_y , and a_z plotted against time from first-stage disreef. Time = 0 second corresponds to 34.32 seconds after launch.

Figure 40.- Continued.



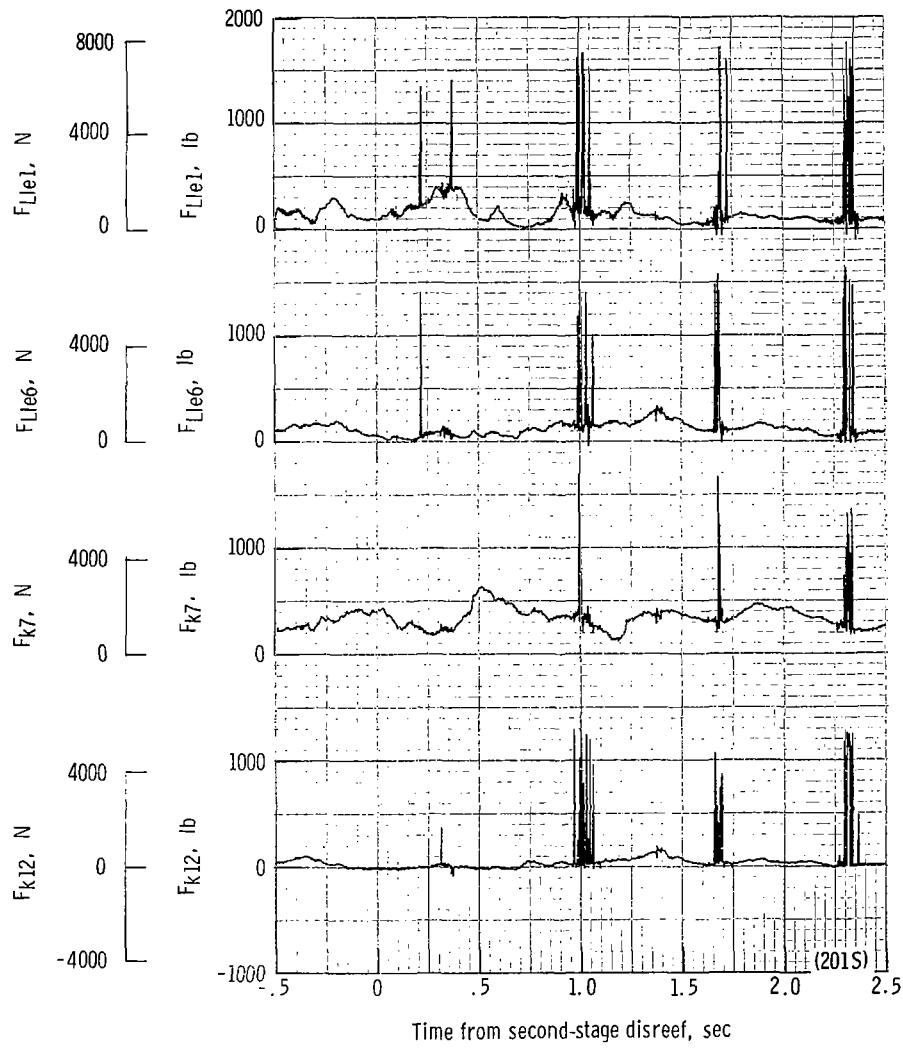
(i) Total force F_t plotted against time from first-stage disreef. Time = 0 second corresponds to 34.32 seconds after launch.

Figure 40.- Continued.



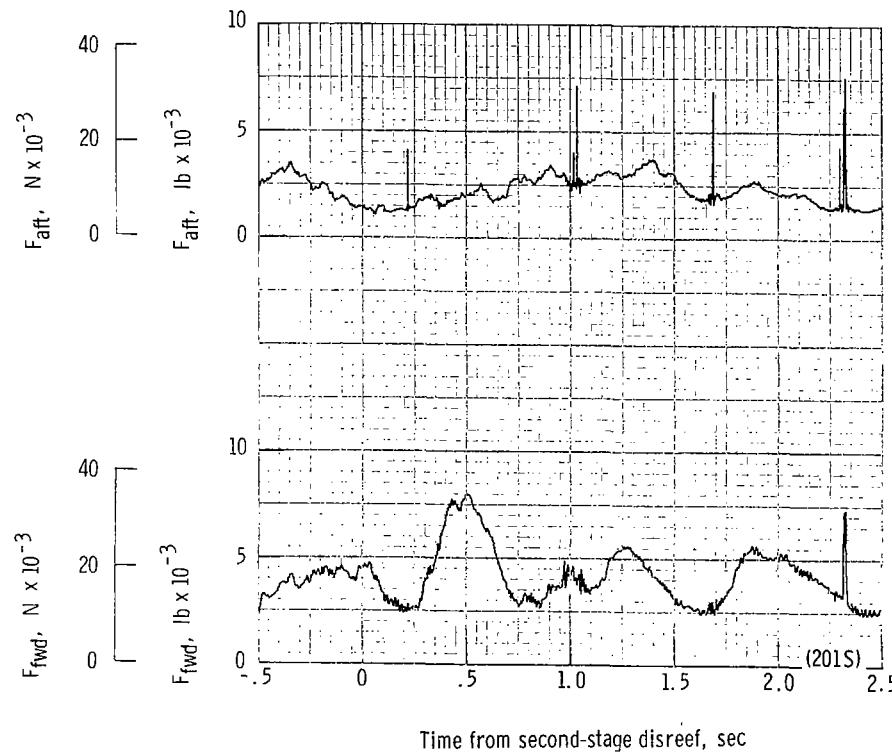
(j) Total force coefficient $C_{F,t}$ and dynamic pressure q plotted against time from first-stage disreef. Time = 0 second corresponds to 34.32 seconds after launch.

Figure 40.- Continued.



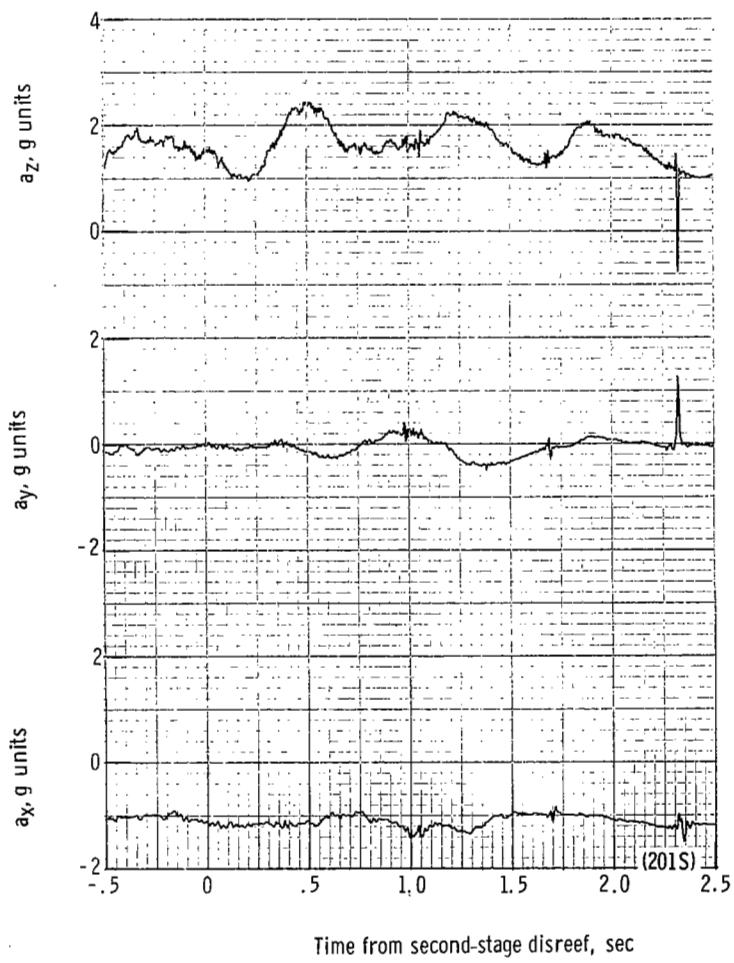
(k) Individual suspension-line loads F_{k12} , F_{k7} , F_{Lle6} , and F_{Lle1} plotted against time from second-stage disreef. Time = 0 second corresponds to 37.99 seconds after launch.

Figure 40.- Continued.



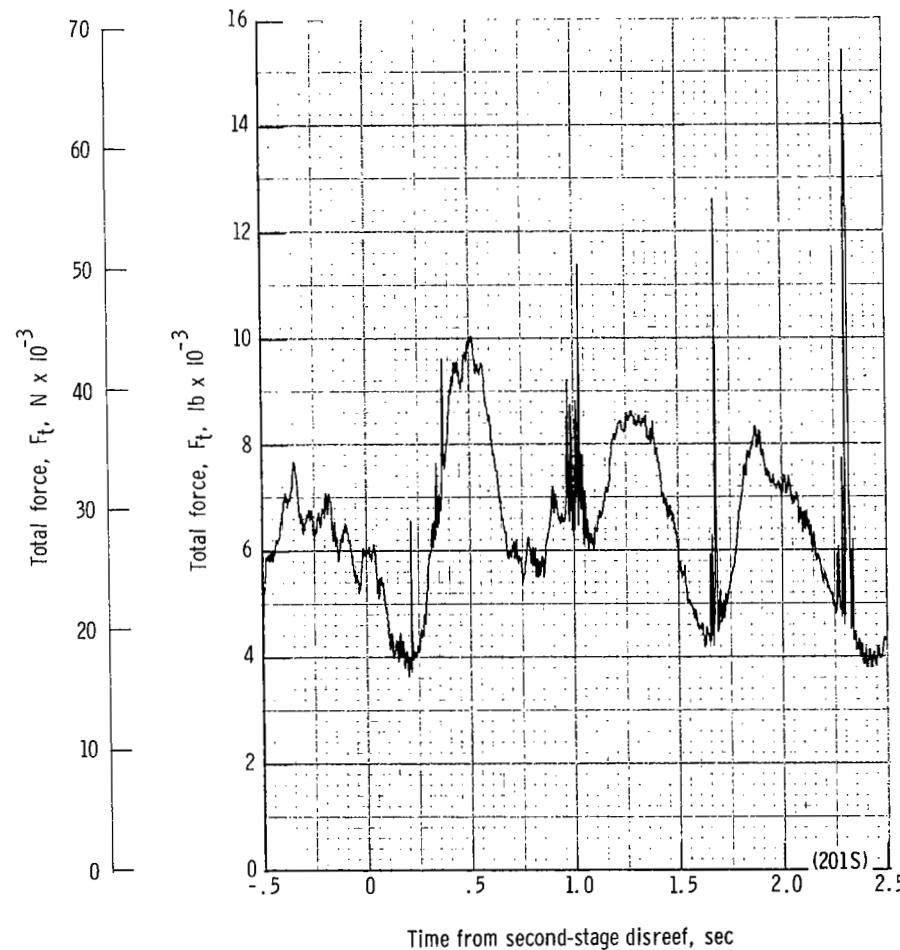
(II) Forward and aft riser loads plotted against time from second-stage disreef. Time = 0 second corresponds to 37.99 seconds after launch.

Figure 40.- Continued.



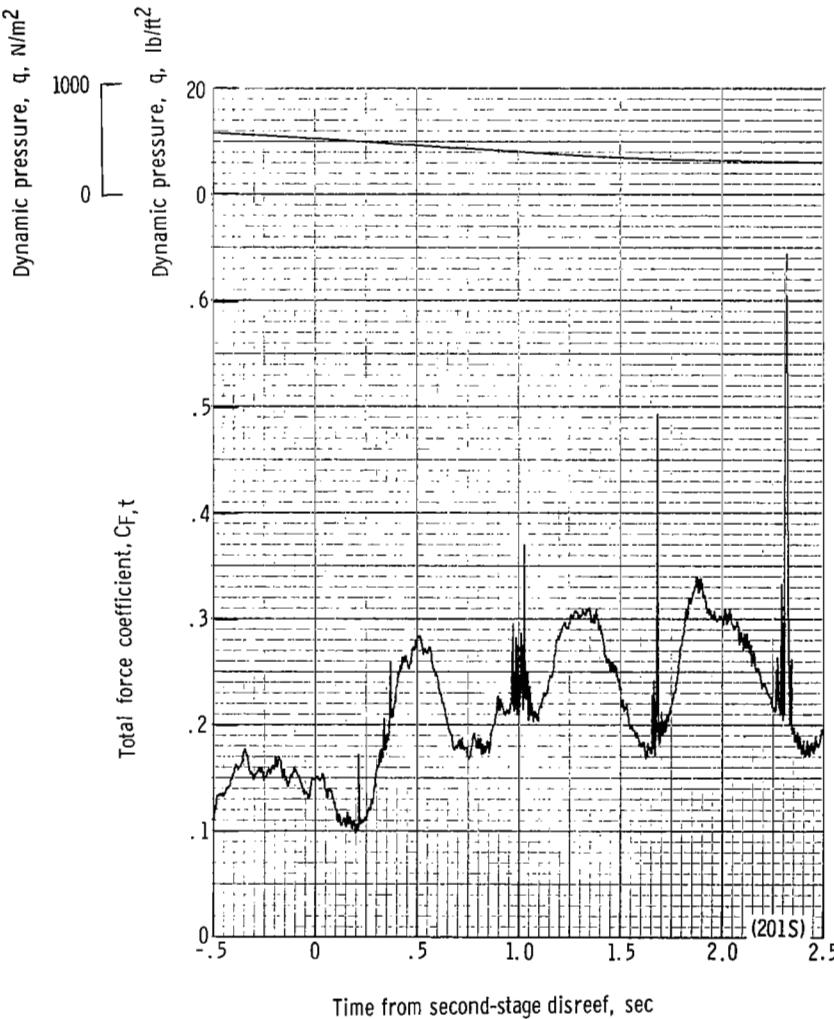
(m) Accelerations a_x , a_y , and a_z plotted against time from second-stage disreef. Time = 0 second corresponds to 37.99 seconds after launch.

Figure 40.- Continued.



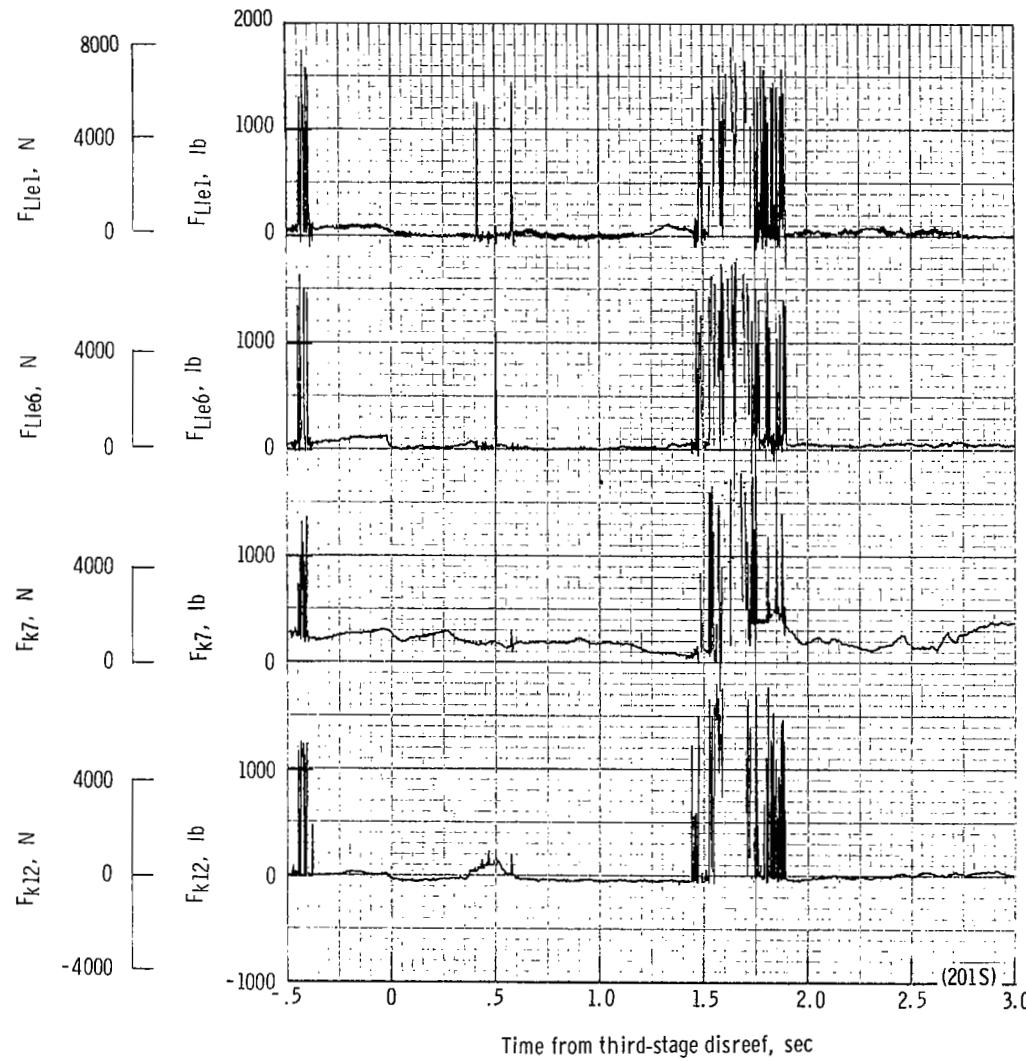
(n) Total force F_t plotted against time from second-stage disreef. Time = 0 second corresponds to 37.99 seconds after launch.

Figure 40.- Continued.



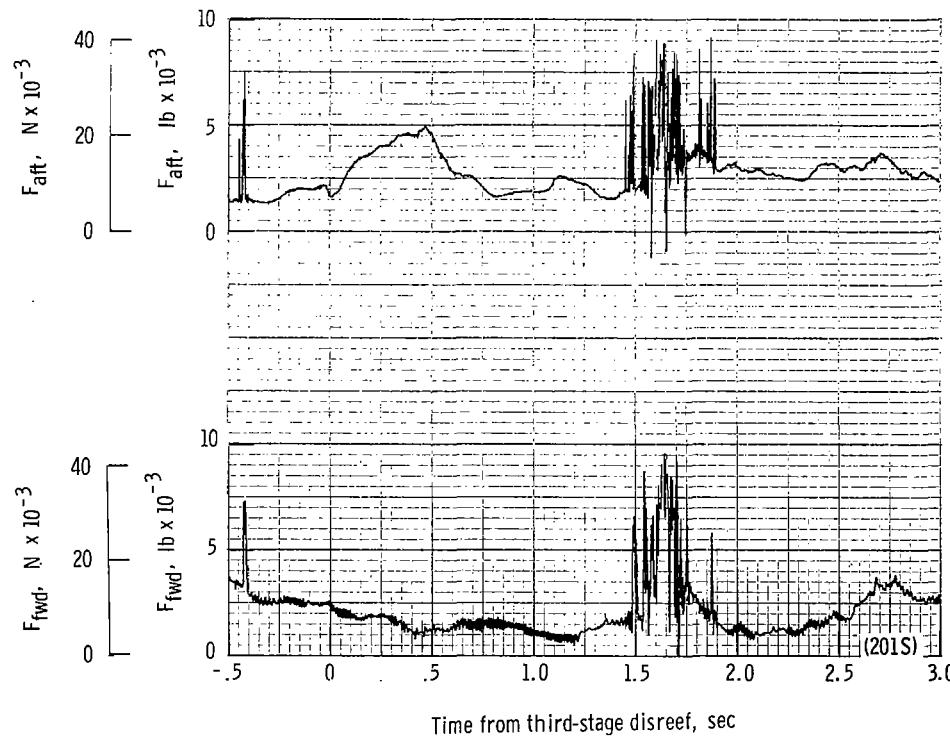
(o) Total force coefficient $C_{F,t}$ and dynamic pressure q plotted against time from second-stage disreef. Time = 0 second corresponds to 37.99 seconds after launch.

Figure 40.- Continued.



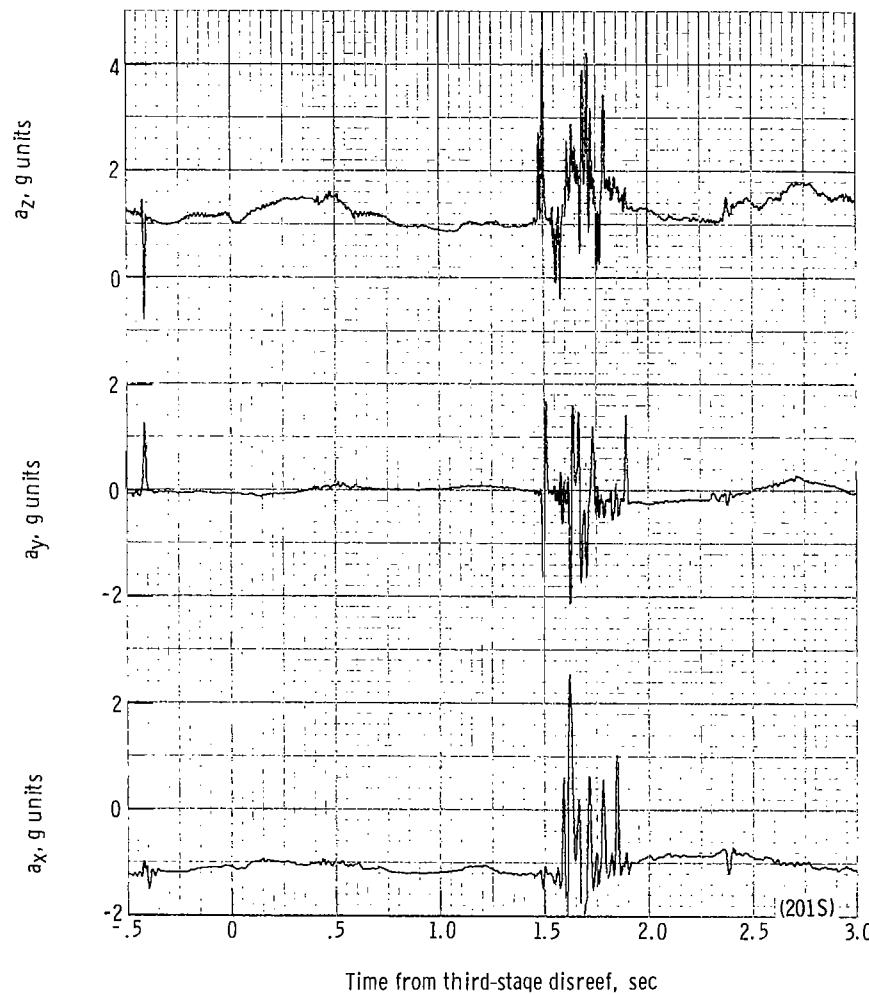
(p) Individual suspension-line loads F_{k12} , F_{k7} , F_{Lle6} , and F_{Lle1} plotted against time from third-stage disreef. Time = 0 second corresponds to 40.74 seconds after launch.

Figure 40.- Continued.



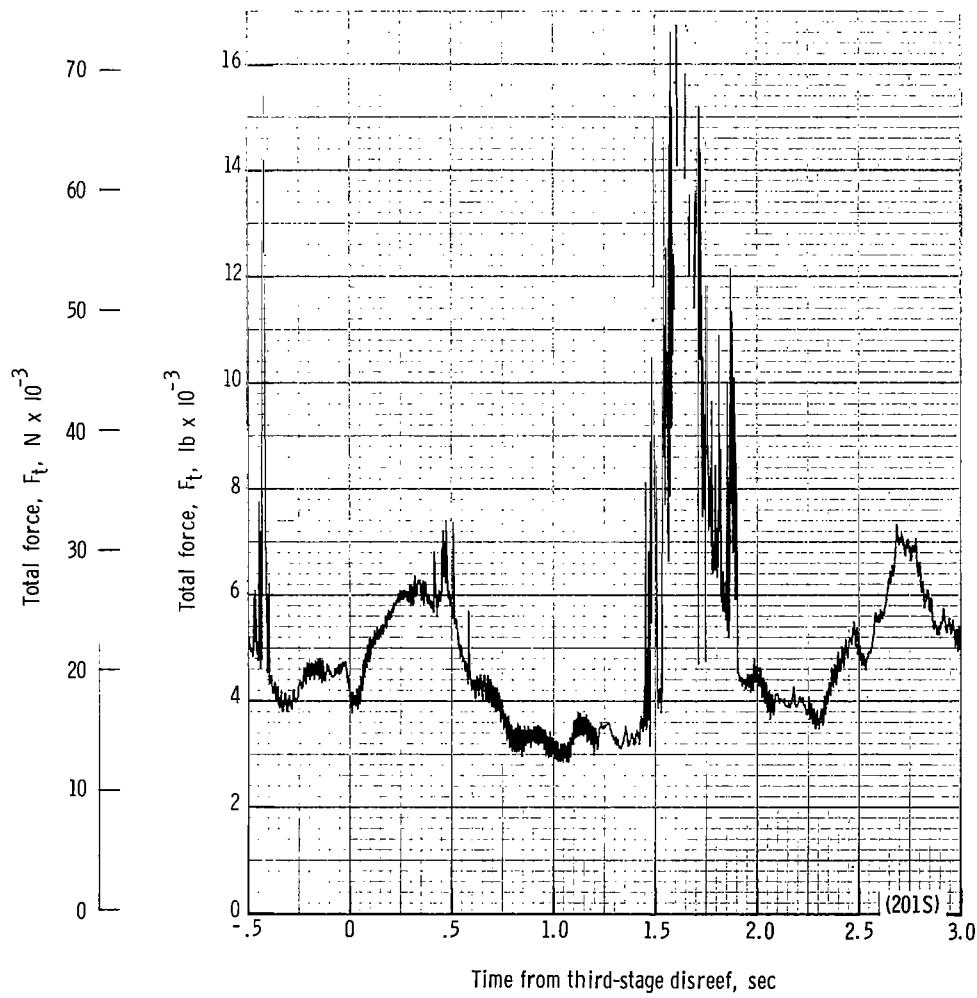
(q) Forward and aft riser loads plotted against time from third-stage disreef. Time = 0 second corresponds to 40.74 seconds after launch.

Figure 40.- Continued.



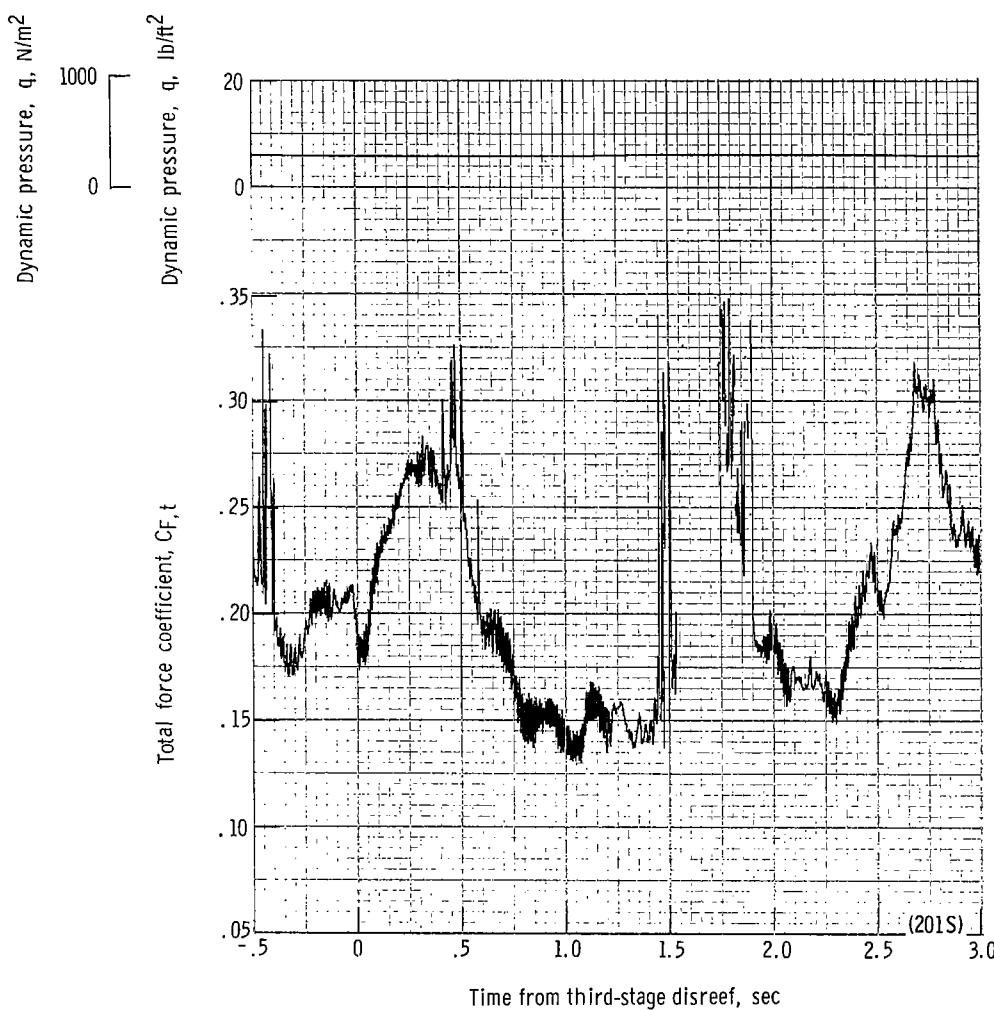
(r) Accelerations a_x , a_y , and a_z plotted against time from third-stage disreef. Time = 0 second corresponds to 40.74 seconds after launch.

Figure 40.- Continued.



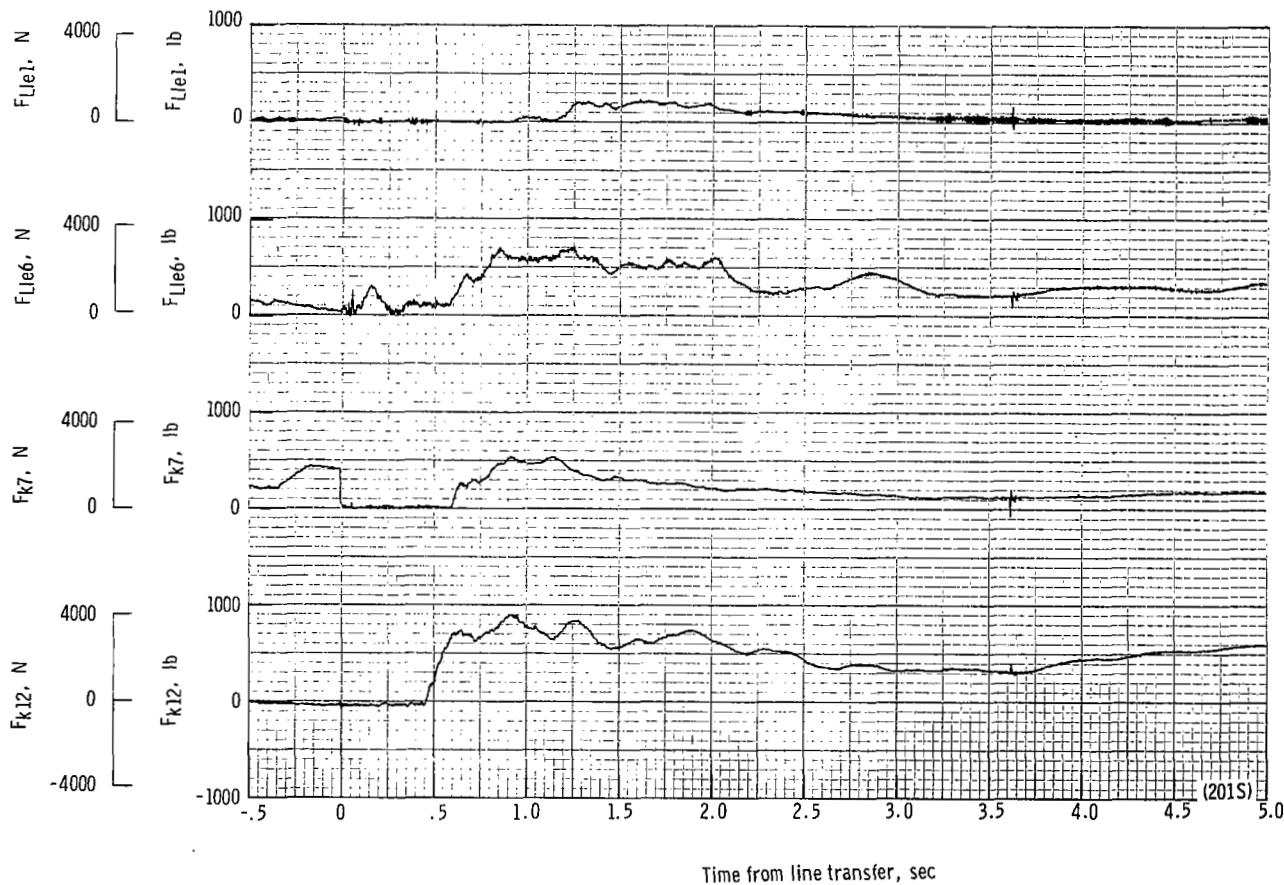
(s) Total force F_t plotted against time from third-stage disreef. Time = 0 second corresponds to 40.74 seconds after launch.

Figure 40.- Continued.



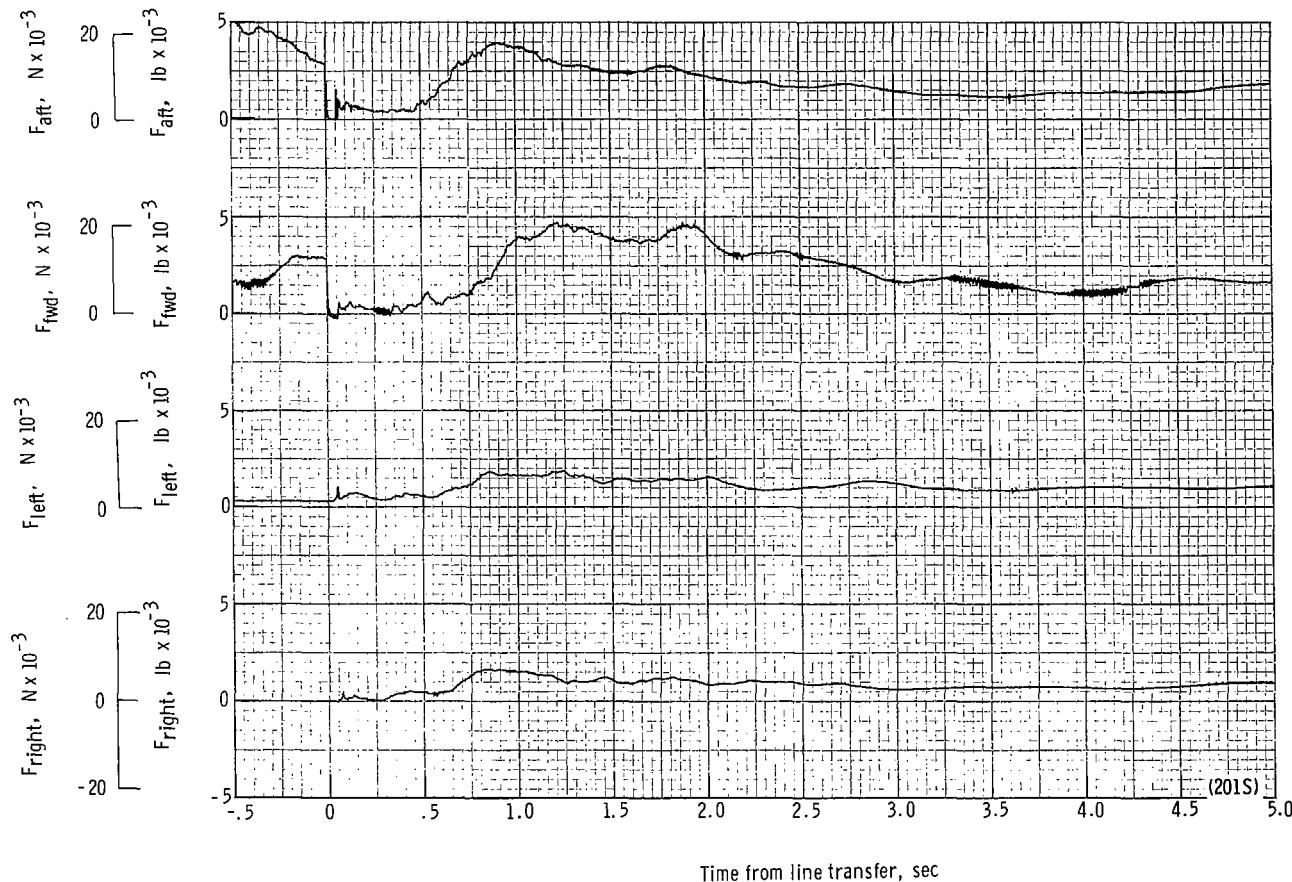
(t) Total force coefficient $C_{F,t}$ and dynamic pressure q plotted against time from third-stage disreef. Time = 0 second corresponds to 40.74 seconds after launch.

Figure 40.- Continued.



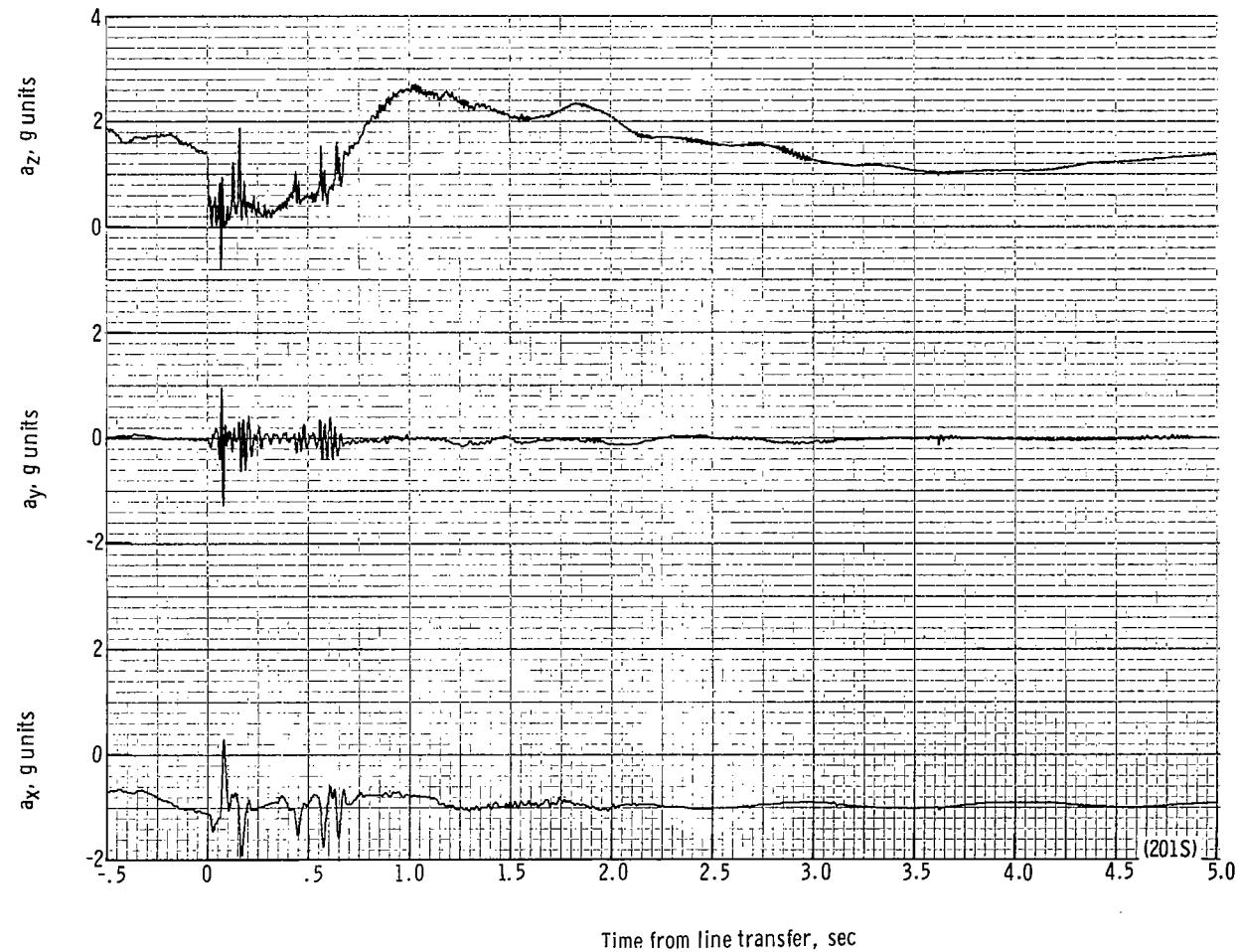
(u) Individual suspension-line loads F_{k12} , F_{k7} , F_{Lle6} , and F_{Lle1} plotted against time from line transfer. Time = 0 second corresponds to 44.87 seconds after launch.

Figure 40.- Continued.



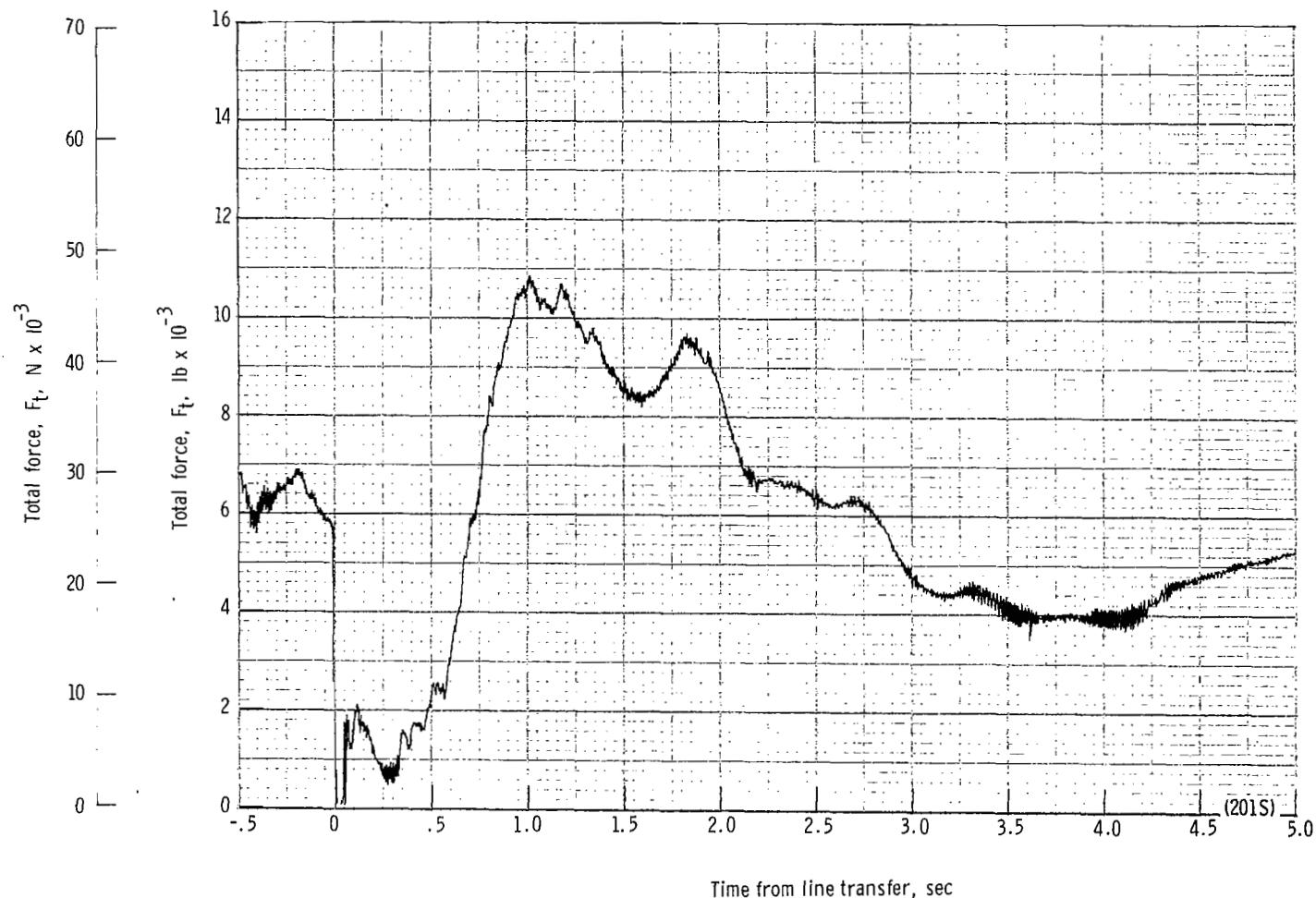
(v) Right, left, forward, and aft riser loads plotted against time from line transfer. Time = 0 second corresponds to 44.87 seconds after launch.

Figure 40.- Continued.



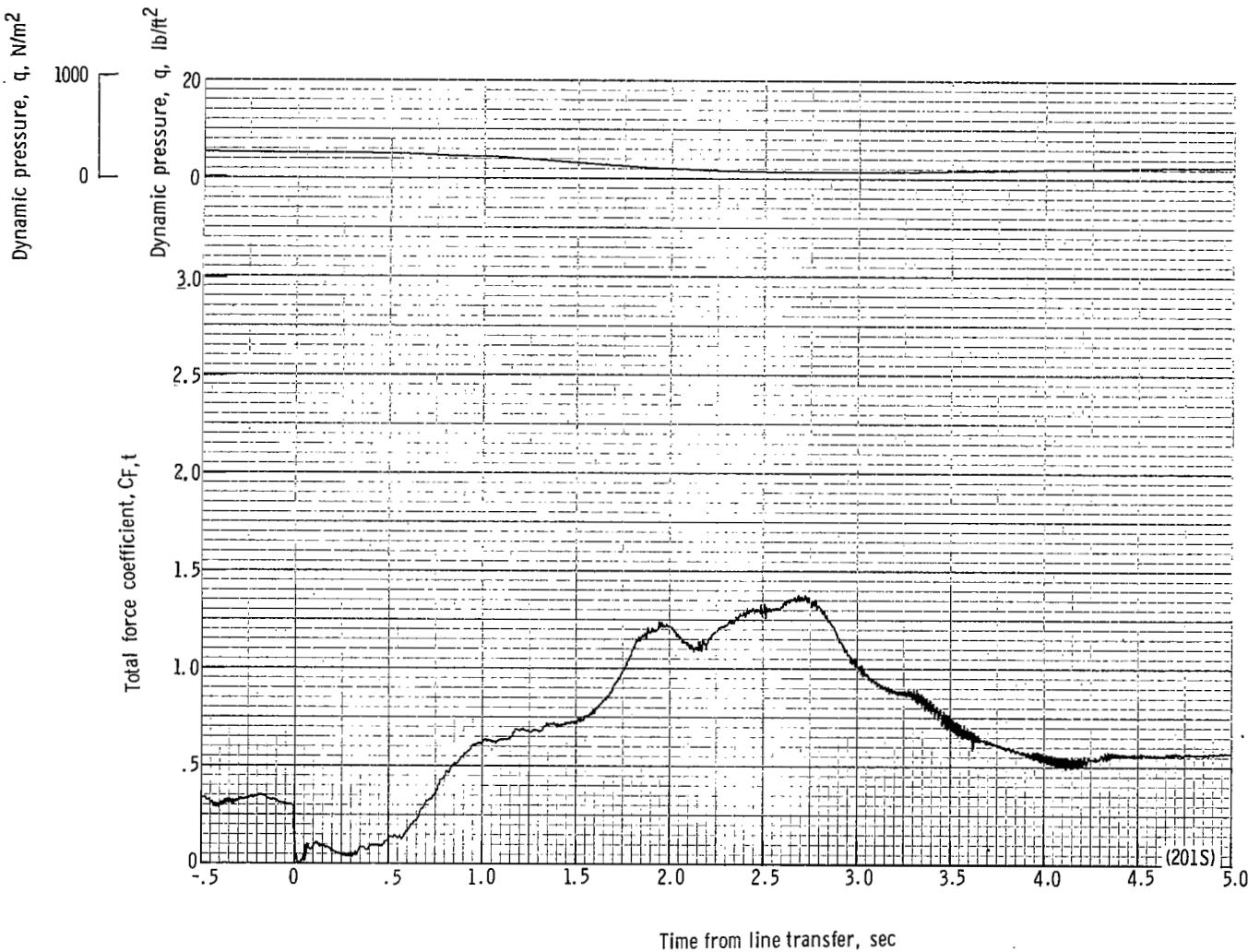
(w) Accelerations a_x , a_y , and a_z plotted against time from line transfer. Time = 0 second corresponds to 44.87 seconds after launch.

Figure 40.- Continued.



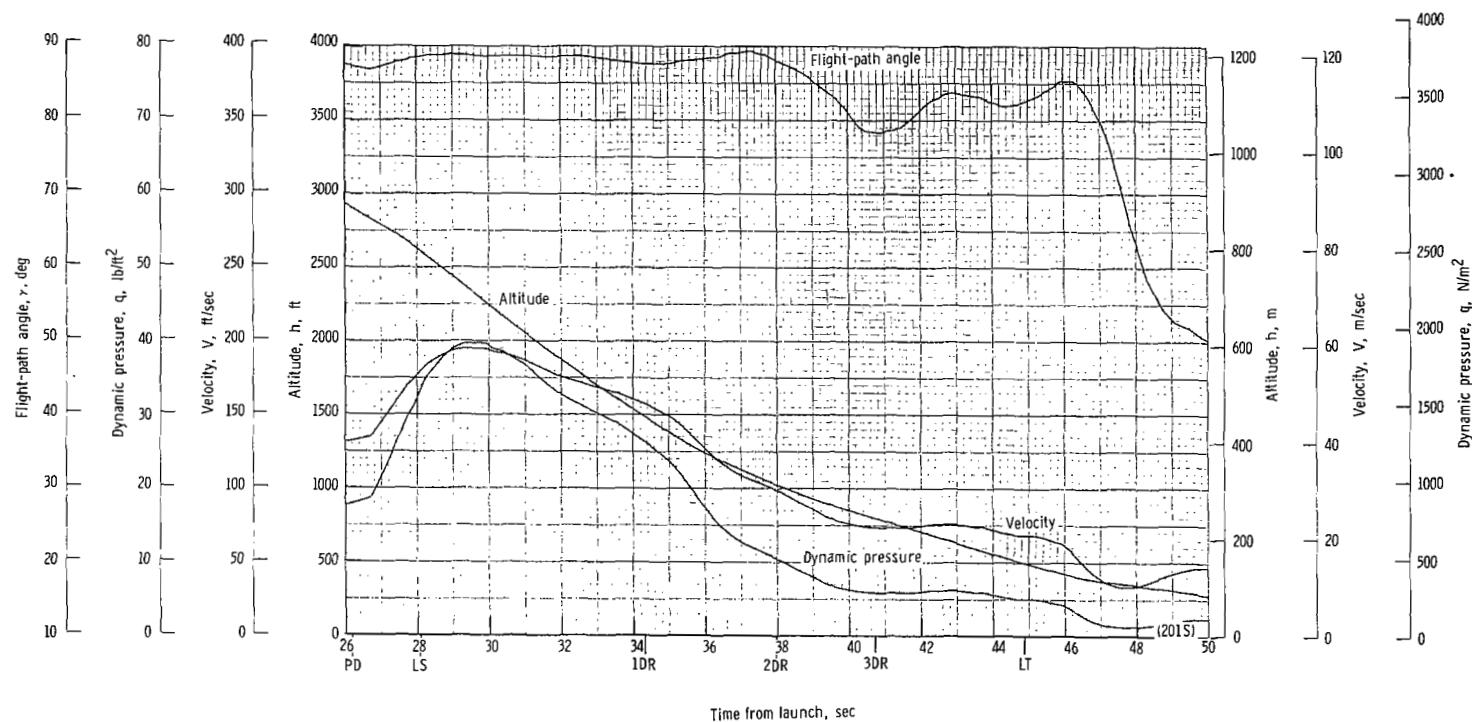
(x) Total force F_t plotted against time from line transfer. Time = 0 second corresponds to 44.87 seconds after launch.

Figure 40.- Continued.



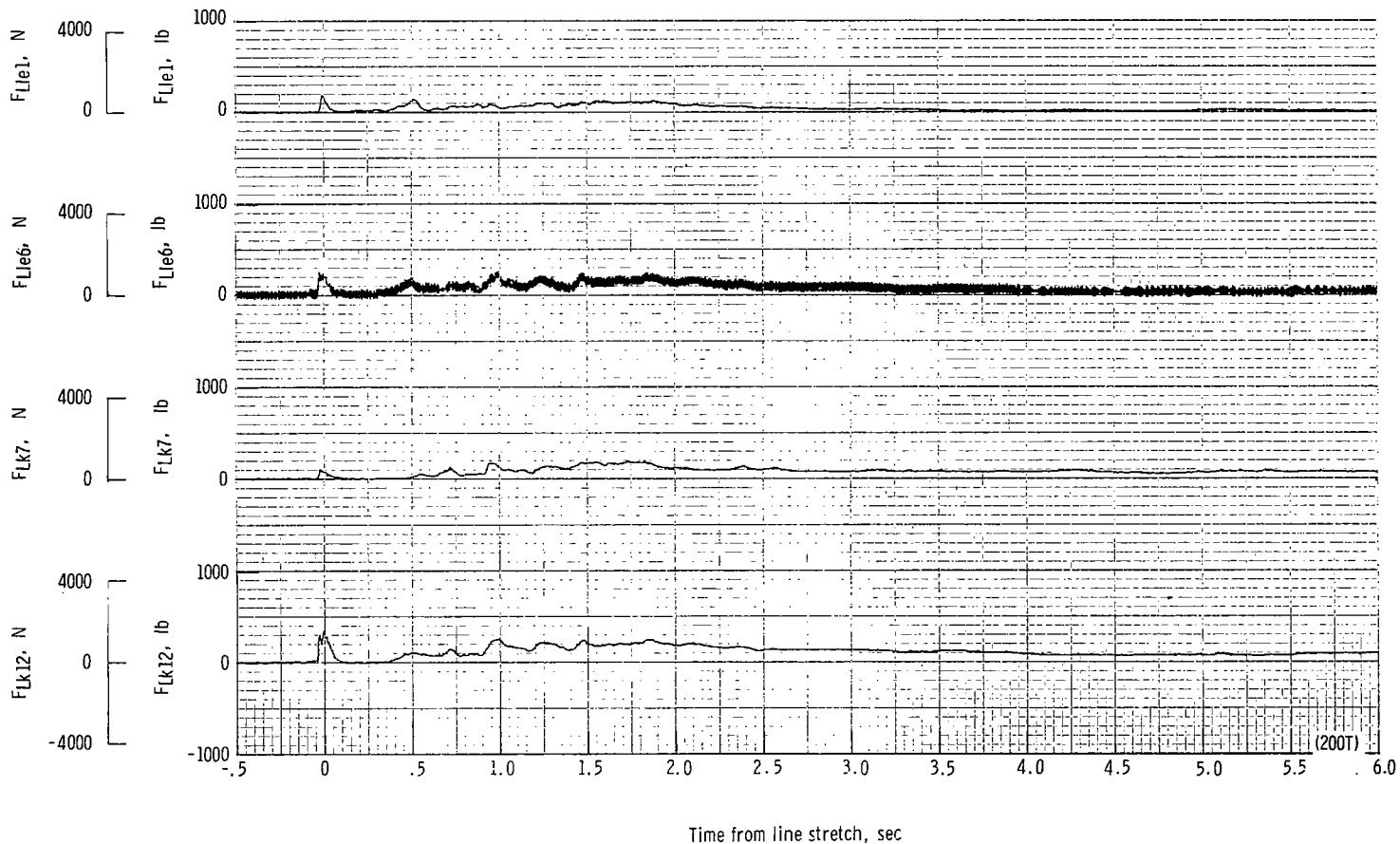
(y) Total force coefficient $C_{F,t}$ and dynamic pressure q plotted against time from line transfer. Time = 0 second corresponds to 44.87 seconds after launch.

Figure 40.- Continued.



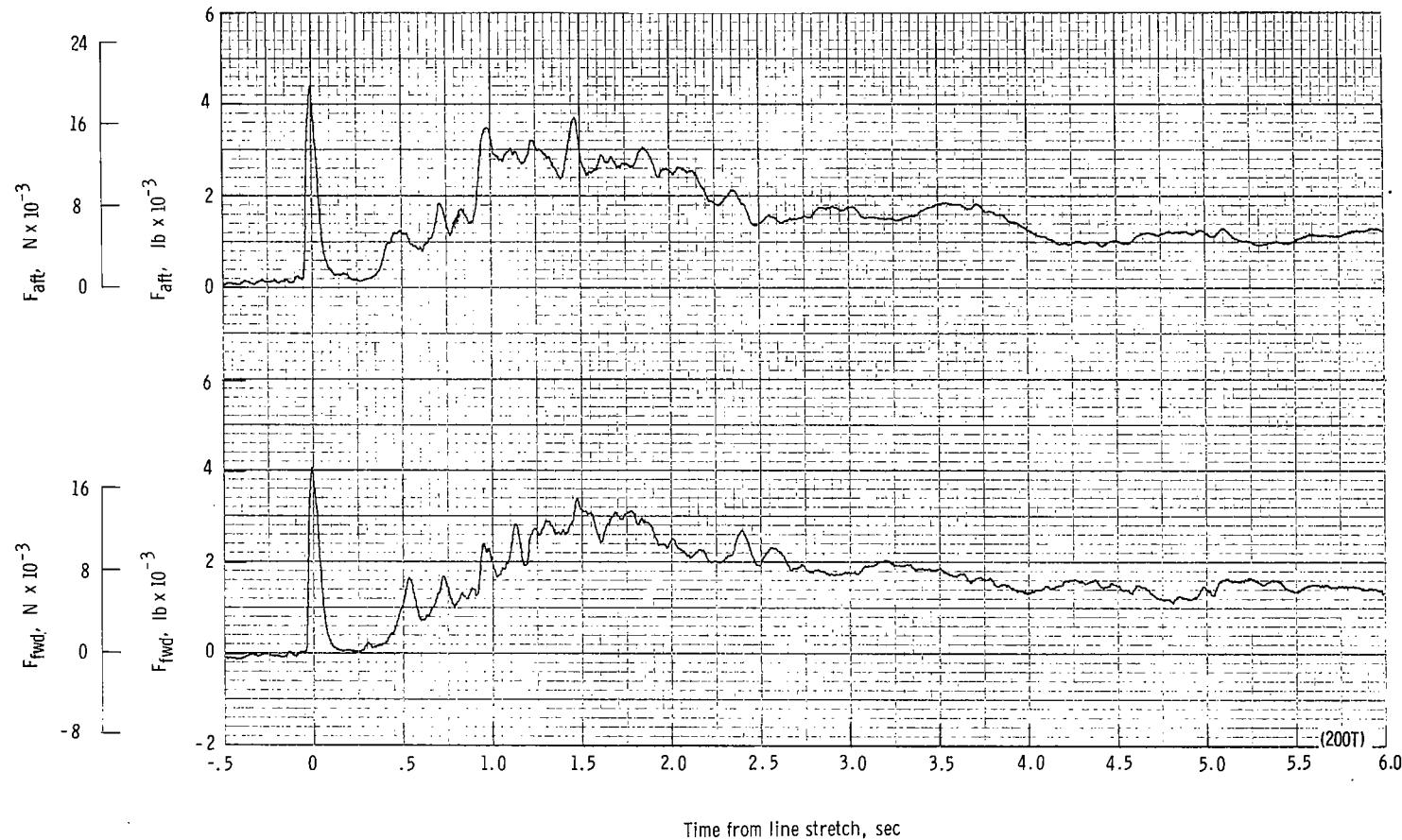
(z) Flight-path angle γ , dynamic pressure q , velocity V , and altitude h plotted against time from launch.

Figure 40.- Concluded.



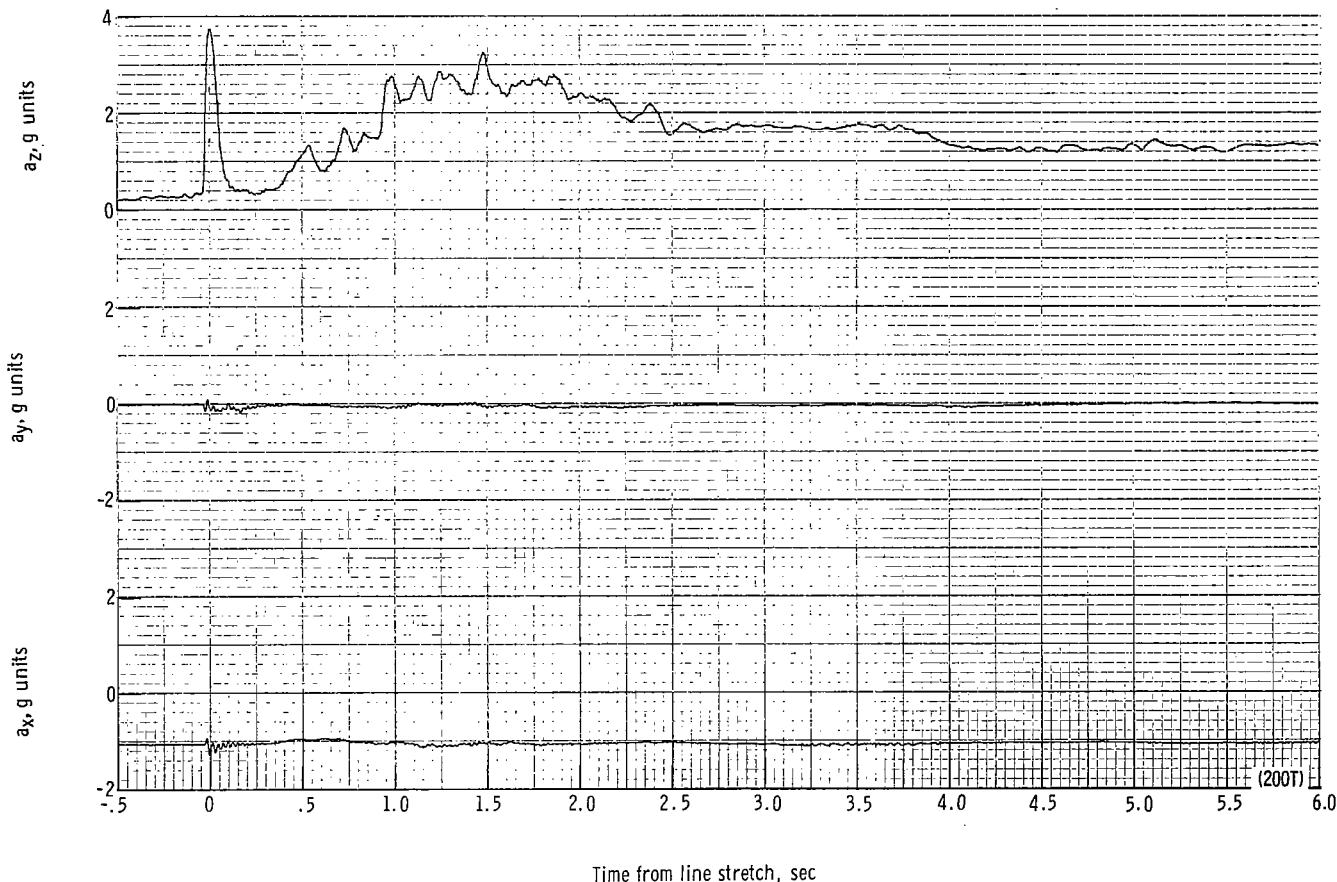
(a) Individual suspension-line loads F_{Lk12} , F_{Lk7} , F_{Lle6} , and F_{Lle1} plotted against time from line stretch. Time = 0 second corresponds to 25.61 seconds after launch.

Figure 41.- Time history of twin-keel parawing deployment data for test 200T. $W_D = 12\ 806\ N$ (2879 lb); $W_p = 11\ 214\ N$ (2521 lb); $q_{PD} = 814.0\ N/m^2$ (17.0 lb/ft²); $h_{PD} = 1524\ m$ (5000 ft); $l_r/l_k = 0.140$, reefing version A.



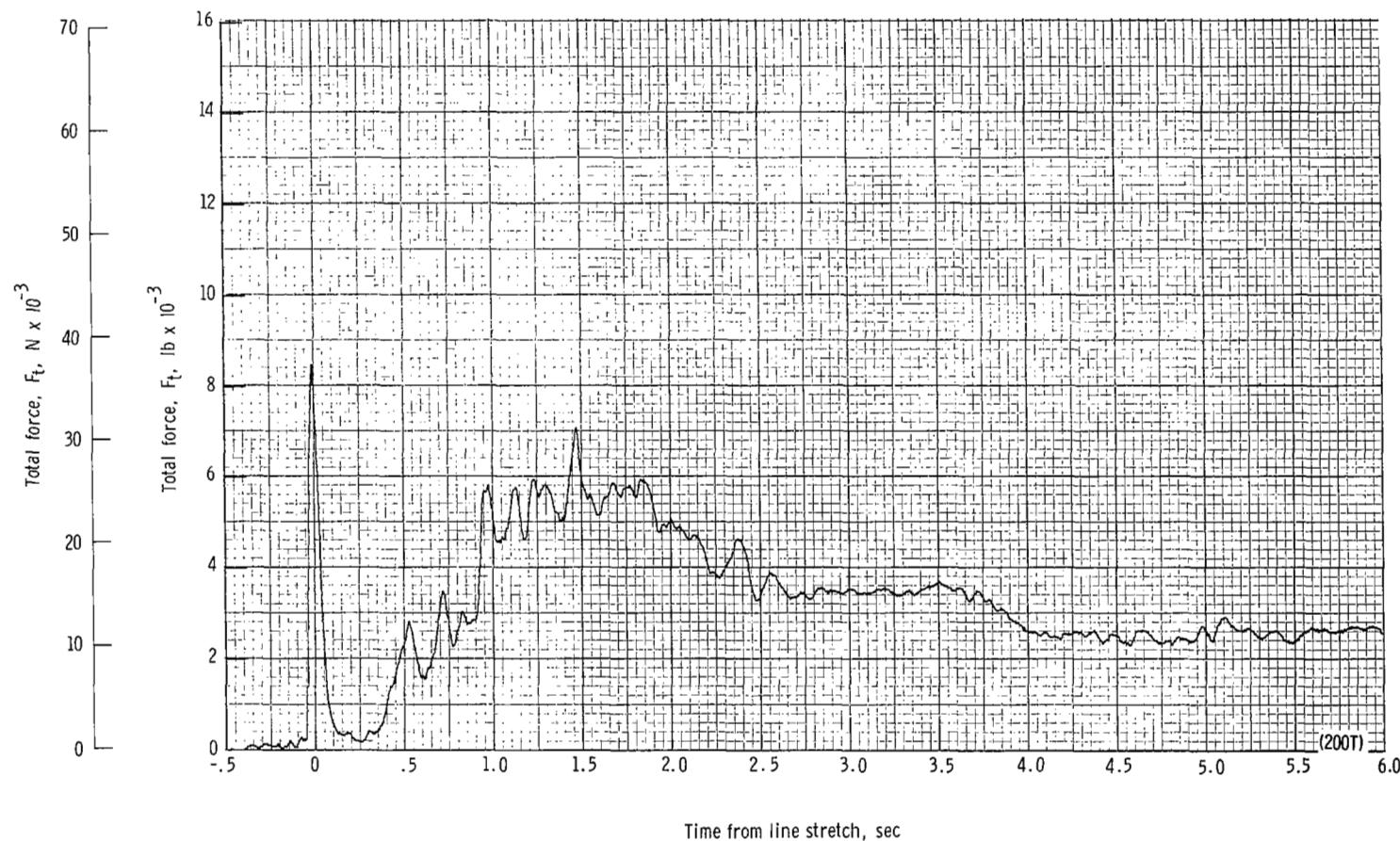
(b) Forward and aft riser loads plotted against time from line stretch. Time = 0 second corresponds to 25.61 seconds after launch.

Figure 41.- Continued.



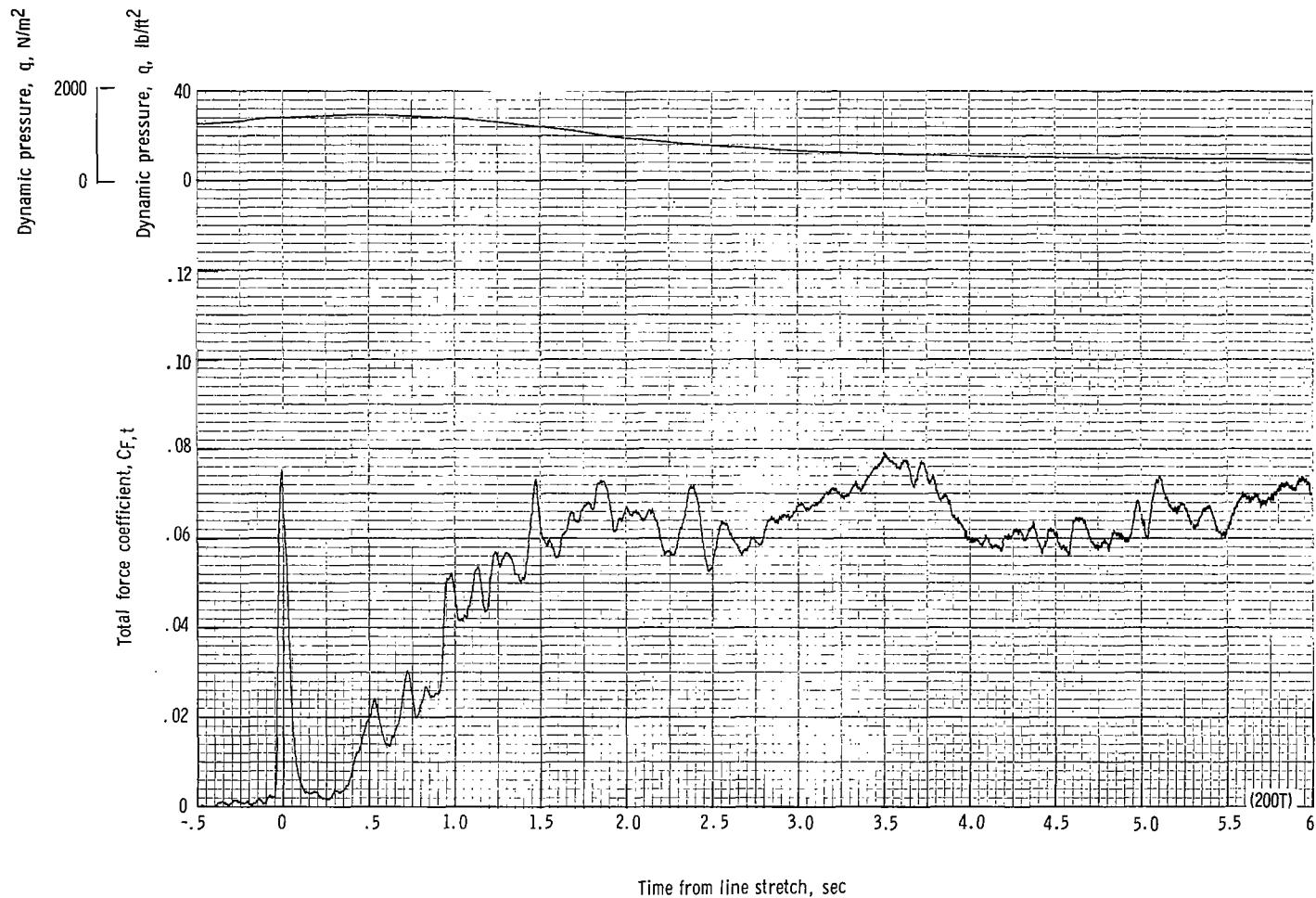
(c) Accelerations a_x , a_y , and a_z plotted against time from line stretch. Time = 0 second corresponds to 25.61 seconds after launch.

Figure 41.- Continued.



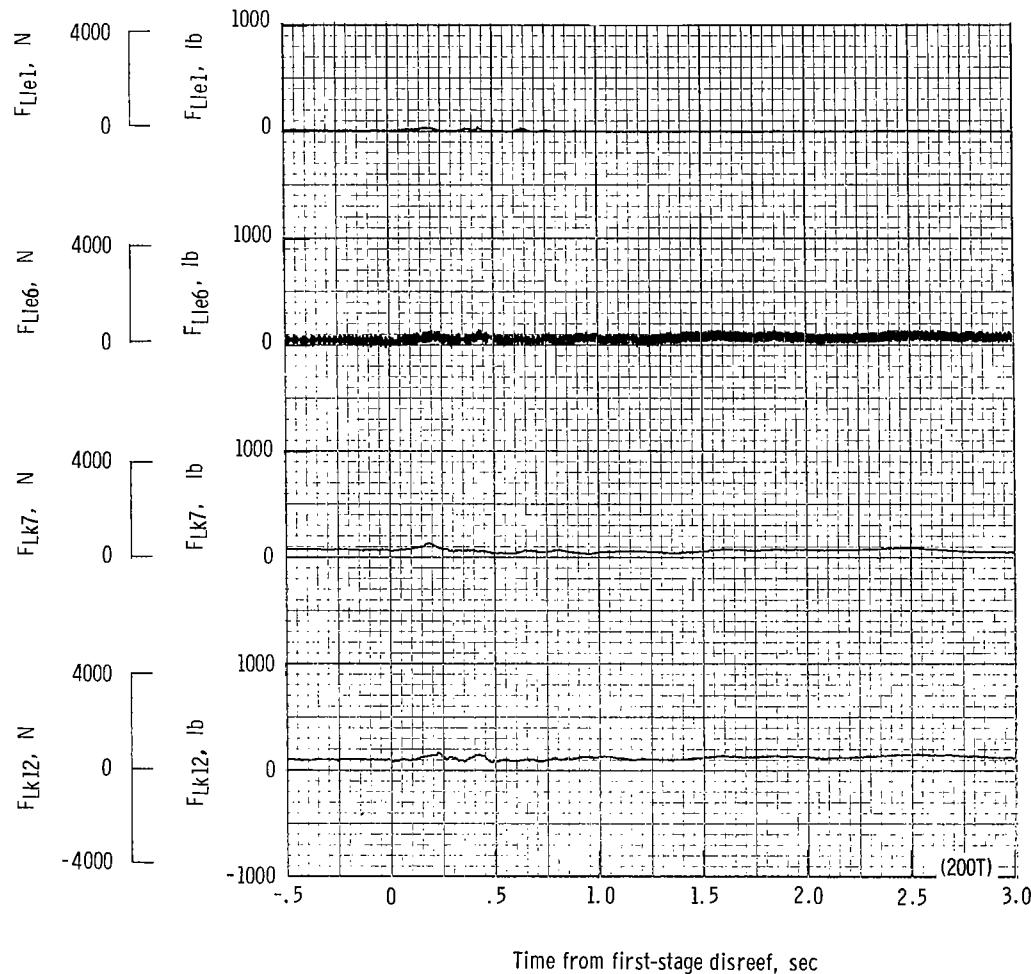
(d) Total force F_t plotted against time from line stretch. Time = 0 second corresponds to 25.61 seconds after launch.

Figure 41.- Continued.



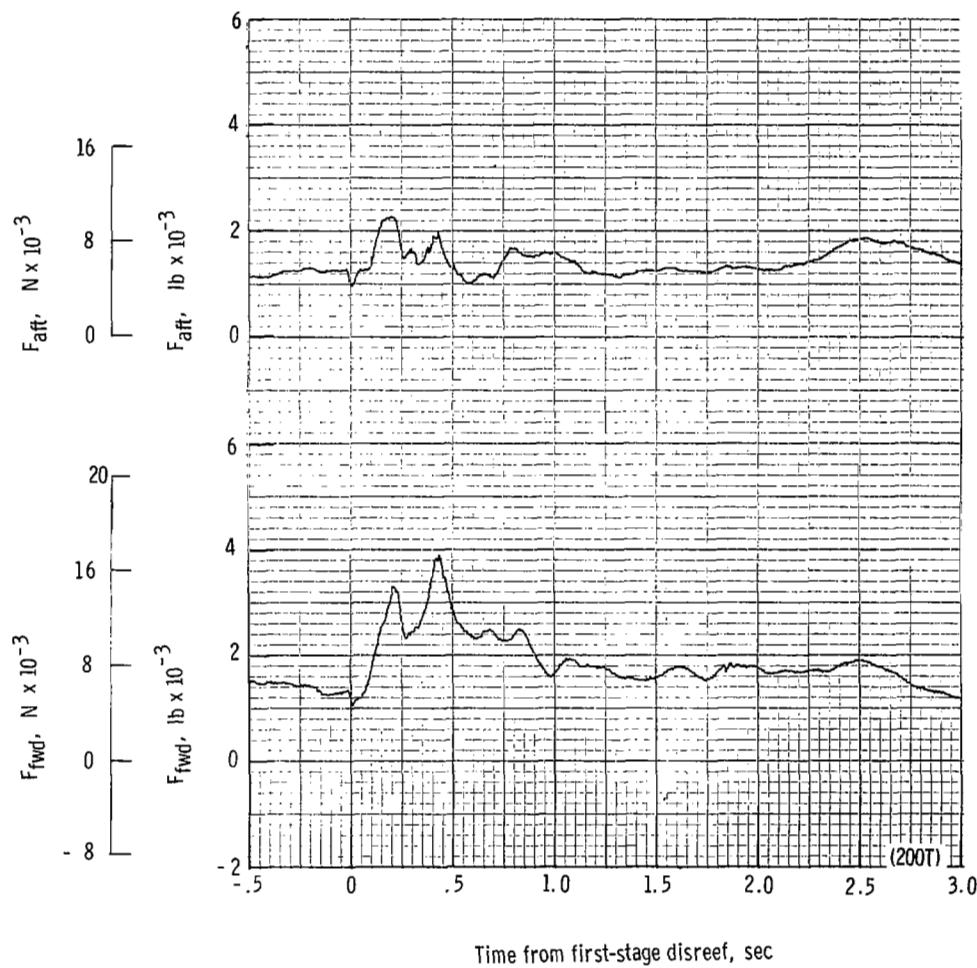
(e) Total force coefficient $C_{F,t}$ and dynamic pressure q plotted against time from line stretch. Time = 0 second corresponds to 25.61 seconds after launch.

Figure 41.- Continued.



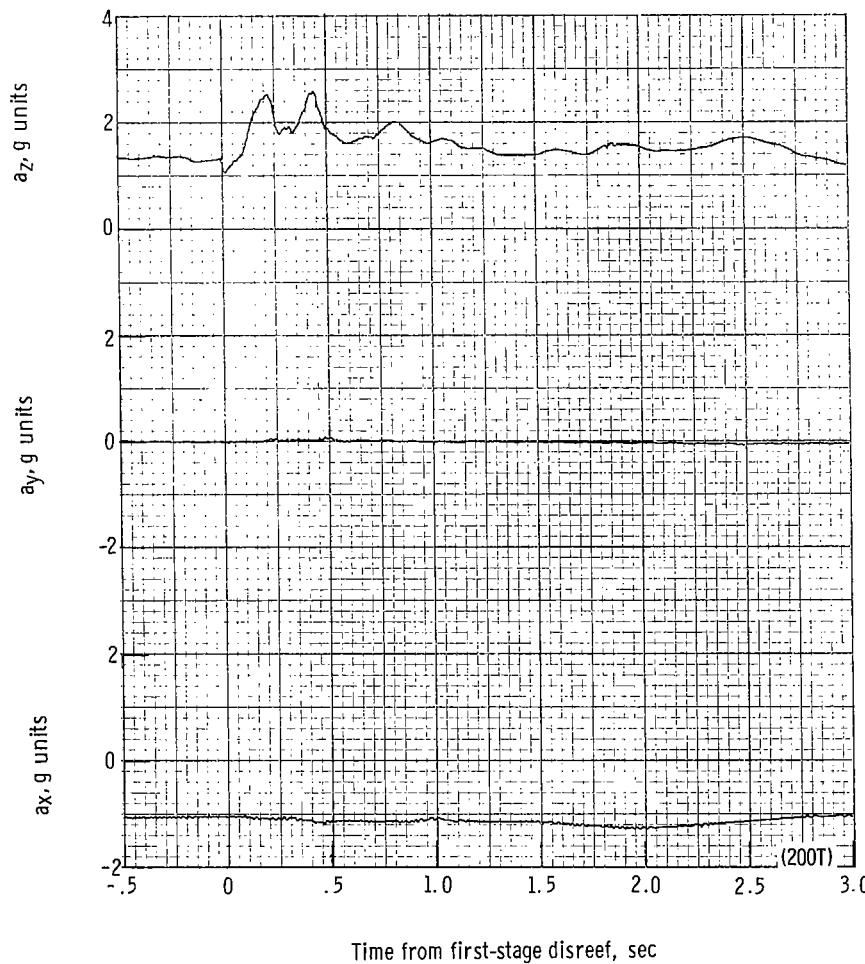
(f) Individual suspension-line loads F_{Lk12} , F_{Lk7} , F_{Lle6} , and F_{Lle1} plotted against time from first-stage disreef. Time = 0 second corresponds to 31.76 seconds after launch.

Figure 41.- Continued.



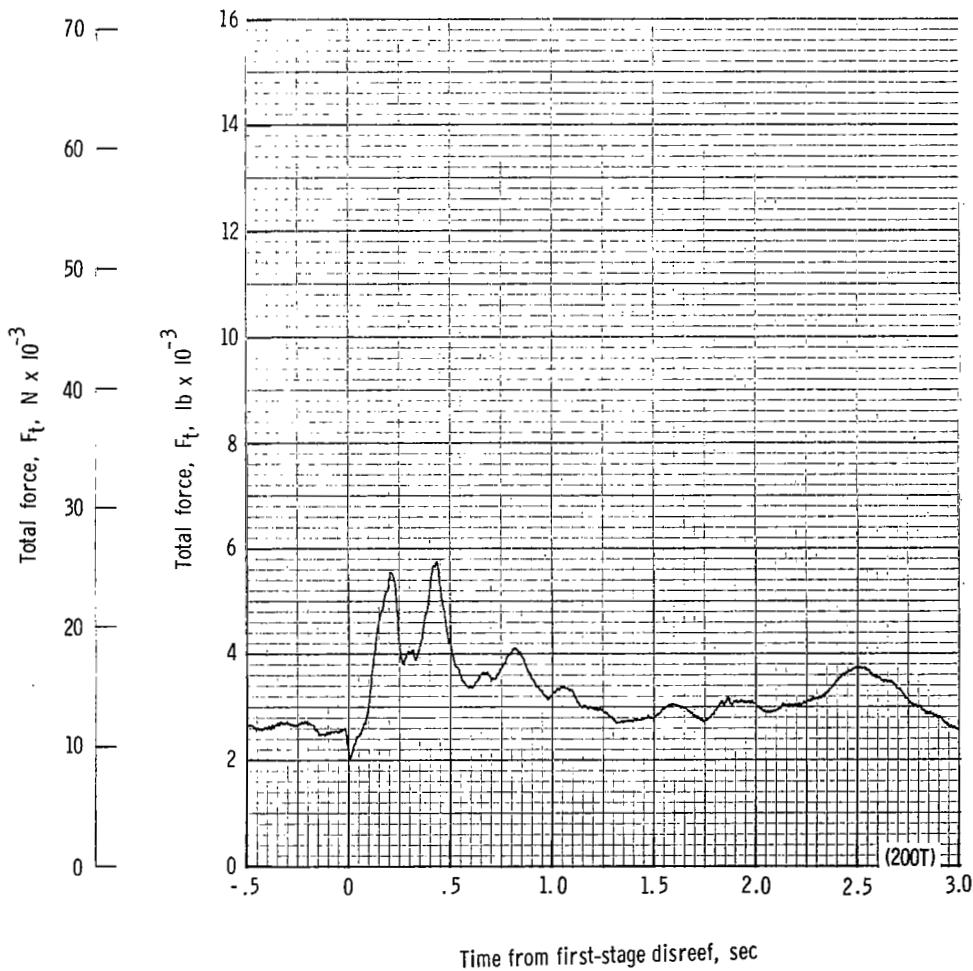
(g) Forward and aft riser loads plotted against time from first-stage disreef. Time = 0 second corresponds to 31.76 seconds after launch.

Figure 41.- Continued.



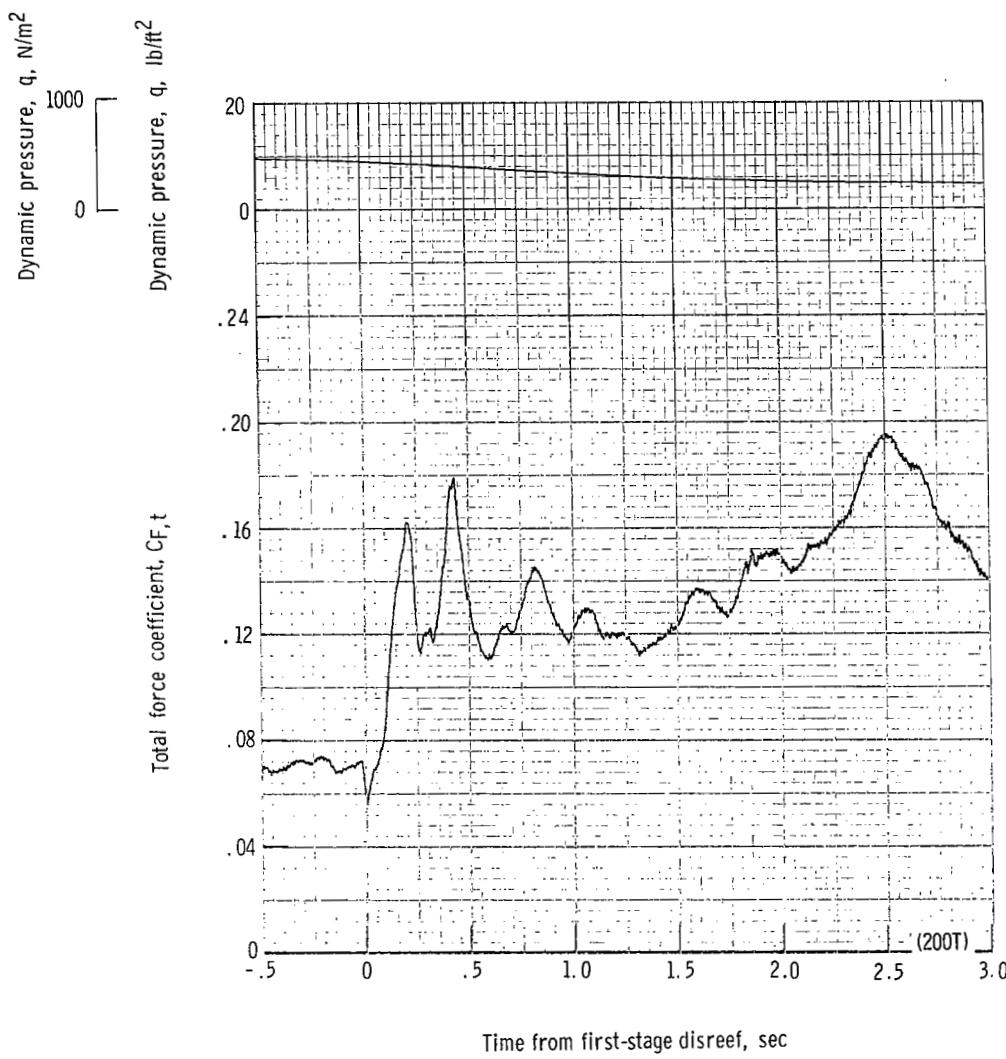
(h) Accelerations a_x , a_y , and a_z plotted against time from first-stage disreef. Time = 0 second corresponds to 31.76 seconds after launch.

Figure 41.- Continued.



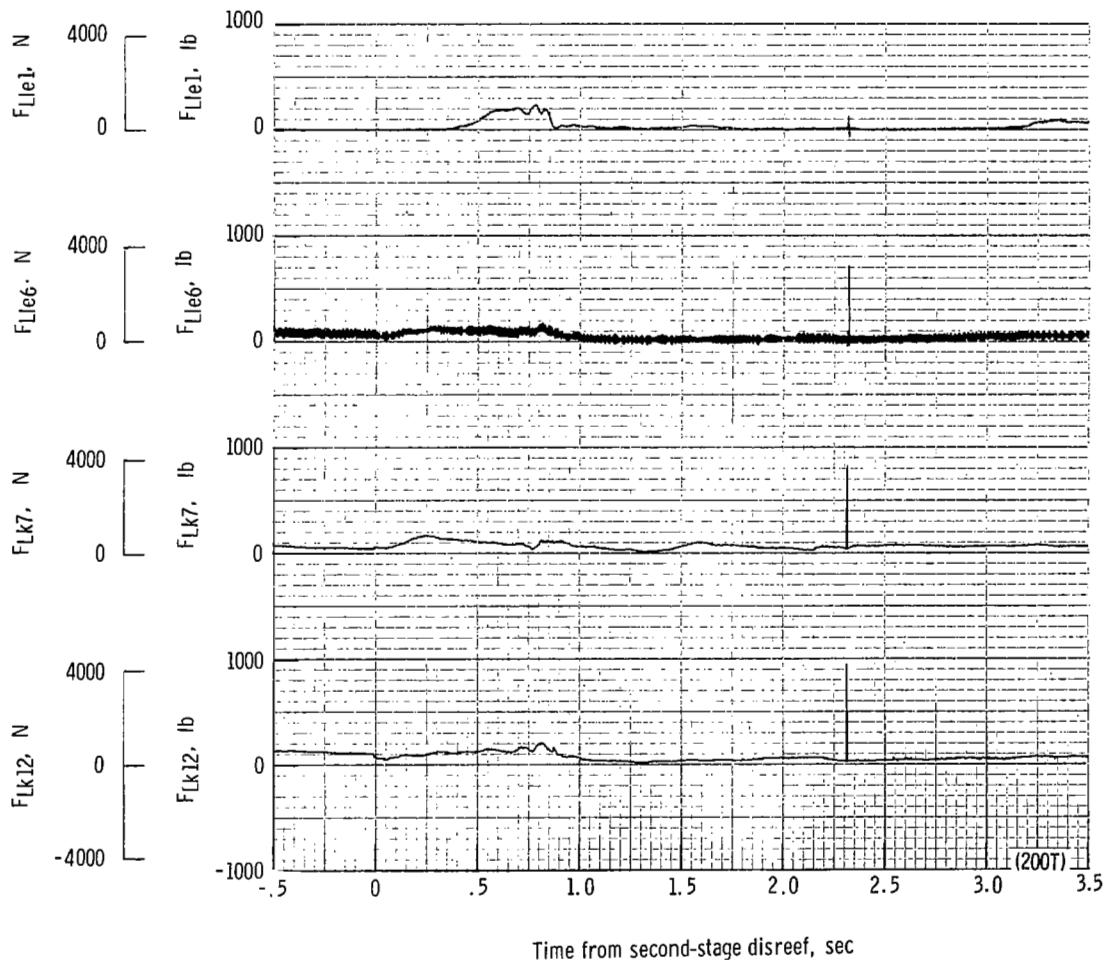
(i) Total force F_t plotted against time from first-stage disreef. Time = 0 second corresponds to 31.76 seconds after launch.

Figure 41.- Continued.



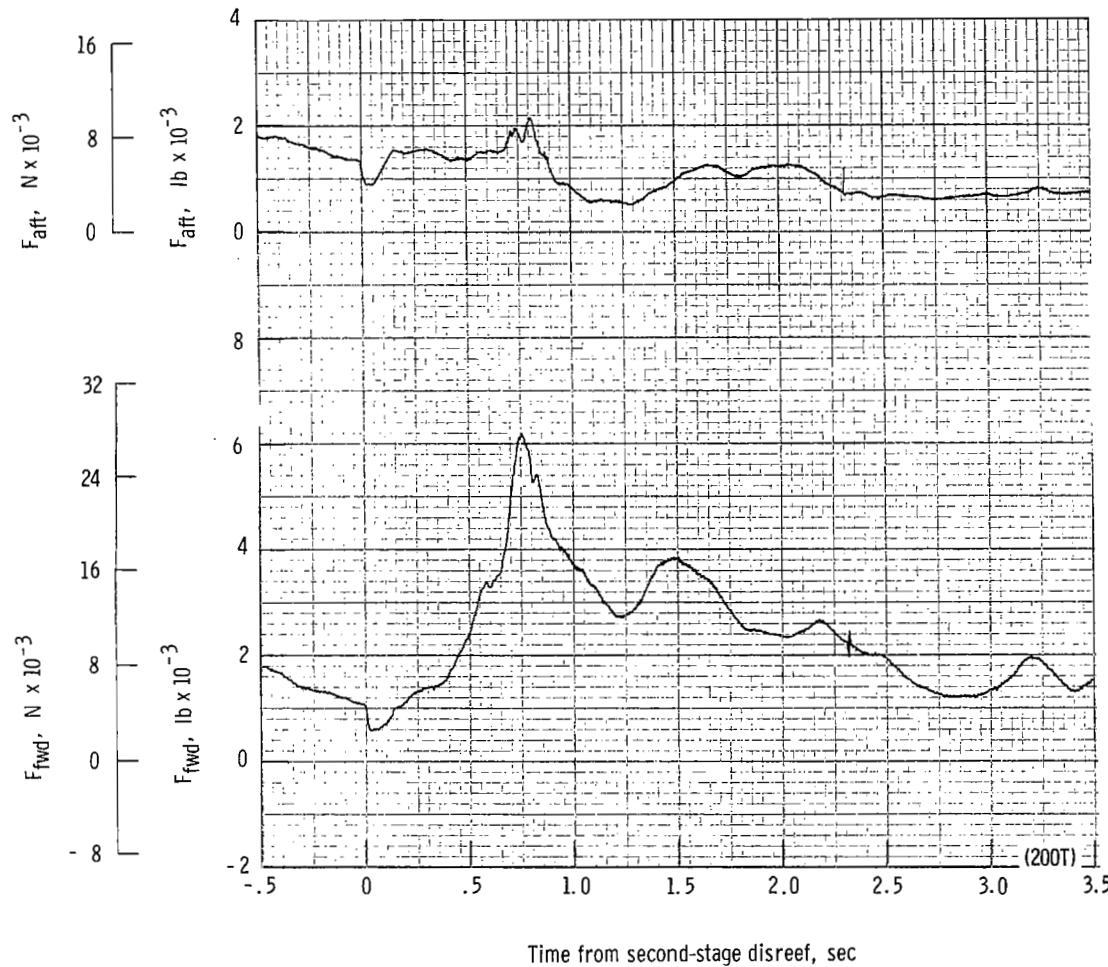
(j) Total force coefficient $C_{F,t}$ and dynamic pressure q plotted against time from first-stage disreef. Time = 0 second corresponds to 31.76 seconds after launch.

Figure 41.- Continued.



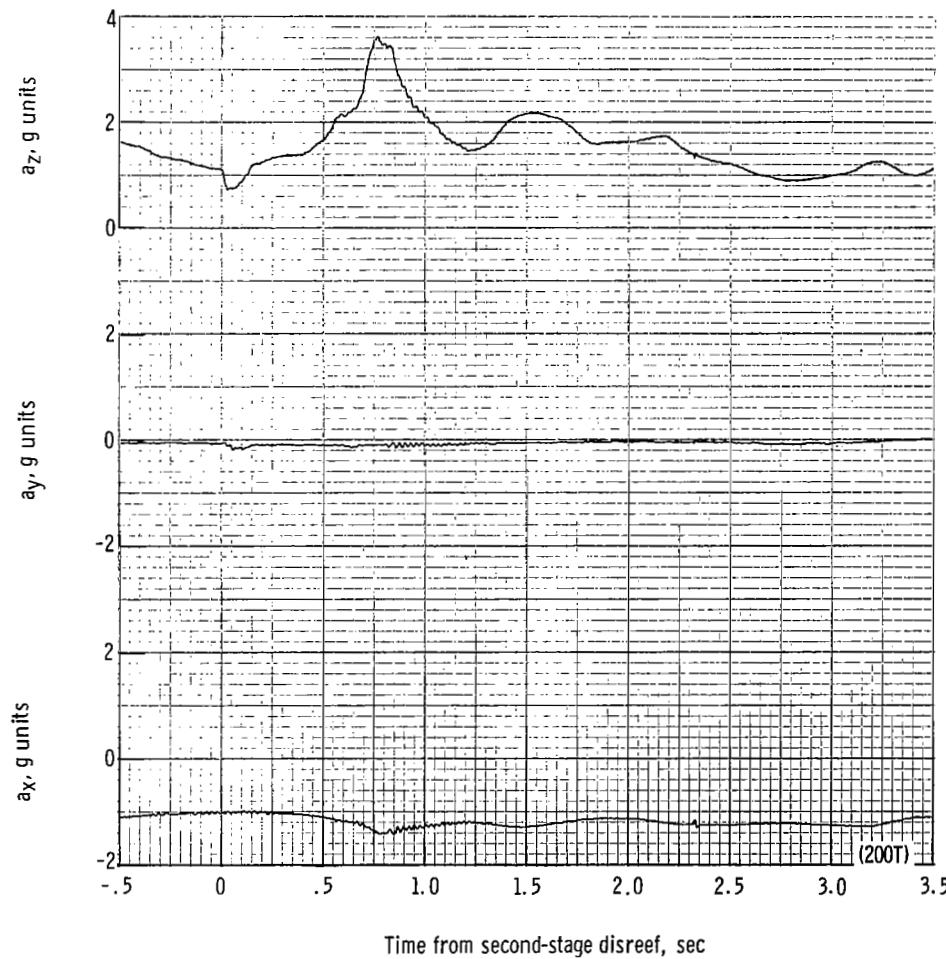
(k) Individual suspension-line loads F_{Lk12} , F_{Lk7} , F_{Lle6} , and F_{Lle1} plotted against time from second-stage disreef. Time = 0 second corresponds to 34.85 seconds after launch.

Figure 41.- Continued.



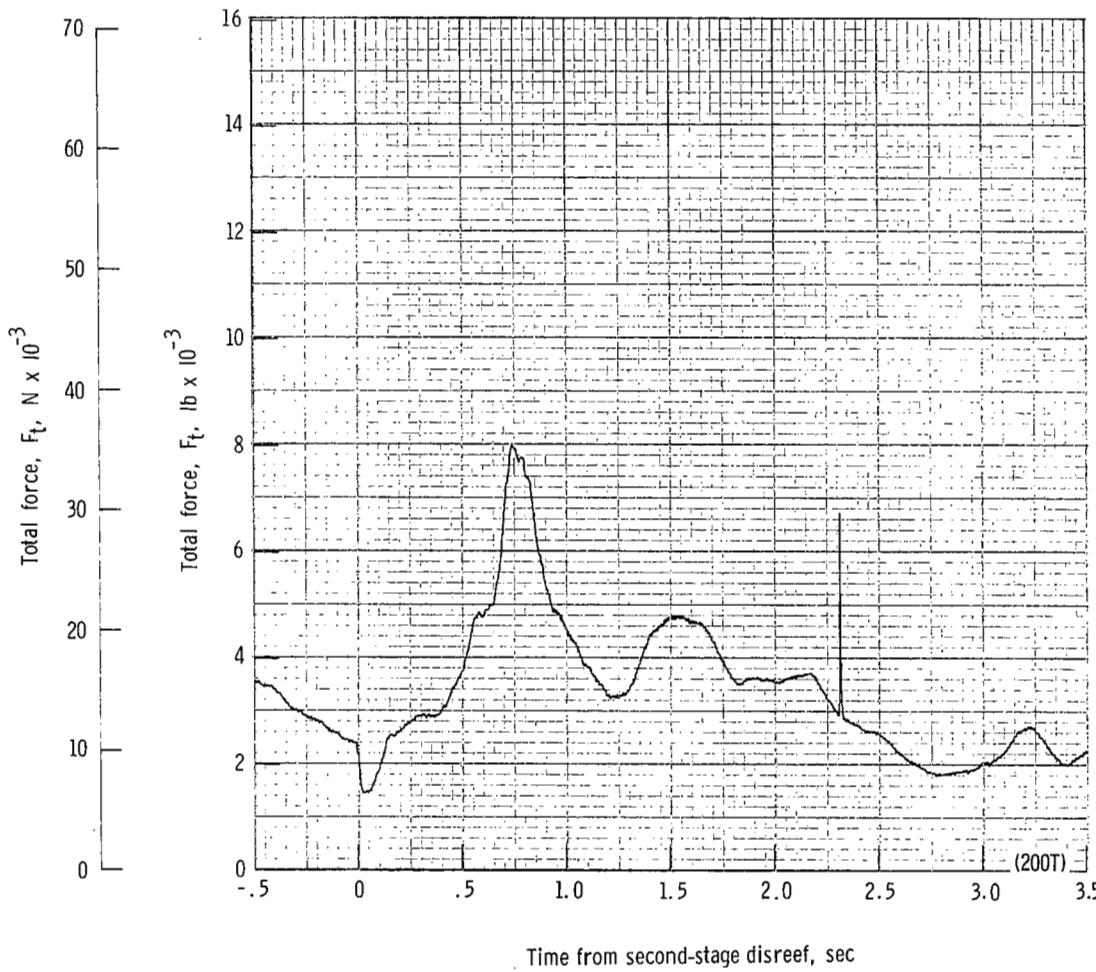
(II) Forward and aft riser loads plotted against time from second-stage disreef. Time = 0 second corresponds to 34.85 seconds after launch.

Figure 41.- Continued.



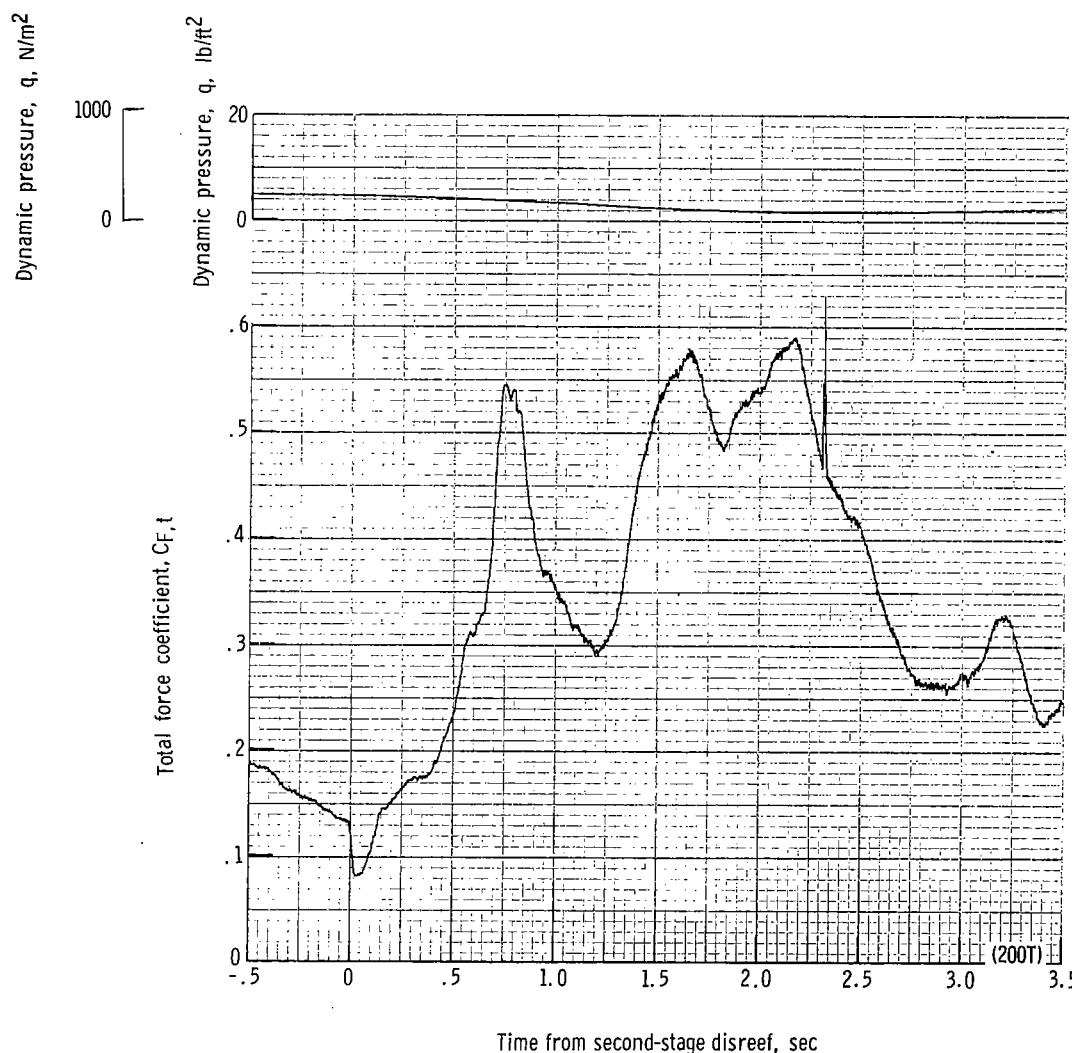
(m) Accelerations a_x , a_y , and a_z plotted against time from second-stage disreef. Time = 0 second corresponds to 34.85 seconds after launch.

Figure 41.- Continued.



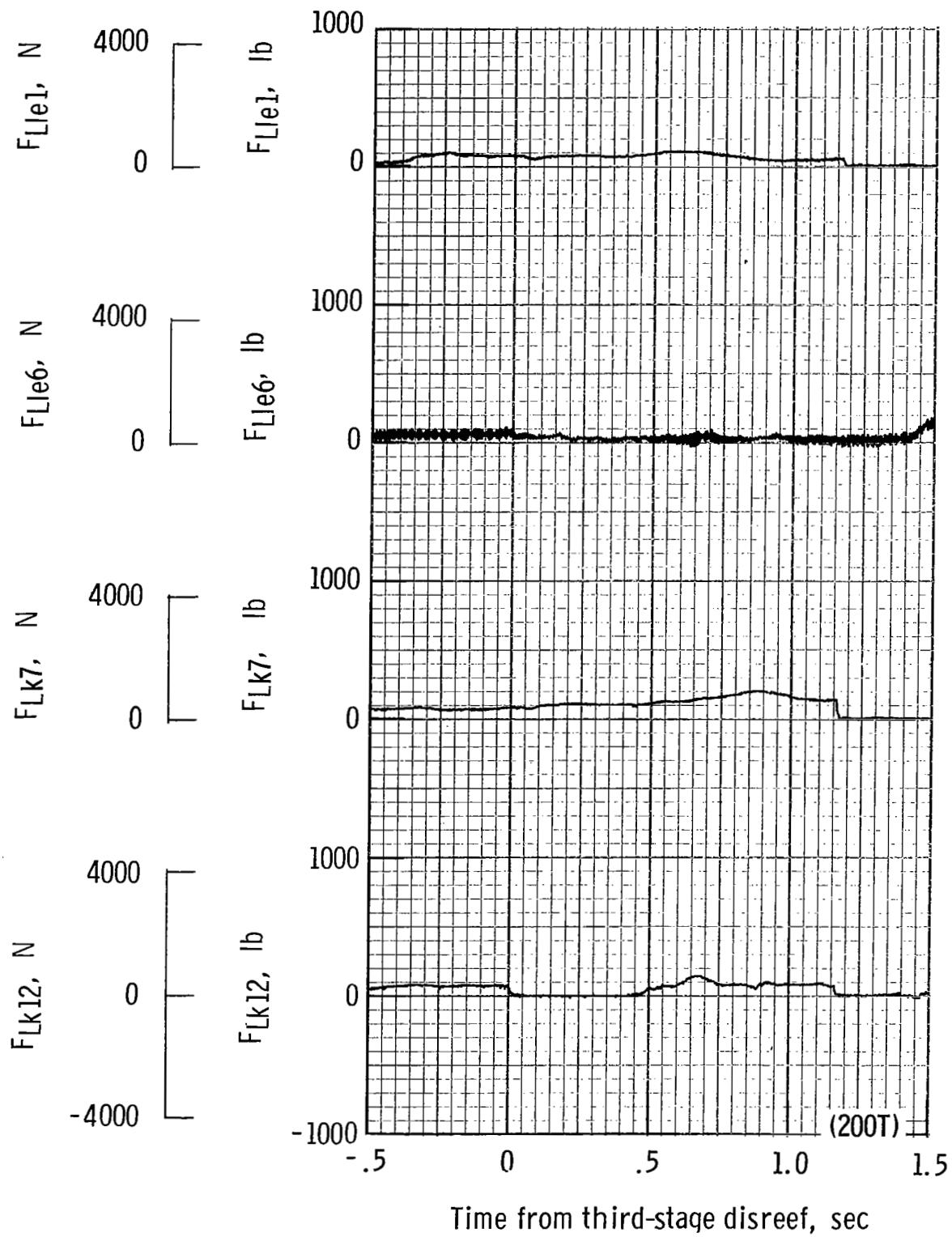
(n) Total force F_t plotted against time from second-stage disreef. Time = 0 second corresponds to 34.85 seconds after launch.

Figure 41.- Continued.



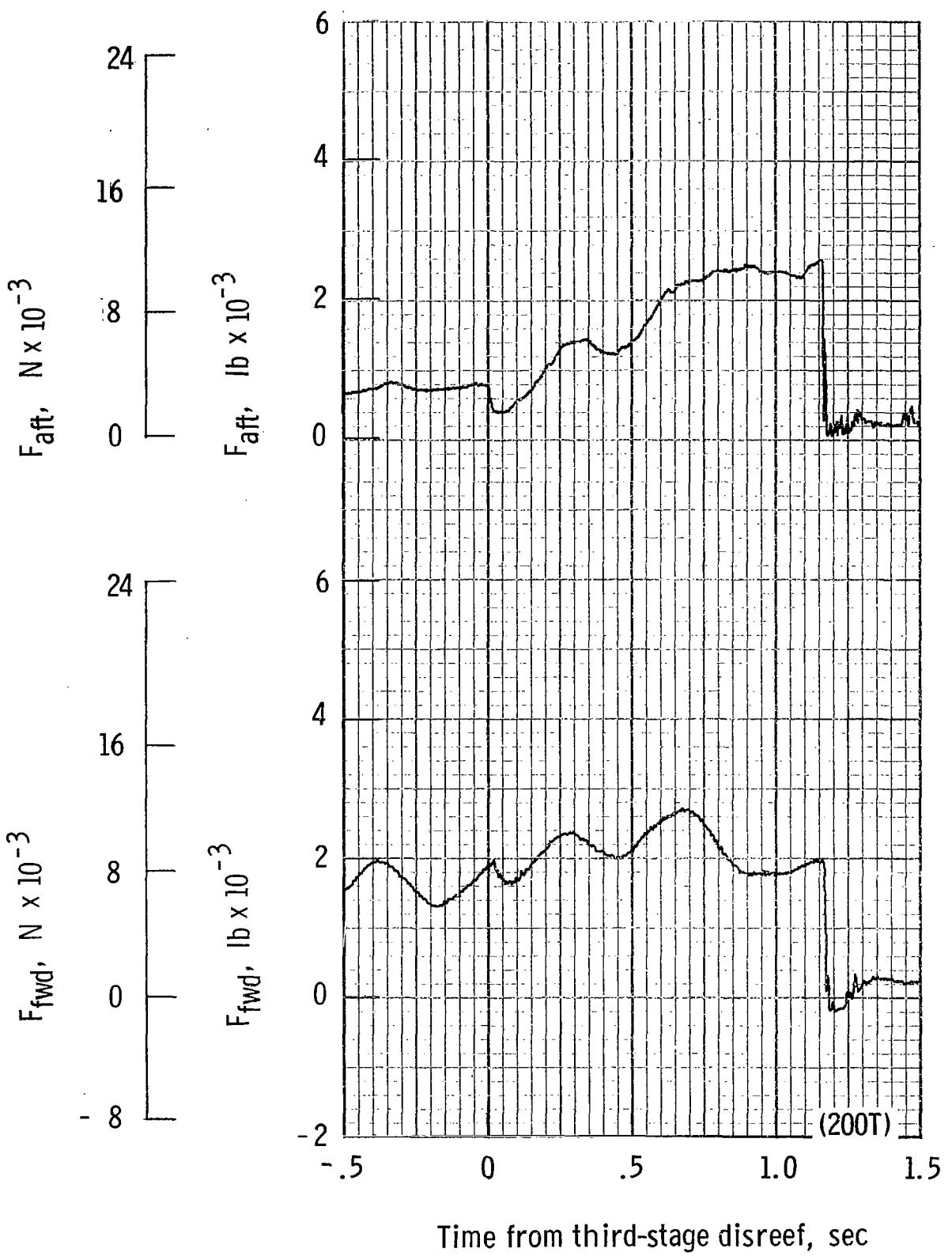
(o) Total force coefficient CF_t and dynamic pressure q plotted against time from second-stage disreef. Time = 0 second corresponds to 34.85 seconds after launch.

Figure 41.- Continued.



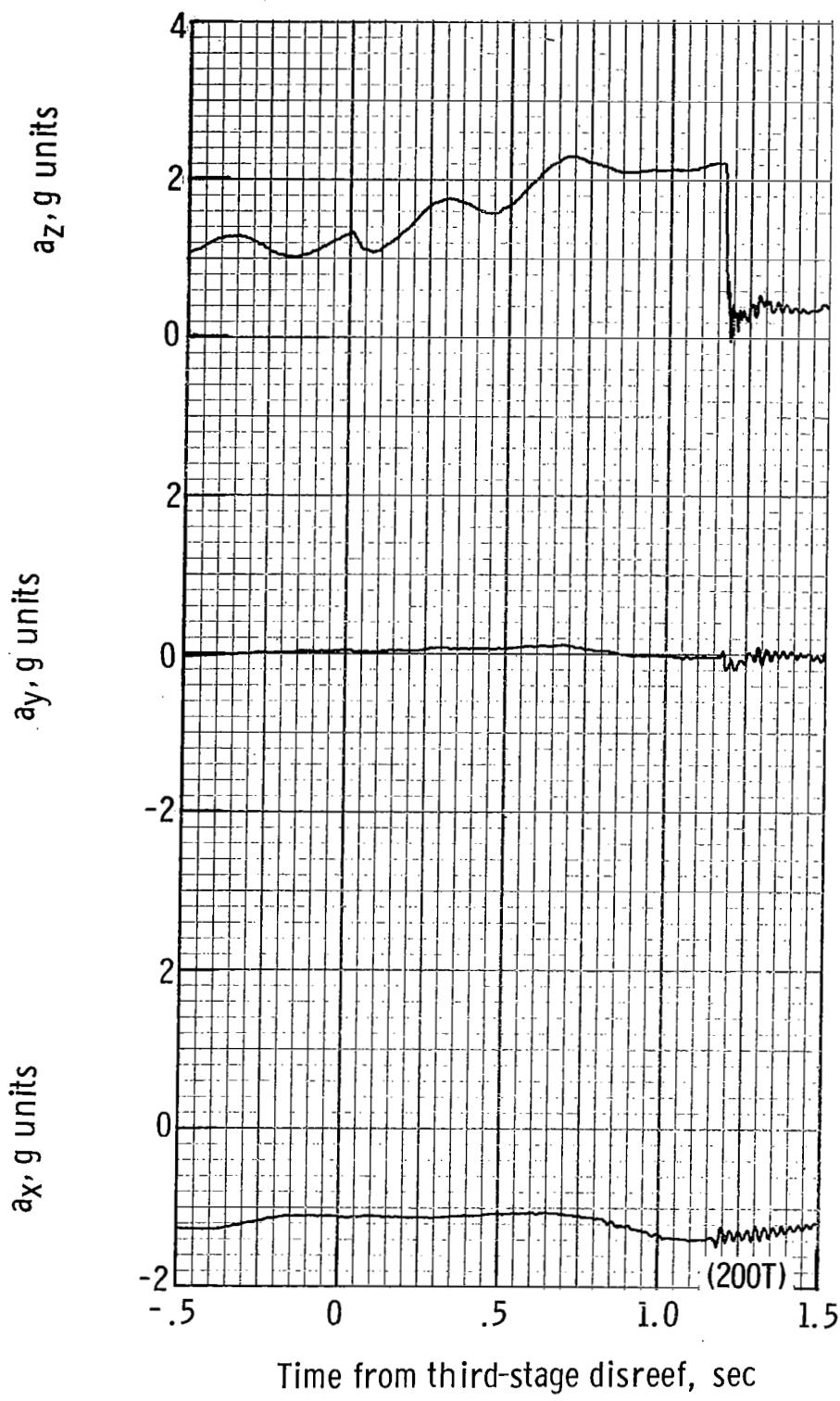
(p) Individual suspension-line loads F_{Lk12} , F_{Lk7} , F_{Lle6} , and F_{Lle1} plotted against time from third-stage disreef. Time = 0 second corresponds to 38.43 seconds after launch.

Figure 41.- Continued.



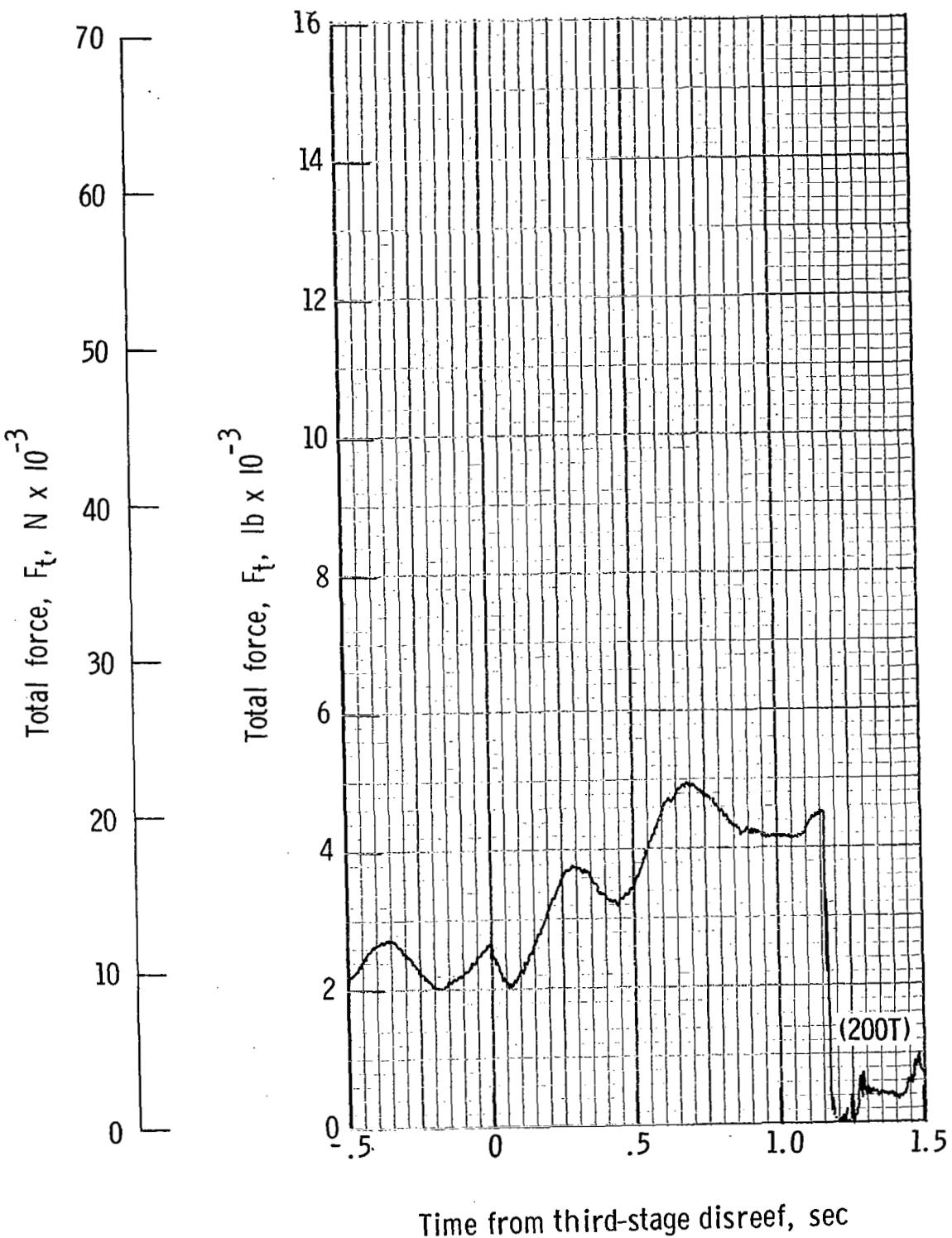
(q) Forward and aft riser loads plotted against time from third-stage disreef. Time = 0 second corresponds to 38.43 seconds after launch.

Figure 41.- Continued.



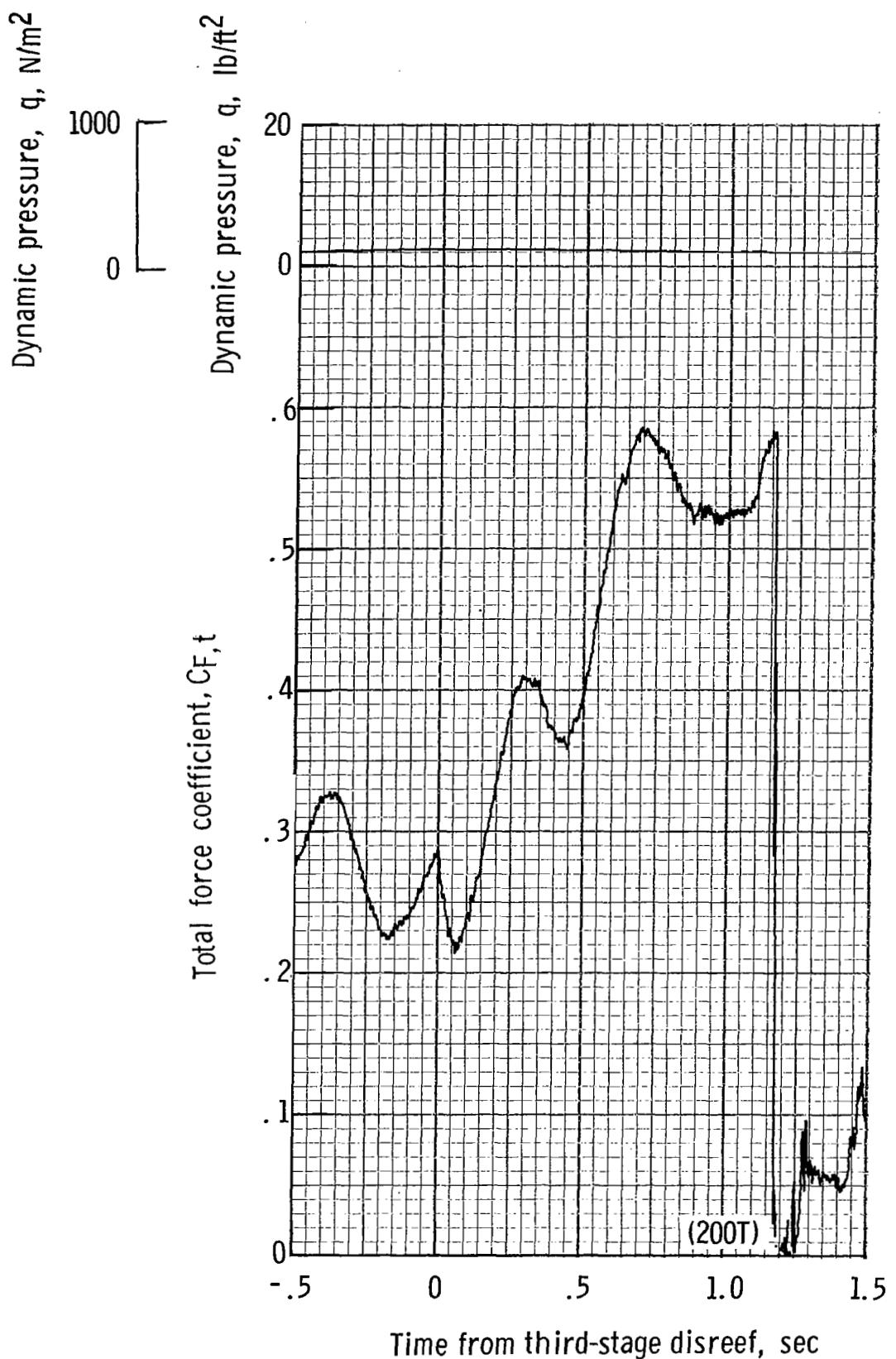
(r) Accelerations a_x , a_y , and a_z plotted against time from third-stage disreef. Time = 0 second corresponds to 38.43 seconds after launch.

Figure 41.- Continued.

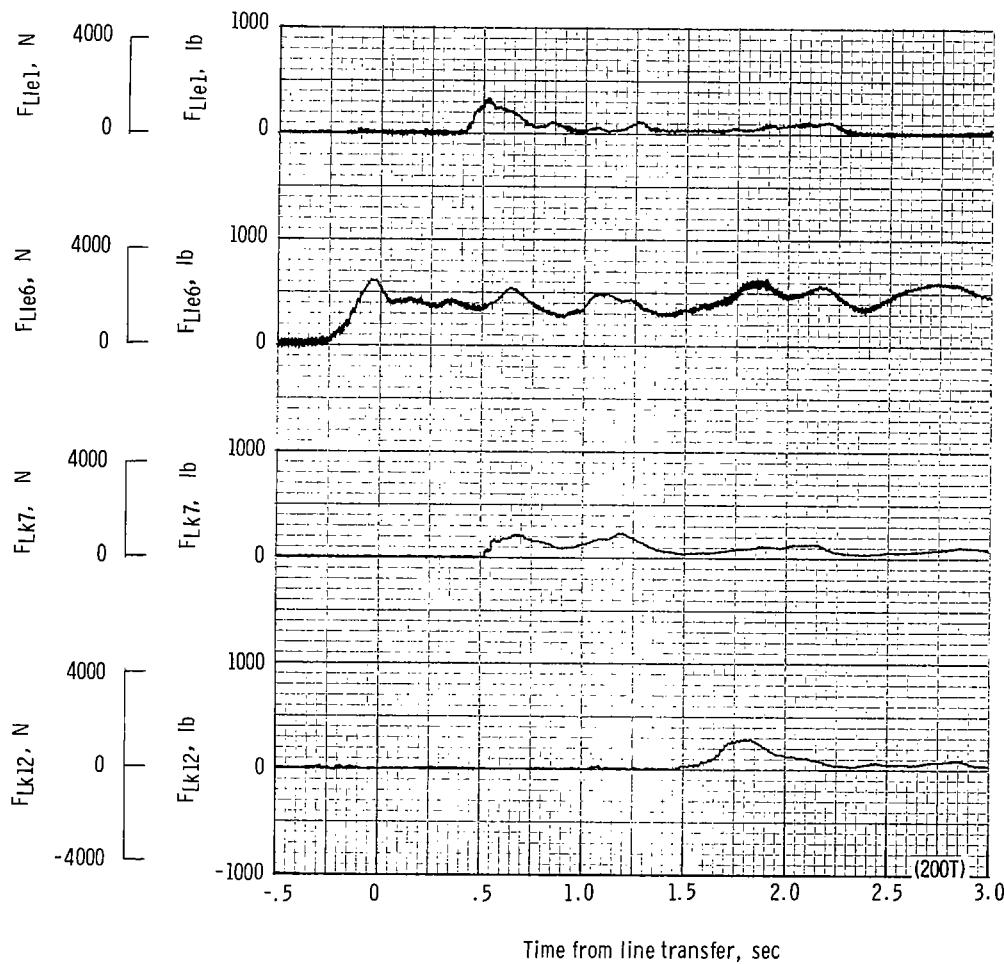


(s) Total force F_t plotted against time from third-stage disreef. Time = 0 second corresponds to 38.43 seconds after launch.

Figure 41.- Continued.

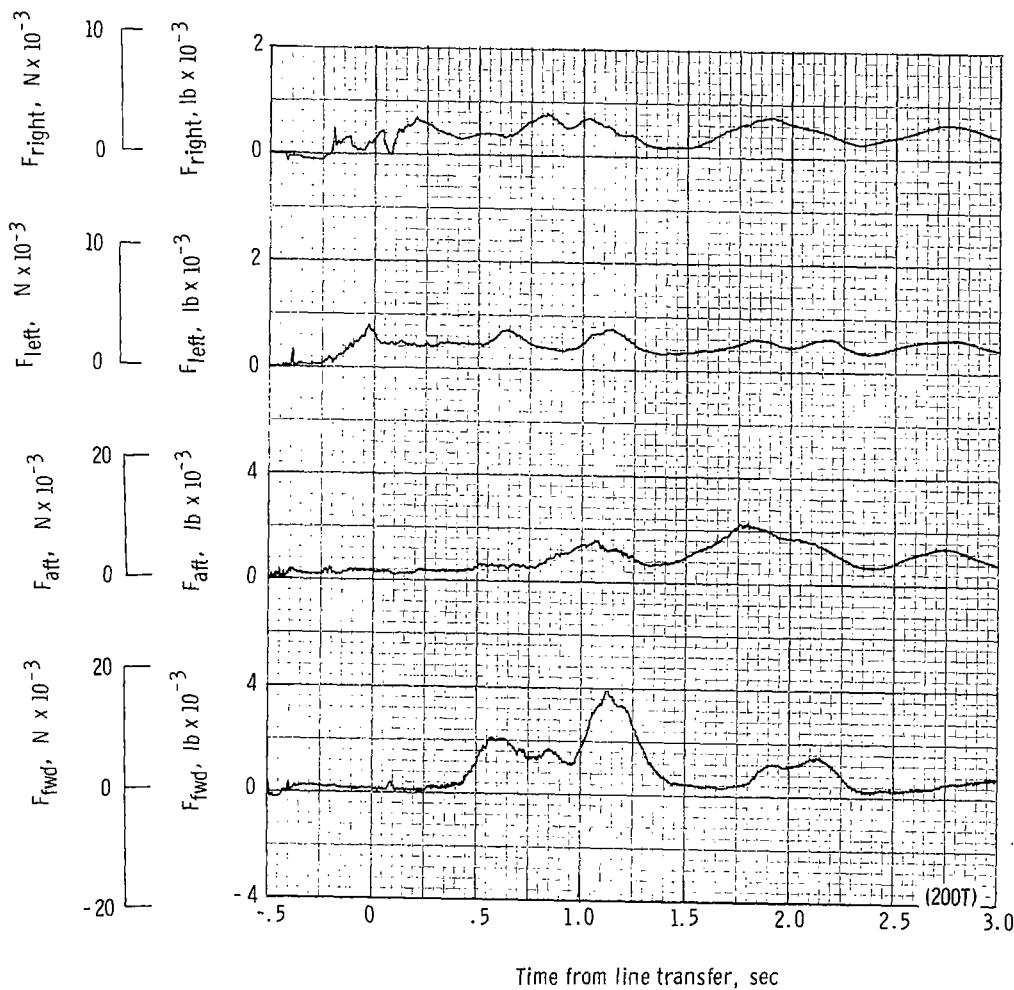


(t) Total force coefficient $C_{F,t}$ and dynamic pressure q plotted against time from third-stage disreef. Time = 0 second corresponds to 38.43 seconds after launch.



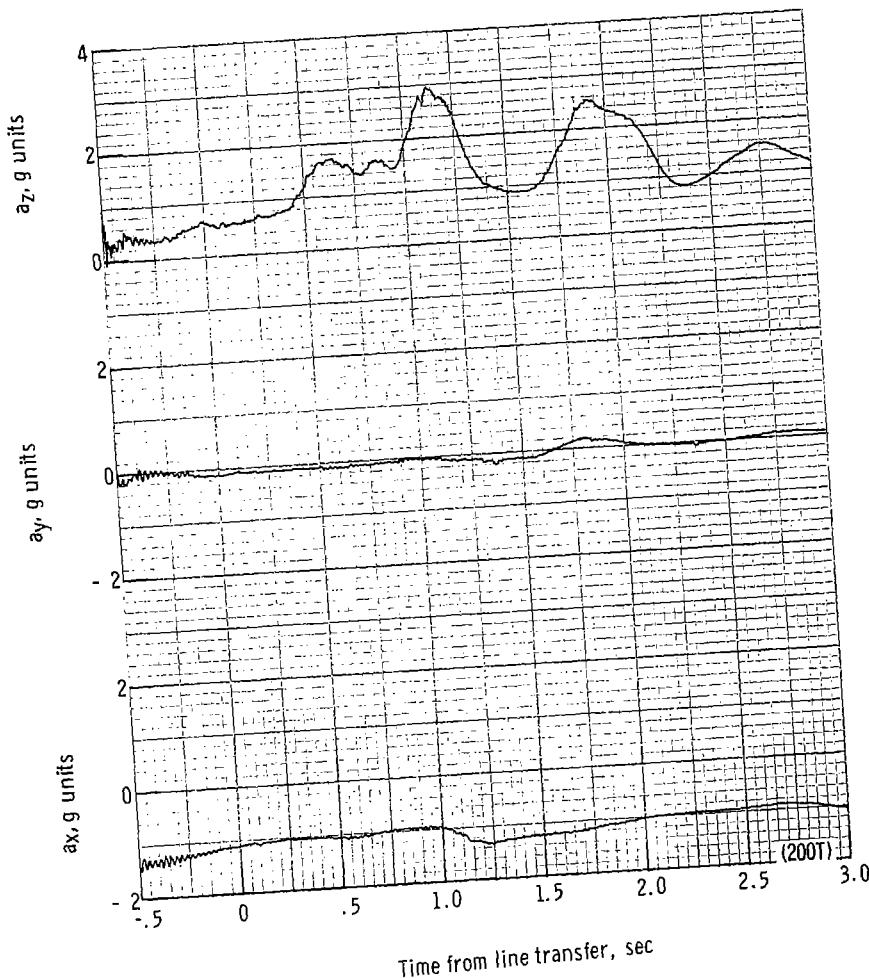
(u) Individual suspension-line loads F_{Lk12} , F_{Lk7} , F_{Lle6} and F_{Lle1} plotted against time from line transfer. Time = 0 second corresponds to 39.61 seconds after launch.

Figure 41.- Continued.



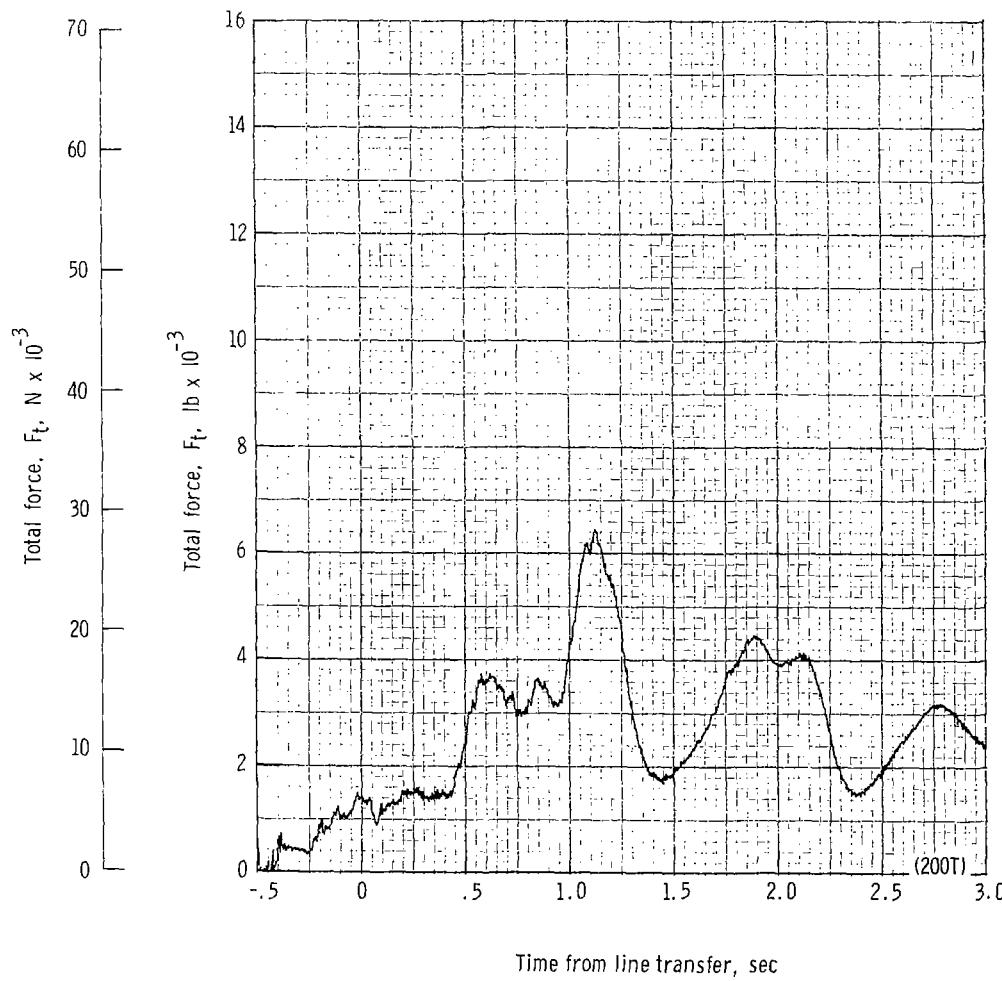
(v) Forward, aft, left, and right riser loads plotted against time from line transfer. Time = 0 second corresponds to 39.61 seconds after launch.

Figure 41.- Continued.



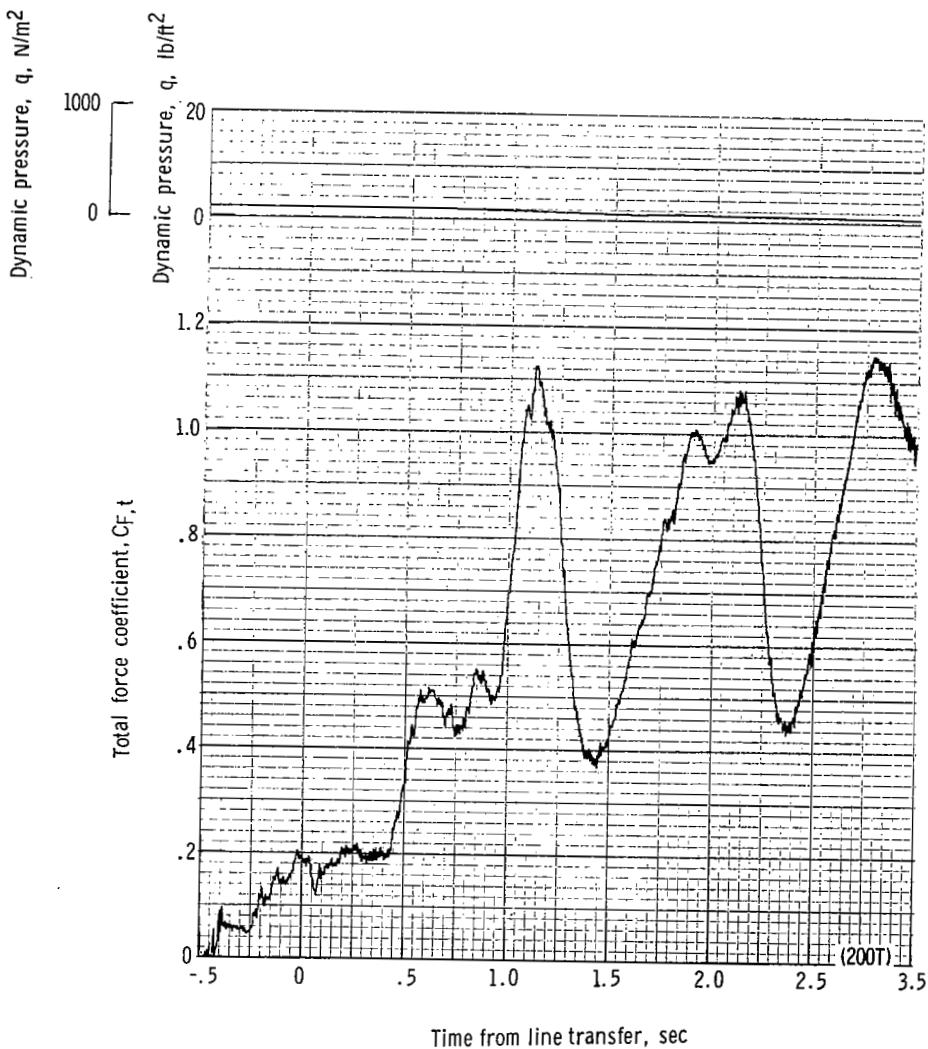
(w) Accelerations a_x , a_y , and a_z plotted against time from line transfer. Time = 0 second corresponds to 39.61 seconds after launch.

Figure 4L.- Continued.



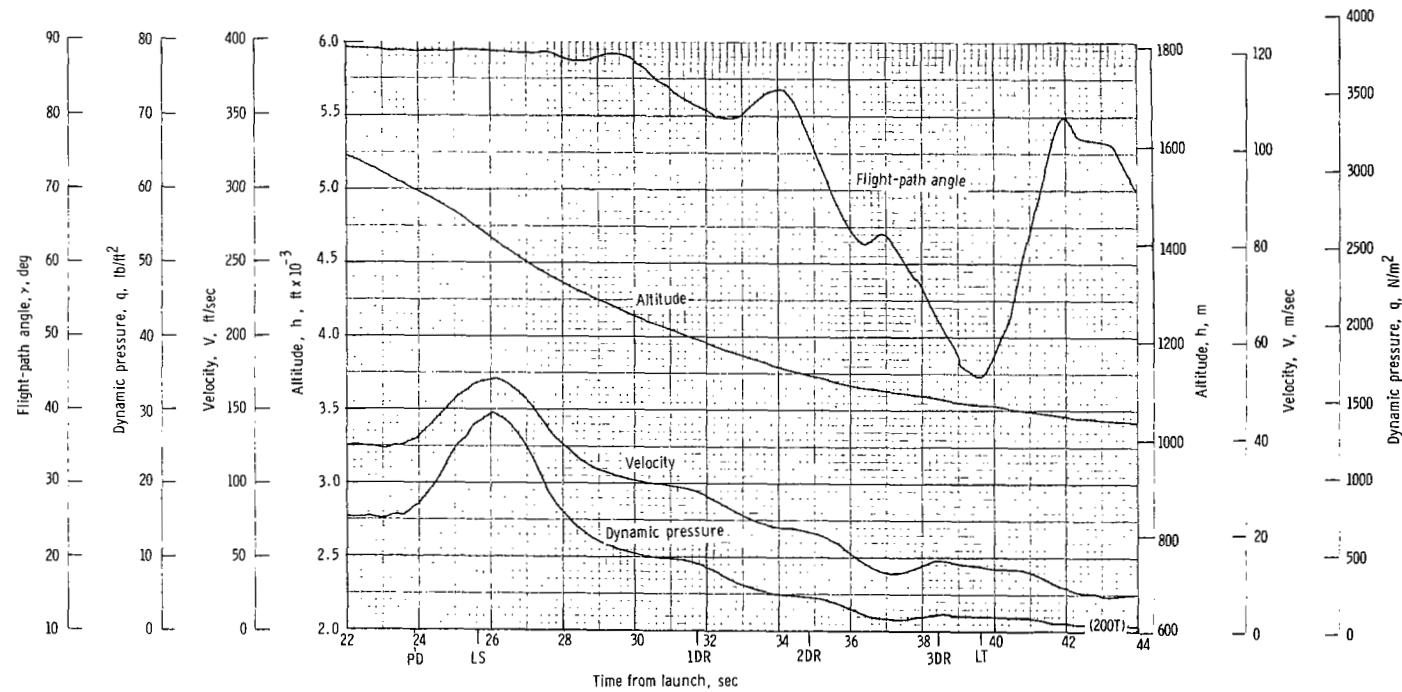
(x) Total force F_t plotted against time from line transfer. Time = 0 second corresponds to 39.61 seconds after launch.

Figure 41.- Continued.



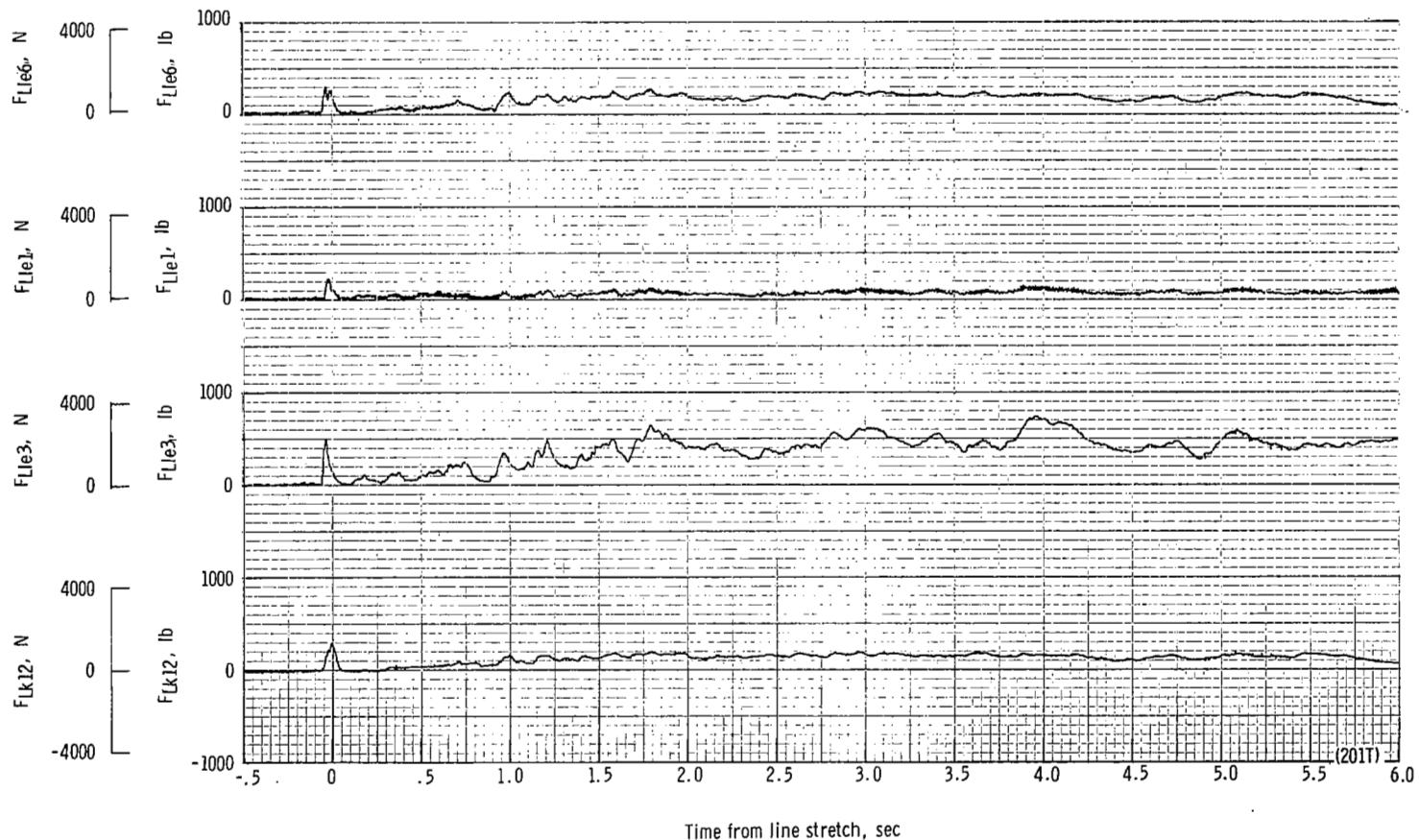
(y) Total force coefficient $C_{F,t}$ and dynamic pressure q plotted against time from line transfer. Time = 0 second corresponds to 39.61 seconds after launch.

Figure 41.- Continued.



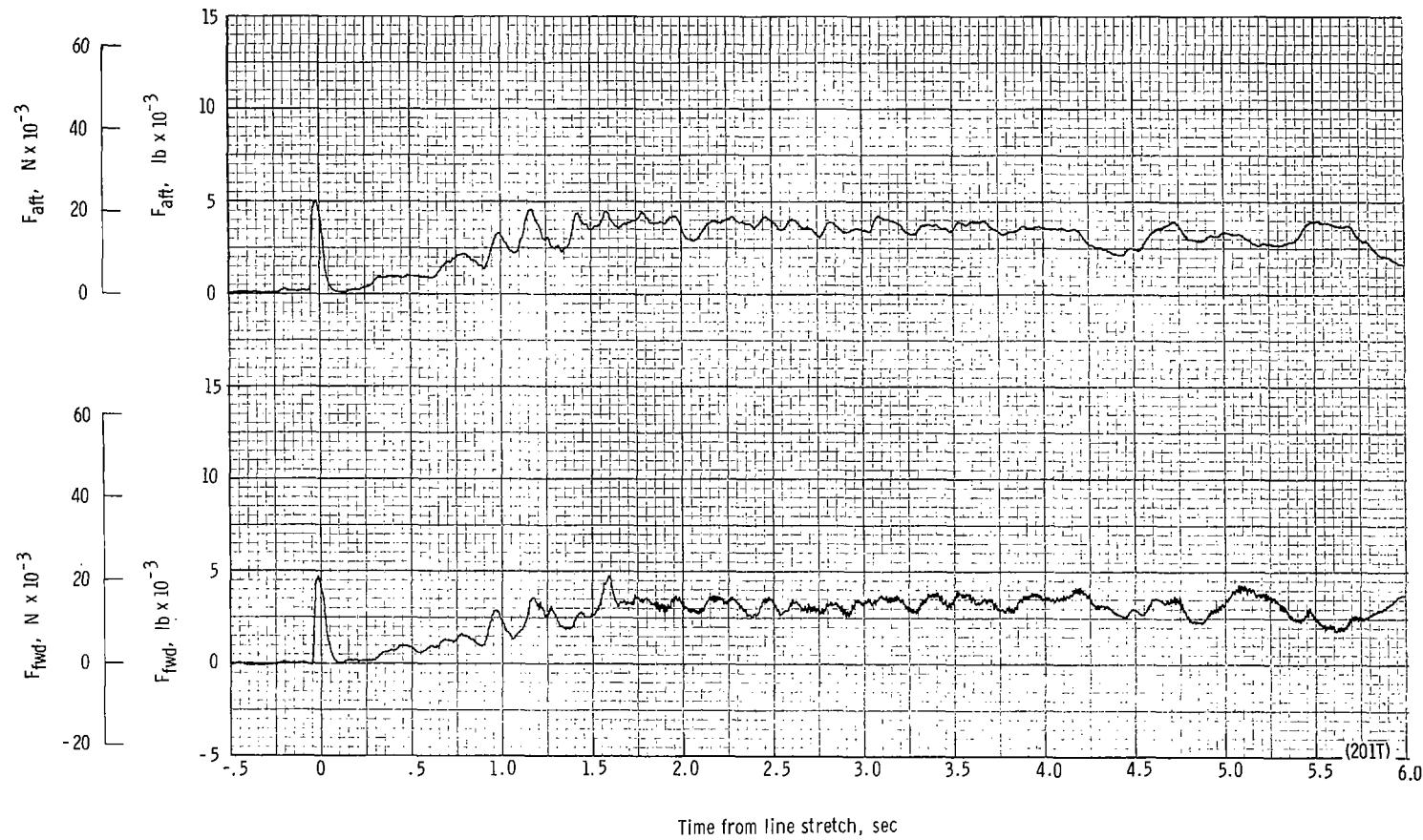
(z) Flight-path angle γ , dynamic pressure q , velocity V , and altitude h plotted against time from launch.

Figure 41.- Concluded.



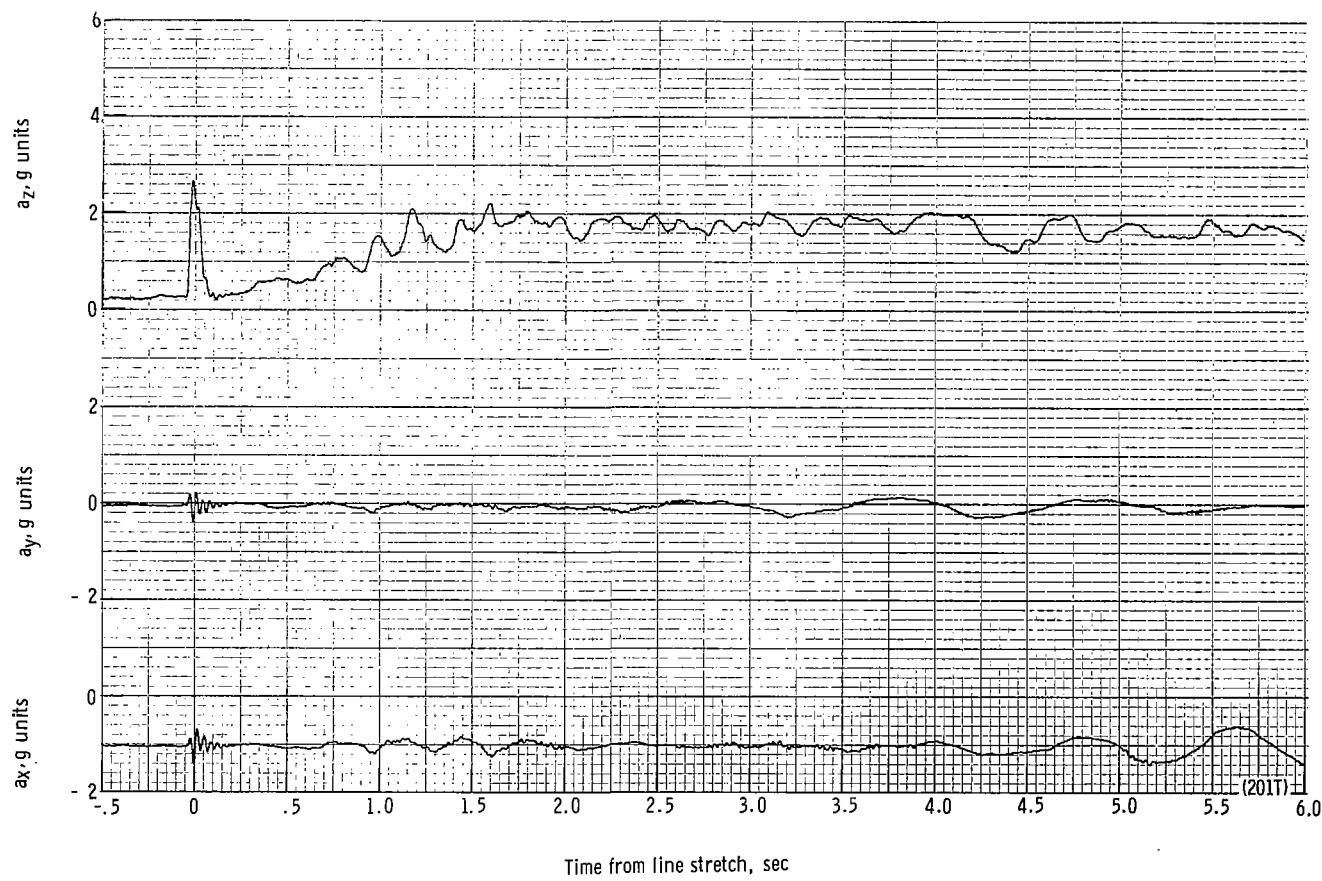
(a) Individual suspension-line loads F_{Lk12} , F_{Lle3} , F_{Lle1} , and F_{Lle6} plotted against time from line stretch. Time = 0 second corresponds to 27.92 seconds after launch.

Figure 42.- Time history of twin-keel parawing deployment data for test 201T. $W_D = 22\ 392\ N$ (5034 lb); $W_p = 20\ 871\ N$ (4692 lb); $q_{PD} = 919.3\ N/m^2$ (19.2 lb/ft²); $h_{PD} = 1227\ m$ (4025 ft); $t_r/t_k = 0.100$; reefing version A.



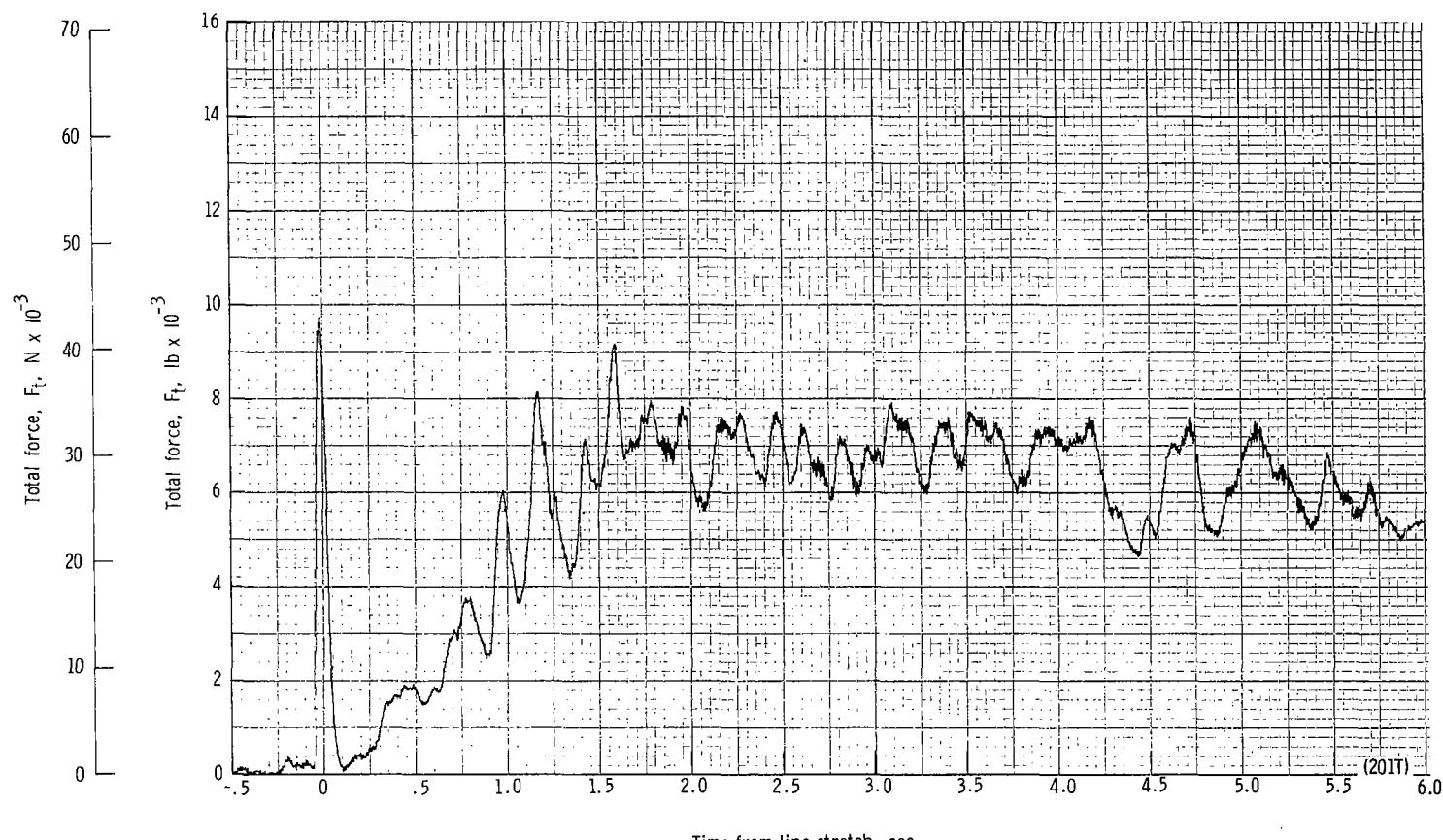
(b) Forward and aft riser loads plotted against time from line stretch. Time = 0 second corresponds to 27.92 seconds after launch.

Figure 42.- Continued.



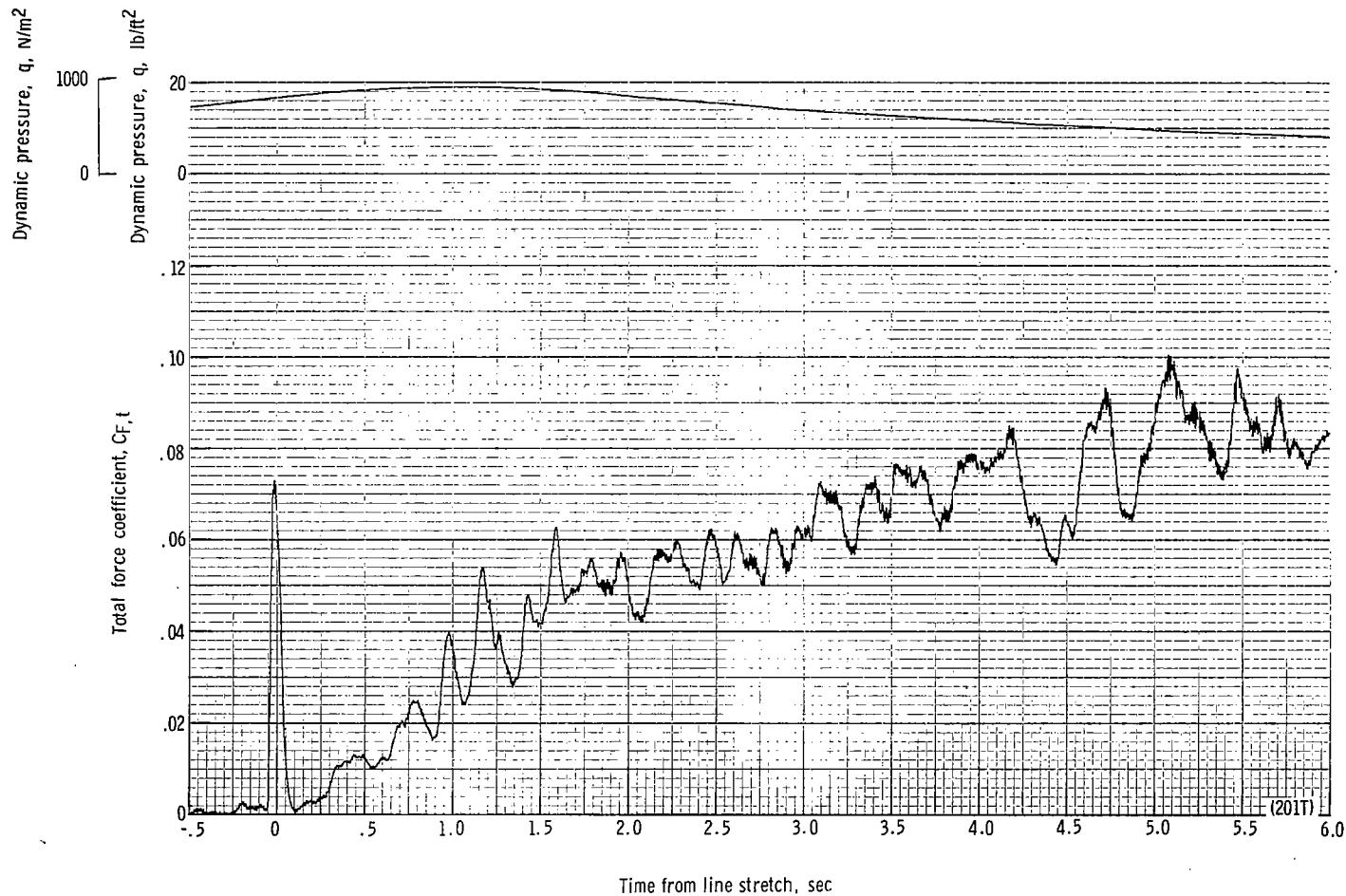
(c) Accelerations a_x , a_y , and a_z plotted against time from line stretch. Time = 0 second corresponds to 27.92 seconds after launch.

Figure 42.- Continued.



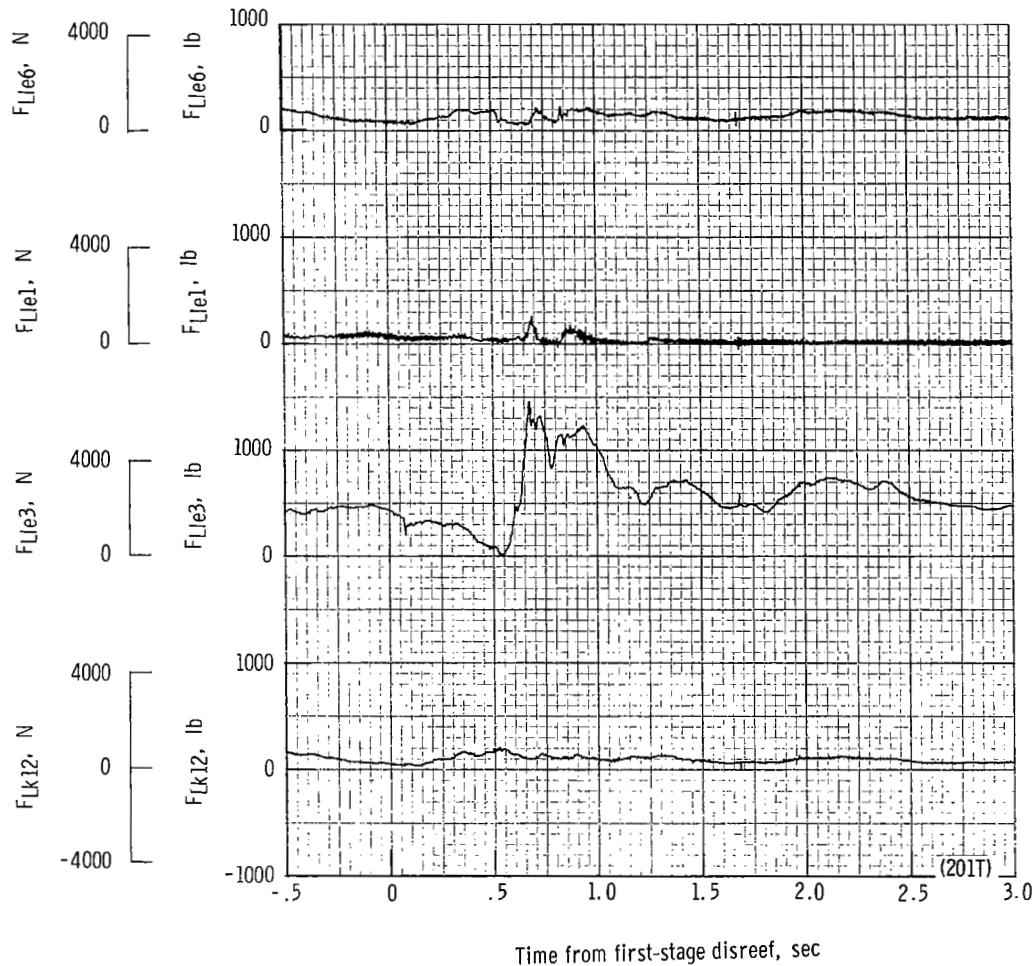
(d) Total force F_t plotted against time from line stretch. Time = 0 second corresponds to 27.92 seconds after launch.

Figure 42.- Continued.



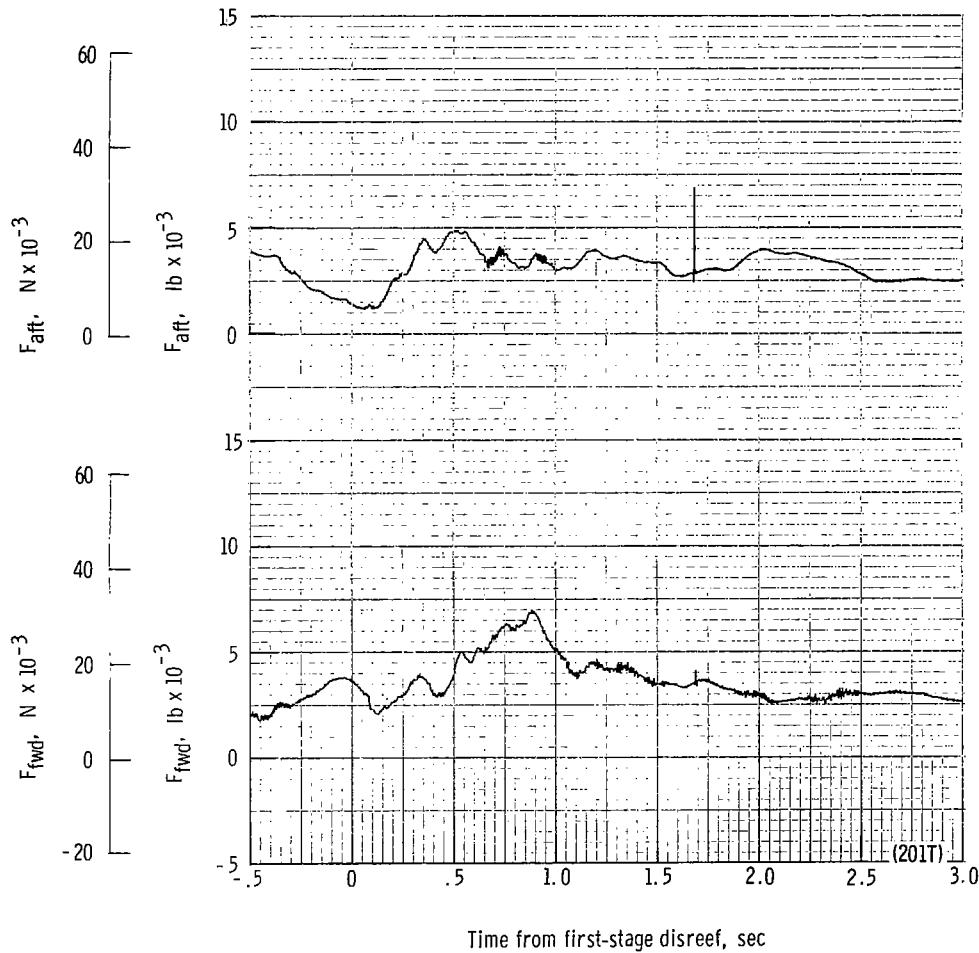
(e) Total force coefficient $C_{F,t}$ and dynamic pressure q plotted against time from line stretch. Time = 0 second corresponds to 27.92 seconds after launch.

Figure 42.- Continued.



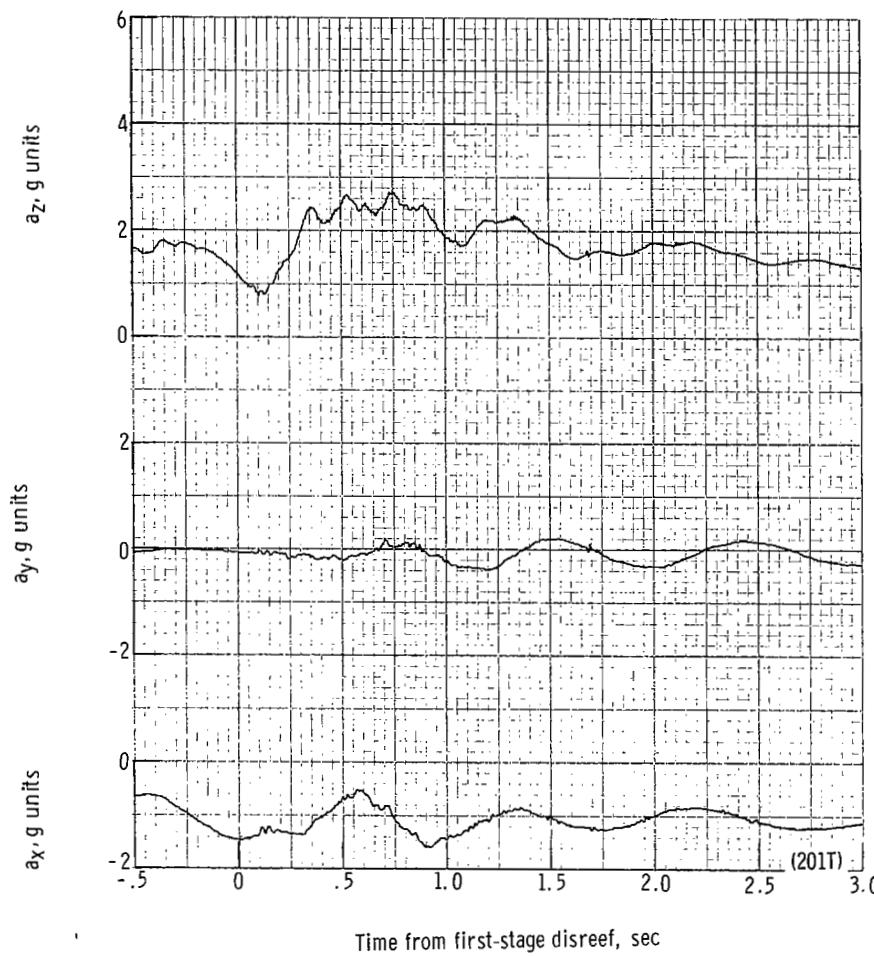
(f) Individual suspension-line loads F_{Lk12} , F_{Lle3} , F_{Lle1} , and F_{Lle6} plotted against time from first-stage disreef. Time = 0 second corresponds to 33.99 seconds after launch.

Figure 42.- Continued.



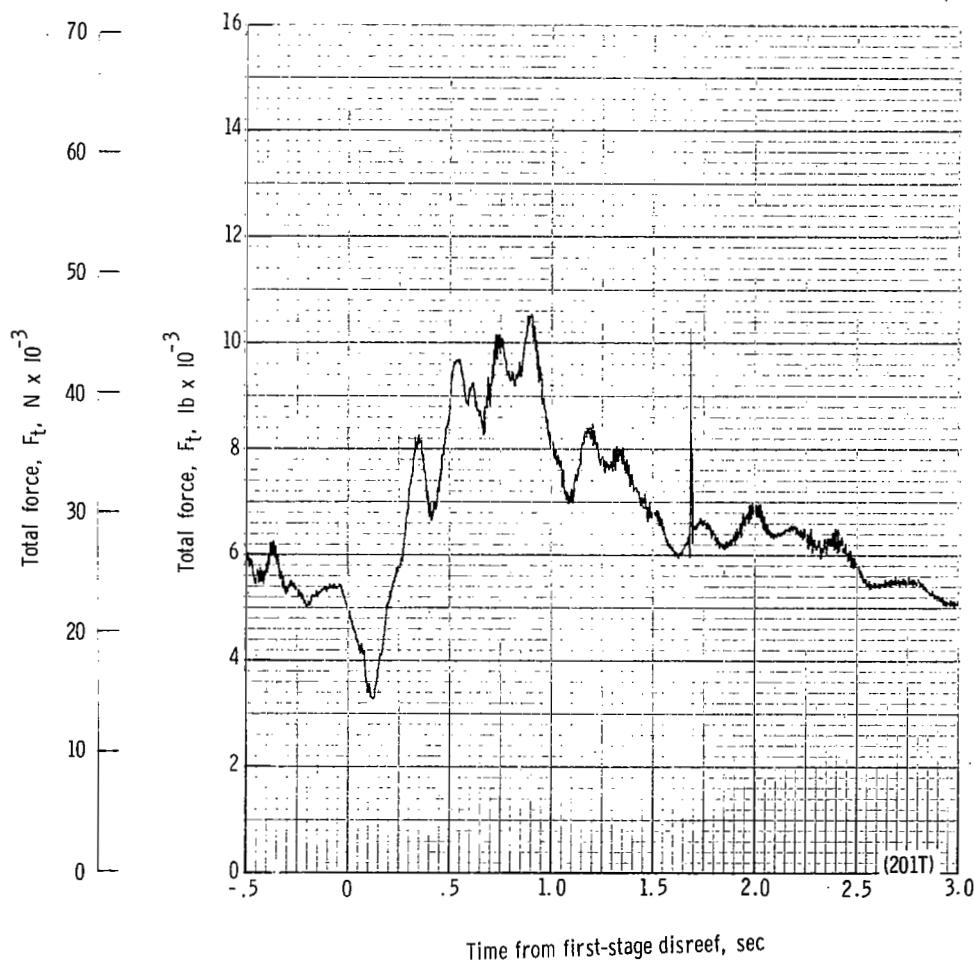
(g) Forward and aft riser loads plotted against time from first-stage disreef. Time = 0 second corresponds to 33.99 seconds after launch.

Figure 42.- Continued.



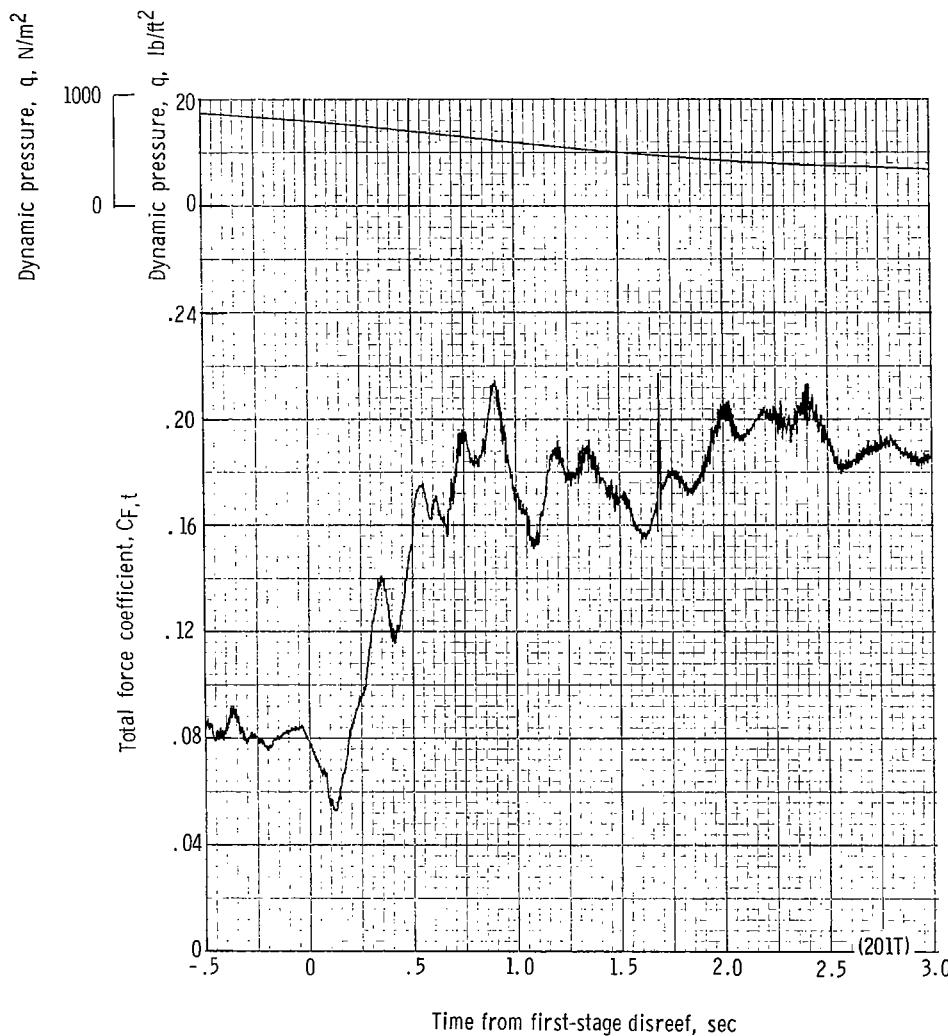
(h) Accelerations a_x , a_y , and a_z plotted against time from first-stage disreef. Time = 0 second corresponds to 33.99 seconds after launch.

Figure 42.- Continued.



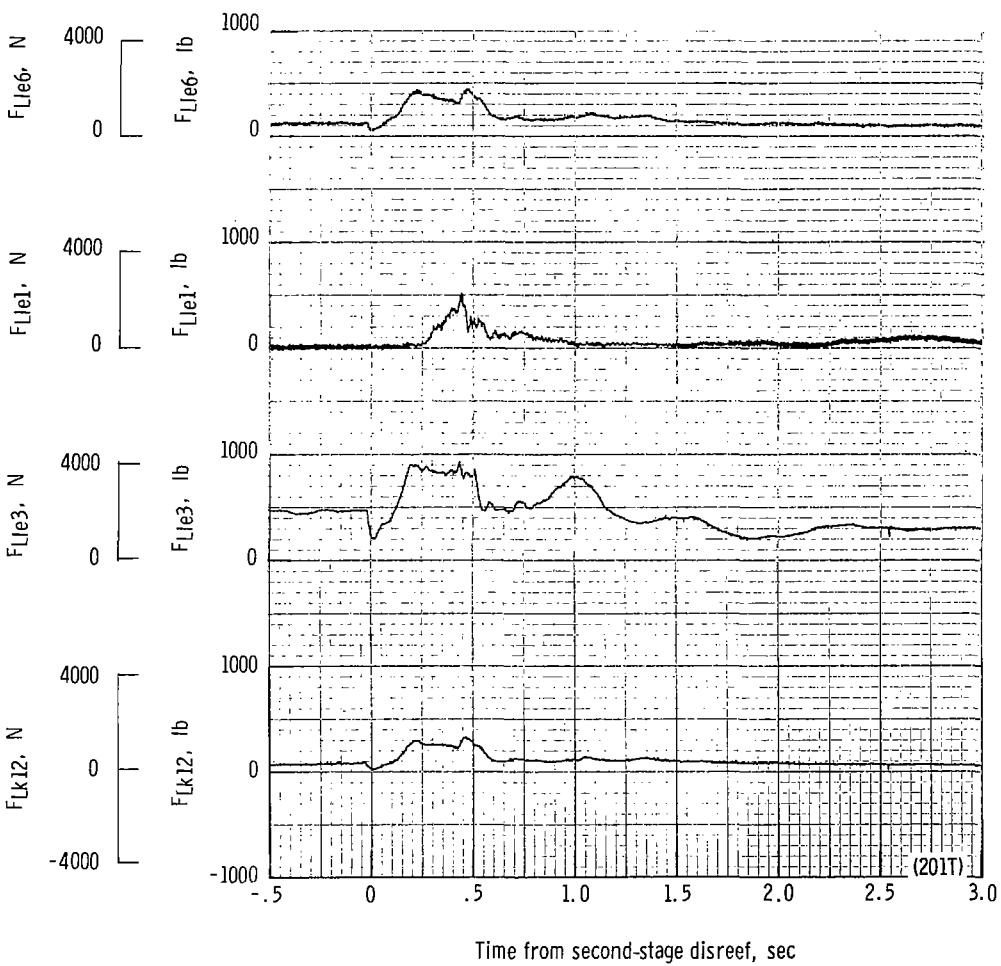
(i) Total force F_t plotted against time from first-stage disreef. Time = 0 second corresponds to 33.99 seconds after launch.

Figure 42.- Continued.



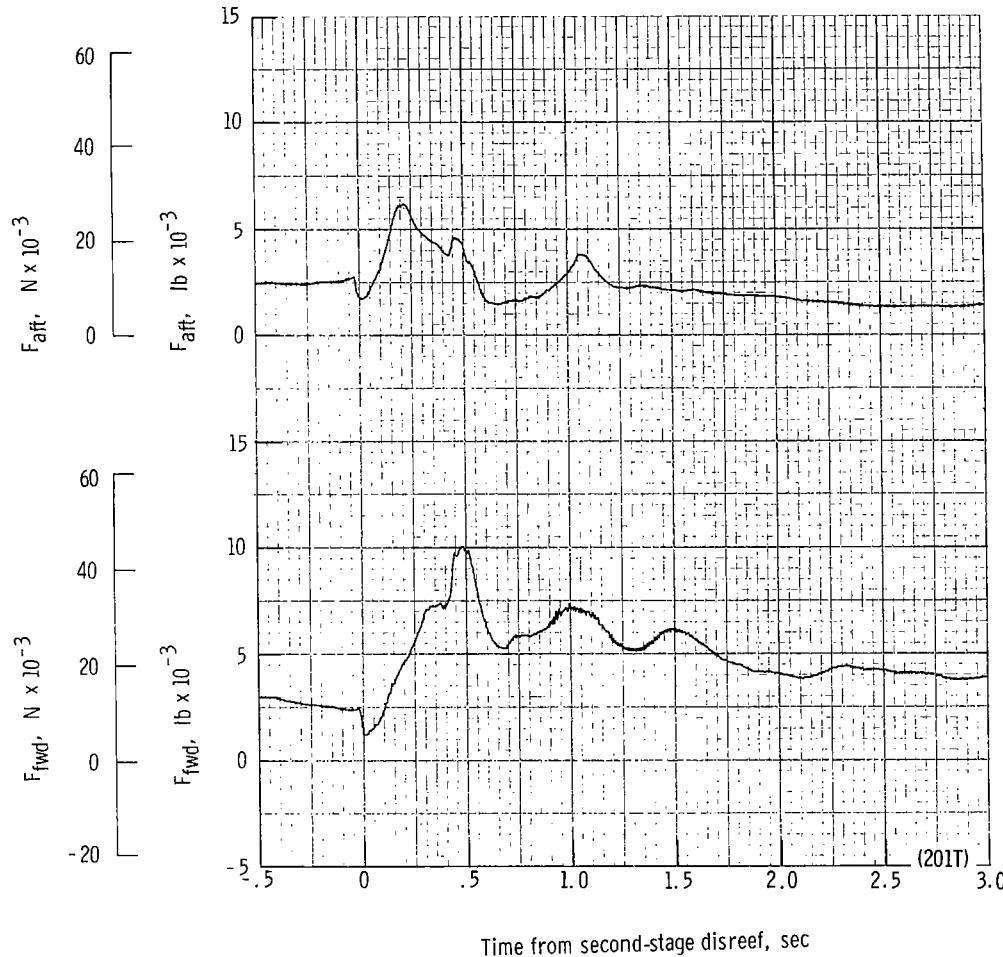
(j) Total force coefficient $C_{F,t}$ and dynamic pressure q plotted against time from first-stage disreef. Time = 0 second corresponds to 33.99 seconds after launch.

Figure 42.- Continued.



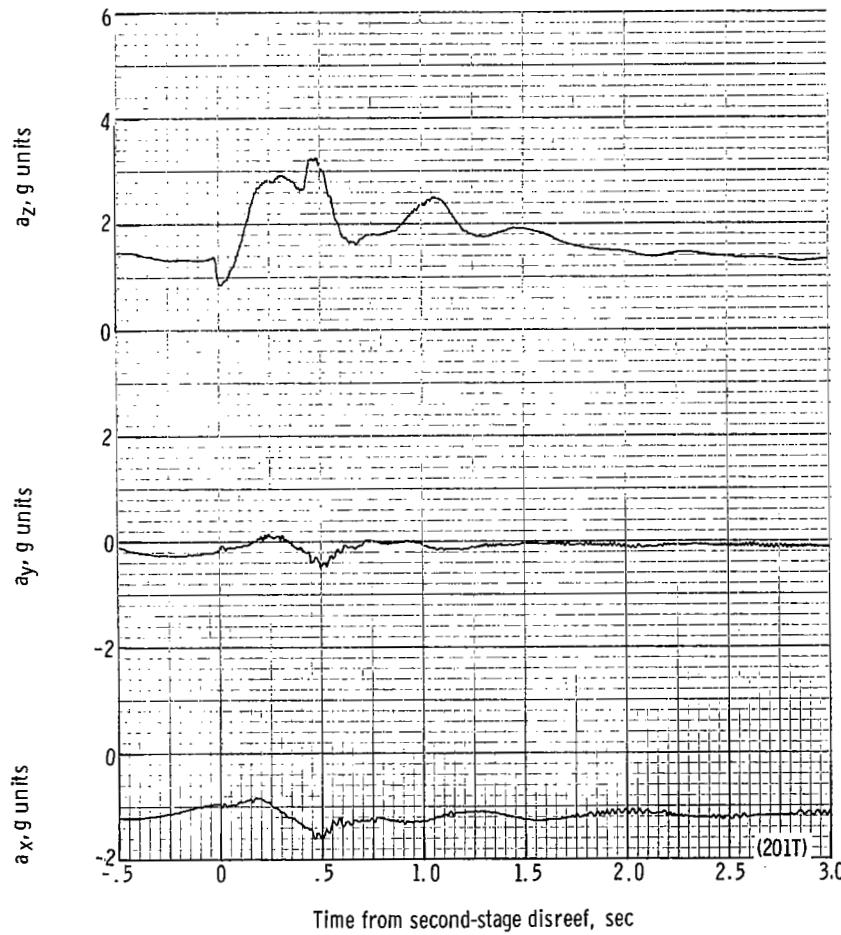
(k) Individual suspension-line loads F_{Lk12} , F_{Lle3} , F_{Lle1} , and F_{Lle6} plotted against time from second-stage disreef. Time = 0 second corresponds to 37.22 seconds after launch.

Figure 42.- Continued.



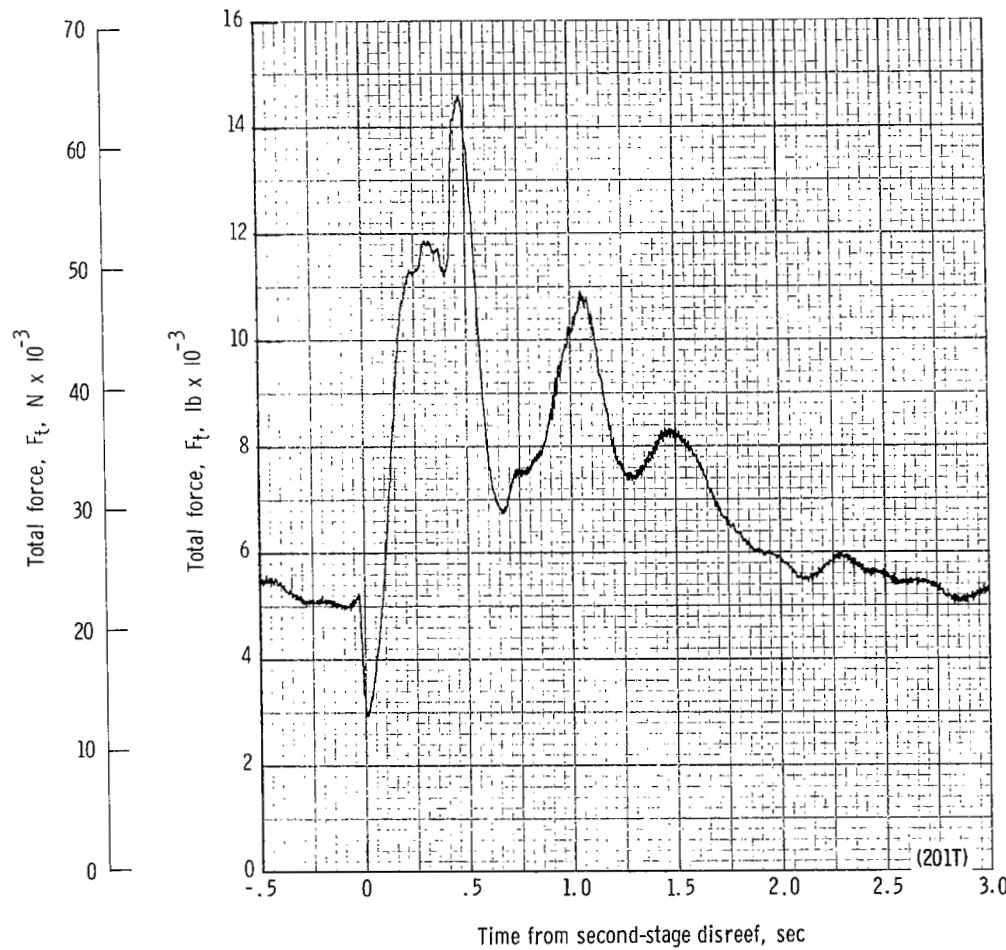
(II) Forward and aft riser loads plotted against time from second-stage disreef. Time = 0 second corresponds to 37.22 seconds after launch.

Figure 42.- Continued.



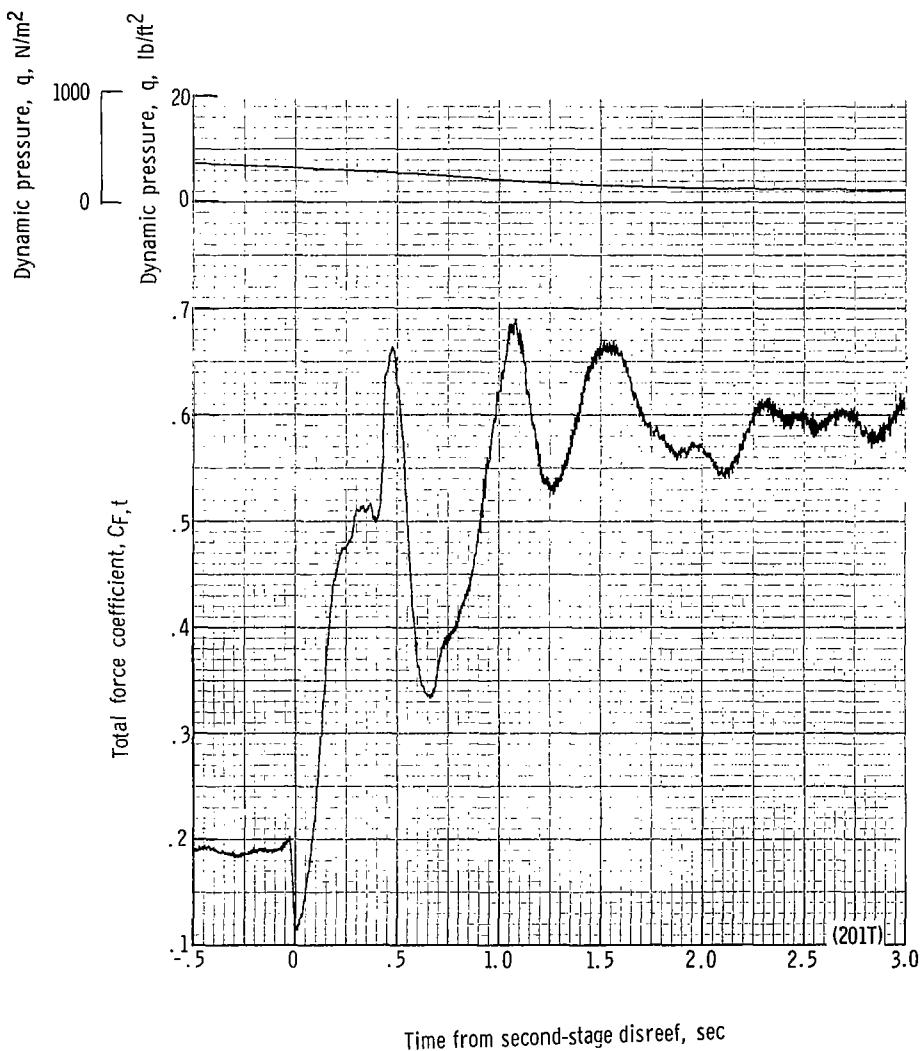
(m) Accelerations a_x , a_y , and a_z plotted against time from second-stage disreef. Time = 0 second corresponds to 37.22 seconds after launch.

Figure 42.- Continued.



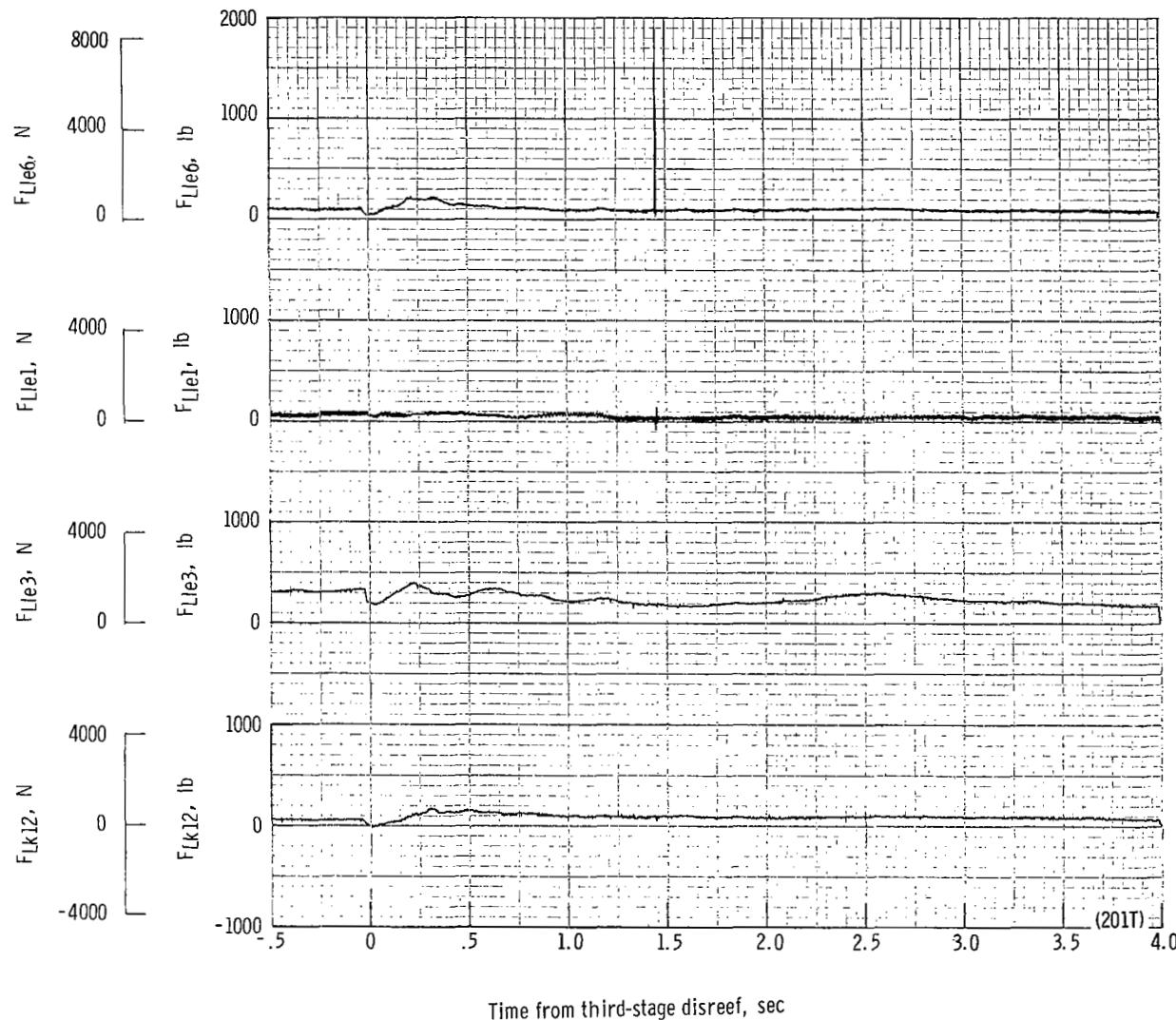
(n) Total force F_t plotted against time from second-stage disreef. Time = 0 second corresponds to 37.22 seconds after launch.

Figure 42.- Continued.



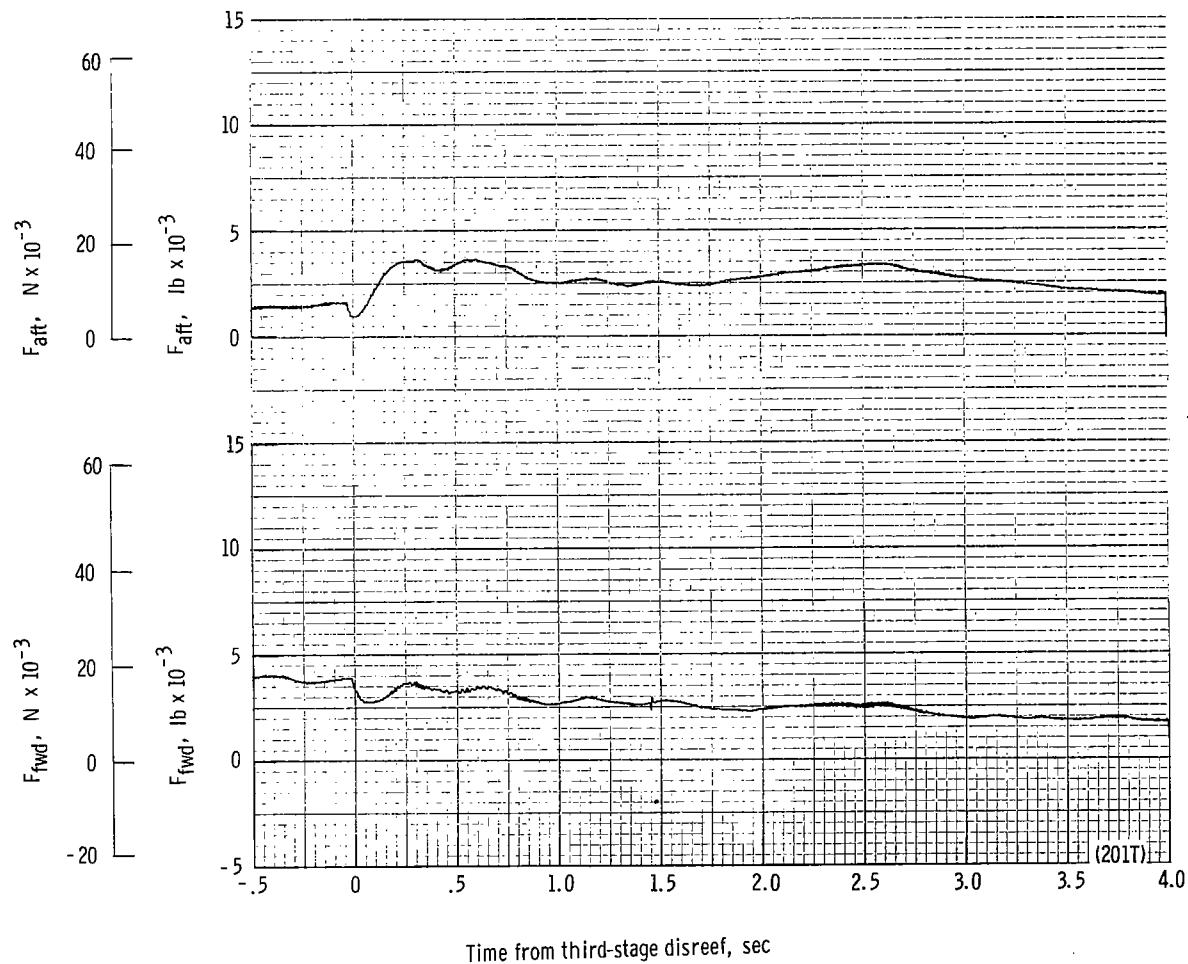
(o) Total force coefficient $C_{F,t}$ and dynamic pressure q plotted against time from second-stage disreef. Time = 0 second corresponds to 37.22 seconds after launch.

Figure 42.- Continued.



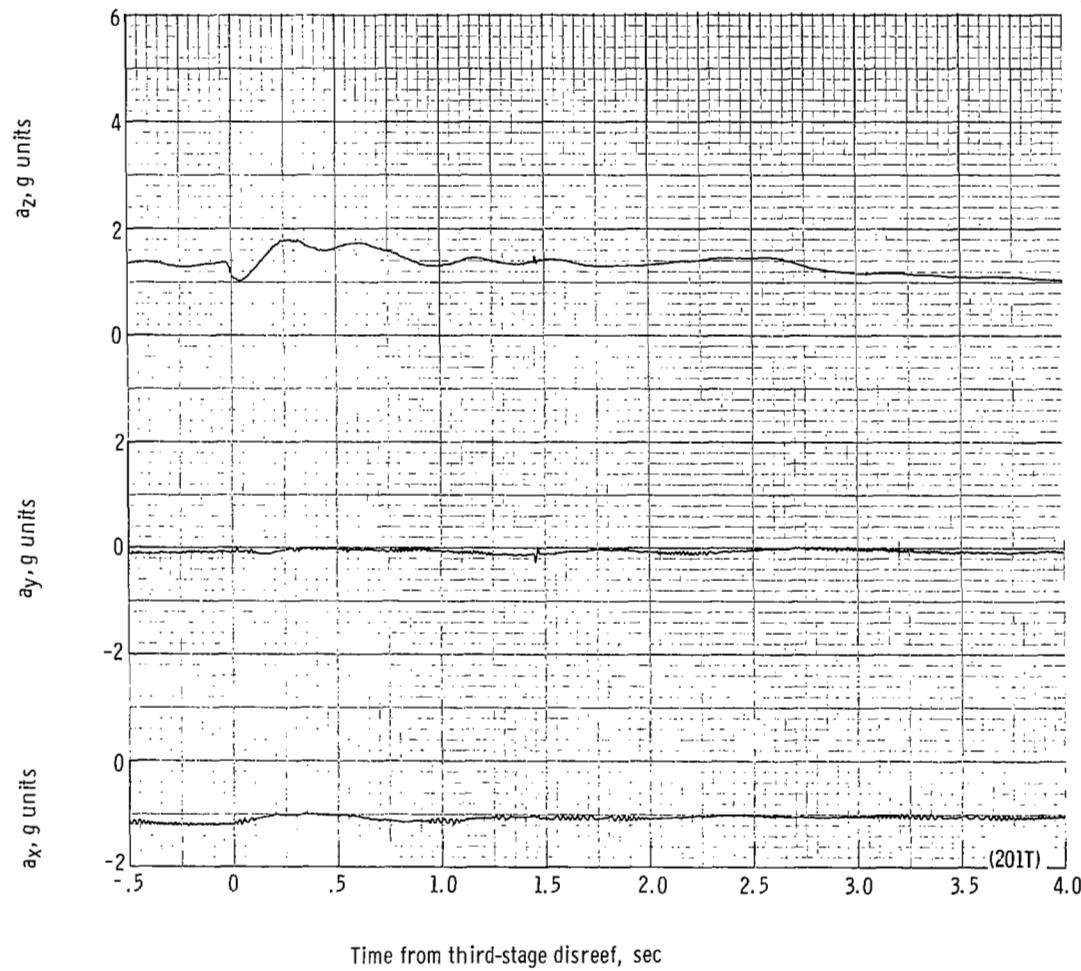
(p) Individual suspension-line loads F_{Lk12} , F_{Lle3} , F_{Lle1} , and F_{Lle6} plotted against time from third-stage disreef. Time = 0 second corresponds to 40.71 seconds after launch.

Figure 42.- Continued.



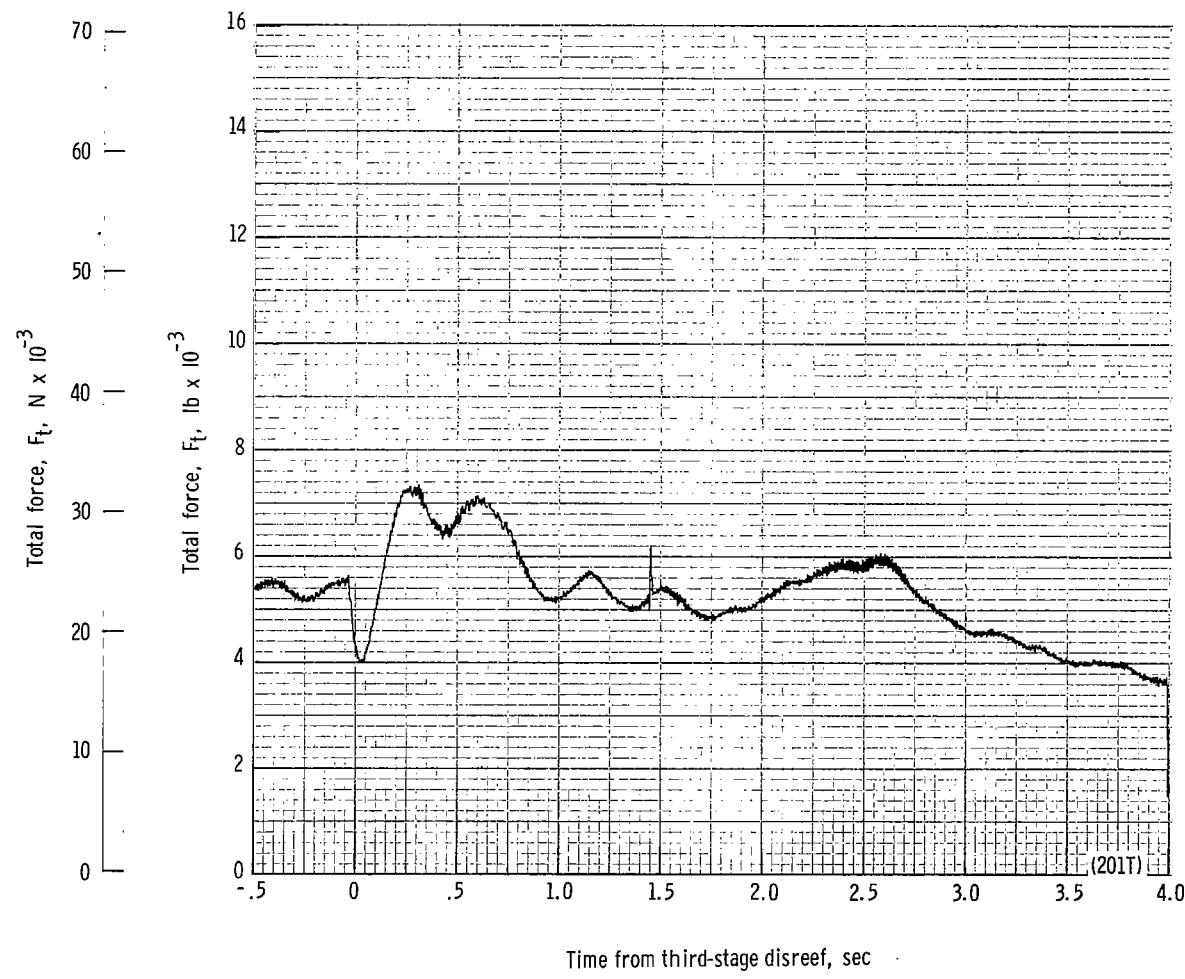
(q) Forward and aft riser loads plotted against time from third-stage disreef. Time = 0 second corresponds to 40.71 seconds after launch.

Figure 42.- Continued.



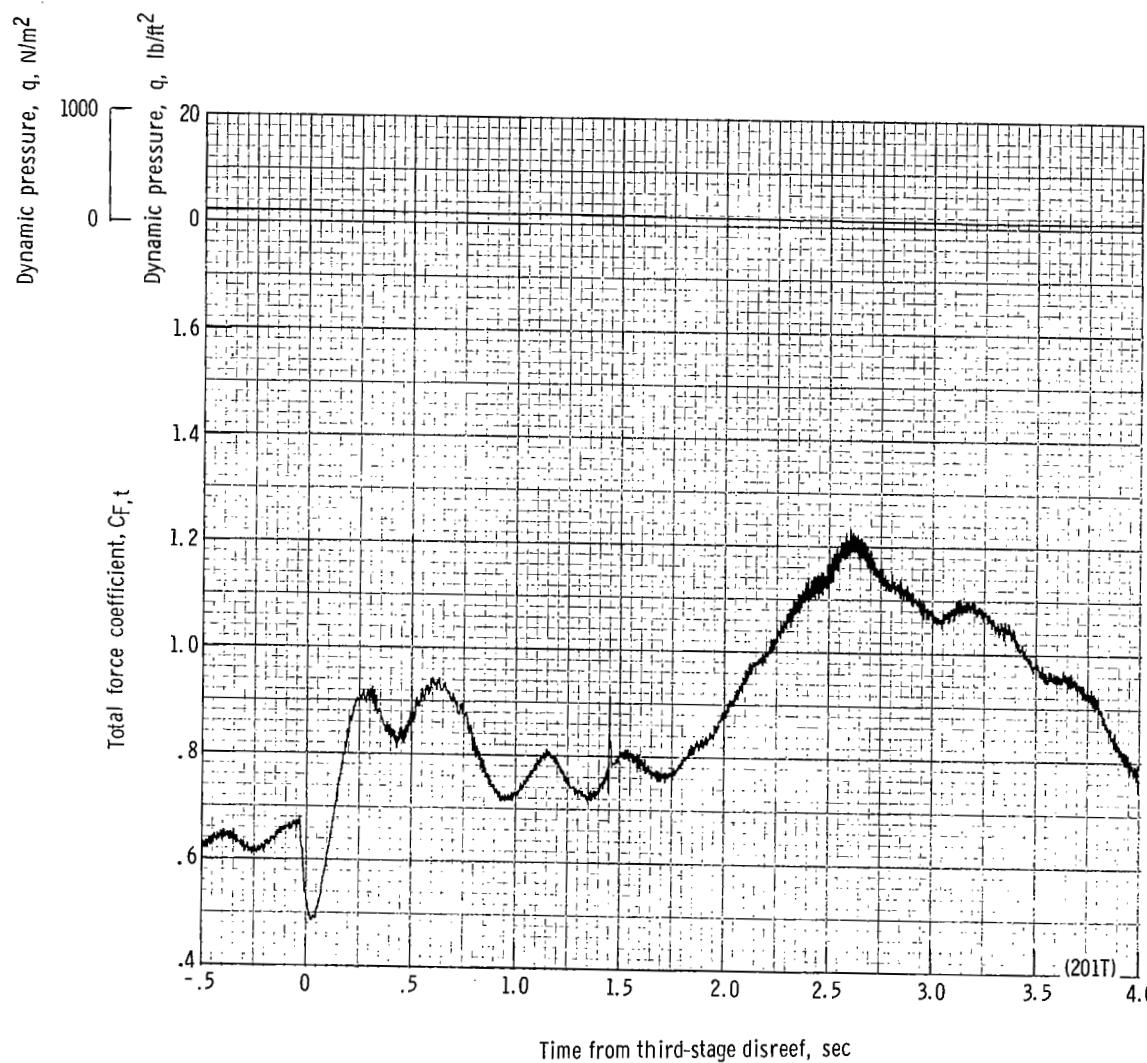
(r) Accelerations a_x , a_y , and a_z plotted against time from third-stage disreef. Time = 0 second corresponds to 40.71 seconds after launch.

Figure 42.- Continued.



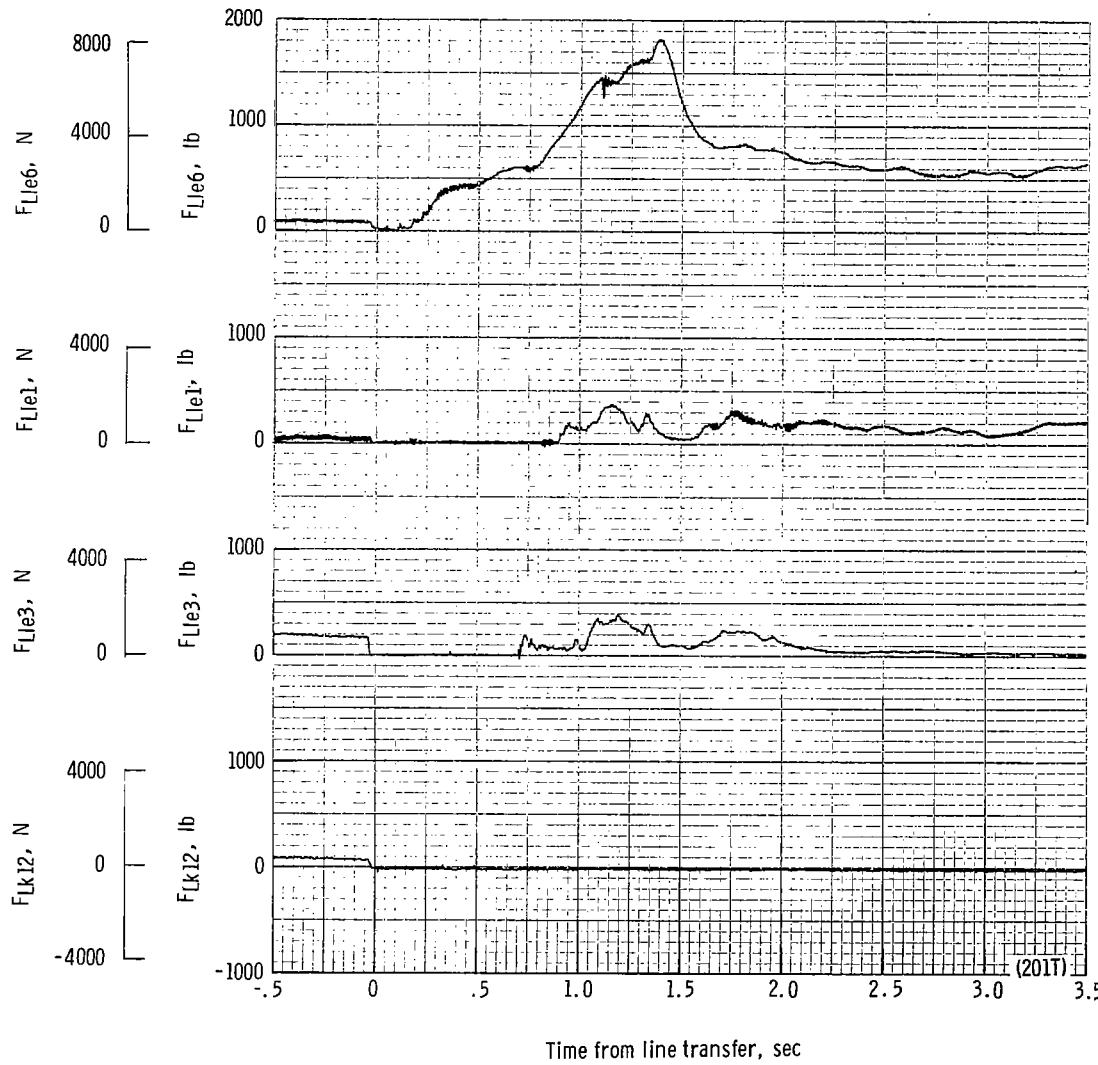
(s) Total force F_t plotted against time from third-stage disreef. Time = 0 second corresponds to 40.71 seconds after launch.

Figure 42.- Continued.



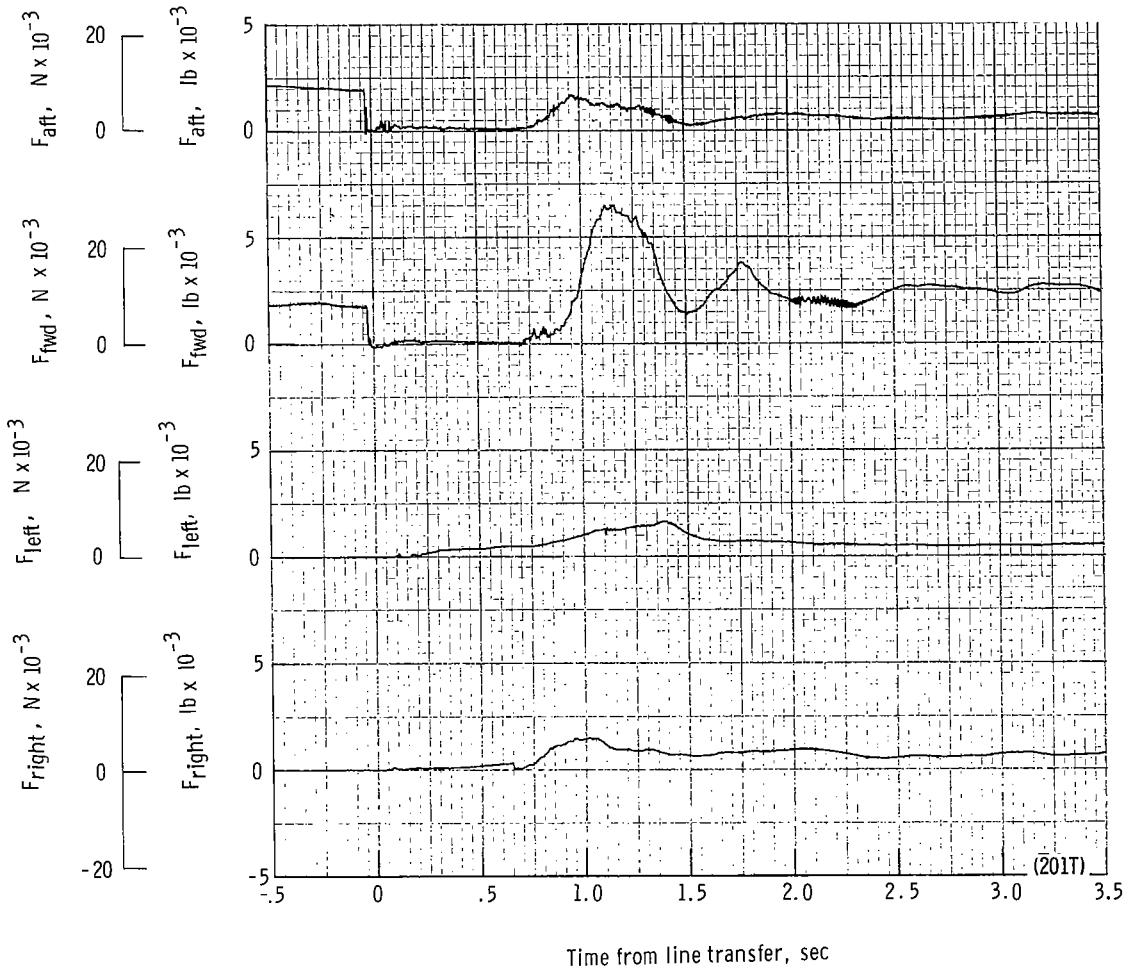
(t) Total force coefficient $C_{F,t}$ and dynamic pressure q plotted against time from third-stage disreef. Time = 0 second corresponds to 40.71 seconds after launch.

Figure 42.- Continued.



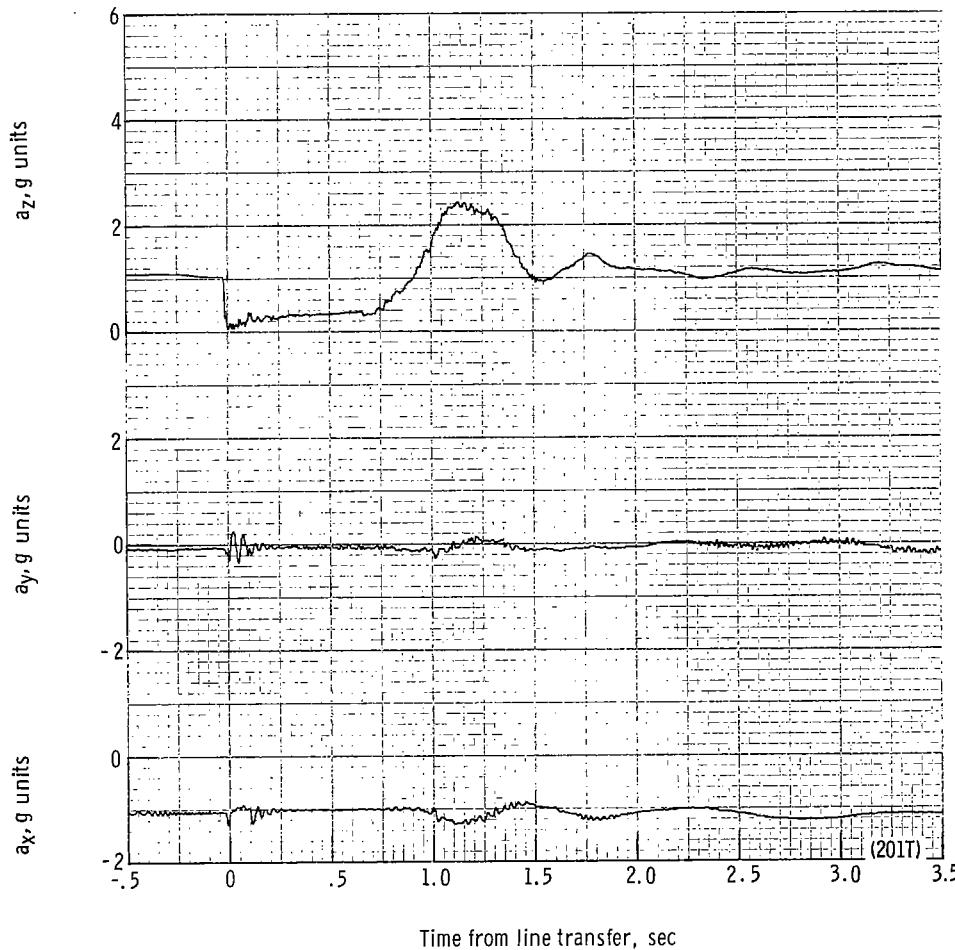
(u) Individual suspension-line loads F_{Lk12} , F_{Lle3} , F_{Lle1} , and F_{Lle6} plotted against time from line transfer. Time = 0 second corresponds to 44.74 seconds after launch.

Figure 42.- Continued.



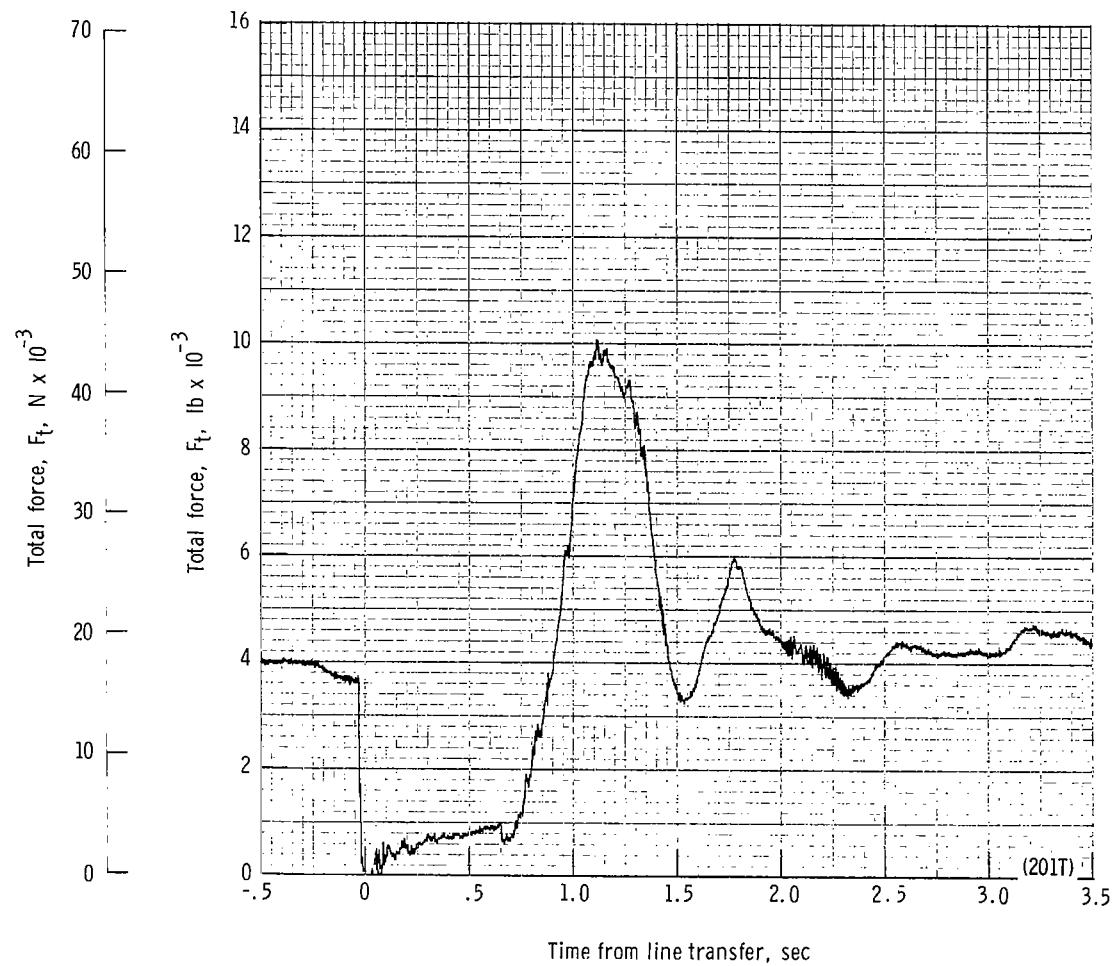
(v) Right, left, forward, and aft riser loads plotted against time from line transfer. Time = 0 second corresponds to 44.74 seconds after launch.

Figure 42.- Continued.



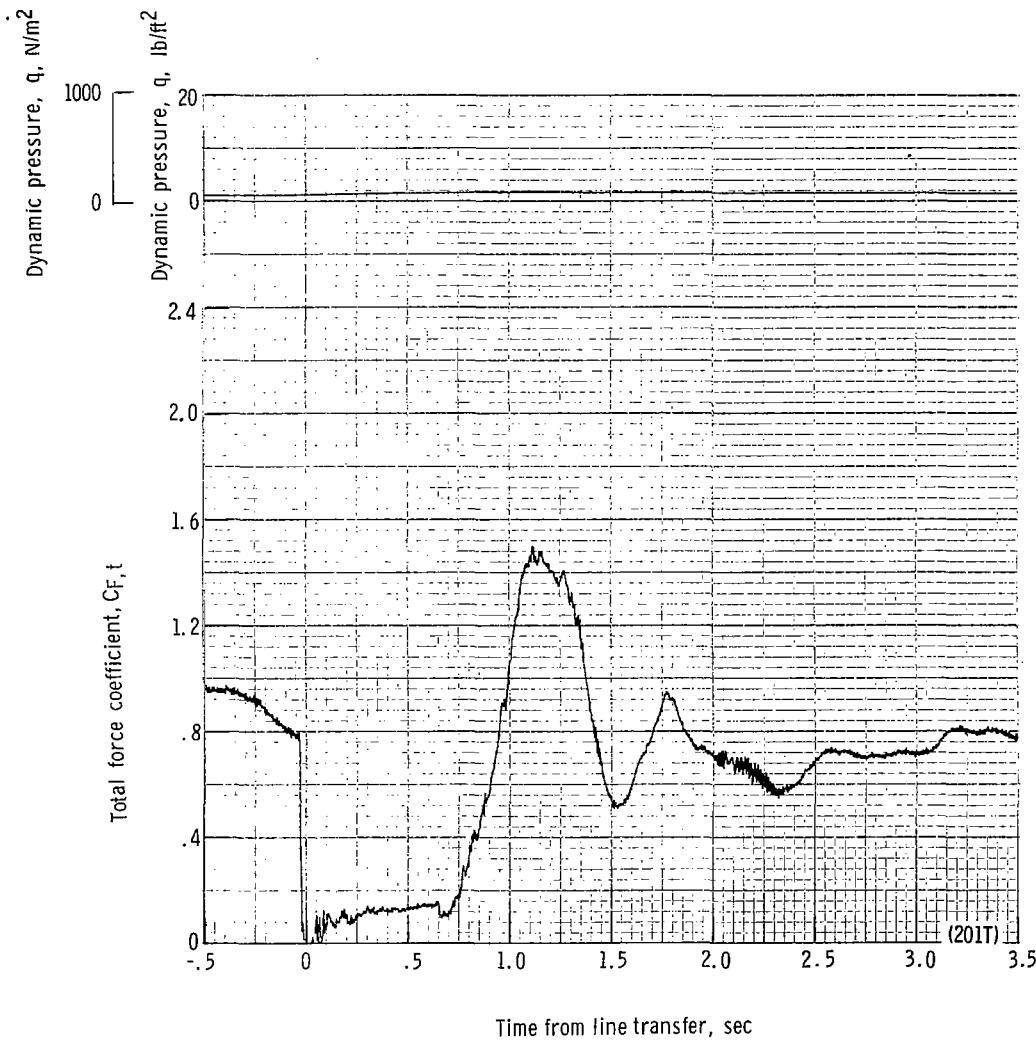
(w) Accelerations a_x , a_y , and a_z plotted against time from line transfer. Time = 0 second corresponds to 44.74 seconds after launch.

Figure 42.- Continued.



(x) Total force F_t plotted against time from line transfer. Time = 0 second corresponds to 44.74 seconds after launch.

Figure 42.- Continued.



(y) Total force coefficient $C_{F,t}$ and dynamic pressure q plotted against time from line transfer. Time = 0 second corresponds to 44.74 seconds after launch.

Figure 42.- Continued.

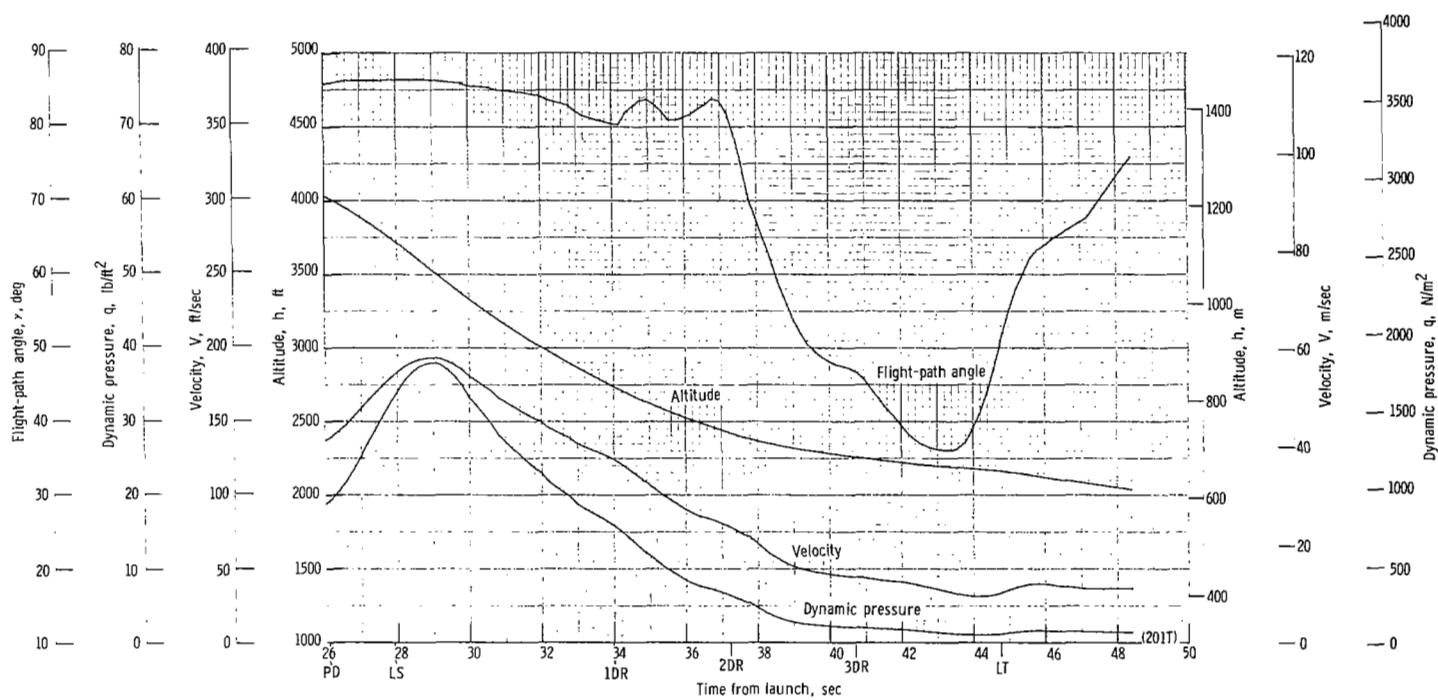
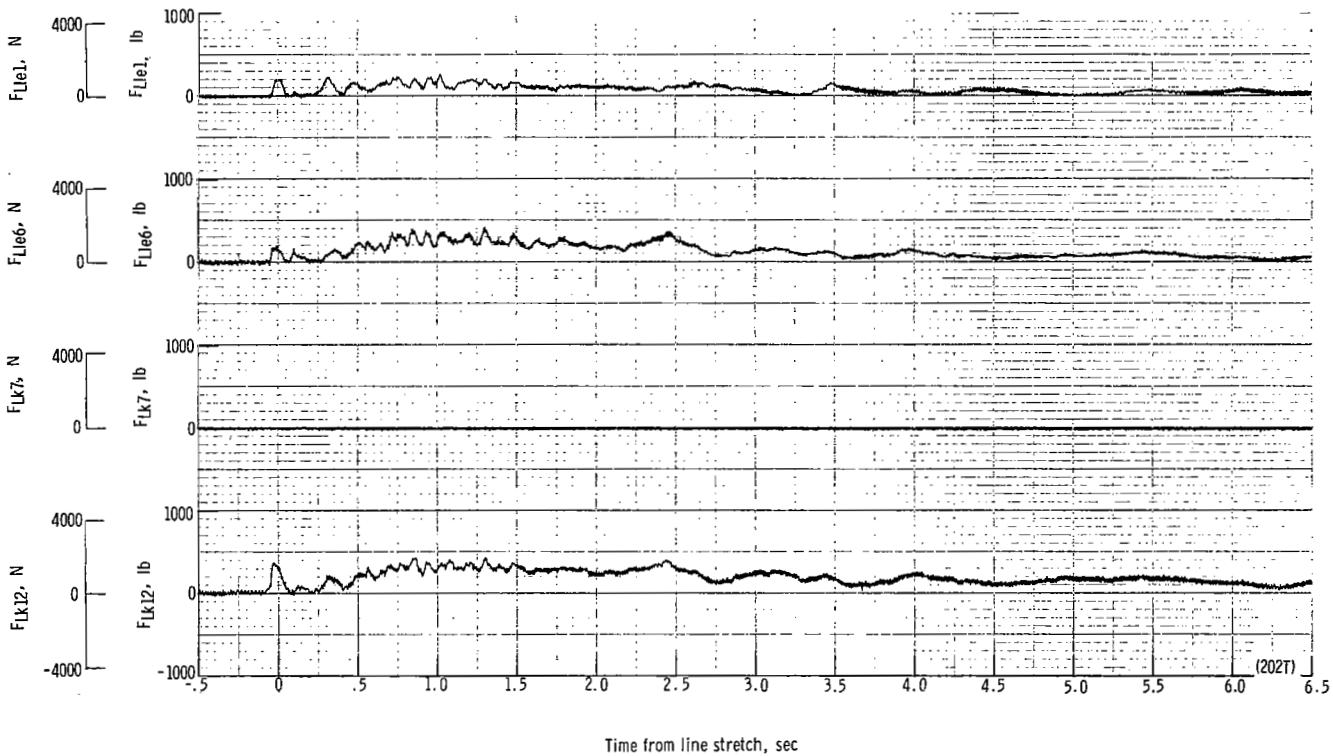
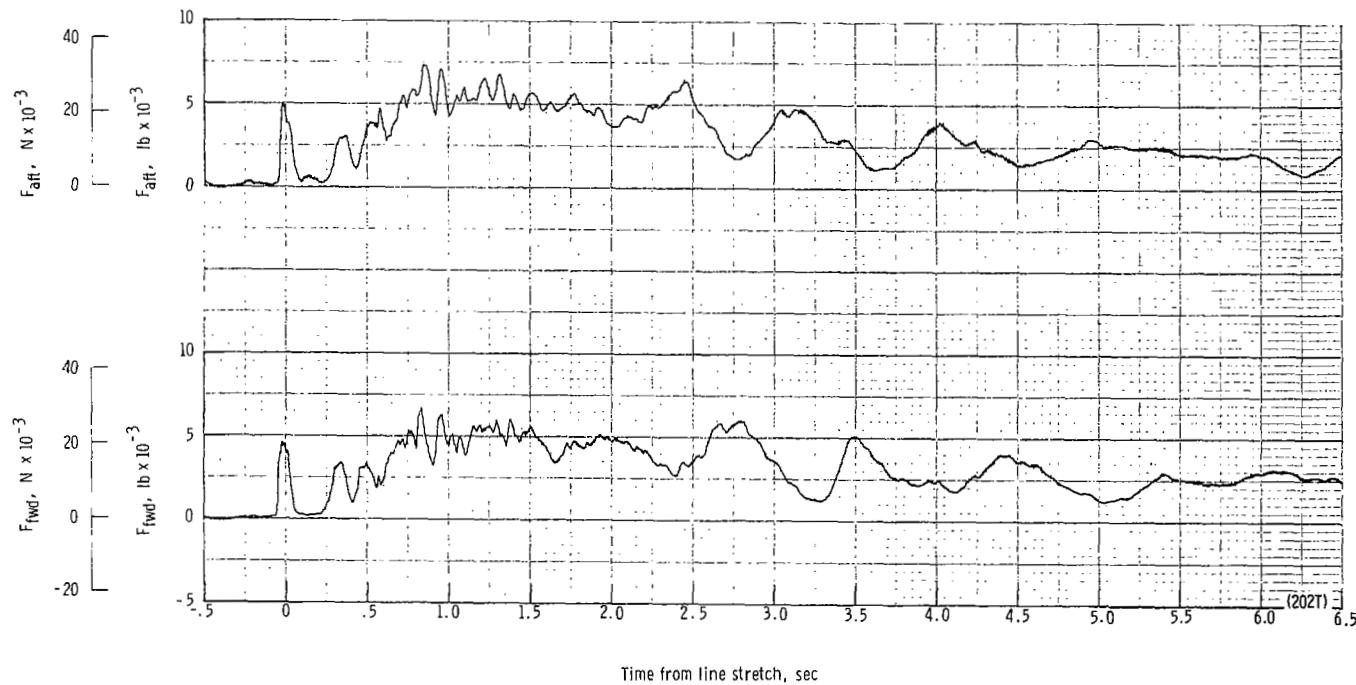
(z) Flight-path angle γ , dynamic pressure q , velocity V , and altitude h plotted against time from launch.

Figure 42.- Concluded.



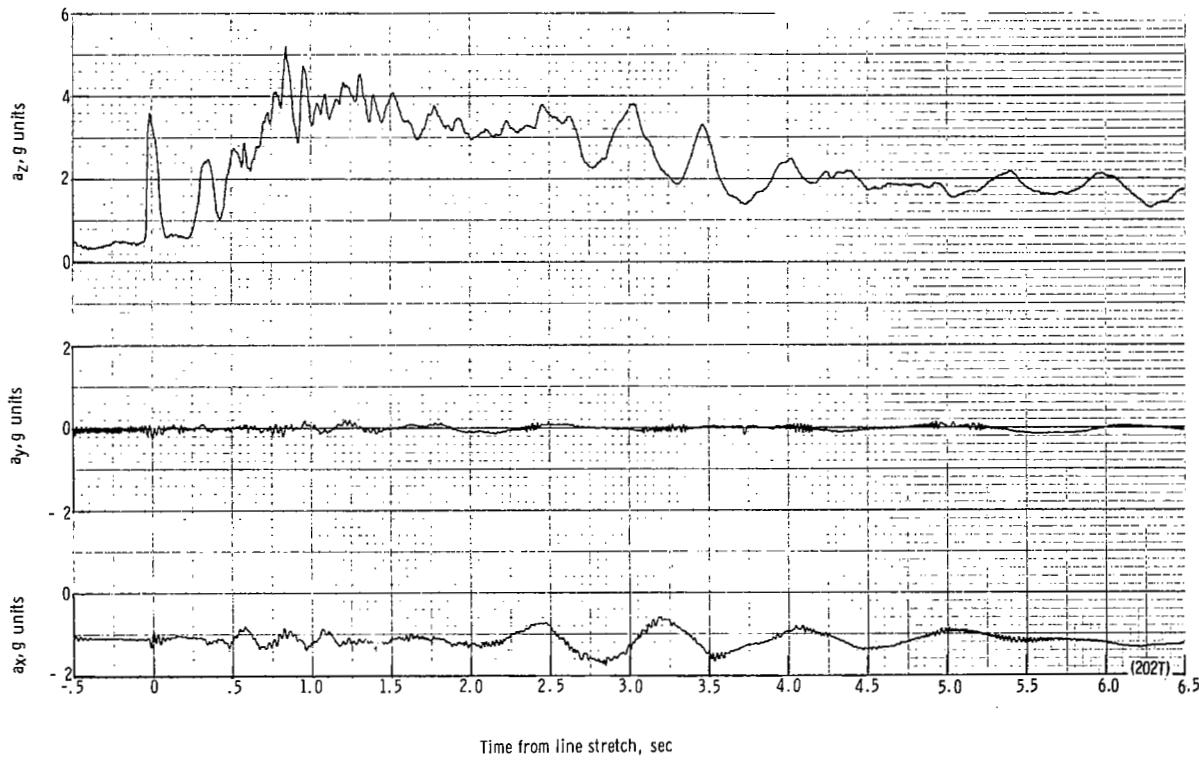
(a) Individual suspension-line loads F_{Lk12} , F_{Lk7} , F_{Lle6} , and F_{Lle1} plotted against time from line stretch. Time = 0 second corresponds to 28.69 seconds after launch.

Figure 43.- Time history of twin-keel parawing deployment data for test 202T. $W_D = 16\ 868\ N$ (3792 lb); $W_p = 15\ 320\ N$ (3444 lb); $q_{PD} = 2734.0\ N/m^2$ (57.1 lb/ft²); $h_{PD} = 4444\ m$ (14 580 ft); $l_r/l_k = 0.100$; reefing version A.



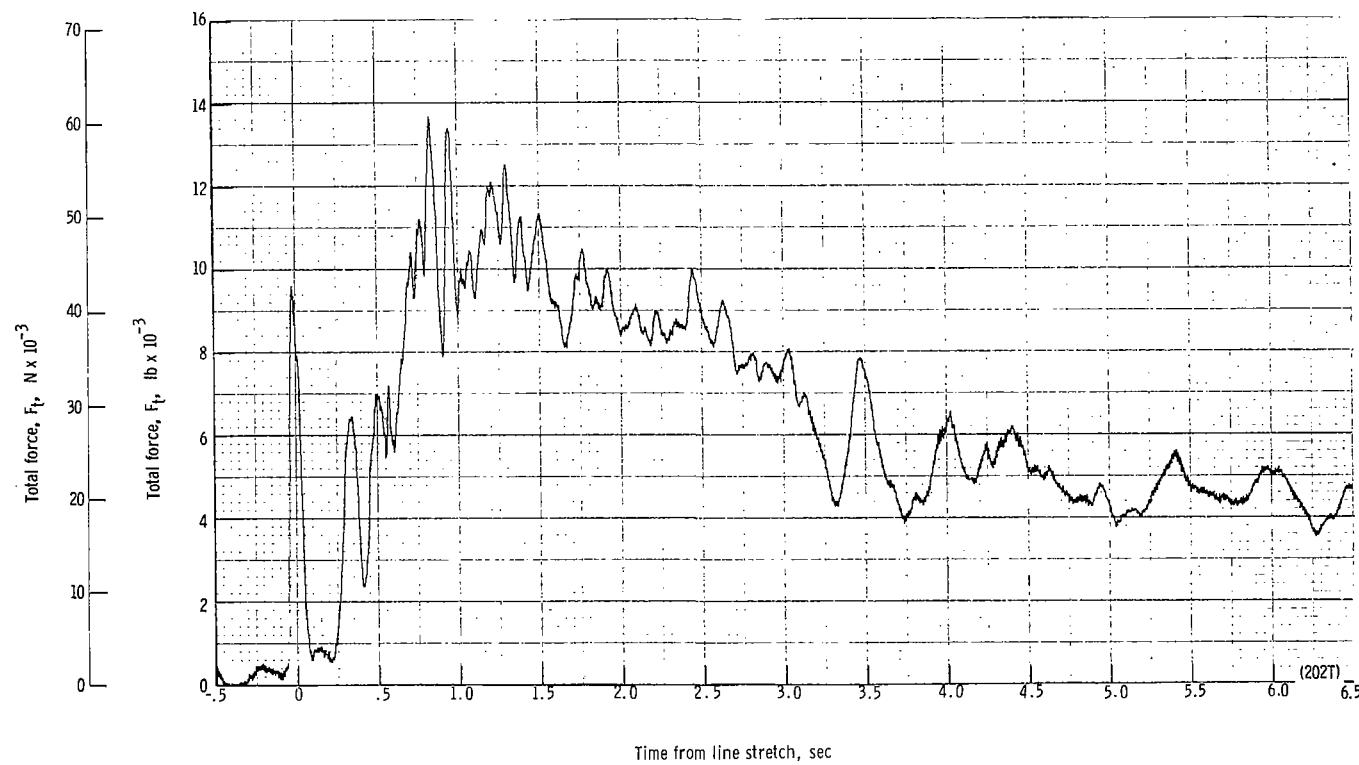
(b) Forward and aft riser loads plotted against time from line stretch. Time = 0 second corresponds to 28.69 seconds after launch.

Figure 43.- Continued.



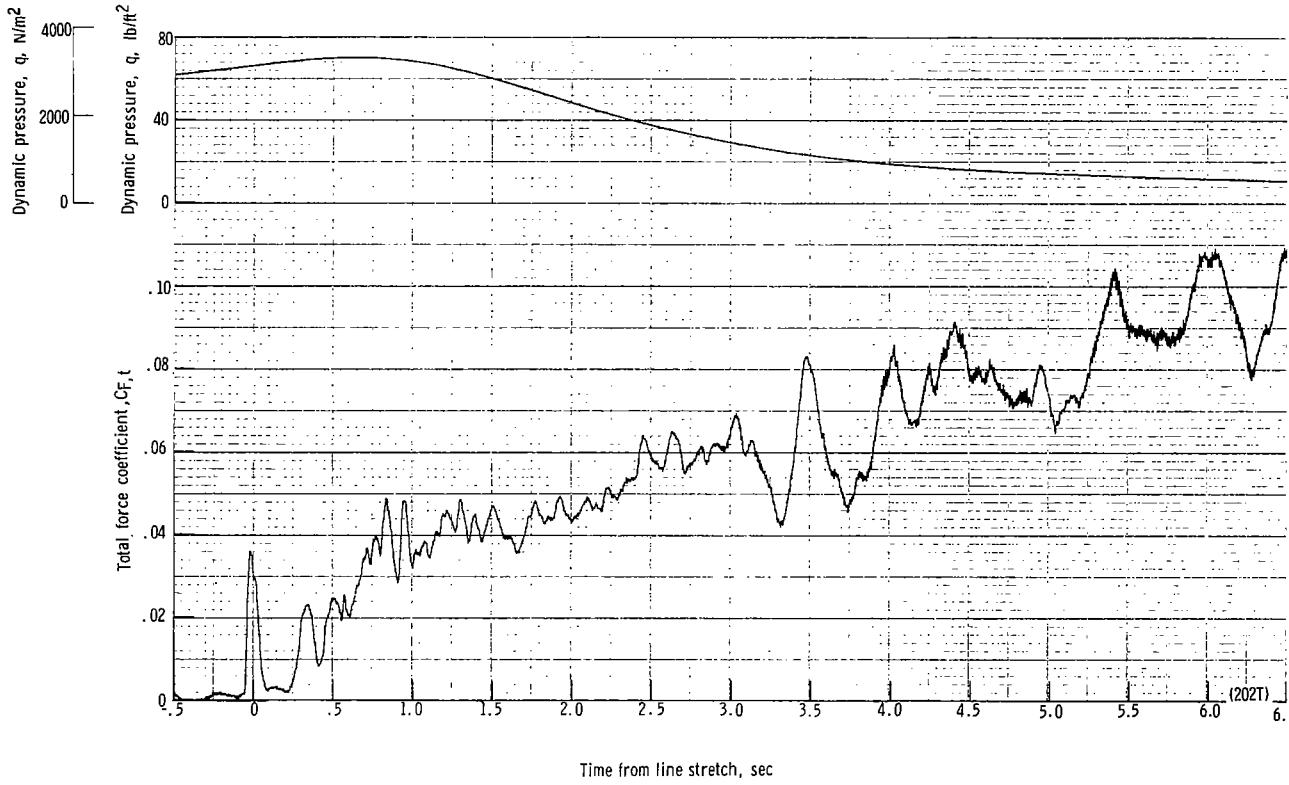
(c) Accelerations a_x , a_y , and a_z plotted against time from line stretch. Time = 0 second corresponds to 28.69 seconds after launch.

Figure 43.- Continued.



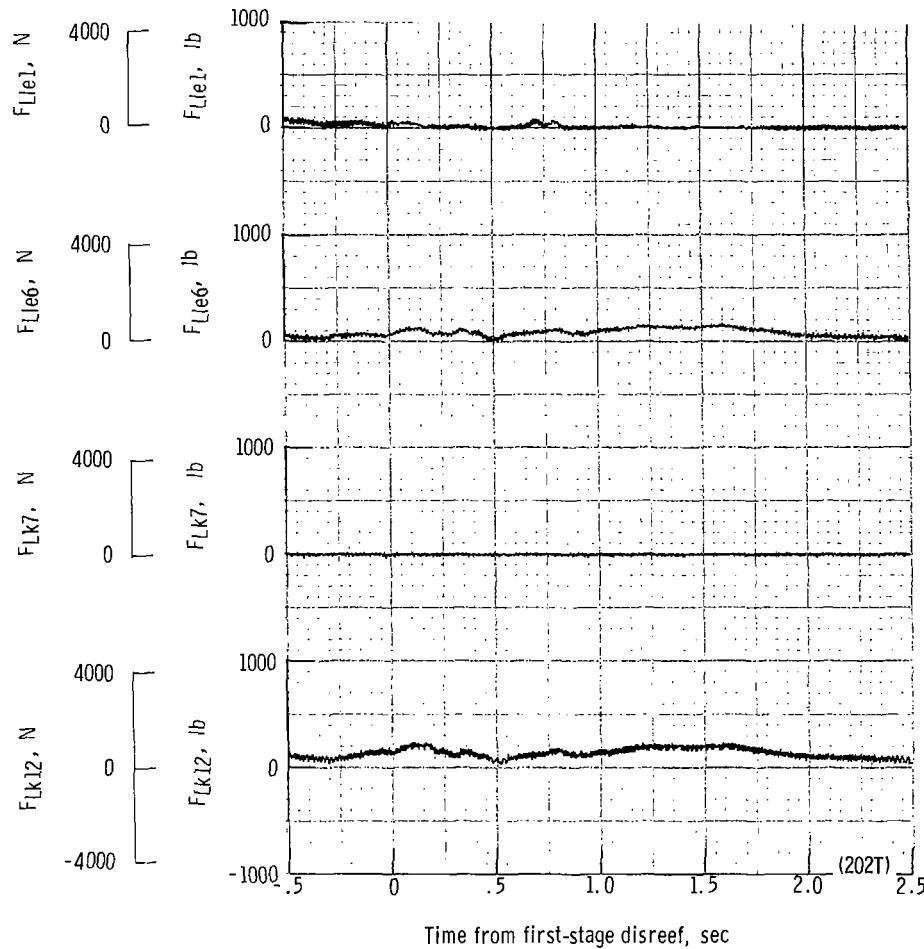
(d) Total force F_t plotted against time from line stretch. Time = 0 second corresponds to 28.69 seconds after launch.

Figure 43.- Continued.



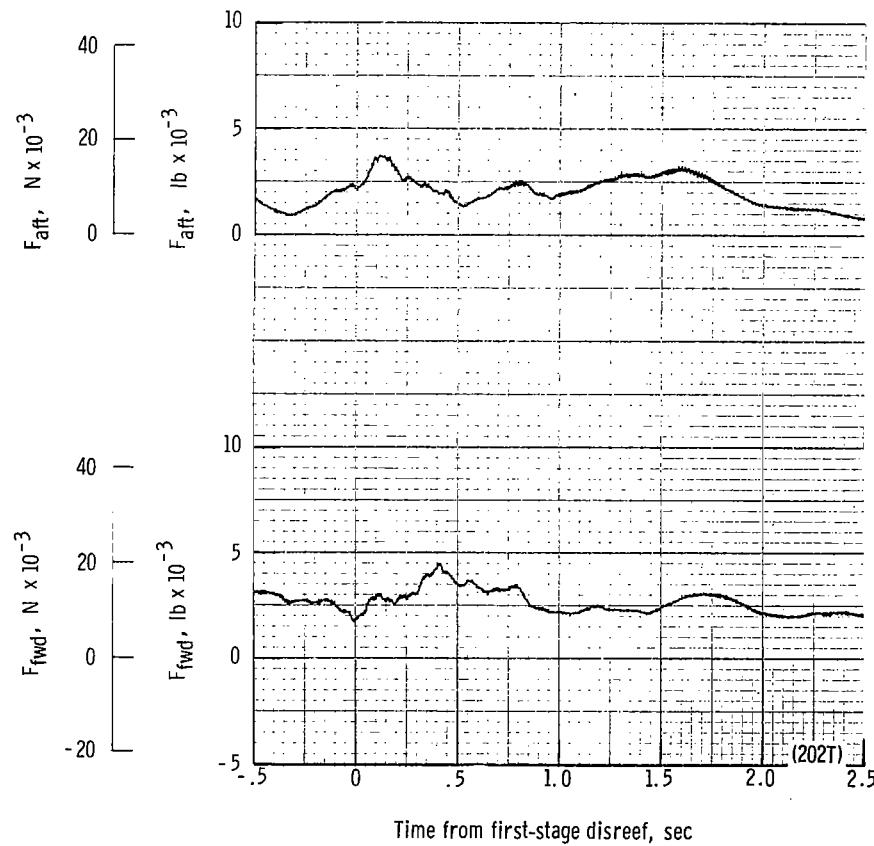
(e) Total force coefficient $C_{F,t}$ and dynamic pressure q plotted against time from line stretch. Time = 0 second corresponds to 28.69 seconds after launch.

Figure 43.- Continued.



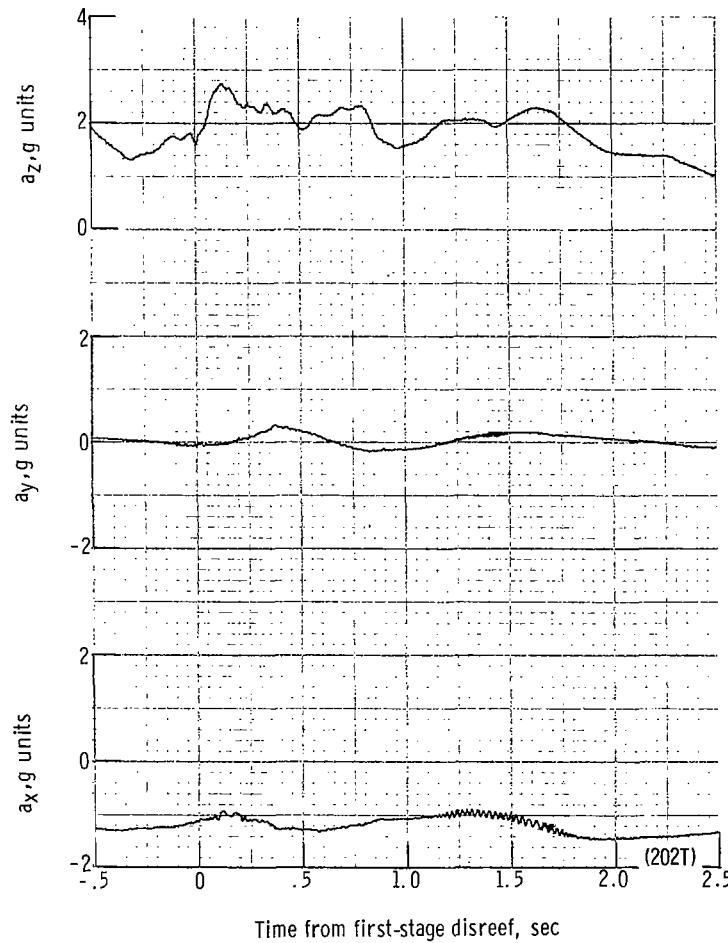
(f) Individual suspension-line loads F_{Lk12} , F_{Lk7} , F_{Lle6} , and F_{Lle1} plotted against time from first-stage disreef.
Time = 0 second corresponds to 35.29 seconds after launch.

Figure 43.- Continued.



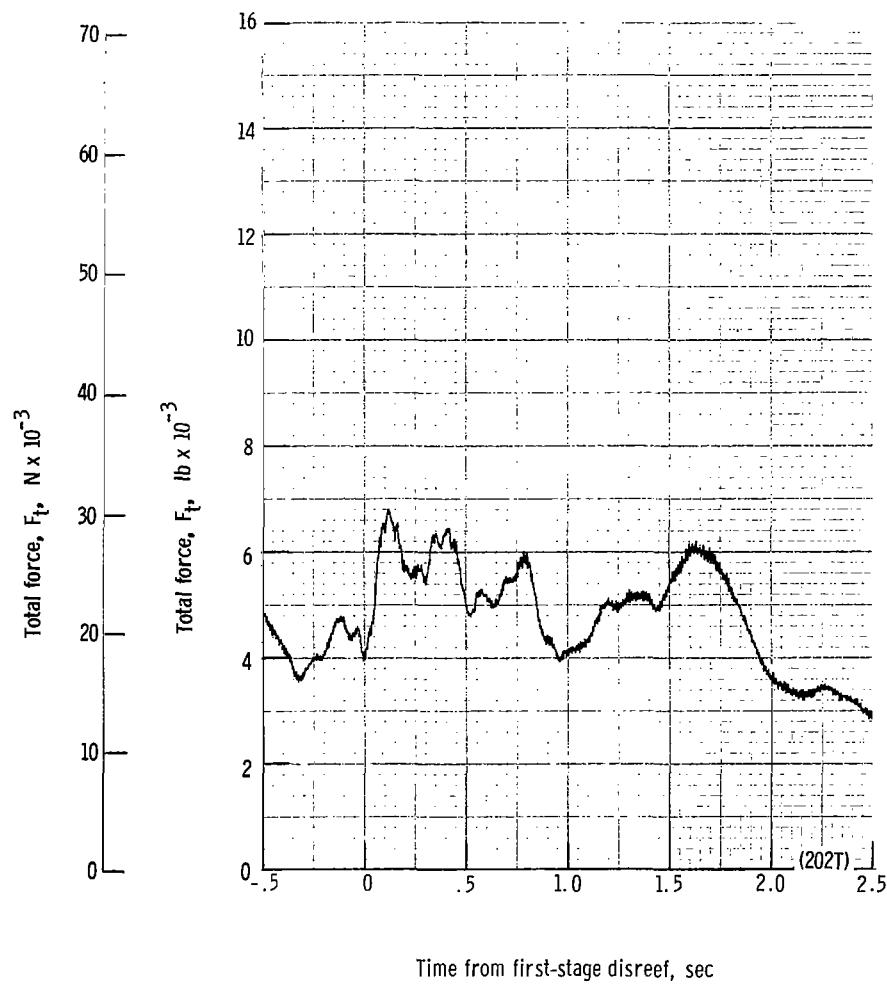
(g) Forward and aft riser loads plotted against time from first-stage disreef. Time = 0 second corresponds to 35.29 seconds after launch.

Figure 43.- Continued.



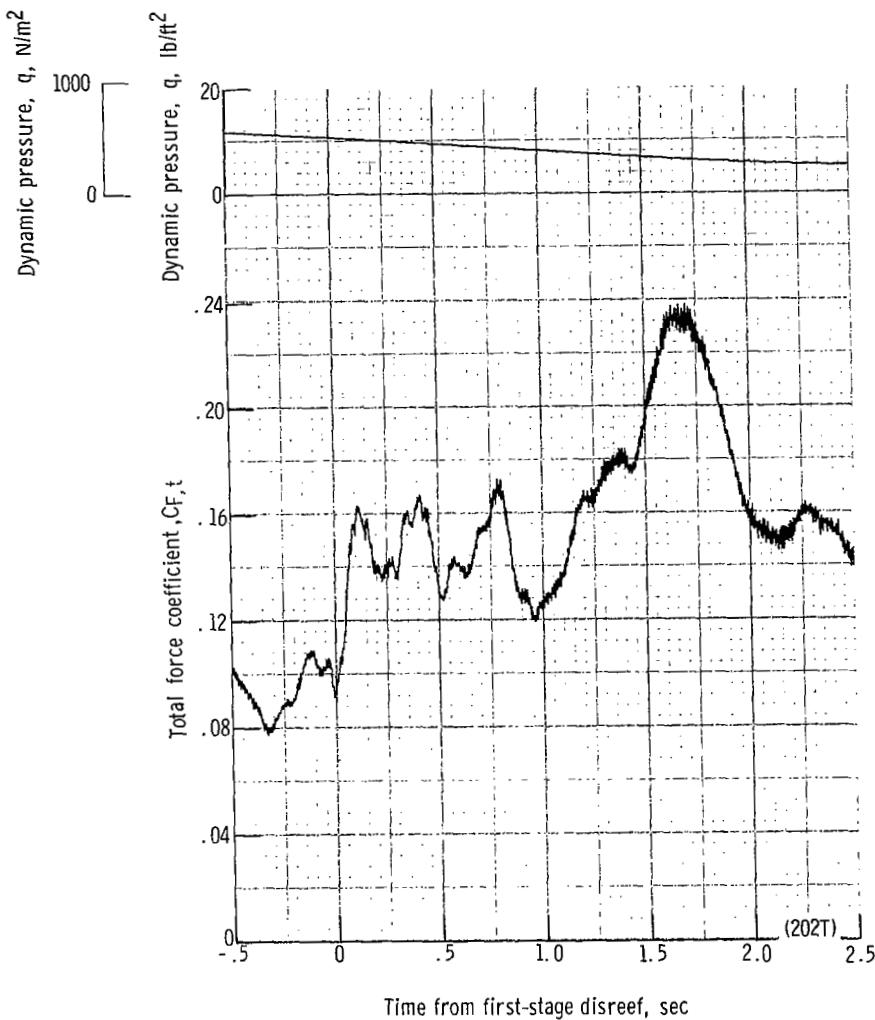
(h) Accelerations a_x , a_y , and a_z plotted against time from first-stage disreef. Time = 0 second corresponds to 35.29 seconds after launch.

Figure 43.- Continued.



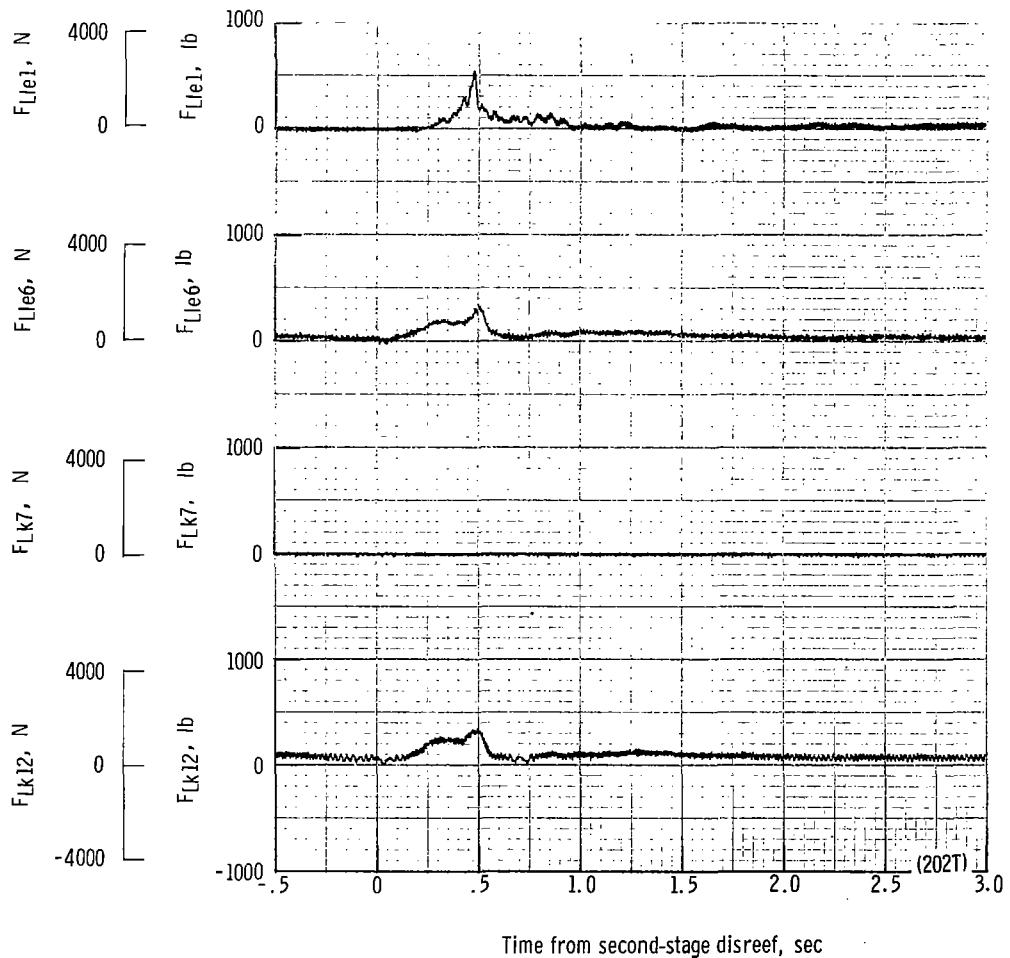
(ii) Total force F_t plotted against time from first-stage disreef. Time = 0 second corresponds to 35.29 seconds after launch.

Figure 43.- Continued.



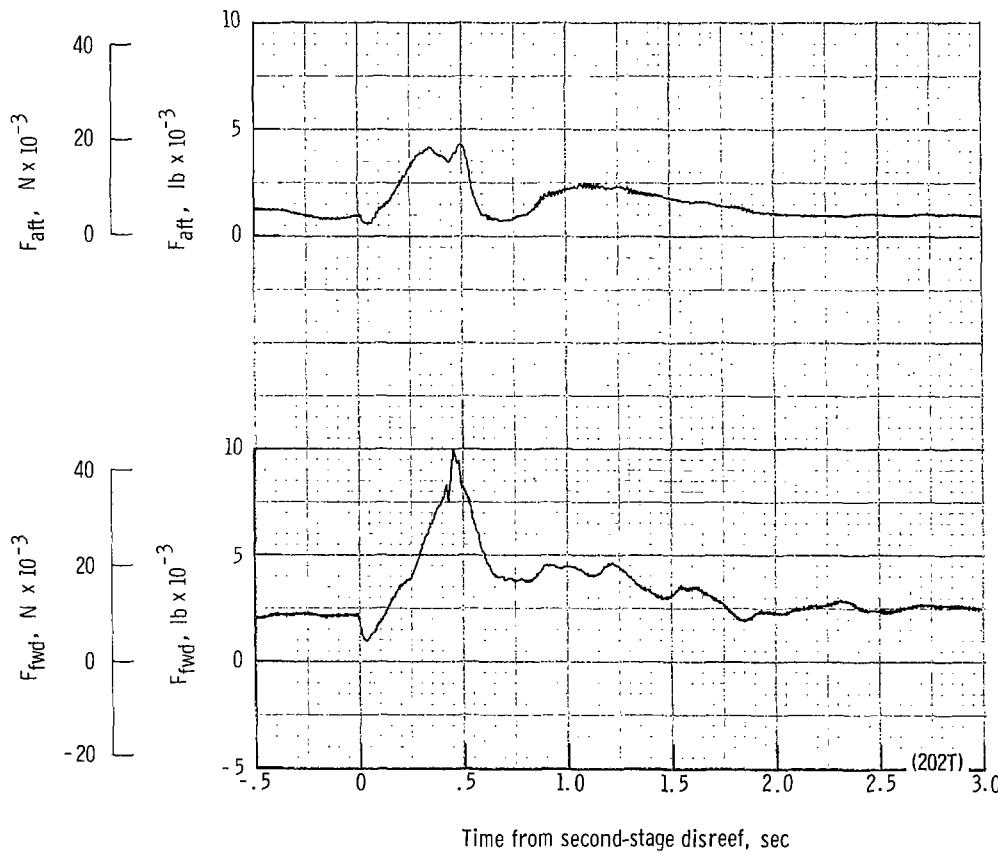
(j) Total force coefficient $C_{F,t}$ and dynamic pressure q plotted against time from first-stage disreef. Time = 0 second corresponds to 35.29 seconds after launch.

Figure 43.- Continued.



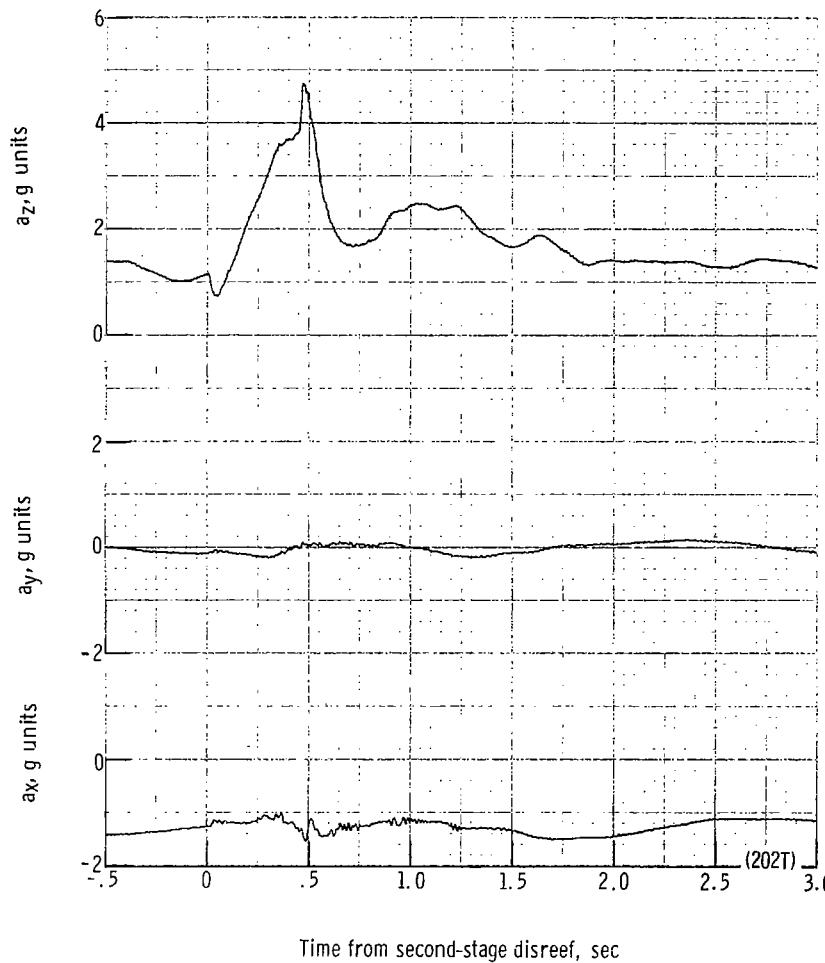
(k) Individual suspension-line loads F_{Lk12} , F_{Lk7} , F_{Lle6} , and F_{Lle1} plotted against time from second-stage disreef. Time = 0 second corresponds to 37.94 seconds after launch.

Figure 43.- Continued.



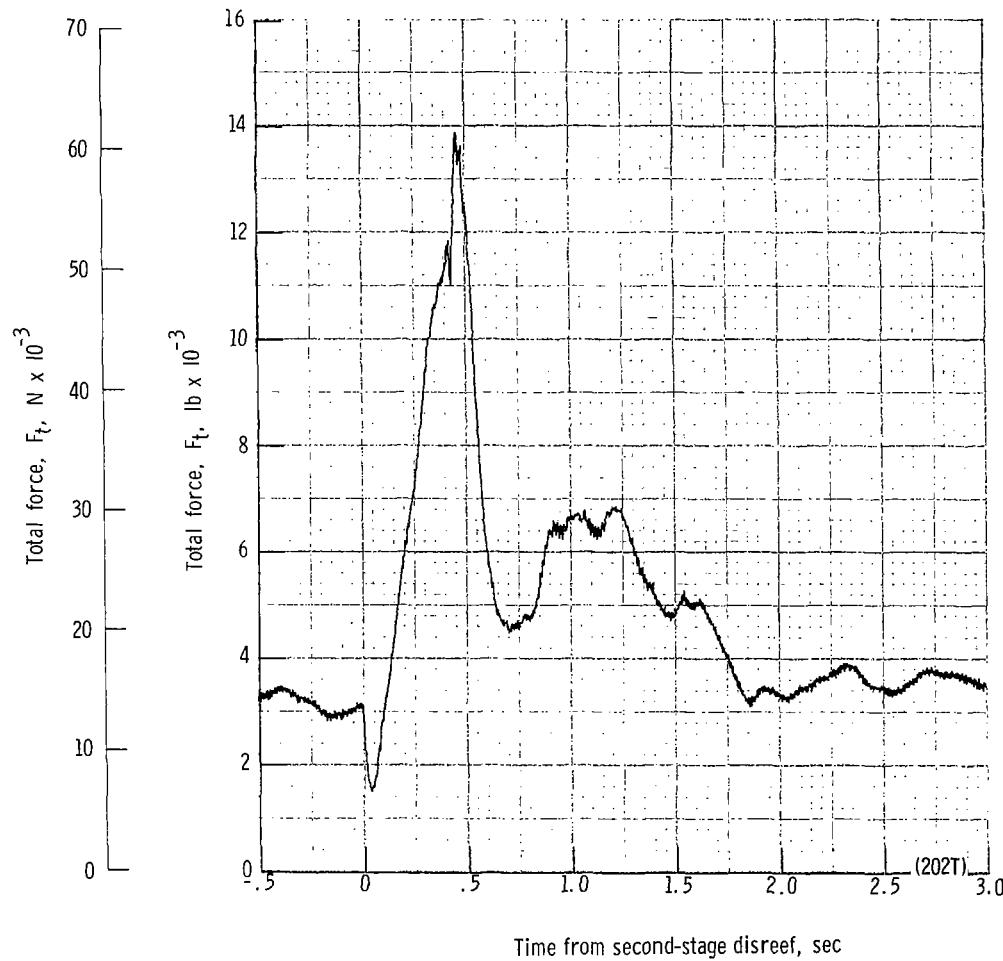
(l) Forward and aft riser loads plotted against time from second-stage disreef. Time = 0 second corresponds to 37.94 seconds after launch.

Figure 43.- Continued.



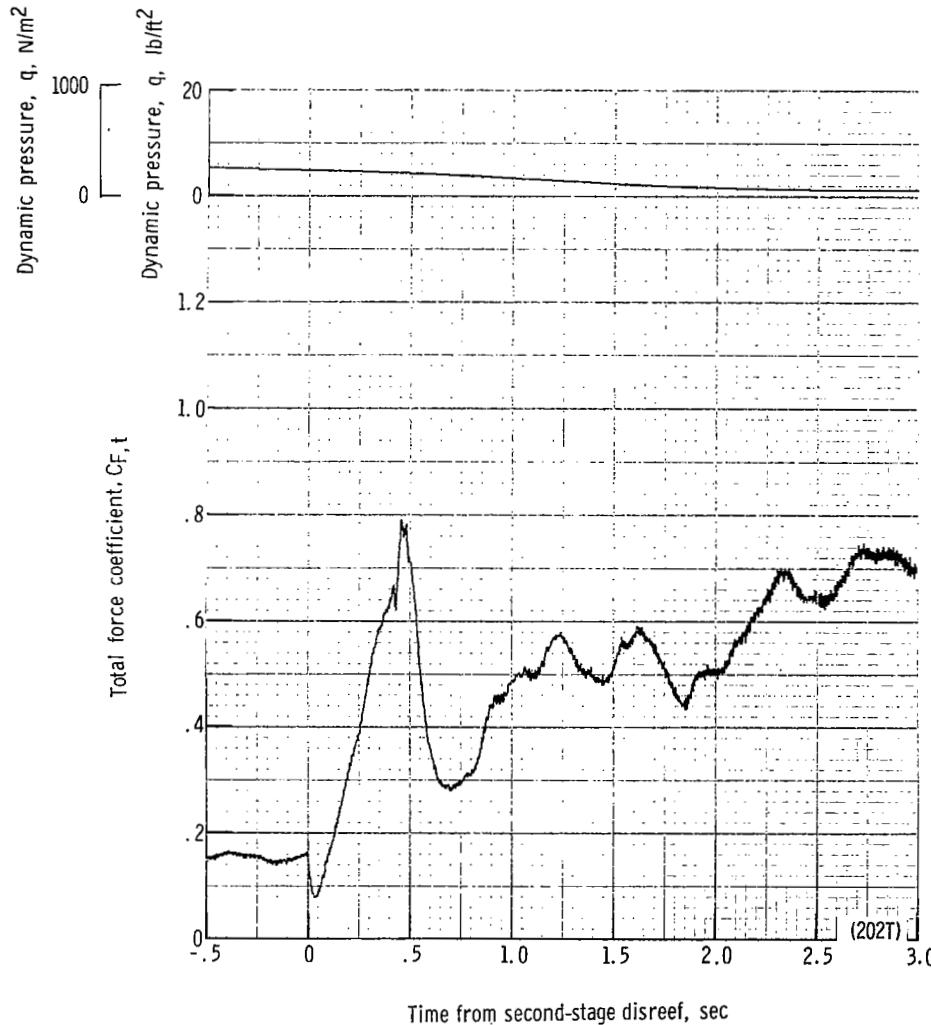
(m) Accelerations a_x , a_y , and a_z plotted against time from second-stage disreef. Time = 0 second corresponds to 37.94 seconds after launch.

Figure 43.- Continued.



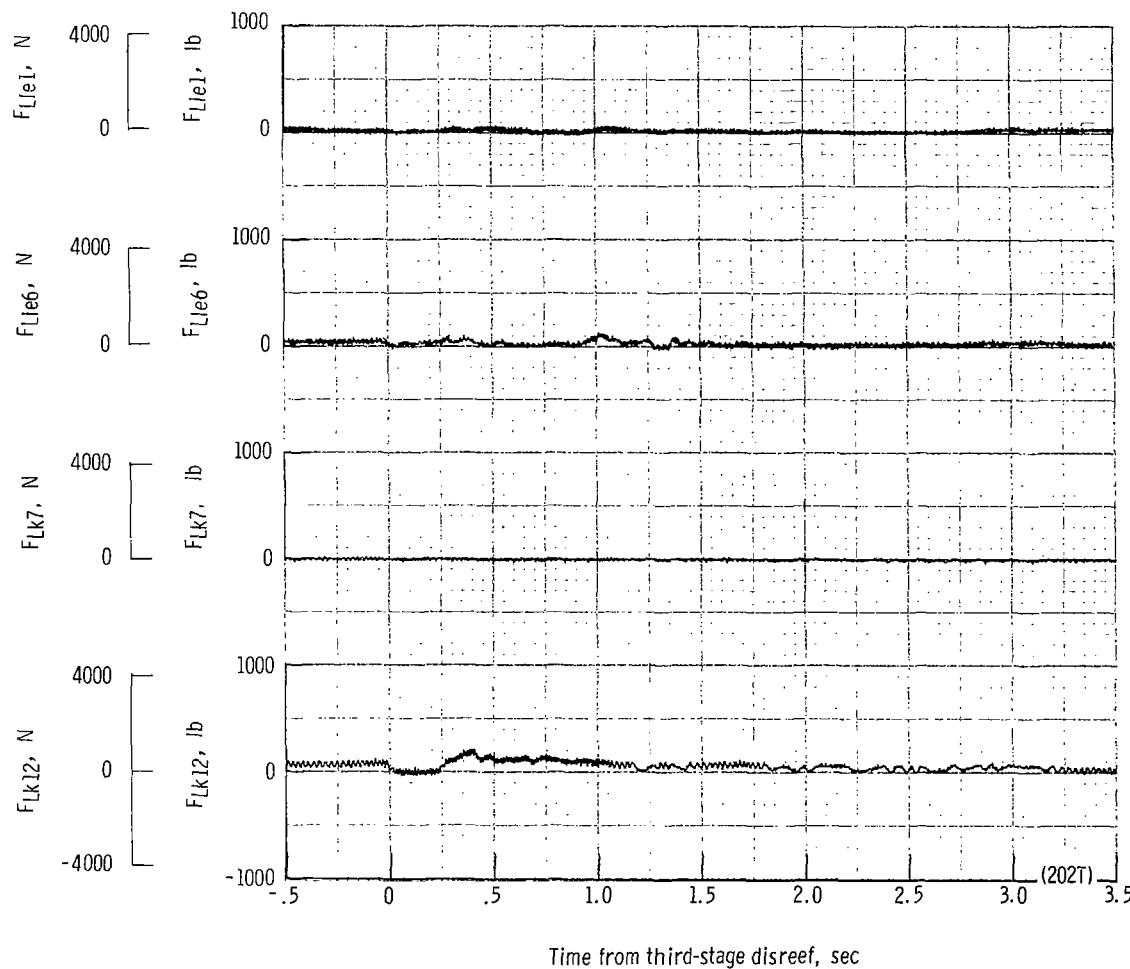
(n) Total force F_t plotted against time from second-stage disreef. Time = 0 second corresponds to 37.94 seconds after launch.

Figure 43.- Continued.



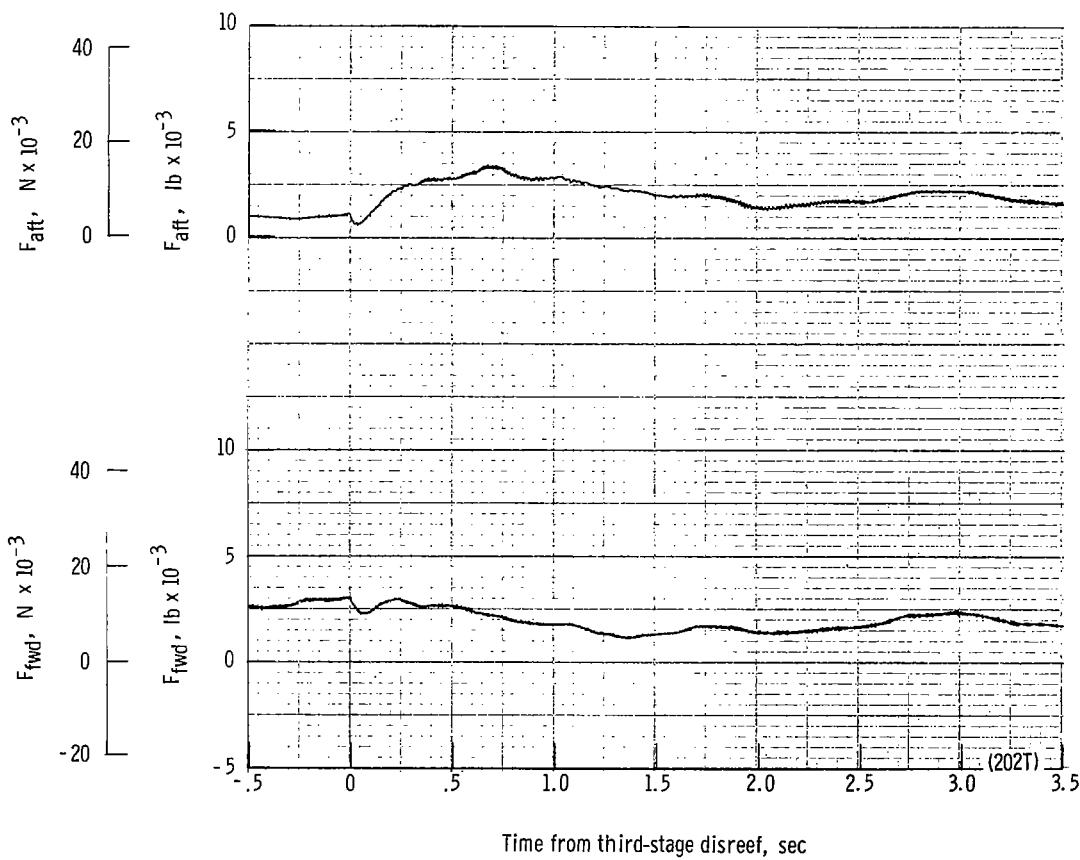
(o) Total force coefficient $C_{F,t}$ and dynamic pressure q plotted against time from second-stage disreef. Time = 0 second corresponds to 37.94 seconds after launch.

Figure 43.- Continued.



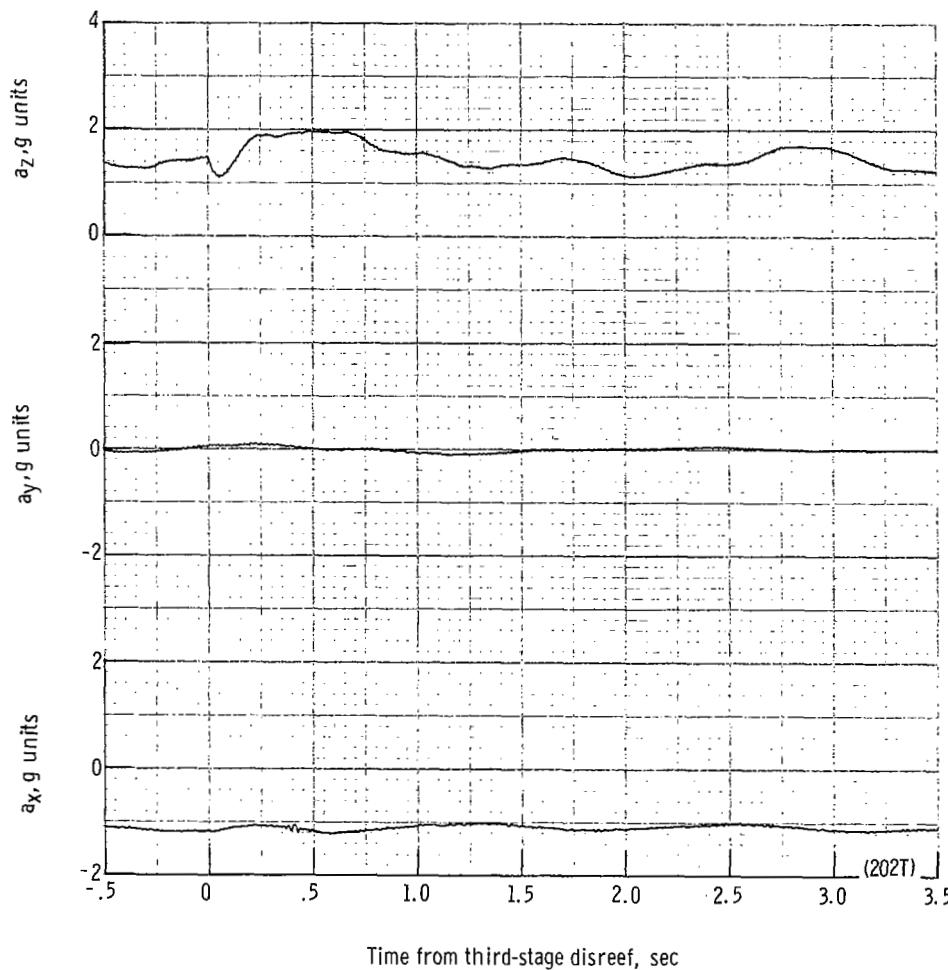
(p) Individual suspension-line loads F_{Lk12} , F_{Lk7} , F_{Lle6} , and F_{Lle1} plotted against time from third-stage disreef. Time = 0 second corresponds to 41.36 seconds after launch.

Figure 43.- Continued.



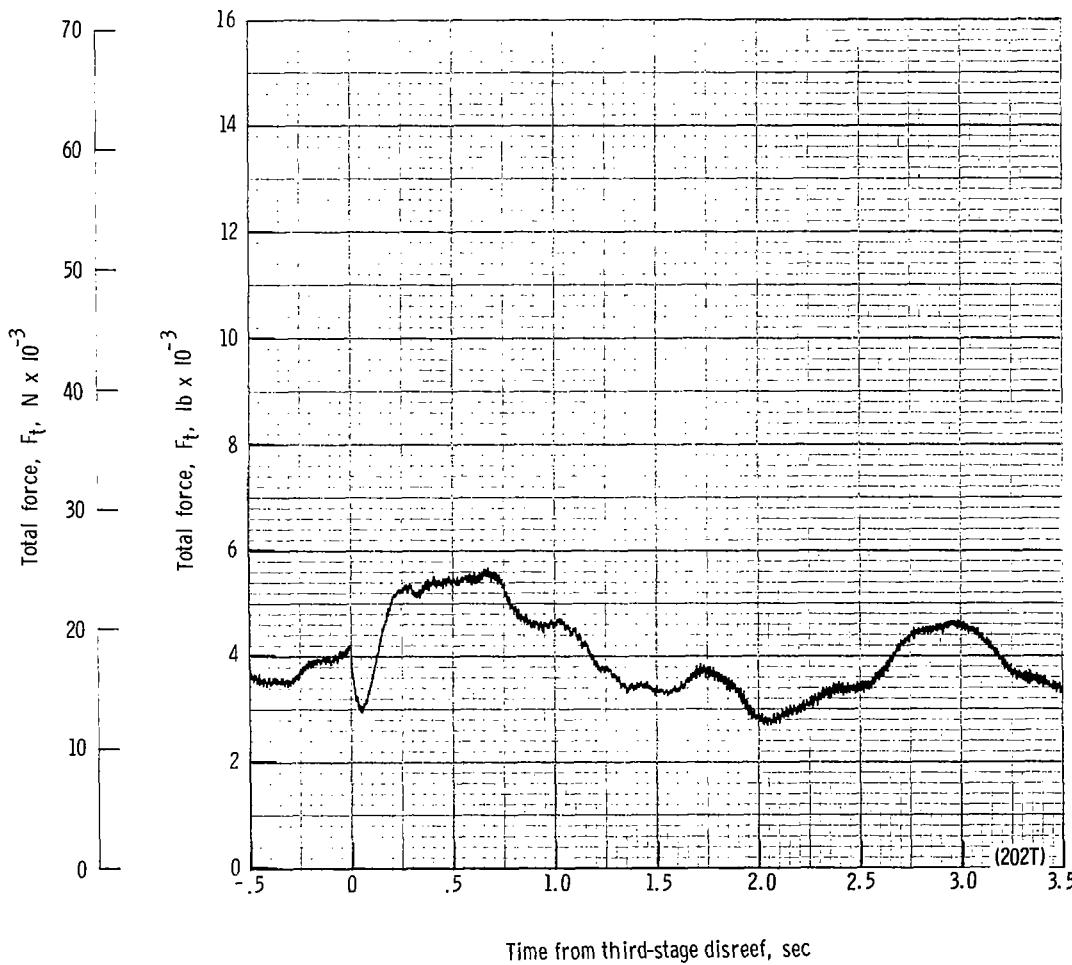
(q) Forward and aft riser loads plotted against time from third-stage disreef. Time = 0 second corresponds to 41.36 seconds after launch.

Figure 43.- Continued.



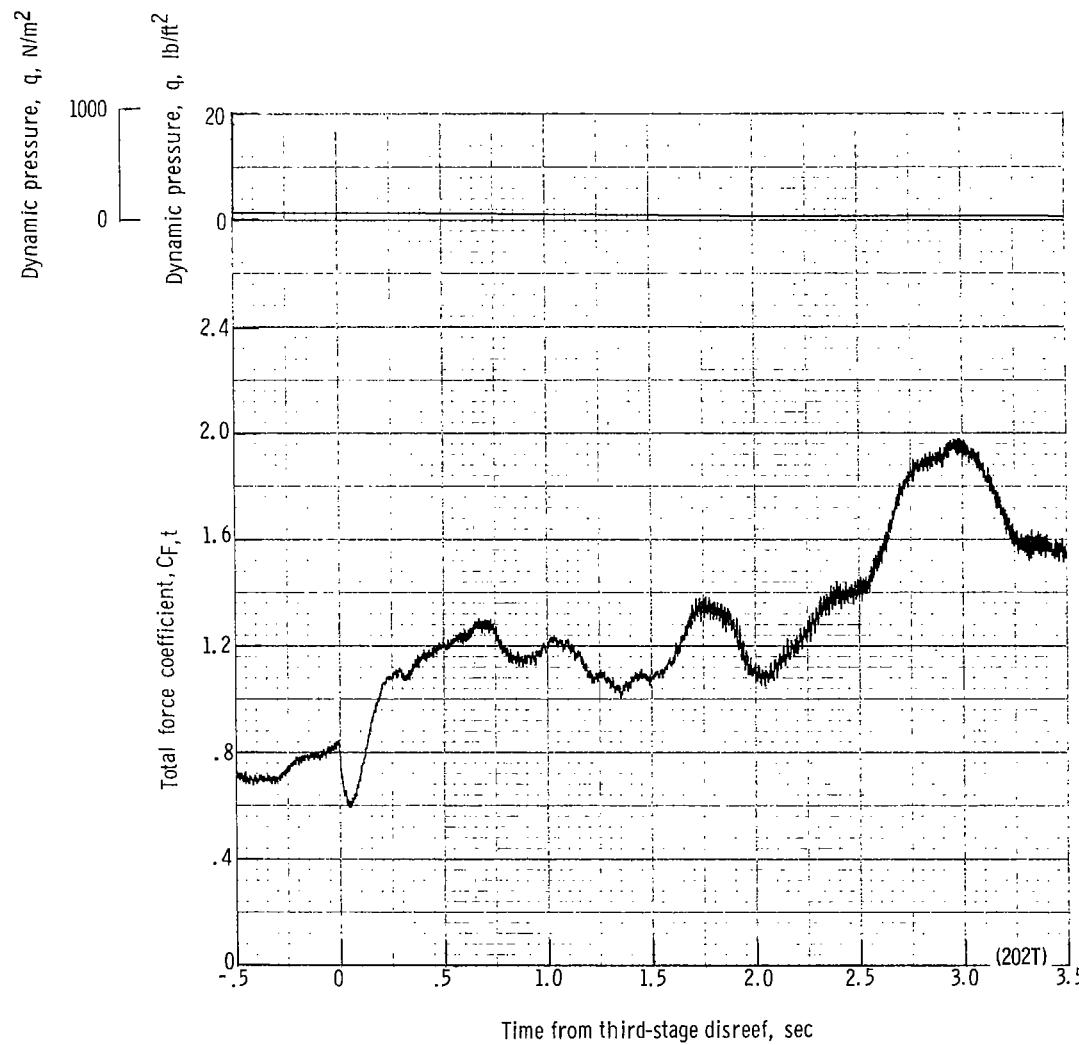
(r) Accelerations a_x , a_y , and a_z plotted against time from third-stage disreef. Time = 0 second corresponds to 41.36 seconds after launch.

Figure 43.- Continued.



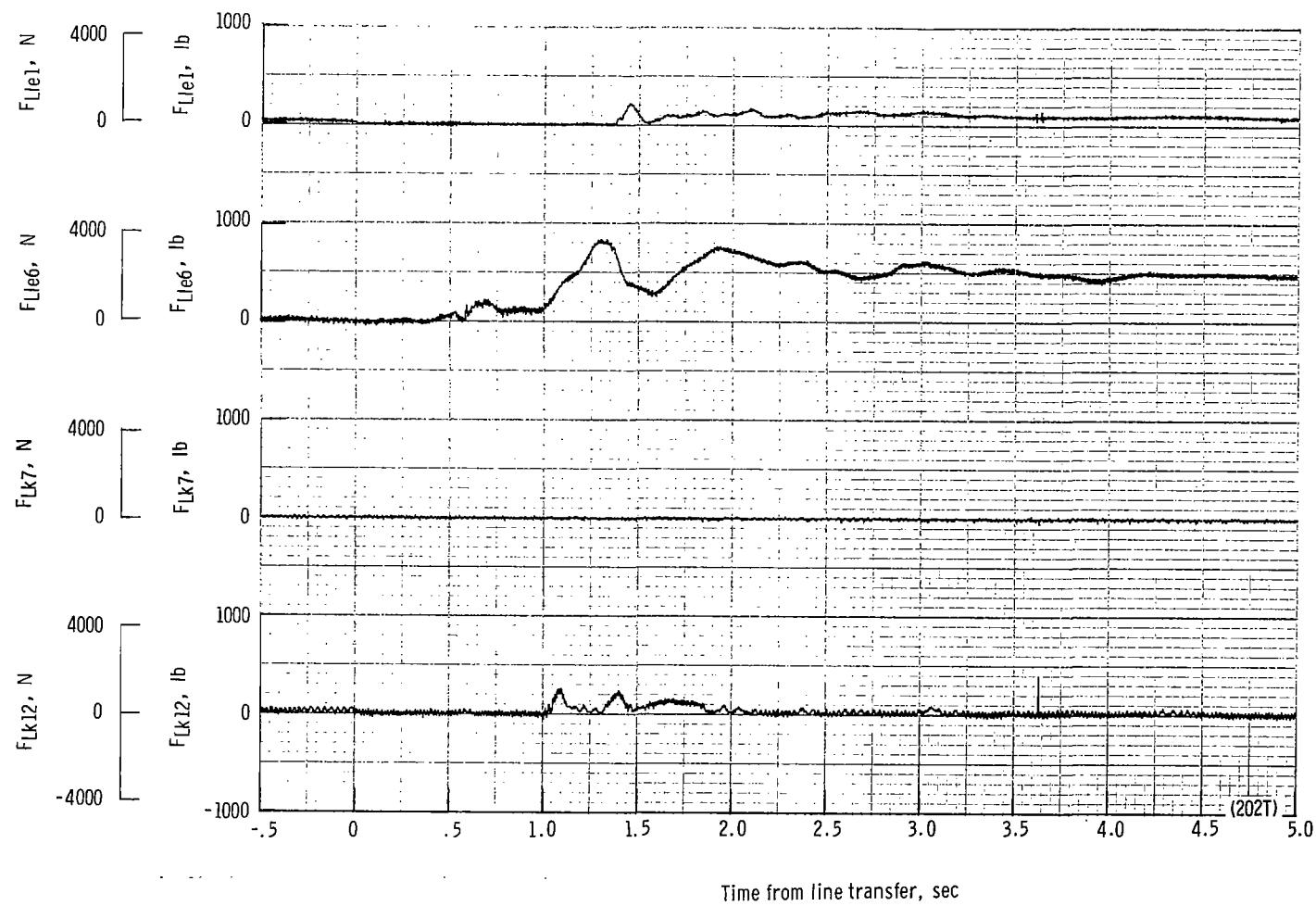
(s) Total force F_t plotted against time from third-stage disreef. Time = 0 second corresponds to 41.36 seconds after launch.

Figure 43.- Continued.



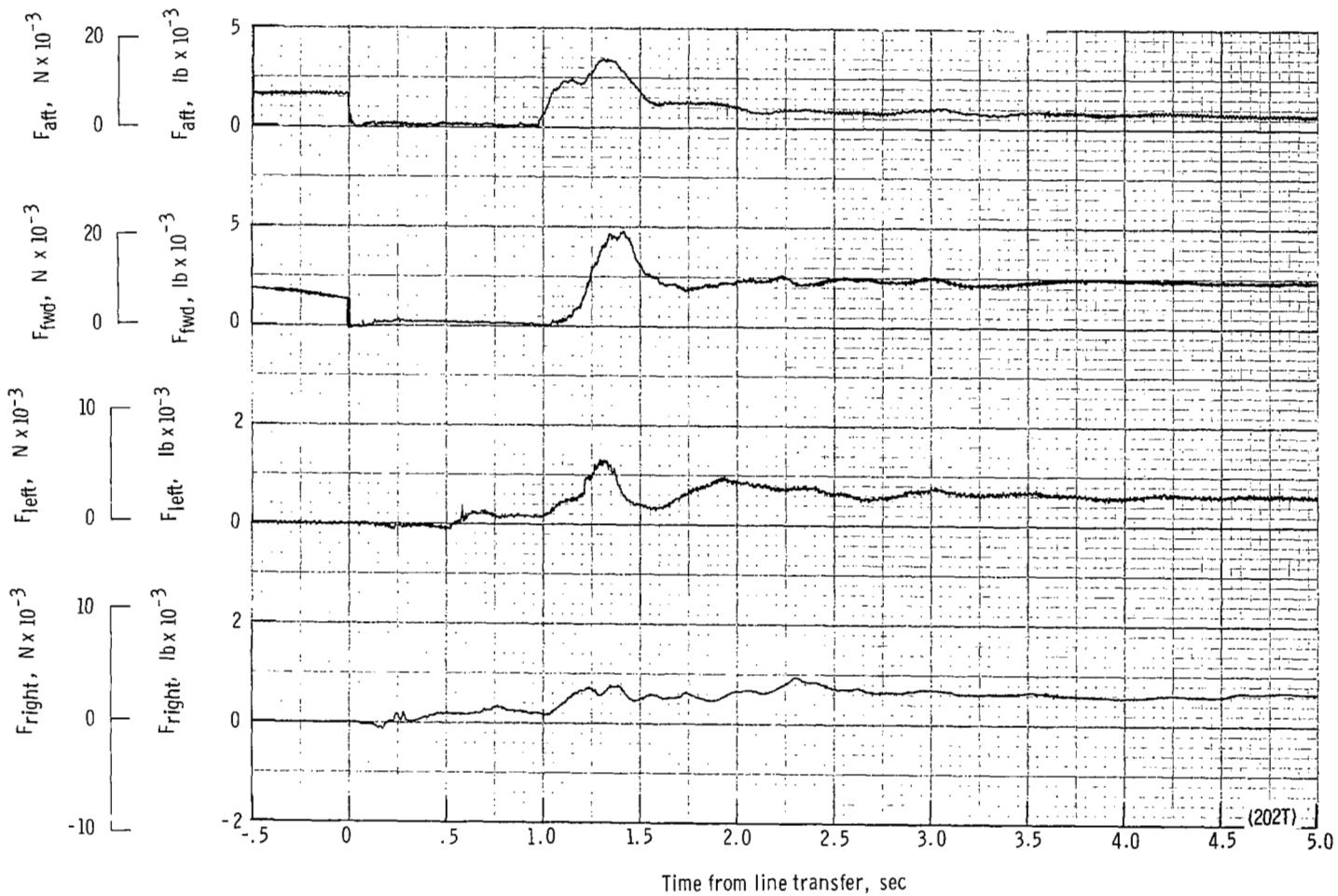
(t) Total force coefficient $C_{F,t}$ and dynamic pressure q plotted against time from third-stage disreef. Time = 0 second corresponds to 41.36 seconds after launch.

Figure 43.- Continued.



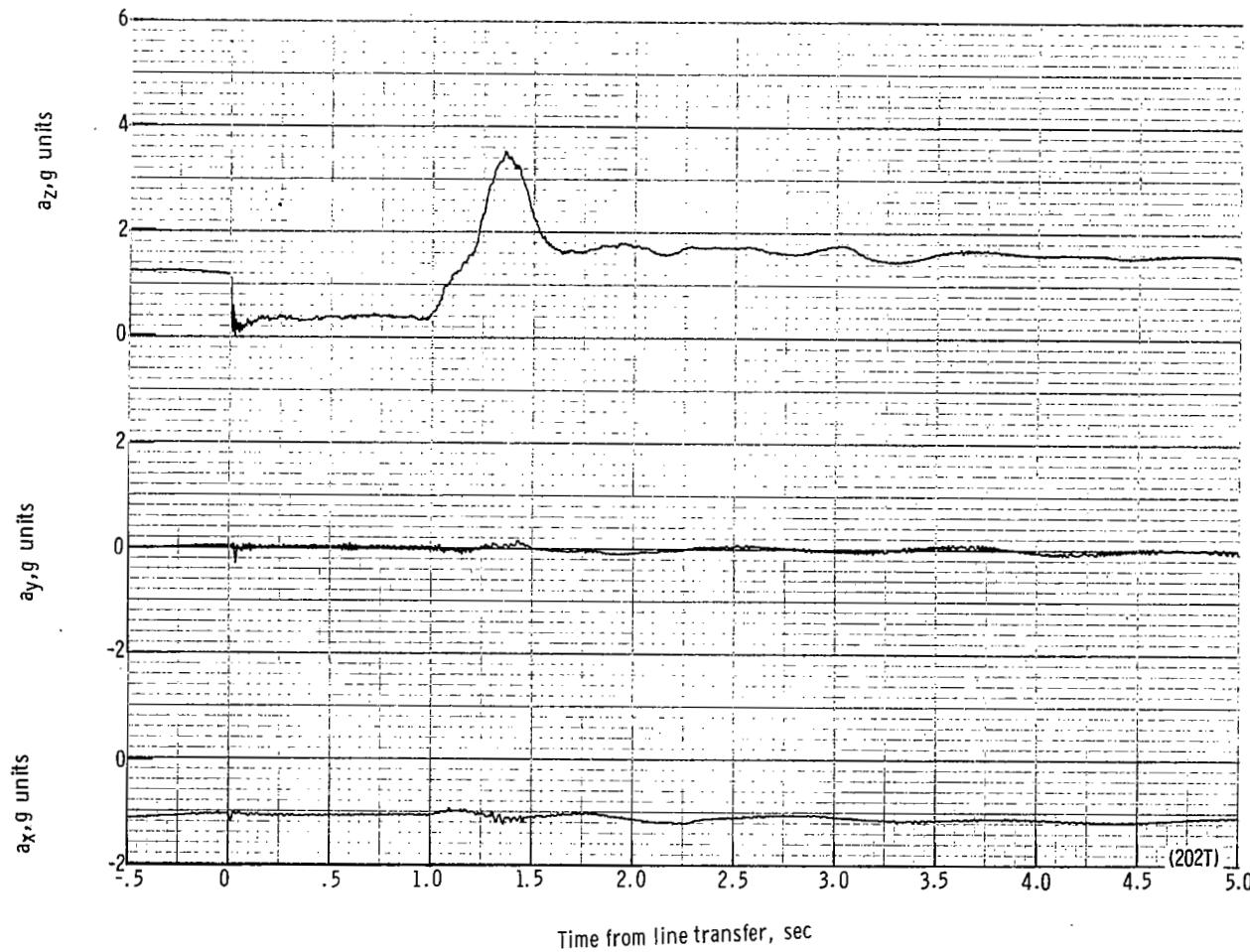
(u) Individual suspension-line loads F_{Lk12} , F_{Lk7} , F_{Lle6} , and F_{Lle1} plotted against time from line transfer. Time = 0 second corresponds to 45.26 seconds after launch.

Figure 43.- Continued.



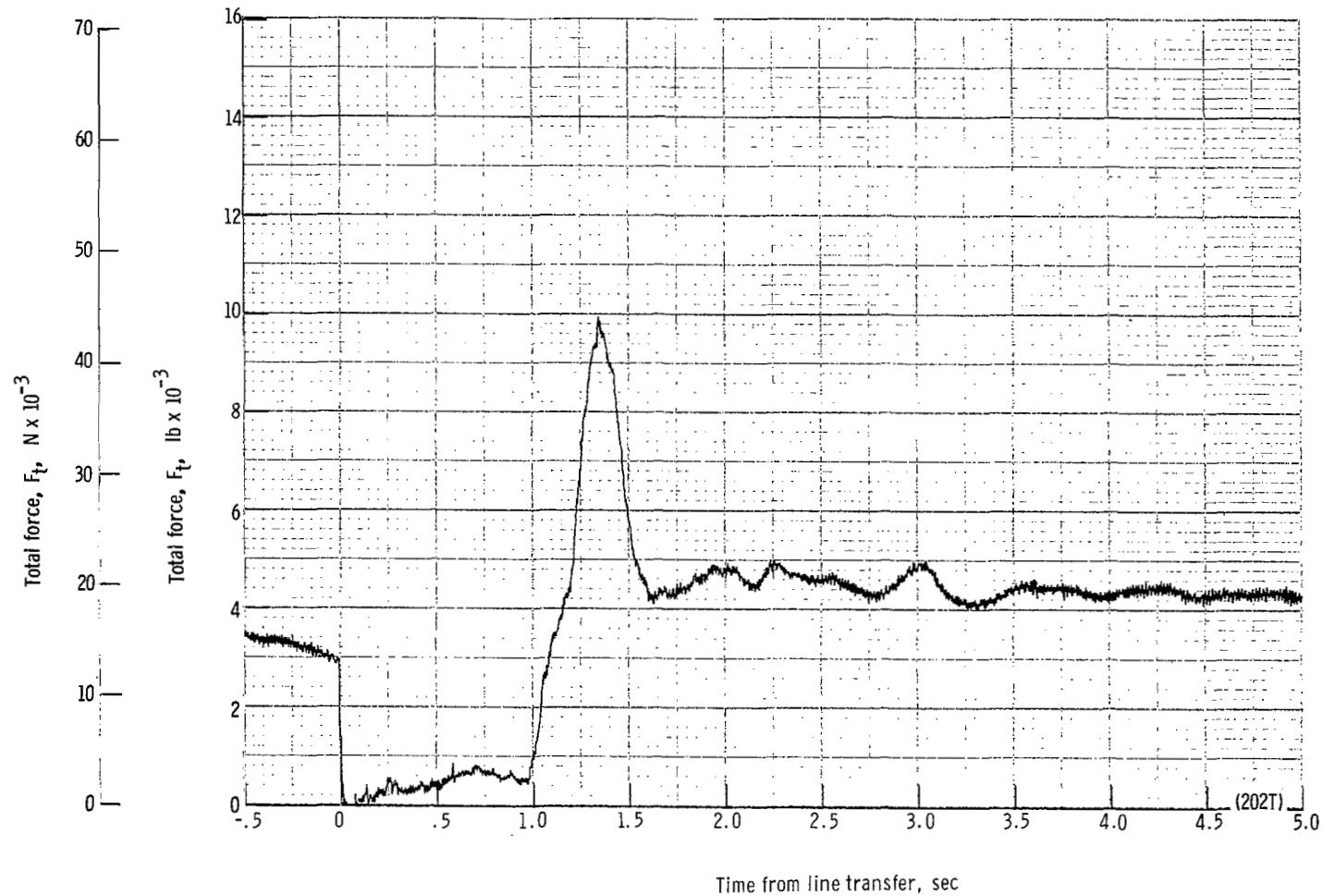
(v) Right, left, forward, and aft riser loads plotted against time from line transfer. Time = 0 second corresponds to 45.26 seconds after launch.

Figure 43.- Continued.



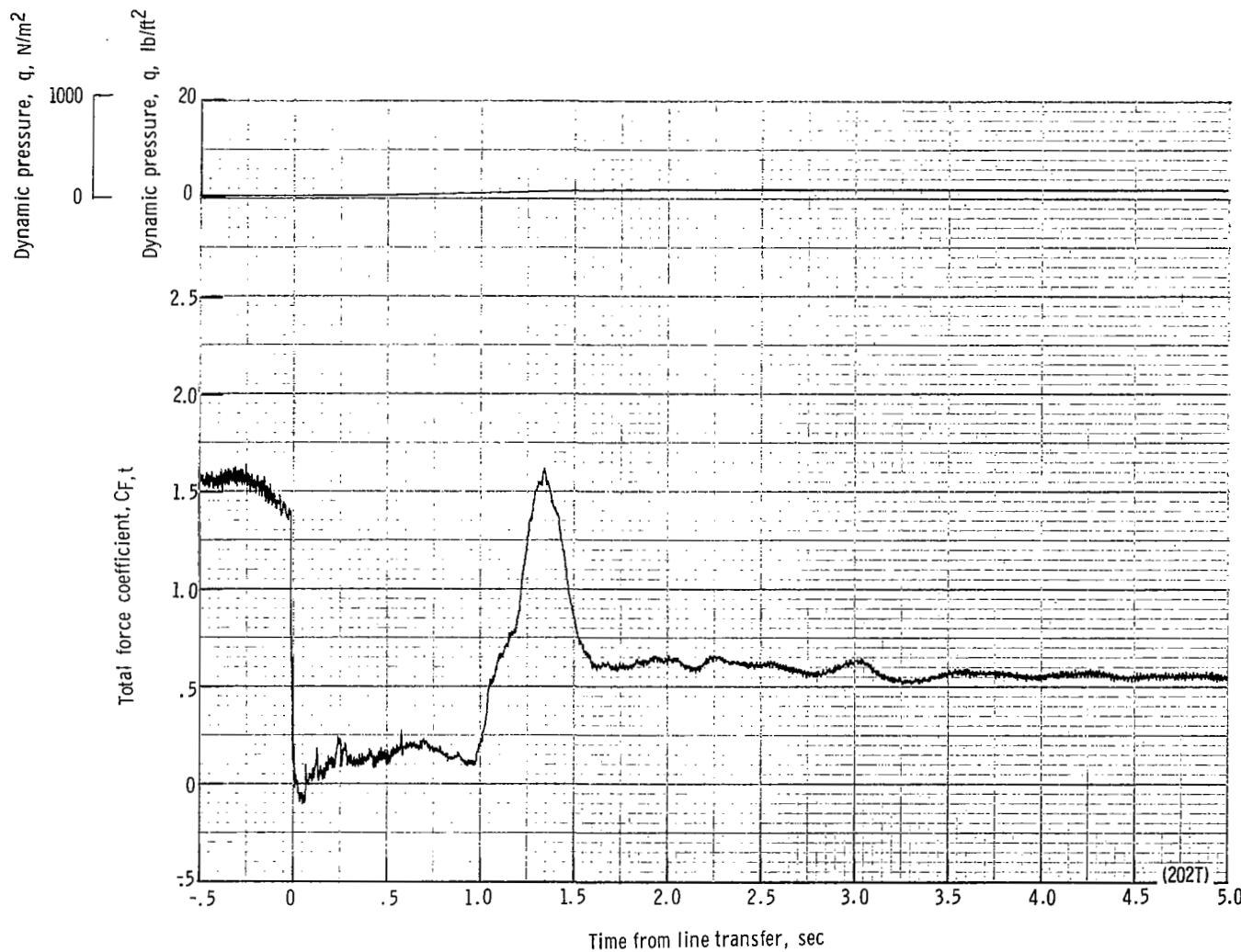
(w) Accelerations a_x , a_y , and a_z plotted against time from line transfer. Time = 0 second corresponds to 45.26 seconds after launch.

Figure 43.- Continued.



(x) Total force F_t plotted against time from line transfer. Time = 0 second corresponds to 45.26 seconds after launch.

Figure 43.- Continued.



(y) Total force coefficient $C_{F,t}$ and dynamic pressure q plotted against time from line transfer. Time = 0 second corresponds to 45.26 seconds after launch.

Figure 43.- Continued.

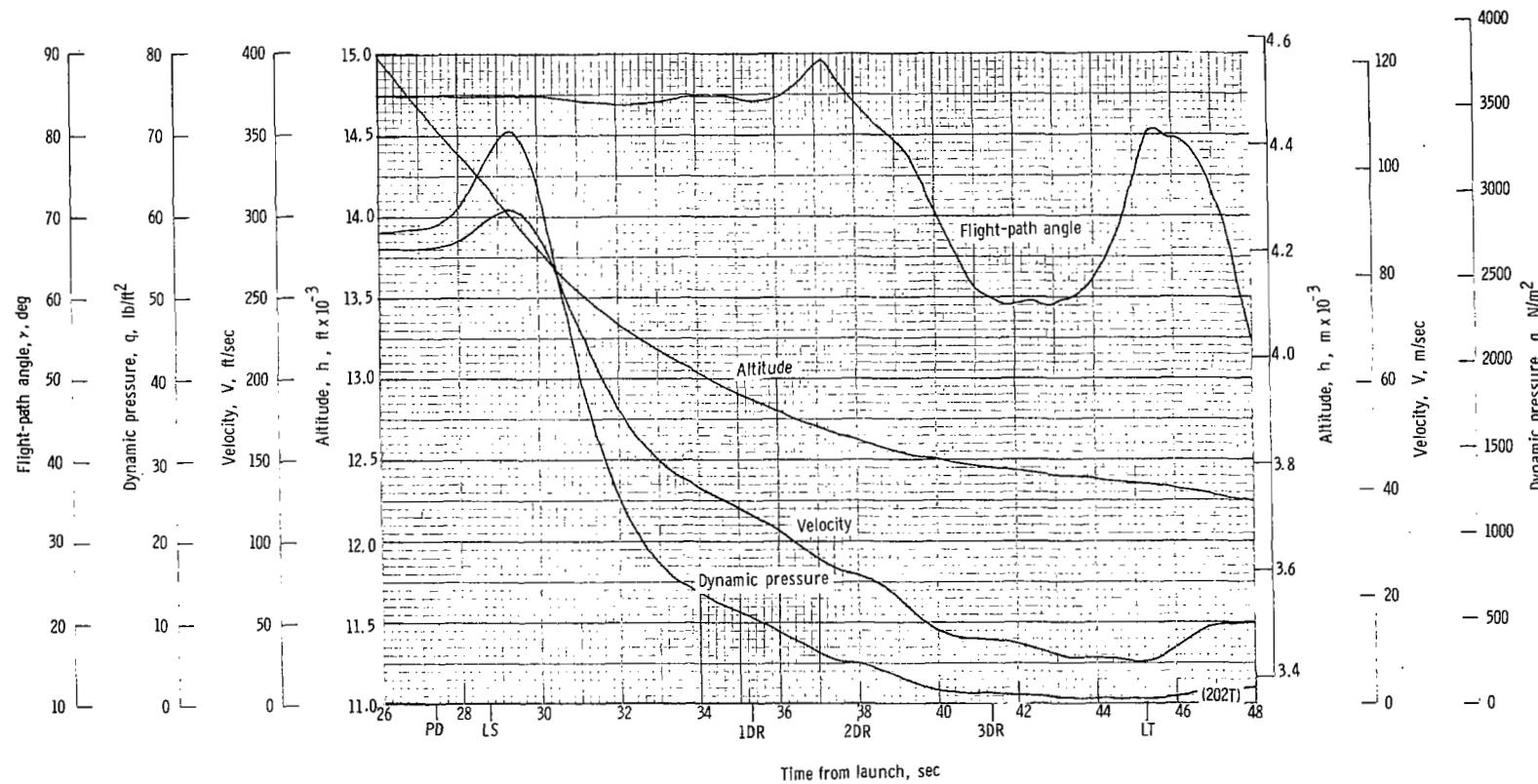
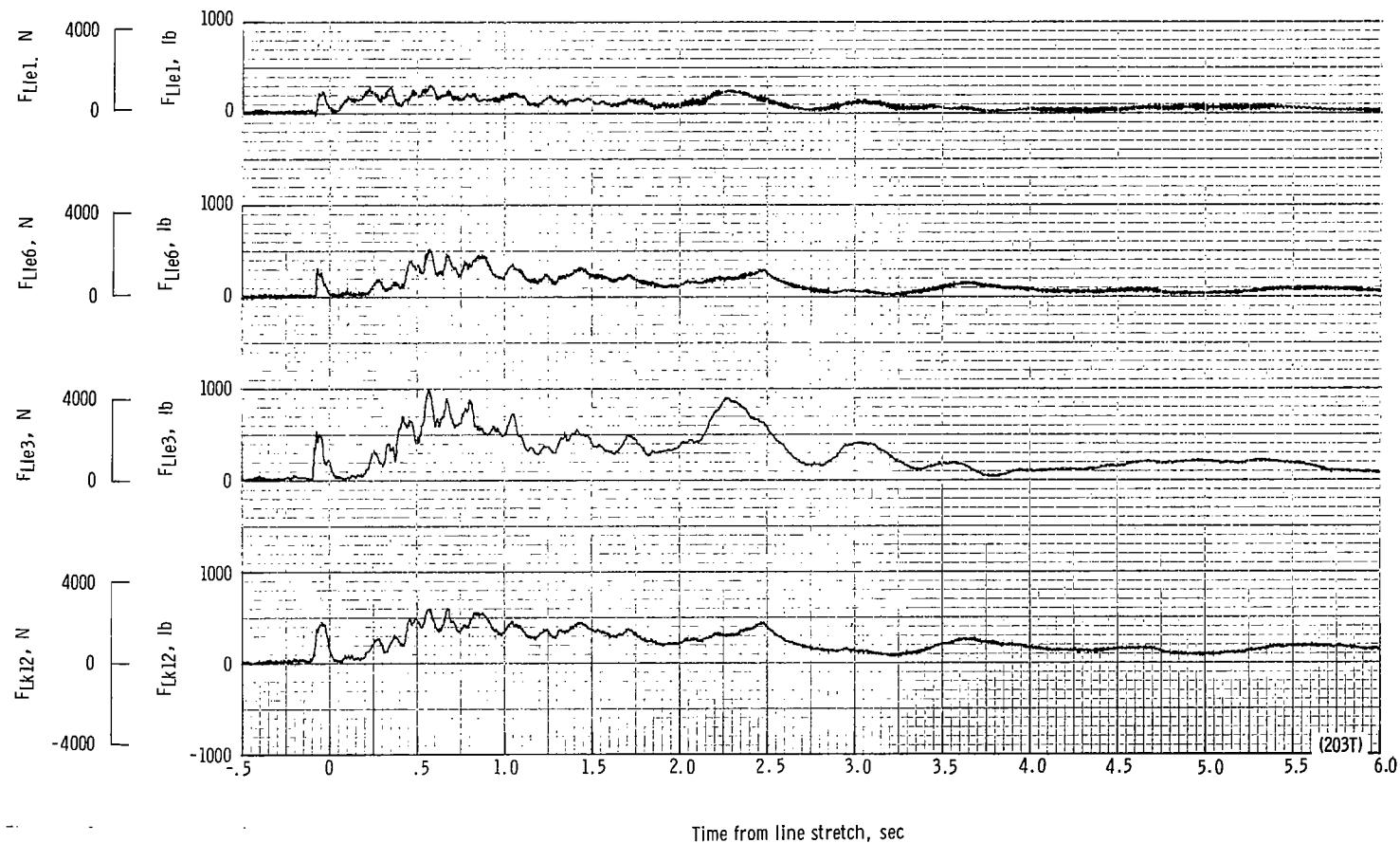
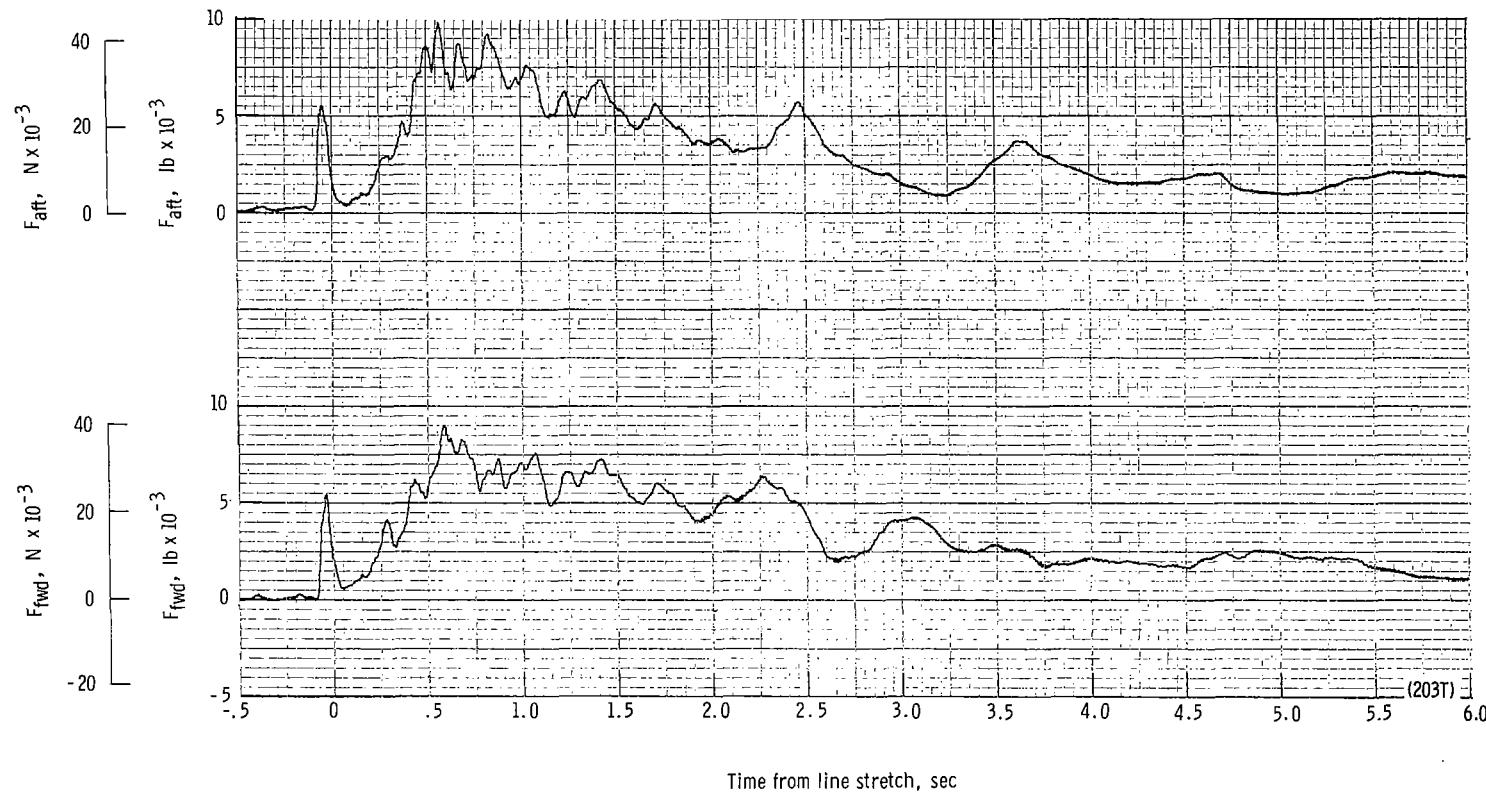
(z) Flight-path angle γ , dynamic pressure q , velocity V , and altitude h plotted against time from launch.

Figure 43.- Concluded.



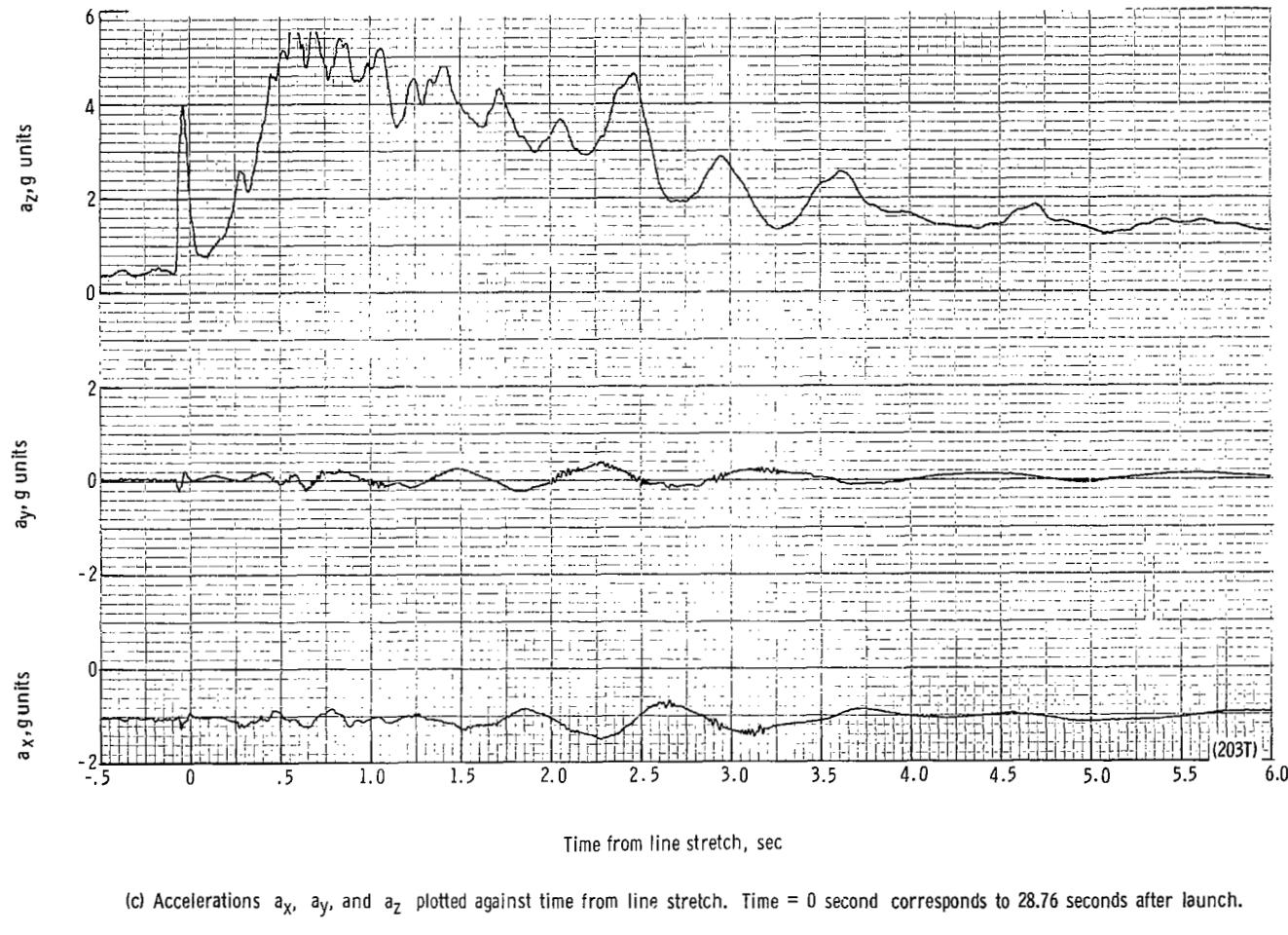
(a) Individual suspension-line loads F_{Lk12} , F_{Lle3} , F_{Lle6} , and F_{Lle1} plotted against time from line stretch. Time = 0 second corresponds to 28.76 seconds after launch.

Figure 44.- Time history of twin-keel parawing deployment data for test 203T. $W_D = 16\ 925\ N$ (3805 lb); $W_p = 15\ 364\ N$ (3454 lb);
 $q_{PD} = 2858.5\ N/m^2$ (59.7 lb/ft²); $h_{PD} = 4560\ m$ (14 960 ft); $t_r/t_k = 0.140$; reefing version A.



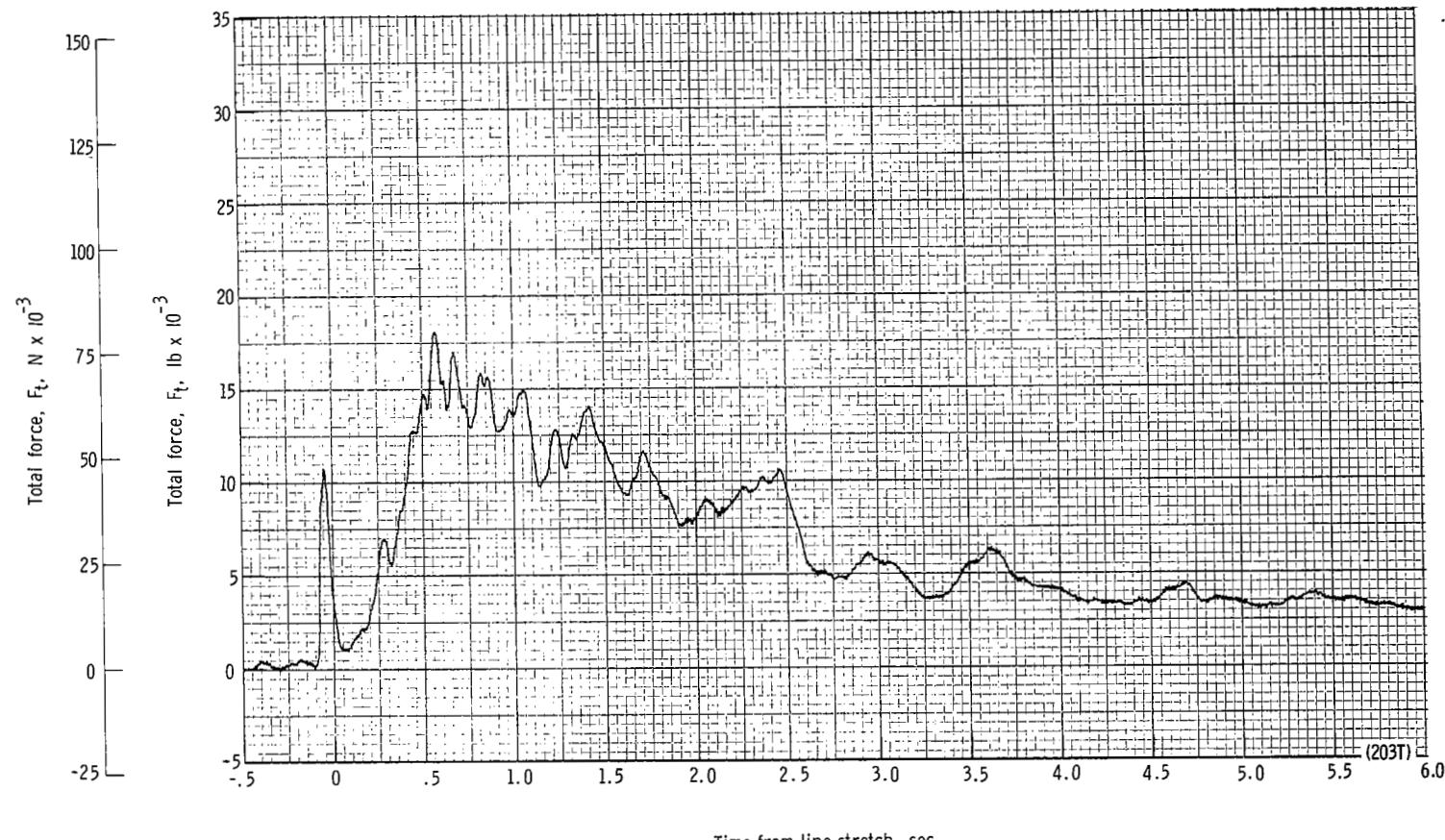
(b) Forward and aft riser loads plotted against time from line stretch. Time = 0 second corresponds to 28.76 seconds after launch.

Figure 44.- Continued.



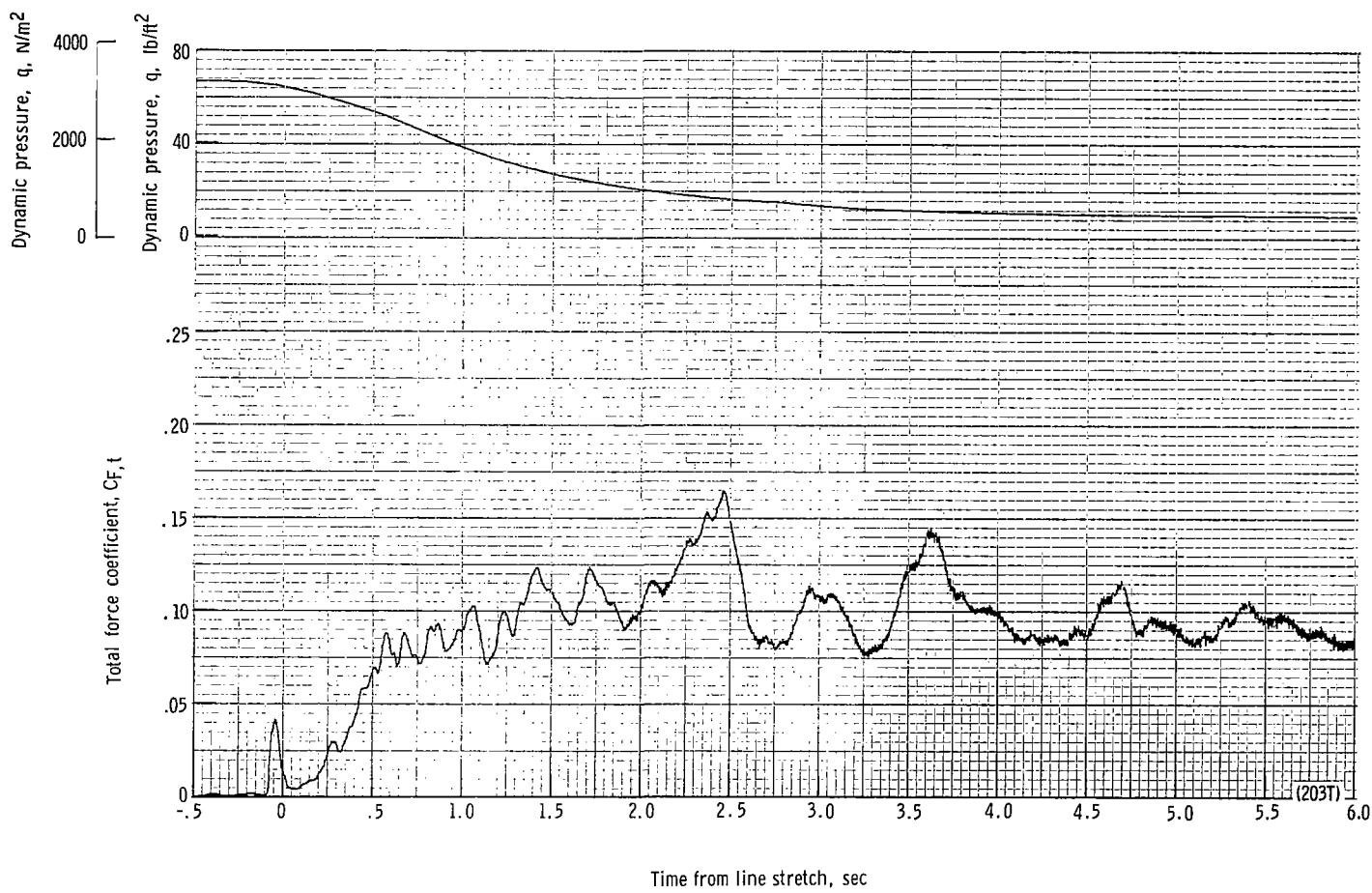
(c) Accelerations a_x , a_y , and a_z plotted against time from line stretch. Time = 0 second corresponds to 28.76 seconds after launch.

Figure 44.- Continued.



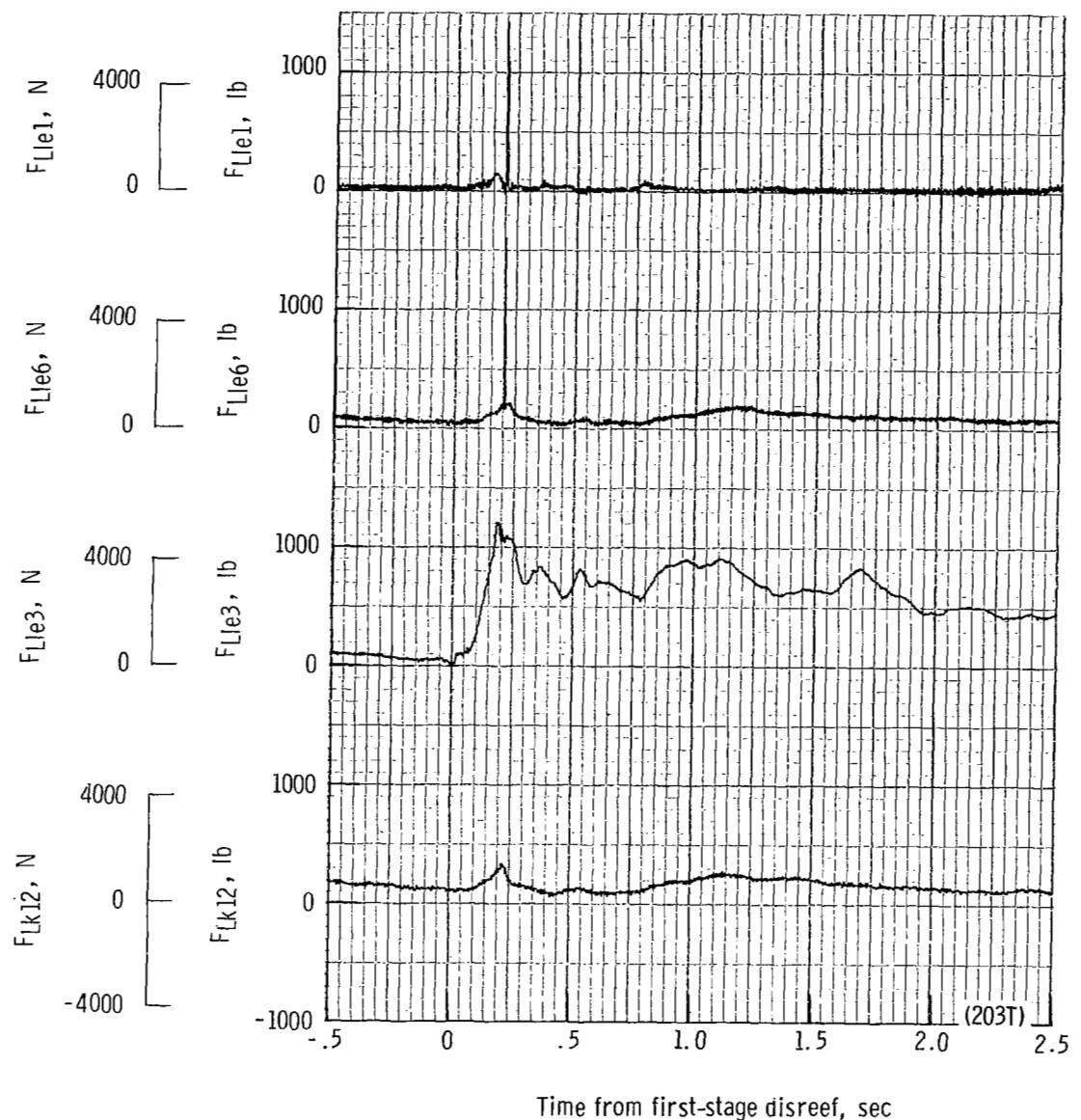
(d) Total force F_t plotted against time from line stretch. Time = 0 second corresponds to 28.76 seconds after launch.

Figure 44.- Continued.



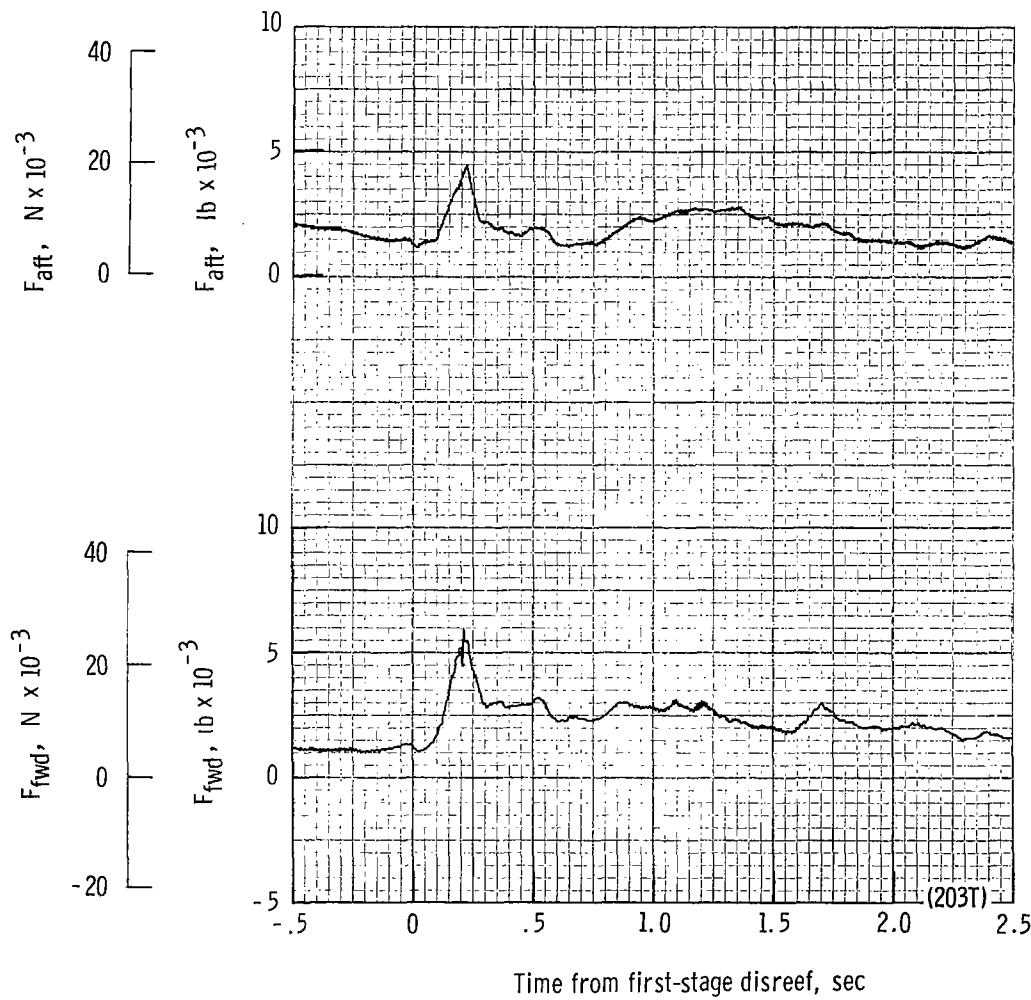
(e) Total force coefficient $C_{F,t}$ and dynamic pressure q plotted against time from line stretch. Time = 0 second corresponds to 28.76 seconds after launch.

Figure 44.- Continued.



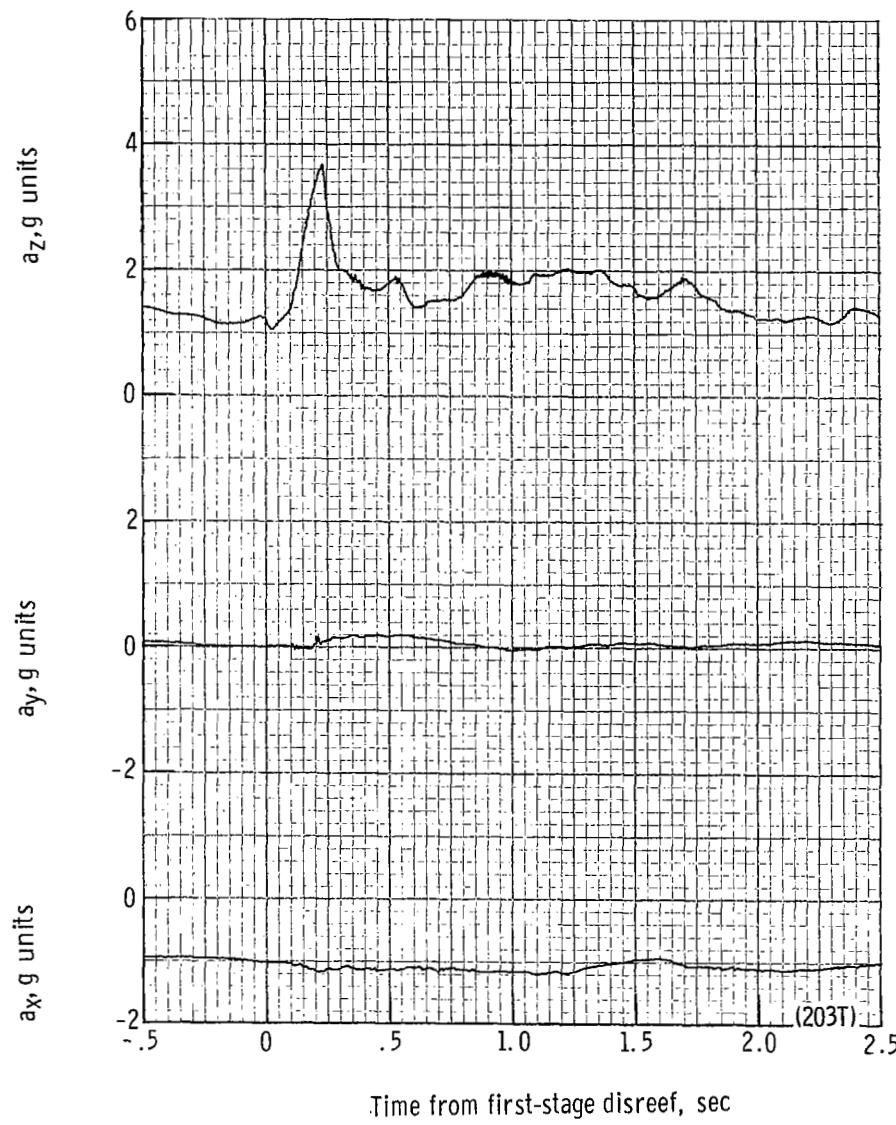
(f) Individual suspension-line loads F_{Lk12} , F_{Lle3} , F_{Lle6} , and F_{Lle1} plotted against time from first-stage disreef. Time = 0 second corresponds to 35.06 seconds after launch.

Figure 44.- Continued.



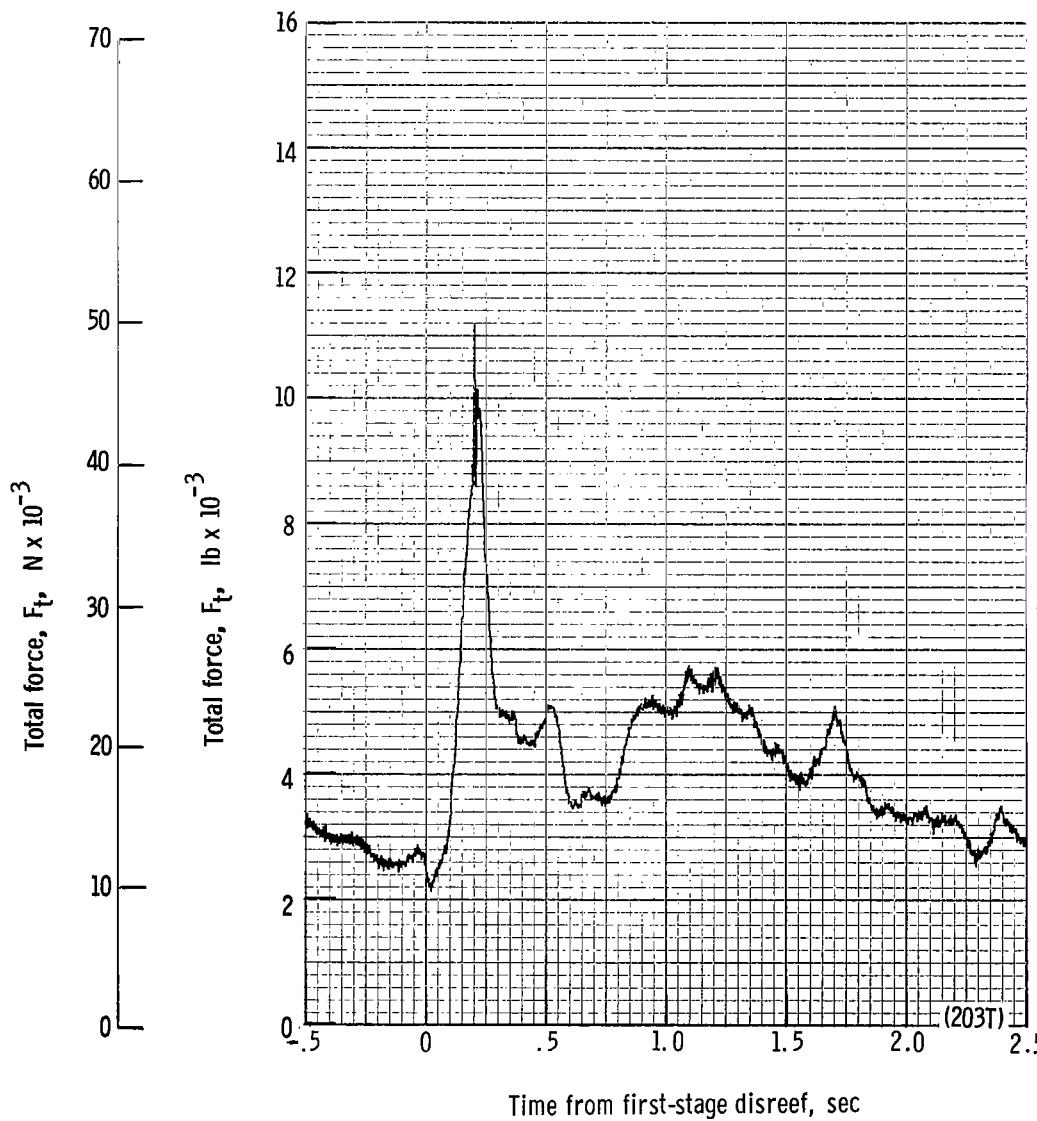
(g) Forward and aft riser loads plotted against time from first-stage disreef. Time = 0 second corresponds to 35.06 seconds after launch.

Figure 44.- Continued.



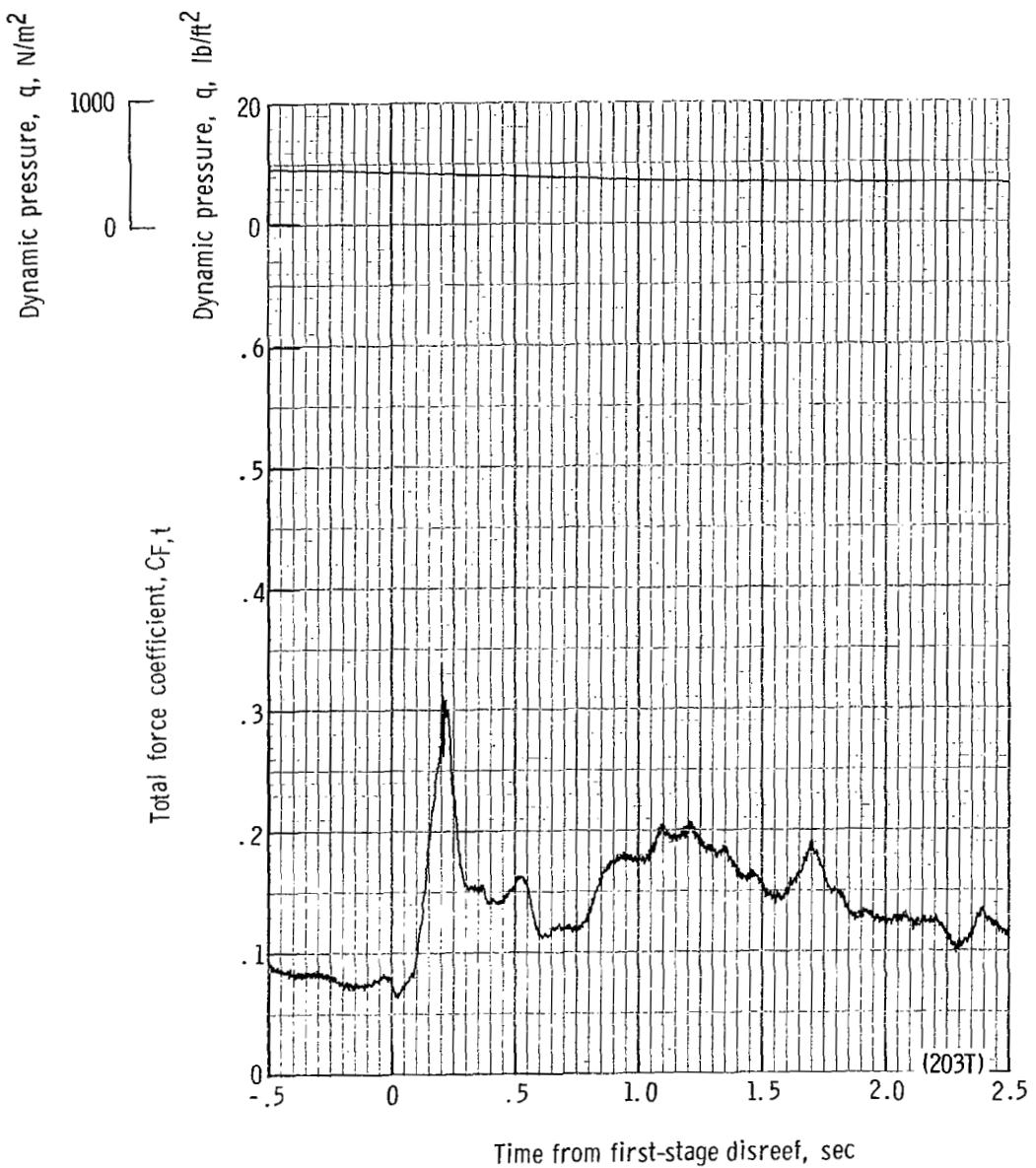
(h) Accelerations a_x , a_y , and a_z plotted against time from first-stage disreef. Time = 0 second corresponds to 35.06 seconds after launch.

Figure 44.- Continued.



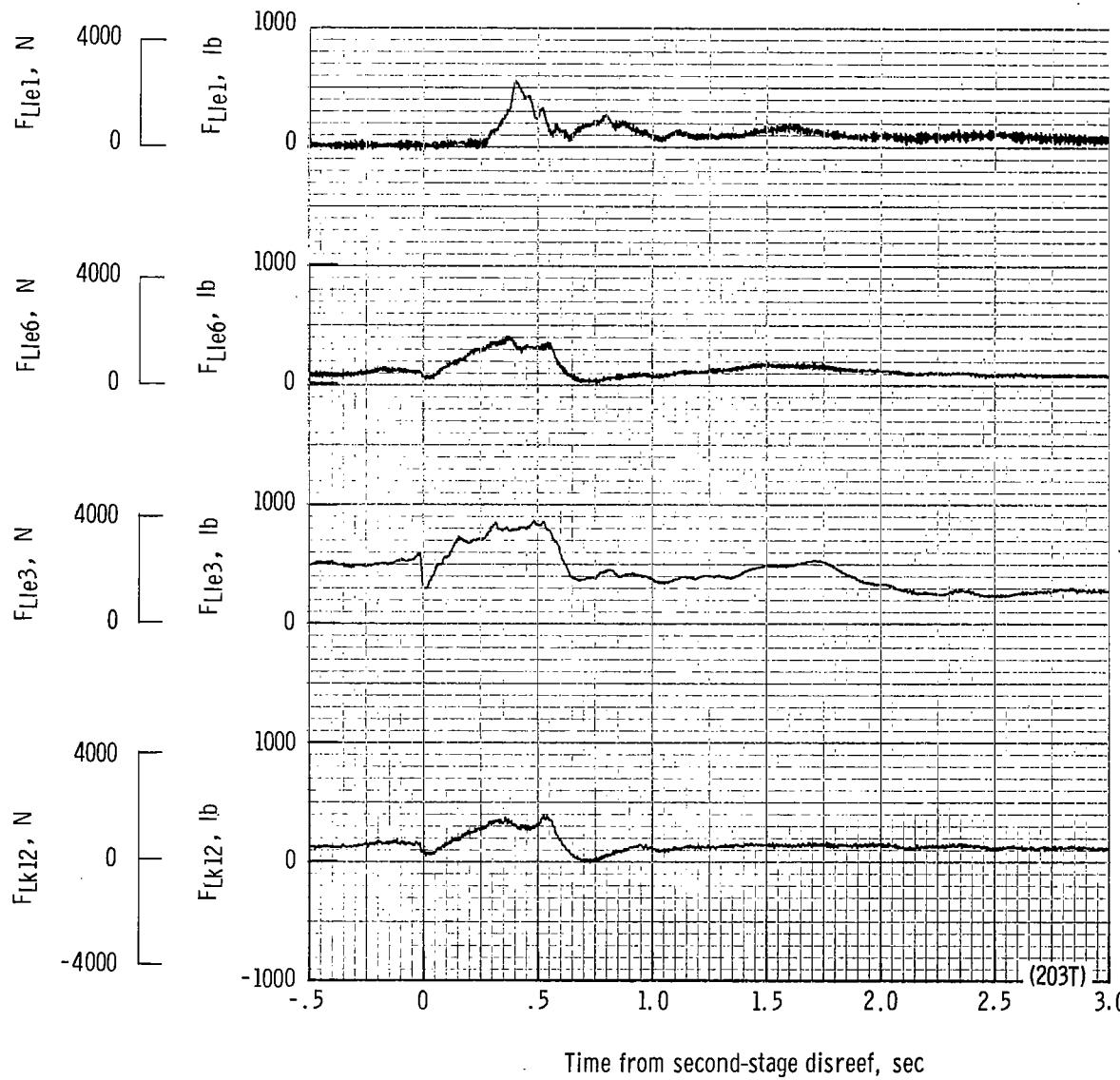
(i) Total force F_t plotted against time from first-stage disreef. Time = 0 second corresponds to 35.06 seconds after launch.

Figure 44.- Continued.



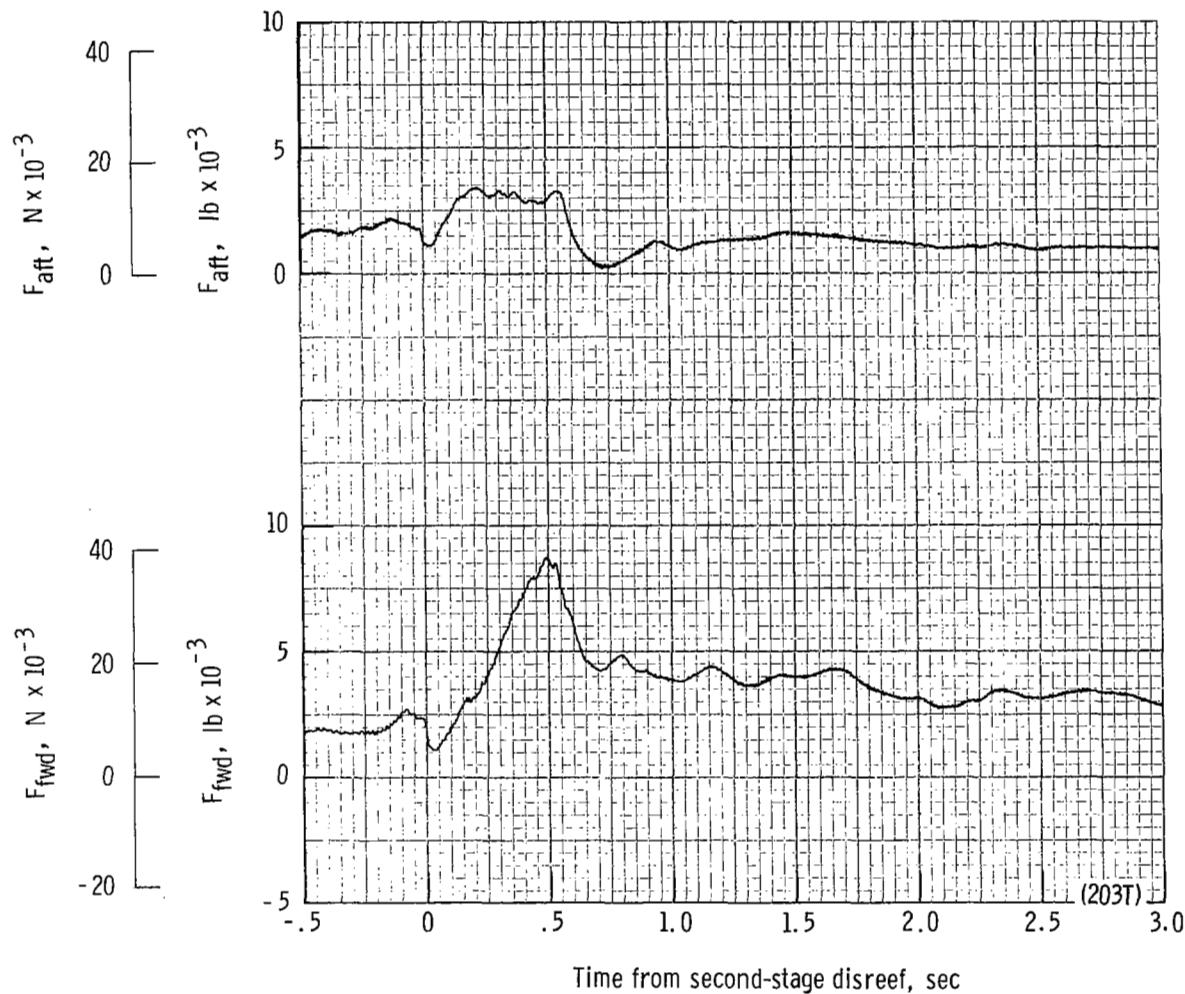
(j) Total force coefficient $C_{F,t}$ and dynamic pressure q plotted against time from first-stage disreef. Time = 0 second corresponds to 35.06 seconds after launch.

Figure 44.- Continued.



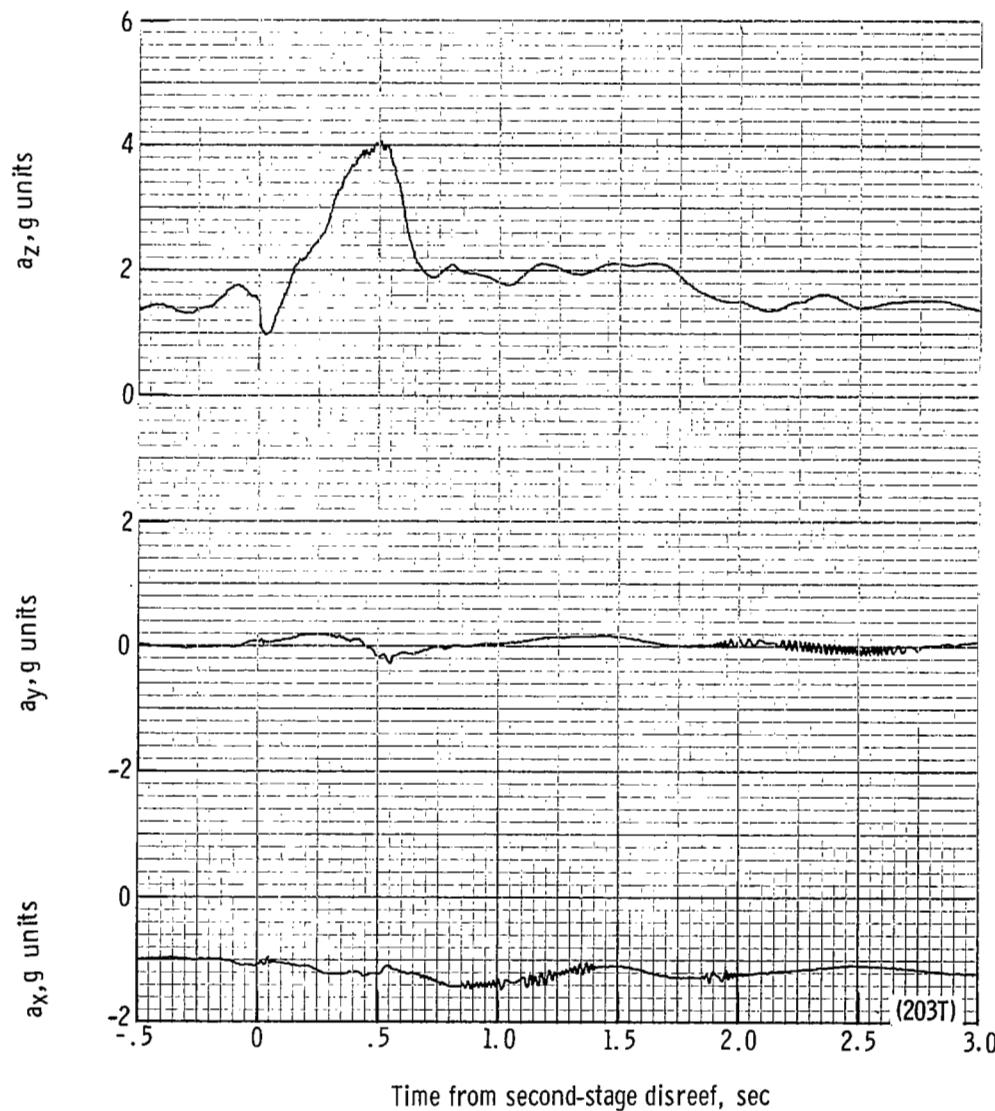
(k) Individual suspension-line loads F_{Lk12} , F_{Lle3} , F_{Lle6} , and F_{Lle1} plotted against time from second-stage disreef. Time = 0 second corresponds to 38.12 seconds after launch.

Figure 44.- Continued.



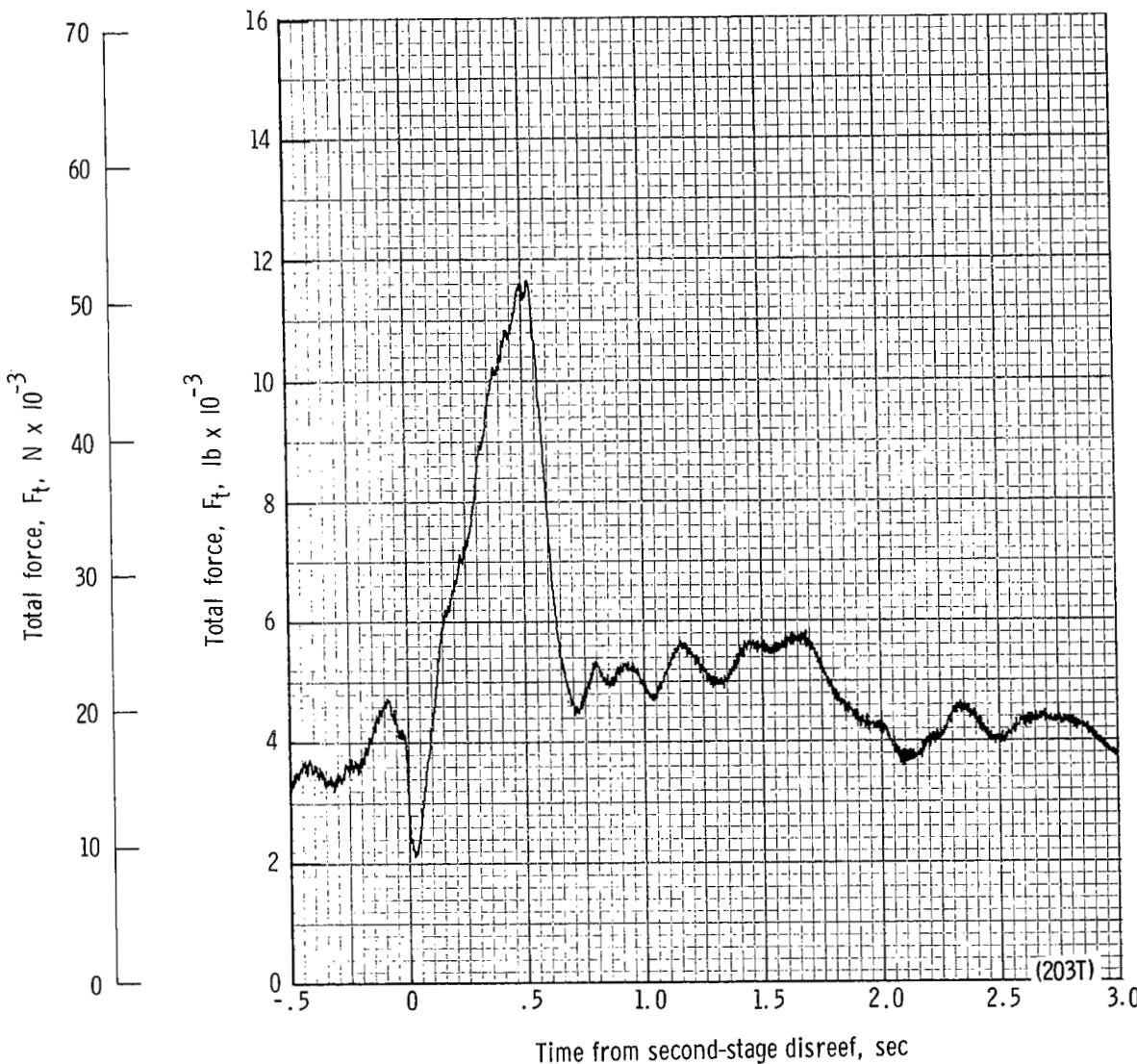
(l) Forward and aft riser loads plotted against time from second-stage disreef. Time = 0 second corresponds to 38.12 seconds after launch.

Figure 44.- Continued.



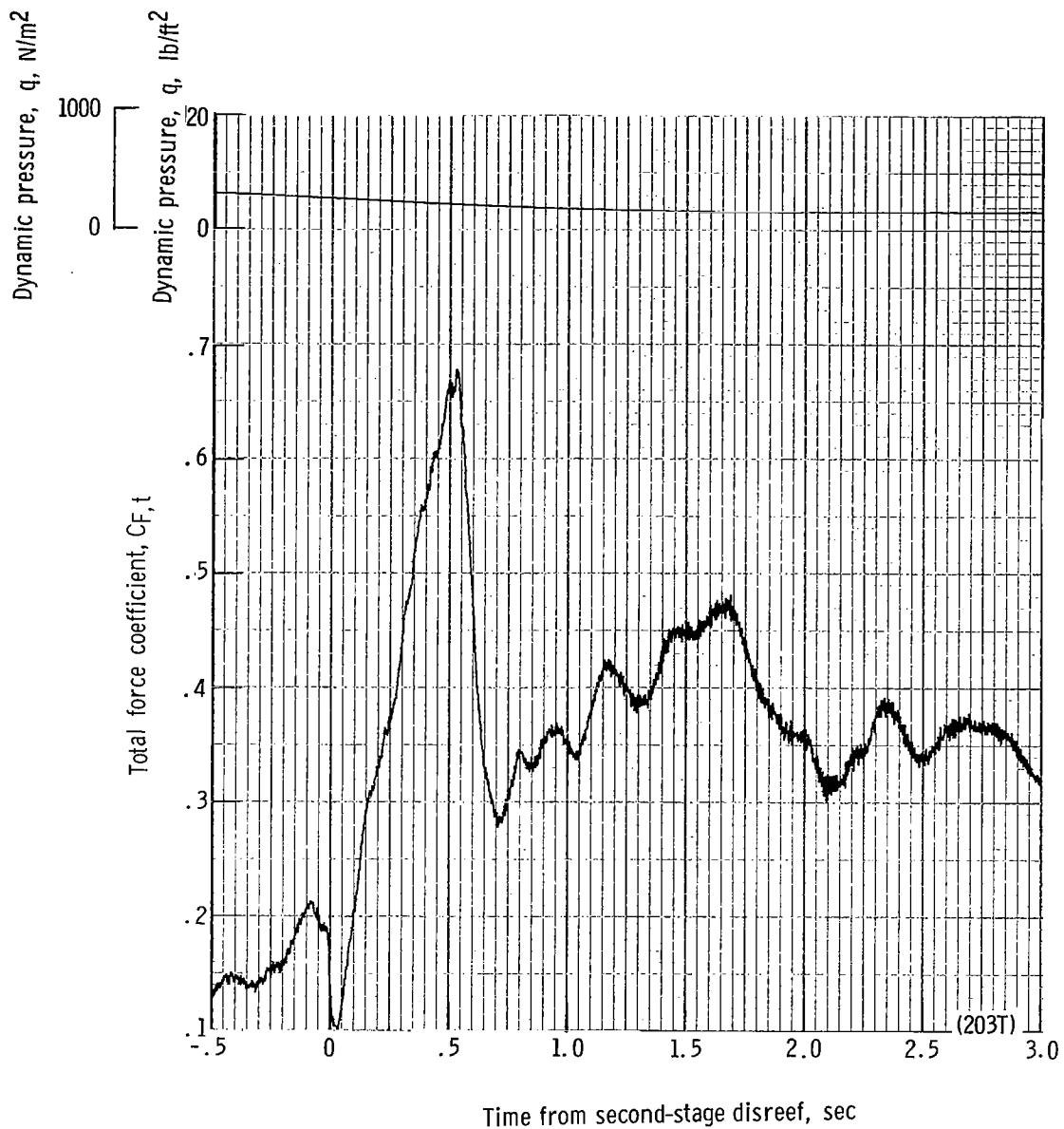
(m) Accelerations a_x , a_y , and a_z plotted against time from second-stage disreef. Time = 0 second corresponds to 38.12 seconds after launch.

Figure 44.- Continued.



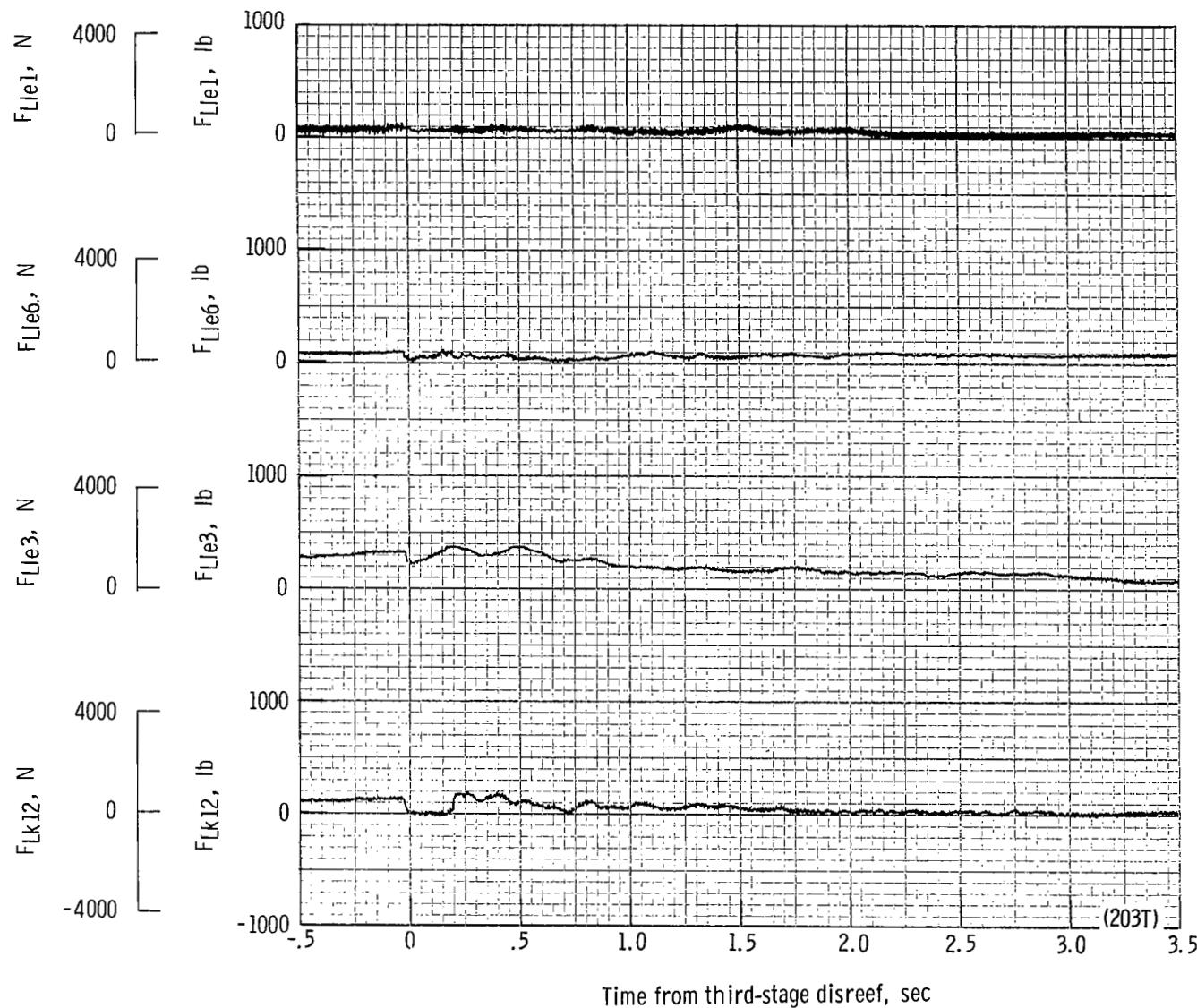
(n) Total force F_t plotted against time from second-stage disreef. Time = 0 second corresponds to 38.12 seconds after launch.

Figure 44.- Continued.



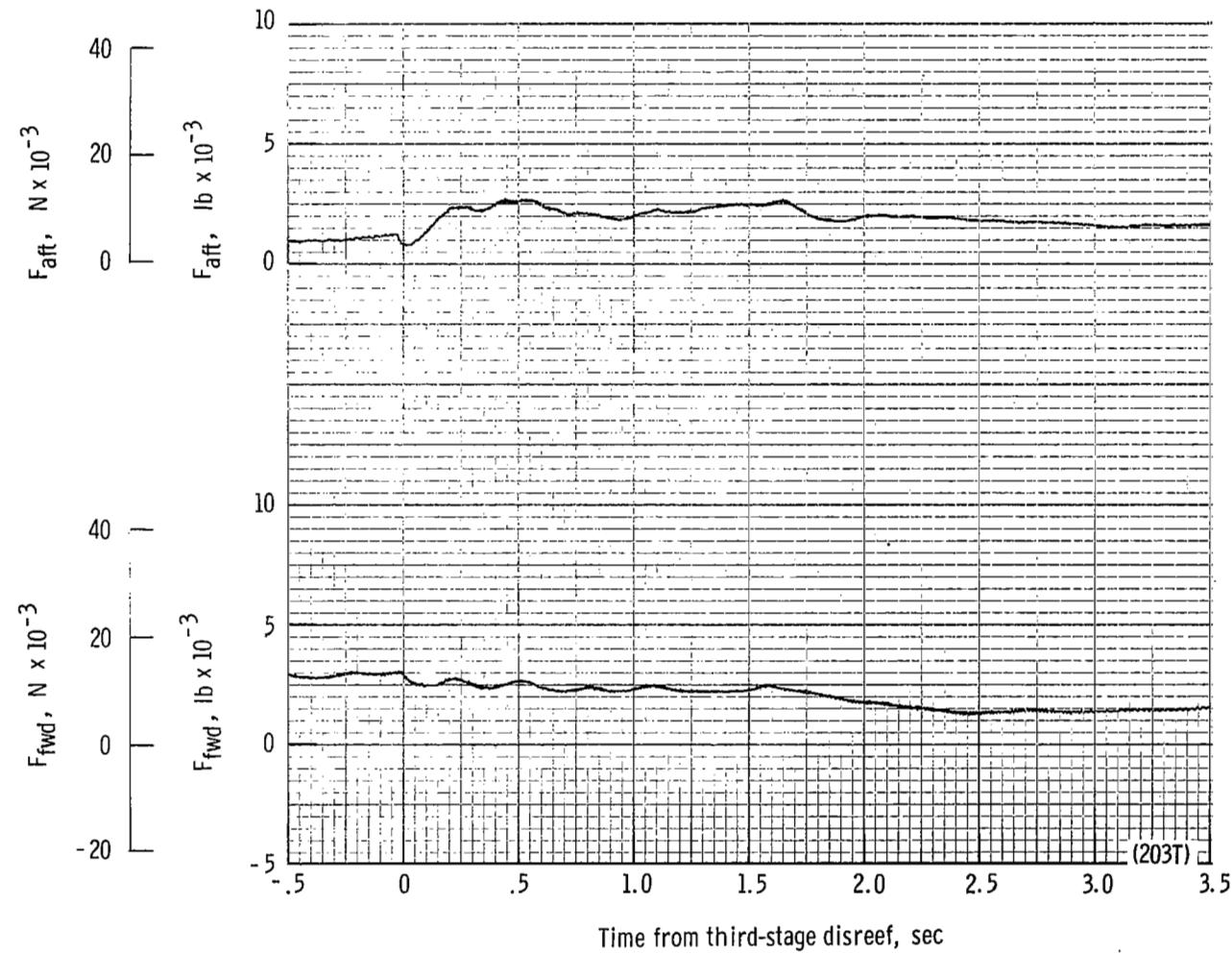
(o) Total force coefficient $C_{F,t}$ and dynamic pressure q plotted against time from second-stage disreef. Time = 0 second corresponds to 38.12 seconds after launch.

Figure 44.- Continued.



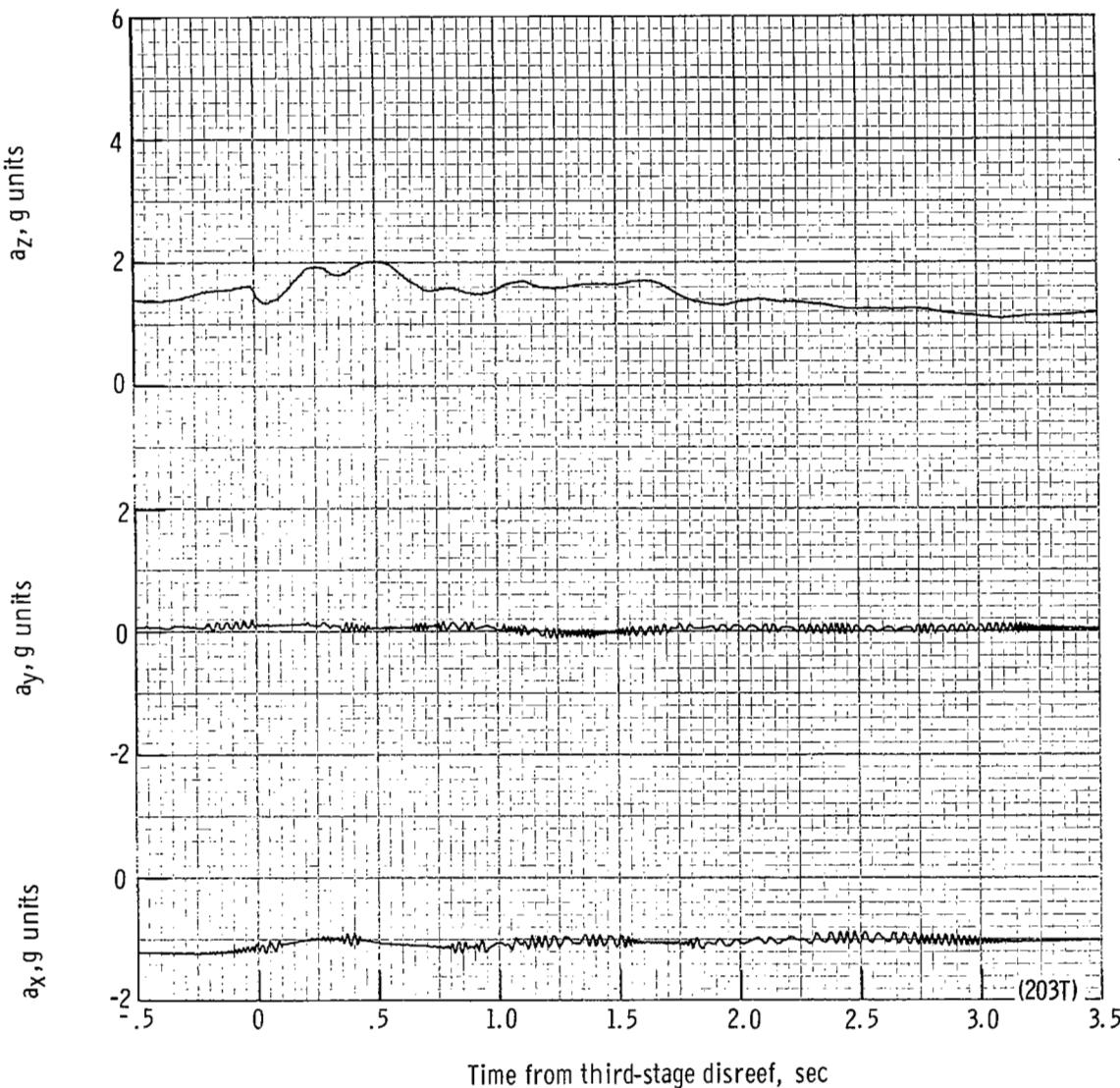
(p) Individual suspension-line loads F_{Lk12} , F_{Lle3} , F_{Lle6} , and F_{Lle1} plotted against time from third-stage disreef. Time = 0 second corresponds to 41.58 seconds after launch.

Figure 44.- Continued.



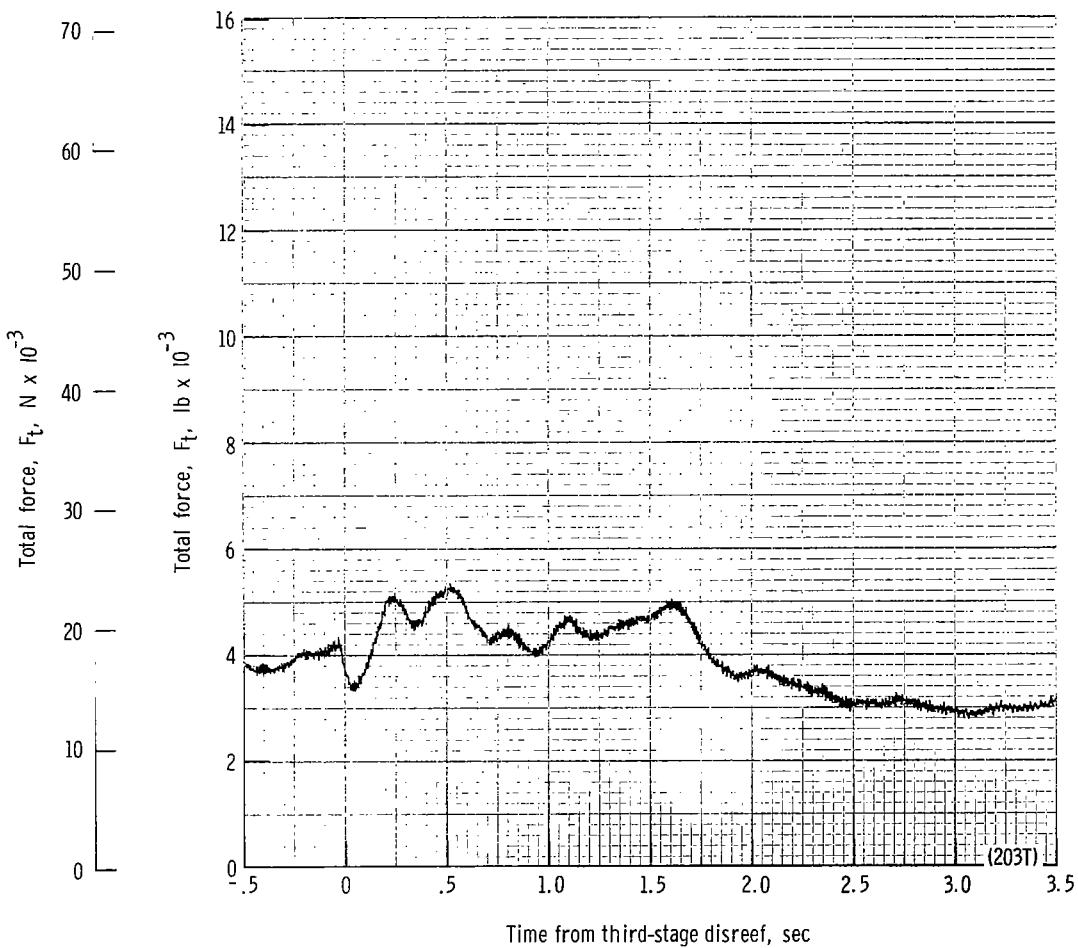
(q) Forward and aft riser loads plotted against time from third-stage disreef. Time = 0 second corresponds to 41.58 seconds after launch.

Figure 44.- Continued.



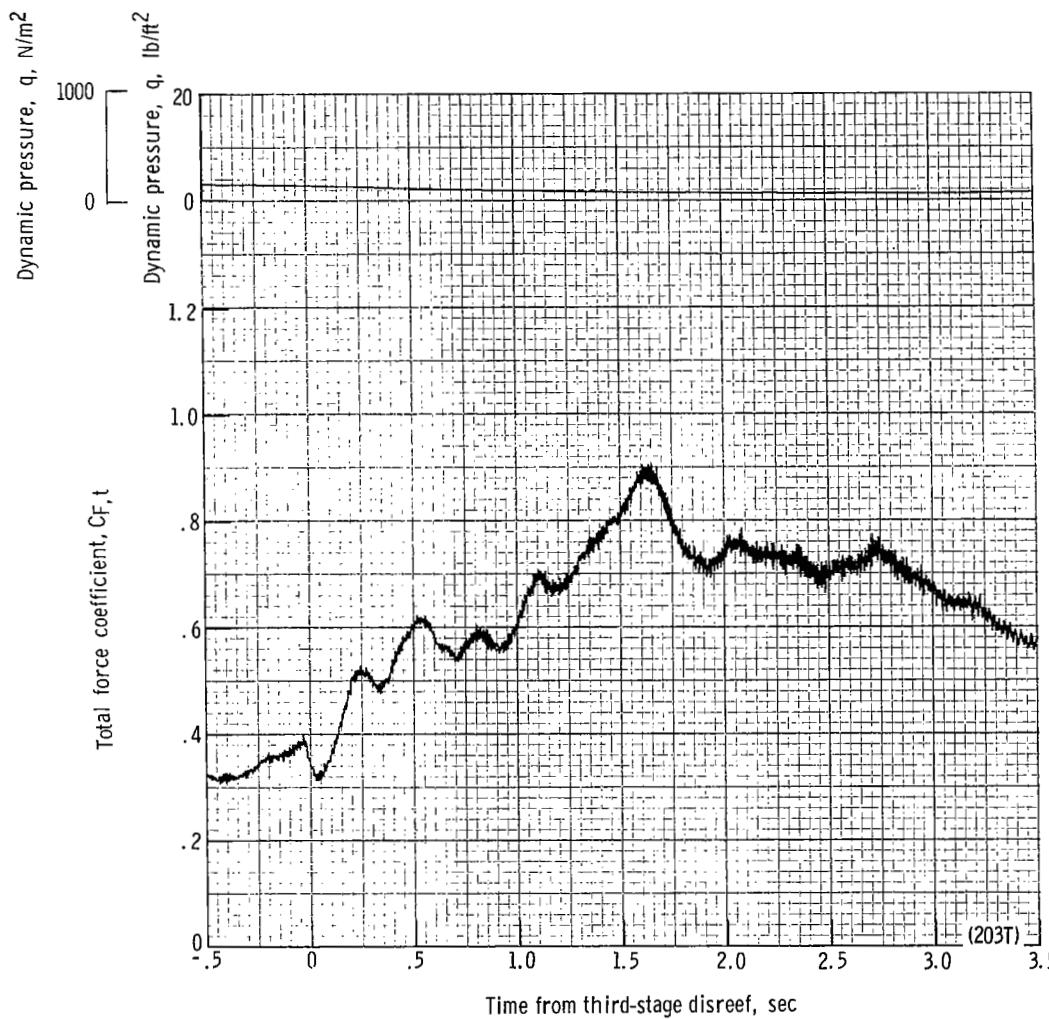
(r) Accelerations a_x , a_y , and a_z plotted against time from third-stage disreef. Time = 0 second corresponds to 41.58 seconds after launch.

Figure 44.- Continued.



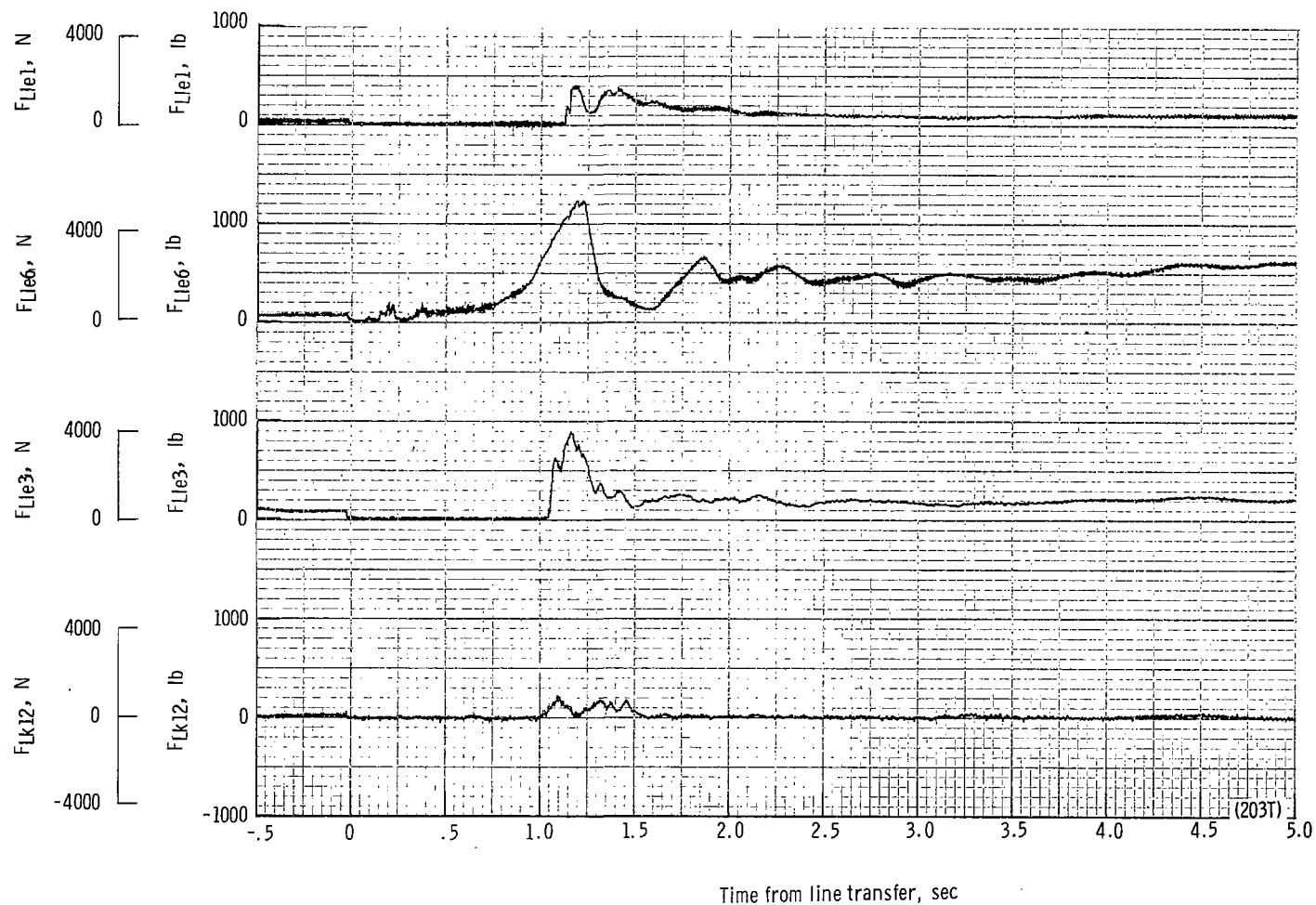
(s) Total force F_t plotted against time from third-stage disreef. Time = 0 second corresponds to 41.58 seconds after launch.

Figure 44.- Continued.



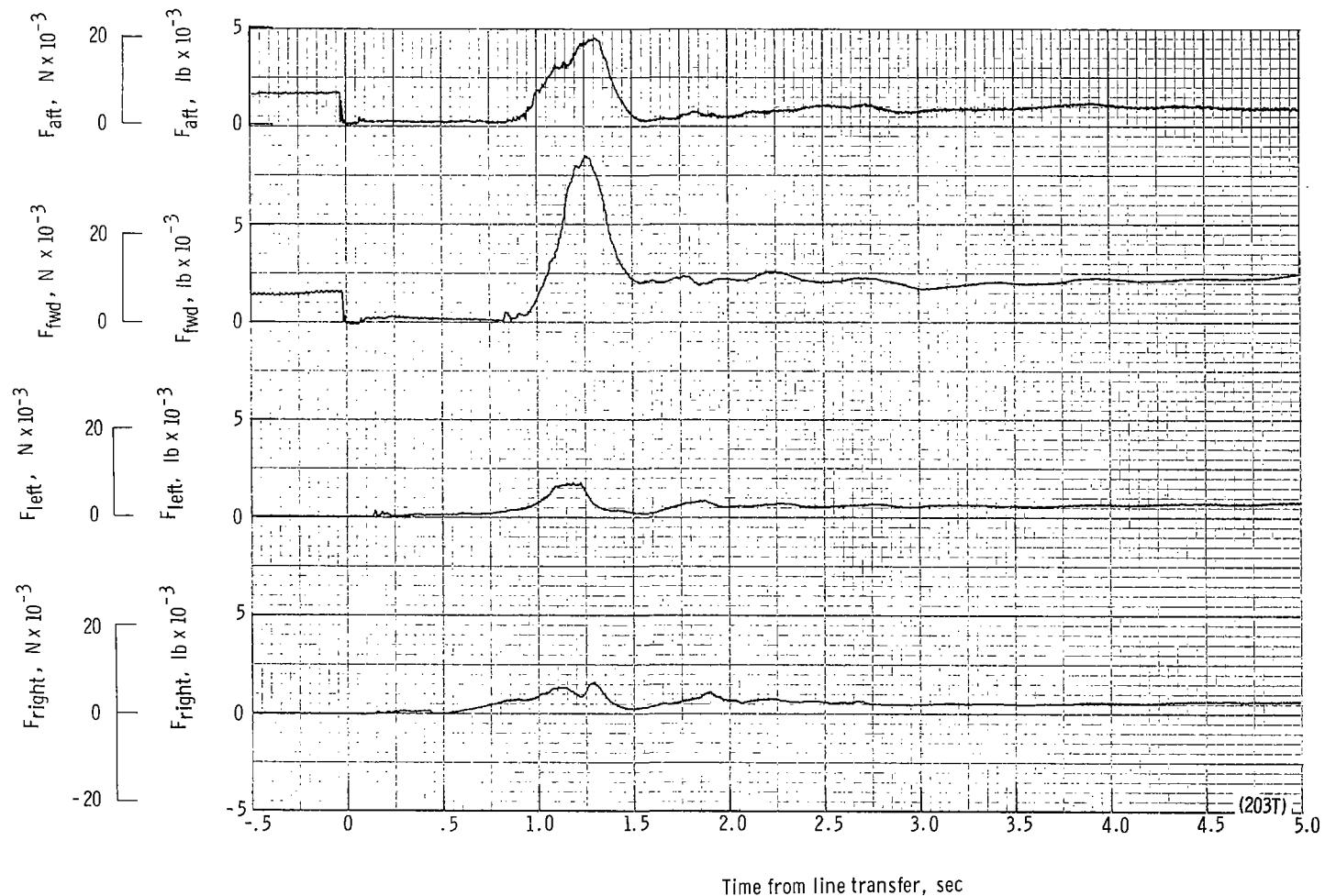
(t) Total force coefficient $C_{F,t}$ and dynamic pressure q plotted against time from third-stage disreef. Time = 0 second corresponds to 41.58 seconds after launch.

Figure 44.- Continued.



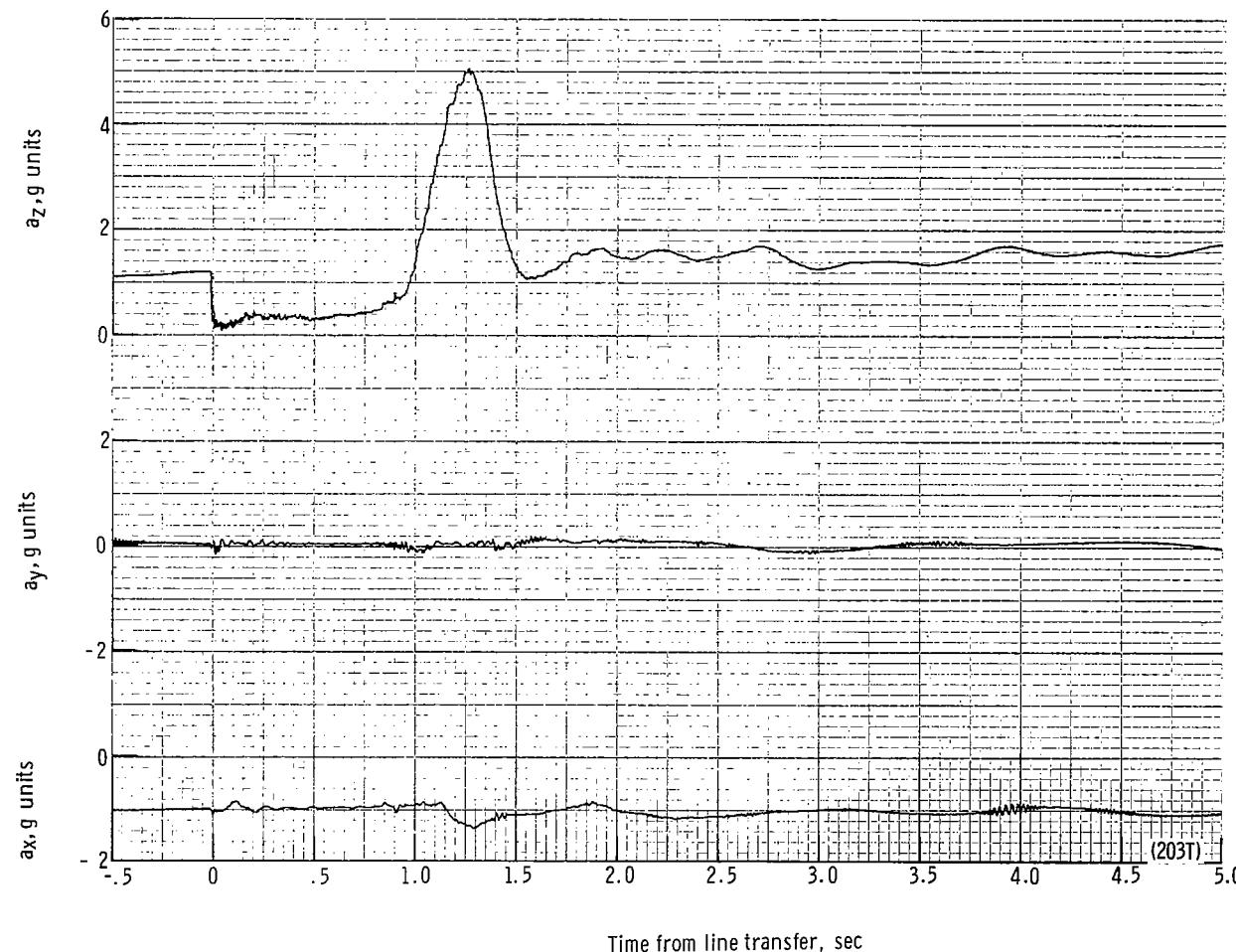
(u) Individual suspension-line loads F_{Lk12} , F_{Lle3} , F_{Lle6} , and F_{Lle1} plotted against time from line transfer. Time = 0 second corresponds to 45.23 seconds after launch.

Figure 44.- Continued.



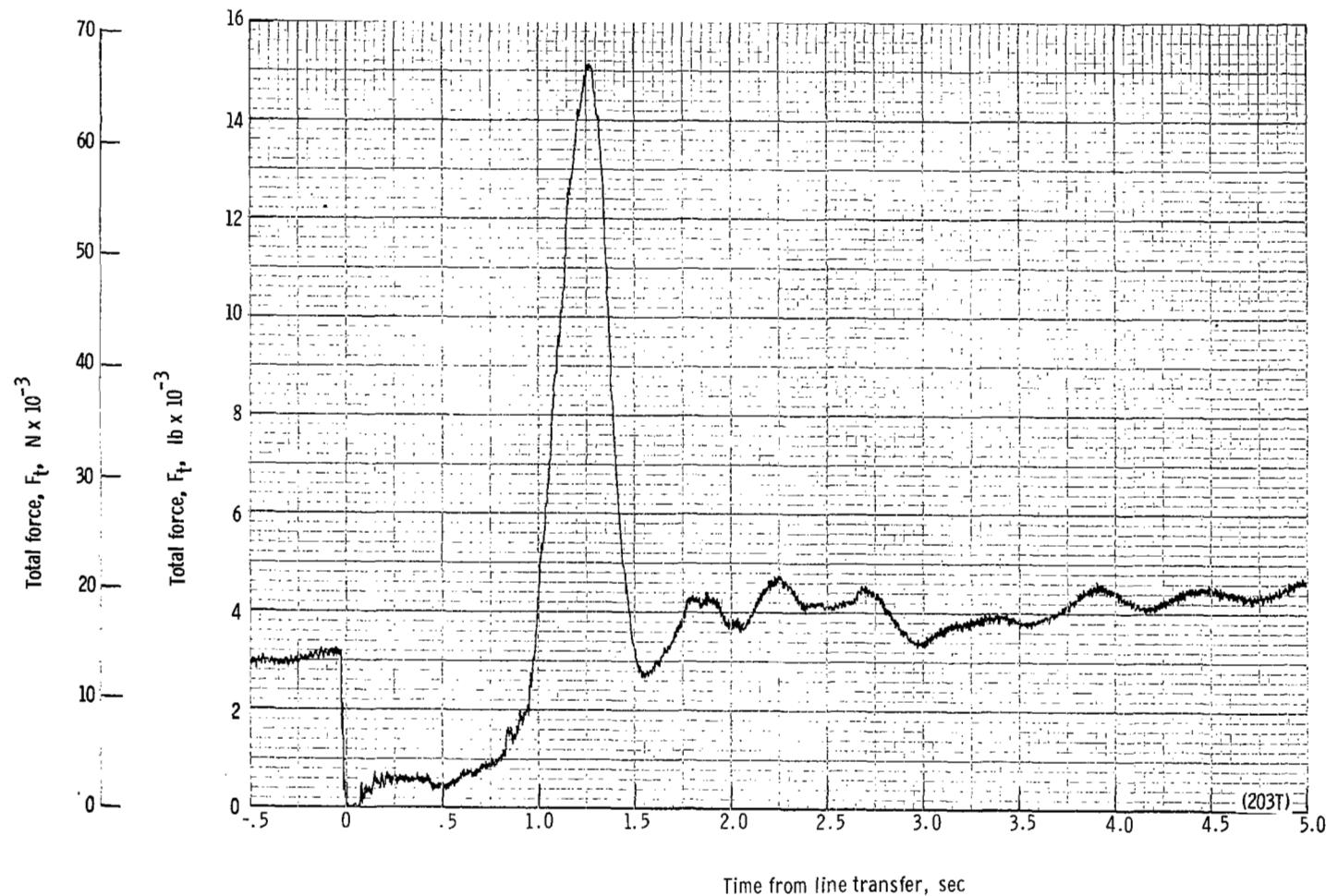
(v) Right, left, forward, and aft riser loads plotted against time from line transfer. Time = 0 second corresponds to 45.23 seconds after launch.

Figure 44.- Continued.



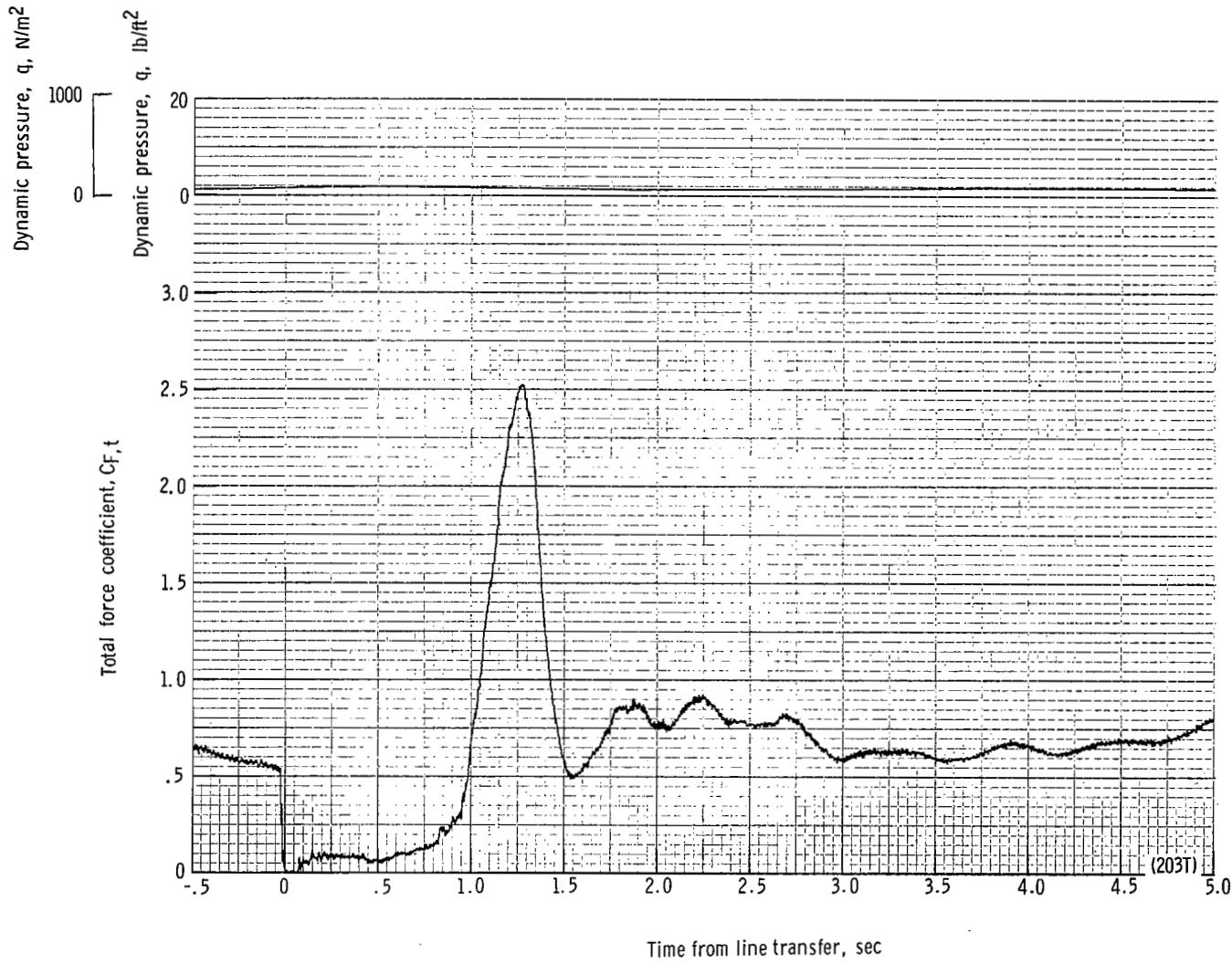
(w) Accelerations a_x , a_y , and a_z plotted against time from line transfer. Time = 0 second corresponds to 45.23 seconds after launch.

Figure 44.- Continued.



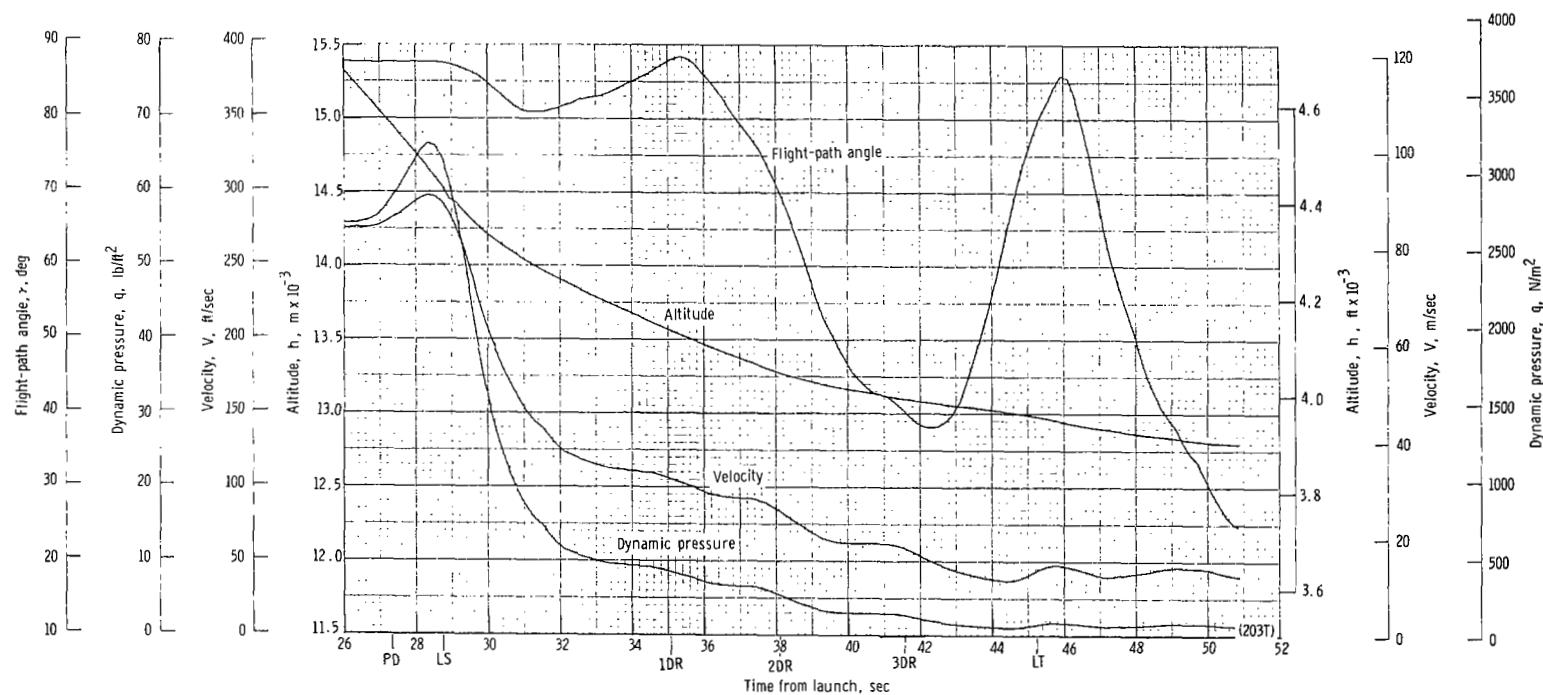
(x) Total force F_t plotted against time from line transfer. Time = 0 second corresponds to 45.23 seconds after launch.

Figure 44.- Continued.



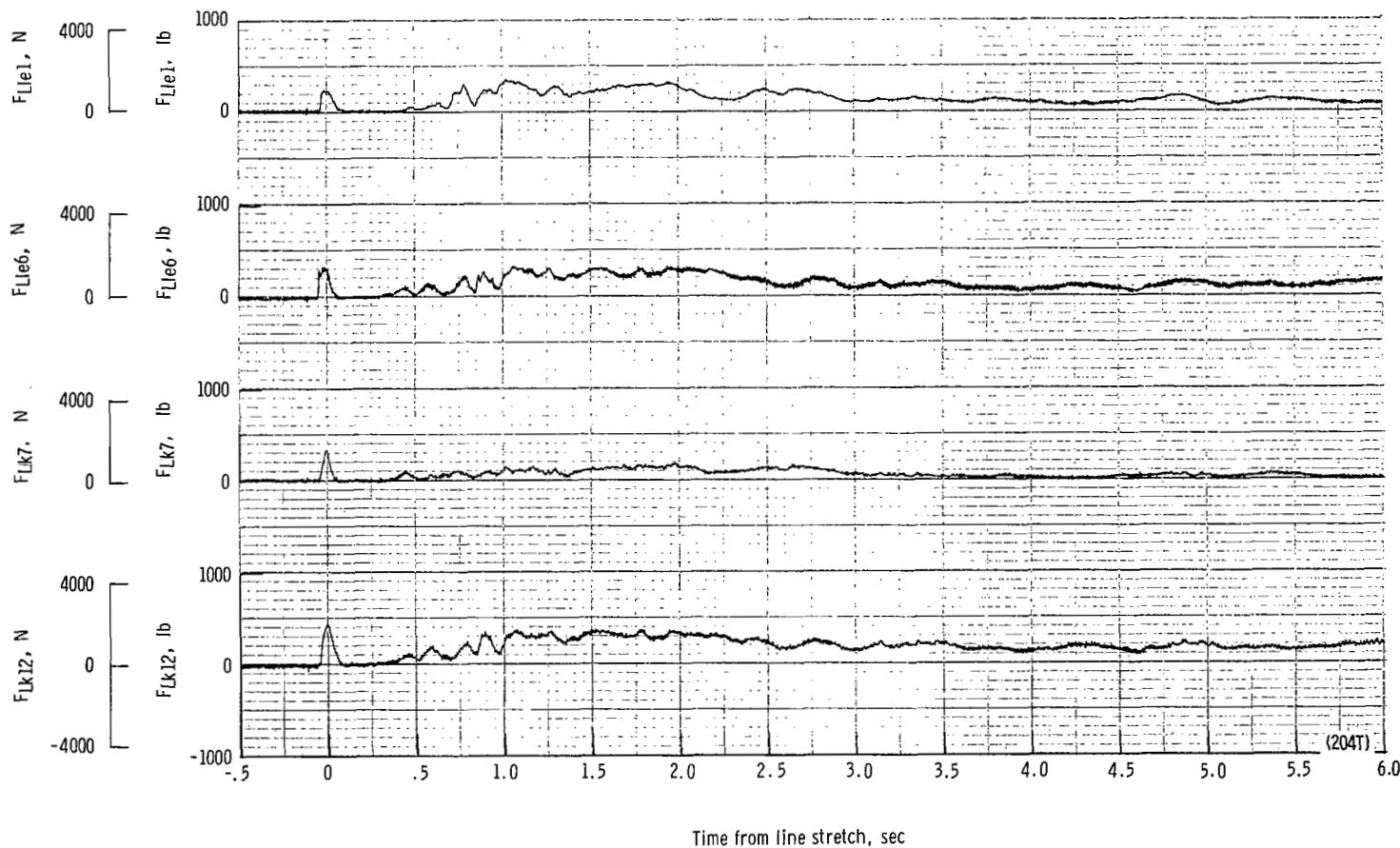
(y) Total force coefficient $C_{F,t}$ and dynamic pressure q plotted against time from line transfer. Time = 0 second corresponds to 45.23 seconds after launch.

Figure 44.- Continued.



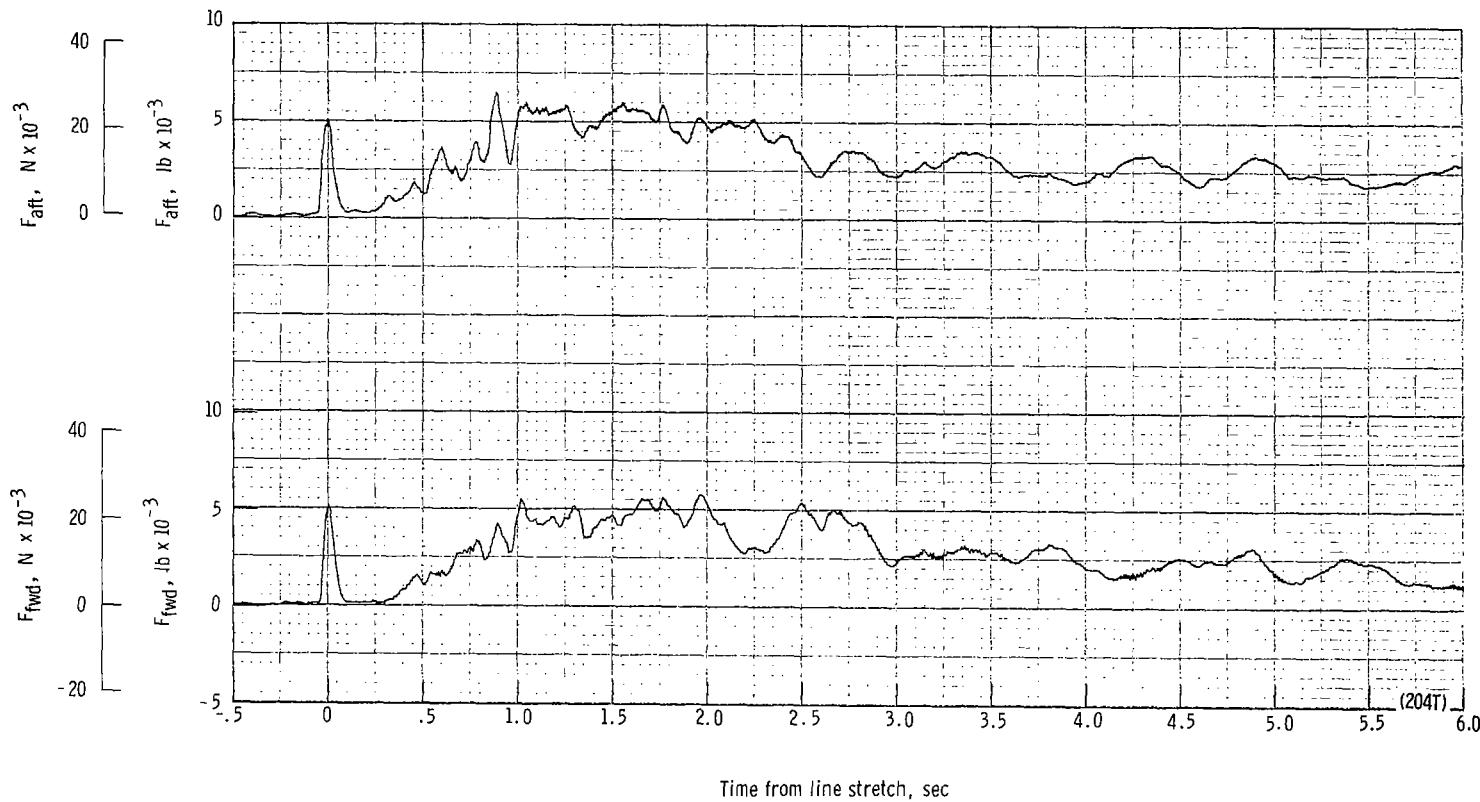
(z) Flight-path angle γ , dynamic pressure q , velocity V , and altitude h plotted against time from launch.

Figure 44.- Concluded.



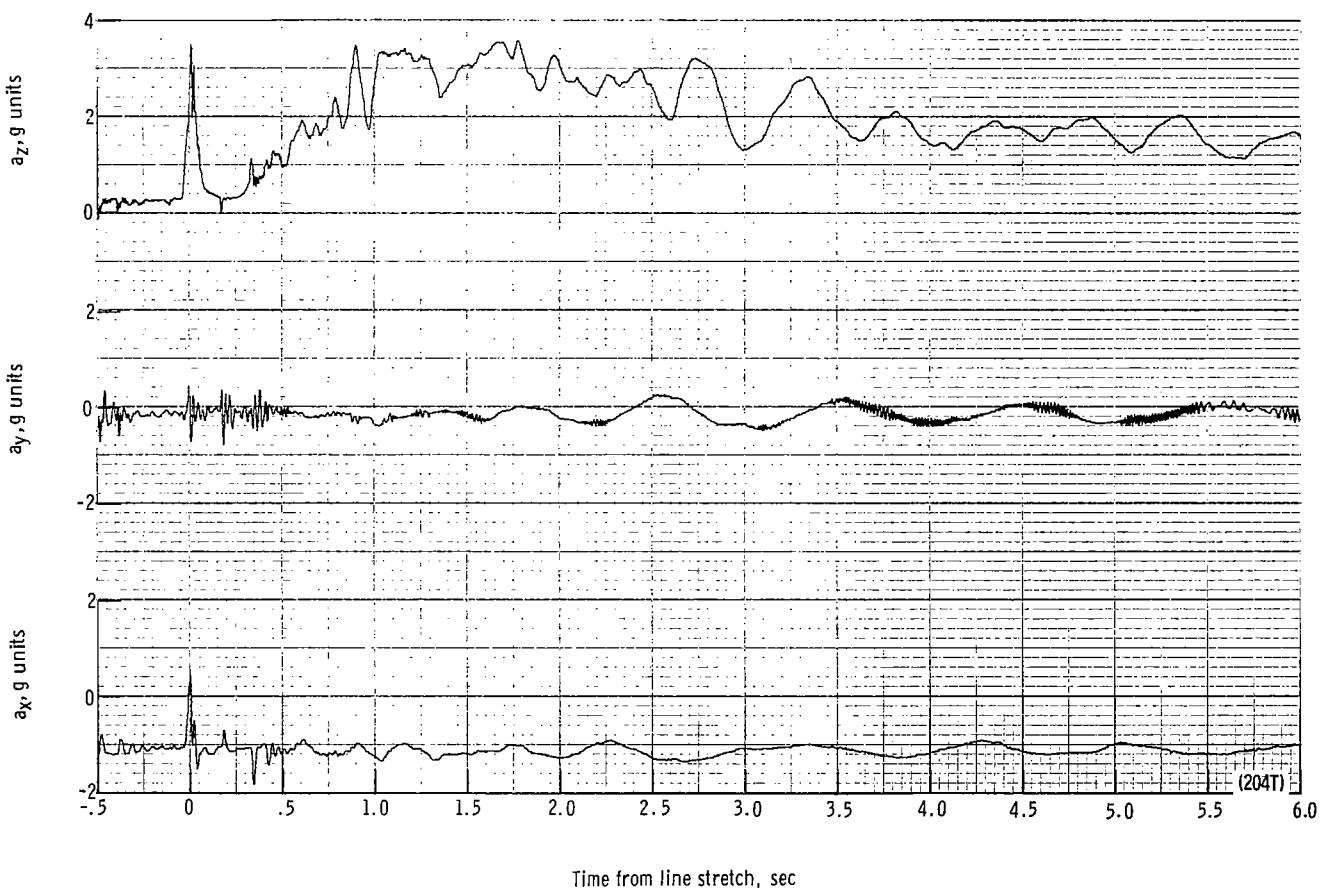
(a) Individual suspension-line loads F_{Lk12} , F_{Lk7} , F_{Lle6} , and F_{Lle1} plotted against time from line stretch. Time = 0 second corresponds to 30.45 seconds after launch.

Figure 45.- Time history of twin-keel parawing deployment data for test 204T. $W_D = 16\ 841\ N$ (3786 lb); $W_p = 15\ 271\ N$ (3433 lb);
 $q_{PD} = 16.231\ N/m^2$ (33.9 lb/ft²); $h_{PD} = 5828\ m$ (19 120 ft); $l_r/l_k = 0.140$; reefing version A.



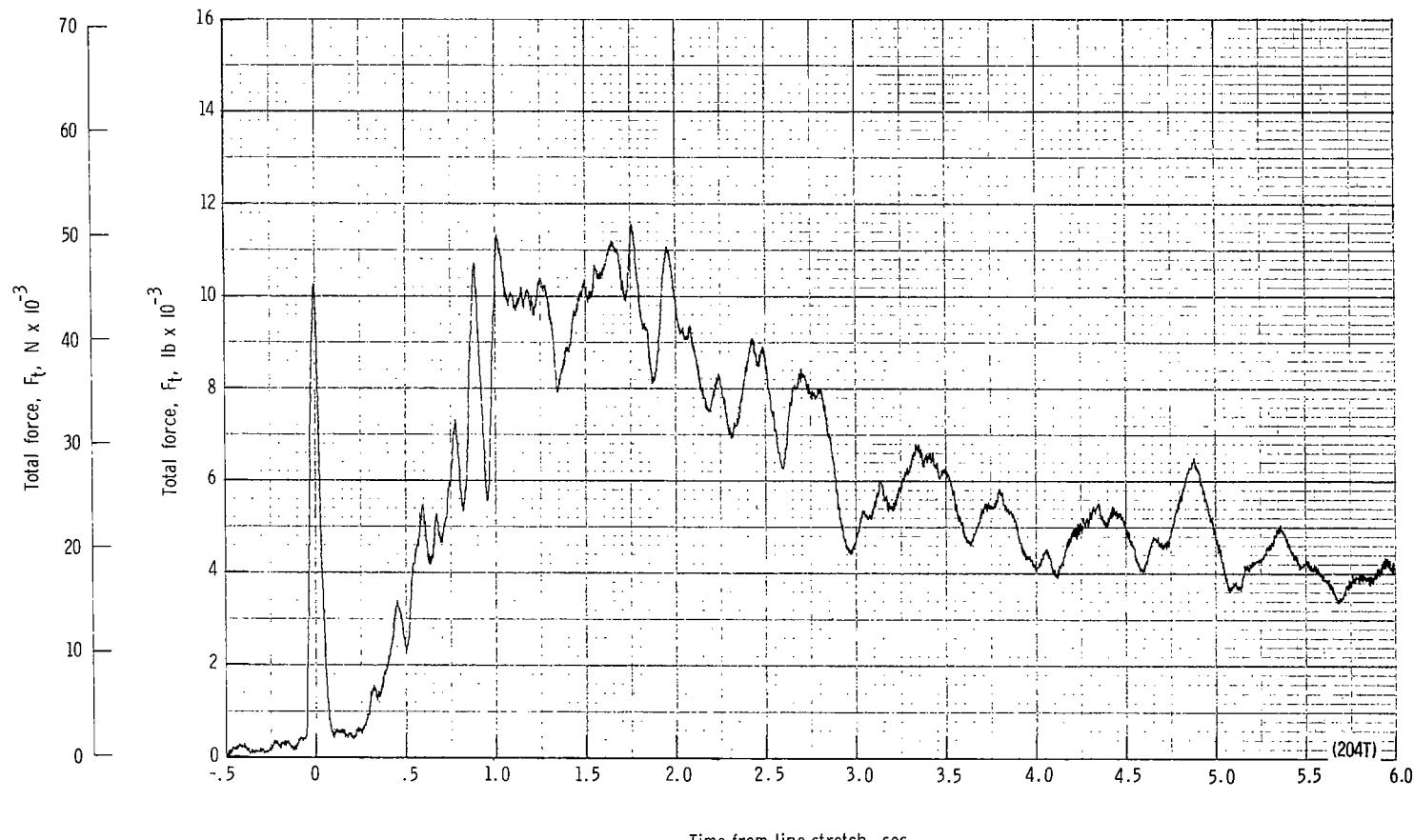
(b) Forward and aft riser loads plotted against time from line stretch. Time = 0 second corresponds to 30.45 seconds after launch.

Figure 45.- Continued.



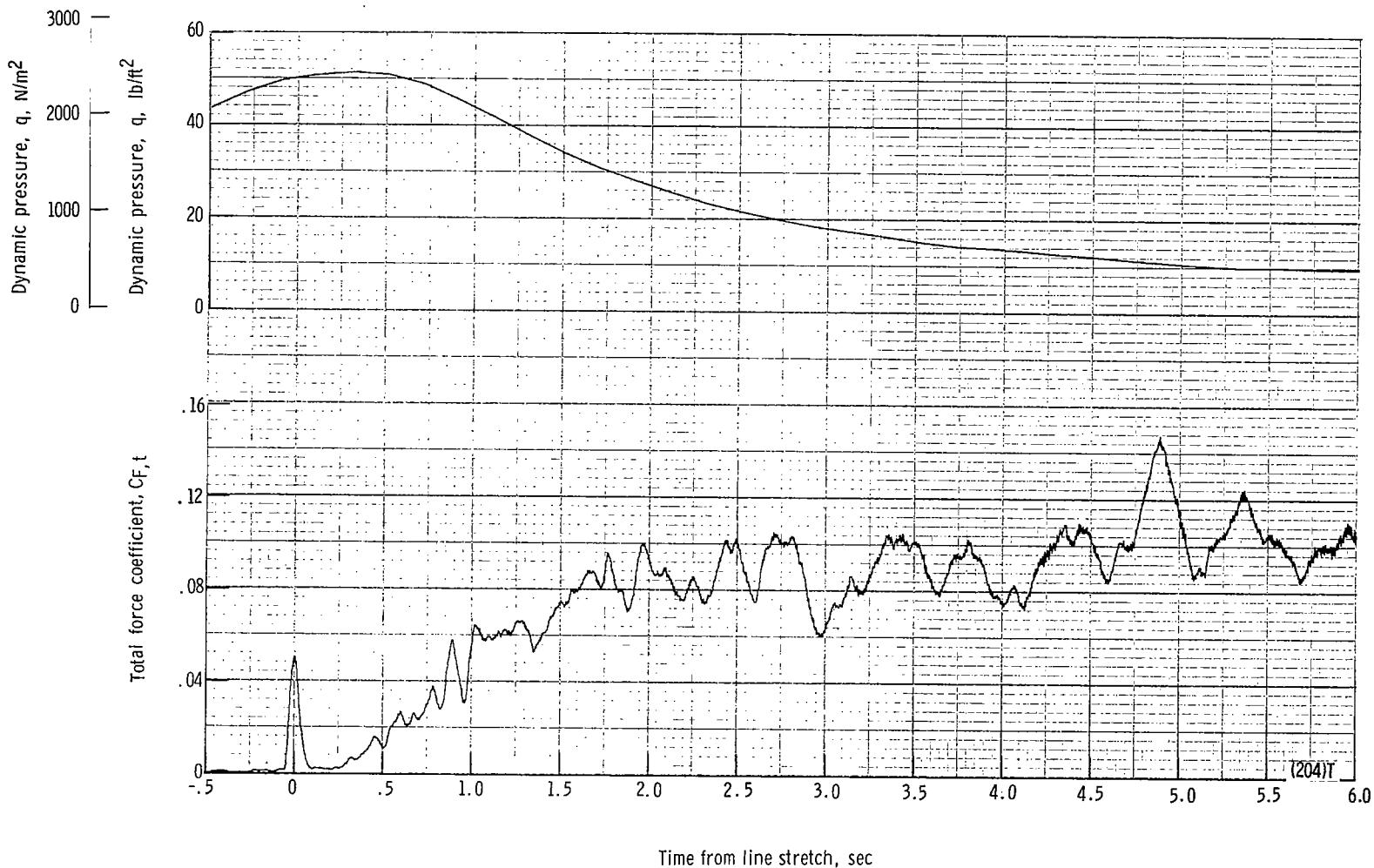
(c) Accelerations a_x , a_y , and a_z plotted against time from line stretch. Time = 0 second corresponds to 30.45 seconds after launch.

Figure 45.- Continued.



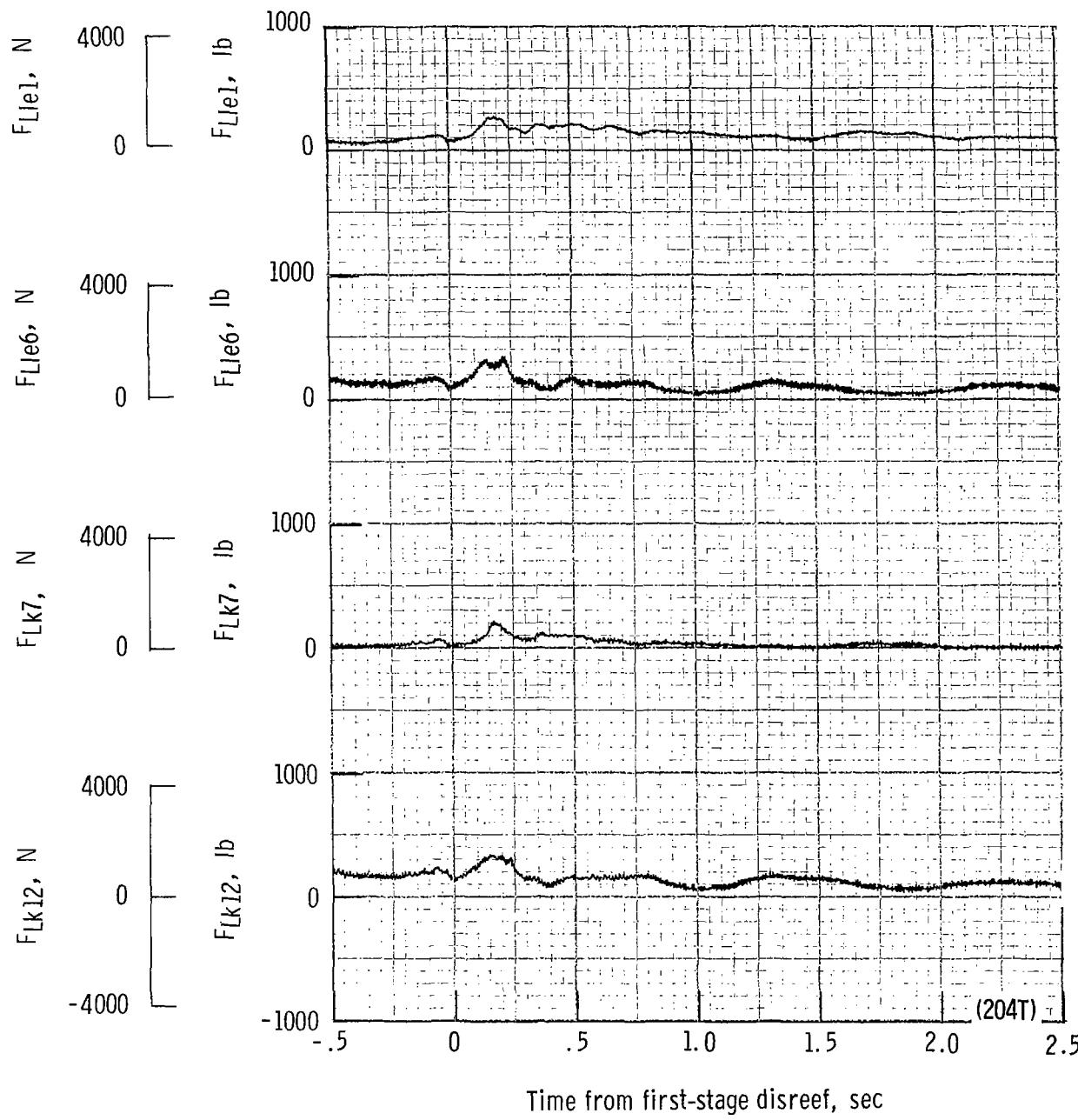
(d) Total force F_t plotted against time from line stretch. Time = 0 second corresponds to 30.45 seconds after launch.

Figure 45.- Continued.

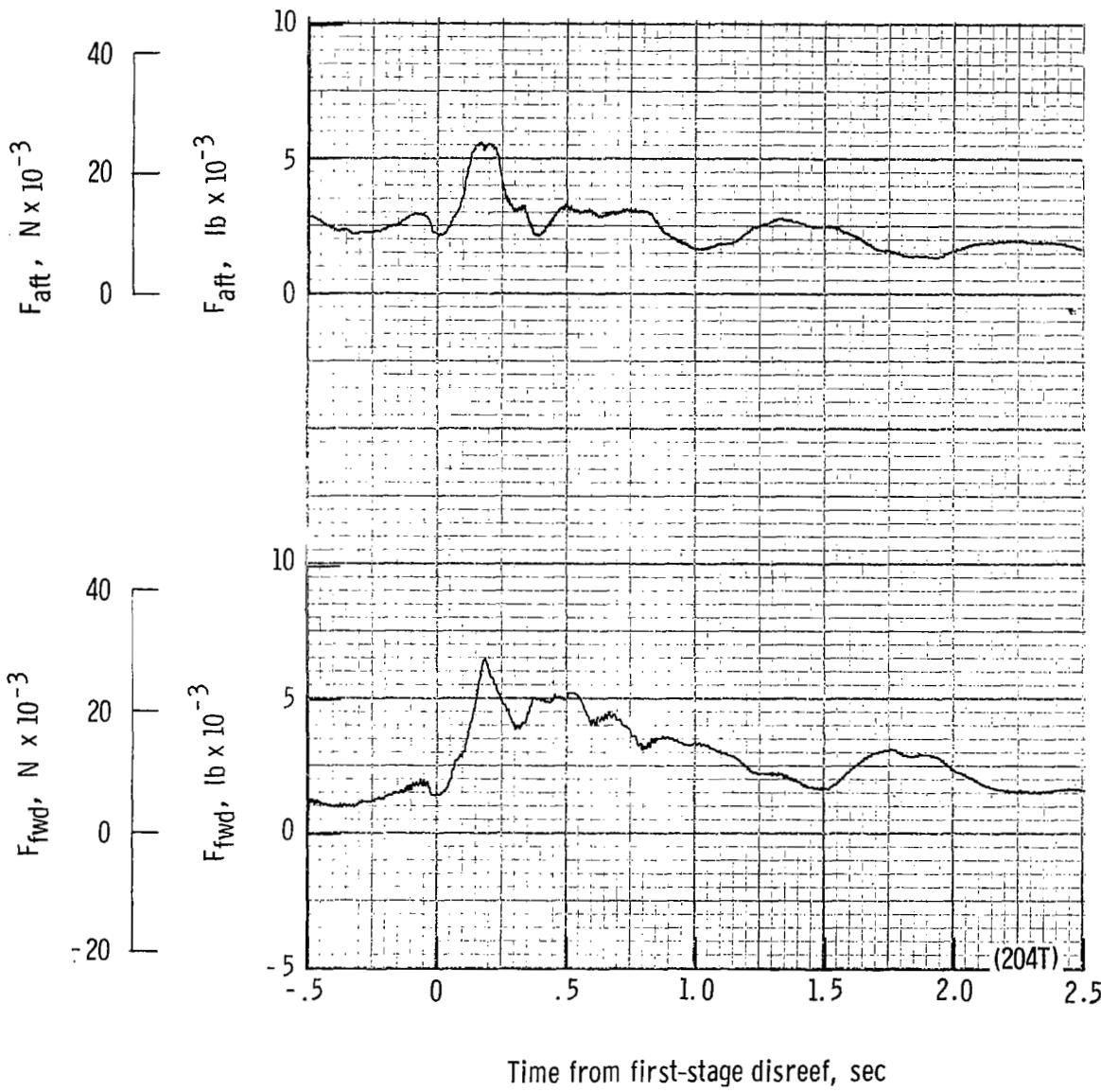


(e) Total force coefficient $C_{F,t}$ and dynamic pressure q plotted against time from line stretch. Time = 0 second corresponds to 30.45 seconds after launch.

Figure 45.- Continued.

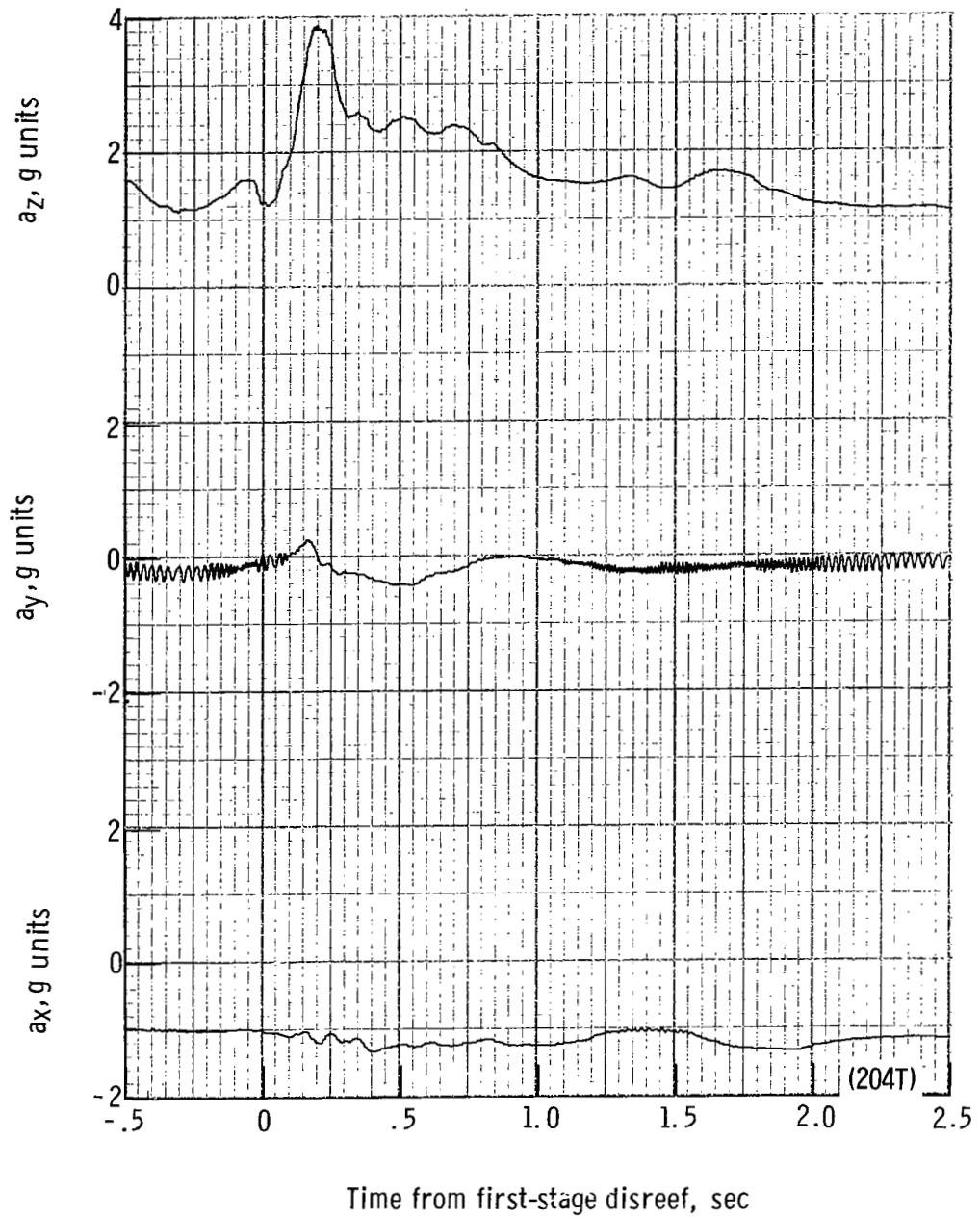


(f) Individual suspension-line loads F_{Lk12} , F_{Lk7} , F_{Lle6} , and F_{Lle1} plotted against time from first-stage disreef. Time = 0 second corresponds to 36.97 seconds after launch.



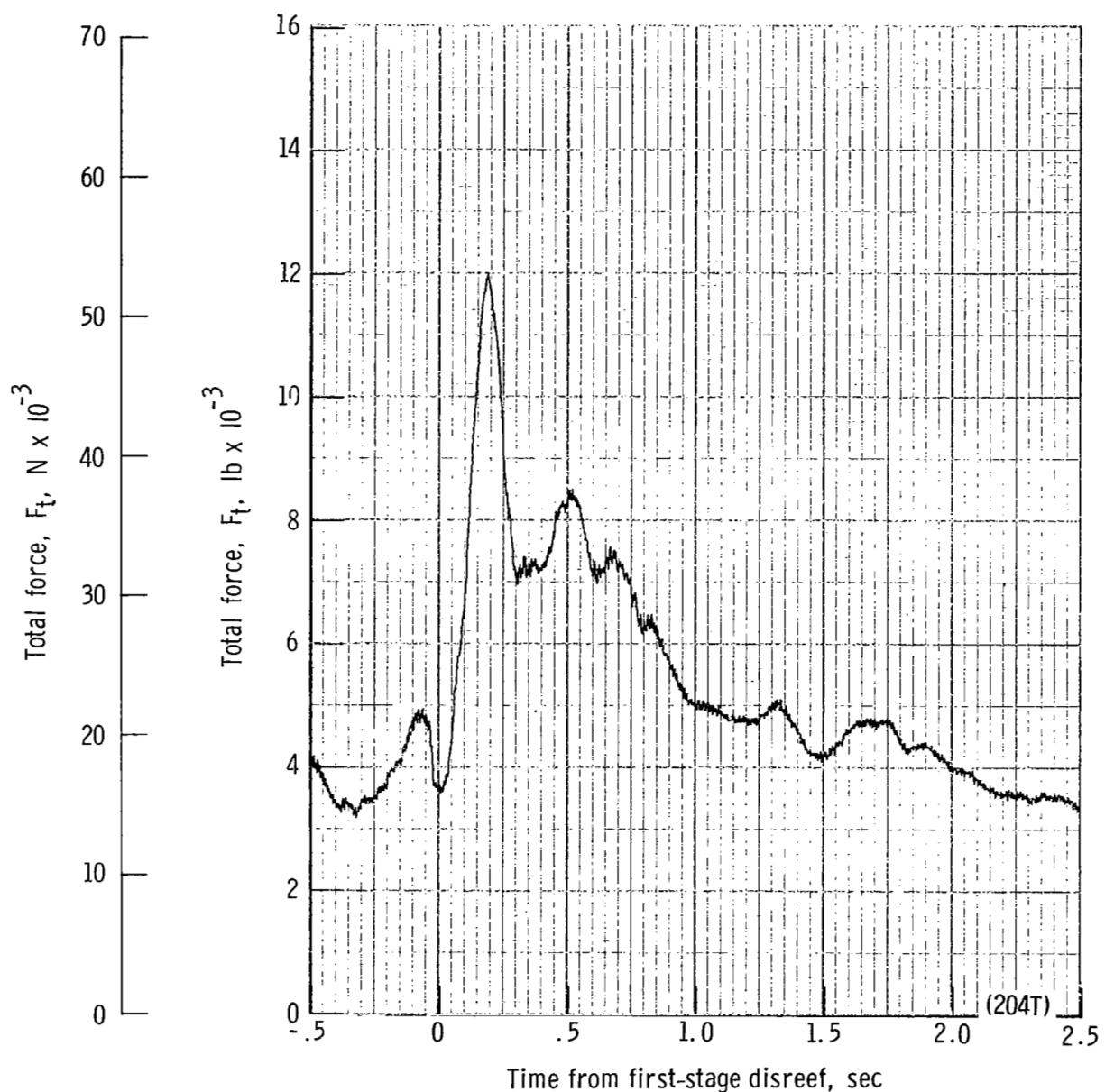
(g) Forward and aft riser loads plotted against time from first-stage disreef. Time = 0 second corresponds to 36.97 seconds after launch.

Figure 45.- Continued.



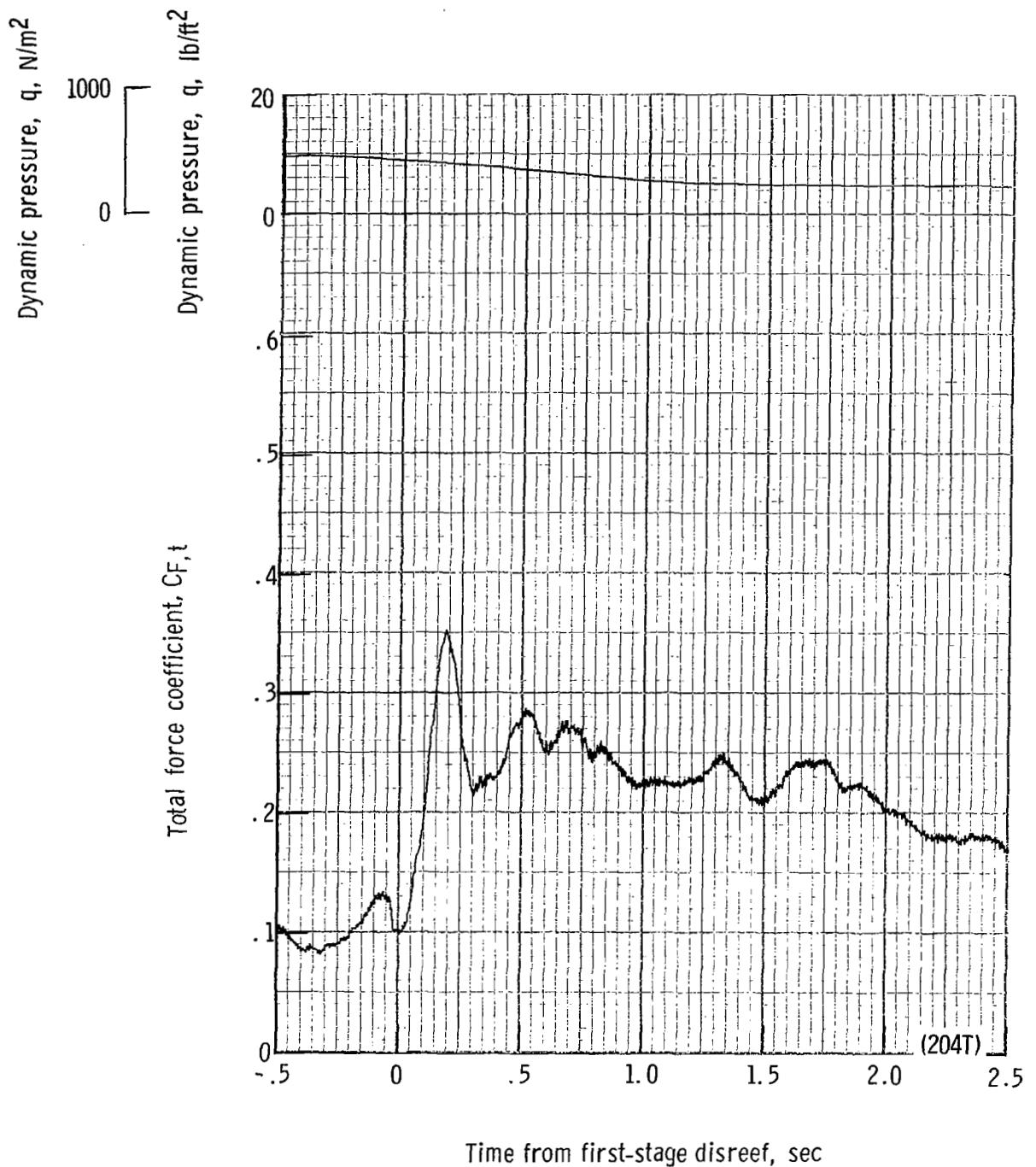
(h) Accelerations a_x , a_y , and a_z plotted against time from first-stage disreef. Time = 0 second corresponds to 36.97 seconds after launch.

Figure 45.- Continued.



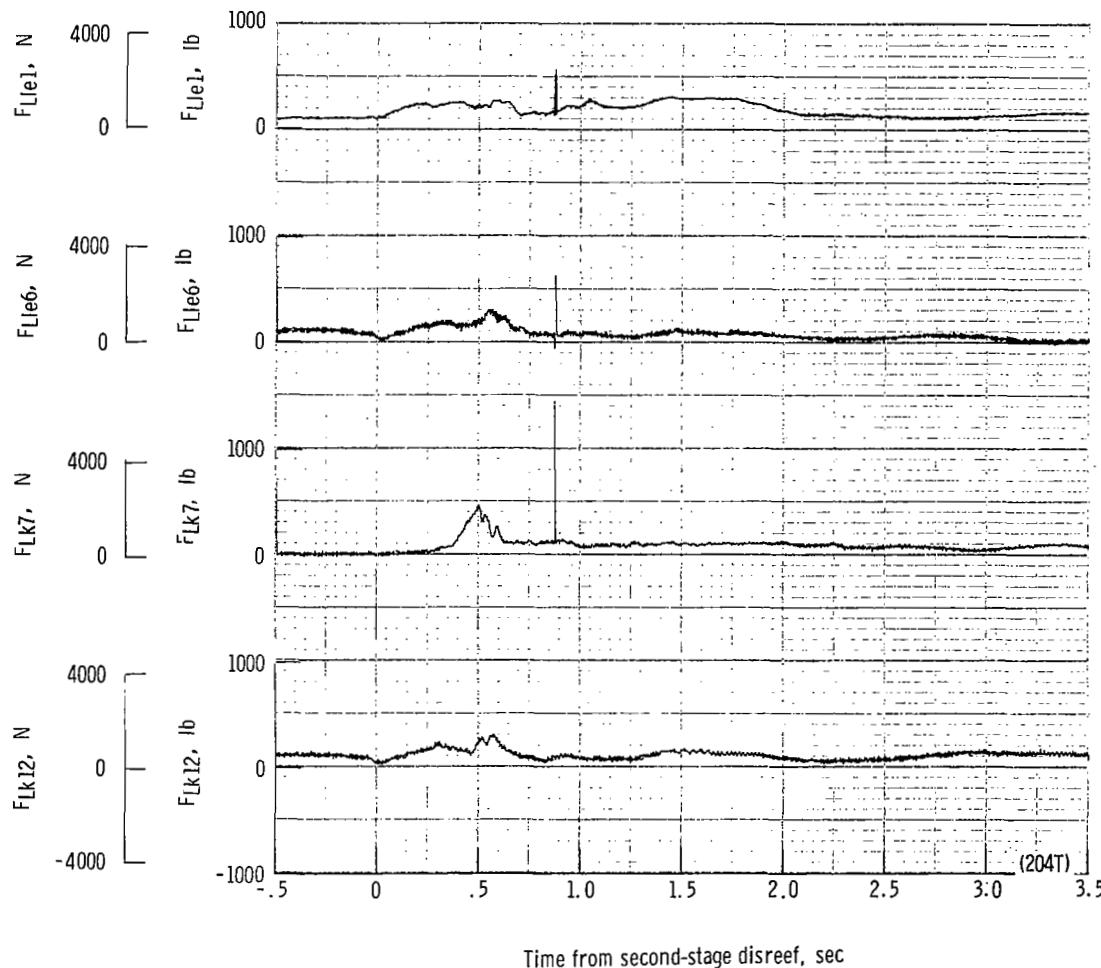
(i) Total force F_t plotted against time from first-stage disreef. Time = 0 second corresponds to 36.97 seconds after launch.

Figure 45.- Continued.



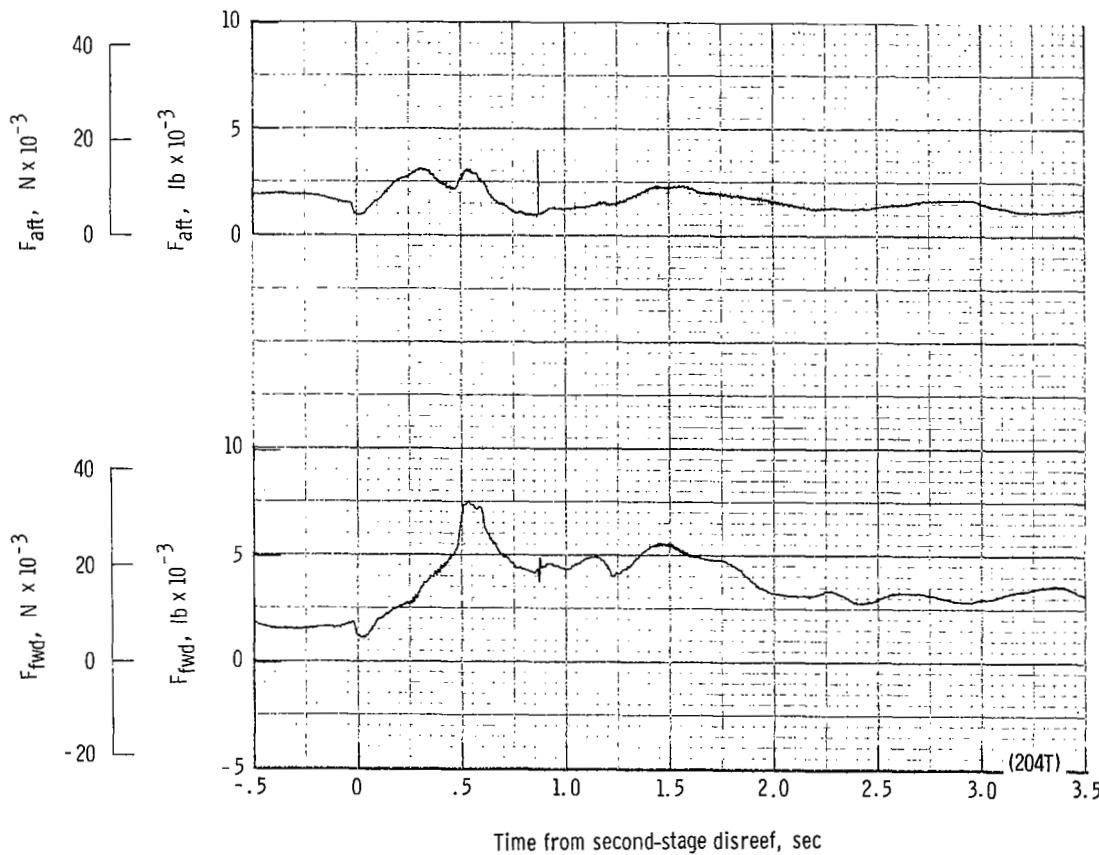
(j) Total force coefficient $C_{F,t}$ and dynamic pressure q plotted against time from first-stage disreef.
Time = 0 second corresponds to 36.97 seconds after launch.

Figure 45.- Continued.



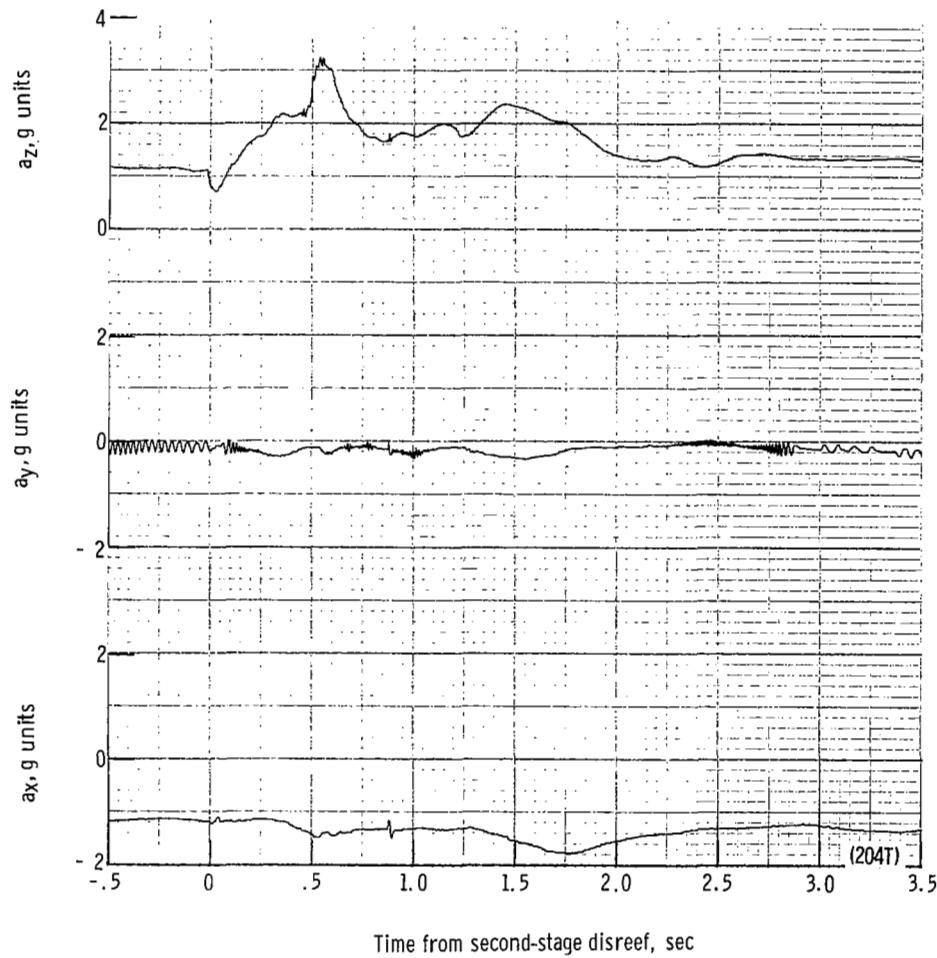
(k) Individual suspension-line loads F_{Lk12} , F_{Lk7} , F_{Lle6} , and F_{Lle1} plotted against time from second-stage disreef. Time = 0 second corresponds to 39.57 seconds after launch.

Figure 45.- Continued.



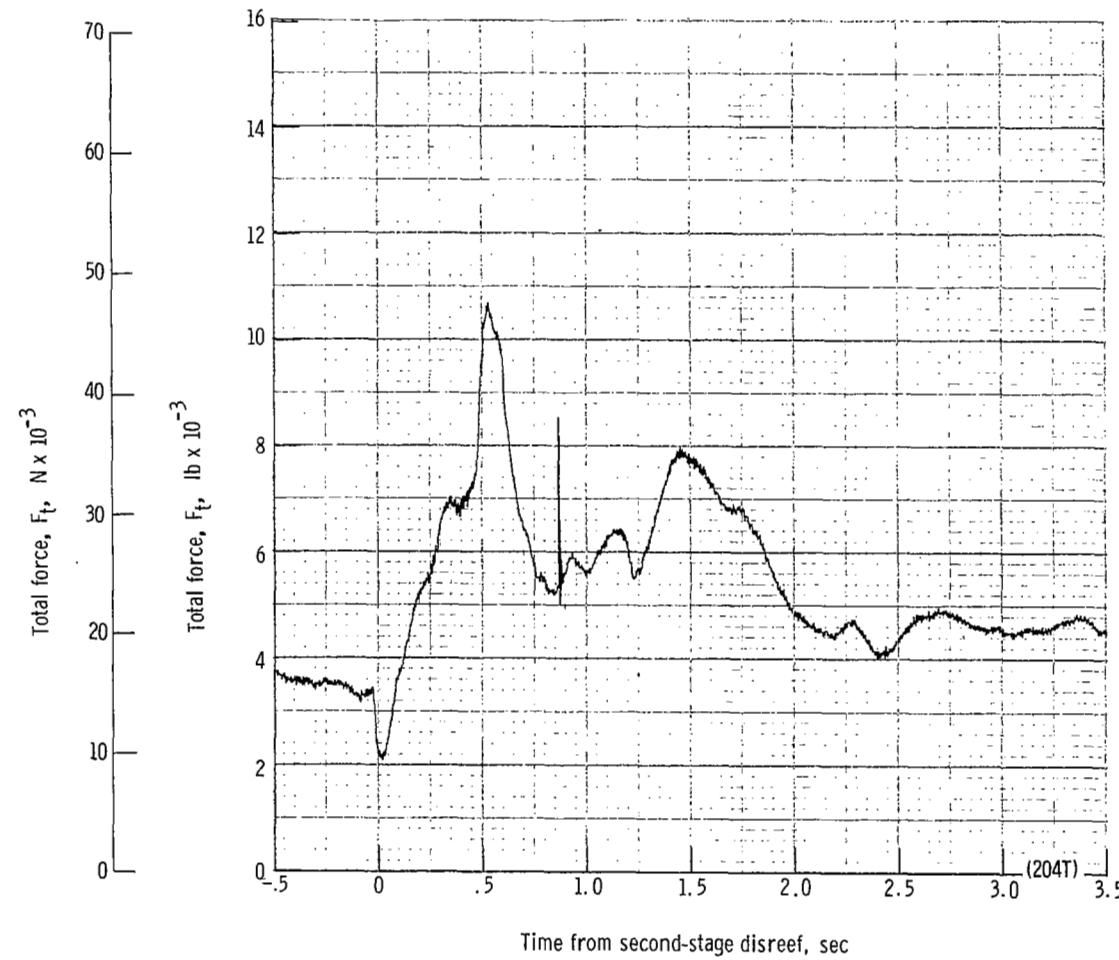
(I) Forward and aft riser loads plotted against time from second-stage disreef. Time = 0 second corresponds to 39.57 seconds after launch.

Figure 45.- Continued.



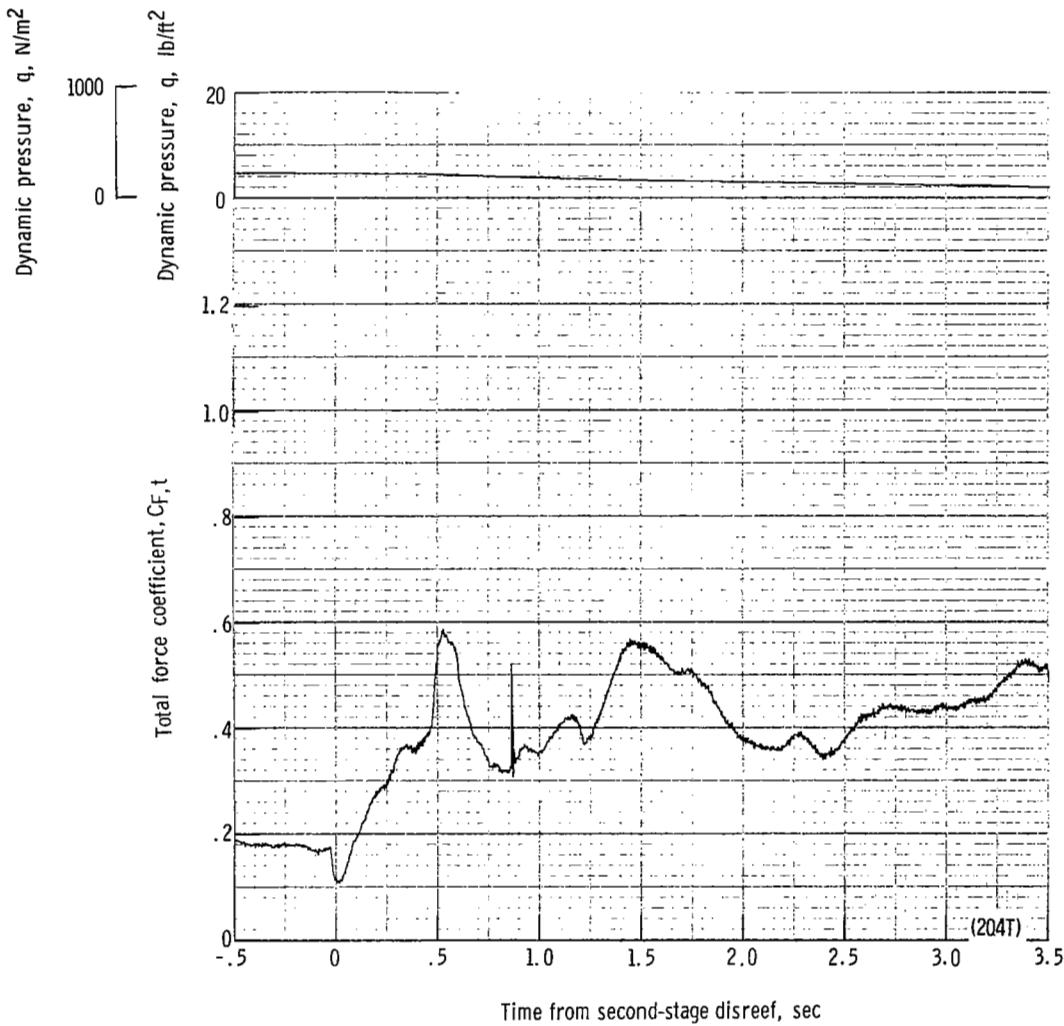
(m) Accelerations a_x , a_y , and a_z plotted against time from second-stage disreef. Time = 0 second corresponds to 39.57 seconds after launch.

Figure 45.- Continued.



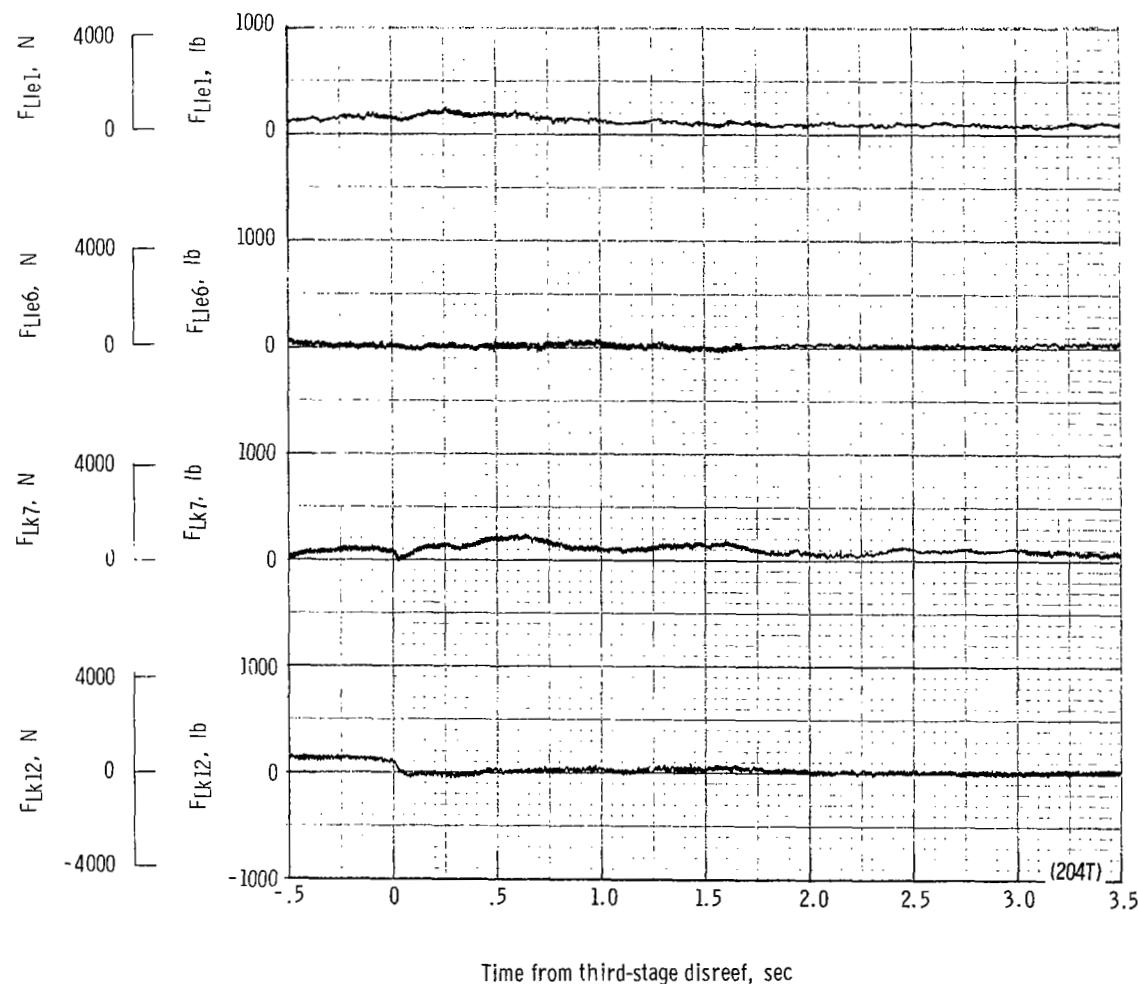
(n) Total force F_t plotted against time from second-stage disreef. Time = 0 second corresponds to 39.57 seconds after launch.

Figure 45.- Continued.



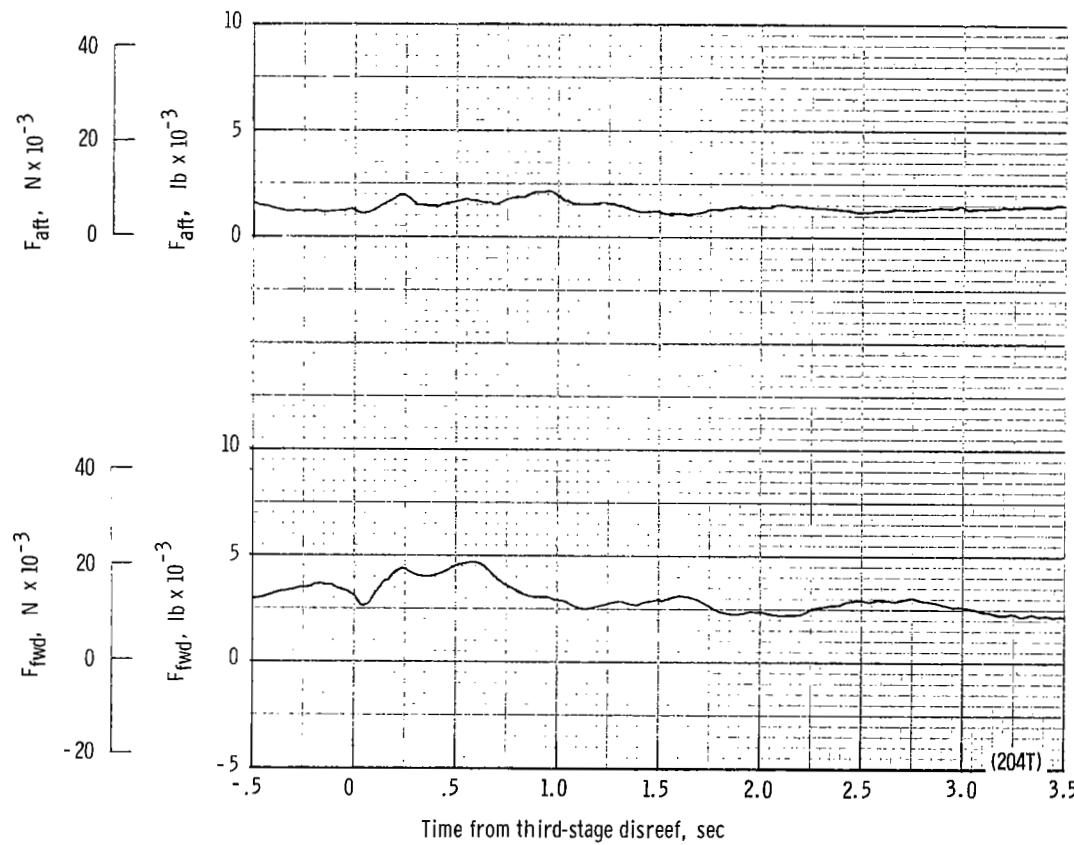
(a) Total force coefficient $C_{F,t}$ and dynamic pressure q plotted against time from second-stage disreef. Time = 0 second corresponds to 39.57 seconds after launch.

Figure 45.- Continued.



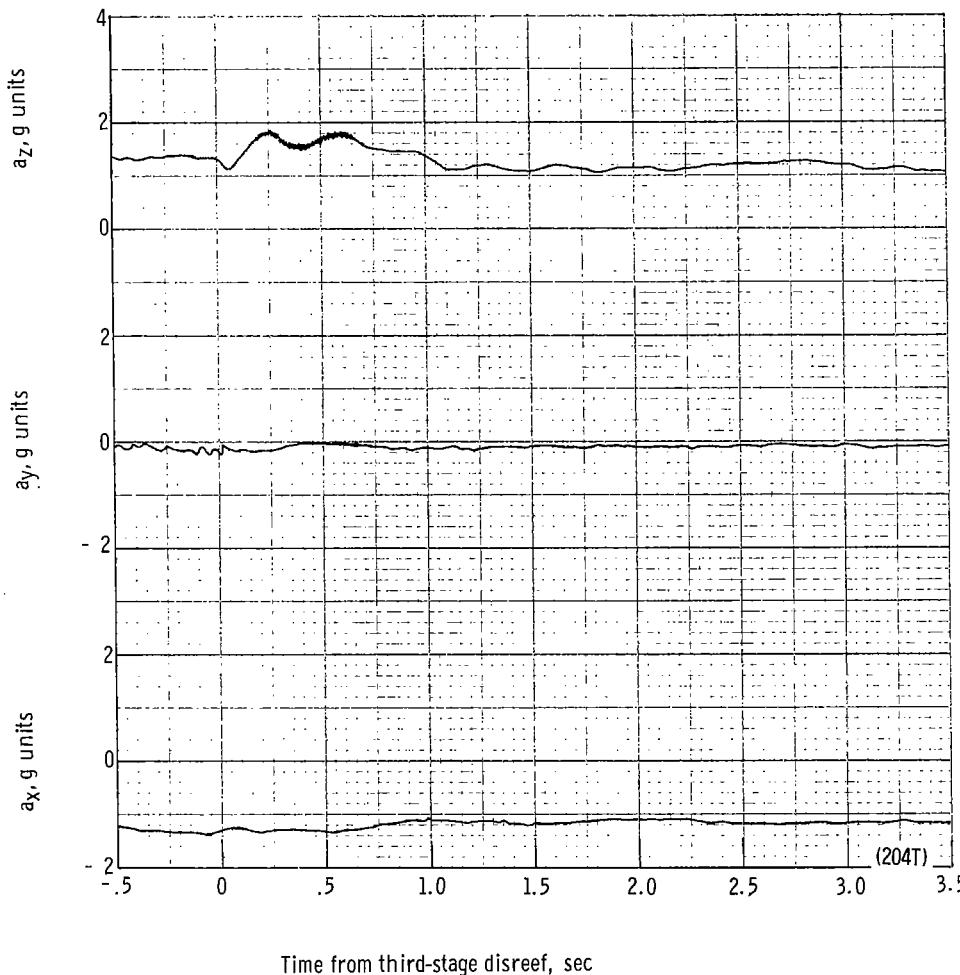
(p) Individual suspension-line loads F_{Lk12} , F_{Lk7} , F_{Lle6} , and F_{Lle1} plotted against time from third-stage disreef. Time = 0 second corresponds to 43.08 seconds after launch.

Figure 45.- Continued.



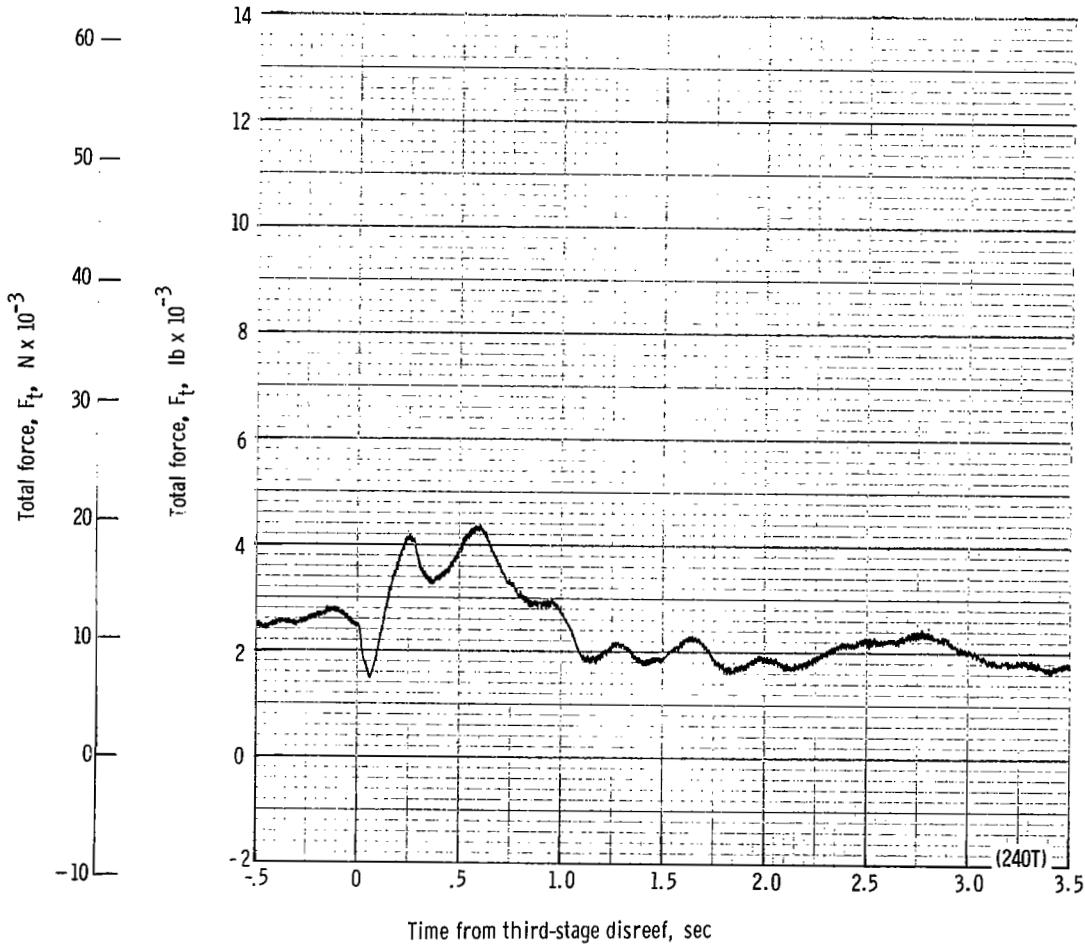
(q) Forward and aft riser loads plotted against time from third-stage disreef. Time = 0 second corresponds to 43.08 seconds after launch.

Figure 45.- Continued.



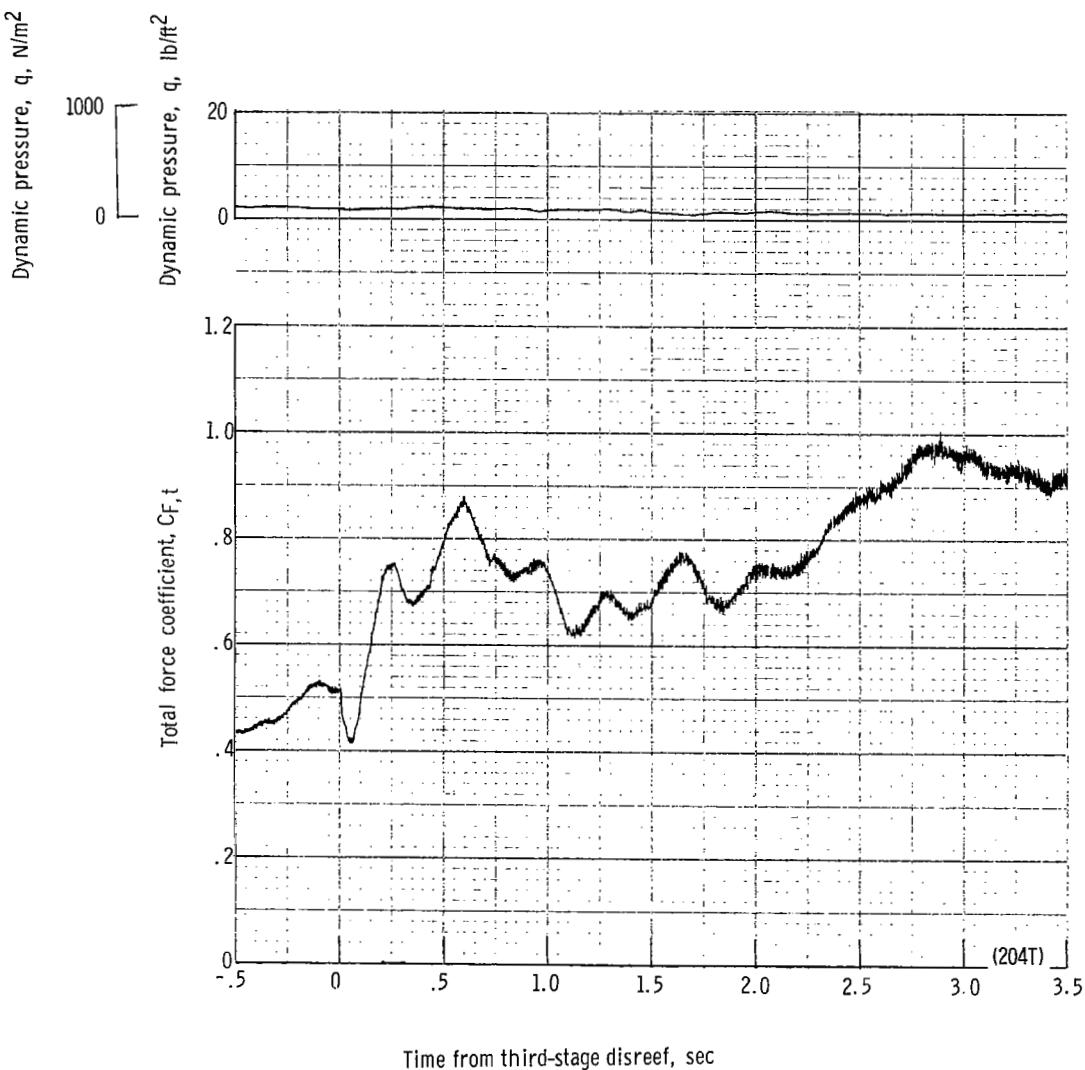
(r) Accelerations a_x , a_y , and a_z plotted against time from third-stage disreef. Time = 0 second corresponds to 43.08 seconds after launch.

Figure 45.- Continued.



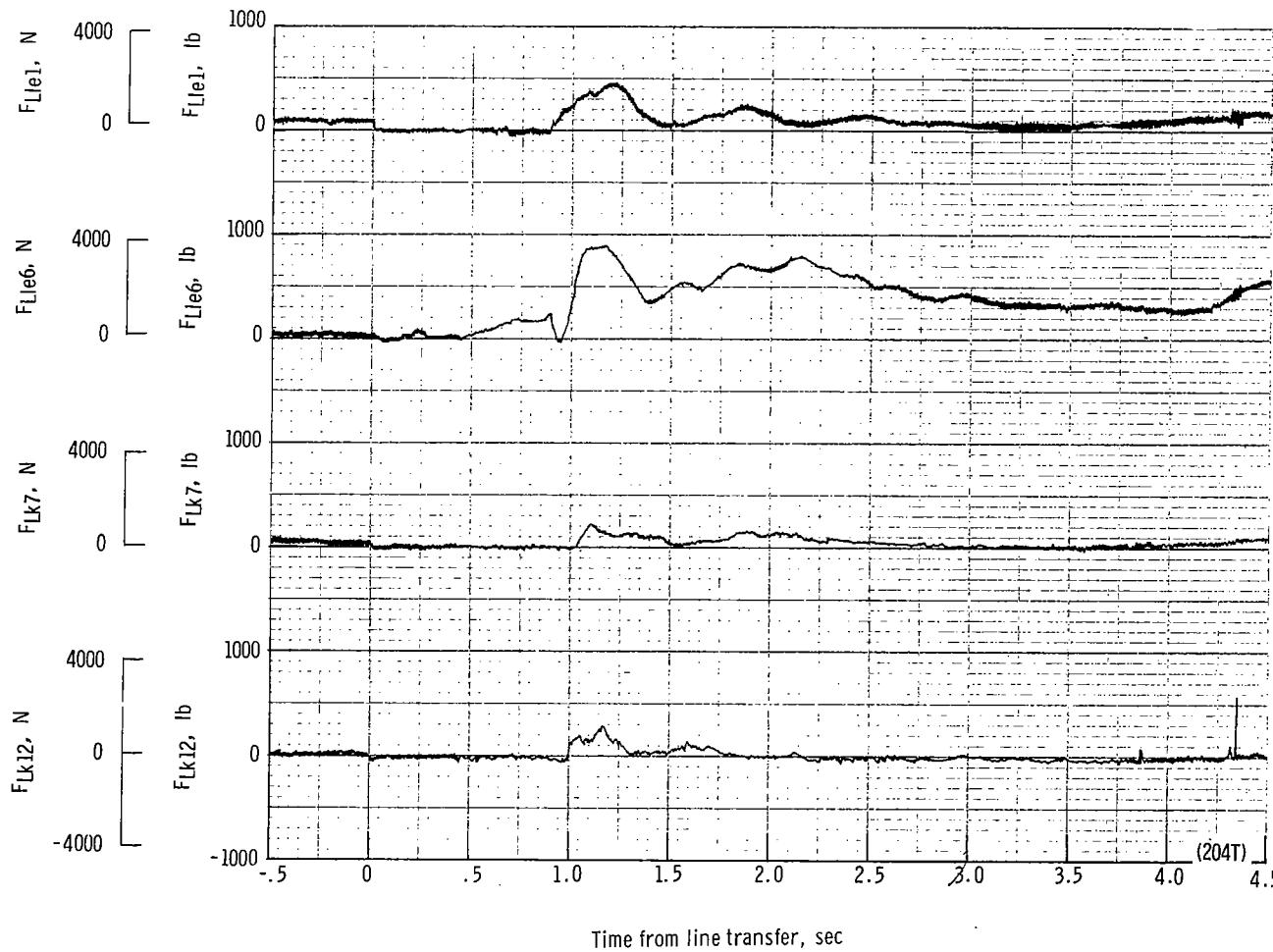
(s) Total force F_t plotted against time from third-stage disreef. Time = 0 second corresponds to 43.08 seconds after launch.

Figure 45.- Continued.



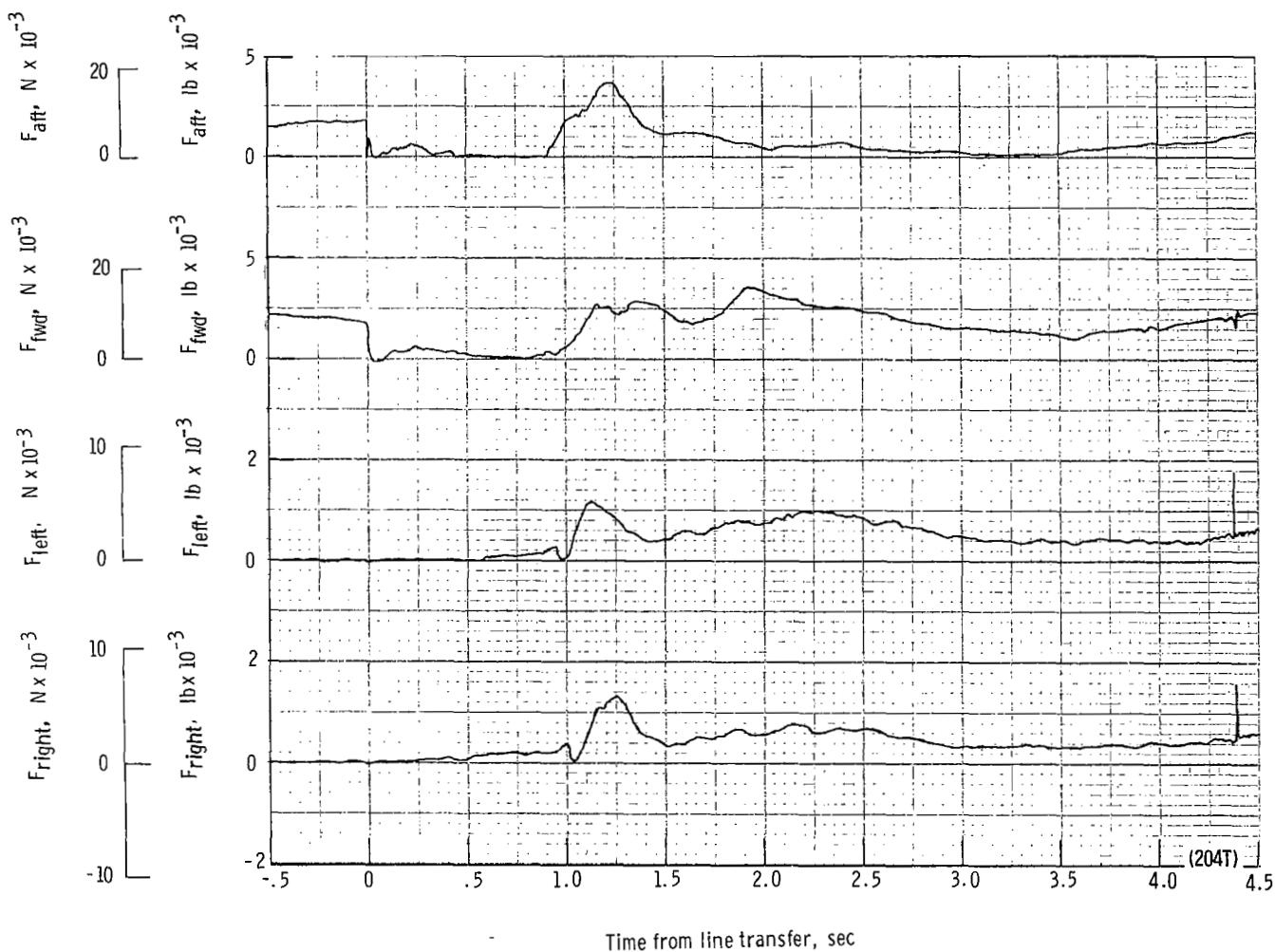
(t) Total force coefficient $C_{F,t}$ and dynamic pressure q plotted against time from third-stage disreef. Time = 0 second corresponds to 43.08 seconds after launch.

Figure 45.- Continued.



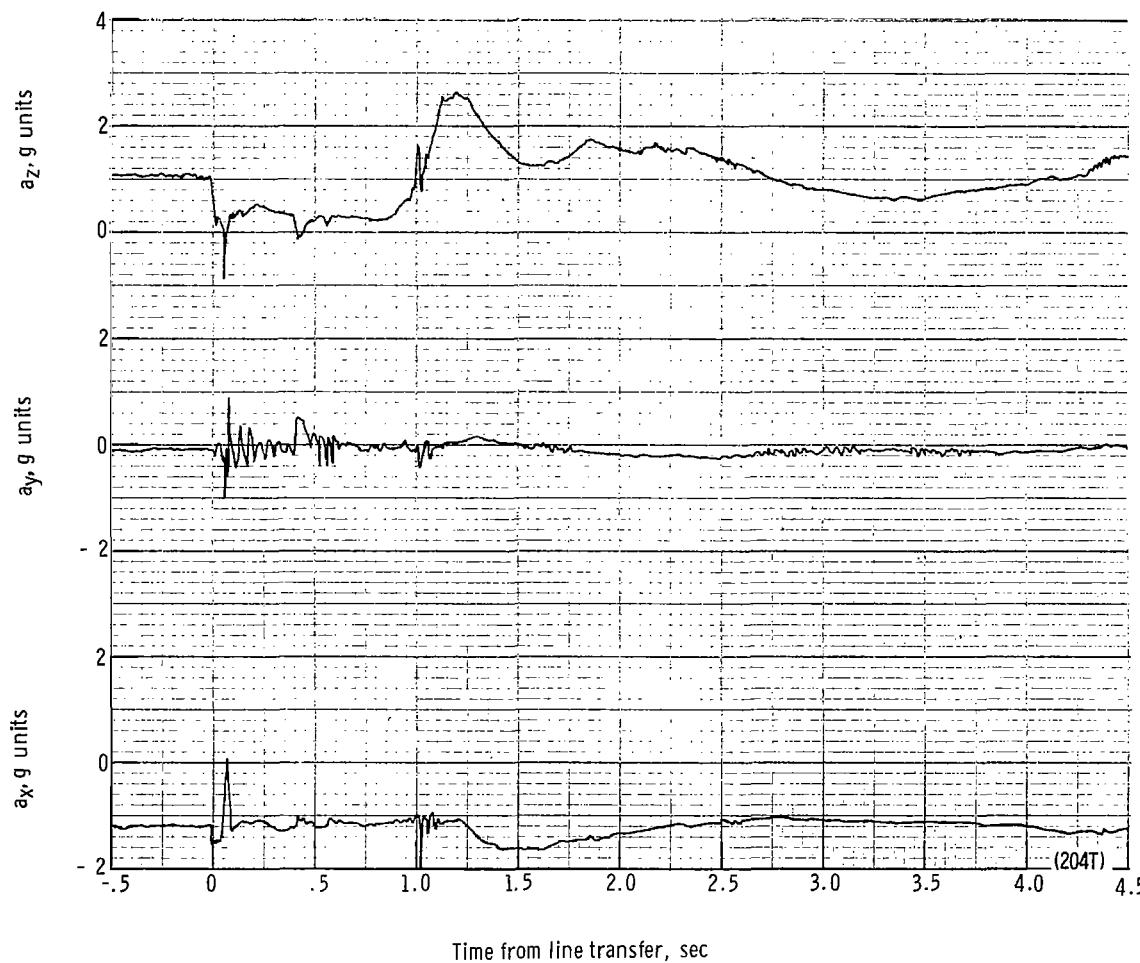
(u) Individual suspension-line loads F_{Lk12} , F_{Lk7} , F_{Lle6} , and F_{Lle1} plotted against time from line transfer. Time = 0 second corresponds to 47.00 seconds after launch.

Figure 45.- Continued.



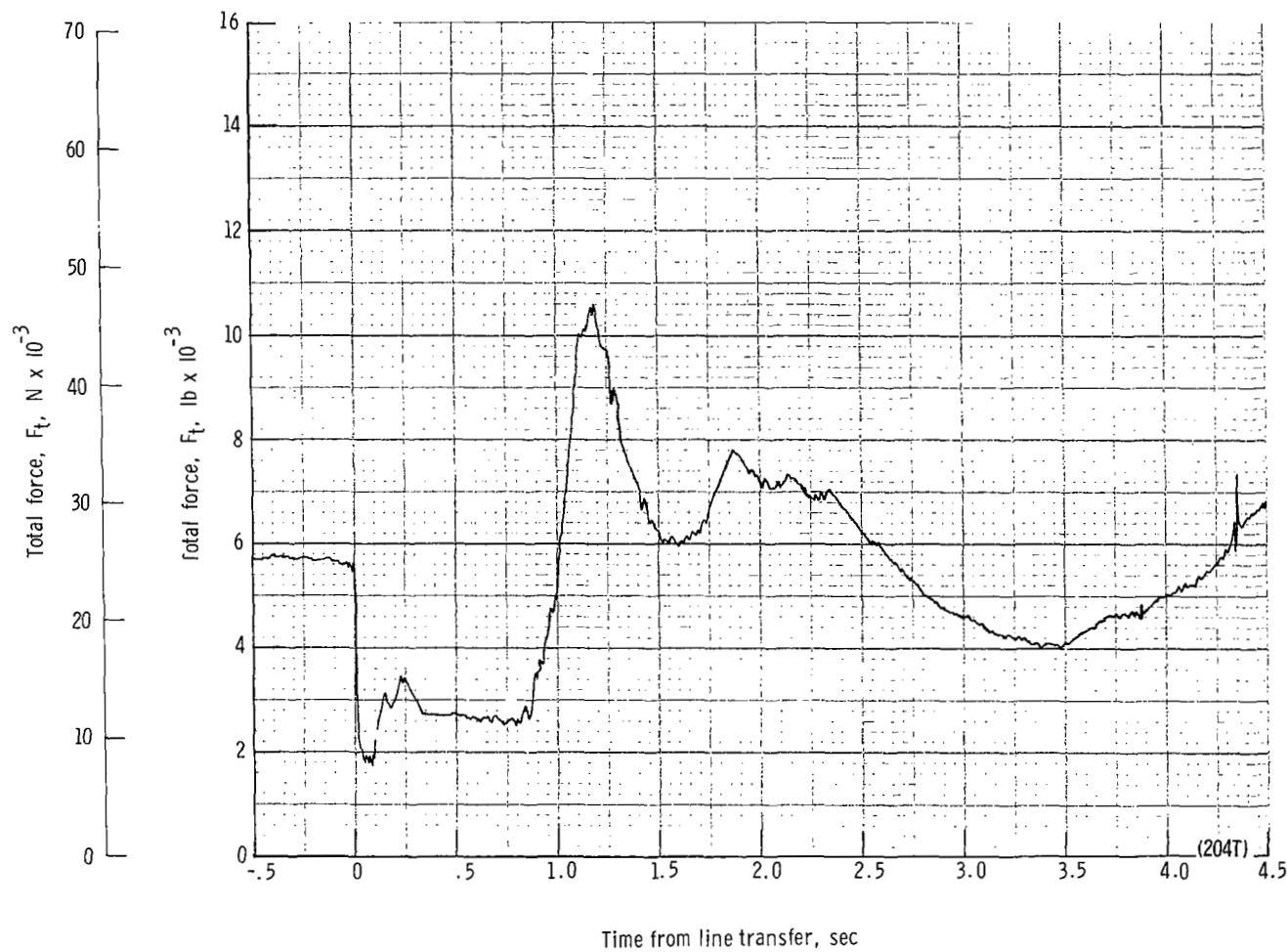
(v) Right, left, forward, and aft riser loads plotted against time from line transfer. Time = 0 second corresponds to 47.00 seconds after launch.

Figure 45.- Continued.



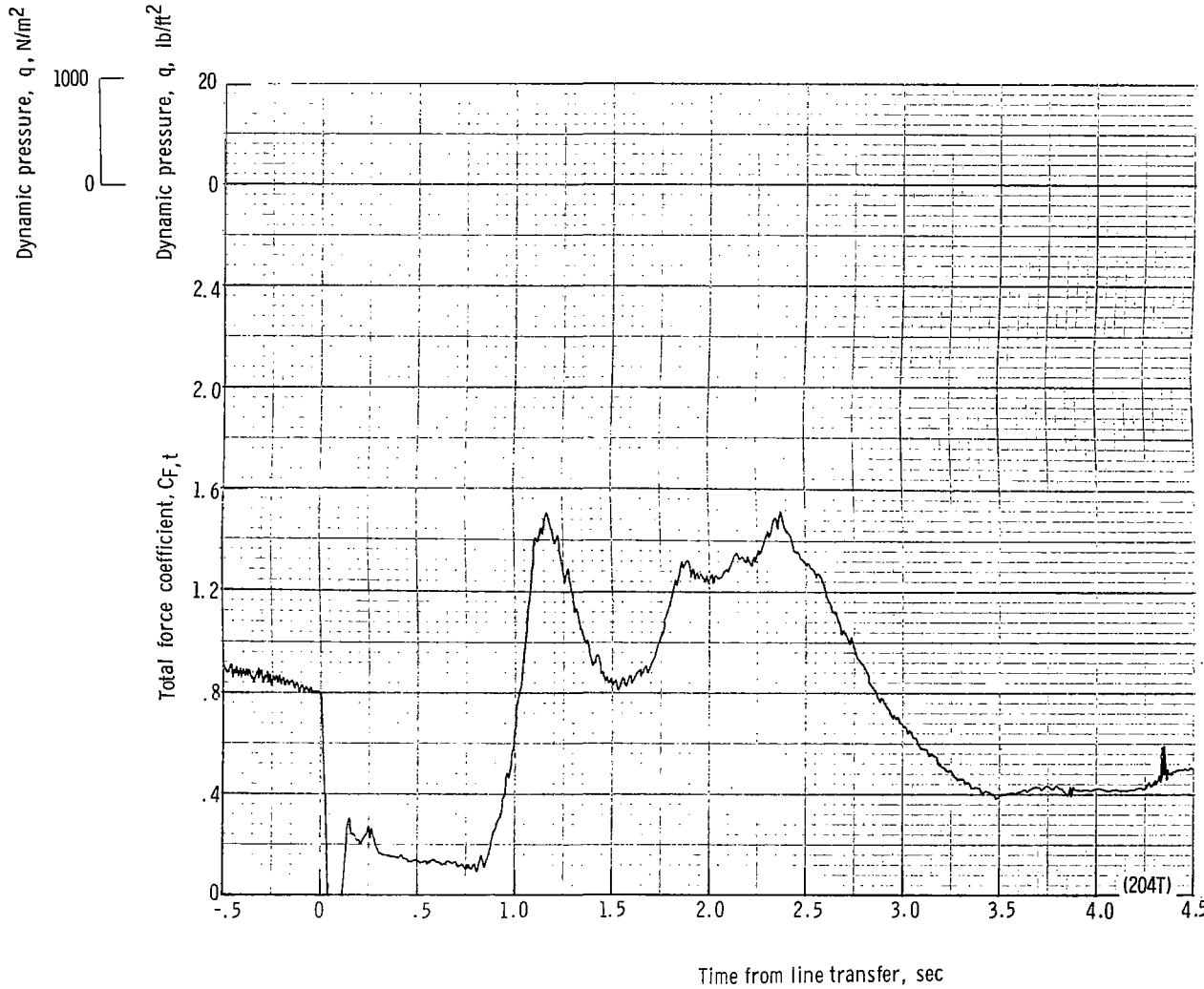
(w) Accelerations a_x , a_y , and a_z plotted against time from line transfer. Time = 0 second corresponds to 47.00 seconds after launch.

Figure 45.- Continued.



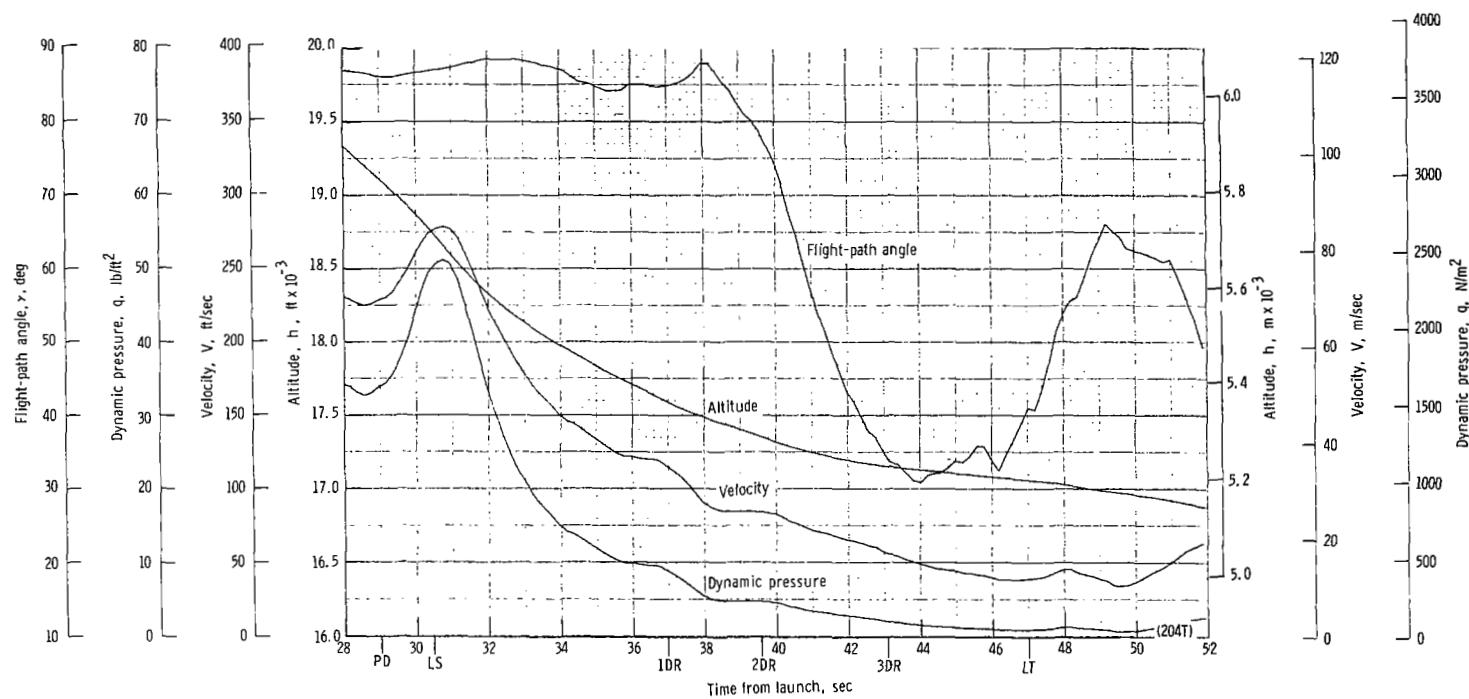
(x) Total force F_t plotted against time from line transfer. Time = 0 second corresponds to 47.00 seconds after launch.

Figure 45.- Continued.



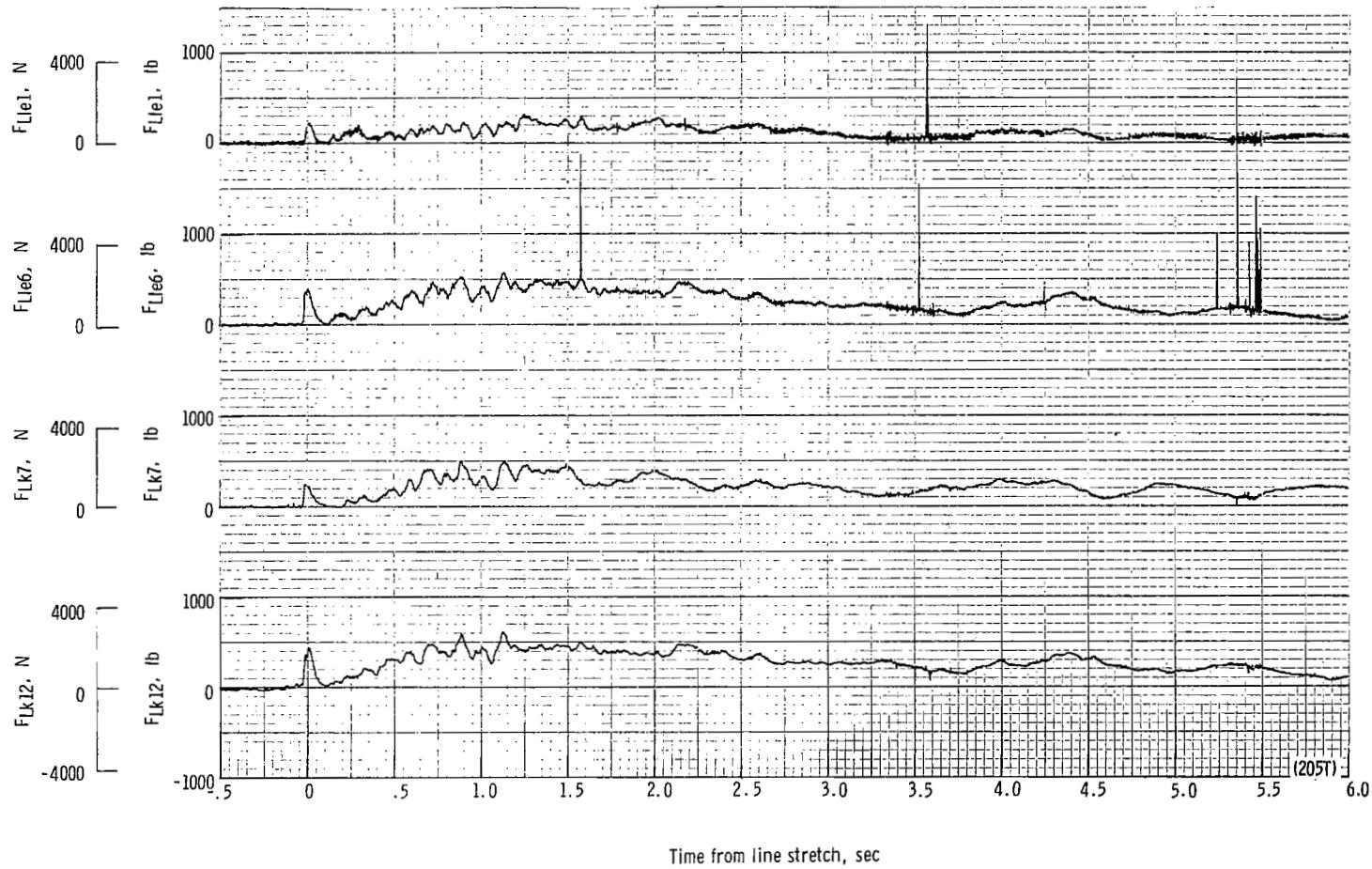
(y) Total force coefficient $C_{F,t}$ and dynamic pressure q plotted against time from line transfer. Time = 0 second corresponds to 47.00 seconds after launch.

Figure 45.- Continued.



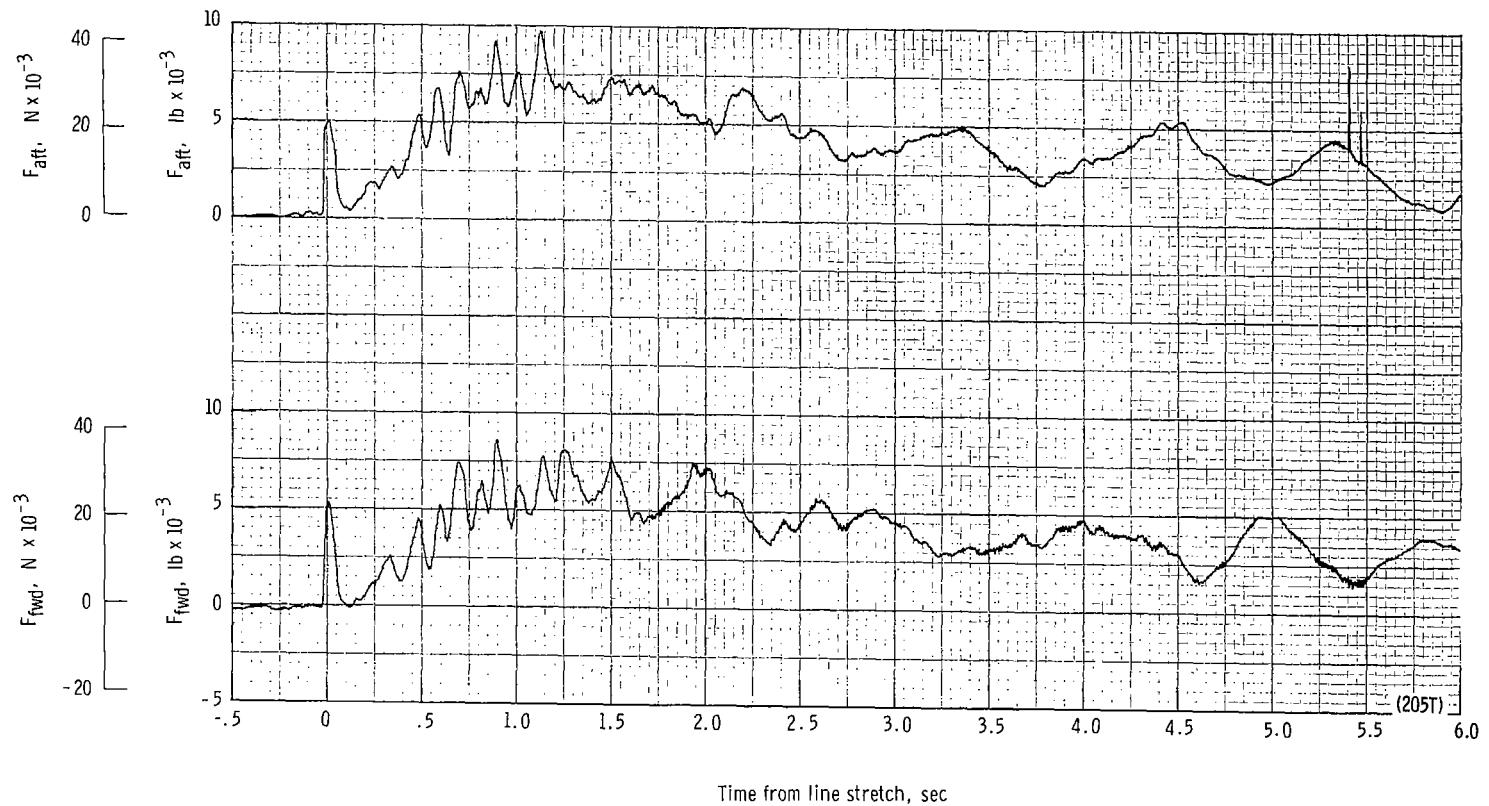
(z) Flight-path angle γ , dynamic pressure q , velocity V , and altitude h plotted against time from launch.

Figure 45.- Concluded.



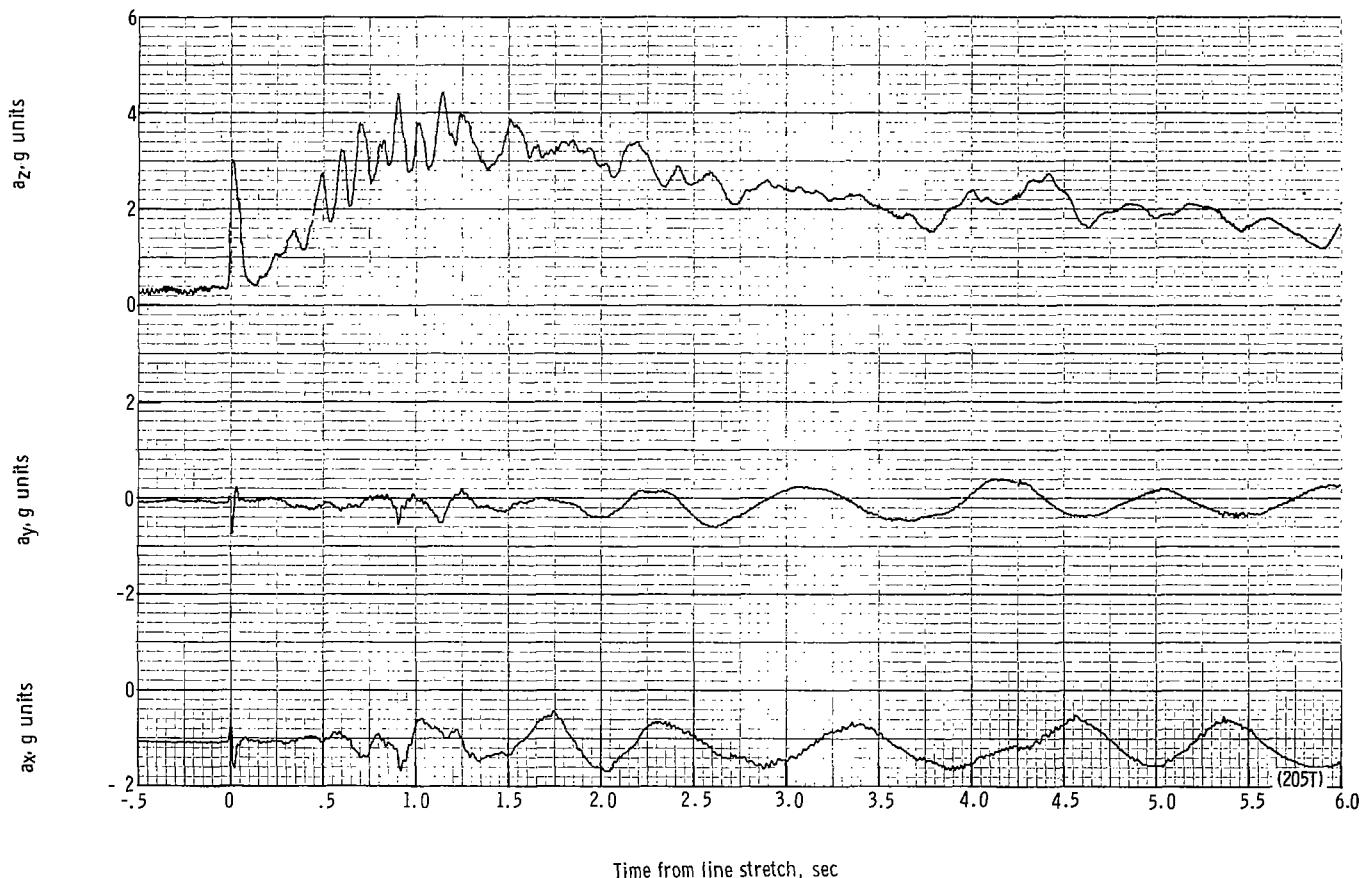
(a) Individual suspension-line loads F_{Lk12} , F_{Lk7} , F_{Lle6} and F_{Lle1} plotted against time from line stretch. Time = 0 second corresponds to 27.57 seconds after launch.

Figure 46.- Time history of twin-keel parawing deployment data for test 205T. $W_D = 22\ 379\ N$ (5031 lb); $W_P = 20\ 809\ N$ (4678 lb);
 $q_{PD} = 3231.9\ N/m^2$ (67.5 lb/ft²); $h_{PD} = 4496\ m$ (14 750 ft); $l_r/l_k = 0.100$; reefing version A.



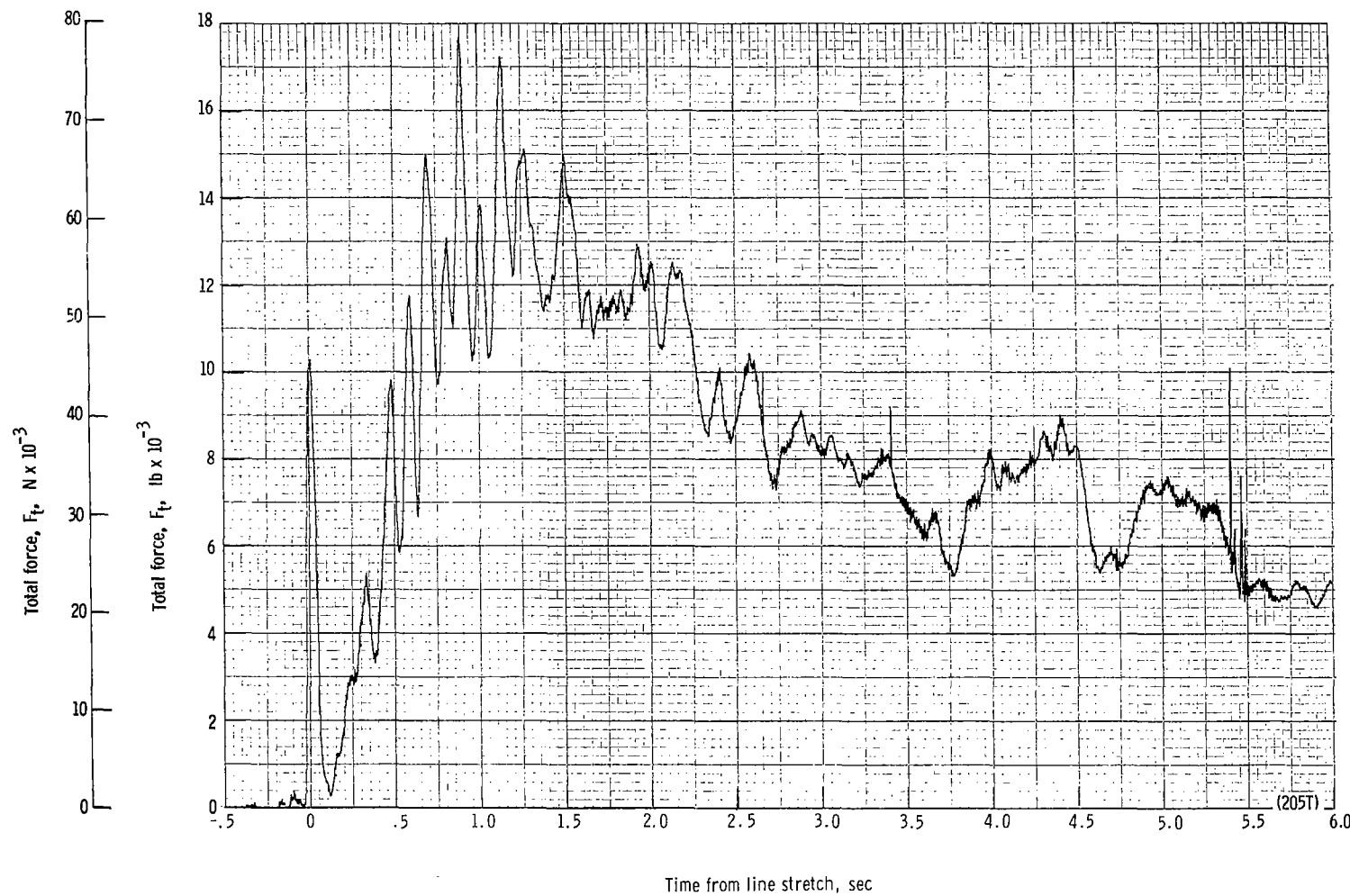
(b) Forward and aft riser loads plotted against time from line stretch. Time = 0 second corresponds to 27.57 seconds after launch.

Figure 46.- Continued.



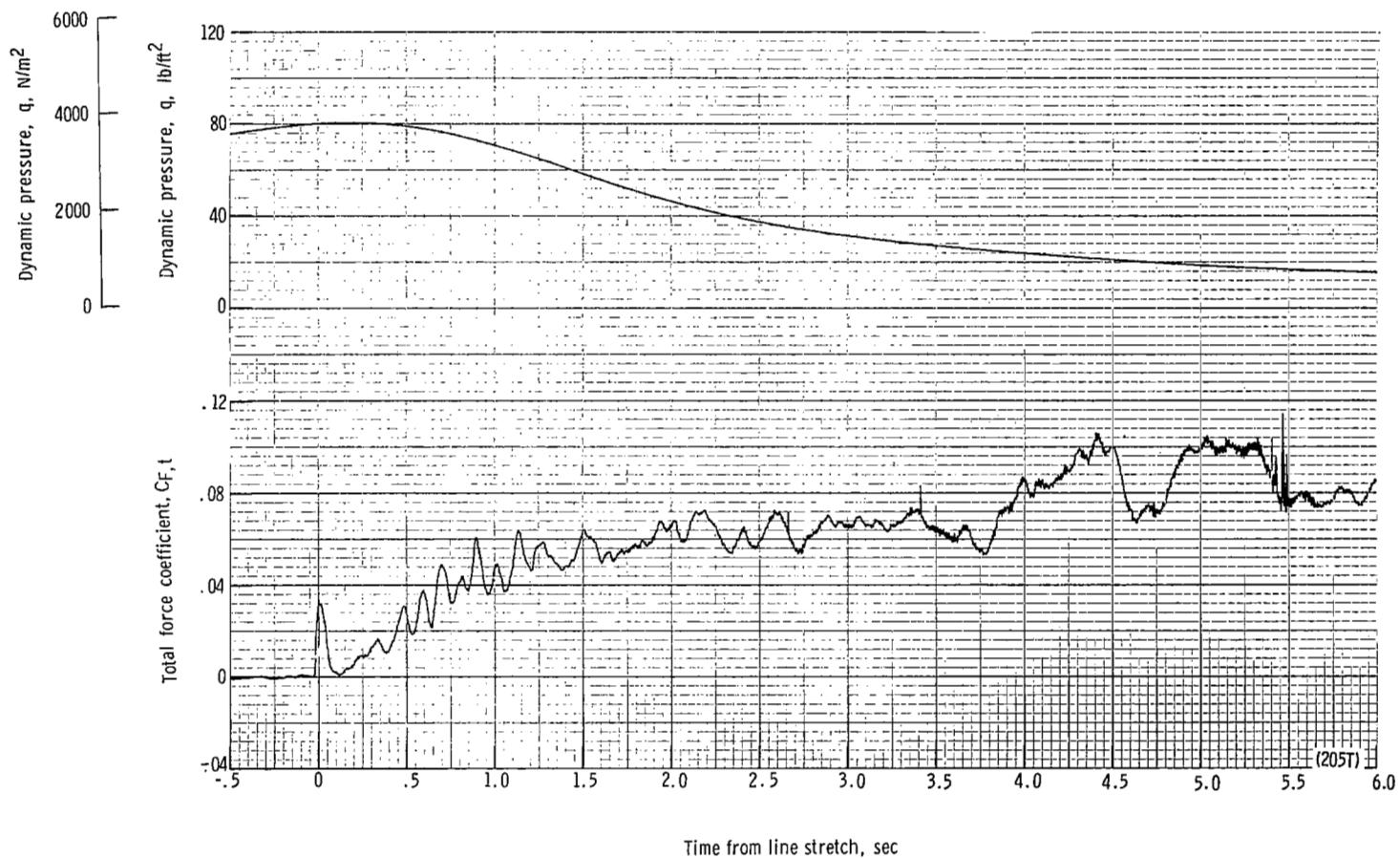
(c) Accelerations a_x , a_y , and a_z plotted against time from line stretch. Time = 0 second corresponds to 27.57 seconds after launch.

Figure 46.- Continued.



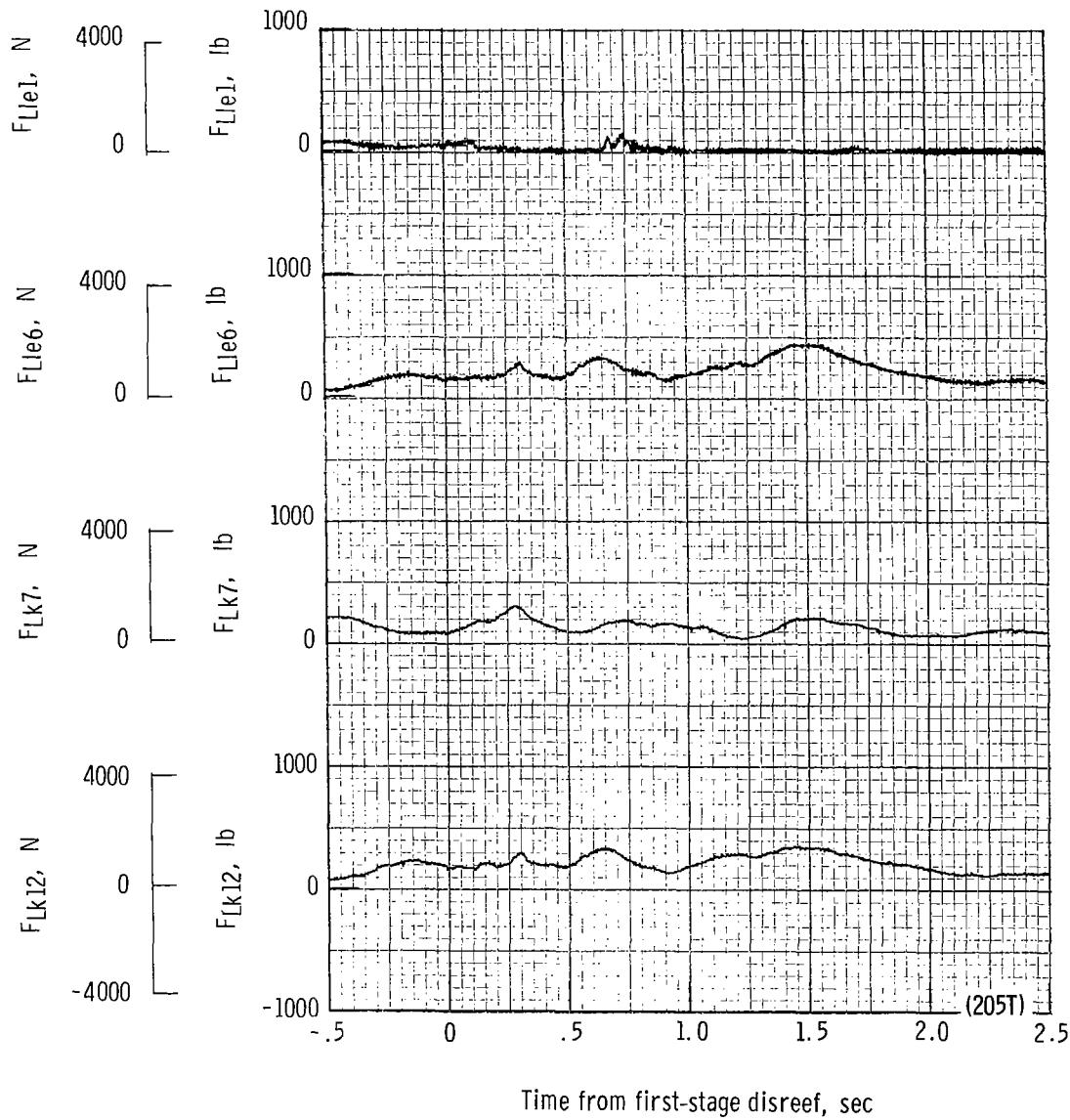
(d) Total force F_t plotted against time from line stretch. Time = 0 second corresponds to 27.57 seconds after launch.

Figure 46.- Continued.



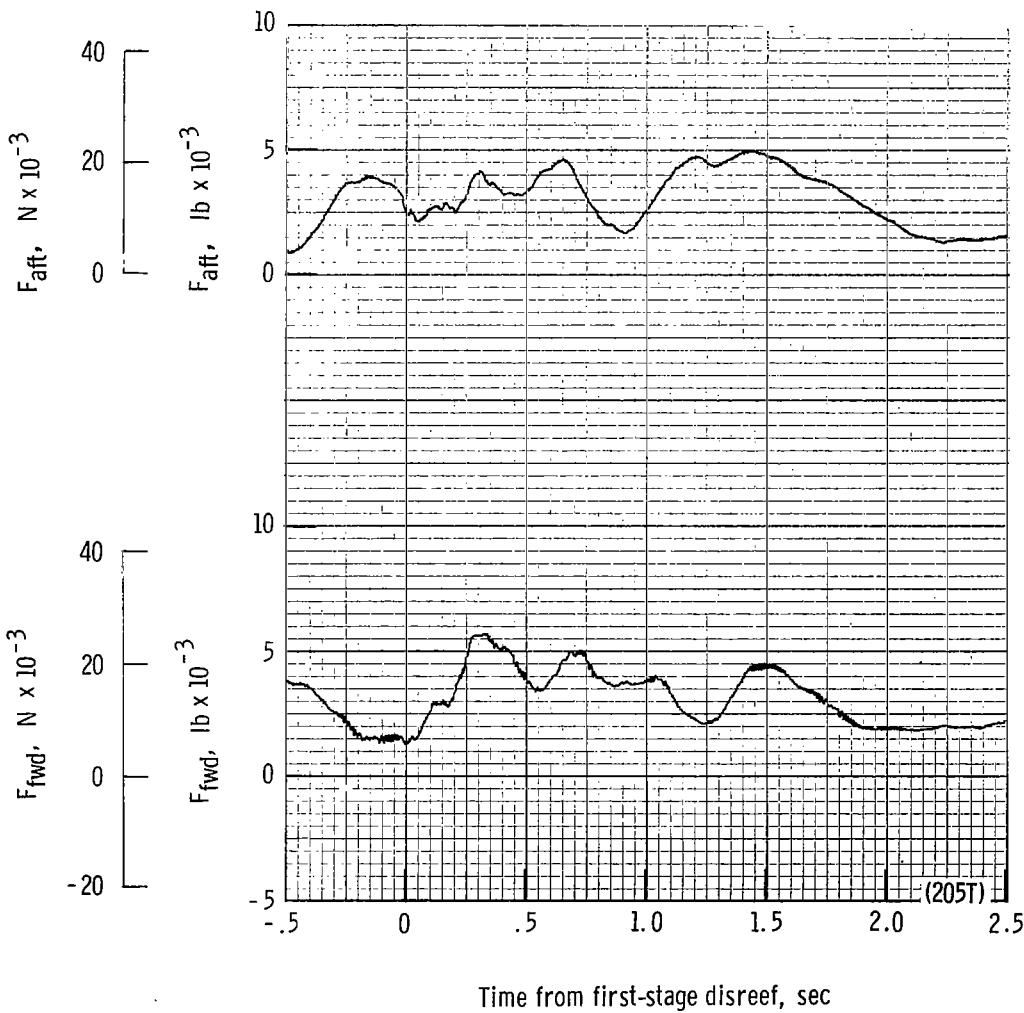
(e) Total force coefficient $C_{F,t}$ and dynamic pressure q plotted against time from line stretch. Time = 0 second corresponds to 27.57 seconds after launch.

Figure 46.- Continued.



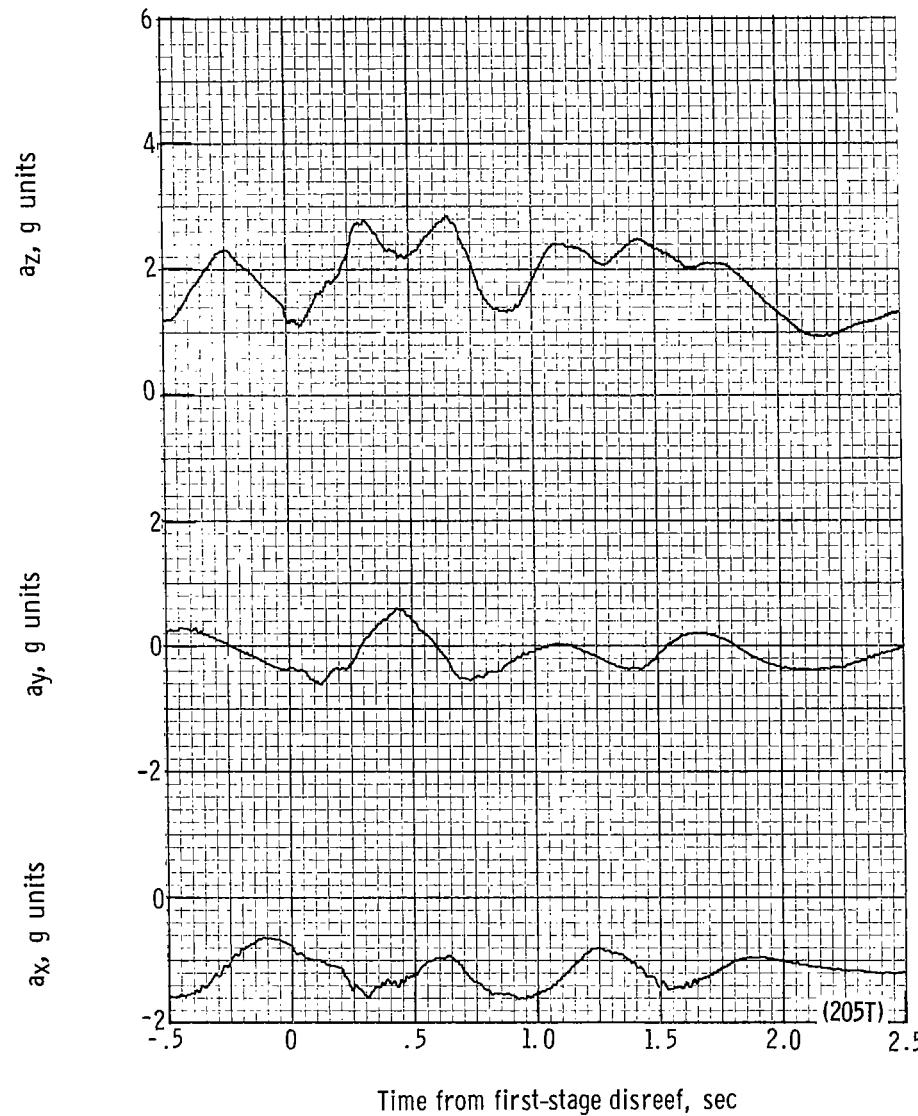
(f) Individual suspension-line loads F_{Lk12} , F_{Lk7} , F_{Lle6} and F_{Lle1} plotted against time from first-stage disreef. Time = 0 second corresponds to 33.96 seconds after launch.

Figure 46.- Continued.



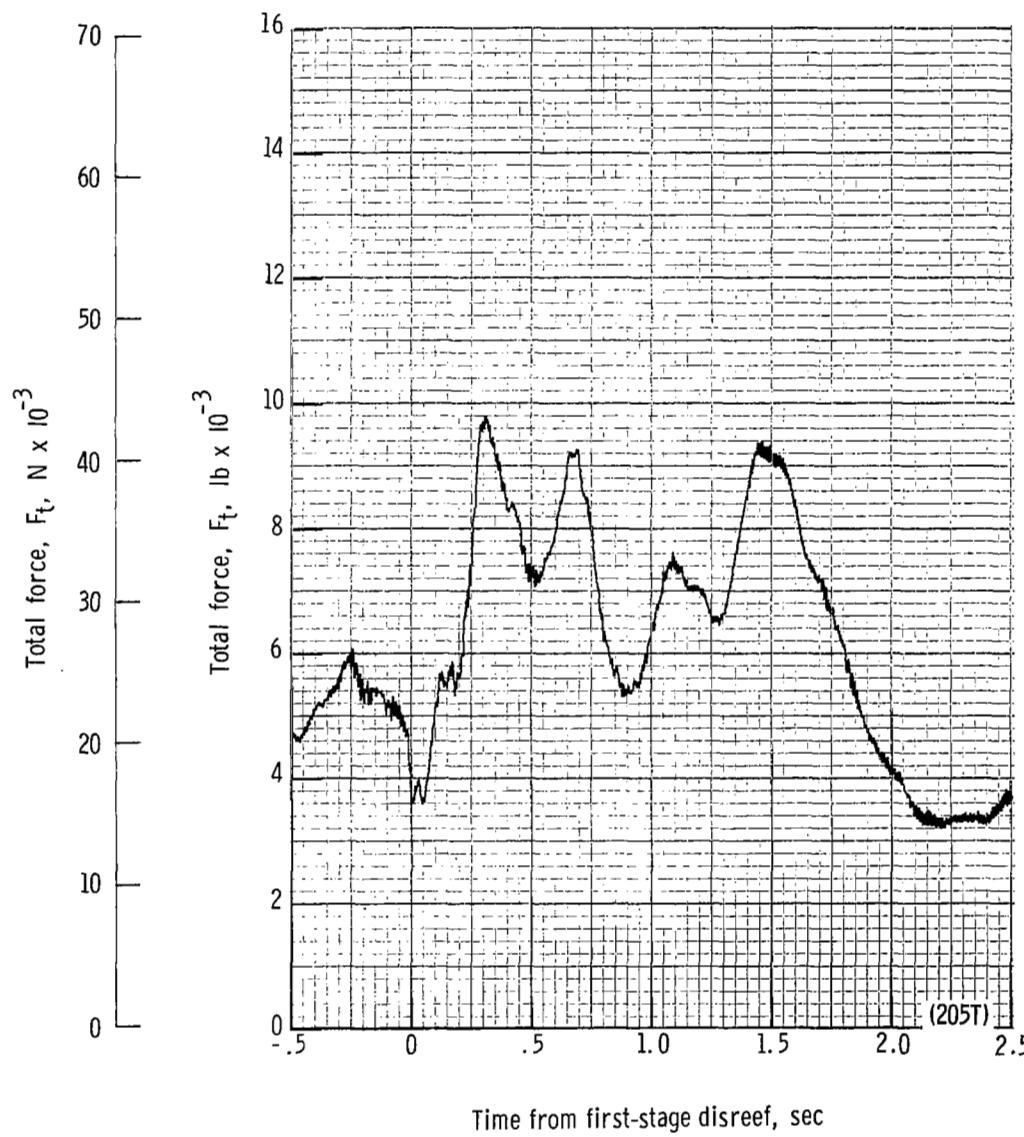
(g) Forward and aft riser loads plotted against time from first-stage disreef. Time = 0 second corresponds to 33.96 seconds after launch.

Figure 46.- Continued.



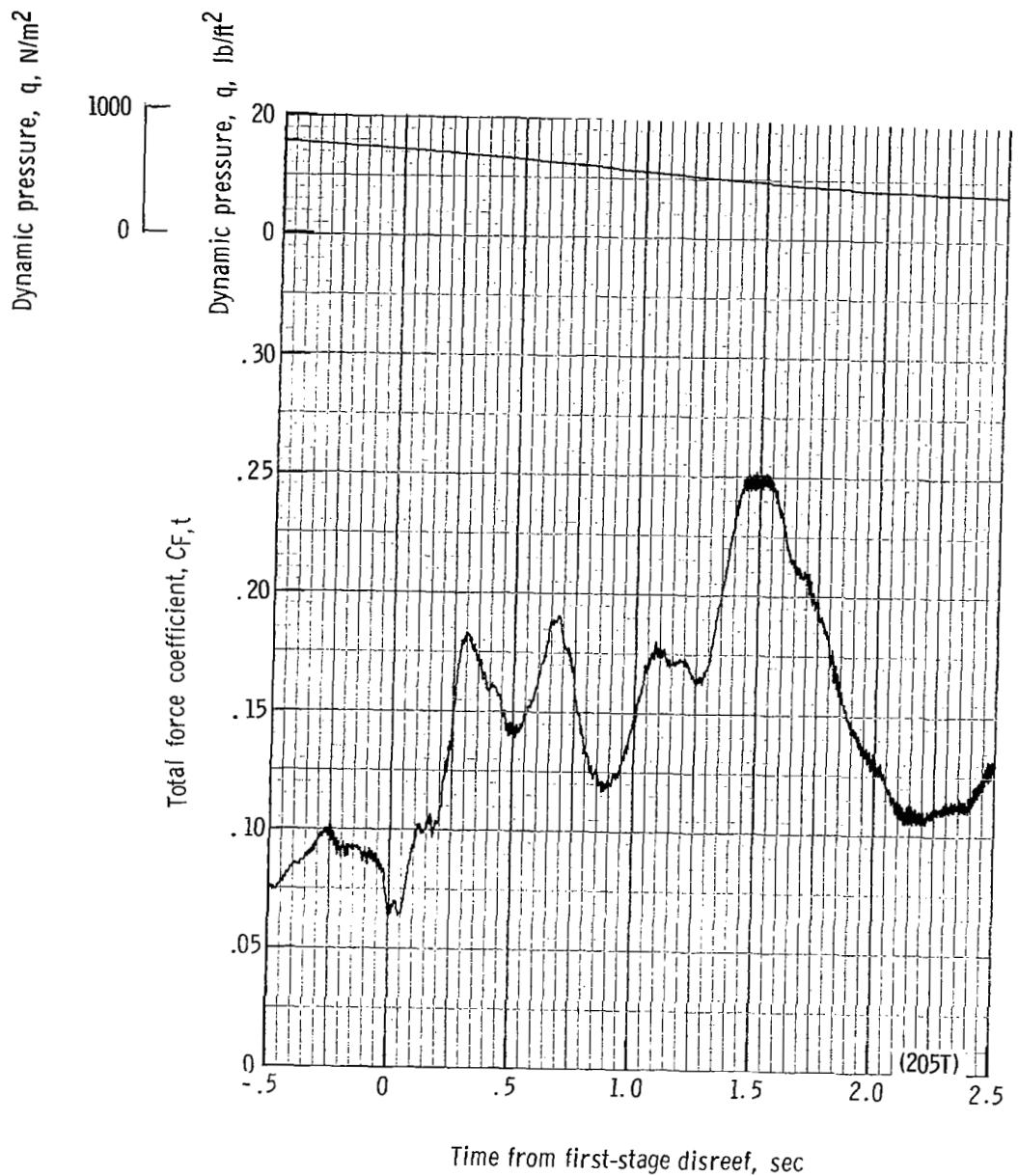
(h) Accelerations a_x , a_y , and a_z plotted against time from first-stage disreef. Time = 0 second corresponds to 33.96 seconds after launch.

Figure 46.- Continued.



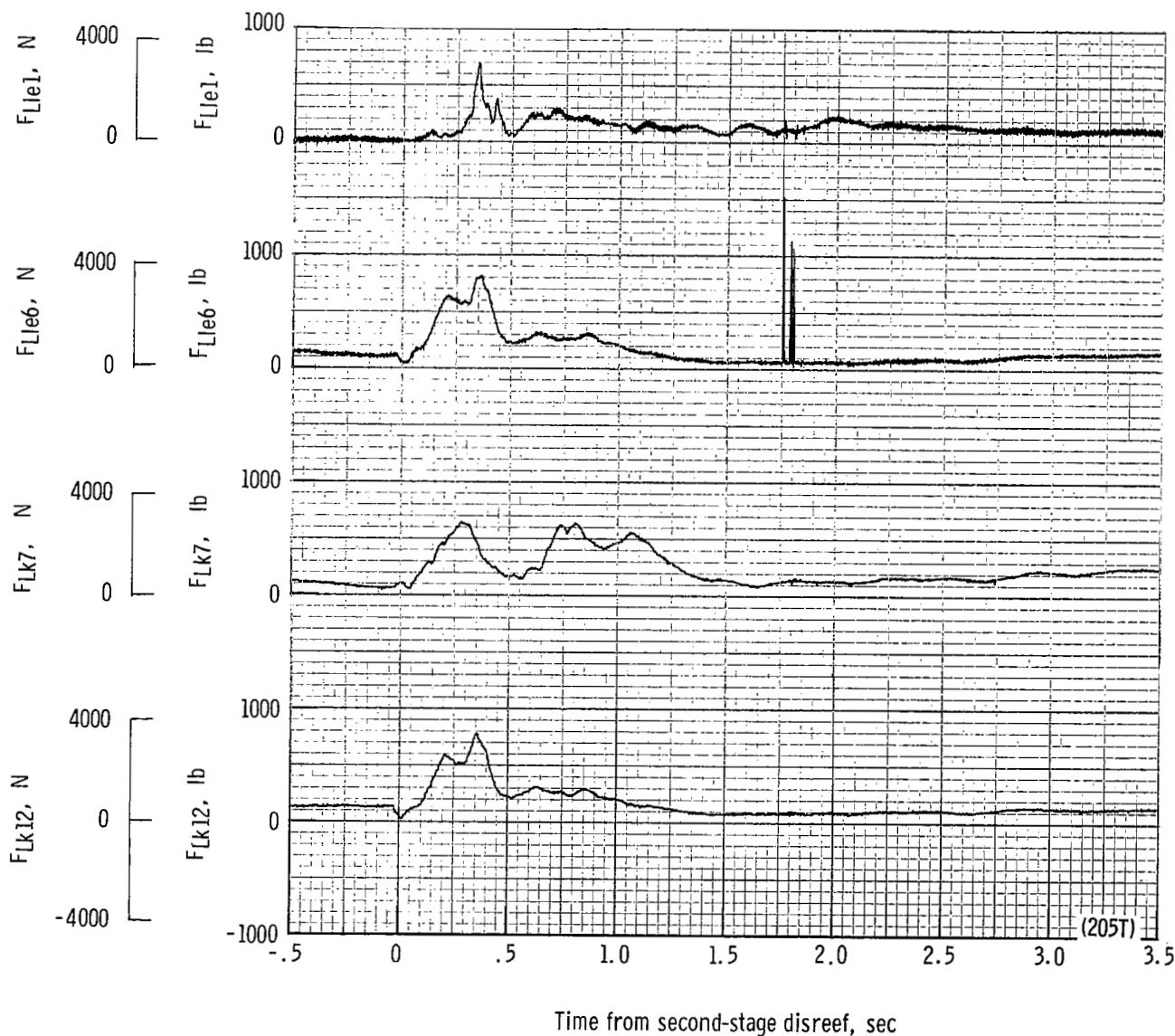
(i) Total force F_t plotted against time from first-stage disreef. Time = 0 second corresponds to 33.96 seconds after launch.

Figure 46.- Continued.

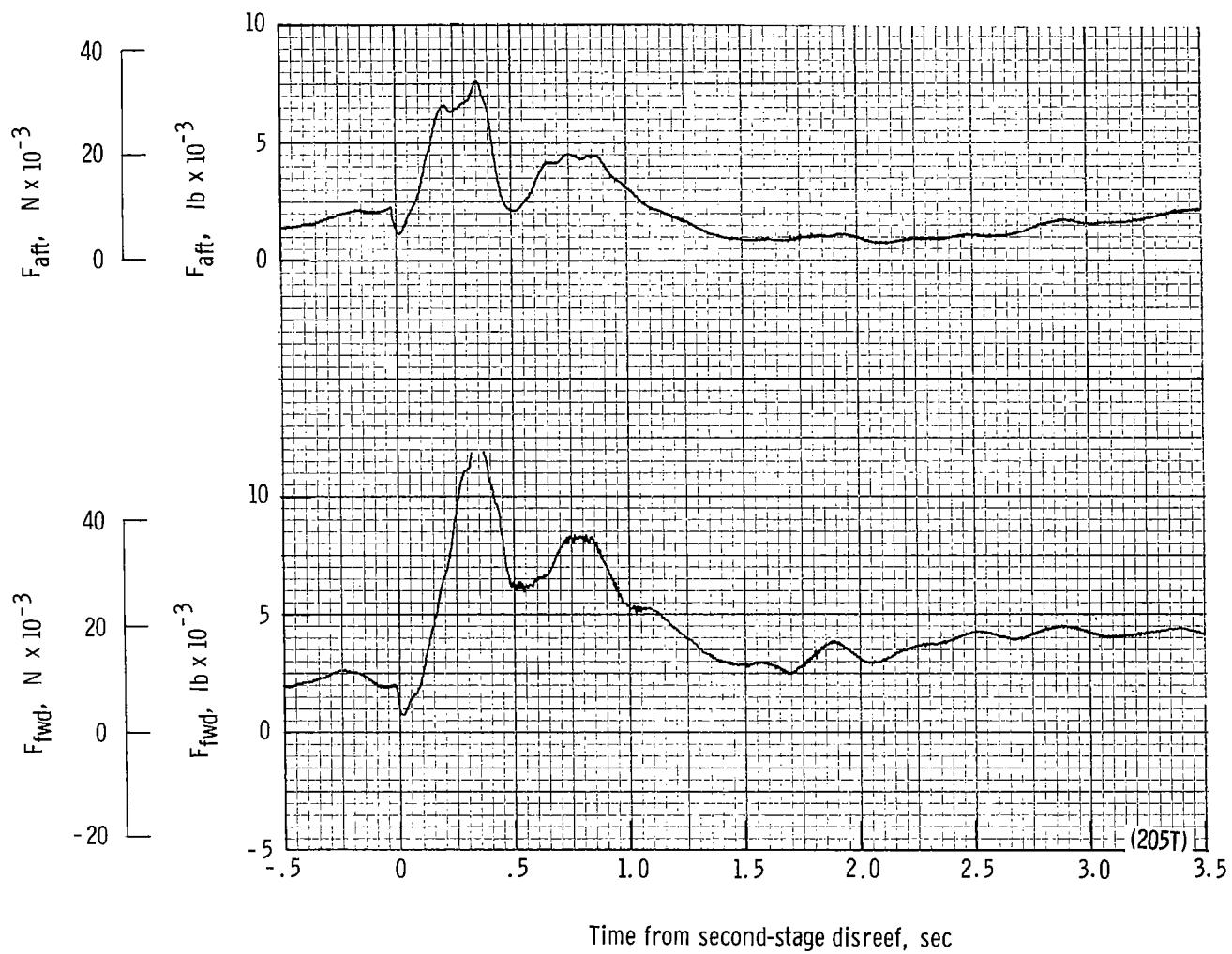


(j) Total force coefficient $C_{F,t}$ and dynamic pressure q plotted against time from first-stage disreef. Time = 0 second corresponds to 33.96 seconds after launch.

Figure 46.- Continued.

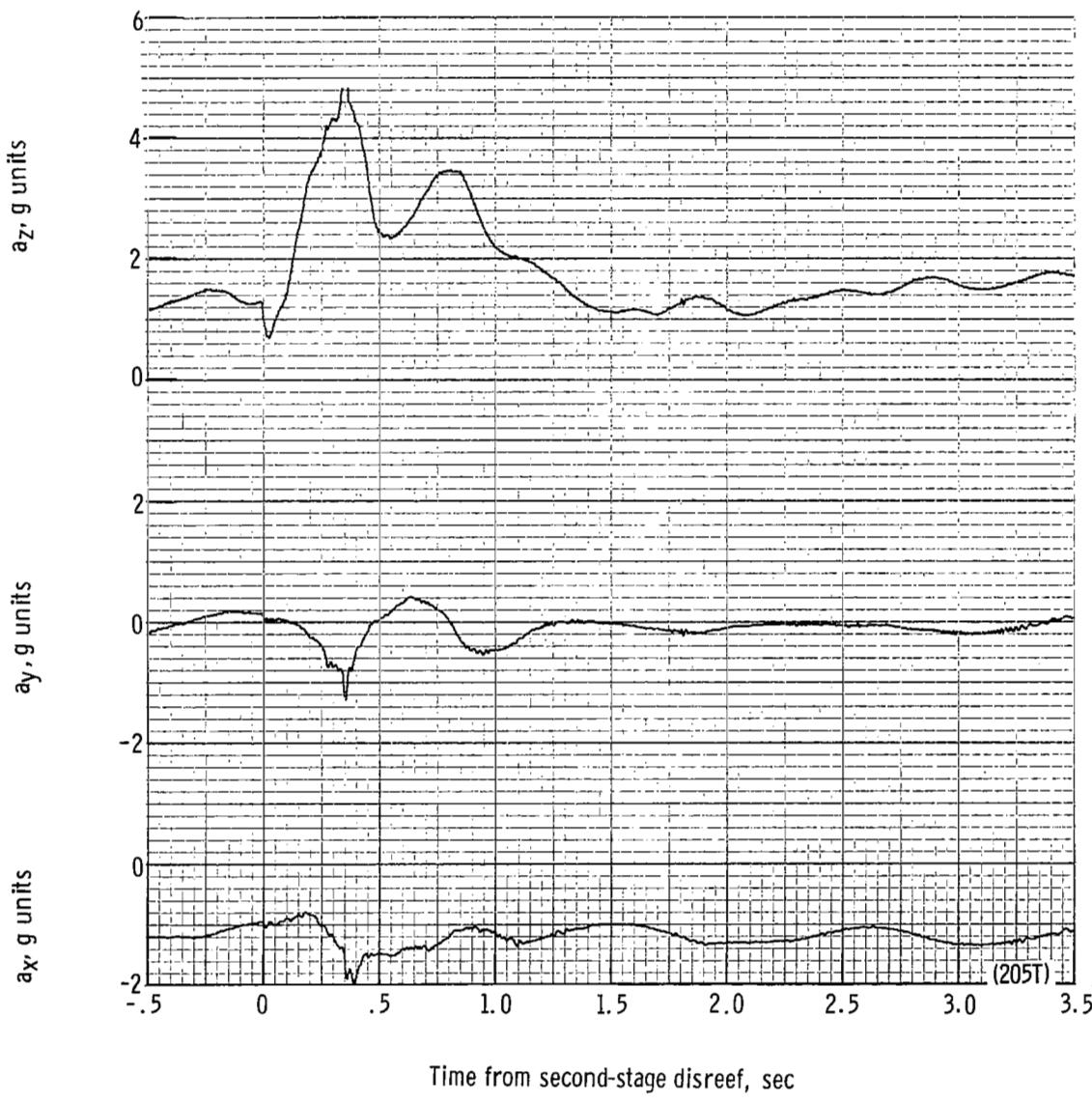


(k) Individual suspension-line loads F_{Lk12} , F_{Lk7} , F_{Lle6} , and F_{Lle1} plotted against time from second-stage disreef. Time = 0 second corresponds to 36.82 seconds after launch.



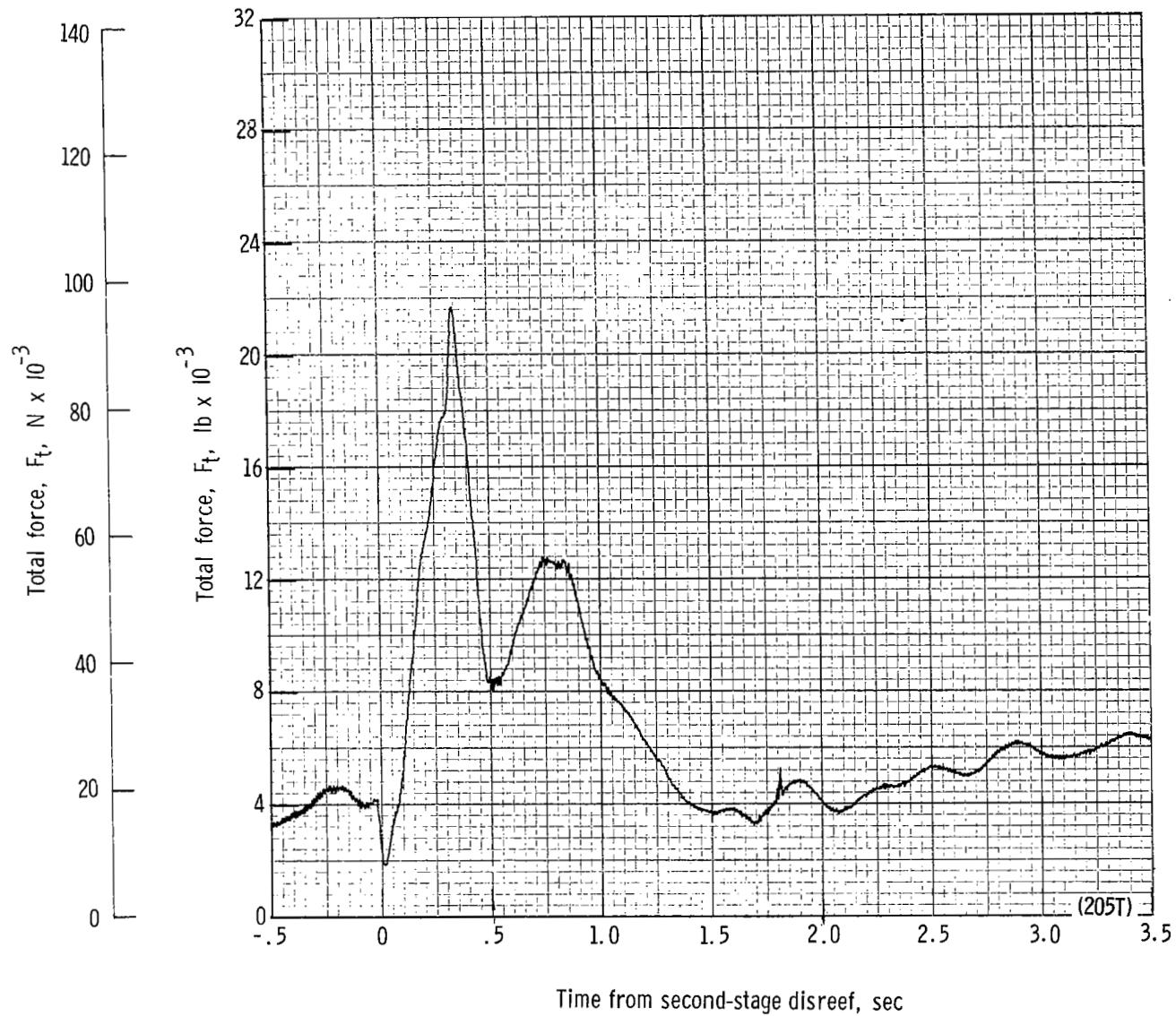
(I) Forward and aft riser loads plotted against time from second-stage disreef. Time = 0 second corresponds to 36.82 seconds after launch.

Figure 46.- Continued.



(m) Accelerations a_x , a_y , and a_z plotted against time from second-stage disreef. Time = 0 second corresponds to 36.82 seconds after launch.

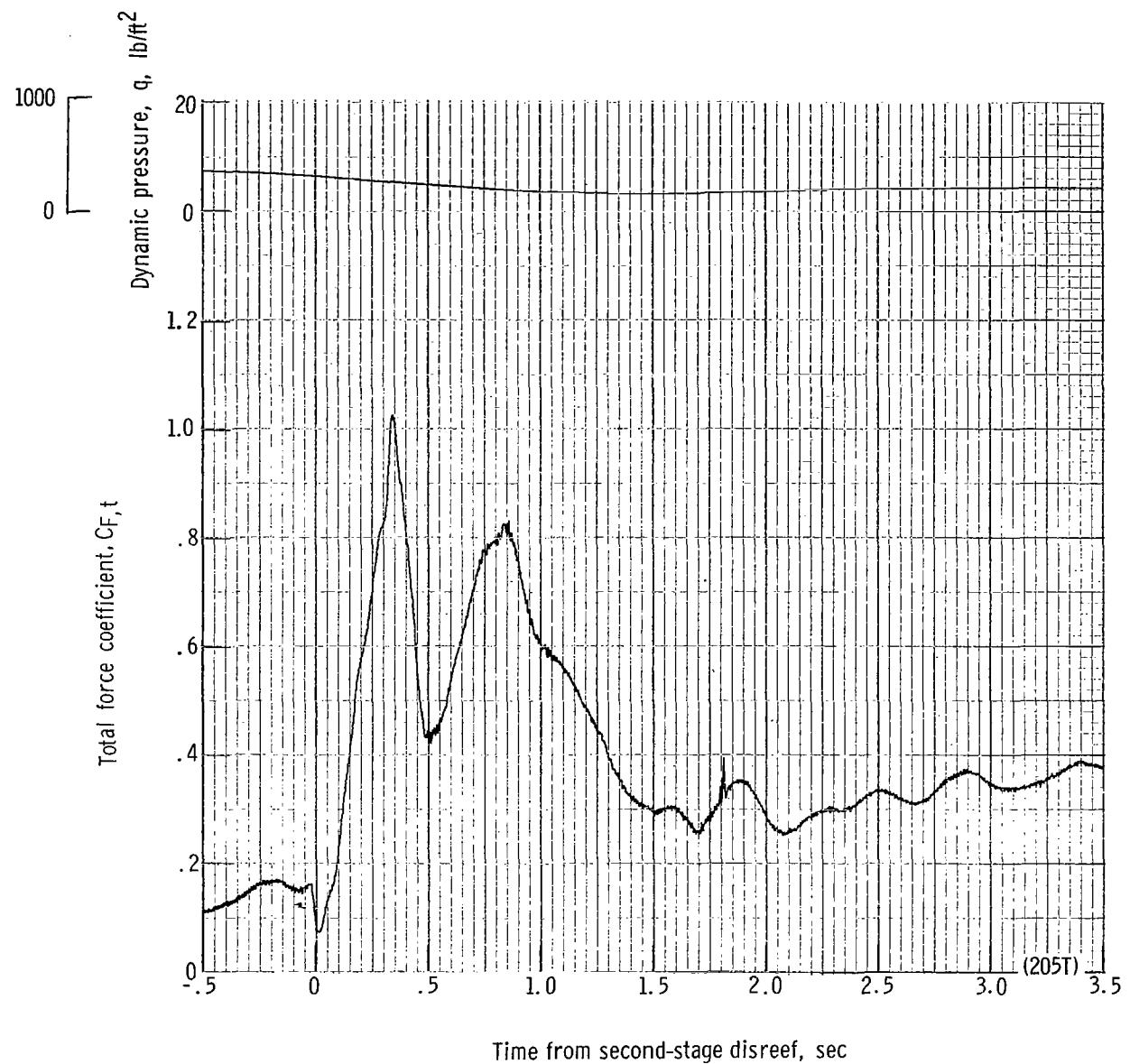
Figure 46.- Continued.



(n) Total force F_t plotted against time from second-stage disreef. Time = 0 second corresponds to 36.82 seconds after launch.

Figure 46.- Continued.

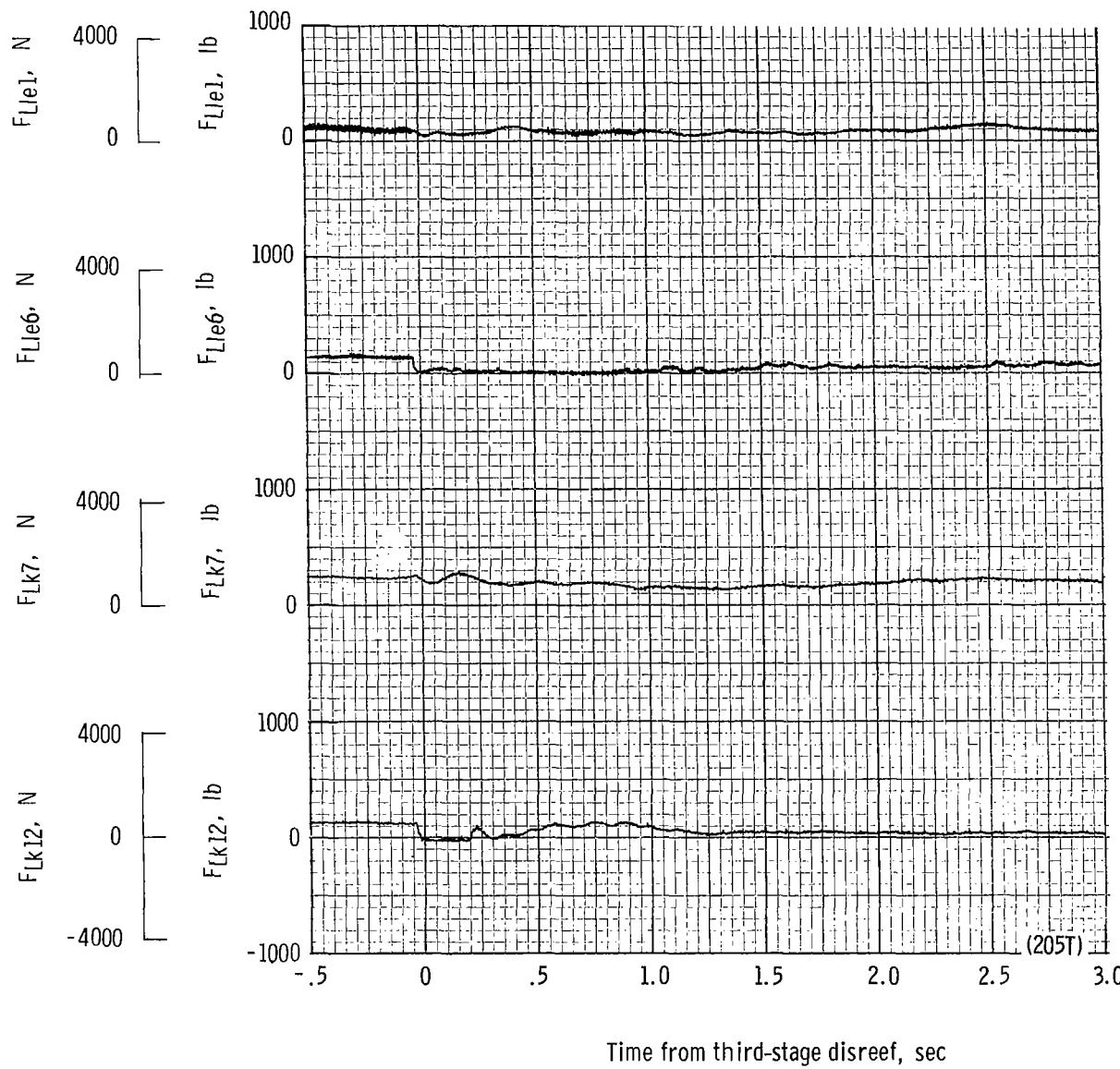
Dynamic pressure, q , N/m²



(o) Total force coefficient CF_t and dynamic pressure q plotted against time from second-stage disreef.

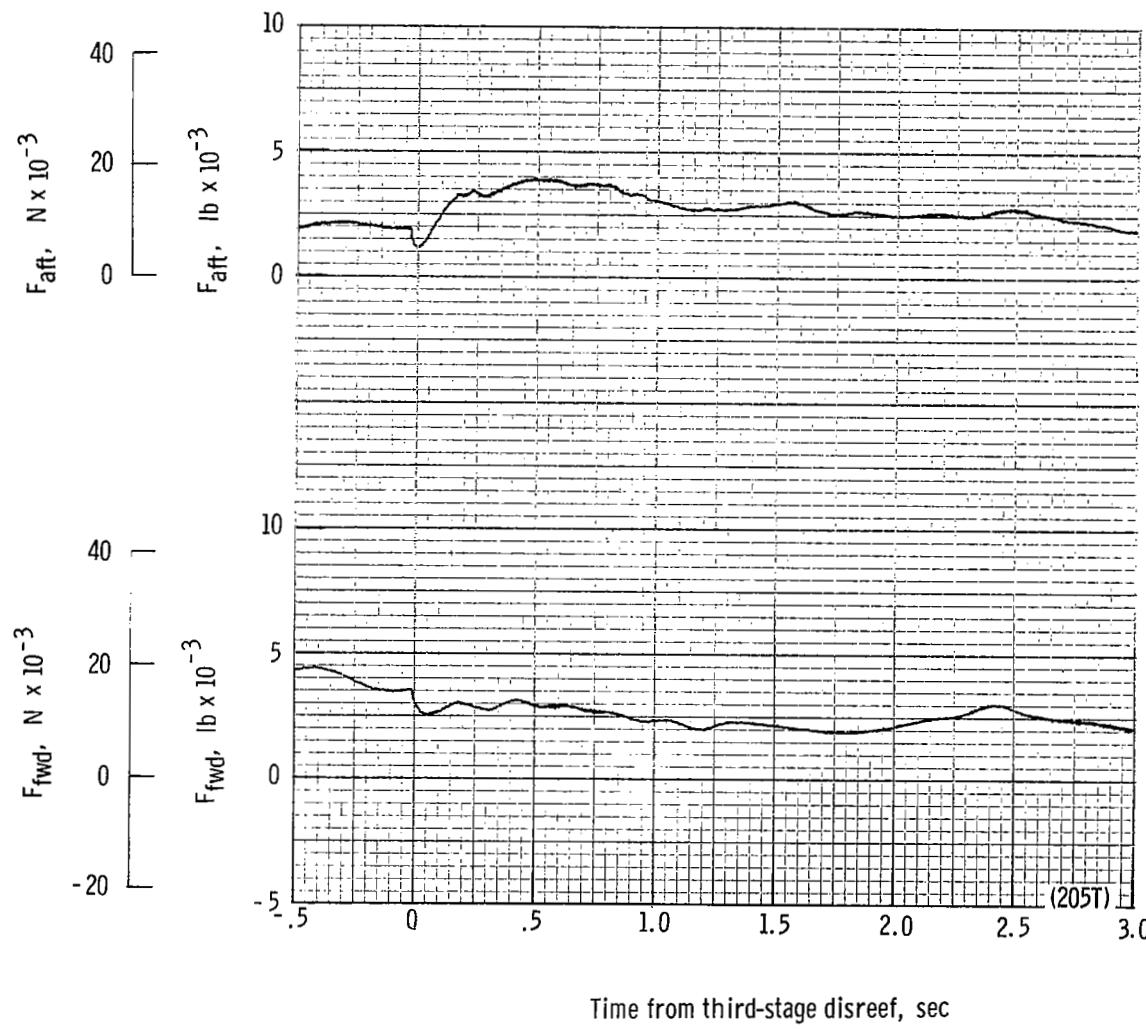
Time = 0 second corresponds to 36.82 seconds after launch.

Figure 46.- Continued.



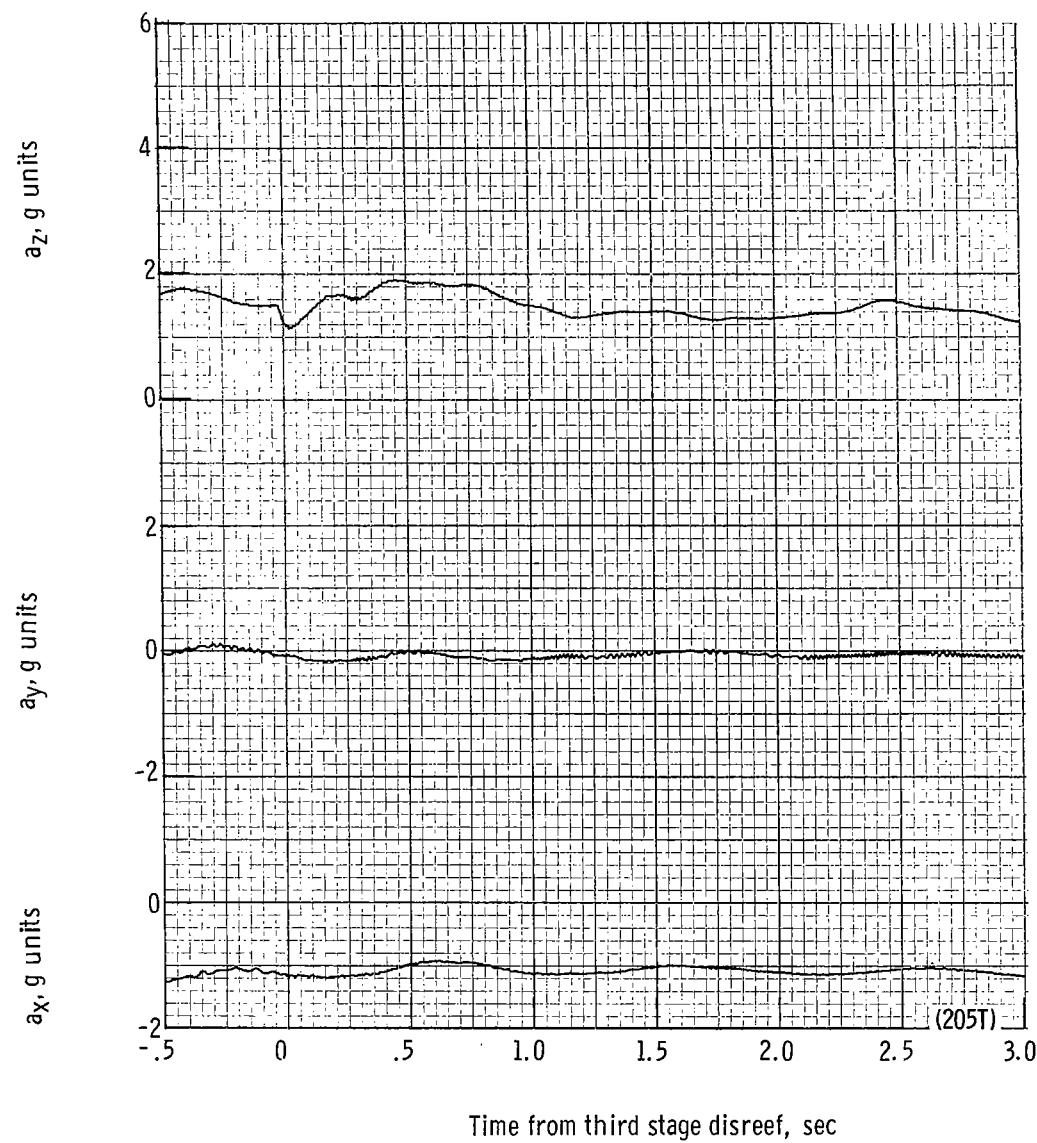
(p) Individual suspension-line loads F_{Lk12} , F_{Lk7} , F_{Lle6} , and F_{Lle1} plotted against time from third-stage disreef. Time = 0 second corresponds to 40.63 seconds after launch.

Figure 46.- Continued.



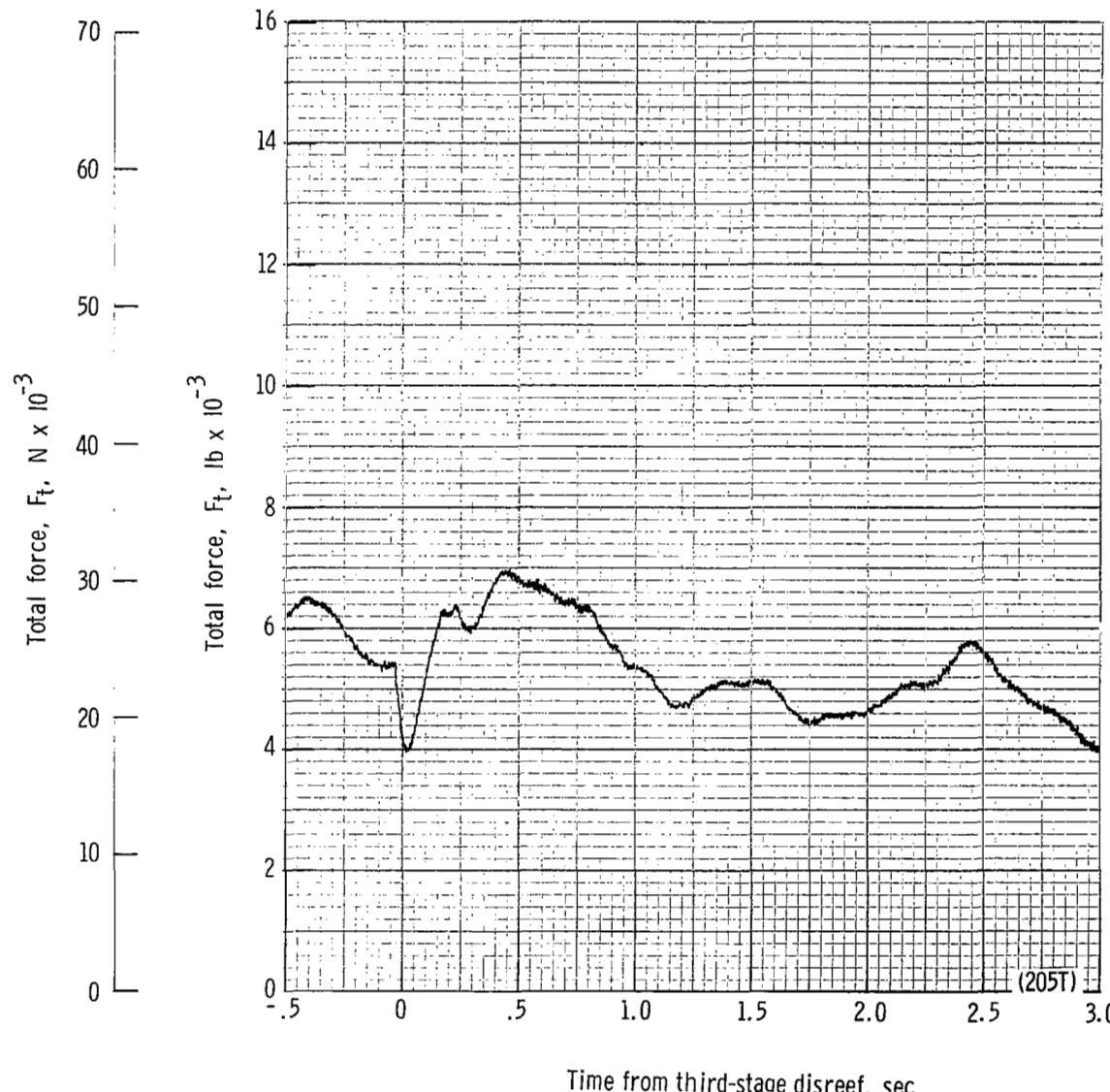
(q) Forward and aft riser loads plotted against time from third-stage disreef. Time = 0 second corresponds to 40.63 seconds after launch.

Figure 46.- Continued.



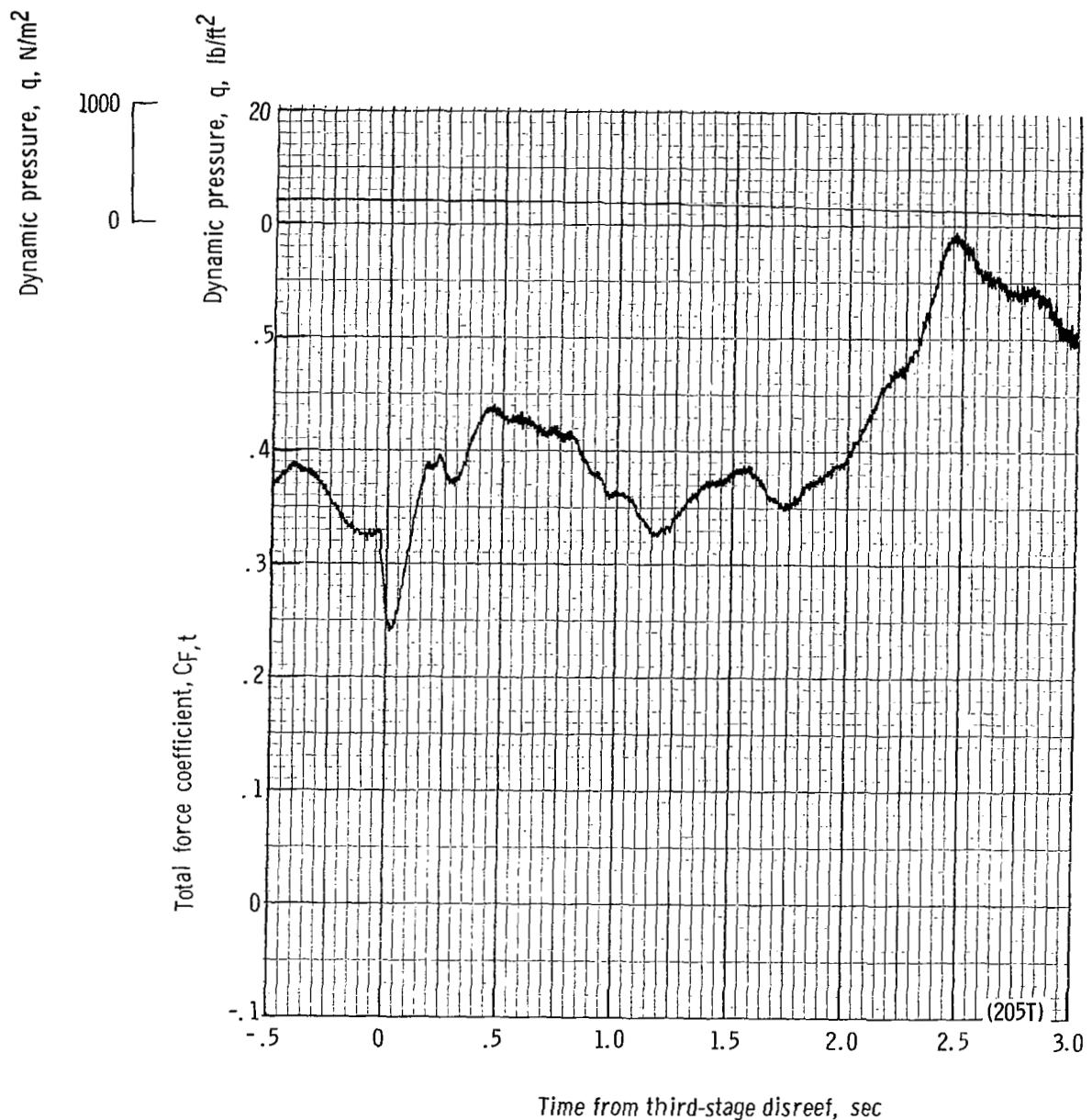
(r) Accelerations a_x , a_y , and a_z plotted against time from third-stage disreef. Time = 0 second corresponds to 40.63 seconds after launch.

Figure 46.- Continued.



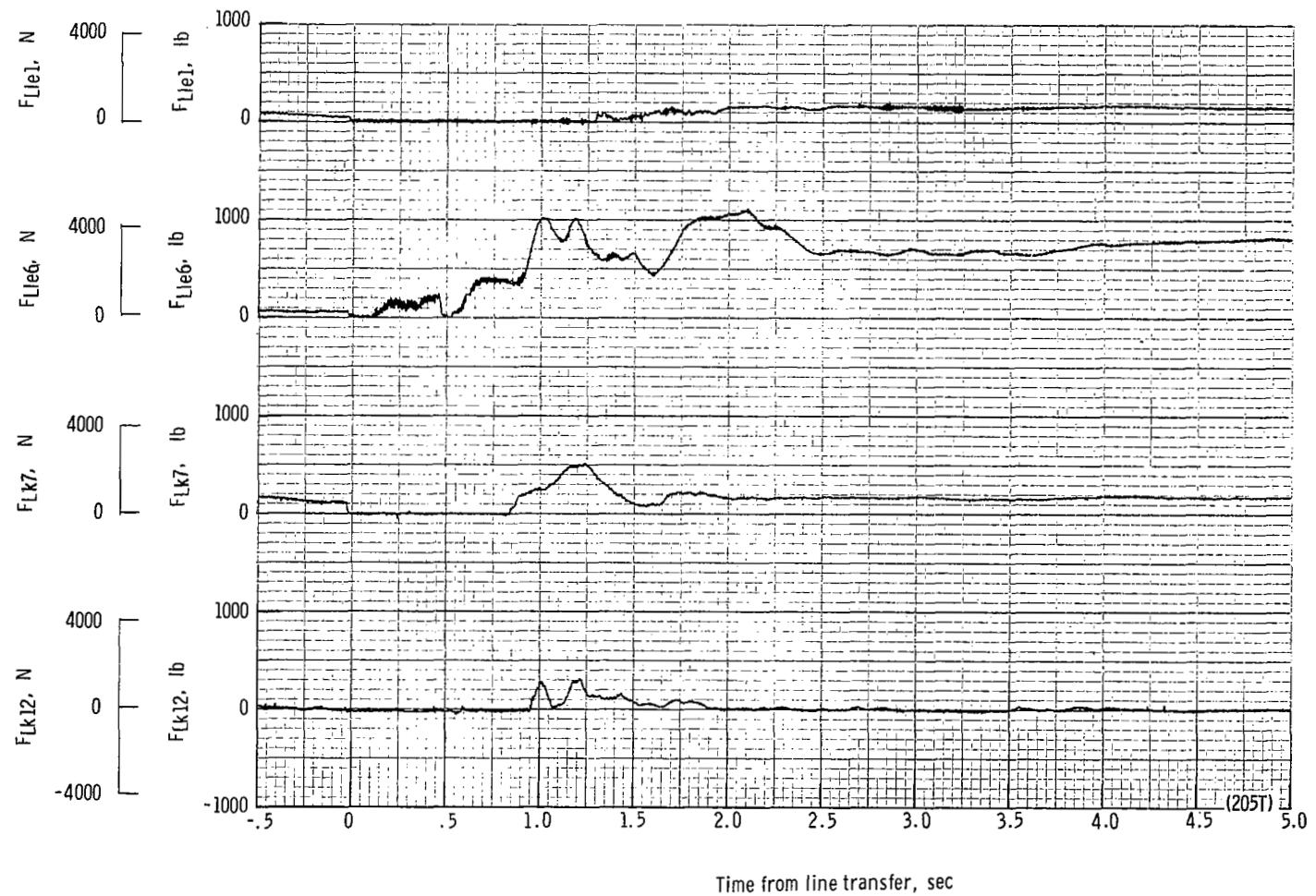
(s) Total force F_t plotted against time from third-stage disreef. Time = 0 second corresponds to 40.63 seconds after launch.

Figure 46.- Continued.



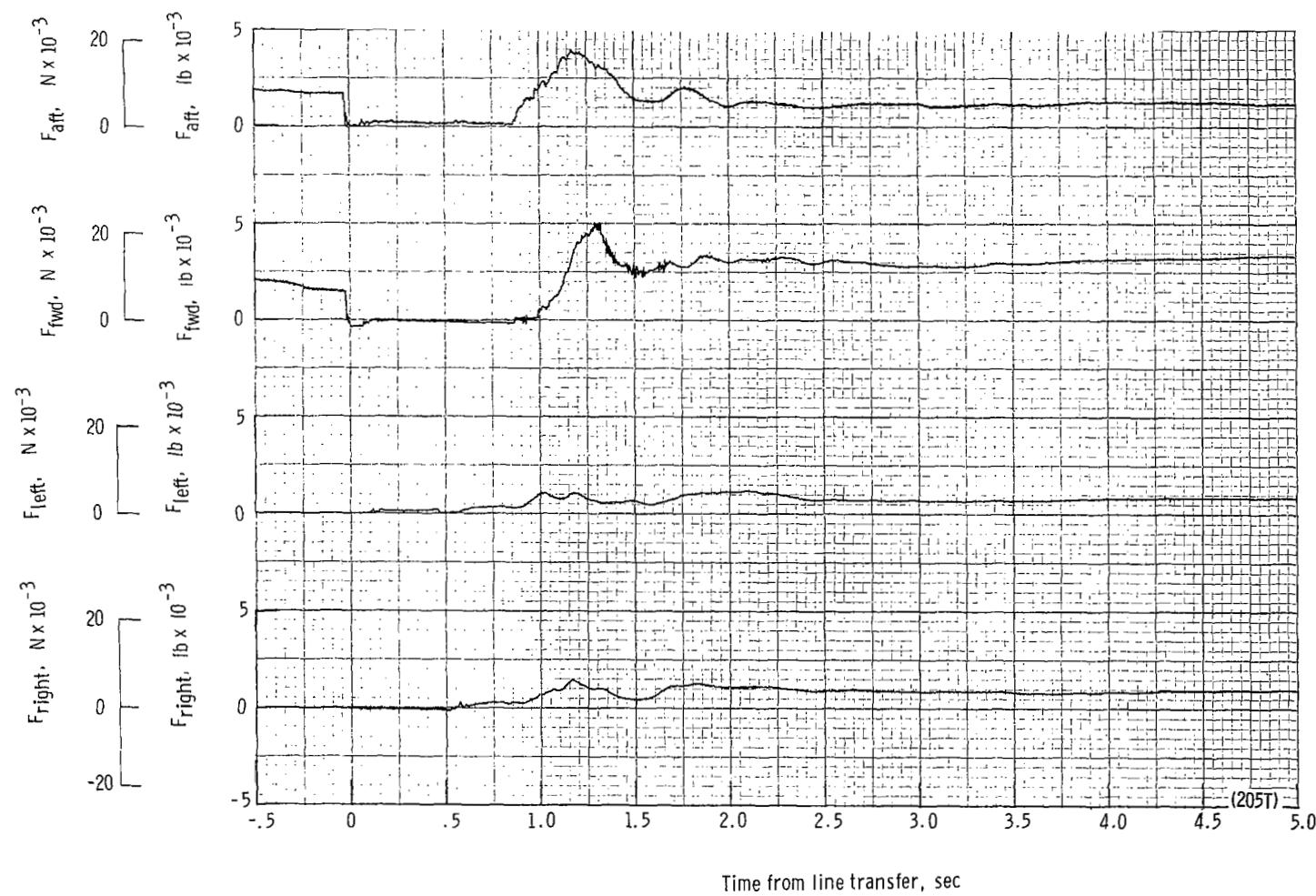
(b) Total force coefficient $C_{F,t}$ and dynamic pressure q plotted against time from third-stage disreef. Time = 0 second corresponds to 40.63 seconds after launch.

Figure 46.- Continued.



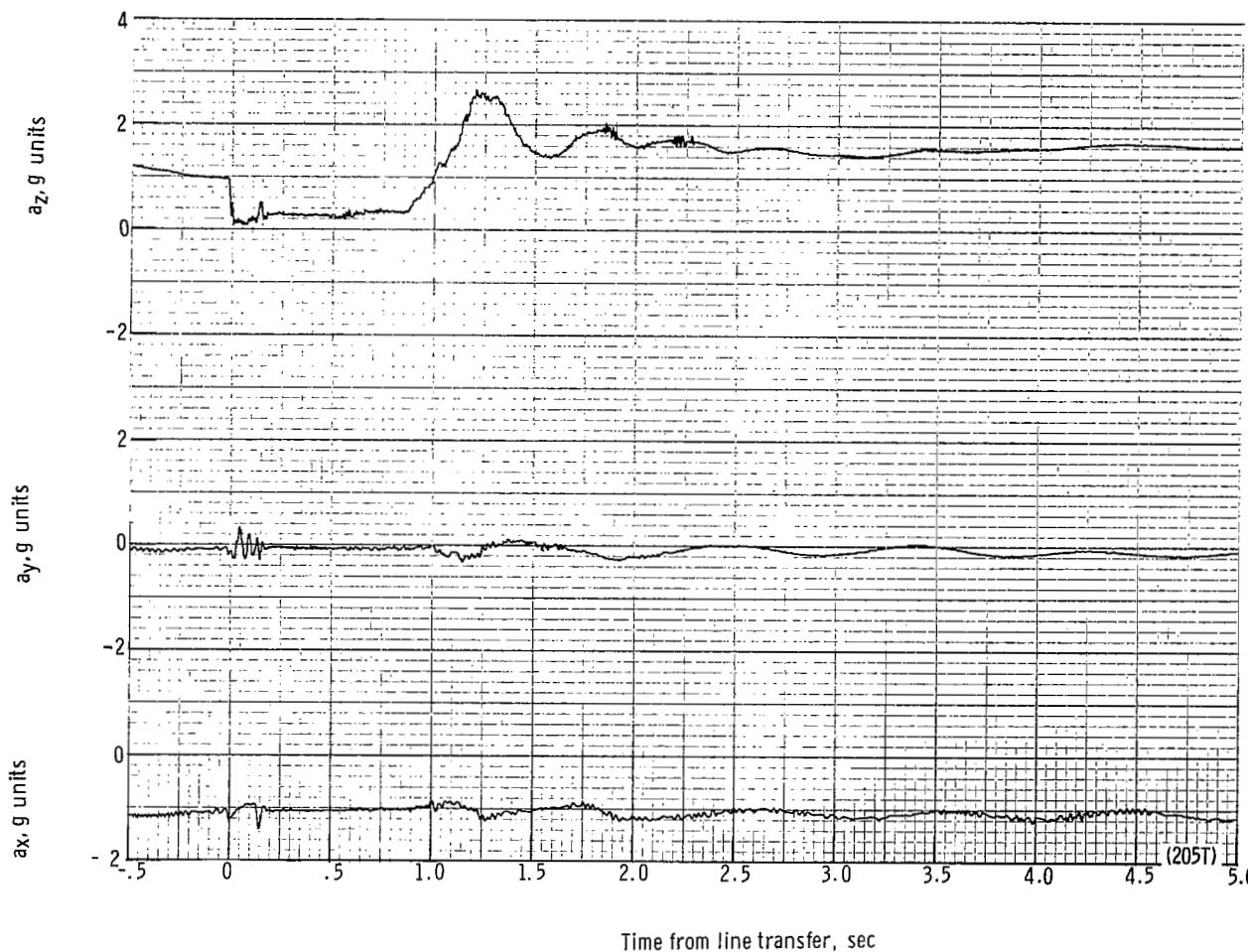
(u) Individual suspension-line loads F_{Lk12} , F_{Lk7} , F_{Lle6} , and F_{Lle1} plotted against time from line transfer. Time = 0 second corresponds to 44.16 seconds after launch.

Figure 46.- Continued.



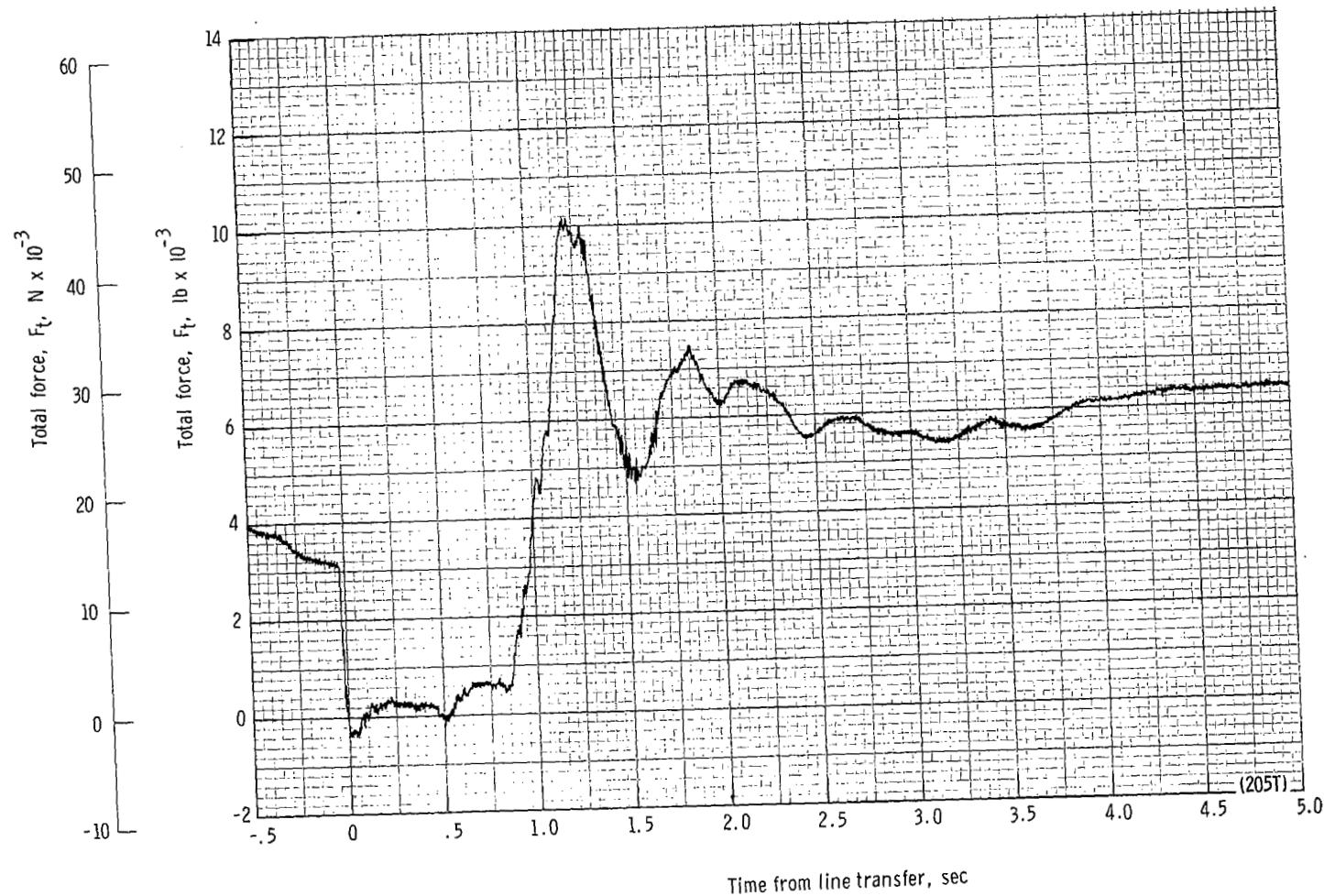
(v) Right, left, forward, and aft riser loads plotted against time from line transfer. Time = 0 second corresponds to 44.16 seconds after launch.

Figure 46.- Continued.



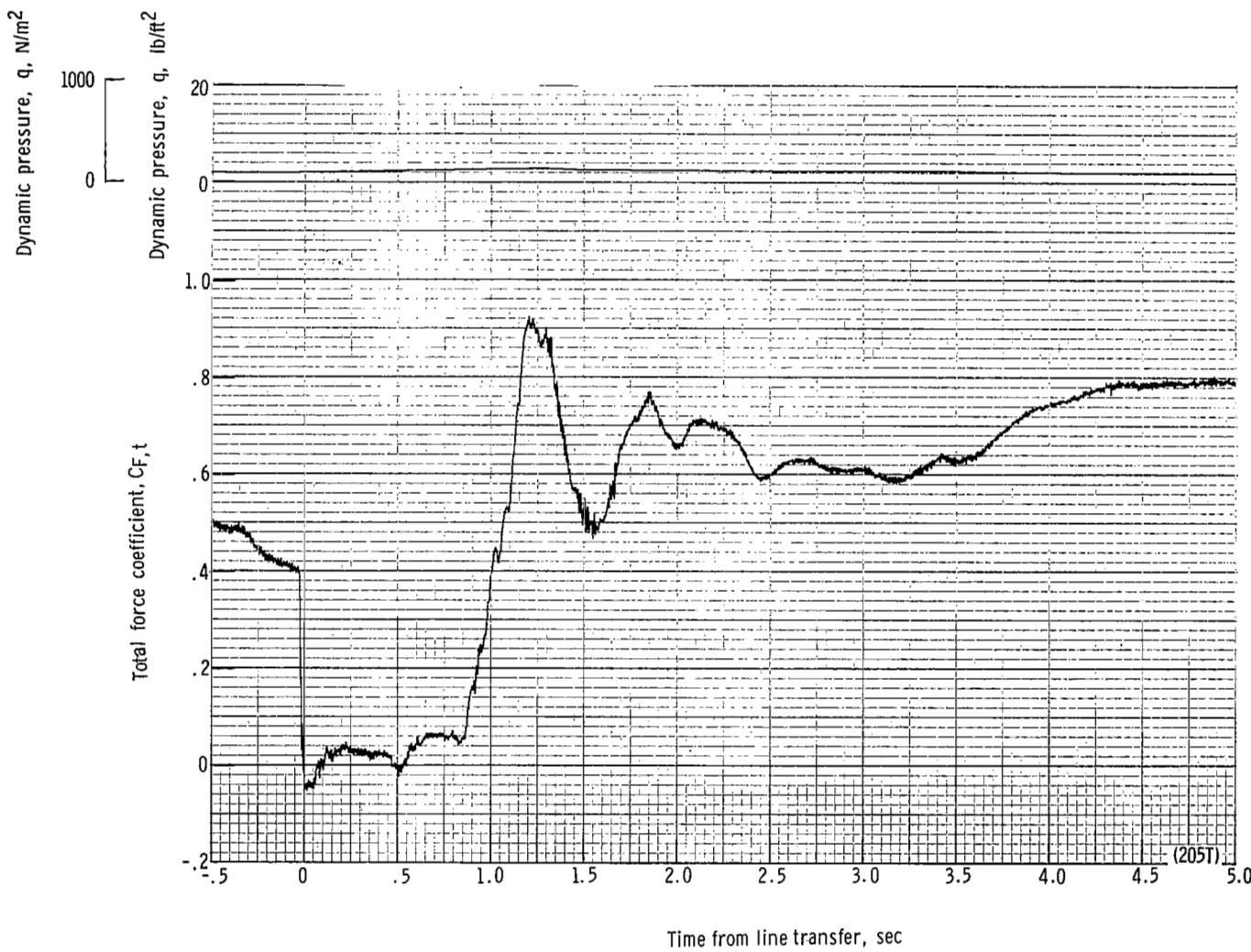
(w) Accelerations a_x , a_y , and a_z plotted against time from line transfer. Time = 0 second corresponds to 44.16 seconds after launch.

Figure 46.- Continued.



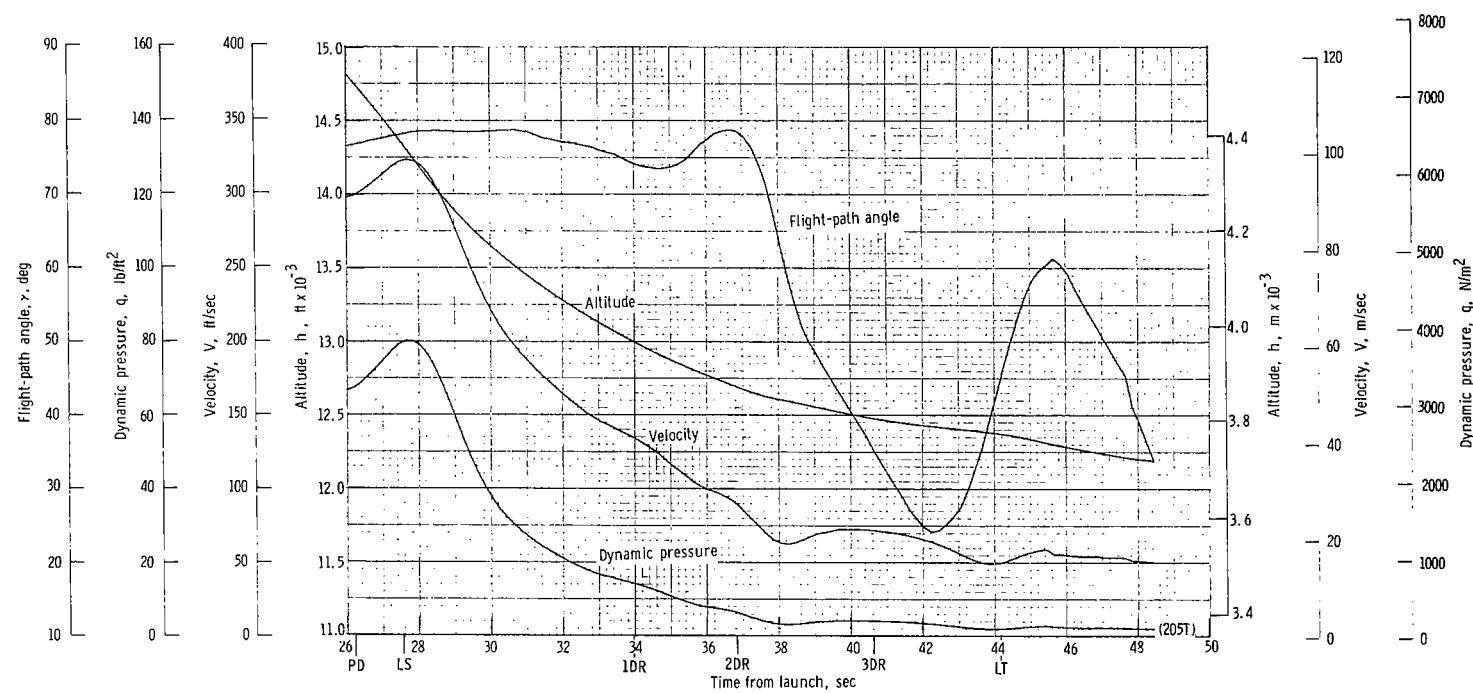
(x) Total force F_t plotted against time from line transfer. Time = 0 second corresponds to 44.16 seconds after launch.

Figure 46.- Continued.



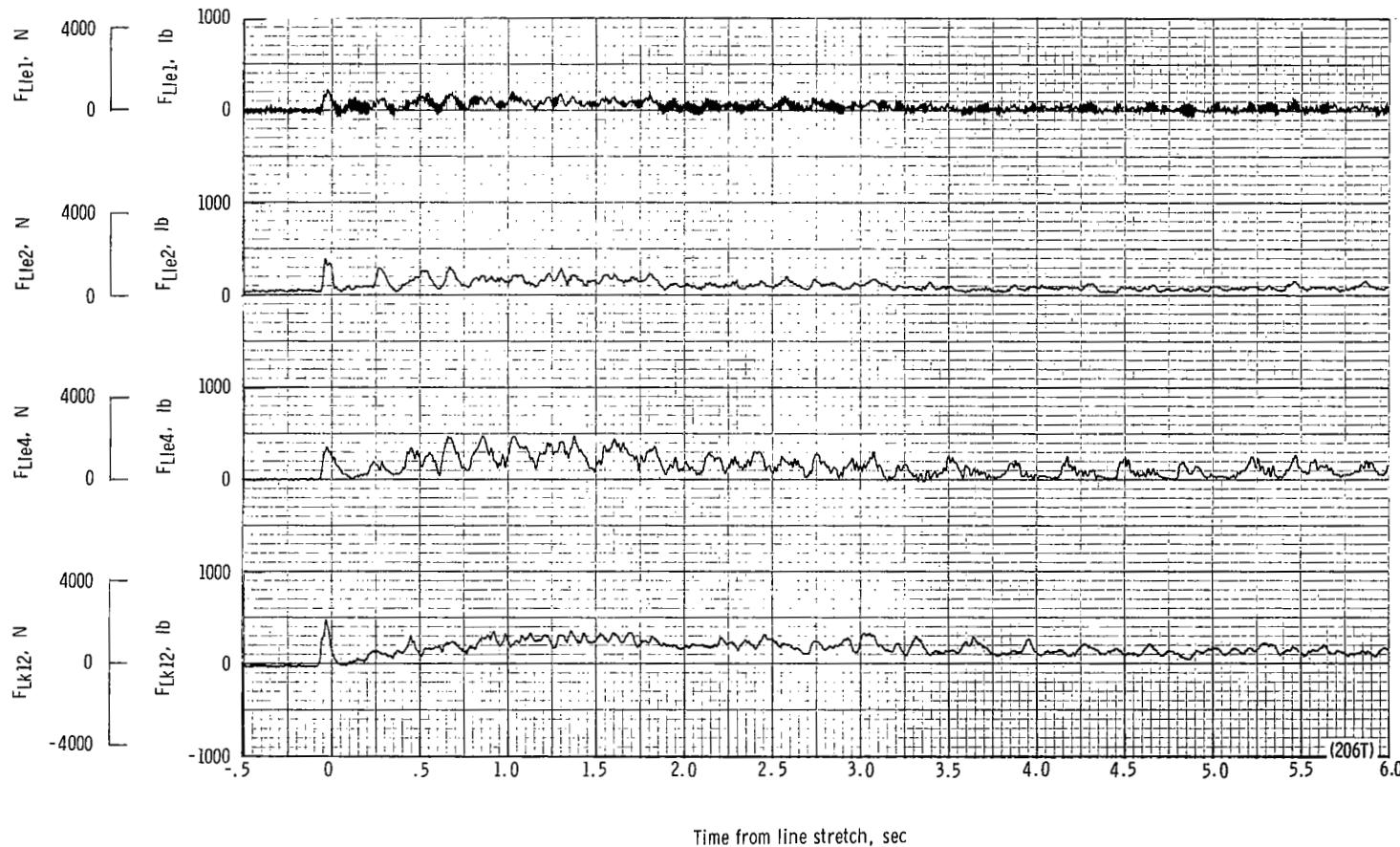
(y) Total force coefficient $C_{F,t}$ and dynamic pressure q plotted against time from line transfer. Time = 0 second corresponds to 44.16 seconds after launch.

Figure 46.- Continued.



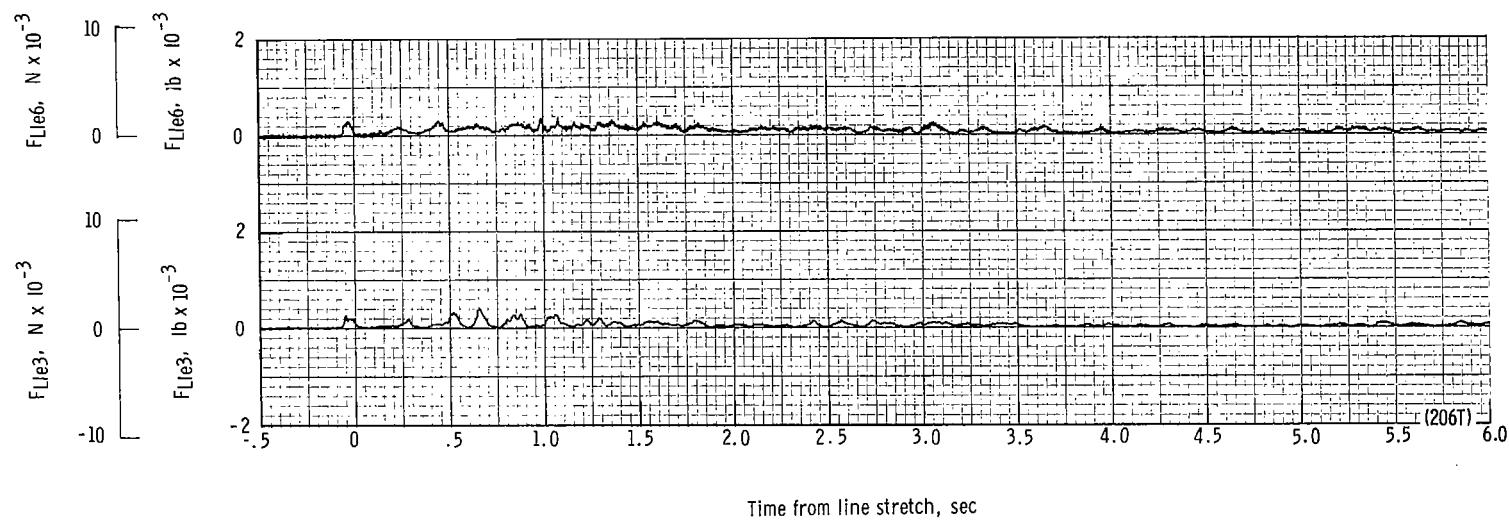
(z) Flight-path angle γ , dynamic pressure q , velocity V , and altitude h plotted against time from launch.

Figure 46.- Concluded.



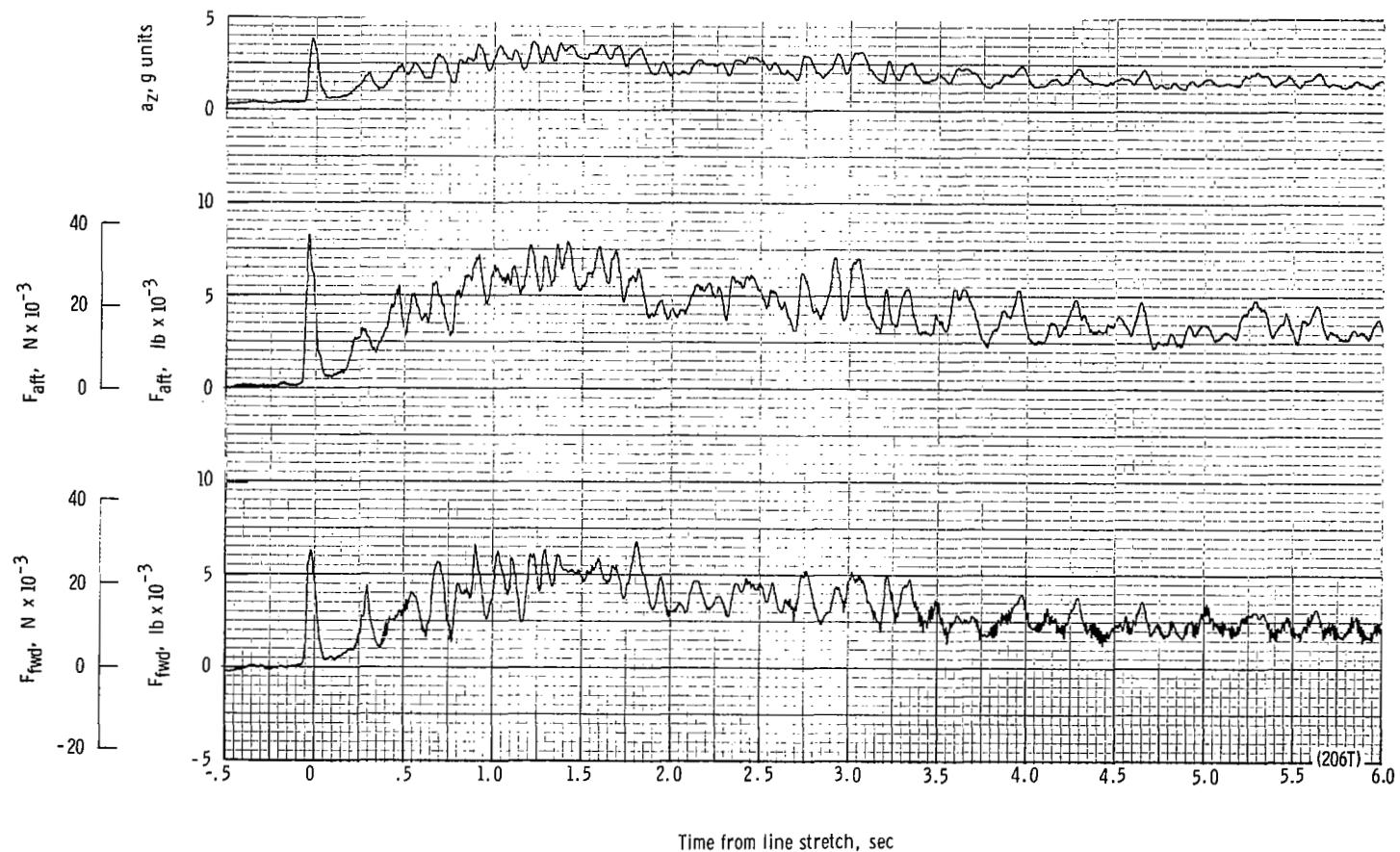
(a) Individual suspension-line loads F_{Lk12} , F_{Lle4} , F_{Lle2} and F_{Lle1} plotted against time from line stretch. Time = 0 second corresponds to 23.86 seconds after launch.

Figure 47.- Time history of twin-keel parawing deployment data for test 206T. $W_D = 22\ 246\ N$ (5001 lb); $W_p = 20\ 395\ N$ (4585 lb);
 $q_{PD} = 4366.7\ N/m^2$ (91.2 lb/ft²); $h_{PD} = 5627\ m$ (18 460 ft); $l_r/l_k = 0.080$; reefing version C.



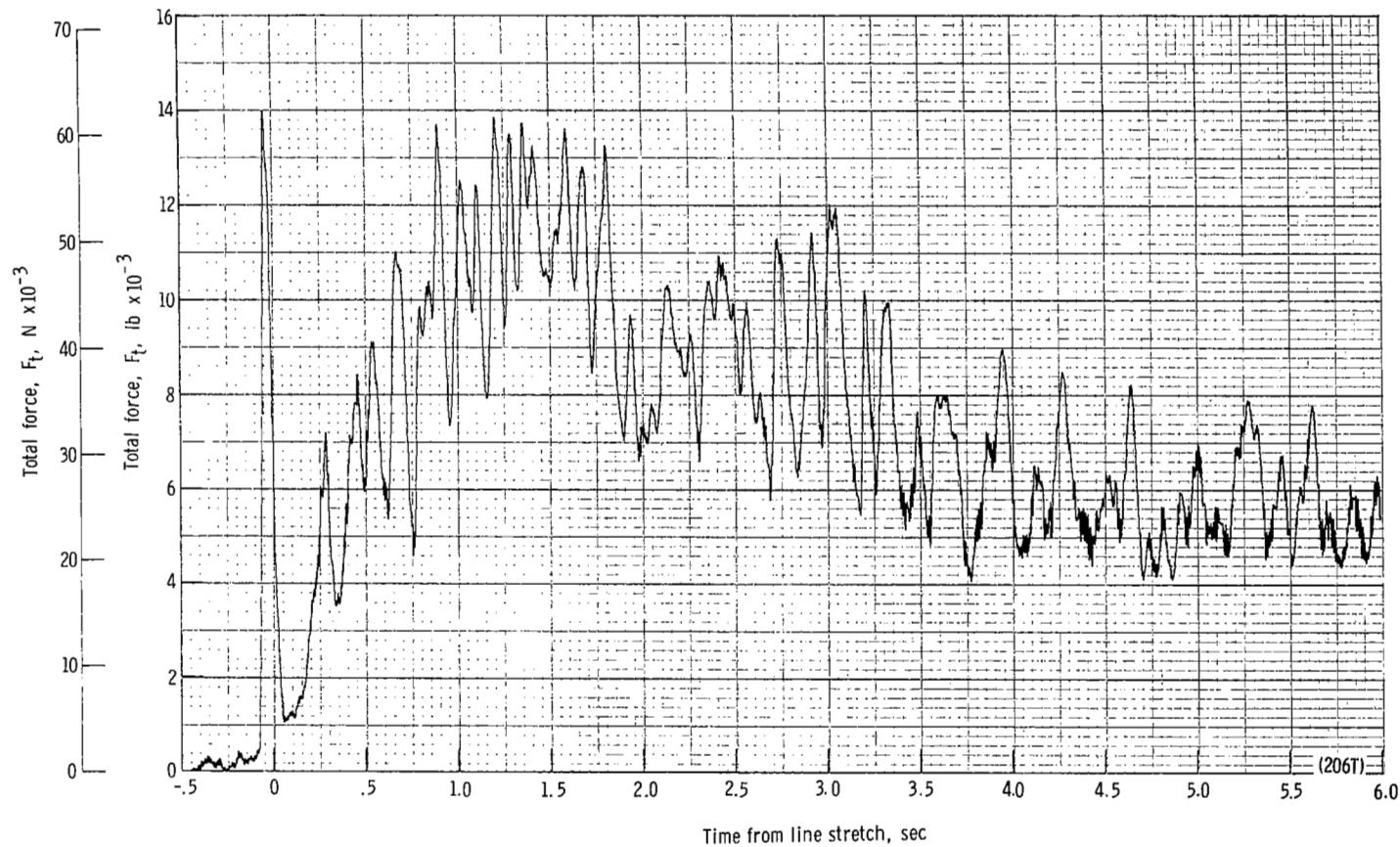
(b) Individual suspension-line loads F_{Lle3} and F_{Lle6} plotted against time from line stretch. Time = 0 second corresponds to 23.86 seconds after launch.

Figure 47.- Continued.



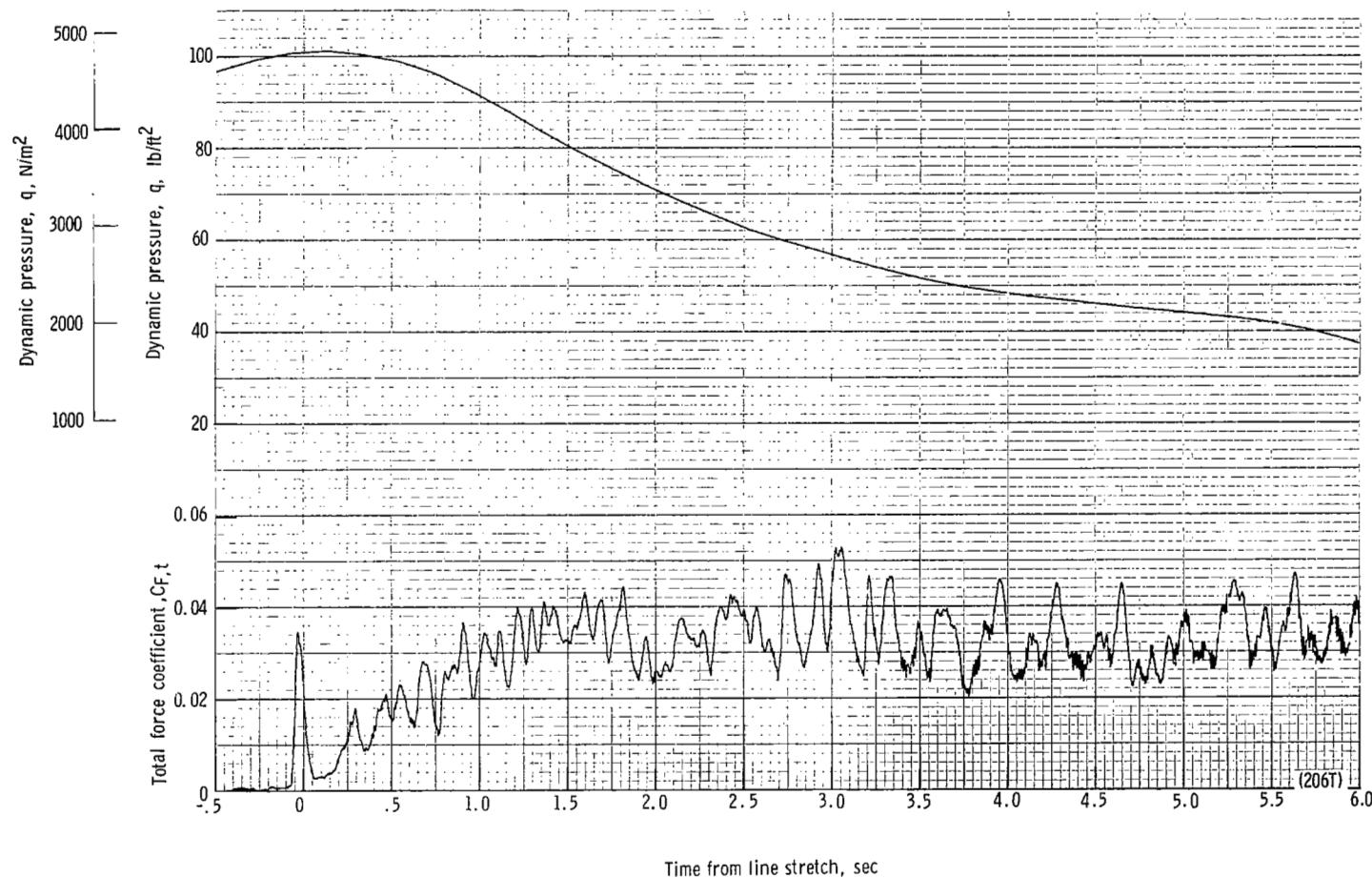
(c) Forward and aft riser loads and acceleration a_z plotted against time from line stretch. Time = 0 second corresponds to 23.86 seconds after launch.

Figure 47.- Continued.



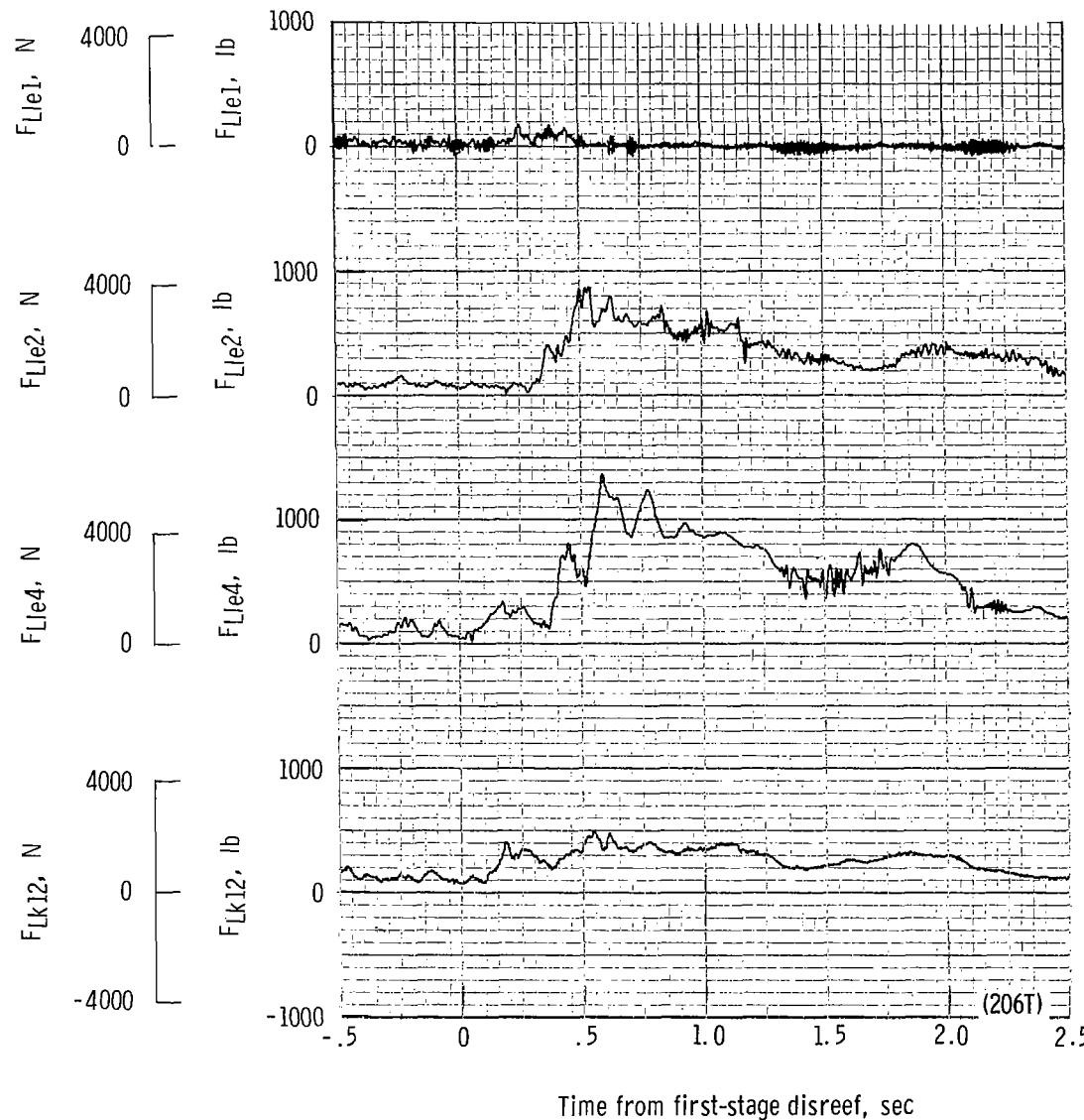
(d) Total force F_t plotted against time from line stretch. Time = 0 second corresponds to 23.86 seconds after launch.

Figure 47.- Continued.



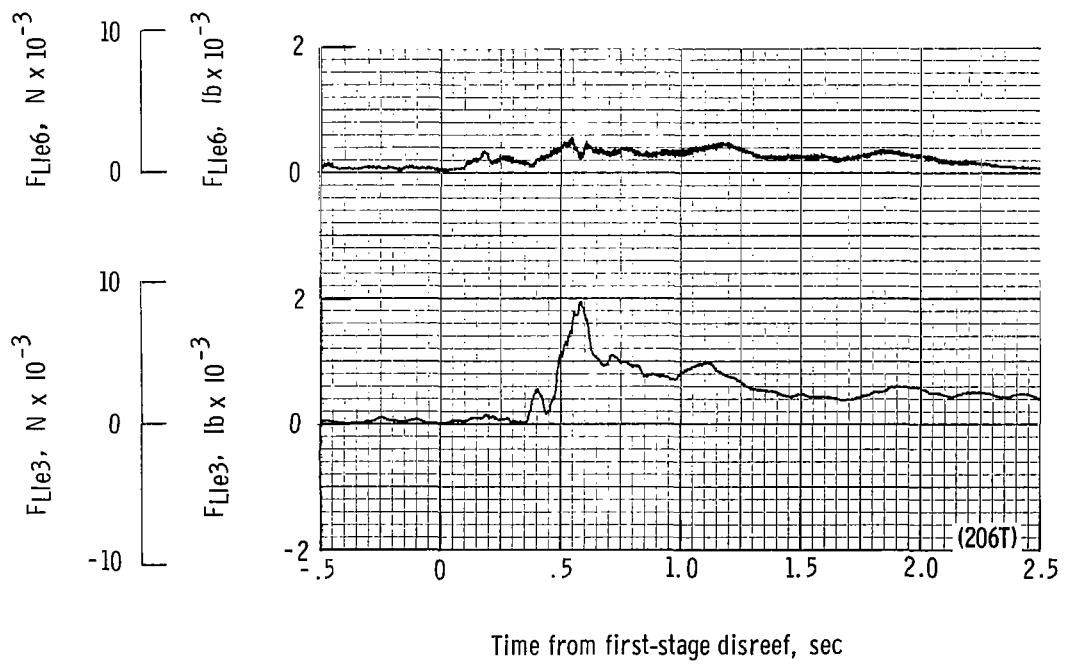
(e) Total force coefficient $C_{F,t}$ and dynamic pressure q plotted against time from line stretch. Time = 0 second corresponds to 23.86 seconds after launch.

Figure 47.- Continued.



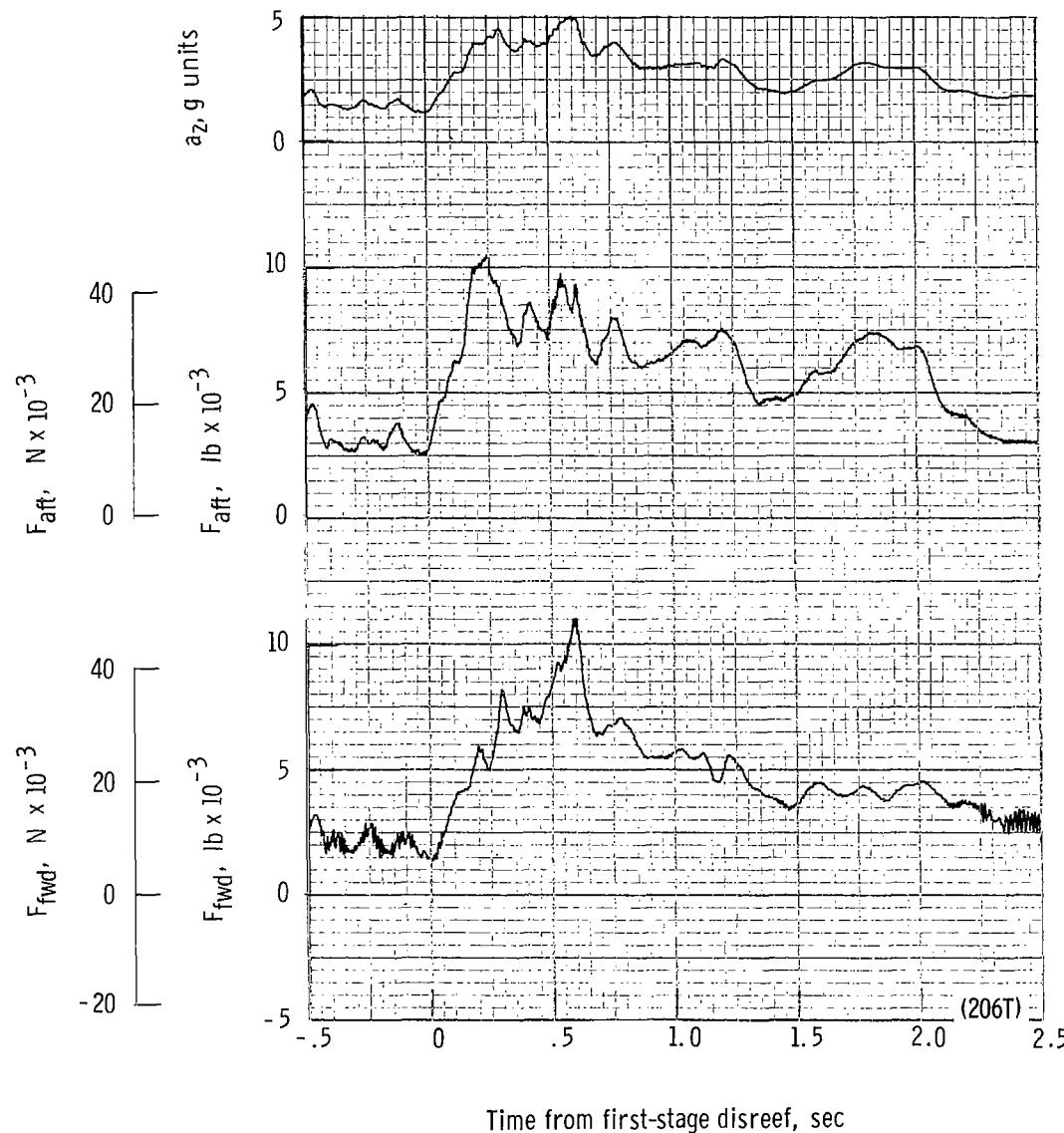
(f) Individual suspension-line loads F_{Lk12} , F_{Lle4} , F_{Lle2} , and F_{Lle1} plotted against time from first-stage disreef. Time = 0 second corresponds to 29.96 seconds after launch.

Figure 47.- Continued.



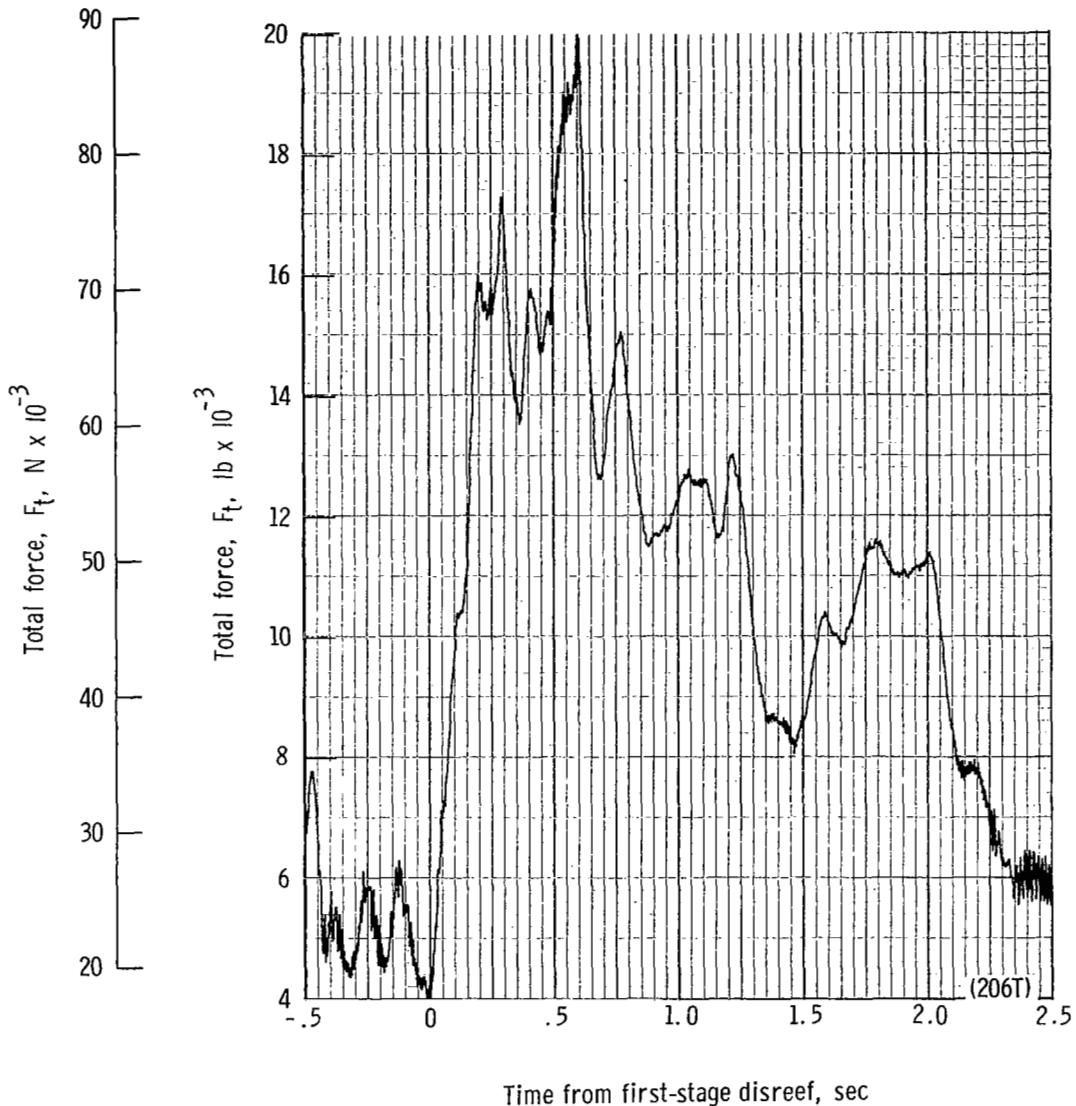
(g) Individual suspension-line loads F_{Lle3} and F_{Lle6} plotted against time from first-stage disreef. Time = 0 second corresponds to 29.96 seconds after launch.

Figure 47.- Continued.



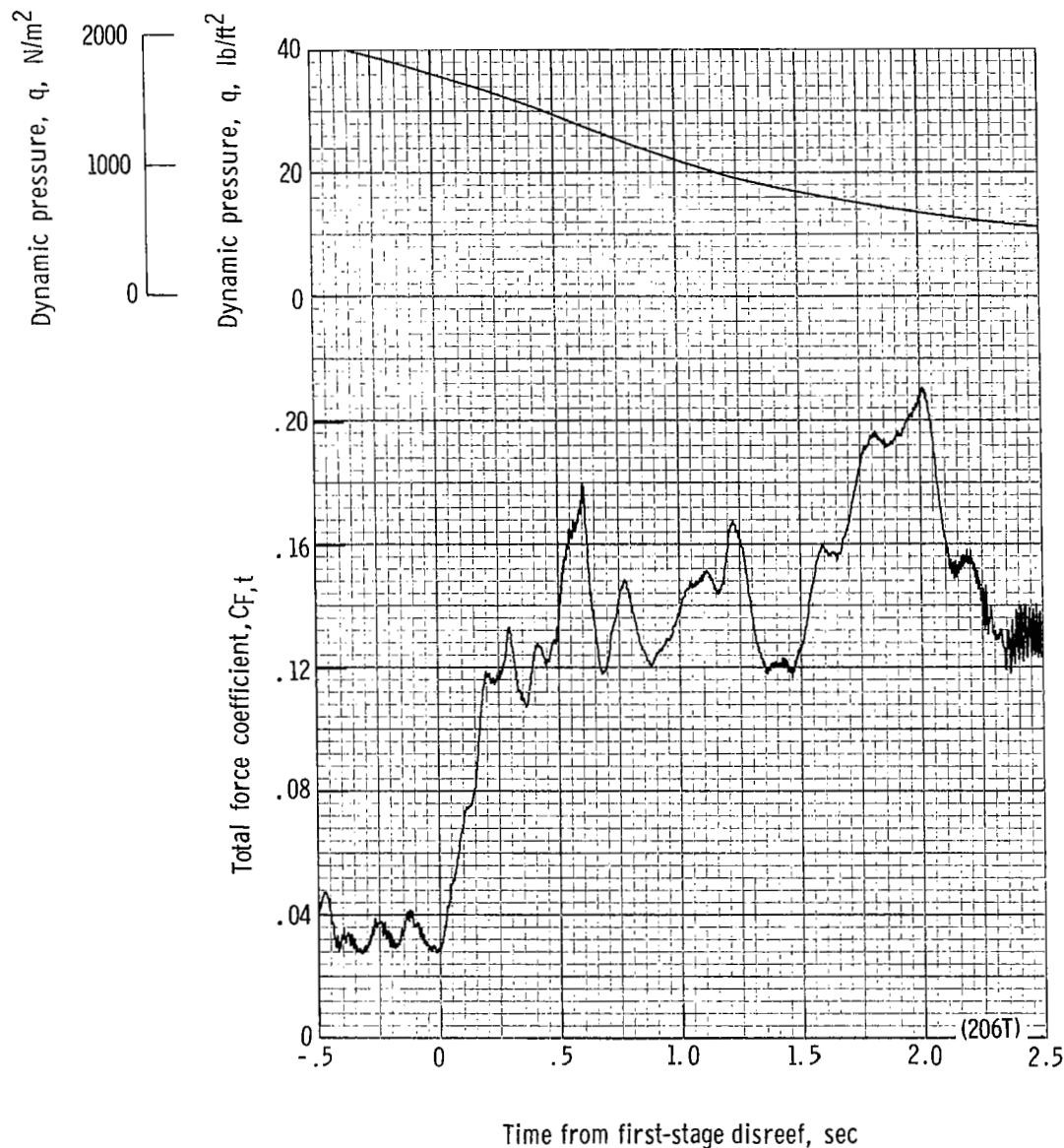
(h) Forward and aft riser loads and acceleration a_z plotted against time from first-stage disreef. Time = 0 second corresponds to 29.96 seconds after launch.

Figure 47.- Continued.



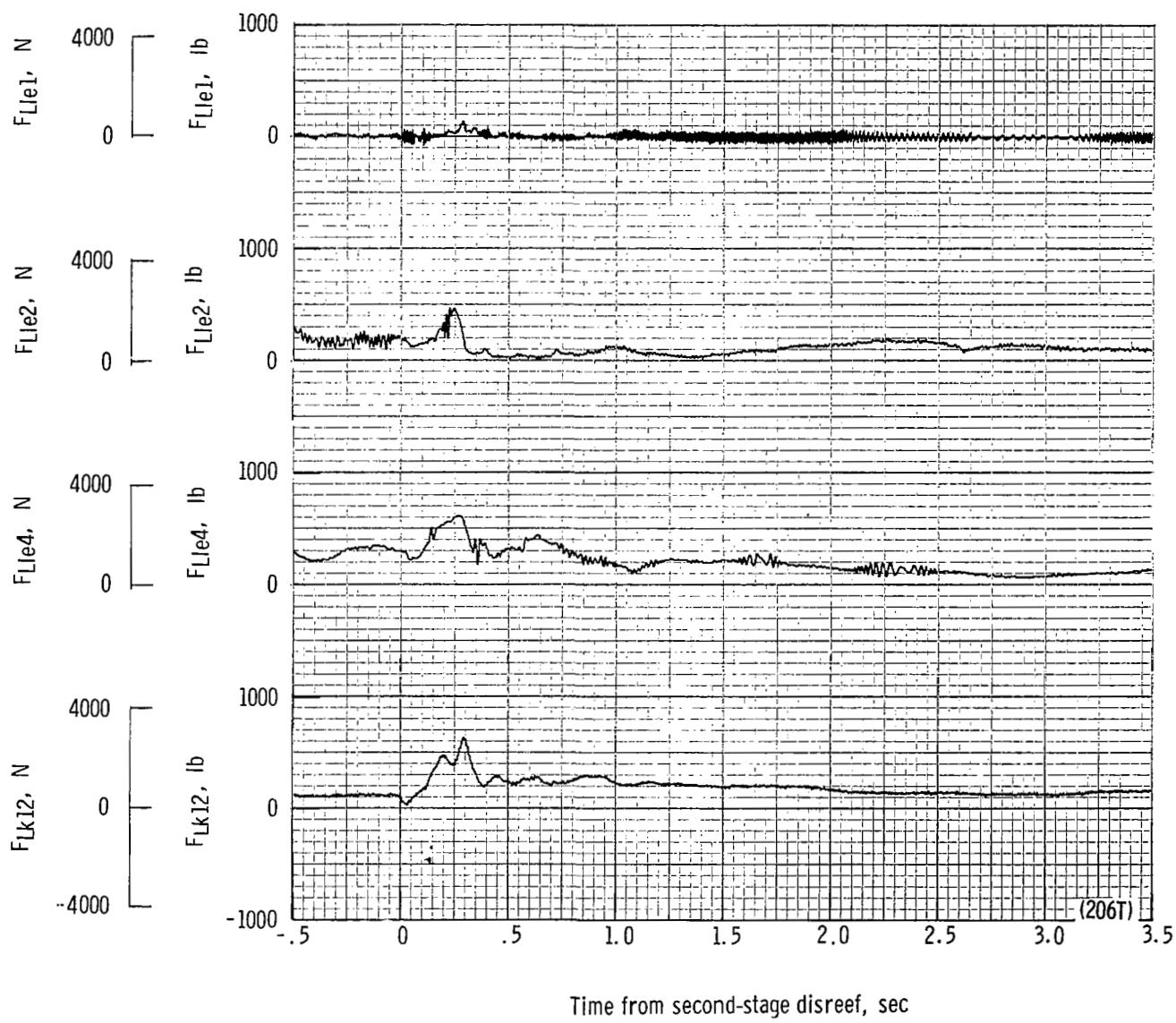
(i) Total force F_t plotted against time from first-stage disreef. Time = 0 second corresponds to 29.96 seconds after launch.

Figure 47.- Continued.



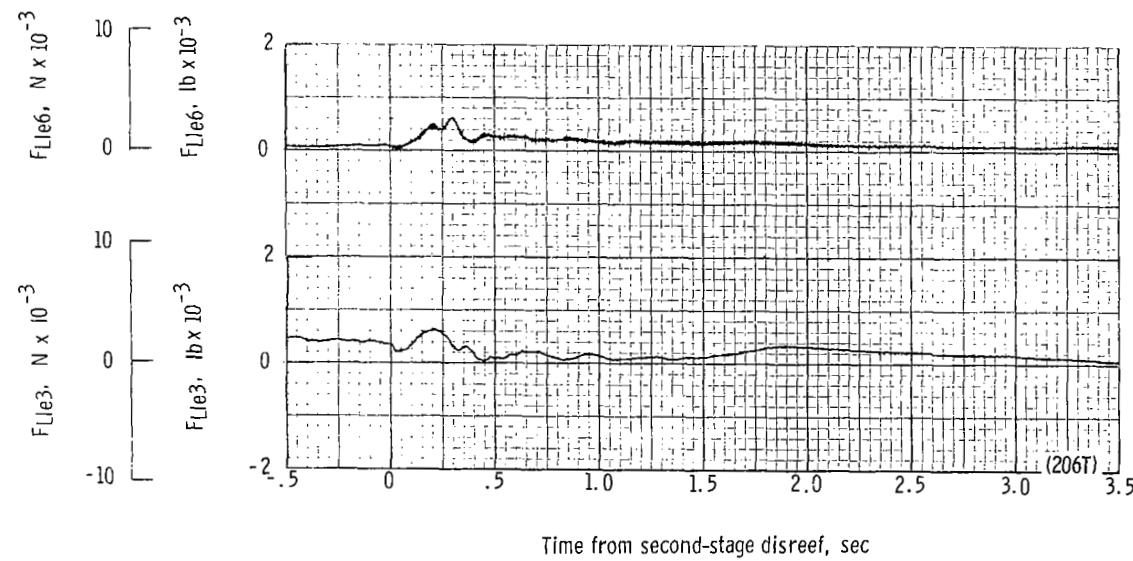
(j) Total force coefficient $C_{F,t}$ and dynamic pressure q plotted against time from first-stage disreef. Time = 0 second corresponds to 29.96 seconds after launch.

Figure 47.- Continued.



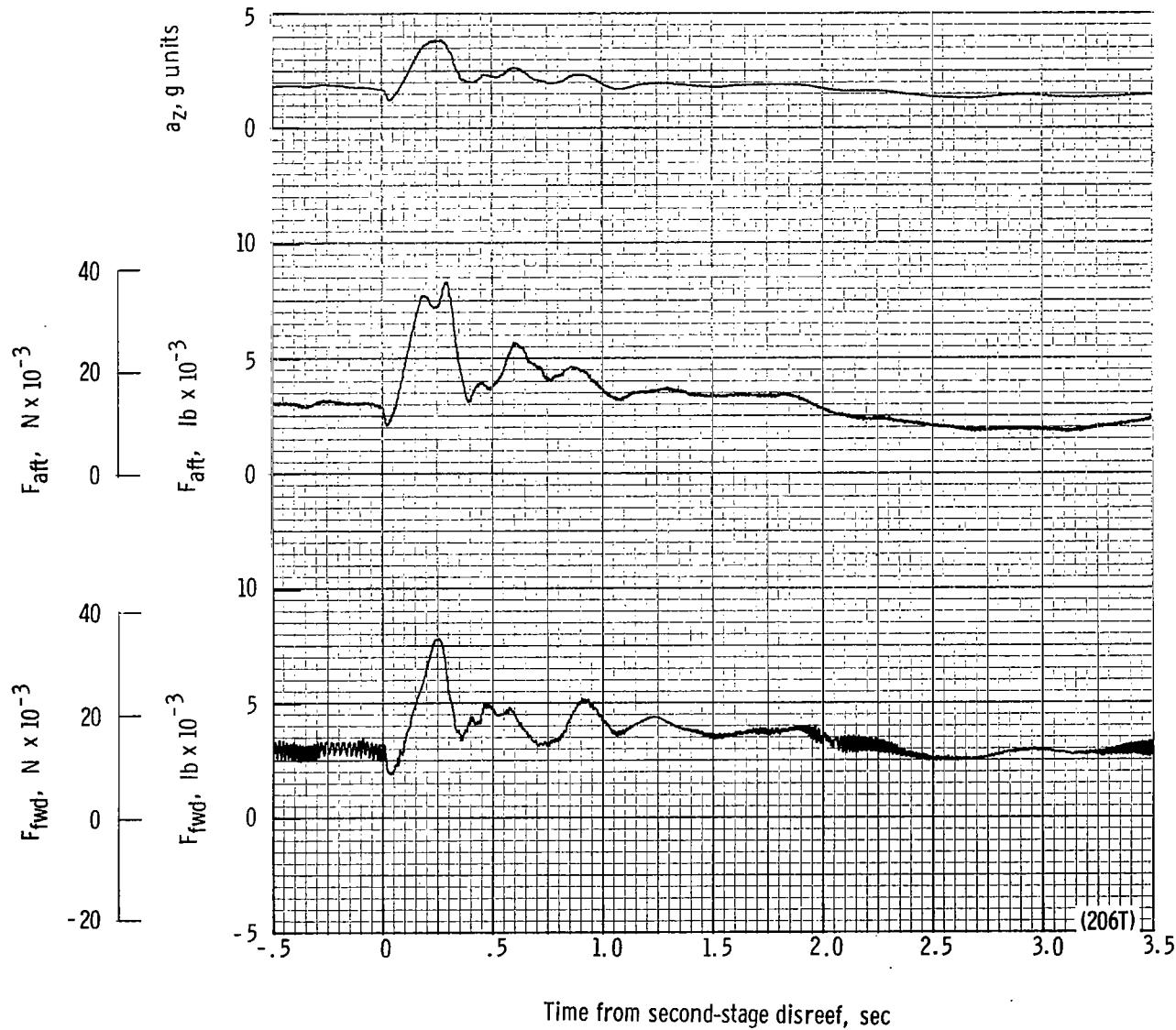
(k) Individual suspension-line loads F_{Lk12} , F_{Lle4} , F_{Lle2} , and F_{Lle1} plotted against time from second-stage disreef. Time = 0 second corresponds to 32.84 seconds after launch.

Figure 47.- Continued.



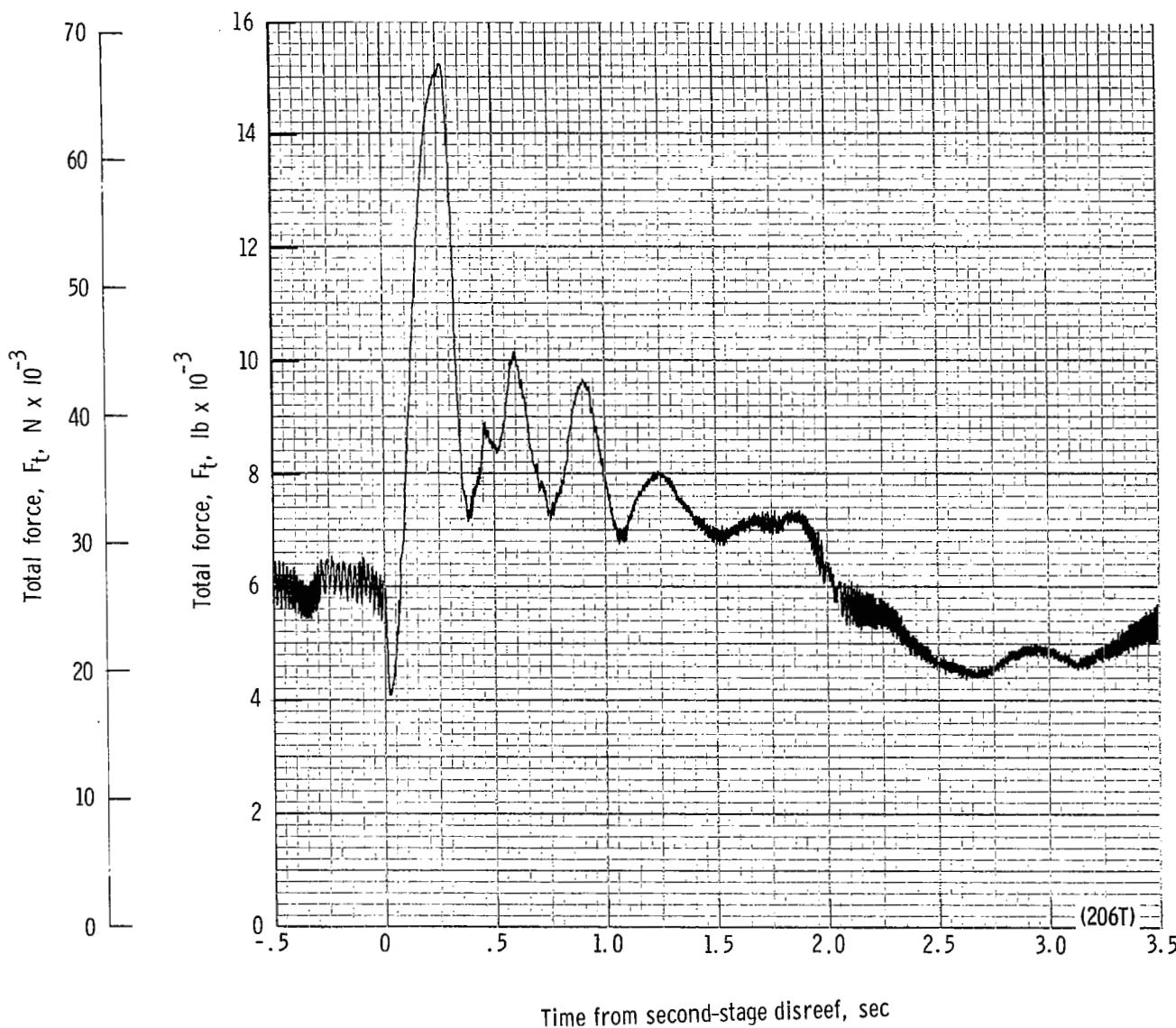
(II) Individual suspension-line loads F_{Lle3} and F_{Lle6} plotted against time from second-stage disreef. Time = 0 second corresponds to 32.84 seconds after launch.

Figure 47.- Continued.



(m) Forward and aft riser loads and acceleration a_z plotted against time from second-stage disreef. Time = 0 second corresponds to 32.84 seconds after launch.

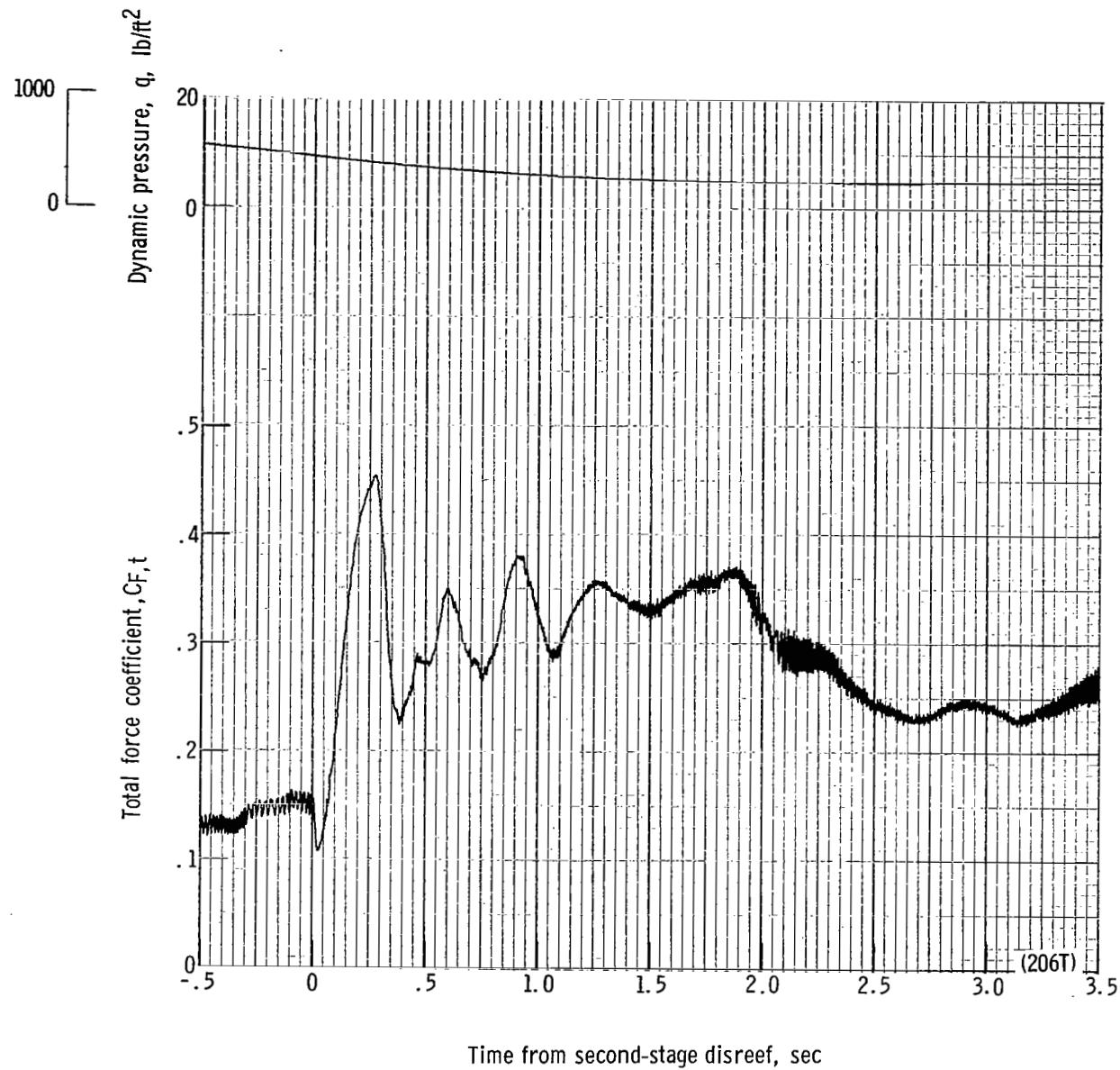
Figure 47.- Continued.



(n) Total force coefficient $C_{F,t}$ and dynamic pressure q plotted against time from second-stage disreef. Time = 0 second corresponds to 32.84 seconds after launch.

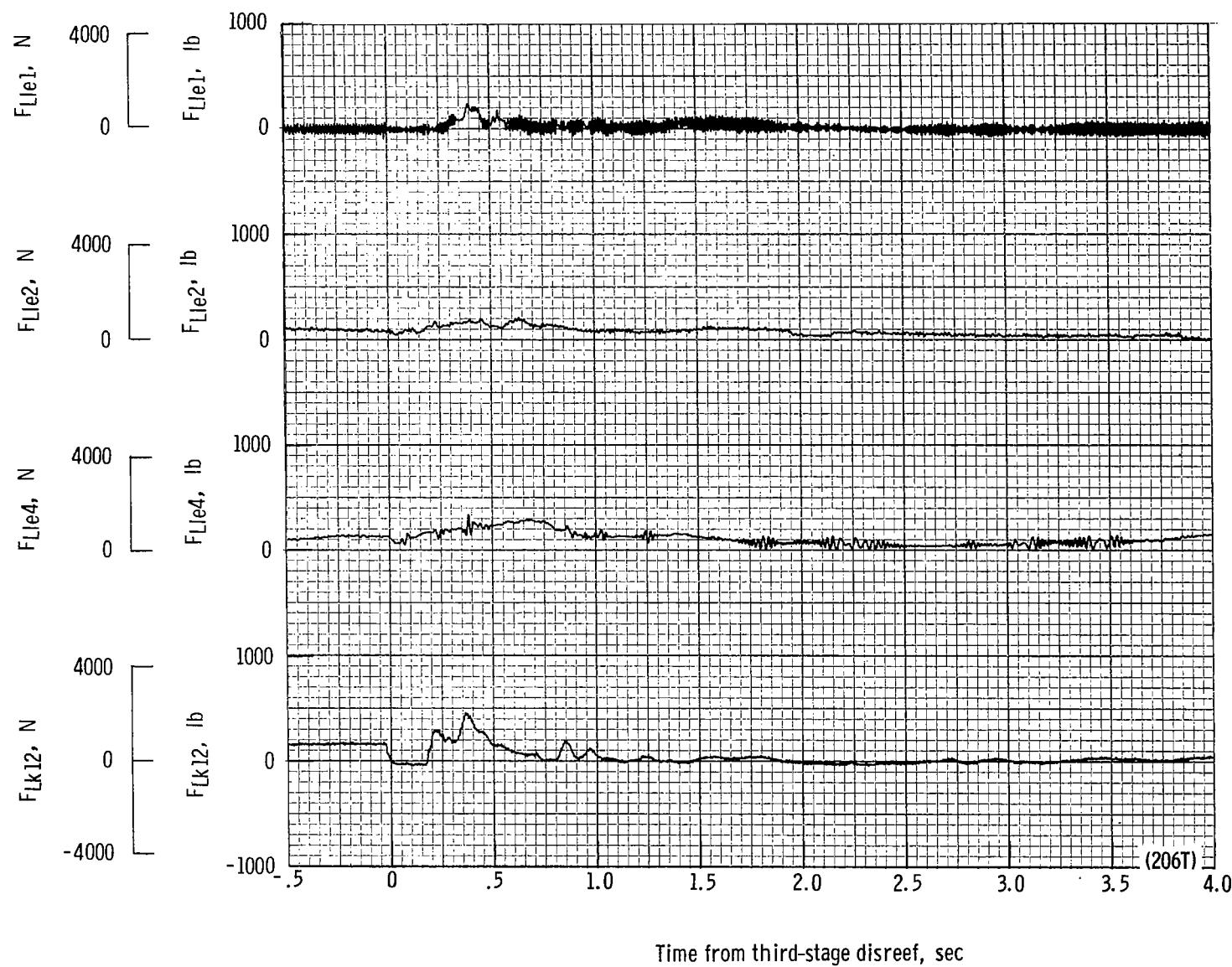
Figure 47.- Continued.

Dynamic pressure, q , N/m²



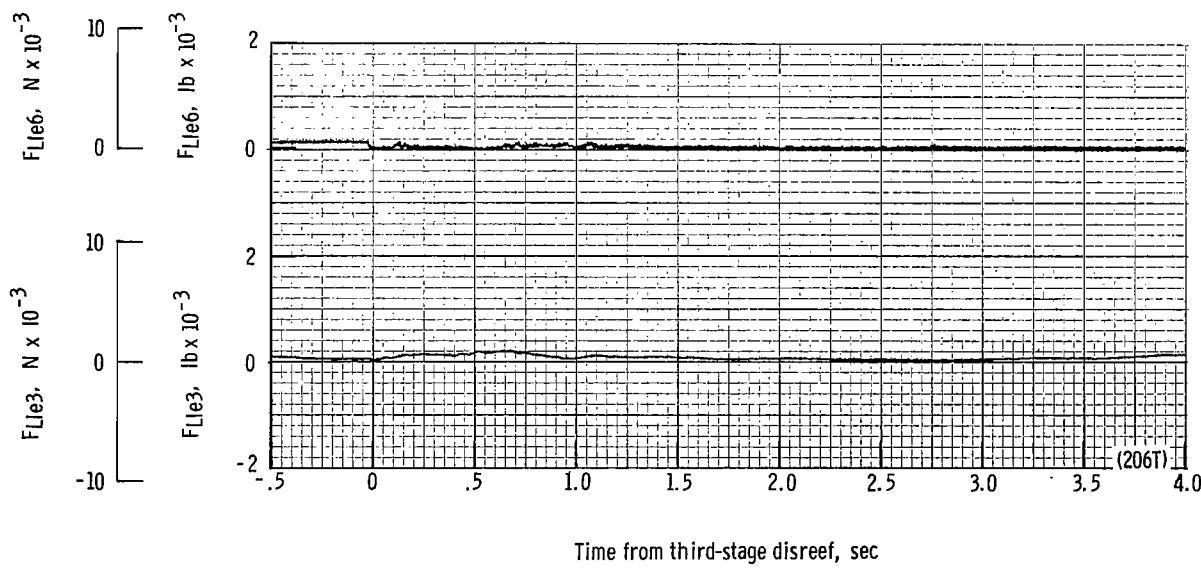
(o) Total force F_t plotted against time from second-stage disreef. Time = 0 second corresponds to 32.84 seconds after launch.

Figure 47.- Continued.



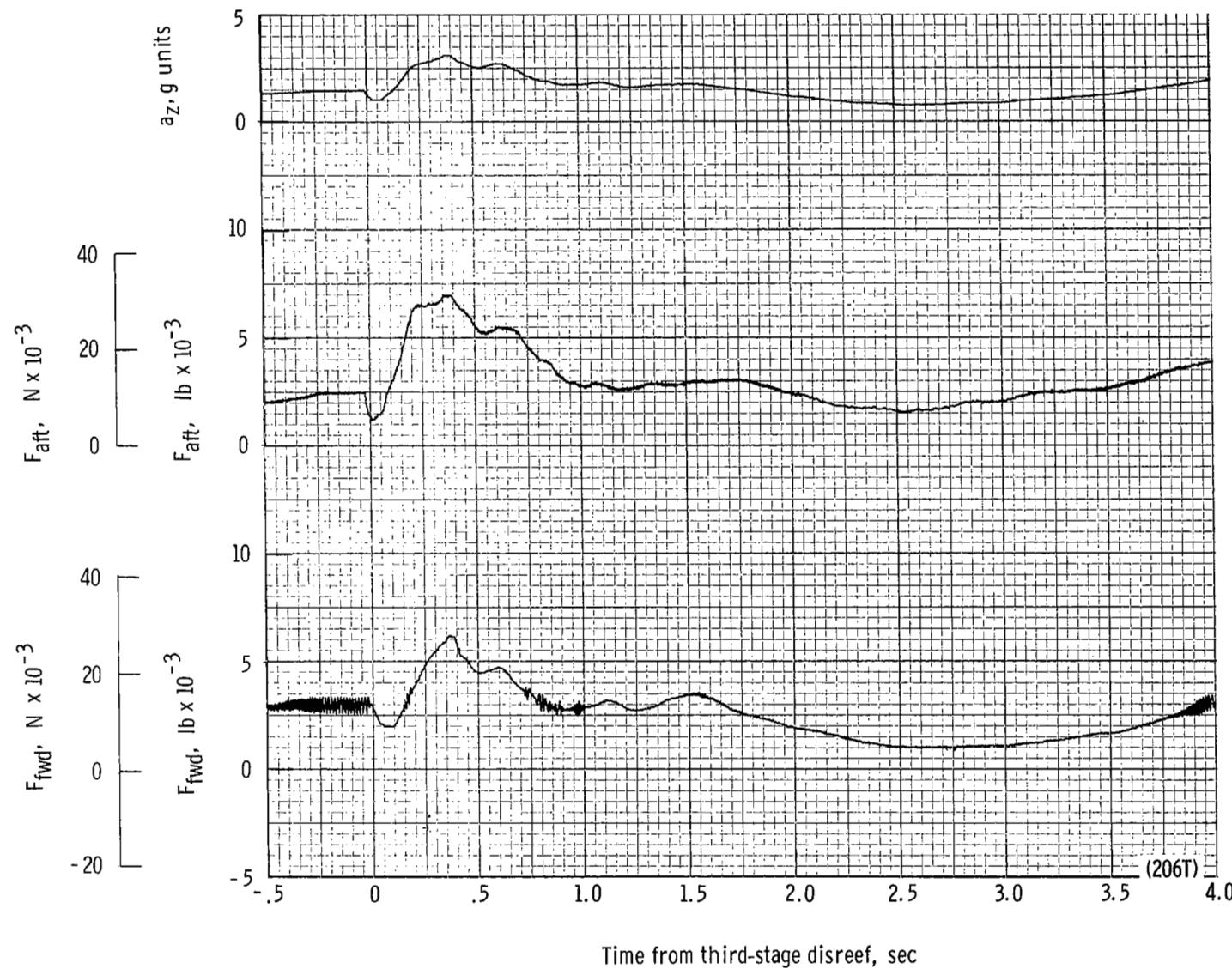
(p) Individual suspension-line loads F_{Lk12} , F_{Lle4} , F_{Lle2} , and F_{Lle1} plotted against time from third-stage disref. Time = 0 second corresponds to 36.62 seconds after launch.

Figure 47.- Continued.



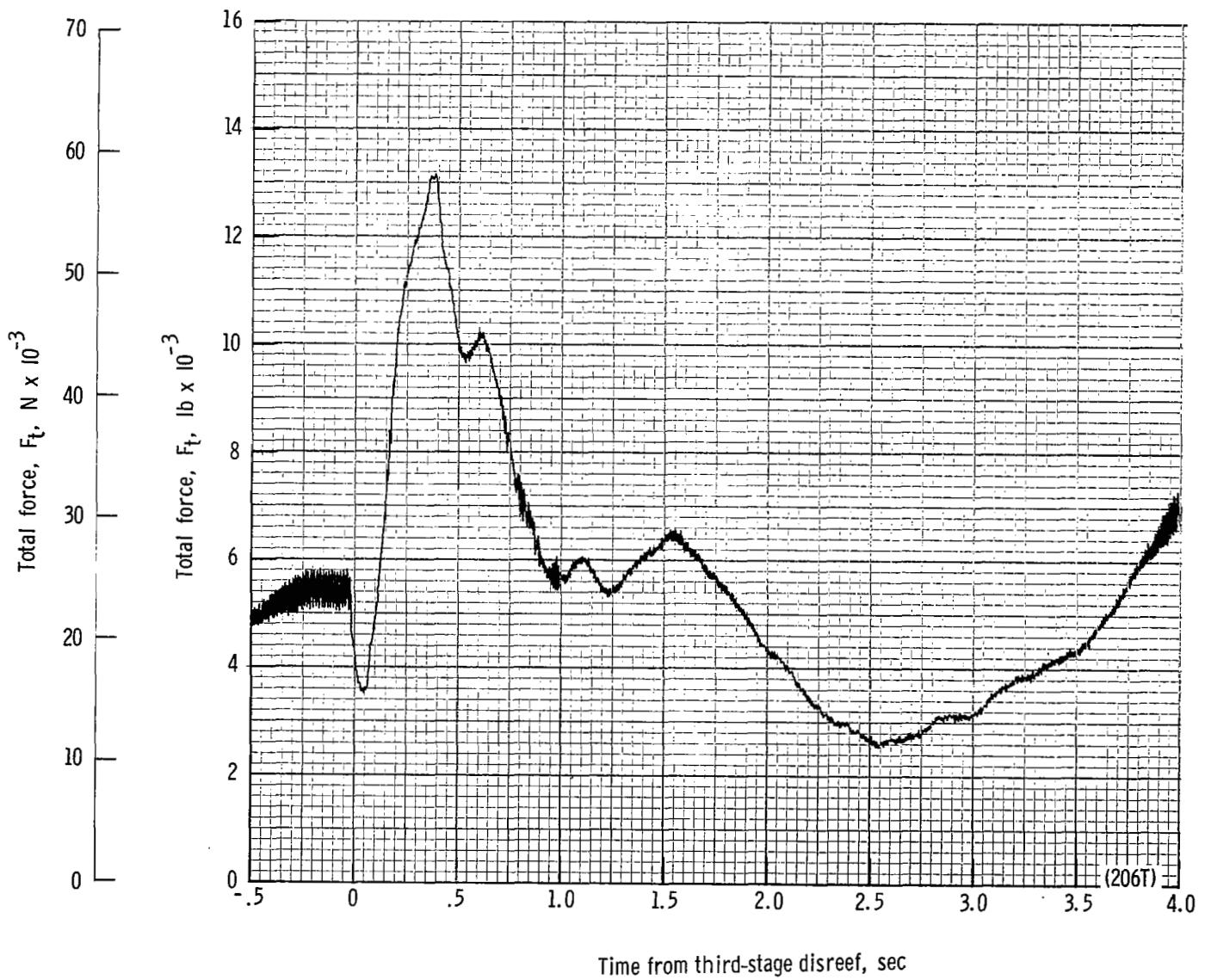
(g) Individual suspension-line F_{Lle3} and F_{Lle6} plotted against time from third-stage disreef. Time = 0 second corresponds to 36.62 seconds after launch.

Figure 47.- Continued.



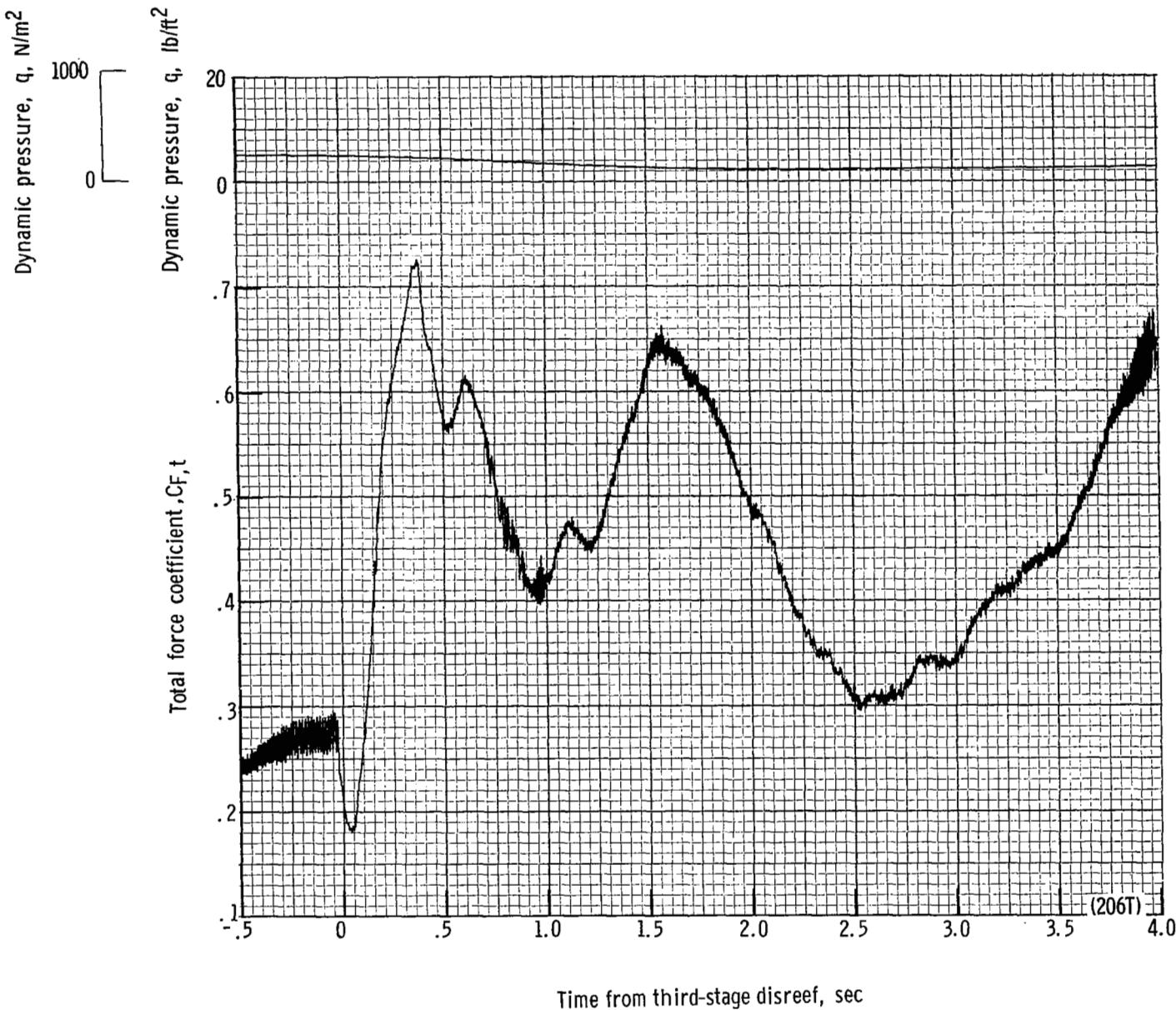
(r) Forward and aft riser loads and acceleration a_z plotted against time from third-stage disreef. Time = 0 second corresponds to 36.62 seconds after launch.

Figure 47.- Continued.



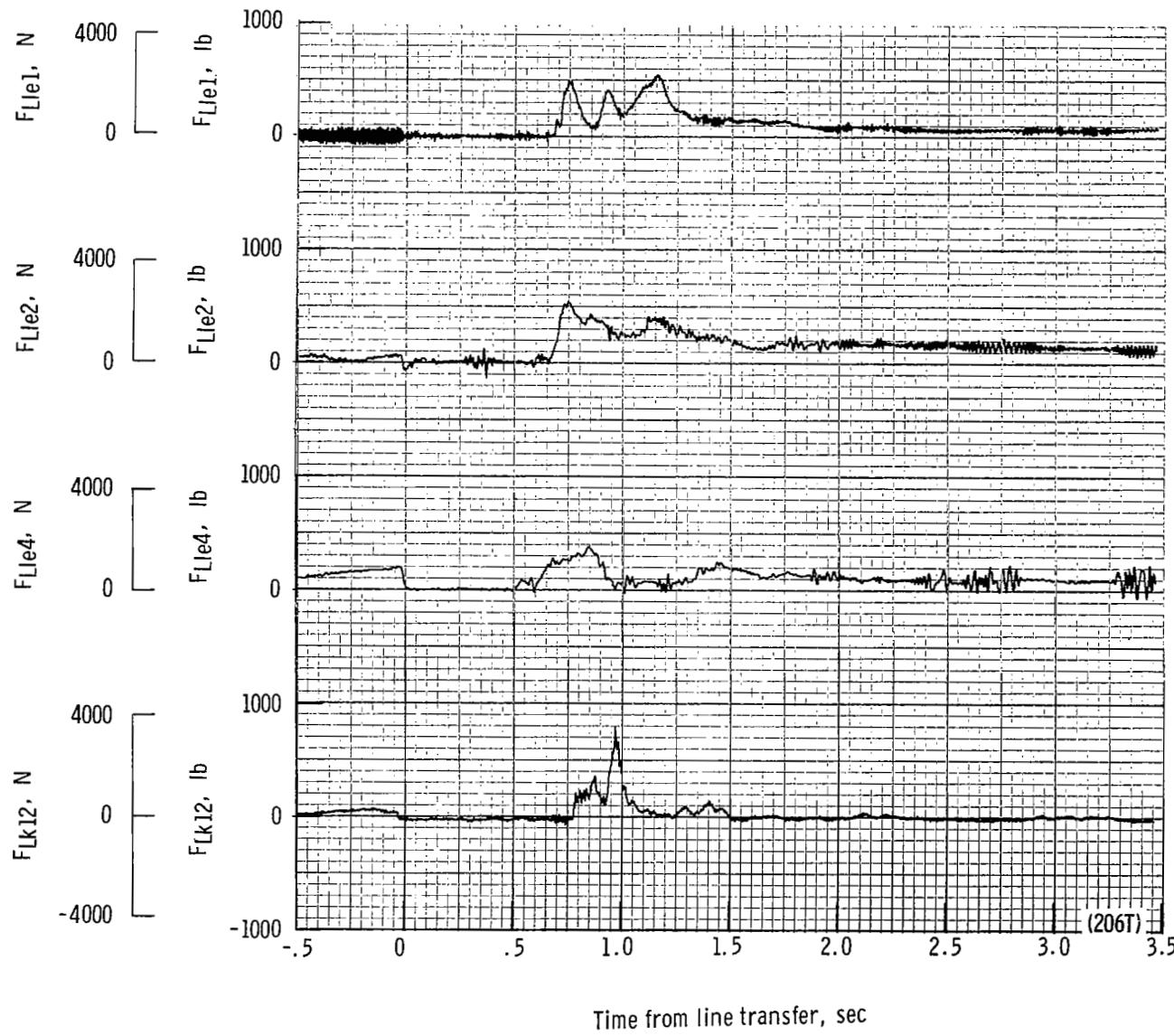
(s) Total force F_t plotted against time from third-stage disreef. Time = 0 second corresponds to 36.62 seconds after launch.

Figure 47.- Continued.

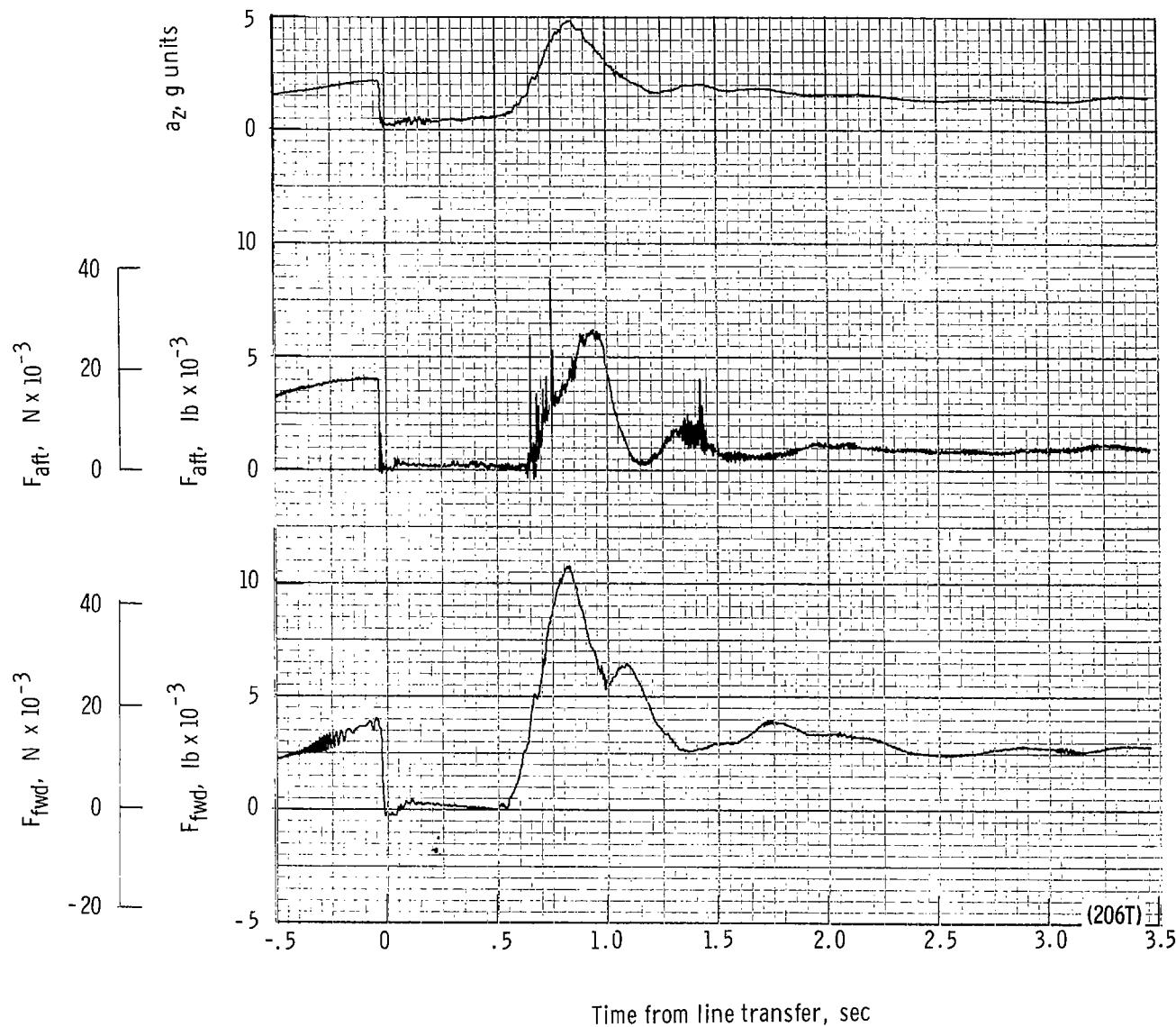


(t) Total force coefficient $C_{F,t}$ and dynamic pressure q plotted against time from third-stage disreef. Time = 0 second corresponds to 36.62 seconds after launch.

Figure 47.- Continued.

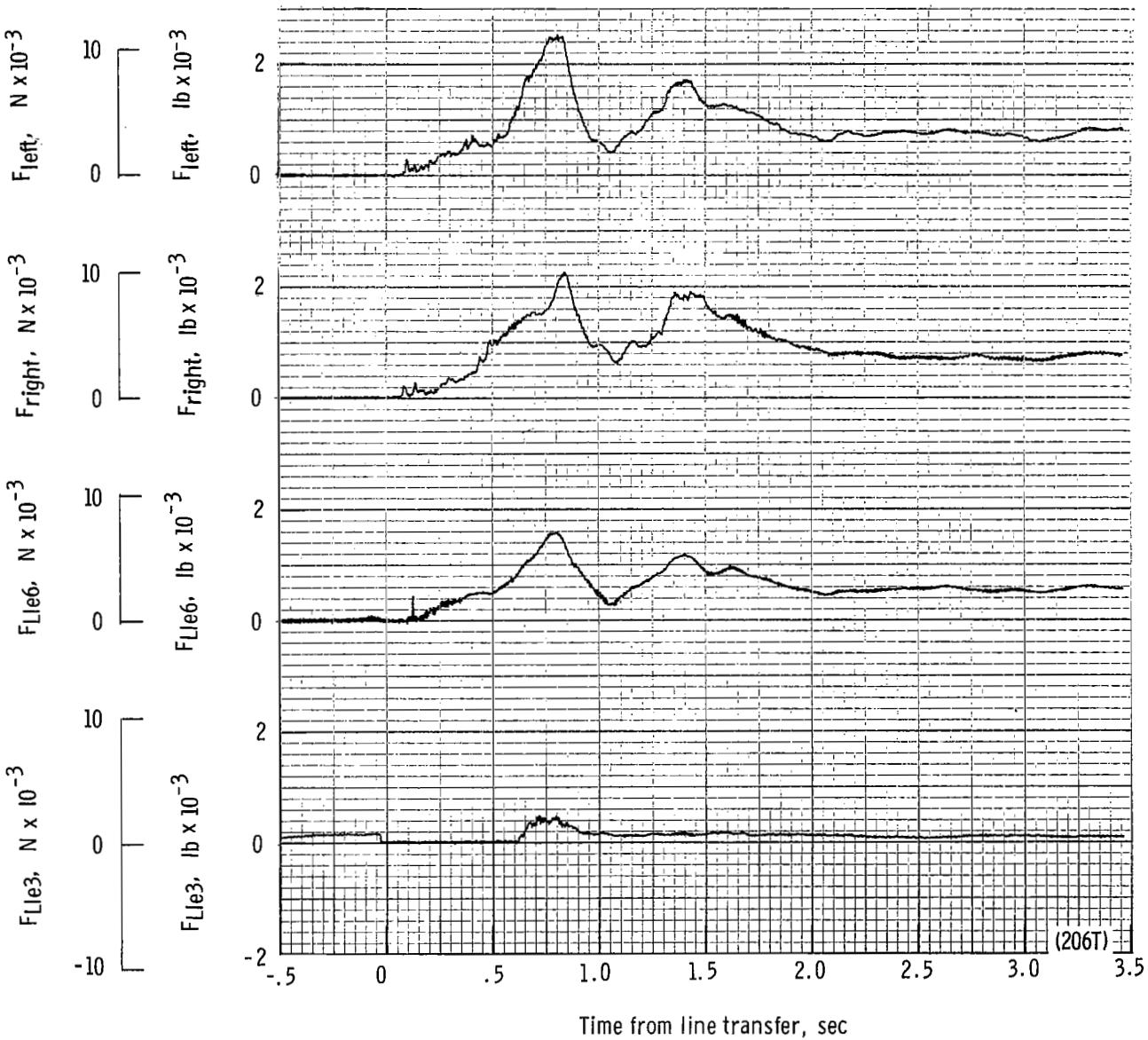


(u) Individual suspension-line loads F_{Lk12} , F_{Lle4} , F_{Lle2} , and F_{Lle1} plotted against time from line transfer. Time = 0 second corresponds to 40.83 seconds after launch.



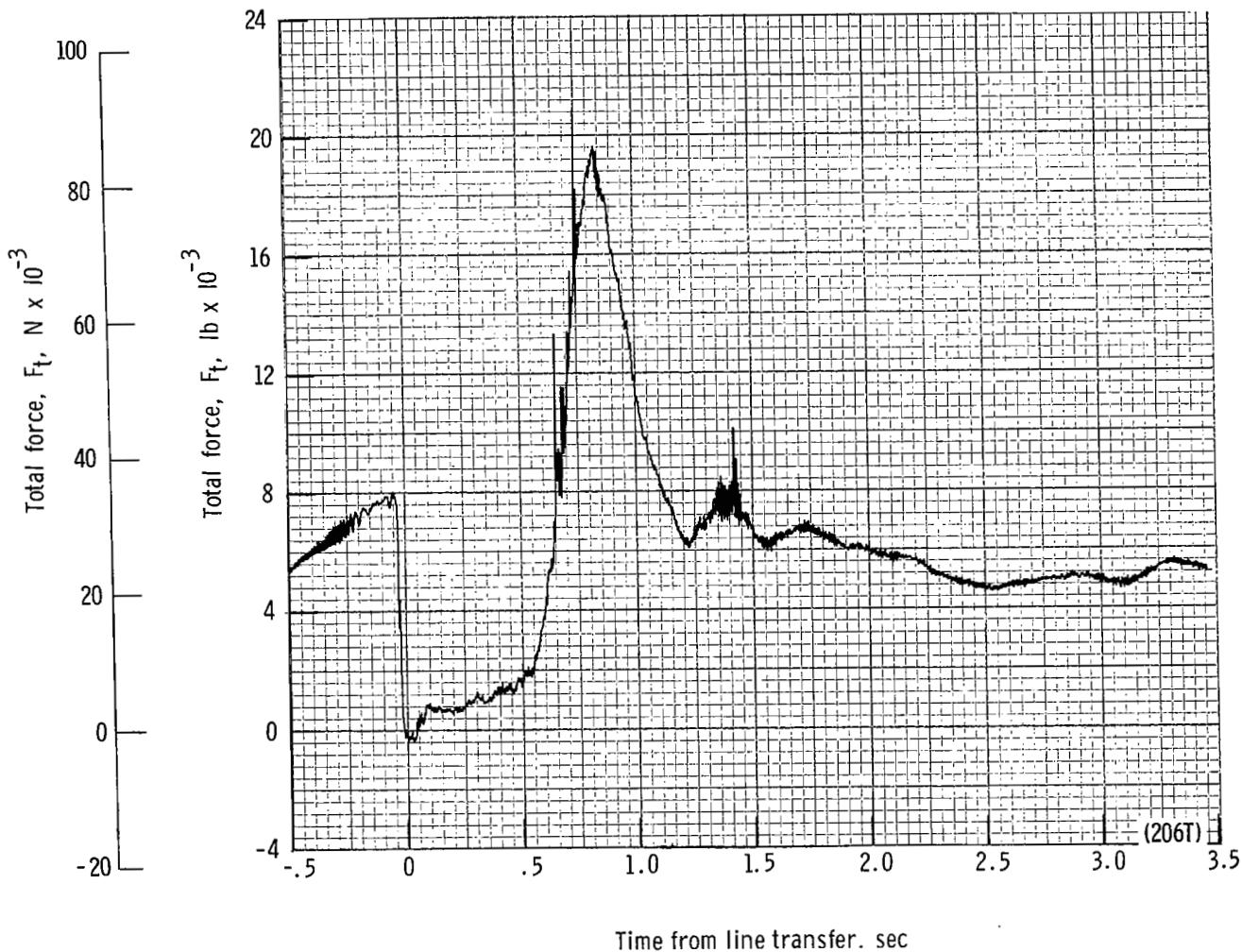
(v) Forward and aft riser loads and acceleration a_z plotted against time from line transfer. Time = 0 second corresponds to 40.83 seconds after launch.

Figure 47.- Continued.



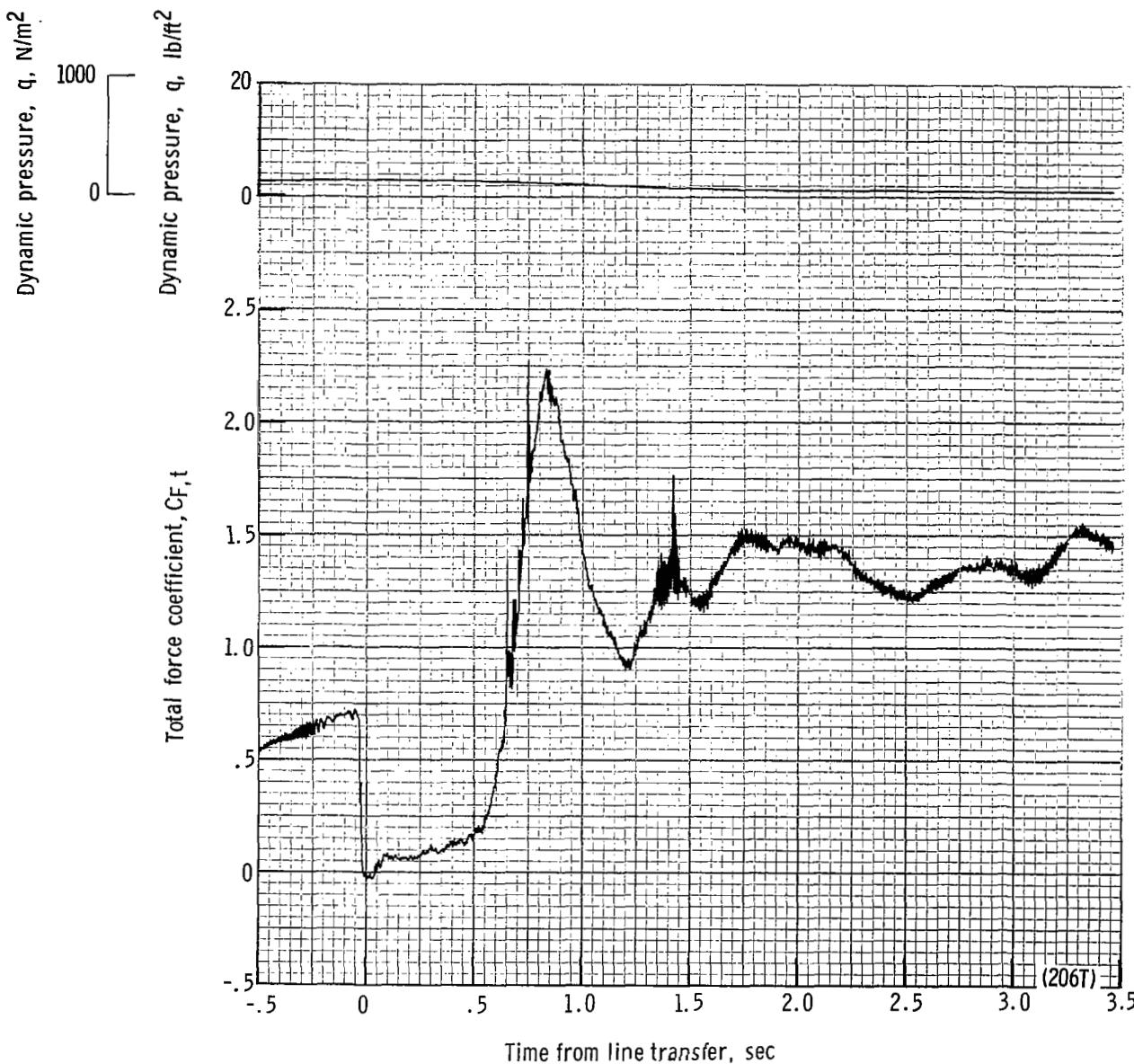
(w) Individual suspension-line loads F_{Lle3} and F_{Lle6} and right and left riser loads plotted against time from line transfer. Time = 0 second corresponds to 40.83 seconds after launch.

Figure 47.- Continued.



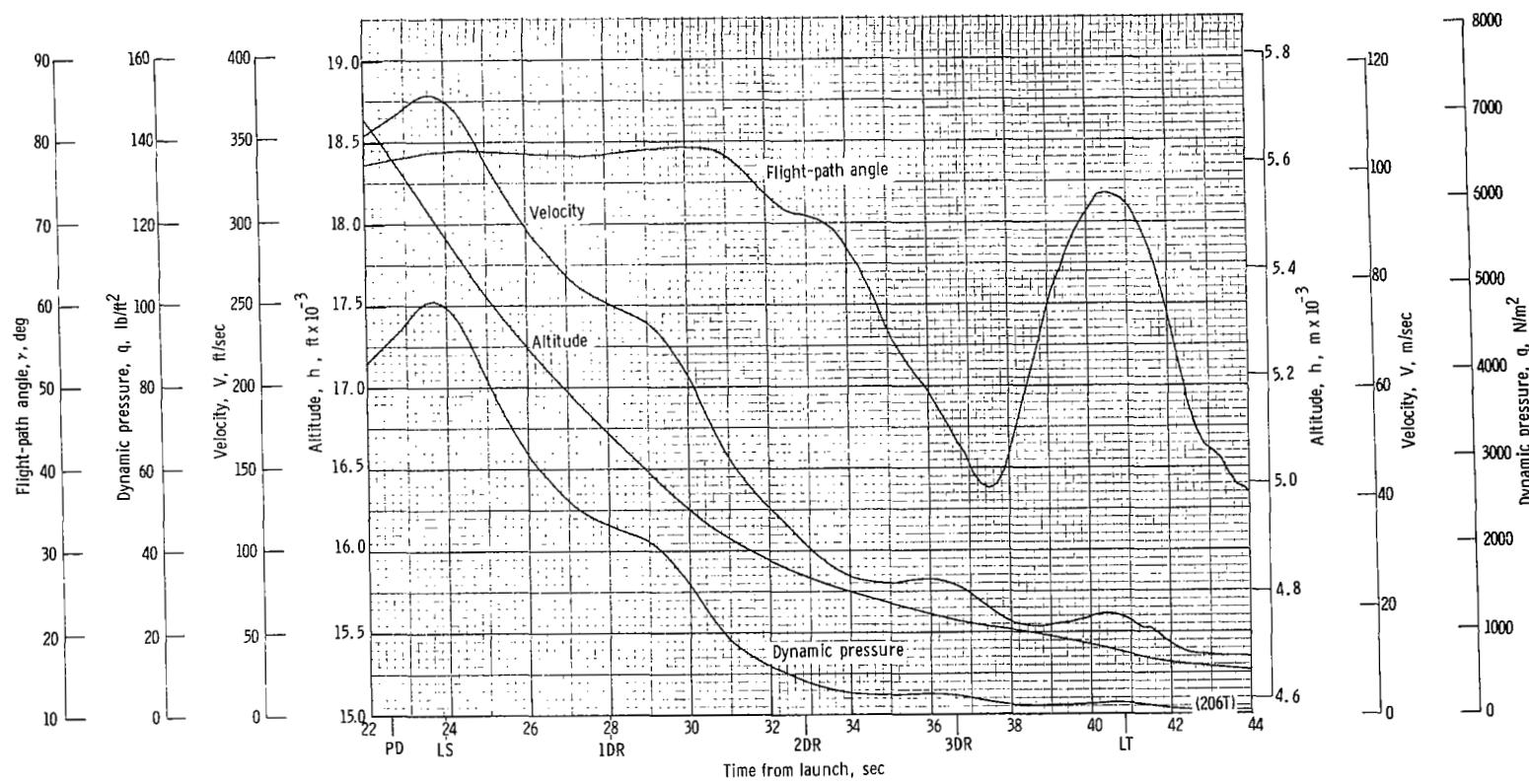
(x) Total force F_t plotted against time from line transfer. Time = 0 second corresponds to 40.83 seconds after launch.

Figure 47.- Continued.



(y) Total force coefficient $C_{F,t}$ and dynamic pressure q plotted against time from line transfer. Time = 0 second corresponds to 40.83 seconds after launch.

Figure 47.- Continued.



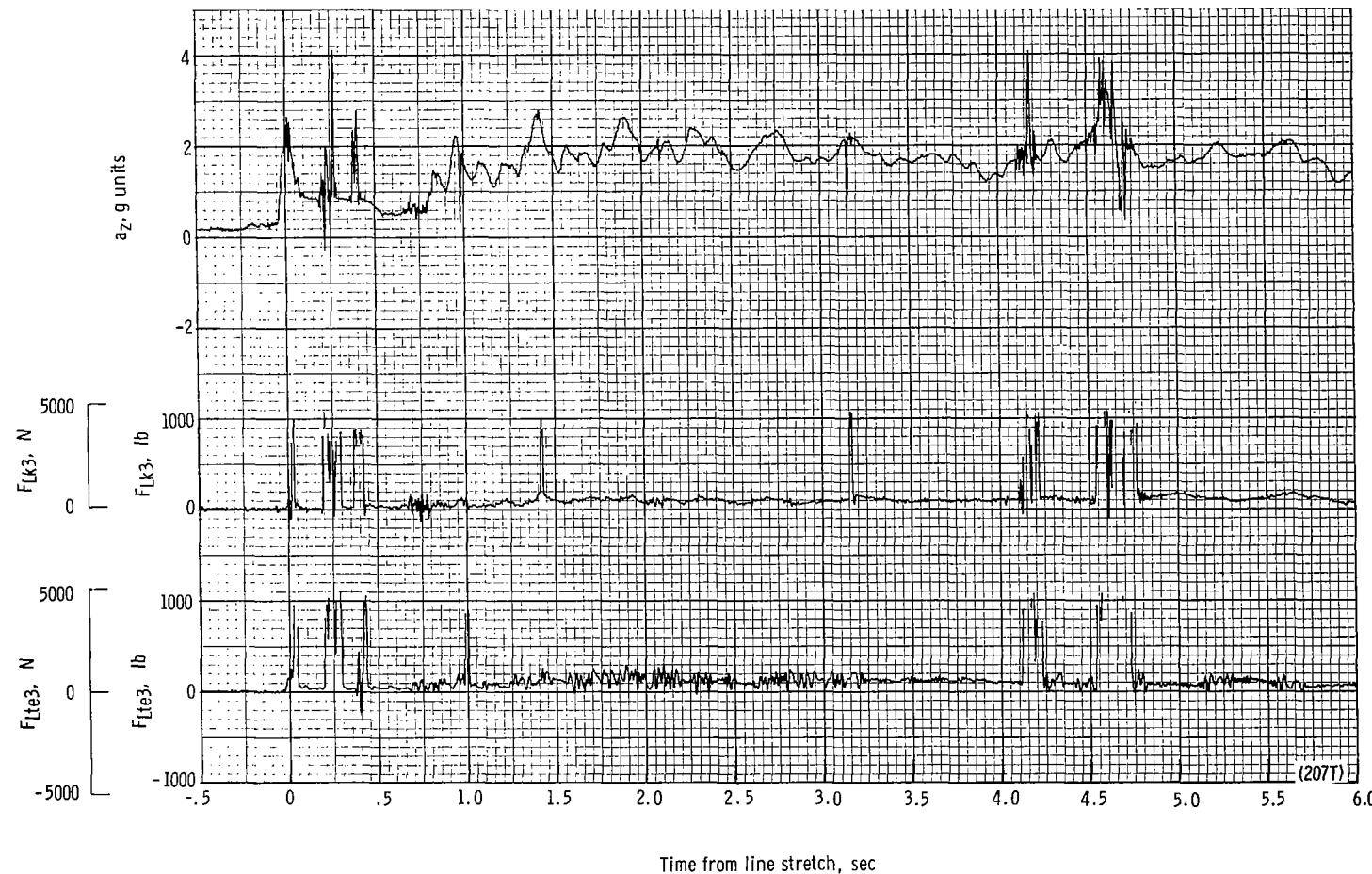
(z) Flight-path angle γ , dynamic pressure q , velocity V , and altitude h plotted against time from launch.

Figure 47.- Concluded.



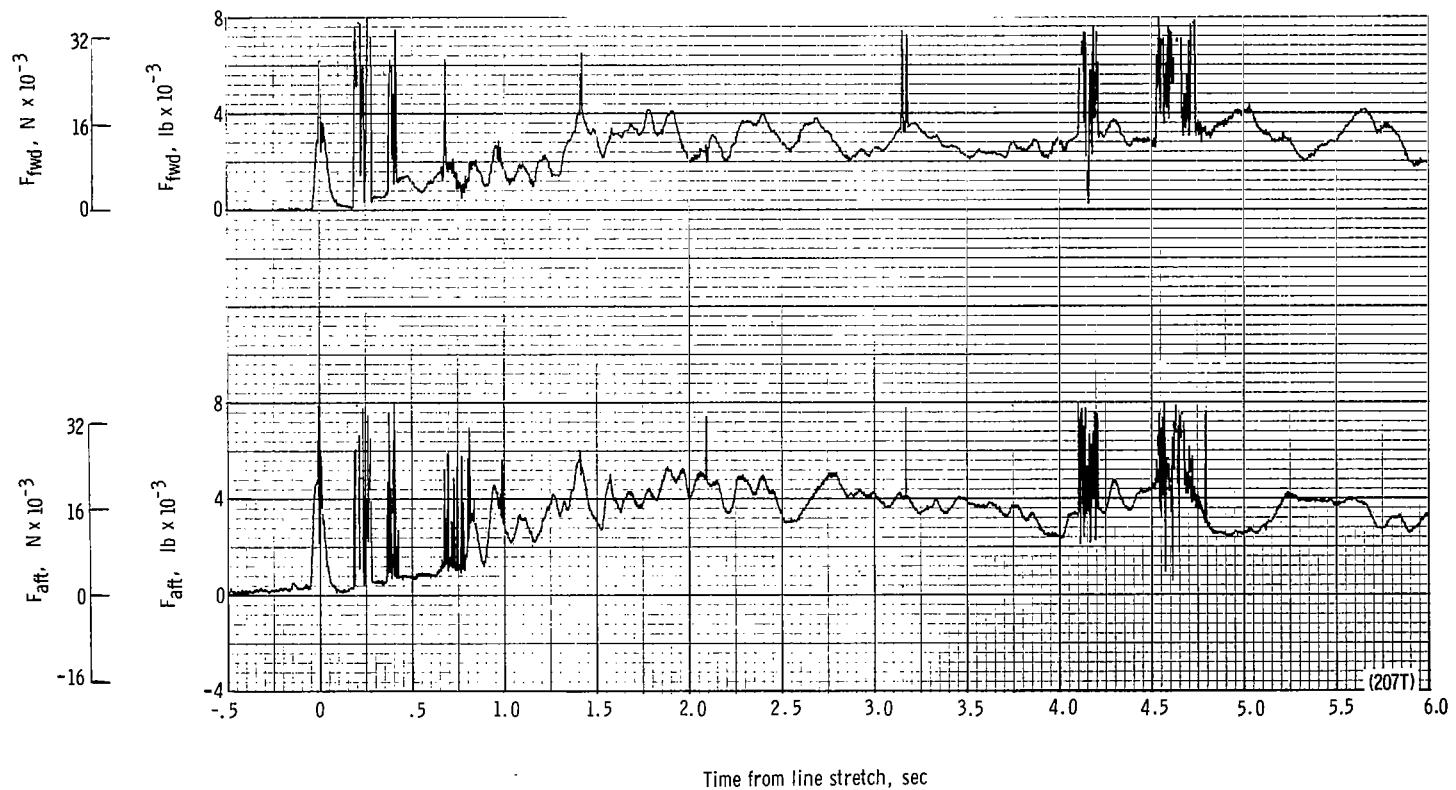
(a) Individual suspension-line loads F_{Llel} , F_{Lle6} , F_{Lk7} , and F_{Lk12} plotted against time from line stretch. Time = 0 second corresponds to 30.02 seconds after launch.

Figure 48.- Time history of twin-keel parawing deployment data for test 2077. $W_D = 22\ 214\ N$ (4994 lb); $W_p = 20\ 502\ N$ (4609 lb); $q_{PD} = 1489.1\ N/m^2$ (31.1 lb/ft²); $h_{PD} = 4625\ m$ (15 175 ft); $l_r/l_k = 0.100$; reefing version B.



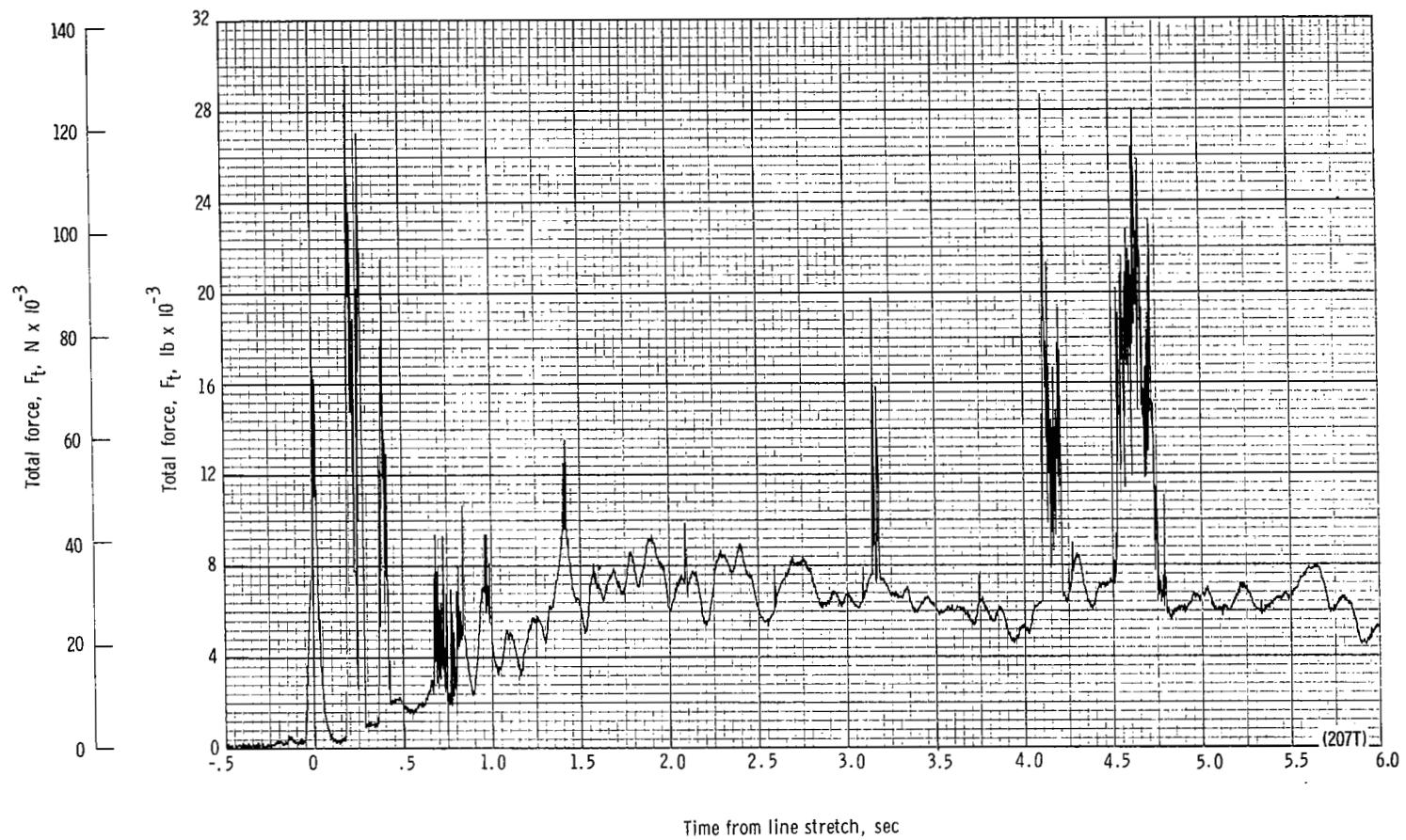
(b) Individual suspension-line loads F_{Lte3} and F_{Lk3} and acceleration a_z plotted against time from line stretch. Time = 0 second corresponds to 30.02 seconds after launch.

Figure 48.- Continued.



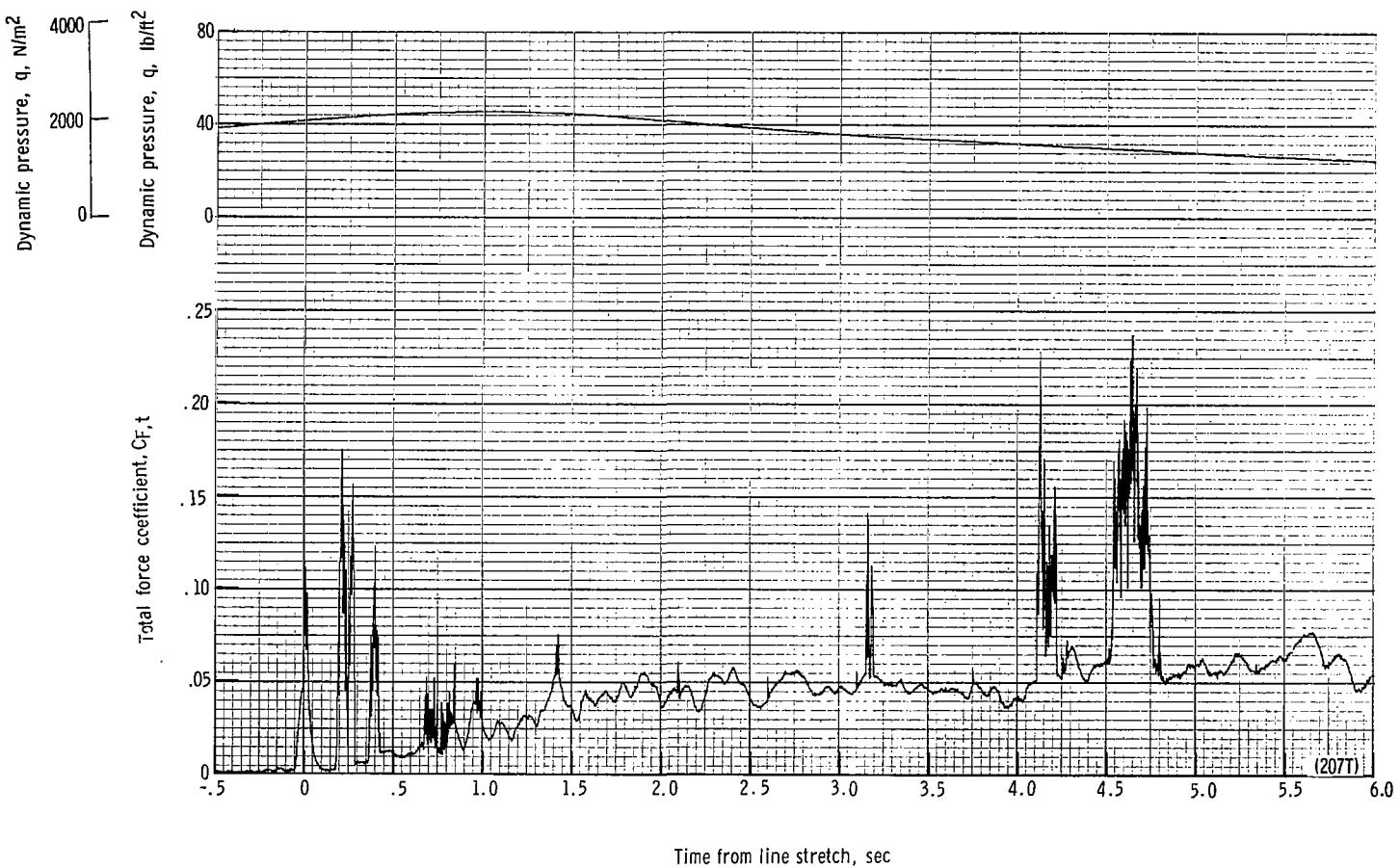
(c) Forward and aft riser loads plotted against time from line stretch. Time = 0 second corresponds to 30.02 seconds after launch.

Figure 48.- Continued.



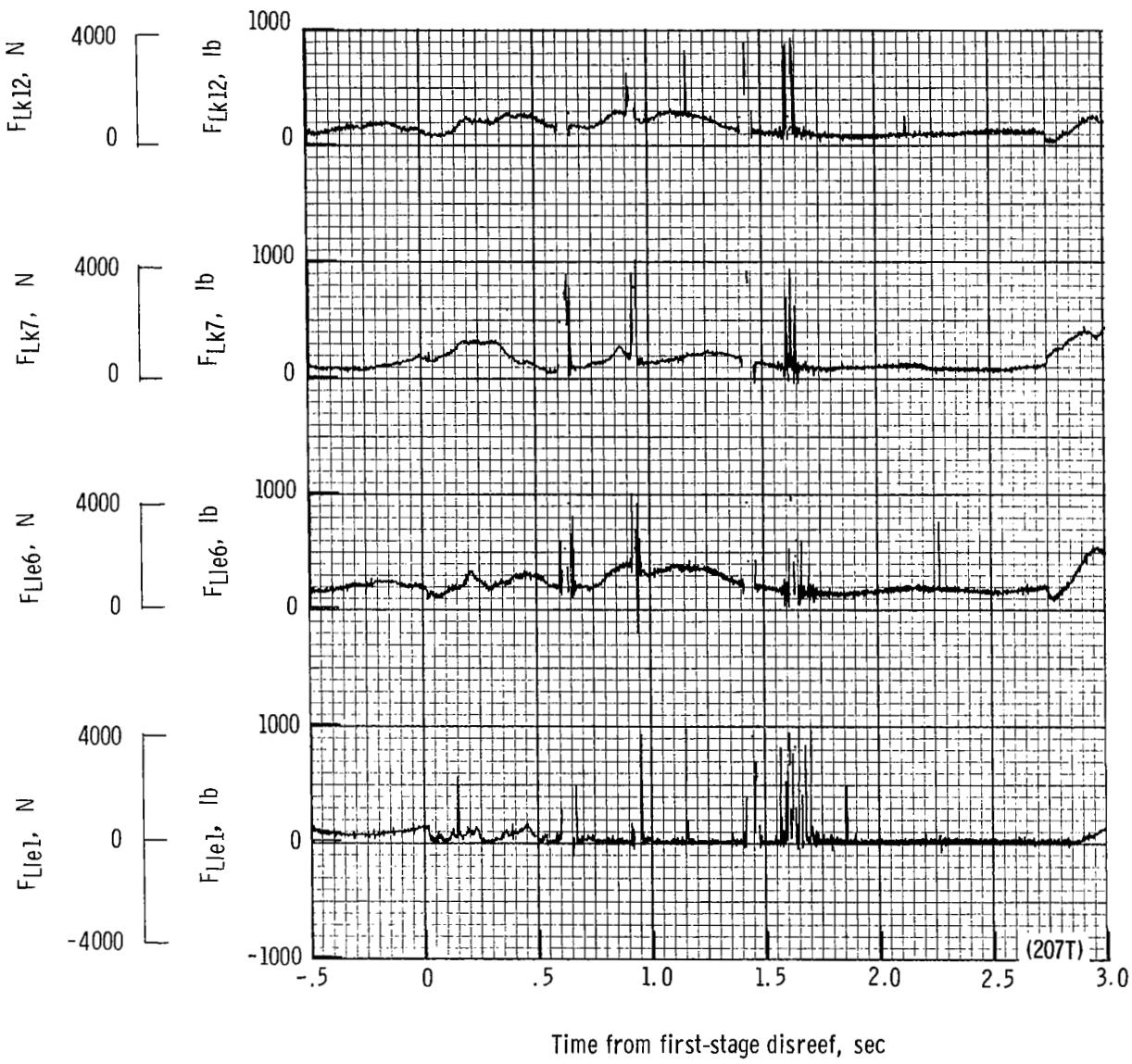
(d) Total force F_t plotted against time from line stretch. Time = 0 second corresponds to 30.02 seconds after launch.

Figure 48.- Continued.



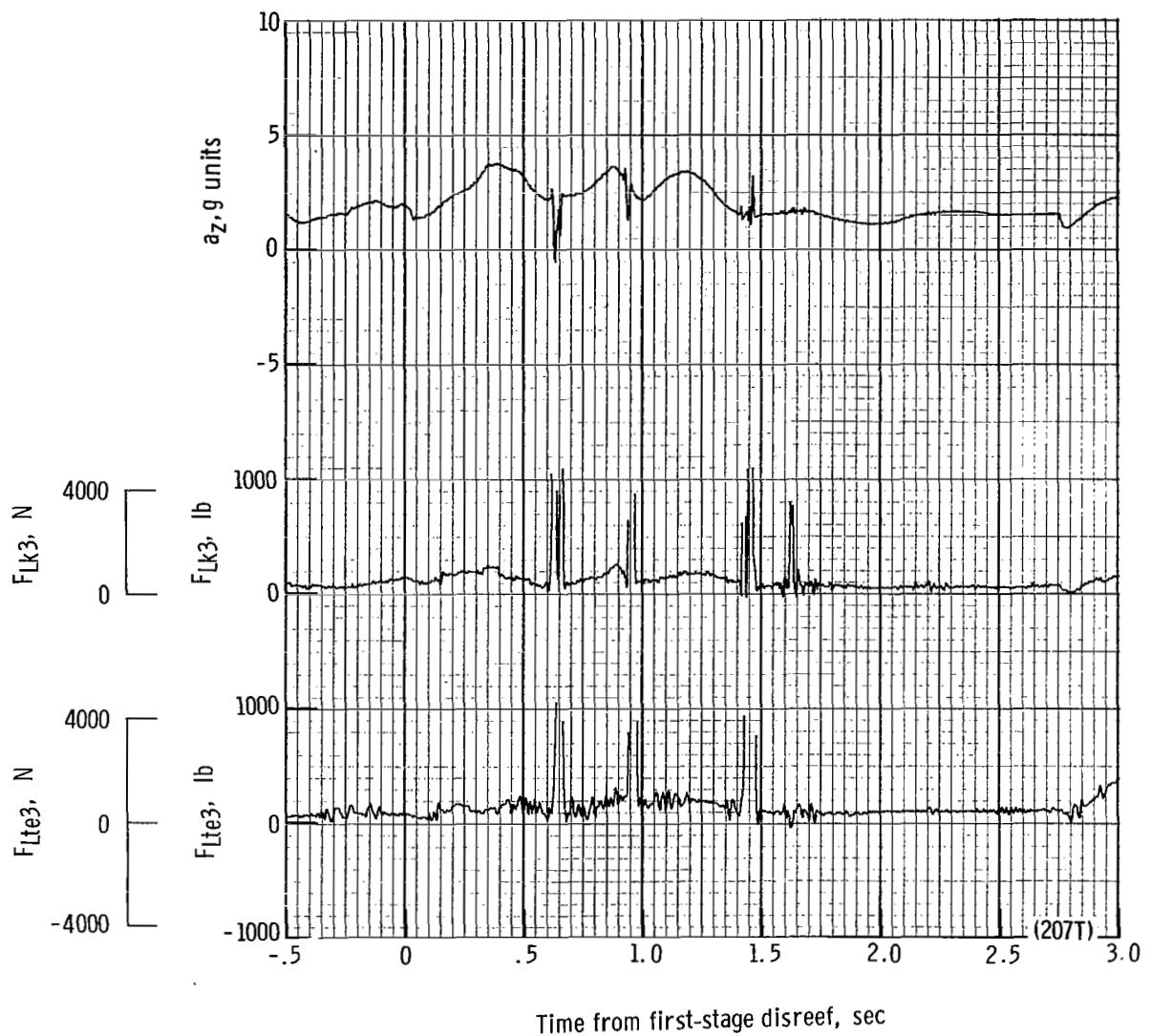
(e) Total force coefficient $C_{F,t}$ and dynamic pressure q plotted against time from line stretch. Time = 0 second corresponds to 30.02 seconds after launch.

Figure 48.- Continued.



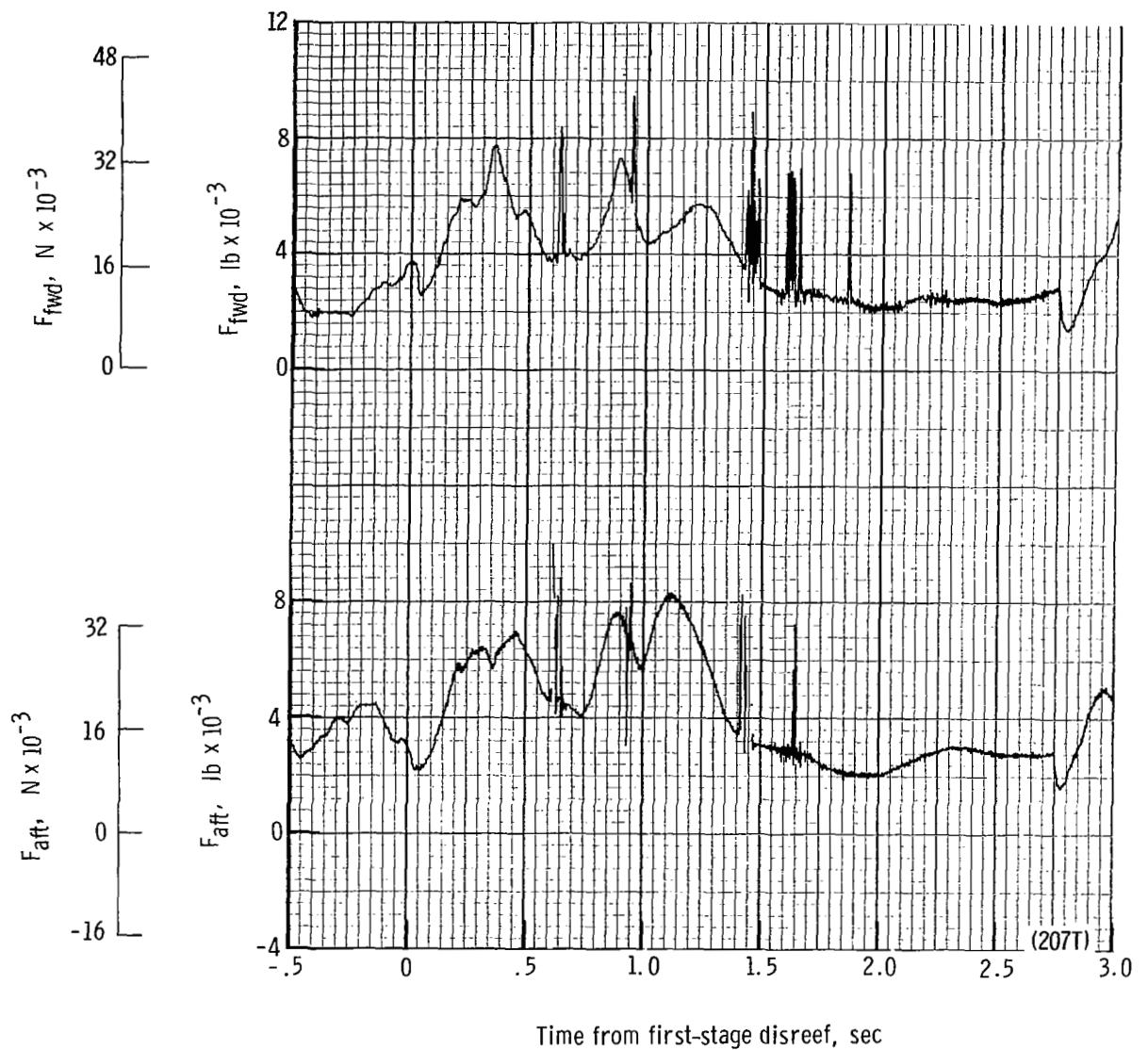
(f) Individual suspension-line loads F_{Lle1} , F_{Lle6} , F_{Lk7} , and F_{Lk12} plotted against time from first-stage disreef. Time = 0 second corresponds to 37.37 seconds after launch.

Figure 48.- Continued.



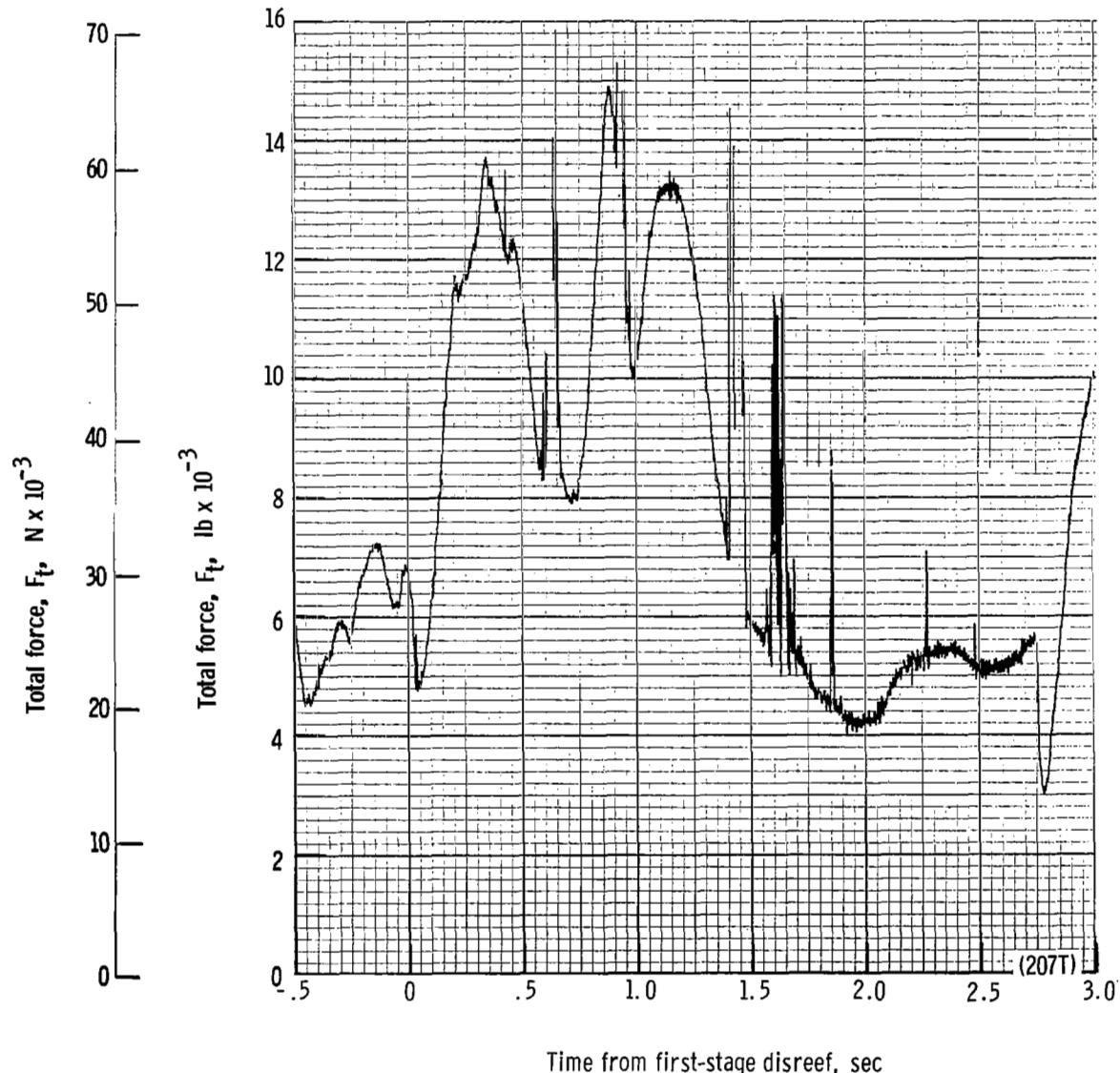
(g) Individual suspension-line loads F_{Lte3} and F_{LK3} and acceleration a_Z plotted against time from first-stage disreef. Time = 0 second corresponds to 37.37 seconds after launch.

Figure 48.- Continued.



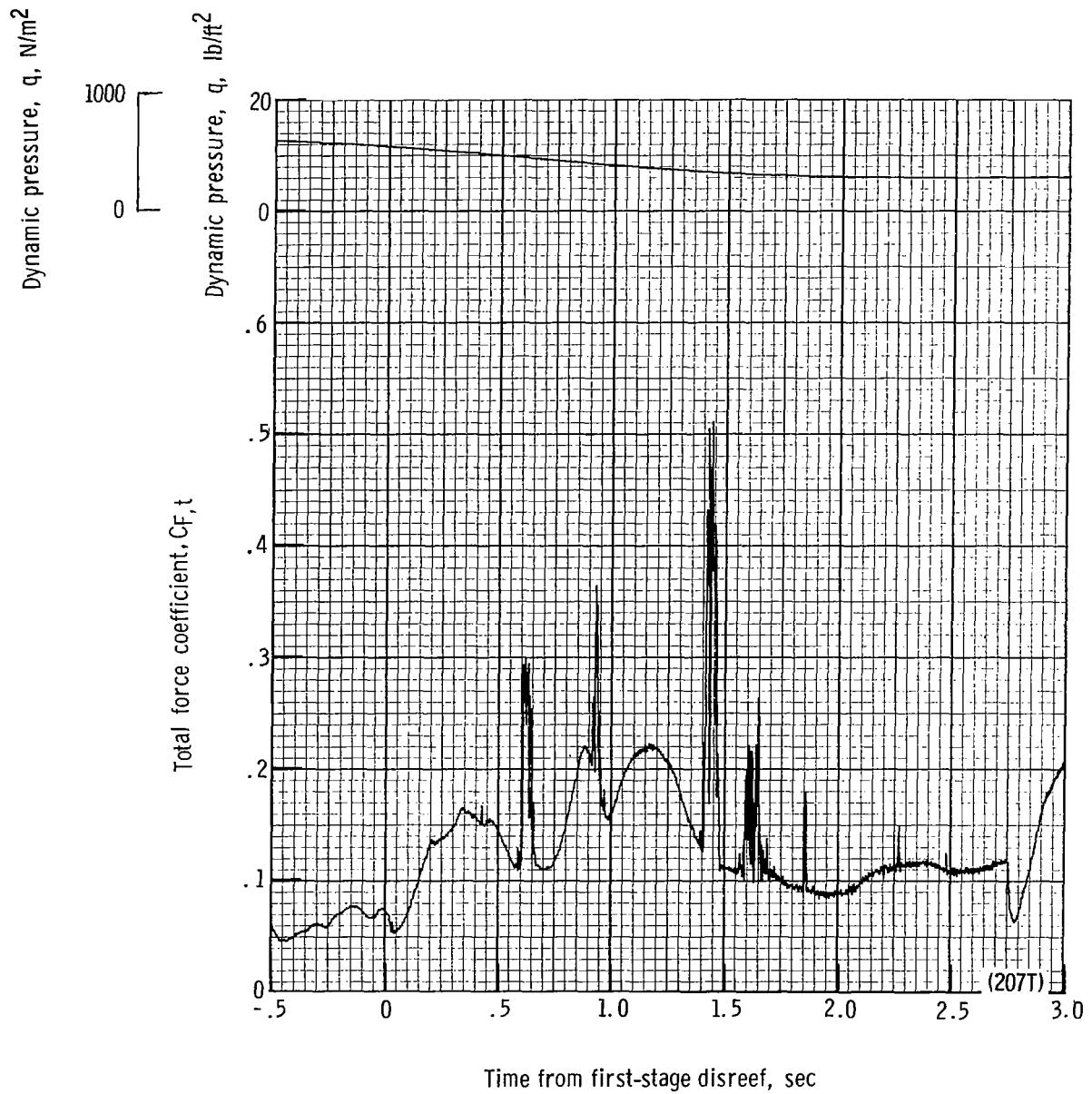
(h) Aft and forward riser loads plotted against time from first-stage disreef. Time = 0 second corresponds to 37.37 seconds after launch.

Figure 48.- Continued.



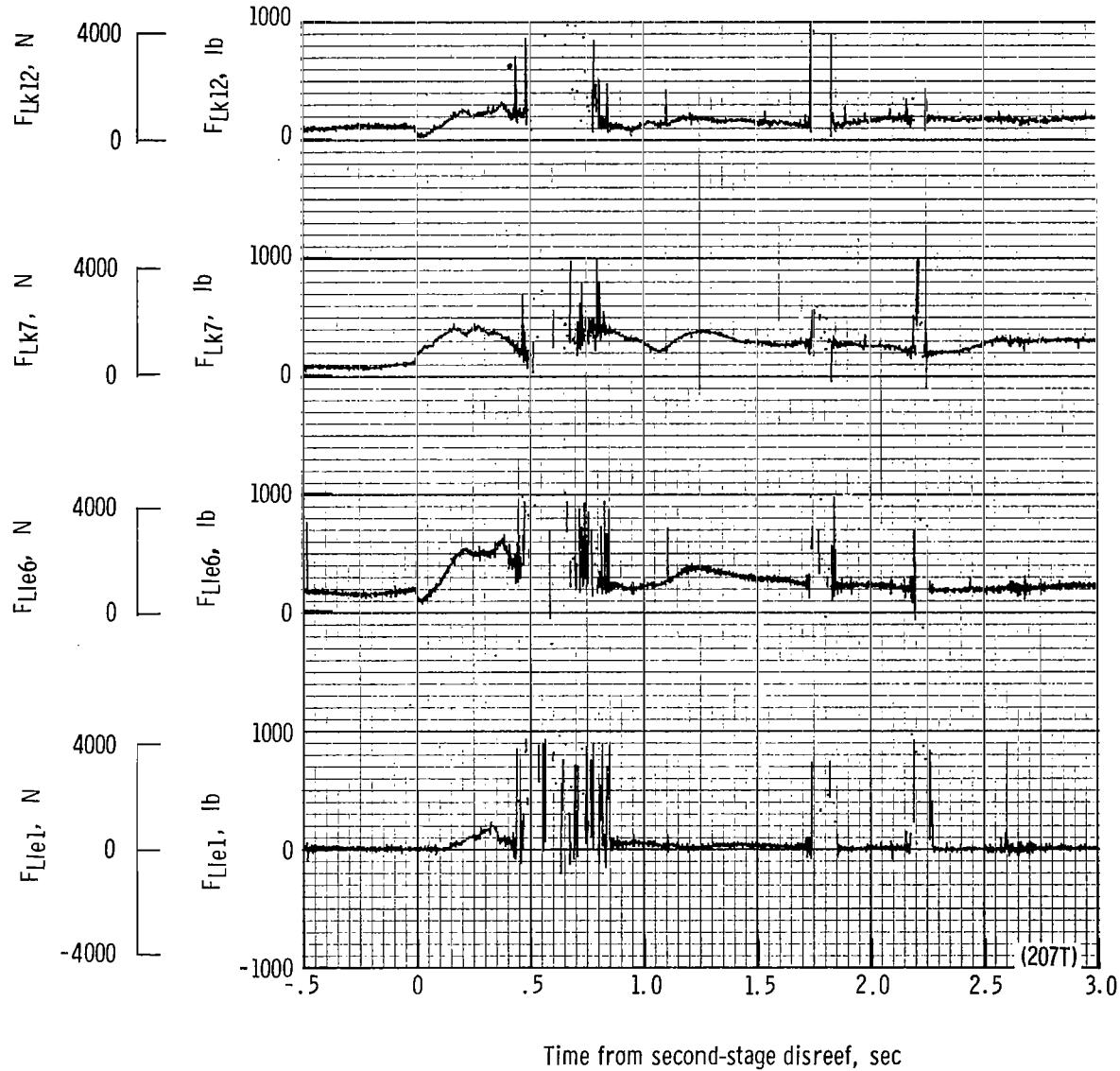
(i) Total force F_t plotted against time from first-stage disreef. Time = 0 second corresponds to 37.37 seconds after launch.

Figure 48.- Continued.



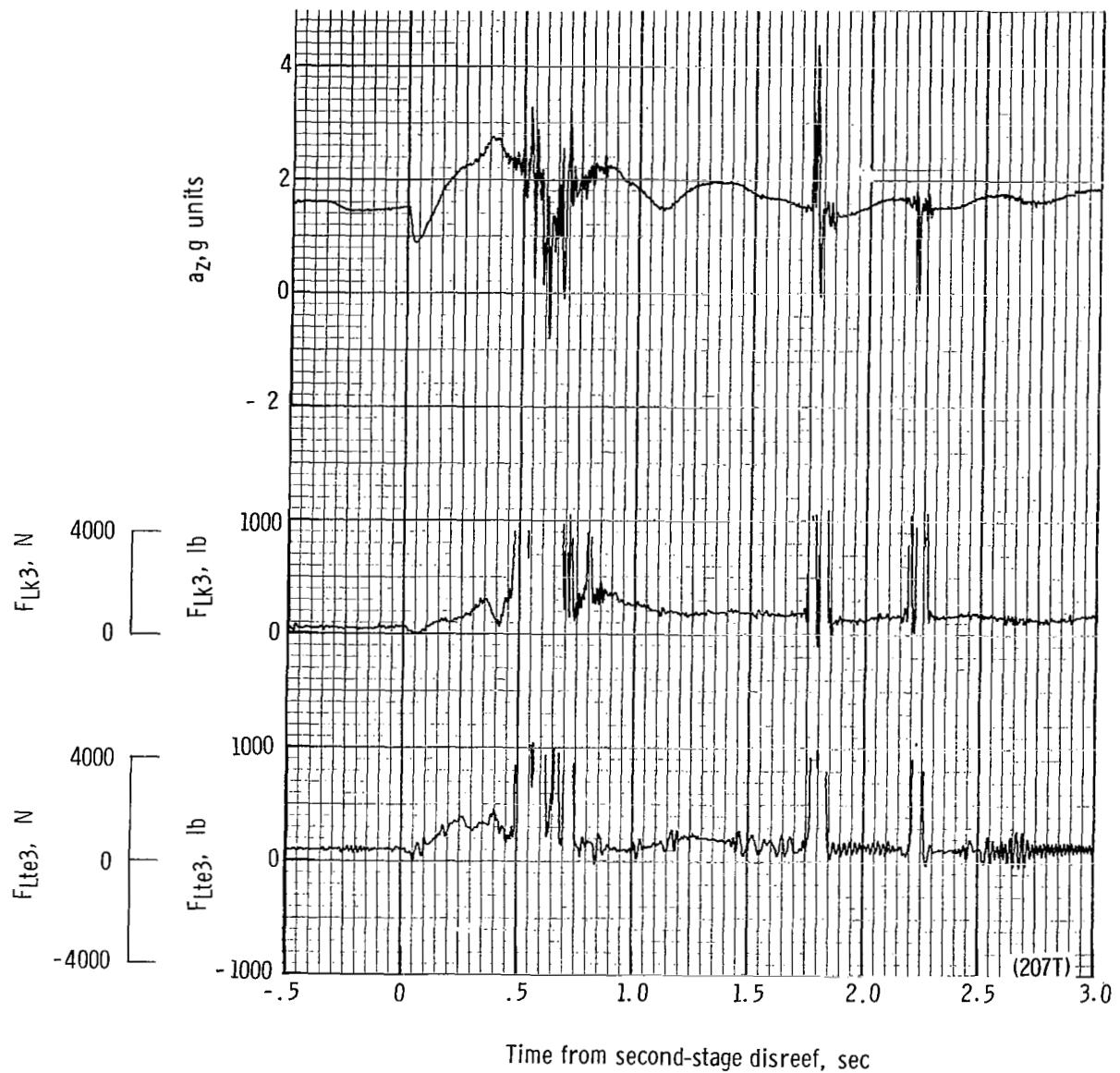
(j) Total force coefficient $C_{F,t}$ and dynamic pressure q plotted against time from first-stage disreef.
Time = 0 second corresponds to 37.37 seconds after launch.

Figure 48.- Continued.



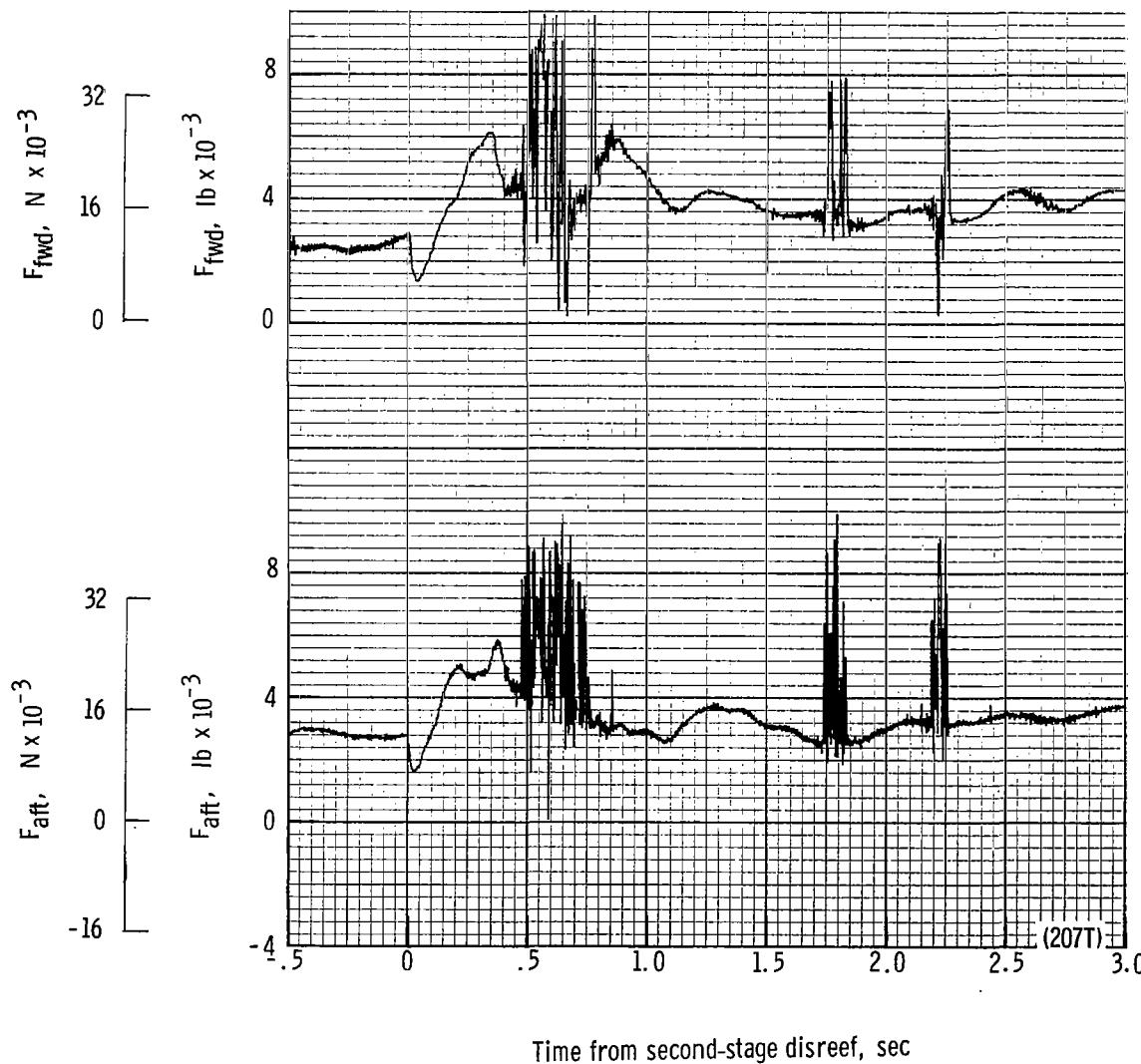
(k) Individual suspension-line loads F_{Lle1} , F_{Lle6} , F_{Lk7} , and F_{Lk12} plotted against time from second-stage disreef. Time = 0 second corresponds to 40.12 seconds after launch.

Figure 48.- Continued.



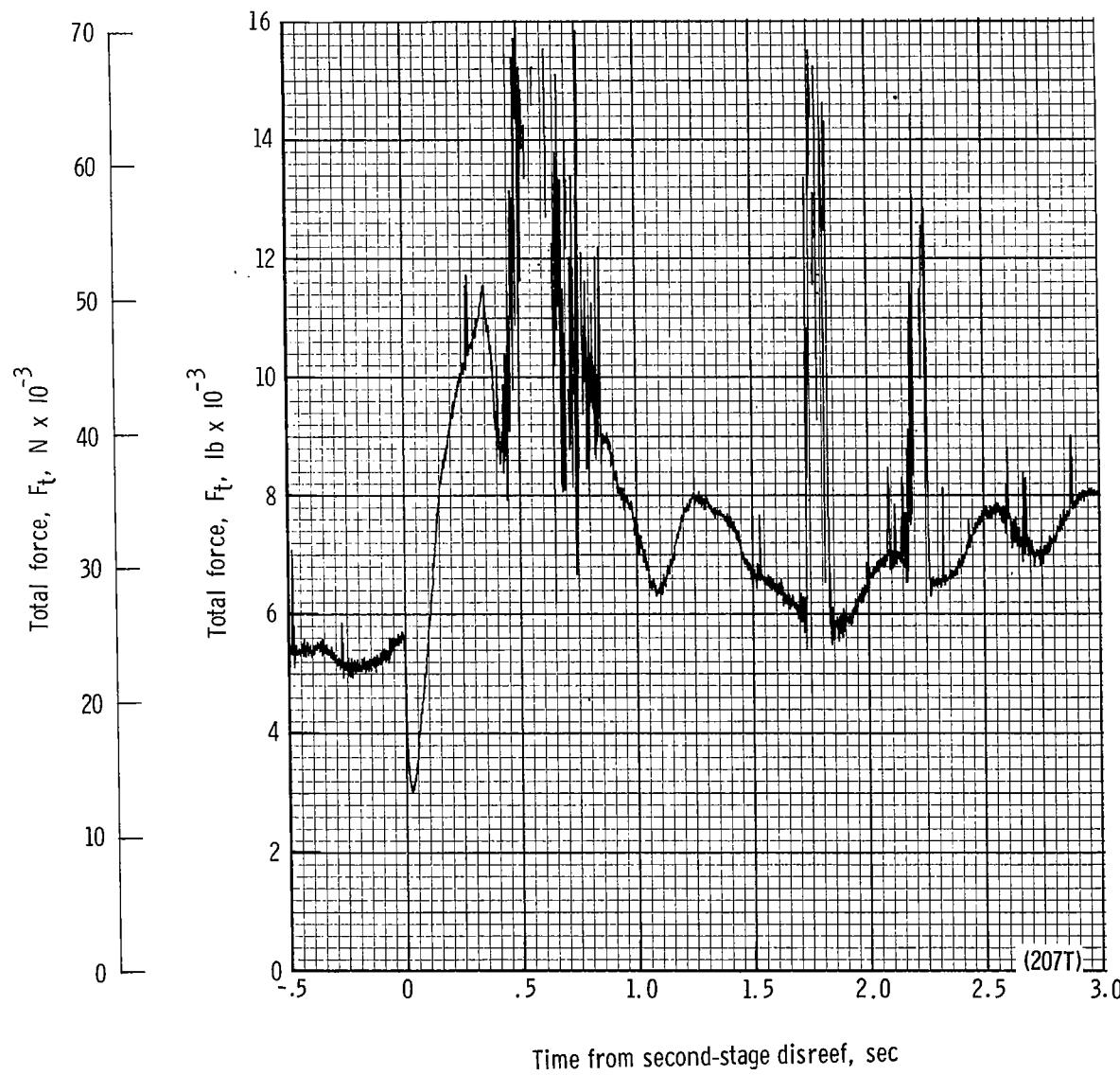
(II) Individual suspension-line loads F_{Lte3} and F_{Lk3} and acceleration a_z plotted against time from second-stage disreef. Time = 0 second corresponds to 40.12 seconds after launch.

Figure 48.- Continued.



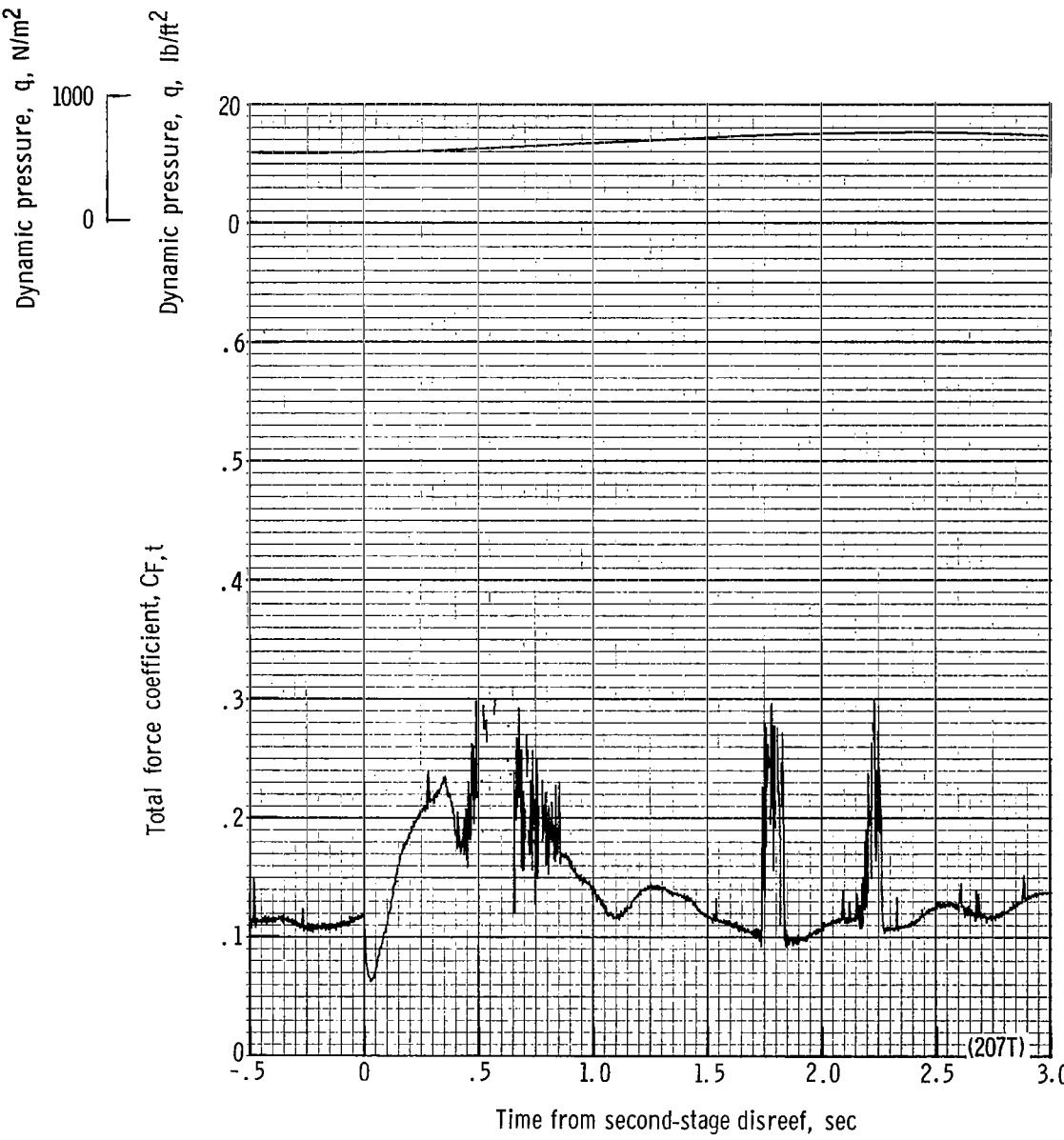
(m) Aft and forward riser loads plotted against time from second-stage disreef. Time = 0 second corresponds to 40.12 seconds after launch.

Figure 48.- Continued.



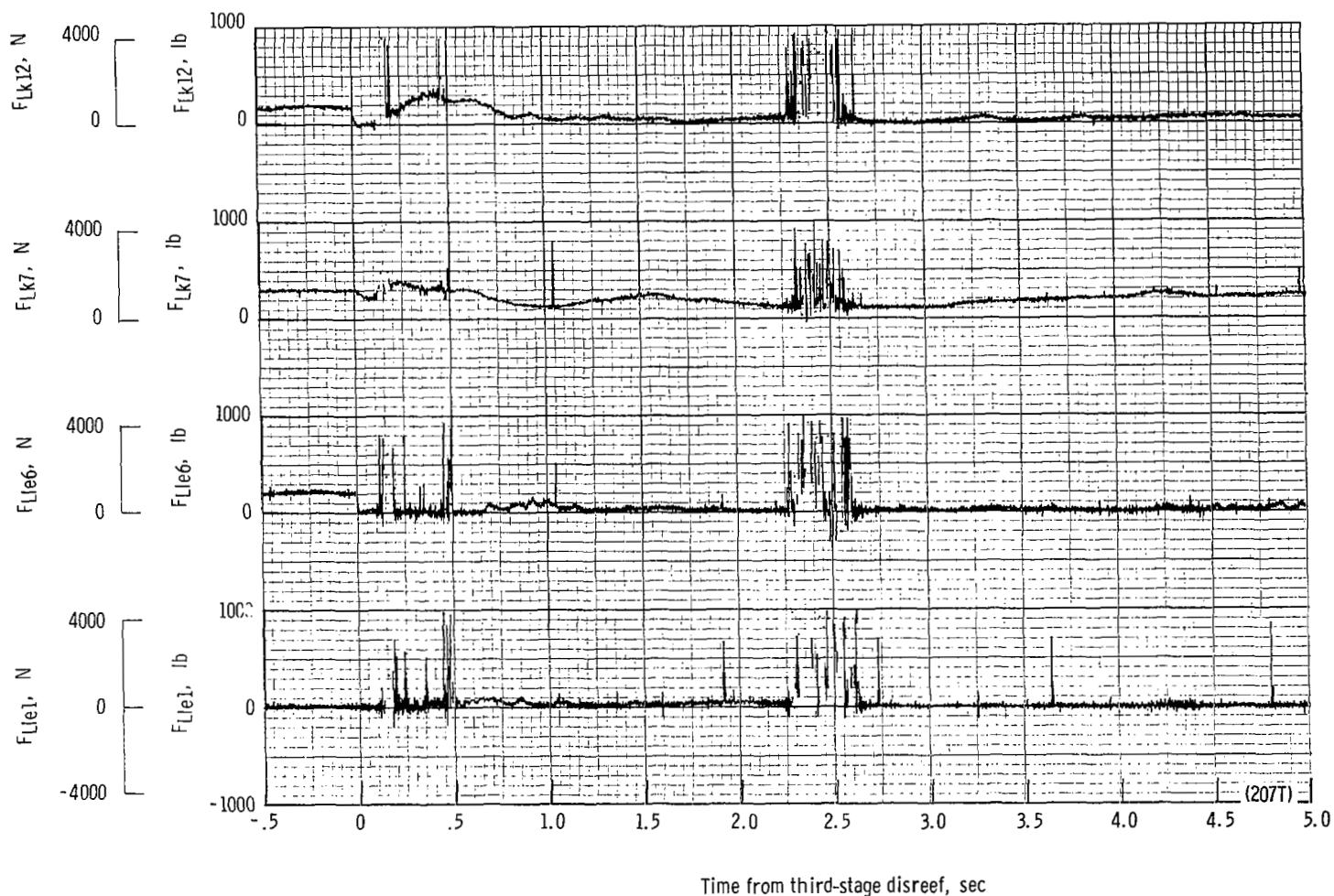
(n) Total force F_t plotted against time from second-stage disreef. Time = 0 second corresponds to 40.12 seconds after launch.

Figure 48.- Continued.



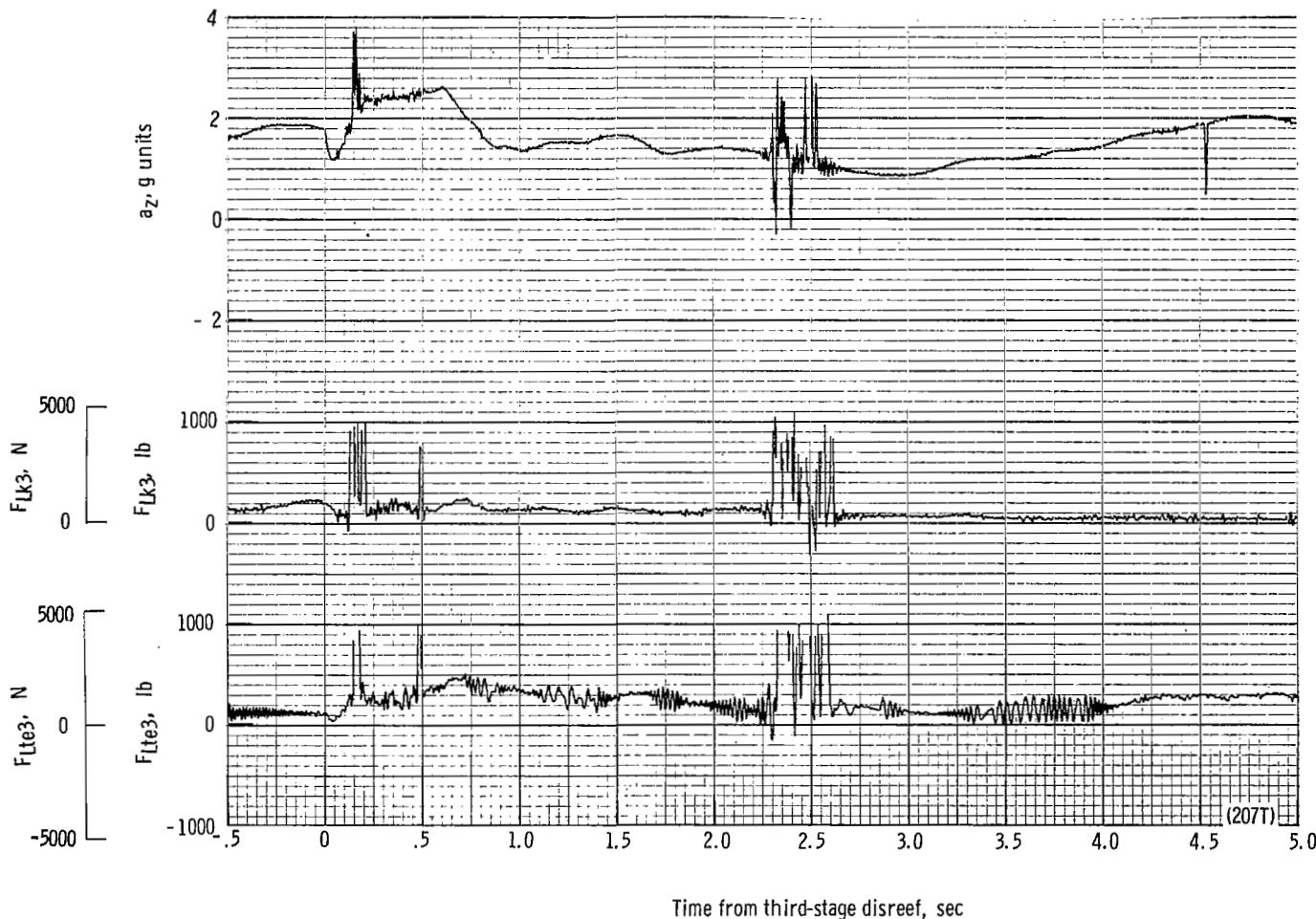
(c) Total force coefficient $C_{F,t}$ and dynamic pressure q plotted against time from second-stage disreef. Time = 0 second corresponds to 4012 seconds after launch.

Figure 48.- Continued.



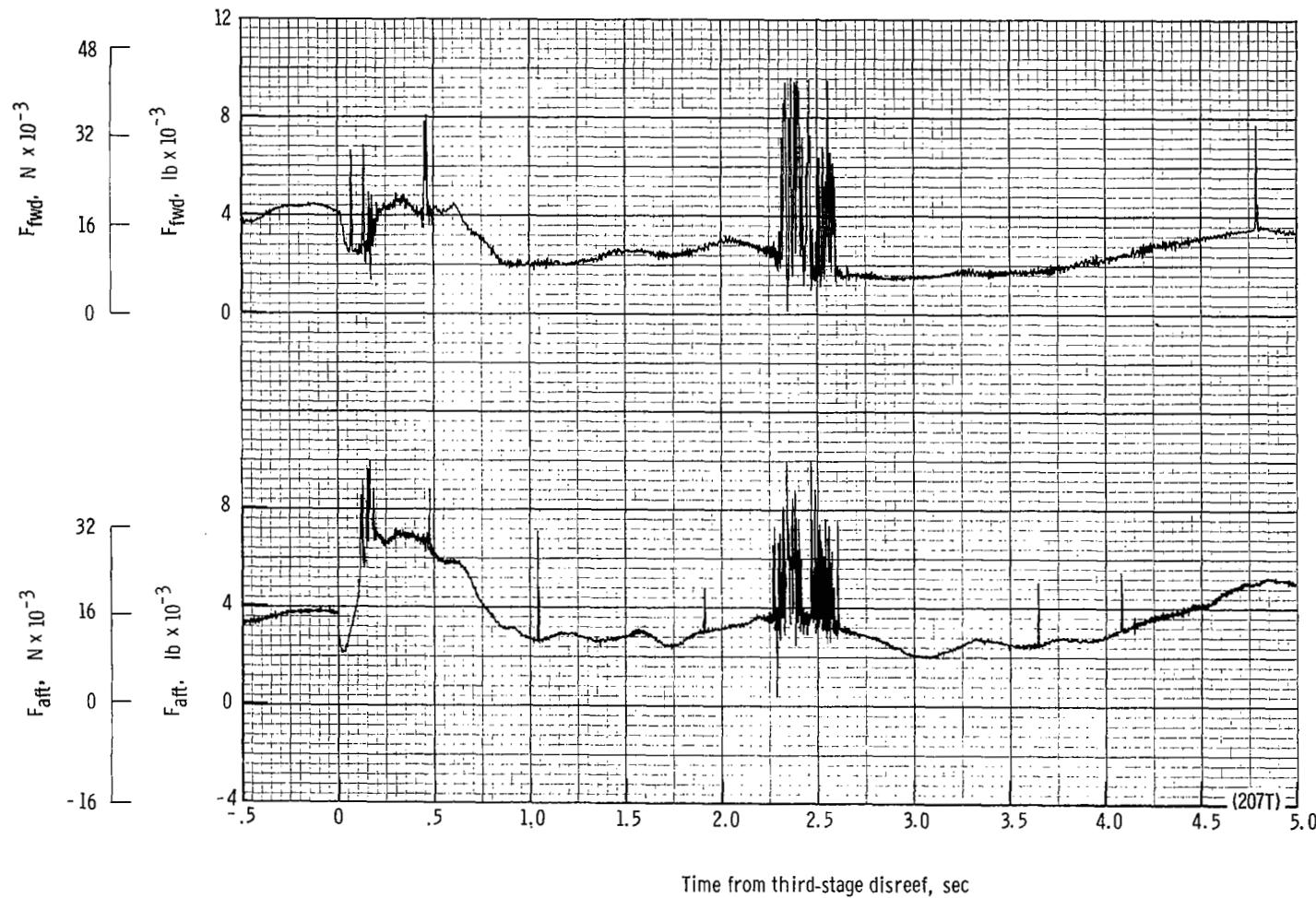
(p) Individual suspension-line loads F_{Lle1} , F_{Lle6} , F_{Lk7} , and F_{Lk12} plotted against time from third-stage disreef. Time = 0 second corresponds to 43.32 seconds after launch.

Figure 48.- Continued.



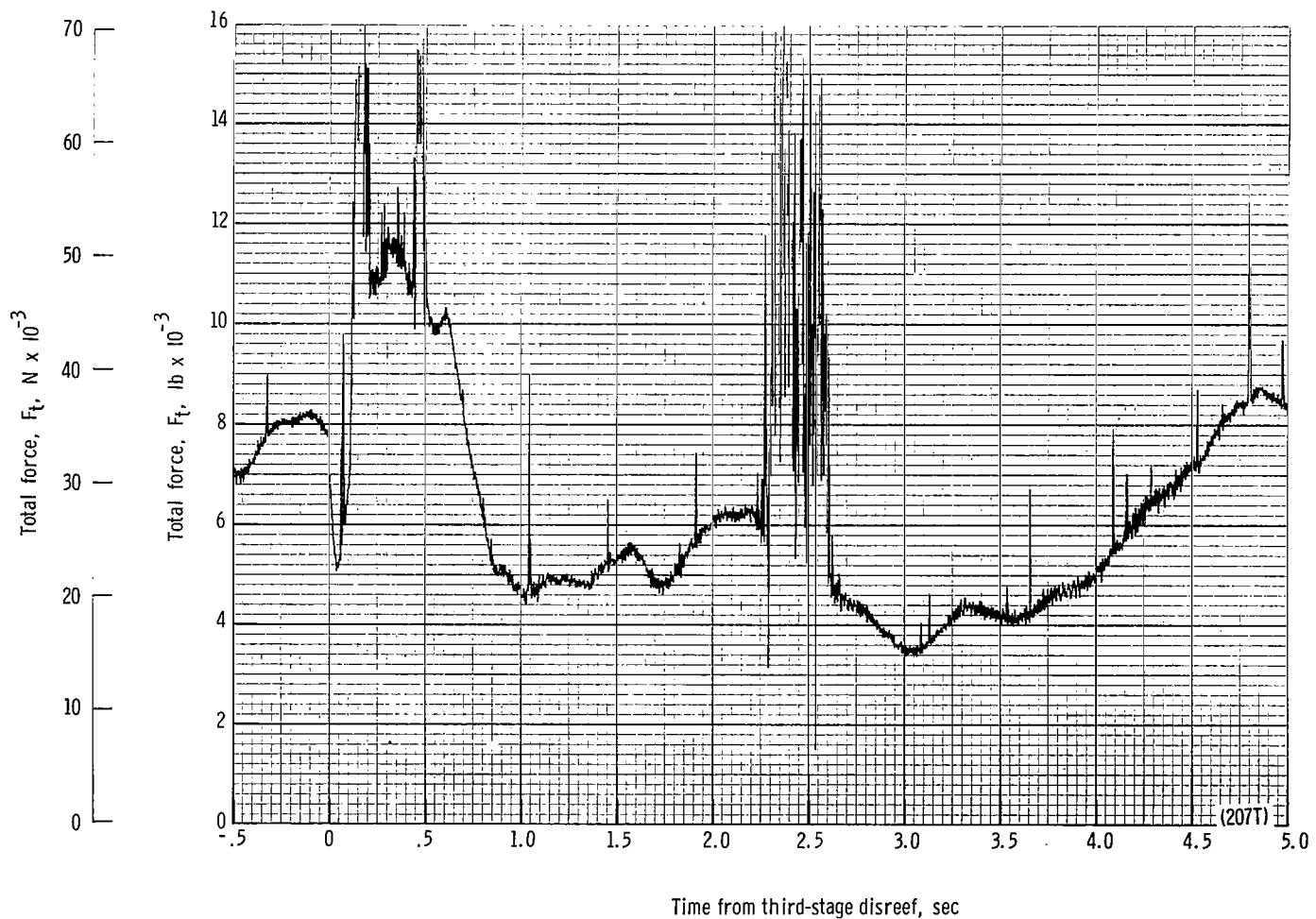
(q) Individual suspension-line loads F_{Lte3} and F_{Lk3} and acceleration a_z plotted against time from third-stage disreef. Time = 0 second corresponds to 43.32 seconds after launch.

Figure 48.- Continued.



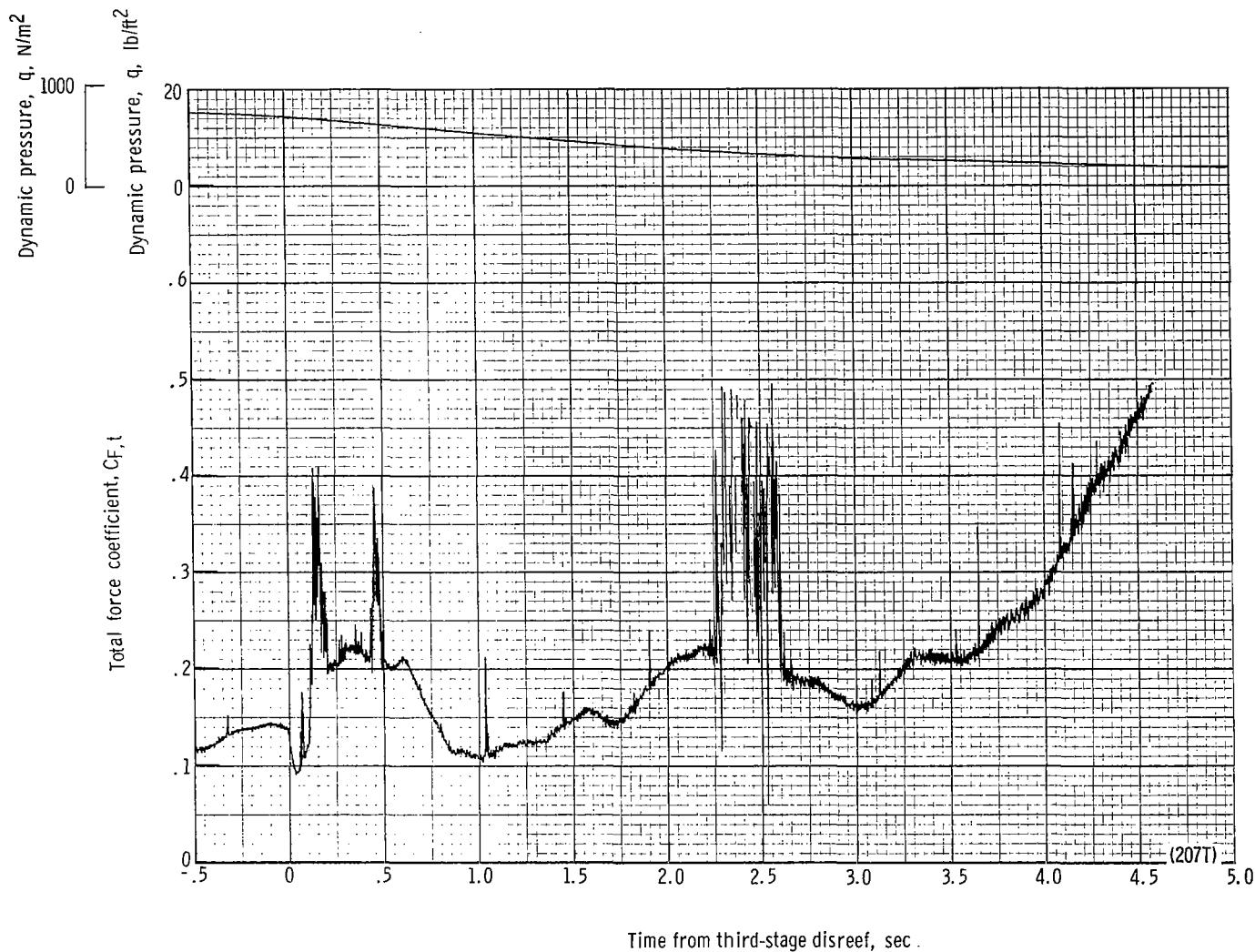
(r) Forward and aft riser loads plotted against time from third-stage disreef. Time = 0 second corresponds to 43.32 seconds after launch.

Figure 48.- Continued.



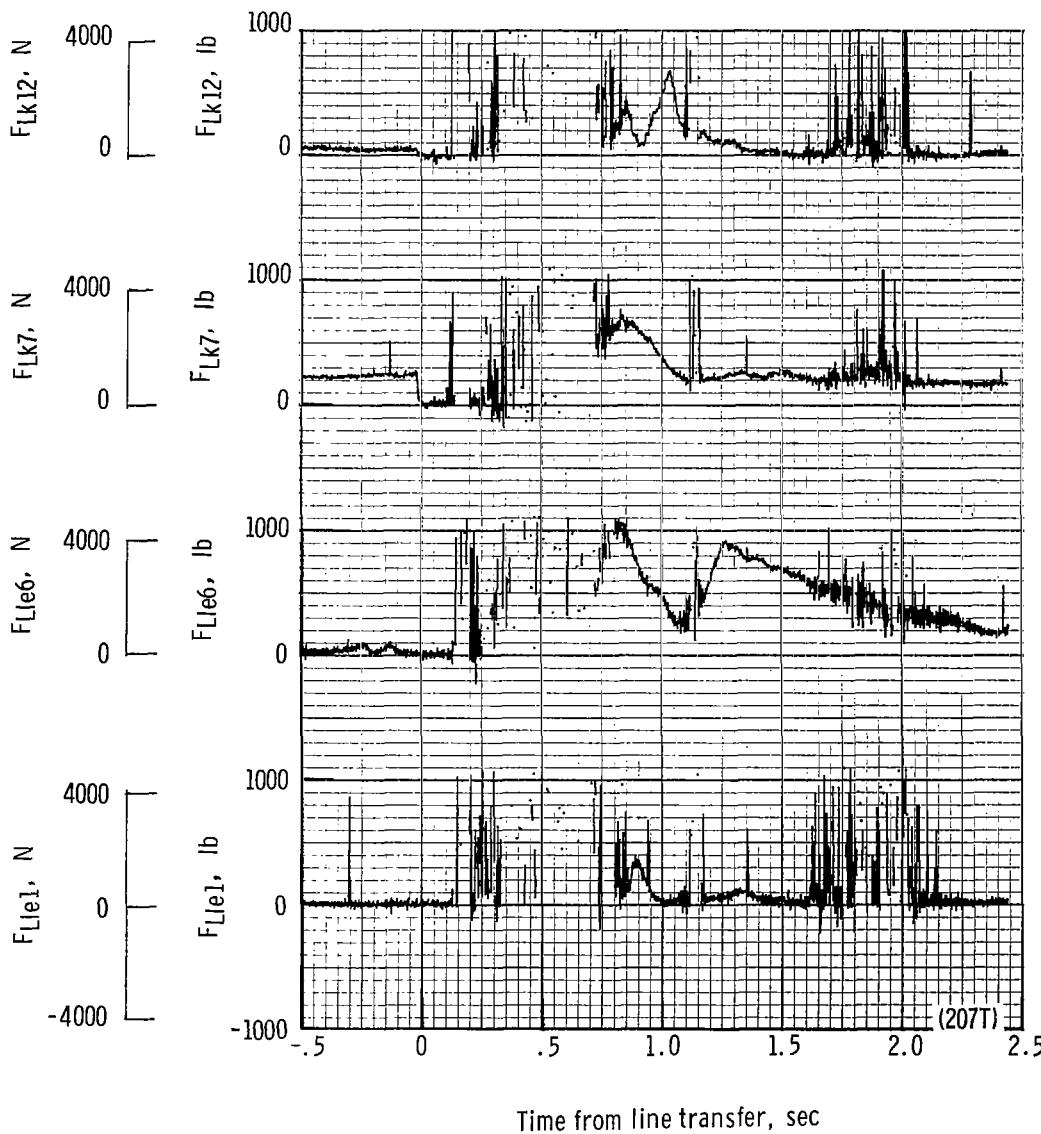
(s) Total force F_t plotted against time from third-stage disreef. Time = 0 second corresponds to 43.32 seconds after launch.

Figure 48.- Continued.



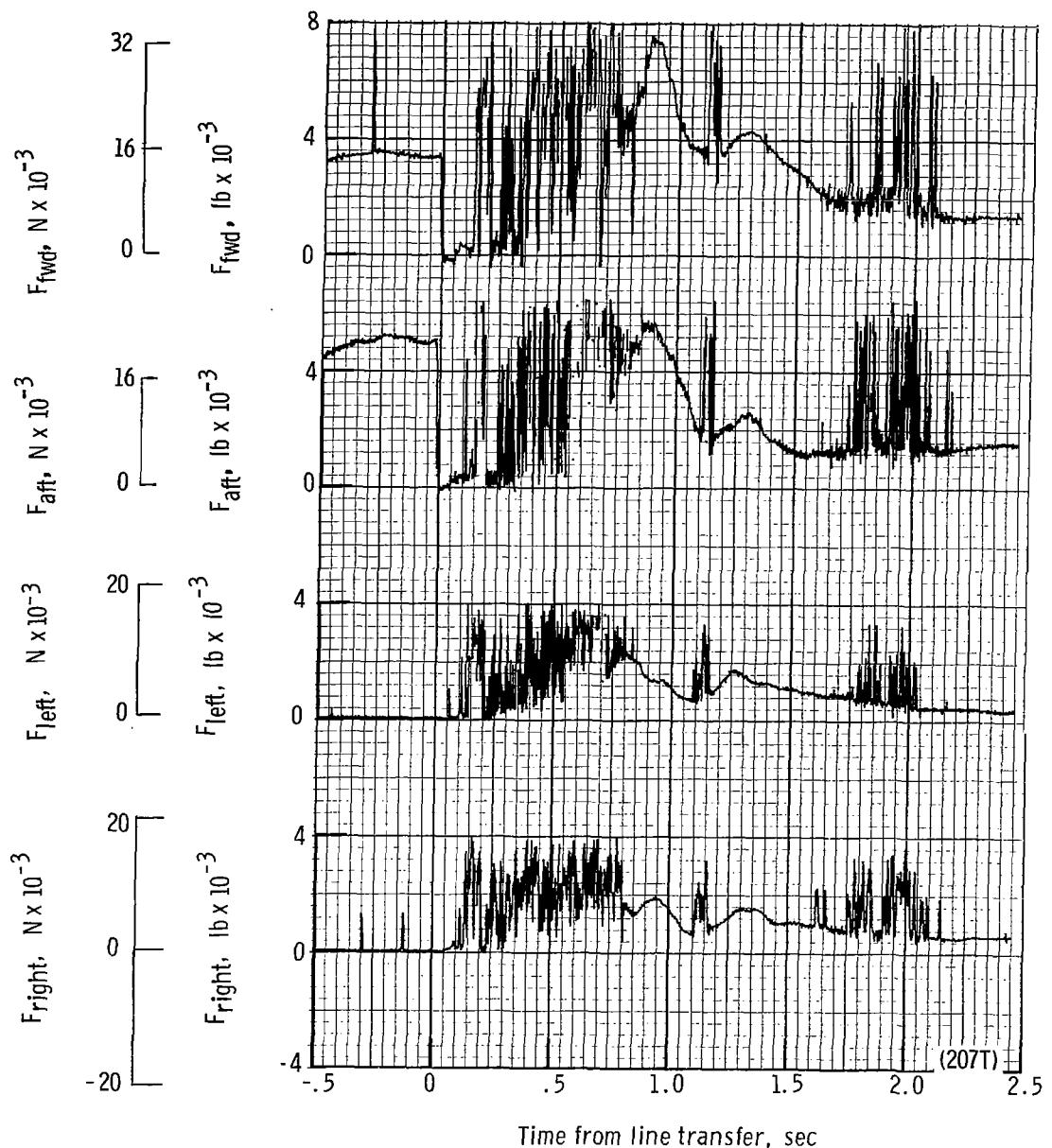
(t) Total force coefficient $C_{F,t}$ and dynamic pressure q plotted against time from third-stage disreef. Time = 0 second corresponds to 43.32 seconds after launch.

Figure 48.- Continued.



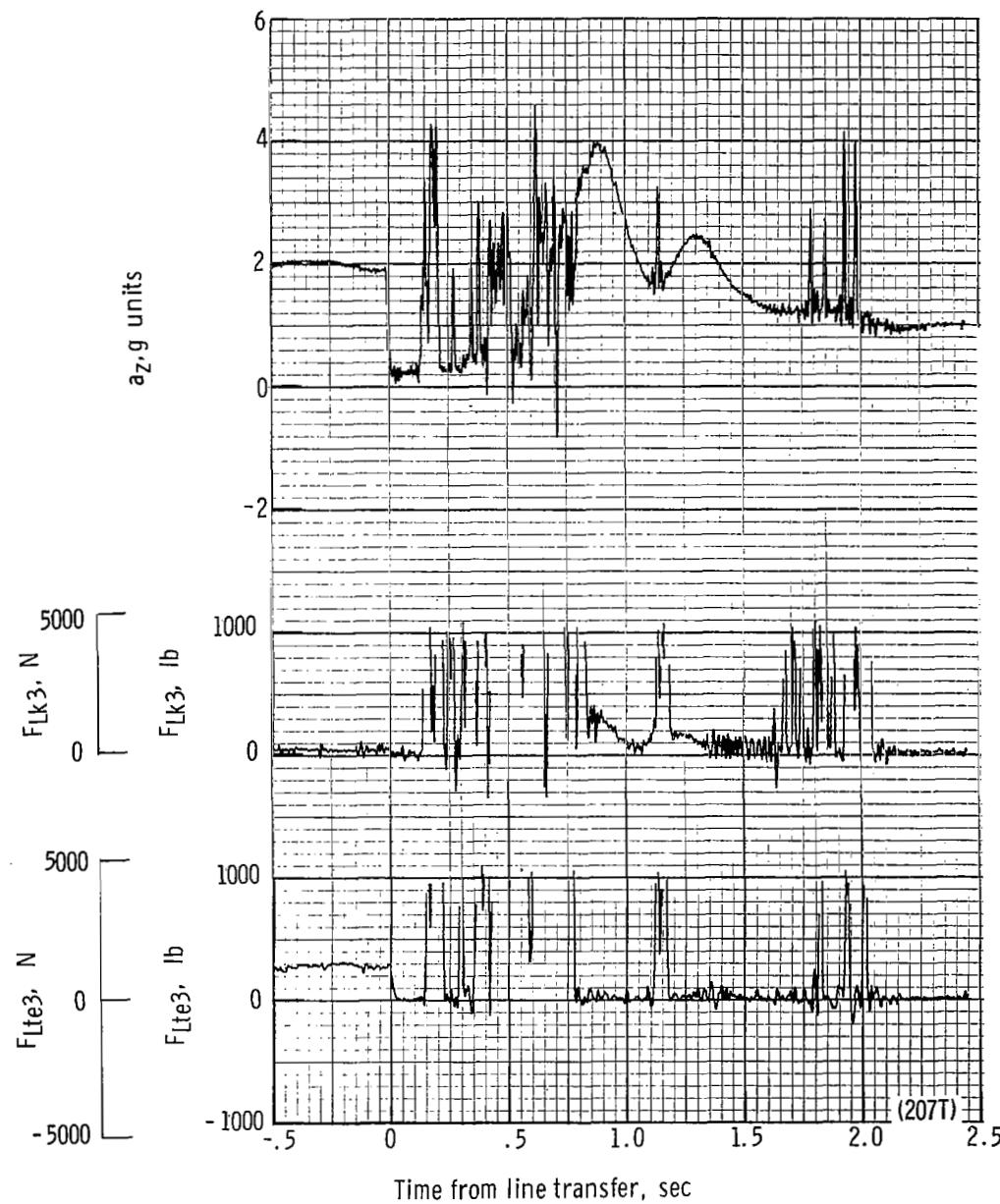
(u) Individual suspension-line loads F_{Ltel} , F_{Lle6} , F_{Lk7} , and F_{Lk12} plotted against time from line transfer. Time = 0 second corresponds to 48.42 seconds after launch.

Figure 48.- Continued.

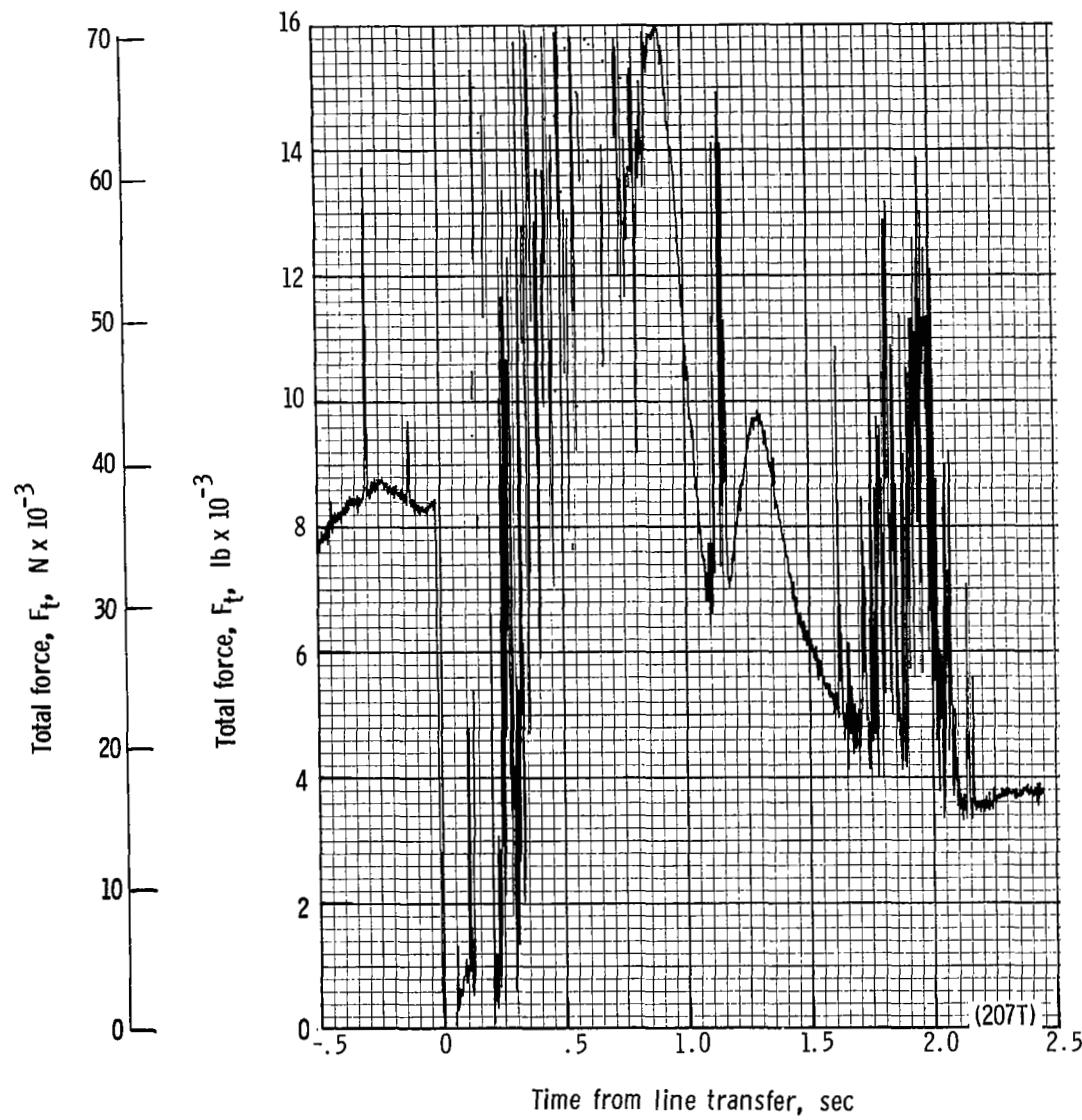


(v) Right, left, aft, and forward riser loads plotted against time from line transfer. Time = 0 second corresponds to 48.42 seconds after launch.

Figure 48.- Continued.

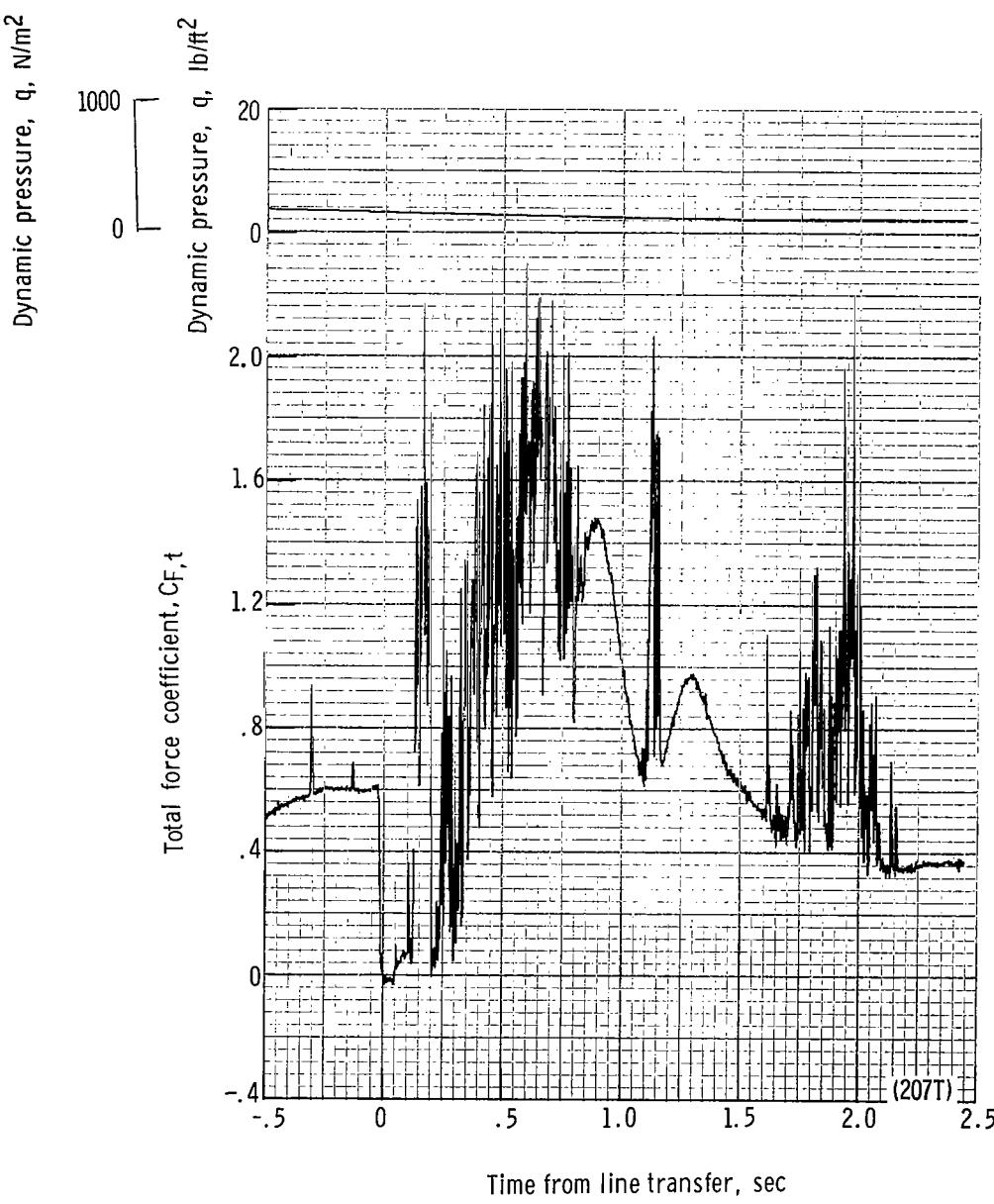


(w) Individual suspension-line loads F_{Lte3} and F_{Lk3} and acceleration a_z plotted against time from line transfer. Time = 0 second corresponds to 48.42 seconds after launch.



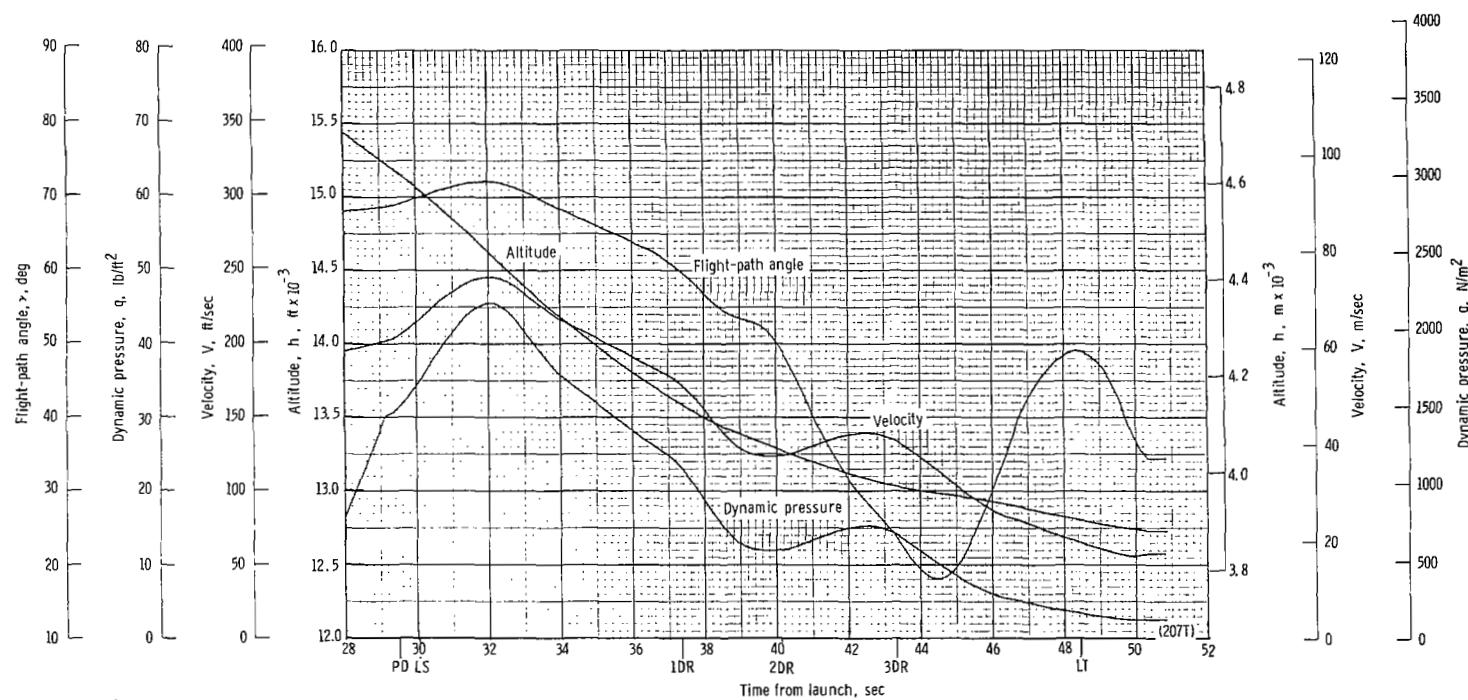
(x) Total force F_t plotted against time from line transfer. Time = 0 second corresponds to 48.42 seconds after launch.

Figure 48.- Continued.



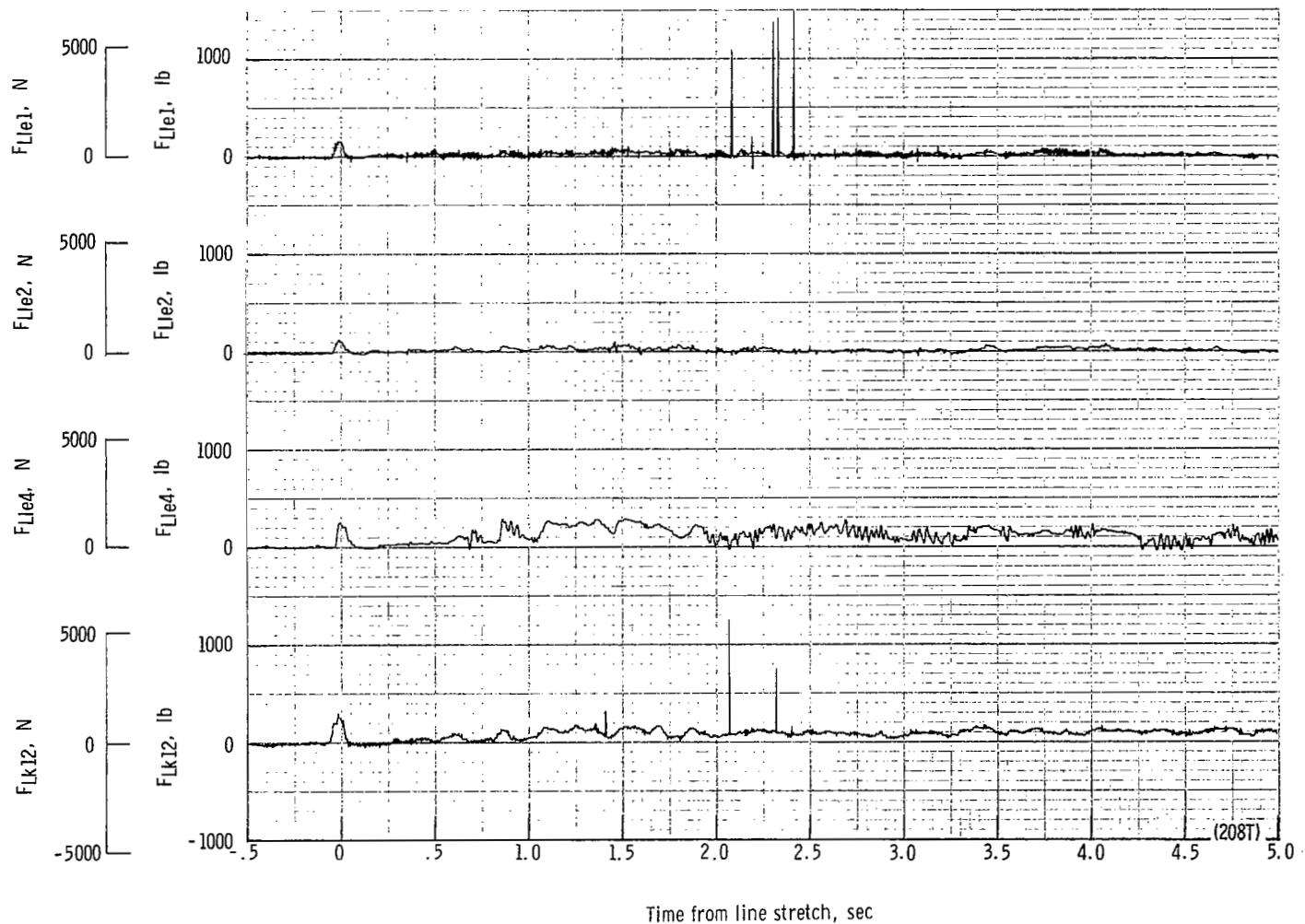
(y) Total force coefficient $C_{F,t}$ and dynamic pressure q plotted against time from line transfer. Time = 0 second corresponds to 48.42 seconds after launch.

Figure 48.- Continued.



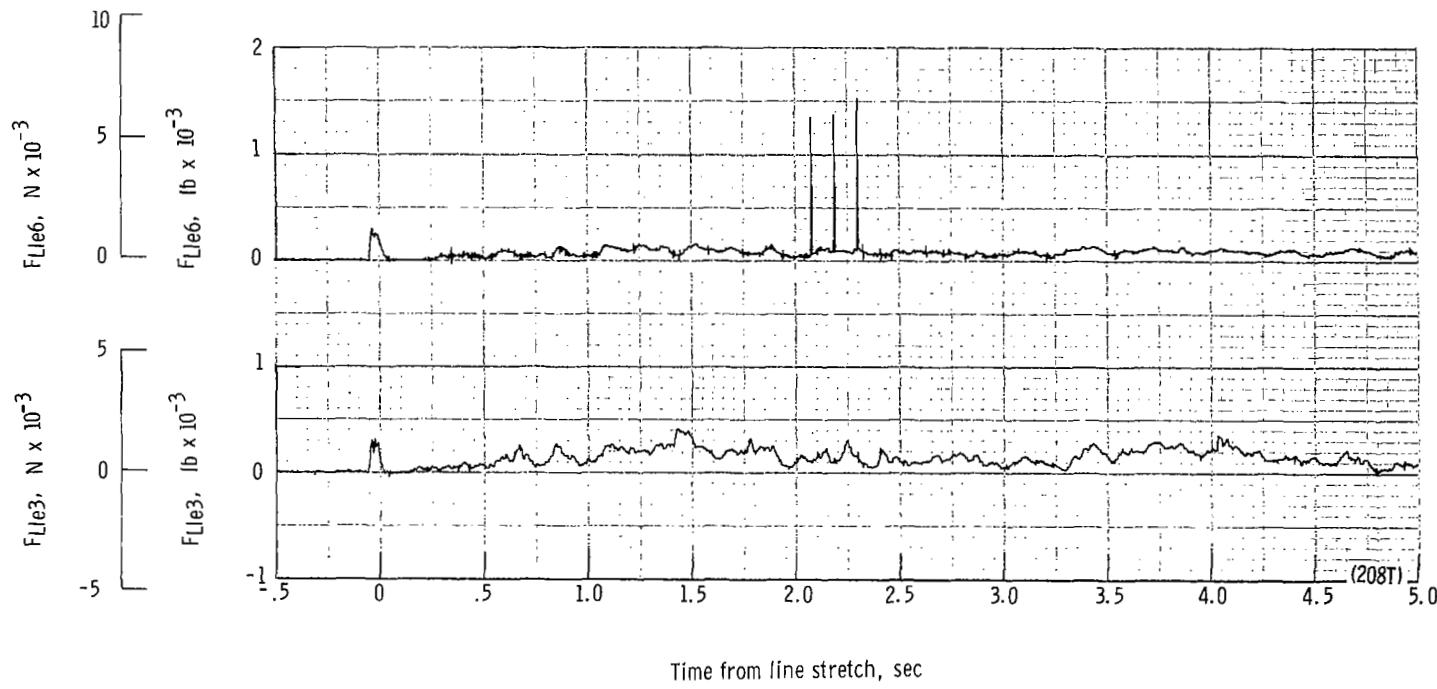
(z) Flight-path angle γ , dynamic pressure q , velocity V , and altitude h plotted against time from launch.

Figure 48.- Concluded.



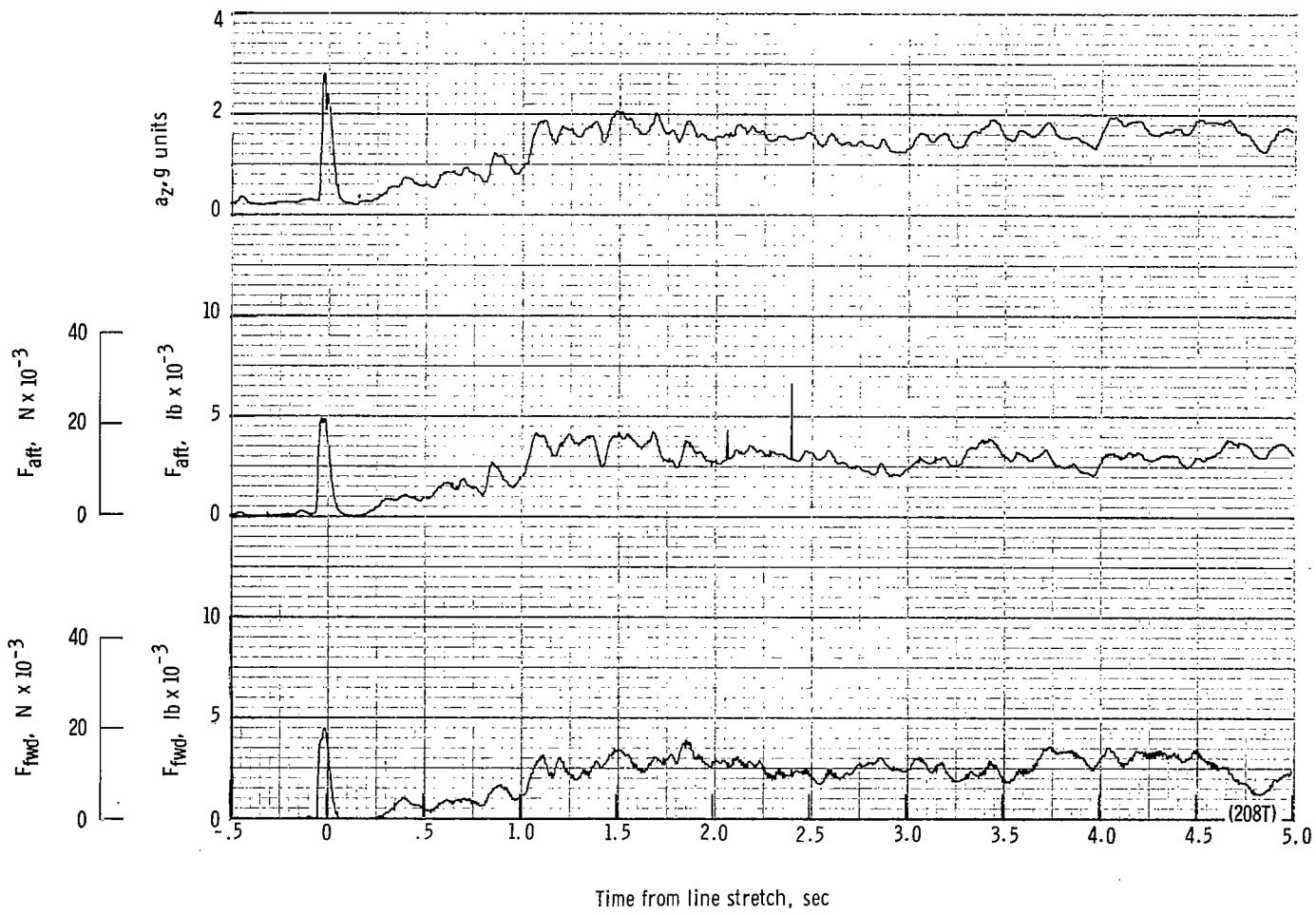
(a) Individual suspension-line loads F_{Lk12} , F_{Lle4} , F_{Lle2} and F_{Lle1} plotted against time from line stretch. Time = 0 second corresponds to 30.99 seconds after launch.

Figure 49.- Time history of twin-keel parawing deployment data for test 208T. $W_D = 22\ 348\ N$ (5024 lb); $W_P = 20\ 764\ N$ (4668 lb); $q_{PD} = 885.8\ N/m^2$ (18.5 lb/ft²); $h_{PD} = 5848\ m$ (19 185 ft); $l_r/l_k = 0.100$; reefing version A.



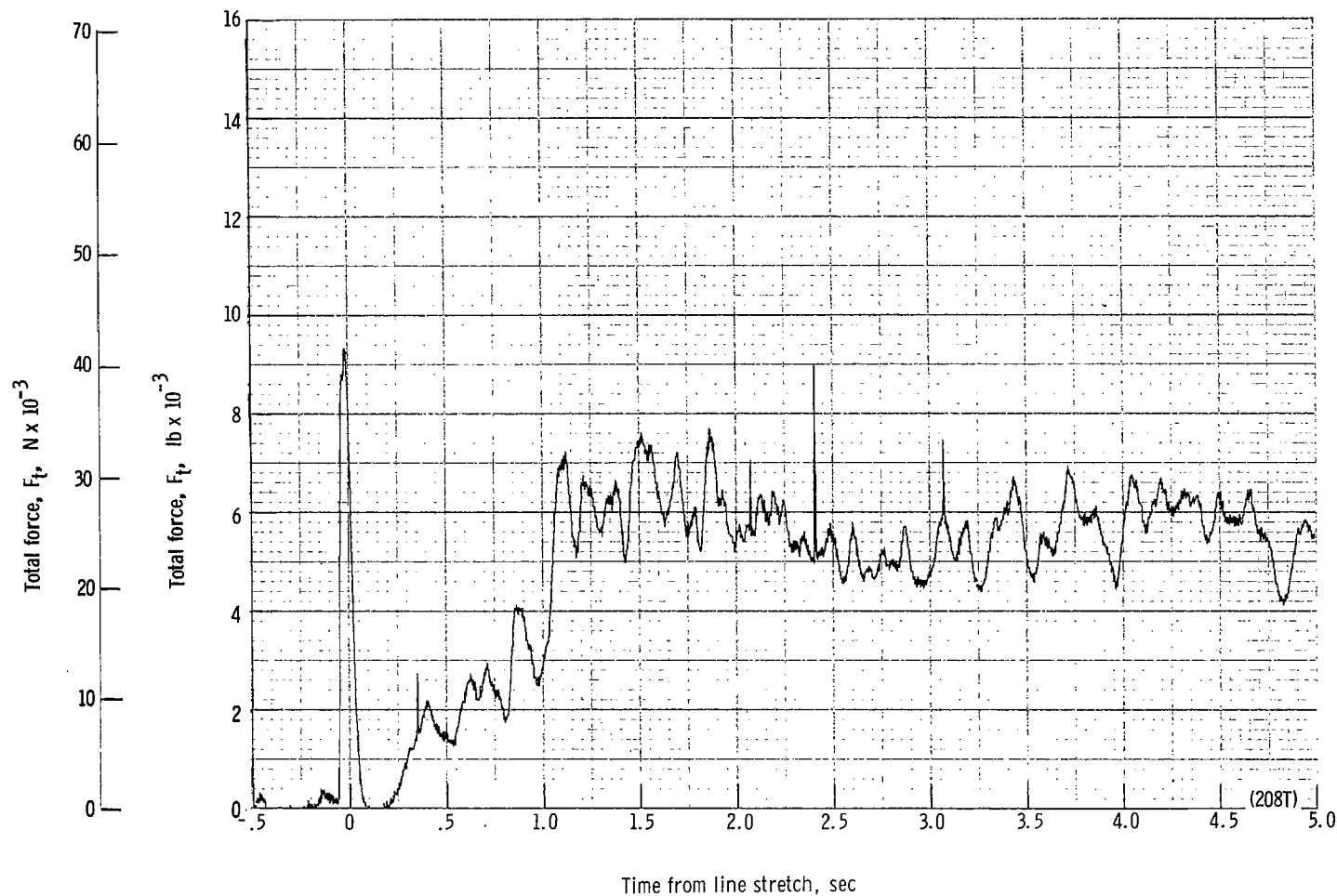
(b) Individual suspension-line loads F_{Lle3} and F_{Lle6} plotted against time from line stretch. Time = 0 second corresponds to 30.99 seconds after launch.

Figure 49.- Continued.



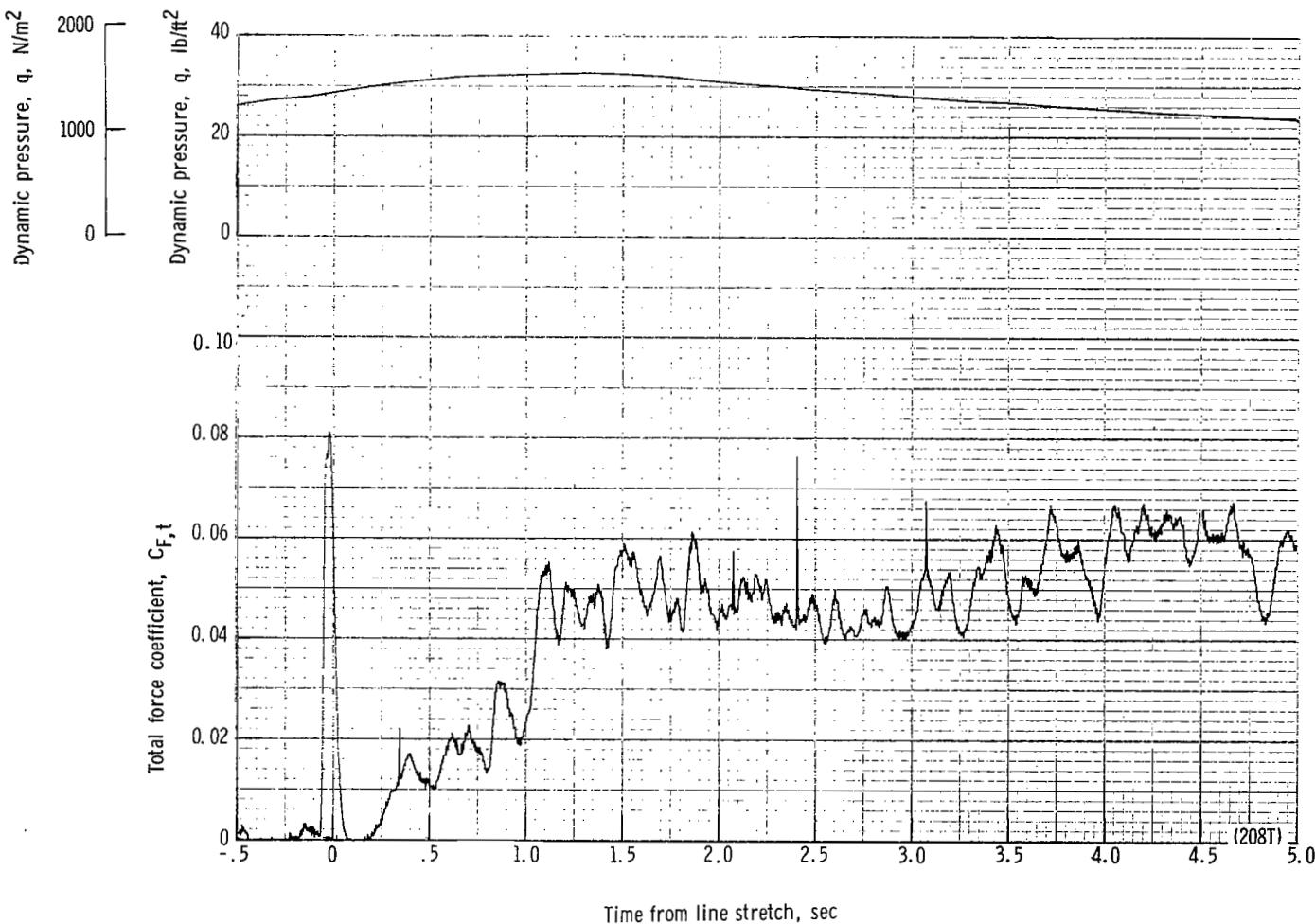
(c) Forward and aft riser loads and acceleration a_z plotted against time from line stretch. Time = 0 second corresponds to 30.99 seconds after launch.

Figure 49.- Continued.



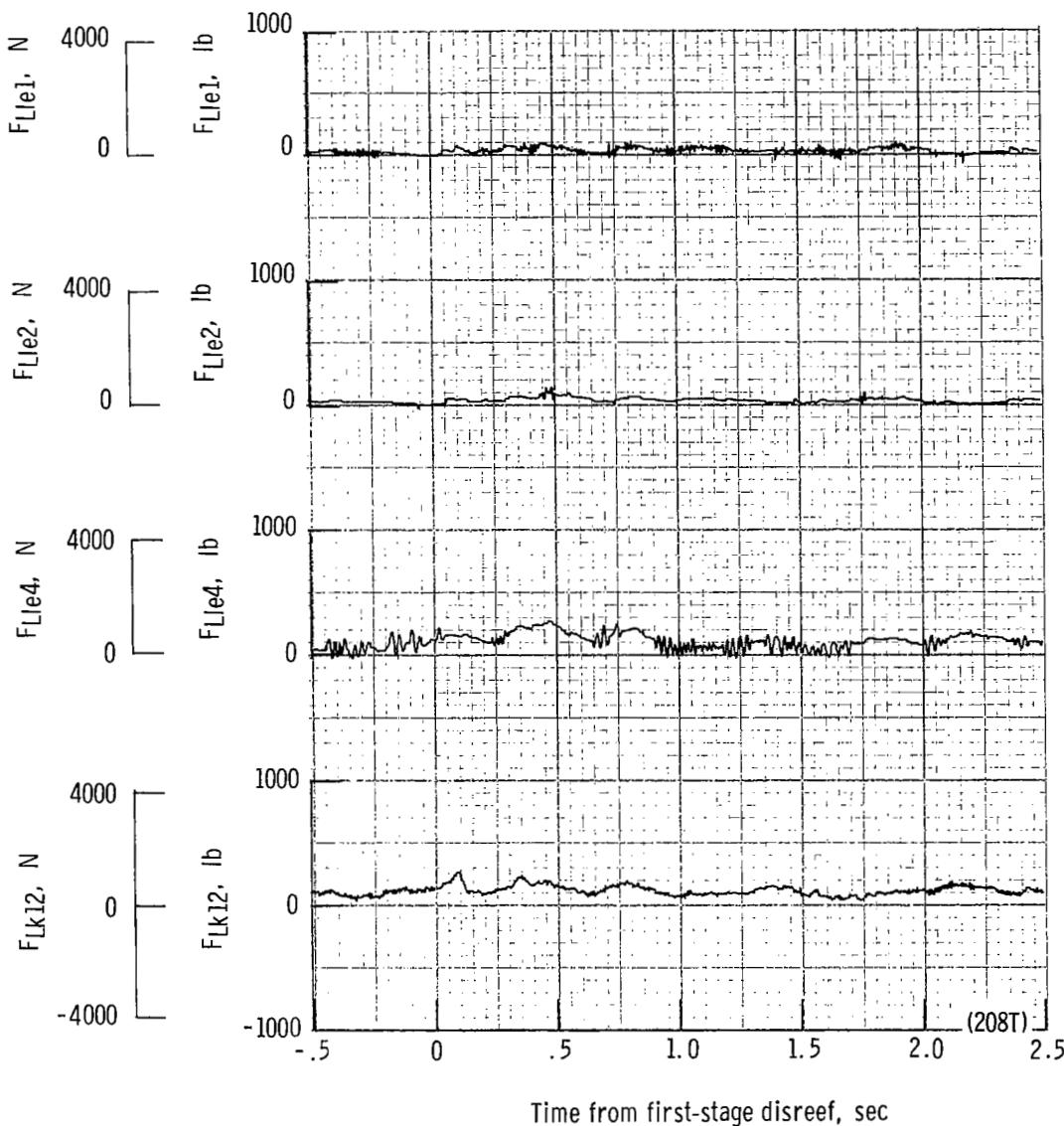
(d) Total force F_t plotted against time from line stretch. Time = 0 second corresponds to 30.99 seconds after launch.

Figure 49.- Continued.



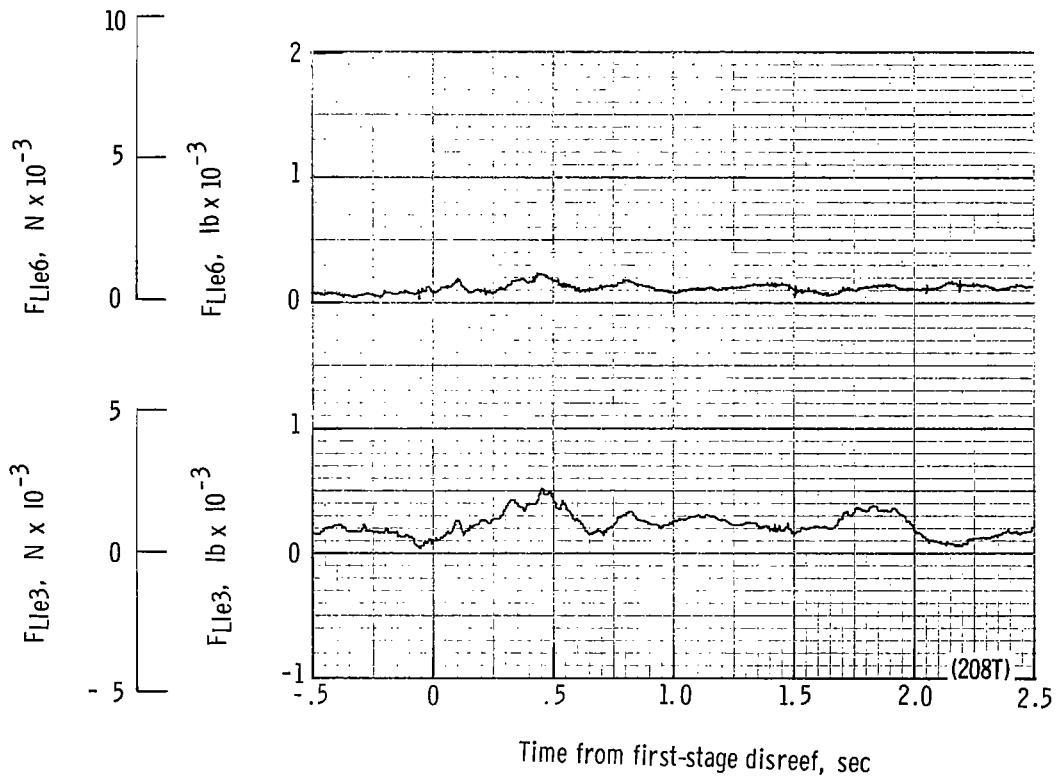
(e) Total force coefficient $C_{F,t}$ and dynamic pressure q plotted against time from line stretch. Time = 0 second corresponds to 30.99 seconds after launch.

Figure 49.- Continued.



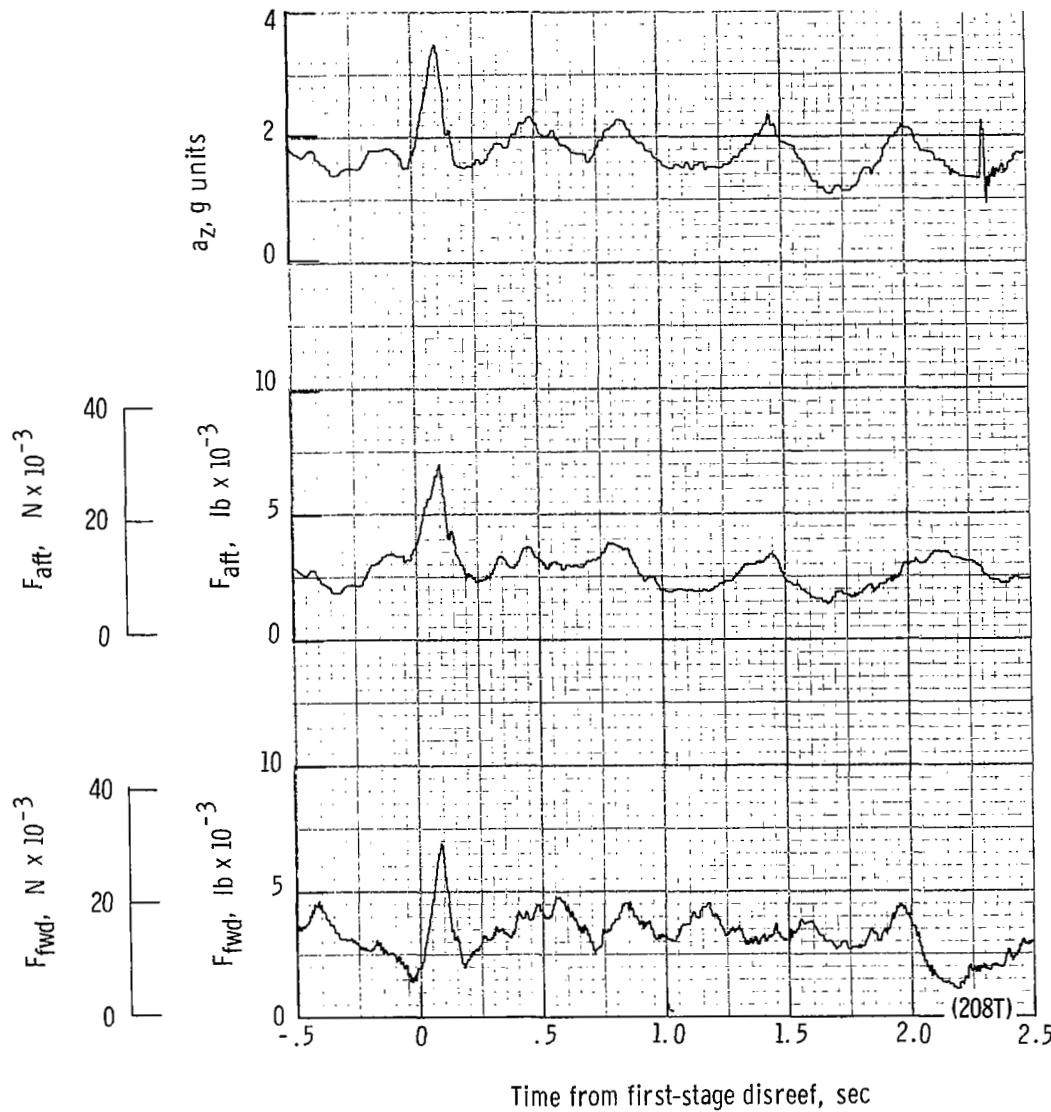
(f) Individual suspension-line loads F_{Lk12} , F_{Lle4} , F_{Lle2} , and F_{Lle1} plotted against time from first-stage disreef. Time = 0 second corresponds to 37.42 seconds after launch.

Figure 49.- Continued.



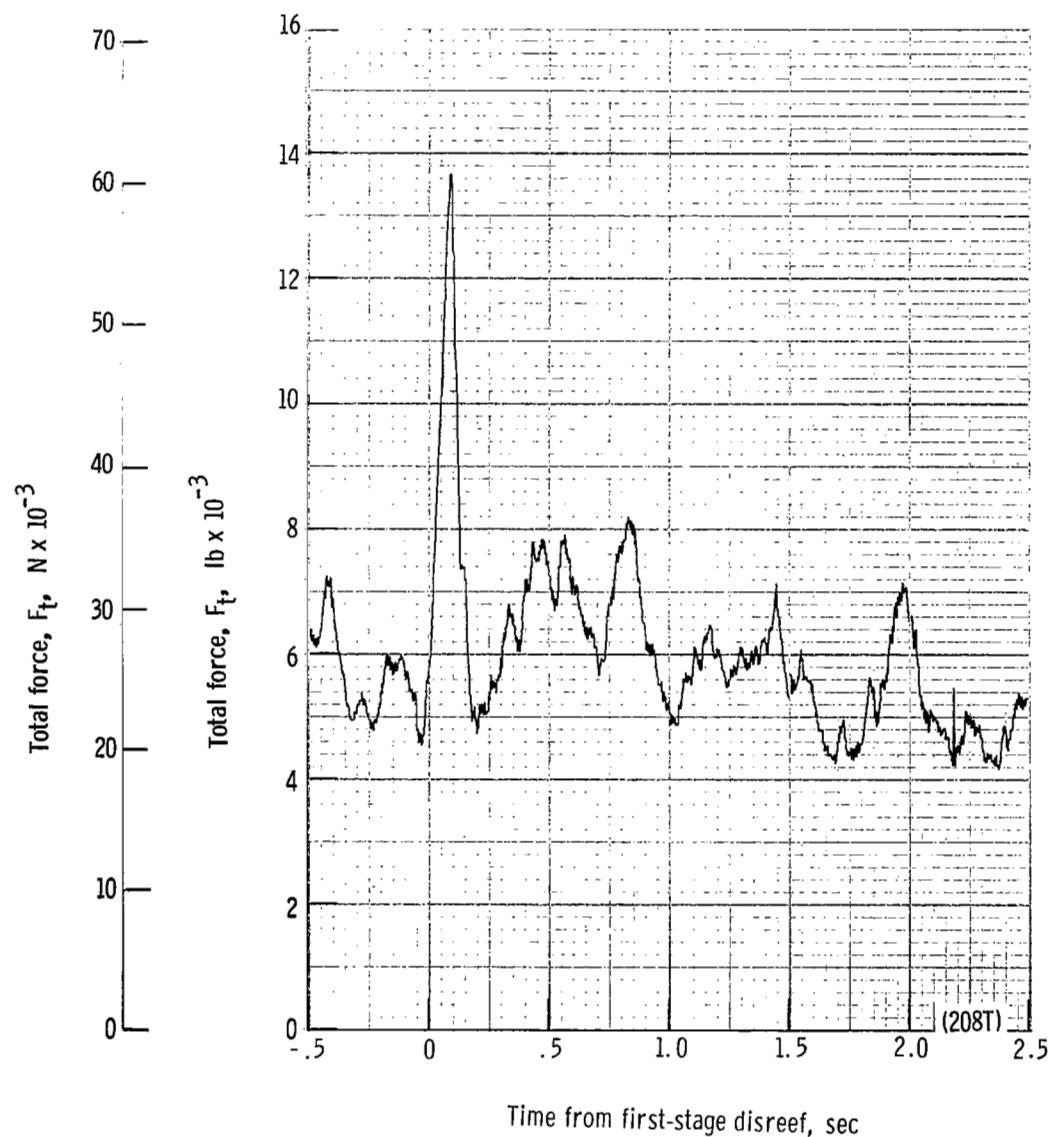
(g) Individual suspension-line loads F_{Lle3} and F_{Lle6} plotted against time from first-stage disreef. Time = 0 second corresponds to 37.42 seconds after launch.

Figure 49.- Continued.



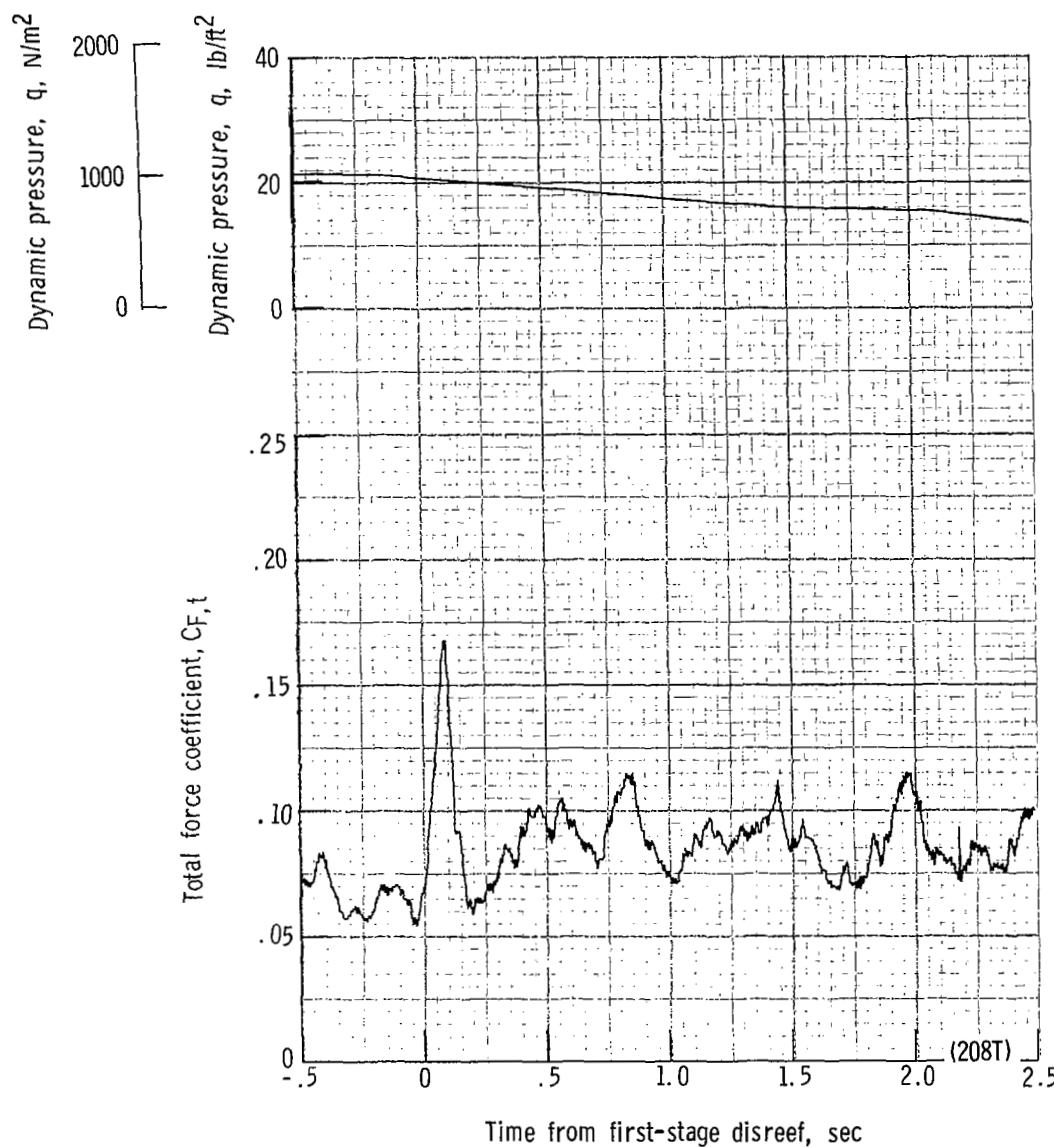
(h) Forward and aft riser loads and acceleration a_z plotted against time from first-stage disreef. Time = 0 second corresponds to 37.42 seconds after launch.

Figure 49.- Continued.



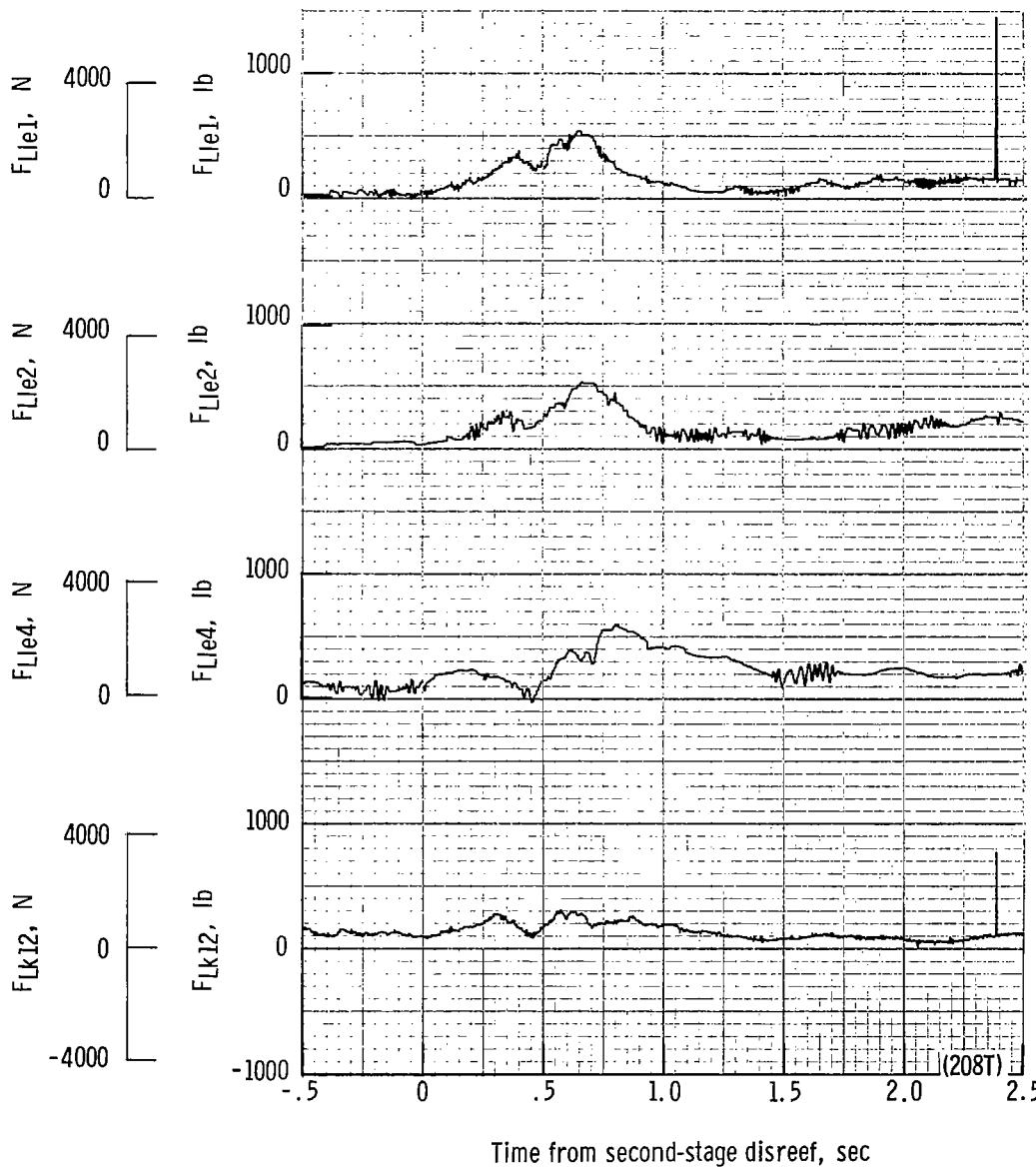
(i) Total force F_t plotted against time from first-stage disreef. Time = 0 second corresponds to 37.42 seconds after launch.

Figure 49.- Continued.



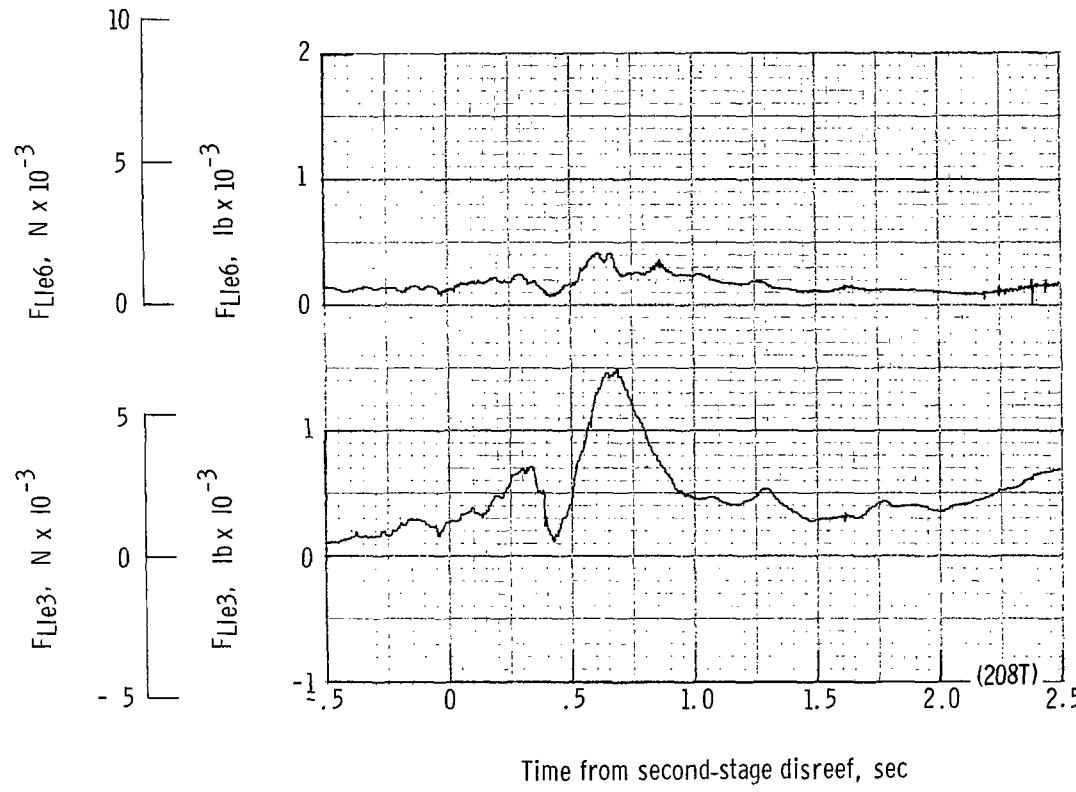
(j) Total force coefficient $C_{F,t}$ and dynamic pressure q plotted against time from first-stage disreef. Time = 0 second corresponds to 37.42 seconds after launch.

Figure 49.- Continued.



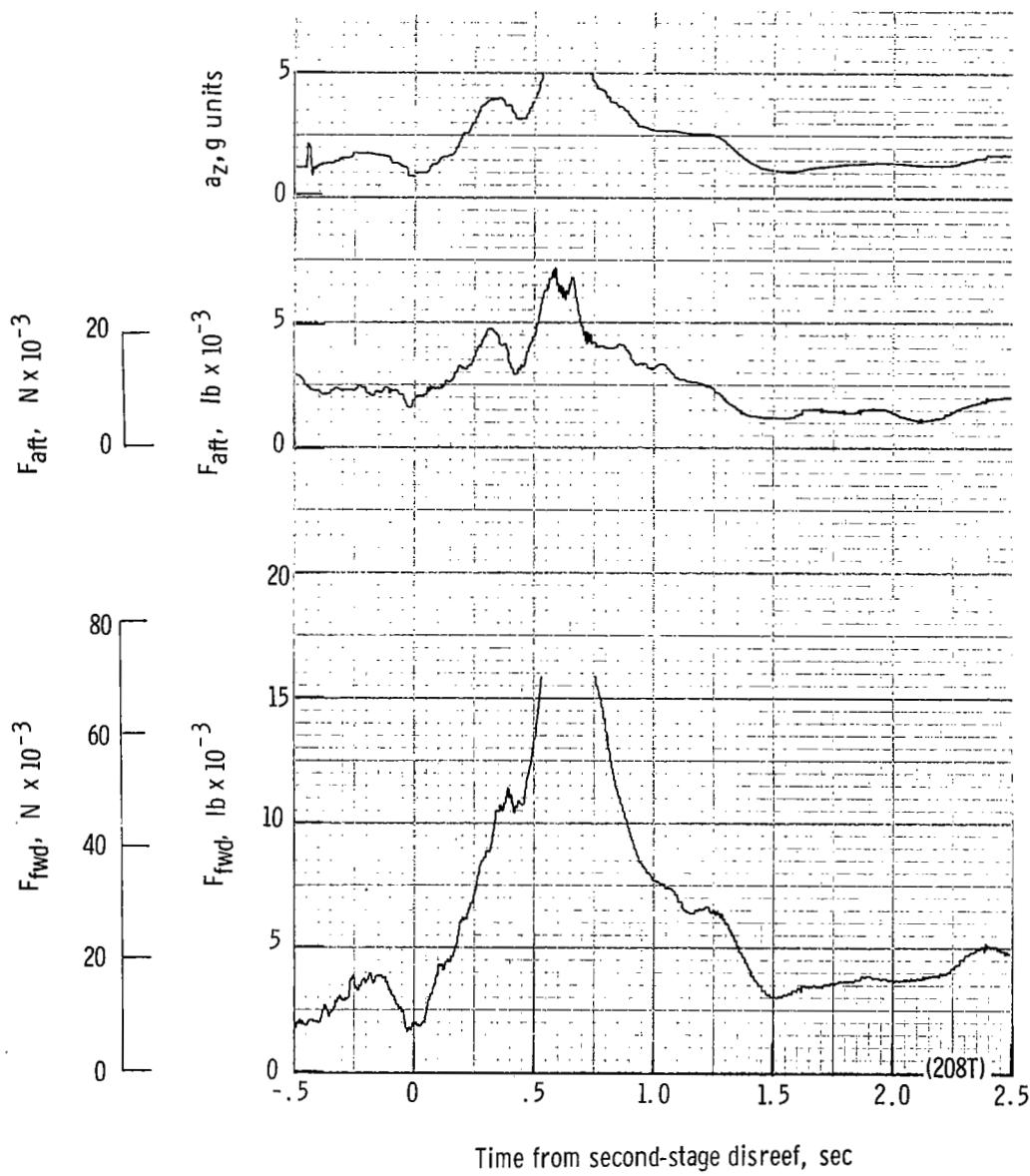
(k) Individual suspension-line loads F_{Lk12} , F_{Lle4} , F_{Lle2} , and F_{Lle1} plotted against time from second-stage disreef. Time = 0 second corresponds to 40.19 seconds after launch.

Figure 49.- Continued.



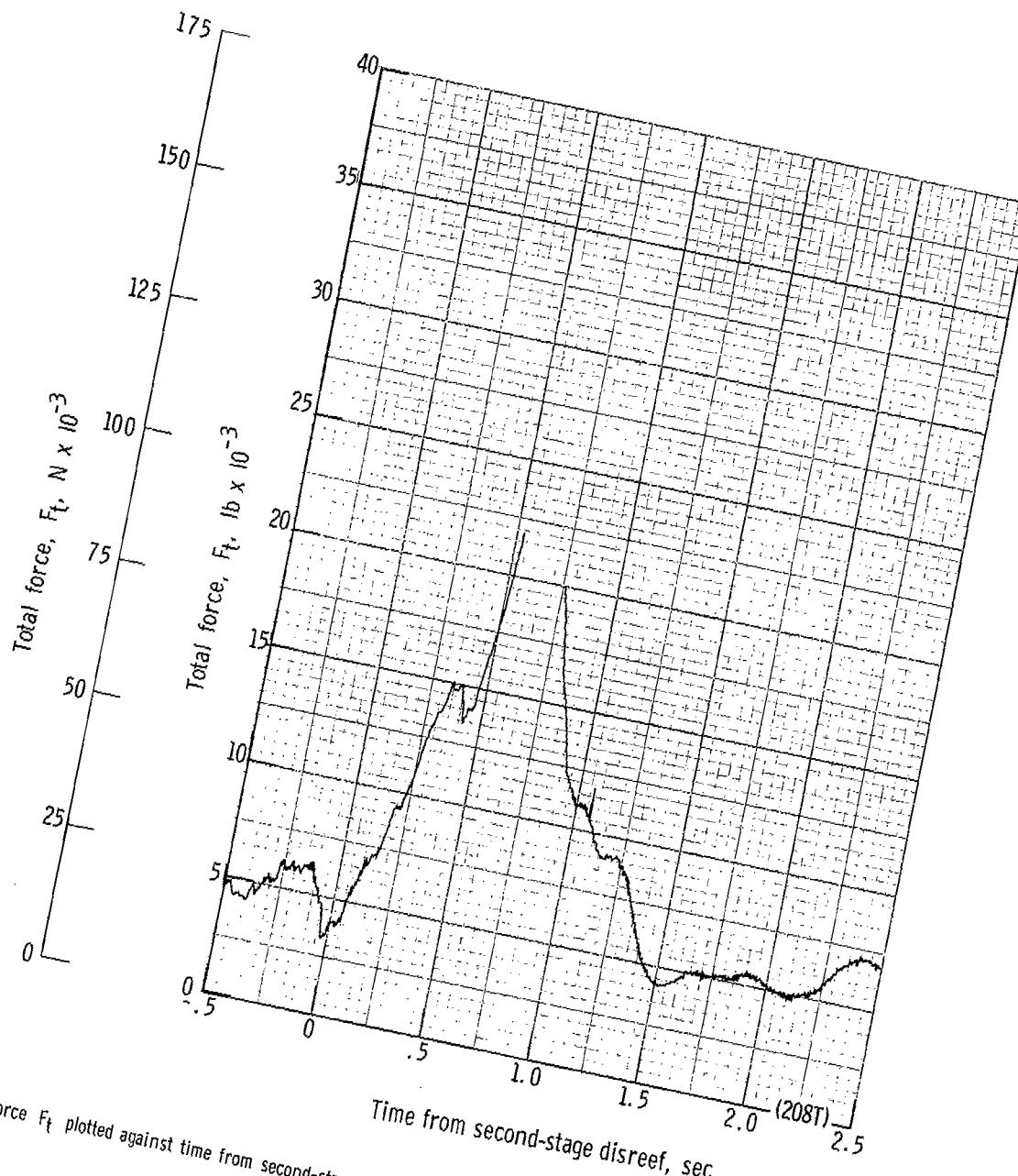
(l) Individual suspension-line loads F_{Lle3} and F_{Lle6} plotted against time from second-stage disreef. Time = 0 second corresponds to 40.19 seconds after launch.

Figure 49.- Continued.



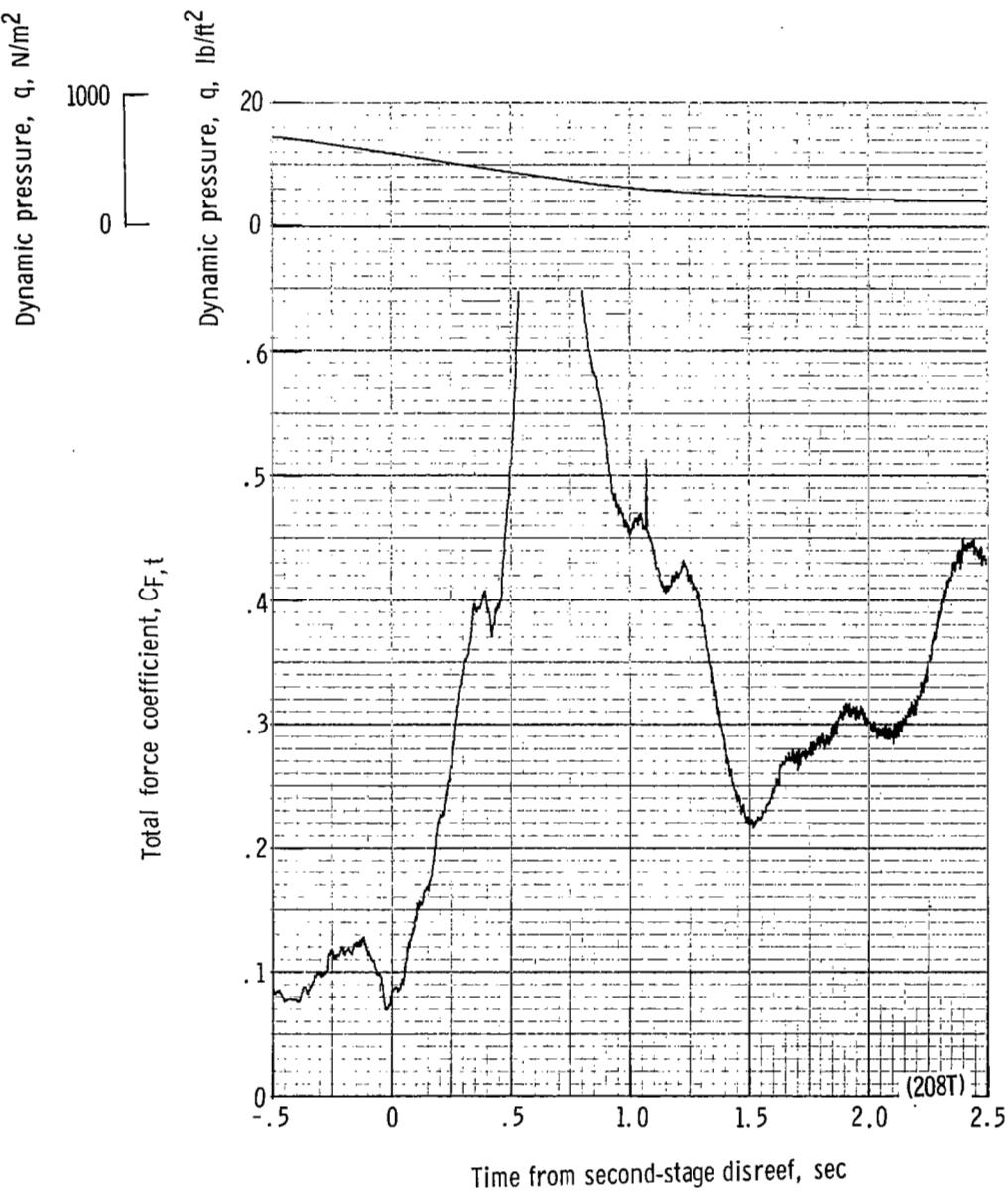
(m) Forward and aft suspension-line loads and acceleration a_z plotted against time from second-stage disreef. Time = 0 second corresponds to 40.19 seconds after launch.

Figure 49.- Continued.



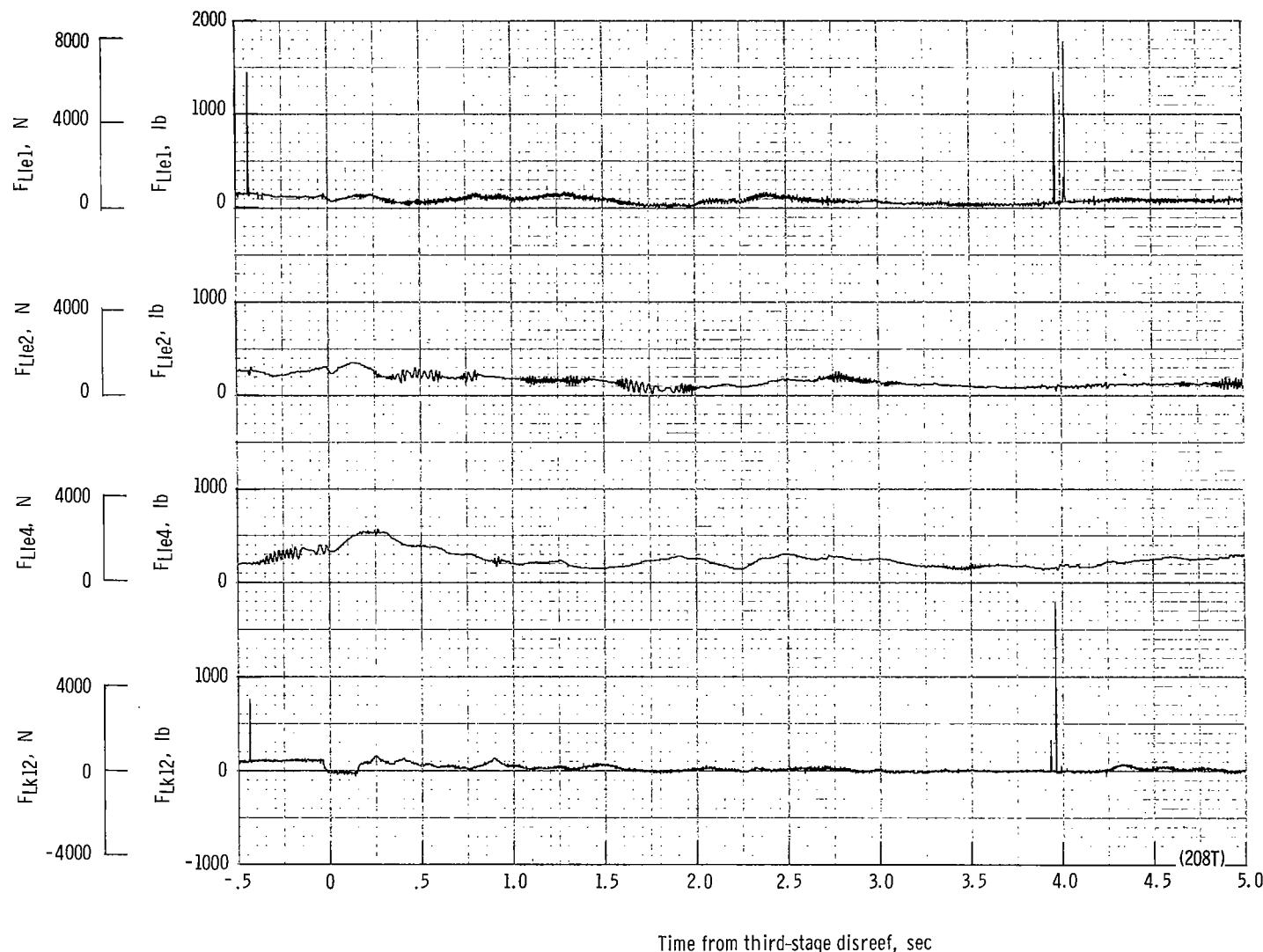
(n) Total force F_t plotted against time from second-stage disreef. Time = 0 second corresponds to 40.19 seconds after launch.

Figure 49.- Continued.



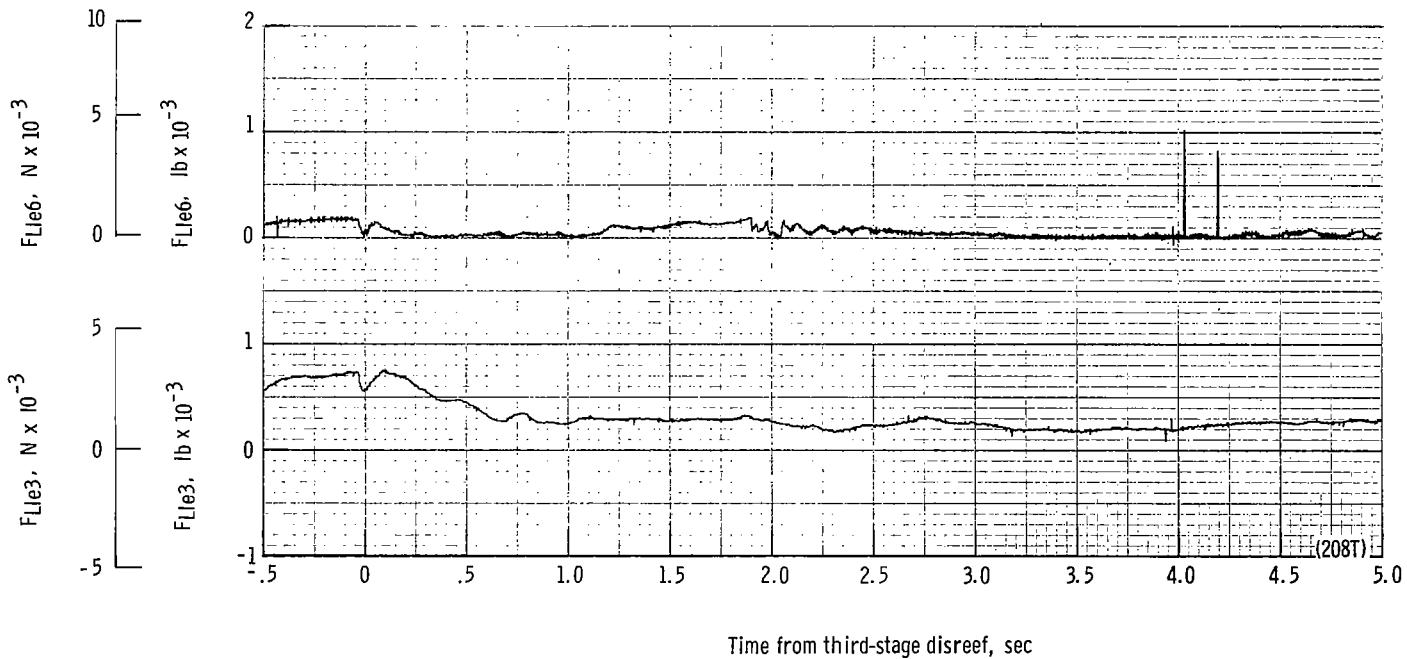
(a) Total force coefficient $C_{F,t}$ and dynamic pressure q plotted against time from second-stage disreef. Time = 0 second corresponds to 40.19 seconds after launch.

Figure 49.- Continued.



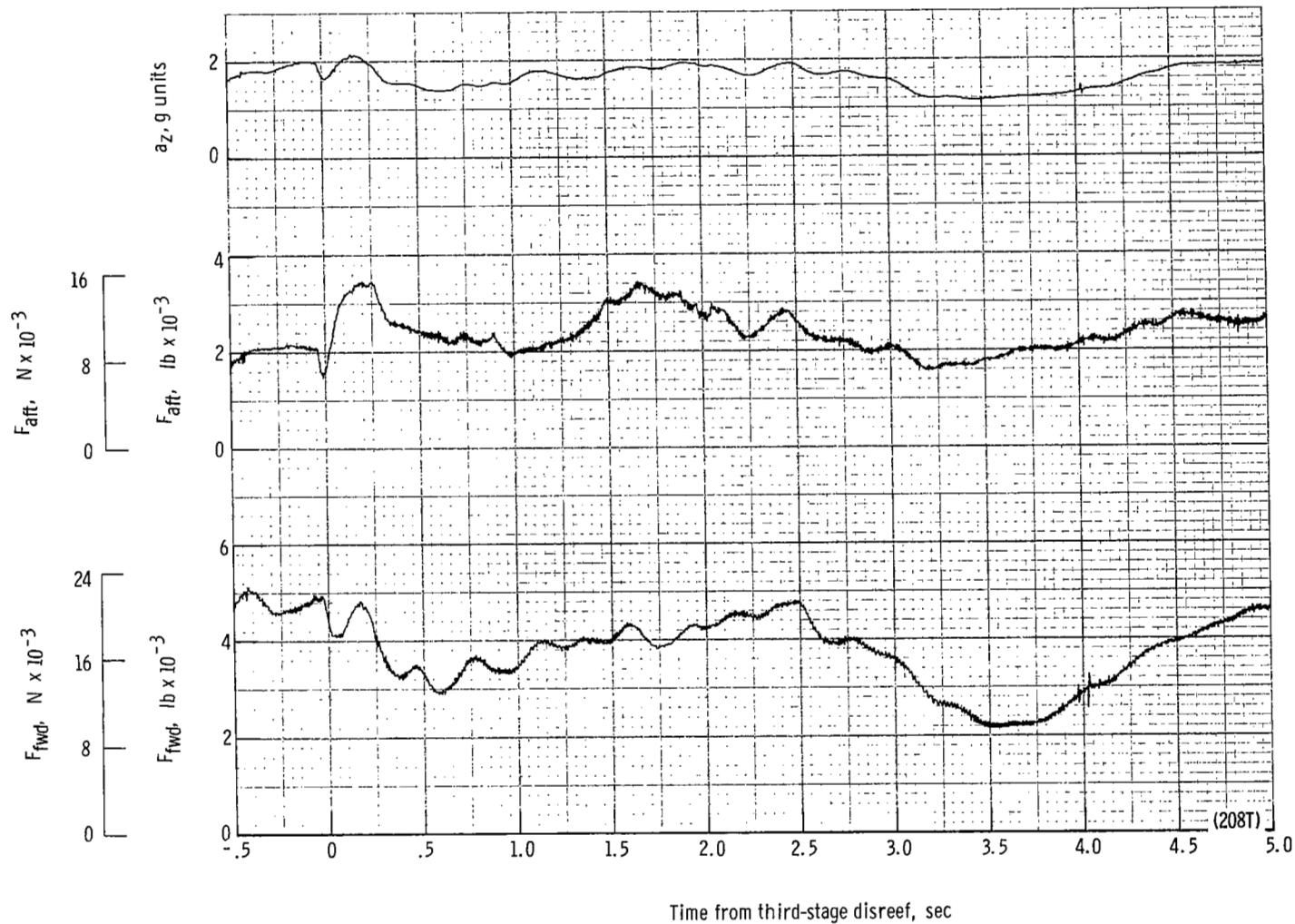
(p) Individual suspension-line loads F_{Lk12} , F_{Lle4} , F_{Lle2} , and F_{Lle1} plotted against time from third-stage disreef. Time = 0 second corresponds to 43.01 seconds after launch.

Figure 49.- Continued.



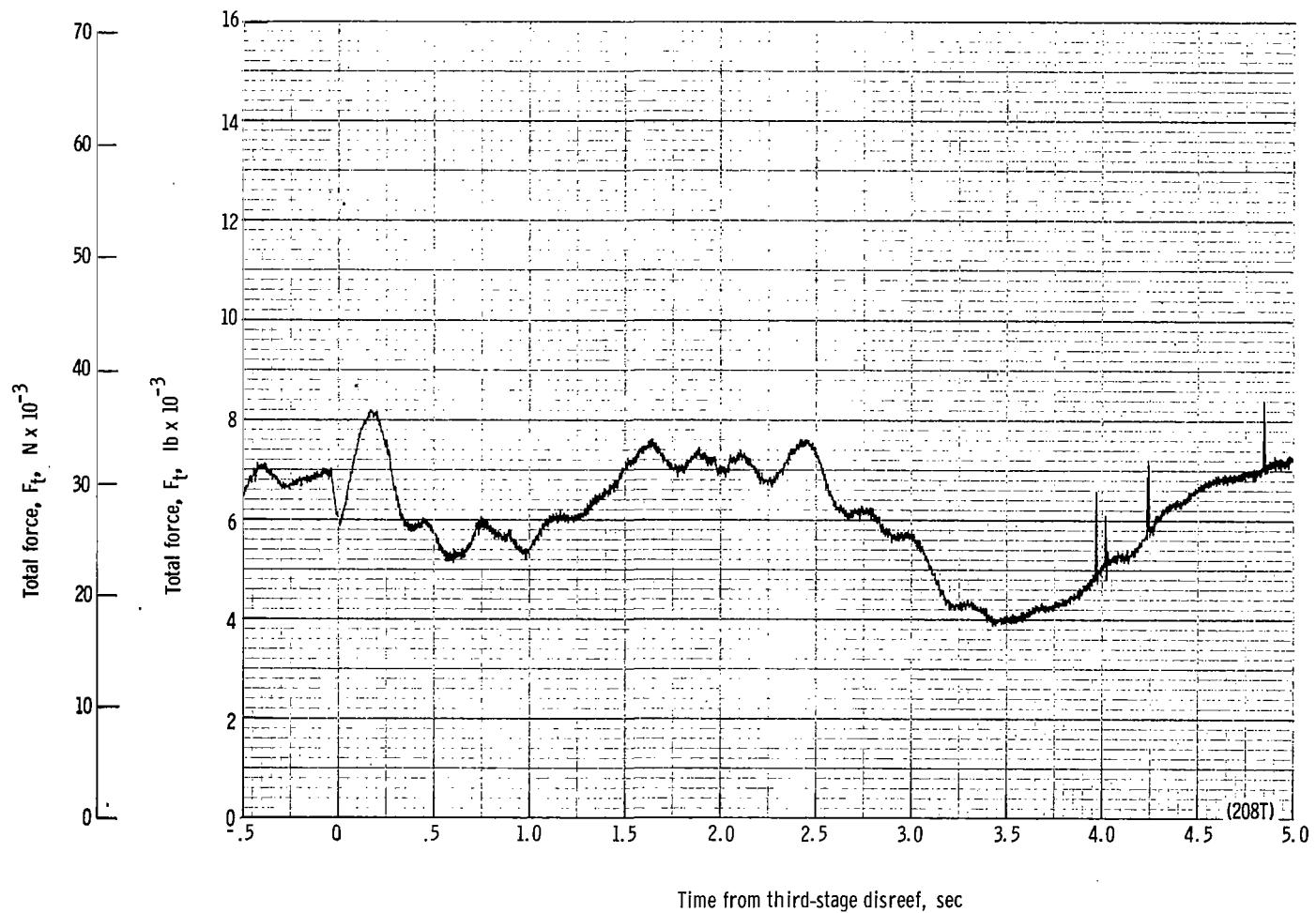
(q) Individual suspension-line loads F_{Lle3} and F_{Lle6} plotted against time from third-stage disreef. Time = 0 second corresponds to 43.01 seconds after launch.

Figure 49.- Continued.



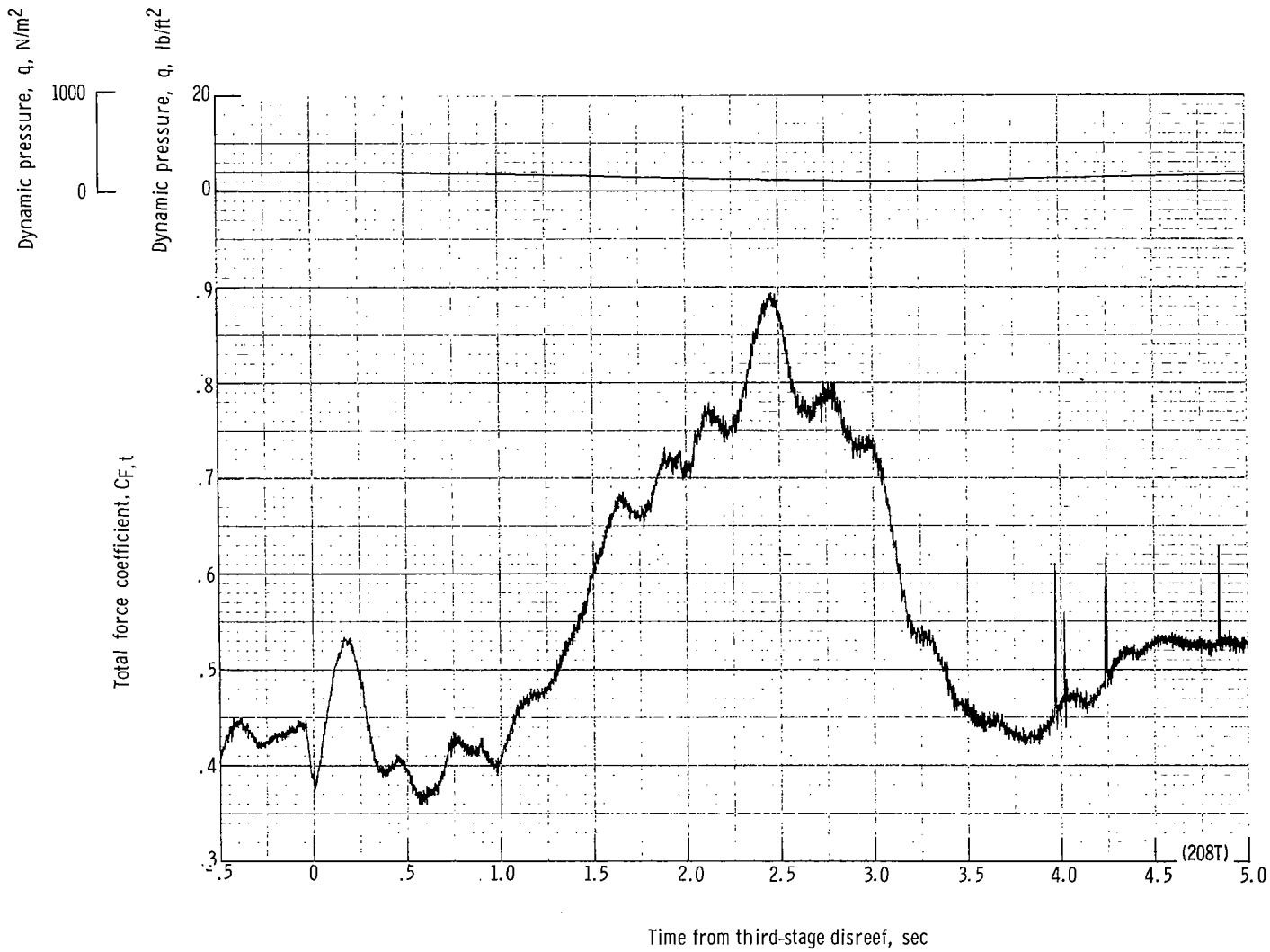
(r) Forward and aft riser loads and acceleration a_z plotted against time from third-stage disreef. Time = 0 second corresponds to 43.01 seconds after launch.

Figure 49.- Continued.



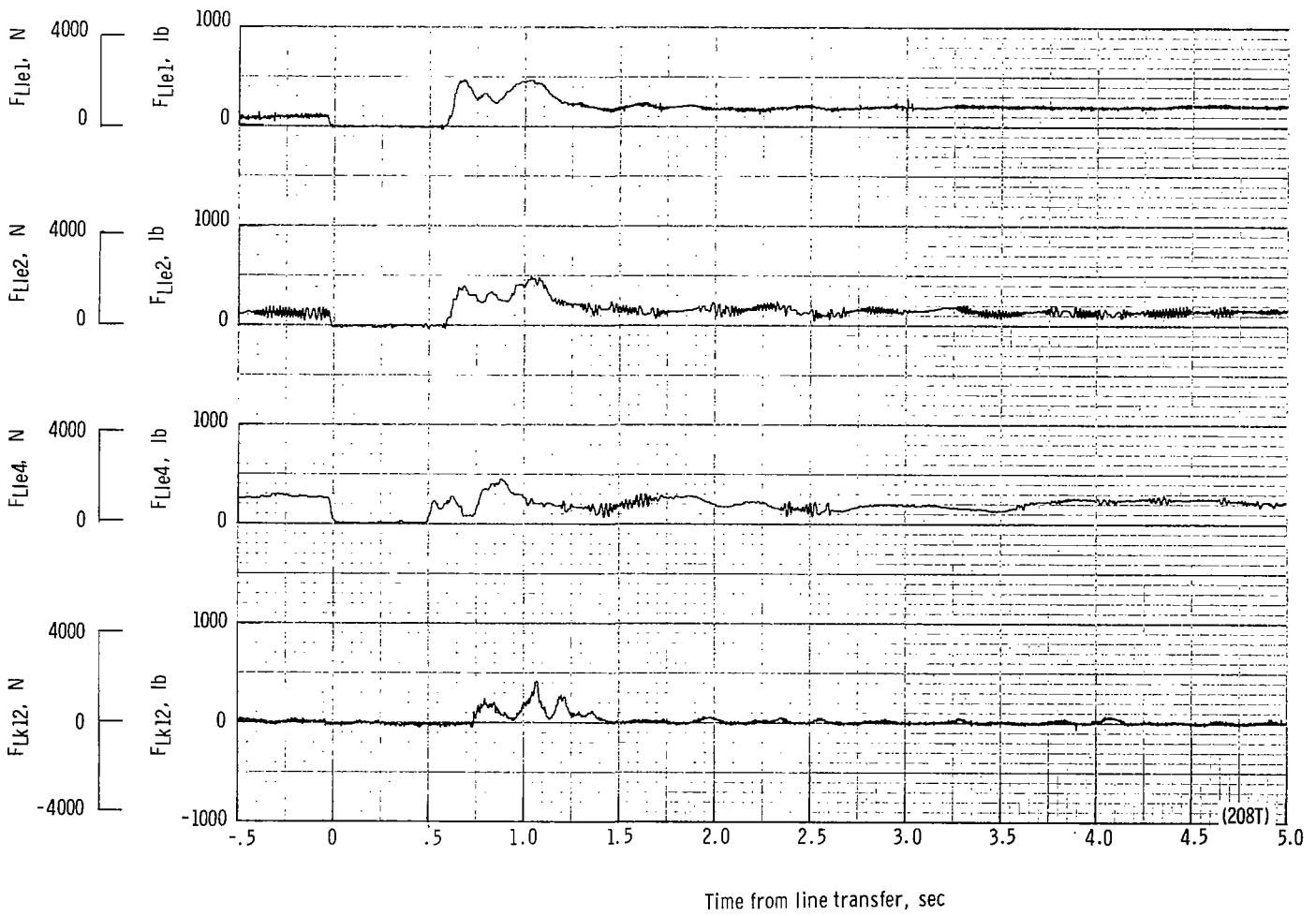
(s) Total force F_t plotted against time from third-stage disreef. Time = 0 second corresponds to 43.01 seconds after launch.

Figure 49.- Continued.



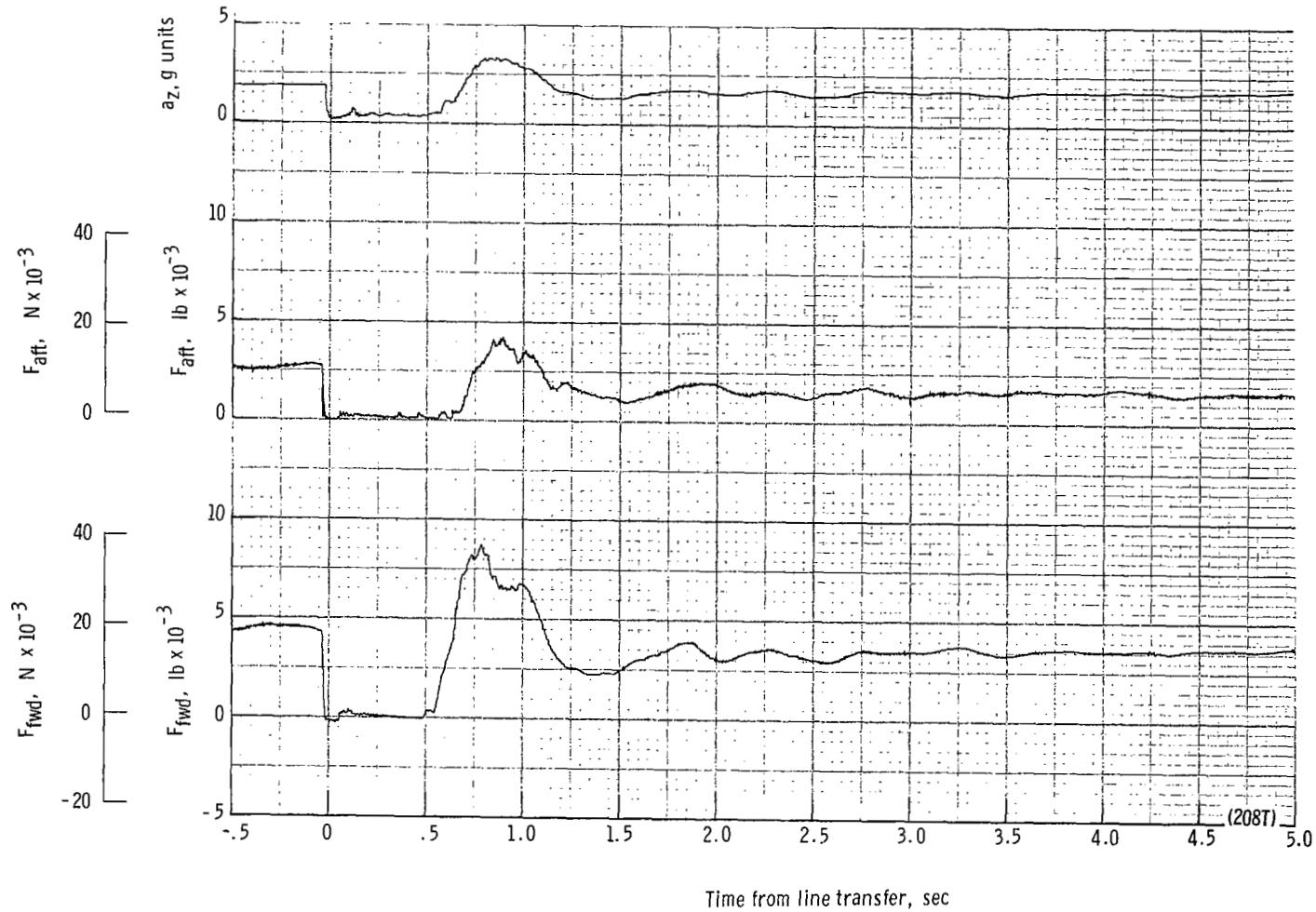
(t) Total force coefficient $C_{F,t}$ and dynamic pressure q plotted against time from third-stage disreef. Time = 0 second corresponds to 43.01 seconds after launch.

Figure 49.- Continued.



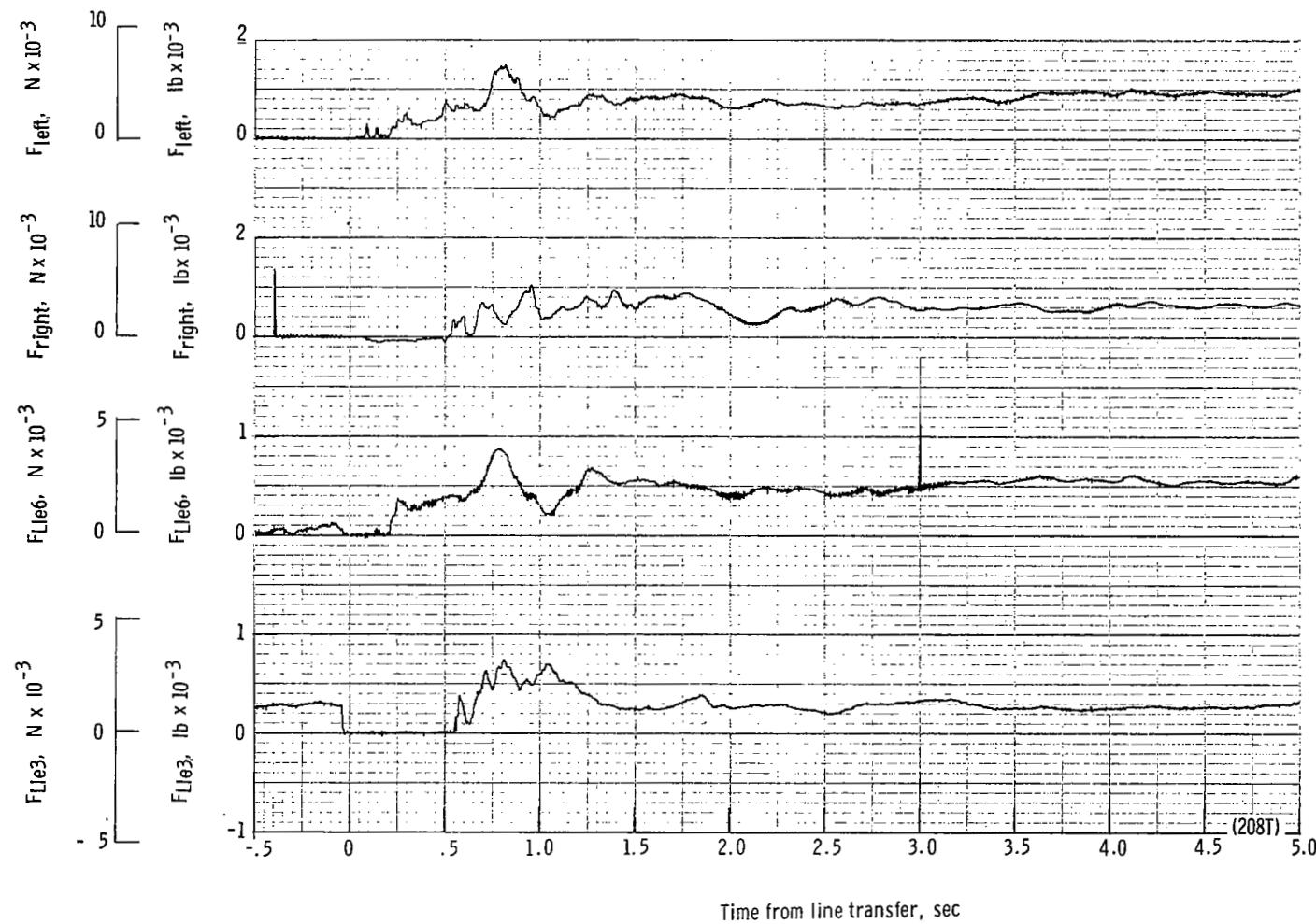
(u) Individual suspension-line loads F_{Lk12} , F_{Lle4} , F_{Lle2} , and F_{Lle1} plotted against time from line transfer. Time = 0 second corresponds to 48.26 seconds after launch.

Figure 49.- Continued.



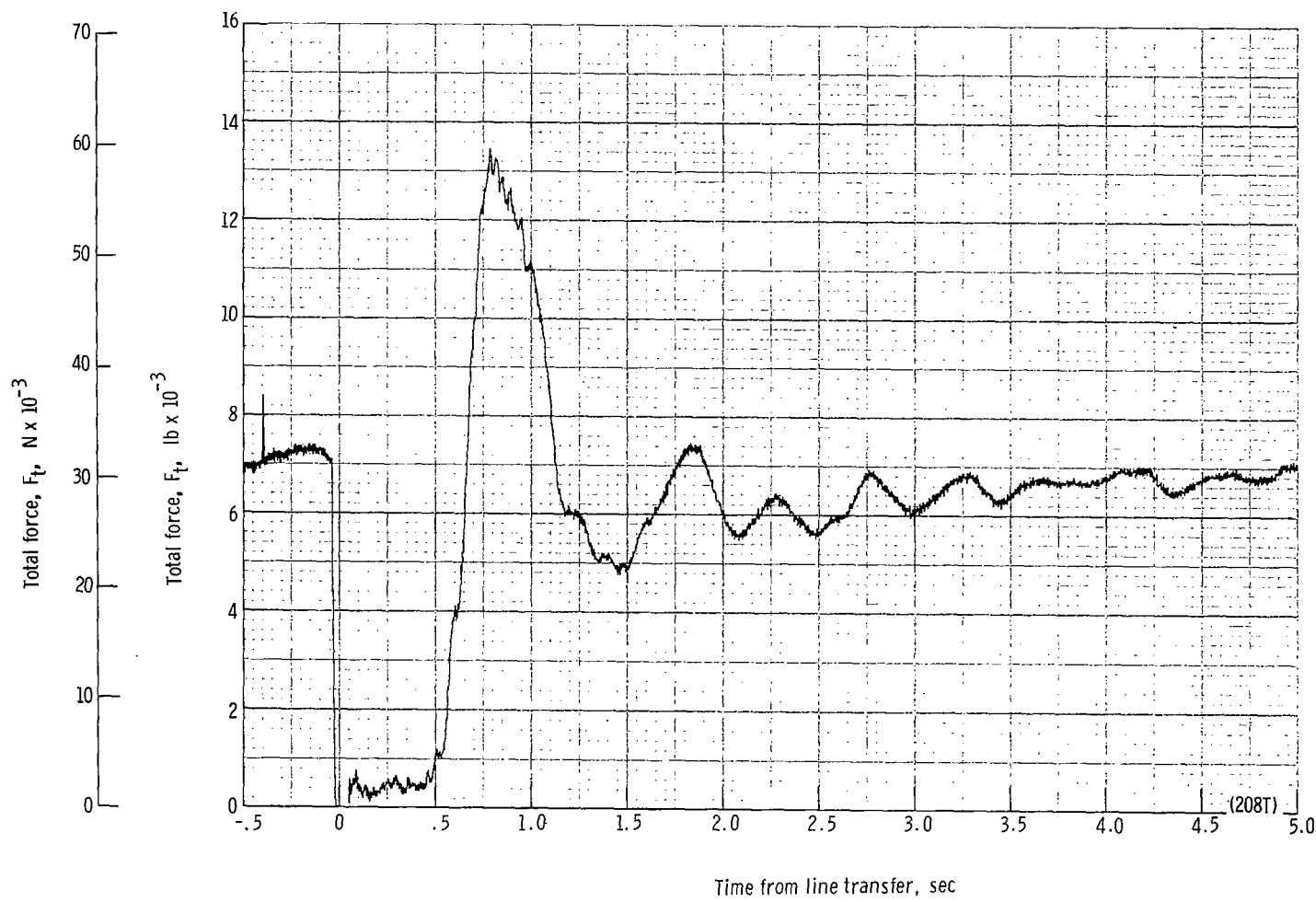
(v) Forward and aft riser loads and acceleration a_z plotted against time from line transfer. Time = 0 second corresponds to 48.26 seconds after launch.

Figure 49.- Continued.



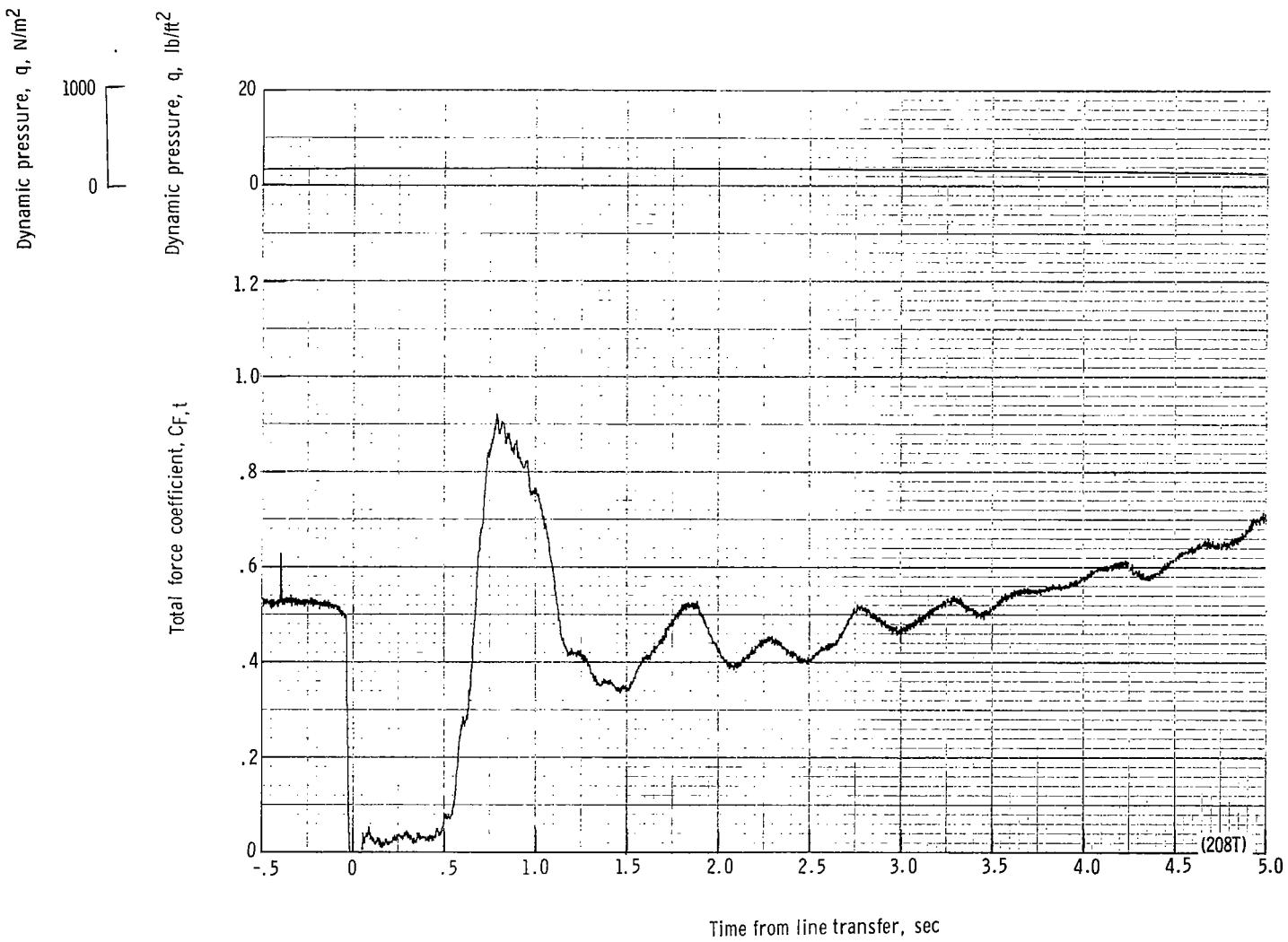
(w) Individual suspension-line loads F_{Lle3} and F_{Lle6} and right and left riser loads plotted against time from line transfer. Time = 0 second corresponds to 48.26 seconds after launch.

Figure 49.- Continued.



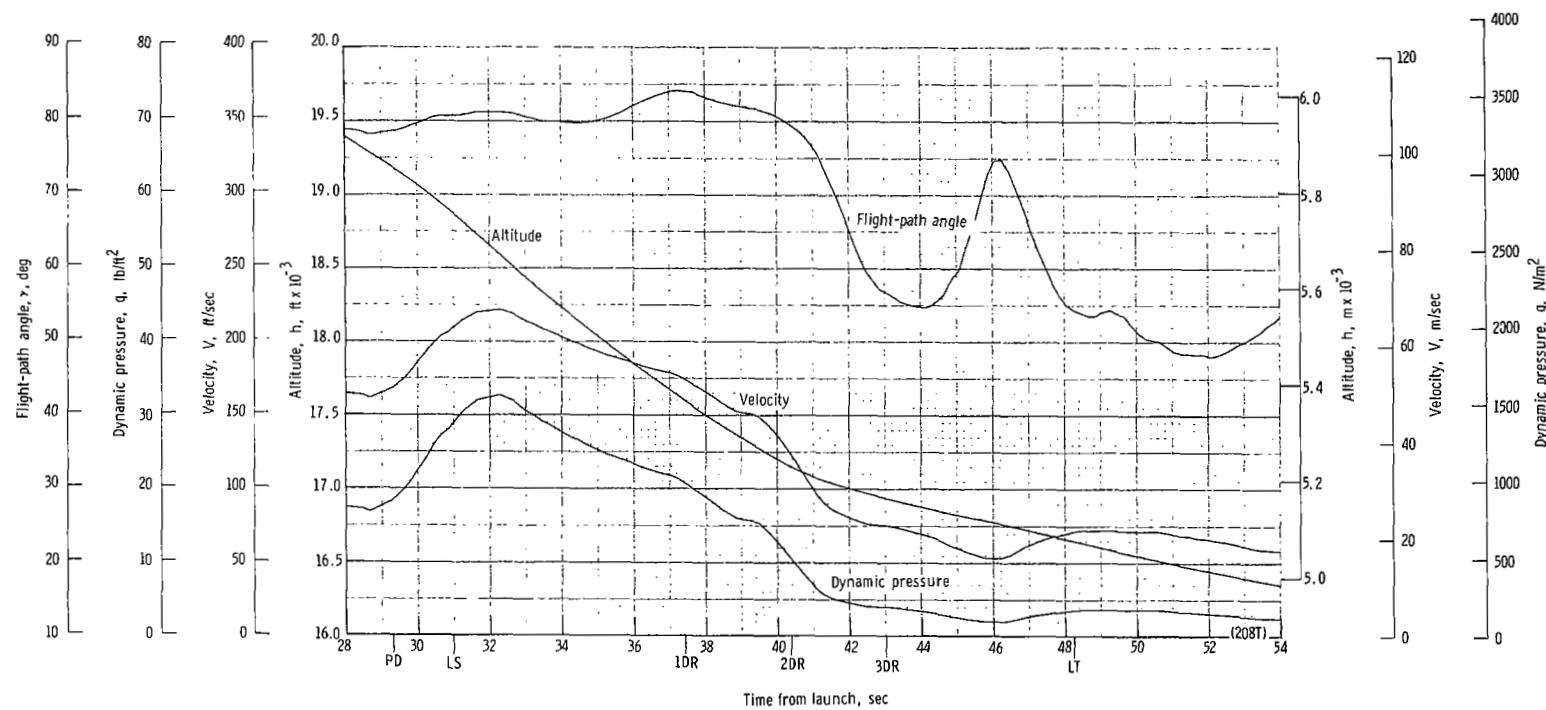
(x) Total force F_t plotted against time from line transfer. Time = 0 second corresponds to 48.26 seconds after launch.

Figure 49.- Continued.



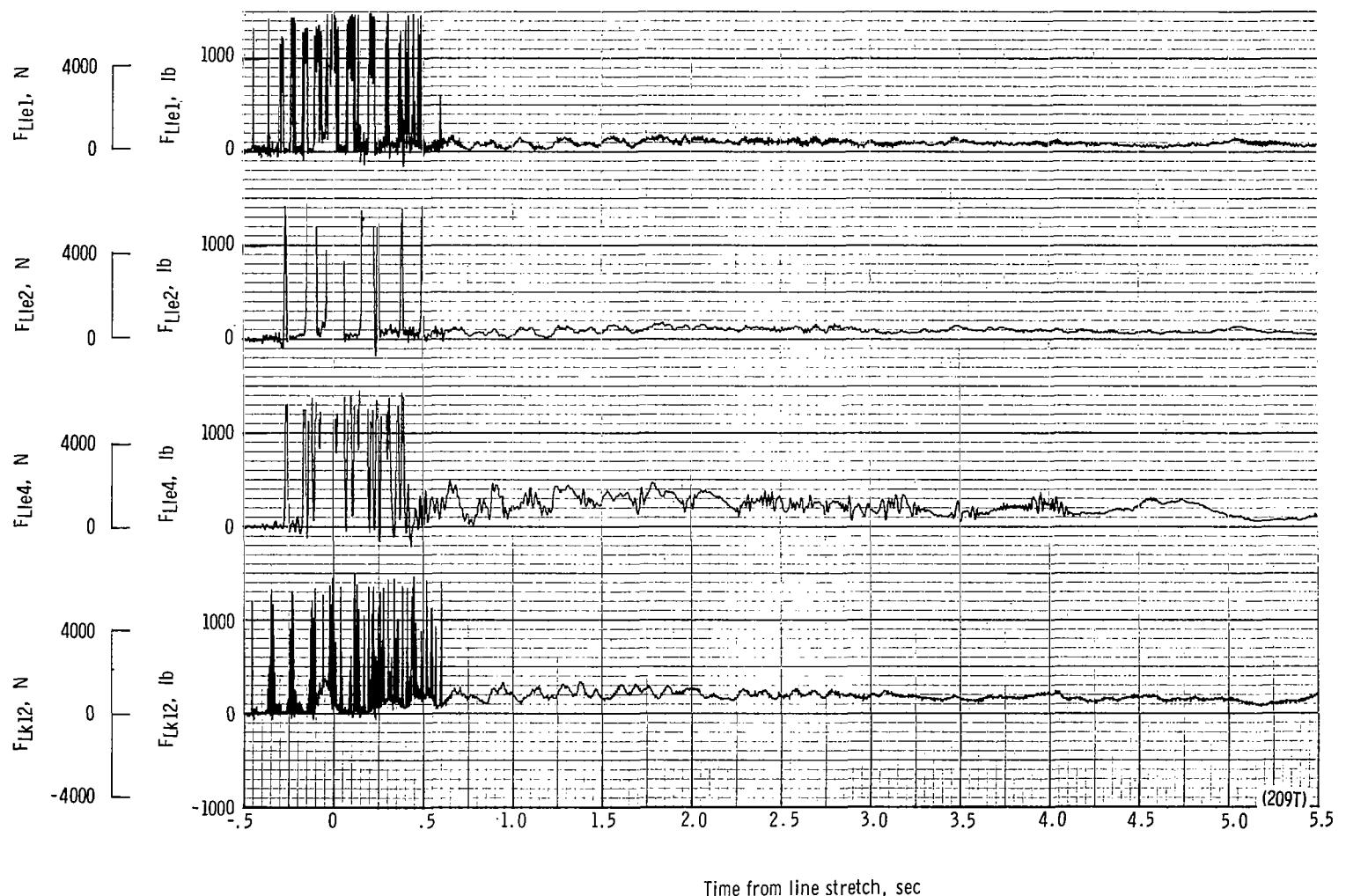
(y) Total force coefficient $C_{F,t}$ and dynamic pressure q plotted against time from line transfer. Time = 0 second corresponds to 48.26 seconds after launch.

Figure 49.- Continued.



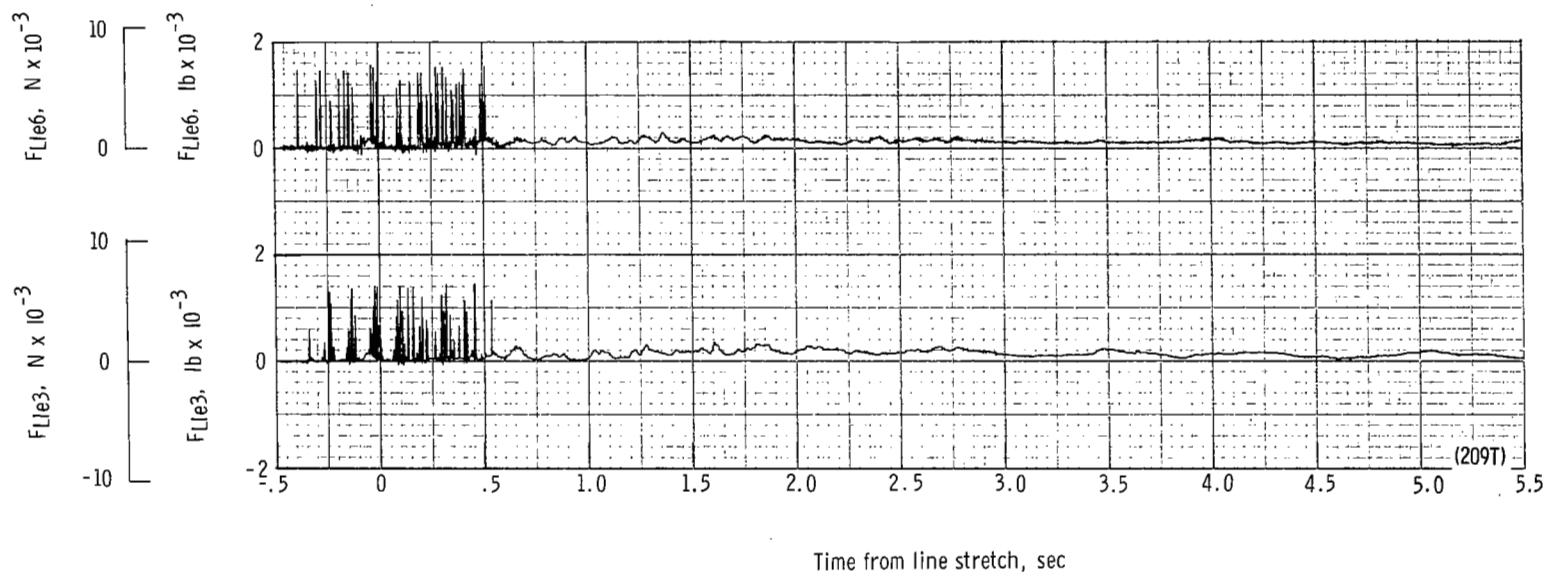
(z) Flight-path angle γ , dynamic pressure q , velocity V , and altitude h plotted against time from launch.

Figure 49.- Concluded.



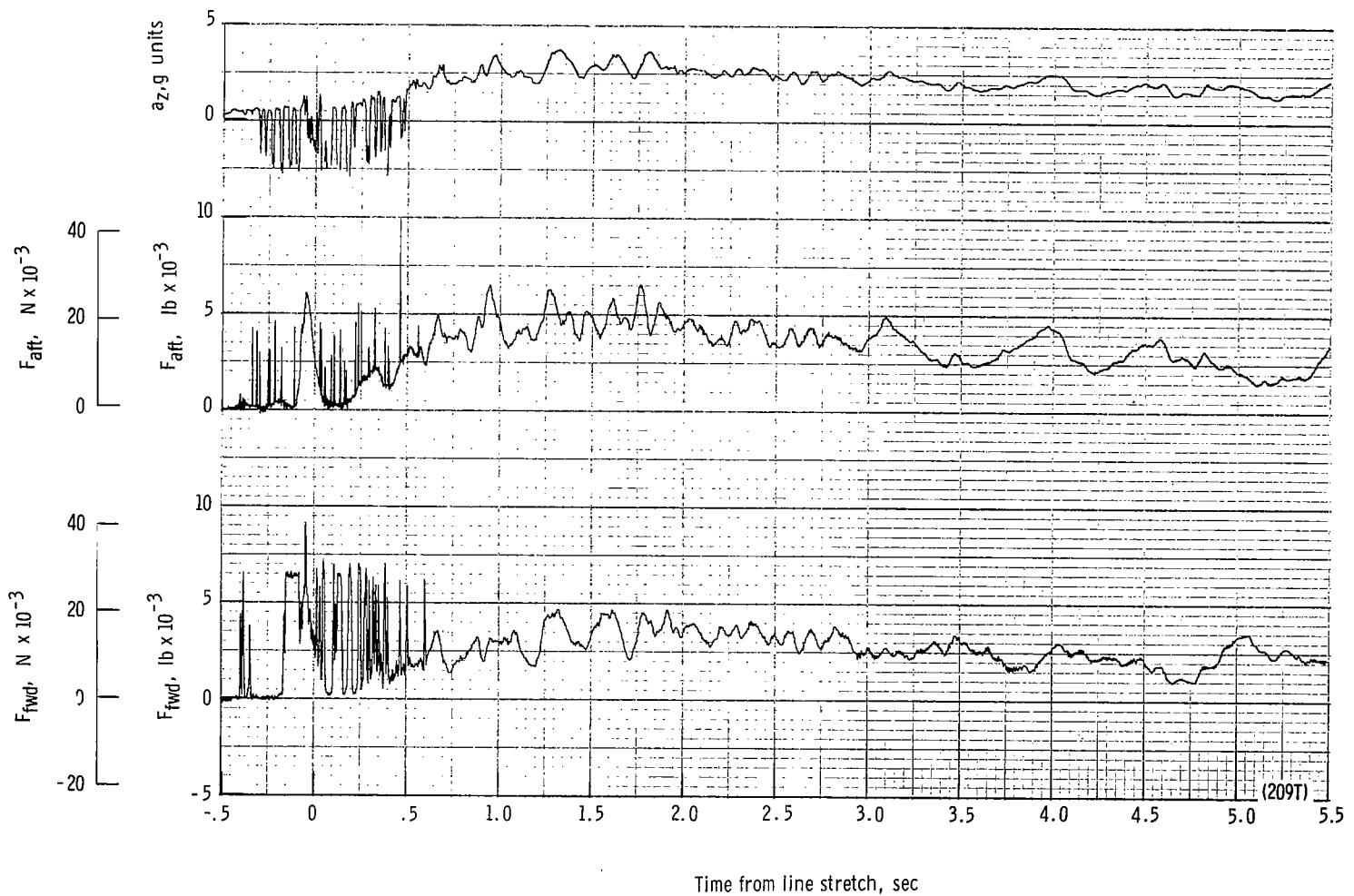
(a) Individual suspension-line loads F_{Lk12} , F_{Lle4} , F_{Lle2} and F_{Lle1} plotted against time from line stretch. Time = 0 second corresponds to 28.82 seconds after launch.

Figure 50.- Time history of twin-keel parawing deployment data for test 209T. $W_D = 16\ 952\ N$ (3811 lb); $W_p = 15\ 106\ N$ (3396 lb);
 $q_{PD} = 2724.4\ N/m^2$ (56.9 lb/ft²); $h_{PD} = 4432\ m$ (14 540 ft); $l_r/l_k = 0.080$; reefing version B.



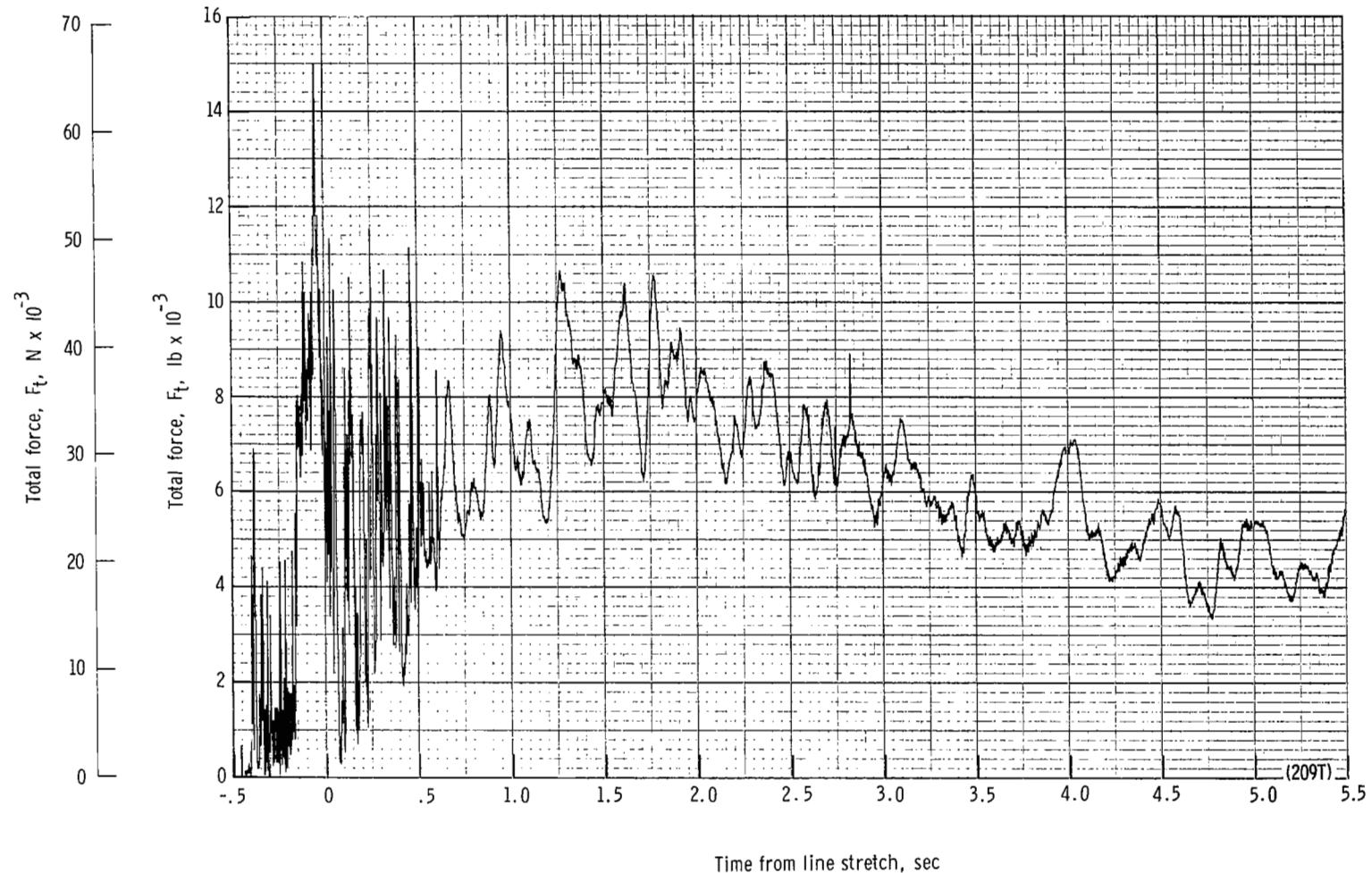
(b) Individual suspension-line loads F_{Lle3} and F_{Lle6} plotted against time from line stretch. Time = 0 second corresponds to 28.82 seconds after launch.

Figure 50.- Continued.



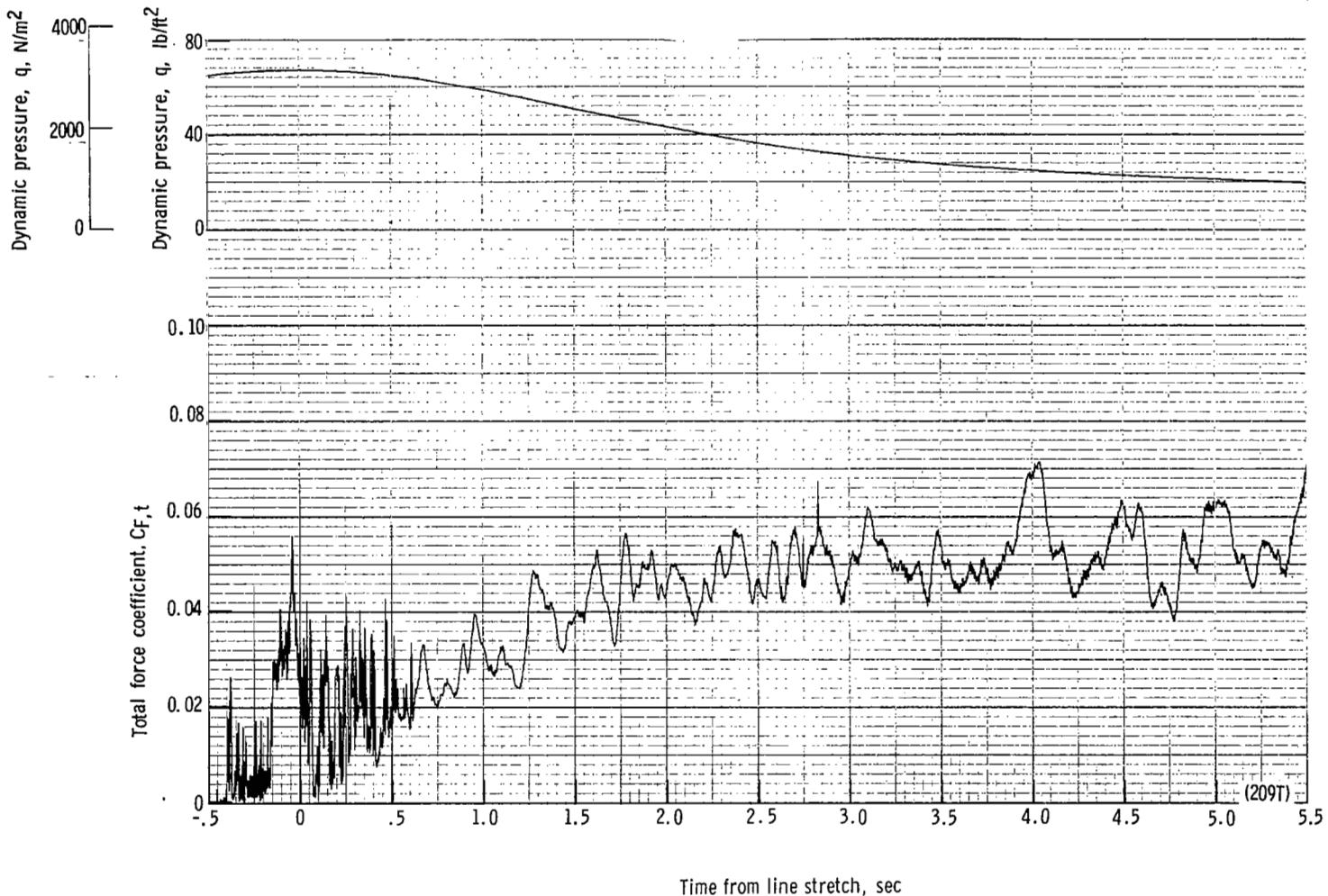
(c) Forward and aft riser loads and acceleration as plotted against time from line stretch. Time = 0 second corresponds to 28.82 seconds after launch.

Figure 50.- Continued.



(d) Total force F_t plotted against time from line stretch. Time = 0 second corresponds to 28.82 seconds after launch.

Figure 50.- Continued.



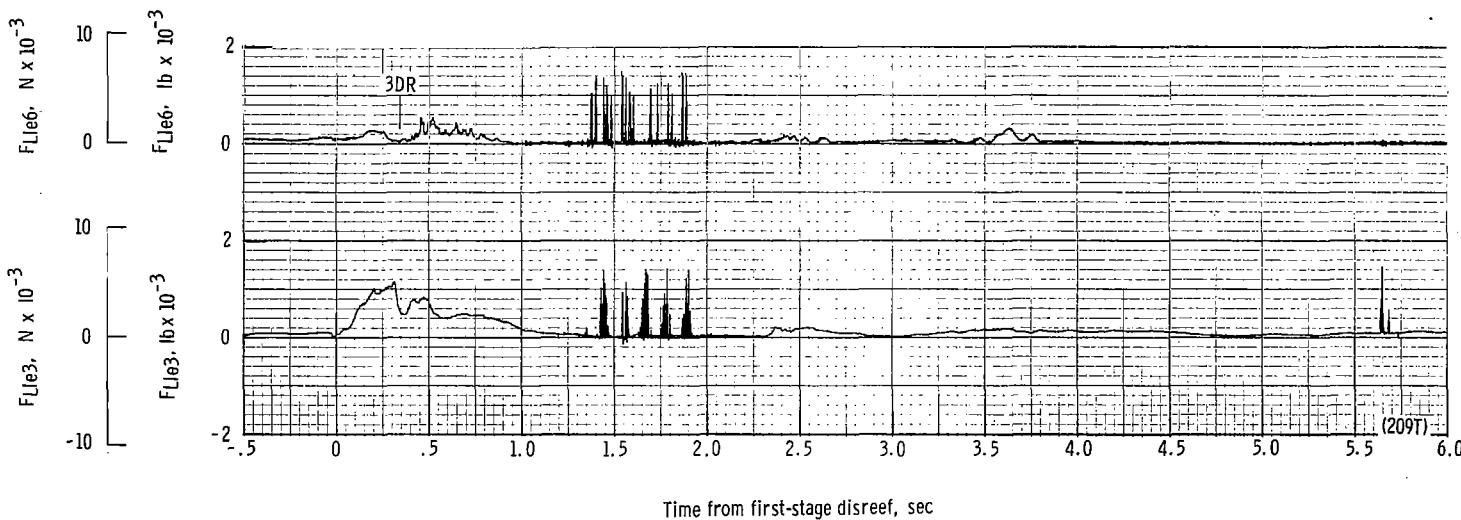
(e) Total force coefficient $C_{F,t}$ and dynamic pressure q plotted against time from line stretch. Time = 0 second corresponds to 28.82 seconds after launch.

Figure 50.- Continued.



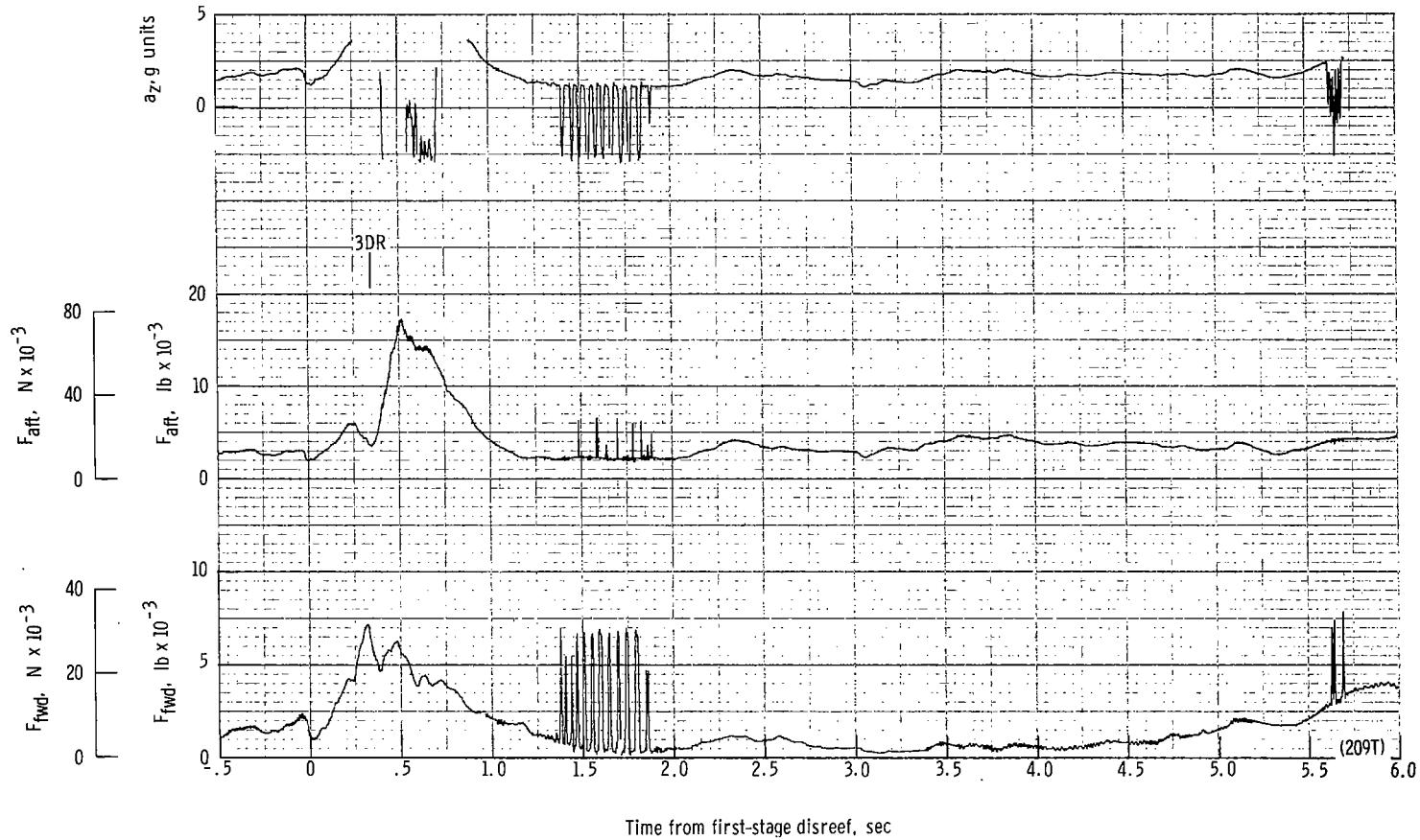
(f) Individual suspension-line loads F_{Lk12} , F_{Lle4} , F_{Lle2} , and F_{Lle1} plotted against time from first-stage disreef. Time = 0 second corresponds to 35.07 seconds after launch.

Figure 50.- Continued.



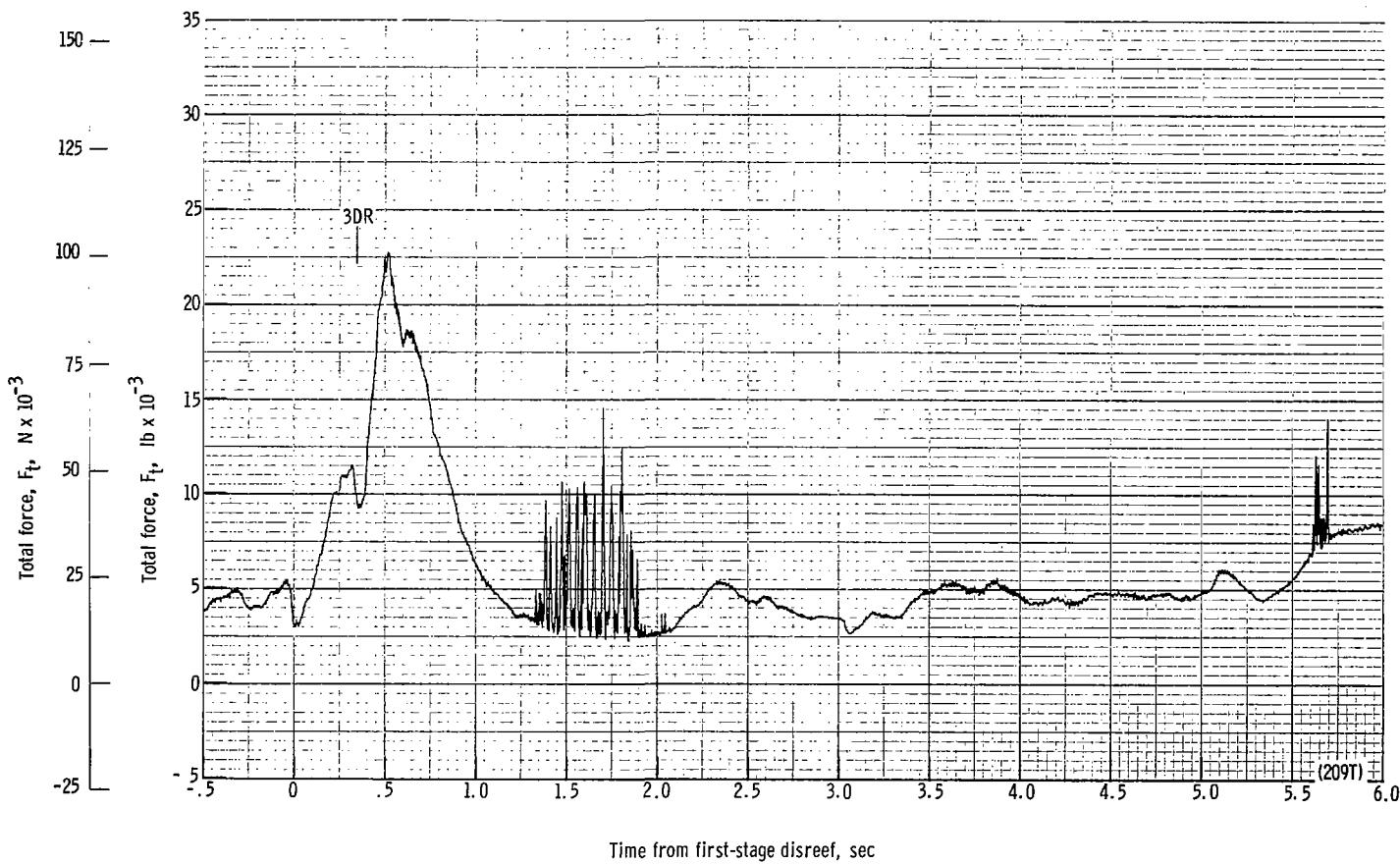
(g) Individual suspension-line loads F_{Lle3} and F_{Lle6} plotted against time from first-stage disreef. Time = 0 second corresponds to 35.07 seconds after launch.

Figure 50.- Continued.



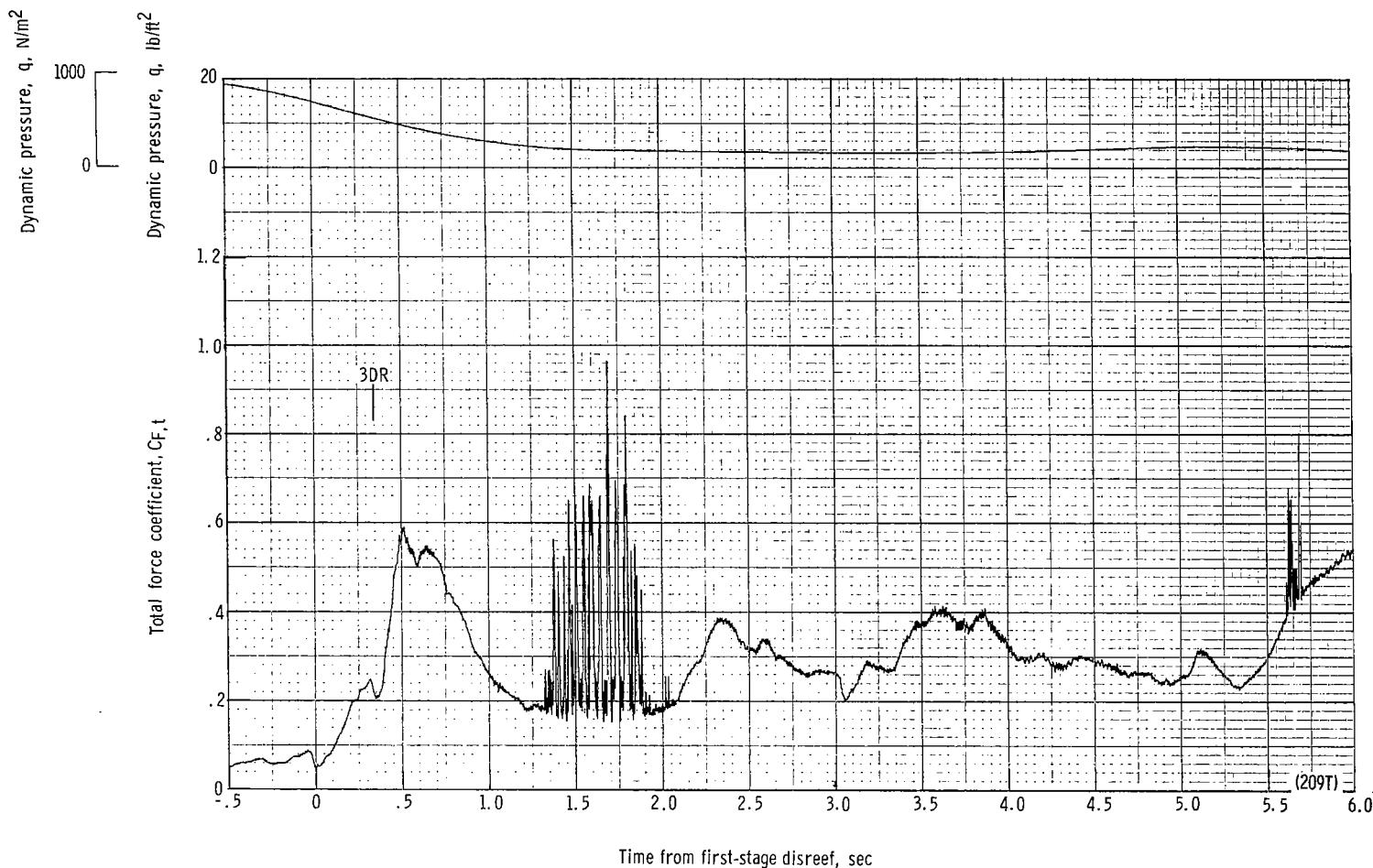
(h) Forward and aft riser loads and acceleration a_Z plotted against time from first-stage disreef. Time = 0 second corresponds to 35.07 seconds after launch.

Figure 50.- Continued.



(ii) Total force F_t plotted against time from first-stage disreef. Time = 0 second corresponds to 35.07 seconds after launch.

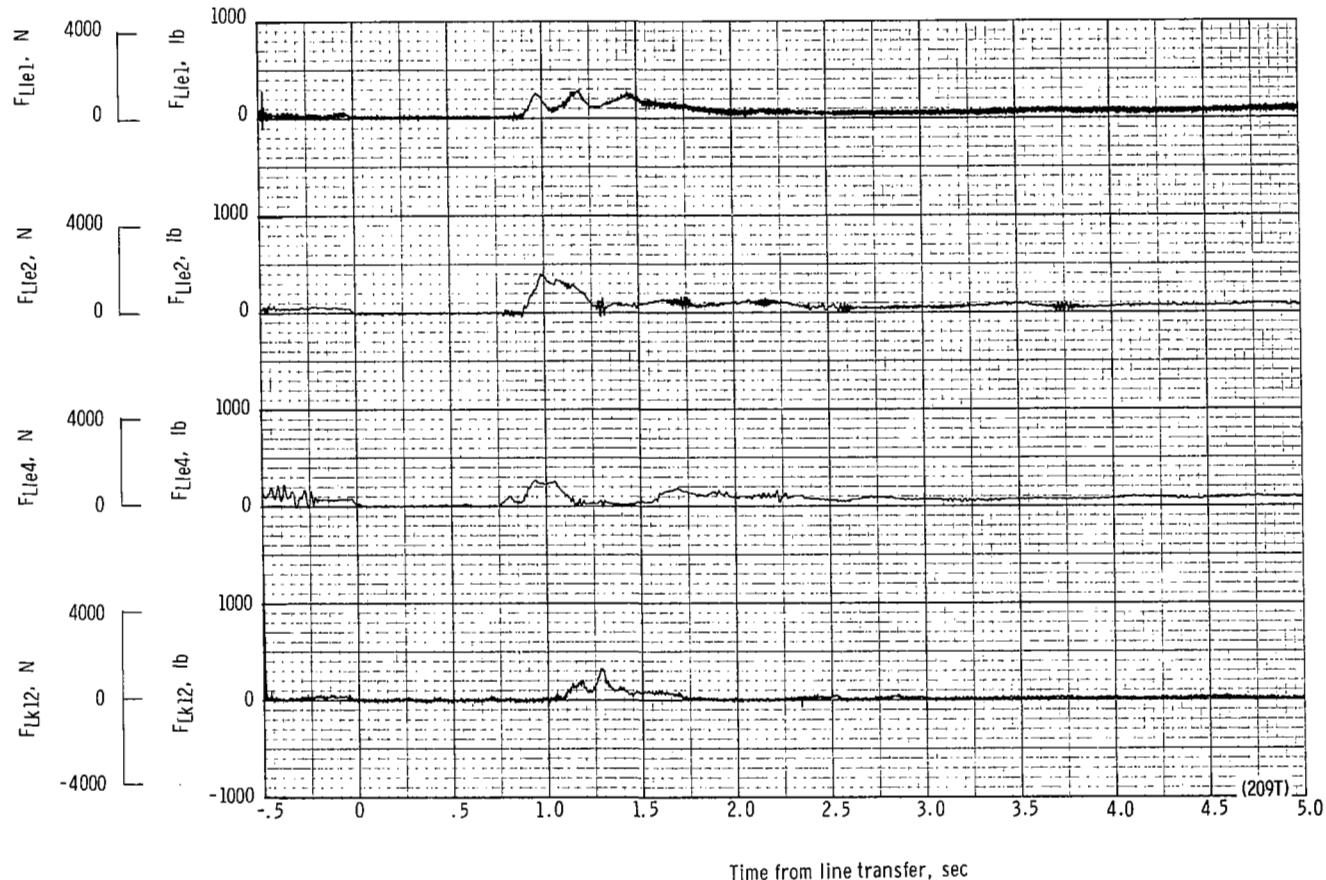
Figure 50.- Continued.



(j) Total force coefficient $C_{F,t}$ and dynamic pressure q plotted against time from first-stage disreef. Time = 0 second corresponds to 35.07 seconds after launch.

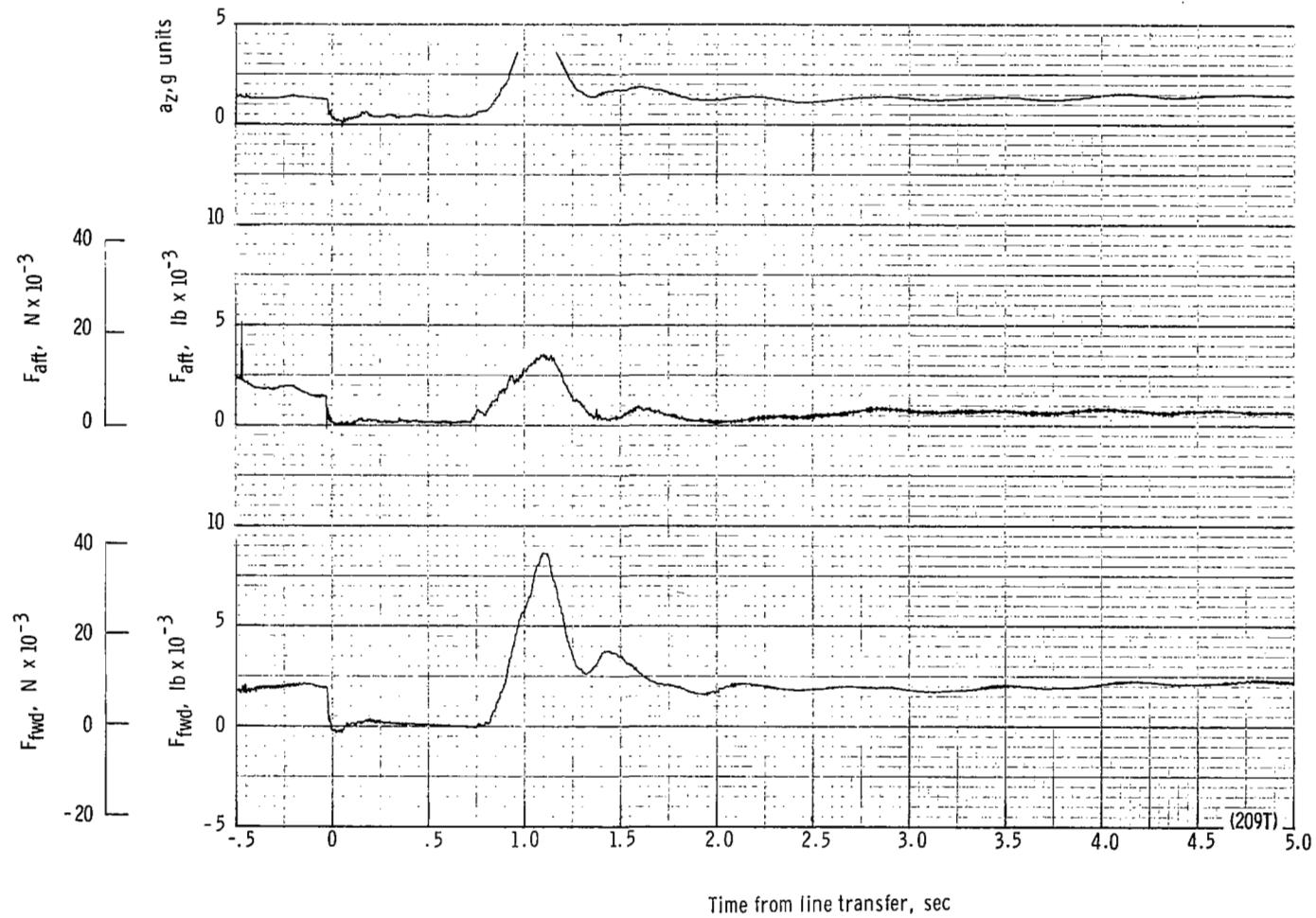
Figure 50.- Continued.

Note: Third-stage trailing-edge gathering line failed at $t = 35.41$ sec, resulting in premature third-stage disreef. Second-stage disreef was not distinguishable. Therefore, parts (k) to (t) of figure 50 are omitted.



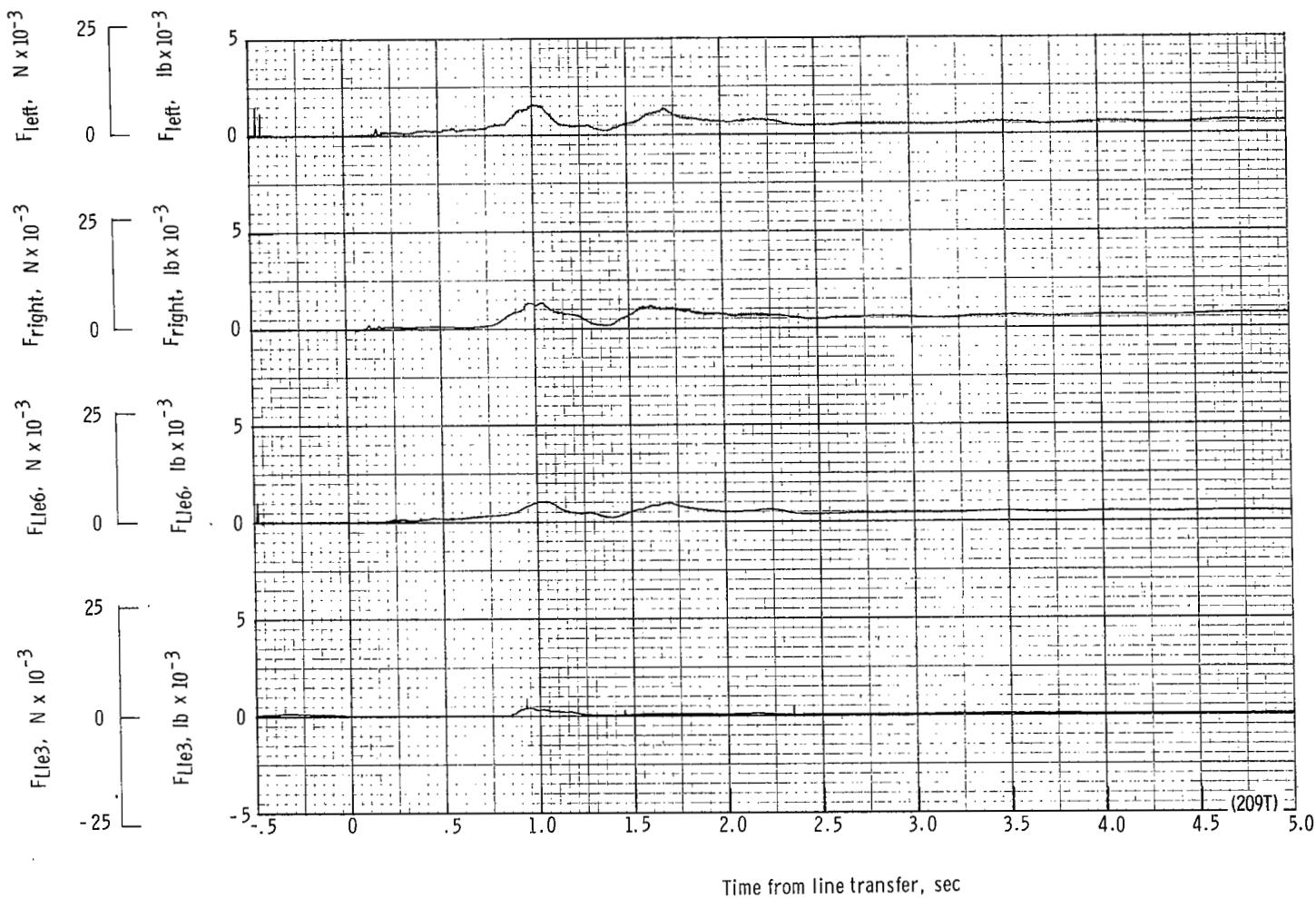
(u) Individual suspension-line loads F_{Lk12} , F_{Lle4} , F_{Lle2} , and F_{Lle1} plotted against time from line transfer. Time = 0 second corresponds to 45.47 seconds after launch.

Figure 50.- Continued.



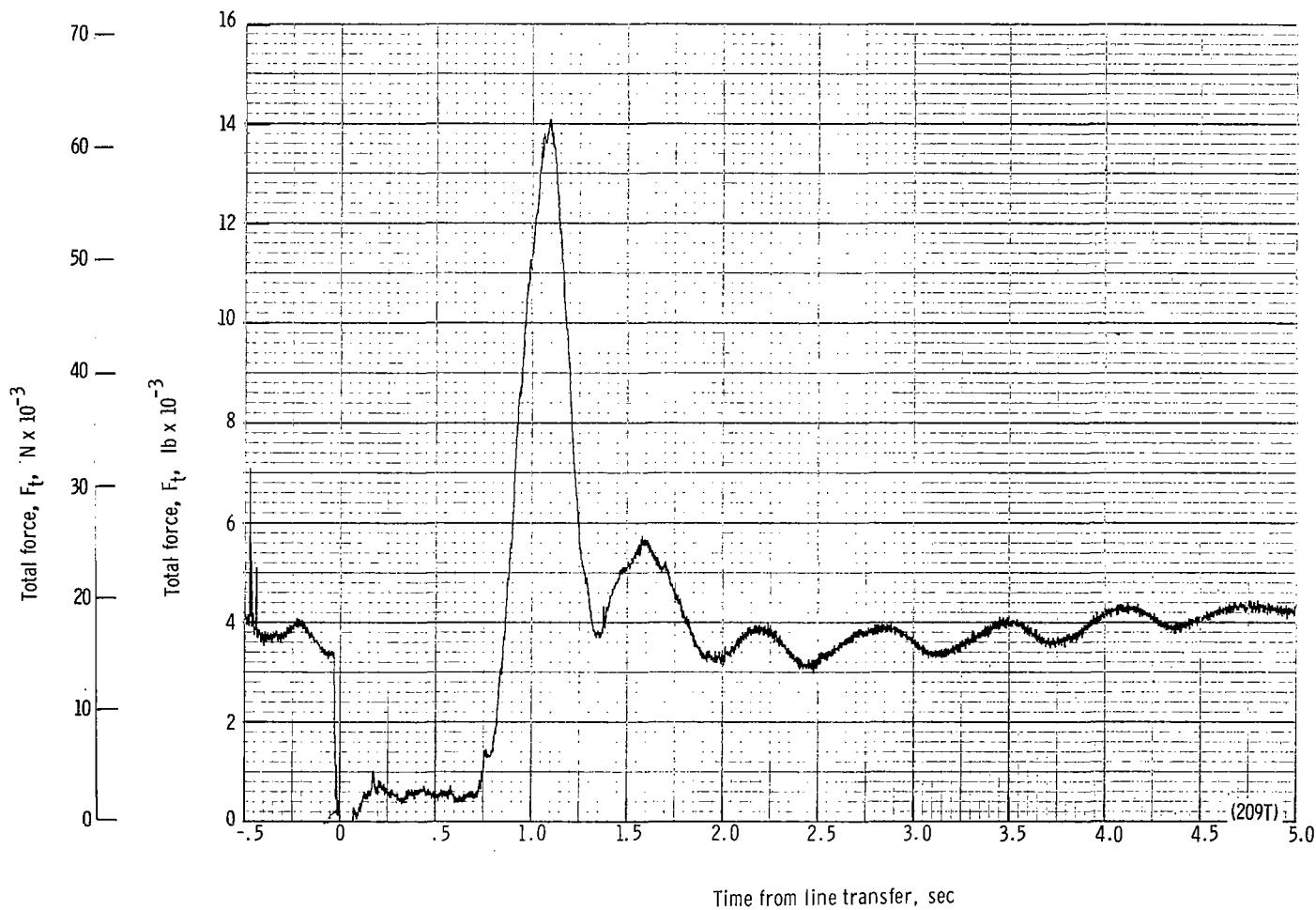
(v) Forward and aft riser loads and acceleration a_z plotted against time from line transfer. Time = 0 second corresponds to 45.47 seconds after launch.

Figure 50.- Continued.



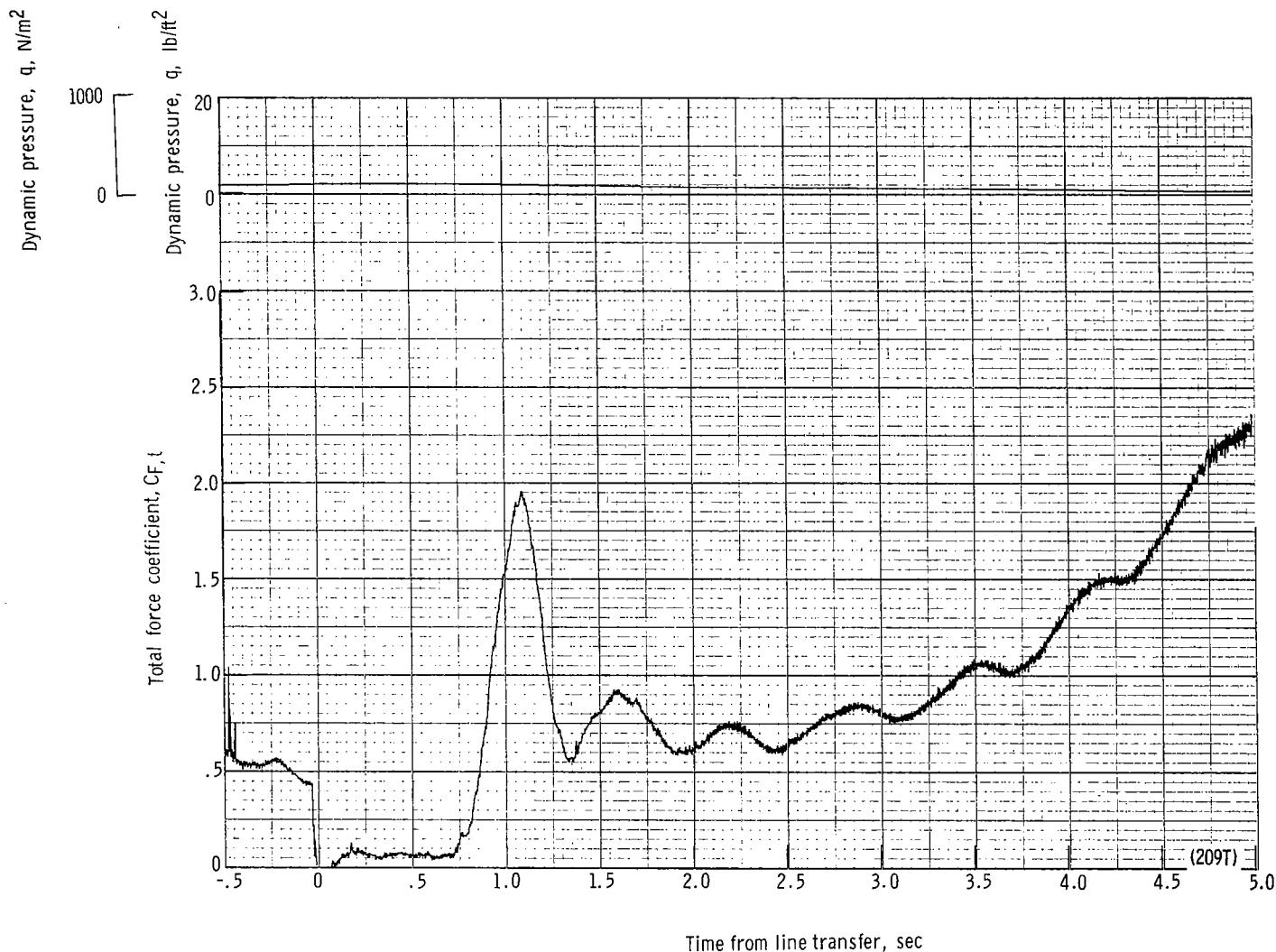
(w) Individual suspension-line loads F_{Lle3} and F_{Lle6} and right and left suspension-line loads plotted against time from line transfer. Time = 0 second corresponds to 45.47 seconds after launch.

Figure 50.- Continued.



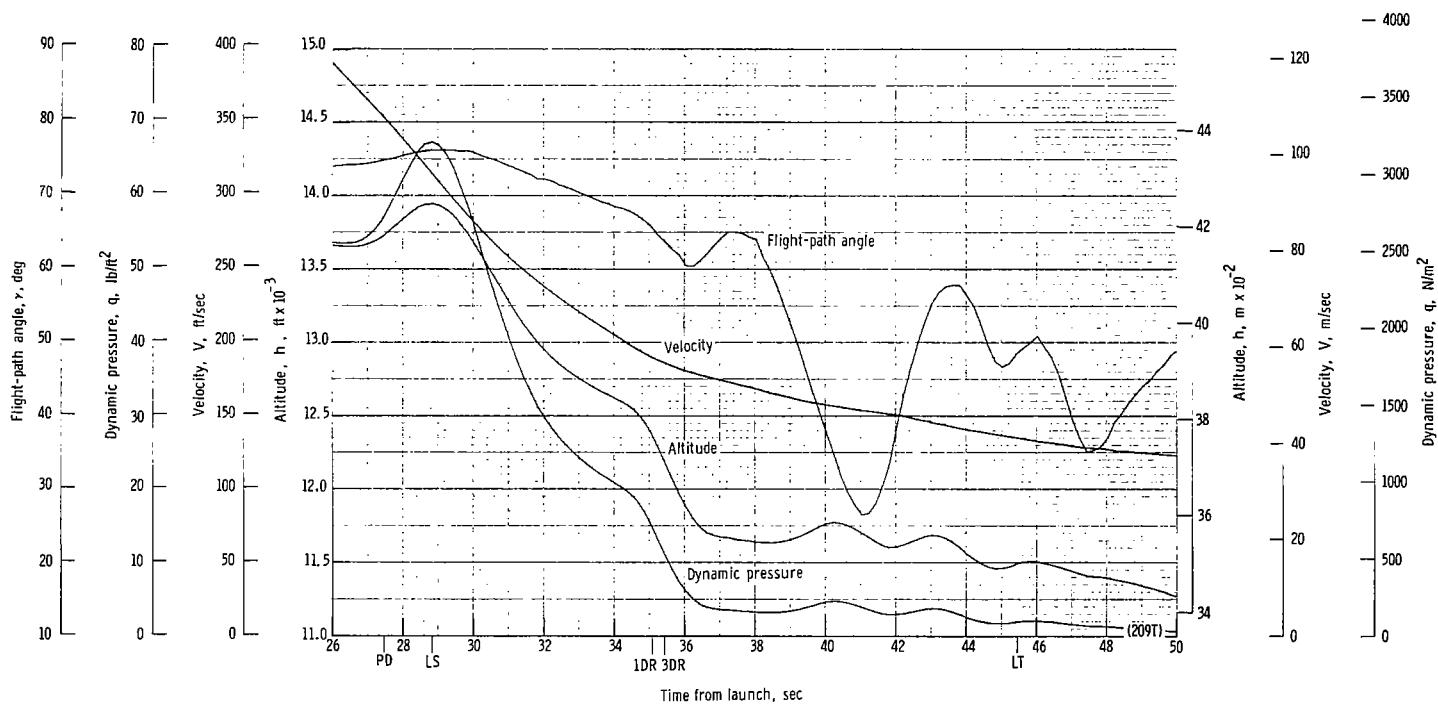
(x) Total force F_t plotted against time from line transfer. Time = 0 second corresponds to 45.47 seconds after launch.

Figure 50.- Continued.



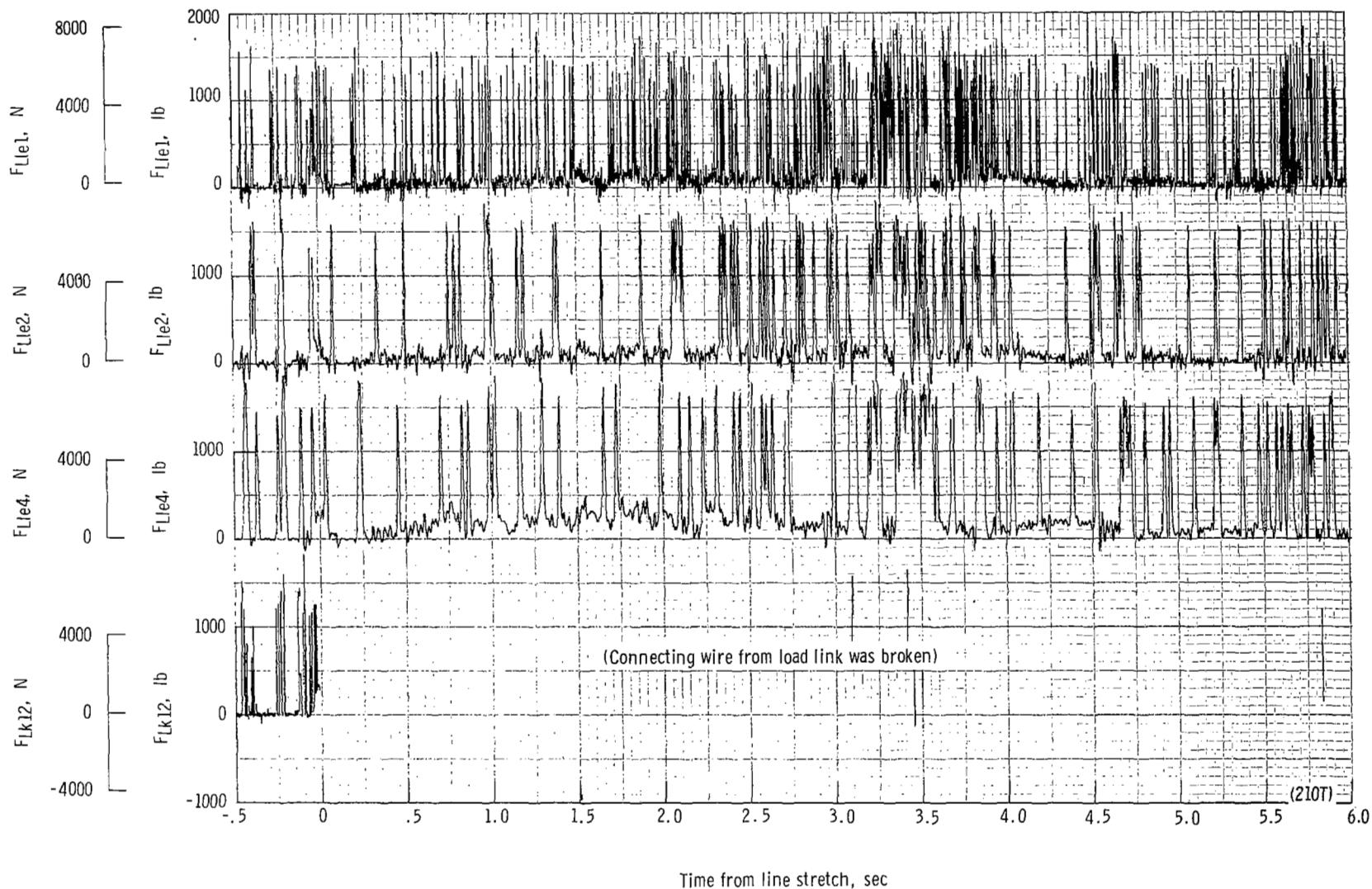
(y) Total force coefficient $C_{F,t}$ and dynamic pressure q plotted against time from line transfer. Time = 0 second corresponds to 45.47 seconds after launch.

Figure 50.- Continued.



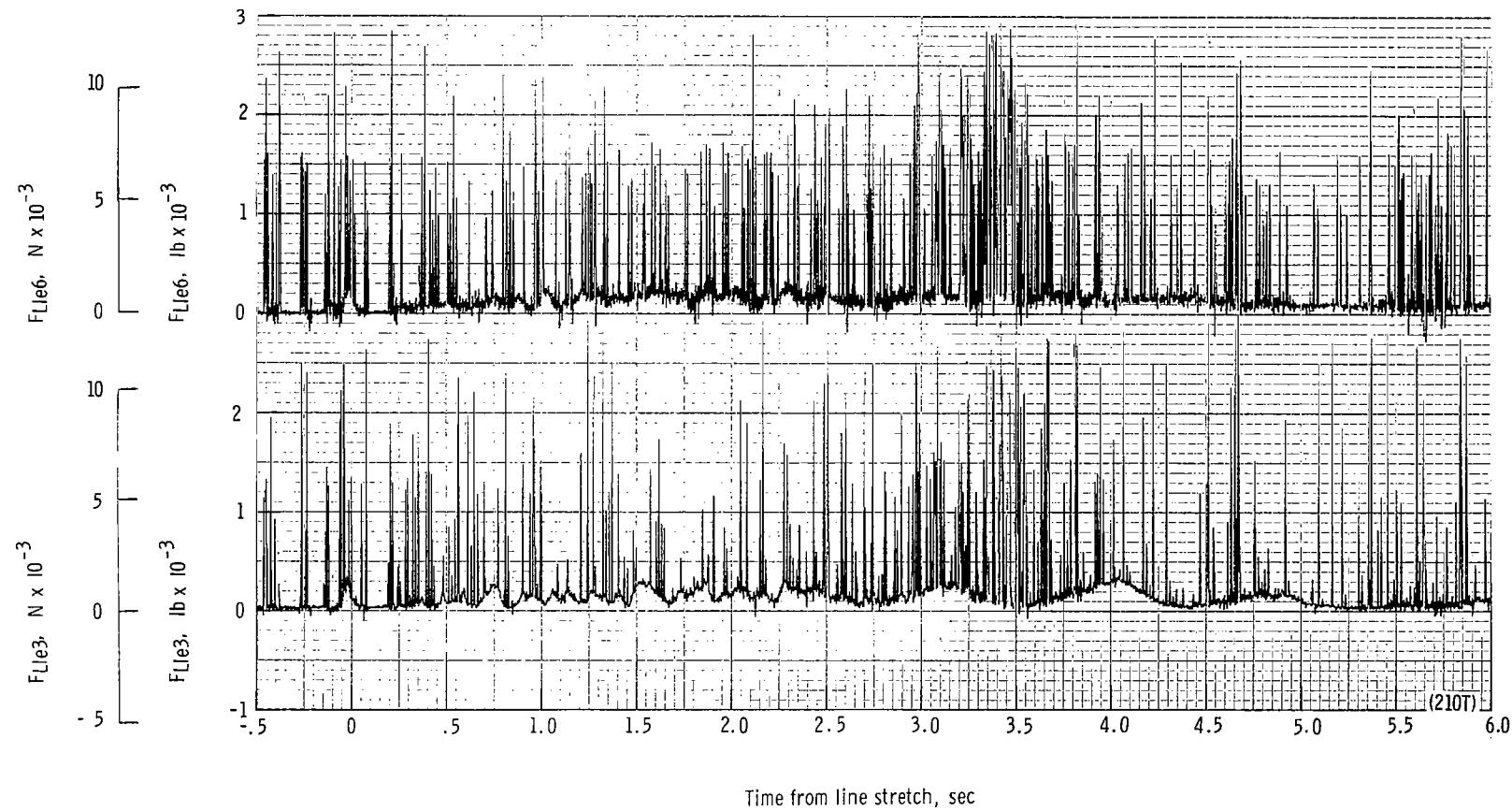
(z) Flight-path angle γ , dynamic pressure q , velocity V , and altitude h plotted against time from launch.

Figure 50.- Concluded.



(a) Individual suspension-line loads F_{Lk12} , F_{Lle4} , F_{Lle2} , and F_{Lle1} plotted against time from line stretch. Time = 0 second corresponds to 24.54 seconds after launch.

Figure 51.- Time history of twin-keel parawing deployment data for test 210T. $W_D = 16\ 961\ N$ (3813 lb); $W_p = 15\ 097\ N$ (3394 lb); $q_{PD} = 2614.3\ N/m^2$ (54.6 lb/ft²); $h_{PD} = 5794\ m$ (19 010 ft); $l_r/l_k = 0.080$; reefing version C.



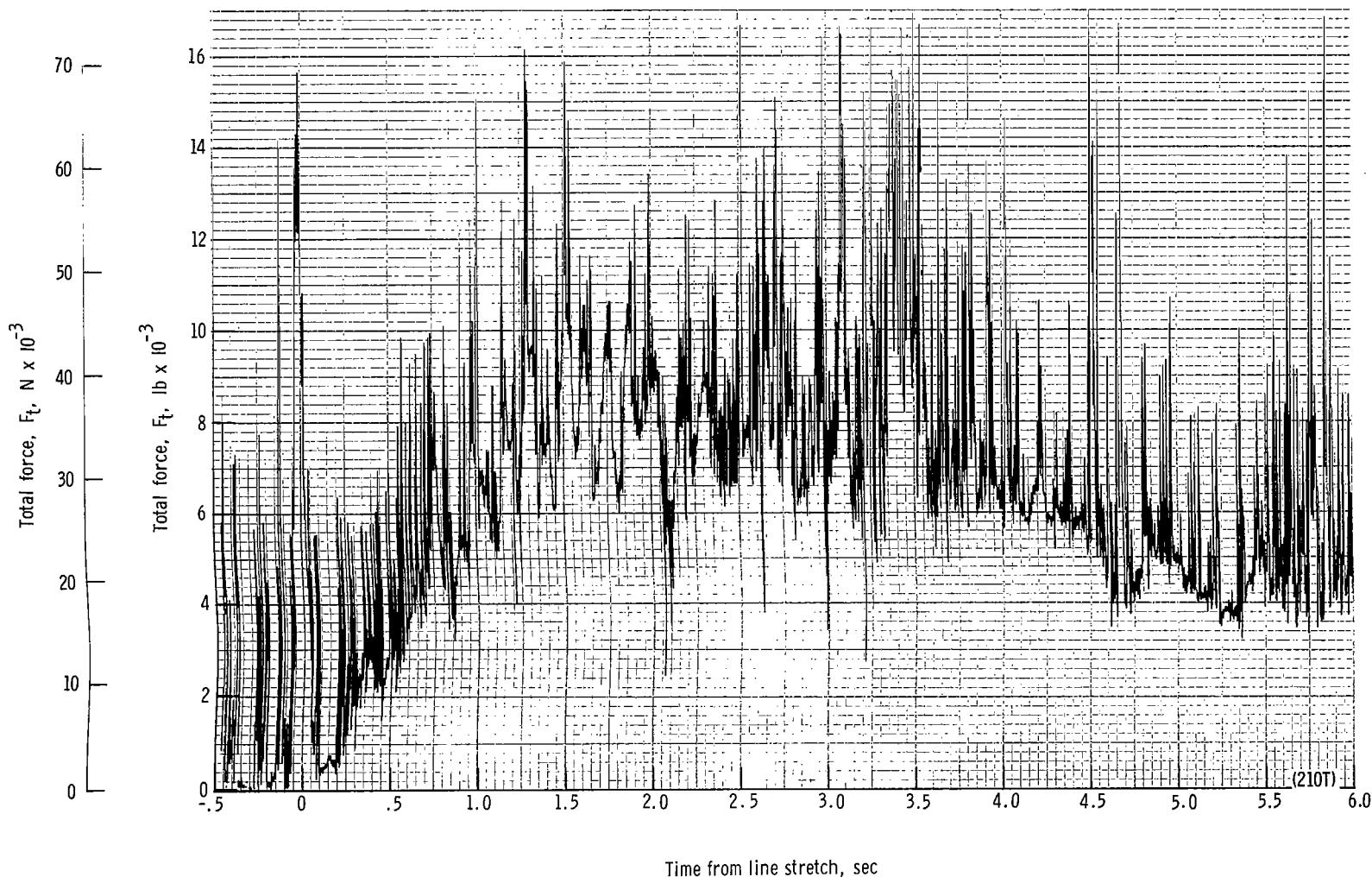
(b) Individual suspension-line loads F_{Lle3} and F_{Lle6} plotted against time from line stretch. Time = 0 second corresponds to 24.54 seconds after launch.

Figure 51.- Continued.



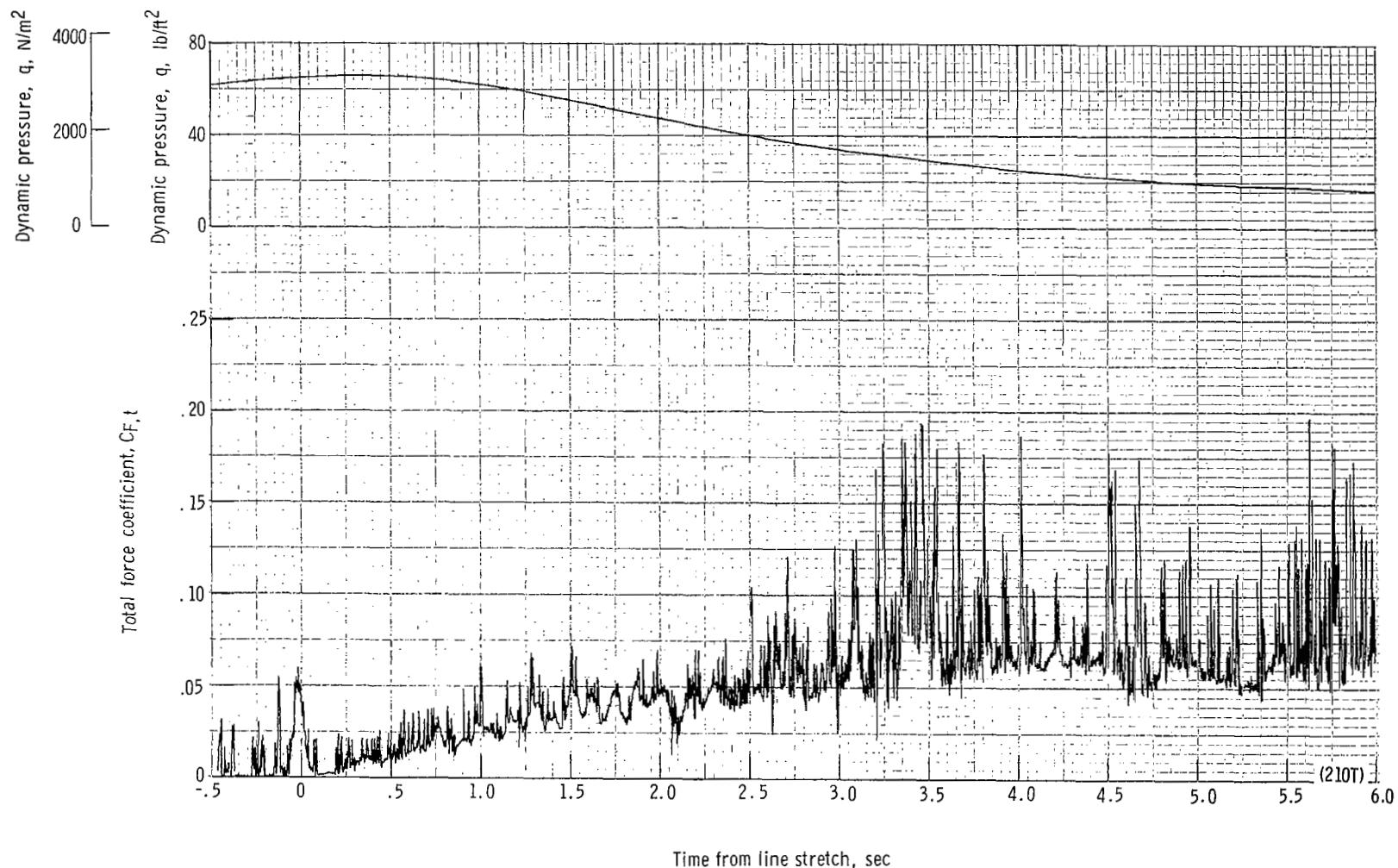
(c) Forward and aft riser loads and acceleration a_z plotted against time from line stretch. Time = 0 second corresponds to 24.54 seconds after launch.

Figure 51.- Continued.



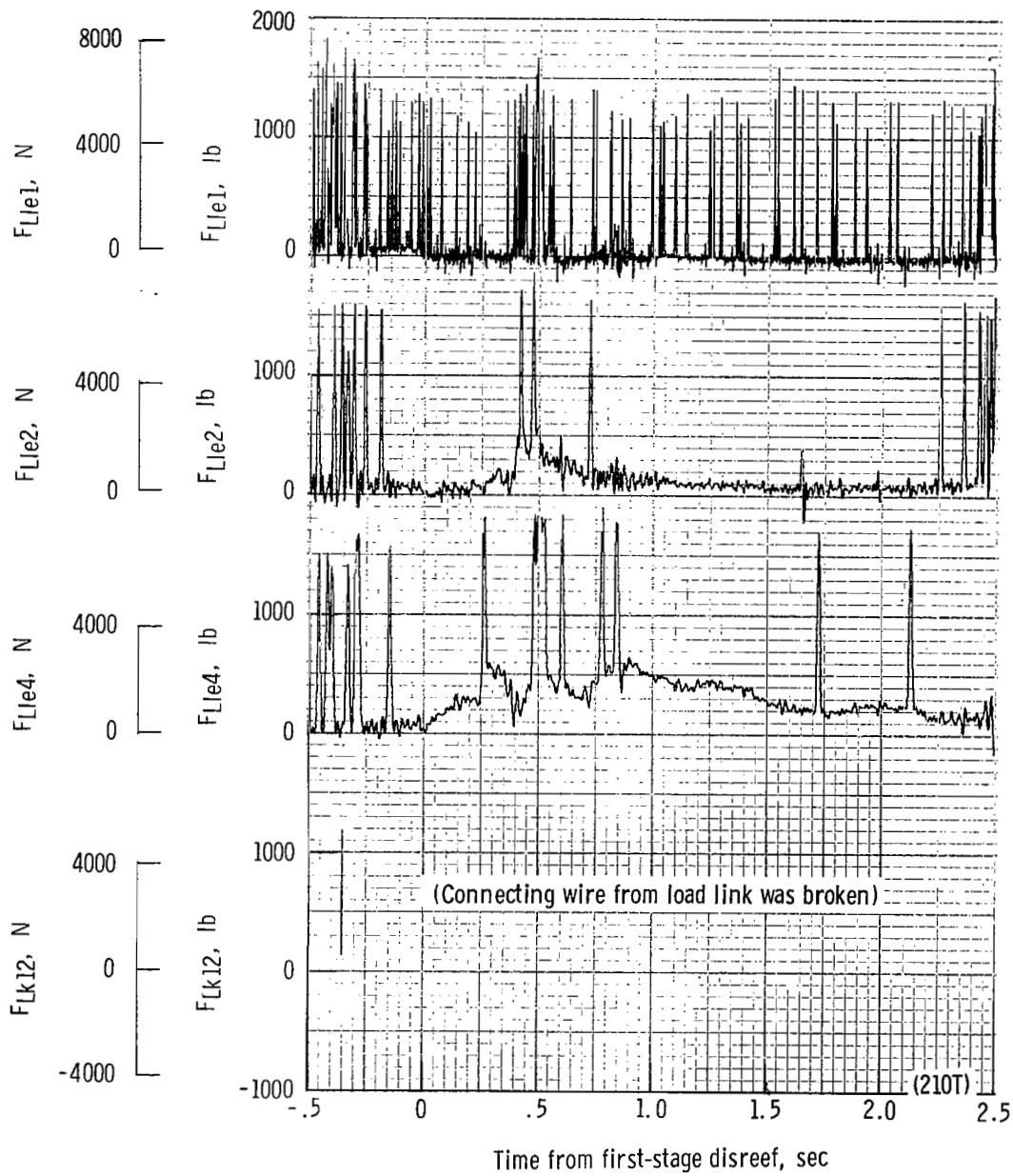
(d) Total force F_t plotted against time from line stretch. Time = 0 second corresponds to 24.54 seconds after launch.

Figure 51.- Continued.



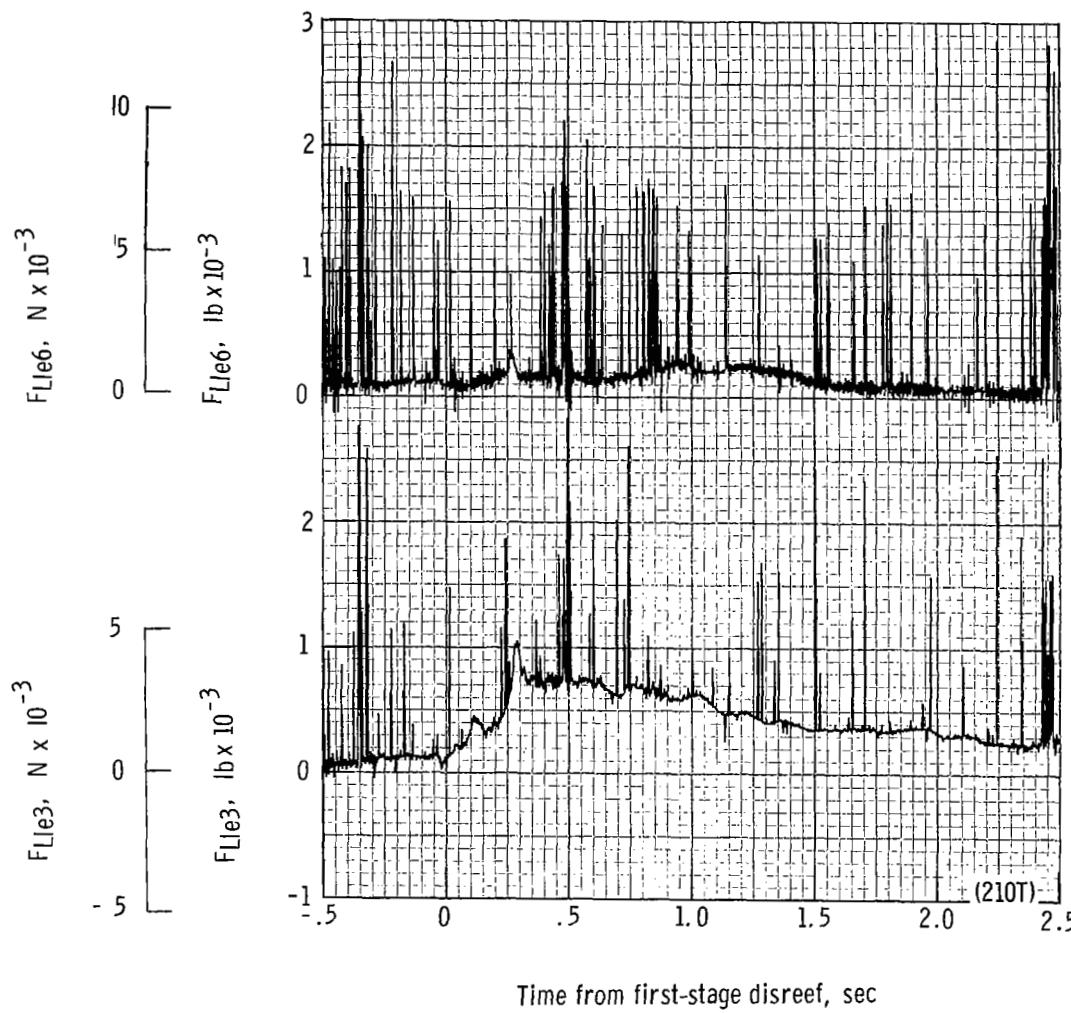
(e) Total force coefficient $C_{F,t}$ and dynamic pressure q plotted against time from line stretch. Time = 0 second corresponds to 24.54 seconds after launch.

Figure 51.- Continued.



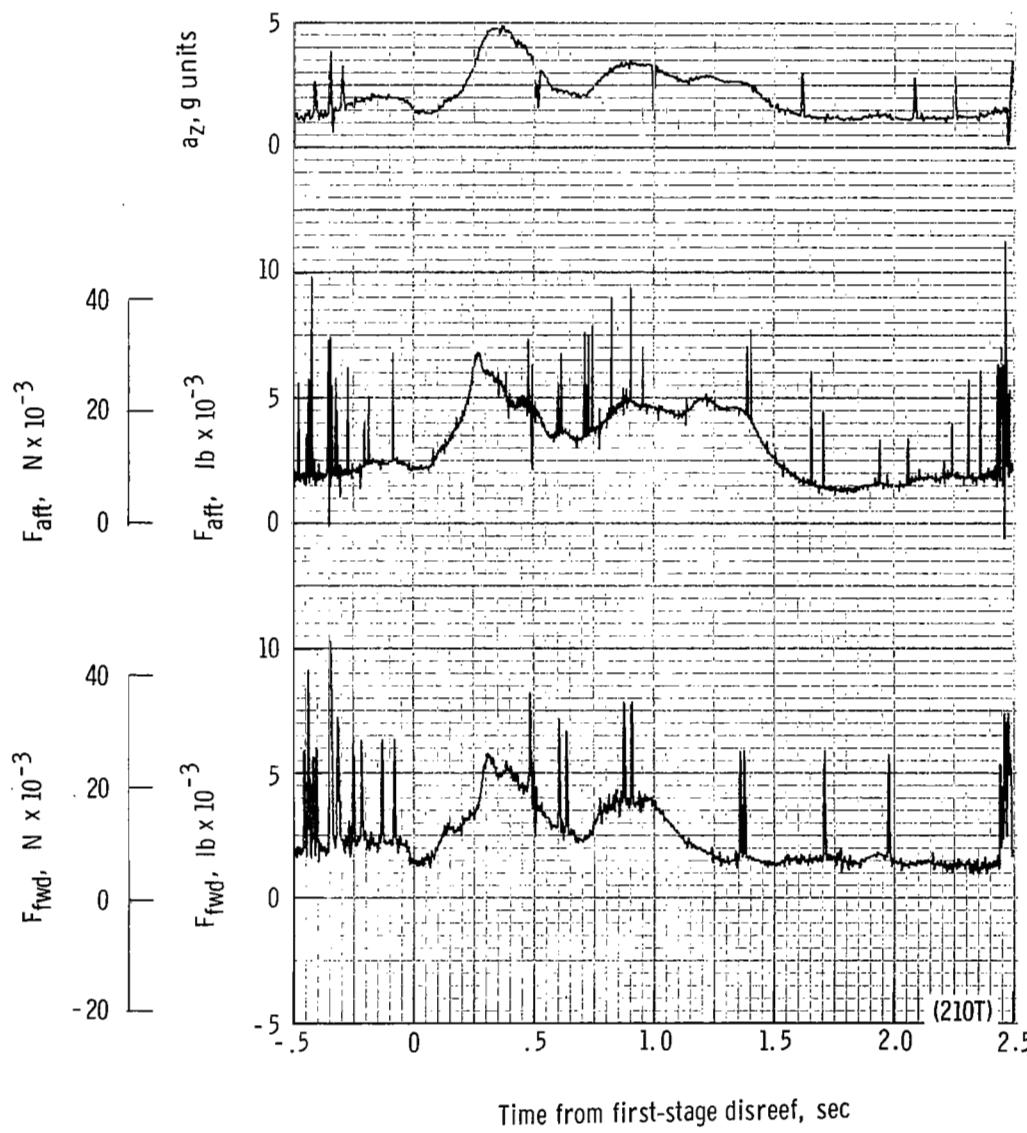
(f) Individual suspension-line loads F_{Lk12} , F_{Lle4} , F_{Lle2} , and F_{Lle1} plotted against time from first-stage disreef. Time = 0 second corresponds to 30.74 seconds after launch.

Figure 51.- Continued.



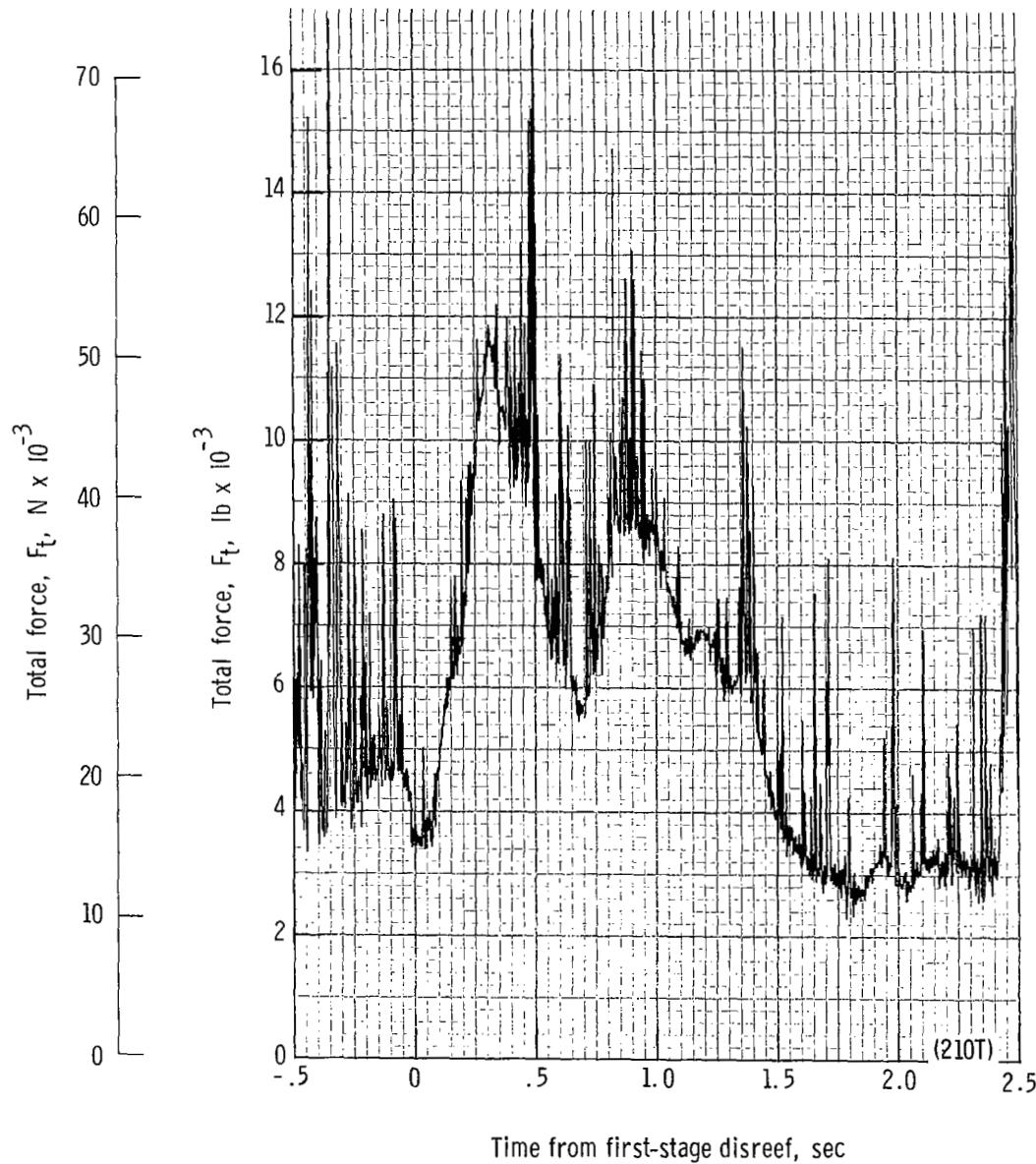
(g) Individual suspension-line loads $F_{Ll e3}$ and $F_{Ll e6}$ plotted against time from first-stage disreef. Time = 0 second corresponds to 30.74 seconds after launch.

Figure 51.- Continued.



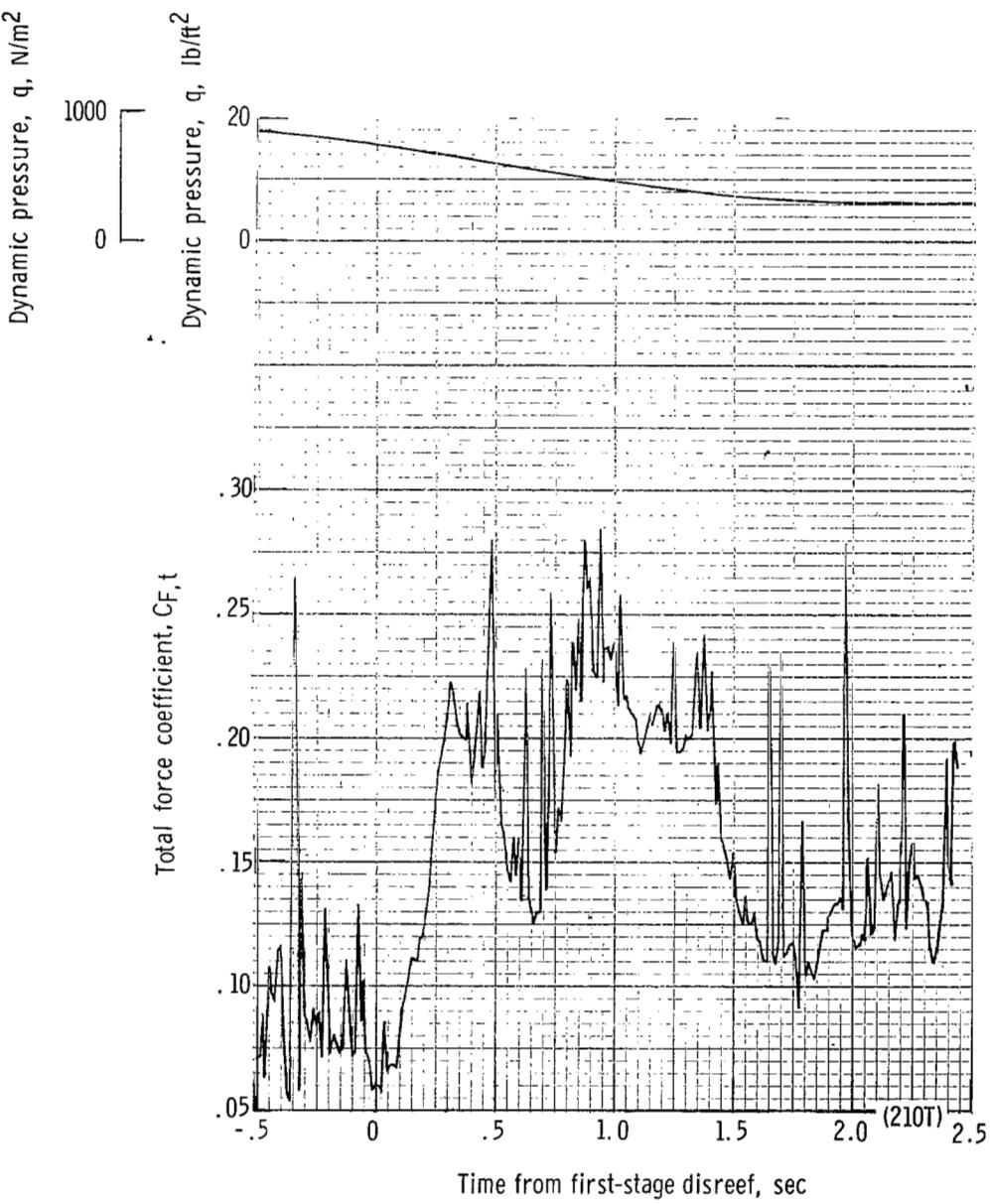
(h) Forward and aft riser loads and acceleration a_z plotted against time from first-stage disreef. Time = 0 second corresponds to 30.74 seconds after launch.

Figure 51.- Continued.



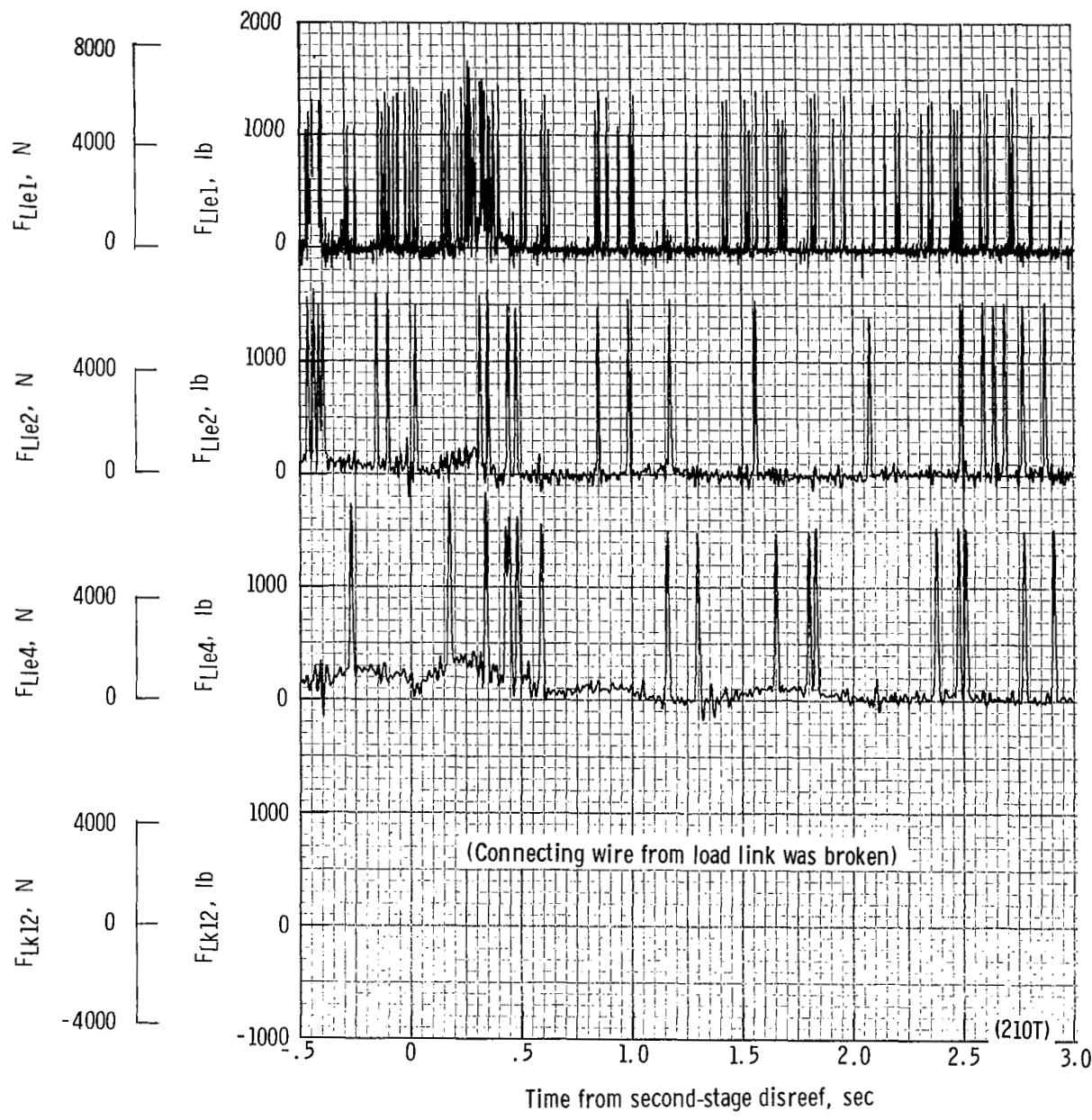
(i) Total force F_t plotted against time from first-stage disreef. Time = 0 second corresponds to 30.74 seconds after launch.

Figure 51.- Continued.



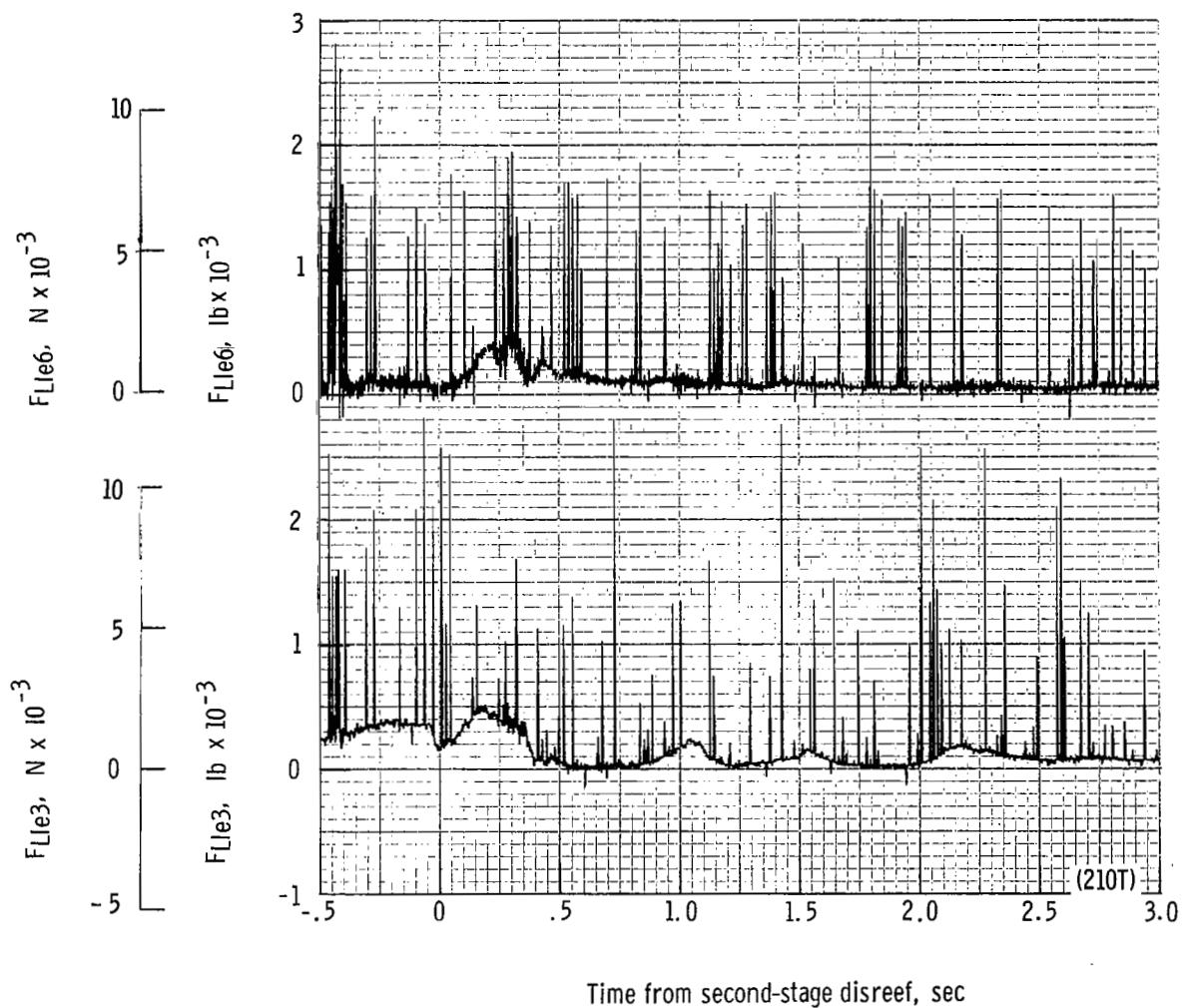
(j) Total force coefficient $C_{F,t}$ and dynamic pressure q plotted against time from first-stage disreef. Time = 0 second corresponds to 30.74 seconds after launch.

Figure 51.- Continued.



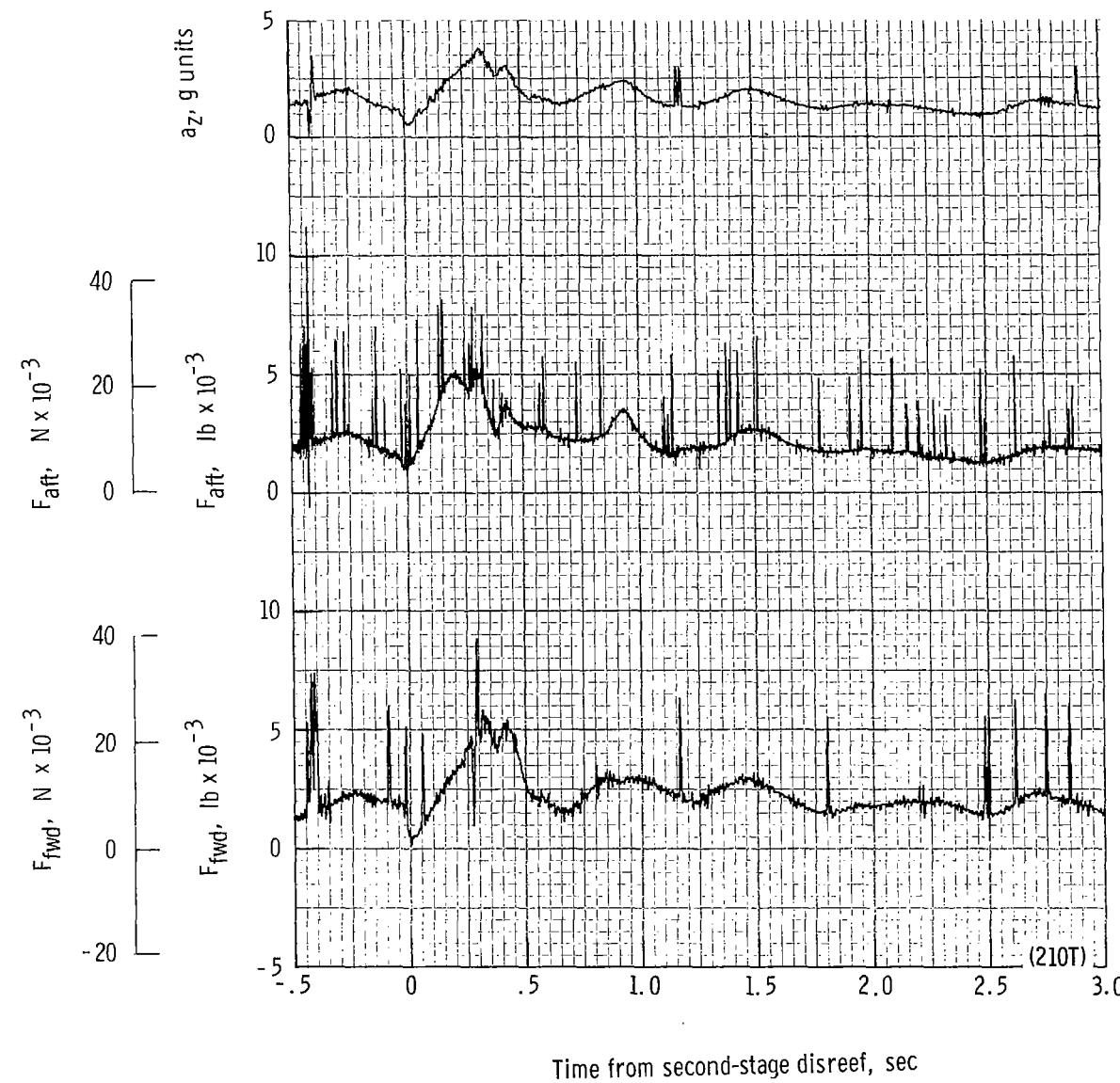
(k) Individual suspension-line loads F_{Lk12} , F_{Lle4} , F_{Lle2} , and F_{Lle1} plotted against time from second-stage disref. Time = 0 second corresponds to 35.64 seconds after launch.

Figure 51.- Continued.



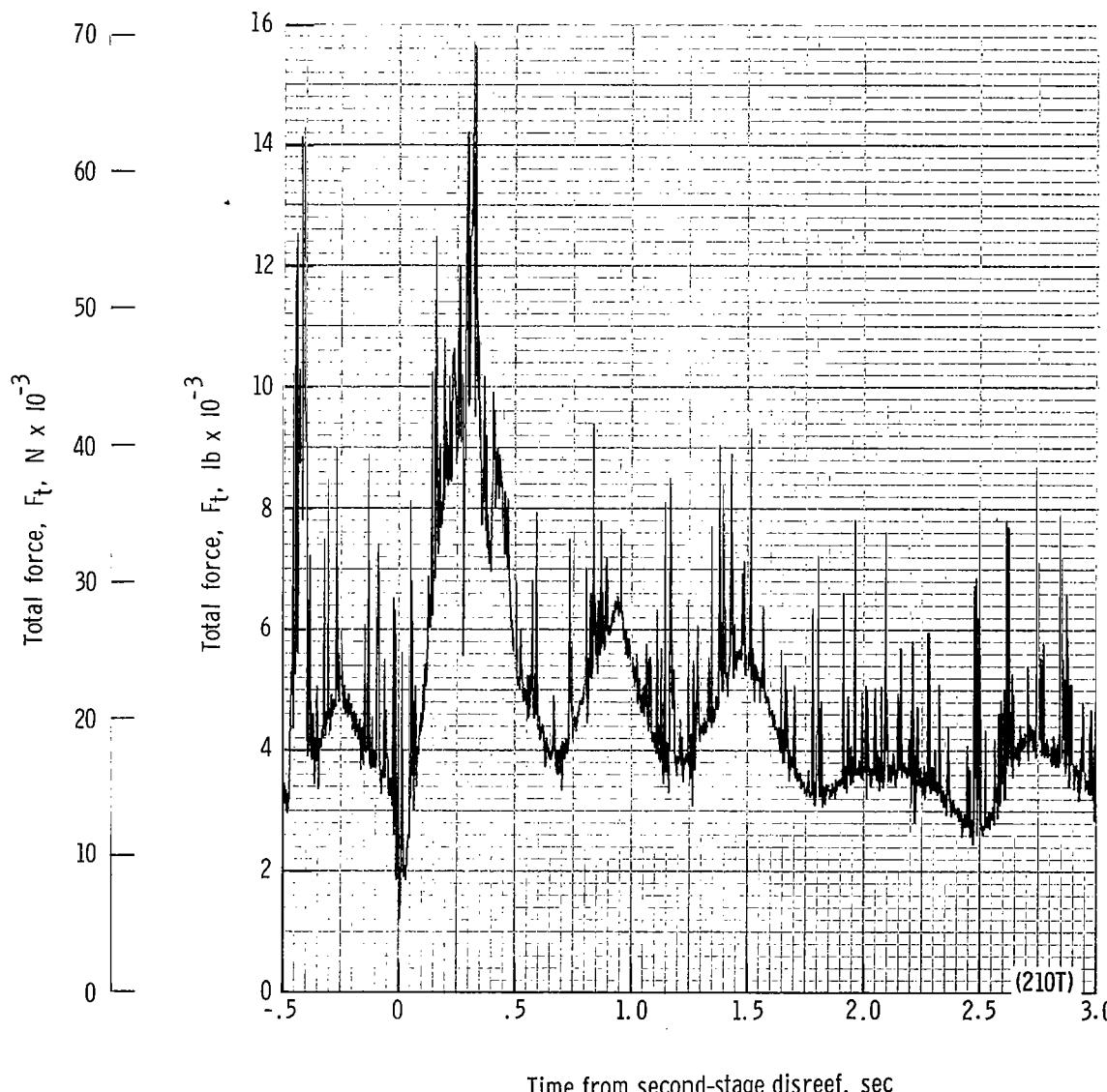
(II) Individual suspension-line loads F_{Lle3} and F_{Lle6} plotted against time from second-stage disreef. Time = 0 second corresponds to 35.64 seconds after launch.

Figure 51.- Continued.



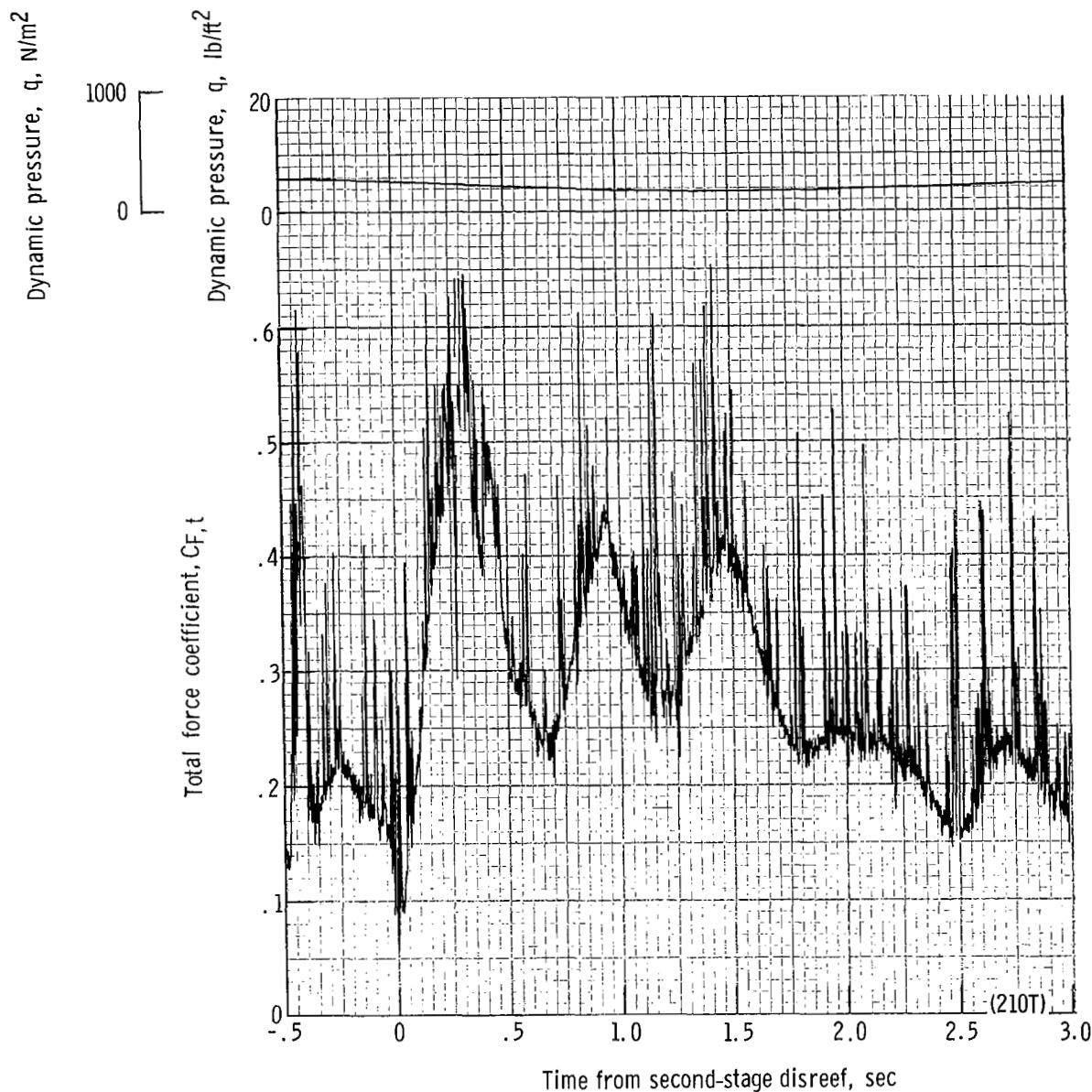
(m) Forward and aft riser loads and acceleration a_z plotted against time from second-stage disreef. Time = 0 second corresponds to 35.64 seconds after launch.

Figure 51.- Continued.



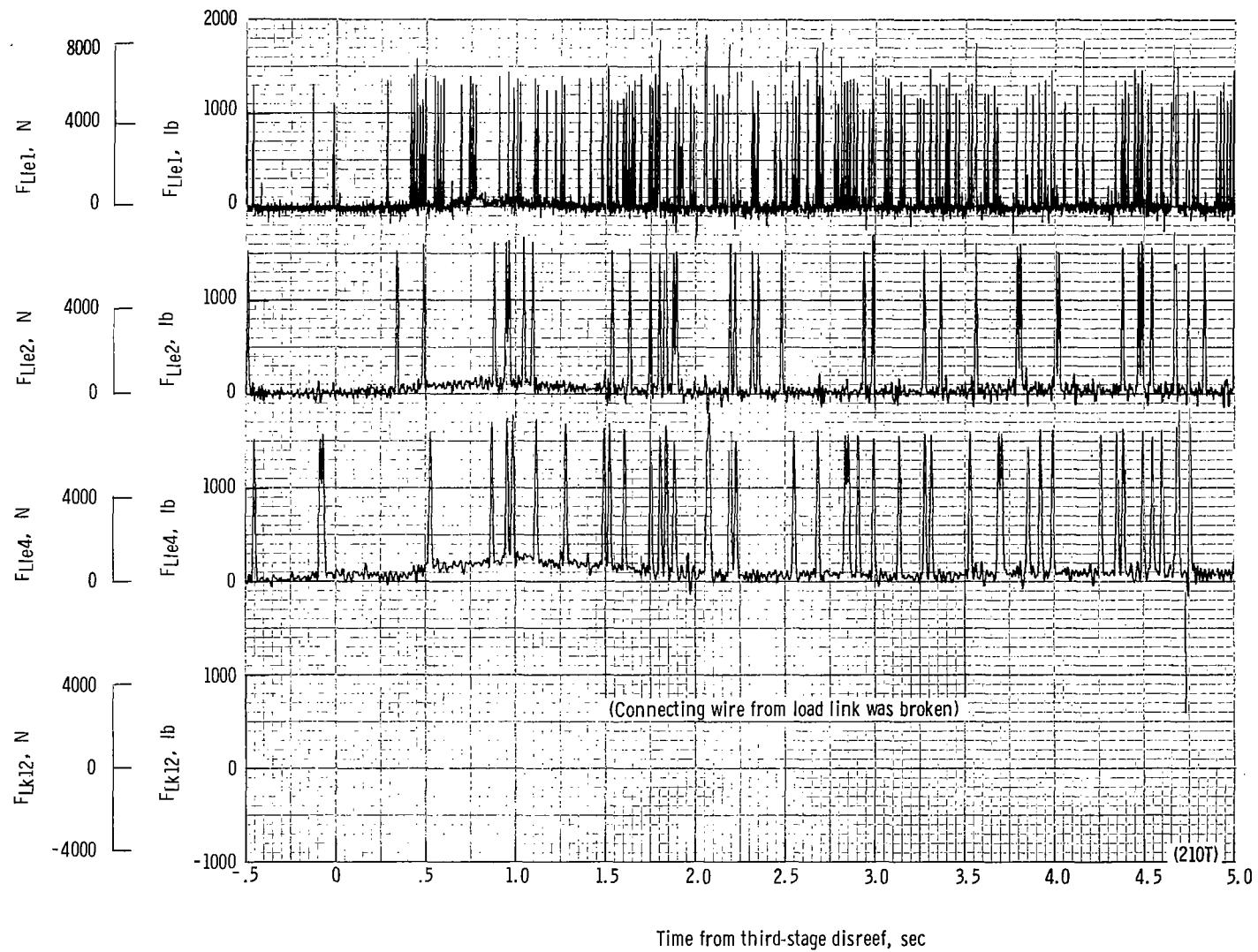
(n) Total force F_t plotted against time from second-stage disreef. Time = 0 second corresponds to 35.64 seconds after launch.

Figure 51.- Continued.



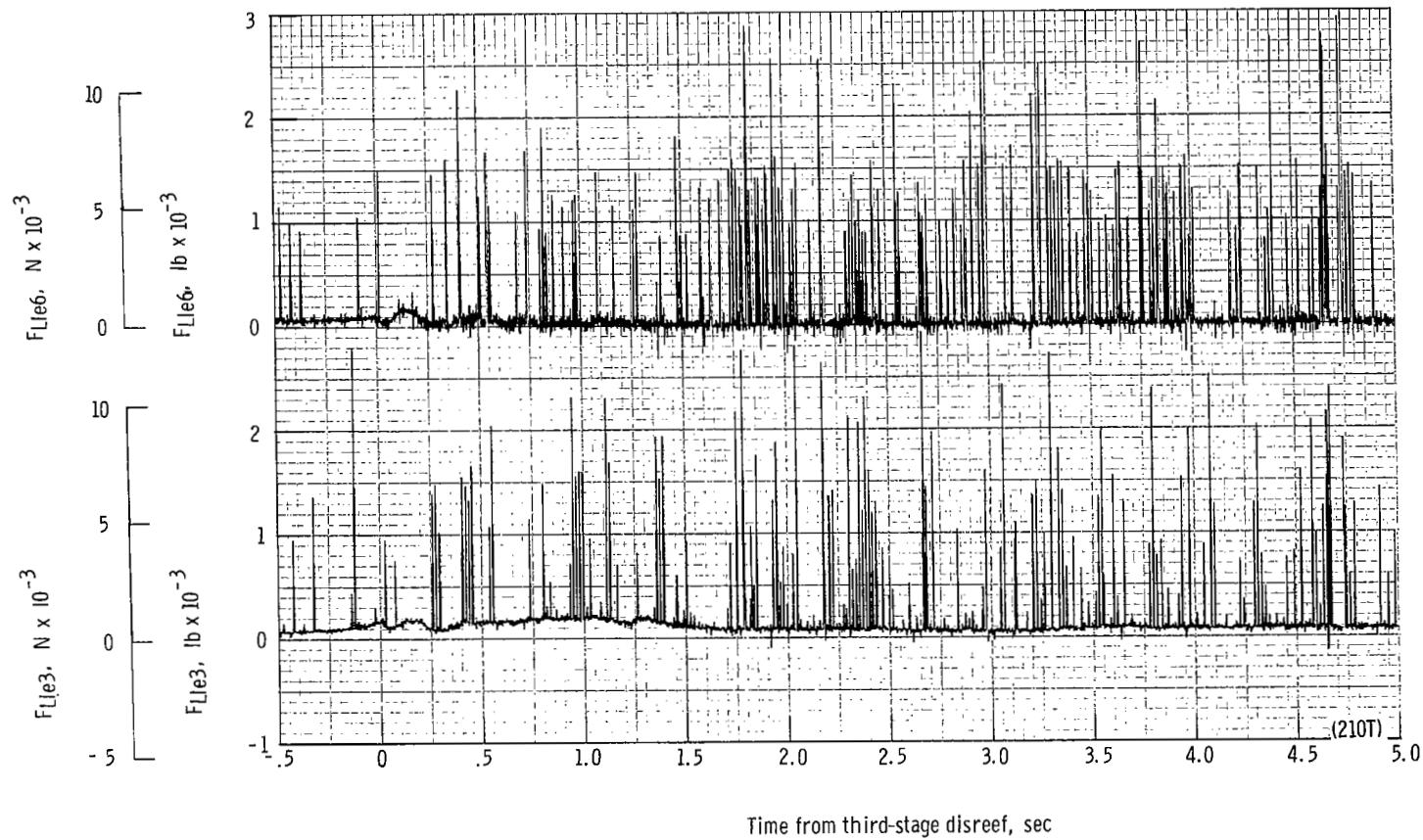
(a) Total force coefficient $C_{F,t}$ and dynamic pressure q plotted against time from second-stage disreef. Time = 0 second corresponds to 35.64 seconds after launch.

Figure 51.- Continued.



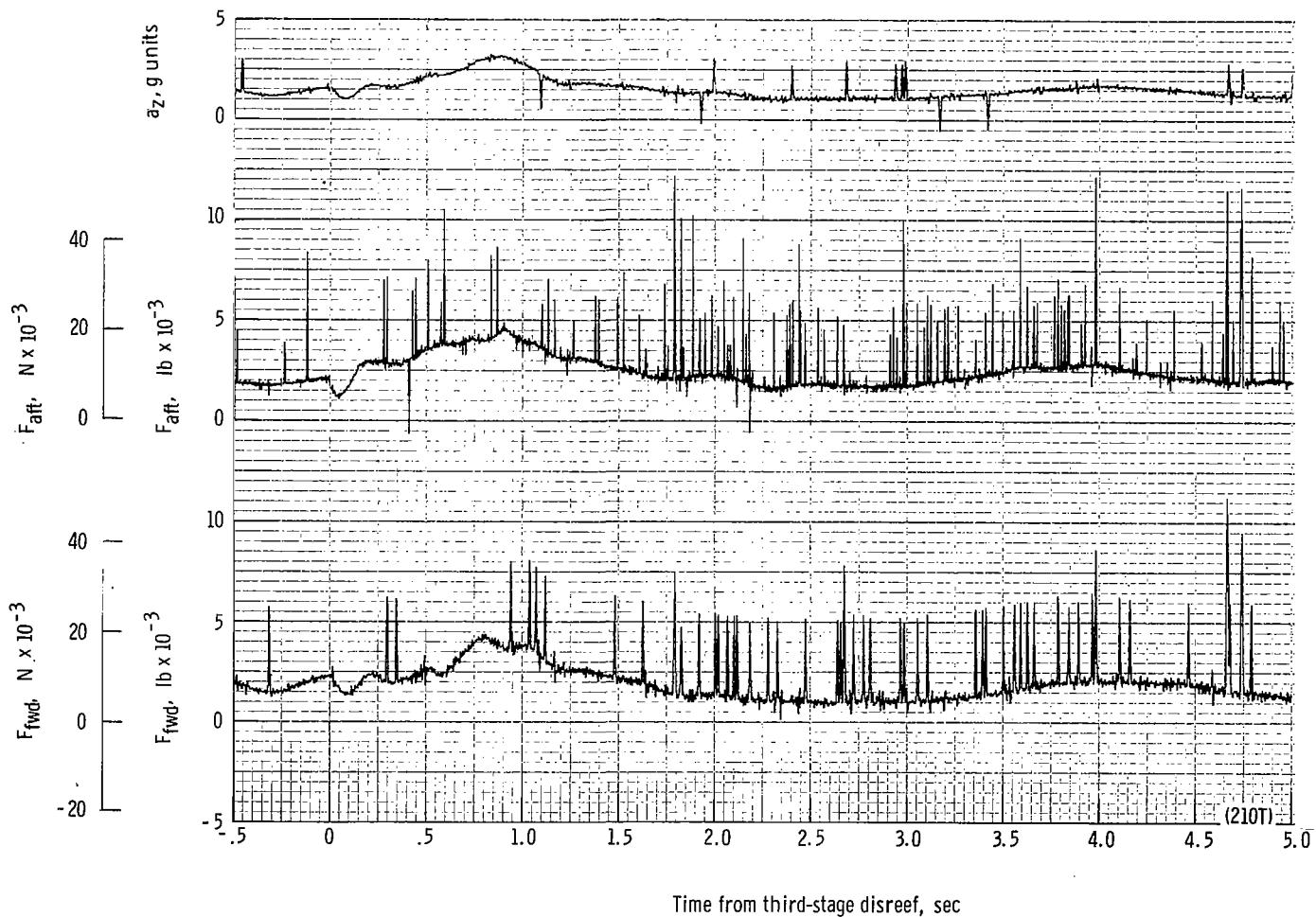
(p) Individual suspension-line loads F_{Lk12} , F_{Lle4} , F_{Lle2} , and F_{Lle1} plotted against time from third-stage disreef. Time = 0 second corresponds to 36.99 seconds after launch.

Figure 51.- Continued.



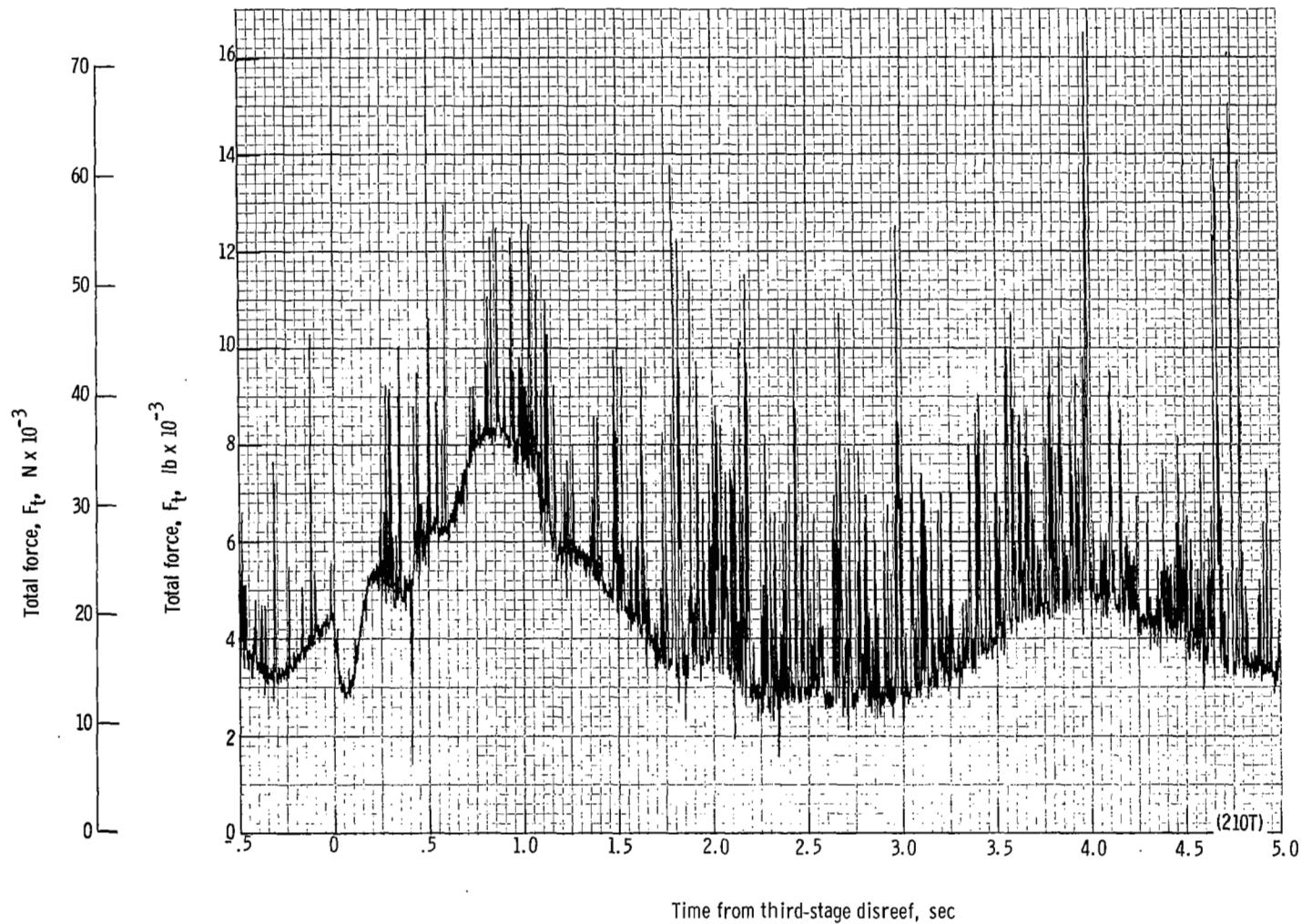
(q) Individual suspension-line F_{Lle3} and F_{Lle6} plotted against time from third-stage disreef. Time = 0 second corresponds to 36.99 seconds after launch.

Figure 51.- Continued.



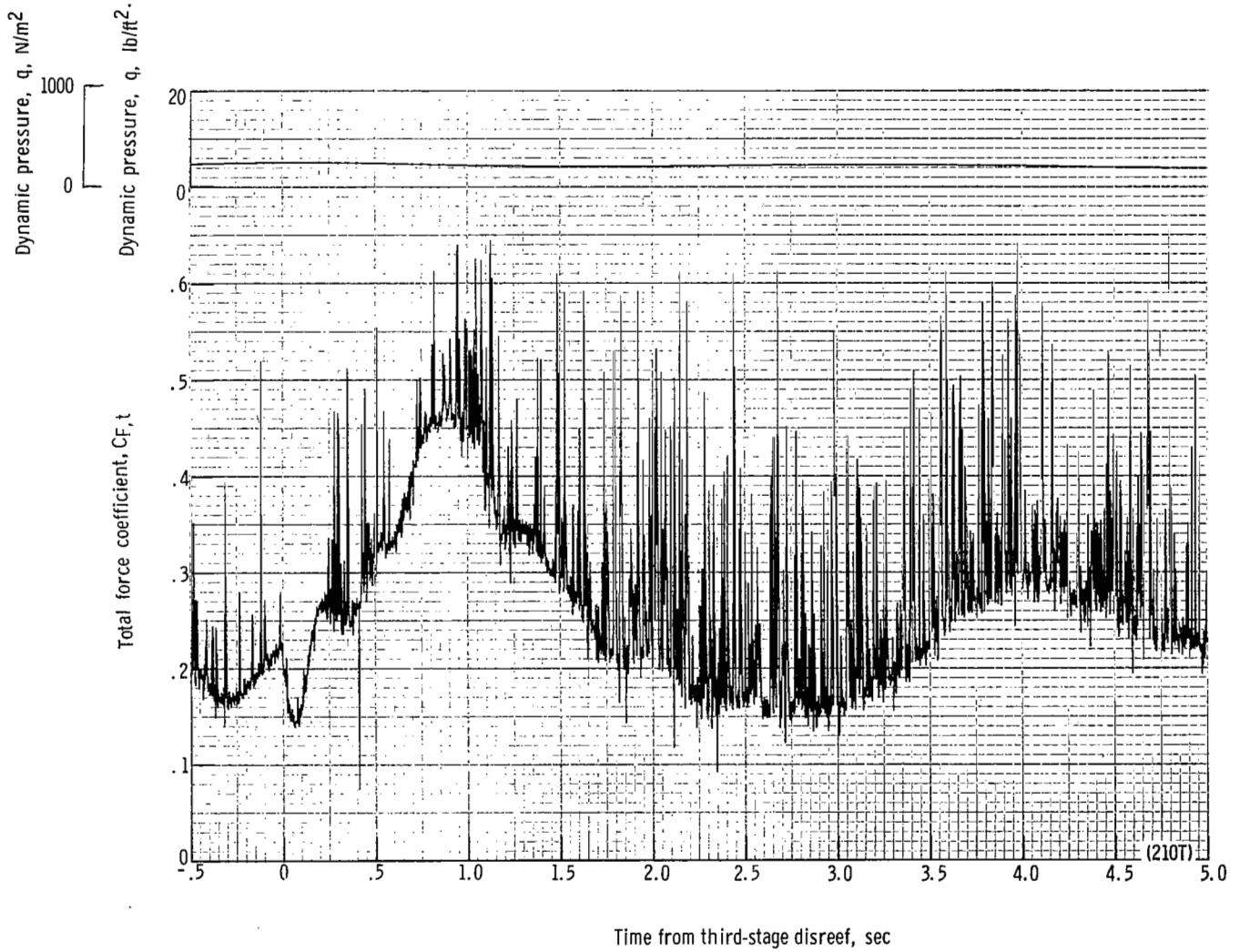
(r) Forward and aft riser loads and acceleration a_z plotted against time from third-stage disreef. Time = 0 second corresponds to 36.99 seconds after launch.

Figure 51.- Continued.



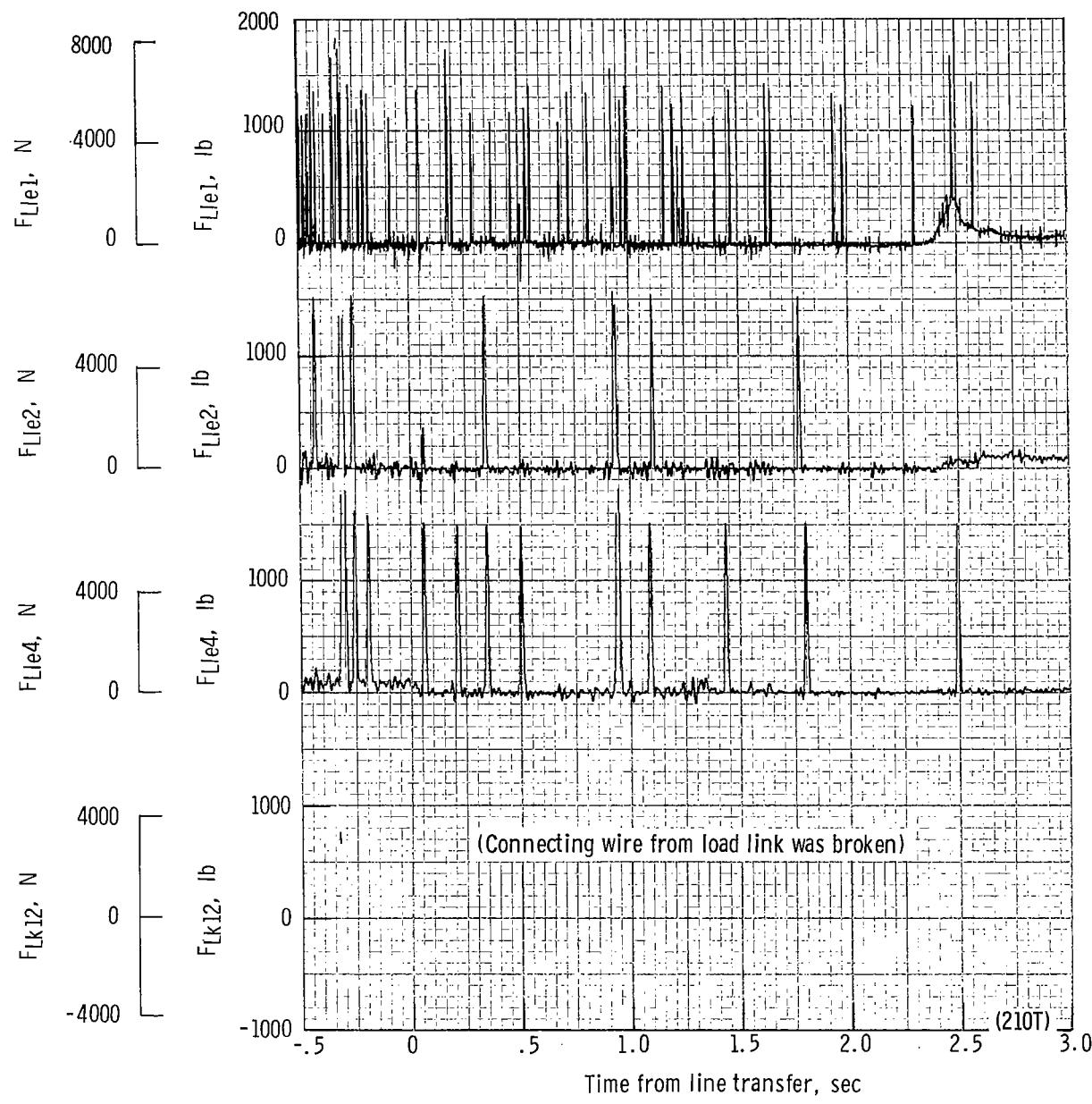
(s) Total force F_t plotted against time from third-stage disreef. Time = 0 second corresponds to 36.99 seconds after launch.

Figure 51.- Continued.



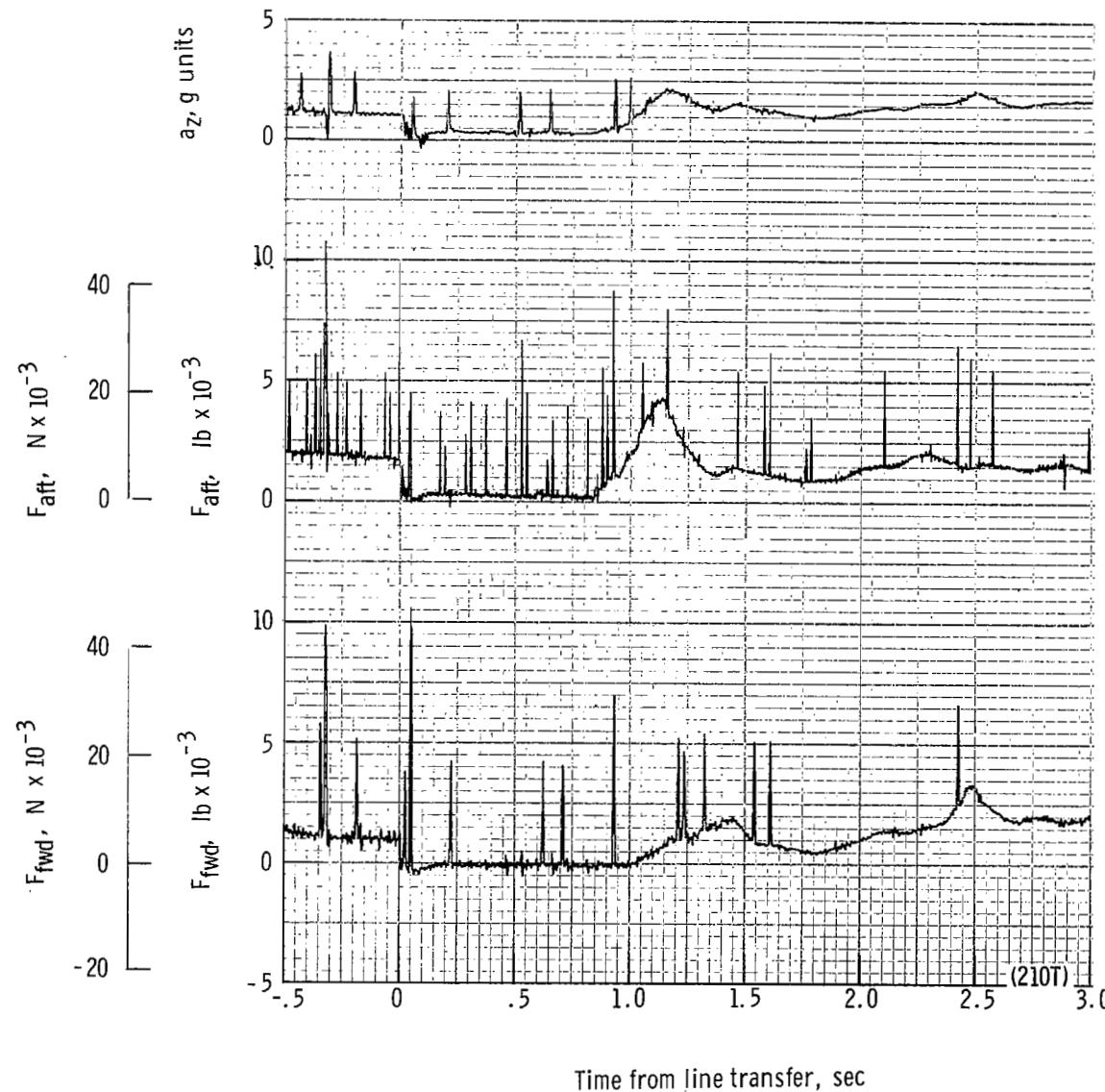
(t) Total force coefficient $C_{F,t}$ and dynamic pressure q plotted against time from third-stage disreef. Time = 0 second corresponds to 36.99 seconds after launch.

Figure 51.- Continued.



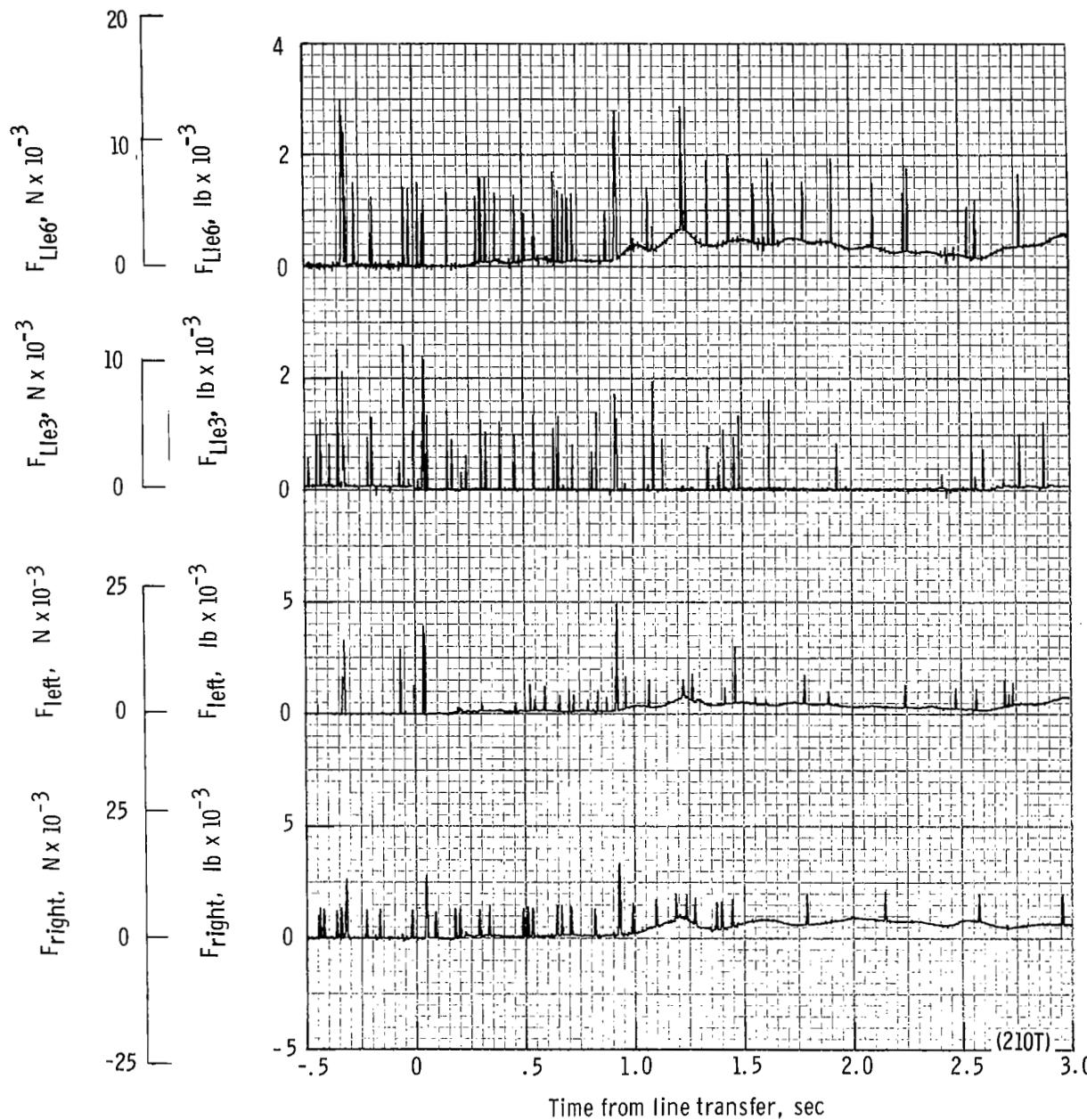
(u) Individual suspension-line loads F_{Lk12} , F_{Lle4} , F_{Lle2} , and F_{Lle1} plotted against time from line transfer. Time = 0 second corresponds to 42.43 seconds after launch.

Figure 51.- Continued.



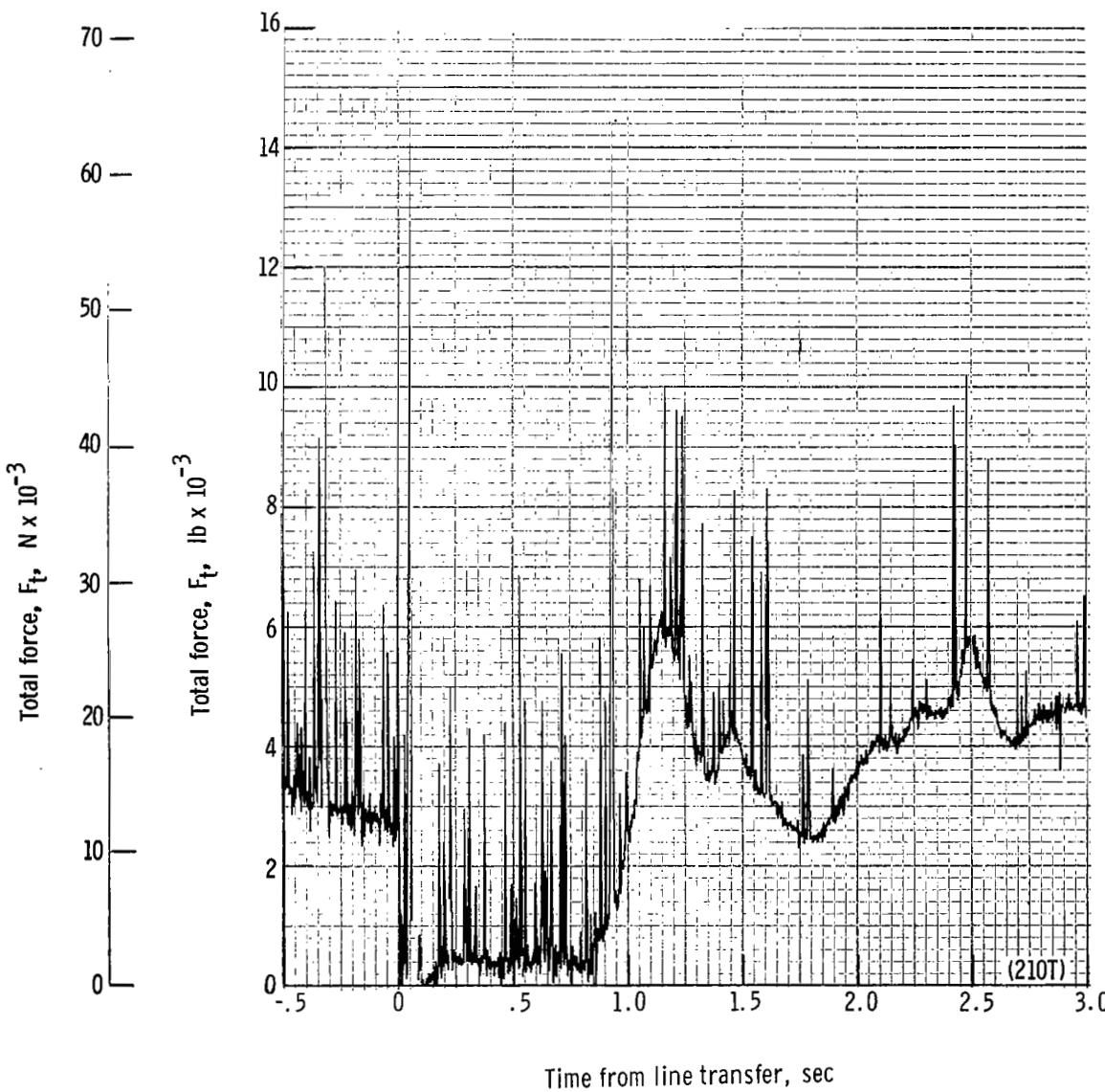
(v) Forward and aft riser loads and acceleration a_z plotted against time from line transfer. Time = 0 second corresponds to 42.43 seconds after launch.

Figure 51.- Continued.



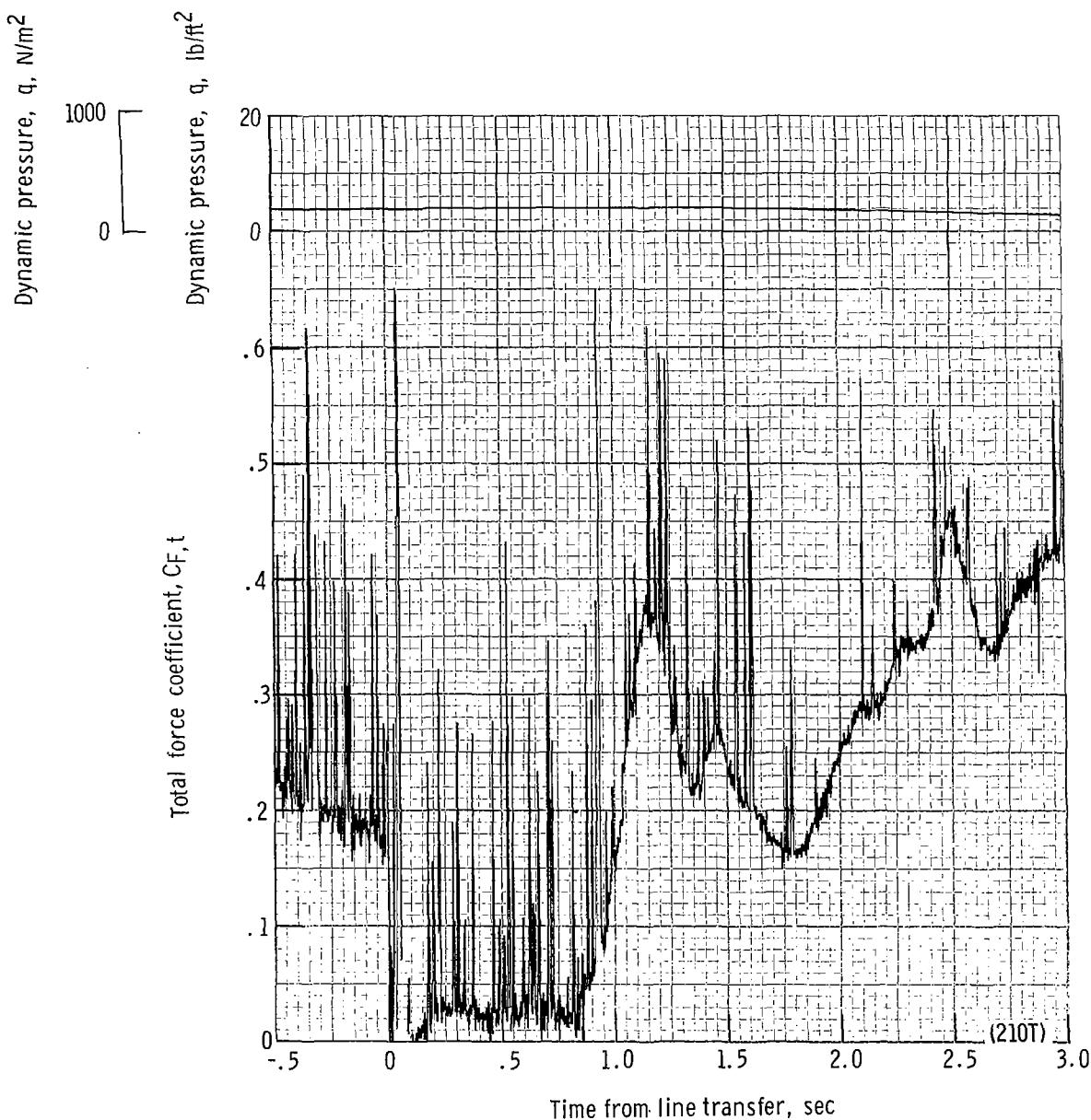
(w) Right and left riser loads and individual line loads F_{Lle3} and F_{Lle6} plotted against time from line transfer. Time = 0 second corresponds to 42.43 seconds after launch.

Figure 51.- Continued.



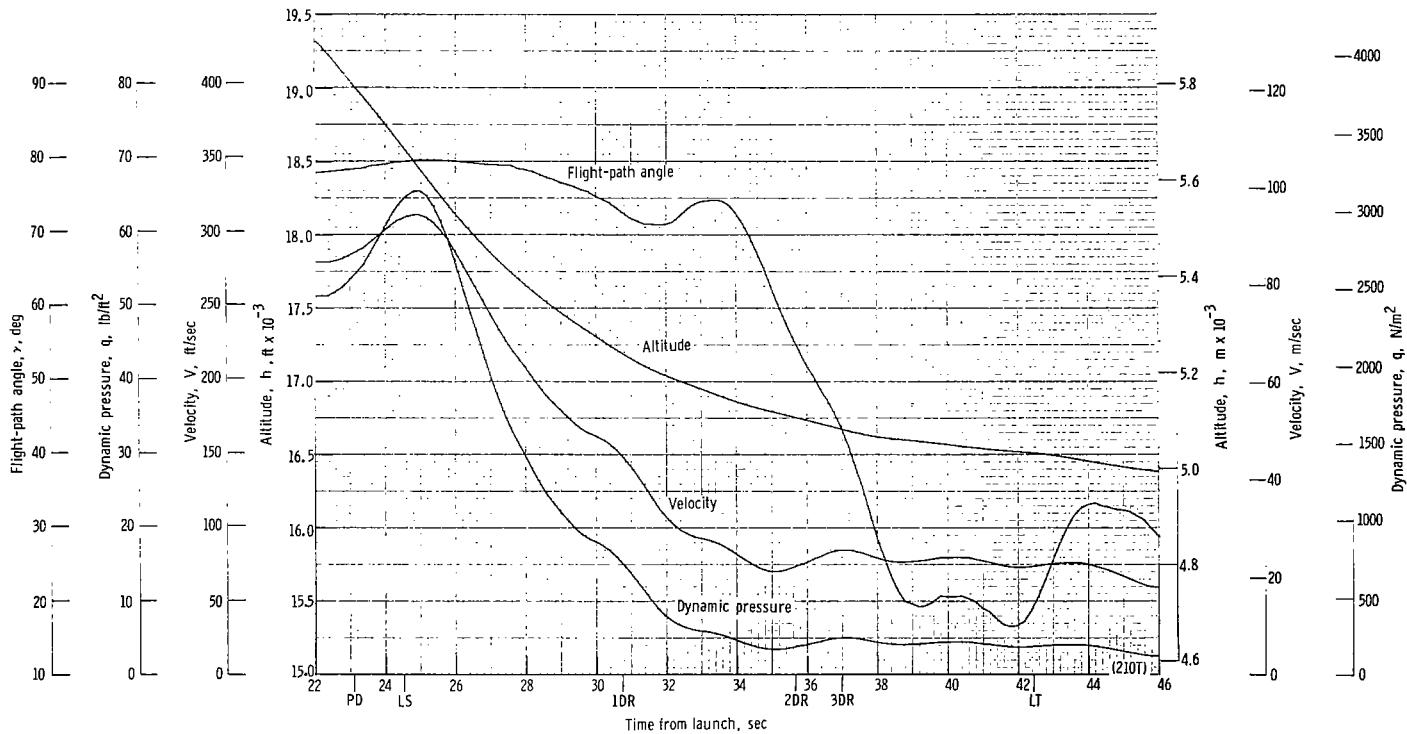
(x) Total force F_t plotted against time from line transfer. Time = 0 second corresponds to 42.43 seconds after launch.

Figure 51.- Continued.



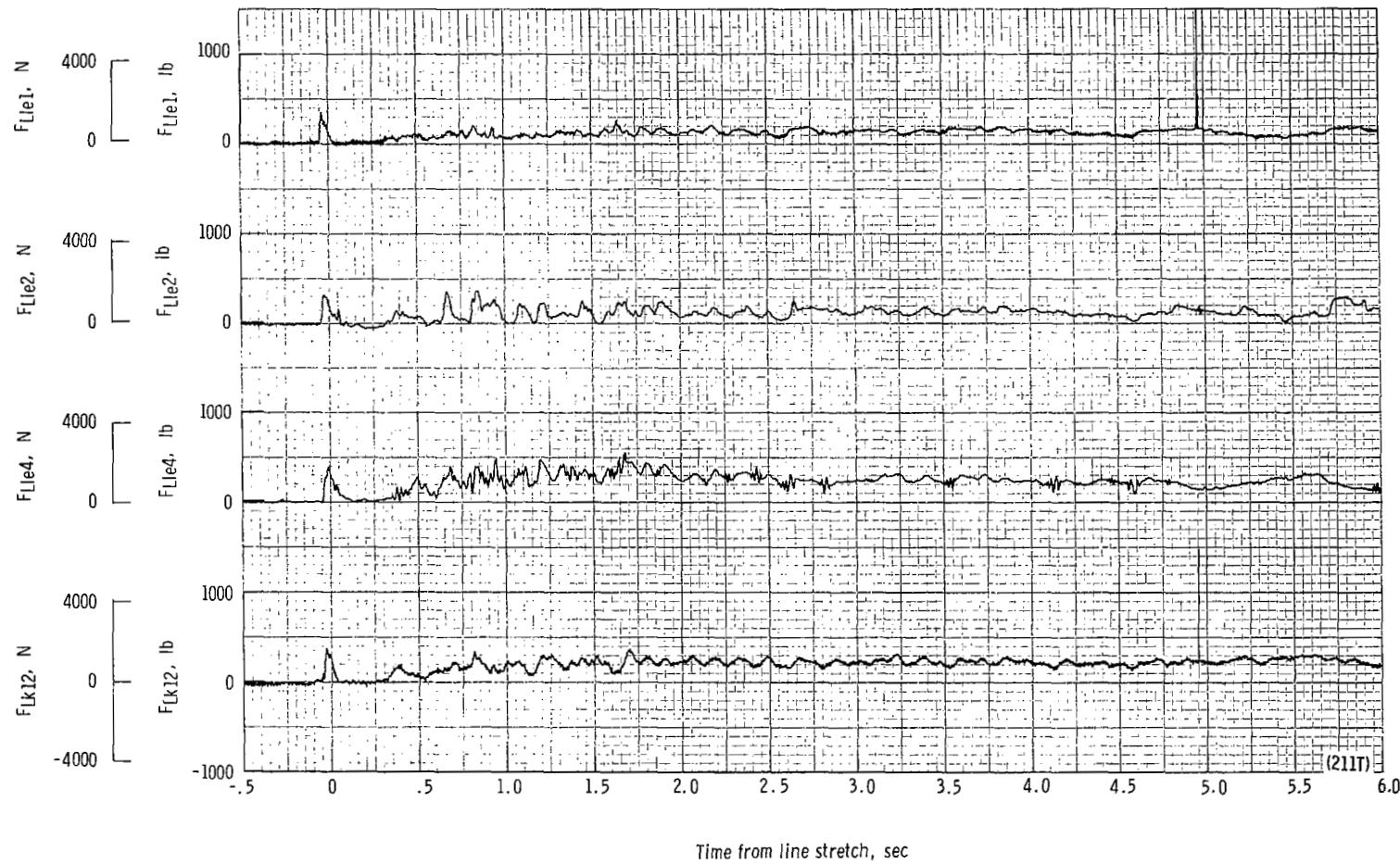
(y) Total force coefficient $C_{F,t}$ and dynamic pressure q plotted against time from line transfer. Time = 0 second corresponds to 42.43 seconds after launch.

Figure 51.- Continued.



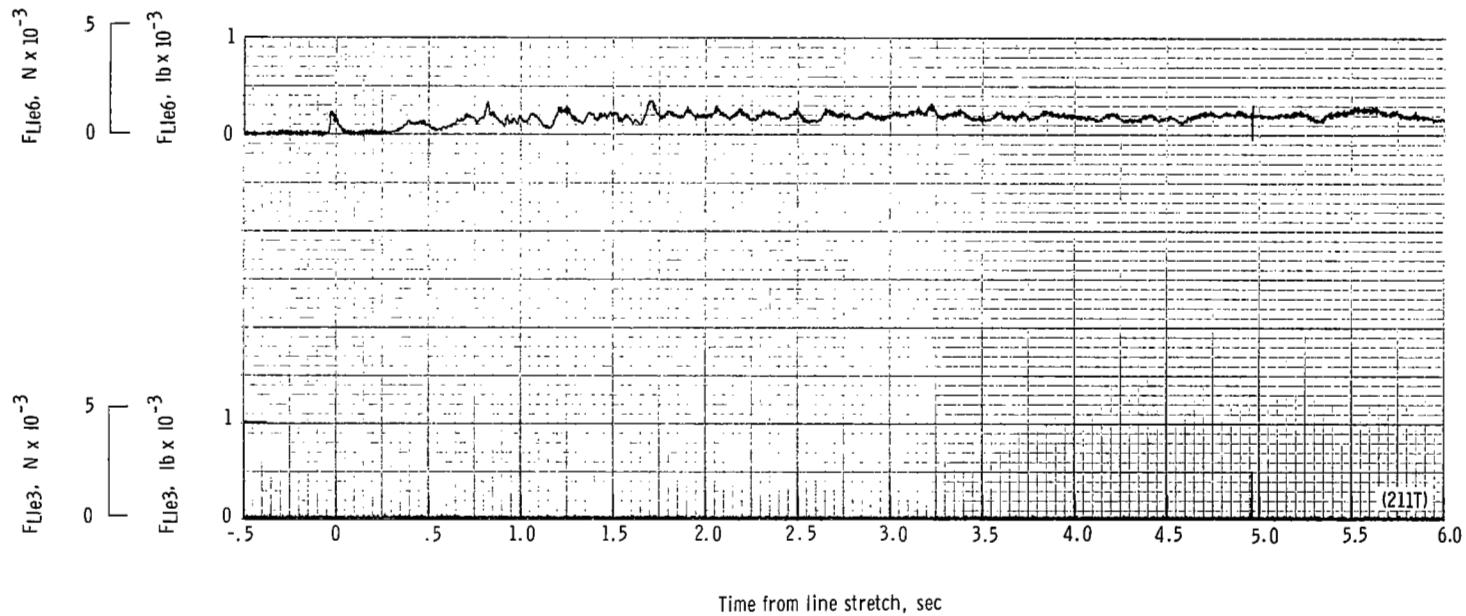
(z) Flight-path angle γ , dynamic pressure q , velocity V , and altitude h plotted against time from launch.

Figure 51.- Concluded.



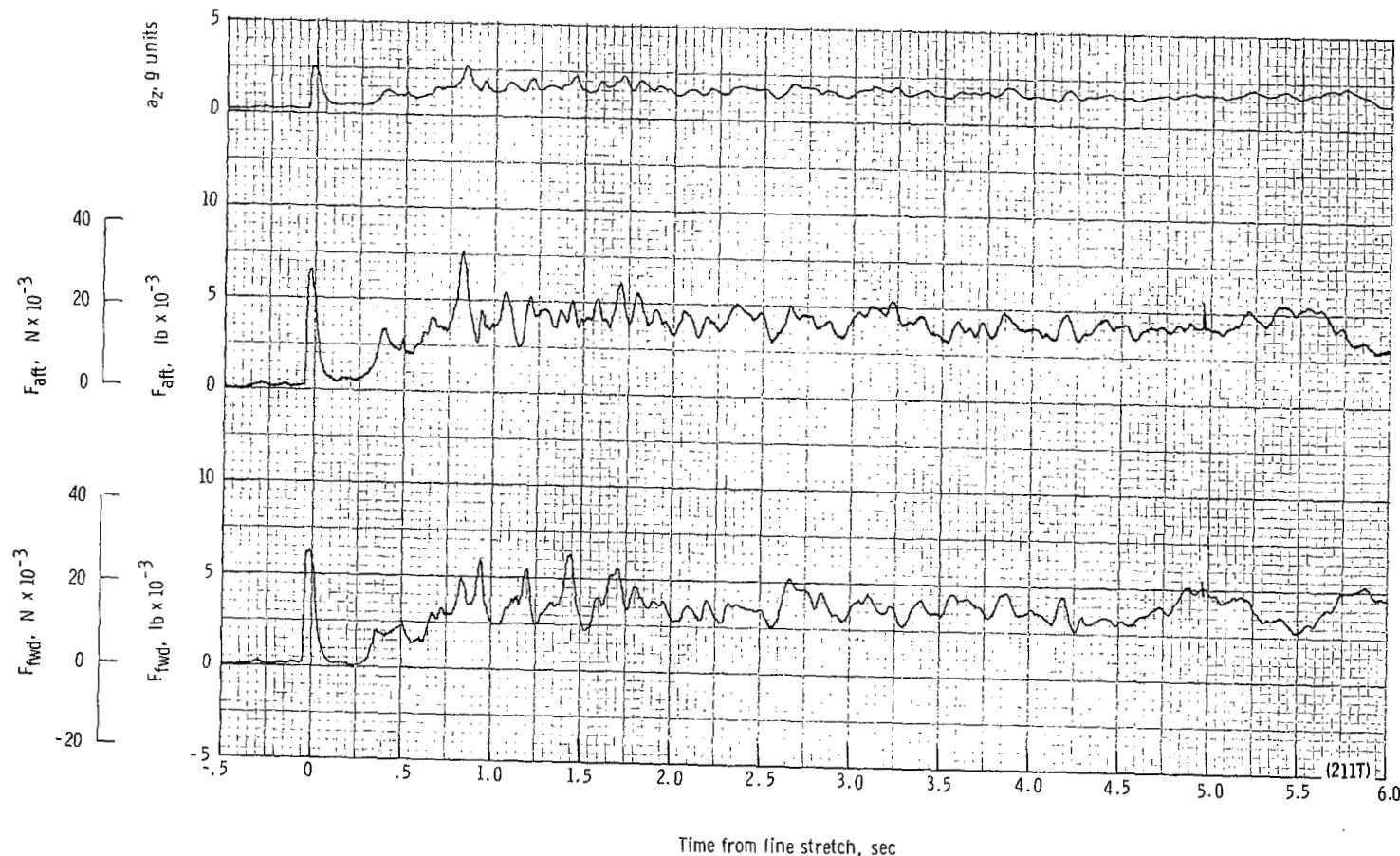
(a) Individual suspension-line loads F_{Lk12} , F_{Lle4} , F_{Lle2} , and F_{Lle1} plotted against time from line stretch. Time = 0 second corresponds to 24.90 seconds after launch.

Figure 52.- Time history of twin-keel parawing deployment data for test 211T. $W_D = 26\ 729\ N$ (6009 lb); $W_p = 24\ 897\ N$ (5597 lb); $q_{PD} = 2034.9\ N/m^2$ (42.5 lb/ft²); $h_{PD} = 5692\ m$ (18 675 ft); $l_r/l_k = 0.100$; reefing version B.



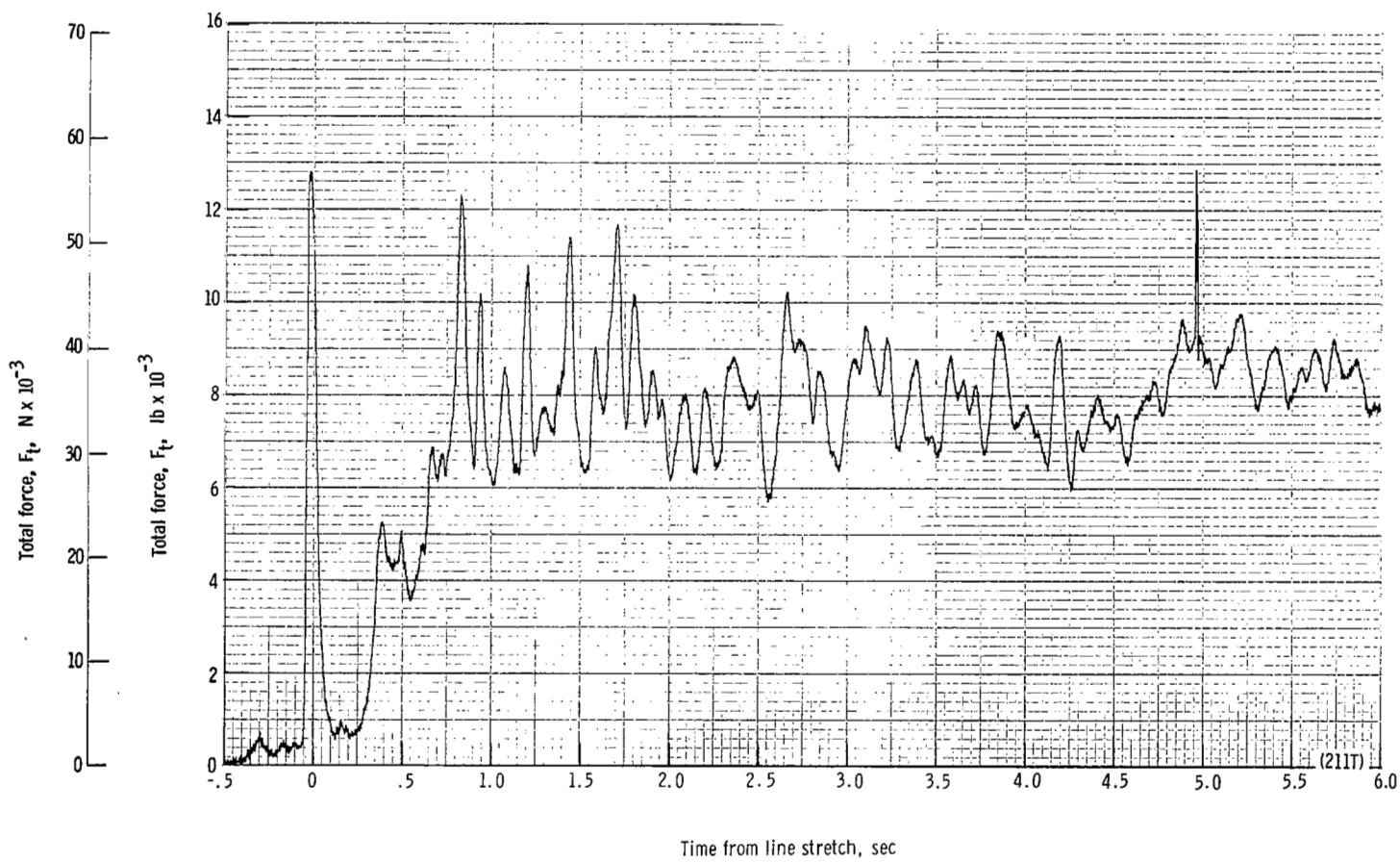
(b) Individual suspension-line loads F_{Lle3} and F_{Lle6} plotted against time from line stretch. Time = 0 second corresponds to 24.90 seconds after launch.

Figure 52.- Continued.



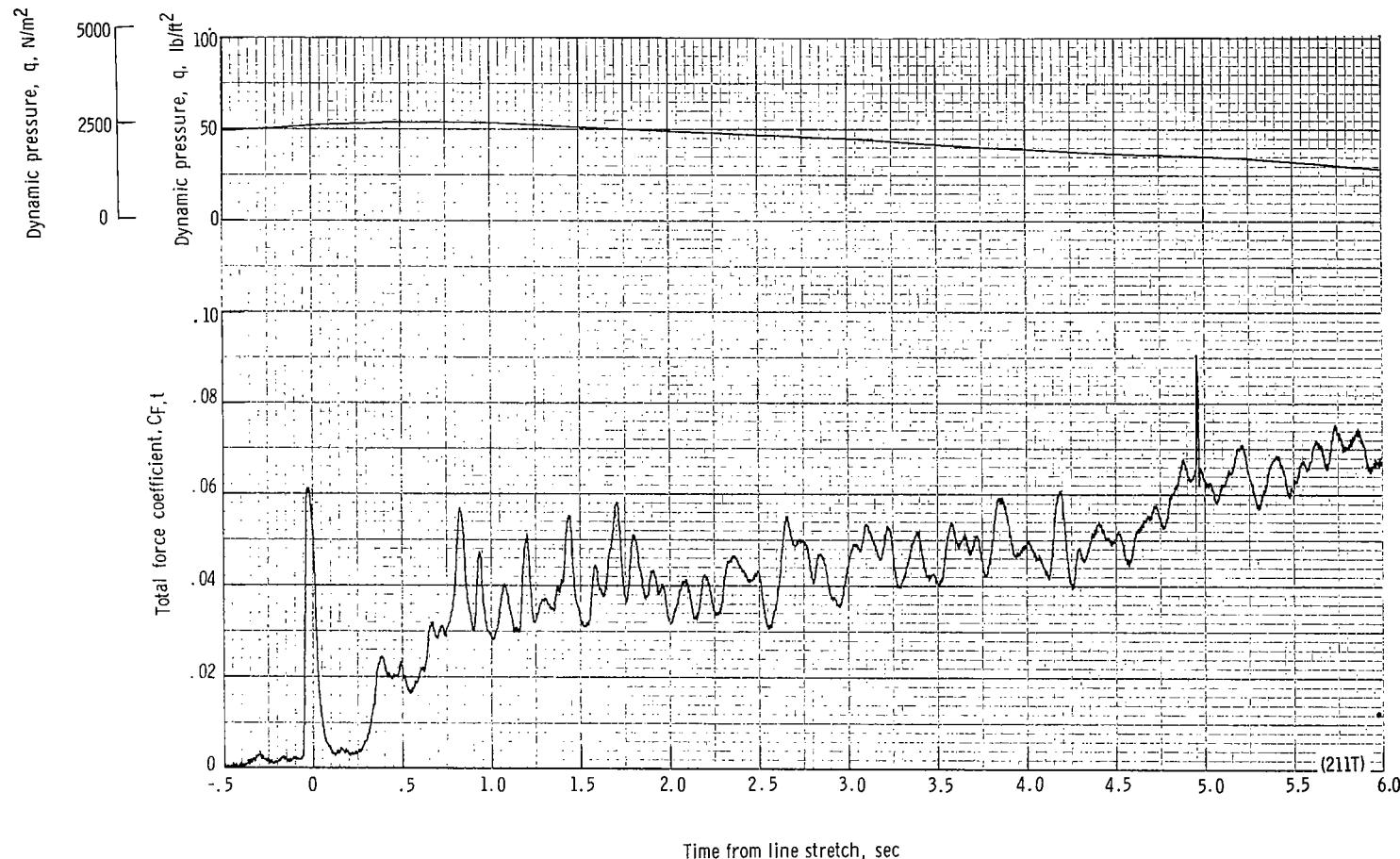
(c) Forward and aft riser loads and acceleration a_z plotted against time from line stretch. Time = 0 second corresponds to 24.90 seconds after launch.

Figure 52.- Continued.



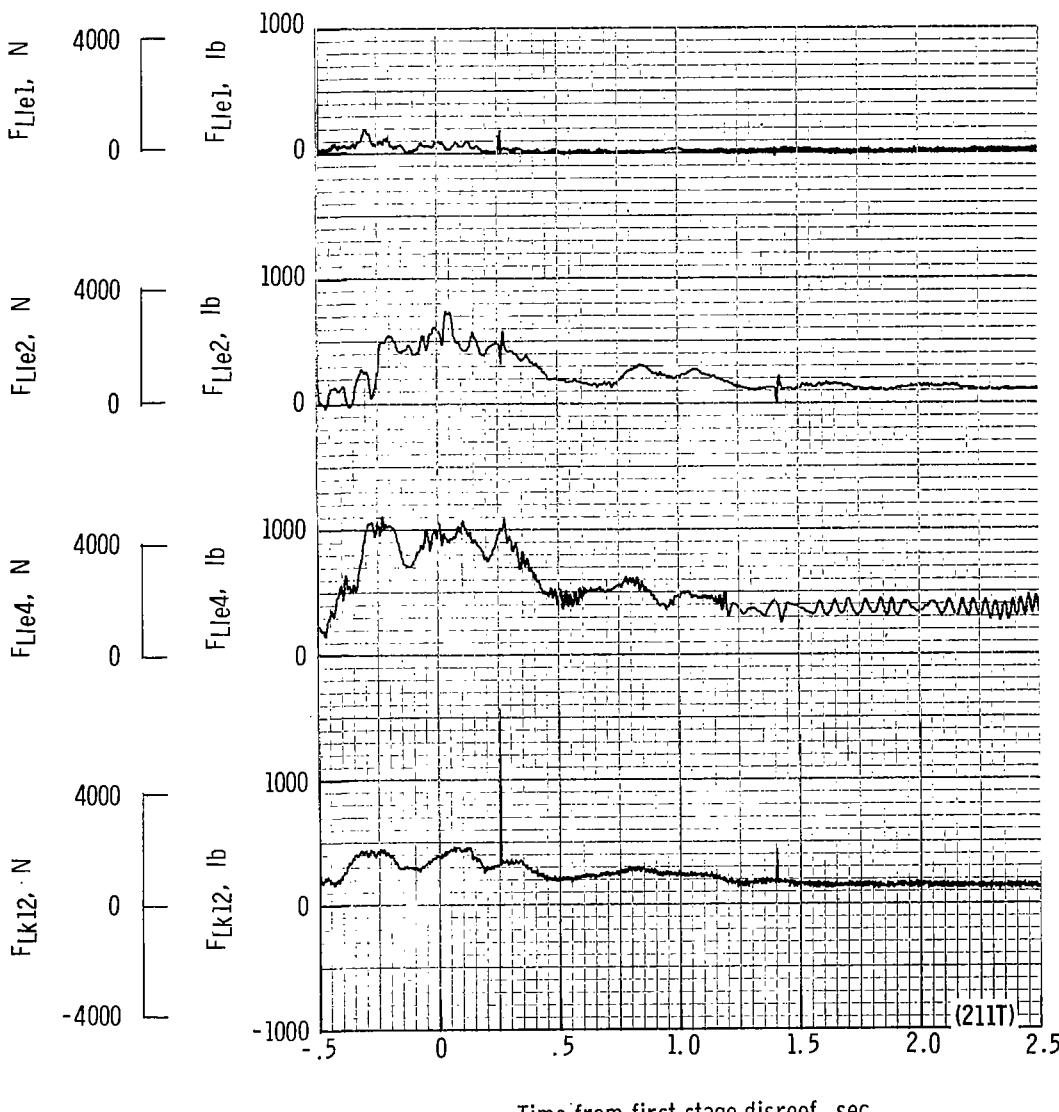
(d) Total force F_t plotted against time from line stretch. Time = 0 second corresponds to 24.90 seconds after launch.

Figure 52.- Continued.



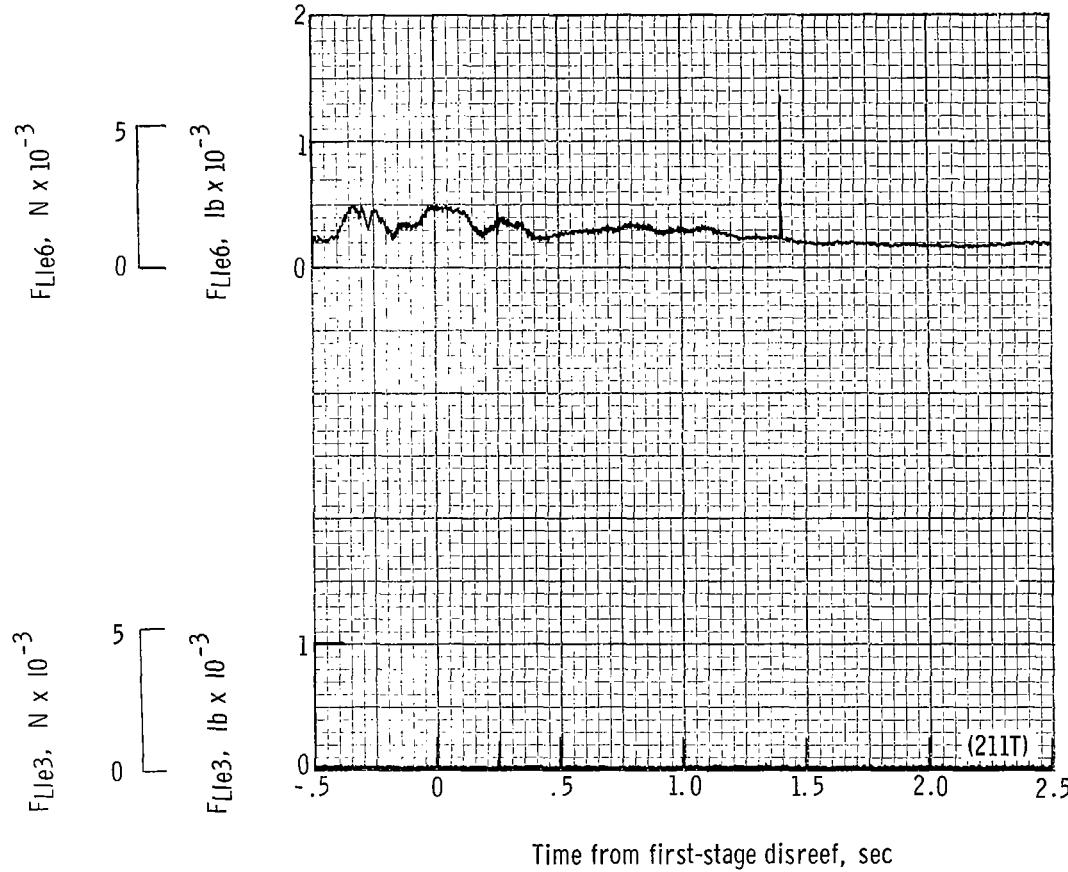
(e) Total force coefficient CF_t and dynamic pressure q plotted against time from line stretch. Time = 0 second corresponds to 24.90 seconds after launch.

Figure 52.- Continued.



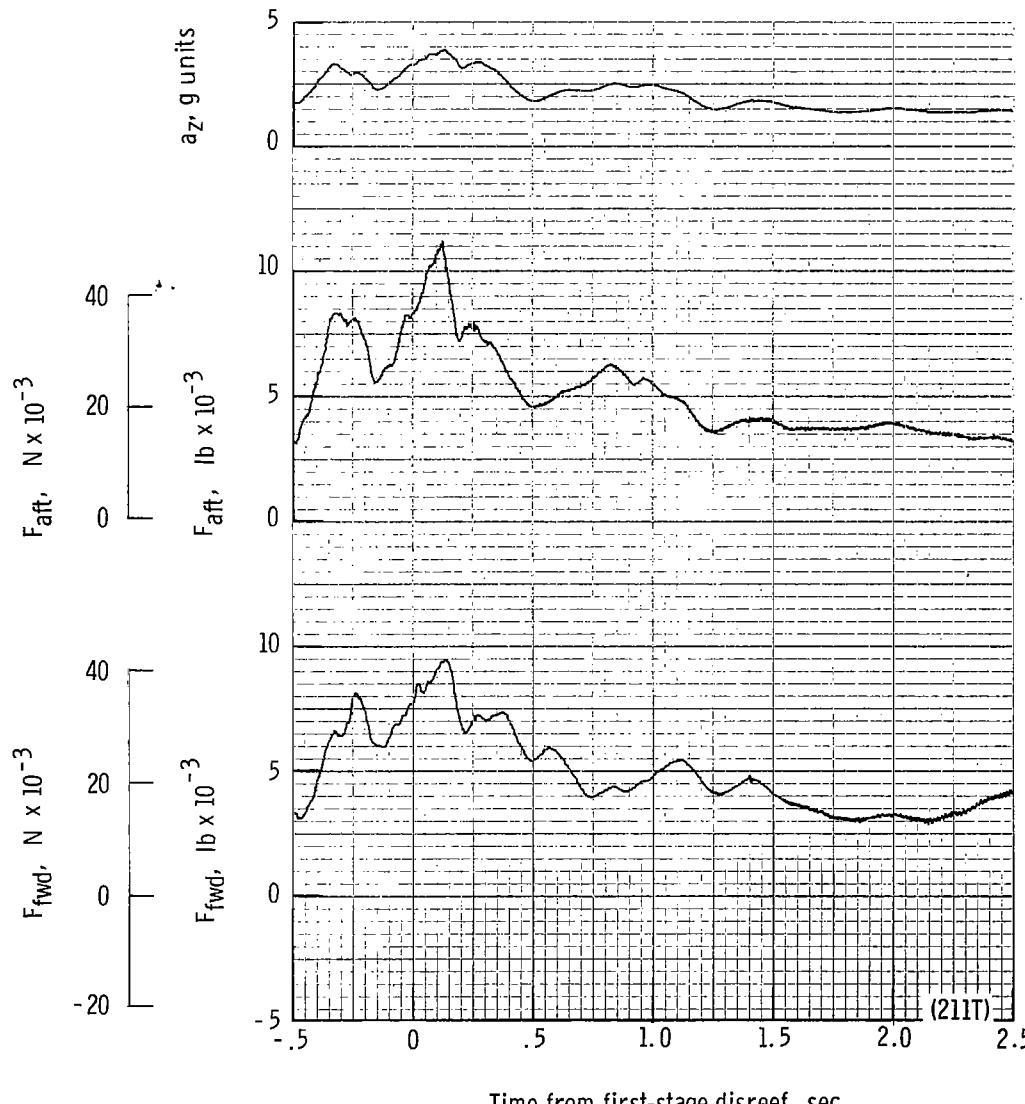
(f) Individual suspension-line loads F_{Lk12} , F_{Lle4} , F_{Lle2} , and F_{Lle1} plotted against time from first-stage disreef. Time = 0 second corresponds to 31.03 seconds after launch.

Figure 52.- Continued.



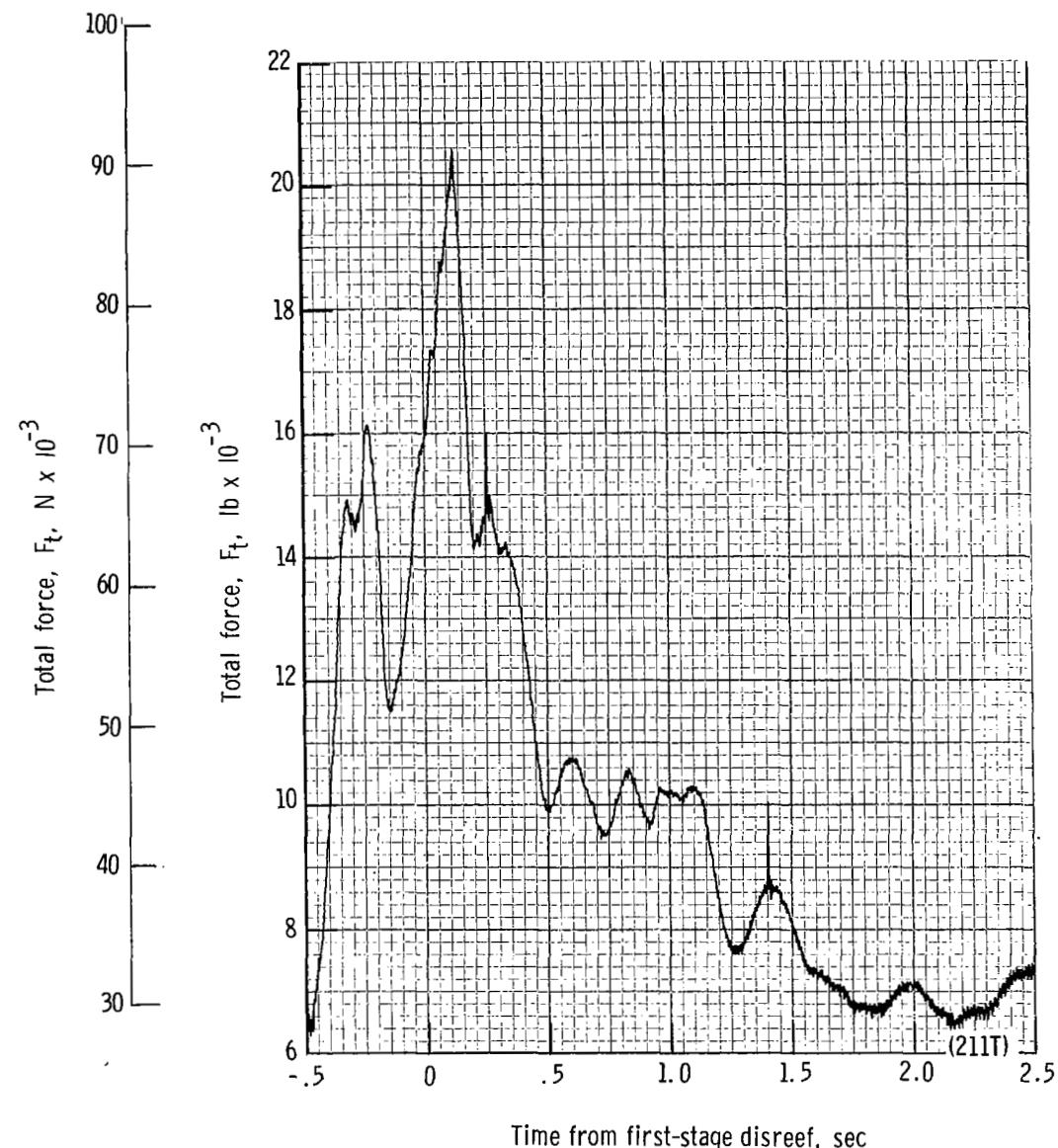
(g) Individual suspension-line loads F_{Lle3} and F_{Lle6} plotted against time from first-stage disreef. Time = 0 second corresponds to 31.03 seconds after launch.

Figure 52.- Continued.



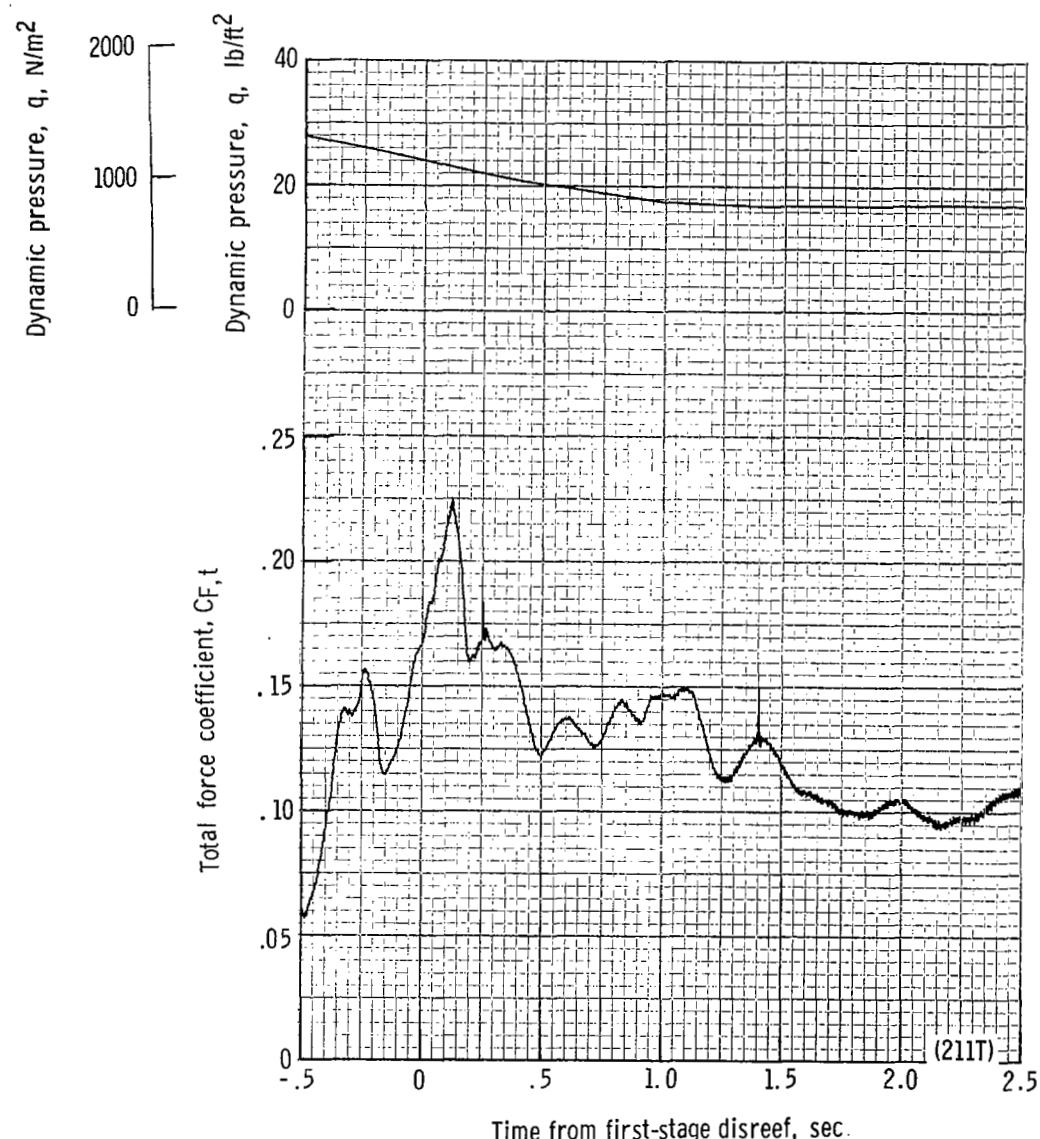
(h) Forward and aft riser loads and acceleration a_z plotted against time from first-stage disreef. Time = 0 second corresponds to 31.03 seconds after launch.

Figure 52.- Continued.



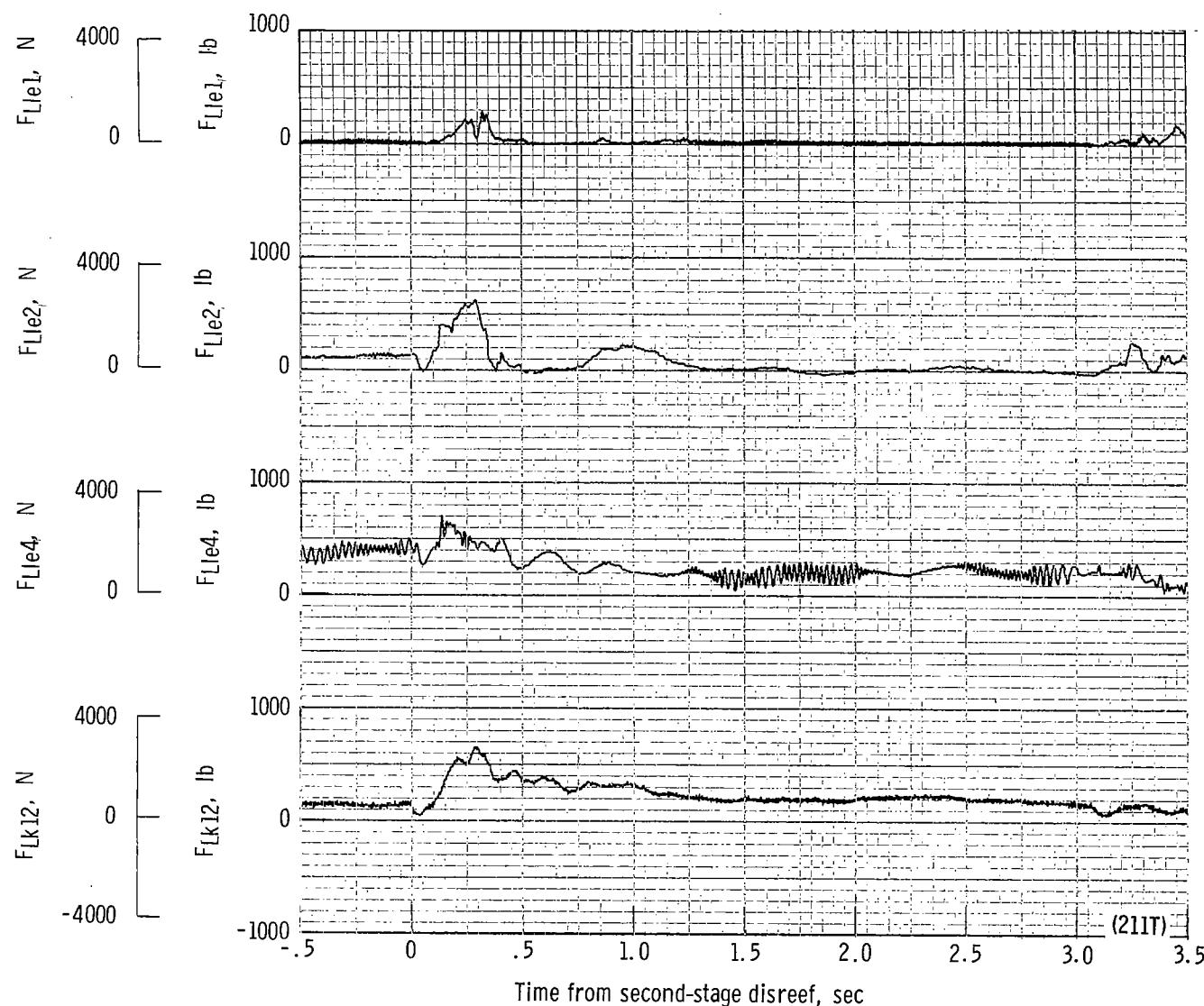
(i) Total force F_t plotted against time from first-stage disreef. Time = 0 second corresponds to 31.03 seconds after launch.

Figure 52.- Continued.



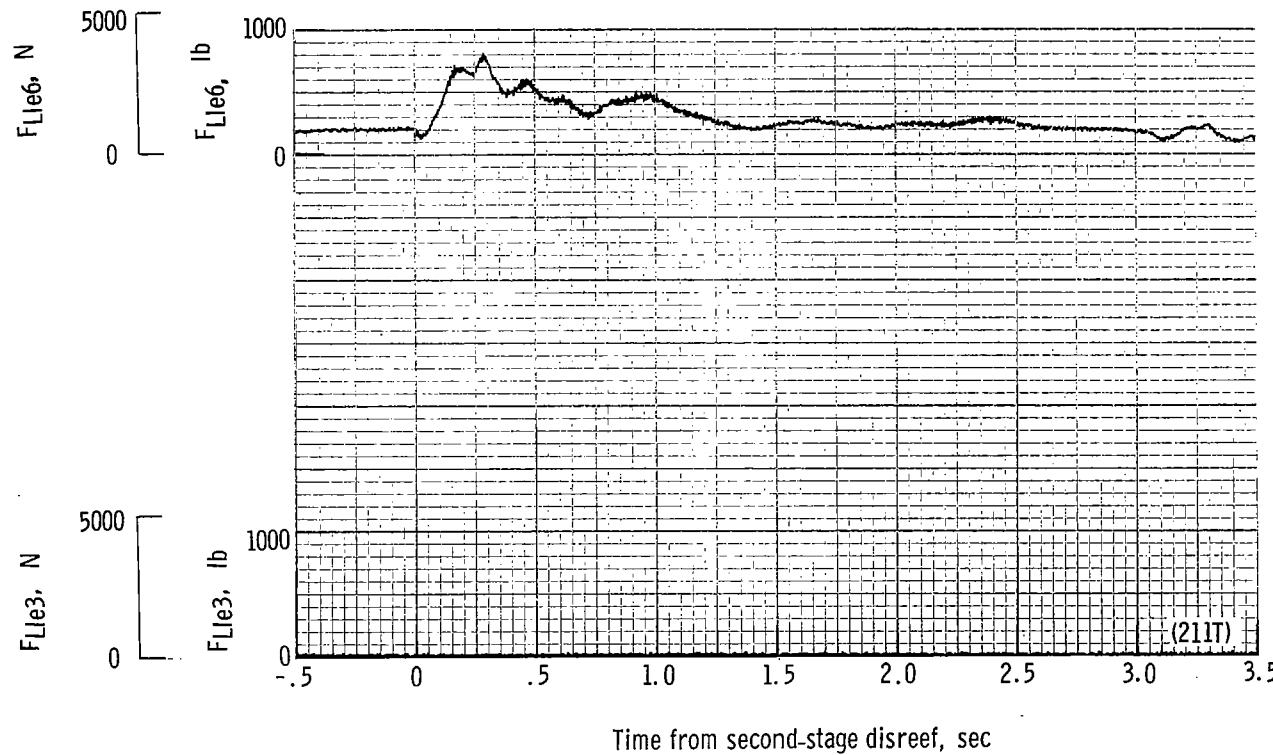
(j) Total force coefficient $C_{F,t}$ and dynamic pressure q plotted against time from first-stage disreef. Time = 0 second corresponds to 31.03 seconds after launch.

Figure 52.- Continued.



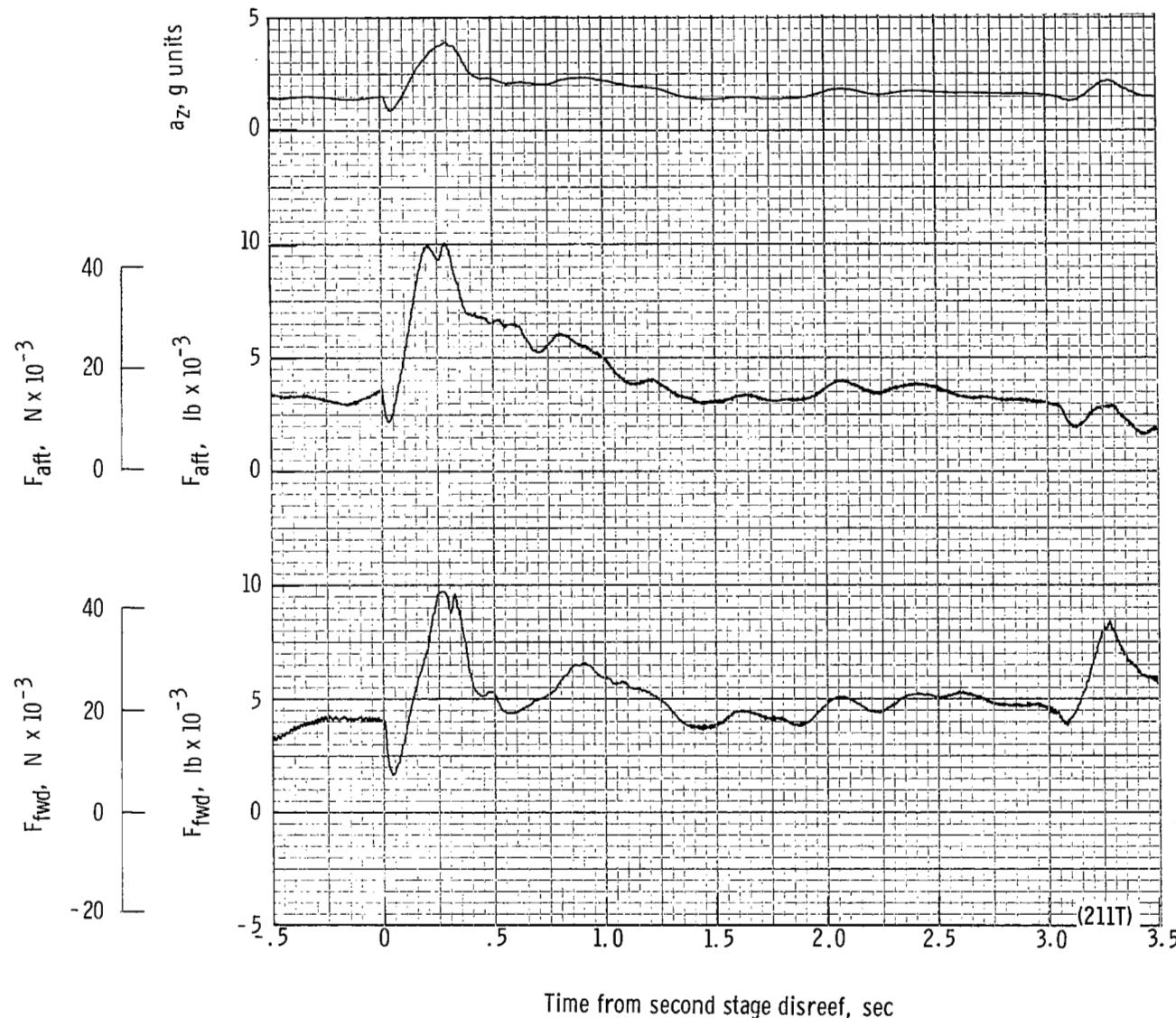
(k) Individual suspension-line loads F_{Lk12} , F_{Lle4} , F_{Lle2} , and F_{Lle1} plotted against time from second-stage disreef. Time = 0 second corresponds to 34.30 seconds after launch.

Figure 52.- Continued.



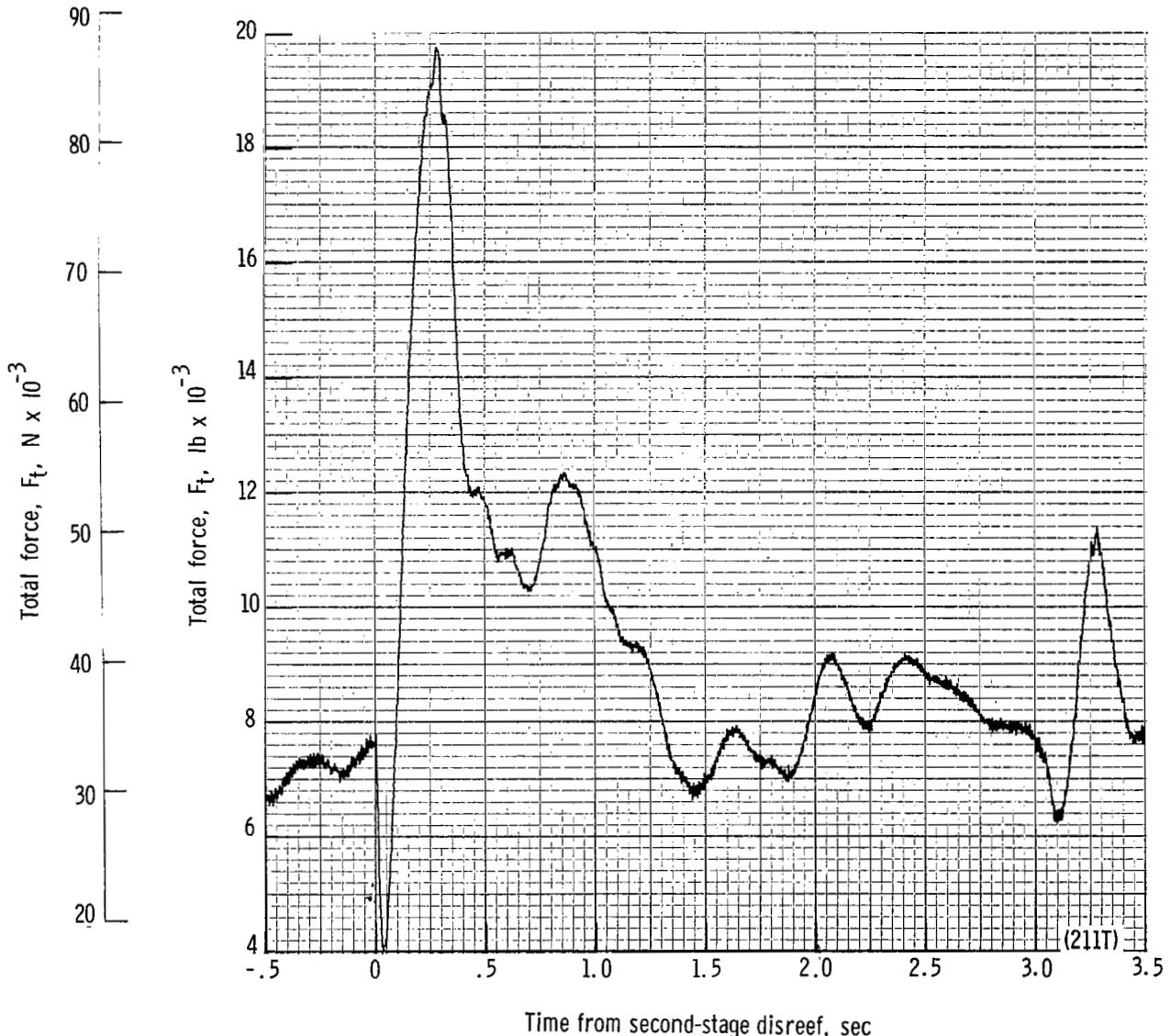
(II) Individual suspension-line loads F_{Lle3} and F_{Lle6} plotted against time from second-stage disreef. Time = 0 second corresponds to 34.30 seconds after launch.

Figure 52.- Continued.



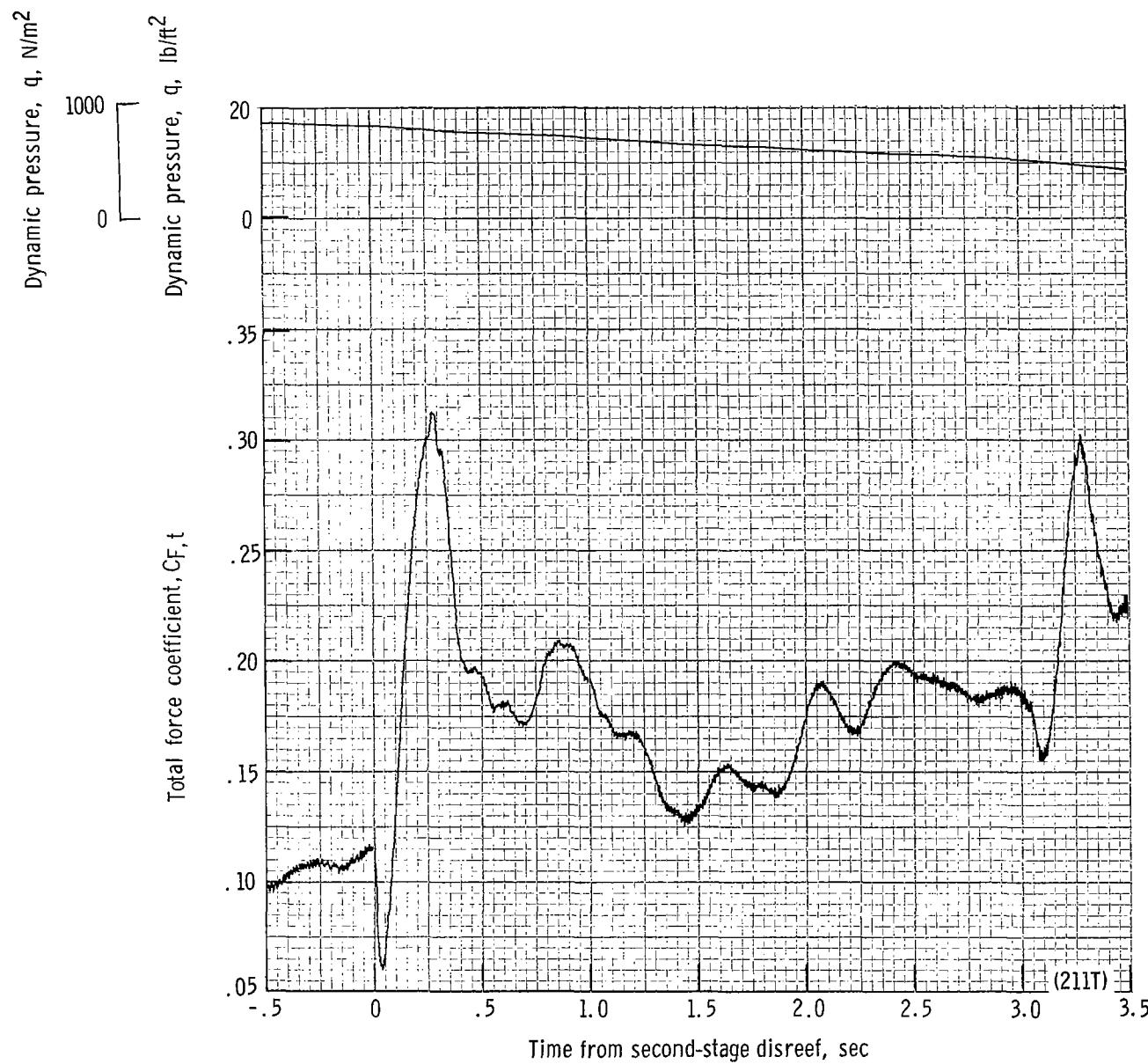
(m) Forward and aft riser loads and acceleration a_z plotted against time from second-stage disreef. Time = 0 second corresponds to 34.30 seconds after launch.

Figure 52.- Continued.



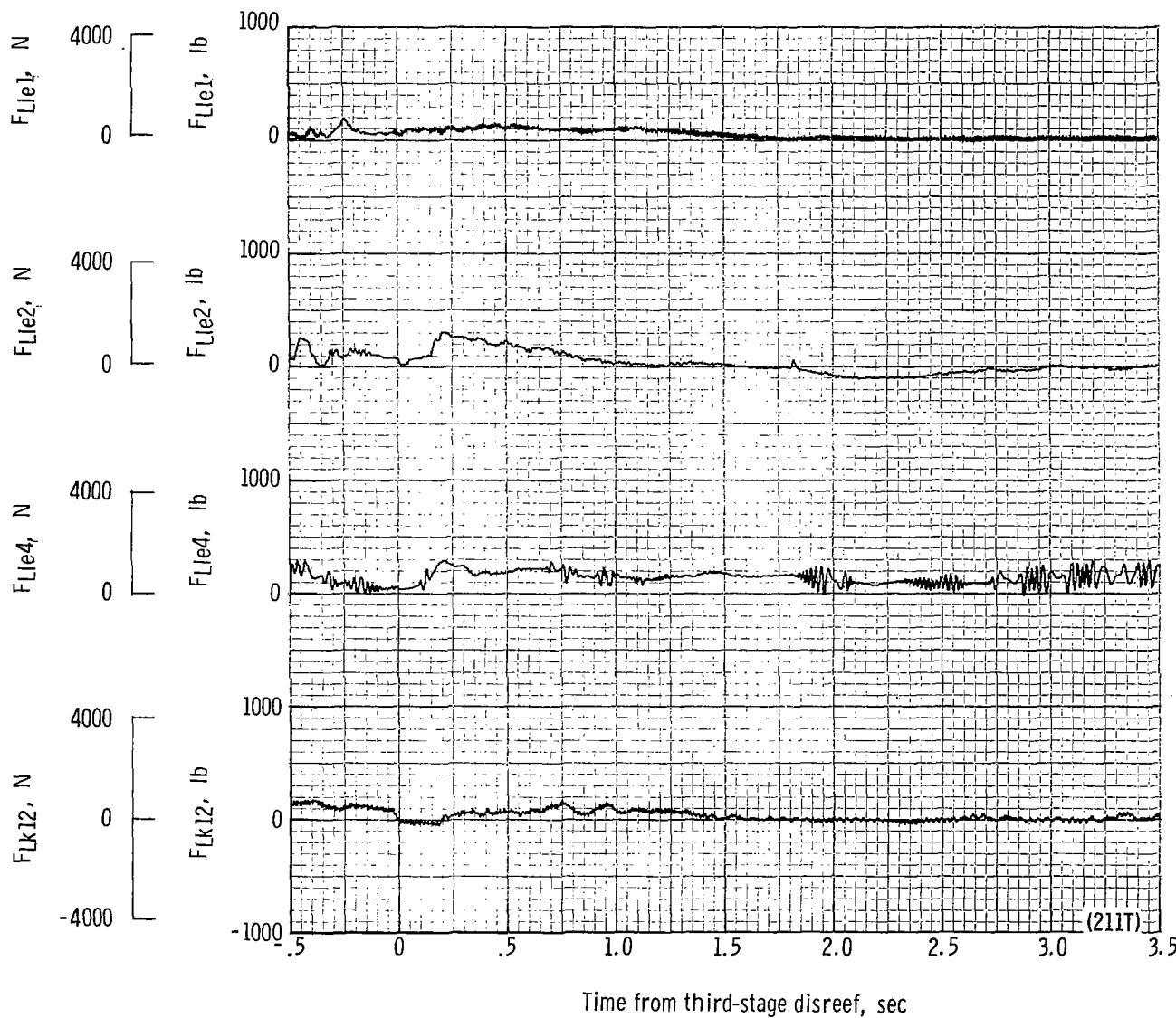
(n) Total force F_t plotted against time from second-stage disreef. Time = 0 second corresponds to 34.30 seconds after launch.

Figure 52.- Continued.



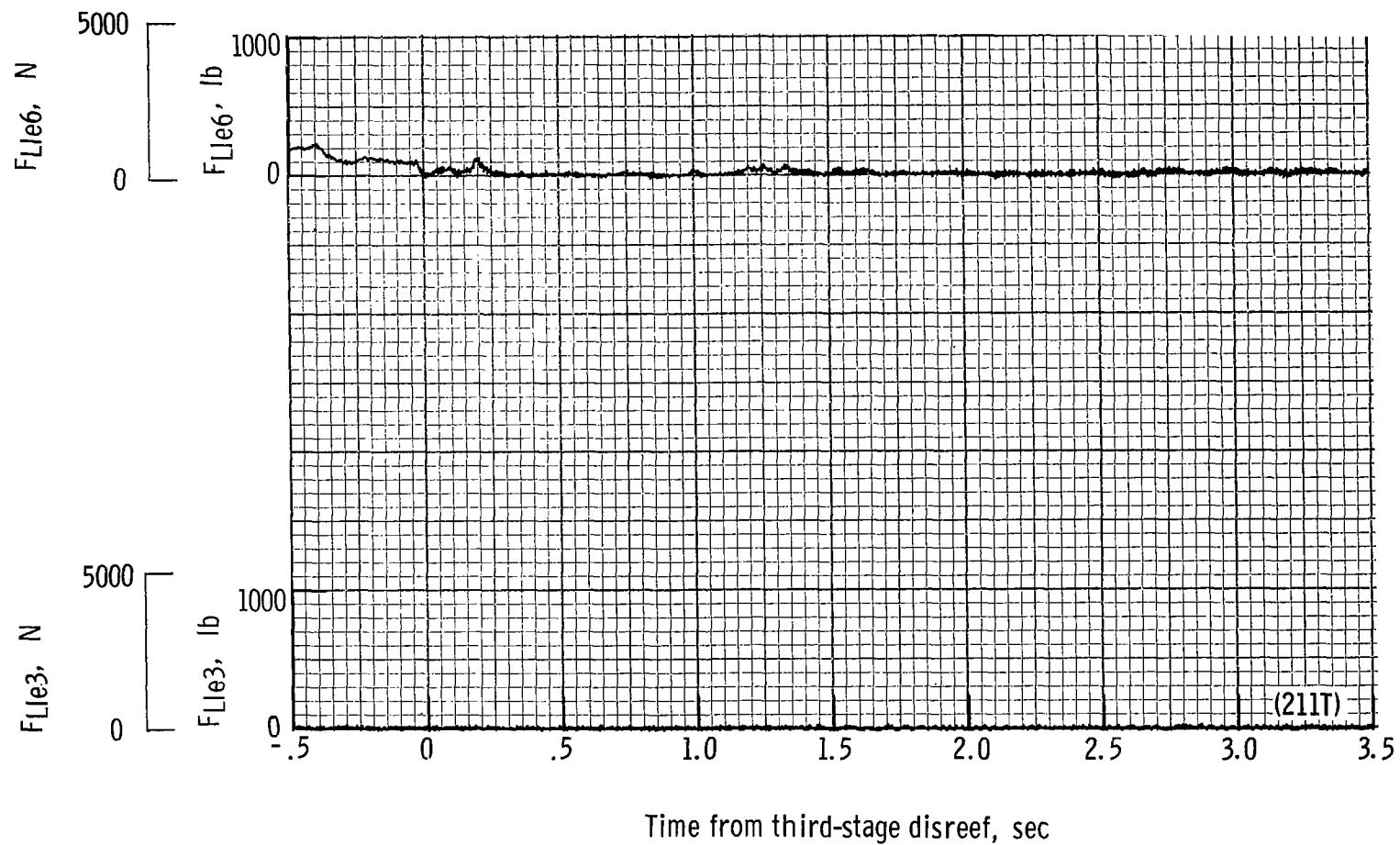
(o) Total force coefficient $C_{F,t}$ and dynamic pressure q plotted against time from second-stage disreef. Time = 0 second corresponds to 34.30 seconds after launch.

Figure 52.- Continued.



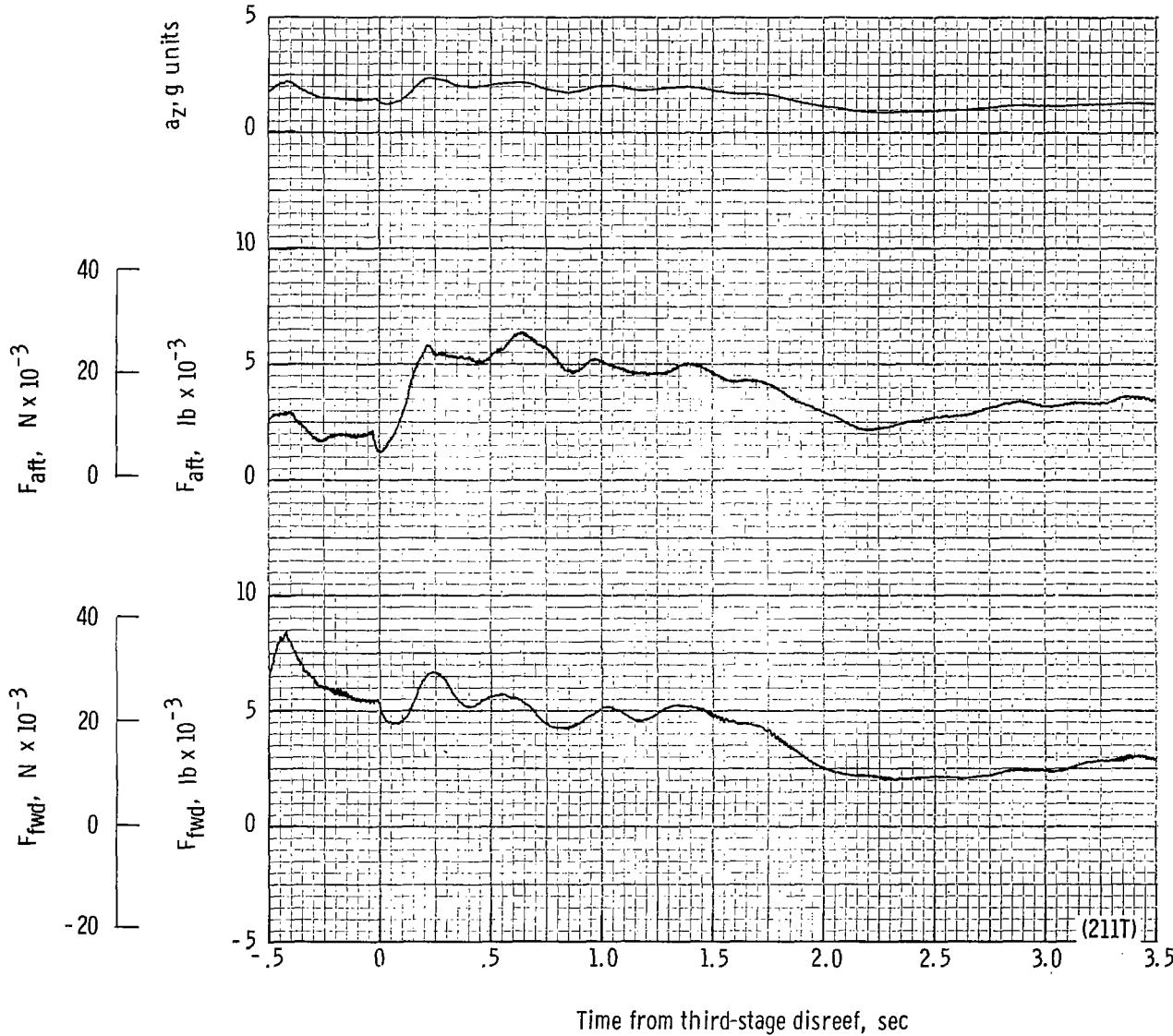
(b) Individual suspension-line loads F_{Lk12} , F_{Lle4} , F_{Lle2} , and F_{Lle1} plotted against time from third-stage disreef. Time = 0 second corresponds to 38.00 seconds after launch.

Figure 52.- Continued.



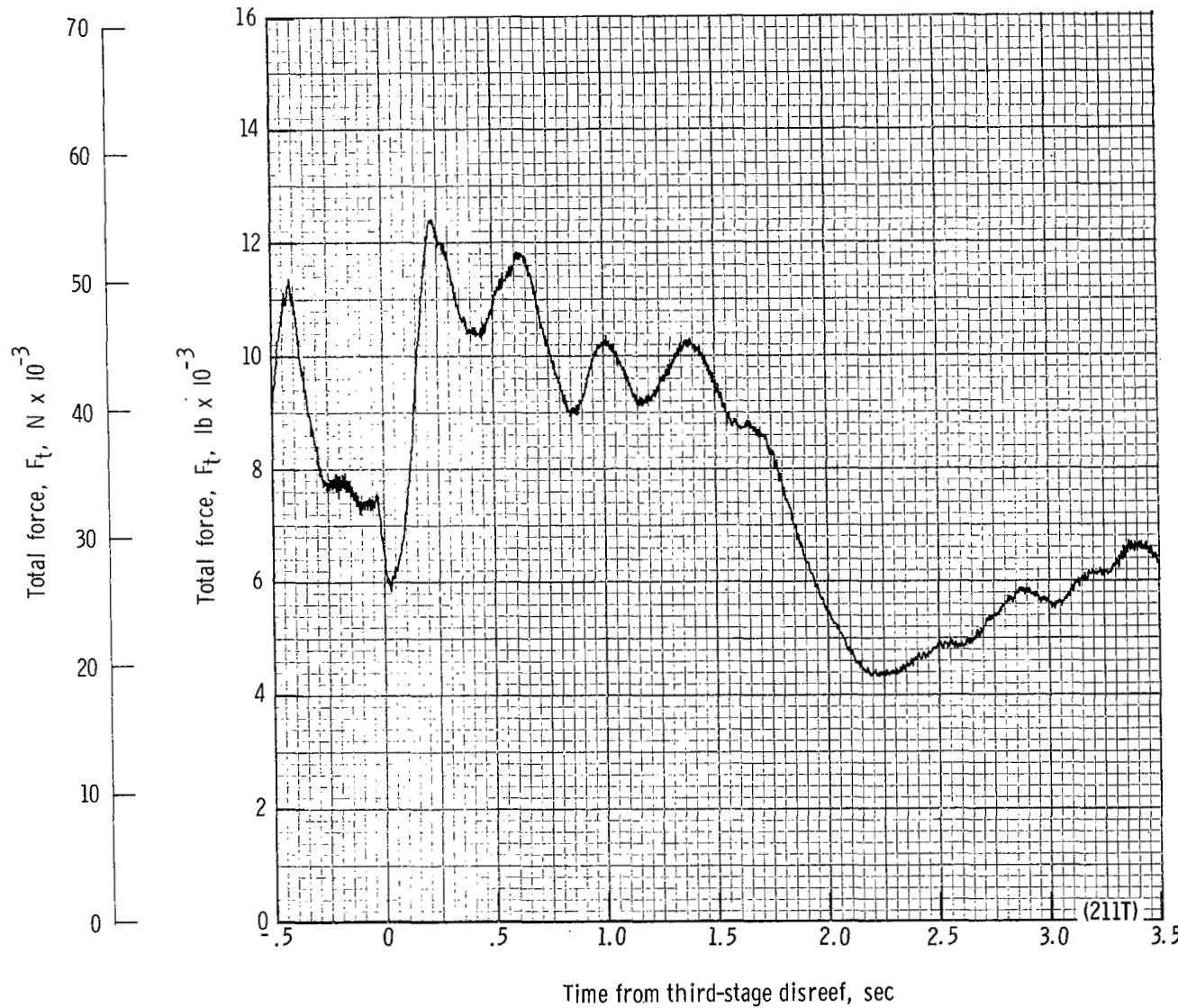
(q) Individual suspension-line loads F_{Lle3} and F_{Lle6} plotted against time from third-stage disreef. Time = 0 second corresponds to 38.00 seconds after launch.

Figure 52.- Continued.



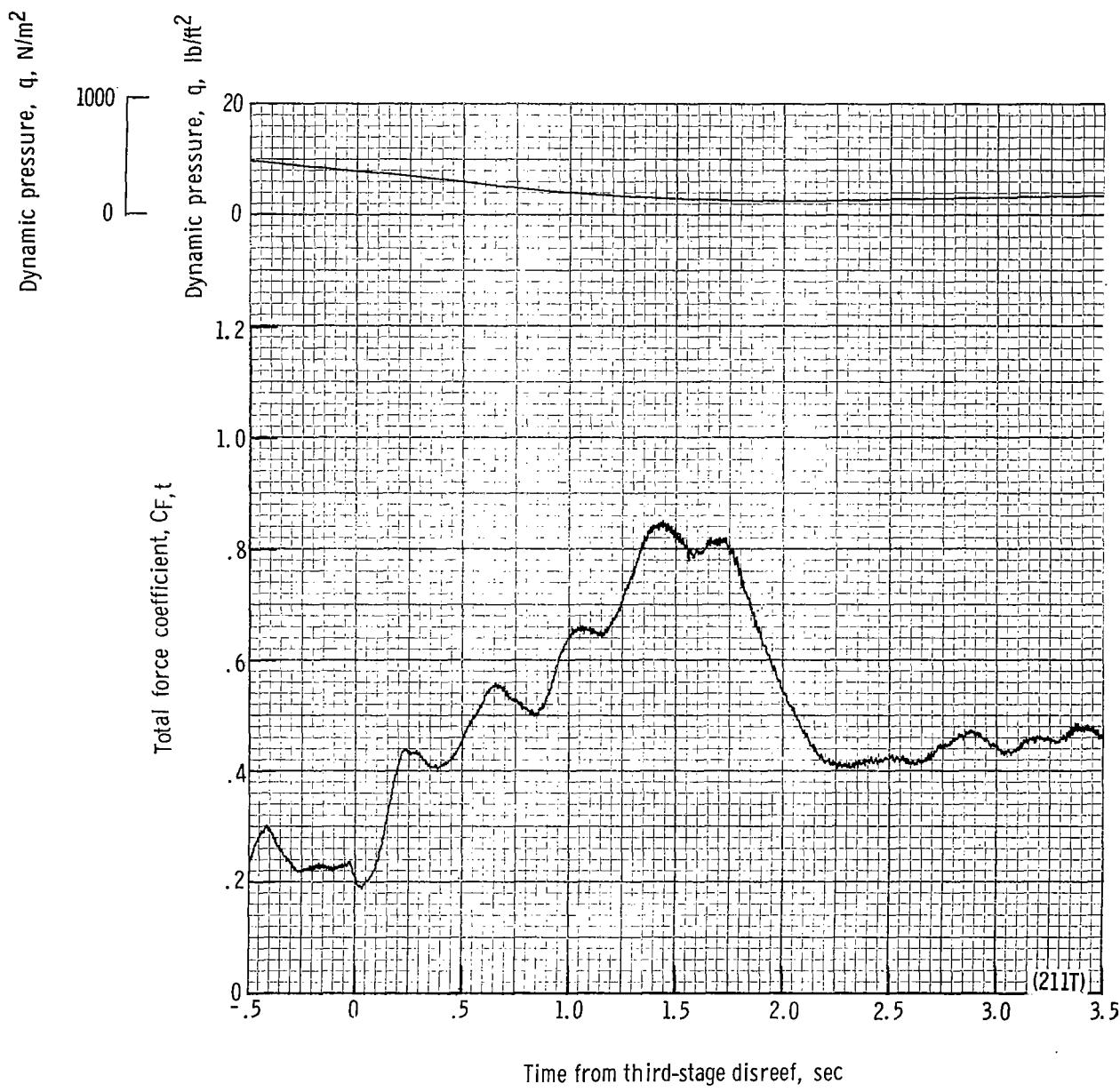
(r) Forward and aft riser loads and acceleration a_z plotted against time from third-stage disreef. Time = 0 second corresponds to 38.00 seconds after launch.

Figure 52.- Continued.



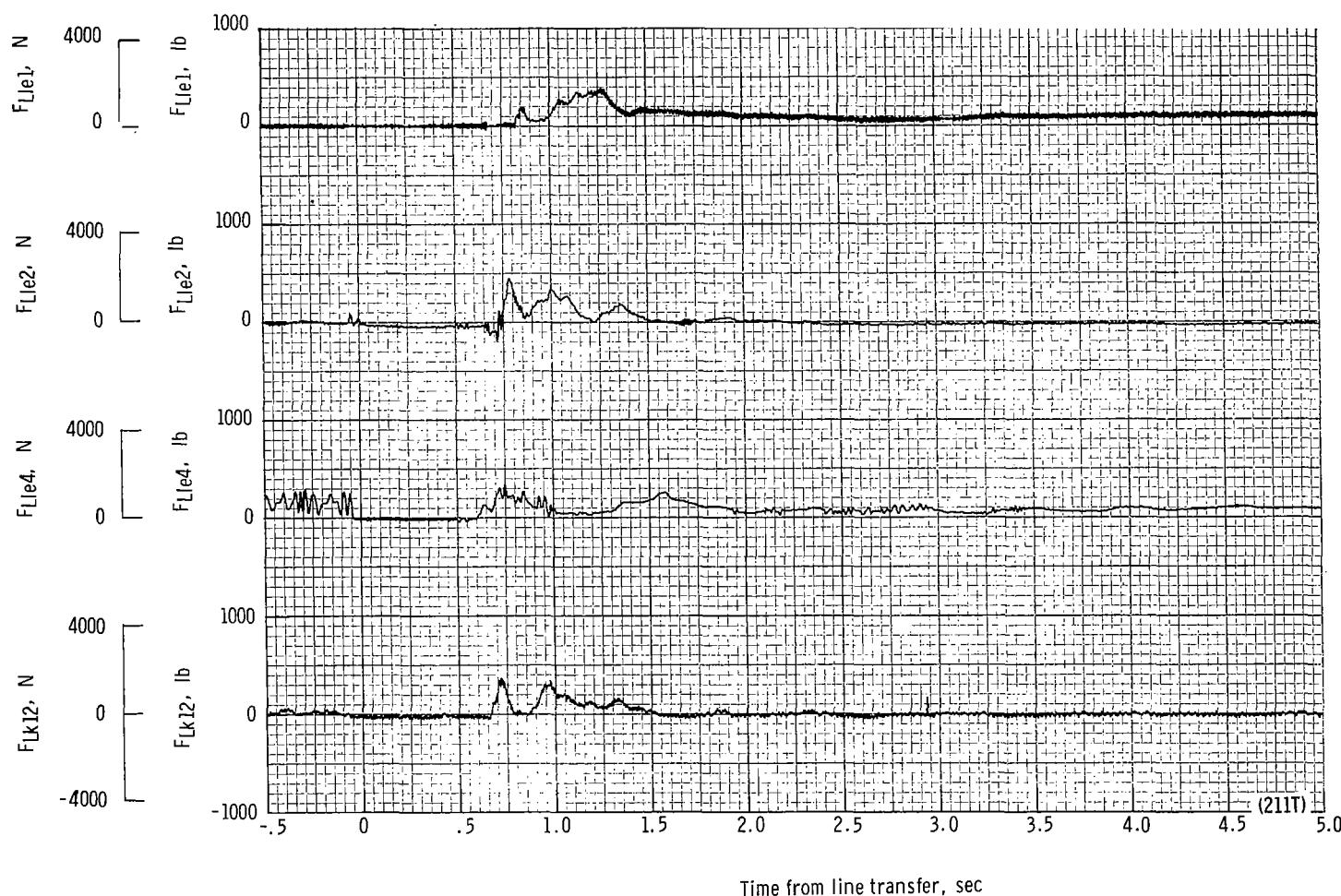
(s) Total force F_t plotted against time from third-stage disreef. Time = 0 second corresponds to 38.00 seconds after launch.

Figure 52.- Continued.



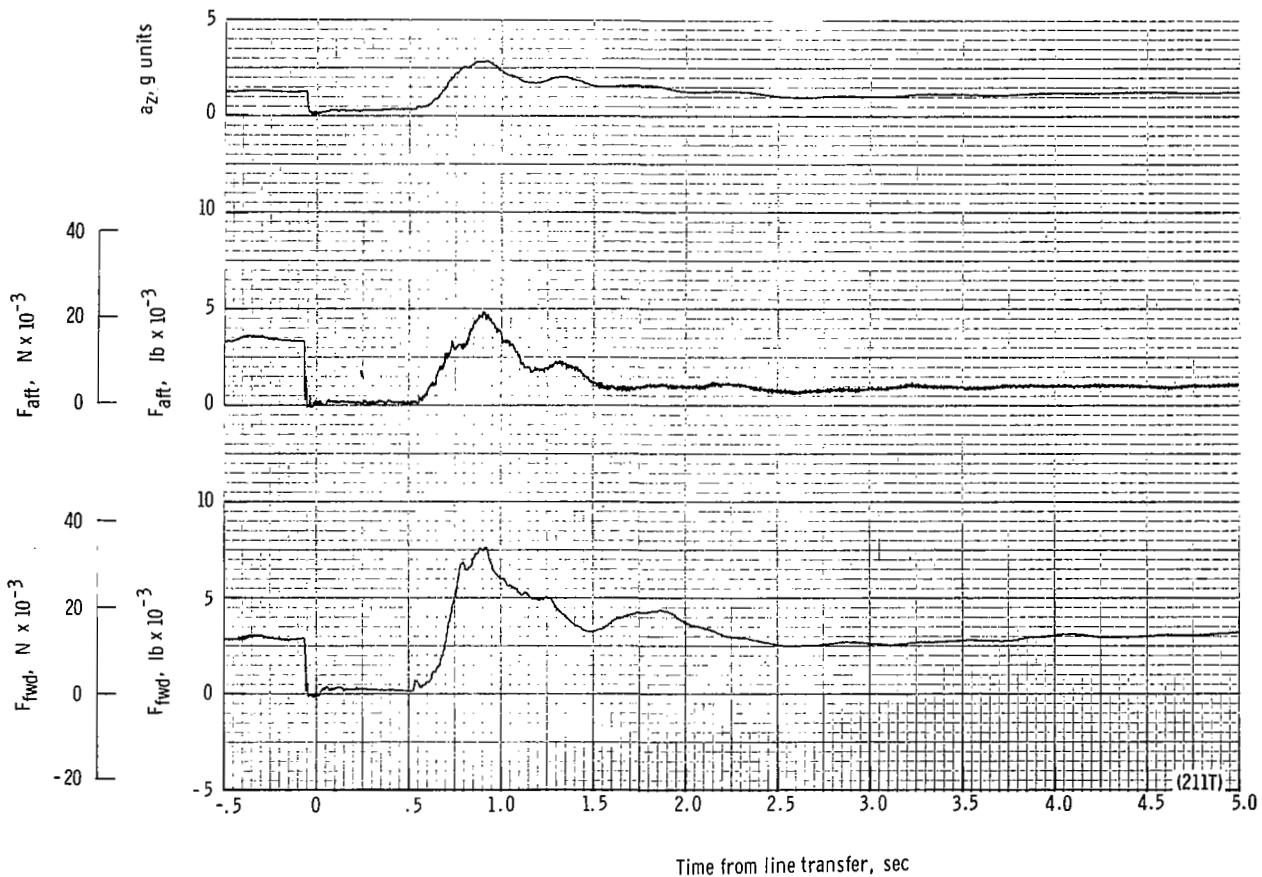
(t) Total force coefficient $C_{F,t}$ and dynamic pressure q plotted against time from third-stage disreef. Time = 0 second corresponds to 38.00 seconds after launch.

Figure 52.- Continued.



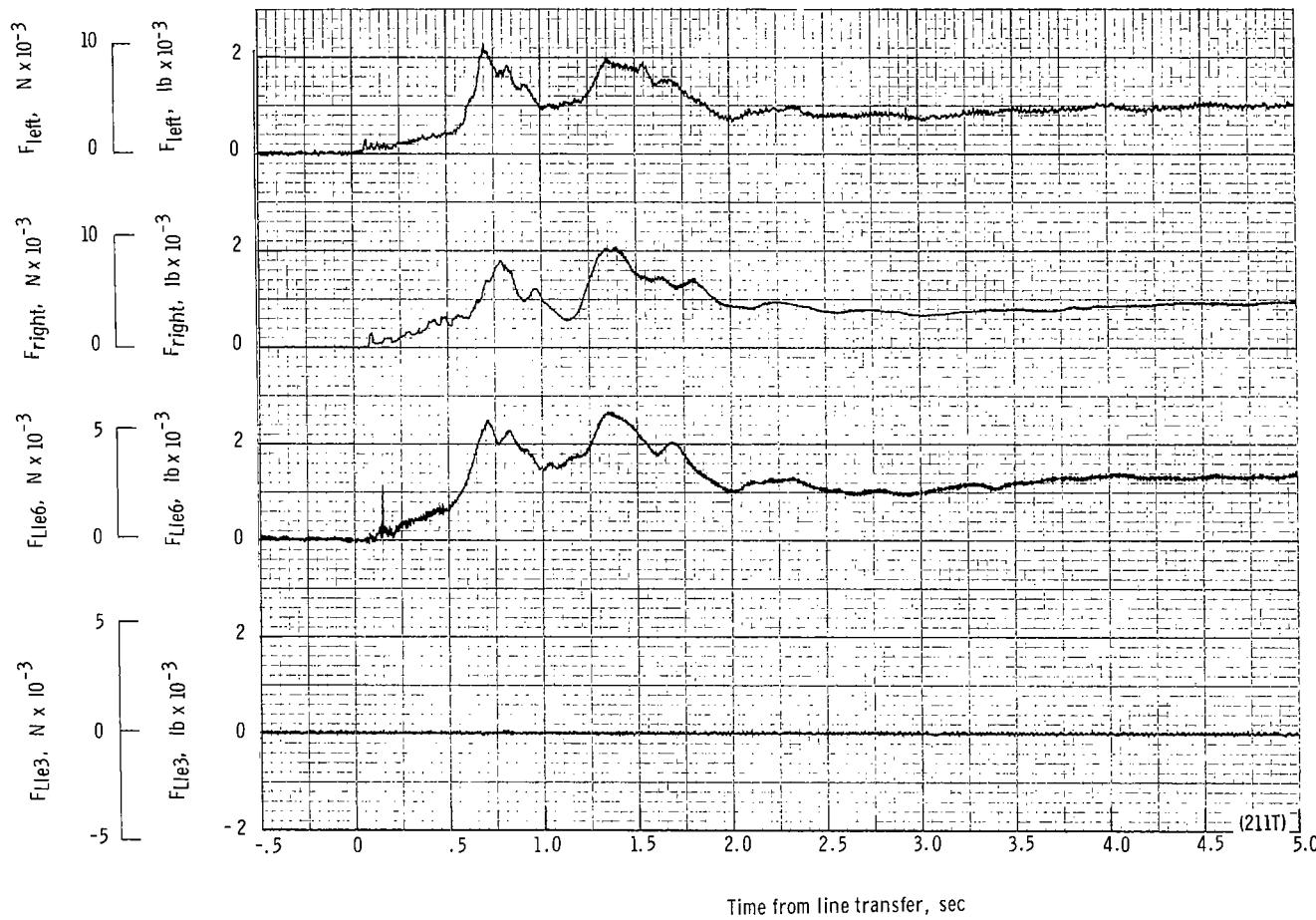
(u) Individual suspension-line loads F_{Lk12} , F_{Lle4} , F_{Lle2} and F_{Lle1} plotted against time from line transfer. Time = 0 second corresponds to 41.68 seconds after launch.

Figure 52.- Continued.



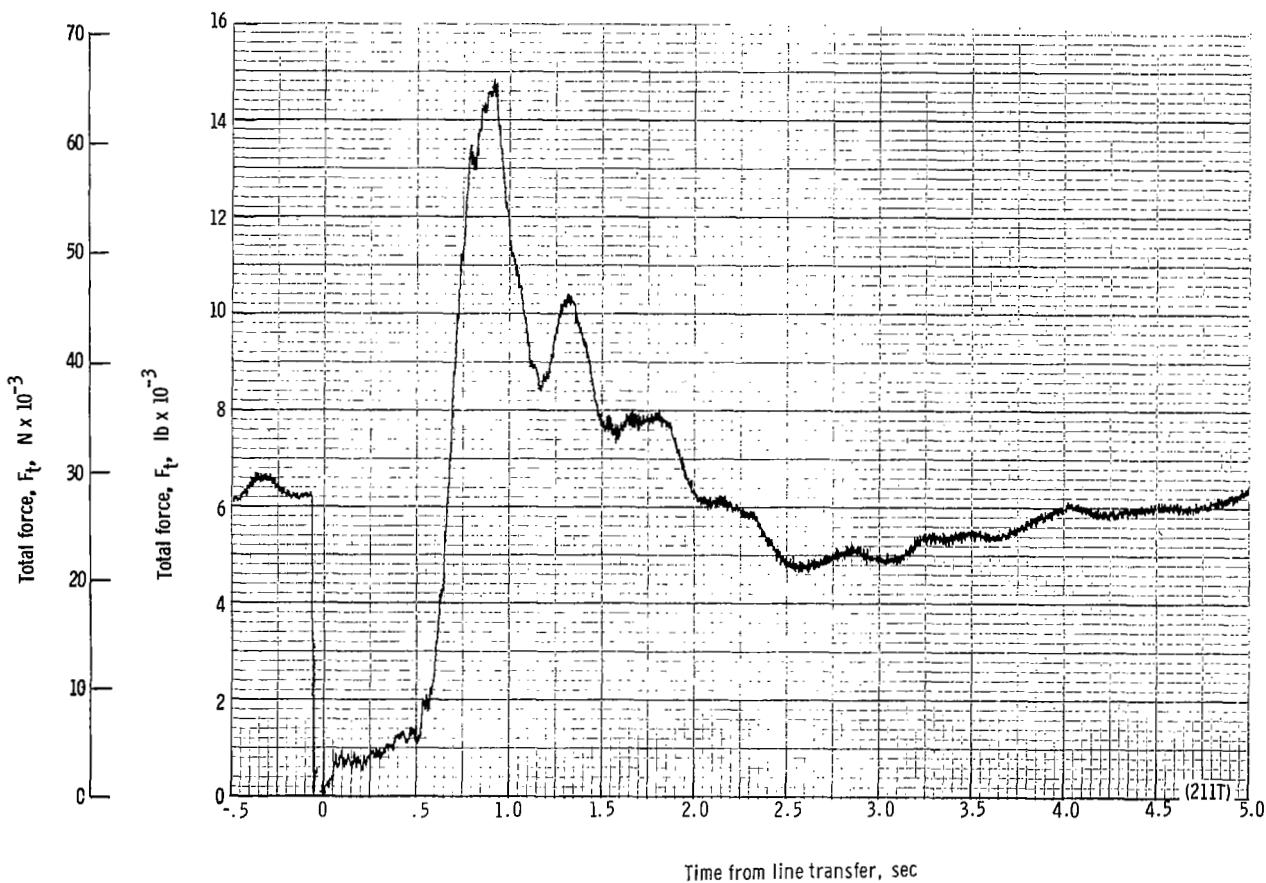
(v) Forward and aft riser loads and acceleration a_z plotted against time from line transfer. Time = 0 second corresponds to 41.68 seconds after launch.

Figure 52.- Continued.



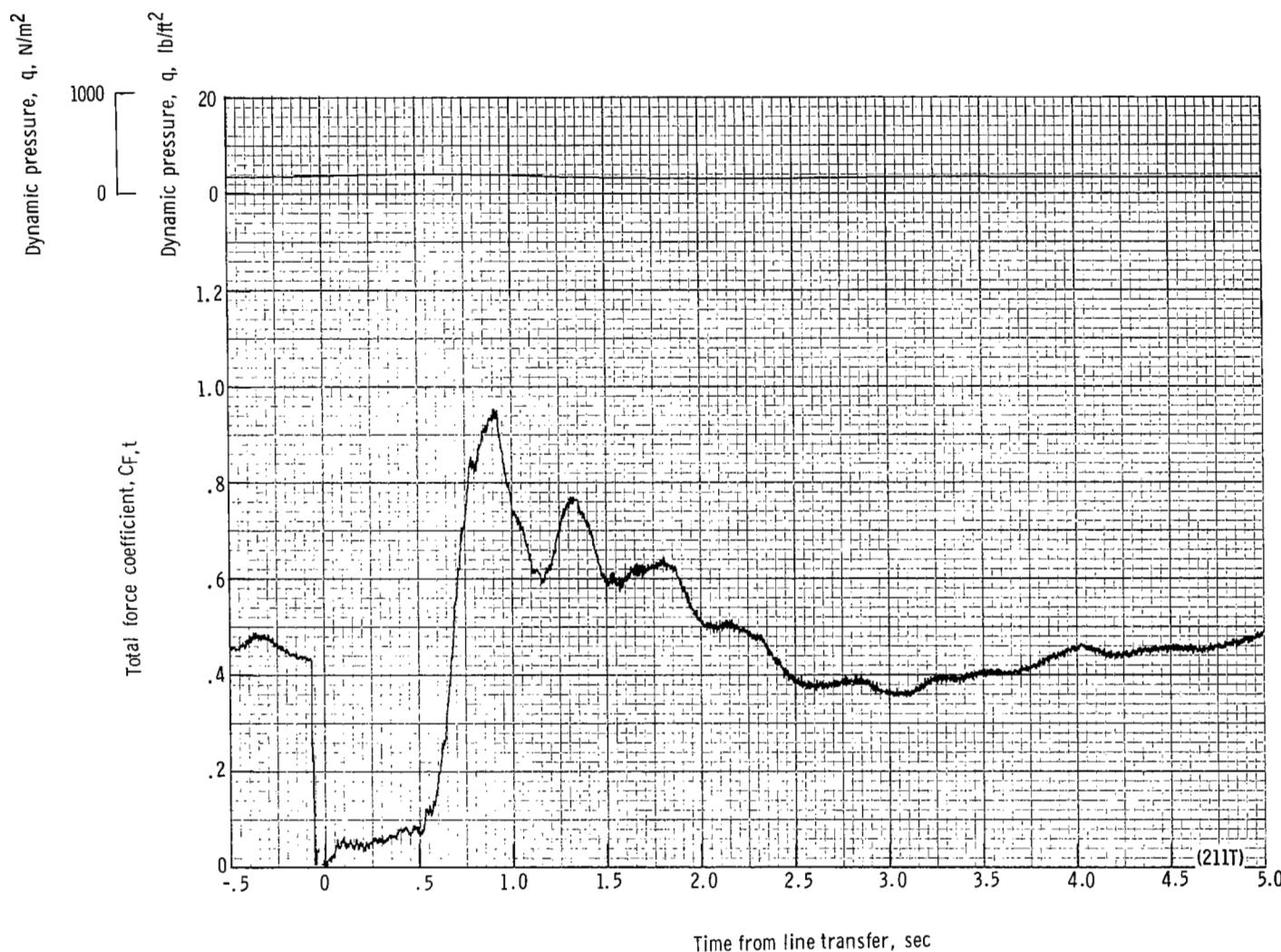
(w) Individual suspension-line loads $F_{\text{Lle}3}$ and $F_{\text{Lle}6}$ and right and left suspension-line loads plotted against time from line transfer. Time = 0 second corresponds to 41.68 seconds after launch.

Figure 52.- Continued.



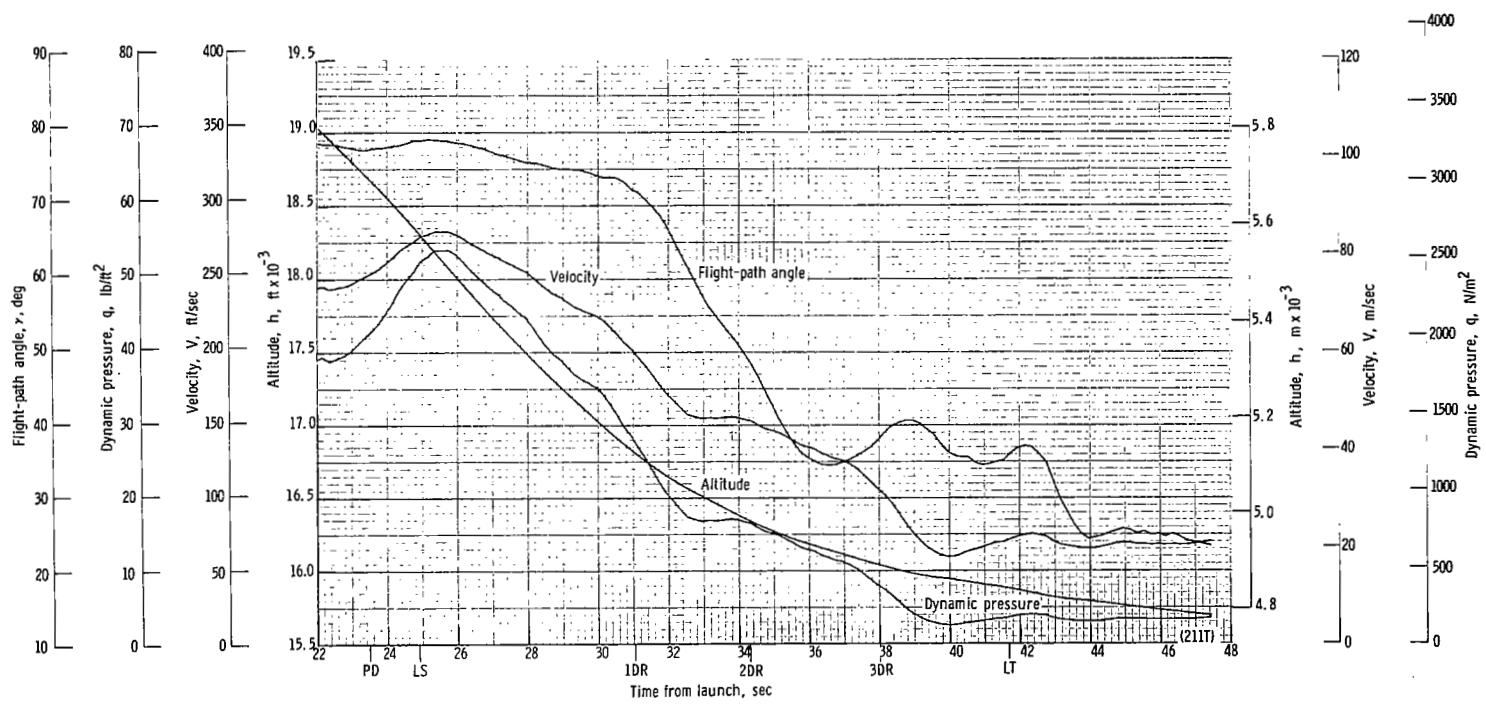
(x) Total force F_t plotted against time from line transfer. Time = 0 second corresponds to 41.68 seconds after launch.

Figure 52.- Continued.



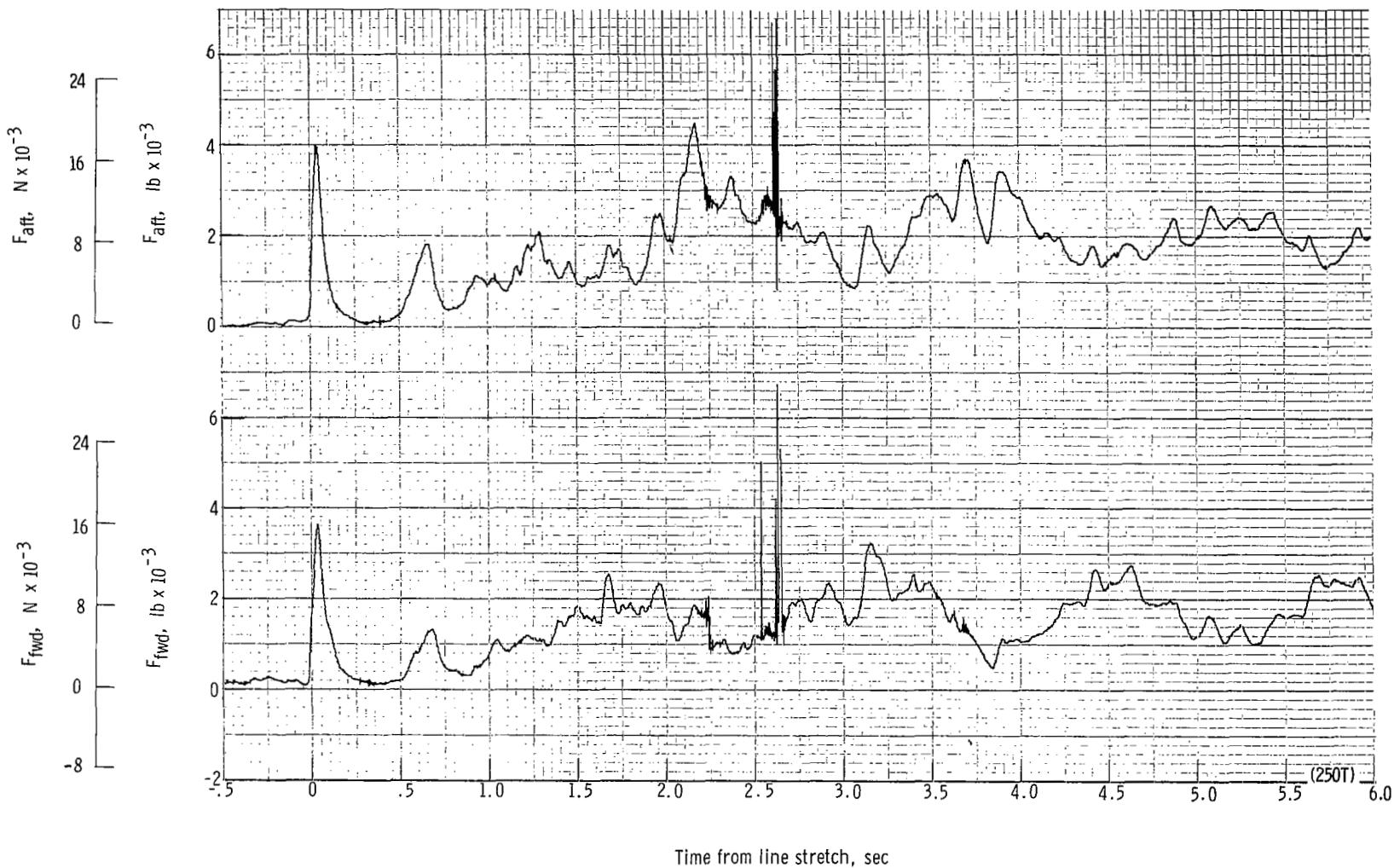
(y) Total force coefficient $C_{F,t}$ and dynamic pressure q plotted against time from line transfer. Time = 0 second corresponds to 41.68 seconds after launch.

Figure 52.- Continued.



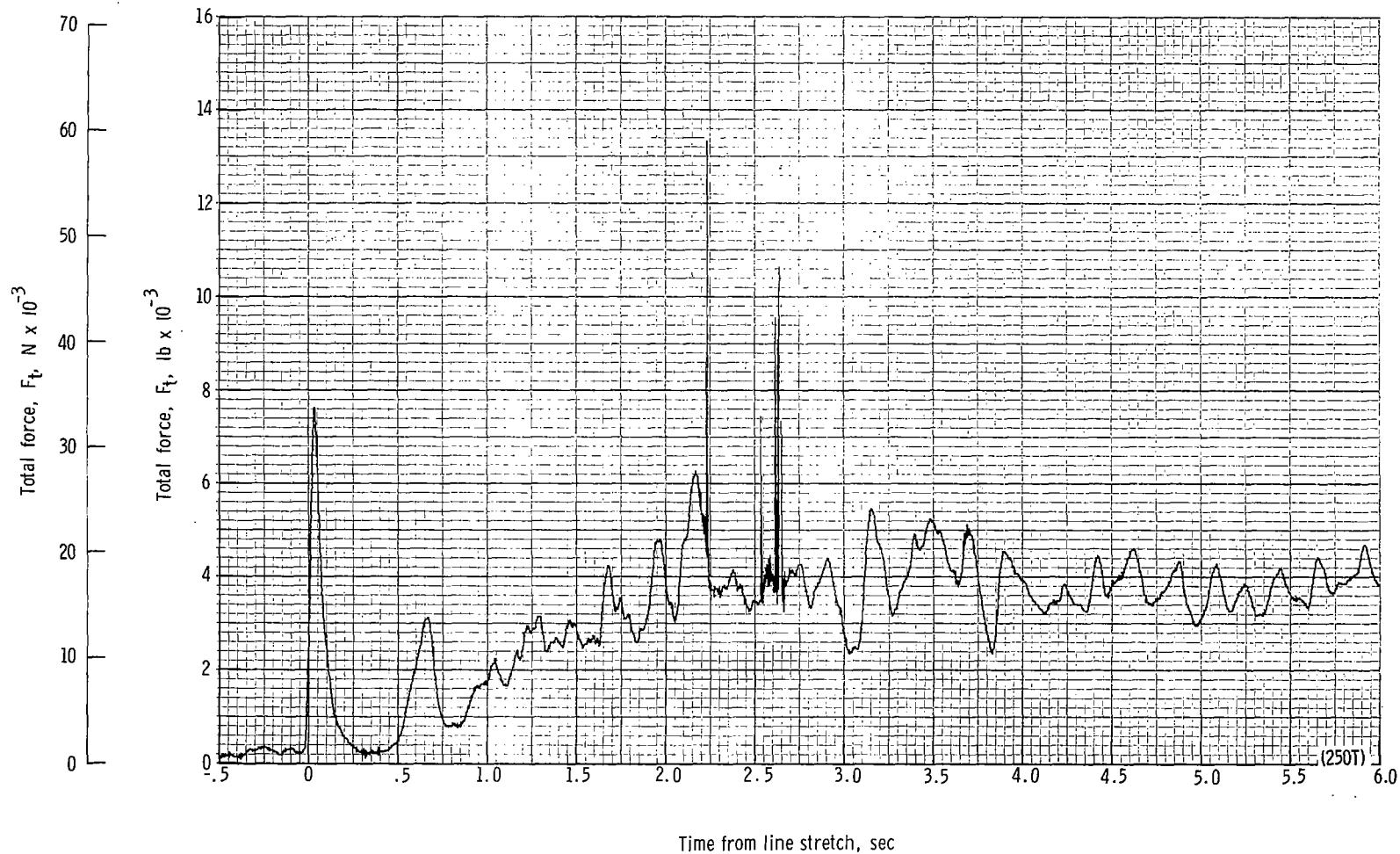
(z) Flight-path angle γ , dynamic pressure q , velocity V , and altitude h plotted against time from launch.

Figure 52.- Concluded.



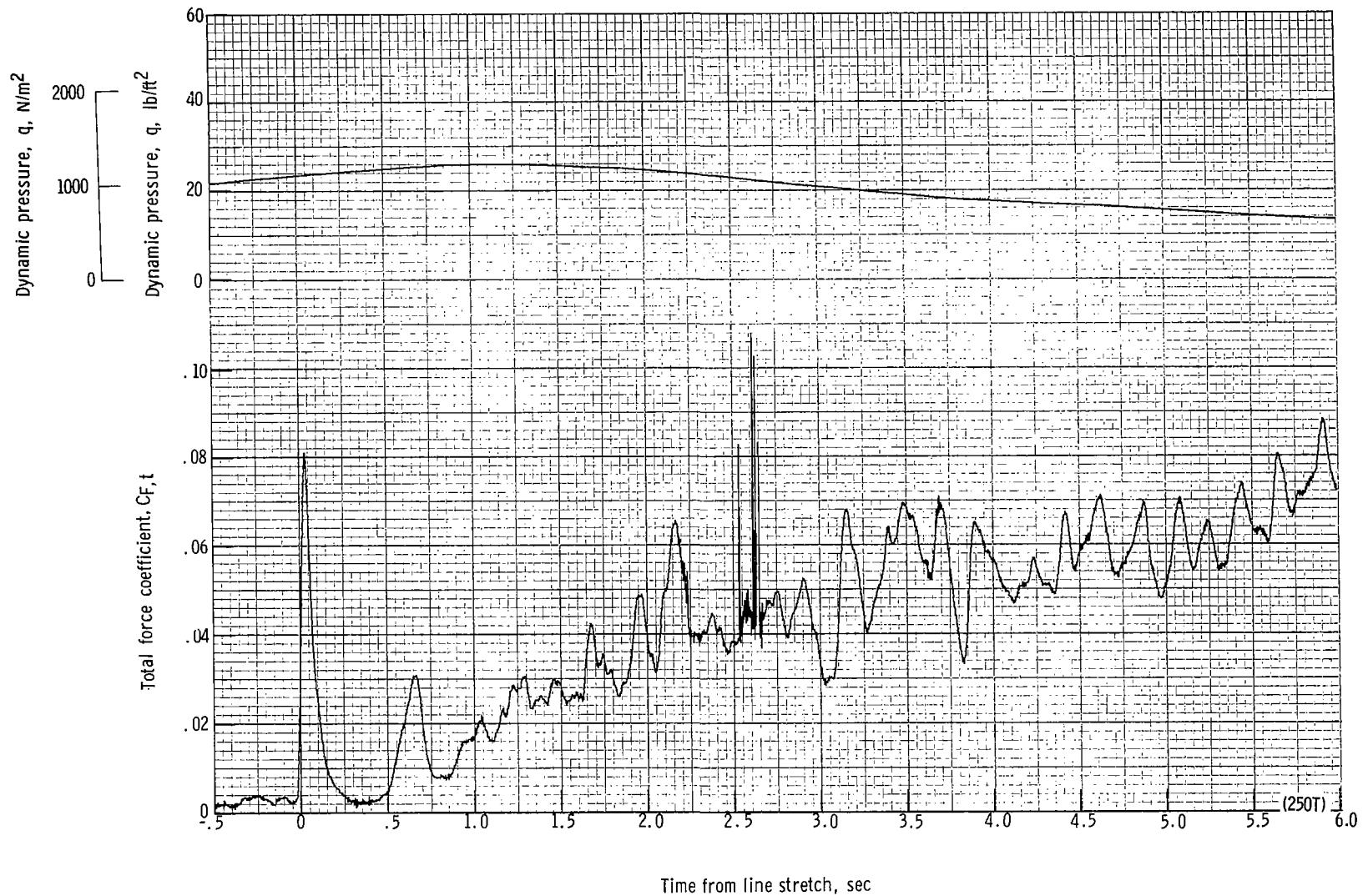
(a) Forward and aft riser loads plotted against time from line stretch. Time = 0 second corresponds to 12.68 seconds after launch.

Figure 53.- Time history of twin-keel parawing deployment data for test 250T. $W_D = 15\ 320\ N$ (3444 lb); $W_P = 13\ 613\ N$ (3060 lb); $q_{PD} = 732\ N/m^2$ (15.3 lb/ft²); $h_{PD} = 5899\ m$ (19 353 ft); $l_r/l_k = 0.100$; reefing version B.



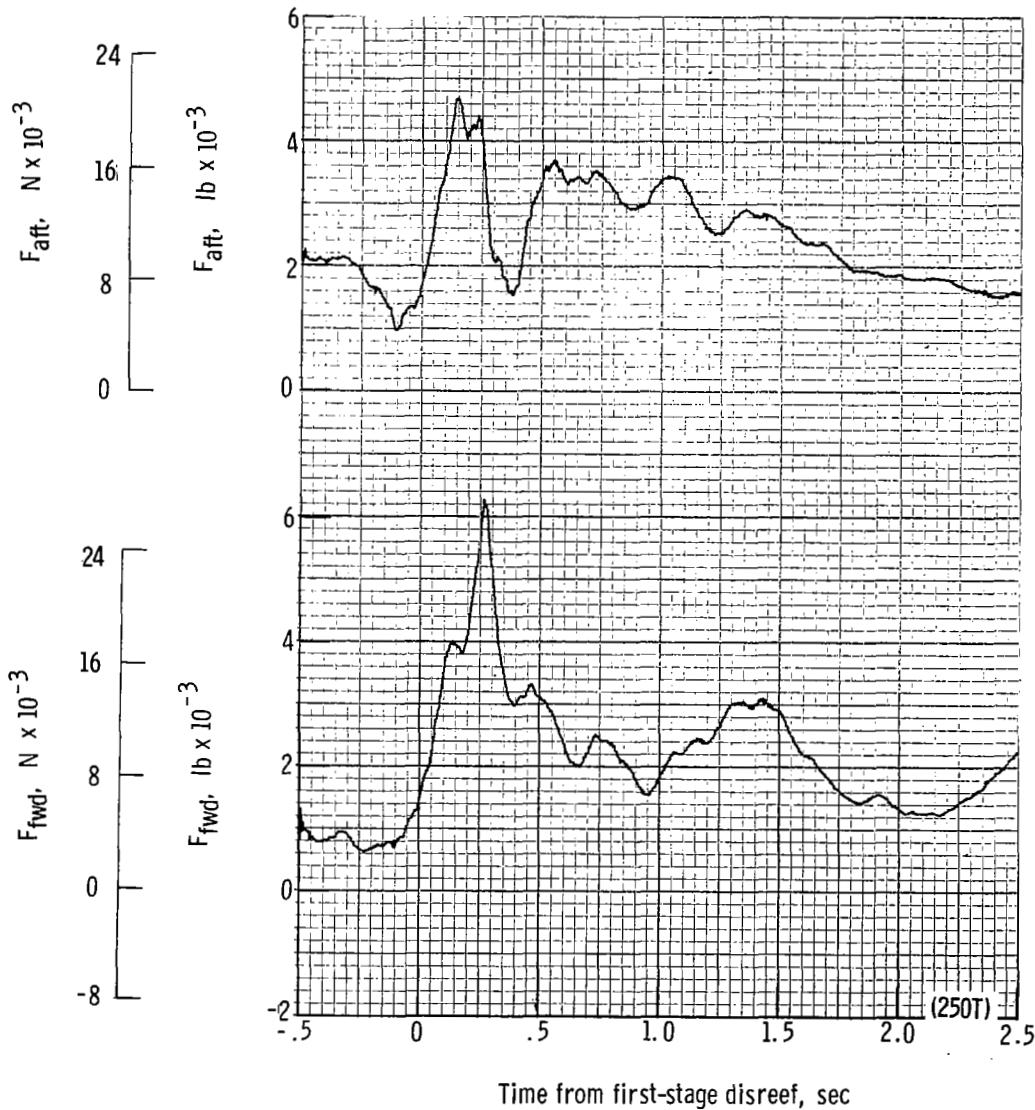
(b) Total force F_t plotted against time from line stretch. Time = 0 second corresponds to 12.68 seconds after launch.

Figure 53.- Continued.



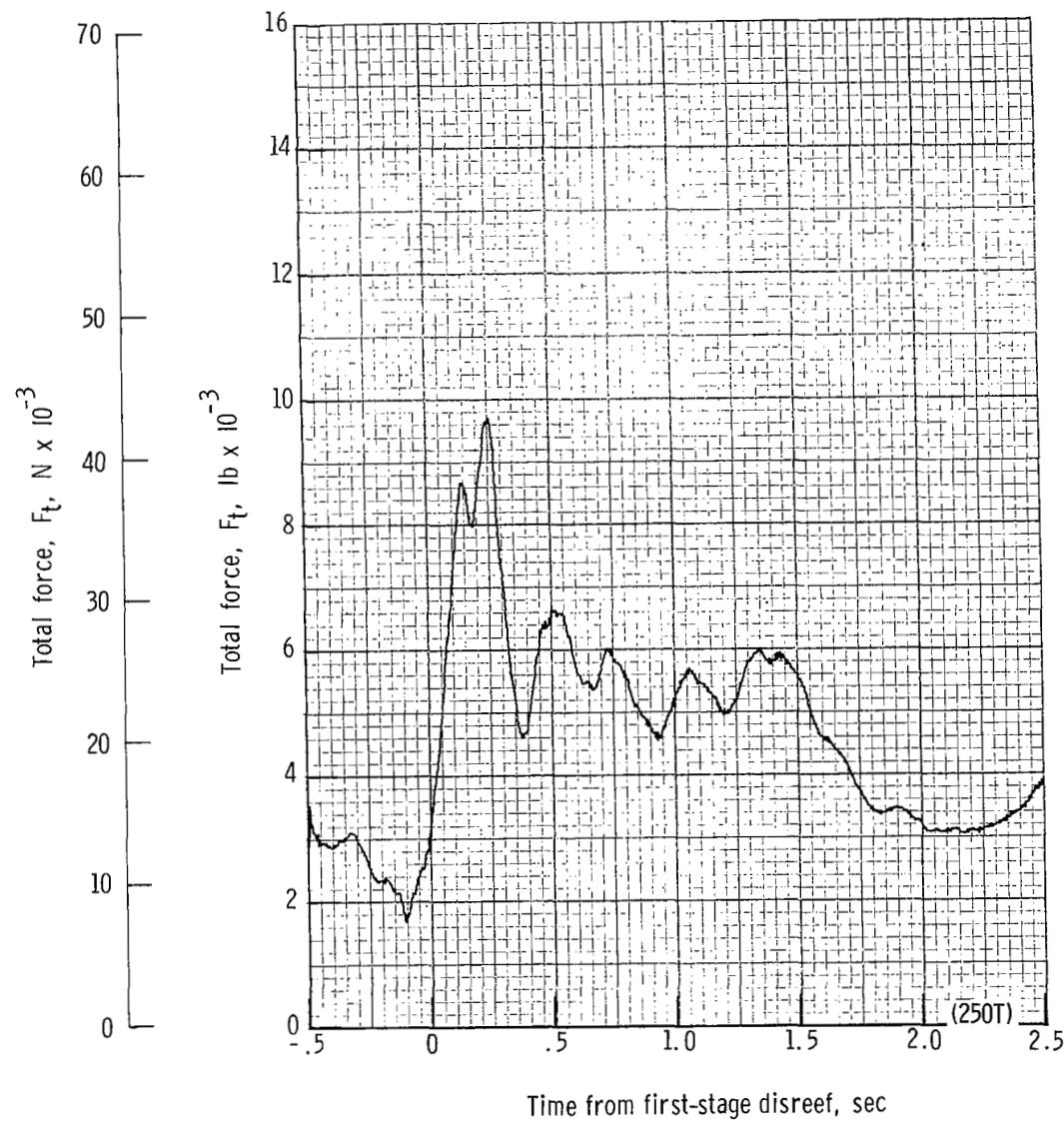
(c) Total force coefficient $C_{F,t}$ and dynamic pressure q plotted against time from line stretch. Time = 0 second corresponds to 12.68 seconds after launch.

Figure 53.- Continued.



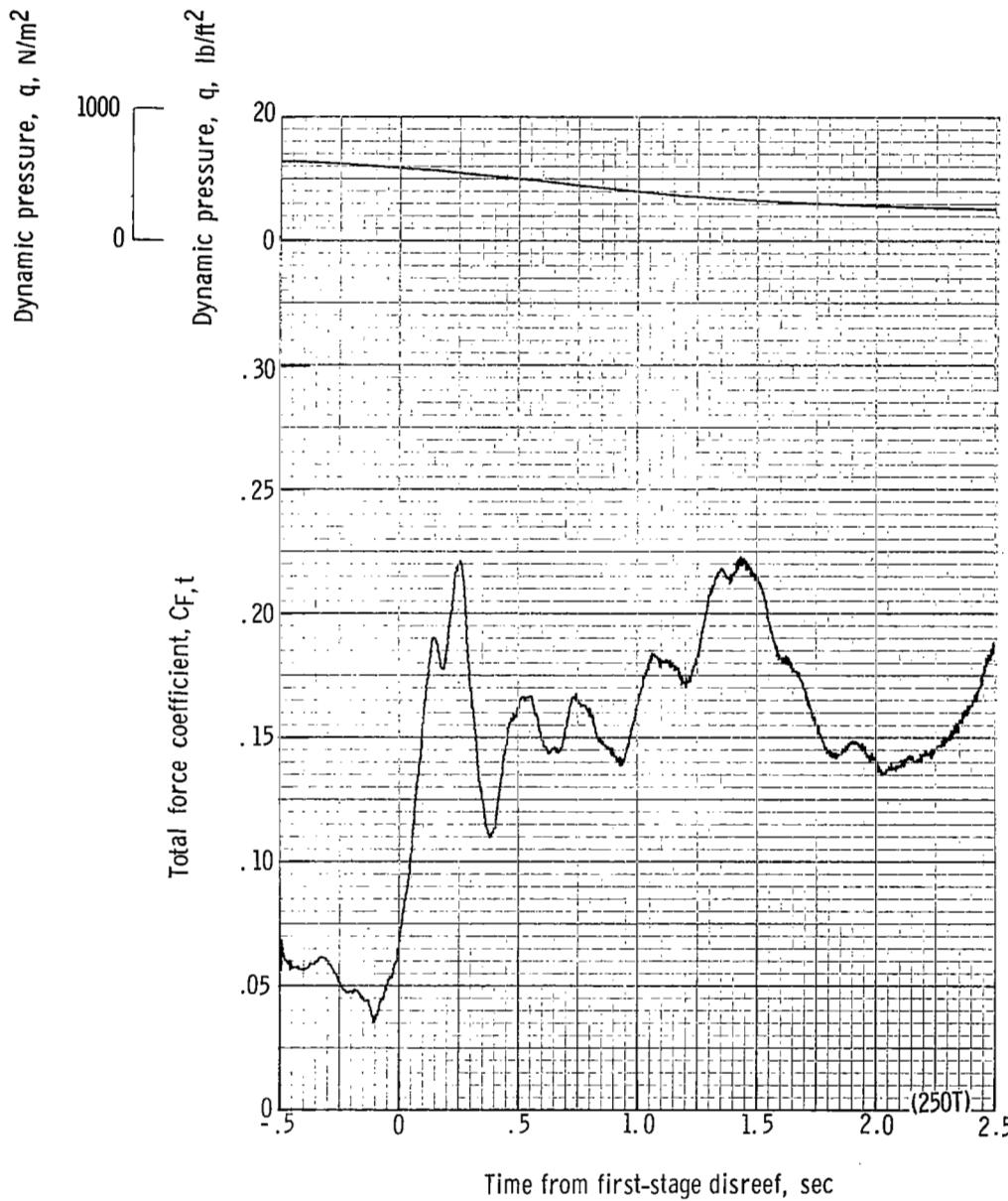
(d) Forward and aft riser loads plotted against time from first-stage disreef. Time = 0 second corresponds to 19.40 seconds after launch.

Figure 53.- Continued.



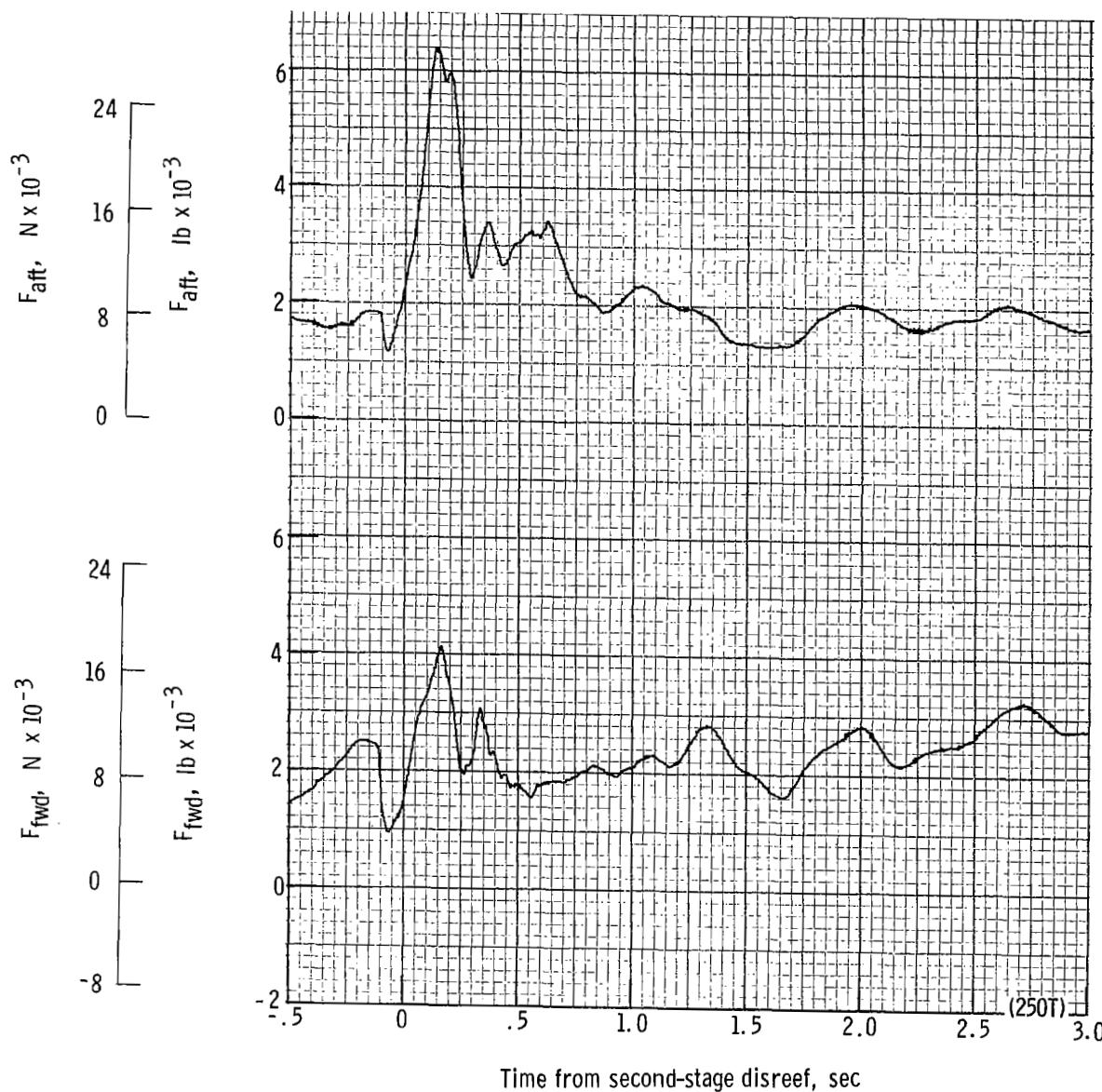
(e) Total force F_t plotted against time from first-stage disreef. Time = 0 second corresponds to 19.40 seconds after launch.

Figure 53.- Continued.



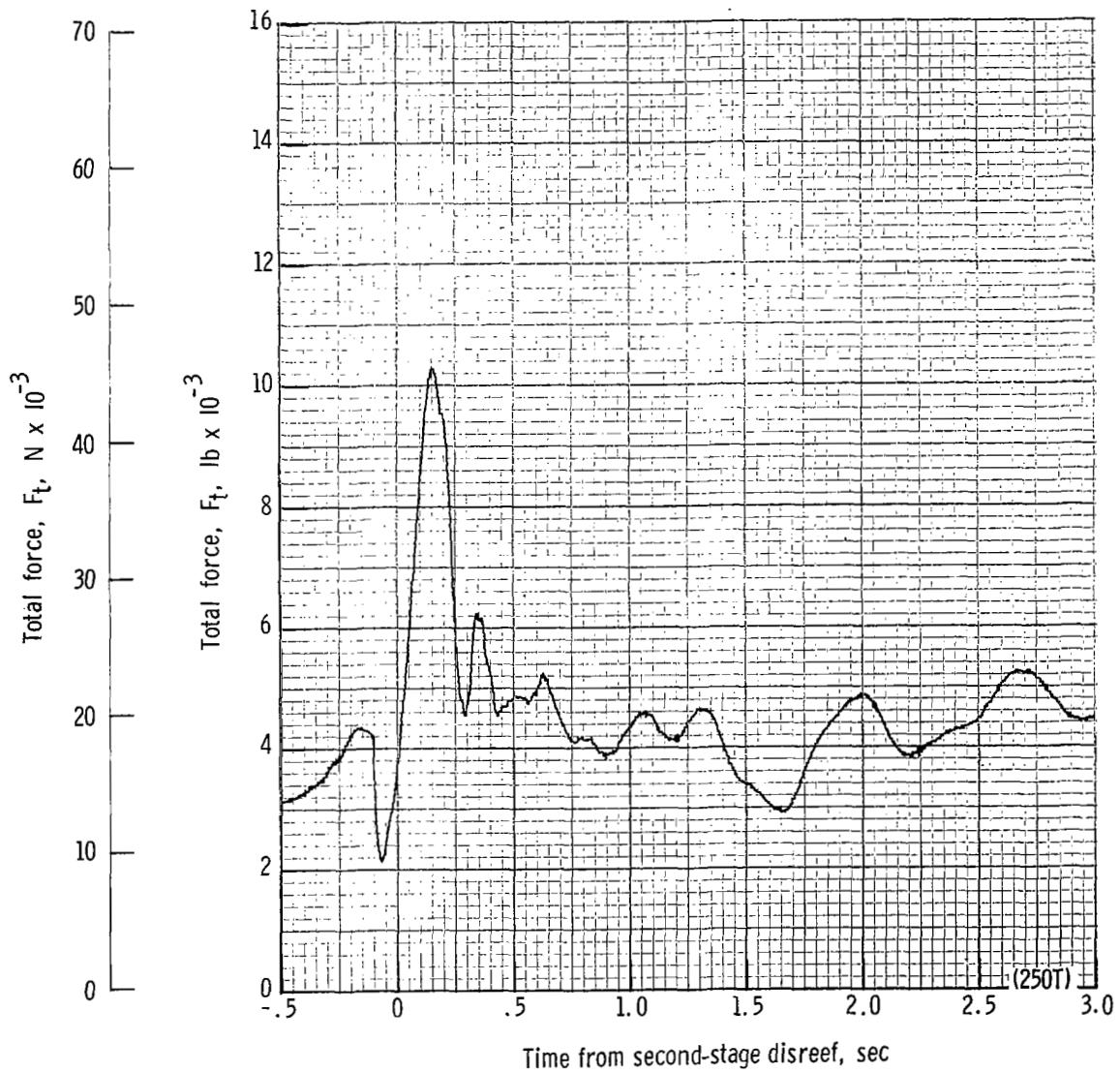
(f) Total force coefficient $C_{F,t}$ and dynamic pressure q plotted against time from first-stage disreef. Time = 0 second corresponds to 19.40 seconds after launch.

Figure 53.- Continued.



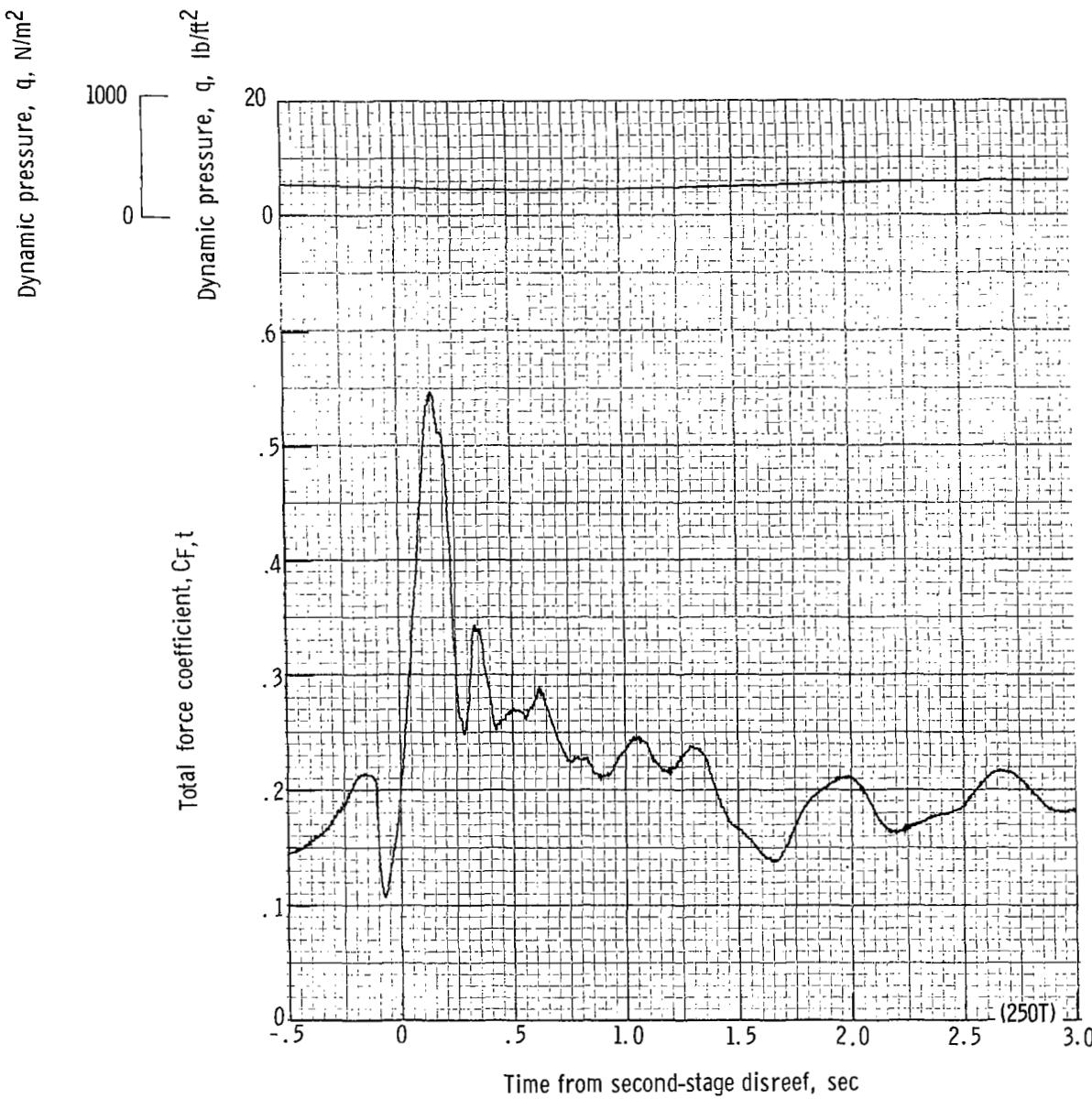
(g) Forward and aft riser loads plotted against time from second-stage disreef. Time = 0 second corresponds to 22.14 seconds after launch.

Figure 53.- Continued.



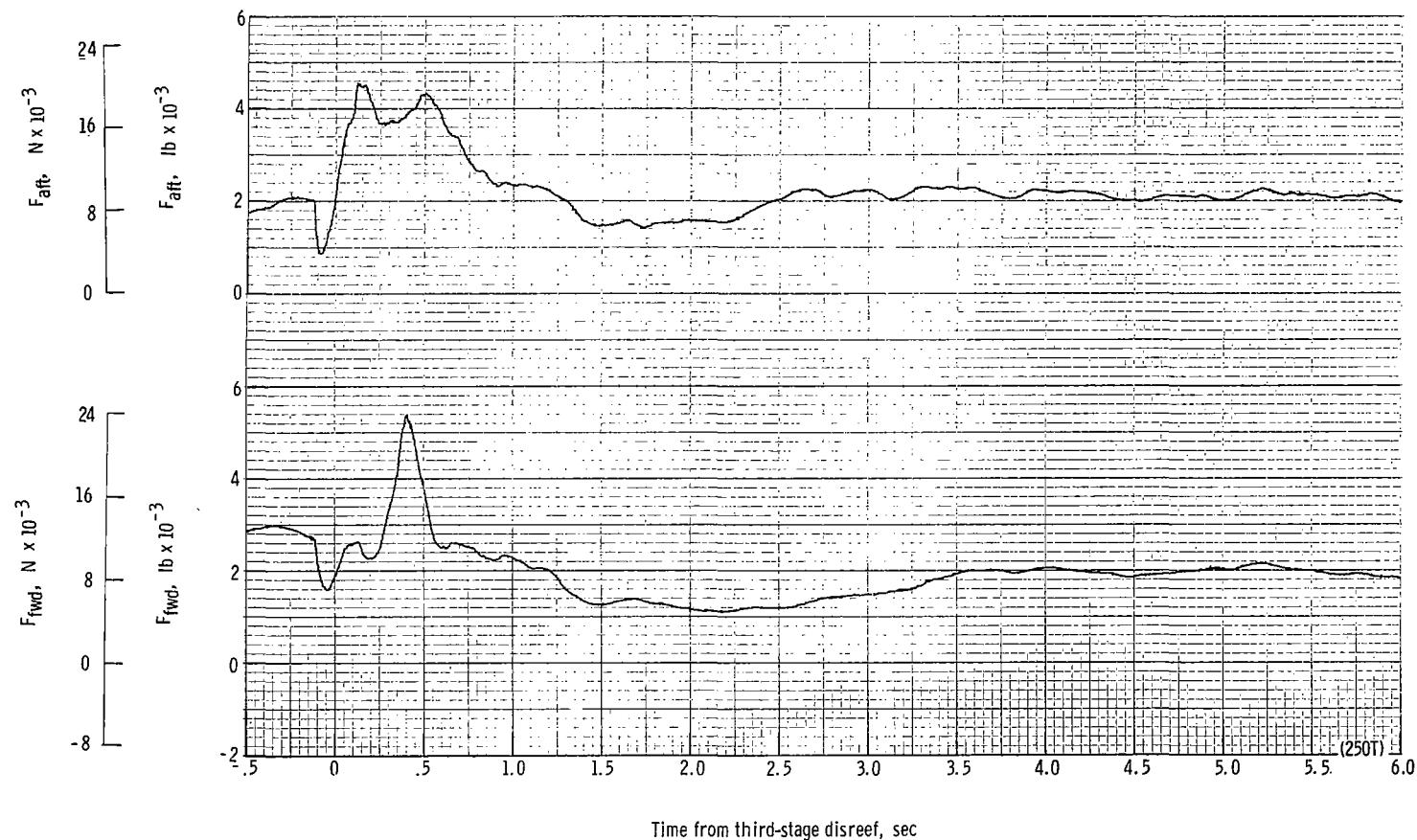
(h) Total force F_t plotted against time from second-stage disreef. Time = 0 second corresponds to 22.14 seconds after launch.

Figure 53.- Continued.



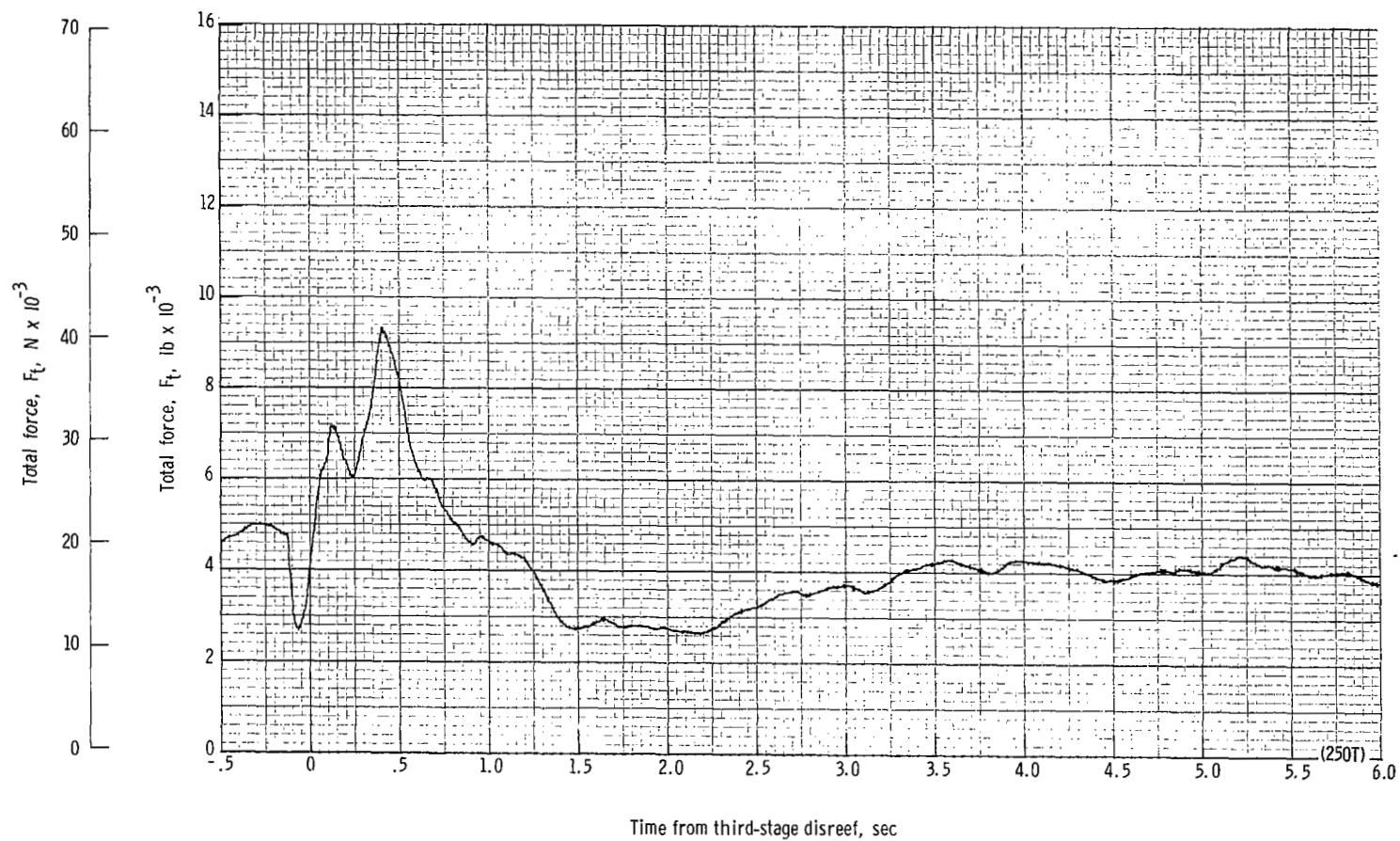
(i) Total force coefficient $C_{F,t}$ and dynamic pressure q plotted against time from second-stage disreef. Time = 0 second corresponds to 22.14 seconds after launch.

Figure 53.- Continued.



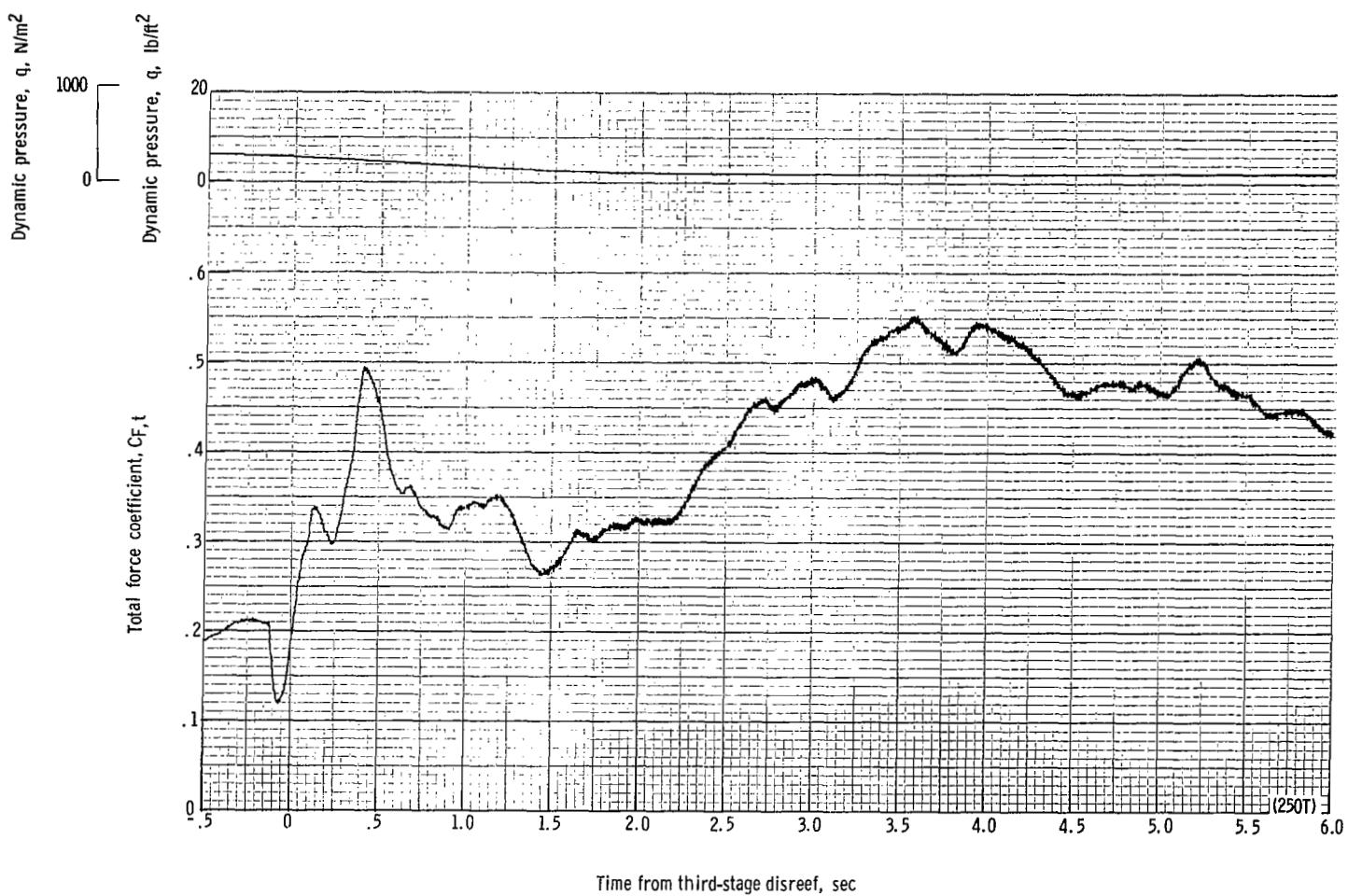
(j) Forward and aft riser loads plotted against time from third-stage disreef. Time = 0 second corresponds to 25.70 seconds after launch.

Figure 53.- Continued.



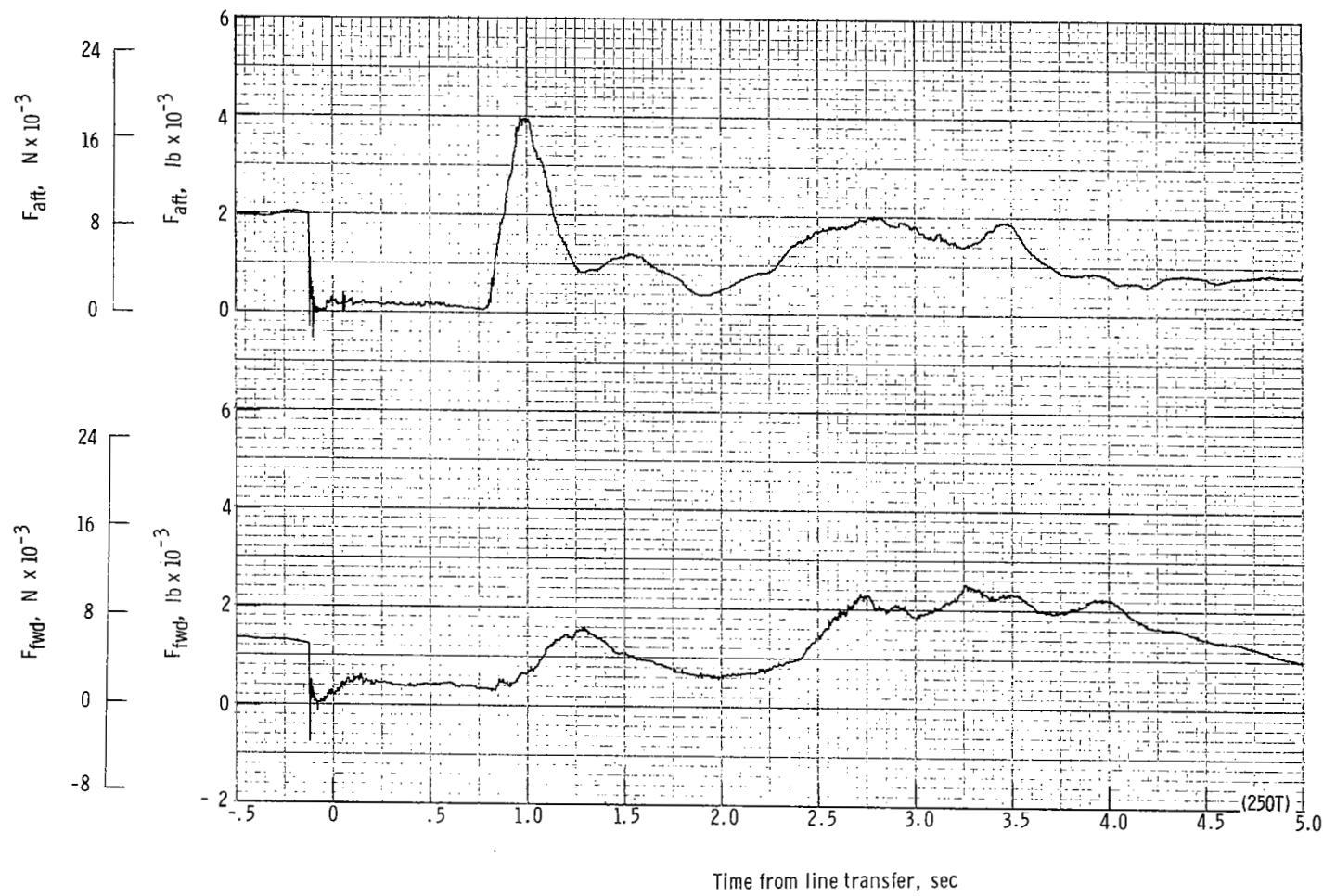
(k) Total force F_t plotted against time from third-stage disreef. Time = 0 second corresponds to 25.70 seconds after launch.

Figure 53.- Continued.



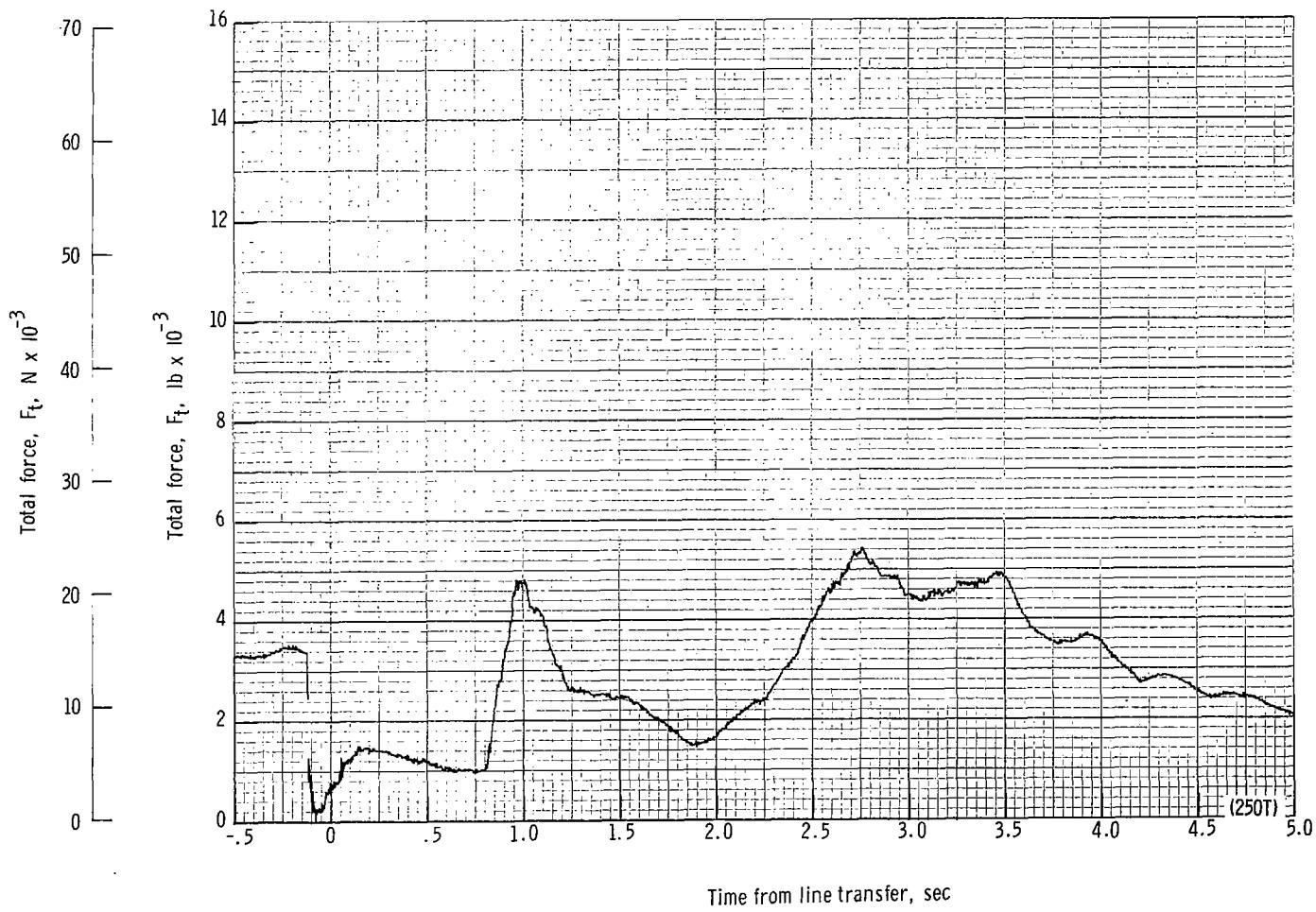
(II) Total force coefficient $C_{F,t}$ and dynamic pressure q plotted against time from third-stage disreef. Time = 0 second corresponds to 25.70 seconds after launch.

Figure 53.- Continued.



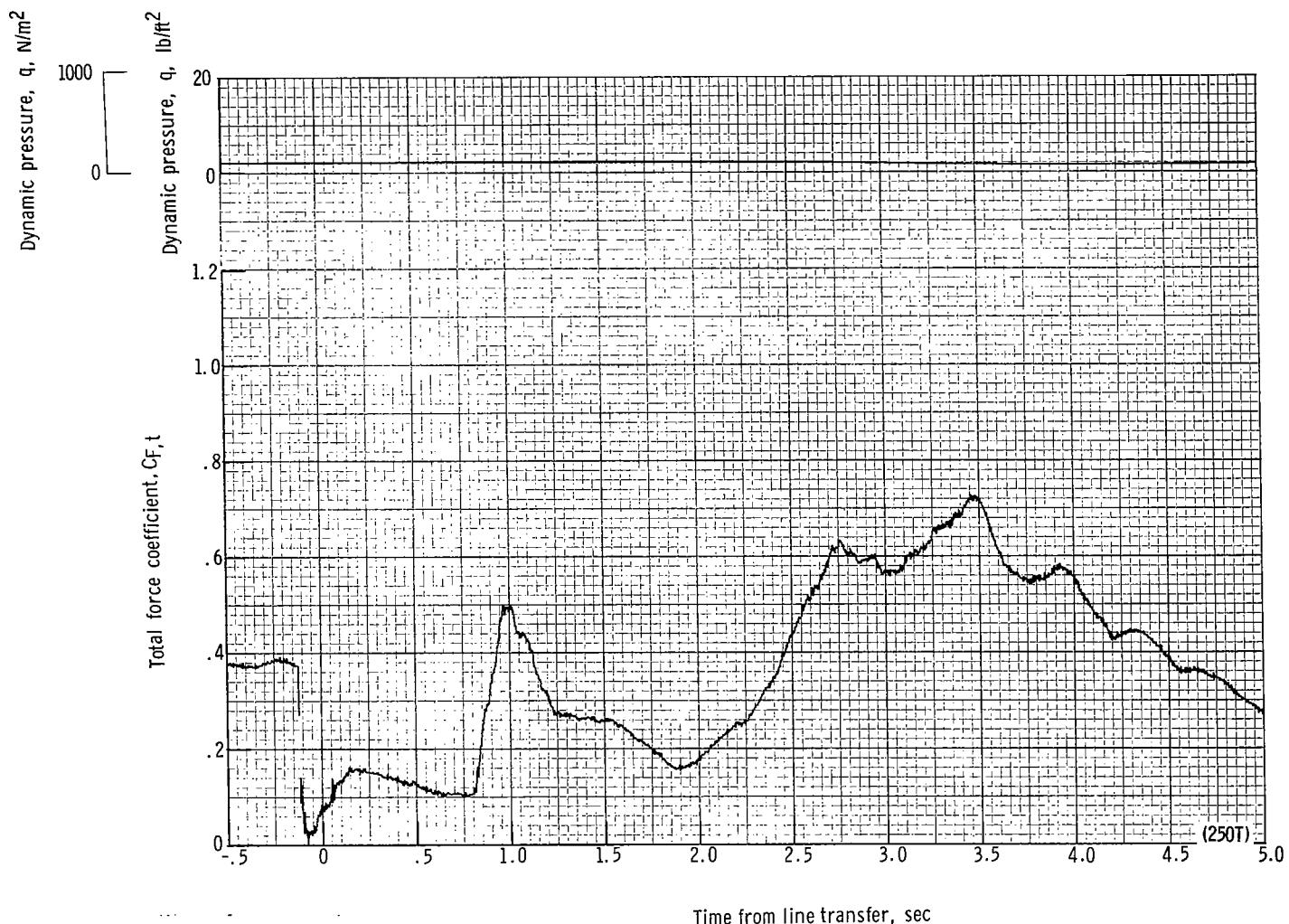
(m) Forward and aft riser loads plotted against time from line transfer. Time = 0 second corresponds to 32.98 seconds after launch.

Figure 53.- Continued.



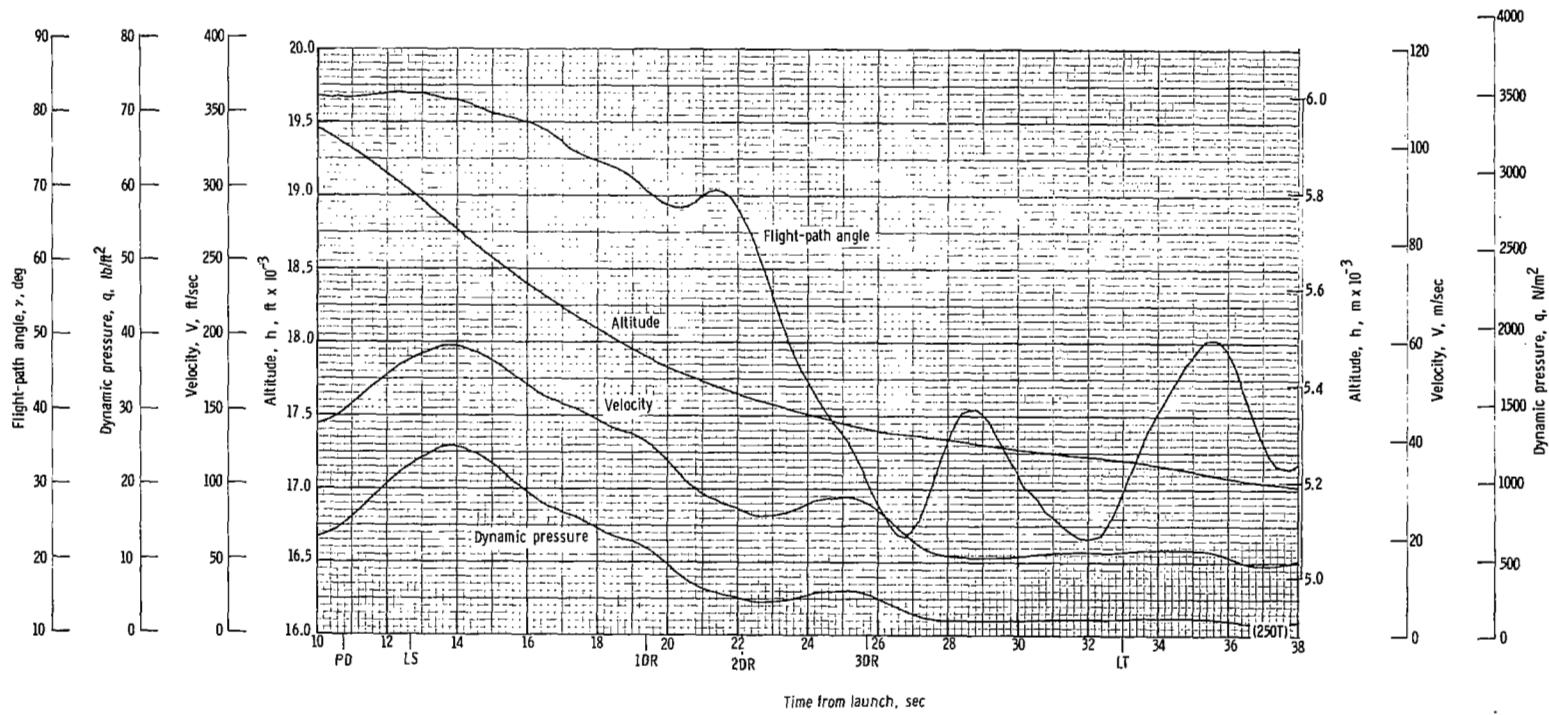
(n) Total force F_t plotted against time from line transfer. Time = 0 second corresponds to 32.98 seconds after launch.

Figure 53.- Continued.



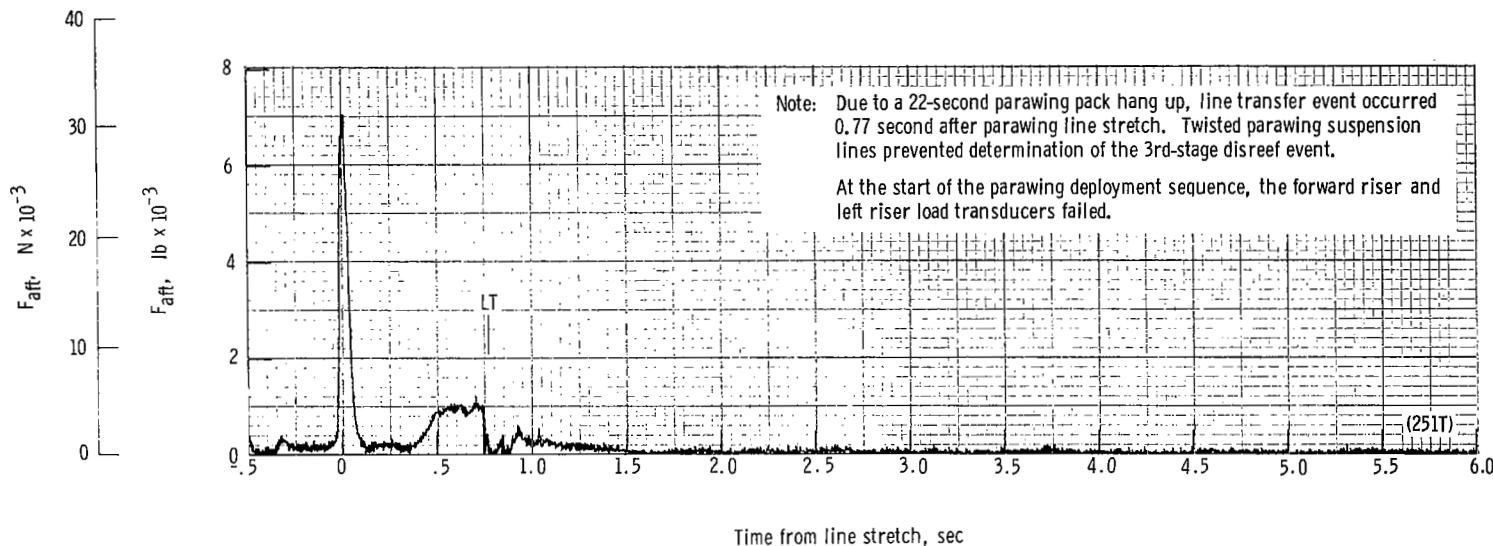
(o) Total force coefficient $C_{F,t}$ and dynamic pressure q plotted against time from line transfer. Time = 0 second corresponds to 32.98 seconds after launch.

Figure 53.- Continued.



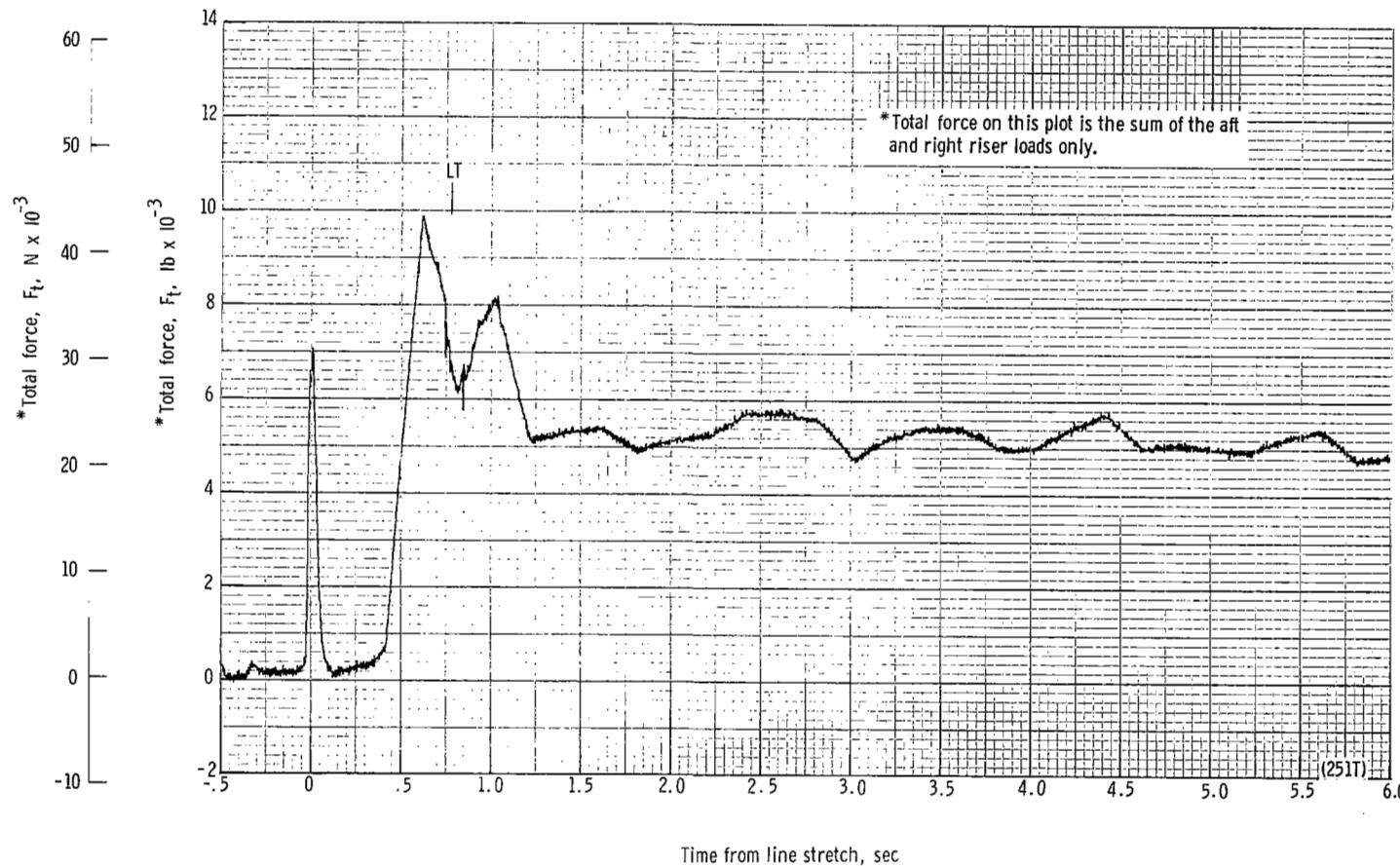
(p) Flight-path angle γ , dynamic pressure q , velocity V , and altitude h plotted against time from launch.

Figure 53.- Concluded.



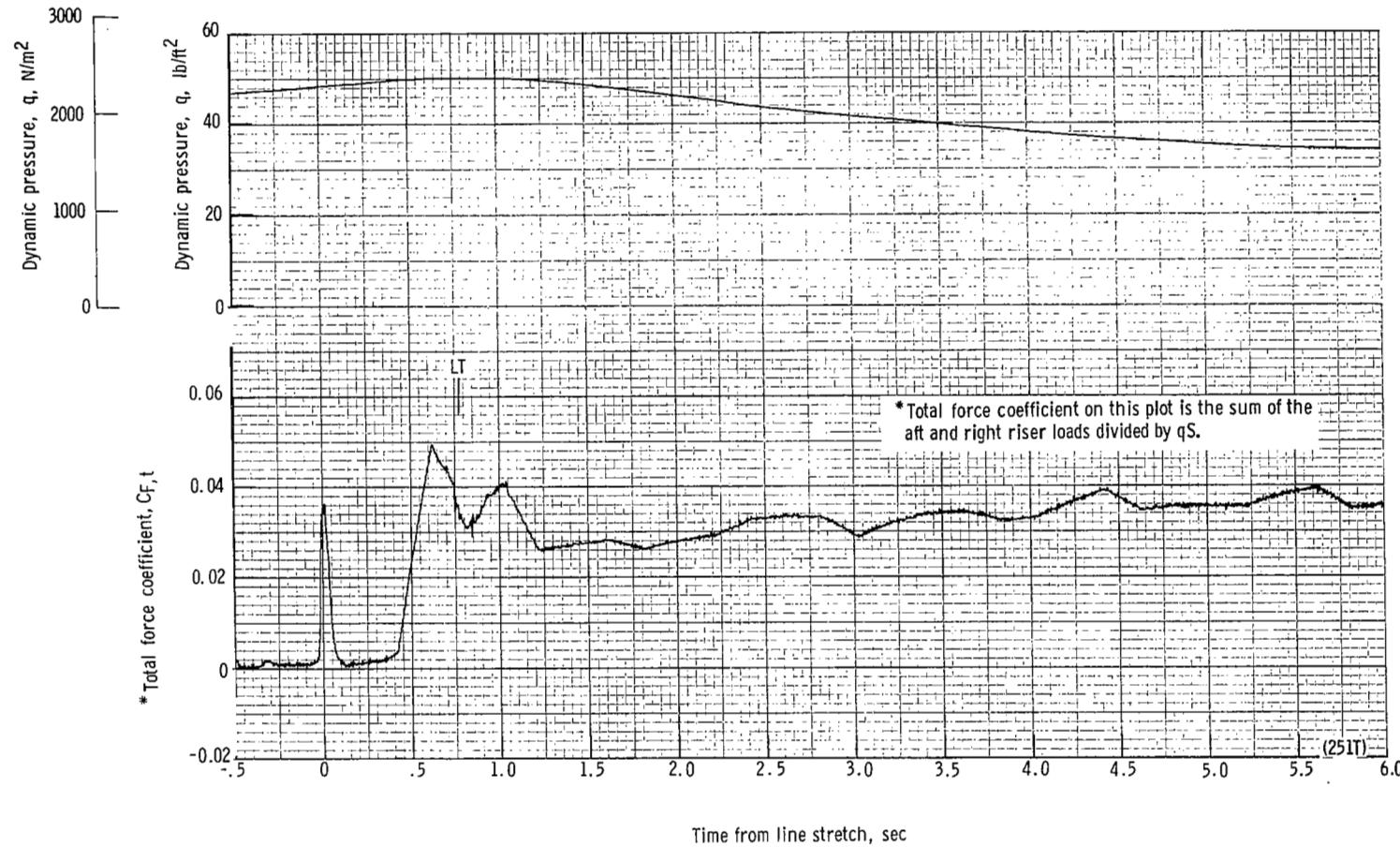
(a) Aft riser load plotted against time from line stretch. Time = 0 second corresponds to 32.99 seconds after launch.

Figure 54.- Time history of twin-keel parawing deployment data for test 251T. $W_D = 17\ 691\ N; $W_p = 15\ 975\ N; $q_{PD} = 1044\ N/m^2; $h_{PD} = 6399\ m; $l_r/l_k = 0.100$; reefing version B.$$$$



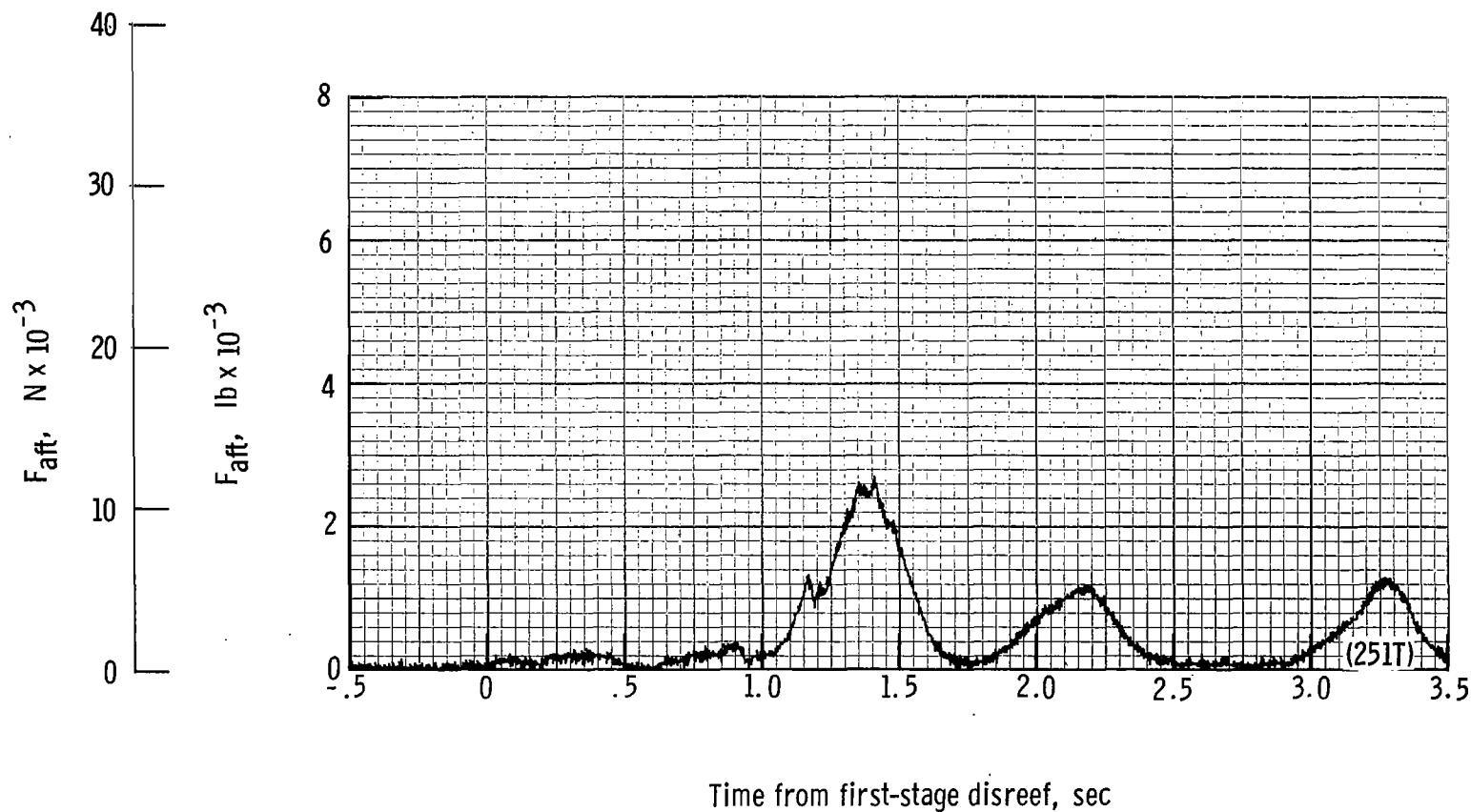
(b) Total force F_t plotted against time from line stretch. Time = 0 second corresponds to 32.99 seconds after launch.

Figure 54.- Continued.



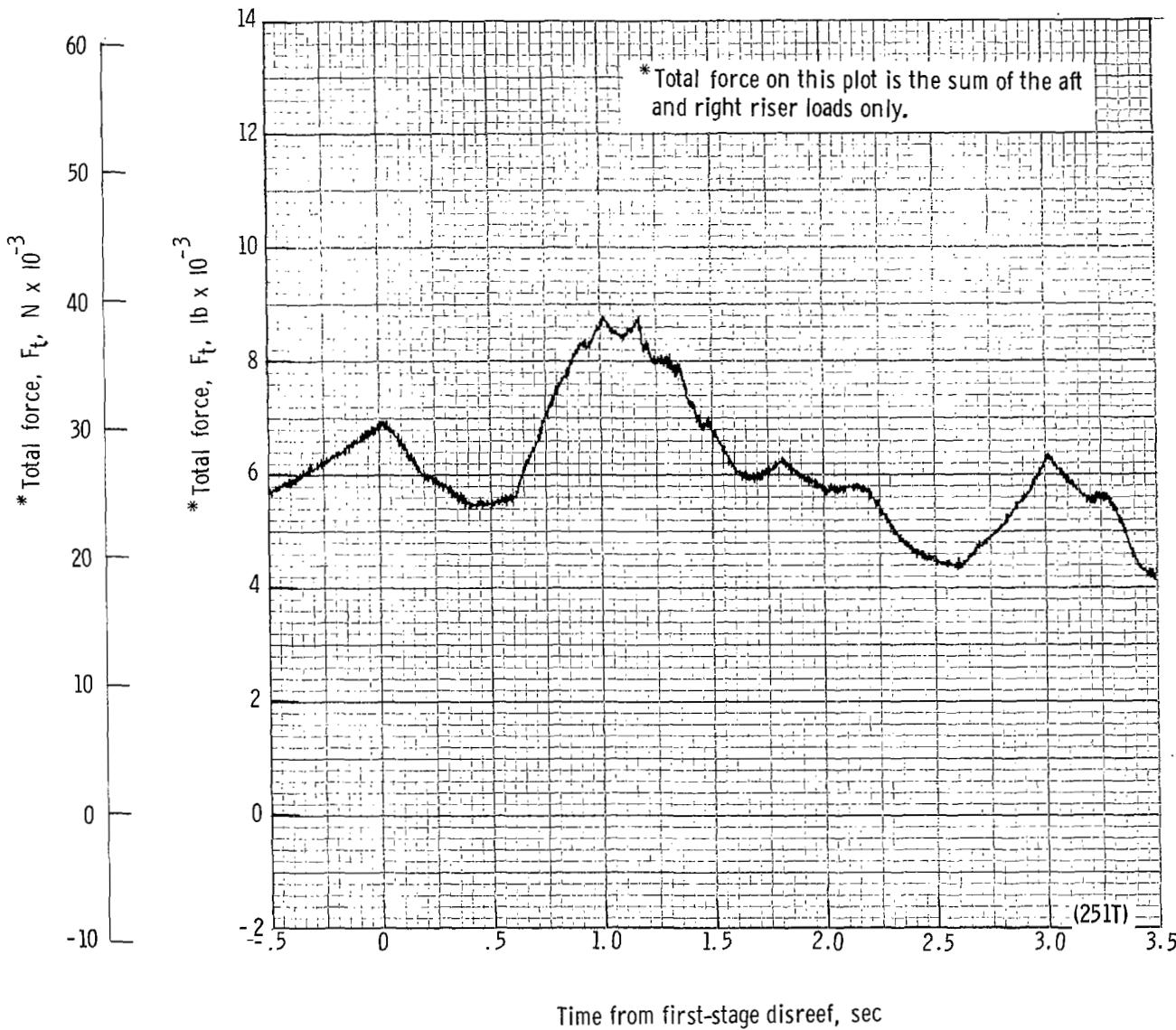
(c) Total force coefficient $C_{F,t}$ and dynamic pressure q plotted against time from line stretch. Time = 0 second corresponds to 32.99 seconds after launch.

Figure 54.- Continued.



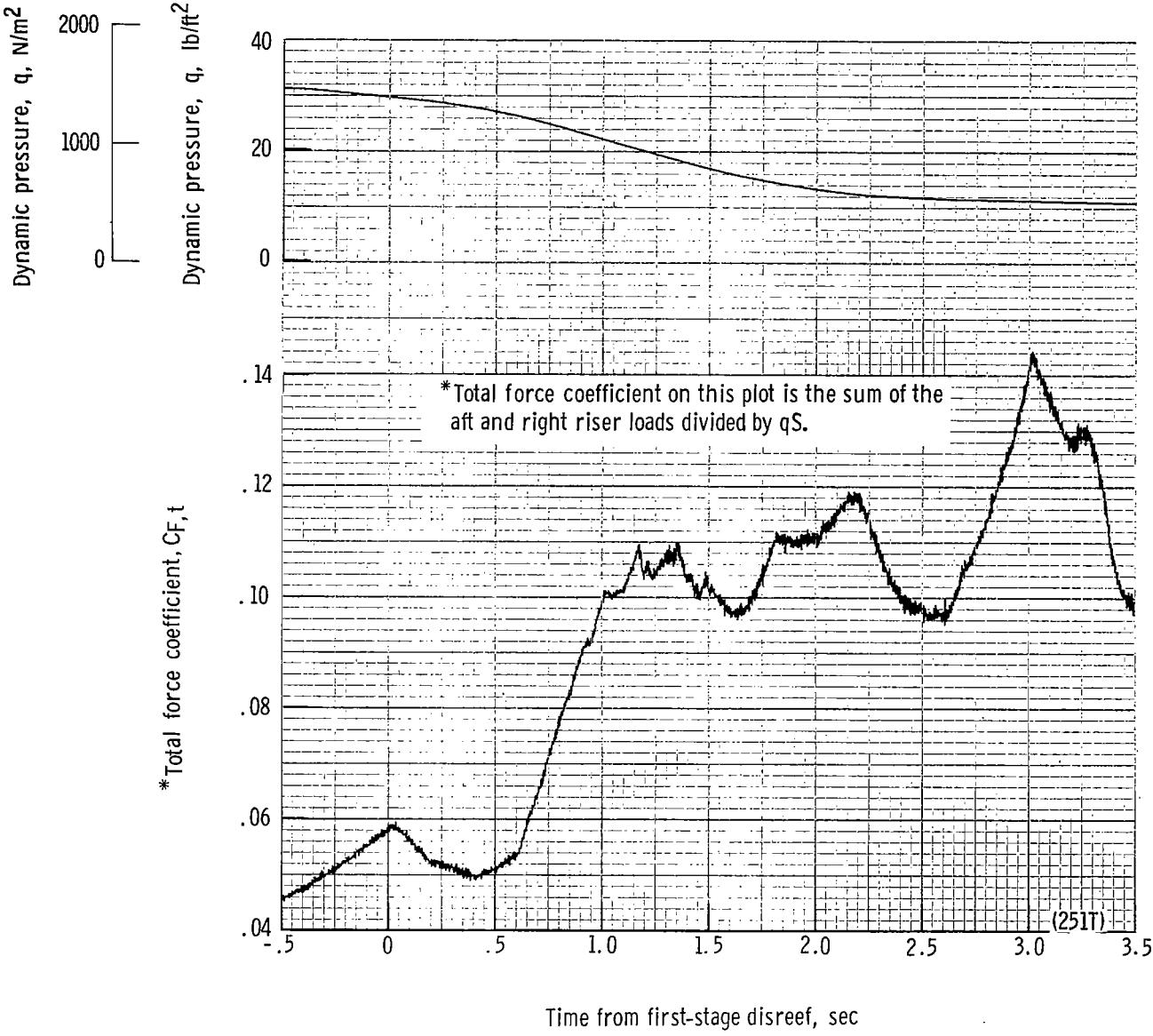
(d) Aft riser load plotted against time from first-stage disreef. Time = 0 second corresponds to 41.99 seconds after launch.

Figure 54.- Continued.



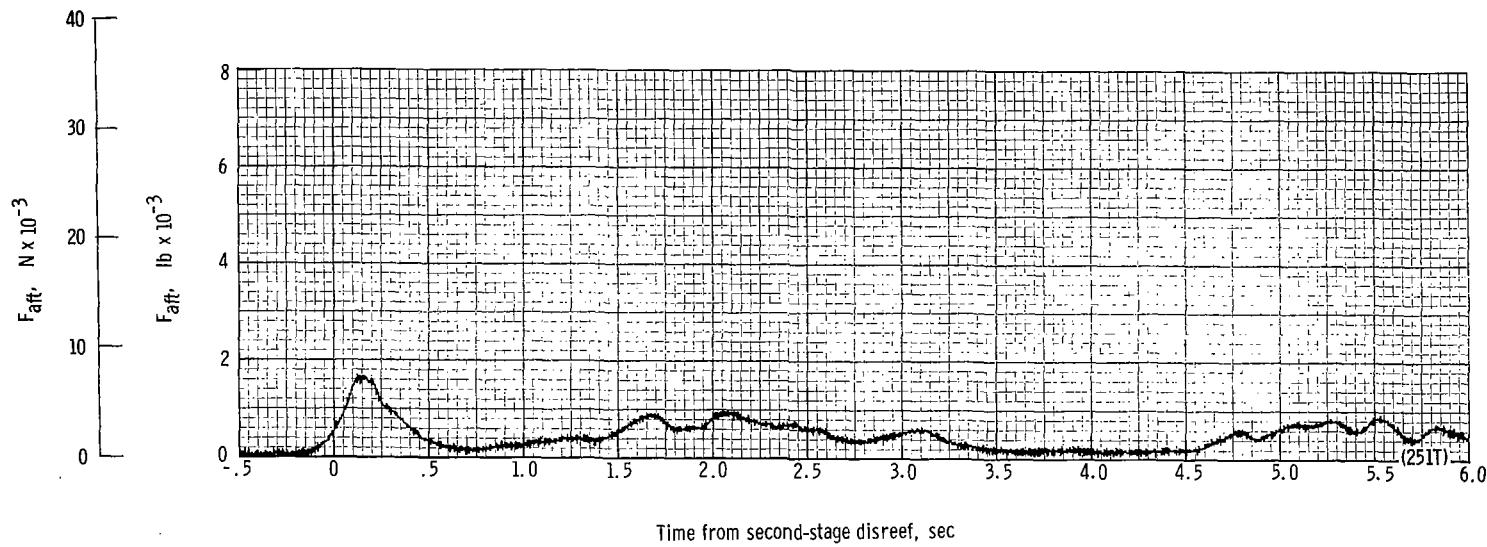
(e) Total force F_t plotted against time from first-stage disreef. Time = 0 second corresponds to 41.99 seconds after launch.

Figure 54.- Continued.



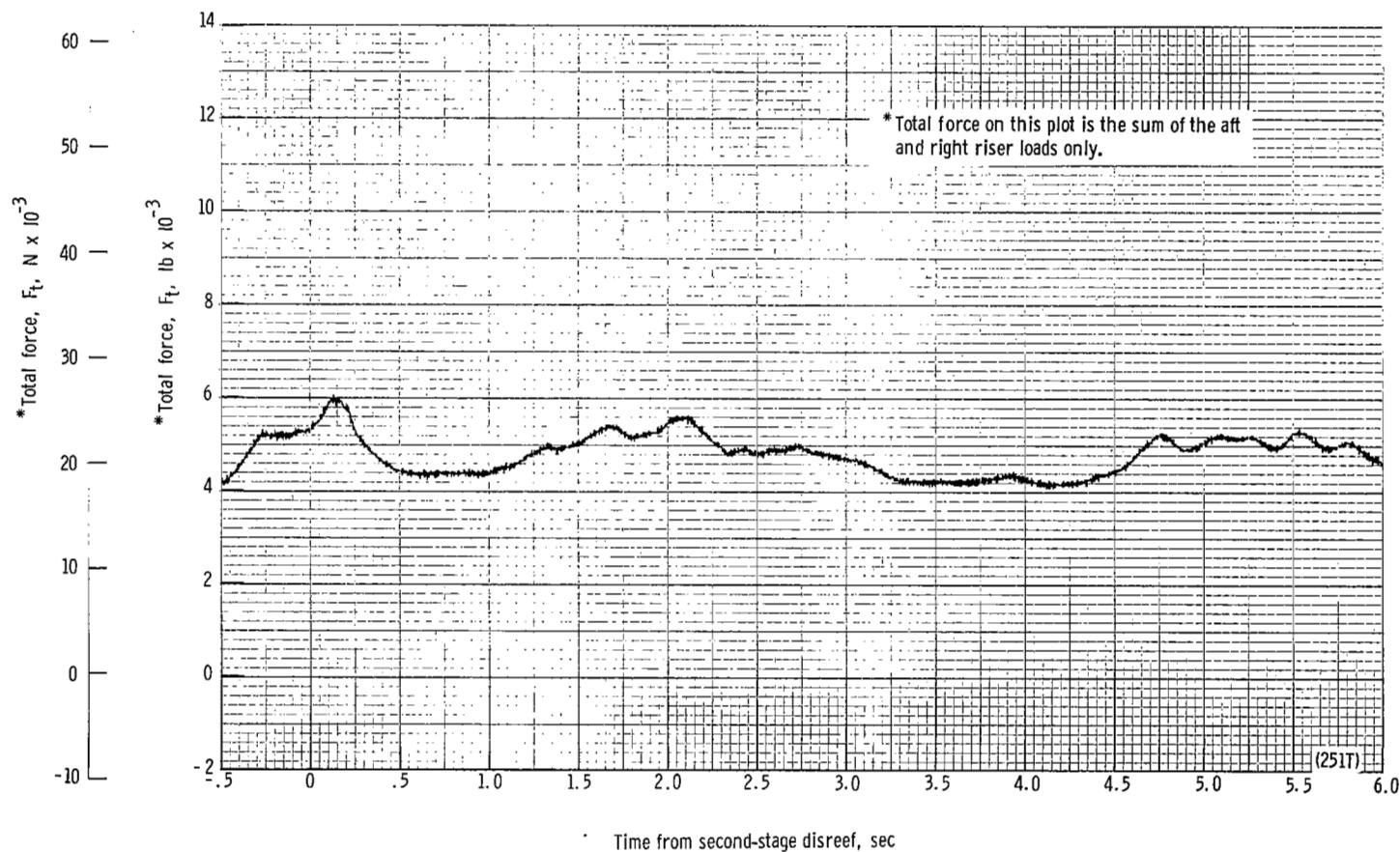
(f) Total force coefficient $C_{F,t}$ and dynamic pressure q plotted against time from first-stage disreef. Time = 0 second corresponds to 41.99 seconds after launch.

Figure 54.- Continued.



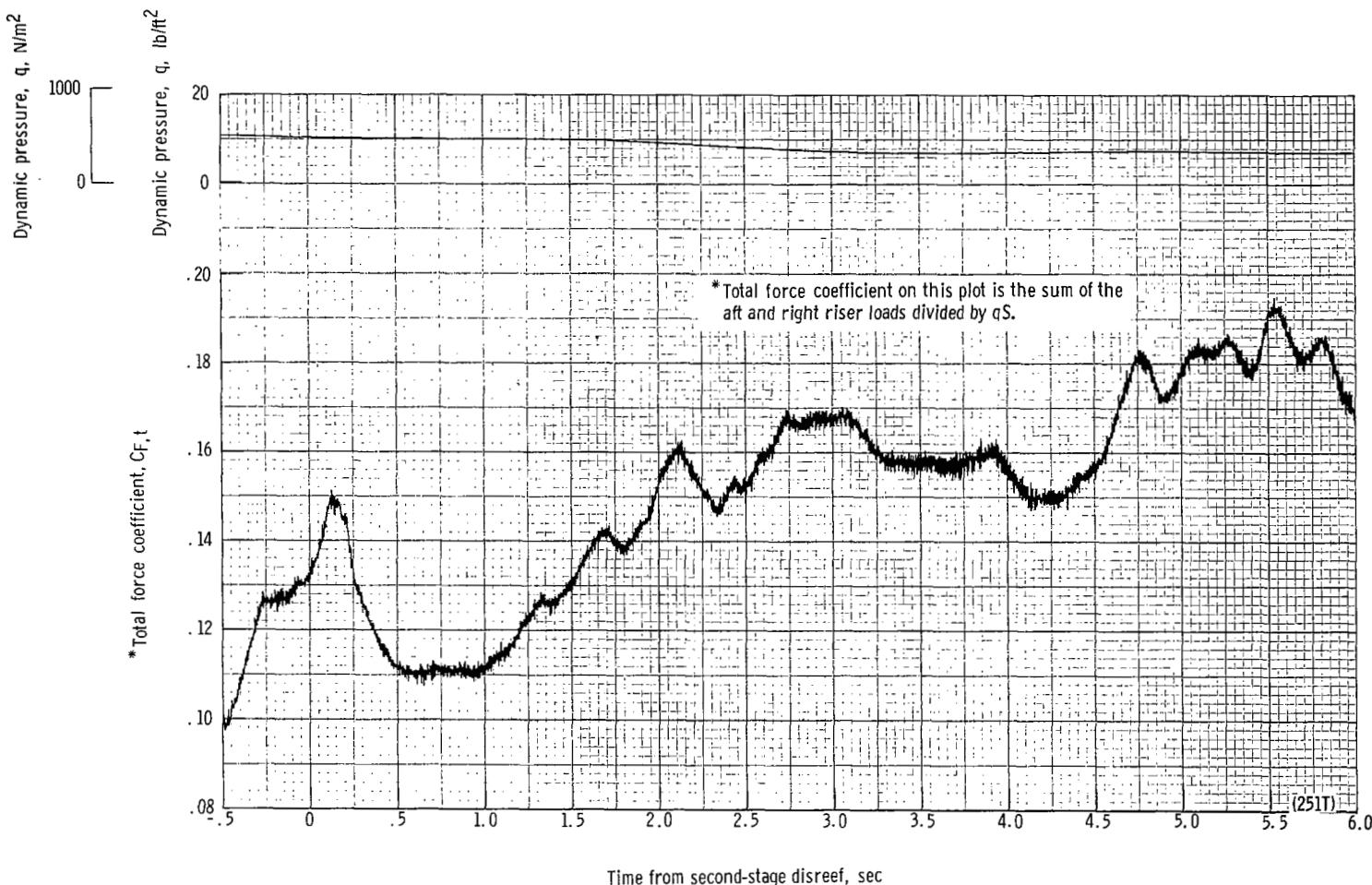
(g) Aft riser load plotted against time from second-stage disreef. Time = 0 second corresponds to 46.08 seconds after launch.

Figure 54.- Continued.



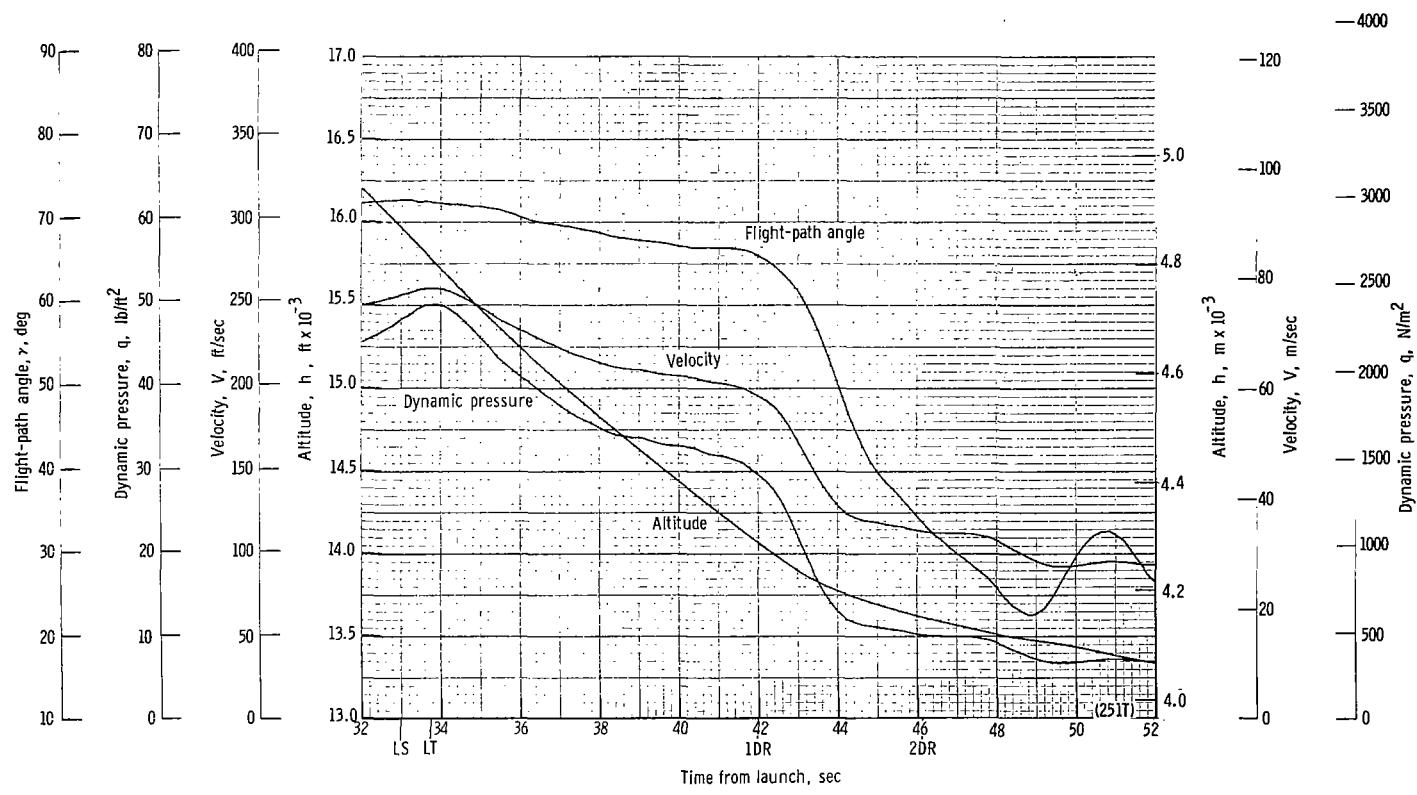
(h) Total force F_t plotted against time from second-stage disreef. Time = 0 second corresponds to 46.08 seconds after launch.

Figure 54.- Continued.



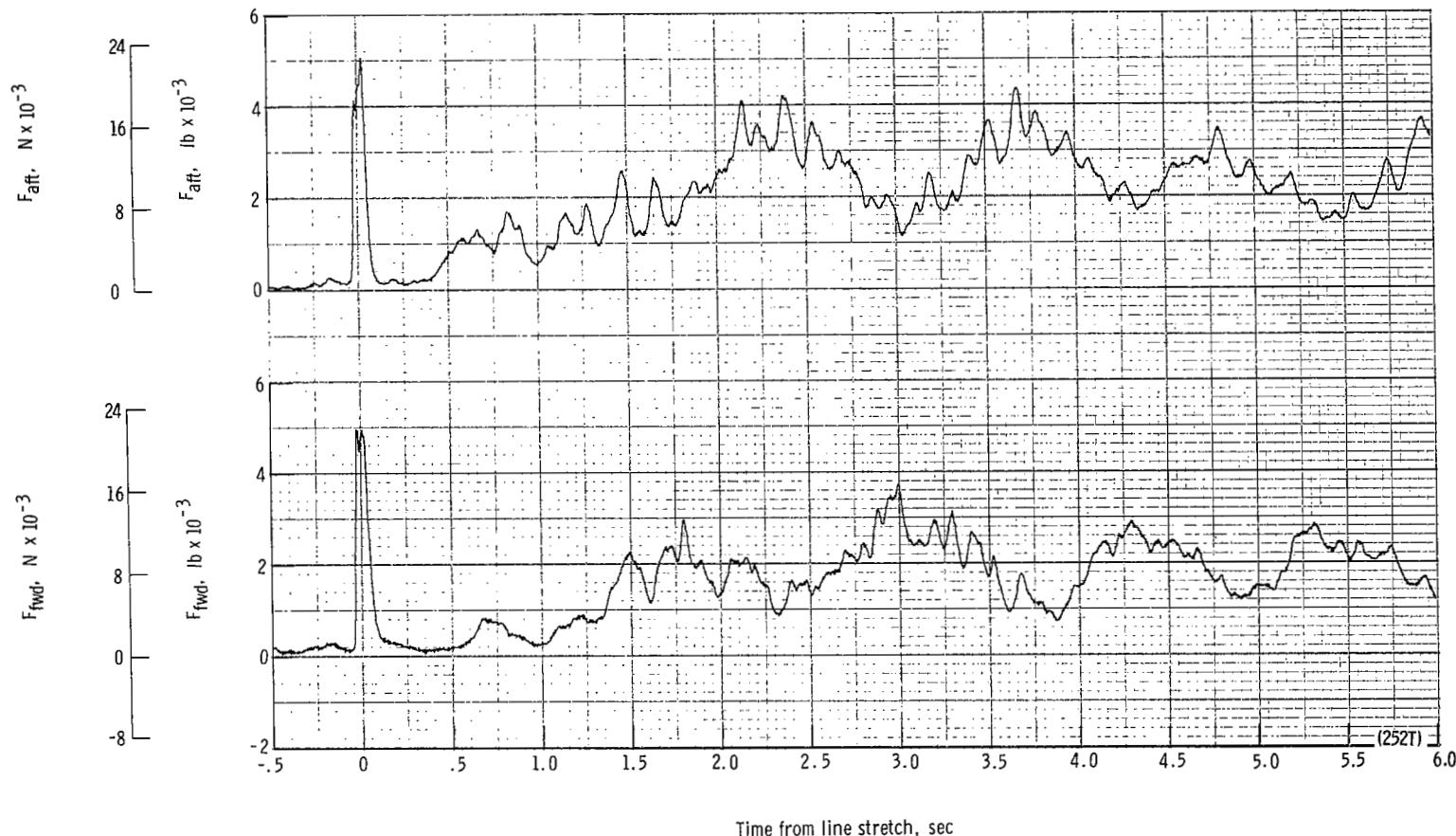
(ii) Total force coefficient $C_{F,t}$ and dynamic pressure q plotted against time from second-stage disreef. Time = 0 second corresponds to 46.08 seconds after launch.

Figure 54.- Continued.



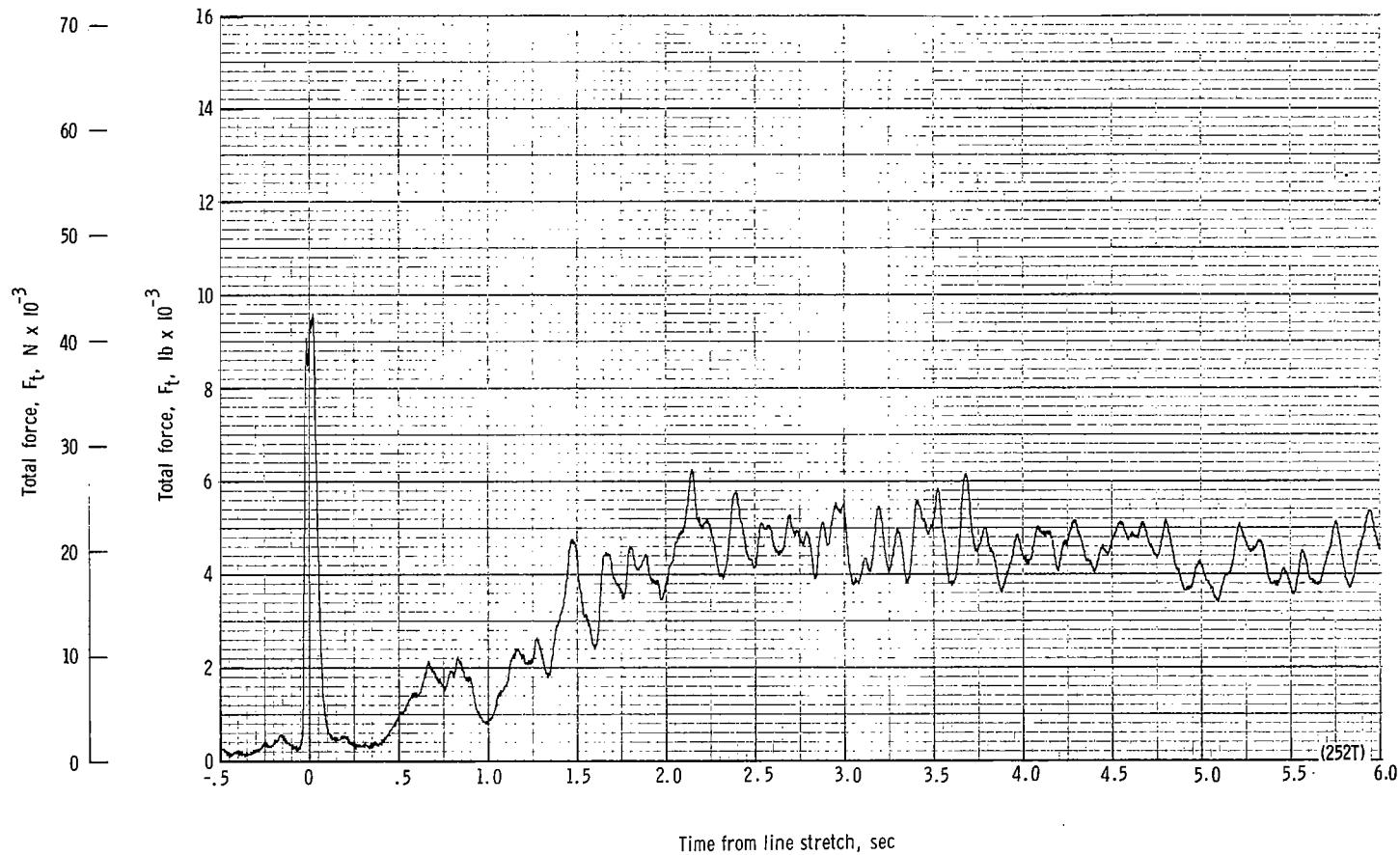
(j) Flight-path angle γ , dynamic pressure q , velocity V , and altitude h plotted against time from launch.

Figure 54.- Concluded.



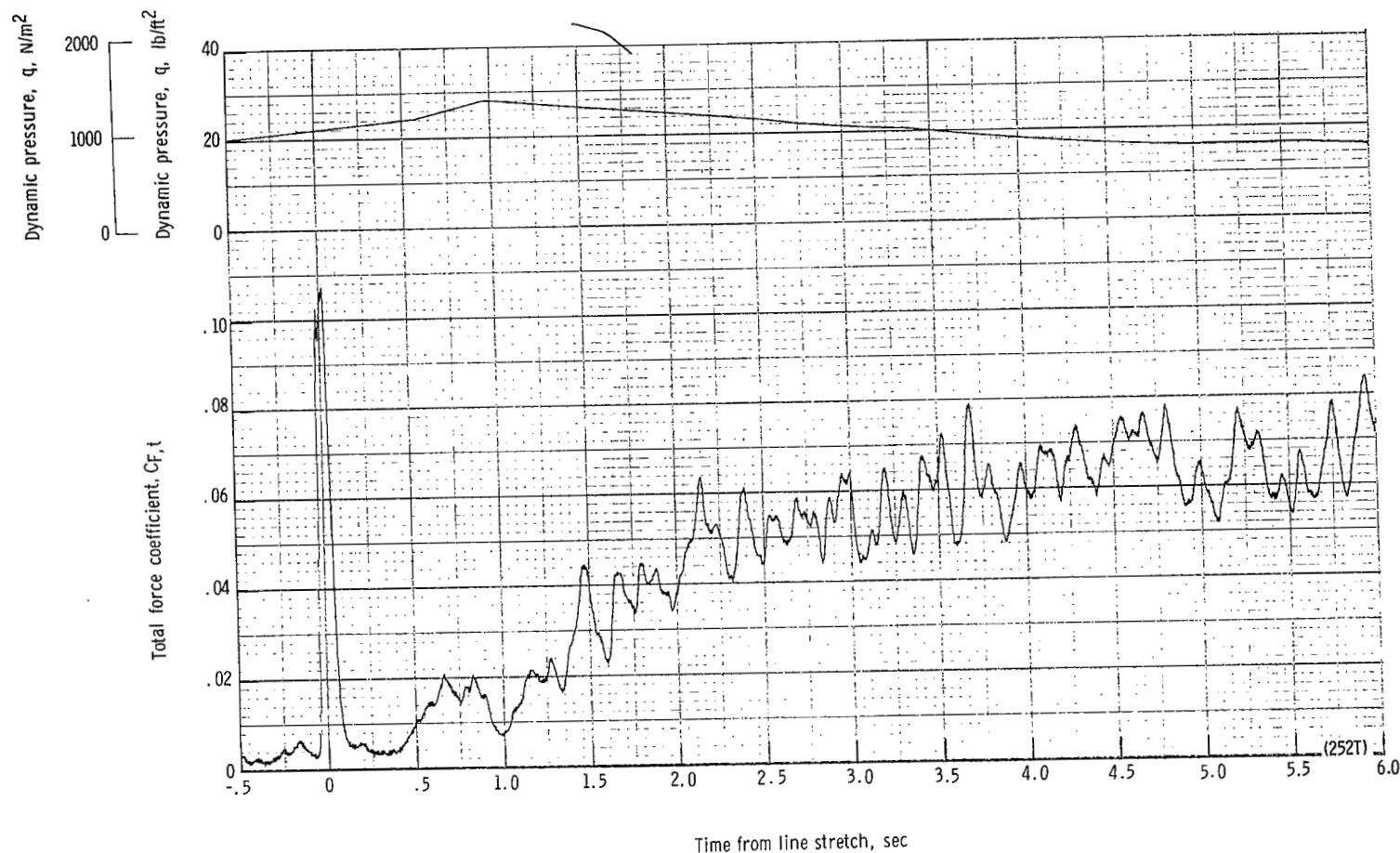
(a) Forward and aft riser loads plotted against time from line stretch. Time = 0 second corresponds to 12.41 seconds after launch.

Figure 55.- Time history of twin-keel parawing deployment data for test 252T. $W_D = 17\ 824\ N; $W_P = 15\ 975\ N; $q_{PD} = 790\ N/m^2; $h_{PD} = 6905\ m; $l_r/l_k = 0.100$; reefing version B.$$$$



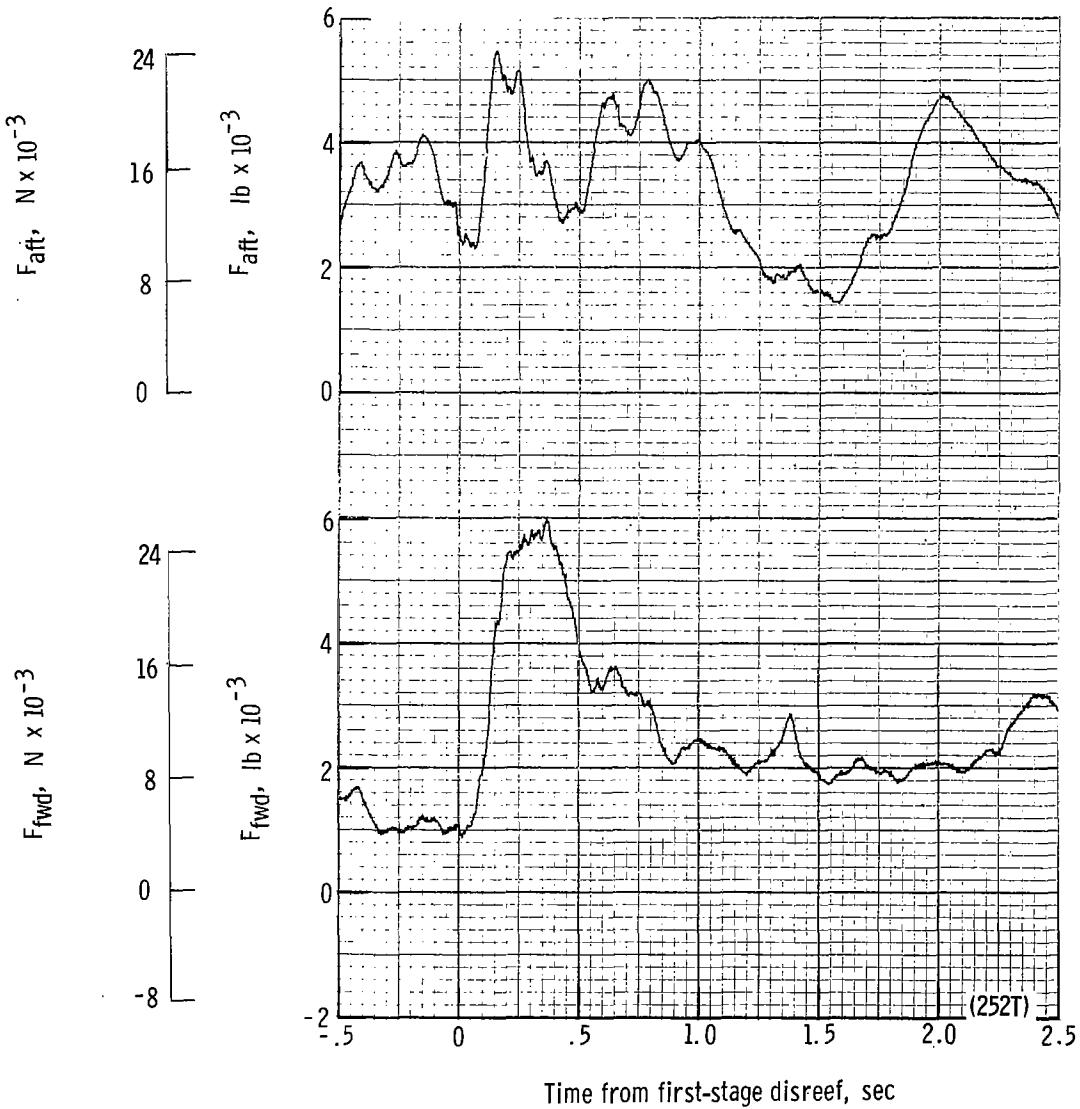
(b) Total force F_t time from line stretch. Time = 0 second corresponds to 12.41 seconds after launch.

Figure 55.- Continued.



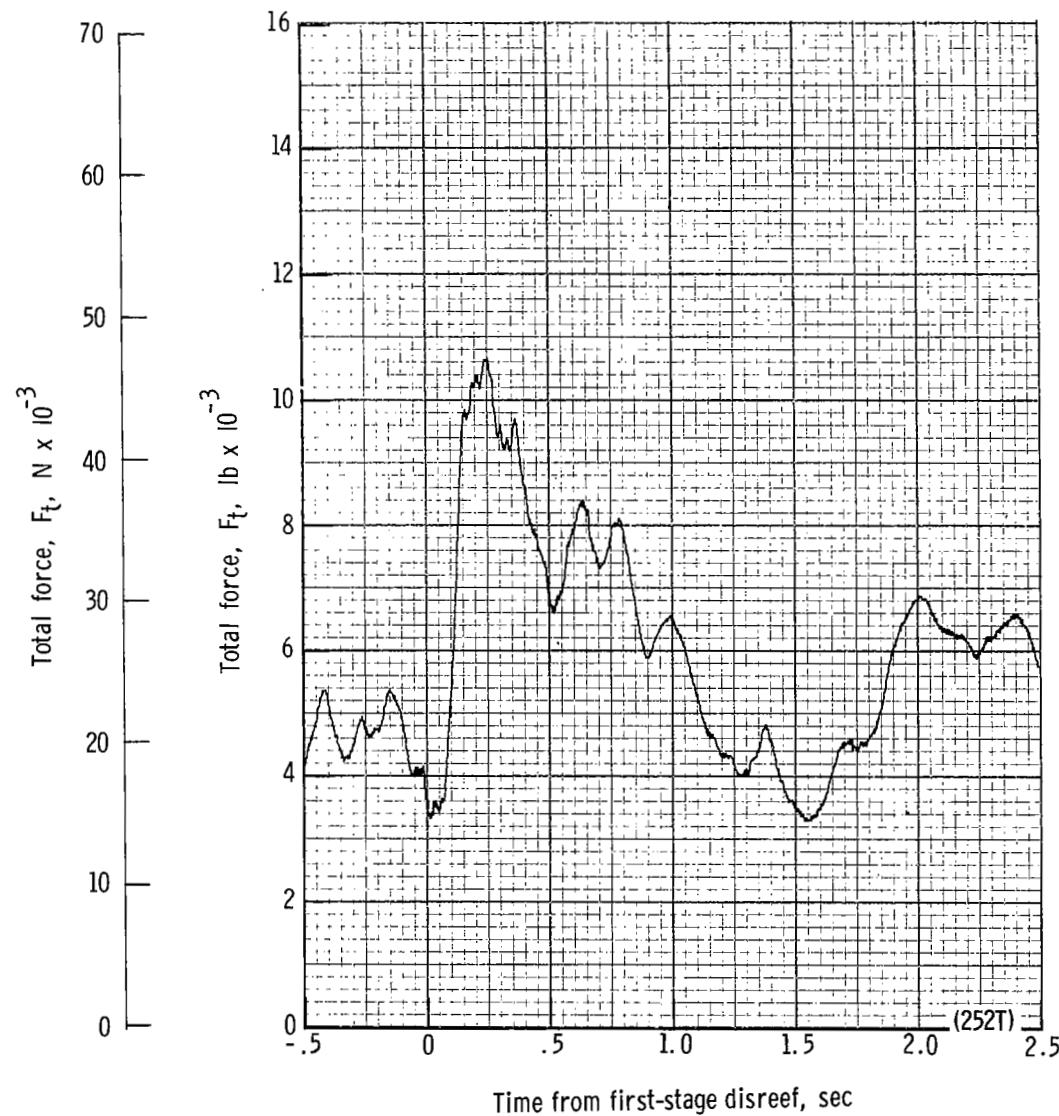
(c) Total force coefficient $C_{F,t}$ and dynamic pressure q plotted against time from line stretch. Time = 0 second corresponds to 12.41 seconds after launch.

Figure 55.- Continued.



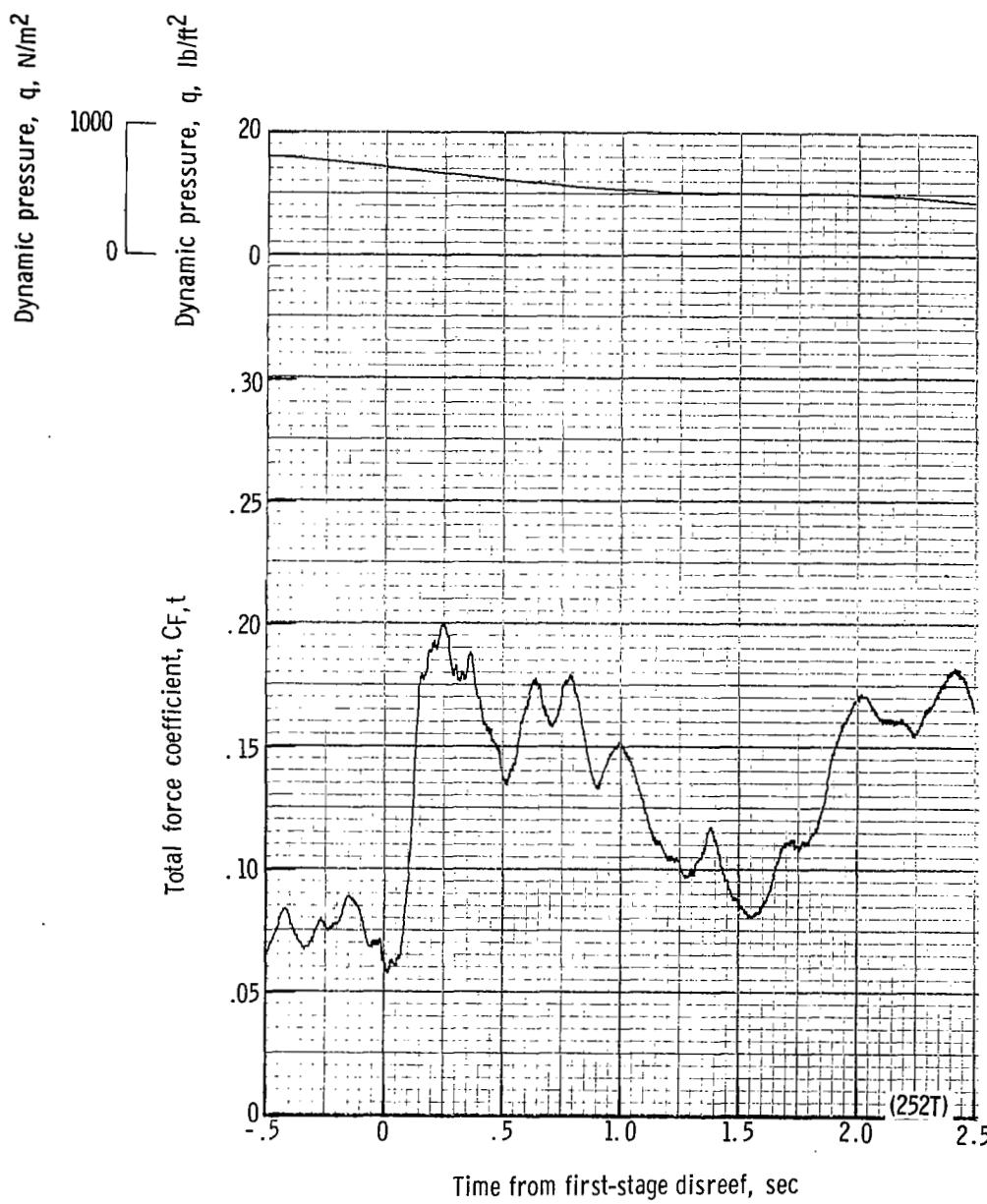
(d) Forward and aft riser loads plotted against time from first-stage disreef. Time = 0 second corresponds to 18.77 seconds after launch.

Figure 55.- Continued.



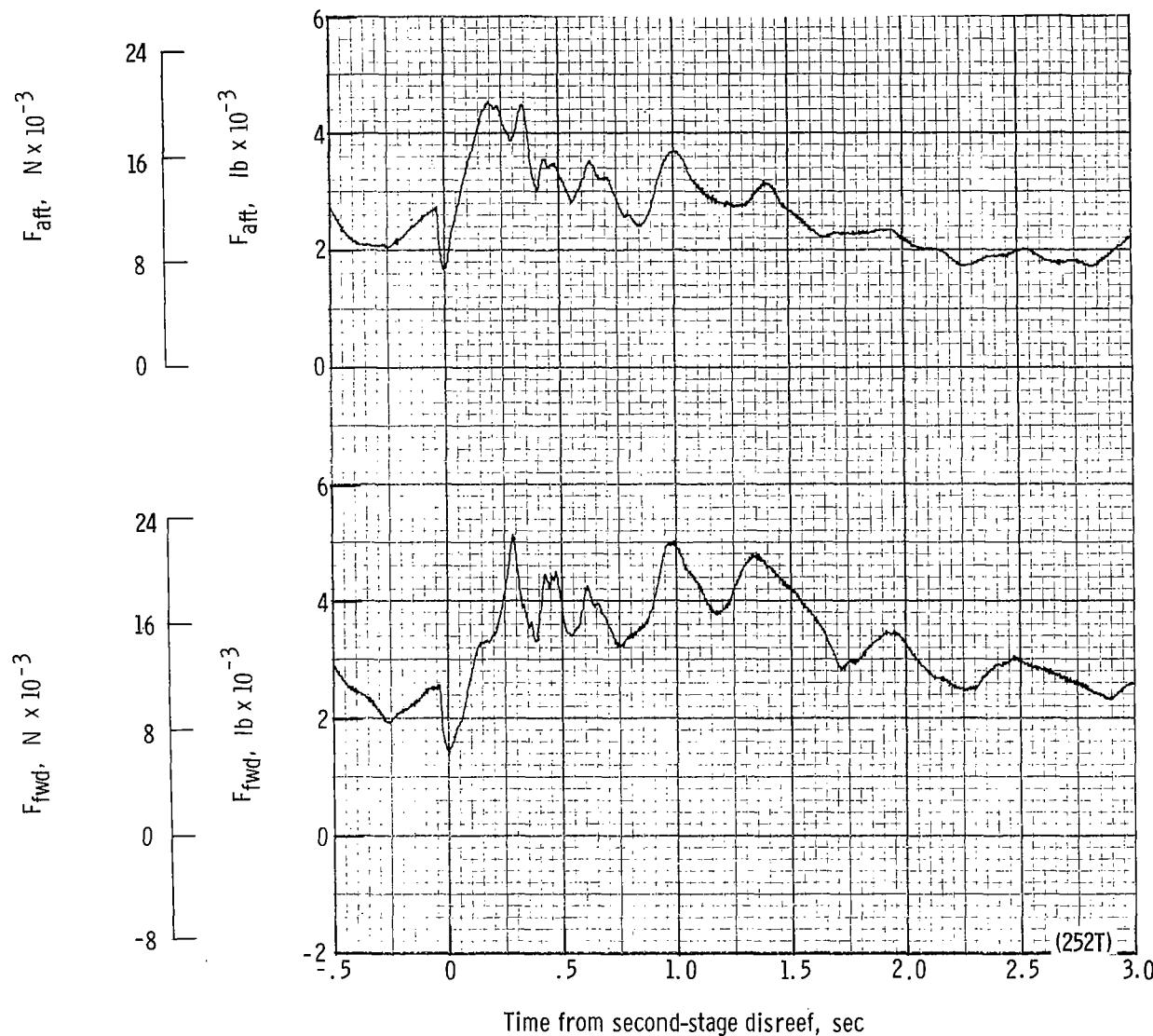
(e) Total force F_t plotted against time from first-stage disreef. Time = 0 second corresponds to 18.77 seconds after launch.

Figure 55.- Continued.



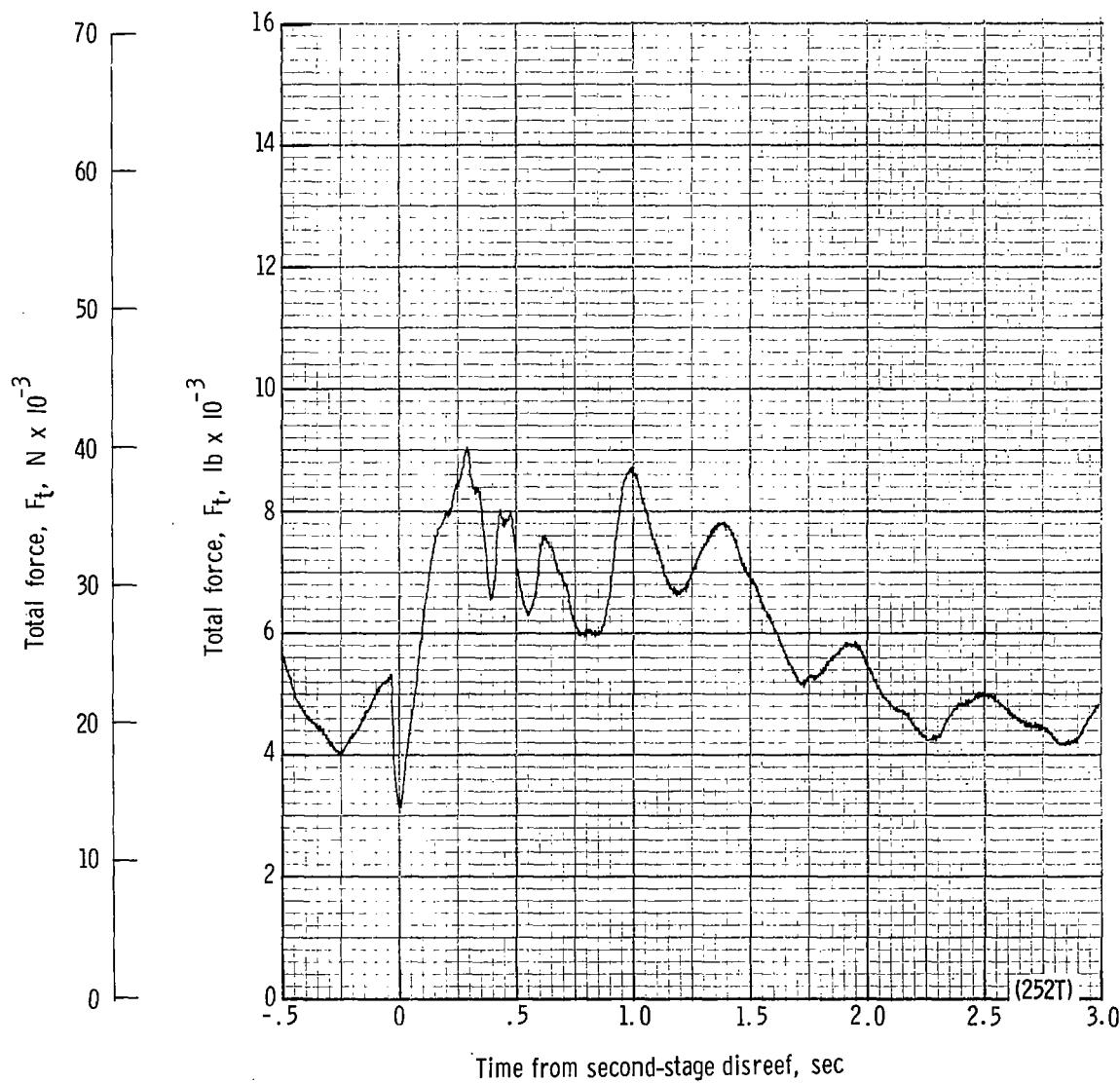
(f) Total force coefficient $C_{F,t}$ and dynamic pressure q plotted against time from first-stage disreef. Time = 0 second corresponds to 18.77 seconds after launch.

Figure 55.- Continued.



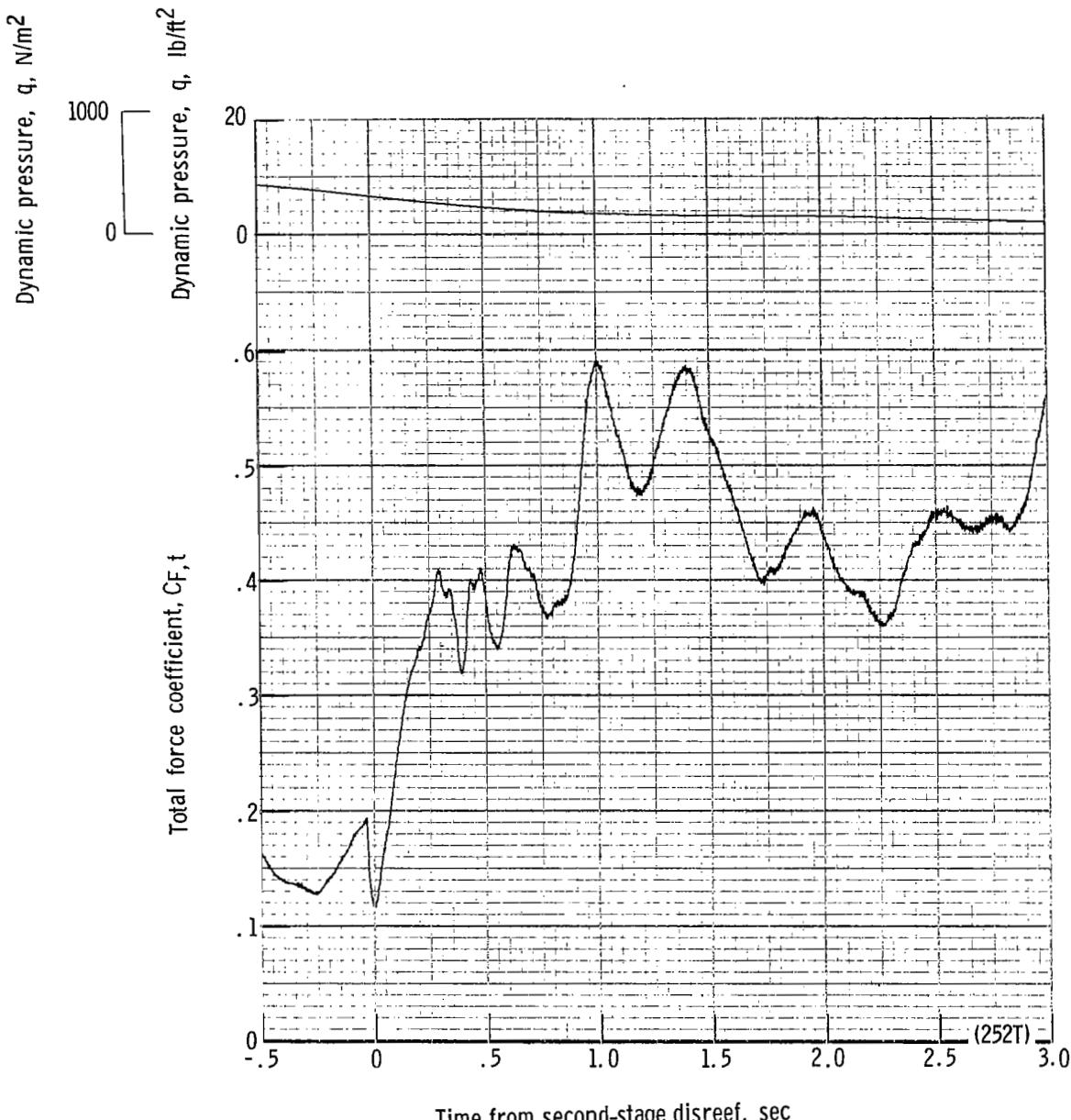
(g) Forward and aft riser loads plotted against time from second-stage disreef. Time = 0 second corresponds to 21.77 seconds after launch.

Figure 55.- Continued.



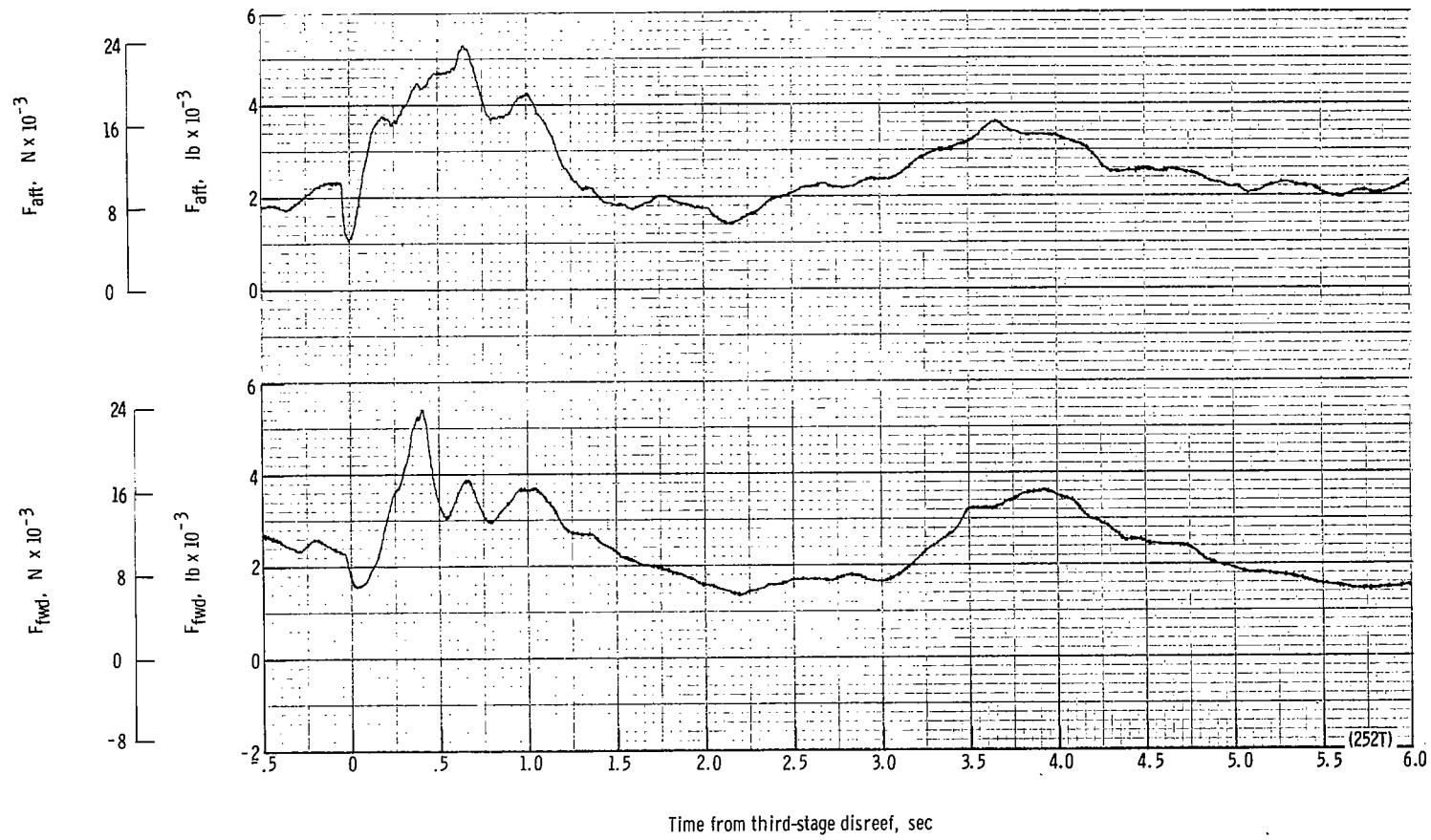
(h) Total force F_t plotted against time from second-stage disreef. Time = 0 second corresponds to 21.77 seconds after launch.

Figure 55.- Continued.



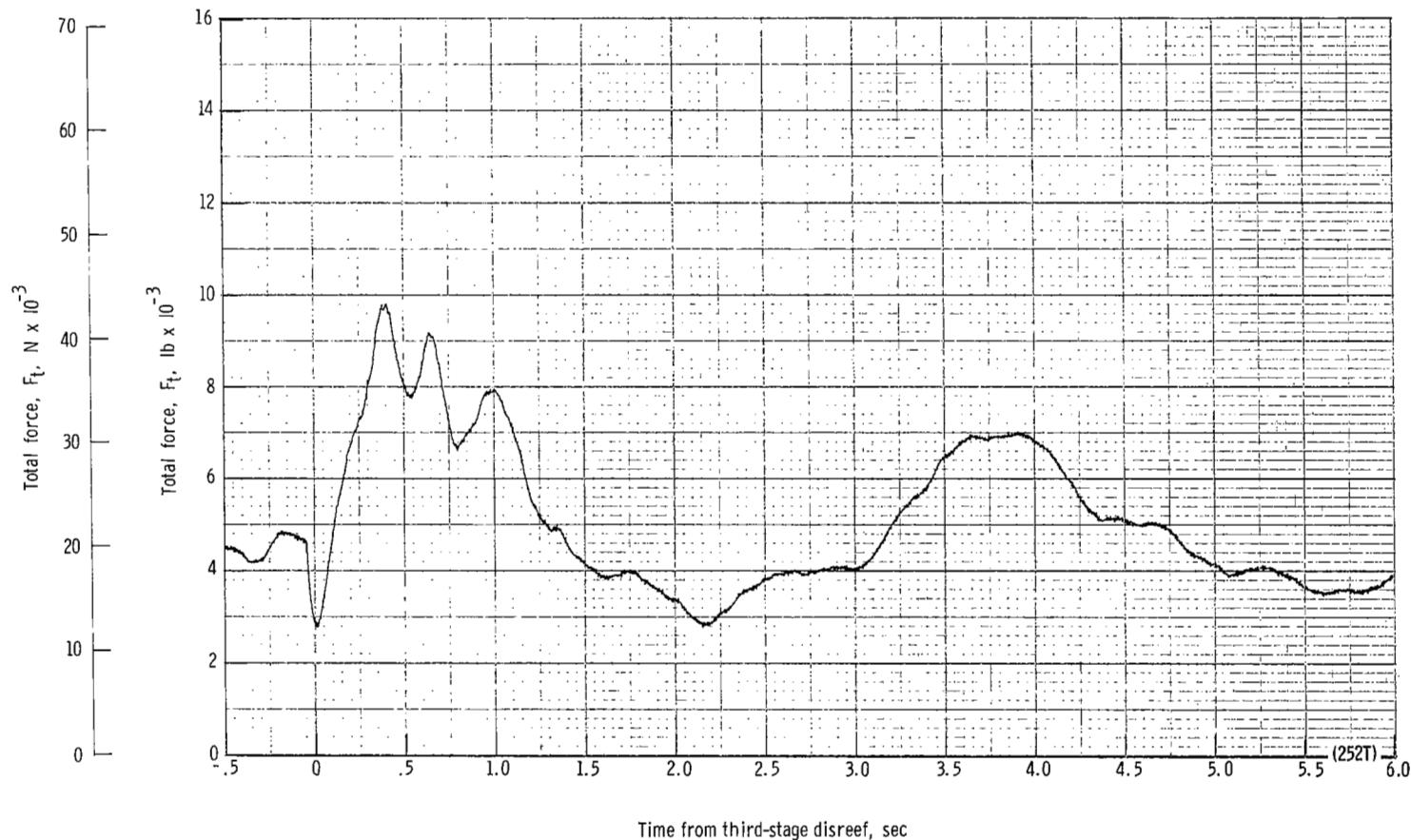
(ii) Total force coefficient $C_{F,t}$ and dynamic pressure q plotted against time from second-stage disreef. Time = 0 second corresponds to 21.77 seconds after launch.

Figure 55.- Continued.



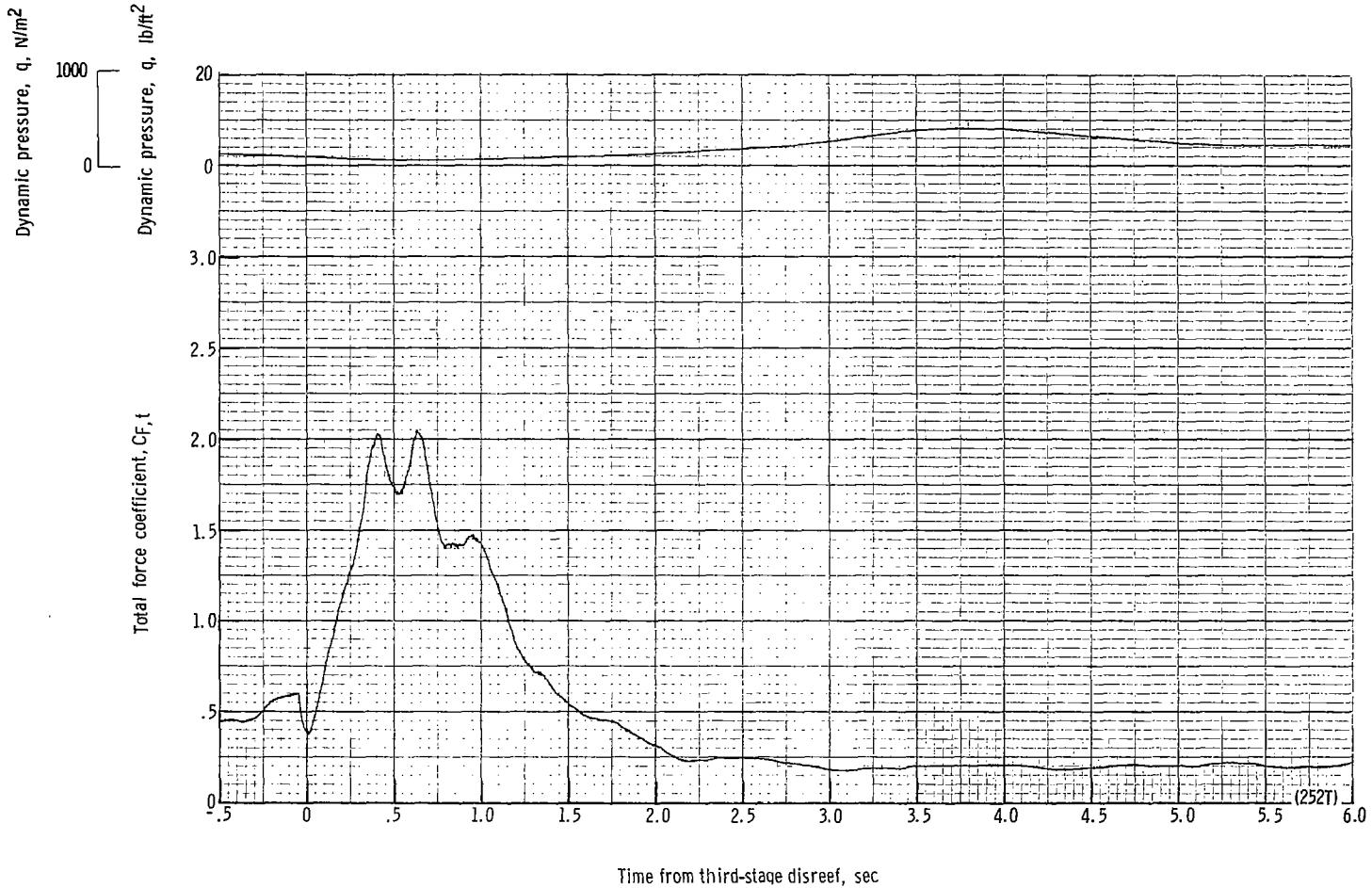
(i) Forward and aft riser loads plotted against time from third-stage disreef. Time = 0 second corresponds to 24.96 seconds after launch.

Figure 55.- Continued.



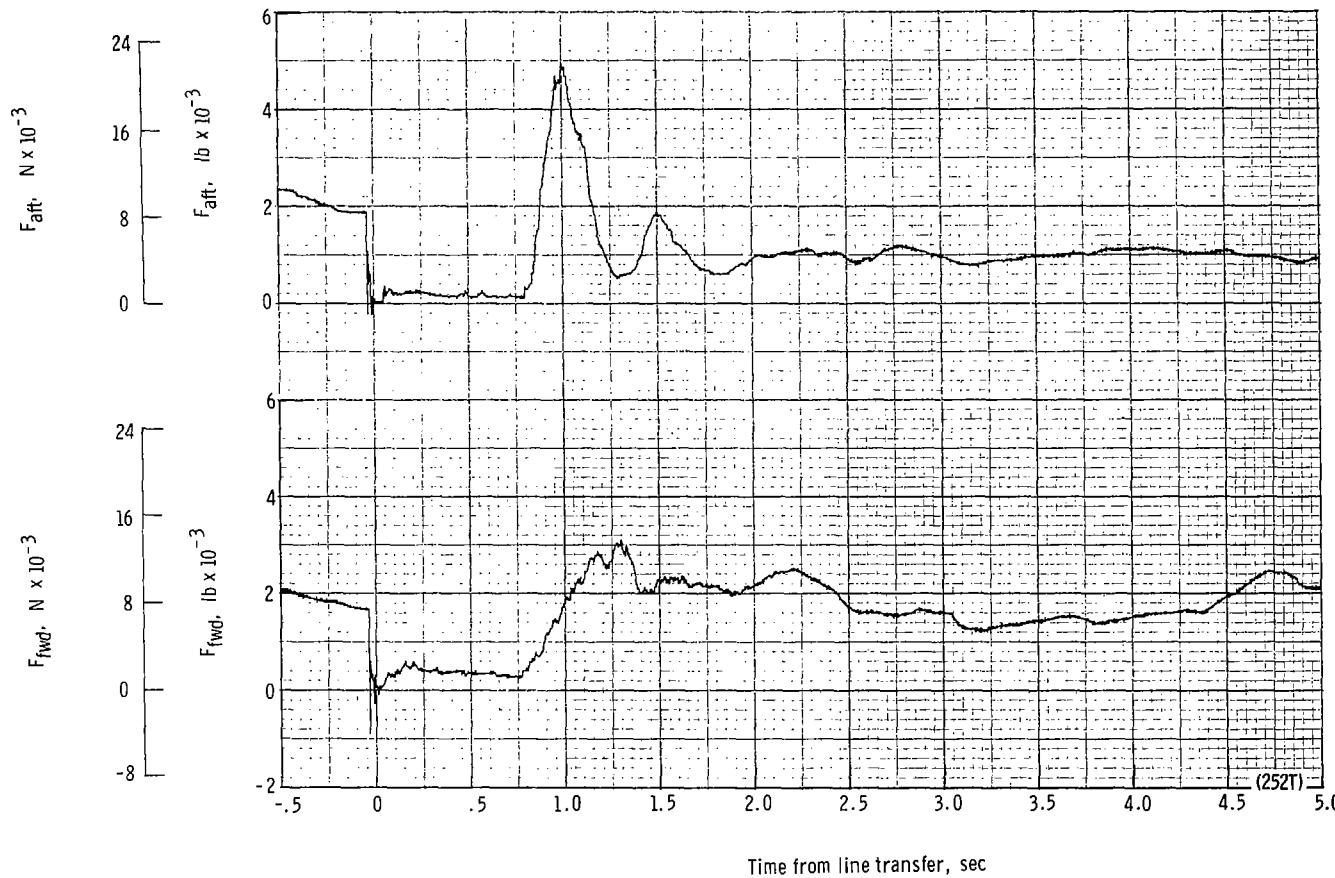
(k) Total force F_t plotted against time from third-stage disreef. Time = 0 second corresponds to 24.96 seconds after launch.

Figure 55.- Continued.



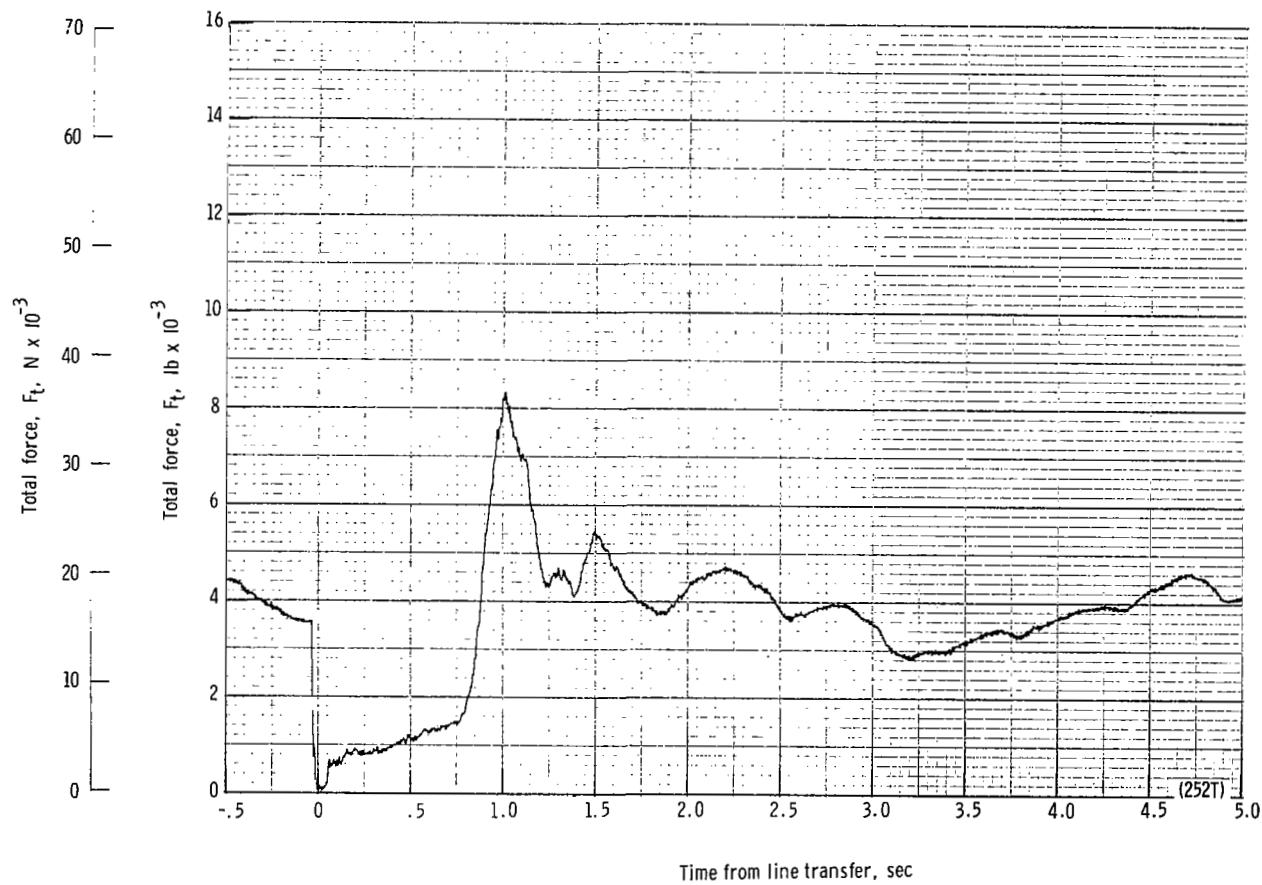
(I) Total force coefficient $C_{F,t}$ and dynamic pressure q plotted against time from third-stage disreef. Time = 0 second corresponds to 24.96 seconds after launch.

Figure 55.- Continued.



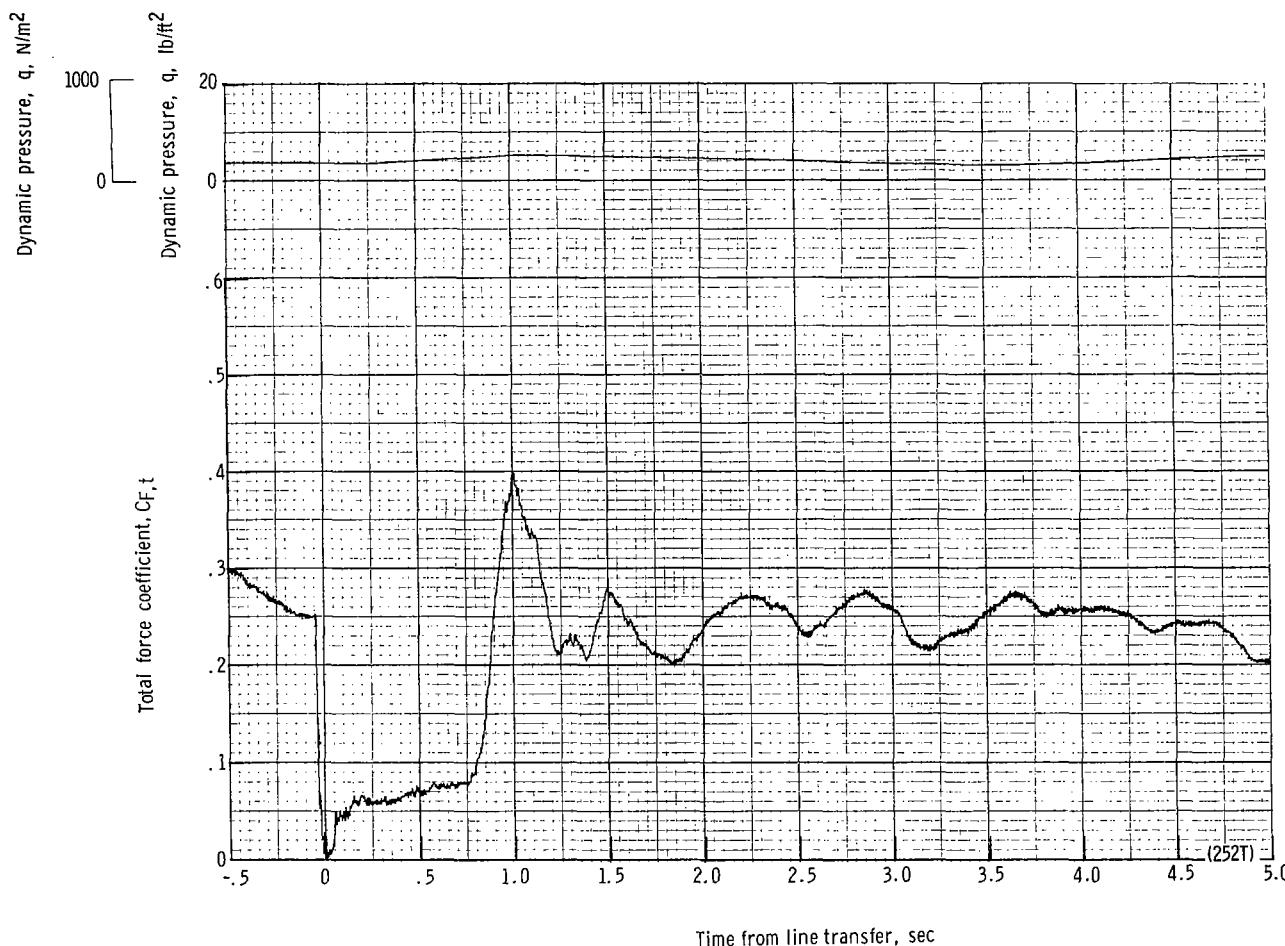
(m) Forward and aft riser loads plotted against time from line transfer. Time = 0 second corresponds to 32.55 seconds after launch.

Figure 55.- Continued.



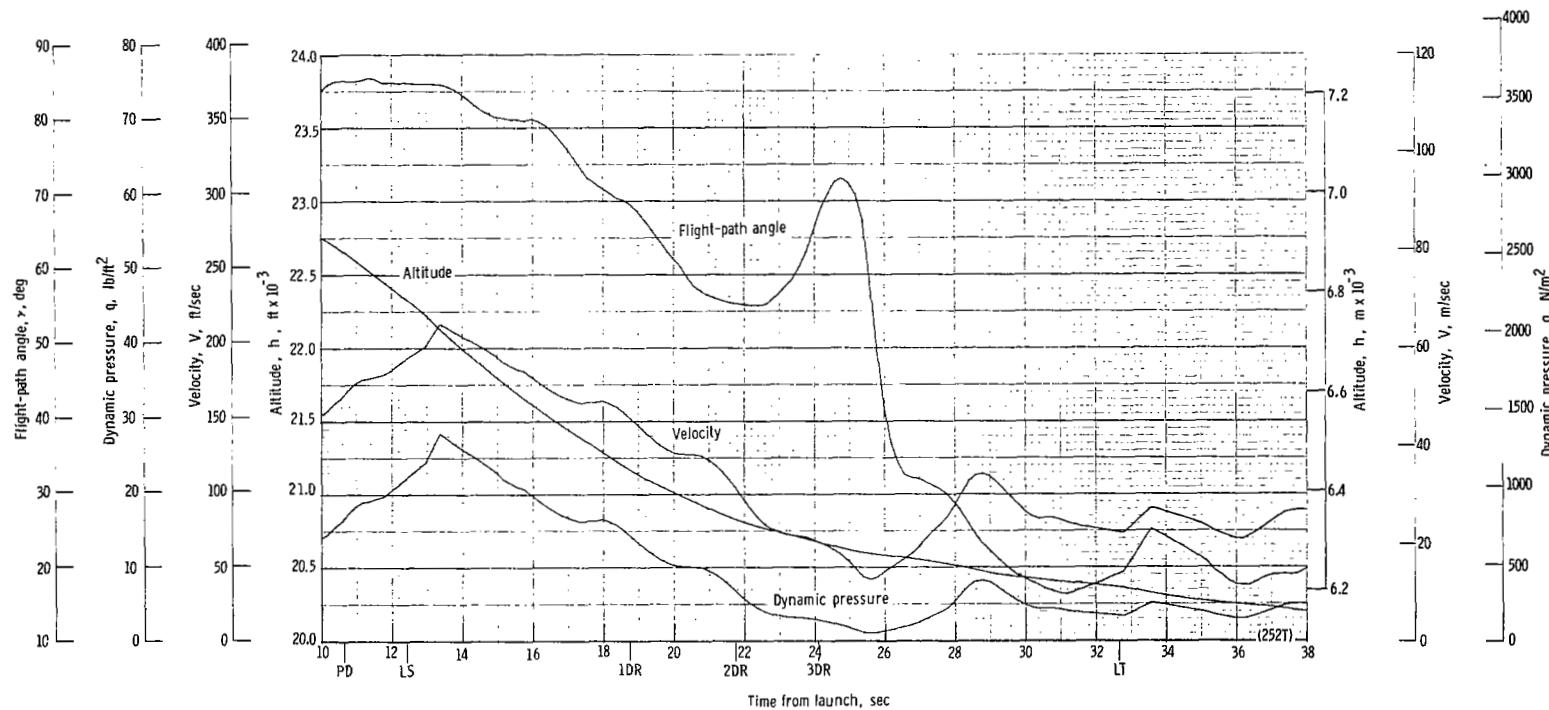
(n) Total force F_t plotted against time from line transfer. Time = 0 second corresponds to 32.55 seconds after launch.

Figure 55.- Continued.



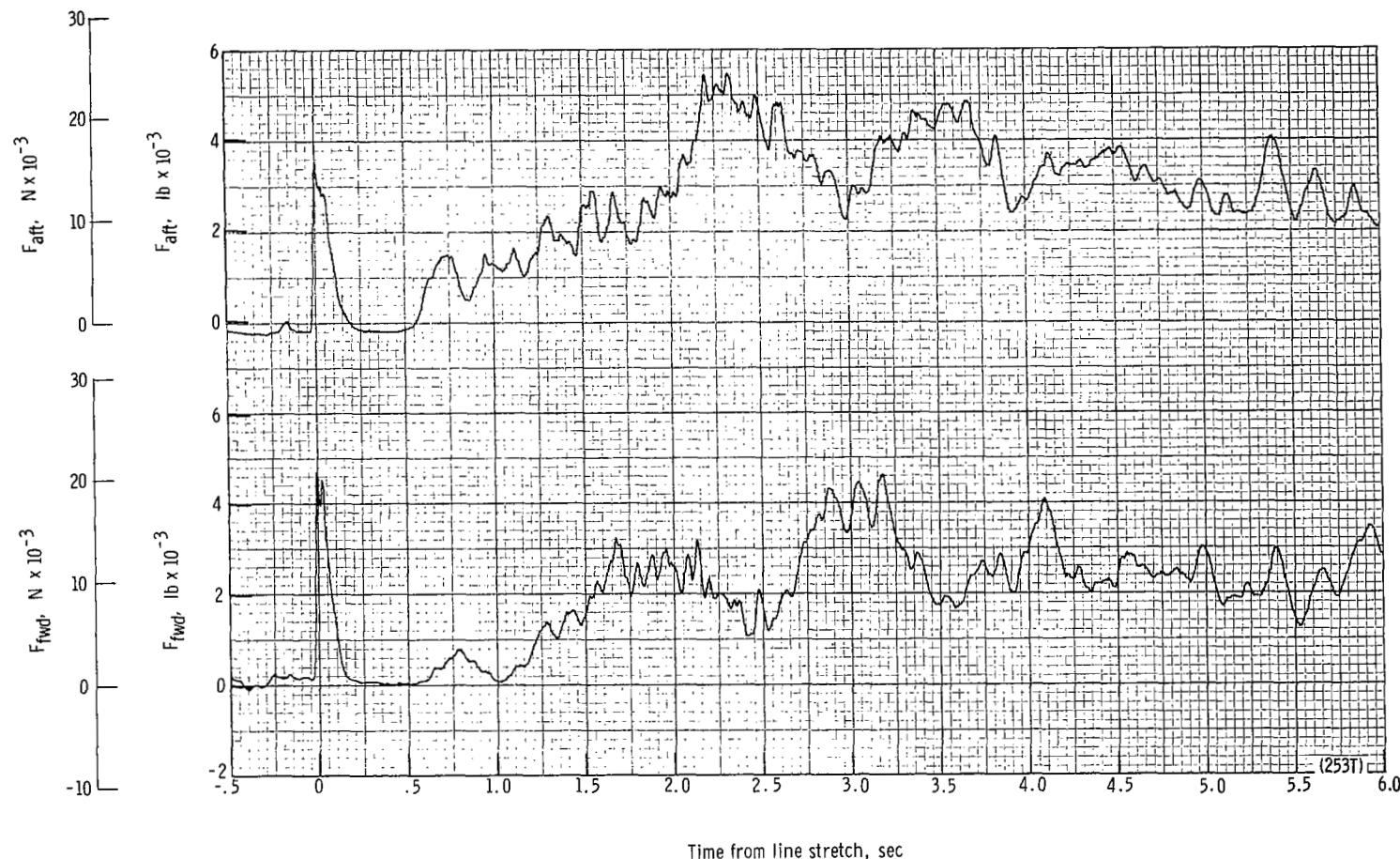
(o) Total force coefficient $C_{F,t}$ and dynamic pressure q plotted against time from line transfer. Time = 0 second corresponds to 32.55 seconds after launch.

Figure 55.- Continued.



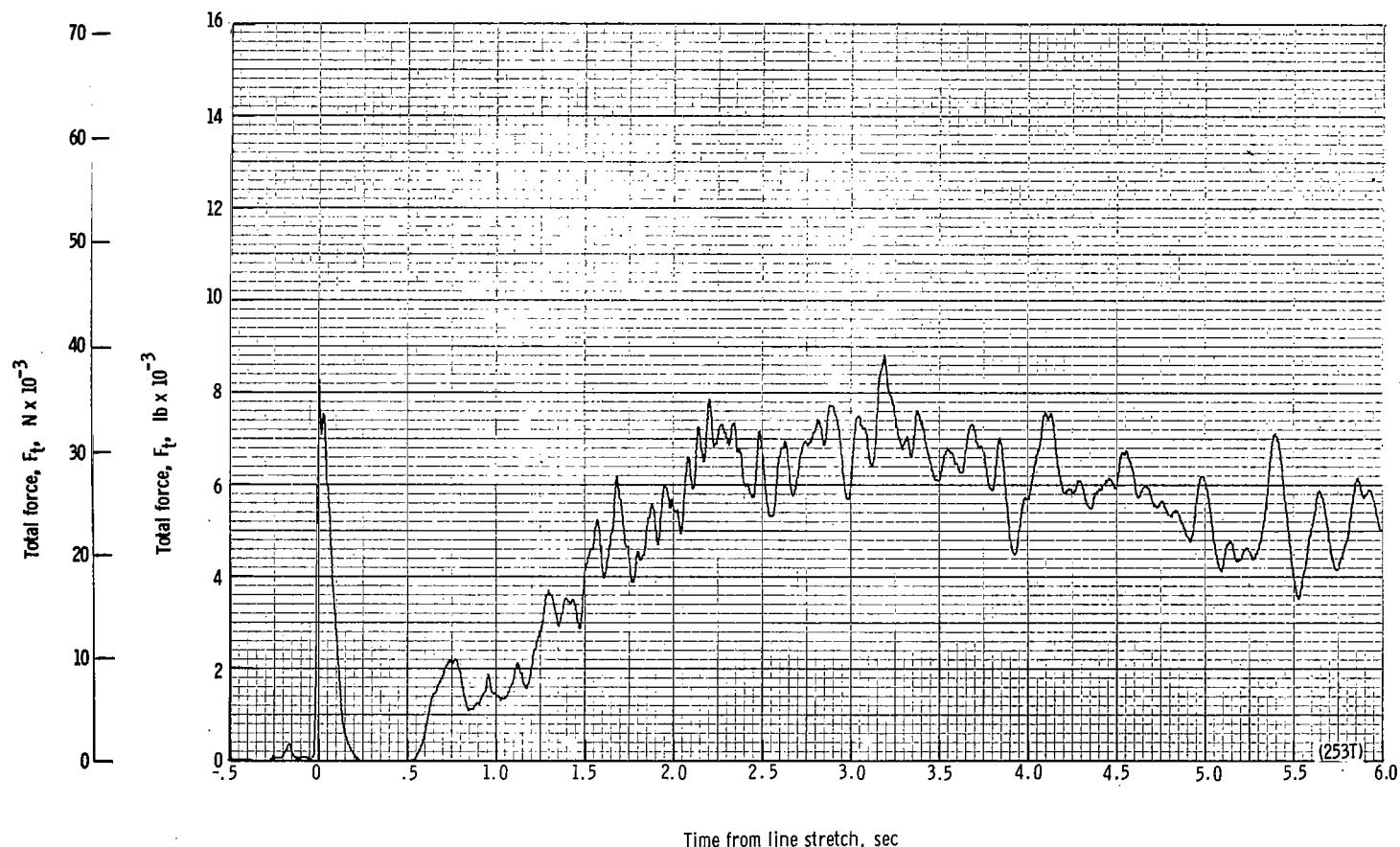
(p) Flight-path angle γ , dynamic pressure q , velocity V , and altitude h plotted against time from launch.

Figure 55.- Concluded.



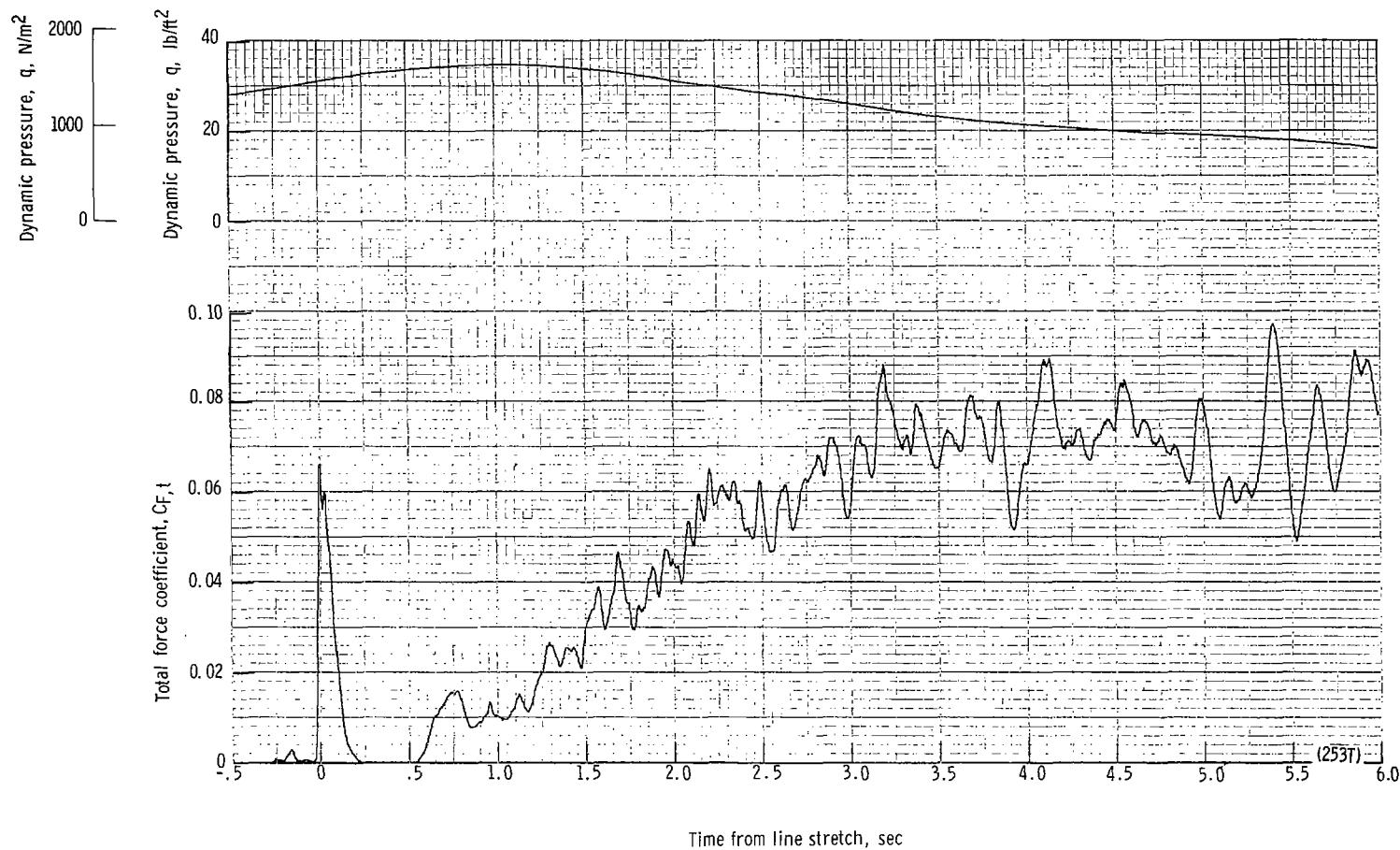
(a) Forward and aft riser loads plotted against time from line stretch. Time = 0 second corresponds to 12.27 seconds after launch.

Figure 56.- Time history of twin-keel parawing deployment data for test 253T. $W_D = 22\ 290\ N$ (5011 lb); $W_p = 20\ 428\ N$ (4592 lb); $q_{PD} = 1139\ N/m^2$ (23.8 lb/ft²); $h_{PD} = 6989\ m$ (22 931 ft); $l_r/l_k = 0.100$; reefing version C.



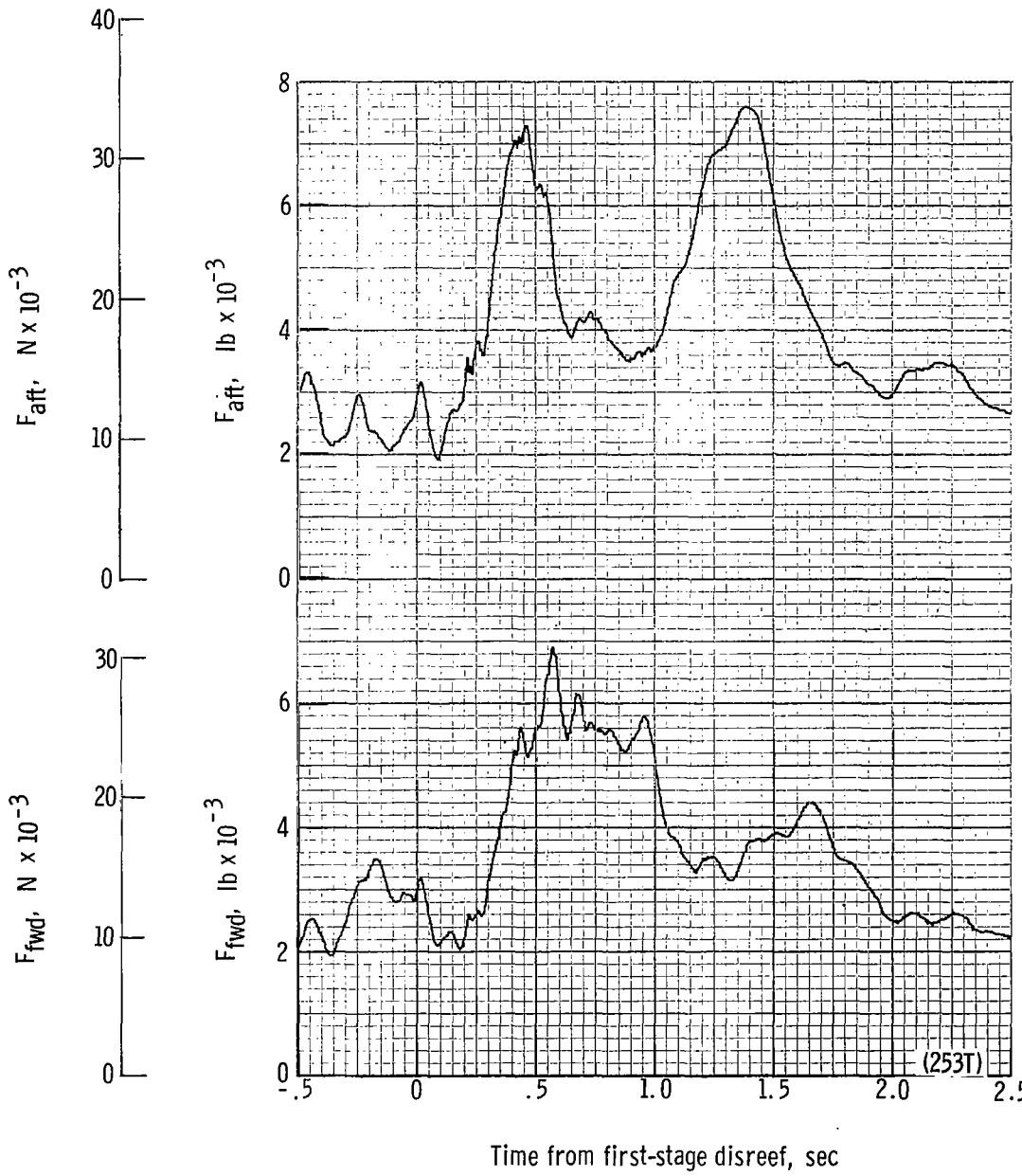
(b) Total force F_t plotted against time from line stretch. Time = 0 second corresponds to 12.27 seconds after launch.

Figure 56.- Continued.



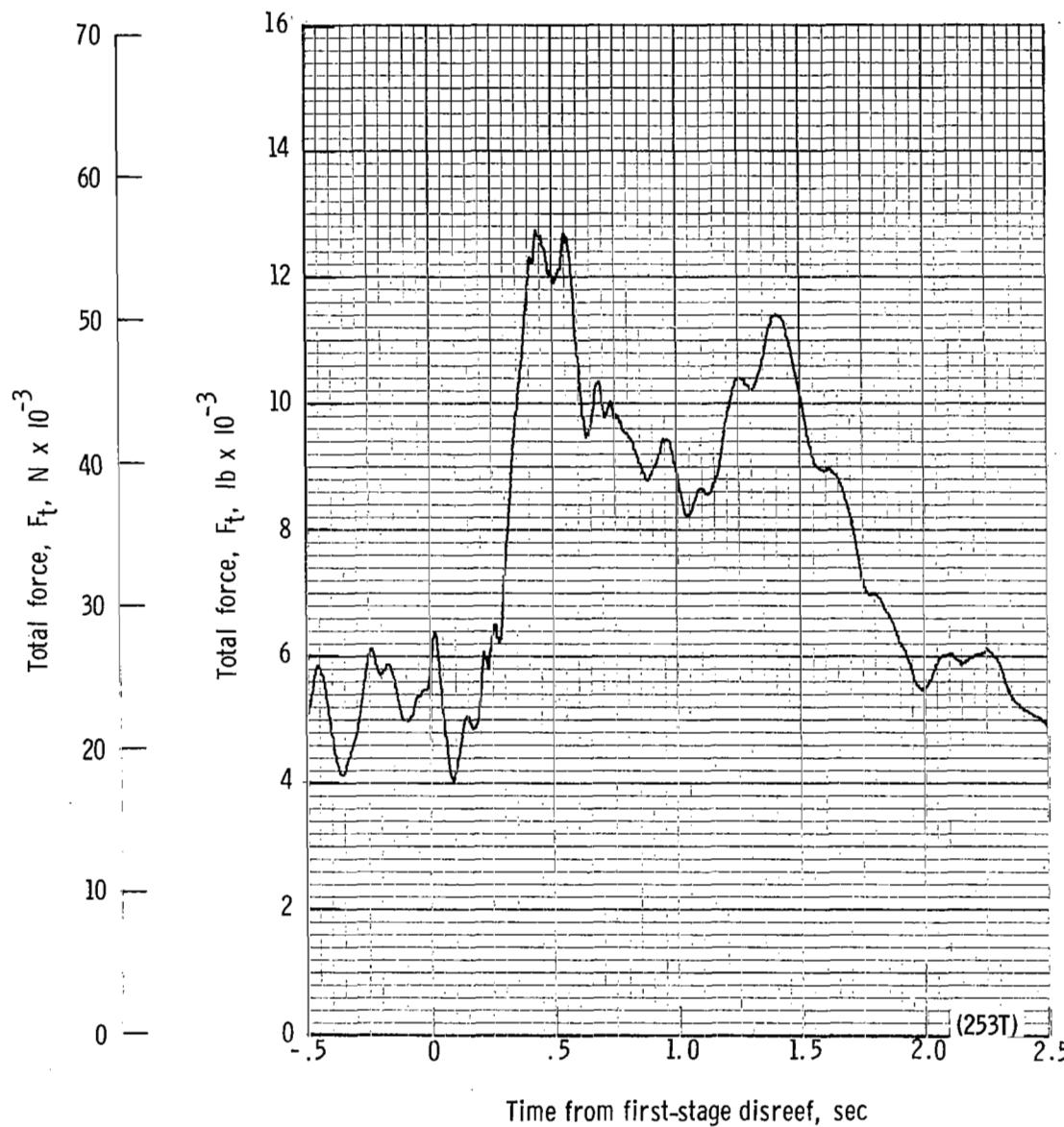
(c) Total force coefficient $C_{F,t}$ and dynamic pressure q plotted against time from line stretch. Time = 0 second corresponds to 12.27 seconds after launch.

Figure 56.- Continued.



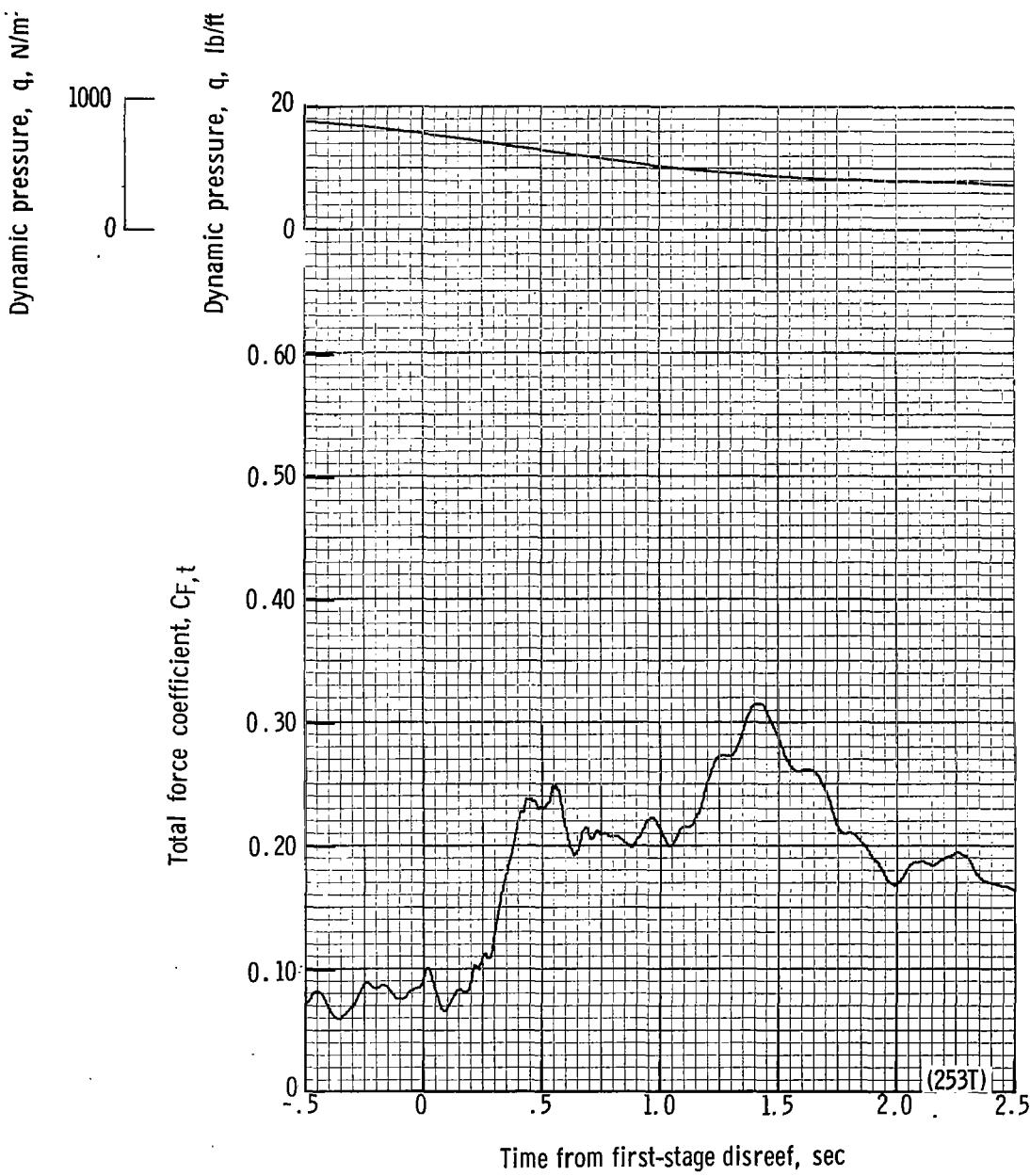
(d) Forward and aft riser loads plotted against time from first-stage disreef. Time = 0 second corresponds to 18.38 seconds after launch.

Figure 56.- Continued.



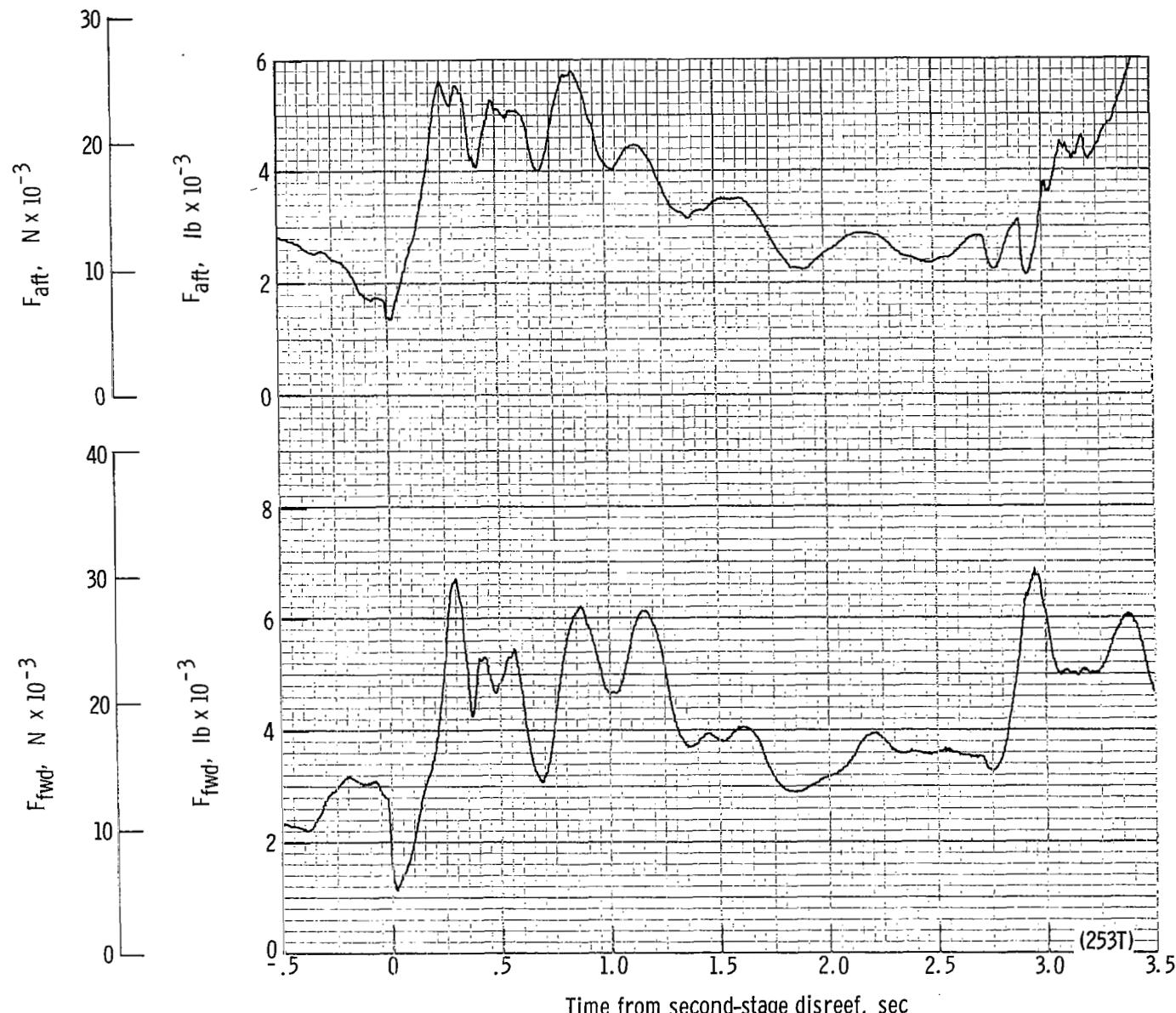
(e) Total force F_t plotted against time from first-stage disreef. Time = 0 second corresponds to 18.38 seconds after launch.

Figure 56.- Continued.



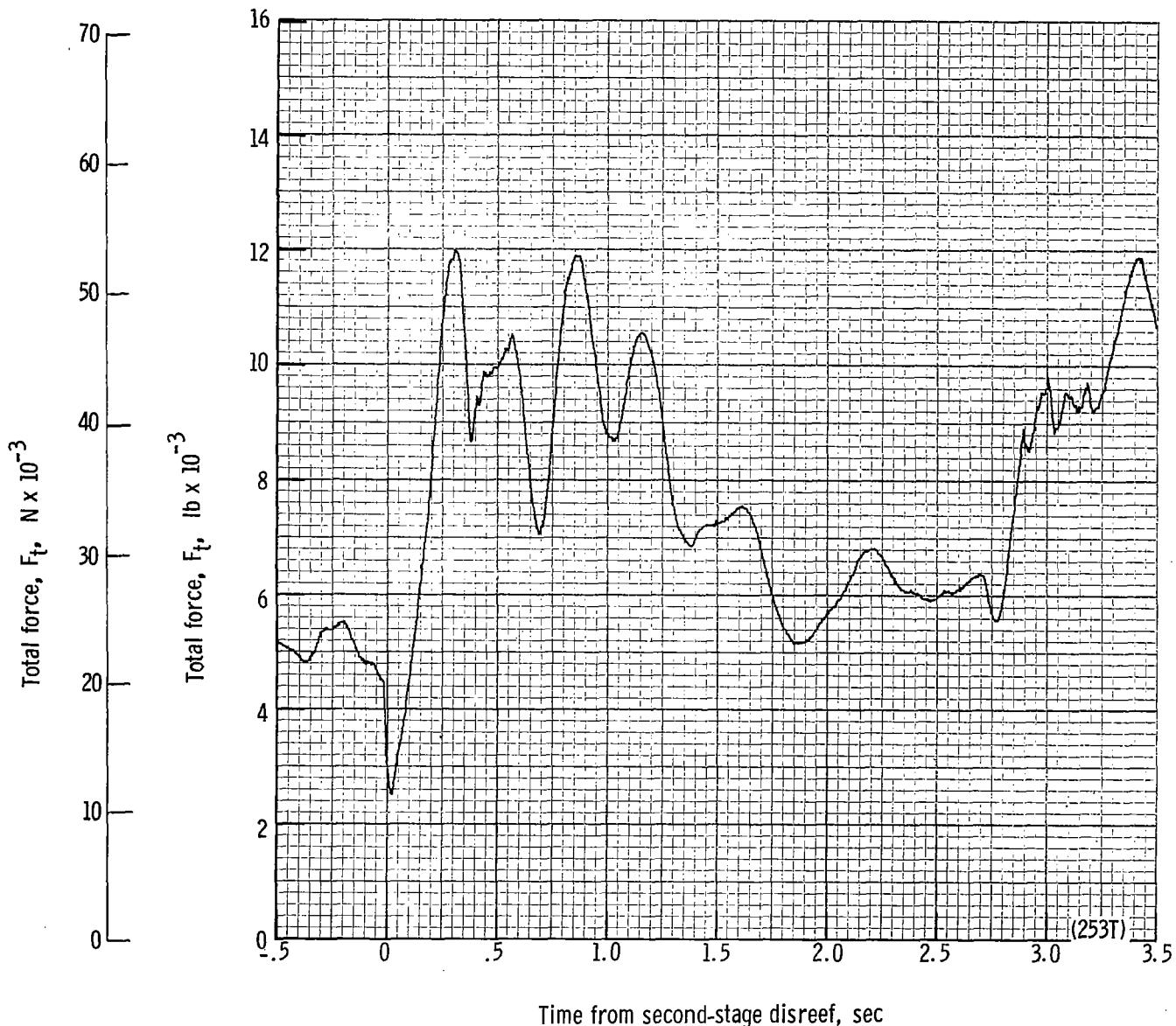
(f) Total force coefficient $C_{F,t}$ and dynamic pressure q plotted against time from first-stage disreef. Time = 0 second corresponds to 18.38 seconds after launch.

Figure 56.- Continued.



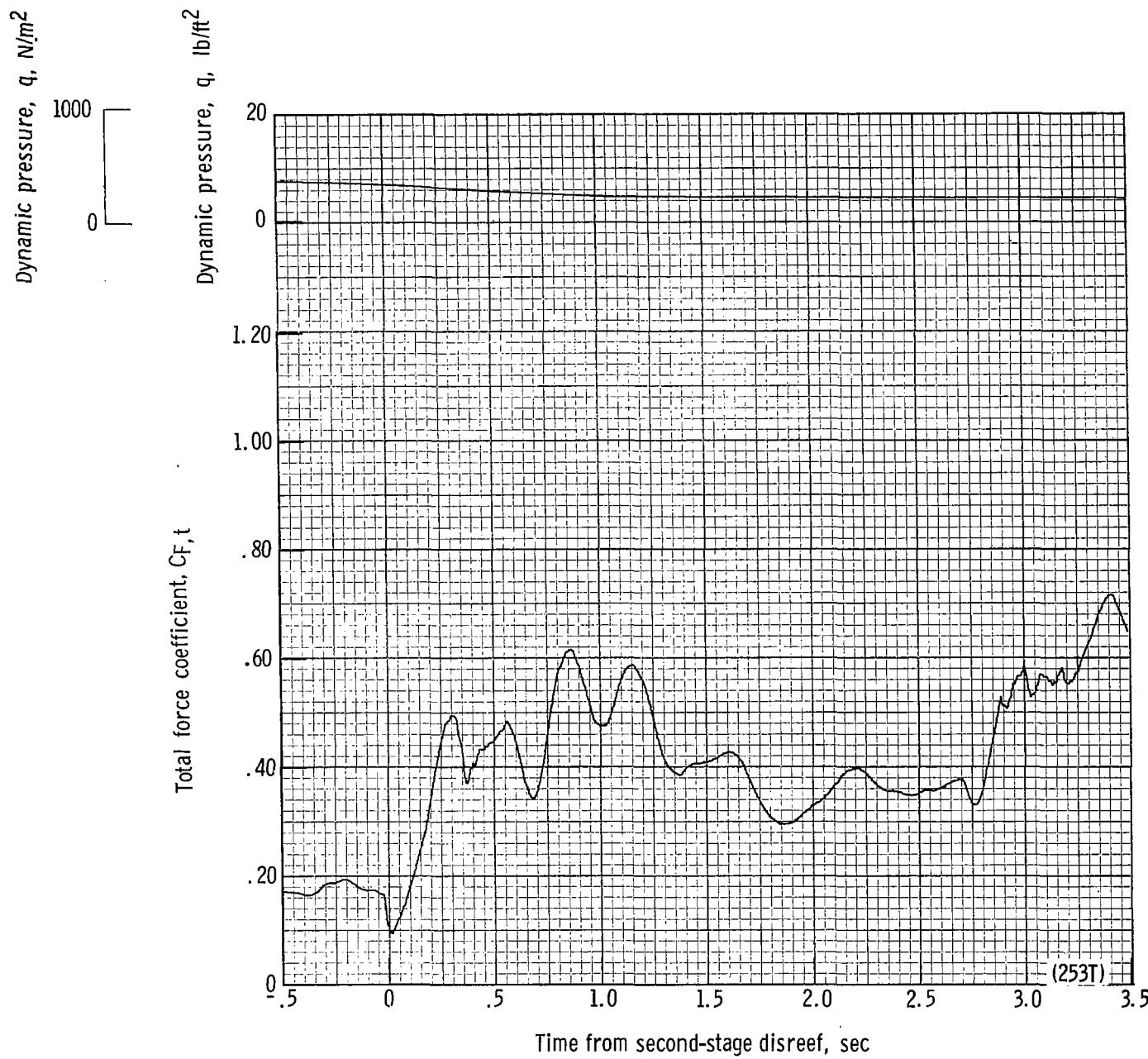
(g) Forward and aft riser loads plotted against time from second-stage disreef. Time = 0 second corresponds to 21.27 seconds after launch.

Figure 56.- Continued.



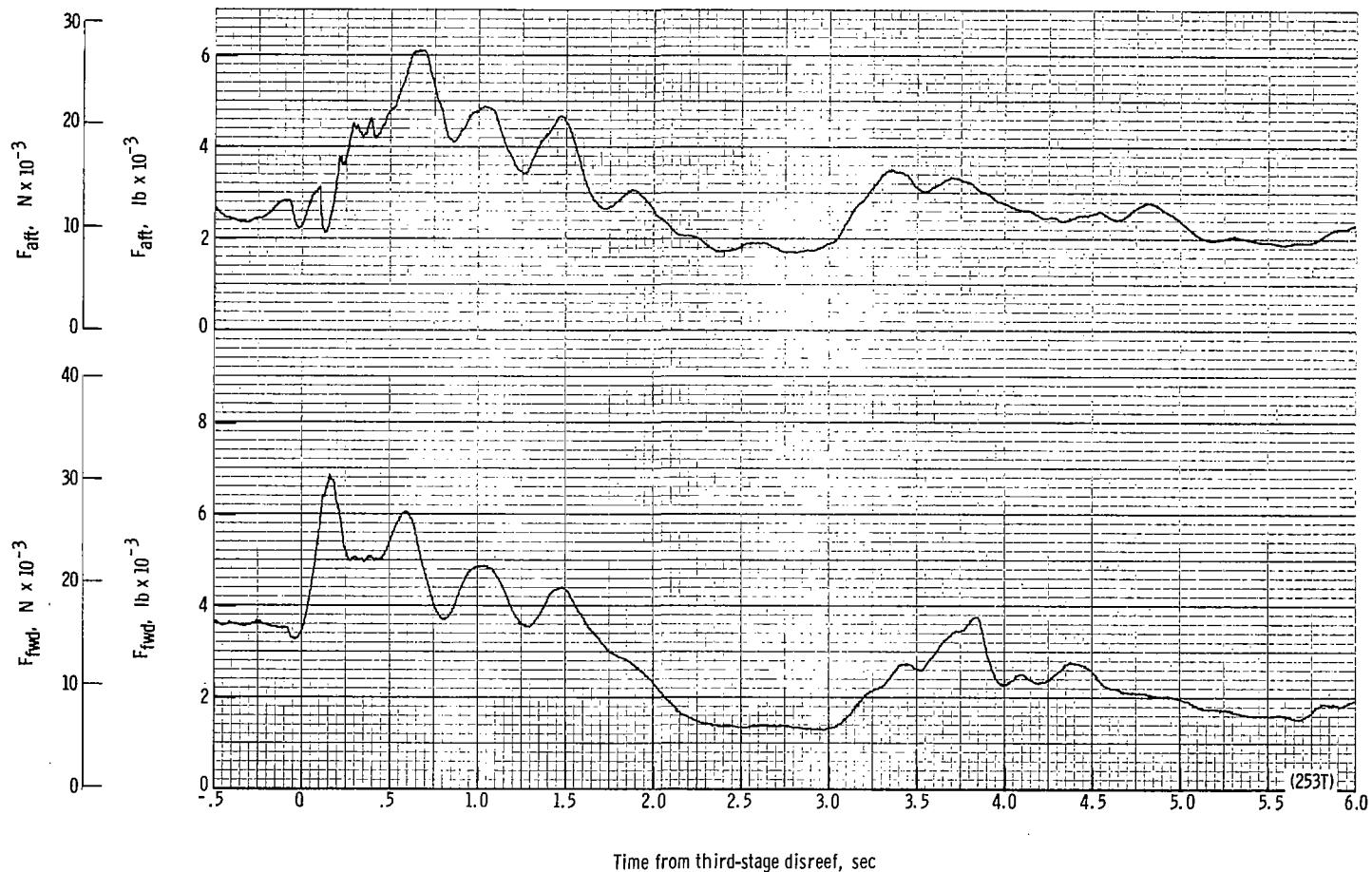
(h) Total force F_t plotted against time from second-stage disreef. Time = 0 second corresponds to 21.27 seconds after launch.

Figure 56.- Continued.



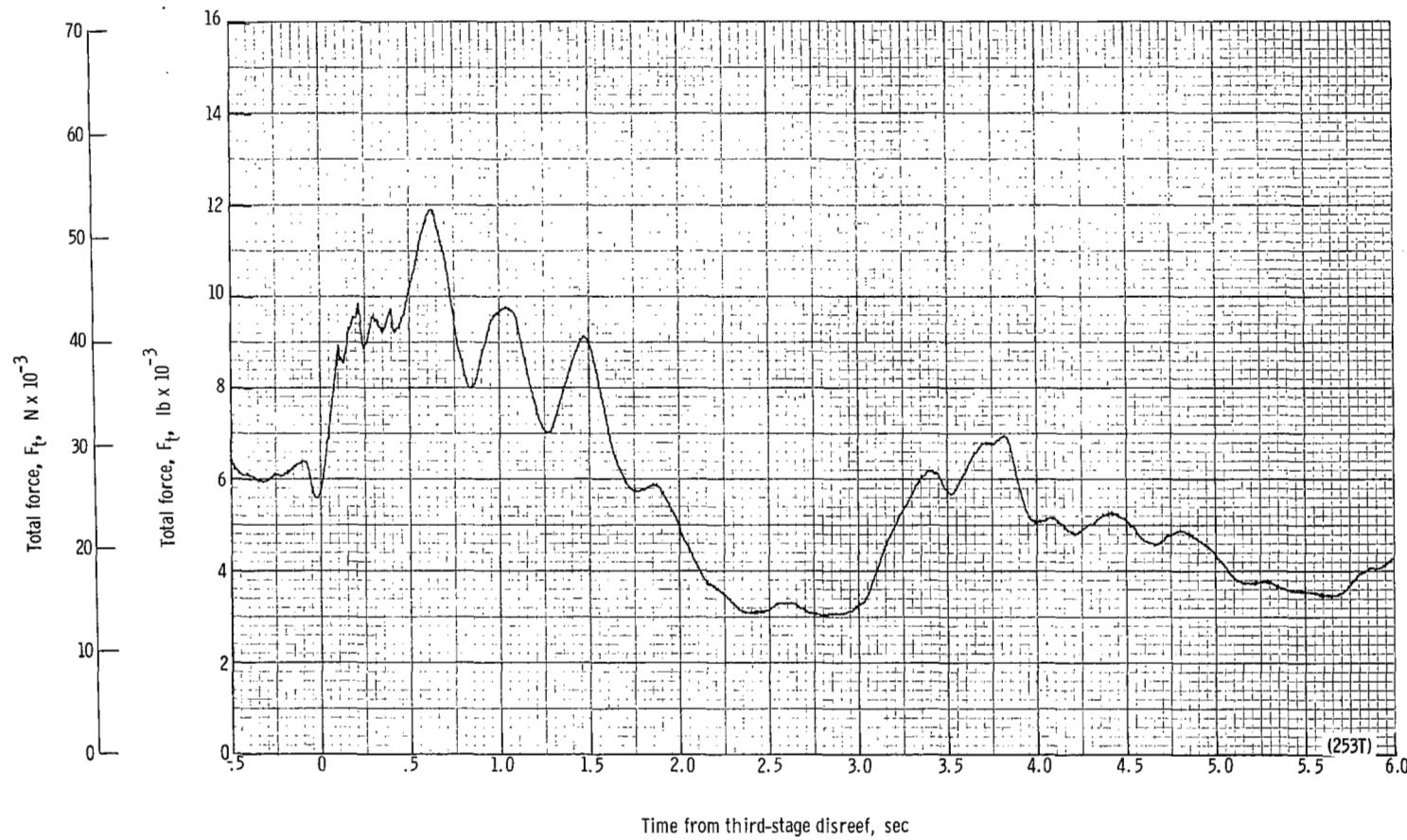
(i) Total force coefficient $C_{F,t}$ and dynamic pressure q plotted against time from second-stage disreef. Time = 0 second corresponds to 21.27 seconds after launch.

Figure 56.- Continued.



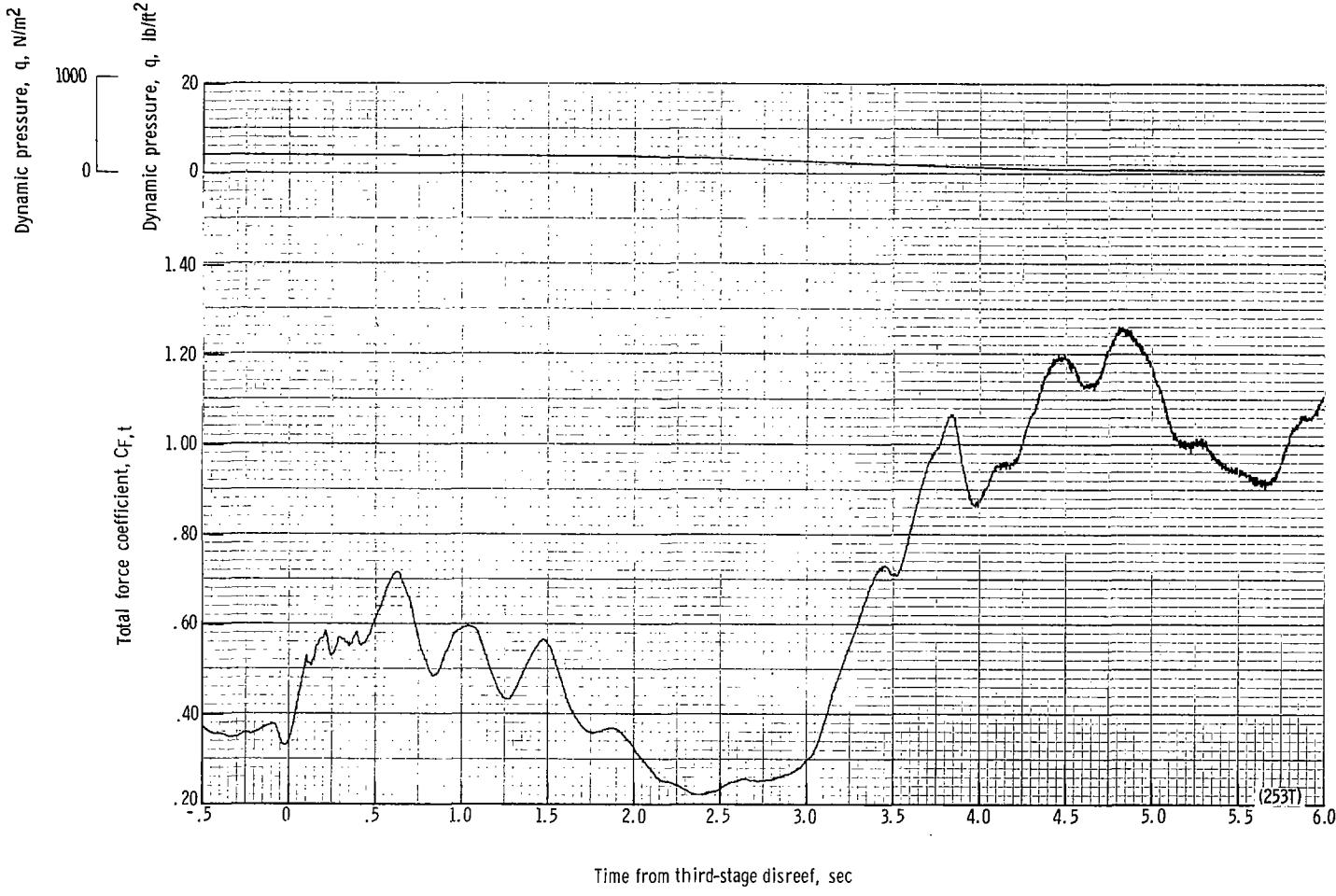
(j) Forward and aft riser loads plotted against time from third-stage disreef. Time = 0 second corresponds to 24.11 seconds after launch.

Figure 56.- Continued.



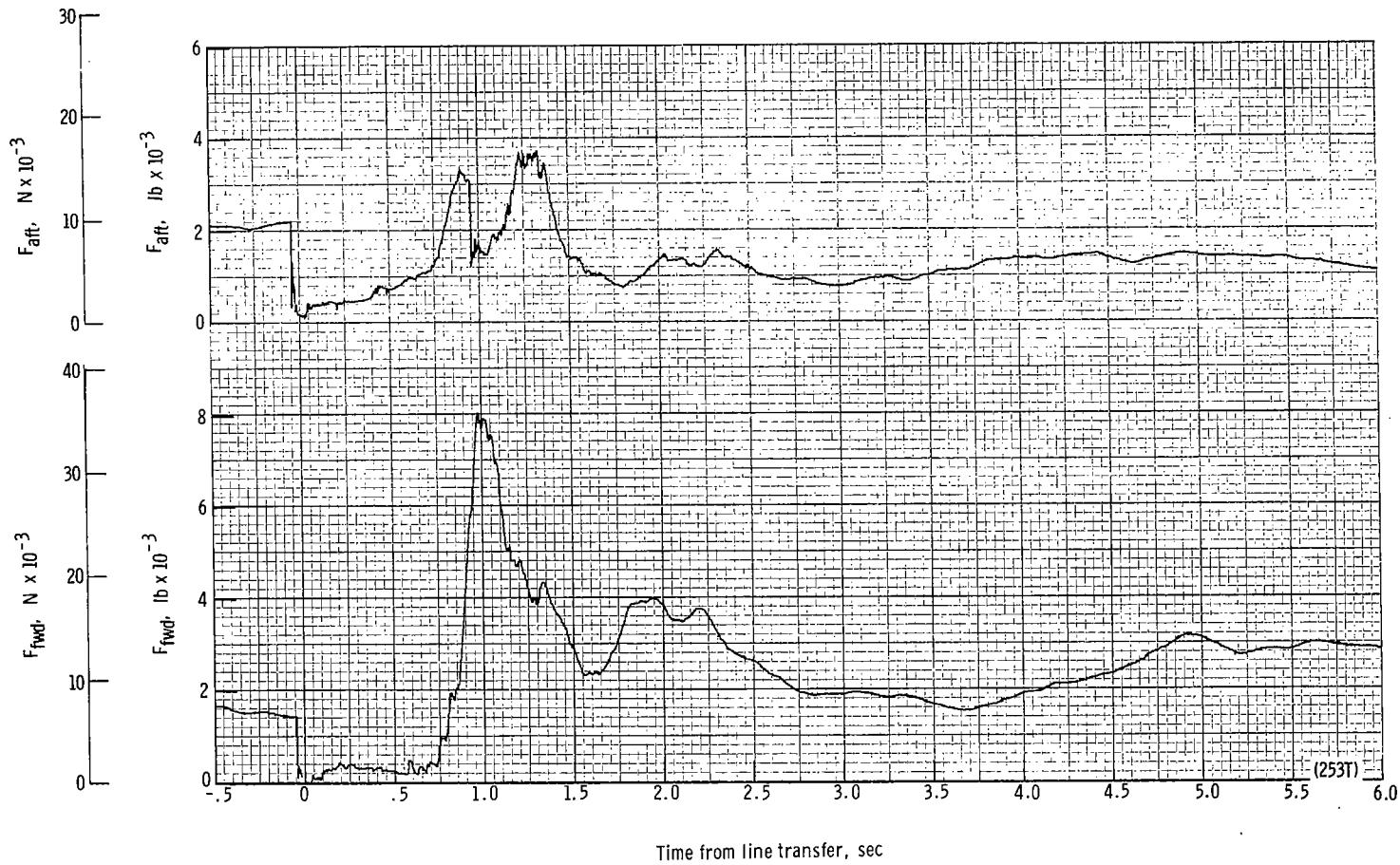
(k) Total force F_t plotted against time from third-stage disreef. Time = 0 second corresponds to 24.11 seconds after launch.

Figure 56.- Continued.



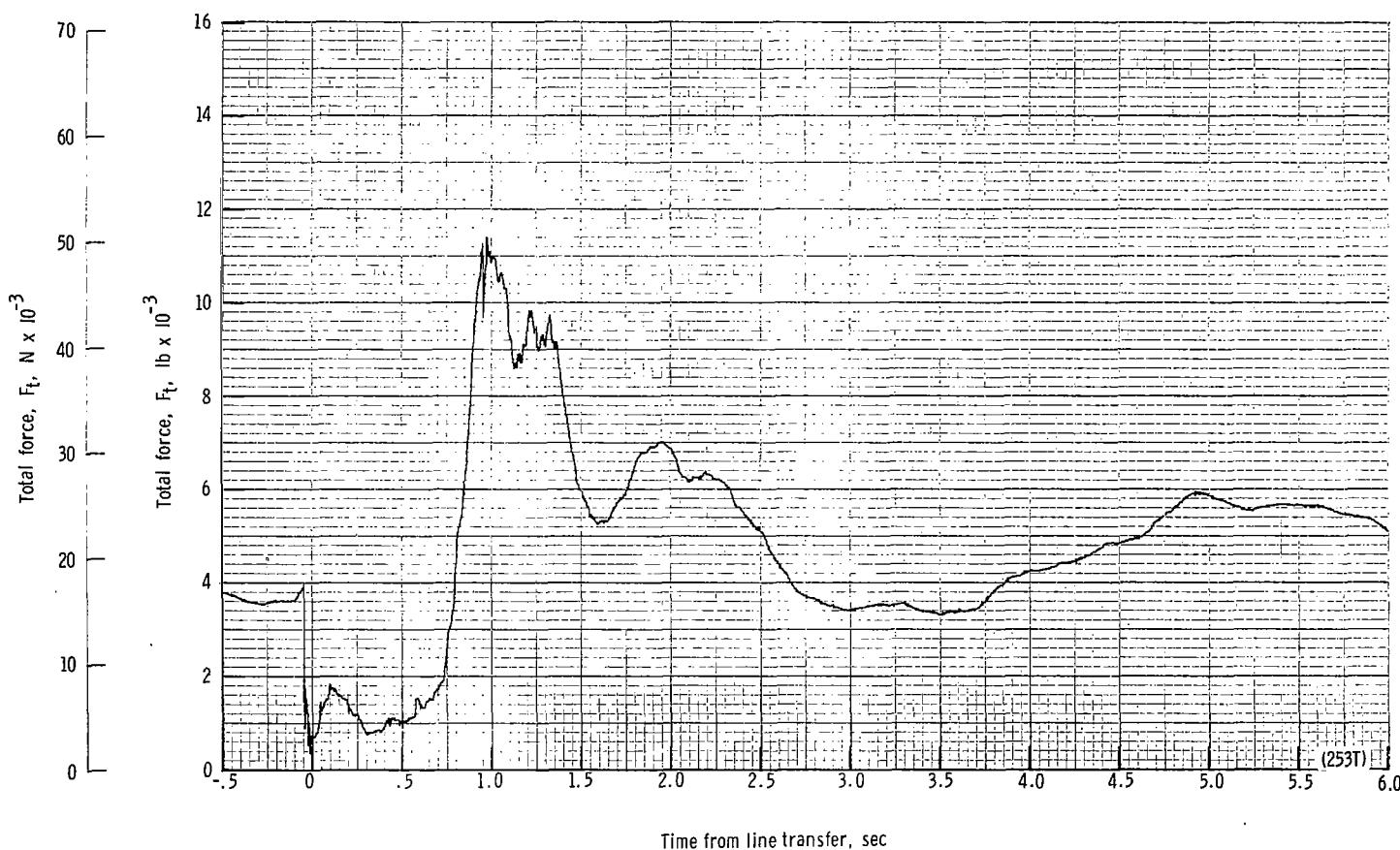
(I) Total force coefficient $C_{F,t}$ and dynamic pressure q plotted against time from third-stage disreef. Time = 0 second corresponds to 24.11 seconds after launch.

Figure 56.- Continued.



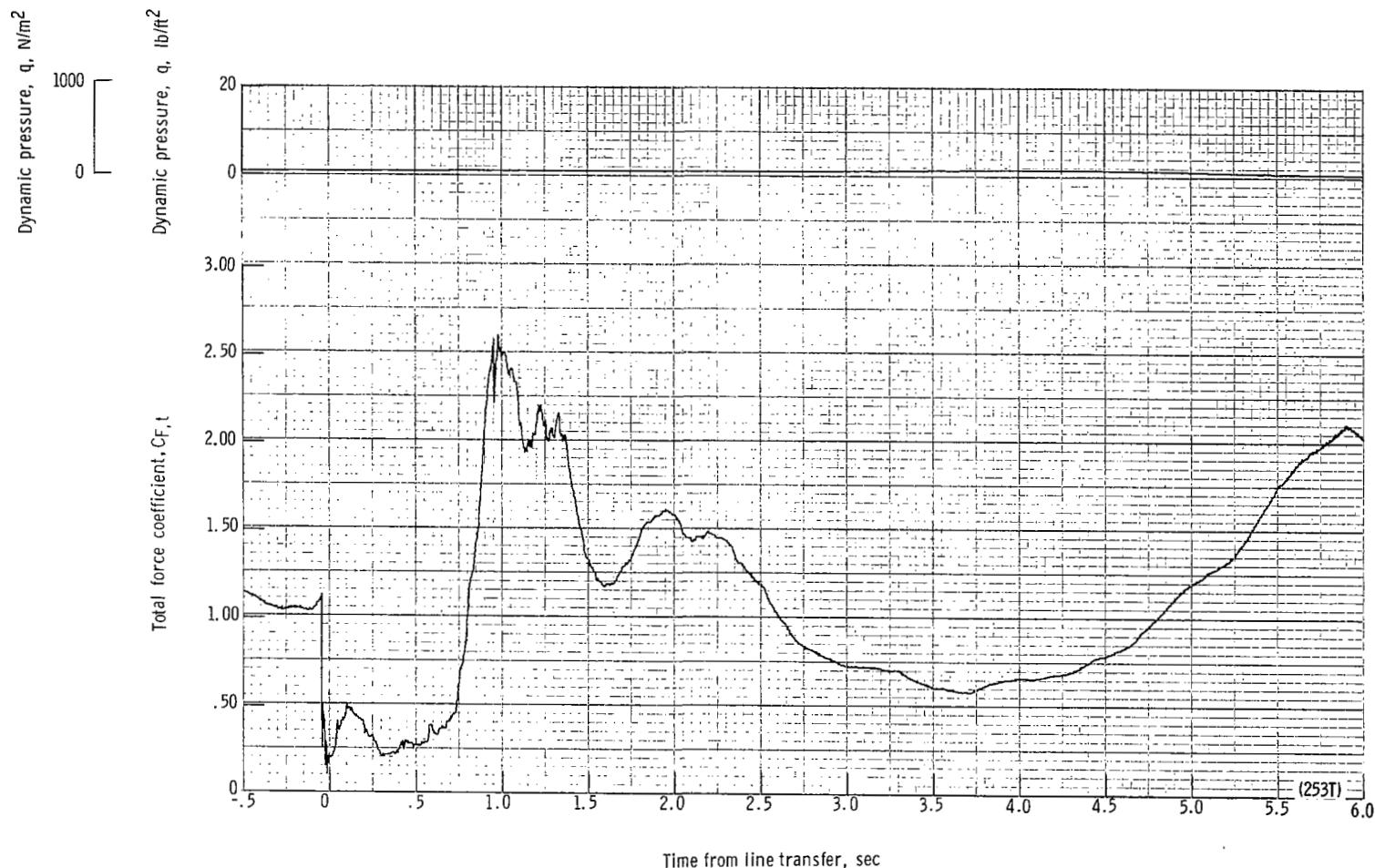
(m) Forward and aft riser loads plotted against time from line transfer. Time = 0 second corresponds to 32.63 seconds after launch.

Figure 56.- Continued.



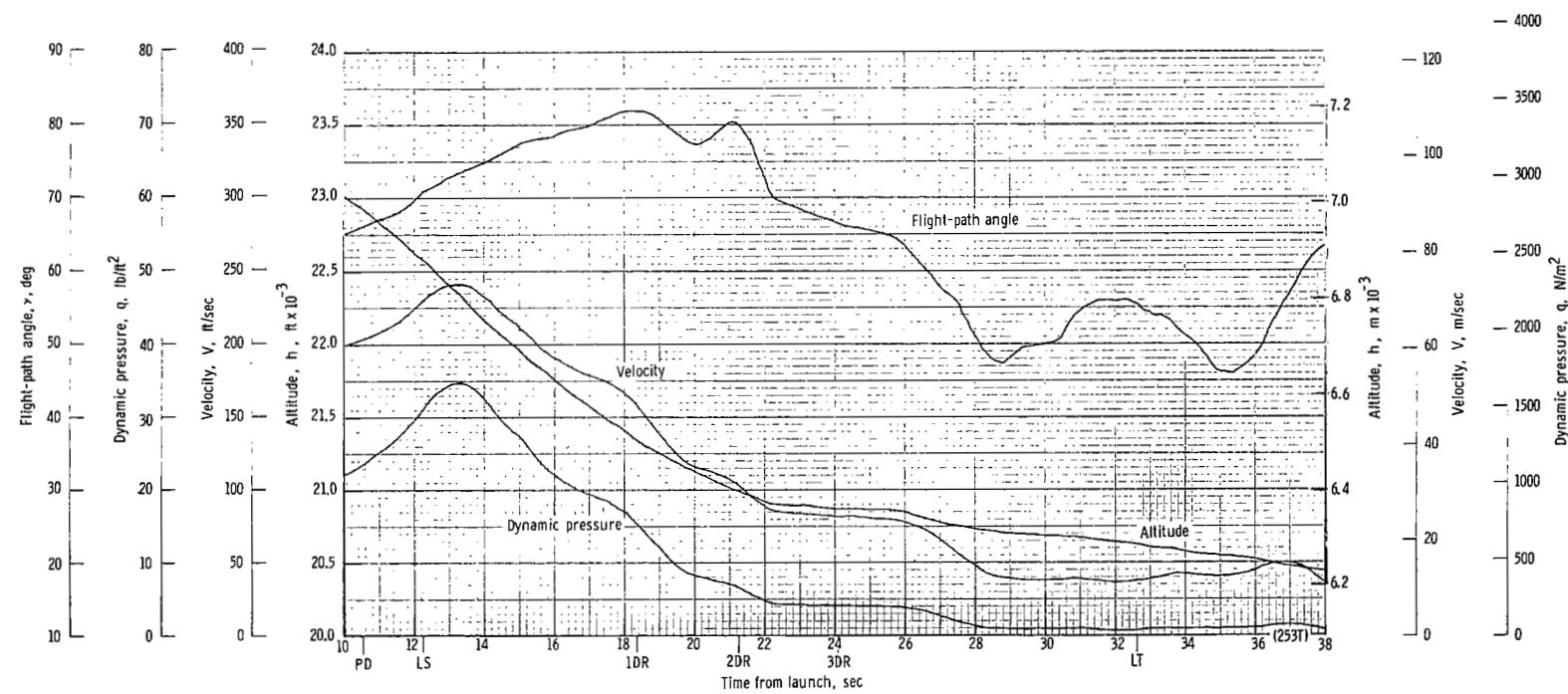
(n) Total force F_t plotted against time from line transfer. Time = 0 second corresponds to 32.63 seconds after launch.

Figure 56.- Continued.



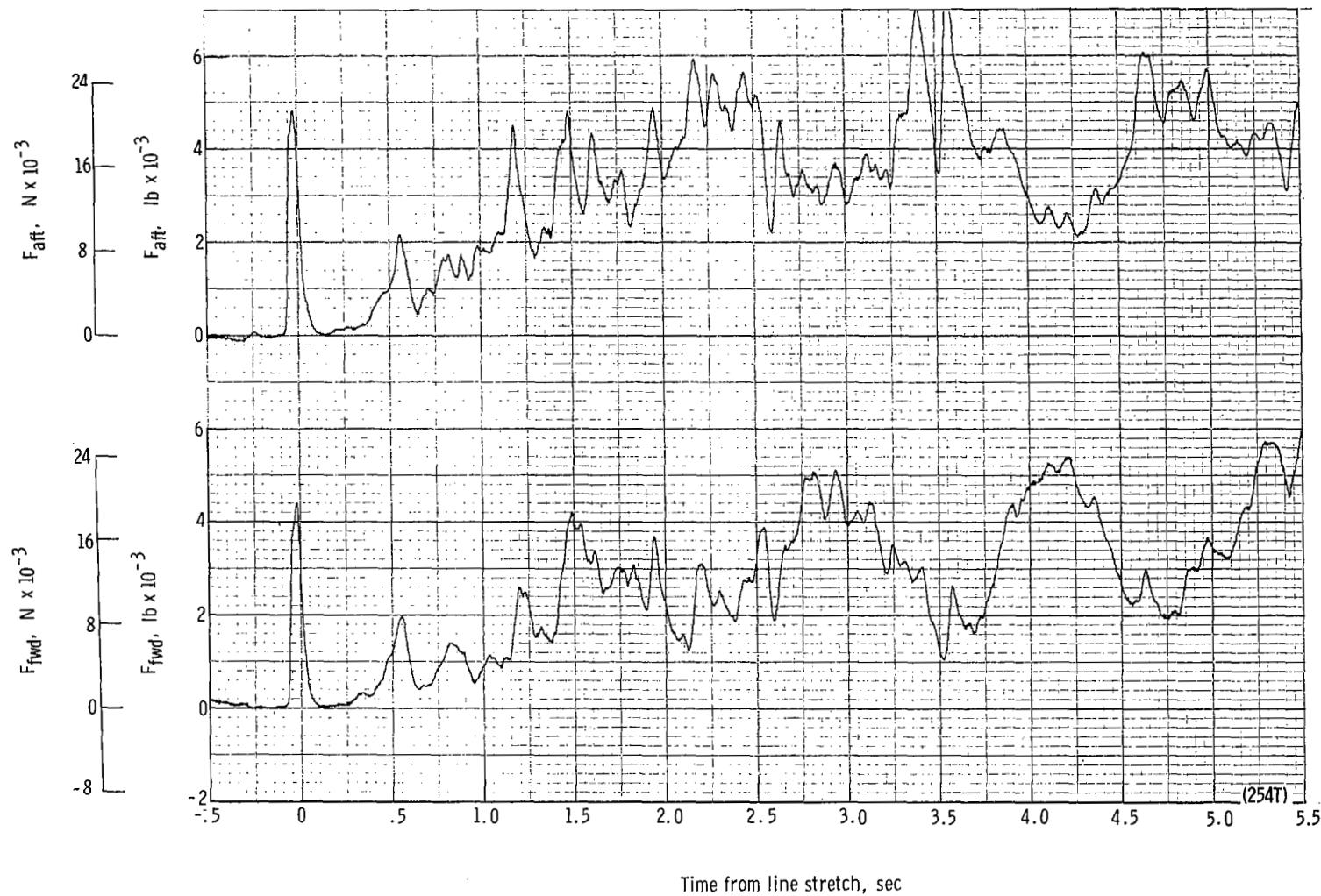
(o) Total force coefficient $C_{F,t}$ and dynamic pressure q plotted against time from line transfer. Time = 0 second corresponds to 32.63 seconds after launch.

Figure 56.- Continued.



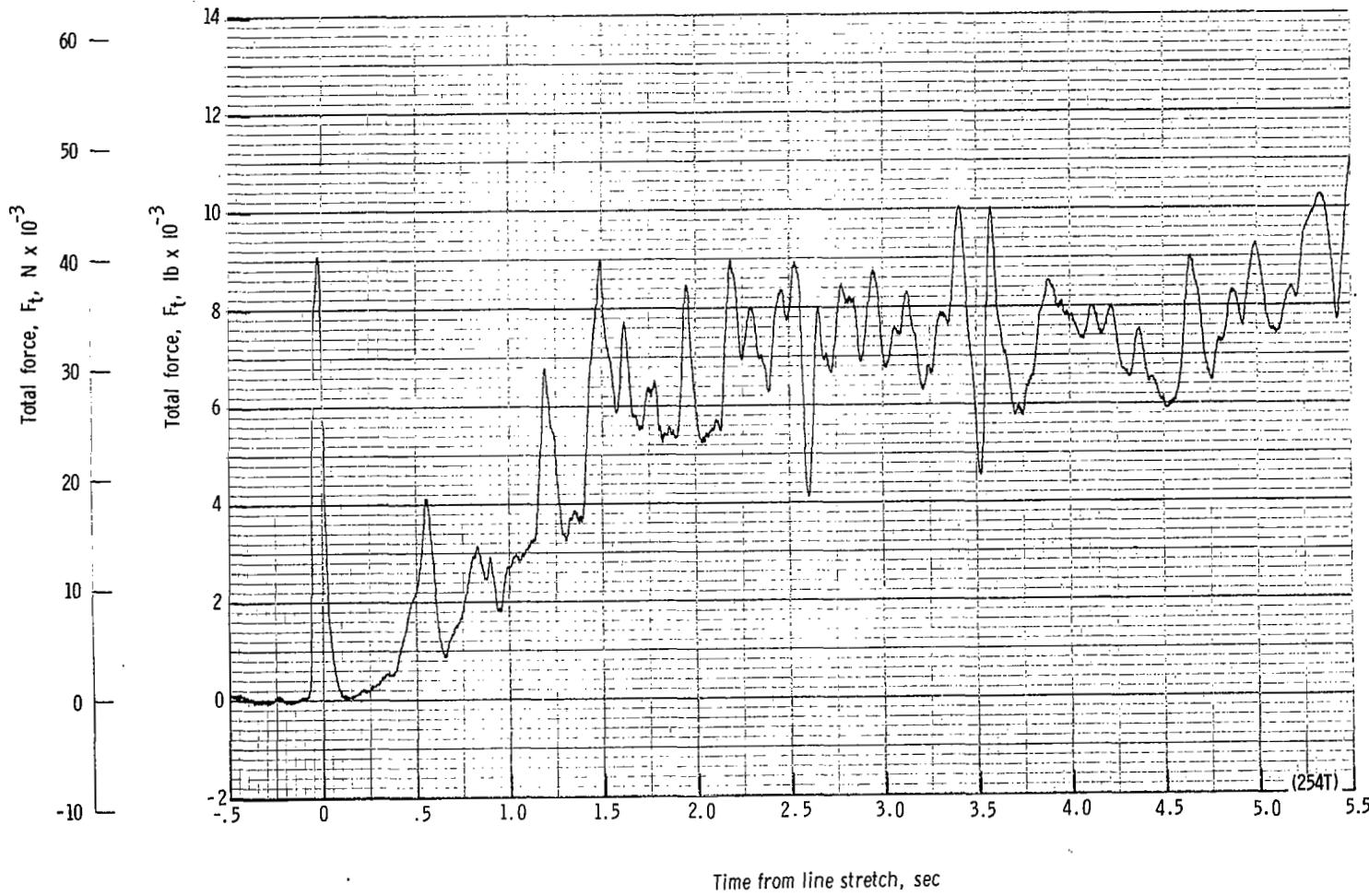
(p) Flight-path angle γ , dynamic pressure q , velocity V , and altitude h plotted against time from launch.

Figure 56.- Concluded.



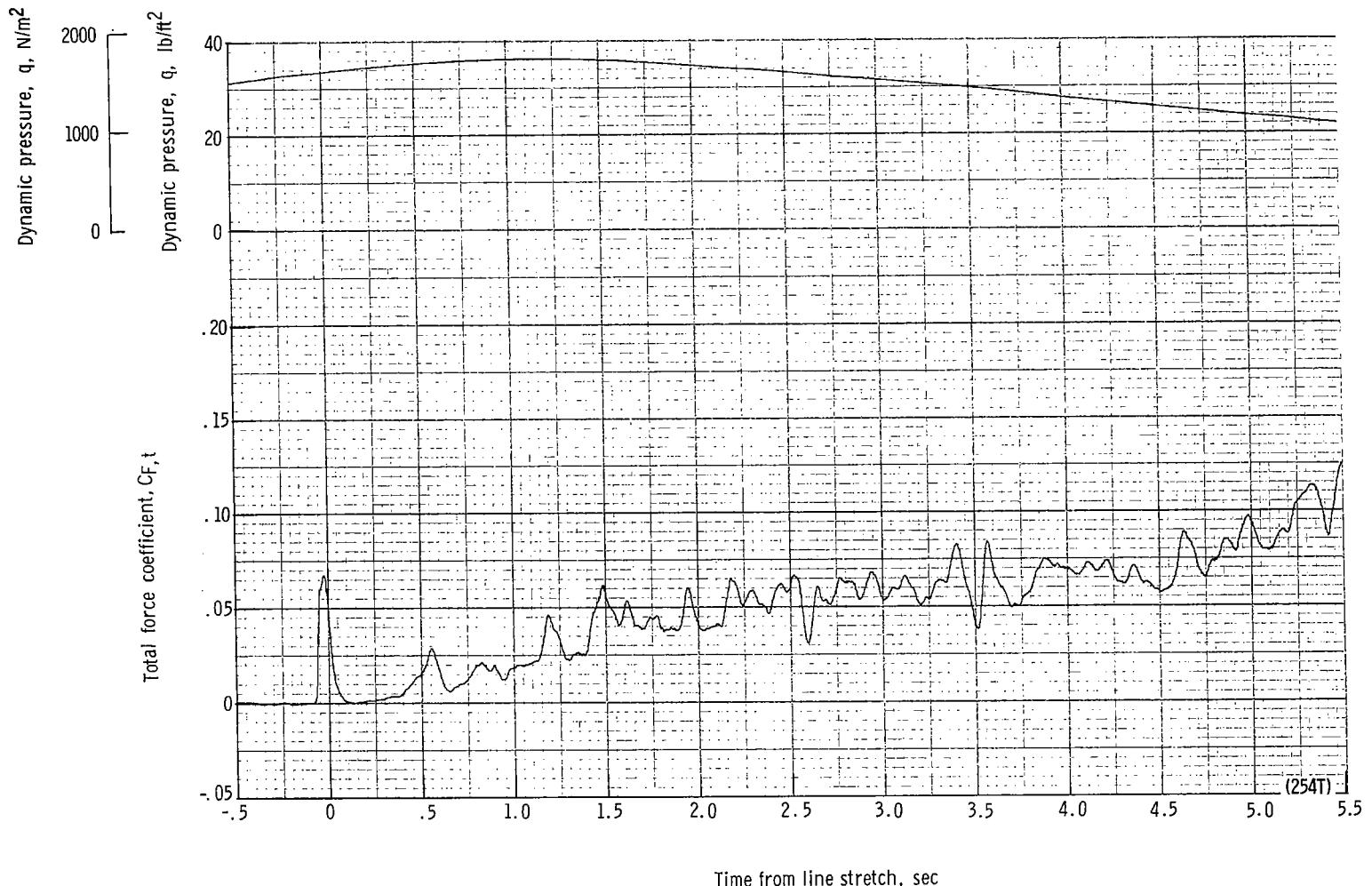
(a) Forward and aft riser loads plotted against time from line stretch. Time = 0 second corresponds to 12.33 seconds after launch.

Figure 57.- Time history of twin-keel parawing deployment data for test 254T. $W_D = 26\ 738 \text{ N}$ (6011 lb); $W_p = 24\ 881 \text{ N}$ (5593 lb); $q_{PD} = 1216 \text{ N/m}^2$ (25.4 lb/ft²); $h_{PD} = 6834 \text{ m}$ (22 420 ft); $l_r/l_k = 0.100$; reefing version C.



(b) Total force F_t plotted against time from line stretch. Time = 0 second corresponds to 12.33 seconds after launch.

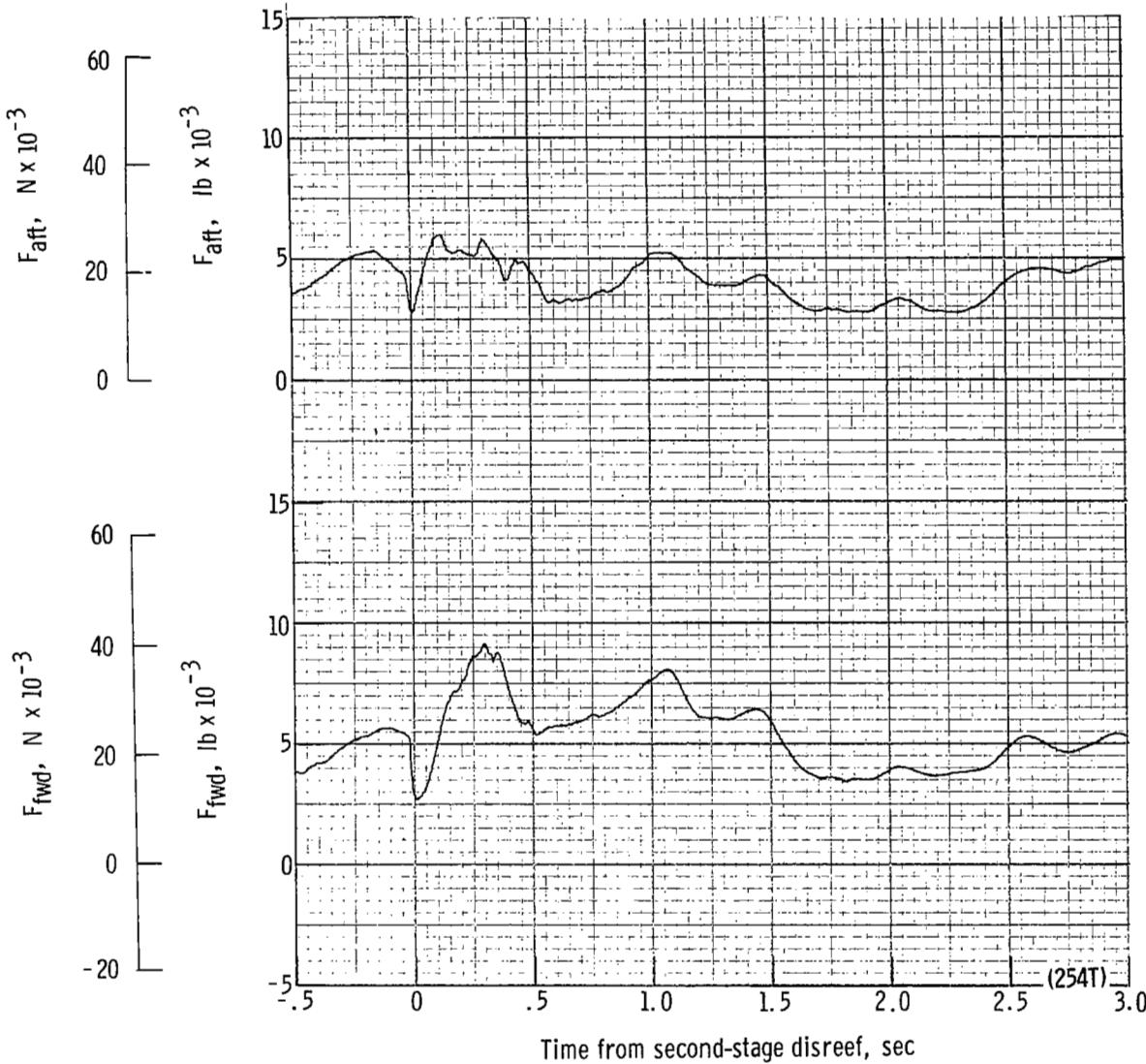
Figure 57.- Continued.



(c) Total force coefficient $C_{F,t}$ and dynamic pressure q plotted against time from line stretch. Time = 0 second corresponds to 12.33 seconds after launch.

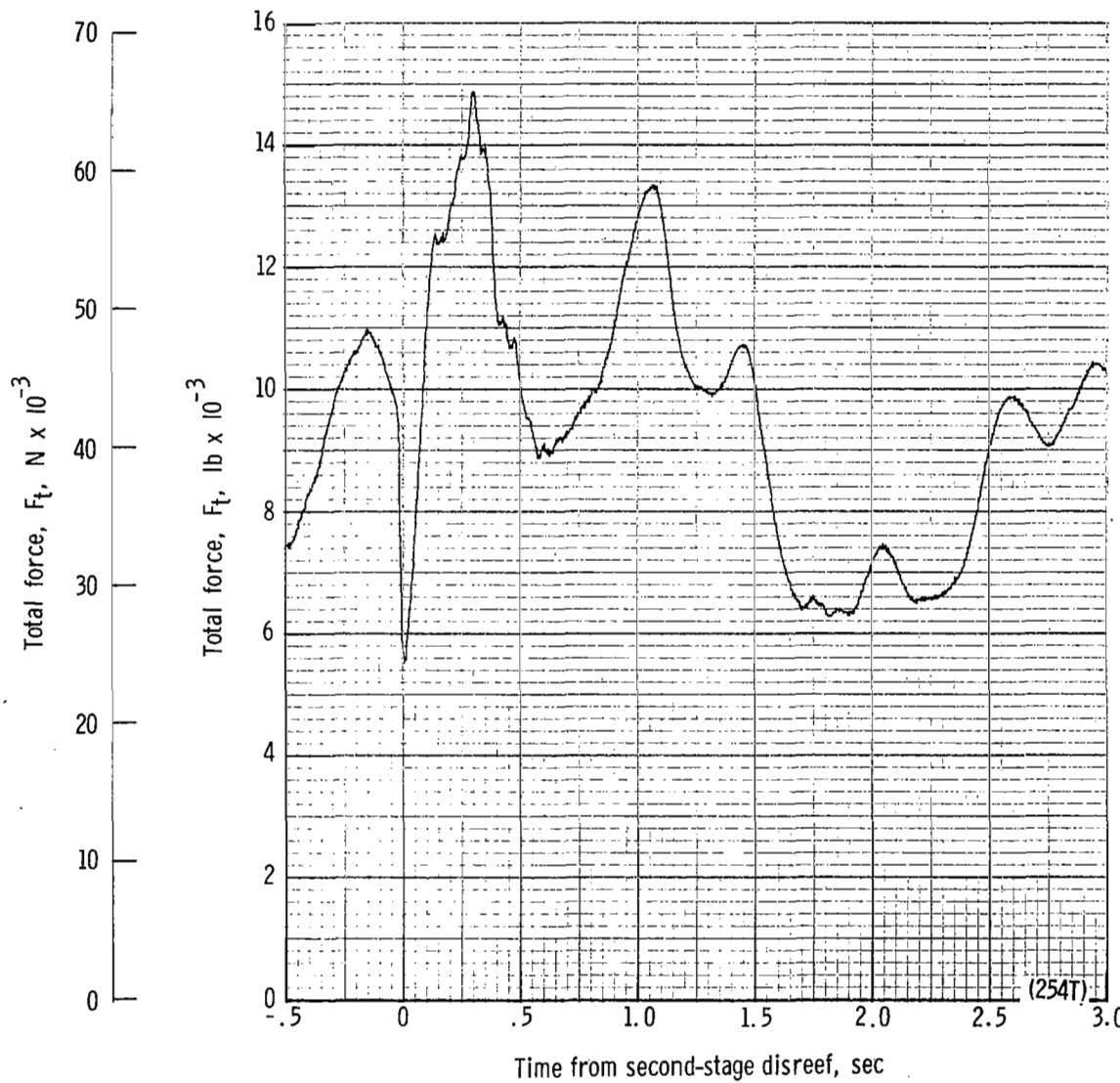
Figure 57.- Continued.

Note: A telemetry calibration signal was initiated approximately 6 seconds after parawing line stretch for a duration of about 2 seconds. This signal obscured the load readings during a significant portion of parawing second-stage reefed inflation. Therefore, parts (d), (e), and (f) of figure 57 are omitted.



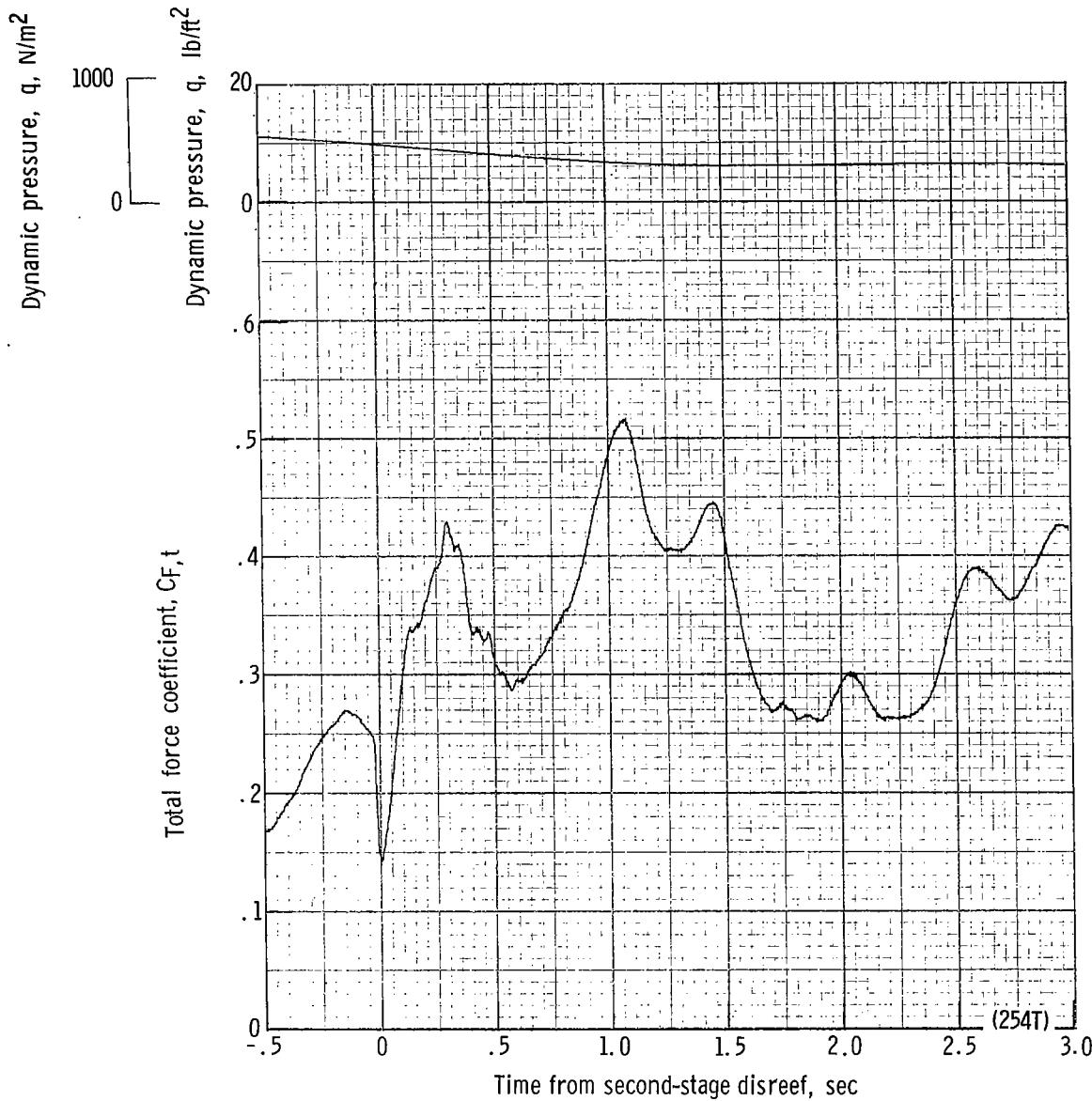
(g) Forward and aft riser loads plotted against time from second-stage disreef. Time = 0 second corresponds to 21.30 seconds after launch.

Figure 57.- Continued.



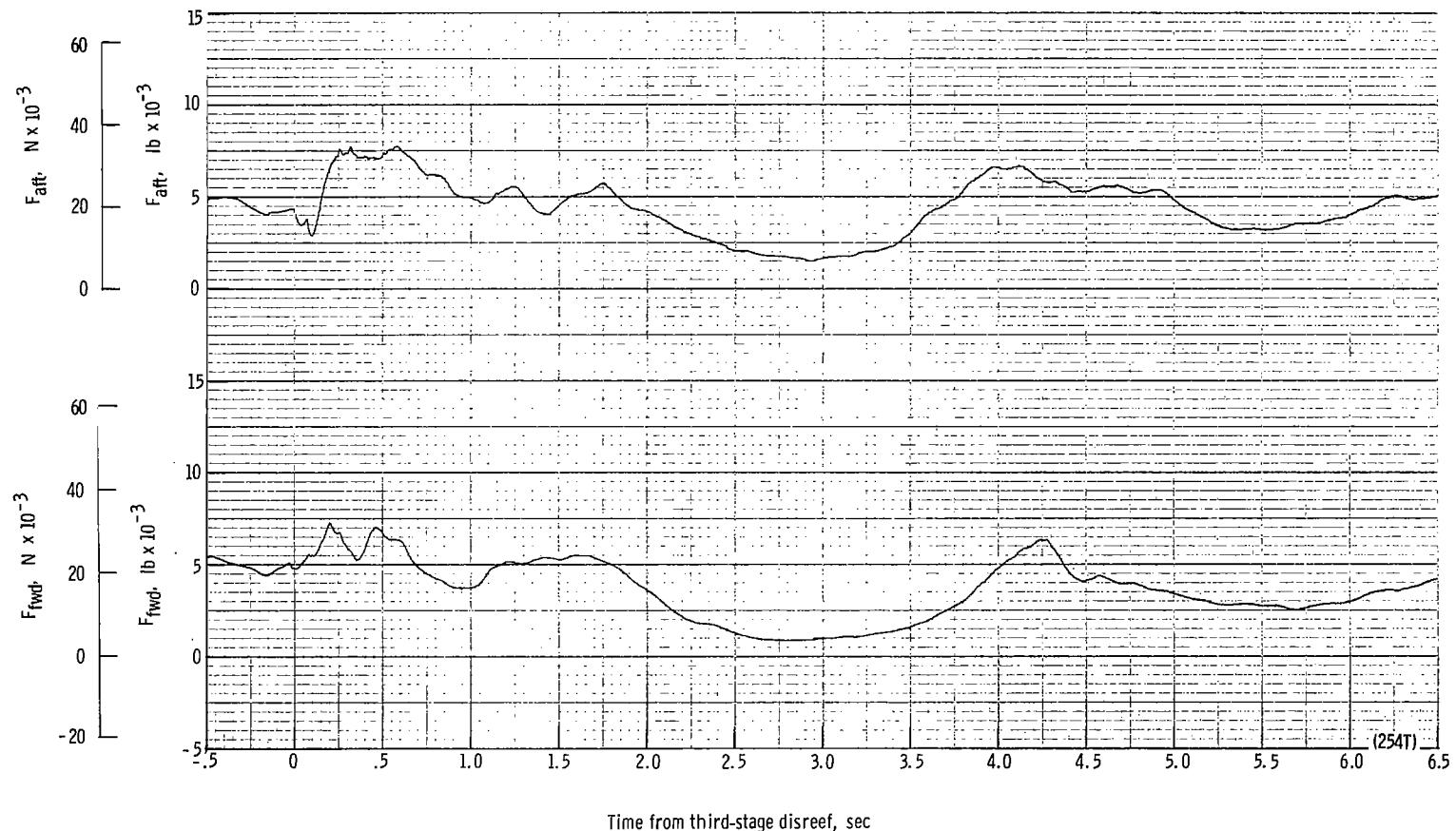
(h) Total force F_t plotted against time from second-stage disreef. Time = 0 second corresponds to 21.30 seconds after launch.

Figure 57.- Continued.



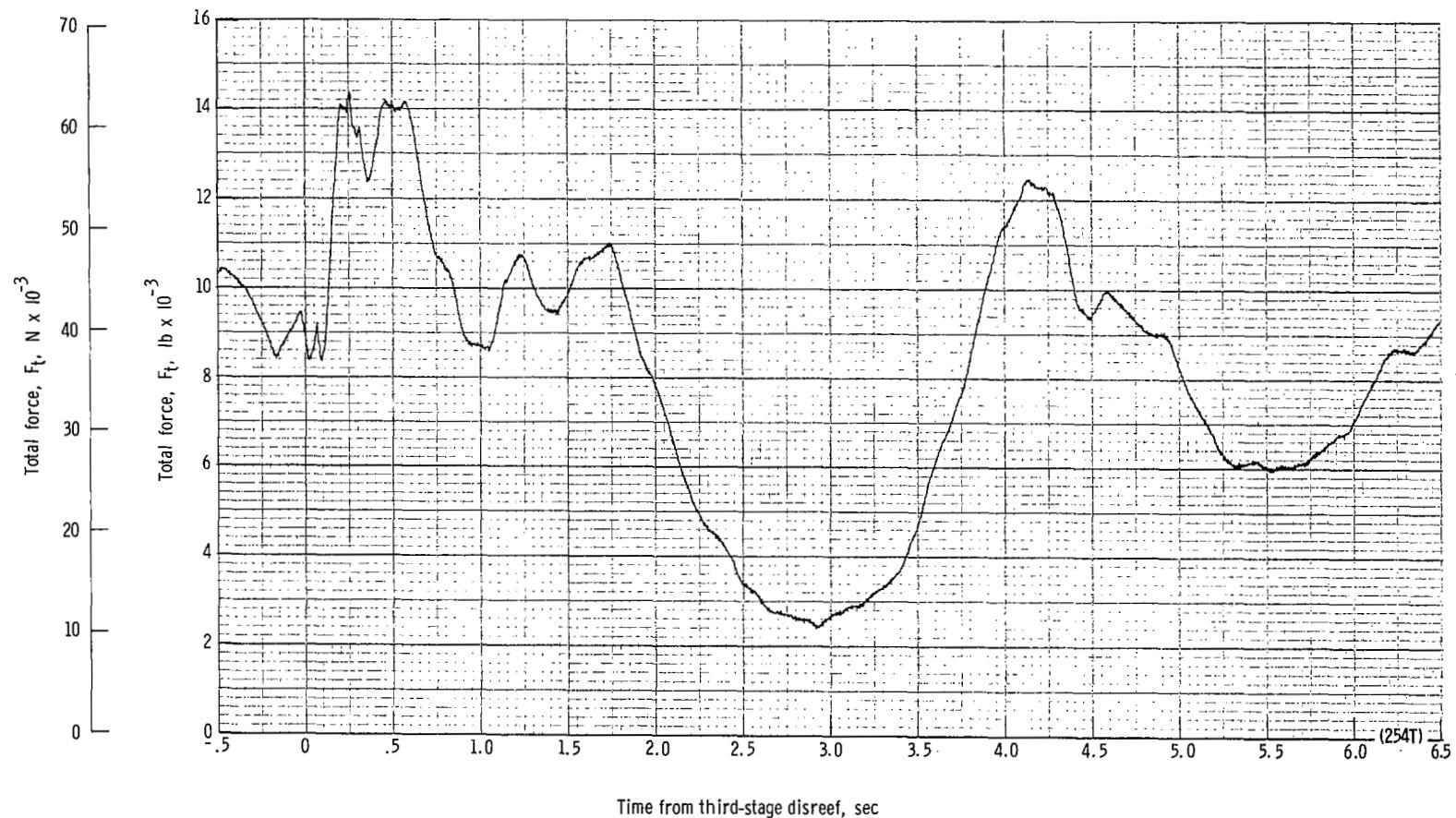
(i) Total force coefficient $C_{F,t}$ and dynamic pressure q plotted against time from second-stage disreef. Time = 0 second corresponds to 21.30 seconds after launch.

Figure 57.- Continued.



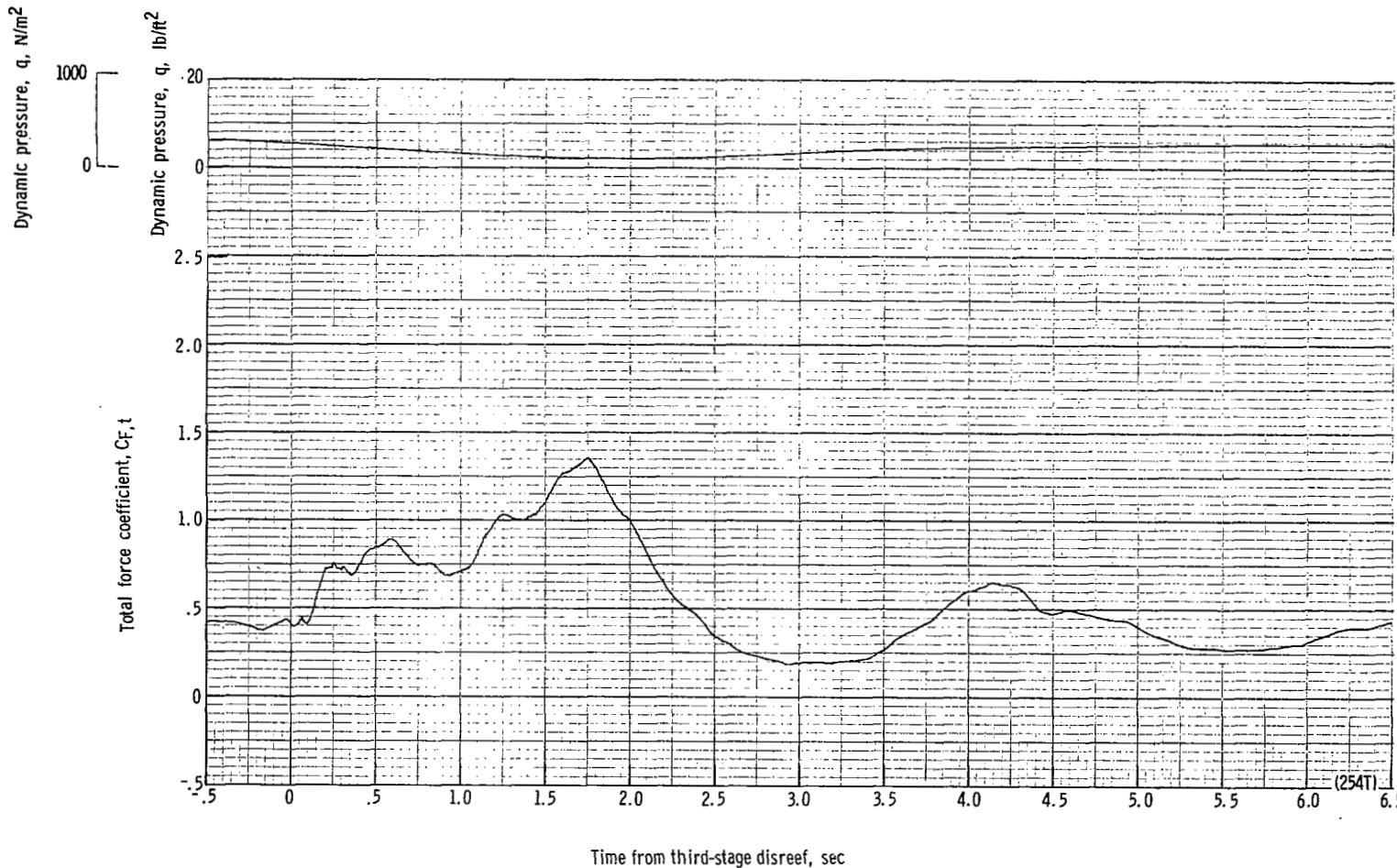
(i) Forward and aft riser loads plotted against time from third-stage disreef. Time = 0 second corresponds to 24.72 seconds after launch.

Figure 57.- Continued.



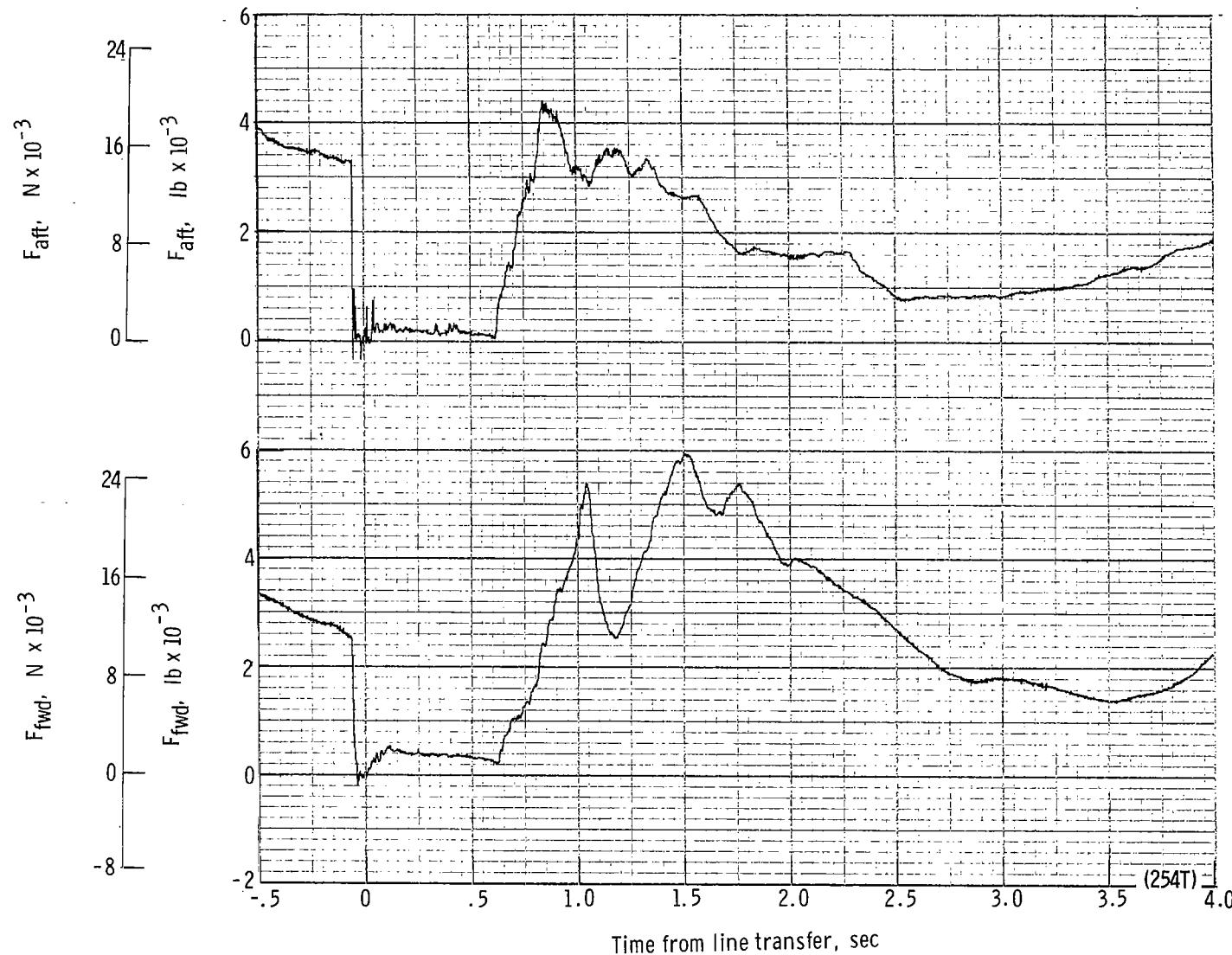
(k) Total force F_t plotted against time from third-stage disreef. Time = 0 second corresponds to 24.72 seconds after launch.

Figure 57.- Continued.



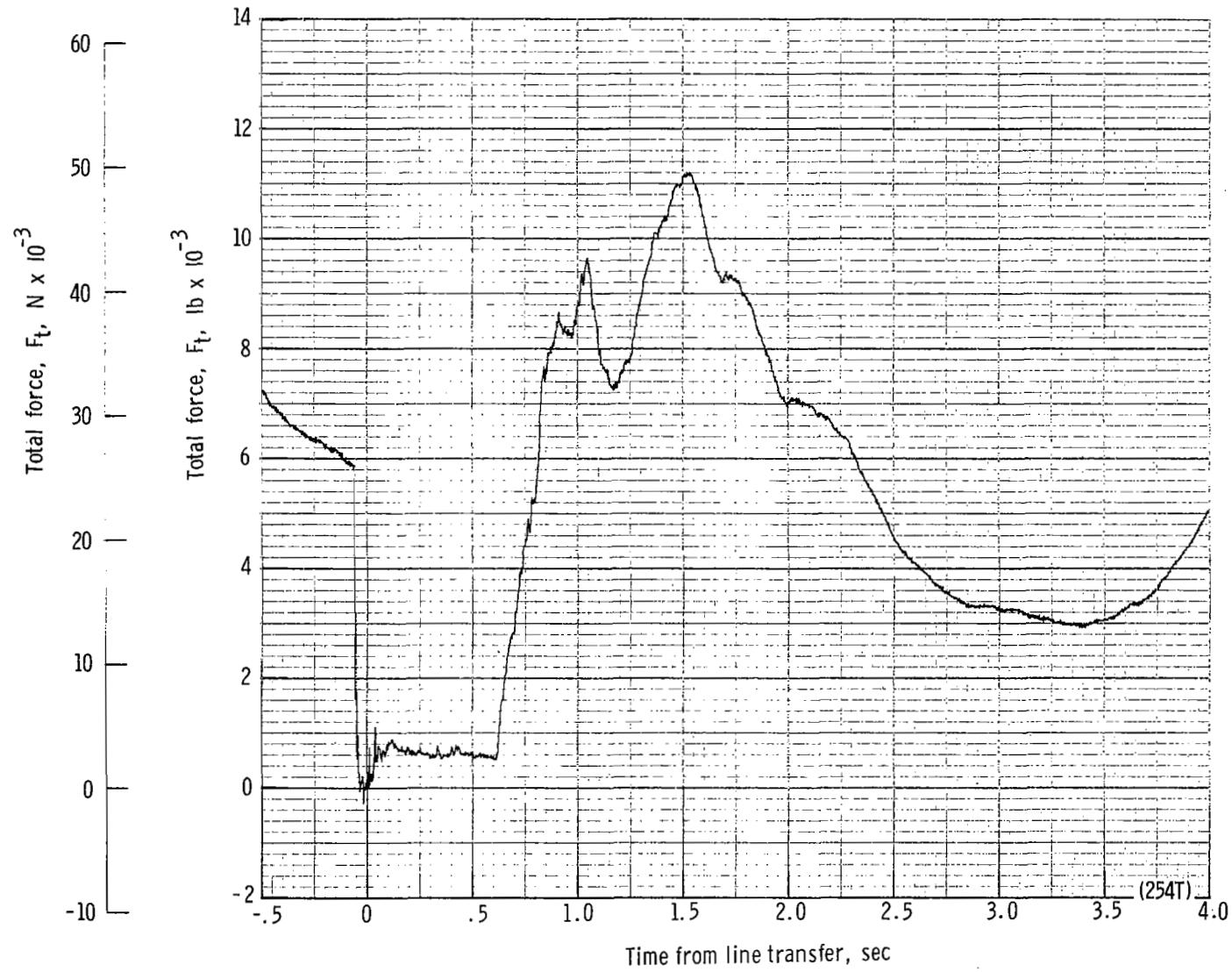
(II) Total force coefficient $C_{F,t}$ and dynamic pressure q plotted against time from third-stage disreef. Time = 0 second corresponds to 24.72 seconds after launch.

Figure 57.- Continued.



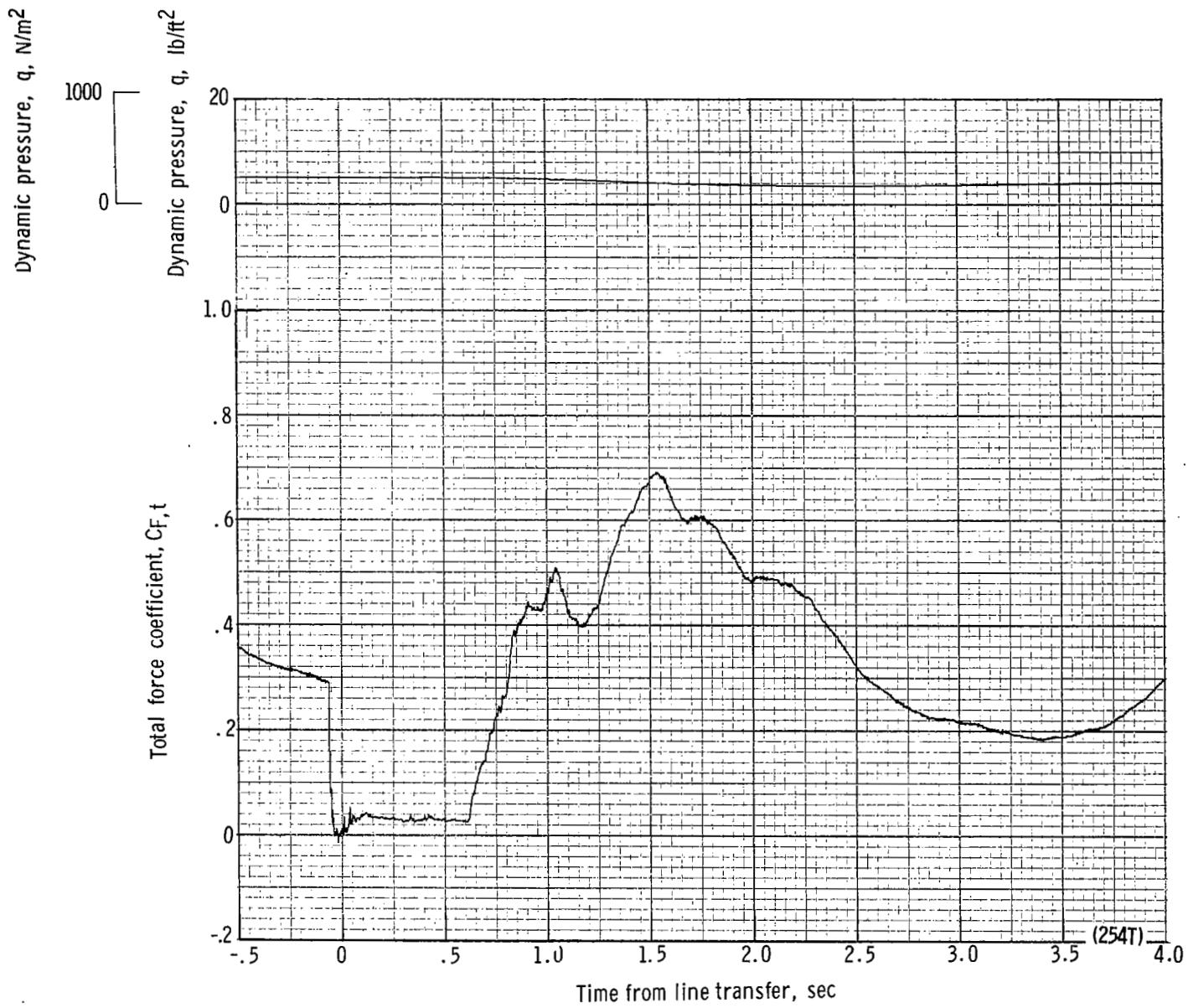
(m) Forward and aft riser loads plotted against time from line transfer. Time = 0 second corresponds to 32.32 seconds after launch.

Figure 57.- Continued.

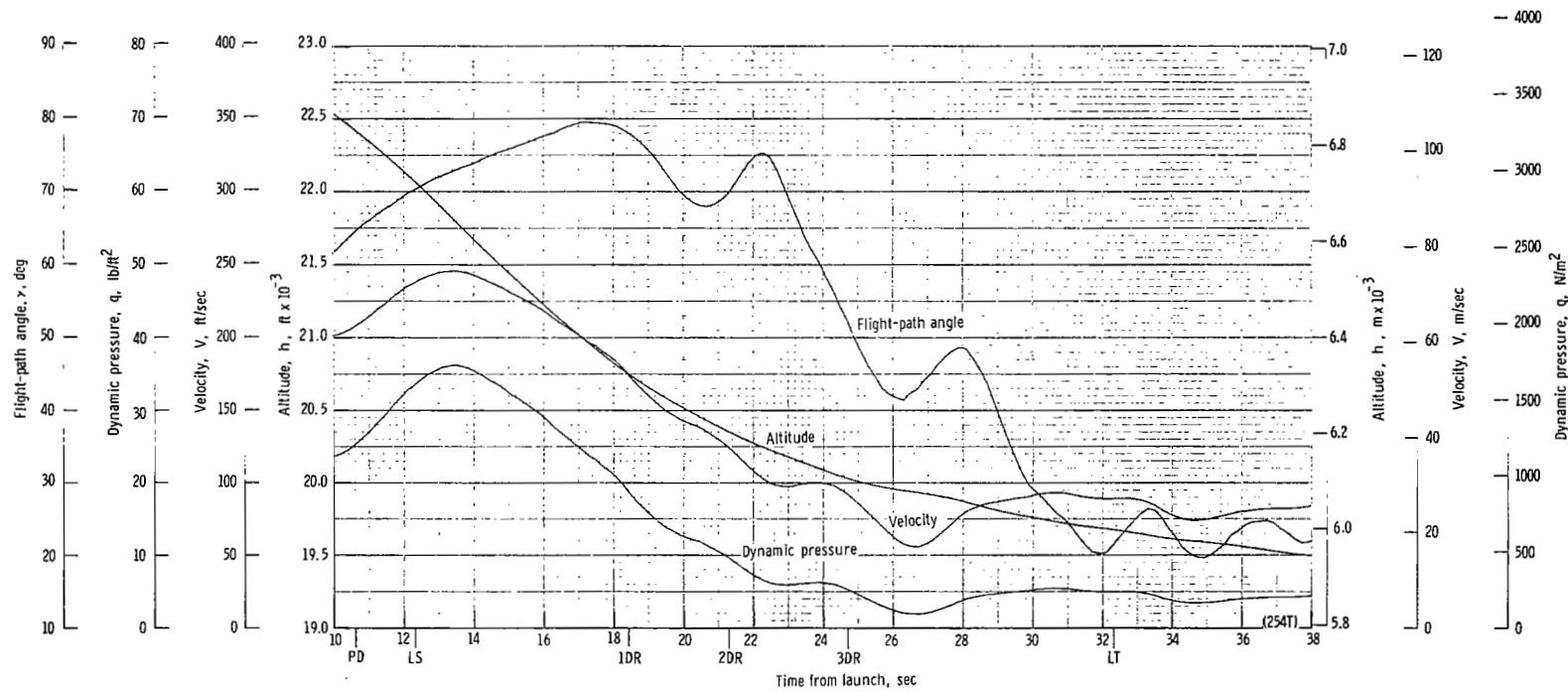


(n) Total force F_t plotted against time from line transfer. Time = 0 second corresponds to 32.32 seconds after launch.

Figure 57.- Continued.

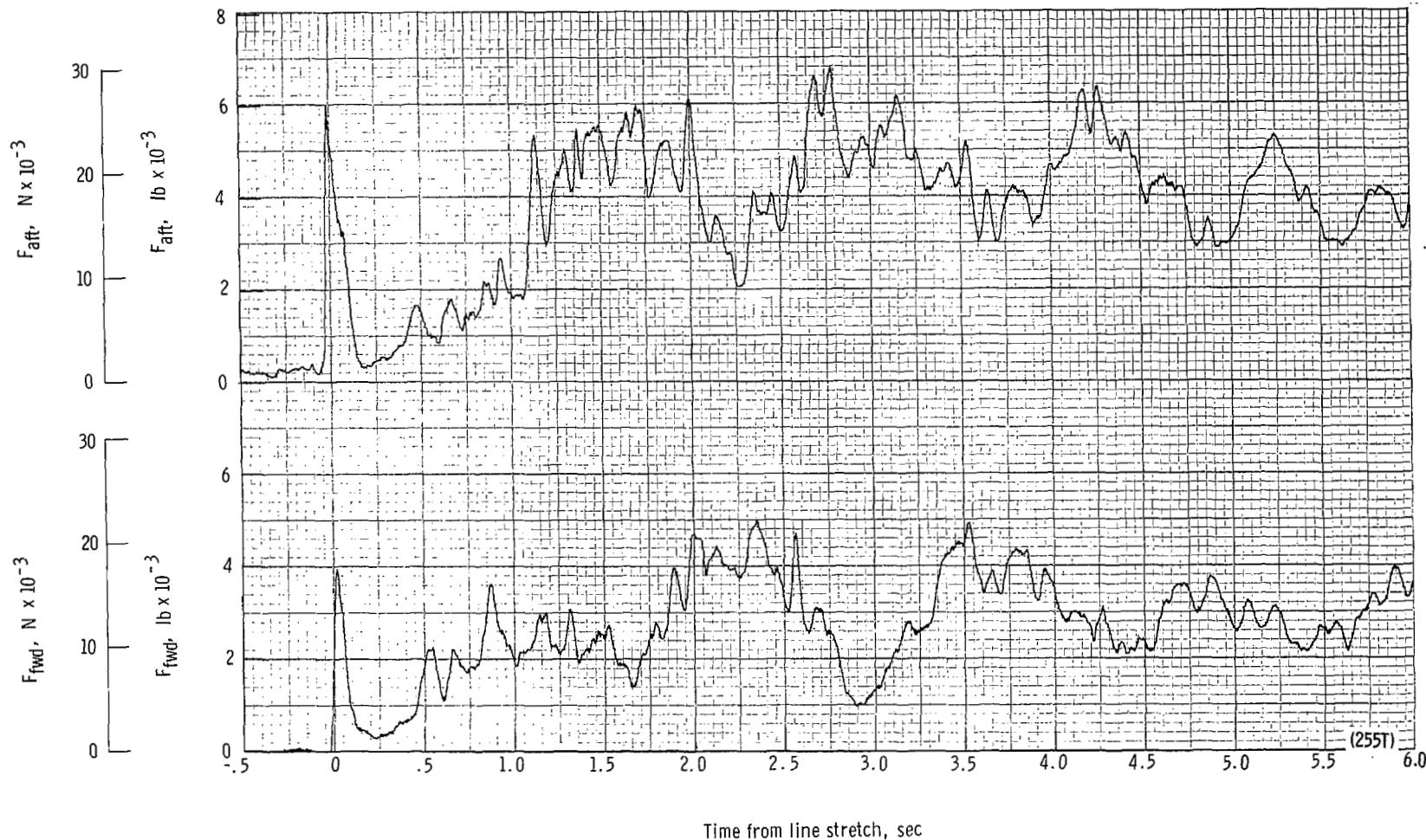


(a) Total force coefficient $C_{F,t}$ and dynamic pressure q plotted against time from line transfer. Time = 0 second corresponds to 32.32 seconds after launch.



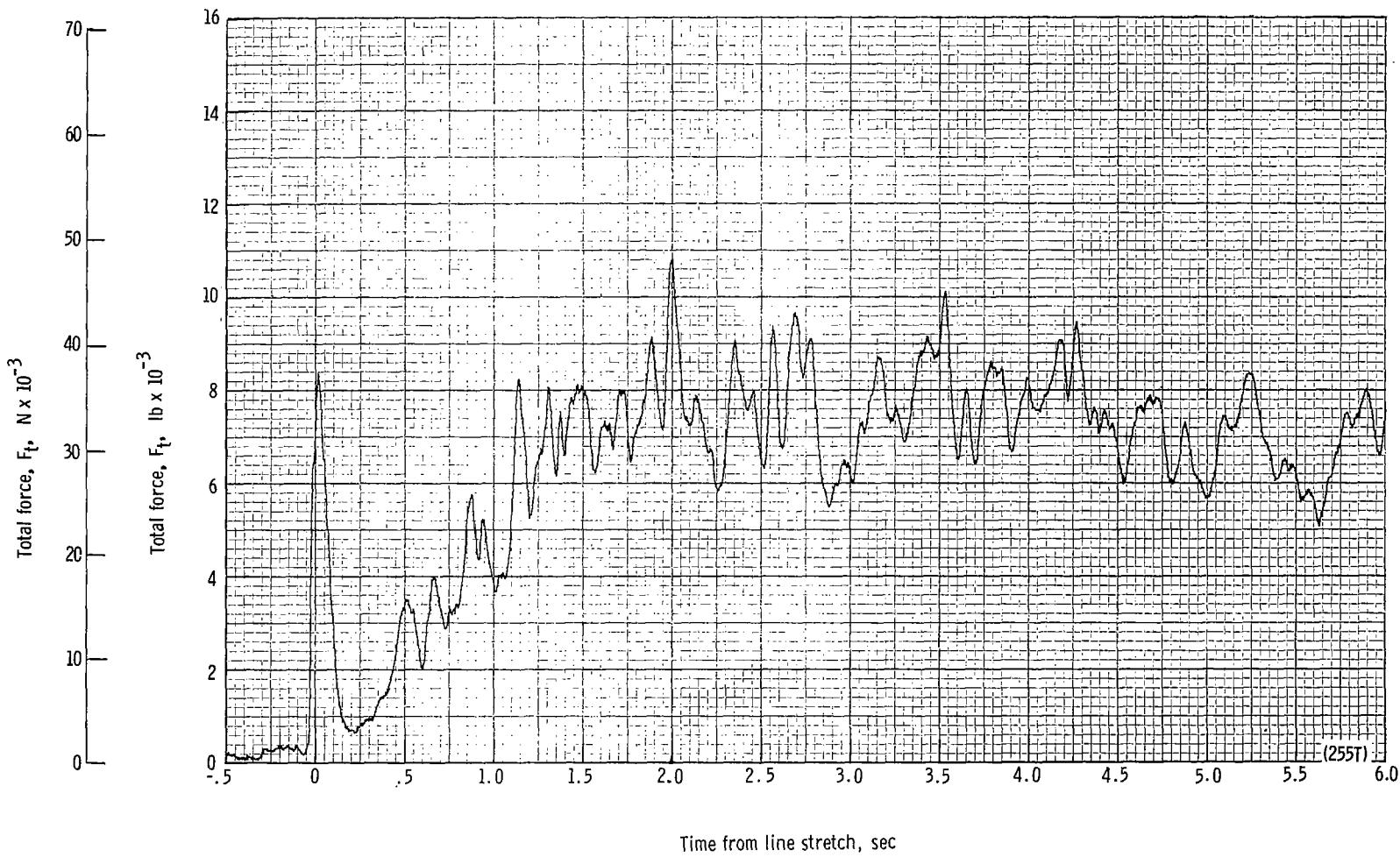
(p) Flight-path angle γ , dynamic pressure q , velocity V , and altitude h plotted against time from launch.

Figure 57.- Concluded.



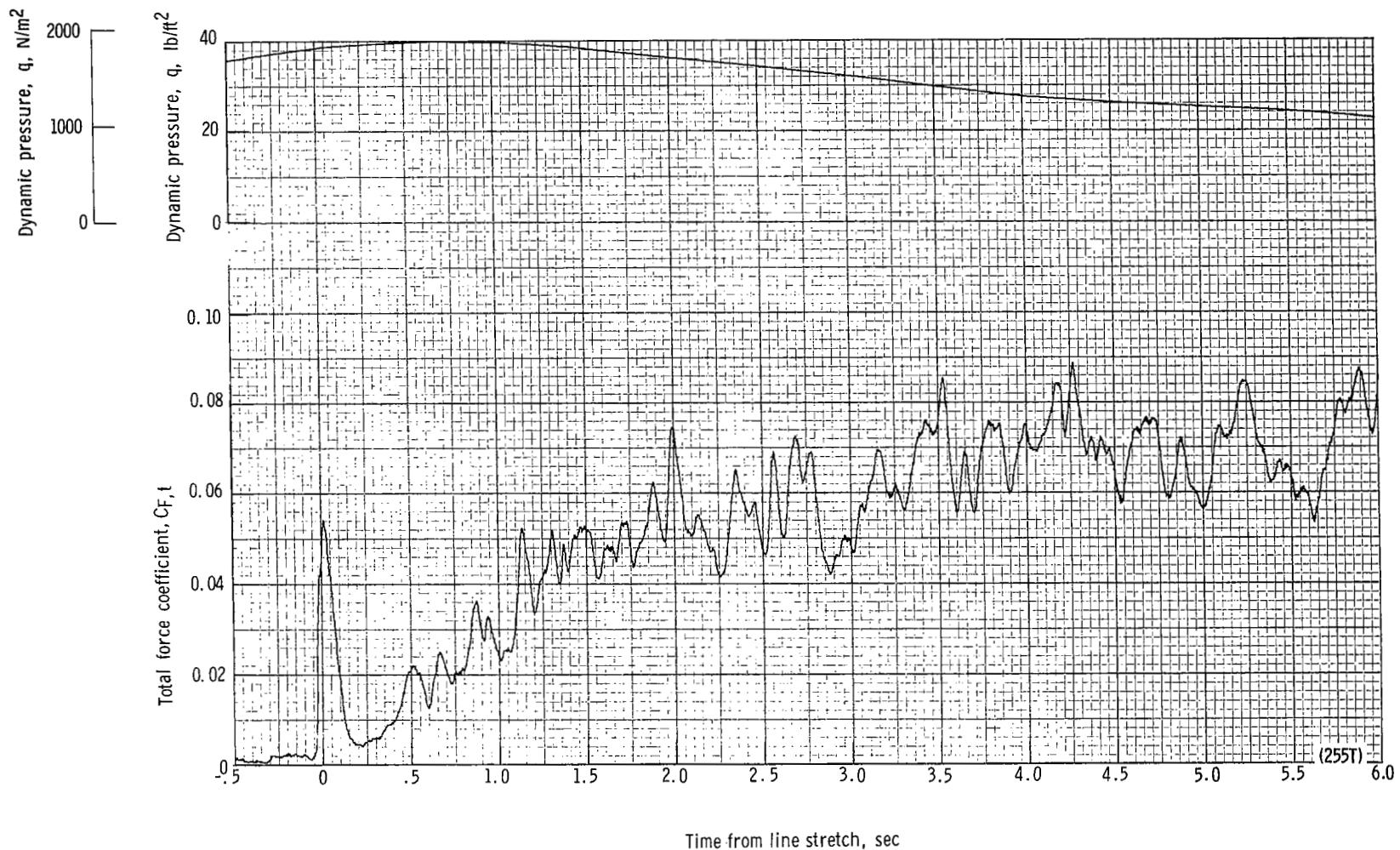
(a) Forward and aft riser loads plotted against time from line stretch. Time = 0 second corresponds to 12.08 seconds after launch.

Figure 58.- Time history of twin-keel parawing deployment data for test 255T. $W_D = 26\ 752 \text{ N}$ (6014 lb); $W_p = 24\ 881 \text{ N}$ (5593 lb); $q_{PD} = 1446 \text{ N/m}^2$ (30.2 lb/ft²); $h_{PD} = 7193 \text{ m}$ (23 600 ft); $l_r/l_k = 0.100$; reefing version C.



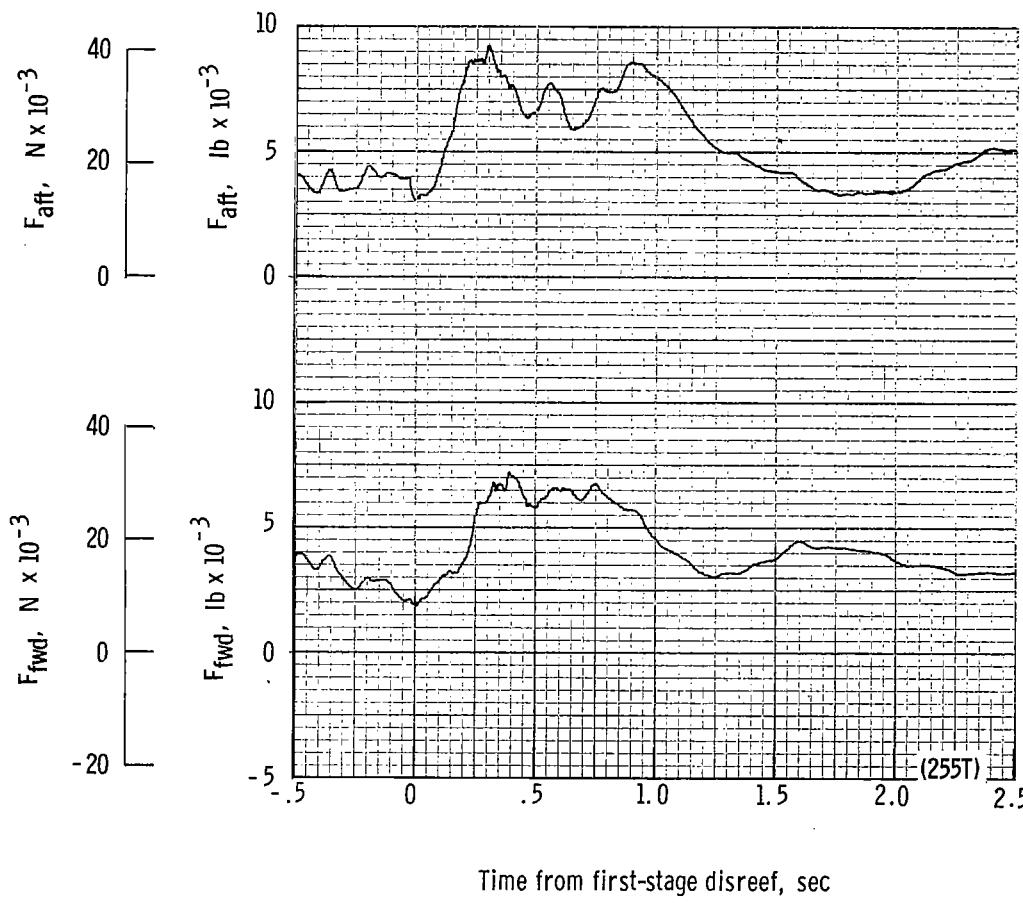
(b) Total force F_t plotted against time from line stretch. Time = 0 second corresponds to 12.08 seconds after launch.

Figure 58.- Continued.



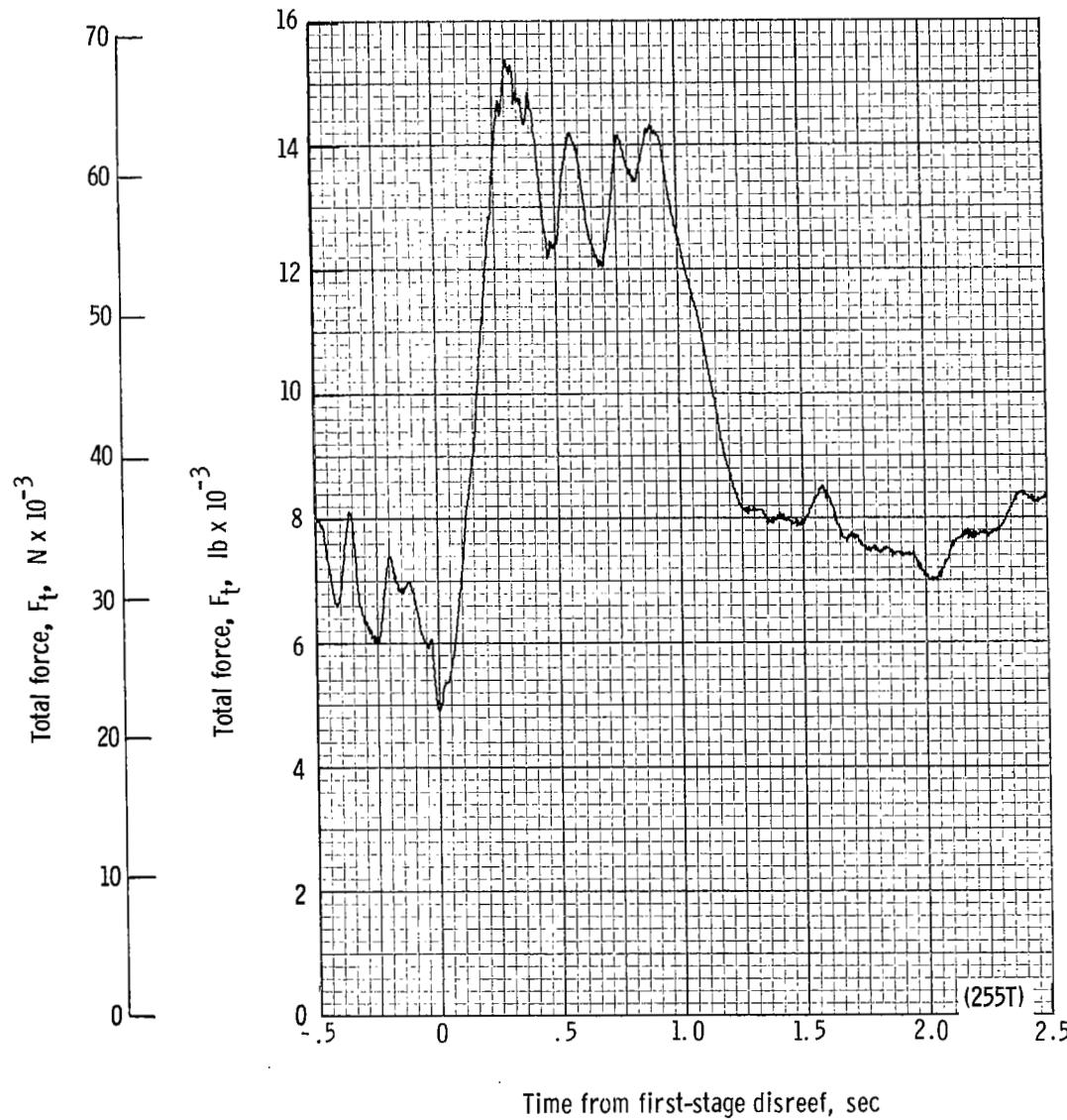
(c) Total force coefficient $C_{F,t}$ and dynamic pressure q plotted against time from line stretch. Time = 0 second corresponds to 12.08 seconds after launch.

Figure 58.- Continued.



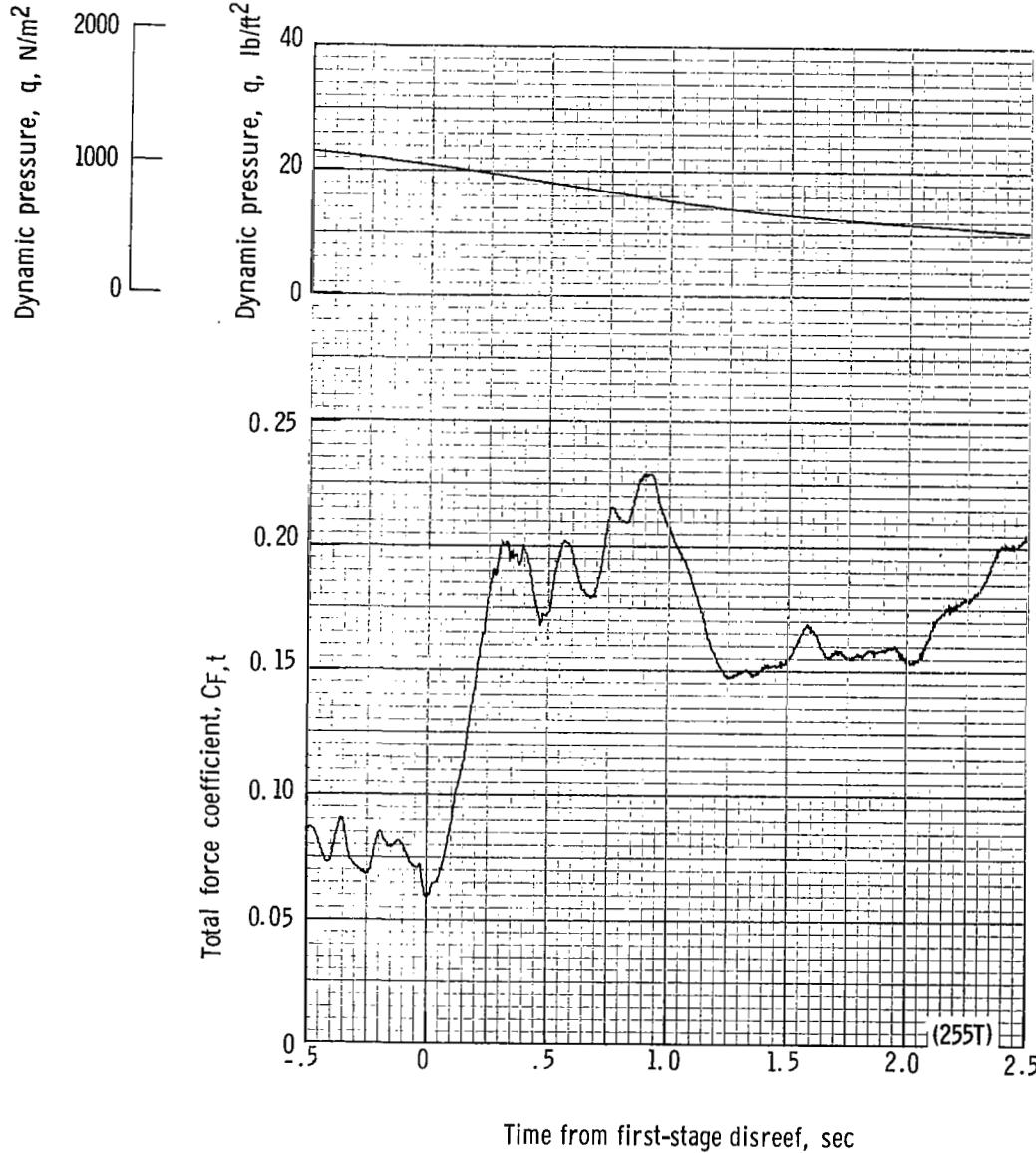
(d) Forward and aft riser loads plotted against time from first-stage disreef. Time = 0 second corresponds to 18.46 seconds after launch.

Figure 58.- Continued.



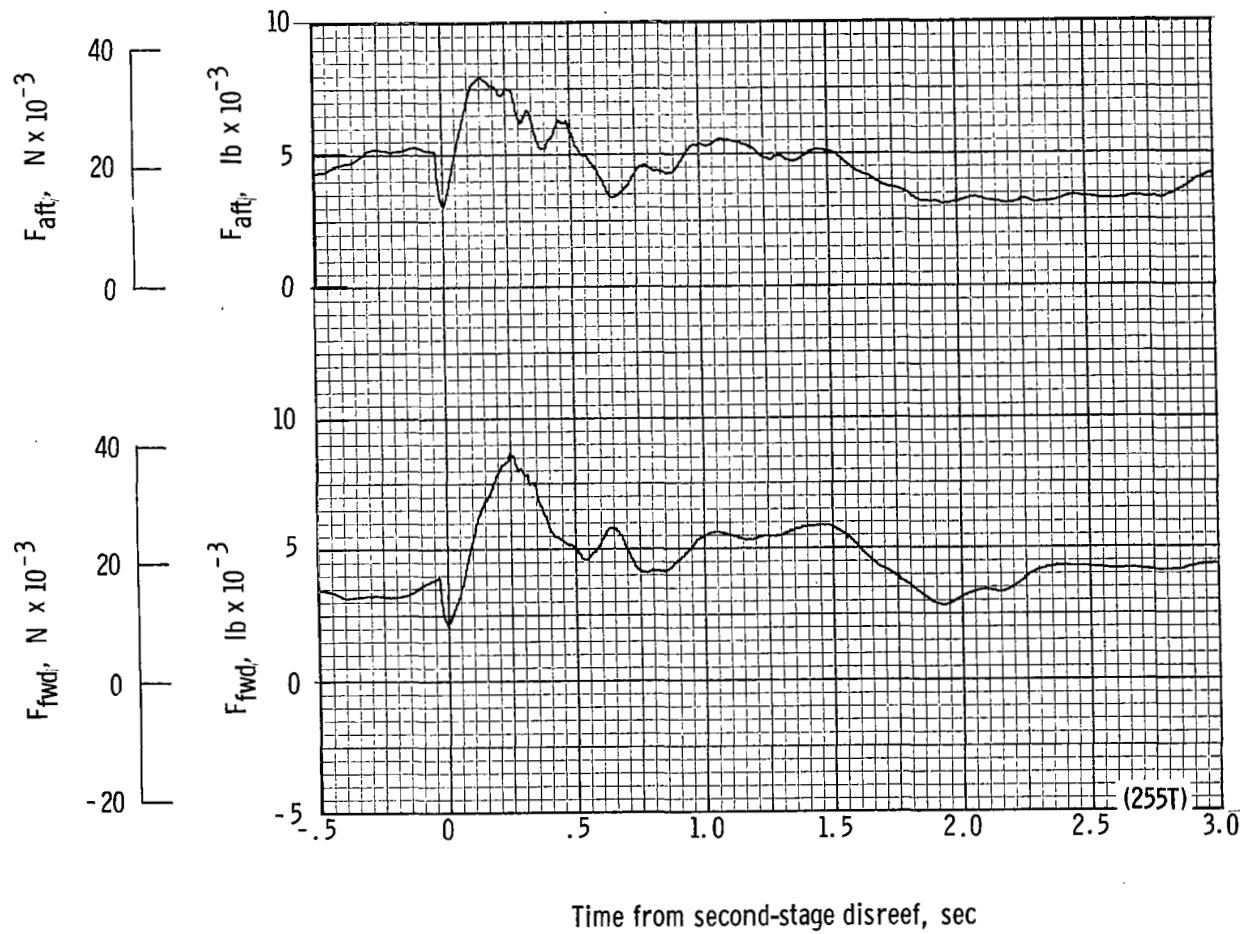
(e) Total force F_t plotted against time from first-stage disreef. Time = 0 second corresponds to 18.46 seconds after launch.

Figure 58.- Continued.



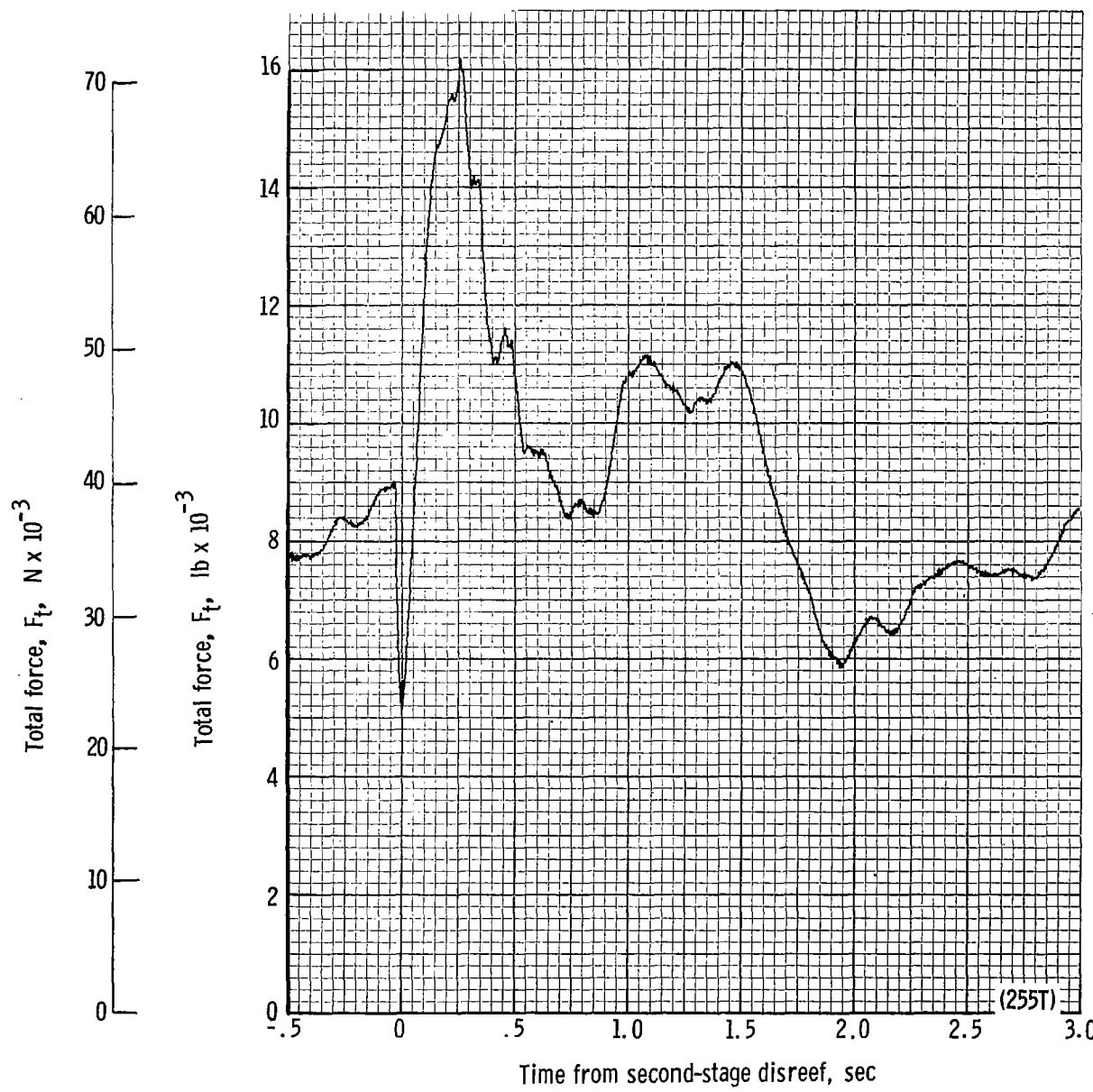
(f) Total force coefficient $C_{F,t}$ and dynamic pressure q plotted against time from first-stage disreef. Time = 0 second corresponds to 18.46 seconds after launch.

Figure 58.- Continued.



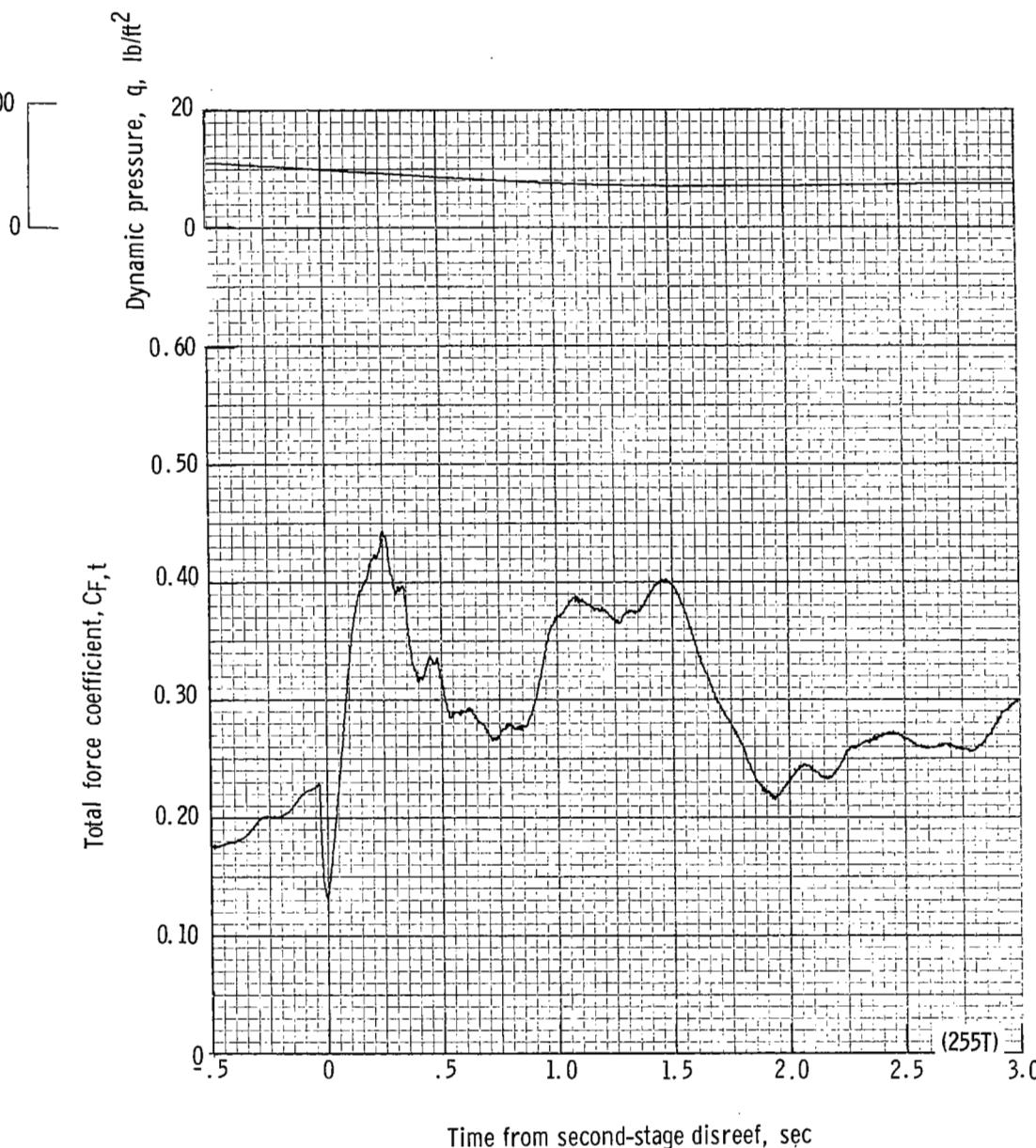
(g) Forward and aft riser loads plotted against time from second-stage disreef. Time = 0 second corresponds to 21.12 seconds after launch.

Figure 58.- Continued.



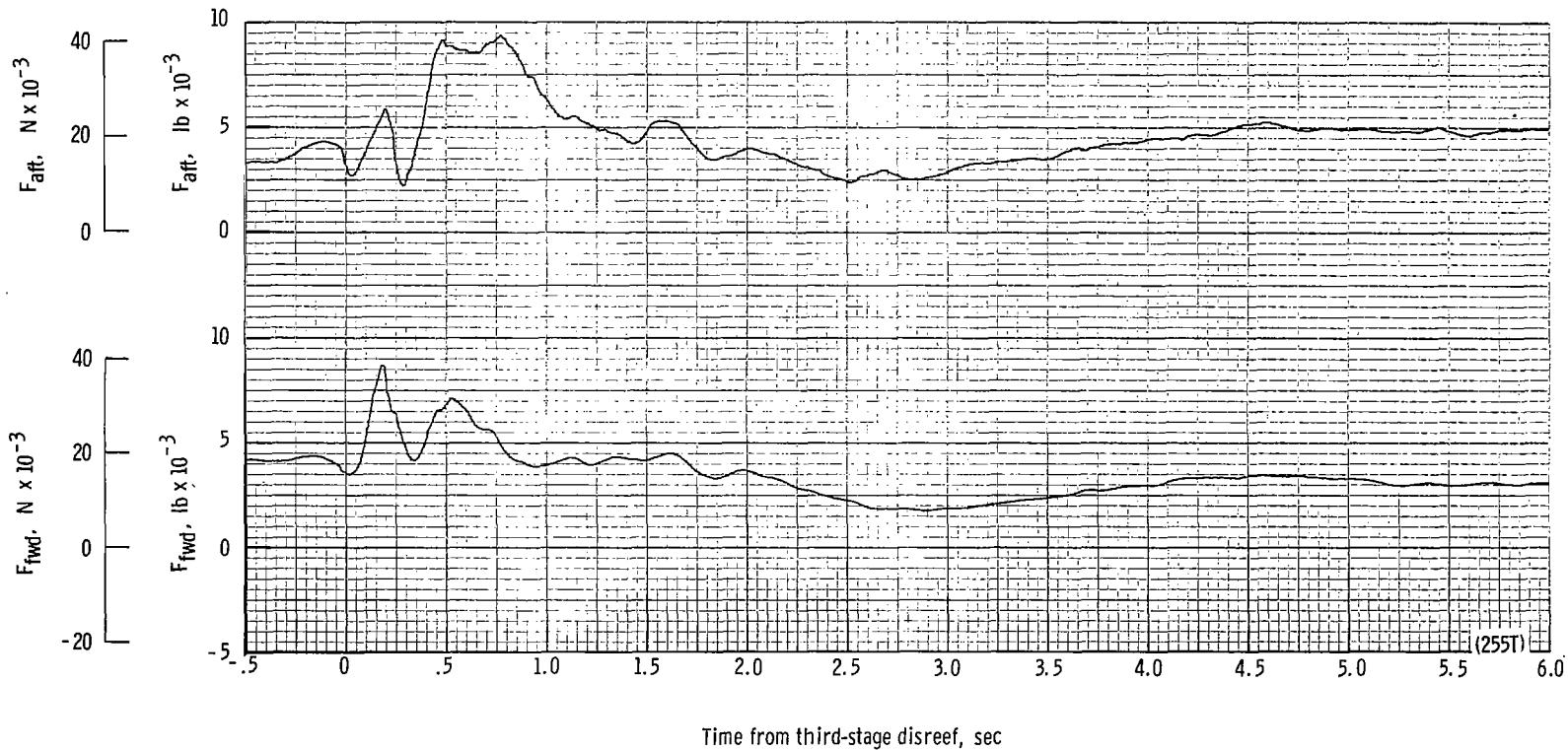
(h) Total force F_t plotted against time from second-stage disreef. Time = 0 second corresponds to 21.12 seconds after launch.

Figure 58.- Continued.



(i) Total force coefficient $C_{F,t}$ and dynamic pressure q plotted against time from second-stage disreef. Time = 0 second corresponds to 21.12 seconds after launch.

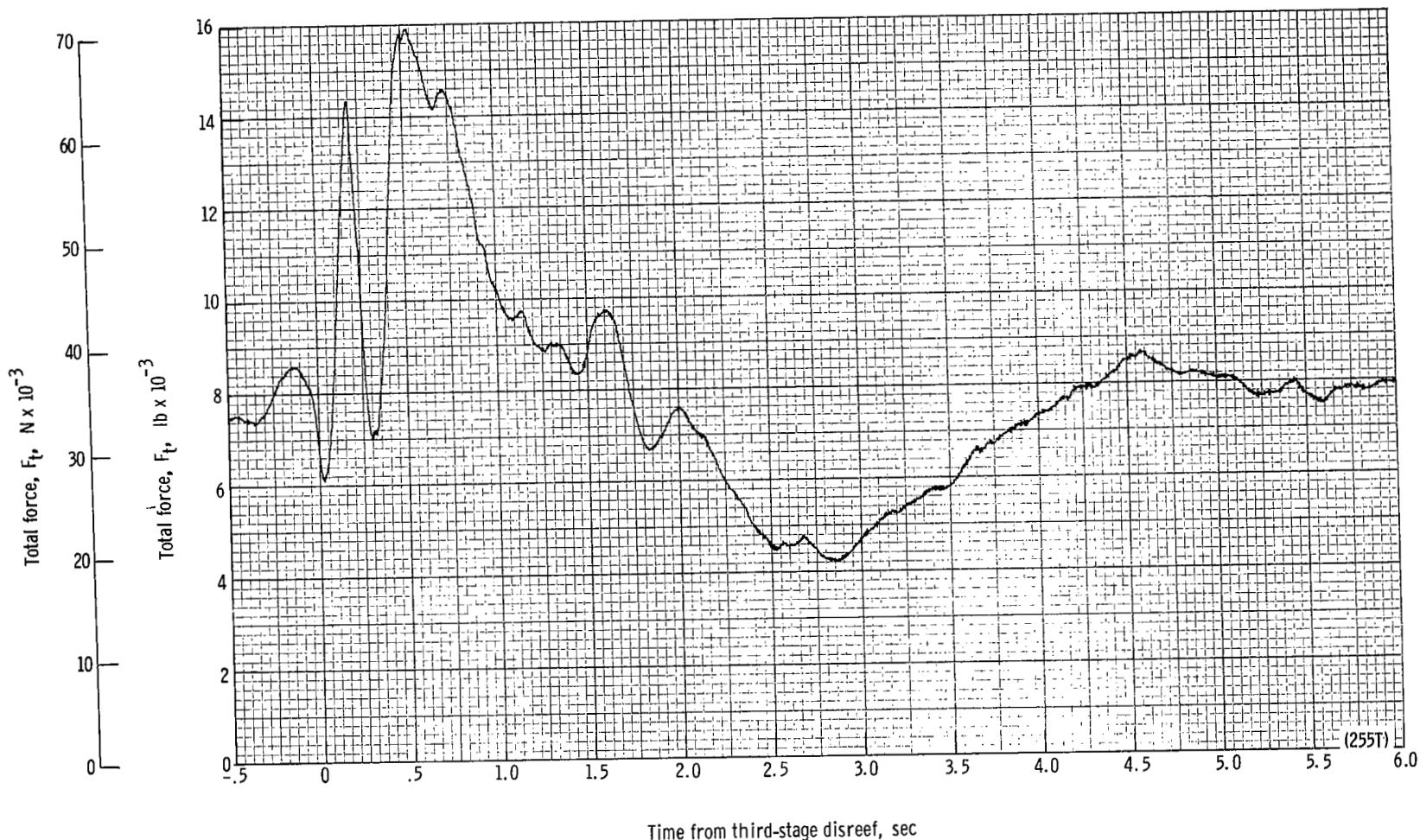
Figure 58.- Continued.



Time from third-stage disreef, sec

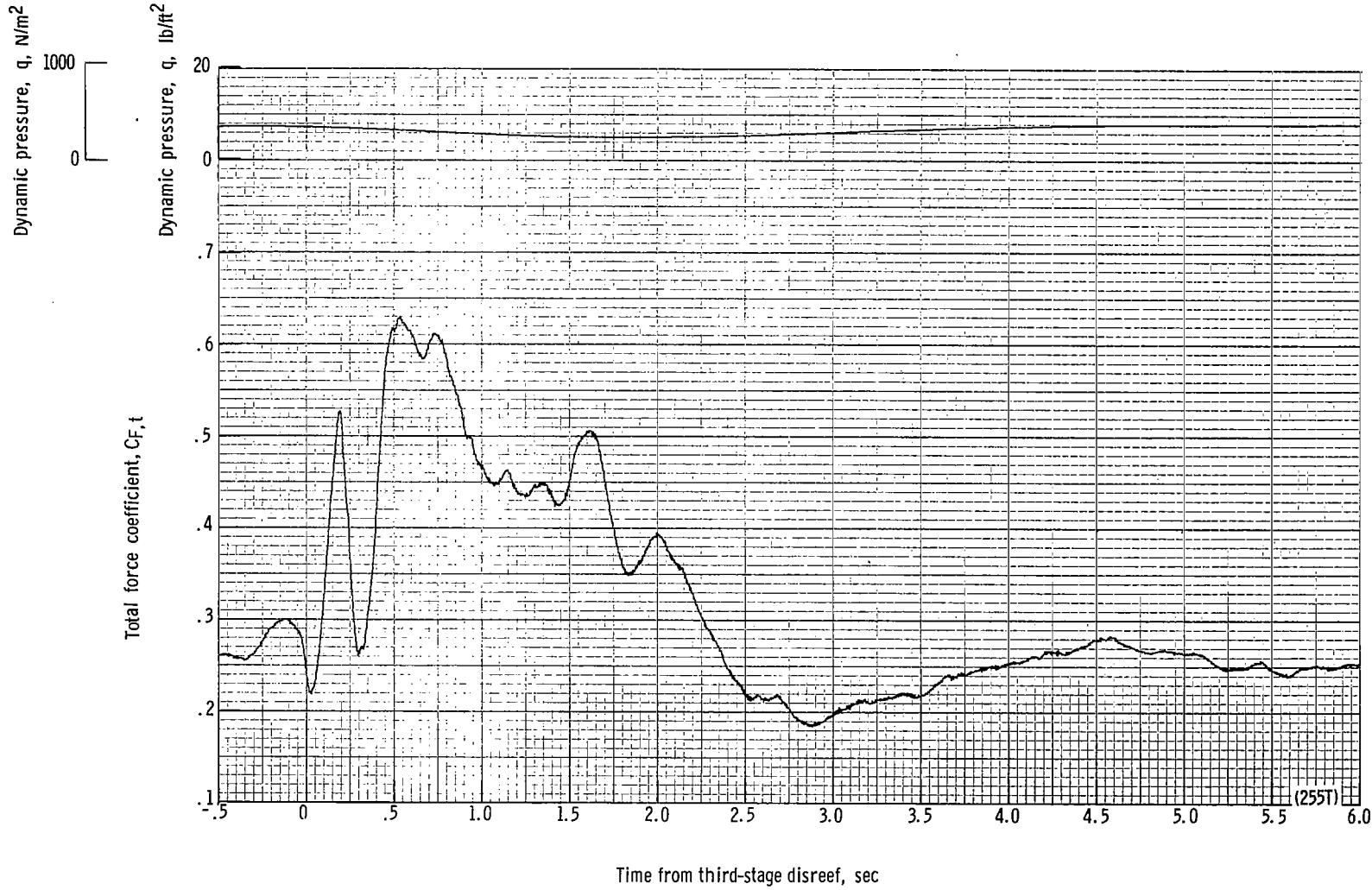
(j) Forward and aft riser loads plotted against time from third-stage disreef. Time = 0 second corresponds to 24.26 seconds after launch.

Figure 58.- Continued.



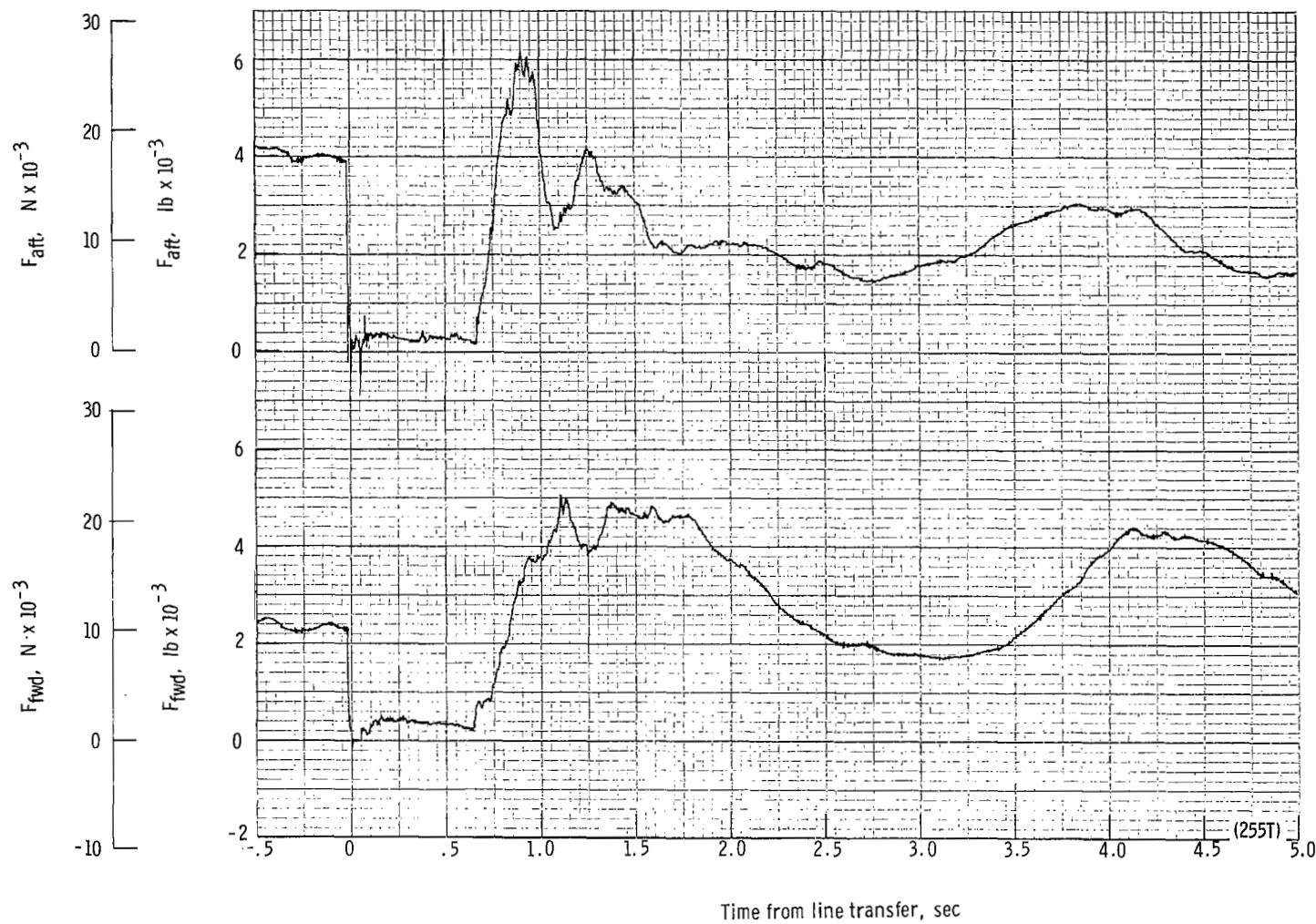
(k) Total force F_t plotted against time from third-stage disreef. Time = 0 second corresponds to 24.26 seconds after launch.

Figure 58.- Continued.



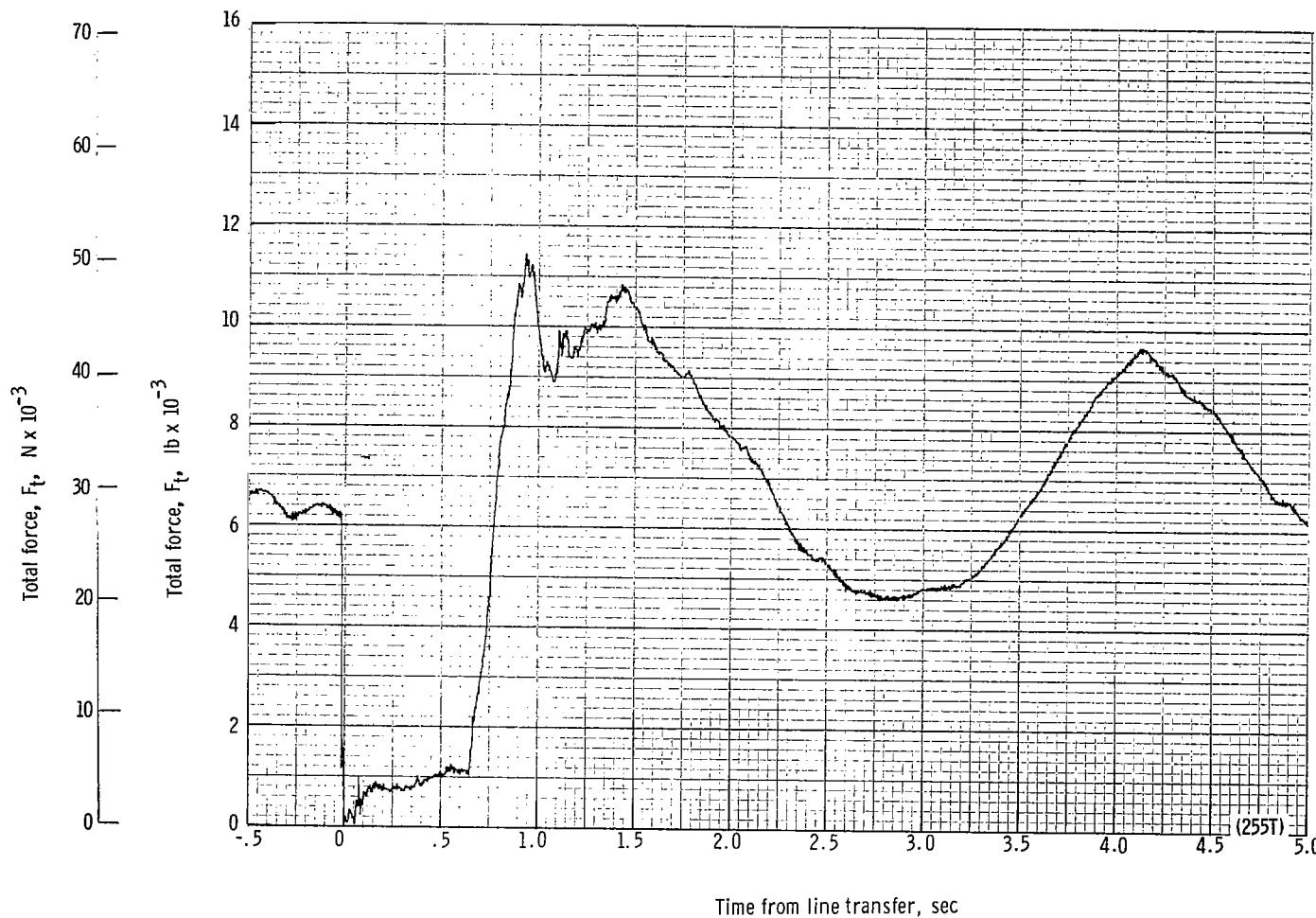
(II) Total force coefficient $C_{F,t}$ and dynamic pressure q plotted against time from third-stage disreef. Time = 0 second corresponds to 24.26 seconds after launch.

Figure 58.- Continued.



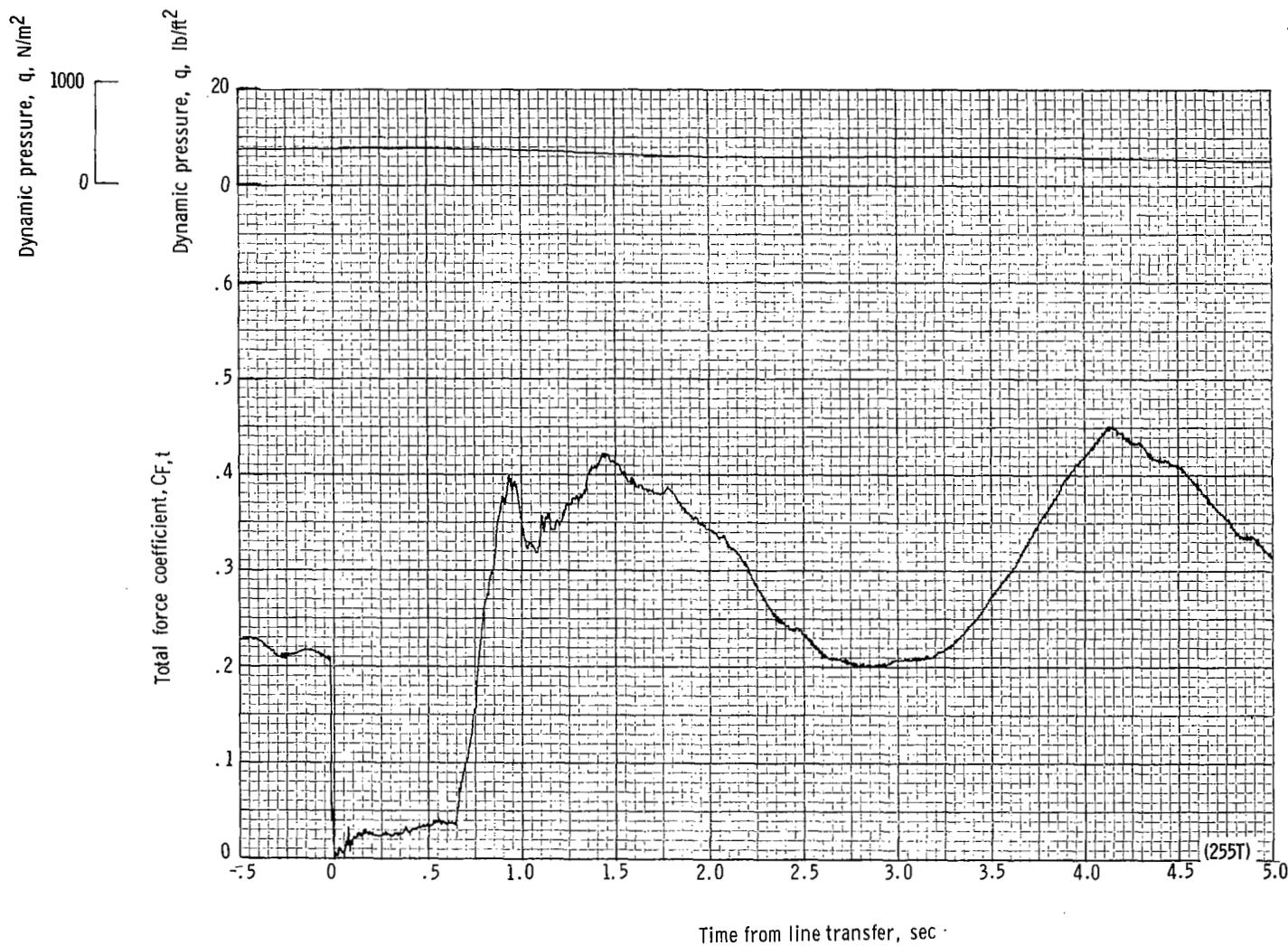
(m) Forward and aft riser loads plotted against time from line transfer. Time = 0 second corresponds to 32.27 seconds after launch.

Figure 58.- Continued.



(n) Total force F_t plotted against time from line transfer. Time = 0 second corresponds to 32.27 seconds after launch.

Figure 58.- Continued.



(o) Total force coefficient $C_{F,t}$ and dynamic pressure q plotted against time from line transfer. Time = 0 second corresponds to 32.27 seconds after launch.

Figure 58.- Continued.

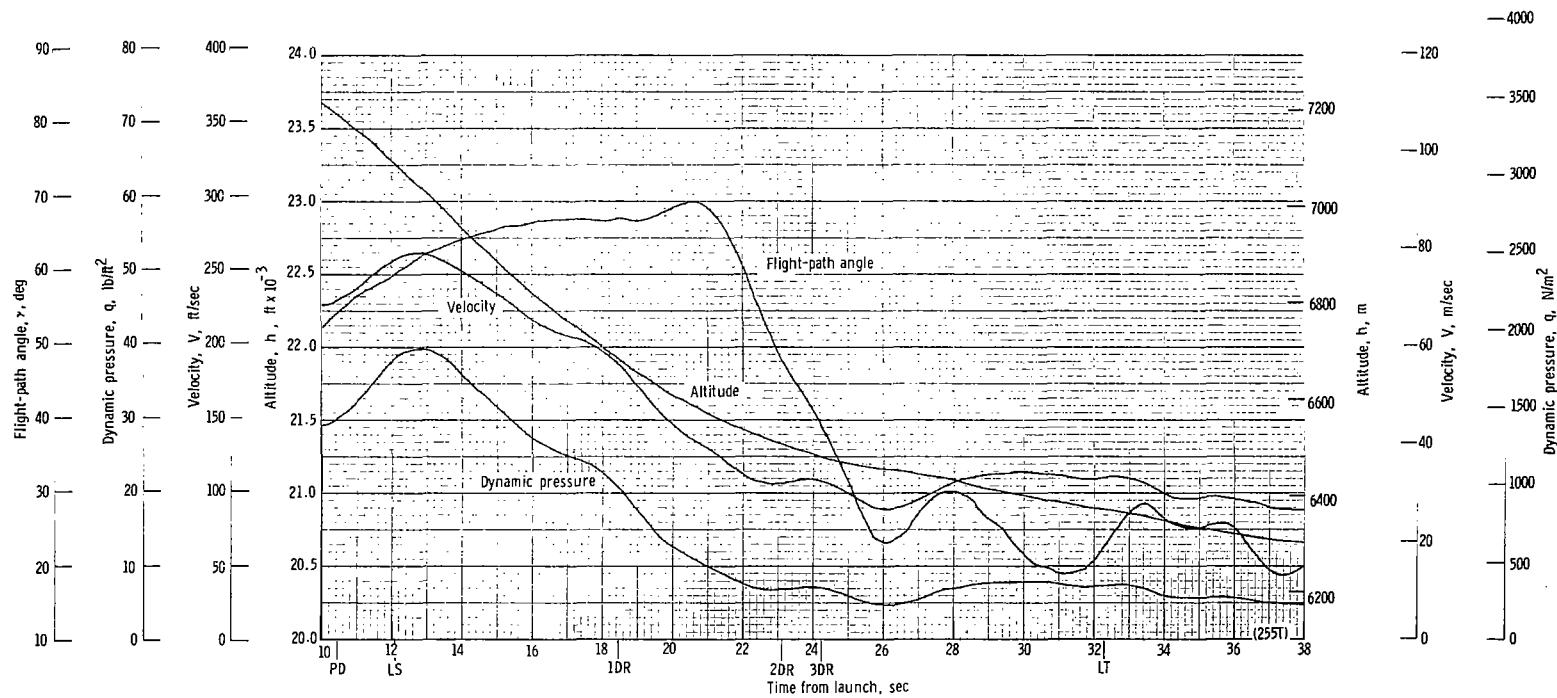
(p) Flight-path angle γ , dynamic pressure q , velocity V , and altitude h plotted against time from launch.

Figure 58.- Concluded.

NATIONAL AERONAUTICS AND SPACE ADMINISTRATION
WASHINGTON, D.C. 20546

OFFICIAL BUSINESS
PENALTY FOR PRIVATE USE \$300

FIRST CLASS MAIL

POSTAGE AND FEES PAID
NATIONAL AERONAUTICS AND
SPACE ADMINISTRATION



009B 01 C2 UL 02 711119 S00903DS 720401
DEPT OF THE AIR FORCE
AF WEAPONS LAB (AFSC)
TECH LIBRARY/WLOL/
ATTN: E LOU BOWMAN, CHIEF
KIRTLAND AFB NM 87117

POSTMASTER: If Undeliverable (Section
Postal Manual) Do Not R

"The aeronautical and space activities of the United States shall be conducted so as to contribute . . . to the expansion of human knowledge of phenomena in the atmosphere and space. The Administration shall provide for the widest practicable and appropriate dissemination of information concerning its activities and the results thereof."

— NATIONAL AERONAUTICS AND SPACE ACT OF 1958

NASA SCIENTIFIC AND TECHNICAL PUBLICATIONS

TECHNICAL REPORTS: Scientific and technical information considered important, complete, and a lasting contribution to existing knowledge.

TECHNICAL NOTES: Information less broad in scope but nevertheless of importance as a contribution to existing knowledge.

TECHNICAL MEMORANDUMS: Information receiving limited distribution because of preliminary data, security classification, or other reasons.

CONTRACTOR REPORTS: Scientific and technical information generated under a NASA contract or grant and considered an important contribution to existing knowledge.

TECHNICAL TRANSLATIONS: Information published in a foreign language considered to merit NASA distribution in English.

SPECIAL PUBLICATIONS: Information derived from or of value to NASA activities. Publications include conference proceedings, monographs, data compilations, handbooks, sourcebooks, and special bibliographies.

TECHNOLOGY UTILIZATION PUBLICATIONS: Information on technology used by NASA that may be of particular interest in commercial and other non-aerospace applications. Publications include Tech Briefs, Technology Utilization Reports and Technology Surveys.

Details on the availability of these publications may be obtained from:

SCIENTIFIC AND TECHNICAL INFORMATION OFFICE

NATIONAL AERONAUTICS AND SPACE ADMINISTRATION

Washington, D.C. 20546